

Volume 10 Issue 4

April 2019



ISSN 2156-5570(Online)

ISSN 2158-107X(Print)



www.ijacsa.thesai.org

Editorial Preface

From the Desk of Managing Editor...

It may be difficult to imagine that almost half a century ago we used computers far less sophisticated than current home desktop computers to put a man on the moon. In that 50 year span, the field of computer science has exploded.

Computer science has opened new avenues for thought and experimentation. What began as a way to simplify the calculation process has given birth to technology once only imagined by the human mind. The ability to communicate and share ideas even though collaborators are half a world away and exploration of not just the stars above but the internal workings of the human genome are some of the ways that this field has moved at an exponential pace.

At the International Journal of Advanced Computer Science and Applications it is our mission to provide an outlet for quality research. We want to promote universal access and opportunities for the international scientific community to share and disseminate scientific and technical information.

We believe in spreading knowledge of computer science and its applications to all classes of audiences. That is why we deliver up-to-date, authoritative coverage and offer open access of all our articles. Our archives have served as a place to provoke philosophical, theoretical, and empirical ideas from some of the finest minds in the field.

We utilize the talents and experience of editor and reviewers working at Universities and Institutions from around the world. We would like to express our gratitude to all authors, whose research results have been published in our journal, as well as our referees for their in-depth evaluations. Our high standards are maintained through a double blind review process.

We hope that this edition of IJACSA inspires and entices you to submit your own contributions in upcoming issues. Thank you for sharing wisdom.

Thank you for Sharing Wisdom!

Managing Editor

IJACSA

Volume 10 Issue 4 April 2019

ISSN 2156-5570 (Online)

ISSN 2158-107X (Print)

©2013 The Science and Information (SAI) Organization

Editorial Board

Editor-in-Chief

Dr. Kohei Arai - Saga University

Domains of Research: Technology Trends, Computer Vision, Decision Making, Information Retrieval, Networking, Simulation

Associate Editors

Chao-Tung Yang

Department of Computer Science, Tunghai University, Taiwan

Domain of Research: Software Engineering and Quality, High Performance Computing, Parallel and Distributed Computing, Parallel Computing

Elena SCUTELNICU

"Dunarea de Jos" University of Galati, Romania

Domain of Research: e-Learning, e-Learning Tools, Simulation

Krassen Stefanov

Professor at Sofia University St. Kliment Ohridski, Bulgaria

Domains of Research: e-Learning, Agents and Multi-agent Systems, Artificial Intelligence, Big Data, Cloud Computing, Data Retrieval and Data Mining, Distributed Systems, e-Learning Organisational Issues, e-Learning Tools, Educational Systems Design, Human Computer Interaction, Internet Security, Knowledge Engineering and Mining, Knowledge Representation, Ontology Engineering, Social Computing, Web-based Learning Communities, Wireless/ Mobile Applications

Maria-Angeles Grado-Caffaro

Scientific Consultant, Italy

Domain of Research: Electronics, Sensing and Sensor Networks

Mohd Helmy Abd Wahab

Universiti Tun Hussein Onn Malaysia

Domain of Research: Intelligent Systems, Data Mining, Databases

T. V. Prasad

Lingaya's University, India

Domain of Research: Intelligent Systems, Bioinformatics, Image Processing, Knowledge Representation, Natural Language Processing, Robotics

CONTENTS

Paper 1: Global and Local Characterization of Rock Classification by Gabor and DCT Filters with a Color Texture Descriptor

Authors: J. Wognin Vangah, Sié Ouattara, Gbélé Ouattara, Alain Clement

PAGE 1 – 10

Paper 2: Adoption of the Internet of Things (IoT) in Agriculture and Smart Farming towards Urban Greening

Authors: A. A. Raneesha Madushanki, Malka N Halgamuge, W. A. H. Surangi Wirasagoda, Ali Sye

PAGE 11 – 28

Paper 3: e-Learning Tools on the Healthcare Professional Social Networks

Authors: Evgeny Nikulchev, Dmitry Ilin, Bladimir Belov, Pavel Kolyasnikov, Alexander Kosenkov

PAGE 29 – 34

Paper 4: Systematic Literature Review (SLR) of Resource Scheduling and Security in Cloud Computing

Authors: Abdullah Sheikh, Malcolm Munro, David Budgen

PAGE 35 – 44

Paper 5: Towards a Mechanism for Protecting Seller's Interest of Cash on Delivery by using Smart Contract in Hyperledger

Authors: Ha Xuan Son, Minh Hoang Nguyen, Nguyen Ngoc Phien, Hai Trieu Le, Quoc Nghiep Nguyen, Van Dai Dinh, Phu Thinh Tru, Phuc Nguyen

PAGE 45 – 50

Paper 6: Dynamic Modification of Activation Function using the Backpropagation Algorithm in the Artificial Neural Networks

Authors: Marina Adriana Mercioni, Alexandru Tiron, Stefan Holban

PAGE 51 – 56

Paper 7: Fault Injection and Test Approach for Behavioural Verilog Designs using the Proposed RASP-FIT Tool

Authors: Abdul Rafay Khatri, Ali Hayek, Josef Börcsök

PAGE 57 – 63

Paper 8: An Efficient Image Haze Removal Algorithm based on New Accurate Depth and Light Estimation Algorithm

Authors: Samia Haouassi, Wu Di, Meryem Hamidaoui, Tobji Rachida

PAGE 64 – 76

Paper 9: Arabic Text Classification using Feature-Reduction Techniques for Detecting Violence on Social Media

Authors: Hissah ALSaif, Taghreed Alotaibi

PAGE 77 – 87

Paper 10: Industrial Financial Forecasting using Long Short-Term Memory Recurrent Neural Networks

Authors: Muhammad Mohsin Ali, Muhammad Imran Babar, Muhammad Hamza, Muhammad Jehanzeb, Saad Habib, Muhammad Sajid Khan

PAGE 88 – 99

Paper 11: Software Artefacts Consistency Management towards Continuous Integration: A Roadmap

Authors: D. A. Meedeniya, I. D. Rubasinghe, I. Perera

PAGE 100 – 110

- Paper 12: A GRASP-based Solution Construction Approach for the Multi-Vehicle Profitable Pickup and Delivery Problem
Authors: Abeer I. Alhujaylan, Manar I. Hosny
PAGE 111 – 120
- Paper 13: Secured Multi-Hop Clustering Protocol for Location-based Routing in VANETs
Authors: K. Sushma Eunice, I. Juvanna
PAGE 121 – 126
- Paper 14: Compound Mapping and Filter Algorithm for Hybrid SSD Structure
Authors: Jin-Young Kim, Se Jin Kwon
PAGE 127 – 132
- Paper 15: Optimal Compression of Medical Images
Authors: Rafi Ullah Habib
PAGE 133 – 140
- Paper 16: Protection of Ultrasound Image Sequence: Employing Motion Vector Reversible Watermarking
Authors: Rafi Ullah Habib, Fayez Al-Fayez
PAGE 141 – 149
- Paper 17: Extended Fuzzy Analytical Hierarchy Process Approach in Determinants of Employees' Competencies in the Fourth Industrial Revolution
Authors: Phuc Van Nguyen, Phong Thanh Nguyen, Quyen Le Hoang Thuy To Nguyen, Vy Dang Bich Huynh
PAGE 150 – 154
- Paper 18: A Recurrent Neural Network and a Discrete Wavelet Transform to Predict the Saudi Stock Price Trends
Authors: Mutasem Jarrah, Naomie Salim
PAGE 155 – 162
- Paper 19: Medical Image(s) Watermarking and its Optimization using Genetic Programming
Authors: Rafi Ullah Habib, Hani Ali Alquhayz
PAGE 163 – 169
- Paper 20: Voltage Variation Signals Source Identification and Diagnosis Method
Authors: Weihown Tee, Mohd Rahimi Yusoff, Abdul Rahim Abdullah, Muhamad Faizal Yaakub
PAGE 170 – 180
- Paper 21: Reliability and Connectivity Analysis of Vehicular Ad Hoc Networks for a Highway Tunnel
Authors: Saajid Hussain, Di Wu, Wang Xin, Sheeba Memon, Naadiya Khuda Bux, Arshad Saleem
PAGE 181 – 186
- Paper 22: Instrument Development for Measuring the Acceptance of UC&C: A Content Validity Study
Authors: Emy Salfarina Alias, Muriati Mukhtar and Ruzzakiah Jenal
PAGE 187 – 193
- Paper 23: Congestion Control Techniques in WSNs: A Review
Authors: Babar Nawaz, Khalid Mahmood, Jahangir Khan, Mahmood ul Hassan, Ansar Munir Shah, Muhammad Kashif Saeed
PAGE 194 – 199

Paper 24: Convolutional Neural Network based for Automatic Text Summarization

Authors: Wajdi Homaid Alquliti, Norjihhan Binti Abdul Ghani

PAGE 200 – 211

Paper 25: Hospital Readmission Prediction using Machine Learning Techniques

Authors: Samah Alajmani, Hanan Elazhary

PAGE 212 – 220

Paper 26: A Comparative Analysis of Wavelet Families for the Classification of Finger Motions

Authors: Jingwei Too, Abdul Rahim Abdullah, Norhashimah Mohd Saad

PAGE 221 – 226

Paper 27: Comparative Analysis of Cow Disease Diagnosis Expert System using Bayesian Network and Dempster-Shafer Method

Authors: Aristoteles, Kusuma Adhianto, Rico Andrian, Yeni Nuhricha Sari

PAGE 227 – 235

Paper 28: Enhanced e-Learning Experience using Case based Reasoning Methodology

Authors: Swati Shekapure, Dipti D. Patil

PAGE 236 – 241

Paper 29: Effect of Correlating ImageThreshold Values with Image Gradient Field on Damage Detection in Composite Structures

Authors: Mahmoud Zaki Iskandarani

PAGE 242 – 251

Paper 30: Images Steganography Approach Supporting Chaotic Map Technique for the Security of Online Transfer

Authors: Yasser Mohammad Al-Sharo

PAGE 252 – 258

Paper 31: ABCVS: An Artificial Bee Colony for Generating Variable T-Way Test Sets

Authors: Ammar K Alazzawi, Helmi Md Rais, Shuib Basri

PAGE 259 – 274

Paper 32: Improving the Performance of {0,1,3}-NAF Recoding Algorithm for Elliptic Curve Scalar Multiplication

Authors: Waleed K. AbdulRaheem, Sharifah Bte Md Yasin, Nur Izura Binti Udzir, Muhammad Rezal bin Kamel Ariffin

PAGE 275 – 279

Paper 33: Novel Software-Defined Network Approach of Flexible Network Adaptive for VPN MPLS Traffic Engineering

Authors: Faycal Bensalah, Najib El Kamoun

PAGE 280 – 284

Paper 34: Big Data Strategy

Authors: Alicia Valdez, Griselda Cortes, Sergio Castaneda, Laura Vazquez, Angel Zarate, Yadira Salas Gerardo Haces Afondo

PAGE 285 – 290

Paper 35: Performance Analysis of Security Mechanism for Automotive Controller Area Network

Authors: Mabrouka Gmiden, Mohamed Hedi Gmiden, Hafedh Trabelsi

PAGE 291 – 297

Paper 36: Feature-based Sentiment Analysis for Slang Arabic Text

Authors: Emad E. Abdallah, Sarah A. Abo-Suaileek

PAGE 298 – 304

Paper 37: Healthcare Management using ICT and IoT based 5G

Authors: Vijey Thayanathan

PAGE 305 – 312

Paper 38: Towards a Conceptual Model to Evaluate usability of Digital Government Services in Malaysia

Authors: Rini Yudesia Naswir, Nurazean Maarop, Mahmudul Hasan, Salwani Daud, Ganthan Narayana Samy, Prithheega Magalingam

PAGE 313 – 322

Paper 39: A Hybrid of Multiple Linear Regression Clustering Model with Support Vector Machine for Colorectal Cancer Tumor Size Prediction

Authors: Muhammad Ammar Shafi, Mohd Saifullah Rusiman, Shuhaida Ismail, Muhamad Ghazali Kamardan

PAGE 323 – 328

Paper 40: Intrusion-Miner: A Hybrid Classifier for Intrusion Detection using Data Mining

Authors: Samra Zafar, Muhammad.Kamran, Xiaopeng.Hu

PAGE 329 – 336

Paper 41: Gene Optimized Deep Neural Round Robin Workflow Scheduling in Cloud

Authors: Shanmugasundaram M, Kumar R, Kittur H M

PAGE 337 – 346

Paper 42: Multi-criteria Intelligent Algorithm for Supply Chain Management

Authors: Mahdi Jemmali, Loai Kayed B.Melhim, Mafawez Alharbi

PAGE 347 – 353

Paper 43: Techniques, Tools and Applications of Graph Analytic

Authors: Faiza Ameer, Muhammad Kashif Hanif, Ramzan Talib, Muhammad Umer Sarwar, Zahid Khan, Khawar Zulfiqar

PAGE 354 – 363

Paper 44: Dual-Cross-Polarized Antenna Decoupling for 43 GHz Planar Massive MIMO in Full Duplex Single Channel Communications

Authors: Muhsin, Rina Pudji Astuti

PAGE 364 – 370

Paper 45: Multimodal Age-Group Recognition for Opinion Video Logs using Ensemble of Neural Networks

Authors: Sadam Al-Azani, El-Sayed M. El-Alfy

PAGE 371 – 378

Paper 46: Performance Evaluation of Completed Local Ternary Pattern (CLTP) for Face Image Recognition

Authors: Sam Yin Yee, Taha H. Rassem, Mohammed Falah Mohammed, Nasrin M. Makbol

PAGE 379 – 387

Paper 47: Quantitative Analysis of Healthy and Pathological Vocal Fold Vibrations using an Optical Flow based Waveform

Authors: Heyfa Ammar

PAGE 388 – 393

Paper 48: A Parallel Hybrid-Testing Tool Architecture for a Dual-Programming Model

Authors: Ahmed Mohammed Alghamdi, Fathy Elbouraey Eassa

PAGE 394 – 400

Paper 49: Efficient Mining of Association Rules based on Clustering from Distributed Data

Authors: Marwa Bouraoui, Amel Grissa Touzi

PAGE 401 – 409

Paper 50: Academic Emotions Affected by Robot Eye Color: An Investigation of Manipulability and Individual-Adaptability

Authors: Kento Koike, Yuya Tsuji, Takahito Tomoto, Daisuke Katagami, Takenori Obo, Yuta Ogai, Junji Sone, Yoshihisa Udagawa

PAGE 410 – 418

Paper 51: Formal Concept Analysis based Framework for Evaluating Information System Success

Authors: Ansar Daghour, Khalifa Mansouri, Mohammed Qbadou

PAGE 419 – 424

Paper 52: Cluster based Hybrid Approach to Task Scheduling in Cloud Environment

Authors: Y. Home Prasanna Raju, Nagaraju Devarakonda

PAGE 425 – 429

Paper 53: How Volunteering Affects the Offender's Behavior

Authors: Momina Shaheen, Tayyaba Anees, Muhammad Imran Manzoor, Shuja Akbar, Iqra Obaid, Aimen Anum

PAGE 430 – 439

Paper 54: Real Time RNA Sequence Edition with Matrix Insertion Deletion for Improved Bio Molecular Computing using Template Match Measure

Authors: Kotteeswaran C, Khanaa V, Rajesh A

PAGE 440 – 444

Paper 55: CMMI-DEV Implementation Simplified

Authors: Maruthi Rohit Ayyagari, Issa Atoum

PAGE 445 – 450

Paper 56: Algorithm for Enhancing the QoS of Video Traffic over Wireless Mesh Networks

Authors: Abdul Nasser A. Moh, Radhwan Mohamed Abdullah, Abedallah Zaid Abualkishik, Borhanuddin Bin Moh. Ali, Ali A. Alwan

PAGE 451 – 456

Paper 57: Cybercrime in Morocco

Authors: M. EL Hamzaoui, Faycal Bensalah

PAGE 457 – 465

Paper 58: A Comprehensive Comparative Analysis of Two Novel Underwater Routing Protocols

Authors: Umar Draz, Tariq Ali, Khurshid Asghar, Sana Yasin, Zubair Sharif, Qasim Abbas, Shagufta Aman

PAGE 466 – 472

Paper 59: Extreme Learning Machine and Particle Swarm Optimization for Inflation Forecasting

Authors: Adyan Nur Alfiyatin, Agung Mustika Rizki, Wayan Firdaus Mahmudy, Candra Fajri Ananda

PAGE 473 – 478

Paper 60: Impact Factors of IT Flexibility within Cloud Technology on Various Aspects of IT Effectiveness
Authors: Salameh A. Mjlae, Zarina Mohamad, Wan Suryani

PAGE 479 – 489

Paper 61: Assistive Technologies for Bipolar Disorder: A Survey
Authors: Yumna Anwar, Dr. Arshia Khan

PAGE 490 – 499

Paper 62: Hybrid Genetic-FSM Technique for Detection of High-Volume DoS Attack
Authors: Mohamed Samy Nafie, Khaled Adel, Hassan Abounaser, Amr Badr

PAGE 500 – 509

Paper 63: Using Space Syntax and Information Visualization for Spatial Behavior Analysis and Simulation
Authors: Sheng-Ming Wang, Chieh-Ju Huang

PAGE 510 – 521

Paper 64: Content based Document Classification using Soft Cosine Measure
Authors: Md. Zahid Hasan, Shakhawat Hossain, Md. Arif Rizvee, Md. Shohel Rana

PAGE 522 – 528

Paper 65: Fuzzy Delphi Method for Evaluating HyTEE Model (Hybrid Software Change Management Tool with Test Effort Estimation)

Authors: Mazidah Mat Rejab, Nurulhuda Firdaus Mohd Azmi, Suriyati Chuprat

PAGE 529 – 535

Paper 66: Efficient MRI Segmentation and Detection of Brain Tumor using Convolutional Neural Network
Authors: Alpana Jijja, Dr. Dinesh Rai

PAGE 536 – 541

Paper 67: Smartphones-Based Crowdsourcing Approach for Installing Indoor Wi-Fi Access Points
Authors: Ahmad Abadleh, Wala Maitah, Hamzeh Eyal Salman, Omar Lasassmeh, Awni Hammouri

PAGE 542 – 549

Paper 68: Data Citation Service for Wikipedia Articles
Authors: Arif Bramantoro, Ahmad A. Alzahrani

PAGE 550 – 556

Paper 69: Software Abstractions for Large-Scale Deep Learning Models in Big Data Analytics
Authors: Ayaz H. Khan, Ali Mustafa Qamar, Aneeq Yusuf, Rehanullah Khan

PAGE 557 – 566

Paper 70: Person Detection from Overhead View: A Survey
Authors: Misbah Ahmad, Imran Ahmed, Kaleem Ullah, Iqbal Khan, Ayesha Khattak, Awais Adnan

PAGE 567 – 577

Paper 71: Towards a Context-Dependent Approach for Evaluating Data Quality Cost
Authors: Meryam Belhiah, Bouchaïb Bounabat

PAGE 578 – 584

Paper 72: Towards Usability Guidelines for the Design of Effective Arabic Websites

Authors: Abdallah Namoun, Ahmad B. Alkhodre

PAGE 585 – 594

Paper 73: Digital Certificate Exchange of Agricultural Products using SOAP Web Services

Authors: Miyanda Chilikwela, Jackson Phiri

PAGE 595 – 603

Paper 74: New Approach based on Model Driven Engineering for Processing Complex SPARQL Queries on Hive

Authors: Mouad Banane, Abdessamad Belangour

PAGE 604 – 609

Paper 75: Improved Cryptanalysis of Provable Certificateless Generalized Signcryption

Authors: Abdul Waheed, Jawaid Iqbal, Nizamud Din, Shahab Ul Islam, Arif Iqbal Umar, Noor Ul Amin

PAGE 610 – 616

Paper 76: Efficient Energy Utilization in Cloud Fog Environment

Authors: Babur Hayat, Muhammad Nauman Ali, Sheraz Yousaf, Mudassar Mehmood, Hammad Saleem

PAGE 617 – 623

Global and Local Characterization of Rock Classification by Gabor and DCT Filters with a Color Texture Descriptor

J. Wognin Vangah¹, Sié Ouattara², Gbélé Ouattara³, Alain Clement⁴

URMI Electronique et Electricité Appliquées (EAA)

Institut National Polytechnique Felix Houphouët-Boigny (INP-HB)

BP 1093 Yamoussoukro, Côte d'Ivoire^{1,2,3}

Laboratoire Angevin de Recherche en Ingénierie des Systèmes (LARIS)

Institut Universitaire de Technologie (IUT) / Université d'Angers

4 Boulevard Lavoisier - BP 42018 - 49016 - ANGERS, France⁴

Abstract—In the automatic classification of colored natural textures, the idea of proposing methods that reflect human perception arouses the enthusiasm of researchers in the field of image processing and computer vision. Therefore, the color space and the methods of analysis of color and texture, must be discriminating to correspond to the human vision. Rock images are a typical example of natural images and their analysis is of major importance in the rock industry. In this paper, we combine the statistical (Local Binary Pattern (LBP) with Hue Saturation Value (HSV) and Red Green Blue (RGB) color spaces fusion) and frequency (Gabor filter and Discrete Cosine Transform (DCT)) descriptors named respectively Gabor Adjacent Local Binary Pattern Color Space Fusion (G-ALBPCSF) and DCT Adjacent Local Binary Pattern Color Space Fusion (D-ALBPCSF) for the extraction of visual textural and colorimetric features from direct view images of rocks. The textural images from the two G-ALBPCSF and D-ALBPCSF approaches are evaluated through similarity metrics such as Chi2 and the intersection of histograms that we have adapted to color histograms. The results obtained allowed us to highlight the discrimination of the rock classes. The proposed extraction method provides better classification results for various direct view rock texture images. Then it is validated by a confusion matrix giving a low error rate of 0.8% of classification.

Keywords—Rock; classification; G-ALBPCSF; D-ALBPCSF; LBP; gabor; DCT; RGB; HSV; color texture

I. INTRODUCTION

In general, the classification and characterization of rocks are done visually following a long process by geologists and mineralogists with many years of experience or through by laboratory tests [1]. Therefore, this so-called manual classification takes time and seems approximate and subjective. However, the automatic classification of rocks could be beneficial and bridge this gap. Today, the analysis and automatic classification of color textures has become one of the areas of active search for shape recognition and computer vision. Several fields of application are covered; let us mention: biomedical [2], facial recognition [3], classification of rocks [4-14]. The automatic classification of rocks is a challenge in the field of image processing with an interest in geologists, universities and specific schools that

study rocks and also these applications in construction (roads, buildings, monuments). This is mainly related to the complex nature of the rocks that make those natural textures are not homogeneous, directional natural textures with very different granularity and color properties, making their classification very difficult. In this classification, the physiological perception of texture and color is very important. Therefore, the color space and texture / color analysis methods to be used, must be chosen to match human vision. A good classification always starts from discriminating methods of extraction of texture / color characteristics that are robust to noise, rotation and change of illumination. Typically, the feature extraction process for texture analysis involves statistical, structural, and multiscale methods. However, statistical and multiscale (frequency) approaches for feature extraction are becoming more popular using co-occurrence matrices, histograms, Gabor filters, and various LBP enhancements with exponential use for facial detection [3]. All these characteristics are derived from the measurement of attributes such as energy, contrast, entropy. Then, they are used by various classification and indexing algorithms such as K nearest neighbors (K-NN) [5, 8], Boosting algorithms (LPBoosting) [6], Support Vector Machine (SVM) [7, 9], Artificial Neural Networks (ANN) [8, 10], Maximum Likelihood (MV) [11] and K-means [21] to result in a better classification. In general, the extraction techniques focus on three forms of analysis of visual attribute: spectral analysis, radiometric analysis and textural analysis in the joint or separate use of color and texture. In [10], Ishikawa and Virginia in 2013, based on these visual attributes (texture and color) and Raman spectroscopy, were able to differentiate minerals in igneous rocks from networks of neurons through the analyze of spectral signature of minerals. However, although the classification of minerals has been largely successful, it is difficult to apply the same methods to all rocks because the spectra may have a combination of signature concurrent. In addition, some minerals that were under-represented with their method, were well identified with radiometric and textural analyzes. In [12], Blake et al. (2012), using X-ray diffraction, required rock samples to be collected and pulverized before chemical analysis. In [9], Galdames et

al. (2017), based on a textural and colorimetric analysis with 3D Laser Range-based features, made a lithological classification to determine the approximate mineralogical composition of rocks. A method for identifying the texture of different basalts in RGB or grayscale images using neural networks has been introduced by Singh et al. (2010) [13]. In [7], Bianconi et al. (2012) presented a classification system for granite tiles incorporating textural and color features. They tested different characteristics and the best performance was obtained with the co-occurrence matrices. A method for classifying limestone types using features based on color image histograms and a probabilistic neural network has been introduced in [14]. Lepisto et al. (2005) [5], succeeded in classifying rocks with textural and colorimetric analysis of visual attributes by applying Gabor filters in different color channels independently. In this study, it has been shown that it is possible to improve the classification of natural rock images by combining the color information with the description of the texture. It is known that rock images are rich in texture and color information. Despite these cited works, the classification of rock texture images remains a real challenge for the image processing scientific community. In recent times, the texture analysis community has developed a variety of different descriptors for the effective capture of textural information for representation and analysis. Local Binary Pattern (LBP) [15] is one of the best texture descriptors for extracting local texture information and has been used in various applications such as face recognition [3] and rock classification [4]. In [4], the performance of LBP, Coordinated Cluster Representation (CCR) and Improved Local Binary Pattern (ILBP) are measured for the classification of granite textures by evaluating the robustness against the rotation of these different LBP descriptors. In 2003, Lepisto et al [16] improved the classification result with the application of K-NN by combining the color information in the HSI space and the extraction of the texture of the rocks by the Gabor filters. The HSI space proved better for this study. Over the past decade, various original LBP extensions have been proposed for classification performance. Attention has been focused on Gabor filters and the LBP operator fusion. Thus Zhang et al. [17] introduced the Local Gabor-based Binary Pattern Histogram Sequence (LGBPHS) by combining LBP and Gabor to enhance the discriminative capacity of LBP descriptors. For the same reasons, Shan et al. [18] proposed Local Gabor Binary Patterns (LGBP) in face recognition. In 2013, Zhihua Xie in [19] showed that integrating global and local characteristics into facial recognition improved performance by comparing the DCT method to the new LGBPH classification method. However, these texture representation methods [17-19] do not consider, on the one hand, the color information in the texture and, on the other hand, its spatial representation in the texture and until now have not yet has been applied to our knowledge to the textures of rock direct view images. To overcome these problems, we propose in this paper two new color texture descriptors that consists in extending LBP color (ALBPCSF) [20] to Gabor Adjacent Local Binary Pattern Color Space Fusion (G-ALBPCSF) by introducing before and impressively the filtering multi-orientation and multi-scale Gabor. And then the DCT Adjacent Local Binary Pattern Color Space Fusion (D-

ALBPCSF) compared to the color LBP considering spatial structure relationships and color characteristics. This paper is organized as follows. Section II refers to previous work on LBP and its merger with Gabor. In section III, we will present the proposed new approach. Finally, the experimental results obtained by the two strategies of our new approach are compared to the different methods used. In section IV, our results will be discussed, and then we end with section V with the conclusion and the perspectives.

II. PREVIOUS WORK ON THE LBP AND ITS MERGER WITH GABOR

In this section, a summary of the LBP algorithms is first presented as well as its merger with Gabor.

A. Brief Review of Original LBP

A common strategy for detecting textures in images is to consider local patches that describe the behavior of the texture around a group of pixels. One of the descriptors that follows this strategy is the LBP descriptor. The LBP operator introduced by Ojala et al. [22] is an effective element of texture description with its discriminating power and simplicity of calculation. As shown in Fig. 1, the operator labels the pixels of an image with decimal numbers, called local bit patterns or LBP codes, which encodes the local structure around each central pixel defined as the threshold for the 3x3 neighborhood. Then each pixel is compared to its eight neighbors by subtracting the value of the central pixel from that of each of these neighbors. The resulting strictly negative values are coded with 0 and the others with 1. Finally, a binary number is obtained by concatenating all the pixels in the direction of the hand of a watch. The decimal value is used for labeling. This process can be expressed mathematically as follows:

$$LBP_{P,R} = \sum_{i=0}^{P-1} s(p_i - p_c) \times 2^i, \quad s(x) = \begin{cases} 1 & \text{if } x \geq 0 \\ 0 & \text{otherwise} \end{cases} \quad (1)$$

where p_c is the gray value of the central pixel, p_i is the gray value of the neighboring pixels, P is the number of neighboring pixels on the circle, R is the radius of the neighborhood circle.

Then primitive extensions considering neighborhoods of different sizes, use of circular neighborhoods, bilinear interpolation of pixel values, and use of uniform patterns are used to estimate pixels that are not exactly in the center pixels:

$LBP_{P,R}^{ri}$ and $LBP_{P,R}^{riu^2}$ are respectively invariant by rotation of LBP and invariant by uniform rotation of LBP. These two improved LBP operators have been proposed by Ojala et al. in 2002 [15].

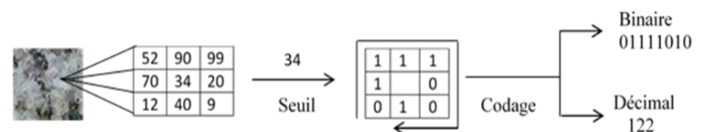


Fig. 1. Example of the Coding Process of the Standard LBP Operator.

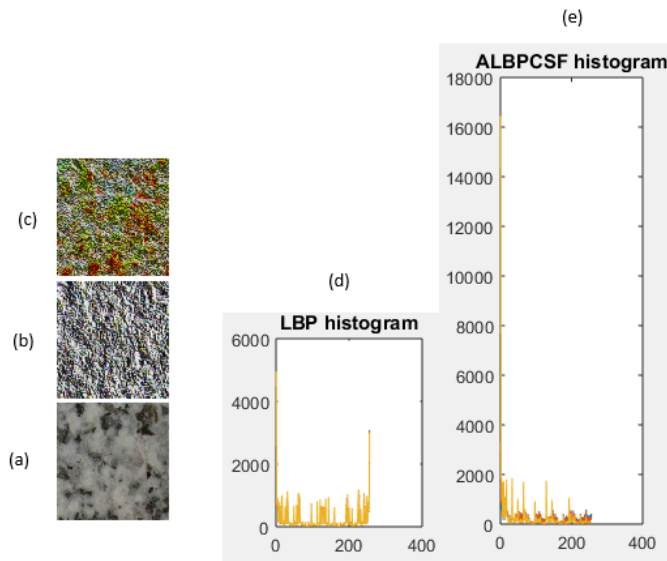


Fig. 2. An Example of an Original Image of Granodiorite (a), Its Image LBP (b), Its Image ALBPCSF (c) (The 3 Superimposed), the Histogram of the Image LBP (d) and the Histogram ALBPCSF (e).

After completing this coding step for the LBP operators, the histogram of these two variants can be created based on the following equation:

$$H_i = \sum_{x,y} I \{ f_i(x, y) = i \}, \quad i = 0, \dots, n-1$$

avec

$$I \{ A \} = \begin{cases} 1, & A \text{ is true} \\ 0, & A \text{ is false} \end{cases} \quad (2)$$

where i is the gray level number i , H_i is the number of pixels in the image with i as the gray level and n is the number of different labels produced by the LBP operators. Other extensions and variants of the LBP operator followed (see Fig. 2) one another with better performances in the extraction of textures, especially for the classification of facial images but will not be treated in this article. However, an exhaustive review of these LBP color and grayscale descriptors is done in [23, 24] for all readers interested in this descriptor which has gained an exponential popularity over the past ten years [2-4, 9, 15, 17-20, 23, 24].

B. Gabor Filter Combined with LBP

To increase the applicability of the LBP operator, modifications of it have been proposed. For example, Zhang et al. [17] proposed the extraction of LBP characteristics from images obtained by filtering a facial image with 40 Gabor filters at different scales and orientations with remarkable results. In [9], the LBP operator was computed on color texture images transformed into the HSV color space after applying Gabor filters on each of the three channels independently. In this same logic, we merge the two RGB and HSV color spaces by putting in the first line the relation between the spatial structure and the color characteristics as in [20].

III. PROPOSED APPROACHES

Inspired in part by the remarkable achievements obtained by combining Gabor's features with the LBP operator, we propose in this paper two new feature extraction algorithms, the first of which is named Gabor Adjacent Local Binary Pattern color space Fusion (G-ALBPCSF) and the second DCT Adjacent Local Binary Pattern Color Space Fusion (D-ALBPCSF). Indeed, the main interest of the combination of the first strategy, that is G-ALBPCSF compared to the original LBP lies in its ability to model the local characteristics of various orientations and scales provided by the transformation of Gabor and the likely consideration of color information. In G-ALBPCSF, the LBP operator applied on the different channels of the RGB and HSV color spaces, is built on the amplitudes of the Gabor filtered image rather than on the intensity of the original image. This coding makes it possible to exploit multi-resolution information and multi-orientations between the pixels, while being robust to the changes of illuminations. Then the second strategy named D-ALBPCSF, another extraction algorithm that combines the characteristics of the DCT and those of LBPcolor (ALBPCSF) to extract the capital information from the rocks.

A. Extraction of Characteristics by Gabor Filters

Gabor multi-resolution and multi-scale filters are frequency filters, located in space and with orientations convenient for the extraction and detection of contours. They are applied for decomposing input images for the sequential extraction of characteristics by changing two characteristic parameters that are: frequency and orientation. The Gabor filters for calculating quantities such as amplitude and phase [9] are defined by equation (3):

$$\Psi_{\nu,\mu}(x, y) = \exp \left(-\frac{\left| \begin{bmatrix} \bar{k}^2 & \bar{r}^2 \end{bmatrix} \right|}{2\sigma^2} \right) \times \rho$$

with

$$\rho = \left(\exp(i\bar{k} \cdot \bar{r}) - \exp(-\sigma^2 / 2) \right) \quad (3)$$

$$\bar{r} = \begin{bmatrix} x \\ y \end{bmatrix} \quad \text{and} \quad \bar{k} = \frac{\pi}{2f^\nu} \begin{bmatrix} \cos(\mu\pi / 8) \\ \sin(\mu\pi / 8) \end{bmatrix},$$

$$f = \sqrt{2}, \sigma = \pi$$

where $\mu = \{0, \dots, 7\}$ and $\nu = \{0, \dots, 4\}$ define respectively the orientations and the scales of the Gabor filters used.

Gabor's transformation of an image that can be called a Gabor image is defined as the convolution of the original image $I(x, y)$ with the Gabor $\Psi_{\mu,\nu}(x, y)$ filters:

$$G_{\mu,\nu}(x, y) = I(x, y) * \Psi_{\mu,\nu}(x, y) \quad (4)$$

The Gabor transformation is a complex function, and can be separated into amplitude $A_{\mu,\nu}(x, y)$ and phase $\theta_{\mu,\nu}(x, y)$ and thus can be rewritten as follows:

$$G_{\mu,\nu}(x, y) = A_{\mu,\nu} \exp(i\theta_{\mu,\nu}(x, y)) \quad (5)$$

Equation (5) is a complex representation of the Gabor transformation of the image and from this transformation a feature vector is created (amplitude, phase).

$$A_{\mu,\nu}(x, y) = |G_{\mu,\nu}(x, y)|$$

$$\theta_{\mu,\nu}(x, y) = \arg(G_{\mu,\nu}(x, y))$$

It should be remembered that since the information phase varies over time (therefore very sensitive), in general, only the amplitude is explored. Thus, for each Gabor filter, an amplitude value is calculated at each position of the pixel, giving a total of 40 amplitudes corresponding to 5 scales and 8 orientations. Fig. 3 shows an image of granite and other images of the same size called Gabor images whose characteristics: amplitude and phase were extracted for two wavelengths and four orientations (16 Gabor images of which 4 are identical so 12 have been represented).

These images clearly show, on the one hand, that the texture information is perceptible and better represented in the Gabor amplitude images, and on the other hand they show that whatever the orientation and / or the scale, the granularity and the structure remain the most important elements and differ significantly from those shown by LBP images (Fig. 3). However, we summarize that Gabor filters transform a given image in only three directions: vertical (0 ° or 180 °), horizontal (90 °) and diagonal (45 ° and 135 °).

B. Extraction of Characteristics by ALBPCSF

To improve the information in the amplitudes, we code the values of the amplitudes of Gabor by the operator ALBPCSF. In G-ALBPCSF, the ALBPCSF operator is driven on the amplitudes produced by the multi-resolution and multi-scale Gabor filters rather than on the intensities of the original images. The LBP operator uses the comparison between the central pixel and its eight neighbors in a 3 * 3 neighbor and their combination with the Gabor images thus exploiting the links between the pixels for several resolutions and orientations has proved to be very robust to enlightenment and change of scale [17]. Fig. 5 illustrates this combination well. It shows the application of ALBPCSF on five Gabor amplitude images for two different frequencies ($\lambda = 4$ for the images of the first line and $\lambda = 8$ for the images of the second line) and five orientations. Fig. 4 shows that the Gabor filters are more informative in the diagonal direction (45° and 135°) and confirms the directional structure of the studied rock.

C. Combination of ALBPCSF with DCT for Extraction of Characteristics

Discrete Cosine Transform (DCT) is a popular technique for imaging and compressing still images and video that transforms spatial representation signals into a frequency representation. As we know, a large amount of information about the original image is stored in a relatively small number of coefficients (in the upper left corresponding to the DCT components at low spatial frequencies of the image) in the image center of Fig. 5. This region contains most of the information, energy, and useful features of the image.

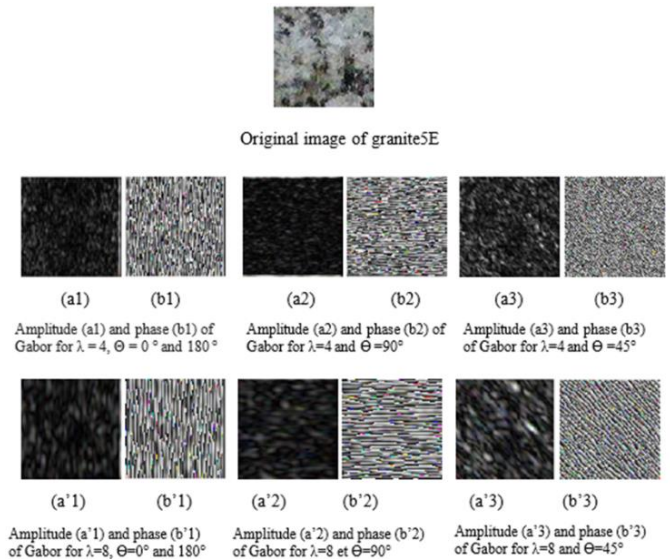


Fig. 3. Examples of an Image Filtered by Four different Gabor Filters: (a1), (a2), (a3), (a'1), (a'2) and (a'3) are the different Images of Amplitudes and (b1), (b2), (b3), (b'1), (b'2) and (b'3) are the Images of the Gabor Phases for Two Wavelengths $\lambda = 4$ and $\lambda = 8$.

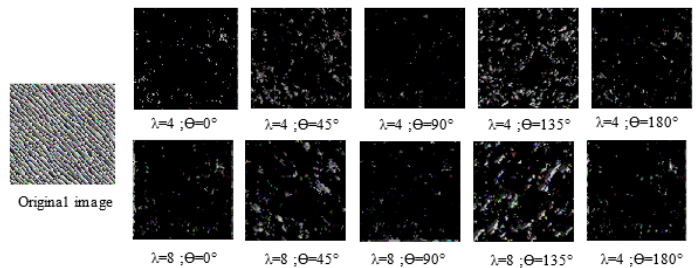


Fig. 4. Gabor_ALBPCSF Image of the Original Granite5E Image for $\lambda = 4$ (Top) and $\lambda = 8$ (Bottom) and for different Orientations (0 °, 45 °, 90 °, 135 °, 180 °).

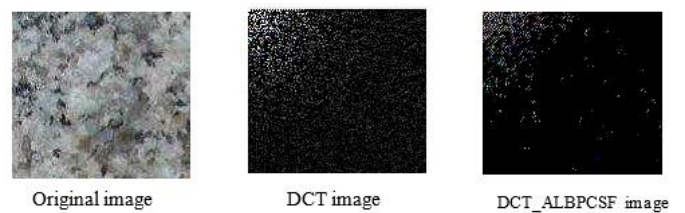


Fig. 5. DCT Image (Middle) of the Original Granite5E Image (Left) and its Combination with ALBPCSF (Right).

For a digital image $f(x, y)$ of resolution $M \times N$, its two-dimensional DCT is defined as follows [19]:

$$A(i, j) = a(i)a(j) \sum_{x=0}^{M-1} \sum_{y=0}^{N-1} f(x, y) \times \cos\left[\frac{(2x+1)i\pi}{2M}\right] \cos\left[\frac{(2y+1)j\pi}{2N}\right]$$

$$i = 0, 1, 2, \dots, M-1; \quad j = 0, 1, 2, \dots, N-1; \quad (6)$$

Where, x and y are the spatial coordinates of the pixels of the image; i and j are the coordinates of the DCT coefficients of the pixels. $A(i, j)$ is the result of the DCT. $a(i)$ and $a(j)$ is defined as follows:

$$a(i)=\begin{cases} \sqrt{1/M} & \text{if } i=0 \\ \sqrt{2/M} & \text{if } 1 \leq i \leq M-1 \end{cases} \quad a(j)=\begin{cases} \sqrt{1/N} & \text{if } j=0 \\ \sqrt{2/N} & \text{if } 1 \leq j \leq N-1 \end{cases} \quad (7)$$

However, the performances of the DCT or the LBP taken independently show some insufficient. In [19], the combination of DCT with LGBP on an ENT database showed better results compared to LGBP applied alone. In this section, we propose a new algorithm for extracting rock texture features named D-ALBPCSF by combining the DCT and ALBPCSF to consider the color information in addition to the advantages already mentioned above. First, the DCT is performed on direct images of rock. Then we select some useful low frequency DCT coefficients to extract the overall characteristics of the rock texture images. In addition, the LBPcolor operator (more precisely ALBPCSF) is executed on these DCT characteristics of rock textures to now extract the local characteristics with high frequencies (see image on the far right in Fig. 5 above). As we know, the analysis of the existing has shown that using a combination of several classifiers of different types can improve the performance of the classification [5]. Indeed, descriptors based on global characteristics can contribute to a discriminant capacity complementary to descriptors based on local characteristics in the recognition of rocks [9].

IV. EXPERIMENTAL RESULTS AND DISCUSSION

In this section we will analyze and comment on the results of our experiments. The selected direct view rock images shown in Fig. 6 below are images from our designed database. This database contains 160 images of magmatic and metamorphic rocks textures. These images have been grouped into eight classes (from class 1 to class 8). These 256x256 resolution images, encoded on eight bits by colorimetric component, present textures that are not homogeneous and often show significant differences in directionality, granularity and color within a given class. Thanks to these texture and color characteristics, the original images were subjectively grouped into eight classes by a geology expert.

A. Averages and Standard Deviation of Gabor and DCT Coefficients

In our study, because of the directionality present in the rock textures, the Gabor filters were applied on these textures. Then, first-order (mean), second-order (standard deviation) were computed on Gabor amplitudes and DCT coefficients, then those of Gabor and DCT combined with ALBPCSF in the different channels. color. Indeed, the calculated average characterizes the luminous intensity of the energies in the image whereas the standard deviation characterizes the variation of the average intensity of all the pixels and corresponds to the changes of contrast of the image. The results are recorded in the tables below.

The analysis of the statistical characteristics used in this work such as average and the standard deviation of the DCT coefficients and Gabor amplitudes for an orientation and a scale (lambda = 4, theta = 135°) indicated in Tables I to VIII shows that magmatic rocks have higher intensity rate than metamorphic rocks. These high intensity rate in magmatic rocks indicate that these rocks have a grainy texture and crystallize at higher temperatures and pressures than metamorphic rocks. Magmatic rocks are characterized by strong energies. However, shale, eclogite, and corneal metamorphic rocks have intensities comparable to those of magmatic rocks when DCT coefficients and Gabor amplitudes are used individually, indicating a lack of such approaches.

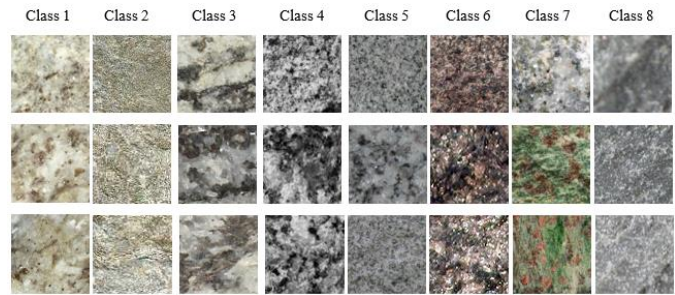


Fig. 6. Examples of the Eight different Classes of Rock Images.

TABLE I. AVERAGE GABOR AMPLITUDE COEFFICIENTS

Average of the coefficients of Gabor amplitudes calculated for different rocks, Lambda = 4, theta = 135°								
	Schiste	Gabbro	Granodiorite	Granite	Eclogite	Migmatite	Corneal	Cipolin
(R,V)	65.3018	46.945	55.5565	57.9142	44.8483	42.2141	57.9337	42.2962
(G,V)	65.4266	45.9711	55.5565	57.9107	44.7356	42.4674	57.9511	42.8727
(B,V)	65.4139	50.1033	55.5565	57.9674	44.7492	42.5286	57.9884	43.7508

TABLE II. AVERAGES OF GABOR_ALBPCSF AMPLITUDE COEFFICIENTS

Mean coefficients of Gabor_ALBPCSF amplitudes calculated for different rocks, Lambda = 4, theta = 135°								
	Gabbro	Granodiorite	Granite	Eclogite	Migmatite	Schiste	Corneal	Cipolin
(R,V)	16.2430	21.4266	15.4365	7.1122	7.8196	6.0078	6.0311	1.3431
(G,V)	15.3746	21.4266	15.4598	7.0253	7.9517	6.0249	6.0753	1.4434
(B,V)	18.3144	21.4266	15.5244	6.9742	7.9593	5.9887	6.0438	1.4487

TABLE III. AVERAGES OF THE DCT COEFFICIENTS

Averages of the DCT coefficients calculated for different rocks								
	Schiste	Gabbro	Granodiorite	Granite	Eclogite	Migmatite	Corneal	Cipolin
(R,V)	13.7518	13.2398	10.7357	8.5716	8.8443	8.0340	6.7993	5.6949
(G,V)	13.7803	12.8244	10.7357	8.5775	8.7991	8.1157	6.8064	5.8441
(B,V)	13.8325	13.8325	10.7357	8.6141	8.8009	8.1050	6.8198	5.9921

TABLE IV. AVERAGES OF THE DCT_LBP COEFFICIENTS

Averages of the DCT_LBP coefficients calculated for different rocks								
	Gabbro	Granodiorite	Granite	Eclogite	Migmatite	Schiste	Corneal	Cipolin
(R,V)	7.2281	5.361	1.797	1.4901	1.1892	0.6873	0.479	0.3811
(G,V)	6.7981	5.361	1.7917	1.4537	1.2444	0.6986	0.4772	0.4472
(B,V)	7.379	5.361	1.8362	1.4636	1.2459	0.7399	0.4808	0.5074

TABLE V. STANDARD DEVIATION OF GABOR AMPLITUDE COEFFICIENTS ON ORIGINAL IMAGES

Mean standard deviations of Gabor coefficients calculated for different rocks, Lambda = 4, Theta = 135 °								
	Schiste	Gabbro	Granodiorite	Granite	Eclogite	Migmatite	Corneal	Cipolin
(R, V)	36.2668	28.2244	33.5475	35.0280	27.5958	29.0953	34.2396	28.0670
(G, V)	36.3339	27.9218	33.5475	35.0924	27.6712	29.3490	34.2445	28.6090
(B, V)	36.3649	30.3900	33.5475	35.0512	27.6677	29.3802	34.2505	28.8726

TABLE VI. STANDARD DEVIATION OF THE COEFFICIENTS OF AMPLITUDES OF GABOR_ALBPCSF (G-ALBPCSF)

Mean standard deviations of G-ALBPCSF coefficients calculated for different rocks, Lambda = 4, Theta = 135 °								
	Schiste	Gab bro	Granodiorite	Granite	Eclo gite	Migmatite	Corneal	Cipolin
(R, V)	27.7572	44.4104	50.9072	43.7388	28.1538	31.2973	26.5383	12.9097
(G, V)	27.7616	43.1394	50.9072	43.7826	27.9202	31.5429	26.6805	13.3843
(B, V)	27.6069	46.5493	50.9072	43.8905	27.8314	31.4801	26.6287	13.3801

TABLE VII. STANDARD DEVIATION OF THE DCT COEFFICIENTS ON THE ORIGINAL IMAGES

Mean standard deviations of the DCT coefficients calculated for different rocks								
	Schiste	Gab bro	Granodiorite	Granite	Eclo gite	Migmatite	Corneal	Cipolin
(R, V)	21.8199	27.2926	26.2376	20.0985	20.8450	19.4737	16.2005	15.5525
(G, V)	21.8907	25.7220	26.2376	20.1102	20.6854	19.8264	16.2257	16.3226
(B, V)	22.1734	26.5375	26.2376	20.3104	20.7362	19.7837	16.2660	17.0531

TABLE VIII. ECART-TYPE DES COEFFICIENTS DCT_ALBPCSF (D-ALBPCSF)

Mean standard deviations of D-ALBPCSF coefficients calculated for different rocks								
	Schiste	Gab bro	Granodiorite	Granite	Eclo gite	Migmatite	Corneal	Cipolin
(R, V)	7.9382	28.0933	24.6956	13.9308	12.2155	11.0881	6.2382	5.9663
(G, V)	8.0066	27.1244	24.6956	13.9060	12.0336	11.3821	6.4121	6.6028
(B, V)	8.2811	28.2027	24.6956	14.1372	12.1098	11.3792	6.4332	7.0632

However, the analysis of the means and the standard deviations of the G-ALBPCSF and D-ALBPCSF coefficients calculated from the combinations of the approaches for these same rocks show a good categorization of the rocks:

- Magmatic rocks with higher intensity rate
- Metamorphic rocks with lower intensity rate than those of magmatic rocks.

These analyzes show that the approach combinations D-ALBPCSF and G-ALBPCSF make it possible to better categorize the rocks, unlike the information with Gabor and DCT taken individually. However, the reflection that this raise is up to what threshold value or limit, we can consider that the average characteristics corresponds to that of a rock belonging to a given class?

B. Comparison D-ALBPCSF and G-ALBPCSF based on the Measurements of Similarity of Intersection of Histograms and chi 2

There are several frequently used metrics for measuring similarity between two histograms for comparing textures. These metrics calculate the distance between the characteristic vectors. In this study, we use the intersection of the histograms and the distance of the Chi 2 defined respectively in equations (8) and (9) below and will allow to compare the efficiency of these two types of characteristics described in Section 3 a little higher.

$$HI(h_i(1), h_i(2)) = 1 - \sum_i \min(h_i(1), h_i(2)) \tag{8}$$

$$\chi^2(h_i(1), h_i(2)) = \sum_i \frac{(h_i(1) - h_i(2))^2}{(h_i(1) + h_i(2))} \tag{9}$$

where h_i are the histograms of the samples of the images of the rocks to be compared. Rock samples can be said to be similar by matching their characteristic histograms (color and / or texture) and when the value obtained is closer to 0 if not

there is no similarity. The same process is followed for Chi2. The results with both metrics show good trends with very low values with the χ^2 . Values between 0 and 1 show that the histograms have been normalized. However, the HI and χ^2 applications have better results in terms of similarity between the rocks with the combination D-ALBPCSF compared to G-ALBPCSF and the other methods used. This shows that the characteristics extracted by the DCT are practically common to all rocks of the same class and show a strong correlation between the rocks of the same class. Tables IX and X show the results of these first experiments.

In this work, we will manly exploit he intersection metric of the histograms with the LBP and D_ALBPCSF approaches given that these approaches make it easier to appreciate the similarity with respect to G_ALBPCSF (see Tables XI and XII).

The analysis of these two methods shows that some metamorphic rocks (migmatite, eclogite, cornea, ...) are like each other and to some magmatic rocks (granite, gabbro, ...). This can be justified by the fact that they have magmatic origins since genesis as it is the case for eclogite for example. The G-ALBPCSF strategy will be especially exploited in our future work. The results are shown in Fig. 7.

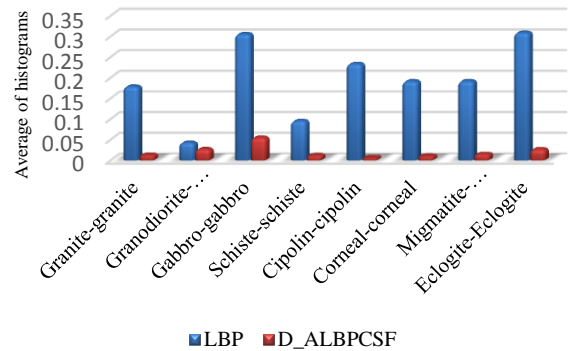


Fig. 7. Intersection of Histograms of Rocks with LBP and D_ALBPCSF.

TABLE IX. MEAN VALUES OF HI FOR THE DIFFERENT METHODS USED

Rocks	Mean HI values of the different methods used				
	ImagRGB	LBP	ALBPCSF	DALBPCSF	GALBPCSF
Schiste	0.4375	0.0977	0.2822	0.0122	0.2422
Granite	0.6737	0.2188	0.3847	0.0143	0.2665
Ciprolin	0.6678	0.2663	0.3945	0.0077	0.5534
Eclogite	0.9283	0.3756	0.5696	0.0799	0.5673
Granodiorite	0.0635	0.0577	0.041	0.0359	0.0843
Migmatite	0.5690	0.2199	0.3805	0.0137	0.3492
Gabbro	0.7345	0.3358	0.4689	0.0764	0.6444
Corneal	0.5457	0.194	0.3680	0.0096	0.3918

TABLE X. AVERAGE VALUES OF χ^2 OF THE DIFFERENT METHODS USED

	Average values of χ^2 of the different methods used				
Rocks	ImagRGB	LBP	ALBPCSF	DALBPCSF	GALBPCSF
Schiste	25,2.10 ⁻⁴	3,59.10 ⁻⁴	14,5.10 ⁻⁴	0,62710 ⁻⁴	10,278.10 ⁻⁴
Granite	44.10 ⁻⁴	7,75.10 ⁻⁴	20,4.10 ⁻⁴	0,62710 ⁻⁴	11,5610 ⁻⁴
Ciprolin	53.10 ⁻⁴	13.10 ⁻⁴	14,25.10 ⁻⁴	0,3229.10 ⁻⁴	33.10 ⁻⁴
Eclogite	71.10 ⁻⁴	13,5.10 ⁻⁴	36.10 ⁻⁴	1,4872.10 ⁻⁴	30,25.10 ⁻⁴
Granodiorite	1,02.10 ⁻⁴	0,44.10 ⁻⁴	0,220.10 ⁻⁴	0,3971.10 ⁻⁴	0,9283.10 ⁻⁴
Migmatite	33,2.10 ⁻⁴	9,014.10 ⁻⁴	20,6.10 ⁻⁴	0,4892.10 ⁻⁴	17.10 ⁻⁴
Gabbro	52,8.10 ⁻⁴	19.10 ⁻⁴	28,6.10 ⁻⁴	2,7523.10 ⁻⁴	44,8.10 ⁻⁴
Corneal	31,6.10 ⁻⁴	7,47.10 ⁻⁴	19,2.10 ⁻⁴	0,3398.10 ⁻⁴	20,8.10 ⁻⁴

The figure shows a good similarity between the rocks of the same class and the D_ALBPCSF method showing the relevance of our proposed method compared to the existing LBP method.

C. Matrix of Confusion

A confusion matrix (Table XIII) was performed with the D_ALBPCSF method discussed in Section 3.2 above, to show the relevance of this method. The effectiveness of the latter is evaluated with the selection of five images of each rock class (8 classes), i.e. 48 images in total for a classification of 320 crossings. For this experiment, the sensitivity (recall), specificity, accuracy and error rate of which the equations are described below and noted respectively (10), (11), (12) and (13) are performance indicators that were chosen to approve the effectiveness of the proposed method and that were also used by Vivek and Audithan in 2014 [6]. Sensitivity is the quality of a class. It indicates the likelihood of a rock to belong to the class knowing that it should belong to it, more simply it is the rate of true positives. Specificity indicates, for its part, the probability that a rock does not belong to its class appropriately, it is the rate of true negatives while the rate of errors corresponds to the general quality of the model.

$$sensitivity = FVP = \frac{VP}{VP + FN} \tag{10}$$

$$specificity = FVN = \frac{VN}{VN + FP} \tag{11}$$

$$precision = \frac{VP}{VP + FP} = \frac{VN}{VN + FN} \tag{12}$$

$$accuracy = \frac{VP + VN}{VP + VN + FP + FN} \tag{13}$$

where VP: True Positive, FP: False Positive; VN: True Negative; FN: False Negative. Here the definitions of the terms assume that one rock is like another if the value of the intersection of their histogram is the lowest. As a result, a true positive is a rock that belongs to a class and whose average

value of the histogram intersections is the smallest. The false positive is a rock that does not belong to a class but has the average value of the smallest inter-sections of histograms. The false negative is a rock that does not belong to a class and does not have the smallest average value of the histogram intersections. The true negative is a non-class rock that does not have the smallest value of the histogram intersections.

Both methods give similar performance at first sight from a general analysis of performance indicators such as sensitivity, specificity and accuracy. However, with a misclassification rate of almost 8% with both the LBP and D_ALBPCSF methods for the 5 classes of metamorphic rocks, the proposed method classifies magmatic rocks better with an error rate of 0.8% against 3.3% for the LBP method. These results show a slightly better performance of our method compared to LBP (see Fig. 8). This is consistent with the observation that can be made of these rock texture images. For images of magmatic rocks, we notice that the texture and the color in these images are somewhat regular in their spatial representation, unlike the case of certain metamorphic rocks where there is no homogeneity in the spatial representation of the tex. and color (examples of eclogite and migmatite). The color texture combination in the rock study has been beneficial for their identification.

As a result, the local and global characteristics used in this study for their extraction have been very useful.

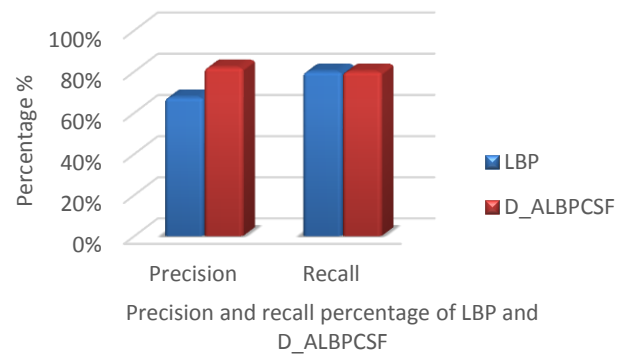


Fig. 8. Precision and Recall of LBP and D_ALBPCSF Methods.

TABLE XI. CONFUSION MATRIX WITH THE D_ALBPCSF METHOD

		Class 1	Class 2	Class 3	Class 4	Class 5	Class 6	Class 7	Class 8
R E A L C L A S S E S	Class 1	4	0	0	0	1	0	0	0
	Class 2	0	5	0	0	0	0	0	0
	Class 3	0	0	5	0	0	0	0	0
	Class 4	0	0	0	5	0	0	0	0
	Class 5	0	0	0	0	5	0	0	0
	Class 6	1	1	0	0	0	2	0	1
	Class 7	0	0	0	0	0	0	4	1
	Class 8	1	0	0	0	2	0	0	2

TABLE XII. PERFORMANCE INDICATORS OF THE TWO METHODS

Assessment indicators		D_ALBPCSF	LBP
Images of rocks textures for different classes	VP	32	32
	VN	272	272
	FP	8	8
	FN	8	8
	Sensitivity	0,8=80%	0,8=80%
	Specificity	0,97=97%	0,97=97%
	Accuracy	0,95=95%	0,95=95%
	Error rate	0,05 = 5%	0,05 = 5%

TABLE XIII. COMPARISON OF LBP AND D_ALBPCSF METHODS

	Parameters of performance	Granite	Granodiorite	Gabbro	Schiste	Cipolin	Eclogite	Migmatite	Corneal
LBP		VP=5	VP=5	VP=5	VP=5	VP=5	VP=0	VP=5	VP=2
		FN=0	FN=0	FN=0	FN=0	FN=0	FN=5	FN=0	FN=3
		VN=31	VN=35	VN=35	VN=35	VN=33	VN=35	VN=33	VN=32
		FP=4	FP=0	FP=0	FP=0	FP=2	FP=0	FP=2	FP=3
	Accuracy by class	90%	100%	100%	100%	95%	87,50%	95%	85%
	Positive accuracy	55,60%	100%	100%	100%	71,40%	0%	71,40%	40%
	Negative accuracy	100%	100%	100%	100%	100%	87,50%	100%	94,10%
Average accuracy	Magmatic rocks : 96,7%				Metamorphic rocks : 92,5%				
DALBPCSF		VP=5	VP=5	VP=5	VP=4	VP=5	VP=2	VP=4	VP=2
		FN=0	FN=0	FN=0	FN=1	FN=0	FN=3	FN=1	FN=3
		VN=34	VN=35	VN=35	VN=33	VN=32	VN=35	VN=35	VN=32
		FP=1	FP=0	FP=0	FP=2	FP=3	FP=0	FP=0	FP=3
	Accuracy by class	97,50%	100%	100%	92,50%	92,50%	92,50%	97,50%	85%
	Positive accuracy	83,30%	100%	100%	66,70%	62,50%	100%	100%	40%
	Negative accuracy	100%	100%	100%	97,10%	100%	92,10%	97,20%	94,10%
Average accuracy	Magmatic rocks : 99,2%				Metamorphic rocks : 92%				

V. CONCLUSION

In this article, we present two new feature extraction methods applied to rock images. We combined the functionalities of Gabor-ALBPCSF and DCT-ALBPCSF to propose two new descriptors G_ALBPCSF and D_ALBPCSF and to better classify rock texture images. In general, this is a very difficult classification task because of the frequent differences observed within samples of the same type of rock. Experimental results on our direct view rock image database show that the G_ALBPCSF and D_ALBPCSF combinations improve the recognition performance compared to the original LBP and ALBPCSF taken separately. That makes it possible to understand that local and global information must be considered for the extraction of rock characteristics.

In perspective, we plan to apply the K-SVD method to the proposed methods and then apply our methods to other types of images such as facial images.

REFERENCES

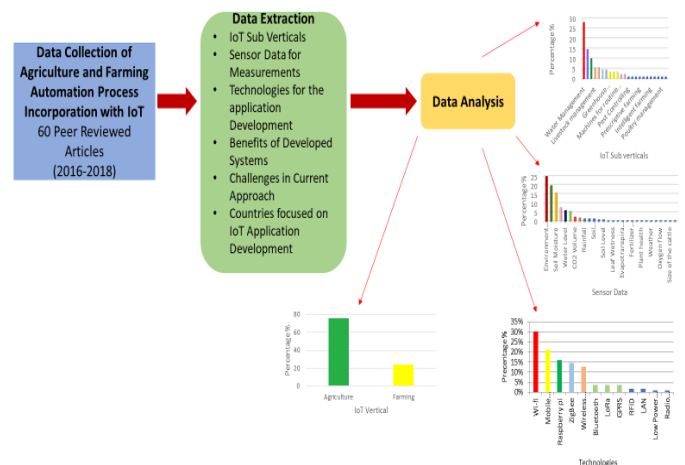
- [1] Chatterjee, S., Bhattacharjee, A., Samanta, B., Pal, S.K., "Image-based quality monitoring system of limestone ore grades", *Computers in Industry*, Vol. 61, no. 5, pp. 391–408, 2010.
- [2] F. Bianconi and A. Fernández : An appendix to "Texture databases – A comprehensive survey", *Pattern Recognition Letters*, Vol. 45, pp. 33-38, 2014.
- [3] Choi JY, Ro YM, Plataniotis KN, "Color local texture features for color face recognition", *IEEE Transactions on Image Processing*. Vol. 21, no. 3, pp. 1366–1380, 2012.
- [4] A. Fernandez, O. Ghida, E. Gonzalez, F. Bianconi, P.F. Whelan, "Evaluation of robustness against rotation of LBP, CCR and ILBP features in granite texture classification", *Machine Vision and Applications*, Vol. 22, pp. 913-926, 2011.
- [5] L. Lepisto, I. Kunttu, and A. Visa, "Rock images classification using color features in Gabor space", *Journal of Electronic Imaging (JEI letters)*, Vol. 14, no. 4, 2005.
- [6] C. Vivek and S. Audithan, "Robust analysis of the rock texture image based on the boosting classifier with Gabor wavelet features", *Journal of Theoretical and Applied Information Technology*, Vol. 69, no. 3, pp. 562-570, 2014.
- [7] F. Bianconi, E. Gonzalez, A. Fernández and S. A. Saetta, "Automatic classification of granite tiles through colour and texture features", *Expert System with Application* Vol. 39, pp. 11212-11218, 2012.
- [8] M. Mlynarczuk, M. Skiba, "The Application of Artificial Intelligence for the Identification of the Maceral Groups and Mineral Components of Coal", *Computers and Geosciences*, Vol. 103, pp. 133-141, 2017.
- [9] F. J. Galdames, C. A. Perez, P. A. Estévez and M. Adams, "Rock Lithological Classification by Laser Range 3D and Color Images", *International Journal of Mineral Processing*, 2017.
- [10] Sascha. T. Ishikawa and Virginia C. Gulick, "An automated mineral classifier using Raman spectra", *Computers & Geosciences*, Vol. 54, pp. 259-268, 2013.
- [11] P. Paclik, S. Verzakov, and R.P.W. Duin "Improving the Maximum-Likelihood Co-occurrence Classifier : A Study on Classification of Inhomogeneous Rock Images", *SCIA*, pp. 998–1008, 2005.
- [12] D. Blake, "The development of the CheMin XRD/XRF ; reflections on building a spacecraft instrument ", In *Aerospace Conference*, IEEE, pp. 1-8, 2012.
- [13] N. Singh, T. N. Singh, A. Tiway and K. M. Sarkar, "Textural identification of basaltic rock mass using image processing and neural network," *Computer and Geosciences*, Vol. 14, pp. 301- 310, 2010.
- [14] A. K. Patel and S. Chatterjee, "Computer vision-based limestone rock-type classification using probabilistic neural network, " *Geoscience Frontiers* 7, pp. 53-60, 2016.
- [15] T. Ojala, M. Pietikainen and T. Maenpaa, "Multiresolution gray-scale and rotation invariant texture classification with local binary patterns, " *IEEE Transactions on Pattern Analysis and Machine Intelligence*, vol. 24, no. 7, pp. 971-987, 2002.
- [16] L. Lepisto, I. Kunttu, J. Autio and A. Visa, " Classification Method for Colored Natural Textures Using Gabor filtering", *IEEE*, 12 th International Conference on Image Analysis and Processing 397- 401, 2003.
- [17] W. Zhang, S. Shan, W. Gao, X. Chen and H. Zhang, " Local Gabor Binary Pattern Histogram Sequence (LGBPHS) : A novel Non-Statistical Model for Face Representation and Recognition", *Proceedings of the Tenth IEEE International Conference on Computer Vision (ICCV05)*, 2005.
- [18] S. Shan, W. Zhang, Y. Su, X. Chen and W. Gao " Ensemble of Piecewise FDA Based on Spatial Histograms of Local (Gabor) Binary Pattern for Face Recognition", *IEEE* 2006, The 18th International Conference on Pattern Recognition (ICPR'06), 2006.
- [19] Zhihua Xie, "Single Sample Face Recognition Based on DCT and Local Gabor Binary Pattern Histogram", *Springer, ICIC* 2013, pp.435- 442, 2013.
- [20] J. Wognin VANGAH, Sié OUATTARA, Alain CLEMENT and Gbélé OUATTARA, "Combination of dictionary learning by k-svd and a colorimetric texture descriptor for improved identification of geological structures : case of rocks", *International Journal of Innovation and Applied Studies (IJIAS)*, Vol. 24, no. 3, pp. 1193-1208, 2018.
- [21] O. Baklanova and O. Shvets, "Methods and Algorithms of Cluster Analysis in the Mining Industry - Solution of Tasks for Mineral Rocks Recognition", In *Proceedings of the 11th International Conference on Signal Processing and Multimedia Applications (SIGMAP-2014)*, pp. 165-171, 2014.
- [22] Ojala, T., Pietikäinen, M., Harwood, D. : A comparative study of texture measures with classification based on feature distributions. *Pattern Recognition*. Vol. 29, pp. 51–59, 1996.
- [23] L. Nanni, A. Lumini and S. Brahmam, "Survey on LBP based texture descriptors for classification", *Expert Systems with Applications*, Vol. 39, pp. 3634-3641, 2012.
- [24] S. Banerji, A. Verma and C. Liu, "Novel color LBP descriptors for scene and image texture classification", in *Proceedings of the 15th International Conference on Image Processing, Computer Vision, and Pattern Recognition, Las Vegas, Nevada*, pp. 537–543, 18-21 July 2011.

Adoption of the Internet of Things (IoT) in Agriculture and Smart Farming towards Urban Greening: A Review

A. A. Raneesha Madushanki¹, Malka N Halgamuge², W. A. H. Surangi Wirasagoda³, Ali Syed⁴
School of Computing and Mathematics, Charles Sturt University, Melbourne, Australia^{1, 3, 4}
Department of Electrical and Electronic Engineering, The University of Melbourne²

Abstract—It is essential to increase the productivity of agricultural and farming processes to improve yields and cost-effectiveness with new technology such as the Internet of Things (IoT). In particular, IoT can make agricultural and farming industry processes more efficient by reducing human intervention through automation. In this study, the aim to analyze recently developed IoT applications in the agriculture and farming industries to provide an overview of sensor data collections, technologies, and sub-verticals such as water management and crop management. In this review, data is extracted from 60 peer-reviewed scientific publications (2016-2018) with a focus on IoT sub-verticals and sensor data collection for measurements to make accurate decisions. Our results from the reported studies show water management is the highest sub-vertical (28.08%) followed by crop management (14.60%) then smart farming (10.11%). From the data collection, livestock management and irrigation management resulted in the same percentage (5.61%). In regard to sensor data collection, the highest result was for the measurement of environmental temperature (24.87%) and environmental humidity (19.79%). There are also some other sensor data regarding soil moisture (15.73%) and soil pH (7.61%). Research indicates that of the technologies used in IoT application development, Wi-Fi is the most frequently used (30.27%) followed by mobile technology (21.10%). As per our review of the research, we can conclude that the agricultural sector (76.1%) is researched considerably more than compared to the farming sector (23.8%). This study should be used as a reference for members of the agricultural industry to improve and develop the use of IoT to enhance agricultural production efficiencies. This study also provides recommendations for future research to include IoT systems' scalability, heterogeneity aspects, IoT system architecture, data analysis methods, size or scale of the observed land or agricultural domain, IoT security and threat solutions/protocols, operational technology, data storage, cloud platform, and power supplies.

Keywords—Internet of Things; IoT; agricultural; smart farming; business; sensor data; automation



Graphical Abstract.

I. INTRODUCTION

IoT is a combination of worldwide data, web associated items or things, and is an integral component of the future Internet. IoT focuses on the automation of processes by lessening human interaction. In the process of automation, IoT collects data using sensors and processes the data using controllers and completing the automation processes by using actuators [1], [2]. IoT in agriculture and farming focus is on automating all the aspects of farming and agricultural methods to make the process more efficient and effective. Traditional approaches in livestock management (such as cattle detection) are not fully automated and have many inefficiencies such as higher human interaction, labour cost, power consumption, and water consumption [1], [3], [4], [5], [6]. The central concept of this review is to analyse the IoT sub-verticals, collected data for measurements and used technologies to develop applications. It is essential to identify the most researched sub-verticals, data collections and technologies to create new IoT applications in the future.

This review provides an overall picture of currently developed IoT applications in agriculture and farming between 2016 and 2018.

As a solution to the existing problems, researchers have focused on smart agricultural and farming automated systems with the help of IoT [7], [8], [9], [10]. IoT is the network of things which identifies elements clearly with the help of software intelligence, sensors and ubiquitous connectivity to the Internet. In IoT, the data that collects from Internet-connected items or things contains with gadgets, sensors and actuators [1]. Many researchers have focused on smart systems for monitoring and controlling agricultural parameters by enhancing productivity and efficiency. Smart systems collect data for measurements to get accurate results that can lead to appropriate actions. Current use of smart agricultural systems relates to collecting data on environmental parameters such as temperature, humidity, soil moisture and pH [11], [12], [13]. With accurate sensor data collection using a range of different sensors, researchers have implemented smart agricultural systems to make the farm process more effective [9], [14]. Research has mainly focused on sub-verticals such as water management, crop management and smart farming to make processes automated by reducing human intervention, costs, power consumption and water consumption.

The automation process of agricultural and farming reduced human interaction and improve the efficiency. The reason for that is every country population depends on agriculture thus consumers of these resources should use water and land resources optimally [19], [20]. Moreover, it is imperative to have good quality production and crop management in order to maximize profitability. Hence, IoT base agricultural management systems are integral for an agriculturally based country. The new systems developed using IoT technologies have reduced the drawbacks associated with traditional approaches and provided many advantages to farmers. For example, IoT-based water management systems collect environmental attributes such as temperature, water level and humidity through the sensors and provide accurate irrigation timing [19], [21]. In addition, crop management systems developed using IoT monitor the temperature, humidity and soil through sensors thus providing adequate information so that farmers can manage the crops appropriately [25]. Overall, these IoT-based systems help to reduce human interaction, power utilization and reduce cost in the field of agriculture. Moreover, IoT-based agricultural related applications have been used in the area of pest control, weather monitoring, nutrient management and greenhouse management.

IoT for agriculture uses sensors to collect big data on the agricultural environment. It discovers, analyses and deals with models built upon big data to make the development of agriculture more sustainable [34]. IoT can provide efficient and low-cost solutions to the collection of data. Weather, Water Scarcity, Soil fertility and Pesticides are the significant players in it. IoT will make agriculture beneficiary. Agriculture and farming depend on water [35]. Farmers depend on rainfall for all their agricultural needs.

Fertilizer also plays a very significant role in the field of agriculture by helping to increase the productivity of plants [36]. By using IoT, farmers can manage soil condition more effectively and at less expense by monitoring them from any location [37]. The primary objective of this study is how IoT and technologies are used in conserving water, fertiliser and energy in the agricultural industry by combining new technologies. This has benefits for the development of the economy of countries as well as the wealth of the people [38]. With the combination of both advanced technologies in hardware and software, IoT can track and count all relevant aspects of production which can reduce the waste, loss and cost [39]. The information needed to make smart decisions can be obtained merely by using electronic devices [40]. IoT transforms the agricultural industry and enables farmers to overcome different challenges. Innovative applications can address these issues and therefore increase the quality, quantity, sustainability and cost-effectiveness of crop production [41], [42], [43]. IoT provides more benefits to the farming industry by improving the health of animals through better food and environment, addressing the labour shortage issue as well cost savings through automation, increase in milk production, and increase in some animals during the breeding period through detection of estrus cycle and additional revenue streams from waste.

Our study has analyzed recently developed IoT applications in the fields of agriculture and farming to address current issues such as unnecessary human interaction leading to higher labour cost, unnecessary water consumption and water-saving measures for the future, higher energy consumption, energy-saving measures for the future and crop monitoring difficulties. According to our analysis, we can identify a focus on water and crop management as sub-verticals in the agriculture and farming sectors. This survey also focusses on other agriculture and farming sub-verticals to identify the gap between IoT application developments in the least researched areas. The IoT generates enormous data, so-called big data (high volume, at a different speed and different varieties of data) in varying data quality. Analysing the IoT system and its key attributes are the key to advancing smart IoT utilization. Therefore, the primary aim of our paper is to explore recently created IoT applications in the agriculture and farming industry to give the more profound understanding about sensor data collection, used technologies, and sub-verticals, for example, water and crop management. The secondary aim of this study is to analyse the current issues such as higher human interaction, high labour cost, higher water consumption and save water for future, higher energy consumption and save energy/electricity for future, crop monitoring difficulties in IoT for agriculture and farming.

The remainder of this paper is as follows: In Section II we include raw data collection methodology, data inclusion criteria, and data analysis methods. Finally, the results of Agriculture and Farming based on IoT Sub verticals, Sensor Data, and Technologies are presented in Section III, and in Section IV we discuss the results. Section V concludes the paper. The raw data collected from 60 peer-reviewed publications used in this paper are summarised in Table I.

II. MATERIALS AND METHODS

Data collection involves identifying important criteria in research articles on the Internet of Things (IoT) in the agriculture and farming sectors.

As shown in Table I, these essential criteria were used to analyse relevant research papers. In particular, 60 peer-reviewed scientific publications on IoT in the agriculture and farming sectors published in scientific journals between 2016 and 2018 were used.

1) *Collection of raw data:* The data gathered for this review is from 60 peer-reviewed publications (2016-2018) that were collected from the IEEE database. All these publications have different data applications that have been studied and analyzed in this survey. The attributes compared were sub-verticals, data collection measurements, used technologies, challenges in current approach, benefits, countries and drivers of IoT.

2) *Data inclusion criteria:* To evaluate the data inclusion criteria a comparison table was drawn to include as the following attributes: Author, Sub vertical, Data collection measurements, Technologies, Benefits, Challenges, Solutions and Drivers of IoT. Nevertheless, in our study, articles were excluded when the selected attributes were not present. In our analysis, the number of sensors, amount of data collected, underlying technologies, sensor topology and other intermediate gateways were not included since no information can find with all the peer-reviewed publications (2016-2018).

3) *Data analysis:* We pooled and analyzed the reported studies based on data collected through peer reviewed articles and displaying emerging themes in a table. The data sets included attributes such as Sub vertical, Data collection measurements, Technologies, Benefits, Challenges, Solutions, Countries focused on automation of the agriculture proses and Drivers of IoT. The descriptive details of the study based on the publication year were analyzed to observe the results from 2016 to 2018.

III. RESULTS

This review aims to analyse the incorporation of IoT for the development of applications in the agriculture and farming sectors. The study focuses on sub-verticals and collecting data for measurements and technologies in the field of agriculture and farming to increase productivity and efficiency with the help of the Internet of Things (IoT). This study of IoT in agriculture and farming focuses on developing a criterion approach with the help of agricultural environmental parameters and IoT measures and technologies. In the field of agriculture, there are many environmental parameters that need to be considered to enhance crops, reduce water consumption and human involvement [44]. Moreover, there are many sub-verticals that can be identified depending on the differences in approach.

In this review, we have gathered articles which have focused on agricultural and farming sub-verticals from 2016 to 2018. As shown in Fig. 1, 23 sub-verticals were found according to the results obtained and the topmost area was water management (28.08%).

As IoT depends on sensor data collections, a vast amount of data needs to be gathered to identify or predict accurate results. This study indicates that many researchers have focused on environmental temperature (24.87%), humidity (19.79%) and soil moisture (15.73%) as environmental measurements. As shown in Fig. 2, 28 types of data were collected for measurements with environmental temperature and humidity being considered the most critical parameters for agriculture and farming.

As shown in Fig. 3, we have categorised all technologies used in the articles. This study has identified Wi-Fi as the most used technology (30.27%) followed by Mobile Technology (21.10%) for both agriculture and farming. ZigBee, another data transfer technology, is also used but to a lesser extent.

According to Fig. 4, the use of IoT was more prominent in the agriculture industry than the farming industry (Agriculture – 76.1%, Farming – 23.8%).

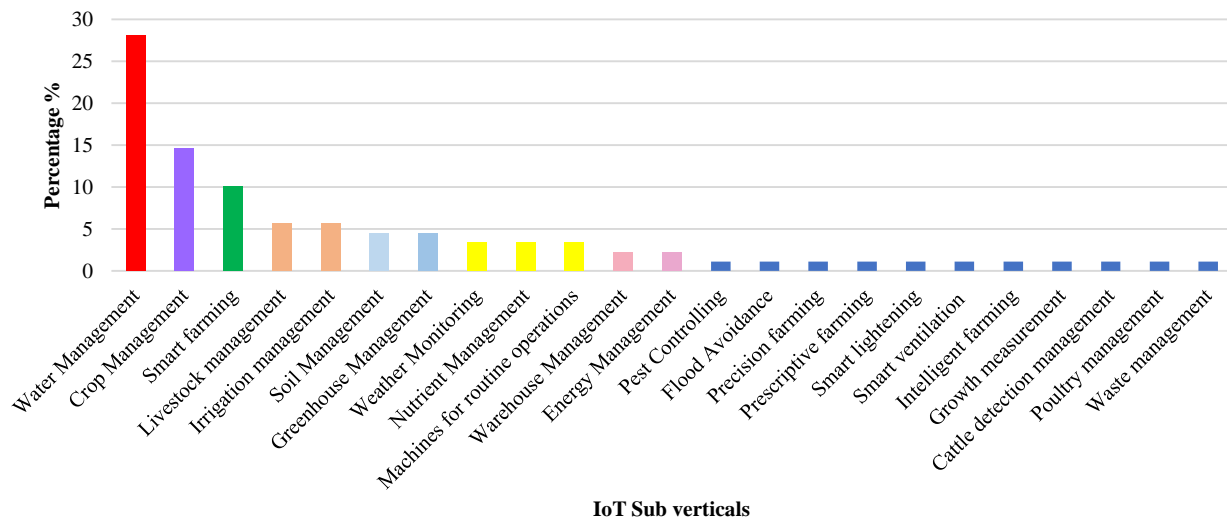


Fig. 1. Agriculture and Farming Sub Verticals: different Agricultural and Farming Sub Verticals Considered to Enhance Efficiency and Productivity–Pooling

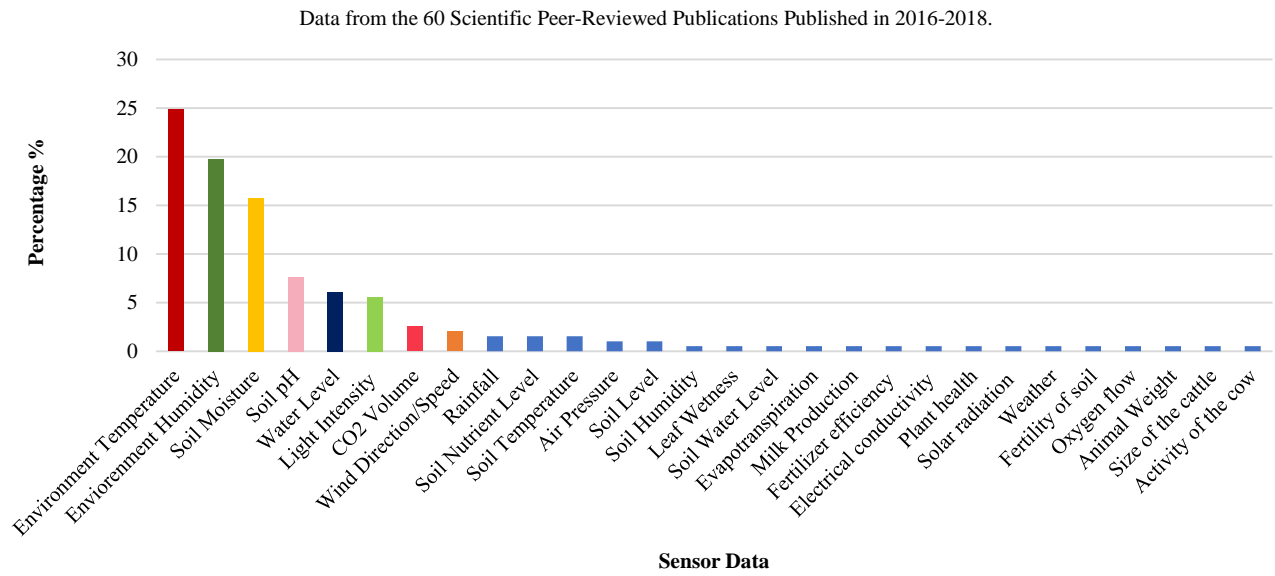


Fig. 2. Utilization of Sensor Data based on Farming Activities Referred to in the Data Pool of 60 Peer Reviewed Published Articles.

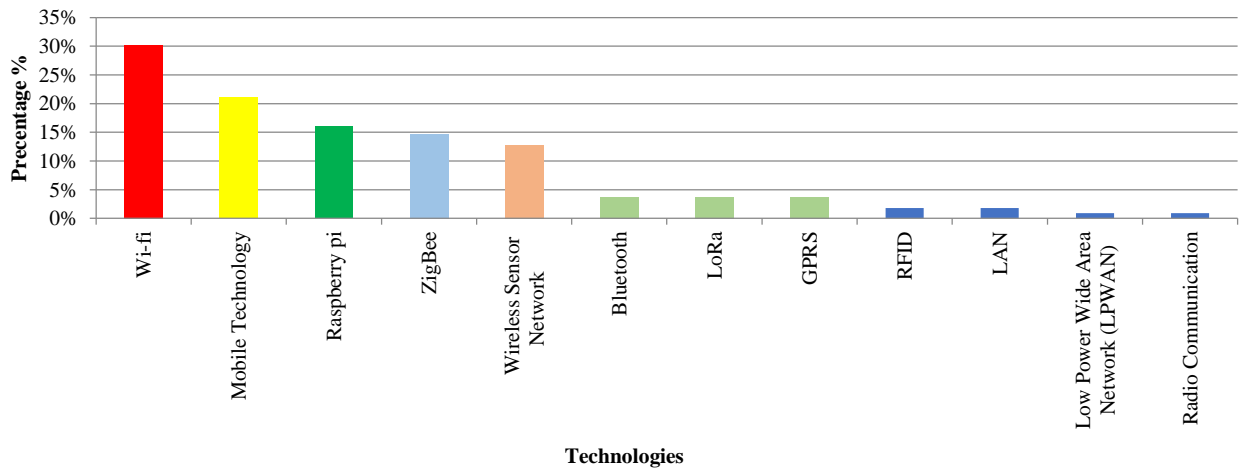


Fig. 3. Overview of different Technologies Referred to in the Data Pool of 60 Peer Reviewed Published Articles and Frequency of Mentions Shown in Order of High Frequency to Low.

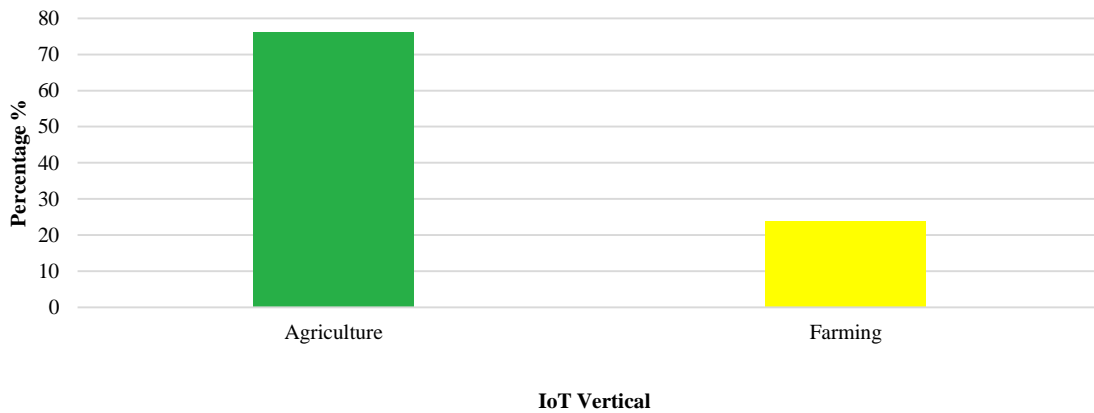


Fig. 4. Overview of Comparing the usage of Internet of Things in two Verticals as Agriculture and Farming in 60 Peer-Reviewed Research Articles to understand which is mostly used Internet of Things from Year 2016-2018.

TABLE I. IOT IN AGRICULTURE AND FARMING CRITERION-APPROACH-DATA EXTRACTED FROM 60 SCIENTIFIC ARTICLES IN 2016-2018

No	Year/Author	IoT Sub Verticals	Measures (Data collection)	Technologies Used	Benefits of Proposed System	Challenges in Current Approach	Solution for Current Issues	Drivers of IoT	Application
1	Venkatesh et al (2017) [1]	✓ Water Management	<ul style="list-style-type: none"> ✓ Environmental temperature ✓ Humidity ✓ Soil ✓ moisture 	<ul style="list-style-type: none"> ✓ Raspberry pi ✓ Wi-Fi. ✓ RFID ✓ Bluetooth ✓ Zigbee 	<ul style="list-style-type: none"> ✓ Can detect the temperature, humidity and moisture. ✓ Continuous monitoring all the places including critical areas. 	<ul style="list-style-type: none"> ✓ Human interaction ✓ Labour cost ✓ Wastage of water ✓ Crop from abnormal irrigation. 	<ul style="list-style-type: none"> ✓ Detect temperature, humidity, moisture using sensors. ✓ Maximize the yield of crop by monitoring agricultural parameters. 	<ul style="list-style-type: none"> ✓ Can deploy it in any type of environment for, ✓ monitoring ✓ flexibility ✓ robust 	✓ Agriculture
2	Athira et al (2017) [2]	<ul style="list-style-type: none"> ✓ Pest controlling ✓ Weather monitoring 	<ul style="list-style-type: none"> ✓ Soil moisture ✓ Temperature ✓ Water level 	✓ ZigBee	<ul style="list-style-type: none"> ✓ Irrigation process is completely controlled by computer-based systems. ✓ System analyses the weather reports. ✓ Keep pest away from the crops. ✓ Help to faster the growth of plants. ✓ Power efficient. 	<ul style="list-style-type: none"> ✓ Only works based on the commands from user 	<ul style="list-style-type: none"> ✓ Low cost ✓ Efficient growth of crops ✓ Faster growth of plants. 	<ul style="list-style-type: none"> ✓ Predict and tackle drought situations to prevent to loss of crops. ✓ Keep monitoring climate conditions. 	✓ Agriculture
3	Zhao et al (2017) [3]	✓ Water Management	✓ Water level	✓ LoRa technology	<ul style="list-style-type: none"> ✓ Can utilize the water usage. 	<ul style="list-style-type: none"> ✓ To identify the appropriate time and in the right amount of water. ✓ High power consumption. ✓ High cost. ✓ Low coverage of ZigBee and Wi-Fi. 	<ul style="list-style-type: none"> ✓ Minimize the cost of deployment and maintenance. ✓ More efficient. ✓ Cover wider area than ZigBee and Wi-Fi. ✓ Energy consumption is low. 	<ul style="list-style-type: none"> ✓ Users can remotely access irrigation system and check the status. 	✓ Agriculture
4	Sagar S et al (2017) [4]	✓ Flood Avoidance	<ul style="list-style-type: none"> ✓ Water level ✓ Soil moisture 	✓ Mobile technology	<ul style="list-style-type: none"> ✓ Lessen the human intercession. ✓ Lessen the probability of the flood occurrences. ✓ Faster the growth of the crops. 	<ul style="list-style-type: none"> ✓ Save water for the future. ✓ Save electricity for the future. 	<ul style="list-style-type: none"> ✓ Flood avoidance. ✓ Power cutoff is being reduced. 	<ul style="list-style-type: none"> ✓ Higher the revenue by faster the growth of crops. ✓ Ensure the durability of the soil. 	✓ Agriculture

5	Saraf et al (2017) [5]	✓ Water Management	<ul style="list-style-type: none"> ✓ Water level. ✓ Soil ✓ Moisture. ✓ Environment temperature. ✓ Humidity 	<ul style="list-style-type: none"> ✓ Wireless sensor network. ✓ ZigBee. ✓ Mobile technology 	<ul style="list-style-type: none"> ✓ Lessen the human interaction. ✓ Efficiently managed the irrigation water system. 	<ul style="list-style-type: none"> ✓ High water consumption. ✓ Human interaction. 	<ul style="list-style-type: none"> ✓ The water consumption is reduced. ✓ Lessen the human interaction. 	<ul style="list-style-type: none"> ✓ Reduced water consumption. 	<ul style="list-style-type: none"> ✓ Agriculture
6	Upadhyaya et al (2017) [6]	✓ Water Management	<ul style="list-style-type: none"> ✓ Soil Moisture ✓ Water requirements 	<ul style="list-style-type: none"> ✓ Wi-Fi ✓ Mobile technology 	<ul style="list-style-type: none"> ✓ Broader coverage. ✓ Notify user when any change happens. 	<ul style="list-style-type: none"> ✓ No attention to water management. ✓ No economic feasibility. ✓ Complicated data for understanding. ✓ Data display is not user friendly. 	<ul style="list-style-type: none"> ✓ Water requirements monitored. ✓ Immediate notification sends to farmer. ✓ User friendly data collection. 	<ul style="list-style-type: none"> ✓ Captured moisture values stored in the cloud. ✓ Compare captured values with predefined moisture values. ✓ Used solar powered battery. 	<ul style="list-style-type: none"> ✓ Agriculture
7	Udhayakumar S et al (2017) [7]	✓ Water Management	<ul style="list-style-type: none"> ✓ Soil moisture ✓ Environment temperature. ✓ Humidity 	<ul style="list-style-type: none"> ✓ Raspberry pi ✓ Mobile technology 	<ul style="list-style-type: none"> ✓ Monitor plants through smart mobile. ✓ Efficient water supply management 	<ul style="list-style-type: none"> ✓ Overhead sprinklers. ✓ Wastage of water. 	<ul style="list-style-type: none"> ✓ Watering crop without human interaction. 	<ul style="list-style-type: none"> ✓ Analyze moisture level of ground. 	<ul style="list-style-type: none"> ✓ Agriculture
8	Kumar et al (2017) [8]	✓ Water Management	<ul style="list-style-type: none"> ✓ Soil moisture ✓ Environment temperature. ✓ Humidity 	<ul style="list-style-type: none"> ✓ Mobile technology 	<ul style="list-style-type: none"> ✓ Higher the crop. ✓ Efficient water supply. ✓ Reduced cost. ✓ Resource optimization 	<ul style="list-style-type: none"> ✓ Hard to water to crop equally due to unequal rain water distribution. ✓ Amount of water not defined. 	<ul style="list-style-type: none"> ✓ Farmers can know field status even they are at home. ✓ Efficient water management. ✓ Provide real time information. 	<ul style="list-style-type: none"> ✓ Automatic plan watering system. 	<ul style="list-style-type: none"> ✓ Agriculture
9	Mathew et al (2017) [9]	✓ Nutrient Management	<ul style="list-style-type: none"> ✓ Environment temperature. ✓ Humidity ✓ Nitrogen level ✓ Prosperous level 	<ul style="list-style-type: none"> ✓ Raspberry pi ✓ Mobile technology ✓ Wi-Fi 	<ul style="list-style-type: none"> ✓ Can monitor whether conditions. ✓ Cost effective ✓ Automatically monitored disease associated with rice species. 	<ul style="list-style-type: none"> ✓ Low or high watering. ✓ Lack of nutrition management. 	<ul style="list-style-type: none"> ✓ Whether conditions detected. ✓ Enhanced the fertilizer amount. 	<ul style="list-style-type: none"> ✓ Can enhance the fertilizer amount. 	<ul style="list-style-type: none"> ✓ Agriculture
10	Suhas et al (2017) [10]	✓ Water Management	<ul style="list-style-type: none"> ✓ Temperature ✓ Moisture level ✓ Humidity ✓ Light Intensity ✓ Nitrogen, ✓ Phosphorus ✓ Potassium 	<ul style="list-style-type: none"> ✓ Bluetooth ✓ Wi-Fi 	<ul style="list-style-type: none"> ✓ Cost effective. ✓ High efficient water management 	<ul style="list-style-type: none"> ✓ Higher water consumption. ✓ High power utilization. ✓ Lack of useful inference. 	<ul style="list-style-type: none"> ✓ Reduced water consumption. ✓ Better power utilization. 	<ul style="list-style-type: none"> ✓ Automated water supply system. 	<ul style="list-style-type: none"> ✓ Agriculture

11	Wicha et al (2017) [11]	✓ Water Management	✓ Soil level ✓ Temperature	✓ Wi-Fi	✓ Efficient water management	✓ High water consumption.	✓ Managed water system effective manner.	✓ Reveals the positive comparison results from the adaptive Wetting Front Detector (WFD).	✓ Agriculture
12	Rajakumar et al (2017) [12]	✓ Crop production	✓ Soil level ✓ Soil nutrient	✓ Mobile technology	✓ Increase the crop production. ✓ Can get current fertilizer requirements.	✓ Due to improper maintenance, the crop becomes damaged which causes a huge loss for a farmer.	✓ Enhance the crop. ✓ Control the agricultural product costs.	✓ Interfacing different soil nutrient sensors.	✓ Agriculture
13	Sachapara et al (2017) [13]	✓ Crop Production ✓ Water Management	✓ Temperature ✓ Humidity ✓ Soil ✓ moisture ✓ Leaf wetness ✓ Wind speed/direction ✓ Rainfall detection ✓ Soil ph. ✓ Seed recognition.	✓ Raspberry pi ✓ Mobile technology	✓ Enhanced crop production. ✓ Enhanced quality. ✓ Reduced costs.	✓ Poor risk management. ✓ Poor water management. ✓ Poor infrastructure. ✓ Poor crops yield and big loss for farmers.	✓ Enhanced crops yield by proper water management.	✓ Seed recognition system helps to know sustainable environmental conditions.	✓ Agriculture
14	Pooja S et al (2017) [14]	✓ Weather Monitoring ✓ Precision Farming	✓ Temperature ✓ Humidity ✓ Soil ✓ Moisture ✓ Light intensity	✓ Raspberry-Pi ✓ Wi-Fi	✓ Improve the crop traceability. ✓ Increase overall yield.	✓ Wastage of crops. ✓ Poor water system management.	✓ Crop productivity increased. ✓ Reduced wastage of crops. ✓ Reduced water use. ✓ Minimal maintenance required. ✓ High accuracy	✓ Use of decision making algorithm.	✓ Agriculture
15	Kavitha et al (2017) [15]	✓ Crop management	✓ Soil moisture ✓ pH level ✓ Temperature ✓ Humidity ✓ Light intensity ✓ Water level	✓ Mobile technology	✓ Improved crop growth. ✓ Efficient watering system.	✓ Difficulties in monitoring. ✓ Harvesting related problems. ✓ Poor crop growth. ✓ Poor power management. ✓ Poor water management.	✓ Effective water management. ✓ Effective power management.	✓ Reduced costs between central server and software.	✓ Agriculture
16	Jawahar et al (2017) [16]	✓ Crop management ✓ Water Management	✓ Temperature ✓ Humidity ✓ Soil moisture ✓ Water level	✓ Mobile technology	✓ Prevent crops from spoilage during rain. ✓ Recycling rain water in an efficient manner.	✓ Wastage of water. ✓ Human interaction. ✓ Hard to monitor field every time to avoid intrusion attacks.	✓ Update farmer with live condition of the field. ✓ Lessen human interaction. ✓ Notify intrusion detections with an alarm.	✓ Excess water from the cultivation field and recycled back to the tank.	✓ Agriculture

17	Nibi K V et al (2017) [17]	<ul style="list-style-type: none"> ✓ Whether management ✓ Crop management 	<ul style="list-style-type: none"> ✓ Soil moisture ✓ Temperature ✓ pH level 	<ul style="list-style-type: none"> ✓ Mobile technology ✓ Wi-Fi 	<ul style="list-style-type: none"> ✓ Provide advice for farmers to properly grow and treat the crops. ✓ Provide suggestions to monitoring crops. ✓ Ex: Irrigation timings ✓ Optimum usage of fertilizers. ✓ Provide whether information. 	<ul style="list-style-type: none"> ✓ High human interaction. ✓ Hard to deal with changing whether parameters. 	<ul style="list-style-type: none"> ✓ Provide efficient suggestions about when and how much to irrigate. ✓ Provide adequate fertilizer information. 	<ul style="list-style-type: none"> ✓ Provide farmer friendly alerts and guidance with their local language. 	<ul style="list-style-type: none"> ✓ Agriculture
18	Tran et al (2017) [18]	<ul style="list-style-type: none"> ✓ Crop management ✓ Nutrient Detection 	<ul style="list-style-type: none"> ✓ Temperature ✓ Humidity 	<ul style="list-style-type: none"> ✓ ZigBee ✓ Raspberry Pi 	<ul style="list-style-type: none"> ✓ Could prevent soil erosion. 	<ul style="list-style-type: none"> ✓ High energy consumption. ✓ Soil and nutrient depletion. 	<ul style="list-style-type: none"> ✓ Reduced energy consumption. ✓ Could react changes in environment and soil. 	<ul style="list-style-type: none"> ✓ Reduce the consumption of energy ✓ Increase the number of sensors 	<ul style="list-style-type: none"> ✓ Agriculture
19	Muhammad et al (2017) [19]	<ul style="list-style-type: none"> ✓ Water Management 	<ul style="list-style-type: none"> ✓ Water level ✓ Soil Moisture 	<ul style="list-style-type: none"> ✓ Wireless Sensor Network ✓ Radio Communication 	<ul style="list-style-type: none"> ✓ Efficient water management 	<ul style="list-style-type: none"> ✓ Climate changes. ✓ Scarcity of water. 	<ul style="list-style-type: none"> ✓ Monitoring water in watercourses. 	<ul style="list-style-type: none"> ✓ Smart water metering system. 	<ul style="list-style-type: none"> ✓ Agriculture
20	Viswanathan et al (2017) [20]	<ul style="list-style-type: none"> ✓ Crop management. ✓ Warehouse Management. 	<ul style="list-style-type: none"> ✓ Temperature ✓ Humidity ✓ Soil Moisture ✓ Rain fall ✓ Light intensity 	<ul style="list-style-type: none"> ✓ Wi-Fi 	<ul style="list-style-type: none"> ✓ Remote controlled processes to perform such tasks as; ✓ Spraying ✓ Weeding ✓ Bird and animal scaring ✓ Keeping vigilance ✓ Provide smart warehouse management ✓ Theft detection in warehouse. 	<ul style="list-style-type: none"> ✓ High cost ✓ Human interaction for all activities. 	<ul style="list-style-type: none"> ✓ Reduced cost. ✓ Lessen human interaction. ✓ High reliability. ✓ Improved crop production. 	<ul style="list-style-type: none"> ✓ Smart warehouse management. 	<ul style="list-style-type: none"> ✓ Agriculture
21	Dai et al (2017) [21]	<ul style="list-style-type: none"> ✓ Water Management ✓ Agricultural Greenhouse Management 	<ul style="list-style-type: none"> ✓ Soil environment: ✓ Temperature ✓ Humidity of soil ✓ Soil CO2 ✓ Soil pH ✓ Environmental: ✓ Temperature ✓ Humidity ✓ Wind speed ✓ Air pressure ✓ Rainfall 	<ul style="list-style-type: none"> ✓ ZigBee 	<ul style="list-style-type: none"> ✓ High irrigation efficiency. ✓ High flexibility. 	<ul style="list-style-type: none"> ✓ Low irrigation efficiency ✓ High labour cost ✓ Low precision ✓ High water consumption. 	<ul style="list-style-type: none"> ✓ Lessen labour cost. ✓ Reduced water wastage. 	<ul style="list-style-type: none"> ✓ Powerful servers to handle storage data. 	<ul style="list-style-type: none"> ✓ Agriculture
22	Yuan et al (2017) [22]	<ul style="list-style-type: none"> ✓ Agricultural Greenhouse Management 	<ul style="list-style-type: none"> ✓ Temperature ✓ Humidity 	<ul style="list-style-type: none"> ✓ ZigBee 	<ul style="list-style-type: none"> ✓ More flexible. ✓ Low power consuming. 	<ul style="list-style-type: none"> ✓ Short distance communication. ✓ High power consumption. 	<ul style="list-style-type: none"> ✓ Lessen power consumption. 	<ul style="list-style-type: none"> ✓ Automated greenhouse management. 	<ul style="list-style-type: none"> ✓ Agriculture

23	Garcia et al (2017) [23]	<ul style="list-style-type: none"> ✓ Water Management ✓ Energy Management 	<ul style="list-style-type: none"> ✓ Irrigation events as: ✓ Flow level ✓ Pressure level ✓ Wind speed 	<ul style="list-style-type: none"> ✓ LoRa ✓ Wi-Fi 	<ul style="list-style-type: none"> ✓ Low cost irrigation control. ✓ Autonomous decision making without human interactions. 	<ul style="list-style-type: none"> ✓ Device scalability is low. ✓ Device manageability is low. 	<ul style="list-style-type: none"> ✓ Lessen human interaction. ✓ Efficient water management. ✓ Efficient power management. 	<ul style="list-style-type: none"> ✓ Autonomous decision making without human interactions. 	<ul style="list-style-type: none"> ✓ Agriculture
24	Janani V et al (2017) [24]	<ul style="list-style-type: none"> ✓ Soil Management ✓ Nutrient Detection 	<ul style="list-style-type: none"> ✓ Soil Measures: ✓ Soil pH ✓ Soil Temperature ✓ Soil Humidity 	<ul style="list-style-type: none"> ✓ Wi-Fi ✓ Raspberry Pi 	<ul style="list-style-type: none"> ✓ Reduced manual monitoring of the field. ✓ Obtained nature of soil. ✓ Can monitored from anywhere. 	<ul style="list-style-type: none"> ✓ Manual field monitoring. ✓ Cost is high. ✓ Difficult to predict the crop for the field. 	<ul style="list-style-type: none"> ✓ Reduces the difficulty for identify the right crop for the field. ✓ Increased agricultural production ✓ Reduced time and money for farmers. 	<ul style="list-style-type: none"> ✓ Soil management with the attention of nutrient, fertilization. 	<ul style="list-style-type: none"> ✓ Agriculture
25	Jyothi et al (2017) [25]	<ul style="list-style-type: none"> ✓ Crop Management 	<ul style="list-style-type: none"> ✓ Temperature ✓ Humidity 	<ul style="list-style-type: none"> ✓ Wi-Fi ✓ GPRS 	<ul style="list-style-type: none"> ✓ Provide accurate changes in the crop yield. ✓ Advance the harvest of the crop. 	<ul style="list-style-type: none"> ✓ Reduced human power. ✓ High cost. ✓ High power consumption. 	<ul style="list-style-type: none"> ✓ Automated monitoring of the crop. ✓ Notify corrective actions to be taken. ✓ Low cost. ✓ Consume less Power. 	<ul style="list-style-type: none"> ✓ Notify agricultural fields with a MMS to the farmer. 	<ul style="list-style-type: none"> ✓ Agriculture
26	Javale et al (2017) [26]	<ul style="list-style-type: none"> ✓ Water Management 	<ul style="list-style-type: none"> ✓ Soil moisture ✓ Soil temperature ✓ Soil pH ✓ Soil water level 	<ul style="list-style-type: none"> ✓ Mobile technology 	<ul style="list-style-type: none"> ✓ Help to irrigate farms efficiently. ✓ Lessen human interaction. 	<ul style="list-style-type: none"> ✓ Water scarcity ✓ Human interaction is high. 	<ul style="list-style-type: none"> ✓ Estimates water as per requirements. ✓ Depending on soil and crop, fertilizer suggestions provided. ✓ Estimate the rainfall based on whether forecast. ✓ Manage water level according to the predicted rainfall. 	<ul style="list-style-type: none"> ✓ Water supply can control by mobile application with the less human interaction. 	<ul style="list-style-type: none"> ✓ Agriculture
27	Sathyadevan et al (2017) [27]	<ul style="list-style-type: none"> ✓ Soil Quality Management ✓ Water Management 	<ul style="list-style-type: none"> ✓ Temperature ✓ Humidity ✓ Soil moisture ✓ Water level 	<ul style="list-style-type: none"> ✓ ZigBee ✓ Wi-Fi ✓ Mobile technology 	<ul style="list-style-type: none"> ✓ Accurate measurements of the velocity of the liquid flowing inside the pipe. ✓ Pump monitoring. 	<ul style="list-style-type: none"> ✓ Water conservation. ✓ High labour cost. ✓ High electricity consumption. ✓ Overdependence on the chemical fertilizers. 	<ul style="list-style-type: none"> ✓ Automated water management. ✓ Lessen labour cost. ✓ Lessen power usage. 	<ul style="list-style-type: none"> ✓ Multiple sensor data collected into IoT framework. 	<ul style="list-style-type: none"> ✓ Agriculture
28	Kulkarni et al (2017) [28]	<ul style="list-style-type: none"> ✓ Soil management ✓ Water Management 	<ul style="list-style-type: none"> ✓ Soil moisture ✓ Soil pH 	<ul style="list-style-type: none"> ✓ Android ✓ Wi-Fi 	<ul style="list-style-type: none"> ✓ Decreased cost in manufacturing. ✓ Reduced cost in maintenance. 	<ul style="list-style-type: none"> ✓ High chemical fertilizer use. ✓ High energy consumption. ✓ High fertilizer costs. 	<ul style="list-style-type: none"> ✓ Save water more efficiently. ✓ Increase the crop yield. ✓ Save energy costs. ✓ Save fertilizer costs. 	<ul style="list-style-type: none"> ✓ Monitor and control plant growth parameters. ✓ Replaces the current system for soil moisture, pH and salinity value testing. 	<ul style="list-style-type: none"> ✓ Agriculture
29	Mahalakshmi et al (2016) [29]	<ul style="list-style-type: none"> ✓ Water Management 	<ul style="list-style-type: none"> ✓ Temperature ✓ Humidity ✓ Soil Moisture 	<ul style="list-style-type: none"> ✓ ZigBee 	<ul style="list-style-type: none"> ✓ Monitor crop field. ✓ Automate 	<ul style="list-style-type: none"> ✓ Water consumption is high. 	<ul style="list-style-type: none"> ✓ Continuous field monitoring 	<ul style="list-style-type: none"> ✓ Reduced water consumption 	<ul style="list-style-type: none"> ✓ Agriculture

		✓ Crop Management	✓ Light Intensity		the irrigation system.	✓ High human interaction.	with the help of low-cost sensors. ✓ Reduces water consumption. ✓ Reduced power consumption. ✓ Increased crop productivity. ✓ Reduced wastage of crops.	n up to great extent.	
30	Zaman et al (2016) [30]	✓ Water Management	✓ Moisture level ✓ Light intensity	✓ Raspberry Pi ✓ Wi-Fi ✓ (Mobile Technology	✓ Detect appropriate time for water supply. ✓ Keep track of water level.	✓ Cannot predict the time for watering.	✓ Improved productivity. ✓ Low cost. ✓ Utilize water resources. ✓ Lessen human interaction.	✓ With the enhanced sensor technology will become more efficient.	✓ Agriculture
31	Biradar et al (2017) [31]	✓ Water Management ✓ Crop management	✓ Temperature ✓ humidity ✓ Soil PH ✓ Evapotranspiration	✓ Wireless Sensor network ✓ Mobile technology ✓ ZigBee ✓ RFID	✓ Helps for decision making process ✓ Can monitor and control the temperature, humidity and soil PH. ✓ It can sense the amount of the change through the integration process of components. ✓ Reduce cost	✓ Unequal distribution of rain water ✓ Differentiation of weather condition. ✓ Different soil types	✓ Crop management by providing required amount of water. ✓ Multidisciplinary monitoring leads to improvement of agricultural management.	✓ Decreases in the cost of sensors ✓ Increasing difficulty of big data analysis	✓ Agriculture
32	Ismail et al (2017) [32]	✓ Soil moisture level monitor	✓ Soil moisture ✓ Water content ✓ Temperature	✓ Wi-Fi	✓ Farmers can face the any environmental challenges easily. ✓ Reduce the harmful risk percentage ✓ Save money and water. ✓ Reduce pest population.	✓ Climatic change. ✓ Take long time to harvesting. ✓ Burnings in land preparation. ✓ Limitation of space.	✓ Monitor and control the soil moisture from the web server.	✓ Decreases in the cost of sensors and actuators. ✓ Recycling the resources.	✓ Agriculture
33	Amandeep et al (2017) [33]	✓ Machines for routine operations ✓ Warehouse management.	✓ Soil moisture ✓ Temperature ✓ Humidity ✓ Water level	✓ ZigBee ✓ Mobile technology ✓ Wi-fi	✓ Increasing the crop productivity ✓ Prevent thefts. ✓ Prevent attacking from birds, animals and other facts.	✓ Manual distribution of seeds. ✓ Pattern of two crops year. ✓ Unscientific system of cultivation. ✓ Unequal watering system.	✓ Using remote control vehicle keeps monitoring the humidity, soil condition and water level in the field.	✓ Improve the green energy concept for better productivity	✓ Farming
34	Dolci (2017) [34]	✓ Precision farming ✓ Prescriptive farming	✓ Temperature ✓ humidity ✓ Soil PH ✓ CO2	✓ Mobile technology	✓ Cost reduction ✓ Reduce the frequency	✓ Unequal distribution of air flow.	✓ Improving malt quality and efficiency in production with using Artificial Intelligence	✓ low cost sensors ✓ open source ✓ applications ✓ ability to increase the level of farming	✓ Farming

								sophistication	
35	Gokul et al (2017) [35]	<ul style="list-style-type: none"> ✓ Livestock management ✓ Smart lightening ✓ Smart ventilation ✓ Water management 	<ul style="list-style-type: none"> ✓ Temperature ✓ humidity ✓ Milk production 	<ul style="list-style-type: none"> ✓ Mobile technology ✓ Wi-Fi 	<ul style="list-style-type: none"> ✓ Identifying the emergency conditions. ✓ Improves location tracking. ✓ Improves cattle health ✓ Improves availability 	<ul style="list-style-type: none"> ✓ Unable to detect illnesses early. ✓ Different environmental conditions ✓ Irregular feeding 	<ul style="list-style-type: none"> ✓ Make ✓ Infrastructure of cattle farming smarter. ✓ implement a noninvasive ✓ wearable to track physiological and biological activities of cattle. 	<ul style="list-style-type: none"> ✓ Improve the smart lightning and ventilation system 	<ul style="list-style-type: none"> ✓ Farming, Agriculture
36	Rajkumar et al (2017) [36]	<ul style="list-style-type: none"> ✓ Irrigation management 	<ul style="list-style-type: none"> ✓ Temperature ✓ humidity ✓ Soil Moisture 	<ul style="list-style-type: none"> ✓ Mobile technology ✓ Wi-Fi 	<ul style="list-style-type: none"> ✓ Provides real time information ✓ Cost reduction ✓ Resource optimization ✓ Reduce water logging and shortage 	<ul style="list-style-type: none"> ✓ Water shortage ✓ Different environmental conditions 	<ul style="list-style-type: none"> ✓ ✓ Developing smart irrigation system to monitor at anywhere. 	<ul style="list-style-type: none"> ✓ Installing a water meter to estimate the amount of water. ✓ Using Wireless sensors. 	<ul style="list-style-type: none"> ✓ Agriculture
37	Sri et al (2017) [37]	<ul style="list-style-type: none"> ✓ Crop management ✓ Irrigation management 	<ul style="list-style-type: none"> ✓ Soil ✓ Temperature ✓ Humidity ✓ Rain fall ✓ Fertilizer efficiency 	<ul style="list-style-type: none"> ✓ Wi-Fi ✓ GPRS ✓ Zig Bee ✓ Raspberry pi ✓ Mobile technology 	<ul style="list-style-type: none"> ✓ ✓ Improve the yield ✓ Low cost 	<ul style="list-style-type: none"> ✓ Unpredictable weather ✓ Water scarcity ✓ Improper water usage 	<ul style="list-style-type: none"> ✓ ✓ Providing reliable and efficient agricultural system to monitor the field 	<ul style="list-style-type: none"> ✓ Improve ✓ by adding several modern techniques like irrigation ✓ Method, solar power source usage. 	<ul style="list-style-type: none"> ✓ Agriculture
38	Rajarsri et al (2017) [38]	<ul style="list-style-type: none"> ✓ Water management 	<ul style="list-style-type: none"> ✓ Water level 	<ul style="list-style-type: none"> ✓ Mobile technology 	<ul style="list-style-type: none"> ✓ Improve the efficiency ✓ Optimize resource ✓ Maximize the profit 	<ul style="list-style-type: none"> ✓ Unequal water distribution 	<ul style="list-style-type: none"> ✓ Build a well-connected farming network and create a knowledge sharing platform. 	<ul style="list-style-type: none"> ✓ Agro loan ✓ Inexpensive Agricultural consultation ✓ better ROI ✓ Agro networking ✓ Low cost products 	<ul style="list-style-type: none"> ✓ Agriculture
39	Ruengittinun et al (2017) [39]	<ul style="list-style-type: none"> ✓ Smart farming 	<ul style="list-style-type: none"> ✓ Temperature ✓ Humidity ✓ PH ✓ Electrical conductivity 	<ul style="list-style-type: none"> ✓ Wi-Fi 	<ul style="list-style-type: none"> ✓ Can farm in less space ✓ Provides many products 	<ul style="list-style-type: none"> ✓ Differential of temperature ✓ Lack of time to manage and plant. 	<ul style="list-style-type: none"> ✓ Build a smart hydroponic eco system 	<ul style="list-style-type: none"> ✓ Symmetrical ✓ plantation to check the accuracy of the HFE across multiple farms in the same area. 	<ul style="list-style-type: none"> ✓ Farming

40	✓ Yoon et al (2018) [40]	✓ Smart farming ✓ Irrigation management	✓ Temperature ✓ Humidity ✓ CO2	✓ Bluetooth ✓ Wi-Fi ✓ LPWAN	✓ can overcome distance ✓ and place constraints. ✓ save maintenance cost of existing devices ✓ provide compatibility with new devices	✓ Power problem ✓ Space limitation ✓ difficulties in installing additional devices	✓ Build a system with using Bluetooth and LPWAN to solve the power problem and space limitation.	✓ System for studying the development of environmental Algorithms	✓ Farming, Agriculture
41	Ezhilazhahi et al (2017) [41]	✓ Smart Farming	✓ Plant health ✓ Soil Moisture ✓ Temperature ✓ Humidity	✓ WSN ✓ Zig Bee ✓ Wi-Fi ✓ Raspberry pi ✓ GPRS	✓ Enrich the productivity of food grains. ✓ Prevent the plant from blight and harmful insects.	✓ water scarcity ✓ unpredictable weather conditions	✓ Developing a system to monitor continuously soil moisture of the plants.	✓ Increasing the number of sensors.	✓ Farming
42	Tanmayee (2017) [42]	✓ Crop management	✓ Temperature ✓ Soil Moisture	✓ Raspberry pi ✓ Mobile technology	✓ Reduces the wastage of pesticides ✓ Reduces the human effort ✓ Increase agricultural productivity	✓ Bacterial diseases ✓ unpredictable weather conditions	✓ Implementing a rice crop monitoring System	✓ Using multicolor detection for detect the disease in any stage.	✓ Agriculture
43	Takecar et al (2017) [43]	✓ Machines for routine operations	✓ Soil Moisture ✓ Temperature ✓ Humidity	✓ Wi-fi.	✓ Increase the income ✓ Cost reduction	✓ Lack of Resource Management	✓ Implementing a system to look after the plantation without disturbing busy schedule.	✓ Improve the components in the PATRIOT system	✓ Farming
44	Krishna et al (2017) [44]	✓ Smart Farming ✓ livestock management	✓ Soil Moisture ✓ Light intensity ✓ Humidity ✓ Temperature ✓ Soil pH	✓ Raspberry pi ✓ Zig Bee ✓ Wi-Fi	✓ Reducing labor costs ✓ Helps to track the changes accurately occurring instantly in real time at the field.	✓ lack of moisture in the fields ✓ salinity ✓ lack of application of fertilizers ✓ Different sowing time.	✓ Using wireless mobile robot performing various operations of the field.	✓ Develop the capabilities of the robot.	✓ Farming
45	Li et al (2017) [45]	✓ Irrigation management ✓ Greenhouse management	✓ Humidity ✓ Temperature	✓ Zig Bee ✓ Wi-Fi ✓ Bluetooth ✓ LAN	✓ Reduce the labour cost. ✓ Improve the efficiency of agricultural production.	✓ low production efficiency ✓ Waste of resources ✓ Environmental pollution.	✓ Green house management to improve the agricultural production.	✓ Implement a comprehensive promotion system.	✓ Agriculture
46	Suciu et al (2016) [46]	✓ Smart Farming	✓ Temperature	✓ Mobile technology ✓ GPRS	✓ Improve the quality and safety of the products ✓ Detecting plant diseases, flood. Etc.	✓ Climatic change ✓ High temperature ✓ Low profit margin	✓ Assist for crop management by using smart agriculture	Allowing system to measure basic parameters for irrigation management.	✓ Farming
47	Putjaika et al (2017) [47]	✓ Intelligent farming	✓ Humidity ✓ Temperature ✓ Soil moisture ✓ Light intensity	✓ Wi-Fi	✓ Improve the production process ✓ Managing resources	✓ Unpredictable weather	✓ Implement a system to monitor the harmful diseases.	✓ Developing the sensor and control system by adding more components.	✓ Farming

48	Okayasu et al (2017) [48]	<ul style="list-style-type: none"> ✓ Growth measurement 	<ul style="list-style-type: none"> ✓ Humidity ✓ Temperature ✓ Solar radiation ✓ CO2 	<ul style="list-style-type: none"> ✓ Wi-Fi 	<ul style="list-style-type: none"> ✓ Reduce production cost ✓ Improve the quality of the products 	<ul style="list-style-type: none"> ✓ High production cost ✓ Less quality in products 	<ul style="list-style-type: none"> ✓ Monitoring the plant growth measurement using smart agriculture. 	<ul style="list-style-type: none"> ✓ Improve the accuracy of measurements. 	<ul style="list-style-type: none"> ✓ Farming
49	Sreekantha et al (2017) [49]	<ul style="list-style-type: none"> ✓ Irrigation management. ✓ Greenhouse management 	<ul style="list-style-type: none"> ✓ Temperature ✓ Soil moisture ✓ Weather ✓ Fertility of soil 	<ul style="list-style-type: none"> ✓ Zig Bee ✓ Mobile technology ✓ Wi-Fi 	<ul style="list-style-type: none"> ✓ Detection of seed, water level, pest, animal intrusion to the field. ✓ Reduce cost and time ✓ Enhance productivity 	<ul style="list-style-type: none"> ✓ Environmental changes ✓ High water consumption 	<ul style="list-style-type: none"> ✓ Enhance the productivity by using crop monitoring system. 	<ul style="list-style-type: none"> ✓ generalize event-condition-action ✓ framework for programming reactive sensor networks 	<ul style="list-style-type: none"> ✓ Agriculture
50	Rajendrakumar et al (2017) [50]	<ul style="list-style-type: none"> ✓ Water management ✓ Crop management 	<ul style="list-style-type: none"> ✓ Soil moisture ✓ Temperature ✓ Humidity ✓ Soil pH 	<ul style="list-style-type: none"> ✓ Mobile technology ✓ Wi-Fi 	<ul style="list-style-type: none"> ✓ Increase harvest efficiency ✓ Decrease water wastage 	<ul style="list-style-type: none"> ✓ Uncertain monsoon ✓ Water scarcity ✓ Climatic variation 	<ul style="list-style-type: none"> ✓ Providing information to understand how to monitor and control the data remotely and apply to the fields. 	<ul style="list-style-type: none"> ✓ Develop multiple systems. 	<ul style="list-style-type: none"> ✓ Agriculture
51	Ferreira et al (2017) [51]	<ul style="list-style-type: none"> ✓ Smart Farming ✓ Machines for routine operations 	<ul style="list-style-type: none"> ✓ Temperature ✓ Soil pH ✓ Oxygen flow 	<ul style="list-style-type: none"> ✓ Mobile technology 	<ul style="list-style-type: none"> ✓ Improve the production. 	<ul style="list-style-type: none"> ✓ Climate changes. ✓ Insufficient available lands. ✓ Air toxins. 	<ul style="list-style-type: none"> ✓ Researching modules related to IoT, event processing, situational awareness and data harmonization 	<ul style="list-style-type: none"> ✓ Developing all the apps and experiment with real cases. 	<ul style="list-style-type: none"> ✓ Farming
52	Vernandhes et al (2017) [52]	<ul style="list-style-type: none"> ✓ Livestock management 	<ul style="list-style-type: none"> ✓ Temperature ✓ Humidity ✓ Light 	<ul style="list-style-type: none"> ✓ Mobile technology ✓ Wi-Fi 	<ul style="list-style-type: none"> ✓ Improve the cultivation 	<ul style="list-style-type: none"> ✓ Limited lands. ✓ Water scarcity 	<ul style="list-style-type: none"> ✓ Smart aquaponic system to monitor and control cultivation 	<ul style="list-style-type: none"> ✓ Increase the manual response speed. 	<ul style="list-style-type: none"> ✓ Farming
53	Vaughan et al (2017) [53]	<ul style="list-style-type: none"> ✓ Livestock management. ✓ Farm management. 	<ul style="list-style-type: none"> ✓ Animal Weight 	<ul style="list-style-type: none"> ✓ Mobile technology 	<ul style="list-style-type: none"> ✓ Can monitor the performance of their animals. ✓ Improve the livestock production 	<ul style="list-style-type: none"> ✓ Weather condition ✓ Maintaining balance ✓ Large number of measurements. 	<ul style="list-style-type: none"> ✓ Gaining data under the hostile conditions of a livestock farm. 	<ul style="list-style-type: none"> ✓ Upstream and downstream the supply chain. 	<ul style="list-style-type: none"> ✓ Farming
54	Padalalu et al (2017) [54]	<ul style="list-style-type: none"> ✓ Water management 	<ul style="list-style-type: none"> ✓ Temperature ✓ Humidity ✓ Light ✓ CO2 ✓ Soil pH 	<ul style="list-style-type: none"> ✓ Mobile technology 	<ul style="list-style-type: none"> ✓ Conserve water ✓ Avoidance of constant vigilance. ✓ Remote automation 	<ul style="list-style-type: none"> ✓ Water scarcity ✓ High power consumption 	<ul style="list-style-type: none"> ✓ Implementing system to make the irrigation system smart, autonomous and efficient 	<ul style="list-style-type: none"> ✓ Estimate the irrigation cost. ✓ Introducing wireless sensor. ✓ Automatic watering 	<ul style="list-style-type: none"> ✓ Agriculture
55	Bellini et al (2017) [55]	<ul style="list-style-type: none"> ✓ Cattle detection management 	<ul style="list-style-type: none"> ✓ Temperature ✓ Milk consumption 	<ul style="list-style-type: none"> ✓ LoRa 	<ul style="list-style-type: none"> ✓ Increase milk production 	<ul style="list-style-type: none"> ✓ Heat detection ✓ Intensification management techniques 	<ul style="list-style-type: none"> ✓ By collecting activity data for heat detection for the cattle. 	<ul style="list-style-type: none"> ✓ Developing power reduction systems. 	<ul style="list-style-type: none"> ✓ Farming
56	Cambra et al (2017) [56]	<ul style="list-style-type: none"> ✓ Energy management ✓ Water management 	<ul style="list-style-type: none"> ✓ Temperature ✓ Humidity 	<ul style="list-style-type: none"> ✓ WSN ✓ Mobile technology ✓ LoRa ✓ Zig Bee 	<ul style="list-style-type: none"> ✓ Energy efficiency ✓ Reduction in fertilizers in products ✓ Saving water 	<ul style="list-style-type: none"> ✓ Scalability ✓ Manageability 	<ul style="list-style-type: none"> ✓ Implement a smart communication system to monitor the agriculture 	<ul style="list-style-type: none"> ✓ Developing irrigation services system in the domain of agricultural decision systems 	<ul style="list-style-type: none"> ✓ Agriculture
57	Moon et al (2017) [57]	<ul style="list-style-type: none"> ✓ Smart farming 	<ul style="list-style-type: none"> ✓ Temperature ✓ Humidity ✓ Rain fall ✓ Wind speed 	<ul style="list-style-type: none"> ✓ Wi-Fi 	<ul style="list-style-type: none"> ✓ Improve crop yield. ✓ Reduce unnecessary 	<ul style="list-style-type: none"> ✓ Managing big data 	<ul style="list-style-type: none"> ✓ Applying lossy compression on IoT big data. 	<ul style="list-style-type: none"> ✓ Use lossy compression techniques 	<ul style="list-style-type: none"> ✓ Farming

					costs.			✓ to reduce the high cost of data storage and transit	
58	Raghudathesh et al (2017) [58]	✓ Poultry management	✓ Temperature ✓ Humidity ✓ Light intensity ✓ Air quality	✓ Raspberry pi ✓ Wi-Fi	✓ Increases poultry production. ✓ optimizes resource utilization. ✓ Saves time ✓ Reduces human intervention	✓ High cost ✓ Maintenance of labour ✓ Wrong knowledge in farming practices.	✓ Develop a poultry management system using low cost commodity hardware and open source software	✓ Making wireless communication between sensor module and coordinator	✓ Farming
59	Maina (2017) [59]	✓ Livestock management ✓ Smart farming	✓ Temperature ✓ Size of the cattle ✓ Activity of the cow	✓ RFID ✓ Raspberry pi	✓ Improve productivity ✓ Can effectively detect heat	✓ Heat detection ✓ Death of livestock	✓ Use prototype sensor to detect the activity of cow.	✓ Improving the system capability to detecting cow activity in real time	✓ Farming
60	Memon et al (2016) [60]	✓ Water management ✓ Waste management	✓ Temperature ✓ Humidity	✓ Wi-Fi ✓ LAN	✓ Provide required feed and water. ✓ Exhaust the excess of biogas of animals ✓ Surveillance of the entire farm	✓ Stock theft	✓ Develop a system to control and monitor the farm remotely	✓ Improve the features of the smart system	✓ Agriculture

IV. DISCUSSION

In this review we have identified important attributes to analyse the research findings in agriculture and farming processes. We have gathered and analyzed data by using 60 recent scientific articles. Our survey shows the most researched sub-verticals are water management, crop management and smart farming. Water management is the most researched sub-vertical for the last few years as most countries mainly focus on the utilization of water resources due to its lack of abundance [61]. Irrigation patterns in agriculture influence crop production making irrigation management a central focus to increase productivity [8], [10]. The second most considered sub-vertical is crop management due to the importance of producing food for a growing global population. It is important to manage the quality, quantity and effectiveness of the agricultural production for sustainability [13]. Although a study [18] discussed that the widely used sensor data collections for measurements are soil conditions as pH and humidity, as per our analysis it shows environmental temperature followed by humidity and soil moisture are the most commonly measured data.

IoT can further be defined as a fusion of heterogeneous networks including chip technology that scopes gradually more and more, expanding due to the rapid growth of Internet applications such as logistics, agriculture, smart community, intelligent transposition, control and tracking systems. According to researchers' analysis, in 2020 IoT objects will be semi-intelligent and an important part of human social life [46]. As analyzed in our review Wi-Fi, mobile technology are the technologies which have a wide range of demand in agriculture and farming domain to monitor land and water resources in contrast to other technologies [33], [35].

Although our results demonstrate the results in such a way, a study [62] analyzed that use of RFID, a Wireless Sensor Network (WSN) technology that can be effectively used to increase the crop production to meet the growing needs of the increasing population. In developing countries with limited Internet speed, the other IoT technologies utilised rather than Wi-Fi include Low-Power, Short-Range IoT Networks, low-rate wireless PAN (LoRaWAN) or Low-Power and Wide-Area Networks.

Further research [61] shows that WSN is used in many applications such as health monitoring, agriculture, environmental monitoring, and military applications whereas our study demonstrates the agriculture sector using IoT in and farming sector using IoT. Our observations show that Agriculture is the primary source of income in developing countries, such as India with the sizeable geographical area when comparing with other countries [9].

Most of the research studies have performed on water management by monitoring such environmental parameters as temperature, humidity and soil moisture [1], [3], [5], [19], [25]. Many of the findings have focused on better water utilization, reduction inhuman intervention and the cost of production [18], [27]. Future research could draw more attention to further automate current processes in waste management, smart lightening and pest controlling sub-verticals by reducing existing drawbacks since it has received the least research attention in the considered period. Fog computing, as an innovation with cross over any barrier between remote data centres and IoT devices, should be considered in future IoT analysis [63], [64], [65], [66], [67]. While IoT has solved many issues related to agriculture and farming there are limitations that we need to consider. Lack of

interoperability and compatibility in devices, network flexibility issues when more devices are connecting, and sensor lifetime is some of the limitations to be addressed in future research.

This study has found that industry 4.0 in agriculture focuses on IoT aspects transforming the production capabilities including the agricultural domain. This study has [68] considered soil quality, irrigation levels, weather, the presence of insects and pests as sensor data. Some of the significant aspects they have been researched are the driver’s assistance to optimise routes and shorten harvesting and crop treatment while reducing fuel consumption CISCO [69]. Producing enough food for the entire world is a big challenge since the global population is rapidly changing as well as climate change and labour shortage. Currently researchers have focused more on robotics to address these problems. A growing number of researchers and companies have focused on Robotics and Artificial Intelligence (AI) to weeding by reducing the amount of herbicide used by farmers.

In contrast to edge computing, cloud computing requires a high-speed internet connection with sending and retrieving data from the cloud. As the process involves transferring and receiving data from the cloud, the process is time-consuming. Since the data capacity is higher than bandwidth, it is always essential to process data locally instead of sending data to the cloud. Edge computing is more efficient than cloud processing when processing data since the capacity doubles faster than the bandwidth doubles [70]. Since IoT uses sensor data collection for decision making, to process collected data, the cloud, or the edge based can be used on the system requirements.

Still, there are some challenges associated with IoT system deployment. Connecting so many devices to the IoT network is the biggest challenge in the future following lack of

technical knowledge among farmers, current centralised architecture to support IoT systems is not much advanced as the growth of the network, centralised systems will turn into a bottleneck. Moreover, sensor battery capacity and lifetime and sensor data storage also more concentrated when IoT system deployment. Smart farming is the association with new advancements in technologies and the different crop and livestock, agriculture and farming in the digital age. Smart farming can deliver agriculture more beneficial for the farmer. This is because decreasing input resources will save farmers' money and labour, and hence, will increase reliability [71] and business outcome [72], [73].

Furthermore, studying diverse approaches for fog computing structure [63], decision making using prediction or pattern analysis [74], [75], [76], big data databases [77] could be an exciting way to make the Internet of Things (IoT) into the future dominating technology.

This survey will fill the gap by the identification of the different IoT sub-verticals and data collections for the measurements in the agriculture and farming process. Results are clearly showing that most considered sub-verticals and data collections for measurements in the field of agriculture and farming. Our study also indicates the technologies used for IoT application development in the reviewed period. To summarise this survey, this has broader knowledge about IoT applications developed for automating the agriculture and farming process. Moreover, this study identifies most considered sub-verticals, collected sensor data and technologies for the development of IoT based applications in agriculture and farming sector towards the significant improvement of the business.

Table II shows the other necessary data collection criteria which were not included in all studies.

TABLE II. IMPORTANT DATA INCLUSION CRITERIA FOR FUTURE IoT STUDIES

Criteria	Information to be Collected in IoT Domain	Addressed in this Review	To be Addressed in Future Research
IoT Sub Verticals	What are the sub-areas addressed?	✓	✓
Measures (Data Collection)	What sort of sensor data collected for measurements?	✓	✓
Technologies Used	Used technologies to develop or to solve problems.	✓	✓
Benefits of Proposed System	Advantages of having the system to address existing issues.	✓	✓
Challenges in Current Approach	Existing issues and problems in the current systems and methods.	✓	✓
Solution for Current Issues	Proposed solution to solve the issues in the current problems.	✓	✓
Drivers of IoT Countries	What are the novelty and future aspects of the proposed systems and methods?	✓	✓
IoT systems' Scalability	Number of sensors are deployed, a variety of sensors, amount of data collection (volume), speed (velocity) of data collection (days-hours, hours-minutes, seconds-microseconds)	x	✓
Heterogeneity Aspects	Are sensors and underlying technologies uniform or heterogeneous in the system?	x	✓

System Architecture	Complex is the adopted IoT architecture, sensors topology, information about intermediate gateways	x	✓
Data Analysis Methods	Business intelligence, Artificial Intelligence, learning algorithms (machine Learning algorithms, Deep learning), big data technologies (Hadoop, Spark) and other protocols	x	✓
Observed System	Size or scale of the observed land or agricultural domain	x	✓
Access to Natural resources	Water resources and weather condition	x	✓
IoT Security and Threat Solutions / Protocols	Encryption techniques for IoT data access, Vulnerable identity (change default passwords), self-error detection and possible cyber attacks	x	✓
Operational Technology	Control and automation hardware, controllers, sensors and actuators	x	✓
Data Storage and Cloud Platform	Public Cloud, Private Cloud, Hybrid Cloud, Cloud (data at rest and centralized data center), Fog (data in motion and distributed data center) or Edge computing	x	✓
Power Supplies	Battery, AC power, and other protocol to optimize energy savings	x	✓

V. CONCLUSION

From our observations from the 60 peer-reviewed publications (2016–2018) in discussing the potential applications of the Internet of Things, it was found that water management is the highest considered IoT sub-vertical followed by crop management, smart farming, livestock management, and irrigation management with the same percentage. As per the observation, the most critical sensor data collection for the measurement is environmental temperature, environmental humidity and also there are some other such sensor data also gathered for IoT applications as soil moisture and soil pH. Wi-Fi has the highest demand of usage in agriculture and farming industry, followed by mobile technology. Other technologies as ZigBee, RFID, Raspberry pi, WSN, Bluetooth, LoRa and GPRS have less demand in the agriculture and farming sectors. When compared to the agricultural sector, farming industry has a lesser percentage amount using IoT for the automation. This survey could be useful for researchers for finding new ways and solution to challenge in the current agricultural era and for agricultural and farming industries to make the automation process more effective and efficient, consequently, to obtain the good businesses outcome.

AUTHORS' PROFILE

R.M., S.W., and M.N.H. conceived the study idea and developed the analysis plan. R.M. and S.W. analyzed the data and wrote the initial paper.

M.N.H. helped to prepare the figures and tables and finalizing the manuscript. R.M. completed the final editing and figures of the manuscript. All authors read the manuscript.

REFERENCES

[1] R. Venkatesan and A. Tamilvanan, "A sustainable agricultural system using IoT," in International Conference on Communication and Signal Processing (ICCSP), 2017.

[2] G. Arvind and V. Athira and H. Haripriya and R. Rani and S. Aravind, "Automated irrigation with advanced seed germination and pest control," in IEEE Technological Innovations in ICT for Agriculture and Rural Development (TIAR), 2017.

[3] W. Zhao and S. Lin and J. Han and R. Xu and L. Hou, "Design and Implementation of Smart Irrigation System Based on LoRa," in IEEE Globecom Workshops (GC Wkshps), 2017.

[4] S. Sagar and G. Kumar and L. Xavier and S. Sivakumar and R. Durai, "Smart irrigation system with flood avoidance technique," in Third International Conference on Science Technology Engineering & Management (ICONSTEM), 2017.

[5] S. Saraf and D. Gawali, "IoT based smart irrigation monitoring and controlling system," in 2nd IEEE International Conference on Recent Trends in Electronics, Information & Communication Technology (RTEICT), 2017.

[6] Rama Chidambaram RM and Vikas Upadhyaya, "Automation in drip irrigation using IOT devices," in Fourth International Conference on Image Information Processing (ICIIP), 2017.

[7] S. Vaishali and S. Suraj and G. Vignesh and S. Dhivya and S. Udhayakumar, "Mobile integrated smart irrigation management and monitoring system using IOT," in International Conference on Communication and Signal Processing (ICCSP), 2017.

[8] M. Rajkumar and S. Abinaya and V. Kumar, "Intelligent irrigation system—An IOT based approach," in International Conference on Innovations in Green Energy and Healthcare Technologies (IGEHT), 2017.

[9] A. Rau and J. Sankar and A. Mohan and D. Das Krishna and J. Mathew, "IoT based smart irrigation system and nutrient detection with disease analysis," in IEEE Region 10 Symposium (TENSymp), 2017.

[10] Sanket Salvi and Pramod Jain S.A and Sanjay H.A and Harshita T.K and M. Farhana and Naveen Jain and Suhas M V, "Cloud based data analysis and monitoring of smart multi-level irrigation system using IoT," in International Conference on I-SMAC (IoT in Social, Mobile, Analytics and Cloud) (I-SMAC), 2017.

[11] P. Surephong and P. Wiangnak and S. Wicha, "The comparison of soil sensors for integrated creation of IOT-based Wetting front detector (WFD) with an efficient irrigation system to support precision farming," in International Conference on Digital Arts, Media and Technology (ICDAMT), 2017.

[12] S. Rajeswari and K. Suthendran and K. Rajakumar, "A smart agricultural model by integrating IoT, mobile and cloud-based big data

- analytics," in International Conference on Intelligent Computing and Control (I2C2), 2017.
- [13] P. Patil and V. Sachapara, "Providing smart agricultural solutions/techniques by using Iot based toolkit," in International Conference on Trends in Electronics and Informatics (ICETI), 2017.
- [14] S. Pooja and D. Uday and U. Nagesh and S. Talekar, "Application of MQTT protocol for real time weather monitoring and precision farming," in International Conference on Electrical, Electronics, Communication, Computer, and Optimization Techniques (ICECCOT), 2017.
- [15] O. Pandithurai and S. Aishwarya and B. Aparna and K. Kavitha, "Agrotech: A digital model for monitoring soil and crops using internet of things (IOT)," in Third International Conference on Science Technology Engineering & Management (ICONSTEM), 2017.
- [16] A. Roselin and A. Jawahar, "Smart agro system using wireless sensor networks," in International Conference on Intelligent Computing and Control Systems (ICICCS), 2017.
- [17] P. Rekha and V. Rangan and M. Ramesh and K. Nibi, "High yield groundnut agronomy: An IoT based precision farming framework," in IEEE Global Humanitarian Technology Conference (GHTC), 2017.
- [18] R. Maia and I. Netto and A. Tran, "Precision agriculture using remote monitoring systems in Brazil," in IEEE Global Humanitarian Technology Conference (GHTC), 2017.
- [19] Z. Ahmad and M. Pasha and A. Ahmad and A. Muhammad and S. Masud and M. Schappacher and A. Sikora, "Performance evaluation of IEEE 802.15.4-compliant smart water meters for automating large-scale waterways," in 9th IEEE International Conference on Intelligent Data Acquisition and Advanced Computing Systems: Technology and Applications (IDAACS), 2017.
- [20] M. Mekala and P. Viswanathan, "A novel technology for smart agriculture based on IoT with cloud computing," in International Conference on I-SMAC (IoT in Social, Mobile, Analytics and Cloud) (I-SMAC), 2017.
- [21] D. Qi and G. Lu and X. Dai, "Design of Urban Greening Intelligent Monitoring System Based on Internet of Things Technology," in 9th International Conference on Intelligent Human-Machine Systems and Cybernetics (IHMSC), 2017.
- [22] Z. Li and J. Wang and R. Higgs and L. Zhou and W. Yuan, "Design of an Intelligent Management System for Agricultural Greenhouses Based on the Internet of Things," in IEEE International Conference on Computational Science and Engineering (CSE) and IEEE International Conference on Embedded and Ubiquitous Computing (EUC), 2017.
- [23] C. Cambra and S. Sendra and J. Lloret and L. Garcia, "An IoT service-oriented system for agriculture monitoring," in IEEE International Conference on Communications (ICC), 2017.
- [24] N. Ananthi and J. Divya and M. Divya and V. Janani, "IoT based smart soil monitoring system for agricultural production," in IEEE Technological Innovations in ICT for Agriculture and Rural Development (TIAR), 2017.
- [25] S. Prathibha and A. Hongal and M. Jyothi, "IOT Based Monitoring System in Smart Agriculture," in International Conference on Recent Advances in Electronics and Communication Technology (ICRAECT), 2017.
- [26] P. Padalalu and S. Mahajan and K. Dabir and S. Mitkar and D. Javale, "Smart water dripping system for agriculture/farming," in 2nd International Conference for Convergence in Technology (I2CT), 2017.
- [27] J. Guruprasadh and A. Harshananda and I. Keerthana and Rachana and K. Krishnan and M. Rangarajan and S. Sathyadevan, "Intelligent soil quality monitoring system for judicious irrigation," in International Conference on Advances in Computing, Communications and Informatics (ICACCI), 2017.
- [28] S. Athani and C. Tejeshwar and M. Patil and P. Patil and R. Kulkarni, "Soil moisture monitoring using IoT enabled arduino sensors with neural networks for improving soil management for farmers and predict seasonal rainfall for planning future harvest in North Karnataka—India," in International Conference on I-SMAC (IoT in Social, Mobile, Analytics and Cloud) (I-SMAC), 2017.
- [29] P. Rajalakshmi and S. Devi Mahalakshmi, "IOT based crop-field monitoring and irrigation automation," in 10th International Conference on Intelligent Systems and Control (ISCO), 2016.
- [30] A. Intej and T. Rahman and M. Hossain and S. Zaman, "IoT based autonomous percipient irrigation system using raspberry Pi," in 19th International Conference on Computer and Information Technology (ICCIT), 2016.
- [31] H. Biradar and L. Shabadi, "Review on IOT based multidisciplinary models for smart farming," in 2nd IEEE International Conference on Recent Trends in Electronics, Information & Communication Technology (RTEICT), 2017.
- [32] M. bin Ismail and N. Thamrin, "IoT implementation for indoor vertical farming watering system," in International Conference on Electrical, Electronics and System Engineering (ICEESE), 2017.
- [33] Amandeep and A. Bhattacharjee and P. Das and D. Basu and S. Roy and S. Ghosh and S. Saha and S. Pain and S. Dey and T. Rana, "Smart farming using IOT", 2017 8th IEEE Annual Information Technology, in Electronics and Mobile Communication Conference (IEMCON), 2017.
- [34] R. Dolci, "IoT Solutions for Precision Farming and Food Manufacturing: Artificial Intelligence Applications in Digital Food," in IEEE 41st Annual Computer Software and Applications Conference (COMPSAC), 2017.
- [35] V. Gokul and S. Tadepalli, "Implementation of smart infrastructure and noninvasive wearable for real time tracking and early identification of diseases in cattle farming using IoT," in International Conference on I-SMAC (IoT in Social, Mobile, Analytics and Cloud) (I-SMAC), 2017.
- [36] C. Yoon and M. Huh and S. Kang and J. Park and C. Lee, "Implement smart farm with IoT technology," in 20th International Conference on Advanced Communication Technology (ICACT), 2018.
- [37] M. Rajkumar and S. Abinaya and V. Kumar, "Intelligent irrigation system—An IOT based approach," in International Conference on Innovations in Green Energy and Healthcare Technologies (IGEHT), 2017.
- [38] S. Ruengittinun and S. Phongsamsuan and P. Sureeratanakorn, "Applied internet of thing for smart hydroponic farming ecosystem (HFE)," in 10th International Conference on Ubi-media Computing and Workshops (Ubi-Media), 2017.
- [39] A. Ezhilazhahi and P. Bhuvanewari, "IoT enabled plant soil moisture monitoring using wireless sensor networks," in Third International Conference on Sensing, Signal Processing and Security (ICSSS), 2017.
- [40] C. Yoon and M. Huh and S. Kang and J. Park and C. Lee, "Implement smart farm with IoT technology," in 20th International Conference on Advanced Communication Technology (ICACT), 2018.
- [41] S. Takekar and S. Takekar, "Plant and taste to reap with Internet of Things implementation of IoT in agriculture to make it a parallel industry," in International Conference on I-SMAC (IoT in Social, Mobile, Analytics and Cloud) (I-SMAC), 2017.
- [42] P. Tanmayee, "Rice crop monitoring system—A lot based machine vision approach," in International Conference on Nextgen Electronic Technologies: Silicon to Software (ICNETS2), 2017.
- [43] A. Moon and J. Kim and J. Zhang and S. Son, "Lossy compression on IoT big data by exploiting spatiotemporal correlation," in IEEE High Performance Extreme Computing Conference (HPEC), 2017.
- [44] Z. Li and J. Wang and R. Higgs and L. Zhou and W. Yuan, "Design of an Intelligent Management System for Agricultural Greenhouses Based on the Internet of Things," in IEEE International Conference on Computational Science and Engineering (CSE) and IEEE International Conference on Embedded and Ubiquitous Computing (EUC), 2017.
- [45] D. Sreekantha and Kavya A.M., "Agricultural crop monitoring using IOT - a study," in 11th International Conference on Intelligent Systems and Control (ISCO), 2017.
- [46] S. Rajendrakumar and Rajashekarappa and V. Parvati and B. Parameshachari and K. Soyjaudah and R. Banu, "An intelligent report generator for efficient farming," in International Conference on Electrical, Electronics, Communication, Computer, and Optimization Techniques (ICECCOT), 2017.

- [47] P. Padalalu and S. Mahajan and K. Dabir and S. Mitkar and D. Javale, "Smart water dripping system for agriculture/farming," in 2nd International Conference for Convergence in Technology (I2CT), 2017.
- [48] D. Ferreira and P. Corista and J. Giao and S. Ghimire and J. Sarraipa and R. Jardim-Goncalves, "Towards smart agriculture using FIWARE enablers," in International Conference on Engineering, Technology and Innovation (ICE/ITMC), 2017.
- [49] T. Okayasu and A. Nugroho and A. Sakai and D. Arita and T. Yoshinaga and R. Taniguchi and M. Horimoto and E. Inoue and Y. Hirai and M. Mitsuoka, "Affordable field environmental monitoring and plant growth measurement system for smart agriculture," in Eleventh International Conference on Sensing Technology (ICST), 2017.
- [50] B. Bellini and A. Amaud, "A 5μ? wireless platform for cattle heat detection," in IEEE 8th Latin American Symposium on Circuits & Systems (LASCAS), 2017.
- [51] C. Cambra and S. Sendra and J. Lloret and L. Garcia, "An IoT service-oriented system for agriculture monitoring," in IEEE International Conference on Communications (ICC), 2017.
- [52] J. Vaughan and P. Green and M. Salter and B. Grieve and K. Ozanyan, "Floor sensors of animal weight and gait for precision livestock farming," in IEEE SENSORS, 2017.
- [53] W. Vernandhes and N. Salahuddin and A. Kowanda and S. Sari, "Smart aquaponic with monitoring and control system based on iot," in Second International Conference on Informatics and Computing (ICIC), 2017.
- [54] G. Raghudathesh and D. Deepak and G. Prasad and A. Arun and R. Balekai and V. Yatnalli and S. Lata and B. Kumar, "Iot based intelligent poultry management system using Linux embedded system," in International Conference on Advances in Computing, Communications and Informatics (ICACCI), 2017.
- [55] C. wa Maina, "IoT at the grassroots—Exploring the use of sensors for livestock monitoring," in IST-Africa Week Conference (IST-Africa), 2017.
- [56] K. Krishna and O. Silver and W. Malende and K. Anuradha, "Internet of Things application for implementation of smart agriculture system," in International Conference on I-SMAC (IoT in Social, Mobile, Analytics and Cloud) (I-SMAC), 2017.
- [57] M. Hunain Memon, "Internet of Things (IoT) Enabled Smart Animal Farm," in Computing for Sustainable Global Development (INDIACom), 2016 3rd International Conference, 2016.
- [58] G. Suci and O. Fratu and A. Vulpe and C. Butca and V. Suci, "IoT agro-meteorology for viticulture disease warning," in IEEE International Black Sea Conference on Communications and Networking (BlackSeaCom), 2016.
- [59] N. Putjaika and S. Phusae and A. Chen-Im and P. Phunchongharn and K. Akkarajitsakul, "A control system in an intelligent farming by using arduino technology," in Fifth ICT International Student Project Conference (ICT-ISPC), 2016.
- [60] S. Prathibha and A. Hongal and M. Jyothi, "IOT Based Monitoring System in Smart Agriculture," in International Conference on Recent Advances in Electronics and Communication Technology (ICRAECT), 2017.
- [61] Rekha B Venkatapur and S Nikitha, "Review on Closed Loop Automated Irrigation System," The Asian Review of Civil Engineering, vol. 6, pp. 9-14, 2017.
- [62] K. Bidua and C. Patel, "Internet of Things and Cloud Computing for Agriculture in India," International Journal of Innovative and Emerging Research in Engineering, vol. 2, pp. 27-30, 2015.
- [63] B. N. B. Ekanayake and M. N. Halgamuge and A. Syed, "Review: Security and Privacy Issues of Fog Computing for the Internet of Things (IoT)," Lecture Notes on Data Engineering and Communications Technologies Cognitive Computing for Big Data Systems Over IoT, Frameworks, Tools and Applications, Springer, vol. 14, p. Chapter 7, 2018.
- [64] J. Gubbi and R. Buyya and S. Marusic and M Palaniswami, "Internet of Things (IoT): A vision, architectural elements, and future directions," Future Generation Computer Systems, vol. 29, no. 7, pp. 1645-1660, 2013.
- [65] Ashkan Yousefpour and Genya Ishigaki and Riti Gour and Jason P. Jue, "On Reducing IoT Service Delay via Fog Offloading," IEEE Internet of Things Journal, Vols. 998 - 1010, no. 2, p. 5, 2018.
- [66] Shigen Shen and Longjun Huang and Haiping Zhou and Shui Yu and En Fan and Qiying Cao, "Multistage Signaling Game-Based Optimal Detection Strategies for Suppressing Malware Diffusion in Fog-Cloud-Based IoT Networks," IEEE Internet of Things Journal, vol. 5, no. 2, pp. 1043 - 1054, 2018.
- [67] Shuang Zhao and Yang Yang and Ziyu Shao and Xiumei Yang and Hua Qian and Cheng-Xiang Wang, "FEMOS: Fog-Enabled Multitier Operations Scheduling in Dynamic Wireless Networks," IEEE Internet of Things Journal, vol. 5, no. 2, pp. 1169 - 1183, 2018.
- [68] [Online]. Available: <https://ec.europa.eu/growth/tools-databases/dem/monitor/content/industry-40-agriculture-focus-iot-aspects>.
- [69] [Online]. Available: <https://newsroom.cisco.com/feature-content?type=webcontent&articleId=1870277>.
- [70] K. Dolui and S. K. Datta, "Comparison of edge computing implementations: Fog computing, cloudlet and mobile edge computing," Global Internet of Things Summit (GloITS), 2017.
- [71] A. Walter and R. Finger and R. Huber and N. Buchmanna, "Opinion: Smart farming is key to developing sustainable agriculture," Proc Natl Acad Science, vol. 114, p. 6148-6150, 2017.
- [72] E. Hakanen, R. Rajala, "Material intelligence as a driver for value creation in IoT-enabled business ecosystems", Journal of Business & Industrial Marketing, September 2018.
- [73] T. Osmonbekov, W. J. Johnston, "Adoption of the Internet of Things technologies in business procurement: impact on organizational buying behavior", Journal of Business & Industrial Marketing, September 2018.
- [74] A. Gupta, A. Mohammad, A. Syed, and M. N. Halgamuge, "A Comparative Study of Classification Algorithms using Data Mining: Crime and Accidents in Denver City the USA", International Journal of Advanced Computer Science and Applications (IJACSA), Volume 7, Issue 7, pp 374 - 381, August 2016.
- [75] C. Wanigasooriya, M. N. Halgamuge, A. Mohamad, "The Analyzes of Anticancer Drug Sensitivity of Lung Cancer Cell Lines by Using Machine Learning Clustering Techniques", International Journal of Advanced Computer Science and Applications (IJACSA), Volume 8, No 9, September 2017.
- [76] A. Singh, M. N. Halgamuge, R. Lakshmiathan, "Impact of Different Data Types on Classifier Performance of Random Forest, Naïve Bayes, and k-Nearest Neighbors Algorithms", International Journal of Advanced Computer Science and Applications (IJACSA), Volume 8, No 12, pp 1-10, December 2017.
- [77] V. Vargas, A. Syed, A. Mohammad, and M. N. Halgamuge, "Pentaho and Jaspersoft: A Comparative Study of Business Intelligence Open Source Tools Processing Big Data to Evaluate Performances", International Journal of Advanced Computer Science and Applications (IJACSA), Volume 7, Issue 10, pp 20-29, November 2016.

e-Learning Tools on the Healthcare Professional Social Networks

Evgeny Nikulchev¹, Dmitry Ilin², Bladimir Belov³
MIREA–Russian Technological University
Moscow, Russia

Pavel Kolyasnikov⁴
Russian Academy of Education
Moscow, Russia

Alexander Kosenkov⁵
Sechenov First Moscow State Medical University
Moscow, Russia

Abstract—According to many studies, professional social networks are not widespread in the health care environment, especially doctors. The article is devoted to two advanced digital tools that can attract the image and increase motivation for professional social networks. The first tool is the inclusion of e-learning, both to increase the level of knowledge and to confirm qualification skills among professionals. The second tool is the developed system of the formation of the tests constructor. The article describes solution of being developed Internet-resources for mass use in professional health care.

Keywords—Healthcare professional social networks; advanced digital tools; e-learning; test constructor; e-learning

I. INTRODUCTION

According to many researches, professional social networks are not widely disseminated in the health care environment [1]. One of the reasons for this seems to be the lack of special advanced digital tools [2, 3] used in the practice of health protection and professional skills training.

There are established trends in the use of social networks. The most widely groups using them are nurses and medical students [4], while doctors are the least likely professional group that use social networks. The reasons for this seem to be inherent in the dichotomies of social technologies nature and the established patterns of doctor's decision-making [5]: it is argued that social technologies are built in accordance with the ideas of egalitarianism, weak ties, co-production and voluntary exchange with the intention of “encouraging a maximum of contributors and of getting the best number of contributions”. However, in the professional field, it is necessary to attract not only idly interested, but specific specialists with certain skills and qualifications [6].

One of the common forms of the social networks use on an equal footing with job search is the increasing education level [7]. The inclusion of educational content into professional social networks can be attractive [8, 9]. In addition, the presence of a certificate and training in a particular network makes the rest of the communication participants a sign of a professional standard, while now the skills are introduced quite arbitrarily [10], confirmed at best by other network participants, like it is in ResearchGate.

There is a wide range of health care professional social networks (HPSN) that are specifically designed for health care providers and the domain of health care. The article [11] shows a significant list of existing health-related HPSN. For the analysis and presentation of commonality and differences between HPSN the common and domain-specific functions can be identified. Common features mean a cohesive set of functionality that can be found in any form of HPSN, such as a personal profile, board, news board, chats, photo and video exchange, documents exchange (articles, presentations, reposts). Domain-specific functions are a set of functionalities that are specifically designed or might be of interest for health care professionals [2, 12], such as a library of medical records or specialized workplaces for medical institutions [13]. In addition to some functional differences, the HPSN is also very different in terms of volume, access, and target groups of users. Although some platforms are open to health care workers around the world, some platforms restrict their access [14]. Some systems give an access to health a specific occupational group. Interprofessional and inter-generational collaboration and knowledge sharing can vary greatly between different HPSN.

Thus, the specificity of the HPSN is to use motivational mechanisms [15, 16] to attract users. It requires the development of reliable digital professional tools necessary for the practice.

The article describes solution of being developed Internet-resources for mass use in professional health care. These are e-learning system. The tool is including e-learning to Internet-resources both for increasing the level of knowledge and confirming professional skills.

The paper consists of two sections, introduction and conclusions. Section II presents the results of developing a learning course for advanced training of cardiac surgeons, the course structure and the specifics of course creation. The Section III describes the developed methodology of tests creation for assessing the course completion. Tests are created in form of the algorithmic description language, which also allows the automatic web interfaces generation, using any modern popular device or browser.

II. E-LEARNING TOOLS

The internal structure of social networks implies that each user of the network can choose the communication topics [17]. It means that there is no clear regulation or control over the topics [18] This is fundamentally contrary to the tasks of creating a professional communication service aimed at the professional and career development of medical specialists in accordance with the standards of their professional activities [19]. It is required to create a tool that allows specialists to improve their professional level, to form new skills and a system of encouragement for the career development of physicians, which would allow to create professional education in professional social networks. In the development process, a number of technological solutions were used [20, 21], in particular, for creating video lectures and recording operations.

To achieve the objectives and to answer the questions raised, following methods were used:

- questioning of physicians of different specialties (815 physicians) on the need and prospects of professional communication services in competence enhancing, career development and their participation in this service;
- questioning of medical specialists of different specialties (342 physicians) on the proper proportion of communication regulation in the professional communication process;
- theoretical research and enhancing the experience of the participation in a number of foreign and domestic social networks for common use;
- theoretical research and enhancing the experience of the participation in social networks for professional use, including the most popular LinkedIn и Gate Research;
- exploring the opportunities of the most common foreign and domestic software for digital learning management.

Methodical work was carried out based on the Department of Hospital Surgery at Sechenov First Moscow State Medical University. Service finalization and initial introduction are carried out with the help of the students of the department.

Currently, the basic implementation principles of professional communication service are developed. Communication in the service are regulated and implemented under centralized control. The issue of themes creating and professional communication level setting was resolved. The accounting, analyses and generalization of users' actions are carried out. Verified user authorization is being worked out.

Management and moderation of every communication topic is carried out by its leader. The leader is one of the professors on the Department of Hospital Surgery at Sechenov First Moscow State Medical University. The topics choice is currently being carried out by the same Department.

The topics are isolated from each other according to the theme. At the beginning, users have to study theory with using

video-lecture and their fragments or reading. Users successfully studied the theory are allowed to complete tests. Tests are divided into two sections: question sets for every part of the topic and questions for the whole topic. After successful tests completion users can communicate with other users and the topic leader. They can ask some questions, share their experience or best practices. The overall sequence of the study and discussion is given on the example of the "Example of professional topic studying and discussing with the use of developed service" (Table I).

Examples of training system screens are shown in Fig. 1 and 2.

Service processes are implemented in Moodle, LMS open source software. So, its functional flexibility and additional features were used.

Methodical work was carried out based on the Department of Hospital Surgery at Sechenov First Moscow State Medical University. Service finalization and initial introduction are carried out with the help of the students of the department.

The material for service was collected with the help of well-organized and delivered video production (video lectures, their fragments, video records of surgical operations, etc.).

In our view, professional communication implemented in such form can be an effective tool for professional and career development of medical specialists, increasing their level of competence and enhancing their skills.

In the future, the service can be used for professional medical specialists' accreditation process that is used in different countries.

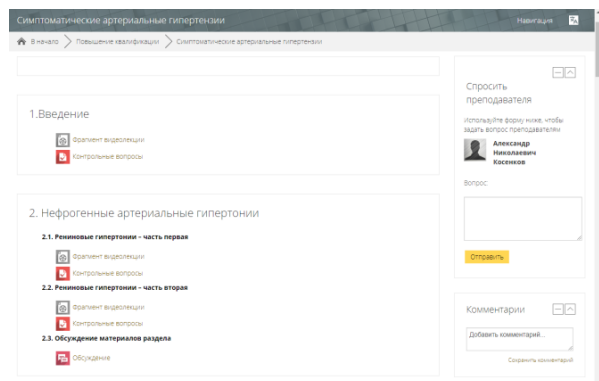


Fig. 1. Example of a Training Course.

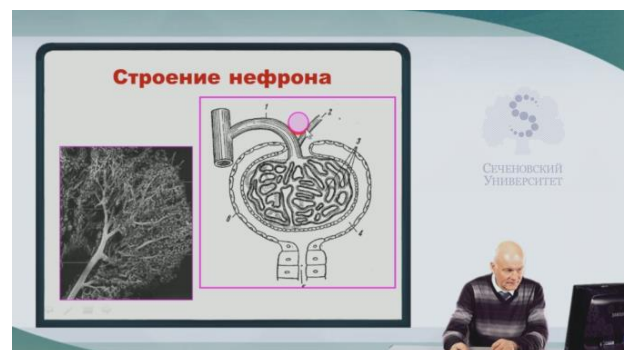


Fig. 2. Example of a Lecture.

TABLE I. EXAMPLE OF PROFESSIONAL TOPIC STUDYING AND DISCUSSING WITH THE USE OF DEVELOPED SERVICE

Topic number	Fragments for video viewing of theory	References on the topic	Testing by subtopics	Discussions under the subtopics	Integration testing on the topic	Integration discussion of the topic
1.	Introduction	* reference to the list of references on the topic	–	–	–	–
2.	renin hypertension – first part		* link to testing for subtopic «2»	* link to forum for subtopic «2»		
	renin hypertension – second part					
3.	Renovascular hypertension definition (RVHT)		* link to testing for subtopic «3»	* link to forum for subtopic «3»		
	RVHT diagnostics – first part					
	RVHT diagnostics – second part					
	RVHT treatment					
	RVHT clinical example					
4.	Neurogenic arterial hypertension, hypercapnia acidosis, exogenous arterial hypertension		* link to testing for subtopic «4»	* link to forum for subtopic «4»		
5.	Arterial hypertension in adrenal cortex tumor – first part		* link to testing for subtopic «5»	* link to forum for subtopic «5»		
	Arterial hypertension in adrenal cortex tumor – second part					
	Arterial hypertension in hyperthyroidism and hyperparathyroidism					
	Arterial hypertension in acromegalia					
6.	Arterial hypertension in insufficiency of aorta valve		* link to testing for subtopic «6»	* link to forum for subtopic «6»		
	Arterial hypertension in atherosclerosis and coarctation of aorta					
7.	Postsurgical arterial hypertension	–	–	* link to testing for the whole topic	* link to the topic-integrated forum	
	Diagnostic formulation					
	Summarizing					

III. TESTS CONSTRUCTOR

The digital approach to tests allows expanding the list of tools available to the learning.

The software implementation for the survey is a web-interface for each test questionnaire included in the methodology. At the same time, an important feature is the need for cross-platform operation of interfaces [22], providing the ability to conduct surveys on a wide range of devices, popular browsers and operating systems Windows, Linux, MacOS, iOS, Android. The report is devoted to the developed standard for describing the interface elements of polls and the corresponding generation technologies on various systems.

For the platform-independent implementation of the test-questionnaire, an internal standard for presenting the test in a

structured form has been developed. It allows using the structure to create a test interface based on previously created elements that have been developed and tested on various devices and operating systems. The presence of the standard makes it possible to develop an interactive designer of test questionnaires to automate the creation of new tests. The developed algorithmic standard for describing the elements includes general test settings (global settings) and consists of three main levels: test, block, and page.

Surveys can be viewed as a hierarchy consisting of three key levels:

- 1) *Test (Fig. 3).*
- 2) *Block (fig. 4).*
- 3) *Page (Fig. 5).*

The test (Fig. 3) is the root element of the hierarchy, consists of one or more blocks, and also has settings related to the entire test as a whole. These settings include, for example, the language of the interface elements.

A block (Fig. 4) is a structure that combines one or more pages that have common parameters. The need to introduce this level of hierarchy will be discussed further on the example of two methods. The parameters of the block, for example, include:

- 1) The number of items that will be displayed on one page (items per page). Using this parameter can make it easier to split a large list of questions into equal parts.
- 2) The order of displaying questions and elements of instructions (items order). There are two main options: fixed and random order.
- 3) Progress display(show progress bar) adjusts whether to show or not to show the percentage of questions in the test.
- 4) Timer display (show timer). It implies three options: no timer, stopwatch and countdown.
- 5) Time limit for passing the block (expected time). If the participant does not fit in the allotted time, it will be asked to proceed to the next block of questions.

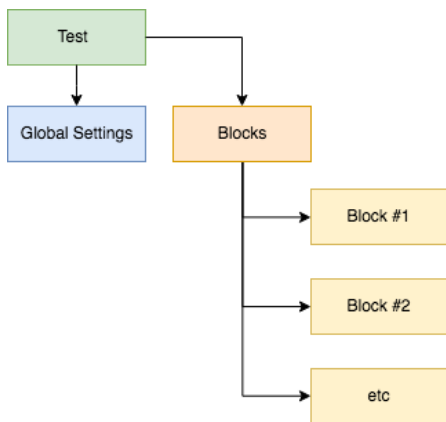


Fig. 3. Hierarchical Representation of the Test.

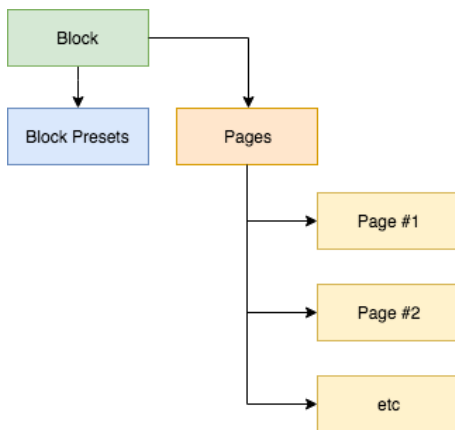


Fig. 4. Hierarchical Block Representation in Test.

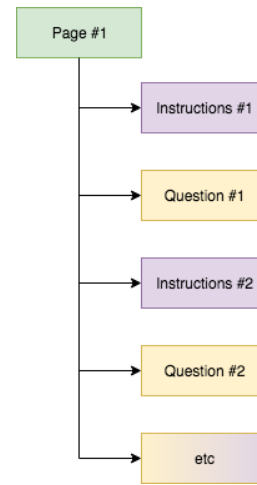


Fig. 5. Hierarchical Presentation of the Page in the Test Block.

A page (Fig. 5) is a collection of elements that directly represent the content of the survey. The page may contain elements of instructions and questions. The elements of the instruction include text blocks and media files presented to the participant.

The software implementation for the survey is a web-interface for each questionnaire included in the methodology. At the same time, it is worth to implement a cross-platform software [1] with providing the ability to conduct surveys on a wide range of devices, popular browsers and operating systems like Windows, Linux, MacOS, iOS, Android. The paper is devoted to the developed standard for describing the interface elements of surveys and the corresponding technologies of generation on different systems.

For the platform-independent implementation of the test-questionnaire, an internal standard for presenting the test in a structured form has been developed. It allows using the structure to create a test interface based on previously created elements that were developed and tested on different devices and operating systems. The standard makes it possible to develop an interactive designer of test questionnaires for creating new tests automatically.

The developed algorithmic standard for describing the elements includes general test settings (global settings) and consists of 3 levels: block, page and question (Fig. 3). Fig. 3 shows the upper level of the standard, which includes the general settings and blocks. The block is necessary to combine questions on their common behavior and display parameters. Each block includes one or more pages. The block structure is shown in Fig. 4. A page is a set of questions and instructions that are displayed together. A diagram of the general structure of the test-questionnaire page is shown in Fig. 5. The question is the basic unit of information that allows receiving and saving the result of the answer. Questions are divided into simple and composite. The answer to a simple question will be saved by a single unique key. A composite question implies more than one answer. Therefore, it will be saved by several different keys.

To carry out calculations based on the answers to questions during data collection, a problem-oriented language was developed. The language includes the following groups of functions:

- Logical functions (and, or, not).
- Comparison functions (equal, greater than, etc.)
- Higher-order functions (map, reduce, etc.)
- Mathematical functions (add, subtract, etc.)
- Functions for working with vectors (sum, size, etc.)
- Data getting functions (getAnswers, getScale, etc.)

According to the developed structure, tests-questionnaires are presented in form of a document with hierarchical links. To form the resulting structure, the JSON Schema solution [23] was chosen, which is the standard for describing the structure of JSON documents.

Fig. 6 shows an example of the questionnaire implementation. On the left, a section of the test structure in JSON Schema, and on the right, an automatically constructed interface based on the described structure is shown.

To solve the problem of correctly displaying interface elements on devices with different screen sizes and image formats, an approach is used that allows automatically adjusting the content to any screen width. This approach is called Responsive Web Design, it rebuilds the interface structure to any screen width due to the pre-written rules in HTML and CSS. A web page can even adapt to a new device with a non-standard resolution.

As a result, a technology was implemented that allows creating a cross-platform interface that works in most modern web browsers and on different types of devices. Fig. 7 shows an example of displaying a questionnaire on different devices: tablet's display is shown on the left side and Android smartphone with Google Chrome browser is on the right side.

The use of technology based on the generation of the interface in accordance with the standard structure of the test description simplifies the process of implementing changes to the interface, since any corrections will be valid for all developed elements.

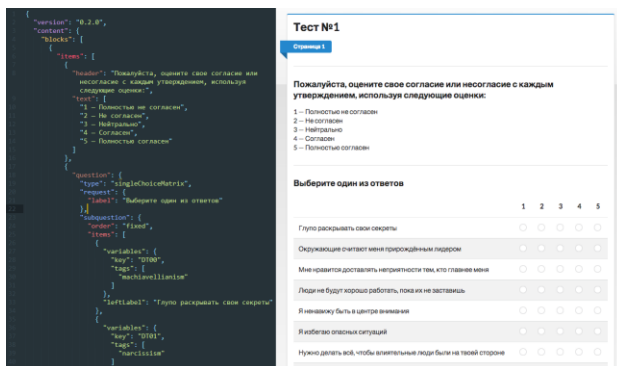


Fig. 6. Example of Test Implementation (on the Left - the Standard for the Elements Description, on the Right - the Generated Interface).

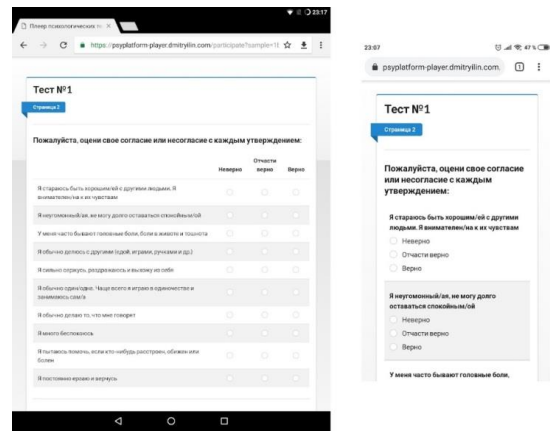


Fig. 7. Example of Respondents Questionnaires Interface Generating on Different Devices (Tablet is on the Left and Smartphone is on the Right).

IV. CONCLUSION

Based on the analysis of the specific functions of social networks in the field of health care, the following features were identified. When targeting the mass use of platforms, there are requirements to restrict access in accordance with professional specialization. This is due to the requirements of professional ethics [24] and rules of access to medical data [25], which makes communication difficult. Thus, although the purpose of portals is to collect and consolidate disparate data, but the motivation of each individual specialist must be high. For each user, the portal data is not fully available. Often there is information that is beyond the scope of scientific or professional interest. Simply filling any data to the system does not motivate specialists, especially in the context of limited communications that are typical for health care field. It needs to develop digital tools for increasing the level of competence and work automation of each user.

The paper presented two tools aimed at developing the motivation of medical specialists to use social networks. These tools include followings: e-learning services aimed at improving skills and increasing the status of proven skills of users of social networks, advanced tools for creating surveys in the field of health. The developed tools are aimed to be used in form of Web service and can be integrated into specialized online health systems. During the testing system developing, the algorithmic standard was developed for describing the interface elements of the questionnaires. This standard will allow to implement cross-platform visualization technology that can generate a Web interface in popular browsers and popular operating systems on different devices.

ACKNOWLEDGMENT

The work was financed by Russian Foundation for Basic Research: project 17-29-02198.

REFERENCES

- [1] R. Heeks, "Health information systems: Failure, success and improvisation", International Journal of Medical Informatics, vol. 75, no. 2, 2006, pp. 125-137.
- [2] D. R. Kaufman, J. Mirkovic & C. Chan, eHealth literacy as a mediator of health behaviors", In Cognitive Informatics in Health and Biomedicine (Springer, Cham), pp. 271-297.

- [3] T. J. Ma & D. Atkin, "User generated content and credibility evaluation of online health information: a meta analytic study", *Telematics and Informatics*, vol. 34, no. 5, 2017, pp. 472-486.
- [4] M. Carpentier, G. Van Hoye, S. Stockman, E. Schollaert, B. Van Theemsche & G. Jacobs, "Recruiting nurses through social media: Effects on employer brand and attractiveness", *Journal of Advanced Nursing*, vol. 73, no. 11, 2017, pp. 2696-2708.
- [5] G. Bruno, F. Dengler, B. Jennings, R. Khalaf, S. Nurcan,... & R. Silva, "Key challenges for enabling agile BPM with social software" *Journal of Software Maintenance and Evolution: Research and Practice*, vol. 23, no. 4, 2011, pp. 297-326.
- [6] Z. Hu, Z. Zhang, H. Yang, Q. Chen, & D. Zuo, "A deep learning approach for predicting the quality of online health expert question-answering services", *Journal of Biomedical Informatics*, vol. 71, 2017, pp. 241-253.
- [7] V. Neville, M. Lam, & C. J. Gordon, "The impact of elearning on health professional educators' attitudes to information and communication technology", *Journal of Multidisciplinary Healthcare*, vol. 8, 2015, pp. 75-81.
- [8] I. V. Osipov, A. A. Volinsky, E. Nikulchev, & A. Y. Prasikova, "Communication and Gamification in the Web-Based Foreign Language Educational System", *International Journal of Web-Based Learning and Teaching Technologies*, vol. 11, no. 4, 2016, pp. 22-34.
- [9] T. A. Demenkova, V. S. Tomashevskaya, & I. S. Shirinkin, "Mobile applications for tasks of distance learning", *Russian Technological Journal*, vol. 6, no. 1, 2018, pp. 5-19.
- [10] E. Nikulchev, D. Ilin, & E. Matishuk, "Scalable service for professional skills analysis based on the demand of the labor market and patent search", *Procedia Computer Science*, vol. 103, 2017, pp. 44-51.
- [11] T. Mettler, "Contextualizing a professional social network for health care: Experiences from an action design research study", *Information Systems Journal*, vol. 28, no. 4, 2018, pp. 684-707.
- [12] C. L. Ventola, "Mobile devices and apps for health care professionals: uses and benefits", *Pharmacy and Therapeutics*, vol. 39, no. 5, 2014, p. 356.
- [13] M. J. Dutta-Bergman, "The impact of completeness and web use motivation on the credibility of e-health information", *Journal of Communication*, vol. 54, no. 2, 2004, pp. 253-269.
- [14] R. S. Mano, "Social media and online health services: A health empowerment perspective to online health information", *Computers in Human Behavior*, vol. 39, 2014, pp. 404-412.
- [15] S. A. Rains, & C. D. Karmikel, "Health information-seeking and perceptions of website credibility: Examining Web-use orientation, message characteristics, and structural features of websites", *Computers in Human Behavior*, vol. 25, no. 2, 2009, pp. 544-553.
- [16] K. P. Hocevar, M. Metzger, & A. J. Flanagin, "Source Credibility, Expertise, and Trust in Health and Risk Messaging", In *Oxford Research Encyclopedia of Communication*, 2017.
- [17] M. Salehan, D. J. Kim, & C. Kim, "Use of online social networking services from a theoretical perspective of the motivation-participation-performance framework", *Journal of the Association for Information Systems*, vol. 18, no. 2, 2017, p. 141.
- [18] S. V. Rehm, L. Goel, & I. Junglas, "Information management for innovation networks—an empirical study on the "who, what and how" in networked innovation" *International Journal of Information Management*, vol. 36, no. 3, 2016, pp. 348-359.
- [19] M. Sprenger, A. Blondiau, P. Rohner, & T. Mettler, "Benefits of Professional Social Networks: Expectations and Design Implications for the Healthcare Domain", *Proceedings of the 17th International Symposium on Health Information Management Research — ISHIMR 2015*, (<https://www.alexandria.unisg.ch/241955/1/ATTCFPVC.pdf>).
- [20] A. A. Alkhatlan, & A. A. Al-Daraiseh, "An Analytical Study of the Use of Social Networks for Collaborative Learning in Higher Education", *International Journal of Modern Education and Computer Science*, vol. 9, no. 2, 2017, pp. 1-13.
- [21] S. Brownson, "Embedding social media tools in online learning courses", *Journal of Research in Innovative Teaching*, vol. 7, no. 1, 2014, pp. 112-118.
- [22] E. Nikulchev, D. Ilin, P. Kolyasnikov, V. Belov, I. Zakharov, & S. Malykh, "Programming technologies for the development of web-based platform for digital psychological tools", *International Journal of Advanced Computer Science and Applications*, vol. 9, no. 8, 2018, pp. 34-45.
- [23] J. L. C. Izquierdo, & J. Cabot, "JSONDiscoverer: Visualizing the schema lurking behind JSON documents", *Knowledge-Based Systems*, vol. 103, 2016, pp. 52-55.
- [24] E. Vayena, M. Salathé, L. C. Madoff, & J. S. Brownstein, "Ethical challenges of big data in public health", *PLoS computational biology*, vol. 11, no. 2, 2015, e1003904.
- [25] J. Sligo, R. Gauld, V. Roberts, & L. Villa, "A literature review for large-scale health information system project planning, implementation and evaluation", *International Journal of Medical Informatics*, vol. 97, 2017 pp. 86-97.

Systematic Literature Review (SLR) of Resource Scheduling and Security in Cloud Computing

Abdullah Sheikh¹, Malcolm Munro², David Budgen³
Department of Computer Science, Durham University
Durham, United Kingdom

Abstract—Resource scheduling in cloud computing is a complex task due to the number and variety of resources available and the volatility of usage-patterns of resources considering that the resource setting is on the service provider. This compounded further when security issues are also factored in. This paper provide a Systematic Literature Review (SLR) that will help to identify as much prior relevant research that has been done in the area of research topic. Also, all papers that are found from the search will be classified into groups to stand on the current situation and to identify possible existing gaps.

Keywords—Cloud computing; security; resource scheduling; systematic literature review; SLR

I. INTRODUCTION

Scheduling in cloud computing is a process or mechanism applied 'to minimise wasting limited resources by efficiently allocating them among all active nodes' [1]. Nodes or virtual machines (VMs) are the virtual resources that are assigned to consumers for running the service and executing tasks [2]. Scheduling is a very complex operation in cloud computing used to allocate resources, improving server utilisation, enhance service performance, and executing tasks [3].

Scheduling can use either static or dynamic methods for scheduling resources in cloud computing. These methods can provide sufficient use of cloud resources to meet Quality of Service (QoS) requirements [4]. Furthermore, using scheduling techniques can avoid conflicts in allocating active resources. For example, scheduling can avoid duplication of allocating the same virtual resource at one time. Also, it can help manage limited resources by handling high demand of requests by using dynamic method that can update the system regularly and to execute tasks over resources based on the resources availability. However, there are some issues need to be considered such as security, limited resources, virtual machines and applications.

Executing and running tasks over the allocated resources raises some security issues that need to be considered such as data security, and service security. Data security includes privacy, integrity, protection from any threats and attacks. Service security includes resource security, and privacy. So, there is a need to consider these issues and the security constraints, including data security, and availability to get an optimised resource scheduling. For this research, the main focus will be on resource scheduling mechanisms when security is factored into the cloud model.

According to Singh and Chana, [5], there are two main objectives for resource scheduling as follows:

- 1) Workloads refer to the tasks that consumers want to run over the resources. So, identifying suitable resources for scheduling workloads on time will help to enhance the effectiveness of resource utilisation.
- 2) To identify heterogeneous multiple workloads to fulfil the Quality of Service (QoS) requirements, such as CPU utilisation, availability, reliability and security.

This paper focuses on searching and reviewing prior research relevant to resource scheduling and security in cloud computing and to identify possible existing gaps.

This paper is organised as follows. Section II gives an over view of cloud computing including cloud definition, cloud architecture, obstacles facing cloud growth, research method, explaining why SLR is important to this research, and research questions and research scope. Section III discusses the search strategy including identifying the search period, search strings, search engines. Section IV describes the inclusion/exclusion criteria, and the procedures of selection. Section V explains the aim of SLR. Section VI presents how the data will be extracted from each paper. Section VII discusses the synthesis strategy and the threats of validity. Section VIII explains limitation and factors that could affect this research. Section IX presents discussion of current finding and proposed solution. Section X concludes with suggestion and future work.

II. BACKGROUND

This section serves as a background and a general view of cloud computing, basic cloud architecture and cloud features. Also, it shows the considered top ten obstacles that are facing the growth of cloud computing and how they related to the security in the cloud. Then it presents the research method for this Systematic Literature Review (SLR). After that, it explains why this SLR need to be performed followed by research questions and the research scope.

A. Cloud Definition

There are many different definitions of cloud computing, the National Institute of Standard and Technology (NIST) [6] gives a basic definition of cloud computing as “a model for enabling convenient, on-demand network access to a shared pool configurable computing resources (e.g. networks, servers, storage, application, and services) that can be rapidly provisioned and released with minimal management effort or service provider interaction”.

To obtain a cloud service a consumer needs to contact a service provider. This communication process makes the

consumer and the provider reach an agreement of the level of the service. This agreement referred to Service Level Agreement (SLA) [7]. This SLA is the basis for the expected level of the service between the consumer and the provider. The provider of a cloud architecture can offer various services to a consumer. Quality of Service (QoS) refers to cloud stakeholders expectation of obtaining a desirable service meeting requirements such as timeliness, scalability, high availability, trust and security specified in the Service Level of Agreement SLA [8]. For this research, Quality of Service (QoS) includes the following concerns:

- **Security:** Security is a shared responsibility between cloud providers and consumers to ensure that the level of security is at a desired level. Consumers need to be aware of security from their side and protect their service from any threats. Cloud providers are able to achieve better scalability by running multiple virtual machines on physical machines. They have to defend the service against any security risks from any unauthorised physical access, data security, security software, and resource security. Other cloud providers who do not use virtual machine have to secure servers and data storage from any security risks. Then any security risks in the virtualisation technology that allows co-occupant virtual machines to make unauthorised access could compromise information assets of consumers [9].
- **Service Performance:** A consumer requires a certain level of the service performance will need provider guarantees to run the require service in the cloud. The Service Level Agreement (SLA) is an agreement between a service provider and a consumer, that specify the level of the service provided [8] [9] [10]. Also, both provider and consumer follow the rules and conditions of this agreement to keep the service secure without any security issues.

These services can vary both in terms of functionality (such as storage capacity or processor count) or in terms of the Quality of Service (QoS) provided [11]. In terms of the QoS a provider will offer a defined SLA which the consumer can use when determining the 'best' provider for their needs.

According to Mell and Grance [6], the cloud architecture is a combination of the following three components:

- **Essential Characteristics:** The essential characteristics refer to a set of cloud features that allow providers and consumers managing, accessing, and measuring the cloud services and resources. These characteristics provide cloud providers and consumers different level of control to measure and provision the service. From a security prospective, each characteristic has a different security concern for both provider and consumers. These security concerns include access control and data security [2]. Access control includes accessing, managing the service, and access availability. Data security includes data confidentiality, date integrity, and data availability.

The five essential cloud characteristics are:

- 1) **On-demand self-service:** A consumer can manage and control the service resources such

as sever time and network storage without any physical interactions by the provider.

- 2) **Broad network access:** Consumers can access and use the cloud service from anywhere across the network.
- 3) **Resource pooling:** Providers can serve consumers with different resources according to consumer demand. Resources such as storage, processing, physical machine, and network bandwidth [2]. Consumers do not need to be concerned about physical location of resources.
- 4) **Rapid elasticity:** Resources can be rapidly scaled outward or inward at any time according to consumers demand.
- 5) **Measured service:** Measured service is the ability to track and control the usage of the resources which can be performed by consumers.

- **Service Models:** Service models in the cloud defines to a consumer the type of the system management and system operations and type of the access to cloud systems. According to Nallur et al. [9] service availability, security and performance are the main elements that are considered to affect cloud service in the service models. Based on SLA, consumers have to trust the provider on the service availability and the only concern is if there is any downtime to the service it will be the time of the service recovery to obtain the service again. The recovery process is the responsibility of the service provider based on the SLA. Both provider and consumers are involve in security such as data security and protection. The provider is concerned about providing a secure and reliable service via the network. Service performance means that the service provided to consumers at a satisfactory level and good quality. There are three types of service model, each service model provides different capabilities to obtain the service:

- 1) **Infrastructure as a Service (IaaS):** To provide a basic form of the service such as a virtual machine (VM), virtual storage and network bandwidth [9]. Consumers have to configure the setting and install any needed operating system and software before running the service. One of the main security concerns in IaaS for the provider is to check that there is no VMs interference while the service is running.
- 2) **Software as a Service (SaaS):** Here, software and applications are provided by the cloud provider which lets consumers use these applications. Consumers can have access to the service from different devices via different interface such as web browser and a program interface. One security concern needs to be considered is web browser security. The level of the browser security is very important, weak browser security can let an attacker get important information or hijack the consumer resources and data.

- 3) Platform as a Service (PaaS): In this form, the cloud provider provides a platform that allows the consumer to develop their application but the cloud provider is still responsible for maintenance and all upgrades of the platform.

Table I shows the main security issues that exists for each service model [12]. From Table I, SaaS has the most security issues because it is more complex than the other service models. PaaS and IaaS have less security issues compared with SaaS because they have better control over the security and they are not involved in the application level.

Table I shows the responsibility perspective for the the security issues for providers and consumers. These issues are different in terms of responsibilities from the providers and consumers. The table shows that most responsibility to ensure the security level of the service is on the providers. The providers responsibilities include data (security, locality, segregation, confidentiality), network security, authentication and authorisation, vulnerability in virtualisation, availability, and identity management. Using secure web applications to access the service is mostly the responsibility of the consumers. The other security issues such as data access, data breaches and backup are shared responsibilities for providers and consumers. These security issues affect differently each service model. These issues are:

- Data Security: Providers need to use good techniques to secure data access such as encryption and decryption.
- Network Security: To secure the data flow through the network from any security breach or leakage.
- Data Locality: To manage storing consumers data in a reliable location and to protect it from any risks.
- Data Integrity: To make sure that data is stored and then it correctly and accurately flow through the database over the service.
- Data Segregation: To secure the data flow, and data storage from any intrusions hacking the system on each level of the service.
- Data Access: To control data access for consumers.
- Authorisation, Authentication: To manage accessing to the service or database.
- Data Confidentiality: To control and protect the data flow on each level of the service.
- Web Application Security: Consumers need to ensure their web applications are secure to access to the service.
- Data Breaches: Providers need to protect data and prevent any indirect access.
- Vulnerability in Virtualisation: Providers need to ensure that each tasks executed separately from each other to reduce security risks that could occur.
- Availability: Providers need to ensure that the service is delivered on demand.

- Backup: The backup information is important and if it has been hacked then any unauthorised accessed will cause a security issues for the consumers. Providers need to ensure that backup is taken regularly and be secured and encrypted to make the service more reliable and fast recovery when it required.
- Identity Management: To control and check the identity of accessing to the service and resources by identifying all information that used to log in.

TABLE I. SECURITY ISSUES IN THE SERVICE MODELS [12]

Security Issues	Service Models			Responsibility Prospective	
	IaaS	PaaS	SaaS	Providers	Consumers
Data Security	✓	✓	✓	✓	
Network Security	✓	✓	✓	✓	
Data Locality	✓		✓	✓	
Data Integrity		✓	✓	✓	
Data Segregation			✓	✓	
Data Access	✓	✓	✓	✓	✓
Authorisation, Authentication	✓		✓	✓	
Data Confidentiality			✓	✓	
Web Application Security			✓		✓
Data Breaches	✓		✓		✓
Vulnerability in Virtualisation	✓	✓	✓	✓	
Availability	✓	✓	✓	✓	
Backup			✓	✓	✓
Identity Management	✓		✓	✓	

Subashini and Kavitha [12] claim that the security issues in the service models such as data security and network security make a significant trade-off to each service model to obtain a reliable, trusted and secure services.

These service models offer different features to customers and providers to operate the service. SaaS offers many significant benefits to customers such as service efficiency improvement and reduced costs. In SaaS providers do all provisioning for hardware, data storage, power, virtual resources. As a result consumers have to pay for what they use, and there is no upfront cost for anything else. With all the benefits that are provided in SaaS, it has some issues such as lack of visibility of data stored and security.

In PaaS users can build their application on top of the platform, but this feature raises the security risks for all the services. Building applications on top of the platform increase security risks such as data security and network intrusion by unlocking the way to intruders trying any unauthorised actions [12]. For example, hackers can attack the applications code and run a very large amount of malicious programs to attack the service. In IaaS, consumers can get services with less cost with basic security configuration and less load balance. Providers have to ensure that the service infrastructure is highly secure for, data storage, data security, data transmission, and network security.

- **Deployment Models:** Deployment models are to describe how the cloud services deliver to consumers. According to [13] there are many security concerns on the cloud deployment models including data privacy and trust, policies, and data transfer. As a result of these concerns providers have to secure cloud services. Also, providers need to apply security policies that can

handle data access and security. The four deployment models, which specify the availability of using cloud service [6], are:

- 1) Public: To specify that cloud services is accessible with no restriction for all users.
- 2) Private: To make cloud services available to particular single group.
- 3) Community: To make cloud services shared between limited group sharing similar concerns.
- 4) Hybrid: A hybrid cloud includes services using multiple cloud combined together, for example joining services and making some parts private and other parts public or community [14].

The common security issues that need to be addressed for these deployment models are authentication, authorisation, availability, access control and data security. These security issues are so important because each deployment model has a different security level. For example, public cloud is less secure than the other cloud model, so it is more likely to be attacked by malicious hackers to get information that can used then to be hack at the private level. Providers are responsible for service security and they have to stop any unauthorised access or any malicious attacks of the service. Suspicious behaviour includes any malicious attacks and abuse of the service. Consumers take responsibility for information security and data security such as integrity, confidentiality, authorisation and authentication.

There is a list of the top ten obstacles facing cloud computing in [2] summarised in Table II. Armbrust et al. [2] indicate that the consideration for each obstacle will vary from one stakeholder to another (consumer and provider). The first obstacle is Service Availability which has multiple sides. One side is cloud providers offer multiple sites to improve availability, however, consumers may choose to use multiple providers to increase availability. As a result, some parts of the services may become unavailable for some consumers for any time.

There are many reasons that can cause service unavailability such as crashed applications, high loads in the service, and service hijack [15]. Then the consumers will think that the service was down and it is not available to be used. However, services with multiple clouds or multiple sites give more opportunities for an attacker to cause a security threat. An attacker can use a public service to get to unauthorised access to resources or by doing many malicious activities that affect the service. One way to defend this issue is to use quick scale-up method and security monitoring [2]. Scaling method in the cloud is used to control cloud resources, which include two type of scaling, horizontal and vertical [16]. The vertical or scale up is used to increase the virtual resources for restoring and improving performance also known as scaling outward. Service Availability is an issue that can be addressed using this method if any virtual resource becomes unavailable. The horizontal method is to scale upward by running the service in one physical resource. Providing the service from one physical resource or one site is an issue of the service availability.

The second, third and fourth obstacles are about data boundaries between platforms and Data Storage, Data Confidentiality, and Data Transfer. There are many security implications should be considered include loosing data, data leakage, transferring data, and data security. The fifth, sixth, seventh, and eighth obstacles are more technical being related to performance, Scalable Storage, removing errors in a large scale distributing system, and how services can be established with quick scaling getting an overview of service costs. Quick scaling could cause unavailability of the service if there is a very high load tasks which needs to be considered as a security implication of this method. The ninth and tenth obstacles are about service policies and Service Level Agreement (SLA) and Software Licence. The concern here is about the eligibility or the authorisation of using the software and to ensure there is no misuse of the licence [2].

TABLE II. THE TOP TEN OBSTACLES AND CATEGORY [2]

No	Obstacles	Category	Stakeholder Prospective
1	Service Availability	Cloud Service Availability	Consumer
2	Data Storage	Data, Data boundaries	Provider
3	Data Confidentiality	Data, Data boundaries	Consumer
4	Data Transfer	Data, Data boundaries	Consumer
5	Performance unpredictability	Performance, Scalability	Consumer
6	Scalable Storage	Performance, Scalability	Consumer
7	Error of large scale	Performance, Scalability	Provider
8	Quick Scaling	Performance, Scalability	Consumer
9	Service Level Agreement (SLA)	Service policies	Provider, Consumer
10	Software Licence	Service policies	Provider, Consumer

B. Research Method

A Systematic Literature Review (SLR) will identify current research topic related to cloud scheduling and security, then to identify existing gaps, and give an overview of research in the area. To identify gaps papers will be classified into groups depending on their main focus. A recent review [17] shows that most models of cloud security classified to Data as a Service (DaaS), Cloud Storage and research for scheduling just focusing on algorithms. A systematic literature review should contain three stages, which are a plan or a protocol, conducting the review, and reporting the review.

The SLR is needed to identify as much prior research that has been performed in this area and the most relevant to the area of the research topic, which is critical to this research direction and methodology. Also, the outcome of this research is to focus on producing a new model for resource scheduling across cloud security boundaries. Then to obtain a list of the previous research, finding gaps to be extended for further research to find an optimal solution.

C. Research Questions

The research questions will be as the following:

- 1) What previous research has been done in terms of Scheduling in the Cloud in the presence of security constraints?

- 2) What constraints other than security need to be considered by each Cloud stakeholder in terms of scheduling in the Cloud?
- 3) What different types of security constraints have been identified and what do these security constraints defend against?
- 4) What evaluation metrics have been used to help to evaluate recent research into Scheduling in the Cloud?
- 5) Based on the research identified, which forms of security aware scheduling merit further research, and why is more research needed and what issues should the further research be addressing?

D. Scope

The following provides the scope for this work using the PICOC model [18].

- **Population:** Published literature papers of scheduling and cloud security.
- **Intervention:** Papers include (Models, surveys, technical report) that address any approaches of scheduling and cloud security.
- **Comparison:** To include comparisons between different scheduling and cloud security models and different approaches.
- **Outcomes of Interest:** The different techniques of scheduling and cloud security models.
- **Context:** To be used by Students and Academic researchers.

III. SEARCH STRATEGY

This section discusses the choice of the search period, search strings, electronic resources to be used, and the possible use of manual searching.

A. Search Period

The developer of cloud computing came from different area. It started with distributed system and utility computing discussed in the 1990s [19].

Cloud computing as a term will be used for initial search criteria and searching over the period 2006, which is the year of the first cloud conference, to the end of 2015 linking what has been done in the area of Cloud Computing and another related topic such as Cloud Security and Scheduling. Additionally, a manual search will be performed to find an earlier date using Cloud Computing as a term or maybe some other phrases that could be related to the topic such as Grid Computing, Utility Computing, and Distributed System.

B. Search Strings

Basic search strings will be used to try to find papers that relate to the topic and will be filtered in the later stage after applying the including and excluding criteria. Also, basic terms will be used for searching for papers such as (Cloud Security, Cloud Security Model, Cloud Scheduling, Resource

Scheduling, Scheduling in the cloud). Then, to find relevant literature reviews using strings as following:

(Cloud Security Model OR Study on Cloud Security, OR Scheduling OR Resource Scheduling) AND (Security in the cloud).

Then:

(((((Cloud) OR (Grid) OR (utilization) AND (Computing))) AND (Security)) AND (Schedul*)) AND (Model*))

C. Search Engines

To obtain a broad prospective the search will be conducted using the following preferred electronic sources. There are preferred because most papers have been found linked to these search engines and the university library:

- IEEE Xplore – since IEEE are a major publisher of relevant conferences and journals.
- ACM Digital Library – for the same reasons as IEEE.
- To check other search engines for manual search to see what they included such as:
 - web of science
 - ScienceDirect
 - Springer link.

D. Other Search

Other search are conducted are a manual search and a Snowball search.

- A manual search of the first IEEE Cloud Conferences and other cloud conferences will be performed to check the electronic searching and to find out what terms have been used. Also, to extend the search and to find the most relevant papers on the topic that might be overlooked and were not indexed by IEEE or ACM.
- A Snowball search consists of following up the references from the papers obtained through other search forms, in order to identify any other papers that might have been missed by keyword searching. The Snowball search will be performed after making the final selection of papers for inclusion. Particularly, to look at papers that are referenced in sections with such titles as 'Background', 'Related Work' and 'Discussion' since this is where a comparison with similar work is likely to be identified.

IV. STUDY SELECTION CRITERIA AND PROCEDURES

This section describes the inclusion/exclusion criteria and the procedures for performing the selection. The scope of this work is confined to those papers that are written in English.

A. Inclusion/Exclusion

The inclusion criteria for selection will be:

- Published Conferences, Workshops, Journals and peer reviewed papers that report on work addressing any aspect of Scheduling in Cloud Security.
- Any previous systematic literature reviews on Scheduling in Cloud Security.
- Where more than one source refers to the same work, the most complete source will be used.
- Where one source refers to more than one piece of work, each relevant work will be counted separately.
- Need to consider the type of research this SLA is interested in - and how the research is conducted - real software implementation, mathematical model or simulation, or thought exercise.

The exclusion criteria will be:

- Sources that are only available as presentations, abstracts, or are otherwise incomplete.
- Forms of publication that have not been subjected to a formal review process, including journals such as ACM Software Engineering Notes (unless containing conference proceedings) and technical reports.
- Opinion paper.

B. Procedures for Selection

After performing the searching phase, the outcomes from the different search engines will be amalgamated into one set of papers. During this process, any obvious duplicates will be removed where a paper has been found by more than one search engine. The inclusion/exclusion criteria will then be applied through the following process.

- Stage 1: Exclusion on the title. This will involve excluding those papers with titles that make it evident that they do not meet the inclusion criteria (e.g. are about some other form of Scheduling or Security).
- Stage 2: Exclusion on abstract. For this, the abstracts were be read and again exclude any papers that are clearly not appropriate.
- Stage 3: Exclusion on full paper. For the remaining candidate papers, obtain the full paper and make a final decision on that basis.
- Stage 4: Resolution of papers and work. This process will identify where the outcomes from a piece of work have been published in more than one paper and where papers are reported.

An initial search has been performed to test the search string on IEEE xplorer, ACM, ScienceDirect, Web of Science, and SpringerLink search engines shown in Fig. 1. In this searching stage the total number of papers from all search engines is 877. Then the search string have been refined to be check that it cover the area and that number of papers found has been increased to 2466.

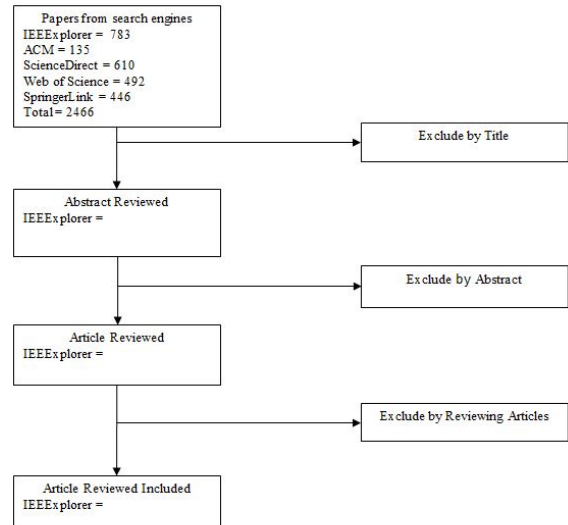


Fig. 1. Procedure for Selection

V. QUALITY ASSESSMENT

The aim of the SLR is to make a decision about the quality of existing work. This depends on the quality score for each paper, and it applies a short quality assessment questionnaires to be completed after performing data extraction. The role of quality assessment is to provide additional information about the primary work that can then be used to assess which ones should be given the greater weighting when drawing any conclusions. This shown as Appendix A.

VI. DATA EXTRACTION

For this work, the following proposed questions shown in Table III will be performed for data extraction from each paper:

TABLE III. QUESTIONS FOR DATA EXTRACTION

No.	Question	Study Types
1	What was the research question(s)?	
2	What sort of models are used to test the ideas in in the paper(s)?	
3	Which security issues (Table I) are they addressing?	
4	What scheduling and cloud security techniques have been used?	
5	Is definition of the cloud made clear, and if so, what is it?	
6	What cloud implementation(s) have been used?	
7	What was the outcome measure(s)?	
8	What was the reported outcome of the research?	
9	Original work or replication	
10	Appropriate data analysis	
11	Was there a clear link between data and conclusion?	
12	What were the research hypotheses?	
13	Was the context discussed?	
14	Was any comparison discussed?	
15	Were the research questions answered?	
16	What is the approach of the paper including the basic design?	

VII. SYNTHESIS

For this work, any reviews found, systematic or otherwise, will be used to help to check completeness.

A. Synthesis Strategy

This process will include the following three steps:

- 1) To look at the final set of papers and identify a set of categories from them.
- 2) Allocating papers to these categories (a paper might fit more than one).
- 3) To examine the papers in each category to see what could be learned about that topic (this could be a form of vote counting, moderated by quality scores).

B. Threats to Validity

The process of the synthesis could be affected by the threats of validity, and the initial assessment of these as follows:

Internal Validity. Following this protocol allows the selection of accurate papers related to the research topic, and the selections criteria could validate that papers are selected correctly or not.

External Validity. To get more reliable papers that are relevant to the research topic the exclusions criteria will exclude any irrelevant research or any non academic work.

VIII. LIMITATIONS

The anticipated outcome of this research may be limited by the following factors:

- The number of work will affect this research, as the previous search did not find that many papers in different areas of the research topic.
- Another limitation is that some work intend to focus on the use of supporting tools and use them just for evaluating their work without discussing the scheduling methodology.
- To consider possible limitation that might arise from the way that this work is conducted (such as missing important papers) and how to mitigate this (such as the use of snowballing, and possibly using a 'gold standard' group of known researches and seeing how many of the searches find).

IX. DISCUSSION

This section discusses the finding of SLR, then it presents the proposed outcome.

This section discusses recent related approaches in the area of cloud security such as Data storage approaches that are related to Data as a Service (DaaS) data storage moving from a single cloud to a multi-cloud, and security models. It also provides some approaches in resource management that used static and dynamic methods focusing on performance.

A review of recent cloud models has been performed to get an overview of the models categories shown in Table IV. Models have been classified to categories related to the main focus of the approaches including Data as a service (DaaS), Infrastructure as a Service (IaaS) and cloud storage. The DaaS models focus on all data security and different from cloud storage which is concerned about data centre security. The IaaS models focus on the infrastructure security.

Table I shows some issues have less attention than others such as Authentication, Accountability, Intrusion, and Reliability. The most focused areas are Integrity, Availability, and Security. Most approaches are related to cloud storage and DaaS which make IaaS need more work especially in security.

The DepSky system [20] addresses the availability and the confidentiality of data in their storage system by using multi-cloud providers, combining Byzantine quorum system protocols, cryptographic secret sharing and erasure codes. Whereas NetDB2-MS [21] is a Model to ensure privacy level in DaaS based on data distributed to different service providers and to employ Shamir's secret algorithm [22].

The BlueSky System [23] has extended the DepSky system to be more reliable and deal with large storage volume from a cloud provider and to avoid a dedicated hardware server. Similarly, the SafeStore system [24] is more focused on availability not on performance and cost which is quite different than the other systems.

Other approaches like HAIL [26], ICStore [27], SPORC [28], Depot [29], Data storage Models [30], [31] have focused on cloud storage including some data security aspects such as security and data integrity and data confidentiality. They also have similar limitations such as data intrusion and availability.

There are some models at the deployment level which deal with the security risks but with limitations in confidentiality and integrity such as Separation Model - Migration Model - Availability Model - Tunnel Model - Cryptography Model [32].

Data privacy is still a big concern in other Models like Jerico Formu's Cloud Cube Model [17], Hexagon model [17], Multi-Tenancy Cloud Model [33], Cloud Risk Accumulation Model [34], and the Mapping Model [17], [33]. The logging approach [35] ensures that the log files can mitigate the risks to benefit both sides of accountability, security, performance, and scalability.

Other work in scheduling such as [3] takes into consideration tasks priorities then assign them to be executed over the allocated resources. If there more than one task for each resource, it will be scheduled with different methods depending on what is better for each resource. Then it will use parallel running for all tasks. This work assigned dependent tasks first to run first then non dependent one that to minimise the deadlock situation.

Table V shows some approaches that related to resource management used static and dynamic methods and focusing on performance.

Approaches by Li et al. [36] and Yazir et al. [37] relate to resource scheduling using static and dynamic mechanism but they did not include any security factors to avoid any security risks. Static scheduling mechanism such as the approach introduced by Jiayin et al. [38] offers a static scheduling solution to improve service performance over virtual machines. The tasks are executed on certain cloud resources based on the static resource allocation. It aims to regulate many resources utilisation of service level objective of applications SLOs. Also, in [38] propose an algorithm that adjust resource

TABLE IV. REVIEW OF CLOUD MODELS

Ref	Category			Main Focus													
	DaaS	IaaS	Cloud storage	Availability	Confidentiality	Reliability	Intrusion	Integrity	Fault tolerance	Recovery fail	Cost	Scalability	Performance	Accountability	Latency	Security	Authentication
DepSky [20]	✓			✓	✓												
Bluesky [23]	✓																
SafeStore [24]	✓				✓												
NetDB2-MS [21]	✓			✓			✓	✓									
NCCloud [25]			✓						✓	✓	✓						
HAIL [26]			✓	✓				✓									
ICStore [27]			✓				✓										
SPORC [28]			✓	✓													
Depot [29]			✓	✓						✓					✓		
Logging Solutions [35]		✓										✓	✓	✓			
Venus [31]			✓					✓									
TCCP [42]		✓		✓				✓									
CCM [17]																✓	
Hexagon Model [17]																✓	
MTCM [17]																✓	
CSA [17]																✓	
Mapping model[17]																✓	
Separation Model [32]									✓								
Migration Model [32]								✓									✓
Availability Model [32]				✓													✓
Tunnel Model [32]								✓									✓
Cryptography Model [32]					✓												✓
NDSM [43]	✓		✓														✓
Cloud Trust Model [44]	✓																✓
DSM [45]	✓				✓												✓
DSSM [30]	✓		✓														✓
SC [3]													✓				✓

allocation based on updating the actual task executions which helps to recalculate the finishing time that assigned to the cloud.

Walsh et al. [39] proposed a utility function as a solution by dividing the architecture into two-layers (local and global). The local layer is responsible for calculating resource allocation dynamically. Whereas, the global layer computes the near optimal configuration of allocating resources based on results provided by the local layer, and to fix the load balancing with the server cluster which also helps applications scalability.

Other approaches that use dynamic mechanism such as

Yazir et al. [37] and Slegers et al. [40] include a comparison of static and four heuristic dynamic policies. They showed some differences and presented benefits and weaknesses of using each type in terms of using and managing cloud resources. A price model was introduced by Sharma et al. [41] for dynamic resource management and low cost of cloud service but they did not include the security factor and indicate saving cost on physical resources and maintenance cost as limitations of their model.

As a result of this SLR, the proposed model by Sheikh et al. [47] has considered the over all security discussed by

TABLE V. APPROACHES FOR RESOURCE SCHEDULING

Ref	Resource Management	Static	Dynamic	Performance
Adaptive management of virtualised resources [36]	✓	✓		✓
Adaptive resource allocation [38]	✓	✓		✓
Dynamic resource allocation [37]	✓		✓	✓
Resource allocation for multi-tier [46]	✓		✓	✓
Resource Allocation Policies [40]	✓		✓	✓

Watson [48] to develop Scheduling Security Model (SSM) to address the issues found in other approaches by this SLR such as security and cost.

X. CONCLUSION

This paper has briefly introduced an over view of cloud computing including definition, architecture, obstacles facing cloud growth. Then presented the research method and explained why SLR is important to this research. After that, it discussed the search strategy identifying the search period, strings, search engines. Also, it described the inclusion/exclusion criteria, and the procedures of selection. Next, it explained the aim of SLR, then presented how the data will be extracted from each paper and it discussed the synthesis strategy and the threats of validity. After, it addressed limitation and factors that could affect this research. Finally, it presented the current finding of SLR from the reviewed paper and proposed solution. The proposed solution SSM has developed to cover some issues.

ACKNOWLEDGEMENTS

This research protocol has been prepared following the structure provided in [49]. Moreover, thanks to Taif University in Kingdom of Saudi Arabia for the funding.

REFERENCES

[1] K. Yang G, W. Yu, P. ByoungSeob and C. Hyo Hyun, *A heuristic resource scheduling scheme in time-constrained networks*, Computers & Electrical Engineering, Elsevier, 54, 1–15, 2016.

[2] M. Armbrust, A. Fox, R. Griffith, A. Joseph, R. Katz, A. Konwinsky, L. Andrew, P. Gunho, A. David, A. Rabkin and I. Stoica, *Above the clouds: a Berkeley view of cloud computing*, University of California at Berkeley, 2009.

[3] L. Tripathy and R.R. Patra, *Scheduling in cloud computing*, International Journal on Cloud Computing: Services and Architecture (IJCCSA), 4(5), pp.21-7, 2014.

[4] Wu. Fuhui, Wu. Qingbo and T. Yusong, *Workflow scheduling in cloud: a survey*, The Journal of Supercomputing, Springer, 71, 9, 3373–3418, 2015.

[5] S. Sing and I. Chana, *A survey on resource scheduling in cloud computing: Issues and challenges*, Journal of Grid Computing, Springer, 14, 2, 217–264, 2016.

[6] P. Mell and T. Grance, *The NIST definition of cloud computing*, Computer Security Division, Information Technology, Laboratory, National Institute of Standards and Technology, Gaithersburg, 2011.

[7] P. Patel, A. Ranabahu and A. Sheth, *Service level agreement in cloud computing*, Citeseer, 2009.

[8] F. Panzieri, O. Babaoglu, S. Ferretti, V. Ghini, and M. Marzolla, *Distributed computing in the 21st century: Some aspects of cloud computing*, Springer, 2011.

[9] V. Nallur and R. Bahsoon, *A decentralized self-adaptation mechanism for service-based applications in the cloud*, Transactions on Software Engineering, IEEE, 39, 5, 591–612, 2013.

[10] A. Abdelmaboud, D. Jawawi, I. Ghani, A. Elsafi and B. Kitchenham, *Quality of service approaches in cloud computing: A systematic mapping study*, Journal of Systems and Software, Elsevier, 101, 159–179, 2015.

[11] R. Shelke and R. Rajani, *Dynamic resource allocation in cloud computing*, International Journal of Engineering Research and Technology, ERSRA, 2, 10, 2013.

[12] S. Subashini and V. Kavitha, *A survey on security issues in service delivery models of cloud computing*, Journal of network and computer applications, Elsevier, 34, 1, 1–11, 2011.

[13] T. Dillon, C. Wu, and E. Chang, *Cloud computing: issues and challenges*, International Conference on Advanced Information Networking and Applications, IEEE, 27–33, 2010.

[14] D. Goutam, A. Verma, N. Agrawal, *The performance evaluation of proactive fault tolerant scheme over cloud using CloudSim simulator*, International Conference on the Applications of Digital Information and Web Technologies (ICADIWT), IEEE, 171–176, 2014.

[15] S. Ramgovind, M. Eloff, and E. Smith, *The management of security in cloud computing*, Information Security for South Africa, IEEE, 1–7, 2010.

[16] R. Patil and RK. Singh, *Scaling in Cloud Computing*, International Journal of Advance Research, IJOAR, 1, 21–27, ISSN:2320-9194, 2013.

[17] V. Chang, D. Bacigalupo, G. Wills and D. De Roure, *A categorisation of cloud computing business models*, Proceedings of the IEEE/ACM International Conference on Cluster, Cloud and Grid Computing, IEEE Computer Society, 509–512, 2010.

[18] M. Petticrew and H. Roberts, *Systematic reviews in the social sciences: A practical guide*, John Wiley & Sons, 2008.

[19] I. Foster, Y. Zhao, I. Raicu and S. Lu, *Cloud computing and grid computing 360-degree compared*, Grid Computing Environments Workshop, IEEE, 1–10, 2008.

[20] A. Bessani, M. Correia, B. Quaresma, F. André and P. Sousa, *DepSky: dependable and secure storage in a cloud-of-clouds*, ACM Transactions on Storage (TOS), ACM, 9, 4, 12, 2013.

[21] M. Alzain, B. Soh and E. Pardede, *A new model to ensure security in cloud computing services*, Proceedings of the 10th ACM conference on Service Science Research, Springer, 4, 1, 49–70, 2012.

[22] A. Shamir, *How to share a secret*, Communications of the ACM, ACM, 22, 11, 612–613, 1979.

[23] M. Vrable, S. Savage, GM. Voelker, *BlueSky: a Cloud-Backed File System for the Enterprise*, Proceedings of the 10th USENIX Conference on File and Storage Technologies, USENIX Association, 19–19, 2012.

[24] R. Kotla, L. Alvisi and M. Dahlin, *SafeStore: a durable and practical storage system*, USENIX Annual Technical Conference, 129–142, 2007.

[25] Tu. Hu, HCH. Chen, P. Lee and Y. Tang, *NCcloud: Applying Network Coding for the Storage Repair in a Cloud-of-Clouds*, FAST, 21, 2012.

[26] K. Bowers, A. Juels and A. Oprea, *HAIL: a high-availability and integrity layer for cloud storage*, Proceedings of the 16th ACM conference on Computer and communications security, ACM, 187–198, 2009.

[27] C. Cachin, R. Haas and M. Vukolic, *Dependable storage in the intercloud*, IBM research, 3783, 1–6, 2010.

[28] AJ. Feldman, WP. Zeller, MJ. Freedman and EW. Felten, *SPORC: Group Collaboration using Untrusted Cloud Resources*, OSDI, 10, 337–350, 2010.

- [29] P. Mahajan, S. Setty, S. Lee, A. Clement, L. Alvisi, M. Dahlin, M. Walfish, *Depot: Cloud storage with minimal trust*, Transactions on Computer Systems (TOCS), ACM, 29, 4, 12, 2011.
- [30] HB. Patel, DR. Patel, B. Borisaniya and A. Patel, *Data storage security model for cloud computing*, International Conference on Advances in Communication, Network, and Computing, Springer, 37–45, 2012.
- [31] A. Shraer, C. Cachin, A. Cidon, I. Keidar, Y. Michalevsky, and D. Shaket, *Venus: Verification for Untrusted Cloud Storage*, Proceedings of the 2010 ACM workshop on Cloud Computing Security Workshop, ACM, 19–30, 2010.
- [32] G. Zhao, C. Rong, MG. Jaatun, FE. Sandnes, *Deployment models: Towards eliminating security concerns from cloud computing*, International Conference on High Performance Computing and Simulation (HPCS), IEEE, 189–195, 2010.
- [33] J. Che, Y. Duan, T. Zhang and J. Fan, *Study on the security models and strategies of cloud computing*, Procedia Engineering, Elsevier, 23, 586–593, 2011.
- [34] G. Brunette and R. Mogull, *Security guidance for critical areas of focus in cloud computing*, Cloud Security Alliance, 2, 1, 1–76, 2009.
- [35] W. Wongthai, F. Rocha, and A. Van Moorsel, *Logging Solutions to Mitigate Risks Associated with Threats in Infrastructure as a Service Cloud*, International Conference on Cloud Computing and Big Data (CloudCom-Asia), IEEE, 163–170, 2013.
- [36] Q. Li, Q. Hao, L. Xiao and Z. Li, *Adaptive Management of Virtualized Resources in Cloud Computing using Feedback Control*, First International Conference on Information Science and Engineering, IEEE, 1, 99–102, 2009.
- [37] YO. Yazir, C. Matthews, R. Farahbod, S. Neville, A. Guitouni, S. Ganti and Y. Coady, *Dynamic resource allocation in computing clouds using distributed multiple criteria decision analysis*, International Conference on Cloud Computing, IEEE, 3, 91–98, 2010.
- [38] J. Li, M. Qiu, JW. Niu, Y. Chen and Z. Ming, *Adaptive Resource Allocation for Preemptable Jobs in Cloud Systems*, International Conference on Intelligent Systems Design and Applications, IEEE, 10, 31–36, 2010.
- [39] WE. Walsh, G. Tesauro, JO. Kephart, and R. Das, *Utility Functions in Autonomic Systems*, Proceedings on International Conference of Autonomic Computing, IEEE, 70–77, 2004.
- [40] J. Slegers, I. Mitrani and N. Thomas, *Static and Dynamic Server Allocation in Systems with on/off Sources*, Annals of Operations Research, Springer, 170, 1, 251–263, 2009.
- [41] B. Sharma, R. Thulasiram, P. Thulasiraman, S. Garg and R. Buyya, *Pricing Cloud Compute Commodities: a Novel Financial Economic Model*, Proceedings of the 2012 12th IEEE/ACM International Symposium on Cluster, Cloud and Grid Computing (CCGRID), IEEE, 451–457, 2012.
- [42] N. Santos, KP. Gummedi and R. Rodrigues, *Towards Trusted Cloud Computing*, HotCloud, 9, 3–3, 2009.
- [43] Sh. Ajoudanian and Mr. Ahmadi, *A novel data security model for cloud computing*, International Journal of Engineering and Technology, IACSIT Press, 4, 3, 326, 2012.
- [44] H. Sato, A. Kanai and S. Tanimoto, *A cloud trust model in a security aware cloud*, International Symposium on Applications and the Internet (SAINT), IEEE, 10, 121–124, 2010.
- [45] Z. Xin, L. Song-qing and L. Nai-wen, *Research on cloud computing data security model based on multi-dimension*, International Symposium on Information Technology in Medicine and Education (ITME), IEEE, 2, 897–900, 2012.
- [46] H. Goudarzi and M. Pedram, *Multi-dimensional SLA-based resource allocation for multi-tier cloud computing systems*, International Conference on Cloud Computing (CLOUD), IEEE, 324–331, 2011.
- [47] A. Sheikh, M. Munro and D. Budgen, *Scheduling Security Model (SSM) for a Cloud Environment*, Conference of Cloud Computing, ACM, 2, 1, pp 1-15, 2018.
- [48] P. Watson, *A multi-level security model for partitioning workflows over federated clouds*, Journal of Cloud Computing, Springer, 1, 1, pp 1-15, 2012.
- [49] D. Budgen, *Protocol for a Systematic Literature Review on Empirical Studies of Software Visualisation*, 2011.

APPENDIX

The questionnaire in Table VI will be used to produce a quality score for each paper. Each question should be answered either yes/no (Y/N) or yes/partially/no (Y/P/Y) and there will provision for a short comment where appropriate. Values will be scored as Y=1, P=0.5 and N=0 to provide an overall quality for each paper.

TABLE VI. QUALITY QUESTIONNAIRE

No.	Question	Score	Comment
1.	Does the paper clearly state the aims of the research?	Y/N	
2.	Does the paper answer the research question?	Y/P/N	
3.	Is there any comparison?	Y/N	
4.	Does the paper adequately describe the research Methodology?	Y/P/N	
5.	Was the scheduling technique(s) adequately defined?	Y/P/N	
6.	Does the paper include defined data collection measures	Y/P/N	
7.	Does the paper defined the data collection procedures	Y/P/N	
8.	Are there any potential confounding factors adequately controlled for the analysis?	Y/N	
9.	Does the paper discuss experiment environments?	Y/N	
10.	Does the paper include and discuss of the limitation of the research?	Y/P/N	
11.	Does the paper explain what security issue is addressed / corrected?	Y/P/N	

Towards a Mechanism for Protecting Seller's Interest of Cash on Delivery by using Smart Contract in Hyperledger

Ha Xuan Son¹, Minh Hoang Nguyen², Nguyen Ngoc Phien³, Hai Trieu Le⁴, Quoc Nghiep Nguyen⁵,
Van Dai Dinh⁶, Phu Thinh Tru⁷, and The Phuc Nguyen⁸

¹FPT University, Can Tho City, Viet Nam

²Hanoi University of Science and Technology, Ha Noi, Viet Nam

³Center for Applied Information Technology, Ton Duc Thang University, Ho Chi Minh City, Vietnam

³Faculty of Information Technology, Ton Duc Thang University, Ho Chi Minh City, Vietnam

^{1, 4, 5, 6, 7}Cantho University of Technology, Can Tho City, Viet Nam

⁸University of Trento, Trento, Italy

Abstract—In emerging economies, with the explosion of e-commerce, payment methods have increasingly enhanced security. However, Cash-on-Delivery (COD) payment method still prevails in cash-based economies. Although COD allows consumers to be more proactive in making payments, it still appears to be vulnerable by the appearance of a third party (shipping companies). In this paper, we proposed a payment system based on “smart contract” implemented on top of blockchain technology to minimize risks for parties. The platform consists of a set of rules that each party must follow including specific delivery time and place, cost of delivery, mortgage money; thereby, forcing parties to be responsible for their tasks in order to complete the contract. We also provided a detailed implementation to illustrate the efficiency of our model.

Keywords—Blockchain; fintech; smart contract; customer; seller; shipper; cash on delivery; hyperledger

I. INTRODUCTION

With the development of Internet, online retail is now growing significantly. As the payment trend is shifting from Cash-on-Delivery (COD) to online payments, COD continues to remain the most preferred type of payment in cash-based economies as customers can control more over online transactions to minimize the risk of fraud. By definition, COD is a type of transaction that payments are completed at the time of delivering. Otherwise, the product would be returned to the seller. According to Nielsen's Global Connected Commerce Survey, about 83% of Indian customers prefer COD instead of online payment. UAE has up to 60% of e-commerce transactions carried out by COD [1]. However, COD poses a major drawback as shopping process might be affected by shipping carriers – a third party. These risks include misplacing parcels, lost/damaged goods or even being hijacked by the delivery company. In addition, as payment is made between the customer and shipper which is not the seller, in case the shipping company has any financial problems, they may take advantage of the clients' collected money instead of returning them to the seller (e.g. bankrupt of City Link [2] in 2014, Hanjin Shipping [3] in 2017, GNN Express – a Vietnamese delivery company – owned customers up to US\$ 230000 [4]).

This situation is becoming more and more popular recently causing damage to the seller and loss of consumer confidence.

Being able to provide high transparency in transactions and e-commerce, blockchain technology recently is becoming the *de facto* technology for financial business worldwide. Blockchain is a digital ledger providing secure options for making and recording transactions, agreements and smart contracts – anything that needs to be recorded and verified as having taken place. With its potential, blockchain enables e-commerce to be faster, safer and more reliable to both sellers and customers. Among applications of blockchain for e-commerce, to resolve the issues of COD, in this paper, we focused on designing a peer-to-peer trading platform between clients and suppliers without the presence of a trusted third-party.

Our system is implemented using the concept of “smart contract”, a core application of blockchain. Smart contract is built on top of a blockchain defining the rules between different parties who agree within the contract. Its mechanism eliminates the needs for trusted third parties as each party have to deposit some digital assets to the contract and the assets automatically get redistributed among the parties according to the contract if and only if all conditions are satisfied. Ethereum [5] uses smart contract to exchange digital assets without a trusted third party. Toward our scenario, the sellers and shipping company will sign a smart contract to ensure interests/rights of the parties: the sellers always receive their payments/goods while the carriers receive his shipping fee.

Our system is built on Hyperledger fabric which is an open source project initiated by the Linux Foundation (on December 2015) [6], [7]. Hyperledger is developed on many sub-projects within it with the general purpose of supporting utilizing blockchain technologies for enterprises. The contribution of this paper is two-fold: (i) providing a framework to ensure the customer's payment; and (ii) reducing the risk of third-party in the COD process.

This paper is organized as follows. In the second section, we briefly review related work. The following section

illustrates the concept of blockchain technology and applied technique in detail. We described our proposed architecture with its main algorithm and describes the experimental designs and discuss the results in section fourth. Finally, Section 5 presents the conclusion and future works.

II. RELATED WORKS

One of the major problems of e-commerce globally is the selling and buying of goods among the parties over the Internet in which the traders may not trust their partners. Krishnamachari et al. [8] proposed the mechanism that executes a transaction with any kinds of assets by using the digital key and these processes do not need a trusted third-party. Additionally, the authors describe a transaction method which signs dual deposit for anti-fraud payment transactions and the delivery between two parties in which the trader can use the digital signature to verify. The seller and the customer use a pair of symmetric keys to verify goods. They use smart contracts to decide and handle sellers and customers by increasing deposits. But this paper has not yet analysis on a problem of shipping, if it is a physical product and the shipper fails to comply with the commitment, then the system is not resolved. For our article, it is recommended that the shipper join the system and mortgage a sum of money to ensure the reliability of the system. Our process is given to not only ensure the benefits of the seller but also prevent shipper's fraudulent. If the shipper has problems, such as loss of goods then the goods of the seller sent at the carrier will still be refunded in cash to the seller.

HR Hasan, K Salah [9] provides a delivery process, participants (sellers, carriers, and buyers) must mortgage a value. This value is double the value of the goods shipped if the successful contract value will be returned for parties. If it fails, Arbitrator will solve the problem when disputing. We provide a time-bound solution to complete the contract if it fails on time, the system will automatically resolve the dispute, based on the contract without Arbitrator.

Two party contracts [10] propose the process using hash and key that is shipped by the seller with goods. The seller will be using the key and hash to compare whether it matches my product. Participants will make a deposit to the contract. But when goods are delivered by the shipper with the same key then it is possible for the carrier to find a way to manipulate or steal a key. Therefore this trust is not guaranteed to affect seller very much.

Deposit on `localethereum.com` [11] is an environment that is implemented by Ethereum smart contract. They introduced a process of three agents including sellers, buyers and third parties funded to deposit. Sellers and buyers trade with each other when they accept the terms of trading. A third party will ensure agreement for the transaction if a dispute happens. Currently, a reliable mediator is always `localethereum.com`. In our approaches, the mediation section is smart contract handling without an additional third party to stand out and such third party generation also increases costs more than primarily.

BitBay [12] is a market that uses decentralized platforms. Sellers and buyers join the transaction and it eliminates the trusted third-party. Therefore, the third-party is its contract.

The smart contract will be responsible for receiving the deposit, all funds will be kept in the contract until the transaction is completed. But when the seller and the buyer sign the contract, they will have to deposit a double amount of that product, it means that the item costs \$1, the buyer will put in the contract is \$2 and the seller is also \$2. So the cost incurred is a consideration.

Our article applies blockchain technology [13] to create an operational chain, and we use distributed networks to ensure the consensus of all participants. The blockchain is applied to Bitcoin [14] to solve double spending problems. Participants trade on the blockchain network using private and public key. With the deployment of blockchain networks, smart contracts are included to make transactions between different users faster and more efficient [15]. We use hyperledger fabric [6] as an open source distributed ledger platform for building applications so the blockchain platform is effective and secure.

III. OUR APPROACH

A. Blockchain and Applied Techniques

1) *BlockChain*: is a technology that enables secure data transmission based on an extremely complex encryption system, similar accounting book of a company where cash is closely monitored. In this case, Blockchain is an accounting ledger operating in the digital field. A special feature of blockchain is that transactions are executed at a high level of trust without disclosing information; security and reliability mechanisms are achieved through special mathematical functions or coding. By 2016, most Blockchain networks were used for digital money transactions. Smart contracts based on blockchain are being considered for a variety of different transaction types, from omnipresent devices to real-time operation management structures for industrial products and in-app data transmission including transaction finance. All types of business and management can participate in the network and use the properties of the blockchain system to ensure the transparency of stakeholders.

2) *Consensus Protocol*: allow parties in the network have permission to validating and maintaining the network. A transactions before submitted to ledger have to send to all node in network to ensure that the transaction is valid, so that transactions can't be tampered without parties's agreement. In addition, consensus protocol keep all node in the network synchronized with each other.

3) *Smart Contract*: is the source code stored within blockchain system and execute predetermined terms and conditions are met. Smart contract allow parties exchange goods, make payment, while avoiding the services of a trusted third parties. Basically, smart contract is developed by programmers and install by administrators. Smart contract of Hyperledger called chaincode written by golang, node.js or java language that interact to database in each block, functions in chaincode are called by client application.

4) *Hyperledger Fabric*: is an open source distributed ledger platform, design for developing permission application enterprise-grade, Fabric provide a platform to building fast, efficient and secure enterprise blockchain applications.

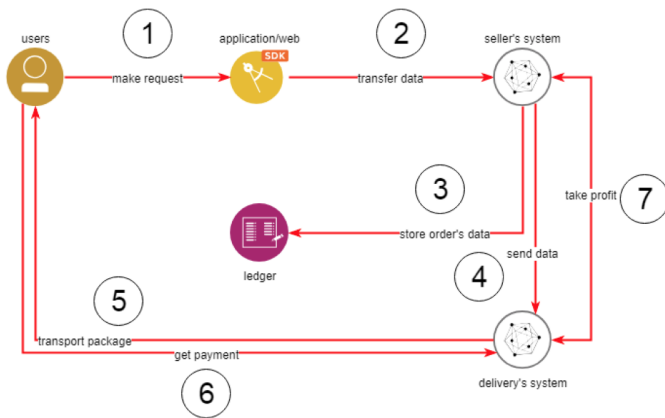


Fig. 1. The COD mechanism for protecting the seller's interest

B. General Model

COD system consist of some object: user (customer), application or website, seller, delivery, smart contract, order, distributed ledger is described in Fig. 1. In the first step, an order is made through website/application, order's information are send to seller's system and store to distributed ledger in step 2 and 3. These information is also send to delivery's system and stores again to the ledger in step fourth. After that delivery packages asset of seller and transport to customer in step 5. Next, the customer pay for asset and finally, seller and delivery take theirs profit in step 7.

IV. THE COD MECHANISM FOR PROTECTING THE SELLER'S INTEREST

A. The COD Model for Protecting the Seller's Interest

In the implementation aspect, COD system contain customer (buyer), application or website, seller's system (seller), delivery system (delivery company), smart contract, order, distributed ledger. All object of COD system are described in Fig. 2. In this picture, the black lines denoted main steps; the green dashed lines describe the delivery companies can't transport package to customer in limit time; and the black dashed lines describe the customer refuse receive package. The customers make an order on website or application (step 1), order's information are send to the seller to confirm. The seller can accept or refuse this order (from step 2 to step 4). If sellers accept the order, a contract is created with a deal to determine the price of goods and the time, location delivery, step 5. After that, the seller finds the delivery company according to the delivery fee, the previous activities of the delivery company. The seller and delivery company will mortgage money including a delivery fee from the seller and the deposit from the delivery company (equal to the goods' value) to virtual account if they agree with the requirement in the contract including time, location, and fees of delivery. This money must be locked at the virtual account in the blockchain system after that the employee of the delivery company (shipper) transports the goods to the customer. Then the seller announces to the customer that the goods are being delivered (step 6 and 7). In the case of the goods are transported within the delivery time period, the locked mortgage money is refunded to the account of the delivery company. Delivery takes customer's

payment and takes profit with seller, seller announce to the customer that the goods have delivered (between step 8 and step 13). If the customer refuses the goods, the shipper resends that goods back to the seller. Then the seller also announce to the customer (7.1 – 7.3). In case of shipper do not complete delivering within delivery time or there some trouble during delivering such as lost goods, damaged goods. The mortgage money is sent to seller's account and seller notify to the customer that the goods have been lost by the shipper from sub-step 6.1 – 6.3.

B. Algorithms

Algorithm 1 createOrder() function

- 1: **if** seller accept request **then**
- 2: **get information:** id, customer's name, seller's name, asset, quantity, price
- 3: store information to distributed ledger
- 4: **else**
- 5: announce to customer that they cannot accept request
- 6: **end if**

We present a smart contract of COD model, this have some functions that interact to database blockchain to demonstrate the operation steps of the COD process. Firstly, customer make an order, order's information is send to seller system, seller store these information to distributed ledger (**Algorithm 1**), if seller don't accept order they must announce to customer. Seller choose which delivery company they want to transport the package, information of order is send to them, if delivery company accept the order they make a mortgage to virtual account, if not delivery transport package to customer, seller store order's information with delivering state, customer pay for asset (**Algorithm 2**). In case of customer refuse the package, deliverer transport back to seller delivery and seller take theirs profit, seller announce to customer that package have delivered (**Algorithm 3**).

Algorithm 2 delivering() function

- 1: get information of order
- 2: **if** delivery accept order **then**
- 3: announces to seller that they accepts the order
- 4: transfers money to virtual account
- 5: transport package to customer
- 6: **if** customer don't receive package within the limit time **then**
- 7: money in virtual account transferred to seller's account
- 8: **end if**
- 9: **else if** delivery refuse the order **then**
- 10: announces to seller that they refuse the order
- 11: choose other delivery
- 12: **end if**

C. Set Up Environment

In this section, we provide describe the environment used to implement the algorithm described above The system configuration for the experiments is a 64-bit machine with 8GB of RAM and 2.5 GHz Intel Core i5 CPU running Ubuntu

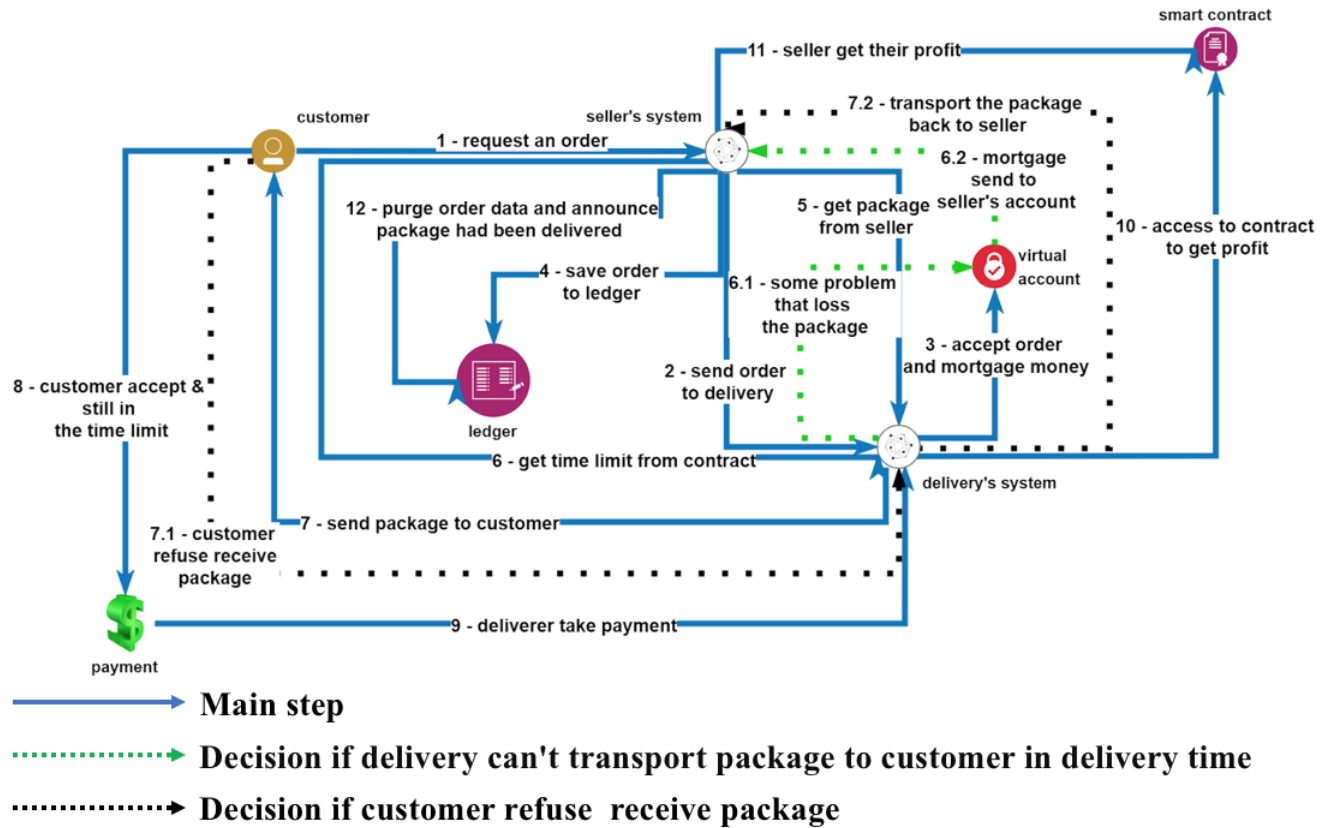


Fig. 2. The COD mechanism for protecting the seller's interest

Algorithm 3 takeProfit() function

- 1: **if** customer accept package **then**
- 2: deliverer receive money
- 3: delivery ad seller take their profit
- 4: **else**
- 5: deliverer take package and give back to seller
- 6: **end if**

18.10 Cosmic Cuttlefish. We have implemented the DeM-CoD framework by using Hyperledger Fabric version 1.4¹ for deploying CoD process on the Blockchain and Golang for implementing CoD's businesses and cryptography functions². The main steps of the COD system are described in detail below.

Open the terminal and go to the directory first-network, execute these command to start network:

```
./byfn.sh down
./byfn.sh up -c mychannel -s couchdb
```

after start the network it will create four peer, public key and private of each peer in two org:

```
peer0.org1.example.com
peer1.org1.example.com
```

```
peer0.org2.example.com
peer1.org2.example.com
```

We just need peer0 of each org to represent seller and delivery of two organization. enter the CLI container.

```
docker exec -it cli bash
```

In default setting, after starting the BYFN network, the active peer is set to: CORE_PEER_ADDRESS=peer0.org1.example.com:7051, in detail it is use public key and private key created when you start network above, so you just install smart contract in peer0 of org1 to represent a seller company by execute the command:

```
peer chaincode install -n COD -v 1.0 -p
github.com/hyperledger/fabric-samples/
chaincode/COD/COD_chaincode/
```

Switching to org2 to install smart contract, note that we just install to peer0 of org1 and org2 because we use only one peer of each organization to represent seller and delivery:

```
export CORE_PEER_LOCALMSPID=Org2MSP
export PEER0_ORG2_CA=/opt/gopath/src/git
hub.com/hyperledger/fabric/peer/crypto/peer
Organizations/org2.example.com/peers/peer0.
org2.example.com/tls/ca.crt
export CORE_PEER_TLS_ROOTCERT_FILE=$PEER0
_ORG2_CA
```

¹<https://hyperledger-fabric.readthedocs.io/en/release-1.4/>
²<https://github.com/xuansonha17031991/CashOnDelevery-Chaincode>

```
export CORE_PEER MSPCONFIGPATH=/opt/gopath/src/github.com/hyperledger/fabric/peer/crypto/peerOrganizations/org2.example.com/users/Admin@org2.example.com/msp
```

Change the active peer to peer0 in org2 and install the chaincode:

```
export CORE_PEER_ADDRESS=peer0.org2.example.com:7051
```

```
peer chaincode install -n marblesp -v 1.0 -p github.com/hyperledger/fabric-samples/chaincode/COD/COD_chaincode/
```

```
peer chaincode instantiate -o orderer.example.com:7050 --tls --cafile $ORDERER_CA -C mychannel -n COD -v 1.0 -c '{"Args":["Init"]}' -P "OR('Org1MSP.member', 'Org2MSP.member')" --collections-config $GOPATH/src/github.com/chaincode/COD/COD_chaincode/collection.json
```

Now the smart contract have installed in two organization represent for seller (org1) and delivery (org2), you can run the functions directly in the smart contract

D. Workflow

Step 1: Create prerequisites information. To participate in the network, companies need to initiates prerequisites information that is assets of sellers, accounts to make payments of seller and delivery, suppose that this information is ready in the network.

query seller's asset

```
{
  "docType": "Seller",
  "name": "seller_1",
  "asset": "Dell_inspiron_5000",
  "quantity": 2, "price": 1560
}
```

query seller's balance

```
{
  "balance": 5000,
  "docType": "balance",
  "name": "seller_1_balance"
}
```

delivery's balance

```
{
  "balance": 5000,
  "docType": "balance",
  "name": "delivery_1_balance"
}
```

Step 2: when customer make an order, customer's information and order's information is created customer's information

```
{
  "docType": "customer",
```

```
  "email": "someone@email.com",
  "location": "Vietnam",
  "name": "customer_1",
  "number": "01234567899"
}
```

order's information

```
{
  "docType": "Order",
  "asset": "Dell_inspiron_5000",
  "customer": "customer_1",
  "delivery": "delivery_1",
  "orderid": "order_1",
  "price": "1560",
  "quantity": 2,
  "seller": "seller_1",
  "status": "waiting"
}
```

Step 3: after order accepted, seller contact to delivery company to make a deal with limit time. The limit time is set up at application layer so it isn't mentioned here, a virtual account is initialized if delivery company agree with that dealing. Finally, delivery make a mortgage to that virtual account, note that the mortgage must equal to asset's price.

query after create virtual account with balance 0

```
{
  "docType": "balance",
  "balance": 0,
  "name": "virtual_account"
}
```

The balance properties of the virtual account is updated to 1560, equivalent to asset's price when delivery mortgage. Now, delivery transport the package to customer the status of package is changed to present that it is delivering.

query's result

```
{
  "docType": "Order",
  "asset": "Dell_inspiron_5000",
  "customer": "customer_1",
  "delivery": "delivery_1",
  "orderid": "order_1",
  "price": "1560",
  "quantity": 2,
  "seller": "seller_1",
  "status": "delivering"
}
```

Step 4: Customer make a payment, delivery take money and receive theirs profit with seller. After that seller announce to customer to confirm that the package have delivered and money in virtual account automatically transfer back to delivery account. The status properties also change to delivered and store to ledger change status of the package the balance of virtual account is transferred to delivery, as mentioned above the rate is 3/7 so delivery take 30% of payment and seller

receive 70%, in detail the seller's balance receive \$1092 (70% of \$1560) and delivery have \$468(30% of \$1560). These rate depend on business mechanism of companies. In case of some problem that causes loss of goods or the delivery company does shipping the goods on time, the amount in the virtual account is automatically transferred to the seller's account.

Query's result after change status of the package to delivered

```
{  
  "docType": "Order",  
  "asset": "Dell_inspiron_5000",  
  "customer": "customer_1",  
  "delivery": "delivery_1",  
  "orderid": "order_1",  
  "price": "1560",  
  "quantity": 2,  
  "seller": "seller_1",  
  "status": "delivered"  
}
```

E. Discussion

The current COD model still has limitations when a mechanism to protect sellers has not been offered, this paper points out those limitations and suggests an additional process to be implemented on smart contract. However, the objects and information is created is only objective reference and will be further studied to build a complete system. Hyperledger fabric is used to build peer to peer applications on blockchain networks and deploy, install smart contracts on that networks. In this paper we presents an additional process of COD model to solve the delivery side issues that directly affect the interests of seller and indirectly reduces the quality of services. Research results is COD process that has been implemented with smart contracts.

This paper presents an additional process of COD model to solve the delivery side issues that directly affect the interests of seller and indirectly reduces the quality of services. Research results is COD process that has been implemented with smart contracts. This is the basis for developing a complete system, from which businesses can consult to apply to their business models. However, the process is only implemented in the form of smart contract, there is not a complete system and has not yet developed the privacy protection feature.

V. CONCLUSION

In summary, this paper focuses on analyzing and outlining existing gaps within the COD process and thereby presenting solutions to address through blockchain technology. There is a worthy solution if they decide to apply COD model in their business this is the basis for developing a complete system, from which businesses can consult to apply to their business models.

However, the process is only implemented in the form of smart contract, there is not a complete system and has not yet developed the privacy protection feature, so we will continue to develop a complete system based on this smart contracts. In the future, we are confident that the number of companies applying COD model will be increased hence the need for blockchain applications in business has become more necessary than ever. Smart contract is the heart of the blockchain system and the infrastructure for businesses to develop their own blockchain-based system.

REFERENCES

- [1] "Cash on delivery the biggest obstacle to e-commerce in uae and region," 2014. [Online]. Available: <https://www.thenational.ae/business/technology/cash-on-delivery-the-biggest-obstacle-to-e-commerce-in-uae-and-region-1.604383>
- [2] "The reason city link went bust on christmas day," 2014. [Online]. Available: <https://www.forbes.com/sites/timworstall/2014/12/27/the-reason-city-link-went-bust-on-christmas-day/>
- [3] "The end of hanjin shipping - officially declared bankrupt," 2017. [Online]. Available: <http://www.seatrade-maritime.com/news/asia/the-end-of-hanjin-shipping-officially-declared-bankrupt.html>
- [4] "Gnn: a prime example of cod payment risk," 2018. [Online]. Available: <https://www.vir.com.vn/gnn-a-prime-example-of-cod-payment-risk-62270.html>
- [5] "Ethereum," 2018. [Online]. Available: <https://ethereum.org/>
- [6] "Hyperledger fabric," 2019. [Online]. Available: <https://hyperledger-fabric.readthedocs.io/en/release-1.4/>
- [7] X. S. Ha *et al.*, "Dem-cod: Novel access-control-based cash on delivery mechanism for decentralized marketplace,"
- [8] A. Asgaonkar and B. Krishnamachari, "Solving the buyer and seller's dilemma: A dual-deposit escrow smart contract for provably cheat-proof delivery and payment for a digital good without a trusted mediator," 2018.
- [9] H. R. Hasan and K. Salah, "Blockchain-based solution for proof of delivery of physical assets," in *International Conference on Blockchain*. Springer, 2018, pp. 139–152.
- [10] "Two party contracts," 2018. [Online]. Available: <https://dappsforbeginners.wordpress.com/tutorials/two-party-contracts/>
- [11] "How our escrow smart contract works," 2018. [Online]. Available: <https://dappsforbeginners.wordpress.com/tutorials/two-party-contracts/>
- [12] "Double deposit escrow," January 2018. [Online]. Available: <https://bitbay.market/double-deposit-escrow>
- [13] J. Bremer and S. Lehnhoff, "Decentralized coalition formation with agent-based combinatorial heuristics," *ADCAIJ: Advances in Distributed Computing and Artificial Intelligence Journal*, vol. 6, no. 3, pp. 29–44, 2017.
- [14] "A peer-to-peer electronic cash system," 2008. [Online]. Available: <https://bitcoin.org/bitcoin.pdf>
- [15] A. González, J. Ramos, J. F. De Paz, and J. M. Corchado, "Obtaining relevant genes by analysis of expression arrays with a multi-agent system," in *9th International Conference on Practical Applications of Computational Biology and Bioinformatics*. Springer, 2015, pp. 137–146.

Dynamic Modification of Activation Function using the Backpropagation Algorithm in the Artificial Neural Networks

Marina Adriana Mercioni¹, Alexandru Tiron², Stefan Holban³
Department of Computer Science
Politehnica University Timisoara, Timisoara, Romania

Abstract—The paper proposes the dynamic modification of the activation function in a learning technique, more exactly backpropagation algorithm. The modification consists in changing slope of sigmoid function for activation function according to increase or decrease the error in an epoch of learning. The study was done using the Waikato Environment for Knowledge Analysis (WEKA) platform to complete adding this feature in Multilayer Perceptron class. This study aims the dynamic modification of activation function has changed to relative gradient error, also neural networks with hidden layers have not used for it.

Keywords—Artificial neural networks; activation function; sigmoid function; WEKA; multilayer perceptron; instance; classifier; gradient; rate metric; performance; dynamic modification

I. INTRODUCTION

The behavior of artificial neural networks has been an area that has been extensively studied over time, providing consistent results. It studied the computational power of artificial neural networks by activating recurring sigmoid. [1] This aspect occurs due to the diversity of systems which are described by datasets used for exercising them.

In applications, the activation function and gradient selection are impacted directly by network convergence. [2].

In this context, the universal behavior of Turing neural networks has been studied for a specific activation function which was called linear function by form:

$$f(x) = \begin{cases} 0, & x \leq 0 \\ x, & 0 < x < 1 \\ 1, & x \geq 1 \end{cases} \quad (1)$$

An activation function in computing of neural artificial networks plays an important role [3, 4].

Neural networks consist of an important method for analysis of activation function because of their capability to deal with data sets which change. For example, in Multilayer Perceptron (MLP), the most common system, neurons are organized in layers [5].

One of the activation functions studied on large scale in the literature is the sigmoid function:

$$g(x) = \frac{1}{1+e^{-x}} \quad (2)$$

These functions represent the main activation functions, being currently the most used by neural networks, representing from this reason a standard in building of an architecture of Neural Network type [6,7].

The activation functions that have been proposed along the time were analyzed in the light of the applicability of the backpropagation algorithm. It has noted that a function that enables differentiated rate calculated by the neural network to be differentiated so and the error of function becomes differentiated [8].

The main purpose of activation function consists in the scalation of outputs of the neurons in neural networks and the introduction a non-linear relationship between the input and output of the neuron [9].

By the other hand, the sigmoid function is used usually for hidden layers because it combines the linear, curvilinear and constant behavior depends by the input value [10].

Also, it has demonstrated that sigmoid function is not efficiently for a single hidden unit, but when more hidden units are involved, it becomes more usefully [11].

Our approach in this paper consists in dynamic modifying of activation function using backpropagation algorithm for training an artificial neural network.

II. BACKPROPAGATION ALGORITHM

It is the most common algorithm used to train neural networks regardless of the nature of the data set used. The Neural network architecture is determined by repeat trials, the goal is to obtain the best possible classification of data set used in this context [8, 12].

Backpropagation algorithm is a supervised learning algorithm and his purpose is to correct the error. It compares the computed output value with the real value, and it tries to change the weights through the calculated error, and in analog manner until the size of obtained error becomes smaller than the error obtained in the first round. The backpropagation network composition is detailed in Fig. 1 [13].

As learning strategy, the backpropagation algorithm proved to be effectively in that it ensures a classification whose accuracy is generally satisfactory [14, 15].

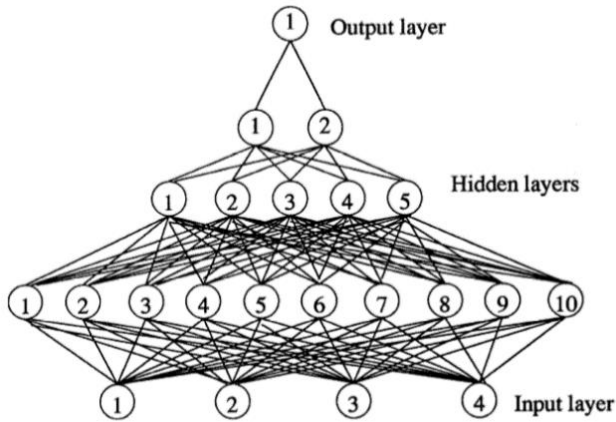


Fig. 1. Backpropagation Network [12].

The main disadvantage of this learning technique is the fact that they are required repeated attempts to establish network architecture, number of hidden layers and number of neurons in each hidden layer, in the context in which training requires a lot of resources as memory and runtime, as in Fig. 2.

The classical backpropagation algorithm is divided in two phases: the first phase consists in the propagation of useful information from the input layer toward the exit, then spread in the reverse direction of errors, and the second phase consists in updating the weights.

- In the first phase, the input data propagate through the network to generate the output values, then calculate the error and propagate back toward the hidden layers and toward the entry to generate the differences between the obtained values and actual values for each neuron.
- In the second phase, for each weight calculates the gradient of error using generated differences in the first step. This weight is updated in the opposite direction to the error by a coefficient of learning.

Backpropagation algorithm has been focused on theorems which have guaranteed „universal approximation”, a property of neural networks [16].

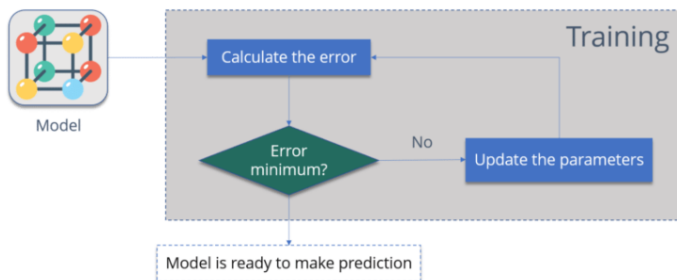


Fig. 2. Backpropagation Algorithm (Source: <https://d1jnx9ba8s6j9r.cloudfront.net/blog/wp-content/uploads/2017/09/Training-A-Neural-Network-Backpropagation-Edureka-768x314.png>).

III. BACKPROPAGATION ALGORITHM WITH DYNAMIC ACTIVATION FUNCTION

The main element of an artificial neural network is artificial neuron, which can be represented by a sum and a function, so the network will be composed of several interconnected functions. More clearly, these functions are the filters through which the information passes. And depending on how we want to learn neural network, these functions have specific characteristics to the chosen purpose [17,19].

One of the most important characteristics of an artificial neural network is the activation function [7].

One of the most important activation functions is sigmoid function. From point of view of evolution, this function has developed from Heaviside function as it is showed in Fig. 3.

The sigmoid function can be calculated as it is showed in Fig. 4; respectively its curve can be seen.

Among the most commonly available types of activation functions we mention them in Fig. 5:

Whatever type of activation function and its characteristics, it remains unchanged during the training process.

We consider that this aspect represents a serious restriction. How learning is a process of dynamic change of weights which characterize numerically the connections between neurons of network, it is normally that this learning process to be reflected in the dynamic activation function by dynamic changing of its characteristics [20].

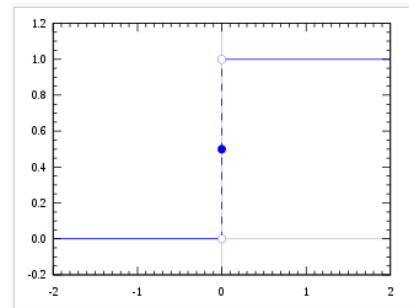


Fig. 3. Heaviside Function (Source: https://upload.wikimedia.org/wikipedia/commons/thumb/d/d9/Dirac_distribution_CDF.svg/1280px-Dirac_distribution_CDF.svg.png).

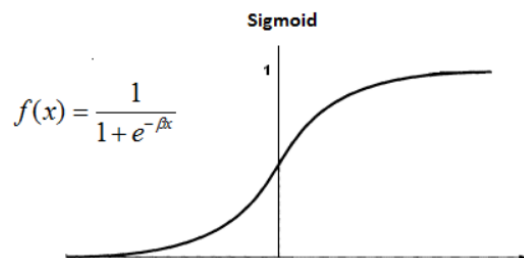


Fig. 4. Sigmoid function (Source: https://cdn-images-1.medium.com/max/1200/1*8SJcWjxz8j7YtY6K-DWxKw.png).

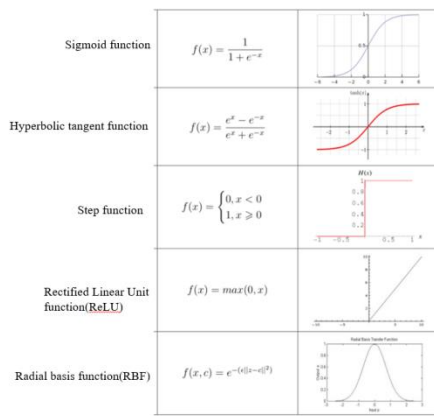


Fig. 5. Activation Function Types (Source: <https://www.code-it.ro/wp-content/uploads/2018/11/Screenshot-2018-11-12-at-22.36.39.png>).

In other words, learning is both dynamic modification of weights and also dynamic modification of activation function characteristics.

To achieve this goal we start from a classical activation function, more exactly sigmoid function (Fig. 4) wherein the β coefficient value is set dynamically during each epoch of learning simultaneously with the adjustment of the weights.

The initial value was considered to be 1 so that this value can change (increase or decrease) depending on the error level of present gradient in each of the learning epochs. The percentage change of this coefficient and its direction of adjustment (increase or decrease) is set by the user at the beginning of the learning process.

IV. EXPERIMENTAL EXPERIMENTS

In this study we took in consideration an activation function by sigmoid type in the context of a neural network architecture without hidden layers. The study has been done considering:

- The β coefficient value of activation function decreases if the error increases during an epoch, respectively it increases. The direction can reverse (β coefficient value of activation function increases if the error increases during an epoch, respectively decreases, if the error decreases) is defined at the start of training.
- Percentage to scale this coefficient is set at the beginning of the training. It is defined by user.

In our experiments we consider the scenario:

- The β coefficient of activation function decreases if the error value increases during an epoch, the coefficient increases, if the error decreases.
- The percentage of modification for β coefficient was 10%, respectively 5% from actual value during training epoch.

To achieve the scenario above, Multilayer Perceptron Classifier has been changed through Weka 3.8.3 platform provided by adding a parameter that determines the direction of change of β value for activation function as the coefficient which is modified. The two parameters are:

- **modRate** which specifies the percentage of modification for β coefficient.
- **variant** which defines the direction of change for β value (True - in case the value of β coefficient for activation function decreases, if the error increases during an epoch, respectively it increases, if the error decreases and False otherwise).

Added code can be viewed in Fig. 6:

From point of view of user, the modification sets initial settings for training process which can be visualized in Fig. 7 with the implicit values which are $\beta=10\%$ and modification direction variant=True.

The study was performed taking into account a total of 10 sets of data provided by this platform as follows.

For these data sets we can observe the experimental results in the following tables and diagrams, which are centralized in Tables 1 and 2 and Fig. 8.

```

if(m_variant == true) { // varianta 1
    for (int i=0 ; i < m_neuralNodes.length ; i++) {
        crt_node = m_neuralNodes[i];
        m_sigmodUnit.set2(sigm_m[i]);
        crt_err = crt_node.errorValue(true);
        if(crt_err < prev_err_per_neuron[i])
            m_sigmodUnit.set2(m_sigmodUnit.get2()+(m_sigmodUnit.get2()*getModRate()));
        if(crt_err > prev_err_per_neuron[i])
            m_sigmodUnit.set2(m_sigmodUnit.get2()-(m_sigmodUnit.get2()*getModRate()));
        prev_err_per_neuron[i] = crt_err;
    }
}

if(m_variant == false) { // varianta 2
    for(int i=0 ; i < m_neuralNodes.length ; i++) {
        crt_node = m_neuralNodes[i];
        m_sigmodUnit.set2(sigm_m[i]);
        crt_err = crt_node.errorValue(true);
        if(crt_err > prev_err_per_neuron[i])
            m_sigmodUnit.set2(m_sigmodUnit.get2()+(m_sigmodUnit.get2()*getModRate()));
        if(crt_err < prev_err_per_neuron[i])
            m_sigmodUnit.set2(m_sigmodUnit.get2()-(m_sigmodUnit.get2()*getModRate()));
        prev_err_per_neuron[i] = crt_err;
    }
    //m_sigmodUnit.set2(0); // for debugging
}
    
```

Fig. 6. Changes Added to Multilayer Perceptron Class..

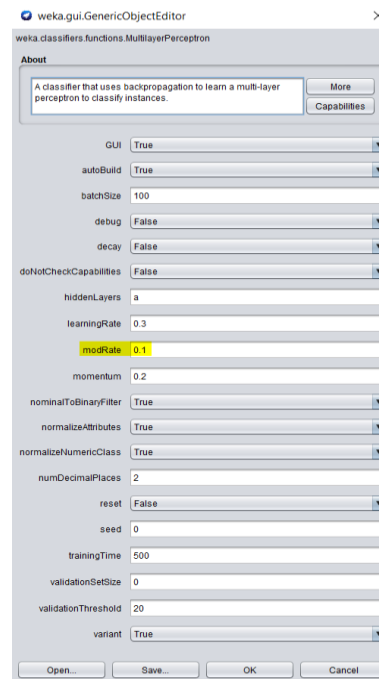


Fig. 7. β Values Set (modRate) and Modification Direction (Variant).

TABLE I. ERROR PER EPOCH

Data set	Variation Error per Epoch $\beta=5\%$ %	Variation Error per Epoch $\beta=10\%$ %
diabetes.arff	0.064609	2.172752
iris.arff	-0.4377358	-0.398922
credit_g.arff	27.853203	13.34323
zoo.arff	136.95652	-30
mushroom.arff	-25	-80
anneal.arff	-2.3637525	-85.01997
balance_scale.arff	0.3788186	1.084578
glass.arff	0.9818232	2.139382
sonar.arff	1.0156026	1.707687
car.arff	-1.2320329	-15.19507
letter.arff	2.1341222	1.921839

TABLE II. INSTANCE CLASSIFICATION

Data set	Dynamic Variation of Instances Classified Correctly $\beta=5\%$ %	Dynamic Variation of Instances Classified Correctly $\beta=10\%$ %
diabetes.arff	0.646161863	-1.777069
iris.arff	0	0
credit_g.arff	-0.201409869	-0.100705
zoo.arff	0	0
mushroom.arff	0	0
anneal.arff	1.283500796	4.426815
balance_scale.arff	-0.173611111	-0.173611
glass.arff	0.543490271	-1.086981
sonar.arff	0	0
car.arff	0	0
letter.arff	-0.891395307	-0.770117

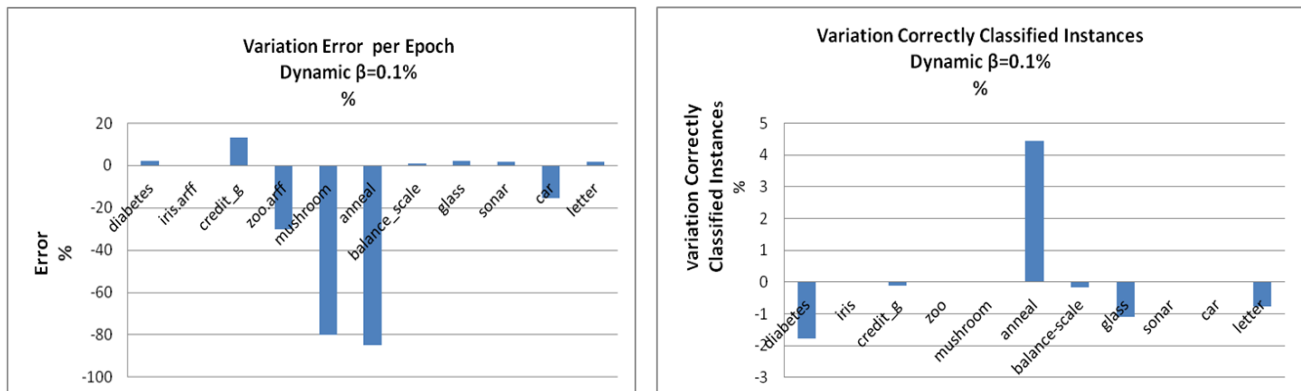


Fig. 8. Variation Error Per Epoch and Correctly Classified Instances in Dynamic Mode.

V. EVALUATION IMPACT OF TRAINING PROCESS BY DYNAMIC INTRODUCING ACTIVATION FUNCTION

After analyzing the experimental results several observations can be made:

1) Introduction of the concept according to the dynamic activation leads to a change in drive definite process that quickly leads to a reduction of the error learning.

For example, this aspect is visible in the graph of error evolution in the case of using the iris.arff data set ($\beta = 10\%$, variant = True) as it is showed in Fig. 9.

It can be seen in the first 50 epochs the modification of characteristics activation function leads to a search process directed toward a lower error in the training process. This aspect is present also in the case ($\beta=5\%$, variant=True), it can be visualized in the graph in Fig. 10.

2) For a number of four data sets (zoo.arff, mushroom.arff, anneal.arff, carr.arff) reveals a definite reduction of the error obtained at the end of the 500 epochs of training.

The error of training is reduced as follows: 30% for zoo.arff, 80% for mushroom.arff, 85% for anneal.arff data set respectively with 15 for carr.arff compared to the situation where the training to perform a static activation function whose features remain constant in the training process.

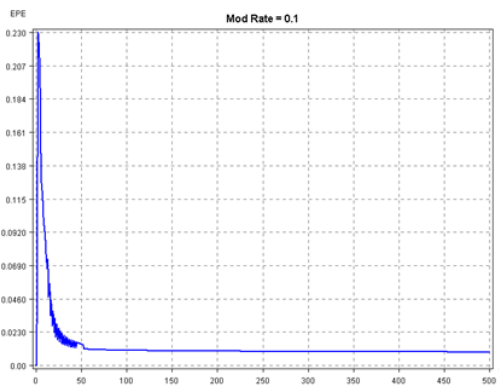


Fig. 9. The Graph of Error Variation/Epoch ($\beta=10\%$, Variant=True).

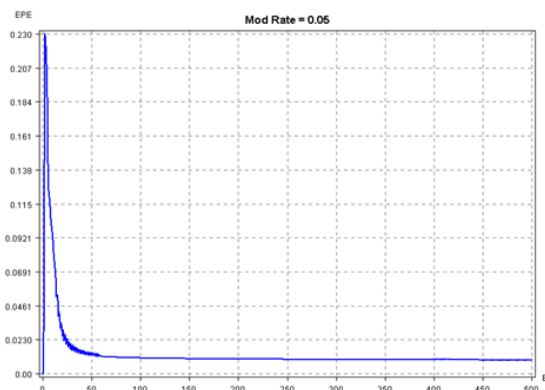


Fig. 10. The Graph of Error Variation / Epoch ($\beta=5\%$, Variant=True).

The only data set where error of training increases is credit_g.arff, whose error increases by 15%. For other datasets variation of error is insignificant.

3) An interesting aspect is related to the following thing: for credit_g.arff data set, whose error increases, we can see that in testing phase it keeps the same number of instance correct classified as in the case of using an unchanged activation function. This aspect is remarked for zoo.arff data set, which for $\beta=5\%$ coefficient we have on the hand an increase of training error equal to 136.9%, but on the other hand when we pass to testing phase, doesn't appear any variation in the number of instances classified correctly. This aspect looks to be a result in fact the instances from data set for a static activation function aren't classified correctly, so in the case of activation function some data set are classified correctly meanwhile other instances are incorrectly classified.

4) We can see that significant differences occur between a dynamic activation of function with $\beta = 10\%$ and a dynamic activation of function with $\beta = 5\%$. But what we can also see in both cases is an improvement in accuracy of classification. It is also specified that will be necessary to find the optimal of dynamic modification for activation function from a training epoch to another training epoch.

VI. CONCLUSIONS

Introducing the concept of dynamic modification during the training process leads to an increase of accuracy for classification. We can remark that a classical training algorithm such as backpropagation algorithm becomes more flexible in the meaning that the learning algorithm is faster guided toward a classification error generally lower.

The proposed method is attempted to monitor the error and check the status for accuracy for different data sets.

Influence of the nature of the data set is no longer reflected in the weights of the neural network but it can be reflected in the activation function. For this reason, the dynamic modification of the activation function may represent a significant way to improve the classification neural network in the wide range of directions where can advance this concept.

REFERENCES

- [1] J. Kilian, H. T. Siegelmann, "The Dynamic Universality of Sigmoidal Neural Networks", New Jersey, Israel, information and computation 128, pp. 48-56, 1996.
- [2] J. Hu, Lili Xu, X. Wang, X. Xu, G. Su, "Effects of BP Algorithm-based Activation Functions on Neural Network Convergence", Journal of Computers Vol. 29 No. 1, pp. 76-85, 2018.
- [3] V. Tiwari, N. Khare, "Hardware implementation of neural network with Sigmoidal activation functions using CORDIC, Microprocessors and Microsystems", 39(6), pp. 373-381, 2015.
- [4] Z.J. Jia, Y.D. Song, D.Y. Li, P. Li, "Tracking control of nonaffine systems using bio-inspired networks with autotuning activation functions and self-growing neurons", Information Sciences pp. 388-389, 191-208, 2017.
- [5] A. F. Sheta, S. E. M. Ahmed, H. Faris, "A Comparison between Regression, Artificial Neural Networks and Support Vector Machines for Predicting Stock Market Index", (IJARAD) International Journal of Advanced Research in Artificial Intelligence, Vol. 4, No.7, 2015.

- [6] Siegelmann, H. T., and Sontag, „Turing computability with neural networks”, *Appl. Math. Lett.* 4, 6, 1991.
- [7] C. Özkan, F. S. Erbek, “The Comparison of Activation Functions for Multispectral Landsat TM Image Classification”, *Istanbul Photogrammetric Engineering & Remote Sensing* Vol. 69, No. 11, pp. 1225–1234, 2003.
- [8] R. Rojas, „Neural Networks”, Berlin, Springer-Verlag, 1996.
- [9] Oda, Tetsuya, et al, “A Neural Network Based User Identification for Tor Networks: Comparison Analysis of Different Activation Functions Using Friedman Test”, *Network-Based Information Systems (NBIS)*, 19th International Conference on. IEEE, 2016.
- [10] M. Cilimkovic, „Neural Networks and Back Propagation Algorithm”, Ireland, 2015.
- [11] K. Hara, K. Nakayama, „Comparison of activation functions in multilayer neural network for pattern classification”, *Proceedings of 1994 IEEE International Conference on Neural Networks (ICNN'94)*, Orlando, USA, pp. 2997-3002 vol.5. doi: 10.1109/ICNN.1994.374710, 1994.
- [12] J. Roman, A. Jameel, “Backpropagation and Recurrent Neural Networks in Financial Analysis of Multiple Stock Market Returns”, Xavier University of Louisiana, *Proceedings of the 29th Annual Hawaii International Conference on System Sciences – 1996*.
- [13] Z. Soltani, A. Jafarian, „A New Artificial Neural Networks Approach for Diagnosing Diabetes Disease Type I”, (IJACSA) International Journal of Advanced Computer Science and Applications, Vol. 7, No. 6, 2016.
- [14] P. Koehn, “Combining Genetic Algorithms and Neural Networks: The Encoding Problem”, A Thesis Presented for the Master of Science Degree The University of Tennessee, Knoxville, 1994.
- [15] V. N. Manohar, G.U. Chaudhari, B. Mohanty, “Function approximation using back propagation algorithm in artificial neural networks”, Rourkela, 2007.
- [16] Han J., Moraga C. „The influence of the sigmoid function parameters on the speed of backpropagation learning”, Berlin, Heidelberg, In: Mira J., Sandoval F. (eds) *From Natural to Artificial Neural Computation. Lecture Notes in Computer Science*, vol 930. Springer, 1995.
- [17] Siegelmann, H. T., and Sontag, E. D., „On the computational power of neural networks”, *J. Comput. System Sci.* 50, 132150, 1995.
- [18] T.Jayalakshmi, Dr.A.Santhakumaran, “Statistical Normalization and Back Propagation for Classification”, *International Journal of Computer Theory and Engineering*, Vol.3, No.1, pp. 1793-8201, 2011.
- [19] A. Gupts, M. Lam, “The Weight Decay backpropagation for generalizations with missing values”, *Annals of Operations Research*, Science publishers, pp.165-187, 1998.
- [20] Liu, Qiang, Yu, Feng, Wu, Shu, Wang, Liang, „A convolutional click prediction model. *Proceedings of the 24th ACM International on Conference on Information and Knowledge Management*”, pp. 1743–1746, 2015.

Fault Injection and Test Approach for Behavioural Verilog Designs using the Proposed RASP-FIT Tool

Abdul Rafay Khatri¹, Ali Hayek², Josef Börcsök³
Department of Computer Architecture and System Programming,
University of Kassel, Kassel, Germany

Abstract—Soft-core processors and complex Field Programmable Gate Array (FPGA) designs are described as an algorithmic manner, i.e. behavioural abstraction level in Hardware Description Languages (HDL). Lower abstraction levels add complexity and delays in the design cycle as well as in the fault injection approach. Therefore, fault simulation/emulation techniques are demanded to develop an approach for testing of design and to evaluate dependability analysis of FPGA designs at this abstraction level. Broadly, the fault injection techniques for FPGA-based designs at the HDL code level are categorised into emulation and simulation-based techniques. This work is an extension of our previous methodologies developed for FPGA designs written at data-flow and gate abstraction levels under the proposed RASP-FIT tool. These methodologies include fault injection by code parsing of the SUT, test approach for finding the test vectors using dynamic and static compaction techniques, fault coverage, and compaction ratio directly at the code level of the design. In this paper, we described the proposed approaches briefly, and the enhancement of a Verilog code modifier for the behavioural designs is presented in detail.

Keywords—Behavioural designs; code parsing; fault injection; test approach; Verilog HDL

I. INTRODUCTION

During the last few decades, the Very Large Scale Integrated (VLSI) systems and soft-core processors have been developed and implemented on the Field Programmable Gate Array (FPGA). These systems are written in Hardware Description Languages (HDL). HDL is also involved in enhancing several methodologies associated with digital system testing and fault simulation/emulation applications. When a new method is devised and fabricated for a particular design, it requires testing which can confirm the accuracy of the design and the testing technique itself. These testing procedures are carried out in the design laboratory rather than in a factory. Therefore, it requires the involvement of the design and test engineers. The design engineer first converts the system specifications in an HDL language such as Verilog. The design engineers can verify the design & apply advanced testing techniques at an early stage by using HDL and testing can directly be applied to the designs. It diminishes the passageway between the tools and methodologies which are used at the time of development of design and testing [1]. It also contributes a rival service by lessening the cost and production time for a system [2].

One of the most popularly accepted HDL language for implementing soft-core processors and Application Specific Integrated Circuit (ASIC) is Verilog HDL. These designs are implemented on the FPGA [1], [3]. In a Register Transfer Level (RTL) design process, the designer first formulates the design specification in an RTL level language such as

Verilog. RTL is a combination of data-flow and behavioural modelling, which characterises the design [2]. For vast and intricate designs, the highest level of abstraction is applied, i.e. behavioural abstraction level. The plan is to develop some methods to bring the testability approaches and dependability evaluation techniques to achieve cost-effectiveness and reduce time solution directly at the code level of the target design.

Testing of digital circuits has traditionally been accomplished using fault models at lower abstraction level or subsequently. Testability is one of the most crucial dependability factors which should be investigated during the development flow stages along with reliability, speed, power consumption and cost for the end user [4]. The integrated circuit has been extended in both size and complexity by the passing days with the continually progressing technology. Fault simulation and testing methods at higher levels of abstraction have a greater chance of being integrated well into the overall design flow.

Fault Injection (FI) method performs an indispensable role in different testability approaches and dependability analysis of FPGA-based designs. FI method injects faults in the System Under Test (SUT) and then the responses of the golden (fault-free) system are matched with the responses of the faulty SUT. After that results are used in the evaluation of the SUT for verification and robustness [1], [5]. We introduced the term “hardness analysis”. It is an algorithm, developed under the proposed tool, which is used to find the sensitive location of the design and then to apply redundancy to those locations to achieve high reliability in terms of the reduction in Soft-Error Rate (SER) [6]. However, in this work, the hardness analysis is not discussed.

This work is a continuation of our previous work [7]–[10]. In these works, authors developed an FI tool named RASP-FIT (RechnerArchitektur and SystemProgrammierung-Fault Injection Tool). The first part of the tool’s name is the German name of the institute. There are three major components of the proposed RASP-FIT tool discussed in this paper:

- 1) Verilog code modifier (code parser) based on instrumentation technique.
- 2) Fault injection control unit provides full controllability and observability about fault locations.
- 3) Result analyser consists of test vector compaction and Fault Coverage (FC) estimation.

In this work, fault injection modifier is upgraded to deal with the vast and complicated design written at the behavioural level. Once, the faulty design is achieved then the proposed

fault injection testing approach is applied and obtained the small number of test vectors for maximum FC.

The organisation of the paper is as follows: The background is explained in Section II. The improvement of the RASP-FIT tool to modify the behavioural designs is introduced in Section III, and it also illustrates the proposed functionalities of the result analyser. Results of fault injection algorithm, test vectors, fault coverage and compaction are presented in Section IV. Lastly, Section V concludes the paper and presents some directions for future work.

II. BACKGROUND

Fault injection and fault simulation approaches are utilised to investigate the consequence of a fault on an embedded hardware/programming framework. As a rule, fault injection is performed on abstract models of the SUT either to recoup early outcomes when the realisation of the system is not finished up yet or to accelerate the runtime for fast fault simulation on explicit models. The higher level of abstraction is RTL, which can not cover all the gate level faults [4]. Fault simulation applications at the RTL level can, for the most part, beat the computational expenses. However, existing higher level fault simulation applications does inadequately relate to RTL fault simulation. For assessing a design concerning robustness against soft-errors, for example, injected by radiation, the system is simulated while artificial faults are incorporated [11]. Authors in [12] demonstrated that RTL fault models could be used for the robustness evaluation of FPGA-based designs. In this work, new RTL fault models are developed and inserted to perform fault injection campaign. Fault injection tool "TSIM" [13] has viewed as a minimal cost, adaptable and accurate framework for fault injection experimentation at the RTL level of the designs.

Concurrent fault simulation is applied to the RTL designs, finds fault coverage, test vectors and developed RTL fault models are presented in [14]. Sandia et al. showed in their work that fault injection experiment at the RTL level is very close to the real-time experiment using radiations cause faults [11]. An approach to reduce the computational expense is to initiate fault injection at a higher level of abstraction. Numerous techniques have been proposed in the last couple of decades, in which faults are deliberately introduced at the different level of abstractions such as, RTL and gate levels [15]. As the size of components on the integrated circuits is reduced, so it makes the test, verification and debugging very complicated. Authors in [16] presented an auto-correction mechanism for the digital design to debug it. It reduces the time-to-market and debugging budget because more than 60% of the verification effort is spent on debugging.

Authors in [17] presented the characterisation method for Single Event Transient (SET) sensitivity of gates for varying pulse widths. In this method, they explained a weighted fault injection drive and calculated the SET sensitivity of combinatorial design. They also proposed that SET analysis can be obtained at the RTL level of design. The correlation between RTL testability and gate-level stuck-at fault coverage is carried out and observed. RTL testability was achieved by TASTE tool whereas FlexTest is used to obtain fault coverage. The design methodology is developed for performing fault modelling, and

enumeration of various statements are taken place for fault injection. In this work, the mutation technique is used for developing faulty circuit [4]. In comparison with this work, authors injected saboteur models for bit-flip, stuck-at 1 & 0 fault models [18].

In this work, a tool (RASP-FIT) is developed for fault injection testing and fault simulation applications. The tool works on the instrumentation technique for any Verilog design by injecting saboteur. These saboteurs consist of logic gates, e.g. XOR, OR and AND with an inverter for bit-flip, stuck-at 1 & stuck-at 0 fault models respectively.

III. THE RASP-FIT TOOL AND ITS COMPONENTS

The RASP-FIT tool can modify the FPGA-based designs, written in Verilog HDL. This tool includes Verilog code modifier (Fault Injection Algorithm), which changes the code by introducing faults. The way of modifying code at each abstraction level is separate. Therefore, fault models must be defined at that abstraction level. The bit-flip, stuck-at 1 & 0 fault models, are adopted for target system modification. In the proposed fault injection technique, fault models are developed using few logic gates such as XOR, OR and AND with NOT added in the HDL code. Verilog code modifier reads the code line by line and extracts keyword, operators or variables. The criterion for fault injection is particularised for every keyword and operator. It also includes the fault injection manager (i.e. Fault Injection, Selection and Activation (FISA) control unit) in each copy of the SUT to elect and stimulate faults [1], [7], [8].

In this paper, behavioural designs are considered for fault modification, obtaining test vectors, fault coverage and compaction analysis under the RASP-FIT tool. A tabbed-based standalone Graphical User Interface (GUI) is developed. Fig. 1 shows the fault injection analysis tab.

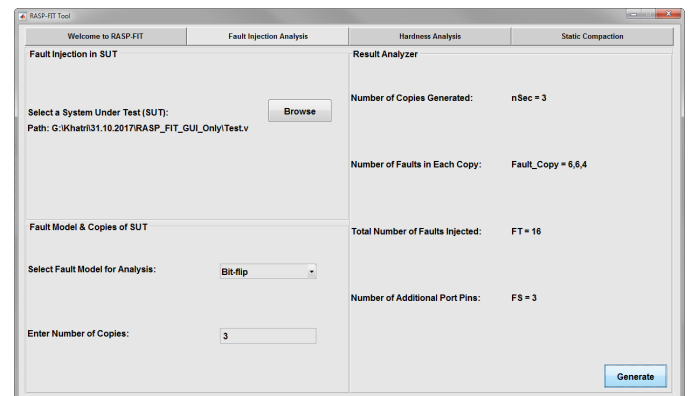


Fig. 1. Graphical window for FIA of the RASP-FIT tool.

A. Flowchart of FIA for Behavioural Designs

Behavioural modelling gives a convincing way to express design functionality algorithmically. Therefore, the soft-core processor and intricate FPGA-based designs are written at this level [19]. It is the highest level of abstraction, which describes the functional operation of the design. This level does not provide any information about the implementation of the design. The behaviour of the design is expressed by procedural

constructs, e.g. `initial` and `always`. The `initial` block statements run only one time, and `always` constructs execute again and again when the sensitivity list parameter changes their value [20], [21]. These constructs control the simulation and handle variables of different data types. The code parsing technique (fault injection mechanism) is different for each abstraction level, e.g. behavioural. The prototypes of following constructs, for example, `always-initial` blocks, blocking and non-blocking assignments, case, if-else construct are added to the RASP-FIT tool [10]. A few more features are also appended which inject fault in user-defined functions, vectors and a part-select/bit-select of vector variables in this work.

Modification of the code manually is a very challenging task. Therefore, the automatic code parser (FIA) under the RASP-FIT tool is devised for FPGA-based designs. Fig. 2 shows the fault injection algorithm flowchart. The synthesizable Verilog design file is applied to the RASP-FIT tool to the fault injection modifier as an input which parses the code line by line. This tool neglects and eliminates the single as well as multi-line comments. When it parses a line of the code (the line ends with a terminator “;”), it extracts the Verilog keyword and operator from it [8]. At behavioural abstraction level, the whole `always` construct read first by the tool and then analysed for the fault injection modification.

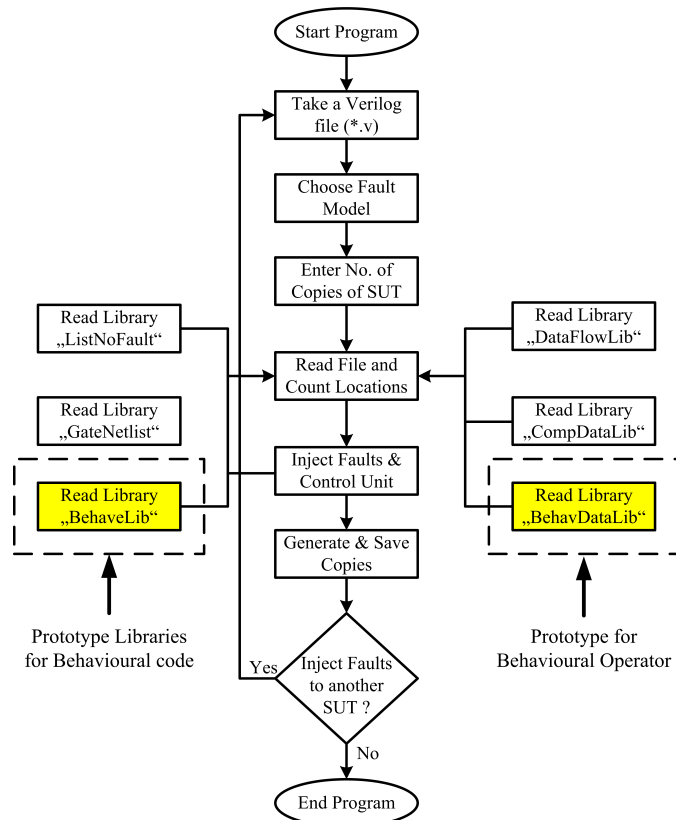


Fig. 2. Flowchart of the RASP-FIT code modifier (FIA).

Two more libraries (*BehaveLib* and *behaveDataLib*) are added in this work for behavioural designs as shown in Fig. 2 (shaded by the colour). The first library “*BehaveLib*” consists of the `always`, `initial` keywords. There are following statements which are used with procedural constructs, e.g.

TABLE I. VERILOG HDL OPERATORS FOR BEHAVIOURAL LEVEL [22]

Verilog Behavioural Operators	Operator Name	Functional Group Name
[]	Bit or Part Select	-
!, ~	Logical Negation, Negation	Logical, Bit-wise
&, , ~&, ~ , ^, ~^or ^^	AND, OR, NAND, NOR, XOR, XNOR	Reduction
+, -	Unary plus and minus	Arithmetic
{}, {() }	Concatenation, Replication	-
*	Multiply	Arithmetic
/	Divide	
%	Modulus	
+	Binary Plus	
-	Binary Minus	Shift
<<	Shift Left	
>>	Shift Right	Relational
>	Greater than	
>=	Greater than or Equal to	
<	Less than	
<=	Less than or equal to	Equality
=, !=	Equality, Inequality	
&, , ^	AND, OR, XOR	Bit-wise
&&,	AND, OR	Logical
?:	Conditional	Conditional

`always`. The way to inject faults in these statements is explained in the sequel.

1) *Blocking and Non-blocking Statements*: Block statements are executed differently in the sequential block and parallel block. In sequential block, they executed before the execution of the statement following it whereas, in the parallel block, the statements do not prevent their executions. Other procedural statements are called non-blocking assignments. In these assignments, numerous variable assignments within the same time step are made without consideration of order or declaration arrangement. The fault injection techniques in these statements inside the `always` constructs are shown in Fig. 3 [21]. Expression in Fig. 3 can be a single bit variable, vector, bit-select/part-select of vector, boolean expression using operators given in Table I.

```

module nameSUT (inputs , outputs);
...
...;
// non-blocking
Var_lvalue <= Expr; //fault-free
Var_lvalue <= (fn ^ Expr); //faulty

// similarly for blocking
Var_lvalue = Expr; //fault-free
Var_lvalue = (fn ^ Expr); //faulty

```

Fig. 3. Prototypes for blocking and non-blocking assignments.

2) *Vector Bit-select and Part-select*: Bit-select extracts a particular bit from an input vector, a vector net, a vector reg, integer, or time variable, or parameter. Instead of a single bit, many adjacent bits in a vector net, vector reg, integer, or time variable, or parameter are chosen and are known as part-select. The part-select is distinguished into two types, an indexed part-select and a constant part-select. Fig. 4 shows the fault modification in the code for bit-select and part-select.

```
module module_name (a,...);  
.  
.  
input [3:0] a;  
.  
.  
// Bit-select  
Var_lvalue <= a[2]; //fault-free  
Var_lvalue <= (fn ^ a[2]); // Single fault at  
    a[2] in a.  
  
// Part-select  
Var_lvalue = a[2:1]; //fault-free  
Var_lvalue = ({fn,fn+1} ^ a[2:1]);  
//Two faults at a[2] and a[1].
```

Fig. 4. Prototypes for bit-select and part-select for fault injection under RASP-FIT.

3) *Conditional Statement*: The conditional statement (or if-else statement) is used to decide on whether the statement is executed. The expression with *if* or *else-if* may contain a single variable, rVals (right variables) and lVals (left variables) separated by relational operators or combinations of different expressions. Fig. 5 shows the examples of expressions, that can be used with conditional expressions with the fault injection strategy. When the expression is constant, the tool does not inject the fault in the expression.

```
module nameSUT (inputs , outputs);  
...  
...;  
// Prototype 1  
if (Expr1) //fault-free  
if (fn ^ Expr1) //faulty  
  
// Prototype 2  
if (Expr1 == 1'd0) // fault-free  
if ((fn ^ Expr1) == 1'd0) // faulty  
  
// Prototype 3  
if (Expr1) < (Expr2)  
if ((fn ^ Expr1) < ((fn+1 ^ Expr2))
```

Fig. 5. Expression prototypes for *if* and *else if*.

4) *Case Statement*: The case statement is a multi-way decision statement. It examines the expression matches one of many other expressions or branches accordingly. The last option of the case statement is the default which executes when none of the condition is met [4]. The RASP-FIT includes all prototypes of case statements, e.g. *casez* and *casex* statements. Fig. 6 shows a fault injection method for the *case* statement. Faults are injected in statements and expressions.

5) *User-defined Primitives & Functions*: Functions are similar to tasks, except that functions return only a single value to the expression from which they are called. A user-defined file (named *user_defined_netlist.csv*) is created and added with the RASP-FIT tool folder. This file consists of two columns; the first column contains the names of user-defined primitives or functions used in the modules with I/O

```
// Case Statement  
case (Expr)  
    Expr : statement  
    Expr { , Expr } : statement  
    default : statement  
endcase  
  
// Faulty Case Statement  
case (fn ^ Expr)  
    Expr : fn+1 ^ statement  
    Expr { , Expr } : statement  
    default : fn+N ^ statement  
endcase
```

Fig. 6. Prototypes for *case* statement under RASP-FIT.

ports. Whereas, the second column consists of the positions of inputs in the function or primitives for fault insertion locations. Both columns are separated by a semi-colon ‘;’. When RASP-FIT is run, the contents of the file are read and added to the predefined libraries for the keywords for each abstraction level.

B. Result Analyser

As described earlier, authors developed the Automatic Test Pattern Generation (ATPG) with hybrid compaction techniques and a method to find the critical nodes of the SUT at the code level under the proposed tool and presented in the previous work [1], [7], [8]. In the previous works, the FC and compact Test Vectors (TV) were calculated for the Verilog HDL designs written at gate-level and data-flow. Firstly, behavioural designs are modified, and faulty code is generated. The proposed test method is applied to the behavioural designs, and test vectors and compaction analysis are carried out and presented in the paper. A small description of the proposed approaches is added to recall the idea briefly.

1) *Test Approach: Fault Injection Testing*: Testing of design becomes essential to guarantee the fault-free operation of devices. Various techniques have been introduced which can test the digital systems realised on FPGA, and are generally acknowledged as test pattern generation methods [7]. The Verilog file is applied to the tool as an input, and the tool modifies the code to generate the faulty copies of the Verilog design, along with the top module file. The top file contains instantiations of the golden model, and faulty models, comparator block (compare the responses), dynamic compaction block (select qualified test vectors) and memory (to store responses in a text file). All these components of the top module are programmed by the RASP-FIT tool in Verilog HDL during the FIA process. Fig. 7 shows all components of the top module file and components of the proposed ATPG approach. Xilinx ISE project navigator tool is used to do the project and simulate the design using Modelsim tool. In order to simulate a design, a test bench is needed, which contains input stimuli signals such as fault selector signal and random pattern generator utilising a Linear Feedback Shift Register (LFSR). In this paper, all proposed approaches are applied to some simple behavioural designs. FC and compaction (C) are calculated by Eq. 1 and Eq. 2, respectively:

$$FC = \frac{F_D}{F_T} \times 100\% \quad (1)$$

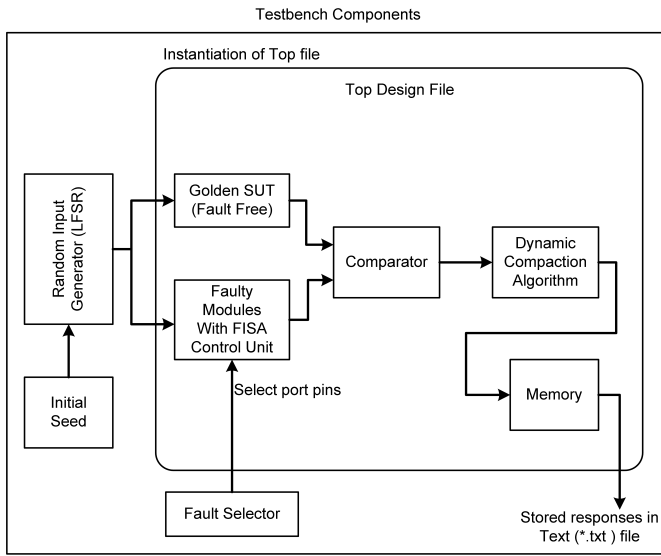


Fig. 7. Simulation environment for proposed fault injection testing.

$$C = \left(1 - \frac{T_{\text{Static compact}}}{T_q} \right) \times 100\% \quad (2)$$

During the ATPG process, a mechanism is defined which can reduce the number of test vector generation. It is widely known as dynamic compaction, and it is a part of an ATPG procedure described step by step shortly in Algorithm 1. Using this algorithm, we obtained the efficient test vectors which detect more faults. Static compaction is a simple approach, and it is not part of the ATPG procedure. Static compaction is used to reduce the test vector count further which were obtained during the ATPG method with dynamic compaction. It is described in Algorithm 2.

Algorithm 1 Proposed dynamic compaction algorithm [1]

- 1: Run the simulation by applying random input pattern and perform fault injection experiment
- 2: Count the fault detections for each pattern
- 3: Compare the sum with the set-point value
- 4: **if** Is sum greater than or equal to set-point value **then**
- 5: Save as qualified test vectors T_q
- 6: Increase the T_q count by one
- 7: **else**
- 8: Apply another pattern
- 9: **end if**
- 10: Go to step 2
- 11: Stop the simulation design when T_q count reaches 100
- 12: Stored all qualified vectors T_q in the text files

2) *System Under Test (SUT)*: To validate the proposed techniques, the authors developed various simple designs at behavioural abstraction level. The purpose of these designs is to utilise all possible operators and keywords specifically used for behavioural modelling and validate the fault injection capability of RASP-FIT tool for behavioural designs. These operators are depicted in Table I. Verilog commands, and their prototypes for fault injection are described in Section III. The

Algorithm 2 Proposed static compaction algorithm

- 1: Detection of faults is summed for each T_q .
- 2: Based on step 1, TVs are sorted in descending order.
- 3: **for** Perform logical OR operation **do**
- 4: Calculate new_FC
- 5: **if** Is new_FC greater than old_FC **then**
- 6: Saved pattern as compact TV
- 7: **else**
- 8: Repeat step 3 for next vector
- 9: **end if**
- 10: Repeat step 3 to 9, stop when new_FC reaches 100% or all T_q checked
- 11: **end for**
- 12: Compact test vectors for maximum FC

target designs consist of all prototypes of statements used in always construct.

IV. RESULTS AND DISCUSSION

The RASP-FIT tool is upgraded, and now it can handle the Verilog HDL designs written at gate, data-flow and behavioural levels. In this paper, behavioural circuits are generated, and code modification is performed on these designs. These designs are simple Verilog designs at the behavioural level and cover nearly all types of Verilog operators and keywords. The sequel presents the results for fault injection, obtaining test vectors, FC, and the compaction ratio.

A. Results: FIA for Behavioural Designs

The RASP-FIT tool is simple, fast and user-friendly. Fault injection analysis is carried out for behavioural designs and the time is measured. It shows the advantage of representing the design at higher abstraction levels. The tool took a fraction of a second to generate the faulty copies of the SUTs. Table II shows the Verilog behavioural designs along with the number of look-up tables, the number of total faults and the time in seconds. The whole design can be represented in fewer lines of code at a higher level of abstraction.

TABLE II. TIMING ANALYSIS FOR FAULTY MODULES GENERATION OF BEHAVIOURAL DESIGNS

S.No.	Behavioural Designs	No. of Slices LUTs	Total Faults	Time (in Seconds)
1	Adder (32-bit)	32	64	0.467
2	Circuit_Bitwise	04	09	0.137
3	Relational_Ops	04	27	0.190
4	Boolean_Ckt	04	10	0.121
5	Mux_Case	06	22	0.143

B. Results: Compact Test Vectors and Fault Coverage

The number of test vectors obtained and fault coverage is calculated for behavioural designs and presented in Table III. The second column shows the number of input and output of the system under test; however, the number of faults detected F_D is shown in 3rd column. FC is calculated for each fault model (bit-flip, stuck-at 1, stuck-at 0). One value entry in F_D & FC columns shows the same value is obtained for each fault

model in the analysis. However, Table IV shows the number of qualified vectors obtained after dynamic compaction T_q . In the proposed dynamic approach, we stop the simulation when the T_q count reaches 100 test vectors. The proposed method is fast and memory efficient. On these vectors, authors applied static compaction scheme and obtained the reduced TV without compromising the FC and mentioned in the 3rd column of Table IV.

TABLE III. RESULT OF FAULT COVERAGE FOR FEW BEHAVIOURAL DESIGNS

System Under Test	No. of Inputs / Outputs (Original Circuits)	Fault Detected (F_D)	Fault Coverage FC (%)
Adder (32-bit)	64/33	64	100
Circuit_Bitwise	9/5	09	100
Relational_Ops	6/4	27	100
Boolean_Ckt	4/2	10	100
Mux_Case	14/3	22	100

C. Results: Compaction

In this work, authors obtained the compaction analysis of the Verilog designs written at behavioural abstraction level. For each design, the qualified test vectors are obtained during the ATPG and stored in a text file. These text files are applied to the RASP-FIT tool to perform static compaction. After static compaction, authors obtained the short test vectors. Fig. 8 shows the static compaction achieved for the various fault models. Table IV contains the test vectors obtained after dynamic compaction and static compaction for bit-flip, stuck-at 0 (SA-0) and stuck-at 1 (SA-1) fault models. Single value entry shows that the number of test vectors are the same for each fault model.

TABLE IV. HYBRID COMPACTION SCHEMES FOR FEW BEHAVIOURAL DESIGNS

SUT	Dynamic Compaction (T_q)	Static Compaction (TV)	Compaction (%) Bit-flip,SA-1,SA-0
Adder (32-bit)	100	2	98
Circuit_Bitwise	100	2	98
Relational_Ops	100	2	98
Boolean_Ckt	100	2,3,3	98,97,97
Mux_Case	100	3,5,4	97,95,96

V. CONCLUSION

In this work, the automatic code-parser is enhanced to inject faults in behavioural HDL designs under the RASP-FIT tool. Previously, the tool can modify the gate level and data-flow designs only. Behavioural HDL codes algorithmically represent designs. It is possible to test, evaluate fault injection and simulation techniques directly at the code level using the RASP-FIT tool. In this way, the tool assists design and test engineers to obtain the small number of TV, FC, and compaction of the designs at an early stage of the development flow, hence reduce the cost and time-to-market. Few behavioural designs are tested, and FC is calculated. It is shown that maximum FC is achieved for fewer test vectors.

In future, result analyser will be upgraded to obtain the compact test vectors for sequential circuits along with the enhancement of ATPG approach. At this time, the tool work

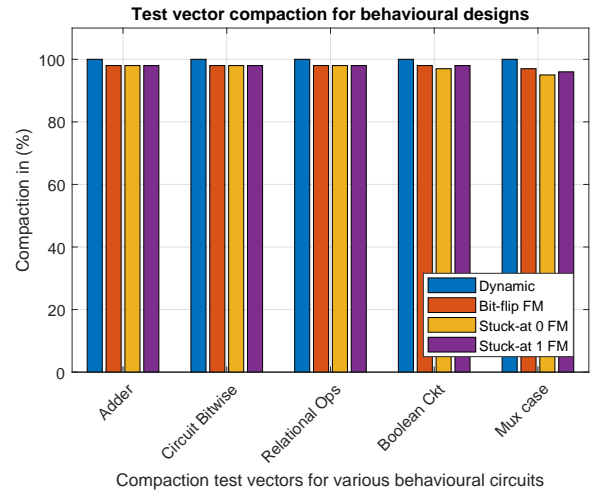


Fig. 8. Compaction ratio for behavioural circuits.

on a single module of design. Multiple modules are also a way to write a hierarchical behavioural design, and it is considered for the RASP-FIT tool.

REFERENCES

- [1] A. R. Khatri, A. Hayek, and J. Börcsök, "Validation of the Proposed Fault Injection, Test and Hardness Analysis for Combinational Data-Flow Verilog HDL Designs Under the RASP-FIT Tool," in *2018 IEEE 16th Intl Conf on Dependable, Autonomic and Secure Computing, 16th Intl Conf on Pervasive Intelligence and Computing, 4th Intl Conf on Big Data Intelligence and Computing and Cyber Science and Technology Congress (DASC/PiCom/DataCom/CyberSciTech)*, (Athens, Greece), pp. 544–551, IEEE, Aug 2018.
- [2] J. Cavanagh, *Computer arithmetic and Verilog HDL fundamentals*. California, USA: Taylor & Francis Group, LLC, 2010.
- [3] H. Ben Fekih, A. Elhossini, and B. Juurlink, *Applied Reconfigurable Computing*, vol. 9040 of *Lecture Notes in Computer Science*. Cham: Springer International Publishing, 2015.
- [4] M. Karunaratne, A. Sagahayroon, and S. Prodhuturi, "RTL fault modeling" in *48th Midwest Symposium on Circuits and Systems, 2005.*, pp. 1717–1720 Vol. 2, IEEE, 2005.
- [5] Z. Navabi, *Digital System Test and Testable Design*. Boston, MA: Springer US, 2011.
- [6] A. R. Khatri, A. Hayek, and J. Börcsök, "Validation of the Proposed Hardness Analysis Technique for FPGA Designs to Improve Reliability and Fault-Tolerance," *International Journal of Advanced Computer Science and Applications*, vol. 9, no. 12, pp. 1–8, 2018.
- [7] A. R. Khatri, A. Hayek, and J. Börcsök, "ATPG method with a hybrid compaction technique for combinational digital systems," in *2016 SAI Computing Conference (SAI)*, (London, UK), pp. 924–930, IEEE, Jul 2016.
- [8] A. R. Khatri, A. Hayek, and J. Börcsök, *Applied Reconfigurable Computing*, vol. 9625 of *Lecture Notes in Computer Science*. Cham: Springer International Publishing, 2016.
- [9] A. R. Khatri, A. Hayek, and J. Borcsok, "Validation of selecting SP-values for fault models under proposed RASP-FIT tool," in *2017 First International Conference on Latest trends in Electrical Engineering and Computing Technologies (INTELLECT)*, (Karachi, Pakistan), pp. 1–7, IEEE, nov 2017.
- [10] A. R. Khatri, A. Hayek, and J. Börcsök, "RASP-FIT: A Fast and Automatic Fault Injection Tool for Code-Modification of FPGA Designs," *International Journal of Advanced Computer Science and Applications*, vol. 9, no. 10, pp. 30–40, 2018.
- [11] T. Flenker, J. Malburg, G. Fey, S. Avramenko, M. Violante, and M. S. Reorda, "Towards Making Fault Injection on Abstract Models a More Accurate Tool for Predicting RT-Level Effects," in *2017 IEEE Computer*

- Society Annual Symposium on VLSI (ISVLSI)*, pp. 533–538, IEEE, Jul 2017.
- [12] R. Champon, V. Beroulle, A. Papadimitriou, D. Hely, G. Genevrier, and F. Cezilly, “Comparison of RTL fault models for the robustness evaluation of aerospace FPGA devices,” in *2016 IEEE 22nd International Symposium on On-Line Testing and Robust System Design (IOLTS)*, pp. 23–24, IEEE, Jul 2016.
- [13] J. Espinosa, C. Hernandez, and J. Abella, “Modeling RTL fault models behavior to increase the confidence on TSIM-based fault injection,” in *2016 IEEE 22nd International Symposium on On-Line Testing and Robust System Design (IOLTS)*, pp. 60–65, IEEE, Jul 2016.
- [14] Li Shen, “RTL concurrent fault simulation,” in *Proceedings of the 7th International Conference on Properties and Applications of Dielectric Materials (Cat No 03CH37417) ATS-03*, p. 502, IEEE, 2003.
- [15] A. L. Sartor, P. H. E. Becker, and A. C. S. Beck, “Simbah-FI: Simulation-Based Hybrid Fault Injector,” in *2017 VII Brazilian Symposium on Computing Systems Engineering (SBESC)*, pp. 94–101, IEEE, Nov 2017.
- [16] B. Alizadeh and S. R. Sharafinejad, “Incremental SAT-Based Accurate Auto-Correction of Sequential Circuits Through Automatic Test Pattern Generation,” *IEEE Transactions on Computer-Aided Design of Integrated Circuits and Systems*, vol. 38, pp. 245–252, Feb 2019.
- [17] A. Evans, D. Alexandrescu, E. Costenaro, and Liang Chen, “Hierarchical RTL-based combinatorial SER estimation,” in *2013 IEEE 19th International On-Line Testing Symposium (IOLTS)*, pp. 139–144, IEEE, Jul 2013.
- [18] A. R. Khatri, M. Milde, A. Hayek, and J. Börcsök, “Instrumentation Technique for FPGA based Fault Injection Tool,” in *5th International Conference on Design and Product Development (ICDPD '14)*, (Istanbul, Turkey), pp. 68–74, 2014.
- [19] S. Palnitkar, *Verilog HDL A guide to Digital Design and Synthesis*. SunSoft Press, 1996.
- [20] Joseph Cavanagh, *Digital Design Verilog and HDL Fundamentals*. Taylor and Francis Group, LLC, 2011.
- [21] Sponsored by the Design Automation Standards Committee, *IEEE Standard for Verilog Hardware Description Language*. No. April, IEEE Computer Society, 2006.
- [22] Akshay.sridharan, “Verilog HDL Operators.”

An Efficient Image Haze Removal Algorithm based on New Accurate Depth and Light Estimation Algorithm

Samia Haouassi¹, Wu Di^{*2}, Meryem Hamidaoui³, Tobji Rachida⁴
School of Computer Science and Technology
Dalian University of Technology, Dalian 116000, China

Abstract—Single image Dehazing has become a challenging task for a variety of image processing and computer applications. Many attempts have been devised to recover faded colors and improve image contrast. Such methods, however, do not achieve maximum restoration, as images are often subject to color distortion. This paper proposes an efficient single image Dehazing algorithm that offers satisfactory scene radiance restoration. The proposed method stands on the estimation of two key indices; image blur and atmospheric light that can be employed in the Image Formation Model (IFM) to recover scene radiance of the hazy image. More clearly, we propose an efficient depth estimation method using image blur. Most existing algorithms implement atmospheric light as a constant which often leads to inaccurate estimations, we propose a new algorithm “A-Estimate” based on blur and energy to estimate the atmospheric light accurately, an adaptive transmission map also has been proposed. Experimental results on real and synthesized hazy images demonstrate an improved performance in the proposed method when compared to existing state-of-the-art methods.

Keywords—Image dehazing; Image Formation Model (IFM); depth map; transmission map; atmospheric light; image blur; image energy

I. INTRODUCTION

Outdoor images are often degraded under bad weather conditions (e.g., foggy or hazy) by the turbid medium (e.g., dust, mist or fumes, haze) in the atmosphere during the propagation process. These images usually suffer from poor visibility such as low contrast and blur, resulting from the fact that the light is scattered and absorbed with distance from the camera. Thus, most of the automatic systems (e.g., automatic monitoring system, outdoor recognition system and smart transportation system) which depend on the definition of the input images, such as those used in the surveillance needs to understand and extract useful information, and detect image features, fail to work correctly. Therefore, improving haze removal techniques is an important task in computer vision and its applications such as image classification and aerial imagery.

Despite there are many proposed hazy image enhancement techniques, which can be classified into two classes [1]: (1) image enhancement based on processing techniques, and (2) image restoration based on physical models, the Dehazing performance still has some problems in term of image quality. First, researchers use the traditional image processing techniques to eliminate the haze from a single hazy image (such as methods which stand on histogram processing [2], [3]),

but these techniques produce unacceptable restoration results because the single hazy image can hardly give much useful information. In [4], [5], [6], polarization-based methods were proposed for Dehazing with multiple image degrees. After, Narasimhan et al. [7], [8], [9] use multiple images of the same scene with different weather conditions. However, these techniques also do not perform well the restoration of the single hazy image. Lately, under the hypothesis that the local contrast of hazy images is much lower than that in haze-free images, researchers use image depth information to deal with the haze within a single image using the physical model. In [10], Tan et al. propose a maximization of local contrast approach using Markov Random Field (MRF) to remove the haze, but Tan’s approach produces oversaturated images. Also, Fattal [11] proposes an Independent Component Analysis (ICA) based Dehazing approach. The problem posed by this approach is the time-consuming, and it cannot recover well the scene radiance of images with a dense haze.

To estimate the thickness of haze, He et al. [12] discover the dark channel prior (DCP) and remove the haze using the atmospheric scattering model, nevertheless, DCP method leads to over saturated recovered scene radiance. Many algorithms [1],[13], [14], [15], [16], [17], [18], [19], [20], [21], [22], [23], [24], [25] have introduced to surmount the weakness of the (DCP)-based method. To overcome the problem of time-consuming many attempts have been discovered, Gibson et al. [14], He et al. [26] and Tarel et al. [20] propose to use guided-image filtering instead of standard median filtering. Kratz and Nishino [22] have adapted FMRF (Factorial Markov Random Field) to enhance the Dehazing quality and give more accurate scene radiance estimation. Qingsong et al. [27] propose a simple Dehazing algorithm based on a linear model to restore the scene depth. However, this algorithm is not efficient enough especially for dense-haze images (see Fig. 1).

On the other hand, using machine learning-based techniques (neural networks, Convolutional neural networks, deep learning), Cai et al. [28], Ren et al. [29] and Song et al. [30] propose image Dehazing models built with convolutional neural networks (CNNs) based deep architectures, which achieve some wrong results in term of saturation, the naturalness of restored image because of non-massive data in the learning process, also in term of efficiency because of redundant computations as Song et al. [30] mentions in his conclusion.

In this paper, we propose a novel haze removal algorithm using image blur and atmospheric light to estimate the depth

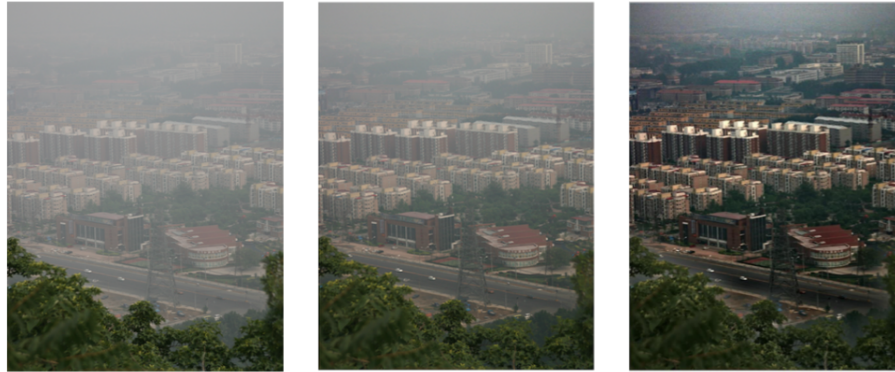


Fig. 1: Example of Quingsong's result with a dense-haze image. Left: Input hazy image. Center: Quingsong's result . Right: our result.

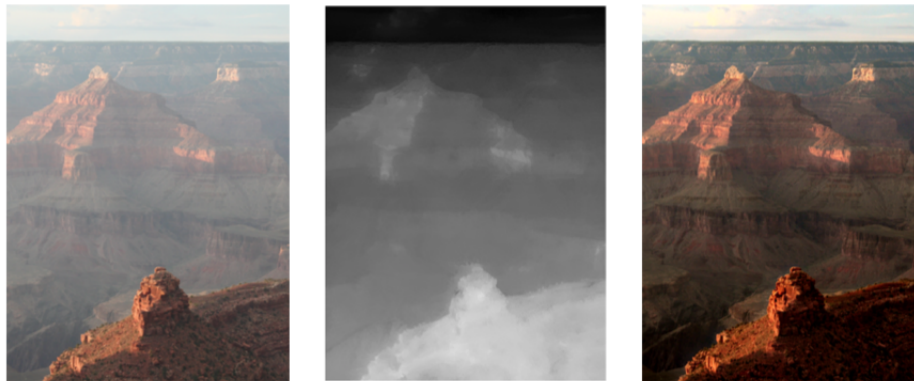


Fig. 2: An overview of our dehazing method. Input hazy image. Restored transmission map. Dehazed image.

and transmission maps (An overview of our proposed method is shown in Fig. 2). The main contributions in our work are:

- We are the first to propose a depth estimation using image blur map estimation for haze removal methods. Because larger scene depth causes object more blurry for hazy images.
- We propose a new and efficient algorithm $A - Estimate$ to estimate the atmospheric light from the most blurry region in the blur map, which is defined by the local patch that has a minimum energy. Then, the light A is selected as the maximum pixel intensity in the patch defined.
- We propose an adaptive transmission map using the distance between the observed intensity and the closest scene point.

The rest of the paper is organized as follow: In Section 2, we review the atmospheric scattering model and the DCP based dehazing method. In Section 3, we describe the proposed method. Qualitative and quantitative experimental results using both real and synthetic hazy images are reported in Section 4. Finally, Section 5 summarizes this paper.

II. RELEVANT BACKGROUND

A. Atmospheric Scattering Model

In [31], McCartney proposes the atmospheric scattering model to illustrate the formation model of a hazy image (Fig. 3). This model is widely used in computer vision and image processing. Later, Narasimhan and Nayer in [8],[32],[33], deduce the model so that it can be expressed as follows:

$$I^c(x) = J^c(x)t(x) + A(1 - t(x)). \quad (1)$$

$$t(x) = e^{-\beta d(x)}. \quad (2)$$

Where $I^c(x)$ is the observed intensity of hazy image at pixel x , J^c is the scene radiance representing the haze-free image, A is the atmospheric light or background light, and $t(x)$ is the transmission medium map that describes the portion of the scene radiance that is not scattered or absorbed and reaches the camera, β is the scattering coefficient of the atmosphere which can be a constant in homogenous atmosphere condition [32], and d is the the depth map of scene. I^c , J^c and A all are represented in RGB color space. Since we have the

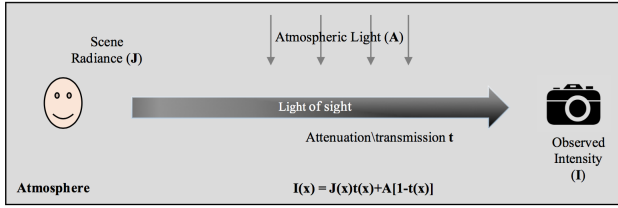


Fig. 3: Hazy Image Formation Model.

input image I^c the problem of dehazing is the estimation of the atmospheric light and the transmission map $t(x)$, and then restore the scene radiance J^c , using the atmospheric scattering model Equation (1). According to the atmospheric scattering model, the depth of the scene is the most important information, after we can easily get the transmission map using Equation (2), and restore the scene radiance.

B. Dark Channel Prior (DCP) based Dehazing Method

To estimate A and $t(x)$, the *DCP* has been proposed. *DCP* based dehazing method serves to find the minimum intensity in the hazy image through a small local patch [12]. We can get the *DCP* of a hazy image using the following formula:

$$I_{dcp}^{rgb}(x) = \min_{y \in p(x)} [\min_{c \in \{r,g,b\}} I^c(y)] \quad (3)$$

Denoted $p(x)$ is a local patch centered at pixel x . For a hazy image, the value of dark channel often increases with depth, which means that the closest scene point has a low value of dark channel and the opposite for a far scene point.

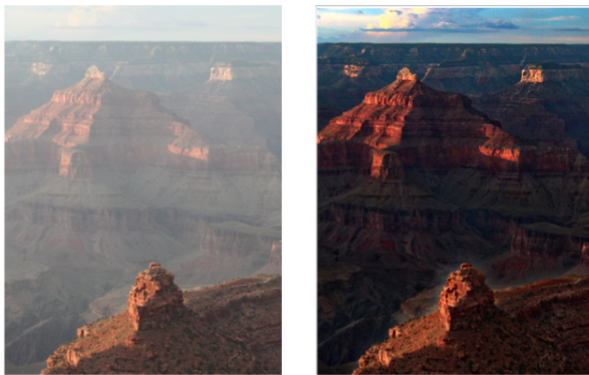


Fig. 4: Example of restoring scene radiance of hazy image using DCP based-Dehazing method

To calculate A , the top 0.1% brightest pixels in I_{dark}^c were picked in [12], where $P_{0.1\%}$ represents their positions in I_{dark}^c . After, A is chosen as the pixel has the highest intensity in the hazy image. The following formula is used to estimated A :

$$A = I^c(\arg \max_{x \in P_{0.1\%}} \sum_{c \in \{r,g,b\}} I^c(x)) \quad (4)$$

In the case of non-hazy images, the transmission $t(x) = 1$ according to Equation (1), so $I^c = J^c$. In addition, under the assumption that for most of the pixels at least one of them has a low intensity in one of color channels within a small local patch p , the *DCP* of the scene radiance J_{dark}^{rgb} generally equals to 0 for haze-free images taken in outdoor scenes. However, this assumption concerned just the outdoor terrestrial haze-free images, and it is not true for pixels of sky area, where nearby pixels also tend to be bright. Therefore it affirms in [12] Equation (5) that for about 75% of the pixels in the dark channels have zero values.

$$J_{dark}^{rgb}(x) = \min_{y \in \omega(x)} \{ \min_{c \in \{r,g,b\}} J^c(y) \} = 0 \quad (5)$$

In order to get the transmission map $t(x)$ both sides of Equation (1) are divided by A , and applying the minimum operator to it. Then we obtain:

$$\min_{y \in \omega(x)} \{ \min_c \frac{I^c(y)}{A} \} = \min_{y \in \omega(x)} \{ \min_c \frac{J^c(y)}{A} t^c(y) \} + 1 - t(x) \quad (6)$$

Note that the estimated TM $t(x) = \min_{y \in \omega(x)} \{ \min_c t^c(y) \}$, and $\min_{y \in \omega(x)} \{ \min_c \frac{J^c(y)}{A} t^c(y) \} = 0$. According to Equation (6) we have:

$$t(x) = 1 - \min_{y \in \omega(x)} \{ \min_{c \in \{r,g,b\}} \frac{I^c(y)}{A} \} \quad (7)$$

In the case of $t(x)$ has negative intensities, it returns to zero. The Equation (7) describes the general approach to estimate TM $t(x)$, and then use it to recover the scene radiance J^c according to Equation (1). Fig. 4 shows the result of DCP based-dehazing method.

III. PROPOSED IMAGE DEHAZING METHOD

We propose a new single image dehazing method based on both image blur map and light scattering. This new method ensures that both estimated A and depth map are more accurate and can provide a well-restored scene radiance. First, we define the most blurry region in the hazy image using image blur map and energy information in a local patch (in our work patch size = 20×20) using A -estimate algorithm after, we select A as the maximum intensity in this patch. Then, based on the A selected and the image blur map, the depth d and the *TM* maps are estimated to recover the scene radiance. The flow diagram in Fig. 5 shows the process of our proposed method.

A. Hazy Image Blur Map Estimation

Blur is the most common undesirable problem and one of the factors that lead to quality degradation which hazy images suffer from, which means that the estimation of the amount of blur presented on a given hazy image can contribute

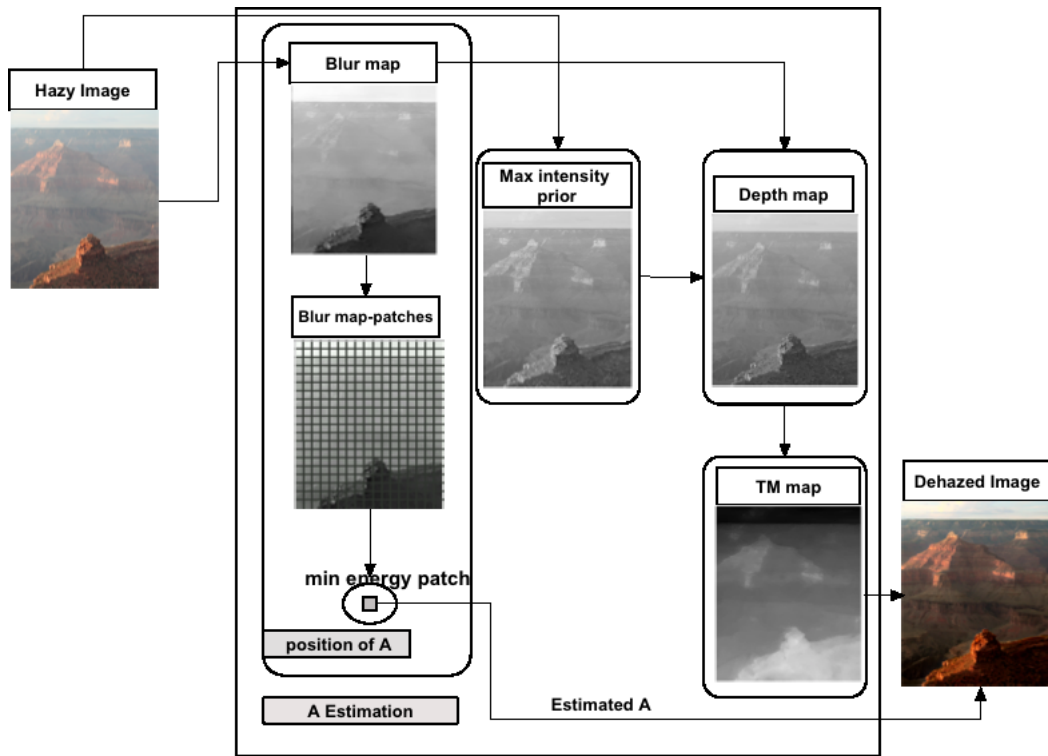


Fig. 5: Diagram chart of our proposed method.

significantly to restore and enhance the visibility of hazy images. To this end, in this section, we propose a blur map estimation method presented in four steps as follows:

- 1) **Blur map estimation:** undoubtedly, that the spatial Gaussian filter is one the most useful filters used to estimate the amount of blur presented on an image and many literature works show the effectiveness of Gaussian filter to quantify and evaluate blur within an image. According to [34], the image blur map can be estimated as the difference between the original image and the multi-scale Gaussian-filtered image. We put $G^{\omega, \sigma}$ as the hazy image filtered by a $\omega \times \omega$ Gaussian filter with variance σ . And then we can estimate the blur map using the formula shown below Equation (8):

$$Blr(x) = \frac{1}{n} \sum_{i=1}^n |I_y - G^{k_i, k_i}(x)| \quad (8)$$

Where I_y is the Y channel of the YCbCr color space of the input image, because it contains the most important gray-scale information about the image, $k_i = 2^i n + 1$, and n set to 3.

- 2) **Detection of brightest pixels:** To find the brightest points within the blur map estimated we apply a grayscale dilation morphological operation with the structuring element SE.

$$B_d(x) = [M_d(Blr(x))] \quad (9)$$

- 3) **Blur map reconstruction:** It consists of filling holes

in the blur map obtained $B_r(x)$ to recover the set of background pixels that cannot be reached by filling in the background from the edge of the image using a morphological reconstruction.

$$B_r(x) = [C_r(B_d(x))] \quad (10)$$

Where C_r is the hole filling morphological reconstruction.

- 4) Finally, we use the guided filter to refine the blur map result. Where F_g is the guided filter function.

$$M_{blr}(x) = F_g[B_r(x)] \quad (11)$$

B. Atmospheric Light Estimation

In most of the previous single image dehazing methods, the atmospheric light A is estimated from the most haze-opaque pixel, for example, the highest intensity pixel is used as a value of atmospheric light in [10] [12] (Fig. 6, the red square). However, the brightest pixel can be one of a white color object within the scene which can lead to dim scene radiance. To overcome the limitation of this method and because the haze changes the tone or the saturation of the atmosphere with distance from the viewpoint, some researchers [27] propose to estimate the A from the farthest point in the scene, but in some cases of outdoor hazy images also the farthest point can be one of the white scene object like clouds in the sky (Fig. 6). In this case, the estimation of the A is not accurate enough.

To deal with this problem, we propose another method to estimate the A which estimates the atmospheric light A from the most blurry region detecting using the blur map mentioned



Fig. 6: Position of atmospheric light in He's, Zhu's and our method respectively (red marks)

in the previous section. To find the most blurry region within the blur map we propose to use energy information and then estimate the atmospheric light we propose a new algorithm *A - Estimate*, more details are explained below (see Fig. 6).

For hazy images, the restored scene radiance J^c varies between inferior and superior bounds [0,1] which are derived by putting $A = 0$ and $A = 1$ as:

$$\max\left(\frac{I(x) - 1 + t(x)}{t(x)}, 0\right) \leq J(x) \leq \min\left(\frac{I(x)}{t(x)}, 1\right) \quad (12)$$

According to this equation Equation (12), restoring hazy image with wrong estimated atmospheric light leads to undesirable results, for more clarification: dim estimated A leads to a vivid scene radiance, as an opposite result is obtained when the estimated A is bright. For example, when we put $A = 0$ then $J^c = \min\left(\frac{I(x)}{t(x)}, 1\right)$ the recovered scene radiance $J(x)$ could be brighter than the observed intensity $I(x)$. To avoid this problem, *DCP* approach and color variance have been adapted by Emberton et al. [35] to estimate A . However, this proposition does not provide accurate results. Also, Peng et al. in [34] propose to use image variance and blurriness information in a candidate selection method to estimate the light BL for underwater images. Nevertheless, this approach is adopted for underwater images and does not work well with hazy images. In contrast, we adopt the image blur and energy information to estimate the A . We propose an A selection method, which selects the most blurry region from the hazy image using blur map and energy indices. First, to detect the most blurry region, we use a patch-based method to calculate the local energy through each patch within the blur map. In our work we set patch-size = [21 × 21]. The patch that has minimum energy represent the lucky region which contains the value of A . Then, we take 0.1% brightest pixels founded in the patch selected as an estimated A . The detail of the selection algorithm is described in Algorithm 1.

C. Depth Estimation

Objects far from the camera are blurry more than those near the camera, which means that the amount of blur in a given hazy image increases with the distance from the camera. In

Algorithm 1 *A - Estimate*

- 1: Input: input image I , Blur map P_{blr} .
 - 2: Output: Estimated A .
 - 3: **Function** *AL_Estimate*(I, P_{blr})
 - 4: $A_1 \leftarrow avg_x[detect - most - blurry - region(I, P_{blr})]$;
 - 5: $A_2 \leftarrow \frac{1}{|P_{0.1\%}|} \sum_{x \in P_{0.1\%}} I(x)$;
 - 6: $A \leftarrow A_2$;
 - 7: **return** A ;
 - 8: **End Function**
 - 9: **Function** *detect - most - blurry - region*(I, P_{blr})
 - 10: $I_{gray} \leftarrow rgb2ycbcr(I)$;
 - 11: $I_{gray} \leftarrow I_{gray}(:, :, 1)$;
 - 12: Patch-size = [21,21];
 - 13: Divide $P_{blr}(x)$ to set of patches;
 - 14: n = number of patches;
 - 15: **for** $k : 1 : n$ **do**
 - 16: Calculate energy E of pixels within each patch
 - 17: $E = \frac{1}{N} \sum_x (P_{blr}(x))^2$;
 - 18: Pick p with minimum energy E and largest blur;
 - 19: **end for**
 - 20: **return** $I(position(patch))$;
 - 21: **End Function**
-

contrast, we have that the depth of the image is defined by the distance from the camera viewpoint to the farthest point in the image, thus, the amount of blur in a given hazy image increases with depth. Therefore, the estimation of depth is relative to the blur estimation. In this section, we propose a scene depth estimation based on image blur and light scattering as an initial depth map. After, we propose a combination depth method to get the final depth map.

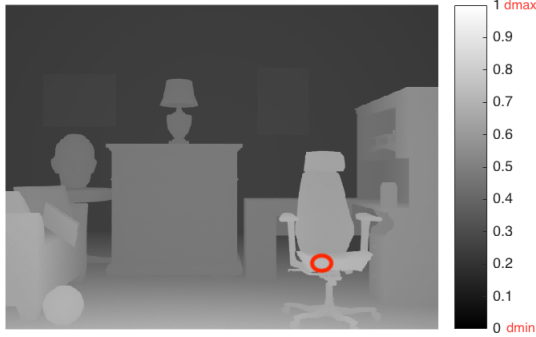


Fig. 7: Scene depth intensities distribution.

For the first method we use the image blur presented before in Equation (11) to estimate the scene depth:

$$d_B = 1 - (P_{blr}) \quad (13)$$

For the second method is the maximum intensity prior based depth estimation (derived from *DCP*-based method assumption) denoted d_D , is defined as:

$$d_D = 1 - (d_{Max}). \quad (14)$$

where d_{max} defined by the following equation:

$$d_{Max} = \max_{y \in \omega(x)} \{ \max_{c \in \{r,g,b\}} \{I^R(y), I^G(y), I^B(y)\} \} \quad (15)$$

Where I^R, I^G, I^B are the three channels Red, Green, and Blue of the image I in *RGB* color space.

This estimation is a combination of two depth estimation methods, which are sigmoidally combined to get the scene depth of a hazy image. By combining Equation (14), and Equation (15), we introduce an efficient scene depth estimation method considering blur and light scattering, as follows:

$$d_n(x) = \alpha_2[\alpha_1 F_s(d_D(x))] + (1 - \alpha_1)F_s(d_B(x)) \quad (16)$$

where F_s is an intensity normalization function to normalize the intensity range given as:

$$F_s = \frac{I - \min(I)}{\max(I) - \min(I)}. \quad (17)$$

Note that I is a two-dimensional image.

Where $\alpha_1 = S(\text{avg}(A), 0.5)$ and $\alpha_2 = S(\text{avg}(I^c), 0.1)$ are defined by the logistic function mentioned in Equation (18):

$$F(x, y) = \frac{1}{1 + e^{-(x,y)}} \quad (18)$$

The final step, we refine and smooth the depth map obtained d_n using soft matting [36] or guided filter [26]. More clarification: when a hazy image has brighter A (For example $A \gg 0.5$), then d_D is more efficient and faithful to estimate the scene depth. The red, green, and blue lights are more absorbed and scattered in far scene points. Therefore when the hazy image has a moderate level of red, green, blue global content ($\text{avg}(I^c) \gg 0.1$), with the atmospheric light is comparatively brilliant ($\text{avg}_c(A) \gg 0.5$), then d_D alone can represent well the scene depth well. In this case, $\alpha_1 \approx 1$, $\alpha_2 \approx 1$, then $d_n(x) \approx d_D(x)$.

Finally, when the red, green and blue lights are very little in the scene, means ($\text{avg}(I^s) \ll 0.1$), then d_D fails to represent well the scene depth. So $\alpha_1 \approx 1$, $\alpha_2 \approx 0$, $d_n(x) \approx d_B(x)$, signify that the blur map can estimate the scene depth well when $\alpha_1 \approx 1$, $\alpha_2 \approx 0$. In the other cases, the combination of the two approaches is the good way to estimate the scene depth.

D. Transmission Map Estimation *TM*

In the *DCP*-based methods, the transmission map *TM* estimation is base on Equation (7). On the other side, the *TM* estimation of hazy image using *IFM* is based on Equation (2) which needs the estimation of the depth from the viewpoint to each spot within the scene. In addition, the distance δ between the camera and the nearest scene point must be defined. In contrast, Peng et al. [34] introduce a metric-based distance estimation to calculate δ according to Equation (19).

$$\delta = 1 - \max_{y,c \in \{r,g,b\}} \frac{|A - I^c|}{\max(A^k, 1 - A^k)} \quad (19)$$

Note that $k = \arg \max_{c \in \{r,g,b\}} (\max_x |A^c - I^c|)$ and A is the estimated light. In the case of a small $\max_{y,c \in \{r,g,b\}} \frac{|A - I^c|}{\max(A^k, 1 - A^k)}$, δ tends to be large. For that reason they propose the final scene depth d_f which can be estimated according to the following equation:

$$d_f = d_{sc} \times (d_n(x) - \delta) \quad (20)$$

Note that d_{sc} is defined as a transforming scale used to get the real distance. However, this estimation is relative with air light estimation and needs to an accurate estimated A and a wrong estimation can leads to color saturation in the closest parts. To this end, we propose to use the scene depth estimated in the previous section as an easy way to estimate the distance between the closest scene point and the camera, Fig. 7 for more understanding:

According to Fig. 7 and the definition of image depth, we have that the closest point of the scene is that has maximum intensity within the depth map, instead of this, we propose to estimate the distance between the observed intensity and the pixel has a maximum intensity in the depth map $I(x)$ in each color channel c . We can calculate δ using the formula below:

$$\delta = 1 - \max_{c \in \{r,g,b\}} (d_{max} - I^c(x)) \quad (21)$$

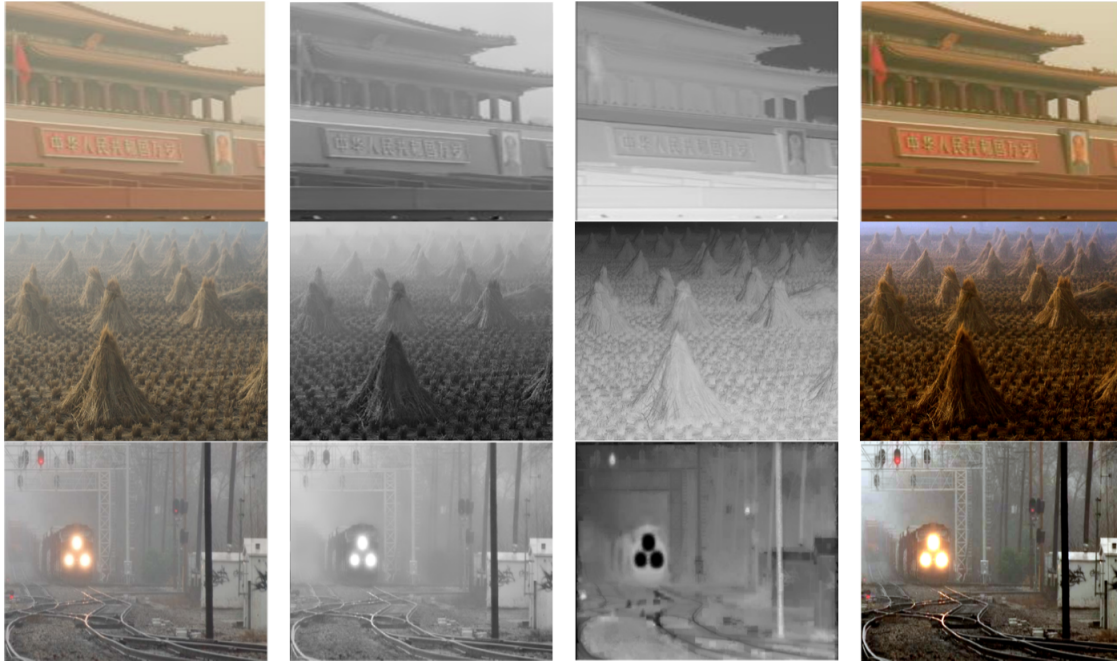


Fig. 8: Examples of Hazy images, their depth maps, transmission maps and recovered scene radiance. Left: Input hazy image. Center: Restored depth and transmission maps, respectively. Right: Dehazed image.

Where dm_{max} is maximum intensity in the depth map. Finally, to find the the scene depth D using distance δ we use the following equation:

$$D = 1 - sc(dn(x) - \delta) \quad (22)$$

Where sc is the scaling constant to transform the relative distance to absolute distance, in our work we set $sc=6$ meters (Fig. 8 the second column represents the final scene depth estimated).

By contrast, using Equation (23) we can get the transmission map TM as:

$$t(x) = e^{-\beta D(x)} \quad (23)$$

Where β is regarded as constant in homogenous atmosphere conditions. In this paper we set ($\beta= 0.8$). With the parameters chosen in this paper, we can see that the proposed method can properly restore the hazy image as Fig. 8. Finally, we use Equation (1) to recover the scene radiance. In the next section, we can show the effectiveness and robustness of the proposed method, by discussing the experimental results.

IV. RESULTS AND DISCUSSION

In order to verify the effectiveness and reliability of the proposed Dehazing method, we test it on a wide range of hazy images (more than 500 real-world and synthetic hazy images), and then compare the results with four state-of-the-art methods, He et al. [12], Quingsong et al. [27], Berman et

al. [37] and Wang et al. [38]. Three ways of evaluation are used to rate the performance of our proposed algorithm:

- Qualitative Evaluation on both Real-World and Synthetic Hazy Images.
- Quantitative Evaluation on both Real-World and Synthetic Hazy Images.
- Computational Time Complexity Comparison.

A. Qualitative Evaluation on both Real-World and Synthetic Hazy Images

1) *Qualitative Evaluation on Real-World Hazy Images:* Most of the existing dehazing algorithms, are able to effectively remove haze and recover scene radiance of outdoor hazy images, thereby rendering it difficult to visually rank and compare them. In an attempt to facilitate such ranking, some challenging images (containing regions of white and gray) are selected for testing.

Fig. 9 illustrates the qualitative comparison of the previous four Dehazing algorithms [12], [27], [37], and [38] on outdoor hazy images. Fig. 9(a) highlights the hazy images chosen to be recovered. Fig. 9(b-e) shows the Dehazed images using the previous Dehazing methods [12], [27], [37], and [38], respectively and Fig. 9(f) demonstrates the results of the proposed method.

As shown in Fig. 9(b), the method proposed by the authors was able to remove most of the haze and rendered well-recovered scene objects. However, the achieved results have led to the issue of over-enhancement, (for example, the top of the mountain in the second image tends to be orange and for

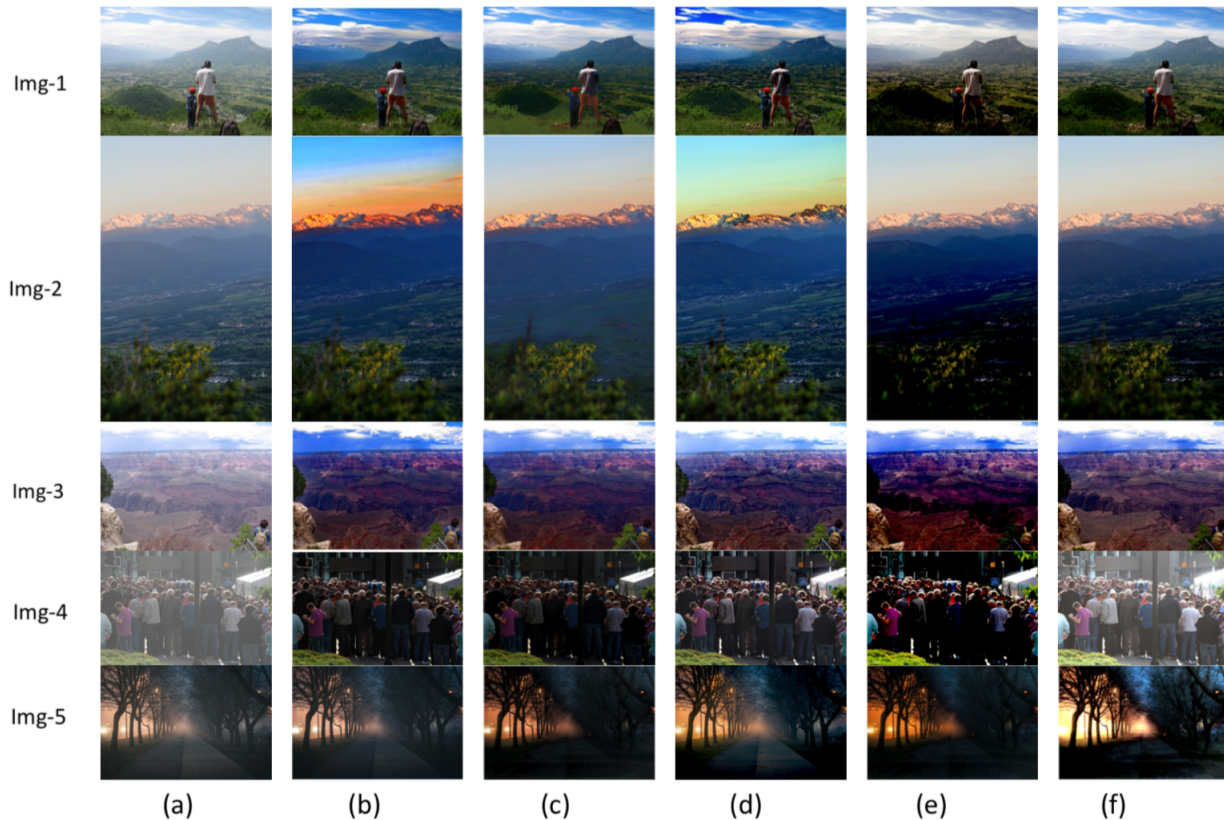


Fig. 9: Qualitative Comparison of Different Methods on Real-World Images. (a) the hazy images. (b) He et al.'s results. (c) Quingsong et al.'s results. (d) Berman et al.'s results. (e) Wang et al.'s results. (f) Our results

the first image, the sky region is much darker than it should be). This problem ensues from overestimating the transmission medium. The results of the second method [27] are much better visually (Fig. 9(c)). However, some parts of white objects are distorted (for instance, the whiteness of the shirt in the first image is darker). Moreover, for select regions in the second image, some edges are not preserved well and become invisible (see the green ground area), so we can deduce that this method can not preserve well the edges. In contrast, Berman's [37] method (Fig. 9(d)) removes the haze gradually and recovers the scene effectively. However, it suffers from the same issue as Quingsong's [27] method, some white regions are distorted (the white shirt in the first image is darker). The local contrast also seems saturated (as shown in the second image at the top of the mountain). While that Wang's [38] method performs well in term of haze removal, but it shows a big distortion in visibility and colors. Comparing the results of the four previous methods [12], [27], [37], and [38], our proposed method shows satisfactory results free from over-saturation, and can preserve edges and whiteness of objects. As shown in Fig. 9(f), the sky and clouds are clearly visible in the first image with details of all objects being enhanced (particularly the mountain in the third image).

2) *Qualitative Evaluation on Synthetic Hazy Images:* In order to further evaluate the performance of the proposed method, comparisons were made on synthesized hazy images

collected from the Middlebury dataset [39], [40], [41], with their respective ground truth images. Fig. 10(a) shows the synthesized hazy images, the results of compared methods are given in 10(b-f), and the last column represents the ground truth of the synthesized images. The haze-free images are taken from the Middlebury stereo datasets [39], [40], [41]. By observing the images in Fig. 10, it is clear that the results in Fig. 10(b) are far from the the ground truth images and appear much darker (particularly the first image, the pig and the face of the doll with red hair). Results of Fig. 10(c) show a slight haziness of distant objects (particularly the distant toys, the map in the background and the pink toy in the second image). Berman's method (Fig. 10(d)) shows results that seem to be more similar to the ground truth images. However, some inaccuracies and over-enhancement can be observed (particularly the third image has a darker background). Wang et al.'s method [38] also removes all the haze presented, however color distortion is evident (particularly in the last image). By comparison, the issue of over-saturation is absent and scene radiance is recovered in our proposed method (Fig. 10(f)).

B. Quantitative Evaluation on both Real-World and Synthetic Hazy Images

In the previous section, a qualitative comparison was presented to assess and rank the algorithms visually. This section proceeds to quantitatively assess and rank the algorithms in

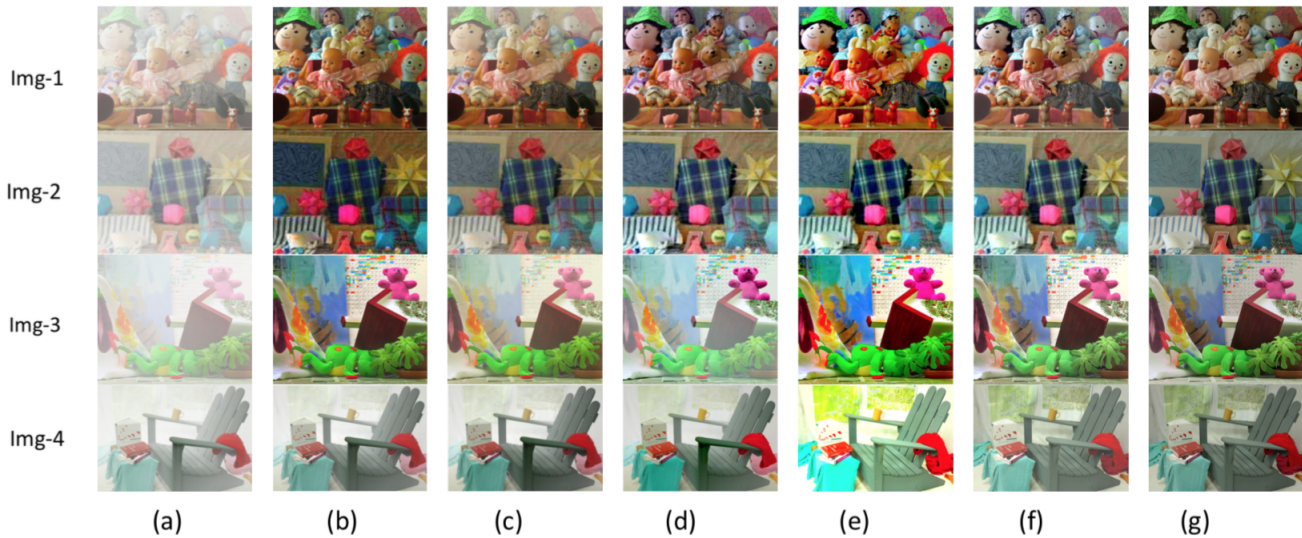


Fig. 10: Qualitative Assessment of Different Methods on Synthetic Images. (a) The hazy images. (b) He et al.'s results. (c) Quingsong et al.'s results. (d) Berman et al.'s results. (e) Wang et al.'s results. (f) Our results. (g) Ground truth.

terms of visibility enhancement, preservability of structural information, naturalness of the image and haze removability, using two categories of IQA(Image Quality Assessment): (NR-(No reference)-IQA and FR(Full reference)-IQA.)

1) NR-IQA on both Real-World and Synthetic Hazy Images:

For NR-IQA, we adopt four widely used metrics e , r , $FADE$ and $BRISQUE$ the most of them are designed for dehazing quality assessment and correlate well with human perception ($e, r, FADE$). The indicators e and r are proposed by Hautière et al. in the well-known approach of blind contrast enhancement assessment [44], where e measures the rate of new visible edges, and r verifies the average visibility enhancement before and after restoration. $FADE$ is a haze removability assessment which is proposed in [43]. $BRISQUE$ Blind/Referenceless Image Spatial Quality Evaluator, is an image quality assessment tool for rating possible loss of the naturalness of an image [42]. Generally, lower values of $FADE$ and $BRISQUE$ indicate that the results are satisfactory (low $FADE$ value indicates a greater dehazing ability) while high values of which, are not acceptable. By contrast, higher values of e and r imply better visual improvement after Dehazing. Tables I-IV contain the values of indicators ($FADE$, $BRISQUE$, e , and r respectively), of the dehazing results of state-of-the-art methods and our proposed method for both real-world and synthetic images (as shown in 9 and 10).

From the values of the $FADE$ indicator listed in Table I, it is observed that our proposed method achieves the best results with respect to haze removability for figures (Fig. 9(1-3), Fig. 10(1,2)), and the second-best values for figures (Fig. 9(4,5)). From these results, we deduce that the efficiency and performance of our proposed Dehazing method are proved, and it outperforms the other state-of-the-art Dehazing methods.

In order to verify the naturalness of the restored hazy images, $BRISQUE$ scores are computed for all compared

dehazing methods (including ours). As shown in Table II and according to $BRISQUE$ values, our Dehazing results produce the least-loss of naturalness for most of the images (9(1,2,4), Fig. 10(1,2)). Thereby indicating that our method preserves the naturalness of images after restoration. It also achieves the second-best score for Fig. 9(3). By contrast, our method fails to preserve the naturalness in the nighttime hazy image (Fig. 9(5)) while He et al. method [12] achieves the best score $BRISQUE$. In accordance with Table III, our results attain the highest value for only the image (Fig. 9(5)) that is a nighttime hazy image, while it realizes the second highest results for the images (Fig. 9(1,2), Fig. 10(4)), and it ranks the third top for the images (Fig. 9(3,4), Fig. 10(1)). It is known that the number of new visible edges after restoration must be balanced to avoid noise amplification, and our method represents this characteristic well, as noise amplification is avoided. In contrast, the results of Wang et al. [38] and Berman et al. [37] achieve the best values of e for the images (Fig. 9(2), Fig. 10(1,4)) and (Fig. 9(1,4)), respectively. This is a result of the over-saturation and over-enhancement of local contrast.

As mentioned previously, the indicator r verifies the average visibility enhancement after the restoration. Table IV shows the r values of Dehazing results for all of the compared methods (including our proposed). According to these results, our proposed method outperforms state-of-the-art methods for most of the images (Fig. 9(1,2,3), Fig. 10(1,4)), where it achieves the best values of r , and second-best result for the image (Fig. 9(4)). Despite the results of He et al. [12] and Berman et al. [37] attain the second-best score of r for the images (Fig. 9(5,3)), respectively, the over-enhancement problem is obvious in their results.

As a recapitulation of result analysis, the power and the performance of our proposed method to remove haze, enhance the visibility, and preserve the naturalness of an image has thus

TABLE I: *FADE* value of All the Compared Methods on Real-world and Synthetic Images (Fig. 9 and Fig. 10)

FADE	He et al. [12]	Quingsong et al. [27]	Berman et al. [37]	Wang et al. [38]	Ours
Fig.9 Img-1	0.3437	0.5246	0.3269	0.5379	0.2724
Fig.9 Img-2	0.5602	0.7923	0.6490	0.4257	0.3065
Fig.9 Img-3	0.3500	0.2132	0.4908	0.3206	0.1992
Fig.9 Img-4	0.2372	0.4022	0.2023	0.2969	0.2344
Fig.9 Img-5	0.6570	0.2700	0.3079	0.4024	0.3670
Fig.10 Img-1	0.3182	0.4830	0.2938	0.2781	0.2582
Fig.10 Img-4	0.5218	0.4583	0.3762	0.3092	0.2871

TABLE II: *BRESQUE* Score of All the Compared Methods on Real-world and Synthetic Images (Fig. 9 and Fig. 10)

<i>BRESQUE</i>	He et al. [12]	Quingsong et al. [27]	Berman et al. [37]	Wang et al. [38]	Ours
Fig.9 Img-1	37.11	32.52	35.08	27.98	24.07
Fig.9 Img-2	30.67	31.86	32.76	36.72	26.27
Fig.9 Img-3	33.40	34.54	30.58	34.68	30.89
Fig.9 Img-4	30.02	29.24	31.06	29.58	22.80
Fig.9 Img-5	29.58	30.08	30.90	35.88	37.83
Fig.10 Img-1	24.62	32.58	25.67	33.70	21.60
Fig.10 Img-4	27.81	22.32	20.98	30.27	19.68

TABLE III: *e* value of All the Compared Methods on Real-world and Synthetic Images (Fig. 9 and Fig. 10)

<i>e</i>	He et al. [12]	Quingsong et al. [27]	Berman et al. [37]	Wang et al. [38]	Ours
Fig.9 Img-1	2.1796	2.0692	3.7521	2.4709	3.0691
Fig.9 Img-2	32.0827	30.0827	39.7003	46.9503	40.6098
Fig.9 Img-3	2.7869	1.5072	1.9806	2.7243	2.6570
Fig.9 Img-4	0.9524	0.7093	1.9260	0.3298	0.7608
Fig.9 Img-5	0.2517	0.3675	0.8072	1.2983	1.3027
Fig.10 Img-1	48.9072	37.8025	45.7053	50.7291	46.5079
Fig.10 Img-4	48.3713	47.9073	50.3208	53.8824	52.6470

TABLE IV: *r* value of All the Compared Methods on Real-world and Synthetic Images (Fig. 9 and Fig. 10)

<i>r</i>	He et al. [12]	Quingsong et al. [27]	Berman et al. [37]	Wang et al. [38]	Ours
Fig.9 Img-1	3.7921	2.9571	3.4960	2.5043	5.2067
Fig.9 Img-2	3.1504	1.8586	3.2607	2.3179	3.9508
Fig.9 Img-3	2.7982	1.2974	1.9527	1.6052	3.9175
Fig.9 Img-4	1.7580	1.6873	2.7613	1.4570	2.0723
Fig.9 Img-5	2.0893	1.7989	1.9720	1.9052	1.7082
Fig.10 Img-1	1.8671	1.9340	2.1436	2.1703	2.3680
Fig.10 Img-4	1.9870	1.7629	1.8605	2.0712	3.1507

TABLE V: *C-SSIM* value of All the Compared Methods on Synthetic Images (Fig. 10)

<i>C-SSIM</i>	He et al. [12]	Quingsong et al. [27]	Berman et al. [37]	Wang et al. [38]	Ours
Fig.10 Img-1	0.8095	0.7965	0.8502	0.7264	0.8973
Fig.10 Img-2	0.7320	0.7534	0.8363	0.8093	0.8209
Fig.10 Img-3	0.8711	0.8462	0.8219	0.7838	0.9185
Fig.10 Img-4	0.8217	0.8913	0.8641	0.8168	0.8874

been proved.

2) *FR-IQA on Synthetic Hazy Images*: For the FR-IQA we select the color-based structural similarity index (*C-SSIM*)

proposed by Ahmed et al. in [45], which is an image quality assessment metric designed for color images. In addition, it is known to have high correlation with human evaluation.

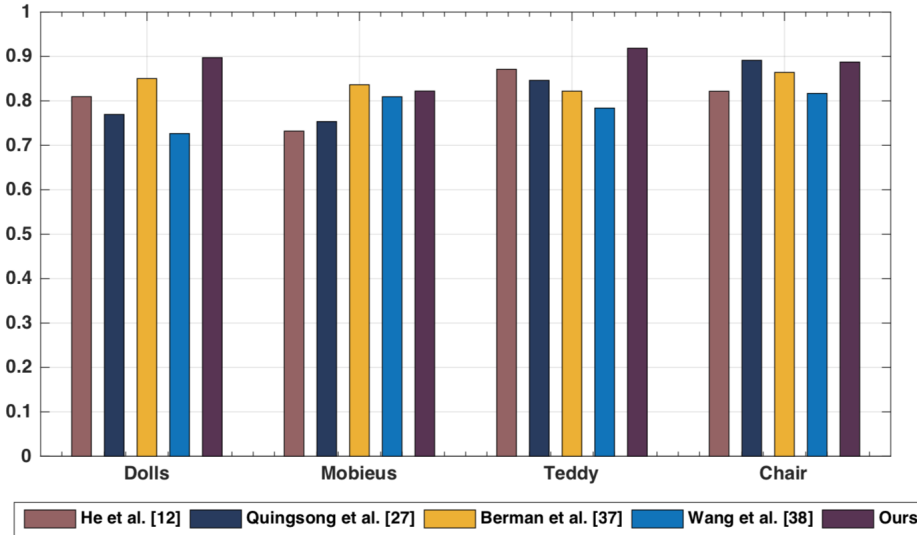


Fig. 11: Distribution of C -SSIM values of all the algorithms

TABLE VI: Computational time for Figures (Fig. 9 and Fig. 10) using different Dehazing methods

Computational time (s)	He et al. [12]	Quingsong et al. [27]	Berman et al. [37]	Wang et al. [38]	Ours
Fig.9 Img-1 (768 × 576)	130.32	2.97	87.96	10.16	3.12
Fig.9 Img-2 (511 × 768)	87.93	2.27	62.77	8.57	1.82
Fig.9 Img-3 (768 × 576)	107.80	2.53	79.22	10.84	2.96
Fig.9 Img-4 (768 × 512)	104.27	2.14	76.81	9.71	1.98
Fig.9 Img-5 (4117 × 2745)	211.64	5.07	99.14	11.21	6.36
Fig.10 Img-1 (695 × 555)	85.70	1.92	60.03	8.13	1.97
Fig.10 Img-4 (2880 × 1988)	190.04	5.12	97.19	10.20	5.28

The goal of which is to assess the ability of an algorithm to preserve structural information. In order to implement the C -SSIM experiments on synthetic hazy images presented in Fig. 10, the ground truth images are adopted as the reference images. The values of C -SSIM corresponding to the results of all the compared Dehazing algorithms are listed in Table V and distributed in Fig. 11. A high score of C -SSIM (close to 1) represents a high similarity between a result of Dehazing method and its ground truth, The converse is true for low values of C -SSIM.

As it can be seen from Table V, that our results are ranked the best among other algorithms for (Fig. 10(1,3)), and the second-best for the images (Fig. 10(2,4)). These results prove that our proposed method can effectively preserve the structural information for images after Dehazing. Despite Berman et al. and Quingsong et al. achieve the best C -SSIM

for the images (Fig. 10(2,4)) respectively, the haze residual is evident especially in Quingsong's result Fig. 10(4). This is confirmed by the $FADE$ value in Table I. By contrast, Wang et al's. results achieve the lowest values of C -SSIM for the majority of the images, and this indicates the loss of significant structural information in most of the images.

C. Computational Time Complexity Comparison

undoubtedly that the time complexity also is an important index to evaluate and rank the algorithms. Because of that, we list the run times of each algorithm in Table VI. The software used to implement and run our proposed algorithm is MATLAB, using a MacBook with 1.2GHz Intel Core M processor and 8 GB RAM. For a given hazy image of size $[N \times M]$, the complexity of our proposed Dehazing algorithm is $O(N \times M)$. According to Table VI, the running time

increases with respect to the size of the image. Also, Our proposed method demonstrates a remarkable computational time efficiency, and it is much faster than most of the other methods. Quinsong et al.'s method also shows an efficient computational time.

FAILURE CASE

As any Dehazing method based on the hazy model, our proposed Dehazing method has a limitation. Based on the experimental results presented in the section "Results and Discussion", we deduce that despite the good performance of our method on a wide range number of synthetic and real-world hazy images, our method performs poorly in case of nighttime hazy images. Example of the failure case is shown in Fig. 9(Img-5(f)), and this problem will be addressed in our future work.

V. CONCLUSION

In this paper, we have proposed a novel single haze removal method based on both image blur and atmospheric light estimation. We propose to use blur and atmospheric light to estimate the depth and transmission maps of hazy image for the first time, instead of the *DCP* based Dehazing method. Where we propose a new simple and powerful method to estimate the blur presented on the hazy image, and a new algorithm to estimate the atmospheric light based on blur and energy of image. To demonstrate the satisfaction of restoration of this proposed method we test it with real and synthesized hazy images. A large number of hazy images are well recovered using our proposed Dehazing method. Both subjective and objective comparison results showed that the proposed method can recover well the scene radiance of hazy image compared with other IFM-based Dehazing methods.

ACKNOWLEDGMENT

The work presented in this paper was supported by the National Natural Science Foundation of China under Grant no. 61370201

REFERENCES

- [1] B. Xie, F. Guo, Z. Cai, "Single Image Dehazing Using Dark Channel Prior and Multi-Scale Retinex," 2010 International Conference on Intelligent System Design and Engineering Applications, 2010.
- [2] T. K. Kim, J.K. Paik, B.S. Kang, "Contrast Enhancement System Using Spatially Adaptive Histogram Equalization with Temporal Filtering," IEEE Transactions on Consumer Electronics, pp. 82-87, 1998.
- [3] J.Y. Kim, L.S. Kim, S.H. Hwang, "An Advanced Contrast Enhancement Using Partially Overlapped Sub-Block Histogram Equalization," IEEE International Symposium on Circuits and Systems Emerging Technologies, 2000.
- [4] Y.Y. Schechner, S.G. Narasimhan, S.K. Nayar, "Instant Dehazing of Images Using Polarization," IEEE Computer Society Conference on Computer Vision and Pattern Recognition CVPR 2001, 2001.
- [5] Y.Y. Schechner, S.G. Narasimhan, S.K. Nayar "Blind Haze Separation," IEEE Computer Society Conference on Computer Vision and Pattern Recognition CVPR2006, 2006.
- [6] Y.Y. Schechner, S.G. Narasimhan, S.K. Nayar, "Polarization-Based Vision through Haze," Applied Optics, pp. 511, 2003.
- [7] S.G. Narasimhan, S.K. Nayar, "Chromatic Framework for Vision in Bad Weather," IEEE Conference on Computer Vision and Pattern Recognit. CVPR 2000, 2000.

- [8] S.K. Nayar, S.G. Narasimhan, "Vision in Bad Weather," IEEE International Conference on Computer Vision, 1999.
- [9] S.G. Narasimhan, S.K. Nayar, "Contrast Restoration of Weather Degraded Images," IEEE Transactions on Pattern Analysis and Machine Intelligence, pp. 713-724, 2003.
- [10] R.T. Tan, "Visibility in Bad Weather from a Single Image," IEEE International Conference on Computer Vision and Pattern Recognition, 2008.
- [11] Fattal, Raanan. "Single Image Dehazing," ACM SIGGRAPH, 2008.
- [12] K. He, J. Sun, X. Tang, "Single Image Haze Removal Using Dark Channel Prior," IEEE Transactions on Pattern Analysis and Machine Intelligence, pp. 2341-2353, 2011.
- [13] S.C. Pei, T.Y. Lee, "Nighttime Haze Removal Using Color Transfer Pre-Processing and Dark Channel Prior," IEEE International Conference on Image Processing, 2012.
- [14] K.B. Gibson, D.T. Vo, T.Q. Nguyen, "An Investigation of Dehazing Effects on Image and Video Coding," IEEE Transaction on Image Processing, pp. 662-673, 2012.
- [15] J. Yu, C.B. Xiao, D. Li, "Physics-Based Fast Single Image Fog Removal," International Conference on Signal Processing, 2010.
- [16] Q. Zhu, S. Yang, P.A. Heng, X. Li, "An Adaptive and Effective Single Image Dehazing Algorithm Based on Dark Channel Prior," IEEE International Conference on Robotics and Biomimetics, 2013.
- [17] C. Xiao, J. Gan, "Fast Image Dehazing Using Guided Joint Bilateral Filter," The Visual Computer, pp. 713-721, 2012.
- [18] Y.Y. Xiang, R.R. Sahay, M.S. Kankanhalli, "Hazy Image Enhancement Based on the Full-Saturation Assumption," IEEE International Conference on Multimedia & Expo Workshops, 2013.
- [19] J.P. Tarel, N. Hautiere, "Fast Visibility Restoration from a Single Color or Gray Level Image," IEEE 12th International Conference Computer Vision, 2009.
- [20] J.P. Tarel, N. Hautiere, L. Caraffa, A. Cord, H. Halmaoui, D. Gruyer, "Vision Enhancement in Homogeneous and Heterogeneous Fog," IEEE Intelligent Transportation Systems Magazine, pp. 6-20, 2012.
- [21] C.O. Ancuti, C. Ancuti, C. Hermans, P. A Bekaert, "Fast Semi-Inverse Approach to Detect and Remove the Haze from a Single Image," Computer Vision ACCV, R. Kimmel, R. Klette, A. Sugimoto, Springer, pp. 501-514, 2011.
- [22] L. Kratz, K. Nishino, "Factorizing Scene Albedo and Depth from a Single Foggy Image," IEEE 12th International Conference on Computer Vision, 2009.
- [23] K. Nishino, L. Kratz, S. Lombardi, "Bayesian Defogging," International Journal of Computer Vision, pp. 263-278, 2012.
- [24] G. Meng, Y. Wang, J.Y. Duan, S. Xiang, C.H. Pan, "Efficient Image Dehazing with Boundary Constraint and Contextual Regularization," IEEE International Conference on Computer Vision, 2013.
- [25] K. Tang, J.C. Yang, J. Wang, "Investigating Haze-Relevant Features in a Learning Framework for Image Dehazing". IEEE Conference on Computer Vision and Pattern Recognition, 2014.
- [26] K. He, J. Sun, X. Tang, "Guided Image Filtering," IEEE Transactions on Pattern Analysis and Machine Intelligence, pp. 1397-1409, 2013.
- [27] Q.S. Zhu, J.m. Mai, L. A Shao "Fast Single Image Haze Removal Algorithm Using Color Attenuation Prior," IEEE Transaction on Image Processing, pp. 3522-3533, 2015.
- [28] B. Cai, X. Xu, K. Jia, C. Qing, D. Tao, "DehazeNet: An End-to-End System for Single Image Haze Removal," IEEE Transaction Image Processing, pp. 5187-51982016.
- [29] W. Ren, S. Liu, H. Zhang, J. Pan, X. Cao, M.H. Yang, "Single Image Dehazing via Multi-Scale Convolutional Neural Network," Computer Vision ECCV2016, pp. 154-169, 2016.
- [30] Y. Song, J. Li, X. Wang, X. Chen "Single Image Dehazing Using Ranking Convolutional Neural Network," IEEE Transactions on Multimedia, 2017.
- [31] E.J. McCartney, Hall, F. Freeman, "Optics of the Atmosphere: Scattering by Molecules". Physics Today, pp. 76-77, 1977.
- [32] S.G. Narasimhan, S.K. Nayar "Vision and the Atmosphere," ACM SIGGRAPH ASIA 2008 Courses -SIGGRAPH Asia 08, 2008.

- [33] S.G. Narasimhan, S.K. Nayar, "Removing Weather Effects from Monochrome Images," IEEE Computer Society Conference of Computer Vision Pattern Recognition, CVPR, 2001.
- [34] Y.T. Peng, P.C. Cosman, "Underwater Image Restoration Based on Image Blurriness and Light Absorption," IEEE Transaction on Image Processing, pp. 1579-1594, 2017.
- [35] S. Emberton, L. Chittka, A. Cavallaro "Hierarchical Rank-Based Veiling Light Estimation for Underwater Dehazing," Proceedings Br. Machine Vision Conference, 2015.
- [36] A. Levin, D. Lischinski, Y. A. Weiss "Closed-Form Solution to Natural Image Matting," IEEE Transaction on Pattern Analysis and Machine Intelligence, pp. 228-242, 2008.
- [37] D. Berman, T. Treibitz, S. Avidan "Non-Local Image Dehazing," IEEE Conference on Computer Vision and Pattern Recognition CVPR, 2016.
- [38] J. Wang, K. Lu, J. Xue, N. He, L. Shao "Single image de-hazing based on the physical model and MSRCR algorithm," IEEE Transactions on Circuits and Systems for Video Technology, 2017.
- [39] D. Scharstein, H. Hirschmüller, Y. Kitajima, G. Krathwohl, N. Nešić, X. Wang, P. Westling "High-Resolution Stereo Datasets with Subpixel-Accurate Ground Truth," pp. 31-42, 2014.
- [40] D. Scharstein, C. Pal "Learning Conditional Random Fields for Stereo," IEEE Conference on Computer Vision and Pattern Recognition, 2007.
- [41] D. Scharstein, R. Szeliski "High-accuracy Stereo Depth Maps Using Structured light," IEEE Conference on Computer Vision and Pattern Recognition (CVPR2003), pp. 195-202, 2003.
- [42] Mittal, A.K. Moorthy, A.C. Bovik "No-reference image quality assessment in the spatial domain" IEEE Transactions on Image Processing, pp. 4695-4708, 2012.
- [43] L.K. Choi, J. You, A.C. Bovik "Referenceless prediction of perceptual fog density and perceptual image defogging," IEEE Transactions on Image Processing, pp. 3888-3901, 2015.
- [44] A.N. Hautière, J.p. Tarel, D. Aubert, É. Dumont "Blind contrast enhancement assessment by gradient ratioing at visible edges," Image Analysis and Stereology, pp. 87-95, 2008.
- [45] A.H. Mohammed, S.B. Mazen "Color-based Structural Similarity Image Quality Assessment," 8th International Conference on Information Technology (ICIT), 2017.

Arabic Text Classification using Feature-Reduction Techniques for Detecting Violence on Social Media

Hissah ALSaif¹, Taghreed Alotaibi²

College of Computer and Information Sciences, Shaqra University, Riyadh, Saudi Arabia

Abstract—With the current increase in the number of online users, there has been a concomitant increase in the amount of data shared online. Techniques for discovering knowledge from these data can provide us with valuable information when it comes to detecting different problems, including violence. Violence is one of the significant problems humanity has faced in recent years all over the world, and this is especially a problem in Arabic countries. To address this issue, this research focuses on detecting violence-related tweets to help in solving this problem. Text mining is an important technique that can be used to find and predict information from text. In this study, a text classification model is built for detecting violence in Arabic dialects on Twitter using different feature-reduction approaches. The experiment comprises bagging, K-nearest neighbors (KNN), and Bayesian boosting using different extraction features, namely, root-based stemming, light stemming, and n-grams. In addition, the study used the following feature-reduction techniques: support vector machine (SVM), Chi-squared (CHI), the Gini index, correlation, rules, information gain (IG), deviation, symmetrical uncertainty, and the IG ratio. The experiment showed that the bagging with tri-gram approach has the highest accuracy at 86.61%, and a combination of IG with SVM from reduction features registers an accuracy of 90.59%.

Keywords—Violence; text mining; classification; feature-reduction techniques; Arabic; Twitter posts

I. INTRODUCTION

One of the most important elements in living a normal and stable life is living in peace. Individuals can reach this level of peace when they are removed from any manifestations of violence and persecution, and this will enhance their ability to be successful members of the community. In recent years, the rate of violence has been increasing all over the world, and this is an indicator of danger that communities should be aware of to take the necessary steps to avoid or reduce it. There are different types of acts that can be categorized as violence, including physical, sexual, and psychological violence.

Due to the evolution of technologies and the increasing number of internet users around the world, especially when it comes to using social networks, social media are becoming a significant environment for studying phenomena related to violence; this is because social network users publish events rapidly, and some of them use social media sites to voice complaints and ask for help. From this perspective, this present research focus on studying violence in the Kingdom of Saudi Arabia (KSA) regarding the increased number of violence cases, where the Ministry of Labor and Social Development received more than 11,000 reports in a year [1]. This research is concentrate on Twitter to collect dataset due to the rising

number of Saudi Twitter users, there were about 2.4 million active Twitter users in 2013, representing 41% of individuals online [2] [3]. To study this usage, four regions were choosing in the KSA with the highest populations to collect tweets from Twitter users.

This research is using text mining, which an important topic regarding the knowledge it uncovers. Text mining, defined as a technique of extracting valuable information from text, consists of different processes, specifically, information retrieval, categorization, extraction, textual analysis, and visualization [4][5]. After information extraction, the biggest challenge faced in text classification is the huge number of features that must consider. To solve this problem, feature-reducing techniques are used for selecting the appropriate subset. Feature reduction is a critical step that can positively or negatively affect the accuracy of the classifier according to the selected approaches [6][7]. This study investigated different feature-reduction methods and their effects on accuracy. Moreover, it used machine learning techniques, where machine learning algorithms can be categorized into two approaches—supervised and unsupervised. In the supervised approach, the data are labeled and the algorithm works to predict the output; in contrast, in the unsupervised approach, there is no labeling process for data, and the algorithm works to build structures to understand the data [8]. This study used the following supervised machine learning algorithms: bagging based on support vector machine (SVM), K-nearest neighbors (KNN), and Bayesian boosting using complement naïve Bayes (CNB) with different stemming and n-gram techniques, in addition to different feature-reduction techniques.

This research has the following objectives:

- To detect violence and find the most common cities with high rates of violence in Saudi Arabia;
- To compare the stemming and n-gram techniques to find the best one for the Arabic language;
- To evaluate some reduction features to find the best one for Arabic; and
- To evaluate some ensemble methods of classification algorithms.

This paper is organized as follows: Section 2 gives a general perspective on the Arabic language, while Section 3 presents an overview of violence. Section 4 briefly presents similar studies on text mining and feature-reduction using Arabic. Section 5 illustrates the machine learning algorithms used in this study, and Section 6 describes the methodology of

the work in detail. Section 7 shows the performance measurement used. Section 8 illustrates the results of the research, and finally, Section 9 presents the conclusion of the study.

II. ARABIC

Arabic is one of the most common languages currently in use, with more than 315 million people around the world who speak this language. Moreover, Arabic is the official language of 17 Arabic countries [9], and it is used in other Islamic countries as a second language. Arabic language can be classified into three types, namely, the original version of Arabic, called Classical Arabic (CA); Modern Standard Arabic (MSA); and dialectal Arabic (DA). CA is the basis for Arabic, and it is the version used in the Holy Qur'an; In contrast, MSA is currently used in the media, education, and formal speech. Finally, because Arabic is spoken in different countries, this has allowed for the emergence of different Arabic dialects, which represent spoken rather than written language [10]. The dialects can be classified depending on the countries in which they are spoken; for example, the Gulf dialect is used in Saudi Arabia, Kuwait, Qatar, Bahrain, and the United Arab Emirates. Moreover, while there are different Arabic dialects in different countries, there are also multiple dialects spoken in the same country; for instance, in Saudi Arabia, there are speakers of the Najd, Hijaz, and Qassim dialects, which are used in informal daily communication.

Arabic consists of 28 letters, which are $\text{أ ب ت ث ج ح خ د ذ ر ز س ش ص ض ط ظ ع غ ف ق ك ل م ن و ي}$ and there are additional vowels letters ا و ي . In contrast to many other languages, Arabic is written from right to left; all the letters are lower case, and there is no capitalization. There are some challenges in working with Arabic. For example, a single letter in Arabic can have different styles depending on its position in the word. The letter (ص) is written in one way if it comes at the beginning of a word, such as (صباح) "morning," another way if it comes in the middle of the word, such as (العصفور) "bird," and yet another way if it comes at the end of the word (ص), such as (خاص) "special" [10][11].

In Arabic, there are some diacritics, which called Harakat that can be used with words. These can change the meaning of the word; for example, مُعَلِّم means "teacher" and مَعْلَم means "landmark" [10][11]. In addition, Arabic words can be conjugated differently for feminine or masculine meanings. For numbers of persons, Arabic uses the three following cases: singular for one person, dual for two people, and plural for more than two people; this is shown in Table I.

Arabic contains many words that have more than one meaning depending on the context of the sentence, such as the examples shown in Table II. In addition, there are different synonyms for the same term, for example, "هفوة", "زلة", "سقطه", "عثره", "كبوته" all mean doing something wrong [11].

TABLE I. ARABIC CASES FOR PERSON NUMBER

Verb	Singular	Dual	Plural
لعب (played)	لعب	لعبا	لعبوا

TABLE II. EXAMPLES OF DIFFERENT WORD MEANINGS DEPENDING ON THE CONTEXT OF THE SENTENCE

Meaning	Example	Word
Walking	"وَجَاءَتْ سَيَّارَه"	سياره
Car	ركبت سيارة	

All Arabic words rely on a root, which can be defined as the main part for any words that cannot be removed without losing the meaning of the word. There are more than 11,000 roots in Arabic [12]. Roots can be connected to affixes; these can come at the beginning of the word (prefixes), end of the word (suffixes), or middle of the word (infixes). To illustrate this in details, see the example of the word (العب) in Table III [13][10]. All these features of Arabic show the challenges researchers face when data mining information written in Arabic.

TABLE III. AFFIXES IN ARABIC WORDS

Suffix	Infix	Prefix	Word
-	-	م	ملعب (Stadium)
-	ا	أ	الاعباب (Toys)

• Violence

Violence is one of the biggest problems society faces today. The number of victims of violence is showing an increasing trend around the world. The World Health Organization showed that about 10 million persons lose their life as a result of violence in the age range of 15–44 years [14]. Violence can come in many forms: It can be defined as the premeditated use of force, either physical or emotional, toward the self, other individuals, or a group in such a way that causes harm, injury, or fatality or is likely to do so [14]. From this definition, it is clear that violence can be classified into different types as physical, sexual, or psychological violence [14]. Physical violence consists of any physical harm of people, such as causing injury, beating, or killing them. Sexual violence includes any forcible sexual acts against children, women, or men [14]. Finally, psychological violence includes any intentional action against a person to harm him or her psychologically by coercion or threats[15]. According to the Ministry of Justice, in the KSA, the number of domestic violence cases in 2014 were about 34.3% in Makkah and 23.3% in Riyadh, followed by 12.9% and 5.6% in the Eastern Region of KSA and Asir, respectively [16].

III. RELATED WORK

Text classification is an excellent technique when it comes to discovering new knowledge from text. However, most related research has focused on text mining in English, and thus, there is still a need for more research connected to Arabic, especially DA. In addition, some research has tried to use extraction and selection features for improving the text classification performance. To our knowledge, the present study is first research on detecting violence in Saudi dialect, with the use to feature extraction and selection techniques.

In [17], the authors studied sexual violence on Twitter. The dataset consisted of 700,000 extracted tweets using the #MeToo hashtag in 2017. The study evaluated different

algorithms, such as a Convolutional Neural Network (CNN) and Multilayer Perceptron (MLP), for classifying tweets based on the place and offender. The results showed that the CNN outperformed the other algorithms by 83%. In addition, Subramani et al. [18], extracted Facebook posts and comments as their experimental dataset. The researchers aimed to classify intent for domestic violence discourse on social media. The dataset contained 8,856 posts and 28,873 comments. Four models were applied, namely, SVM, Naïve Bayes (NB), Decision Tree (DT), and KNN with two reduction features: Linguistic Inquiry and Word Count (LIWC) and CHI. The results showed that the accuracy of NB was highest, at 82%, followed by KNN. In [19], the researchers detected religious hate speech on Twitter in Arabic. The data, which were collected using Twitter's Application Programming Interface (API), comprised 600 tweets as the training set and 6,000 tweets as the testing set. They used three different classification models, namely, a lexicon-based model, an N-gram-based model using logistic regression and a deep neural network using Gated Recurrent Units (GRU). For reduction features they used CHI, Pointwise Mutual Information (PMI) and Bi-Normal Separation (BNS). Tweets were classified using help from crowdsourcing workers. The results showed that the GRU-based system with a simple Recurrent Neural Network (RNN) provided the best results, with 79% accuracy.

In [20], a classifier was built to study six Arabic dialects, namely, Shami, Iraqi, Gulf, Sudanese, Moroccan, and Egyptian. The study used 2,000 tweets from Twitter as dataset, while the algorithms used were the NB, rule-based, and DT algorithms. Data collection was done using the Topsy website and Twitter API. As result, the accuracies for the classifiers were 71.18% for Ripper, 57.43% for DT, and 71.09% for NB, but the classifier had difficulty differentiating the Sudanese, Egyptian, and Gulf dialects.

In Raheel and Dichy's [21] research, they studied which types of feature extraction are best for Arabic languages. They chose Arabic articles covering seven categories as their dataset, which comprised 7,034 articles. They classified the dataset into five versions; in each version of the dataset they use one of the following types of feature extraction: 3-gram, 4-gram, root and lemma. In addition, they used 10-fold cross-validation, and for the algorithms, they used SVM and NB networks with two selection features—IG and CHI. For measuring weight, they used term frequency-inverse document frequency (TF-IDF). In each test, they increased the number of features from 400 to 2,000. The results showed that SVM recorded higher accuracy values using the 3-gram approach, at 92.28% for IG and 92.41% for CHI.

In [22], the researchers implemented a method based on two stages for reducing the dimensionality of the features. First, they used IG for ranking the importance of features; then, they applied the Principal Component Analysis (PCA) and Genetic Algorithm techniques for reducing the feature number. The experiments were conducted on two well-known public datasets written in English with two models, namely the C4.5 DT and KNN classifier. The results revealed good improvements in classification accuracy. The experiments in study [23] were conducted on a public dataset consist of 937 reviews in English. The researchers evaluated four

classification methods, including SVM, logistic regression, bagging, and Bayesian boosting with PCA as reduction techniques for decreasing the dimensionality of the dataset and improving the classification accuracy. The results revealed better performance in classification with PCA. In [24], the researchers performed text mining on an Arabic dataset from King Abdulaziz City for Science and Technology (KACST), covering five fields with about 2,243 texts from the Islamic topics of Feqh, Tafseer, Lughah, Aqeedah, and Hadeet. The researchers employed three schemas for representation—Boolean, LTC, and TF-IDF. The CHI and weirdness coefficients were applied as feature selection, with NB and KNN as classifiers. The study used a different number of features each time, starting from 10 and ending at 300. As a result, NB with CHI squared showed high accuracy, which was 89.25% with LTC. In contrast, the weirdness coefficient showed high accuracy with NB and the Boolean scheme, at 85.22%.

In [25], the researchers focused on comparing various types of NB approaches, such as multivariate guess Naïve Bayes (MGNB), Flexible Bayes (FB), and Multinomial Naïve Bayes (MNB). For feature extraction, different techniques were used, such as the light stemmer and term-based n-gram. For feature reduction, several approaches, such as CHI, Odds Ratio (OR), Mutual Information (MI), and the Galavotti, Sebatiani, Simi (GSS) coefficient, were employed. The results revealed that FB had the best performance among the classifiers.

In [26], the researchers built a large corpus for Arabic using different categories of topics from Saudi newspapers, forums, writers, the Saudi Press Agency, Topics in Islam, websites, and Arabic poems. The study experiment was performed using SVM, NB, KNN, MLP neural networks, C4.5, and C5.0. As a result, SVM registered a high accuracy. For feature selection, the researchers used CHI, GSS, the Darmstadt Indexing Approach (DIA), IG, MI, NG, Goh and Low (NGL) coefficient and Relevancy Score (RS), OR and none. The best result were showed by GSS, none, and RS. The researchers also studied the performance using the following weighting terms, TF-IDF, LTC, TFC, Boolean, relative frequency, and entropy. The LTC came first with the best result followed by Boolean and TFC.

For short text documents, Faqeeh et al. [27] implemented a classifier that studied 1,000 Facebook comments in Arabic and English. They chose and filtered comments related to weather and food manually, then applied four algorithms—SVM, NB, KNN, and DT. As a result, the accuracy for the Arabic dataset was higher than that for English, and the SVM classifier showed a better result than the other classifiers did. Moreover, in [28], the authors performed text mining over an Arabic dataset. The dataset contained 1,000 documents from five fields (health, politics, economics, technology, and sport). They used 5-fold cross-validation because of the limitation of their devices. For stemming, they applied a light stemmer and root-based, and for algorithms, they chose NB, SVM, KNN, DT, and decision table. They established three versions of the dataset—one with no stemming, one with a root-based stemmer, and one with a light stemmer separately. As a result, SVM with 10 light stemmers recorded the best accuracy, at 98.20%.

Another study categorized documents according to their contents into four classes, namely, sport, politics, economics, and arts [29]. The dataset consisted of more than 3,000 documents collected from different websites. The classification was evaluated by the KNN algorithm with four types of similarity measures—cosine, Jaccard, dice, and I_{new} —in terms of execution time and accuracy. The results indicated the superiority of I_{new} over the other similarity measures.

A further study considered the influence of Singular Value Decomposition (SVD) on a large dataset containing 4,000 documents in Arabic [30]. Experiments were applied using seven known algorithms, specifically, NB, KNN, Neural Networks, Cosine Similarity, Random Forest, SVM, and DT. The results showed an improvement in the classification process, where the accuracy of the classification increased from 67.25% to 82.50%.Abuhaiba et al. [31] performed a study comparing the performances between a single classification algorithm and a combination of different algorithms for categorizing Arabic text. The study used text documents from

three news networks with different categories. In addition, they built four models for improving the performance, which were bagging, stacking, AdaBoost, and fixed combining rules. For stemming, they tested each model using light and root-based stemming, and for the weighting term, they used TF-IDF. For the last model, the researchers used the average, product, majority, minimum, and maximum rules. As a result, classifier with the majority voting rule registered higher accuracy, at 94.5%; this was superior to that of each single classifier, which were the radial basis function network (RBFN), Nearest-Neighbor-Like, NB, SVM, C4.5, KNN, and Decision Stump. In contrast, the stack model with five classifiers had even higher accuracy, at 99.5%, compared with each single classifier, which were NB, learning vector quantization (LVQ), C4.5, KNN, and decision stump. Then, the AdaBoost model with 10 iterations outperformed the C4.5 classifier, recording 99.5% accuracy. Finally, the bagging model with 10 iterations had 99.4% accuracy, which was higher than that of DT. Tables IV and V summarize the previews mentioned related works.

TABLE IV. COMPARISON OF SIMILAR STUDIES FEATURES EXTRACTION METHODS

Study	Dataset Source	Dataset Language	Features Extraction Methods
Raheel and Dichy [21]	Articles	Modern Arabic	N-gram, Root-based stemming.
Harun Uguz [22]	Articles	English	-
Al-Thubaity et al.[24]	Articles	Modern Arabic	-
Kadhim and Omar [25]	Articles	Modern Arabic	Light- stemming, N-gram
Khorsheed and Al-Thubaity. [26]	Newspapers	Modern Arabic	-
Vinodhini and Chndrasekarn[23]	Reviews	English	-
Faqeeh et al.[27]	Facebook comments	Arabic, English	Light stemming, Root-based stemming.
Hmeidi et al. [28]	Articles	Modern Arabic	Light -stemming, Root-based stemming
Alhutaish and Omar [29]	Articles	Modern Arabic	Light stemming, N-gram
Al-Anzi , Dia AbuZeina [30]	Articles	Modern Arabic	-
Abuhaiba and Dawoud [31]	Articles	Modern Arabic	Light stemming, Root-based stemming
Al-Walaie and Khan. [20]	Twitter post	Dialect Arabic	-
Albadi et al. [19]	Twitter post	Modern Arabic	N-gram.
Subramani et al. [18].	Facebook comments	English	-
Khatua et. Al. [17]	Twitter post	English	-

TABLE V. COMPARISON OF SIMILAR STUDIES FEATURES REDUCTION METHODS AND CLASSIFICATION ALGORITHMS

Study	Features Reduction Methods	Classification Algorithms
Raheel and Dichy [21]	IG, CHI	SVM, Naïve Bayesian Networks
Harun Uguz [22]	PCA, IG, Genetic algorithm	C4.5 DT, KNN
Al-Thubaity et al.[24]	CHI, Weirdness coefficient (W)	NB., KNN.
Kadhim and Omar[25]	CHI, OR, MI, GSS	MGNB, FB, MNB.
Khorsheed and Al-Thubaity. [26]	CHI, GSS, DIA, IG, MI, NGL, RS, OddsR,	SVM, NB, KNN, MLP, C4.5 DT, C5.0 DT.
Vinodhini and Chandrasekaran[23]	PCA	SVM, Logistic Regression, Bagging, Bayesian boosting
Faqeeh et al.[27]	-	SVM, NB, KNN ,DT
Hmeidi et al. [28]	-	NB. SVM, KNN, J84 DT, Decision Table
Alhutaish and Omar [29]	-	KNN
Al-Anzi , Dia AbuZeina [30]	SVD	NB, KNN, NN, Cosine similarity, Random Forest, SVM, DT
Abuhaiba and Dawoud [31]	-	NB, SVM, C4.5, KNN, Decision Stump, LVQ, RBFN.
Al-Walaie and Khan. [20]	-	NB, Ripper, DT
Albadi et al. [19]	CHI, PMI, BNS	Logistic regression, SVM.
Subramani et al. [18].	CHI, LIWC dimensions	NB, DT, KNN, SVM
Khatua et. Al. [17]	-	CNN ,MLP

IV. MACHINE LEARNING

Machine learning algorithms can be classified into the two following types: eager learners and lazy learners. Eager learners construct models using training datasets before they obtain new objects and then use the model to classify the new objects. In this type of learning, a single global hypothesis is constructed that encompasses the entire dataset. In contrast, lazy learners store data for later use, when there is a new object; they are also called instance-based learners. They compare each new instance of data with instances in the training sets that stored memory; this allows them to measure the similarity [32][33]. In this study, two ensemble methods are used to build models, including bagging and Bayesian boosting, as well as KNN, which is one of the most widely used classifiers. In this section, these algorithms are explained briefly.

A. *K-Nearest Neighbors (KNN)*

KNN is a simple algorithm that can be used to construct many local hypotheses for each new object in a dataset using the lazy learning approach. This approach assigns objects based on the majority of voting of its neighbors. KNN is slow in classifying data, requires a large amount of memory space, and is computationally expensive because a hypothesis must be constructed for each new object. There are many measurements used to determine the distance between objects in space. One popular measure in information retrieval is cosine similarity. The basic idea of cosine similarity is measuring the angle between two objects represented as vectors in the space. The following equation represent cosine similarity [34][35]:

$$\text{cosine}(x, y) = \frac{x \cdot y}{\|x\| \|y\|} \quad (1)$$

B. *Bagging*

Bagging is a well-known ensemble method that creates multiple independent hypotheses, then calculates aggregated results that lead to better performance. Bagging is based on the bootstrapping method, which selects a sample set randomly with replacement. This allows the creation of a more accurate and robust model and avoidance of overfitting [34].

In this study, SVM is used as a meta-algorithm in bagging because it is an effective method in the classification task. This is due to the complexity of hypotheses, depending on the size of the margin, unlike other methods, in which the difficulty is associated with the number of features in the document [36].

C. *Bayesian Boosting*

Bayesian boosting is an iterative method in which each model determines which dataset will be used in the next iteration for model building. It uses bootstrapping, but unlike in bagging, the sample selection is based on weight. This allows building a more accurate model and reducing noise [34].

In this study, CNB is used as a meta-algorithm in boosting. CNB is a fast and simple algorithm that is widely used in classification problems. It is considered a highly accurate algorithm because it avoids the overfitting problem found in the original version of NB [34][33].

V. STUDY METHODOLOGY

To implement models for this study, the following steps were followed.

A. *Data Collection*

As mentioned before, Twitter is used to be the dataset source for this study because it is one of the most widely used applications in the KSA. Tweets from 2017–2018 from four regions in the KSA with higher populations were collected. The regions were Riyadh, Makkah, the Eastern Region, and Asir. Each region comprises different cities. The dataset consists of 6,500 violence tweets and 6,000 tweets from various fields written in colloquial Arabic in the Saudi Dialect. To collect the data, the Twitter API is used to obtain tweets from the four identified regions, and the data is extracted to an Excel file for processing. As a result, the tweets are labeled according to three classifications, namely, physical violence, psychological violence, and no violence. The final dataset consisted of 119,296 features with 32,143 unique features.

B. *Data Preprocessing*

To make the dataset more consistent before it was used on the models, the following important preprocessing steps are performed:

- In Arabic, some characters in a word can be written in different ways, such as أكل، اكل، which means “ate.” Because this research is concentrating on a Saudi colloquial dialect, there are some users writing tweets with different spelling problems. To overcome this problem, some letters are normalized { آ، إ، أ } to { ا }, { ع } to { ي }, { ح } to { و }, and { ه } to { ه };
- Removing English characters, punctuation, and symbols like @, #, and _, which are found in Twitter hashtags, and replaced them with spaces to avoid confusion between letters;
- Removing some links (URLs), diacritics, numbers, stop words, and any word with two letters or less because such words do not have meaning; and
- This paper used TF-IDF to produce a composite weight for every term.

C. *Feature Extraction*

To simplify the processing step for machine learning models, this study needs to apply feature extraction. It used two leading approaches, namely, light stemming and root-based stemming. Light stemming works by removing the prefixes and suffixes of words, while root-based stemming returns the word to its root [31][37]. In addition, the research applied bag of words (BOW), bi-gram, tri-gram, and a combination of the latter two. In bow, a list of words is built with their occurrences [32], while bi-gram and tri-gram focus on splitting words regarding the value of n into two and three words [21].

D. *Feature Reduction*

On completion of the extraction process, the number of features extracted was huge. A large number and variety of features leads to a low level of performance in the classification due to the presence of many words that have no

value. To overcome this issue, various feature-reduction techniques are applied for selecting the most appropriate and relevant subset based on specific measurements. The main goal of feature reduction is improving the overall performance of classification, in addition to improving the speed of the processing and memory usage [6][7]. In this section, some feature-reduction techniques are described briefly.

1) *Rule-based feature reduction*: In rule-based feature reduction, the weight of features is calculated regarding the label feature. It builds a single rule for each feature, then calculates the errors. After that, it considers the feature with the highest weight as the pertinent feature [38].

2) *CHI*: CHI weight is a popular statistical method that uses CHI for calculating the weight of features regarding the attribute's class. Features with higher weight are considered more relevant. If CHI has a large value, then the feature is important for the category. This approach is used for measuring the difference between the expected and observed numbers of times the event occurs. The following formula is used for calculating the CHI statistic [39][40].

$$X^2(t, c) = \frac{N(AD-CB)^2}{(A+C) \times (B+D) \times (A+B) \times (C+D)}, \quad (2)$$

where A is the number of occurrences for t with c , N is the number of documents, D is the number that c and t neither occurred, B is the number of occurrences for t only without c , and C is the number of occurrences of c only without t .

3) *Symmetrical uncertainty*: To calculate the feature weight, the symmetrical uncertainty is calculated regarding class and label features. This calculates between the feature and target class, and it is used to calculate the efficiency of features. The following formula can be used to calculate symmetric uncertainty [41][42]:

$$SU(X, Y) = 2 \left(\frac{IG(X|Y)}{H(X)+H(Y)} \right) \quad (3)$$

It is clear that symmetrical uncertainty is based on the IG of features. $H(X)$ and $H(Y)$ are the entropy values of features X and Y , respectively. This approach normalizes features with a large number of different values to the range $[0,1]$, which means that when $SU = 0$, the features are not related to each other, but when $SU = 1$, knowledge of one feature allows predicting the value of the other.

4) *Deviation*: Using deviation-reduction methods, features are weighted based on normalized standard deviation. Features with a higher weight are considered relevant. The standard deviation illustrates how much variance from the mean is present. A low value of standard variance indicates that a feature is extremely close to the mean, whereas a higher value represents a large contrast. The formula for standard deviation is the variance square root [43].

5) *Correlation*: Correlation is another statistical operation used for understanding the relationship between features. For example, if we have A and B features and want to know how close they are to each other, this can be determined by calculating correlation coefficient. This takes a value in the range of -1 to 1 . If the value is positive, this means that when

A has large value, it is related to a large value of B . In contrast, a negative value of correlation shows an inverse relationship. The correlation coefficient can be calculated using the following formula [44]:

$$r_{A,B} = \frac{\sum_{i=1}^n (a_i b_i) - n \bar{A} \bar{B}}{n \sigma_A \sigma_B} \quad (4)$$

where the number of tuples is n , while a_i and b_i represent the values of A and B in each tuple. In addition, σ_A, σ_B and \bar{A}, \bar{B} are the standard deviation and mean values for A and B , respectively.

6) *Gini index*: The Gini Index is another statistical method that calculates the feature weight regarding the class label using the impurity of features [44].

7) *Information Gain (IG)*: The IG is a popular measure that was introduced by J.R. Quinlan for determining the extent to which a specific feature gives informative value about a class. It ranks scores for each feature, then selects the highest score, while lower scores are removed. ID3 uses IG as a split measure for selecting the attribute with the highest information gain value [33][34].

8) *Information gain ratio*: The simple form (IG) can work for most cases, but it works by choosing features with large values as root nodes. The IG by ratio is a new version of IG that is modified to reduce this bias toward choosing features with large values by normalizing IG. It observes the number of branches that will occur and takes this into account before making the split [45].

9) *SVM*: SVM is used as feature selection for selecting the most relevant features based on setting the hyperplane coefficients, which are calculated by an SVM as the weights of features [33].

VI. PERFORMANCE MEASUREMENT

When using different classifiers, there should be an assessment of how the classifier performs when it is predicting class labels. To accomplish this, there are different measurements for evaluation, which are known as recall, precision, and accuracy, also called the recognition rate [44]. In this study, three of these measurements—accuracy, recall, and precision are choosing to be evaluated. Accuracy can be defined as the ratio of the number of tuples a classifier predicted correctly divided by the total number of tuples. Recall is the number of true-positive tuples divided by the sum of true-positive and false-negative tuples. Finally, the precision is the total of true-positive tuples divided by the sum of true-positive and false-negative tuples. Their equations are as follows [27], [44]:

$$Accuracy(a) = \frac{TP+TN}{TP+FP+TN+FN} \quad (5)$$

$$Precision(p) = \frac{TP}{TP+FP} \quad (6)$$

$$Recall(r) = \frac{TP}{TP+FN} \quad (7)$$

where TP is the number of positive tuples predicted correctly by the classifier, TN is the number of negative tuples predicted correctly by the classifier, FN is the number of

positive tuples the classifier predicted incorrectly, and FP is the number of negative tuples the classifier predicted incorrectly. In addition, the study used 10-fold cross-validation to test the model. The data were divided randomly into 10 folds, and in each iteration, one of these folds was used as the test set and the others as the training partition [44].

VII. EXPERIMENTAL RESULTS

The experiments were implemented using the RapidMiner tool. RapidMiner is an open-source tool written in Java that provides a wide range of text-mining techniques and machine learning algorithms. For the experiments, a 64-bit Windows 10 laptop devices are used with 16 GB of memory and Intel core i7.

A. Dataset Analysis

After collecting the datasets, they are analyzed depending on the types of violence and the user’s location. As a result, some tweets did not have a clear location, so they are excluded. The results in Fig. 1 show that the most tweets were collected from Riyadh, at 54.57%, followed by 34.59% from Makkah and 14.67% and 5.17% for the eastern region and Asir, respectively. The high number of tweets from Riyadh can be explained that this city has one of the highest number of Twitter users in the world [46]. In contrast, the psychological violence was found in 65.95% of the tweets, which was higher than the rates of physical and sexual violence, at 30.96% and 3.09% respectively (see Fig. 2). Psychological violence was higher because people find it easier to act on others via coercion or threats. In contrast, people in the Saudi community find it difficult to disclose any information related to sexual violence they faced to other people.

B. Classifier Accuracy

In this section, bagging SVM, KNN, and Bayesian boosting are applied for constructing models with different feature-extraction techniques that was described in section VII to evaluate their performance. Tables VI, VII and VIII represent the results for accuracy, recall and precision that were explained in the previous section.

In KNN, Choosing the appropriate value for K in datasets has a significant influence on the accuracy of classifications. In the experiments, the value of K was 5 because the initial experiments indicated that it would provide better results. In bagging SVM and Bayesian boosting, the number of iterations was set to 10. The results showed a greater superiority of bagging SVM over the other algorithms because it was used for SVM as a meta-algorithm that has been proved to be effective in the classification of texts.

The experiments clearly showed that the tri-gram approach had the best performance, at 86.61%, 82.80%, and 77.09% for bagging SVM, Bayesian boosting, and KNN, respectively. This was because most words in Arabic have a triangular root, which the tri-gram approach contributes to extracting. In contrast, BOW has shown the worst results because it contains a large number of features. Furthermore, light stemming had better accuracy than root-based stemming because it maintained words’ meanings. Bi-gram obtained good results in general, and it was better than tri-gram with KNN because

KNN is influenced by the number of features, which was only 837 for bi-gram, while tri-gram consisted of 8,960 features. Combining bi-gram and tri-gram gave poor results, contrary to expectations.

C. Baseline and Ensemble Methods Comparison

In this section, baseline methods of SVM, CNB and ensemble methods with bagging SVM and Bayesian boosting are compared to evaluate the effective of ensemble methods. Fig. 3 represents a comparison between the baseline methods of SVM and CNB and ensemble methods with bagging SVM and Bayesian boosting in term of accuracy with Tri-gram technique.

The results showed that the bagging SVM improved the performance of baseline SVM well, while the performance of Bayesian boosting decreased significantly, contrary to expectations.

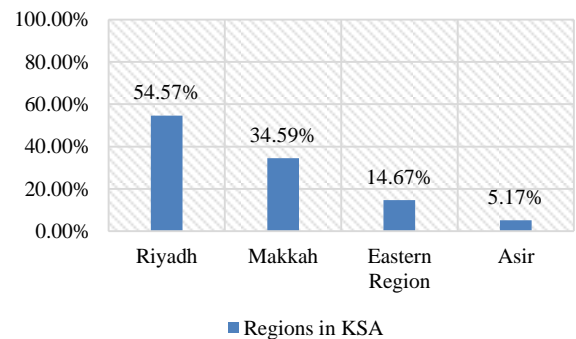


Fig. 1. Percentages of Violence Tweets in Four Regions in the KSA.

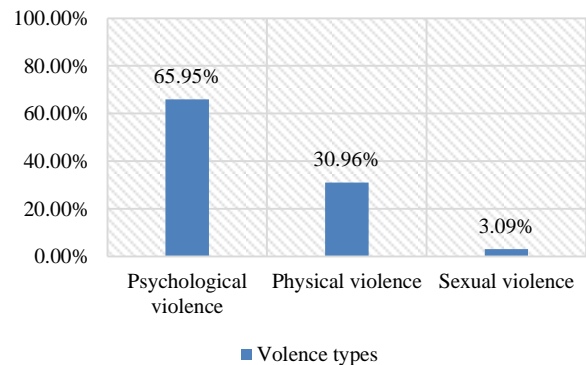


Fig. 2. Violence Tweets Types in Percentages in the KSA.

TABLE VI. EFFECTS OF FEATURES EXTRACTION TECHNIQUES ON BAYESIAN BOOSTING

Bayesian Boosting	Features	Accuracy	Recall	Precision
BOW	32143	68.18	74.37	71.94
Light stemming	16633	69.65	69.67	71.11
Root-based stemming	6677	69.66	69.73	76.28
Bi-gram	837	79.23	79.15	79.13
Tri-gram	8960	82.80	82.76	82.77
Tri-gram + Bi-gram	9506	74.27	74.21	74.37

TABLE VII. EFFECTS OF FEATURES-EXTRACTION TECHNIQUES ON KNN

KNN	Features	Accuracy	Recall	Precision
BOW	32143	68.89	68.82	70.62
Light stemming	16633	69.59	69.59	70.02
Root-based stemming	6677	64.13	64.15	64.43
Bi-gram	837	79.56	79.49	79.53
Tri-gram	8960	77.09	75.09	75.09
Tri-gram + Bi-gram	9506	68.38	68.36	68.44

TABLE VIII. EFFECTS OF FEATURE-EXTRACTION TECHNIQUES ON BAGGING SVM

Bagging	Features	Accuracy	Recall	Precision
BOW	32143	74.89	74.85	75.58
Light stemming	16633	75.3	75.21	75.61
Root-based stemming	6677	72.58	72.52	73.04
Bi-gram	837	85.81	85.76	85.76
Tri-gram	8960	86.61	86.61	86.62
Tri-gram + Bi-gram	9506	76.57	76.60	76.89

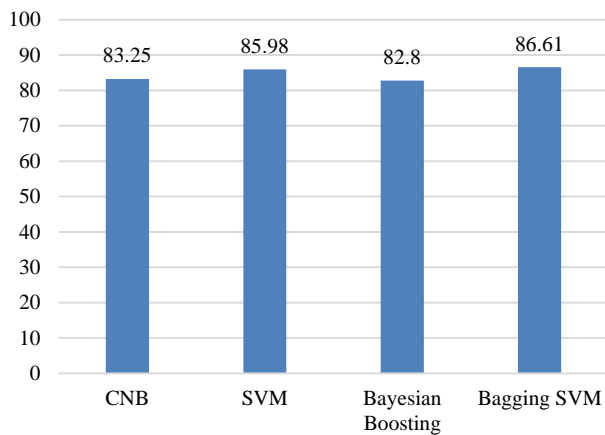


Fig. 3. Results of Ensemble and Baseline Methods.

D. Feature-Reduction Performance

In this section, nine feature-reduction techniques are evaluated to show how they affected bagging SVM. Different number of features are used for each technique at 1,000, 1,500, 2,000, 2,500, 3,000, 3,500 and 4,000 features to see how the number of features affected the performance of each type of feature-reduction techniques. Table IX illustrates the effectiveness of the feature-reduction techniques in term of accuracy, recall, and precision with bagging SVM.

SVM weighting provided the best accuracy, recall, and precision among the investigated methods, confirming SVM’s high capabilities in weighting. The highest score was recorded at 90.41%, when the number of features was 3,000. The rule technique was the worst among them, giving between 60.24% and 78.31%; moreover, the result indicated that the accuracy was positively correlated with the increase in the number of features that means the weakness of its reduction capabilities. It is clear from the results that CHI, deviation, and correlation

had a negative effect on the performance, significantly reducing the accuracy of bagging SVM. The results revealed that the performances of the Gini Index and IG were somewhat similar, reaching the highest level at 3,500 features, with 87.68% and 87.92% for the Gini Index and IG, respectively. The IG ratio resulted in a dramatic declined in accuracy to between 83.30% and 86.34%. The last type of reduction method, symmetrical uncertainty, provided reasonable performance with few features at 1,500 and 2,000. Fig. 4 shows how the number of features affects the accuracy of each type.

Based on the findings, the best results were obtained from the SVM, IG, and Gini Index approaches. These approaches are combined in sequence for evaluating the effects of each combination on the accuracy, recall, and precision of bagging SVM. The value of the number of features on the first side of the sequence has been set to a value that obtained higher accuracy in previous experiments. The results of the first side of the feature-reduction technique will be used on second side. When SVM was the first side, the number of features were 3,000, while for IG and the Gini Index, the values were from 2,500 to 2,000, 1,500, and 1,000. In contrast, when the IG and Gini Index were on the first side, the number of features were 3,500, while in SVM, the value was from 3,000 to 2,500, 2,000, 1,500, and 1,000. Table X illustrates the effectiveness of combinations the feature-reduction techniques in term of accuracy, recall, and precision with bagging SVM.

The overall results of integrating SVM with IG or the Gini Index showed a good influence of SVM on accuracy, recall, and precision. However, the performance of the SVM alone was still better than when integrated with other approaches, except when integrated with IG in the sequence of IG followed by SVM at 90.59% with 1,500 features. In contrast, the performance of merging IG and the Gini Index gave results close to the performance of each one alone, at accuracies of between 86% and 87%. Fig. 5 represents the accuracy of bagging SVM when combinations of feature-reduction techniques were applied.

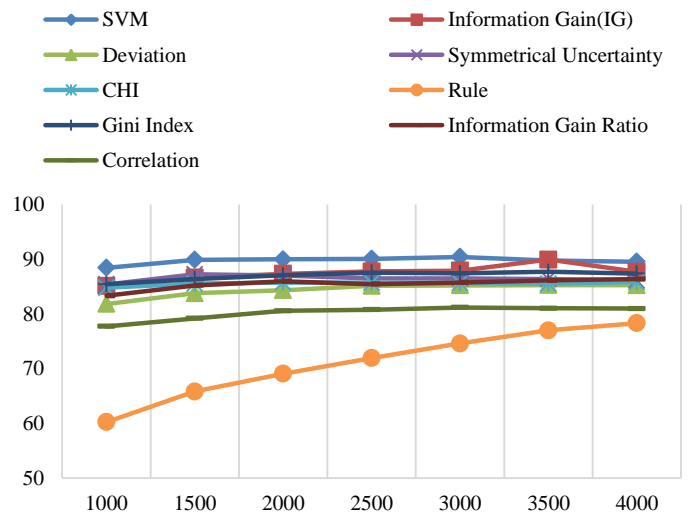


Fig. 4. Effect of K-Features on Bagging SVM Accuracy.

TABLE IX. EFFECTS OF FEATURE-REDUCTION TECHNIQUES ON BAGGING SVM ACCURACY

Features Reduction	Features	Accuracy	Recall	Precision
Information Gain (IG)	1000	85.09	85.12	85.49
	1500	86.63	86.65	86.81
	2000	87.30	87.31	87.72
	2500	87.73	87.73	87.78
	3000	87.37	78.36	87.38
	3500	87.92	87.91	87.93
	4000	87.69	87.70	87.72
Information Gain Raito	1000	83.30	83.37	84.29
	1500	85.21	85.24	85.60
	2000	85.94	85.98	86.27
	2500	85.43	85.44	85.57
	3000	85.74	85.75	85.85
	3500	86.12	86.12	86.17
	4000	86.34	86.34	86.39
SVM	1000	88.42	88.44	88.60
	1500	89.87	89.89	89.94
	2000	89.96	89.96	89.99
	2500	90.05	90.05	90.09
	3000	90.41	90.41	90.43
	3500	89.72	89.72	89.74
	4000	89.53	89.53	89.55
Rule-based	1000	60.24	60.36	61.26
	1500	65.81	65.89	66.45
	2000	69.07	69.12	70.25
	2500	71.92	71.94	72.08
	3000	74.60	74.62	74.82
	3500	77	77.02	77.31
	4000	78.31	78.32	78.44
Symmetrical Uncertainty	1000	85.38	85.41	85.73
	1500	87.21	87.24	87.47
	2000	87.01	87.01	87.11
	2500	86.48	86.49	86.60
	3000	86.48	86.48	86.59
	3500	86.37	86.38	86.44
	4000	86.10	86.10	86.17
Deviation	1000	81.81	81.83	82.17
	1500	83.77	83.77	83.86
	2000	84.31	84.31	84.37
	2500	85.12	85.11	85.16
	3000	85.21	84.86	85.22
	3500	85.26	85.25	85.26
	4000	85.22	85.22	85.23
CHI	1000	84.76	84.73	85.13

	1500	85.53	85.55	85.74	
	2000	85.72	85.73	85.81	
	2500	85.70	85.70	85.80	
	3000	85.65	85.65	85.69	
	3500	85.53	85.53	85.55	
	4000	85.81	85.50	85.83	
	Gini Index	1000	85.41	85.44	85.78
		1500	86.36	86.37	86.54
		2000	87.04	87.05	87.14
		2500	87.55	87.55	87.61
3000		87.42	87.42	87.46	
3500		87.68	87.68	87.71	
4000		87.35	87.35	87.37	
Correlation	1000	77.71	77.58	80.50	
	1500	79.17	79.06	81.62	
	2000	80.54	80.43	82.75	
	2500	80.76	80.66	82.88	
	3000	81.16	81.07	83.02	
	3500	81.02	80.93	82.02	
	4000	80.95	80.87	82.59	

TABLE X. EFFECTS OF FEATURE-REDUCTION COMBINATIONS ON BAGGING SVM

Features Reduction	Features	Accuracy	Recall	Precision
SVM ⇒ IG	1000	86.05	86.08	86.39
	1500	88.33	88.34	88.43
	2000	89.31	89.31	89.42
	2500	89.84	89.84	89.54
IG ⇒ SVM	1000	89.19	89.22	89.42
	1500	90.59	90.60	90.70
	2000	90.30	90.30	90.36
	2500	89.75	89.76	89.79
	3000	88.97	88.97	88.98
SVM ⇒ Gini Index	1000	86.15	86.18	86.42
	1500	88.30	88.30	88.40
	2000	89.29	89.30	89.34
	2500	89.75	89.76	89.79
Gini Index ⇒ SVM	1000	89.74	89.77	89.99
	1500	90.42	90.44	90.54
	2000	90.44	90.39	90.50
	2500	89.86	89.86	89.88
	3000	89.05	89.05	89.08
IG ⇒ Gini Index	1000	86.15	86.18	86.42
	1500	88.30	88.30	88.40
	2000	87.04	87.05	87.14
	2500	87.54	87.55	87.61
	3000	87.54	87.54	87.58
Gini Index ⇒ IG	1000	86.09	86.12	86.49
	1500	86.63	86.65	86.81
	2000	87.30	87.31	87.39
	2500	87.68	87.69	87.75
	3000	87.44	87.44	87.48



Fig. 5. Effect of K-Feature Reduction Combinations on Bagging SVM.

VIII. CONCLUSION

Due to the significant increase in violence in Arab societies, there is a need to discover and study them to find appropriate solutions. This research dealt with expressions of violence on social media in Saudi society.

Dataset collected from Twitter between 2017 and 2018 in colloquial Arabic from the four most densely populated administrative regions in Saudi Arabia, then the results classified. The findings indicated that the most violence is evident in Riyadh. In addition, number of classification algorithms of baseline and ensemble methods was compared in term of accuracy, recall and precision. In addition, multiple ways of extracting features, as well as ways of reducing the number of features are compared. The results showed the superiority of bagging SVM with tri-gram over other approaches at 86.61%; moreover, the combination of SVM weighting and SVM at classification contributed to higher performance at 90.59%.

In the future, the research will extend to cover other administrative regions in Saudi Arabia. In addition, the capabilities of the devices will expand to assess other types of reductions that this research could not implement because of the limitation in memory capabilities, such as PCA and SVD feature-reduction, in addition to extending experiments to other types of ensemble methods, such as stacking.

REFERENCES

[1] M. Alshehri, "11 thousand cases of violence!," Saudi newspaper Okaz.
[2] "Twitter in the Arab Region." [Online]. Available: <http://www.arabsocialmediareport.com/twitter/linechart.aspx>. [Accessed: 30-Mar-2019].
[3] "These Are The Most Twitter-Crazy Countries In The World, Starting With Saudi Arabia (!) | Business Insider." [Online]. Available: <https://www.businessinsider.com.au/the-top-twitter-markets-in-the-world-2013-11>. [Accessed: 16-Mar-2019].
[4] A.-H. Tan, "Text Mining: The state of the art and the challenges.," in Workshop on Knowledge Discovery from Advanced Databases (KDAD'99), 1999, p. 71–76.
[5] A. Hotho, A. Nürnberger, and G. Paaß, "A Brief Survey of Text Mining," *Ldv Forum*, vol. 20, no. 1, pp. 19–62, 2005.
[6] I. Guyon and A. Elisseeff, "An Introduction to Variable and Feature Selection," *J. of Machine Learn. Res.*, vol. 3, pp. 1157–1182, 2003.
[7] H. Liu and H. Motoda, "Feature Selection for Knowledge Discovery and Data Mining," Kluwer Academic, 2011.

[8] J. Maglogiannis, I. Karpouzis, K. Wallace, B.A., Soldatos, *Emerging Artificial Intelligence Applications in Computer Engineering*. 2007.
[9] "Summary by language size | Ethnologue." [Online]. Available: <https://www.ethnologue.com/statistics/size>. [Accessed: 12-Mar-2019].
[10] M. K. Saad, "Arabic Morphological Tools for Text Mining," *Int. Conf. Electr. Comput. Syst.*, pp. 1–6, 2010.
[11] R. Duwairi, "Arabic Text Categorization," *Int. Arab J. Inf. Technol.*, vol. 4, 2007.
[12] M. Al-Zabidi, "The crown bride of the jewels dictionary." 1965.
[13] A. Farghaly and K. Shaalan, "Arabic Natural Language Processing," *ACM Trans. Asian Lang. Inf. Process.*, vol. 8, no. 4, pp. 1–22, 2010.
[14] E. G. Krug, L. L. Dahlberg, J. A. Mercy, A. B. Zwi, and R. Lozano, "World Report on Violence and Health Geneva: World Health Organization, 2002. ISBN 92-4-154561-5.," *Inj. Prev.*, 2002.
[15] "Psychological violence | European Institute for Gender Equality." [Online]. Available: <https://eige.europa.eu/thesaurus/terms/1334>. [Accessed: 15-Mar-2019].
[16] "Makkah region recorded the highest percentage of domestic violence with 34% - Saudi News -Okaz Newspaper." [Online]. Available: <https://www.okaz.com.sa/article/927096>. [Accessed: 15-Mar-2019].
[17] A. Khatua, E. Cambria, and A. Khatua, "Sounds of silence breakers: Exploring sexual violence on Twitter," in *Proceedings of the 2018 IEEE/ACM International Conference on Advances in Social Networks Analysis and Mining, ASONAM 2018*, 2018, no. August, pp. 397–400.
[18] S. Subramani, H. Q. Vu, and H. Wang, "Intent Classification Using Feature Sets for Domestic Violence Discourse on Social Media," in *Proceedings - 2017 4th Asia-Pacific World Congress on Computer Science and Engineering, APWC on CSE 2017*, 2018, pp. 129–136.
[19] N. Albadi, M. Kurdi, and S. Mishra, "Are they Our Brothers? Analysis and Detection of Religious Hate Speech in the Arabic Twittersphere," in *2018 IEEE/ACM International Conference on Advances in Social Networks Analysis and Mining (ASONAM)*, 2018, pp. 69–76.
[20] M. A. Al-Walaie and M. B. Khan, "Arabic dialects classification using text mining techniques," in *International Conference on Computer and Applications, (ICCA)*, 2017, pp. 325–329.
[21] S. Raheel and J. Dichy, "An empirical study on the feature's type effect on the automatic classification of Arabic documents," *Lect. Notes Comput. Sci. (including Subser. Lect. Notes Artif. Intell. Lect. Notes Bioinformatics)*, vol. 6008 LNCS, pp. 673–686, 2010.
[22] H. Uğuz, "A two-stage feature selection method for text categorization by using information gain, principal component analysis and genetic algorithm," *Knowledge-Based Syst.*, vol. 24, no. 7, pp. 1024–1032, 2011.
[23] G. Vinodhini and R. M. Chandrasekaran, "Opinion mining using principal component analysis based ensemble model for e-commerce application," *CSI Trans. ICT*, vol. 2, no. 3, pp. 169–179, 2014.
[24] A. Al-Thubaity, A. Alanazi, I. Hazzaa, and H. Al-Tuwaijri, "Weirdness coefficient as a feature selection method for Arabic special domain text classification," in *Proceedings - 2012 International Conference on Asian Language Processing, IALP 2012*, 2012, pp. 69–72.
[25] M. H. Kadhim and N. Omar, "Bayesian Learning for Automatic Arabic Text Categorization," *J. Next Gener. Inf. Technol.*, vol. 4, no. 3, pp. 1–8, 2013.
[26] M. S. Khorshed and A. O. Al-Thubaity, "Comparative evaluation of text classification techniques using a large diverse Arabic dataset," *Lang. Resour. Eval.*, vol. 47, no. 2, pp. 513–538, 2013.
[27] M. Faqeeh, N. Abdulla, M. Al-Ayyoub, Y. Jararweh, and M. Quwaider, "Cross-lingual short-text document classification for facebook comments," in *Proceedings - 2014 International Conference on Future Internet of Things and Cloud, FiCloud 2014*, 2014, pp. 573–578.
[28] I. Hmeidi, M. Al-Ayyoub, N. A. Abdulla, A. A. Almodawar, R. Abooraig, and N. A. Mahyoub, "Automatic Arabic text categorization: A comprehensive comparative study," *J. Inf. Sci.*, vol. 41, no. 1, pp. 114–124, 2015.
[29] R. Alhutaish and N. Omar, "Arabic text classification using K-nearest neighbour algorithm," *Int. Arab J. Inf. Technol.*, vol. 12, no. 2, pp. 190–195, 2015.

- [30] F. S. Al-Anzi and D. AbuZeina, "Toward an enhanced Arabic text classification using cosine similarity and Latent Semantic Indexing," *J. King Saud Univ. - Comput. Inf. Sci.*, vol. 29, no. 2, pp. 189–195, 2017.
- [31] I. S. I. Abuhaiba and H. M. Dawoud, "Combining Different Approaches to Improve Arabic Text Documents Classification," *Int. J. Intell. Syst. Appl.*, vol. 9, no. 4, pp. 39–52, 2017.
- [32] I. H. Witten, *Text mining, Practical handbook of Internet computing* (CRC Press, Boca Raton). 2005.
- [33] I. H. Witten, E. Frank, and M. a Hall, *Data Mining: Practical Machine Learning Tools and Techniques second edition*. 2011.
- [34] J. Melton, S. Buxton, H. Samet, T. J. Teorey, S. S. Lightstone, T. P. Nadeau, J. Celko, G. Ralf, M. Schneider, J. Celko, E. Cox, T. Halpin, K. Evans, P. Hallock, B. Maclean, J. Melton, J. Melton, A. R. Simon, and M. Chisholm, *Data Mining: Concepts and Techniques*. 1999.
- [35] B. Baharudin, L. H. Lee, and K. Khan, "A Review of Machine Learning Algorithms for Text-Documents Classification," *J. Adv. Inf. Technol.*, vol. 1, no. 1, 2010.
- [36] T. Joachims, "Text Categorization with Support Vector Machines: Learning with Many Relevant Features Thorsten", *Proceeding of the Tenth European Conference on Machine Learning*, pp. 1–7, 1999.
- [37] N. Alami, M. Mekkassi, S. A. Ouatik, and N. Ennahahi, "Impact of stemming on Arabic text summarization," *Colloq. Inf. Sci. Technol. Cist*, pp. 338–343, 2017.
- [38] "Weight by Rule - RapidMiner Documentation." [Online]. Available: https://docs.rapidminer.com/latest/studio/operators/modeling/feature_weights/weight_by_rule.html. [Accessed: 26-Mar-2019].
- [39] Y. Yang and J.P. Pedersen., "Feature selection in statistical learning of text categorization.," *Proc. Fourteenth Int. Conf. Mach. Learn. (ICML'97)*, 1997.
- [40] H. Liu and R. Setiono, "Chi2: feature selection and discretization of numeric attributes," in *Proceedings of the IEEE 7th International Conference on Tools with Artificial Intelligence Chi2:*, 2002, pp. 388–391.
- [41] M. A. Hall and Li. A.Smith, "Practical Feature Subset Selection for Machine Learning ," in *proceedings of the 21st Australasian Computer Science Conference ACSC'98*, 1998, vol. Volume 20, p. 586.
- [42] S. I. Ali, "A Feature Subset Selection Method based on Conditional Mutual Information and Ant Colony Optimization," *Int. J. Comput. Appl.*, vol. 60, no. 11, pp. 5–10, 2012.
- [43] "Weight by Deviation - RapidMiner Documentation." [Online]. Available: https://docs.rapidminer.com/latest/studio/operators/modeling/feature_weights/weight_by_deviation.html. [Accessed: 26-Mar-2019].
- [44] J. Han, M. Kamber, and J. Pei, *Data Transformation by Normalization*. 2011.
- [45] "Weight by Information Gain Ratio - RapidMiner Documentation." [Online]. Available: https://docs.rapidminer.com/latest/studio/operators/modeling/feature_weights/weight_by_information_gain_ratio.html. [Accessed: 26-Mar-2019].
- [46] "The World's Most Active Twitter City? You Won't Guess It." [Online]. Available: <https://www.forbes.com/sites/victorlipman/2012/12/30/the-worlds-most-active-twitter-city-you-wont-guess-it/#4367128655c6>. [Accessed: 16-Mar-2019].

Industrial Financial Forecasting using Long Short-Term Memory Recurrent Neural Networks

Muhammad Mohsin Ali¹, Muhammad Imran Babar², Muhammad Hamza³, Muhammad Jehanzeb⁴, Saad Habib⁵,
Muhammad Sajid Khan⁶

APCOMS, Rawalpindi, Pakistan. UET, Taxila, Pakistan

Abstract—This research deals with the industrial financial forecasting in order to calculate the yearly expenditure of the organization. Forecasting helps in estimation of the future trends and provides a valuable information to make the industrial decisions. With growing economies, the financial world spends billions in terms of expenses. These expenditures are also defined as budgets or operational resources for a functional workplace. These expenses carry a fluctuating property as opposed to a linear or constant growth and this information if extracted can reshape the future in terms of effective spending of finances and will give an insight for the future budgeting reforms. It is a challenge to grasp over the changing trends with an effective accuracy and for this purpose machine learning approaches can be utilized. In this study Long Short-Term Memory (LSTM), which is a variant of Recurrent Neural Network (RNN) from the family of Artificial Neural Networks (ANN), is used for forecasting purposes along with a statistical tool IBM SPSS for comparative analysis. In this study, the experiments are performed on the data set of Pakistan GDP by type of expenditure at current prices - national currency (1970-2016) produced by Economic Statistics Branch of the United Nations Statistics Division (UNSD). Results of this study demonstrate that the proposed model predicted the expenses with better accuracy than that of the classical statistical tools.

Keywords—Financial forecasting; prediction; long-short term memory; recurrent neural networks; artificial neural networks; IBM SPSS

I. INTRODUCTION

Forecasting is concerned with the process of estimating the future trends by doing the analysis on the basis of historical data. Financial forecasting determines the trends by utilizing the previous data and provides valuable information to make future decisions and define strategies for financial management. Financial forecasting is highly vital as different companies and firms are closed due to bankruptcy and the obvious reason behind it was their strategies that were not well-defined and they were unable to compete their rivals. They were not able to see what is coming in the future and when it comes, they were not prepared with the consequences. This looks like a troublesome issue to comprehend however, there is a solution to every problem. As the time goes on, organizations spare their vital data in a very much characterized and appropriate way since it may be useful for them in later phases of the business to analyze the trends. This is where the solution lies.

Whatever, that is occurring in the organization is being spared either it is related to their products or manufacturing or

their finances. Forecasting the financial conditions, in terms of expenses, will be vital for a company to survive and that is the idea of this research. Much of the work is done in the domain of stock market [1-5], power and load [6-9], building energy consumption [10-12], electric price [13-16], weather forecasting [17, 18] and so on. However, the focus of this research is on expense forecasting of the companies to save them from bankruptcy.

In this research a technique is proposed to predict the financial expenses of an organization. The data of the company are analyzed and helpful data are isolated. The legitimacy of the data is highly vital to ensure the results of the proposed intelligent technique for financial forecasting. Different machine learning (ML) techniques are used for financial forecasting. The understanding of the given outcomes is highly vital with the goal that they can be utilized later for various purposes. There are couple of imperative things to consider like the information being utilized is from dependable sources and not fabricated. Secondly, system being designed needs not to be error prone. Forecasting is never 100 % yet it should be as close as it is conceivable. Salaries, business charges, office lease, telephone charges or any other, it appears as though there's no conclusion to the costs related with maintaining a business or to a specific individual. In any case, your capacity to get a firm handle on these money outpourings can assume an imperative part in your definitive achievement or disappointment. Regardless of whether you're contemplating a startup venture or you've been doing business for some time, precisely determining your costs can profit your venture in a number of potential ways.

To improve the procedure of financial forecasting there are different strategies which can be utilized to interface each sort of cost to different factors or cost drivers, for example, income or headcount, which have just been conjecture in the budgetary projections. Obviously, there will be expenses which are settled down and cannot be connected to different factors and should be assessed in total financial terms. There is a need of system that should keep all implying factors in to account and forecast expenses with logical and dependable results. Forecasting helps to create simulation in understanding problems of many sorts for example the weather, a simple analysis can lead us to predict the chances of rain in a particular way that the farmer can sow the seeds accordingly and predicting has led us to many possibilities same can be said in financial sectors and we can consider prediction of the bankruptcies on a corporate level and have counter measure ready at the time of need.

II. RESEARCH BACKGROUND

Forecasting has ever been a hot topic in research horizon. The topic for corporate firm bankruptcies prediction has also been in considerable discussions for the discipline of finance and risk management and various bankruptcies' prediction models are available in the form of light statistical models and artificial intelligence (AI) techniques [19]. The existing techniques involve decision tree, logistics regression and artificial neural networks (ANNs) and among all of them ANN became one of the most popular technique in accurate prediction. The ANN application has also been proven to determine the mortgage applicant solvency, rating of corporate bonds and fraud prevention. The basic intent of all these studies is to compare and contrast the performance and accuracy of the ANN and to justify its usage in the research.

In [19] a comparative analysis of two packages, one is statistical named as SYSTAT [20] and the other is software package named as BRAINMAKER [21], is performed. SYSTAT is a personal statistical package used in discriminant analysis. The test concluded with all variables included in each discriminant analysis. BRAINMAKER software package is based on neural network. After experimentation it was found that neural network outperformed the discriminant analysis resulting in neural network's learning more efficient than the classical methods.

Another study carried out in [22] focuses on the parallelization of the back propagation algorithm over a network that forecasts S&P500 Index in terms of prices of financial instruments, a series prediction problem, the ANN has been used extensively. Stock market forecasting with demands reaching at its peak as people getting more connected to the stock business. The challenge remained for predicting a strong forecast although a few data mining and machine learning techniques are significant enough to do the job. The use of ANN with a windowing operator for prediction is efficiently working along with the time series data [23].

Different techniques are used till now and ANN is the most prominent among them for prediction. Two theories commonly used for stock market prediction are "Efficient market hypothesis (EMH)" and "The random walk theory." Two commonly used approaches for stock market prediction are "Technical analysis" and "Fundamental analysis." All the stated theories and approaches are not of much use to us now but they still provide the foundation for new research. ANN consists of three layers which are helpful in case of nonlinear relationship in between inputs and output. There are several guidelines available that can aid in forecasting [2].

Feedforward NN was first used because of its simple approach and stock price data of IBM for 5000 days was used. Data of 1000 days was used for training and rest for validation purpose. Though it did not provide good results but it gave valuable insight for future experiments that were conducted very later and resulted in an accuracy of nearly 90% by using a three-layered back propagation ANN. When compared with the available statistical models such as GARCH, EGARCH, GJR GARCH, and IGARCH, the ANN performed better than all.

Many experiments were also made where ANN was used along with support of other algorithms like genetic algorithm, fuzzy logic etc. which further improved the results up to 74%. Now a day hybrid methods are being used like back propagation algorithm with Feedforward ANN or with Genetic Algorithm and these hybrid methods resulted up to 98% of accuracy [2].

Without using historical data, load and power forecasting has been proven by using ANN and the electrical energy produced with wind plays a crucial role but the unpredictable nature requires an approach to manage the resources, however, prediction requires a historical dataset to train the neural network for prediction. The drawback exists when there are no historical datasets of the newly created wind farms so the proposed approach requires no extensive historical data set [24]. The model purposed is the self-adaptive artificial network and such prediction model exist using the hidden layer complexity such as Multi-layer Perceptron, Support Vector Machine and Radial Basis Function all of which require high computation power. To overcome the computation complexity the authors used single layered model Functional Link ANN (FLANN) that results in trigonometric base output vector, Chebyshev Neural Network (ChNN) that results in polynomials base output vector and Legendre Neural Network (LeNN) that results in Chebyshev polynomials base output vector having the lower load to process.

Price Forecasting is a useful technique and is constantly being developed because of its benefits. The given research throws some light on the price forecasting of electricity for the day ahead. Different models are present for this purpose, but ANN is preferred because of its dependable results [25]. Support Vector Machine (SVM) Model is developed for price forecasting in case of rapidly changing environment and is used because of its speed and minimizing risks. ANN is used mainly to tackle with the nonlinear relationship in between inputs and output. One thing to be noted is that results were forecasted for a more stable environment with less changes.

For buildings the prediction of demands for its energy consumption holds a great importance. Energy if properly used and managed can be helpful in lowering the operational cost of building. Certain factors are involved in energy demands of a building which includes climate, structure of building and people inside the building. There are few methods available to predict energy demands [26]. Physical method is based on engineering methods for calculating building's energy demands but is less popular because of difficulty in gathering required information like physical parameters of building. With the passage of time different new models based on AI like ANN and SVM were used to obtain better results. However, ANN is used in this research because of its better performance. Data of a building located in Italy was used for experimentation with energy consumption in KWH and an ANN model known as Nonlinear Auto Regressive Neural Network (NAR) was chosen. It has a feedback arrangement and is suitable for forecasting in such cases where only single series of information is present like in the problem of building energy consumption. Results concluded that NAR is an effective model and can give dependable results in case of building energy consumption [26].

ANNs are also widely applicable in weather forecasting. For the past few decades numerous efforts are made to forecast weather. ANNs have played a vital role for prediction purposes and many forecasting models are based on it. The researchers proposed a new approach based on ensemble of neural networks for forecasting [27]. The proposed model intends to solve the redundancy issue by a mutual information sharing process. As a whole the process consists of four basic stages. In the first stage the features were selected from the normalized data. In the second stage an ensemble of four neural networks, which include Multi-layered Perceptron (MLP), Radial Basis Function (RBF), General regression neural network (GRNN) and Time delay neural network (TDNN) was developed for forecasting. The proposed model was applied and compared with existing techniques of SOM and Voting, the proposed model predicts successful results [27].

A research was presented for weather forecasting that includes the technique Back-Propagation Neural Network (BPNN). BPNN has the ability to learn on itself adjusting its weights to achieve the desired results. Different numerical as well as other techniques are present for the purpose of forecasting but still there is a margin of improvement. ANN is brilliant concept when it comes to forecasting [28]. The results conclude that the proposed system is performing very well under the given attributes including Temp. (°C), Dew Point (°C), Humidity (%), Sea Level Pressure (hPa), Visibility (km), Wind (km/h), Gust Speed (km/h) and Precip (cm). Using the BPPN for forecasting on the given attributes produced satisfying results and can result in replicating the existing methods used for forecasting all around the world.

Since weather prediction continues to be a day to day need as it effects over the agriculture and industrial sectors both and is dependent on the predicted data in order to function but the demand is not only limited to that warning for natural disaster can turn out to be a big life saver. The prediction varies for location to location and time as well, to start with to be accurate in regard of time differences for when the data is being recoded and for when it is being used for prediction. A research was presented to predict the temperate weather that included the collection assimilation & analysis of data and the methodology comprises of multi-layer perceptron neural network [29].

The data collected is of historic past of 5 years having the observation or the selected input attributes of temperature, wind speed, wind direction and atmospheric pressure. The analytical data is given to the ANN for the prediction purposes through usage of well-known forecasting models. These models have been known for their effectiveness over predictions, the training is conducted using the back-propagation algorithm and the first set of generated output was parsed through ID3 to generate rules. The ID3 tree had the

outcome from the neural network resulting in to the final output which were the generated rules. The experiment resulted in outcome from the neural network which then given to the ID3 decision tree leading to the conversion of the output to the desired one and through this implementation it is clear demonstration of how effective is the integration of the neural network with the intelligent system as compared to the traditional meteorological approaches [29].

A weather forecast model presented in [30] is based on Multilayer Feedforward Artificial Neural Network (MLFANN) that is based on patterns that are process of conversion from input sets into the outputs. The training of the network is through Resilient Propagation algorithm or RPROP Algorithm. It has proven that it produced the most accurate results during the test periods which were conducted to compare the Conjugate Gradient in terms of the performance [30]. The data considered was for the weather forecasting on a daily basis over in Tiwi, San Rafael, Albay and Philippines. The datasets had the data of between 2012 up to 2015 and the gathered data were provided by the Advanced Science and Technology Institute (DOST – ASTI). With division of the data set resulted into two data set one imputed and the other one with the removed missing values. Three models were created for both the data sets with around 40000 iterations, the networks number of hidden neurons were based through a theorem (the Kolmogorov’s Theorem) the weight training went through first set a random value and then the second set by IWI methodology. The study resulted in a successful 98.96743% accurate prediction although the optimal model contained 10 neurons in the hidden layer and the dataset comprising of removed missing values is utilized.

III. COMPARATIVE ANALYSIS

A detailed comparative analysis of multiple techniques based on the concept of Neural Network is presented in Table I. Table I shows that many techniques like Hybrid Feed Forward and Back Propagation as well as Chebyshev Neural Network (ChNN) show results near to 90 % when it comes to accuracy. Another added benefit is that they also have a very high learning rate among all. For our case expense forecasting which is related to financial forecasting, Hybrid Feed Forward and Back Propagation technique shows perfect results and has been proved. For the purpose of comparative analysis four characteristics are considered like learning rate, effective usage, efficiency and resource requirements. Learning rate describes that how much the proposed technique is efficient in terms of learning, effective usage explains the domain in which the technique is applied, efficiency is based on performance as compared to the contemporary techniques and resource requirements depicts the computational needs of the proposed technique.

TABLE I. COMPARATIVE ANALYSIS OF EXISTING TECHNIQUES

	Learning Rate	Effective usage	Efficiency	Resource Requirements
SYSTAT (DA) [20]	Mid	Financial	88.25% (Ratio With competitor)	High
BRAINMAKER (BP) [21]	High	Financial	97.5% (Ratio With competitor)	High
Parallelization (BP) [22]	High	Generic	61% faster	Mid
Hybrid Feed Forward and Back Propagation [2]	High	Financial	Up 97% more accurate	High
Functional Link ANN (FLANN) [24]	Very High	Power/load	Faster as compared ChNN & LeNN	Low
Chebyshev Neural Network (ChNN) [24]	Very High	Power/load	90% overall performance	Low
Legendre Neural Network (LeNN) [24]	High	Power/load	N/A	Low
Long Short-Term Memory (LSTM) [31]	High	Financial/Pattern Prediction	59% (Average Accuracy)	High

IV. PROPOSED SOLUTION

After going through the detailed literature review, we stumbled upon many methods to setup a neural network. Among those were the classical methods including Back Propagation and more complex mathematical models such as LeNN. As we understand from the study among these stood RNN type method LSTM with a memory to redirect its training under short terms as well as longer terms of time. The proposed model is shown in Fig. 1.

A. LSTM

Conventional Neural Networks were of incredible use to us but they had one issue. Every time they had to start from scratch until the perfect combination was found but what if there is a neural network which can save the output and utilizing it again by feeding it to input. Recurrent Neural Network (RNN) is a type of neural networks that is based on the concept of memory. Once the feed forward network reaches to output the learning rate and error correction are

performed during the back propagation to get the answer right. They have been utilized effectively in taking care of numerous issues like speech recognition, financial solutions and so forth.

Recurrent Neural Networks (RNNs) have been used in and in addition with blend of different models. An example of this is calculating Financial Volatility. Long Short-Term Memory Networks (LSTMs) are a variant of RNN that are now most popular in the field. There are countless examples which can prove its working and usability. LSTMs have been used in multiple fields for prediction purposes and have given noteworthy outcomes.

In transportation, calculating the flow of traffic has been a difficult task because of being highly non-linear in nature. An approach was made to solve this problem using LSTMs. Simply using traffic flow information gave acceptable results but with few other variables like occupancy and speed along with neighboring traffic information showed better results [32].

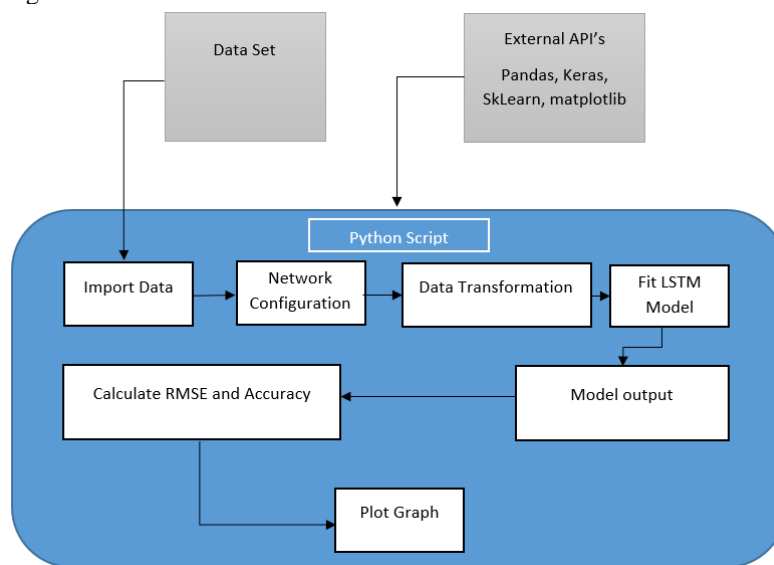


Fig. 1. Proposed Model for Industrial Financial Prediction.

LSTMs were also used in stock market prediction and they came out successful with an average accuracy of 55.9%. It told whether the price of the specific stock is going up or not in the coming 15 minutes and for this purpose the data from 2008 to 2015 were used. Google Tensor Flow was used for performing LSTMs and with such large dimension of input the results were obtained without reducing or handpicking the attributes [31].

RNN was also used for prediction in the field of energy consumption. Short term load forecasting was done on 69 customers of New South Wales. The important part to consider was that the research focused on forecasting on single customer and not as a whole and several experiments resulted that approaches that are successful in grid forecasting may not be very successful in this area and LSTMs produce better results [33].

For calculating the remaining life of Lithium-Ion batteries LSTMs were used. As interesting it may seem, it is of immense use for minimizing battery risks. Different cells were used for this purpose on two different temperatures (25 °C and 40 °C). Different current rates were used to get maximum information and diversity. It is a long-term prediction as it calculates the time of failure for the batteries and the results show that LSTM's give better results than existing techniques like Support Vector Machine (SVM) [34].

LSTMs are a kind of recurrent neural network which can hold the memory of previous prediction and are capable enough for learning long term dependencies. It is widely been used in speech prediction, uses a default squashing function (tanh) which keeps the range of outputs to be in 1 and -1 depending upon the calculated voted outcome. LSTM initially predicts a value and then stores it to be used along with the next value of input. LSTM loops the previous predicted values. It does that by using 4 stages initial prediction, ignoring, forgetting and selection. All 4 states are separate mini networks with the squashing functions.

- 1) *Initial Input*: The first gate where the new information is processed initially.
- 2) *Ignoring*: Should a new information be stored or the information are to be ignored. The gate has a sigmoid function that decides what new information be updated.
- 3) *Forgetting*: Choses what previous output needs to be forget and drop the information of the old subject votes for what not.
- 4) *Selection*: This gate has another sigmoid squashing function which choses the most valid information to be output. Visualization of the above process can be seen in Fig. 2.

Mathematical representation

Input Gate: $f_t = \sigma(W_f \cdot [h_{t-1}, x_t] + b_f)$
 Update Gate: $i_t = \sigma(W_i \cdot [h_{t-1}, x_t] + b_i)$

$$\tilde{C}_t = \tanh(W_C \cdot [h_{t-1}, x_t] + b_C)$$

Forgetting Gate: $C_t = f_t * C_{t-1} + i_t * \tilde{C}_t$

Output Gate: $o_t = \sigma(W_o \cdot [h_{t-1}, x_t] + b_o)$

$$h_t = o_t * \tanh(C_t)$$

B. Tuning the Model

LSTM uses an activation function tanh and a basic RMSprop optimizer. Although the network can function over these basic models but we tend to change the activation functions to sigmoid, Softmax and SELU to better tune the prediction. We also tuned the optimizer to an Adamax Stochastic optimizer with a variable learning rate and shuffle of the population set to be restricted for the efficiency and better performance. In addition to that Equation 1 is used to measure accuracy to better visualize the results.

$$Accuracy = \frac{\sum_{n=0}^n 100 - ((\frac{P_n - E_n}{P_n}) * 100)}{n} \tag{1}$$

The detail of the activation functions is given in Table II.

C. Execution

The model proposed in Fig. 1 is implemented by using Python with Keras API. The script first parses the data through Pandas API. Further the data are transformed from time series to supervised and stationary data. The data are pre-processed. Thus, the training begins based on the configured model of the LSTM. The proposed model forecast financial values and visualizes the results accordingly. Fig. 3 depicts the overall flow chart of the proposed LSTM model.

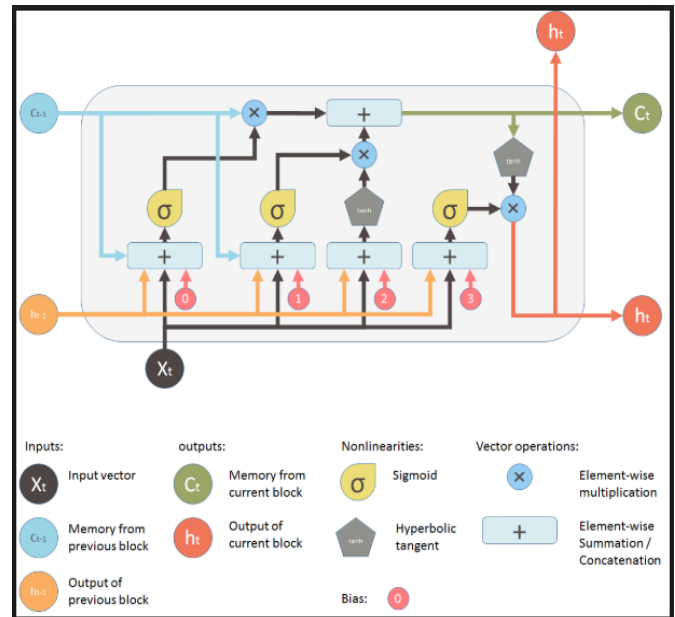
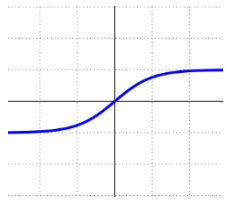
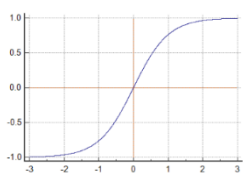
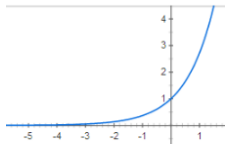
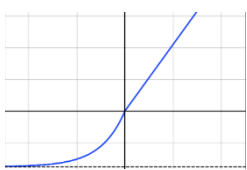


Fig. 2. Architecture of LSTM.

TABLE II. DETAILS OF ACTIVATION FUNCTIONS

Name	Formula	Range	Plot
Tanh	$f(x) = \tanh(x) = \frac{(e^x - e^{-x})}{(e^x + e^{-x})}$	(-1,1)	
Sigmoid	$f(x) = \sigma(x) = \frac{1}{1 + e^{-x}}$	(0,1)	
Softmax	$f_i(\vec{x}) = \frac{e^{x_i}}{\sum_{j=1}^J e^{x_j}}$	(0,1)	
Scaled Exponential Linear Unit (SELU)	$f(\alpha, x) = \lambda \begin{cases} \alpha(e^x - 1) & \text{for } x < 0 \\ x & \text{for } x \geq 0 \end{cases}$	$(-\lambda\alpha, \infty)$	

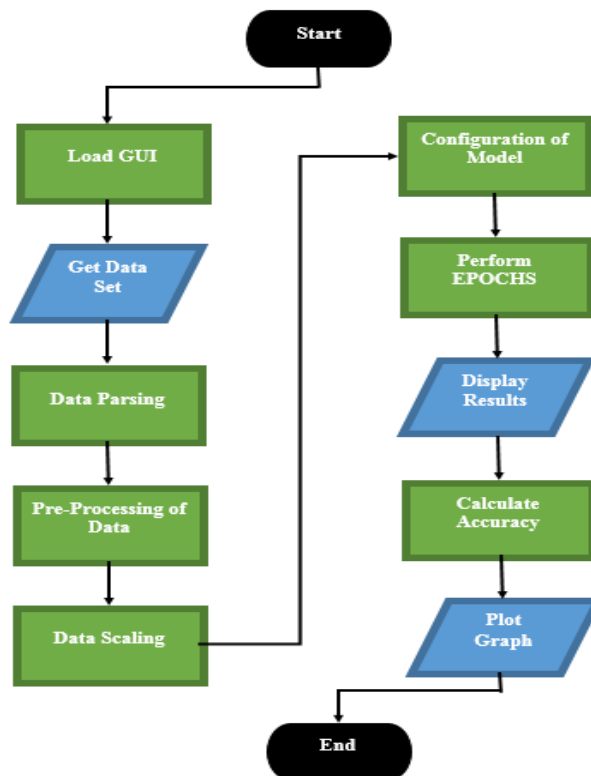


Fig. 3. Flow Chart of the Proposed Model's Execution.

V. RESULTS AND ANALYSIS

For the past years the statistical methods and tools have been used for predication. The financial world has relied upon such techniques as they delivered good results. But what we believe is that the use of machine learning would result in better time series prediction as compared to the classical methods. There are many renowned tools like IBM SPSS. These methods help in recognition of the attributes to be valid and statistically correct. Fig. 4 shows the attribute processing report.

Time series analysis is a sequence of points in a given time. For example, a consumption of electricity at end of every month recorded over a period of time let's say years. We will end up with a time series of monthly based stretching over a number of years. Time series possesses a trend in it, a trend is said to be a change in general direction. Classical methods such as used in SPSS Time Series Analysis failed to fully grasp the change of trend as shown in Fig. 5.

Table V and Fig. 6 shows the results from the system which uses the default activation function (Tanh) for LSTM. In order to maximize the performance, we can use different available activation functions along with making tweaks in Learning Rate, EPOCHS, Number of Neurons in hidden layer and optimizers. This would be done using hit and trial method until we get the best combination to be used for getting the most accurate results. Comparison of Activation Functions (Network Configurations and Plots)

The above graph visualization in Fig. 6 is of the Tanh activation function in terms of expected and predicted values generated by the proposed model resulting in an average accuracy of 90.95%. Table III shows the network configuration used to generate the plot are Number of Neurons 10, Epochs 3000, Learning rate 0.002 and optimizer used is Adamax which are also mentioned in the table above. The graph has two lines of blue and orange color where each color represents expected and predicted values, respectively.

Fig. 7 is visualization of the Sigmoid activation function in terms of expected and predicted values generated by the proposed model resulting in an average accuracy of 89.46%. Table IV shows the network configuration used to generate the plot are Number of Neurons 10, Epochs 3000, Learning rate 0.002 and optimizer used is Adamax which are also mentioned in the Table VI. Fig. 7 represents the expected and predicted values respectively.

Fig. 8 is visualization of the Softmax activation function in terms of expected and predicted values generated by the proposed model resulting in an average accuracy of 91.64%. Table V shows the network configuration used to generate the plot are Number of Neurons 10, Epochs 3000, Learning rate 0.002 and optimizer used is Adamax which are also mentioned in the table above. The graph has two lines of blue and orange color where each color represents expected and predicted values respectively.

Fig. 9 is visualization of the SELU activation function in terms of expected and predicted values generated by the

proposed model resulting in an average accuracy of 92.36%. Table VI shows the network configuration used to generate the plot are Number of Neurons 10, Epochs 3000, Learning rate 0.002 and optimizer used is Adamax which are also mentioned in the table above. The blue and orange lines represent expected and predicted values respectively.

A. Comparison of Activation Functions (Plot)

Fig. 10 and Table VII are helping in understanding the accuracy of all functions used in the experimentation in order to measure the function with highest accuracy. After performing the experiment several time using various activation functions, it is observed that the LSTM model using SELU function outperforms tanh, sigmoid and softmax functions having an average accuracy of 92.34%.

TABLE III. NETWORK CONFIGURATION AND RESULTS OF TANH FUNCTION

Activation Function: Tanh	
Neurons	10
Epochs	3000
Learning Rate	0.002
Optimizer	Adamax
Accuracy	90.945718 %

TABLE IV. NETWORK CONFIGURATION AND RESULTS OF SIGMOID FUNCTION

Activation Function: Sigmoid	
Neurons	10
Epochs	3000
Learning Rate	0.002
Optimizer	Adamax
Accuracy	89.461604%

TABLE V. NETWORK CONFIGURATION AND RESULTS OF SOFTMAX FUNCTION

Activation Function: Softmax	
Neurons	10
Epochs	3000
Learning Rate	0.002
Optimizer	Adamax
Accuracy	91.643963%

TABLE VI. NETWORK CONFIGURATION AND RESULTS OF SELU FUNCTION

Activation Function: Scaled Exponential Linear Unit (SELU)	
Neurons	10
Epochs	3000
Learning Rate	0.002
Optimizer	Adamax
Accuracy	92.356115%

Case Processing Summary

	Cases					
	Included		Excluded		Total	
	N	Percent	N	Percent	N	Percent
Finalconsumptionexpenditure	47	100.0%	0	0.0%	47	100.0%

Report

Finalconsumptionexpenditure		
Mean	N	Std. Deviation
5.013E+12	47	7.3352E+12

Fig. 4. Attribute Processing Report.

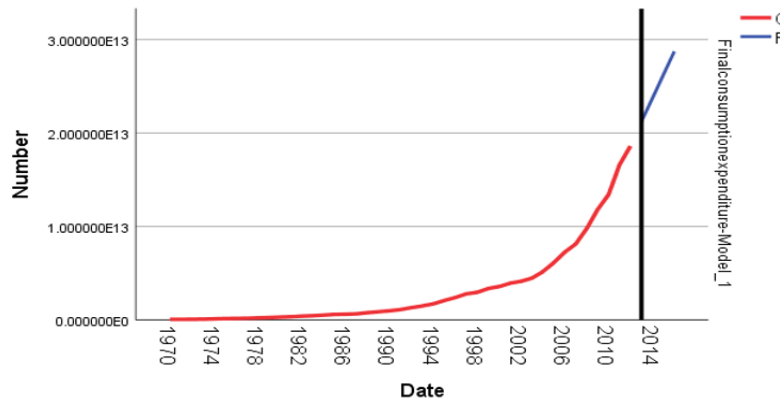


Fig. 5. Statistical Forecasting on Data Set.

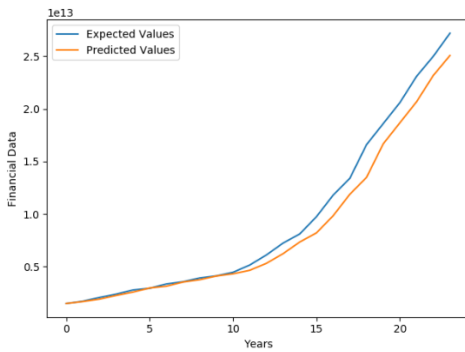


Fig. 6. Graph of Tanh Function Results.

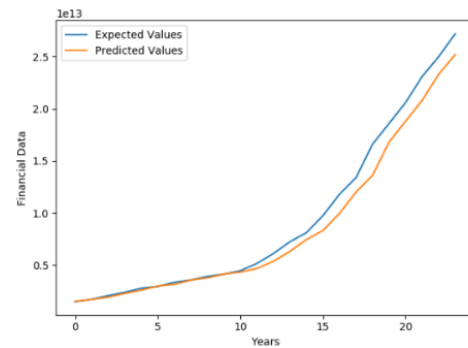


Fig. 8. Graph of Softmax Function Results.

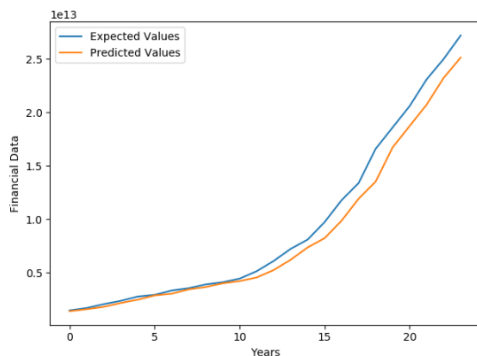


Fig. 7. Graph of Sigmoid Function Results.

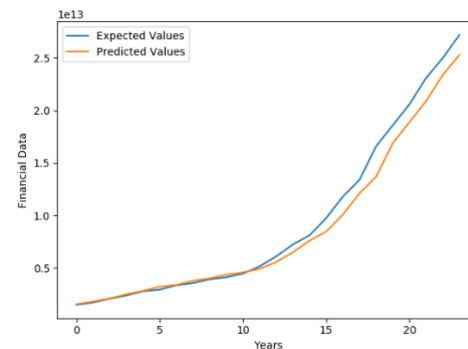


Fig. 9. Graph of Softmax Function Results.

TABLE VII. EXPECTED AND PREDICTED VALUES FROM ALL ACTIVATION FUNCTIONS

Year	Expected “Final consumption expenditure”	Tanh Function	Sigmoid Function	Softmax Function	Scaled Exponential Linear Unit (SELU) Function
1994	1490000000000	1492147941446	1416830417788	1520000000000	1546896795749
1995	1710000000000	1681736572456	1596830417788	1700000000000	1801833265018
1996	2070000000000	1905435251712	1816830417788	1920000000000	2097350911903
-	-	-	-	-	-
2014	23100000000000	20681566936051	20734847291469	20810000000000	20896554042625
2015	25000000000000	23177904562711	23234165990781	23310000000000	23391085687923
2016	27200000000000	25082044218373	25134989737868	25210000000000	25296475122737

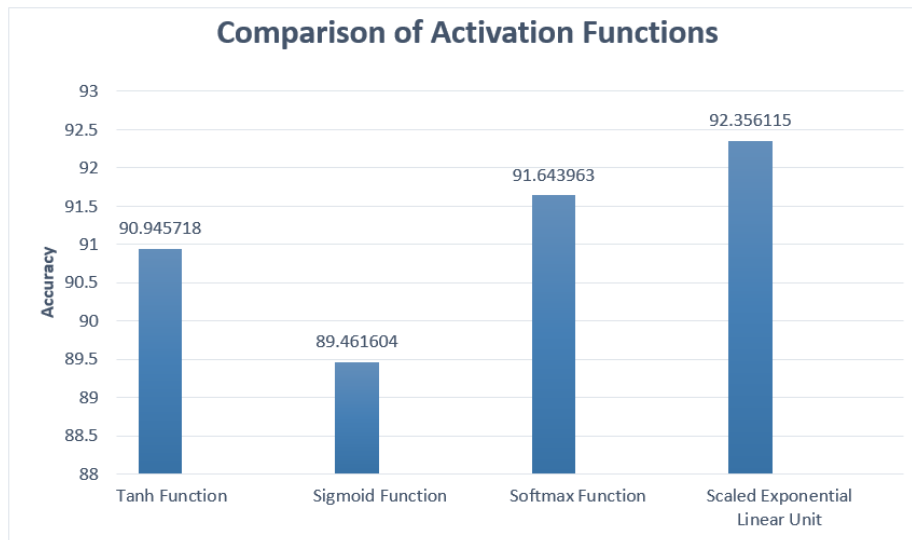


Fig. 10. Comparison of Activation Functions.

VI. EXPERIMENT

The statistical method when tested under the condition was SPSS and expert model of its own best finding. Half of the data was used for it to analyze the trend and make a forecast for the rest of the values so we can compare the expected and predicted values. Fig. 11 show the actual curve and trend of data. Fig. 12 shows the forecasted trend of data.

As it is observed that the analysis failed to grasp upon the curve and didn't follow the trend rather it follows a linear growth path in the positive direction. Table VIII shows the output for the respective forecast in terms of UCL upper limit and LCL lower limit respectively.

A. Experimental Data Set

The experimental data set is used to train and validate the proposed system. The data set needs not to be manufactured rather it should have trends for forecasting purposes. The data set used was “Pakistan GDP by Type of Expenditure at current prices - national currency”. It is produced and maintained by the Economic Statistics Branch of the United Nations Statistics

Division (UNSD). Getting into the particulars of the data, it expands over 48 years beginning from 1970 up to 2016 [35]. It consists of following nine attributes.

- Final consumption expenditure
- Household consumption expenditure
- General government final consumption expenditure
- Gross capital formation
- Gross fixed capital formation
- Changes in inventories
- Exports of goods and services
- Imports of goods and services and
- Gross domestic product (GDP)
- Fig. 13 shows the partial dataset for experimental purposes.

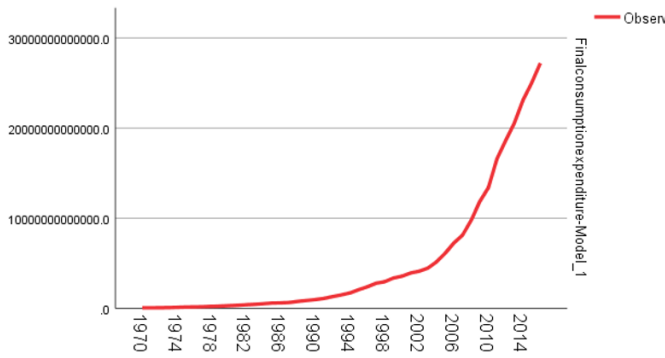


Fig. 11. Actual Curve and Trend of Data.

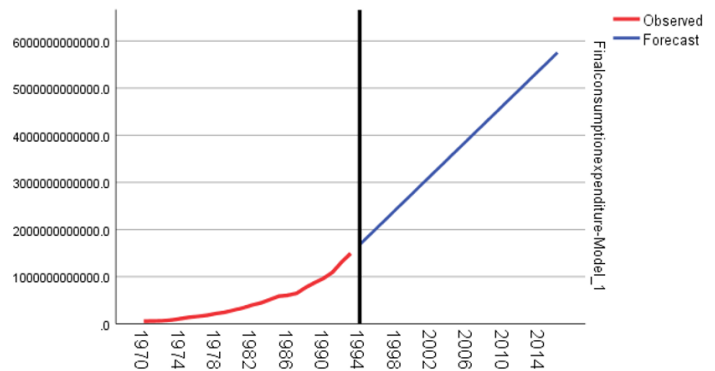


Fig. 12. Forecasted Trend of Data.

TABLE VIII. FORECASTED RESULTS OF 4 YEARS

Forecast					
Model		2008	2009	2010	2011
Finalconsumptionexpenditure-Model_1	Forecast	4270986450158.1	4456215747031.0	4641445043903.8	4826674340776.7
	UCL	6171717092146.6	6541483486414.0	6916855821347.0	7297673656143.6
	LCL	2370255808169.5	2370948007648.0	2366034266460.7	2355675025409.9

	A	B	C	D	E	F	G	H	I	J
1	Date	Final consumpt	Household cc	General gove	Gross capital f	Gross fixed capi	Changes in inv	Exports of good	Imports of go	Gross Domestic
2	31-12-16	2.72055E+13	2.36989E+13	3.50667E+12	4.50177E+12	4.0282E+12	4.73566E+11	2.5734E+12	4.68279E+12	2.95979E+13
3	31-12-15	2.50063E+13	2.19951E+13	3.0112E+12	4.25571E+12	3.81582E+12	4.3989E+11	2.91017E+12	4.67911E+12	2.74931E+13
4	31-12-14	2.31001E+13	2.03912E+13	2.70892E+12	3.68352E+12	3.28082E+12	4.02701E+11	3.08131E+12	4.69616E+12	2.51688E+13
5	31-12-13	2.05549E+13	1.80918E+13	2.46312E+12	3.3483E+12	2.99013E+12	3.58171E+11	2.97218E+12	4.48977E+12	2.23857E+13
6	31-12-12	1.86305E+13	1.65278E+13	2.10263E+12	3.0222E+12	2.70146E+12	3.20744E+11	2.4851E+12	4.09126E+12	2.00465E+13
7	31-12-11	1.66107E+13	1.48313E+13	1.77942E+12	2.58075E+12	2.28833E+12	2.92423E+11	2.55261E+12	3.46763E+12	1.82764E+13

Fig. 13. Partial Data Set.

Subsequent to acquiring the data set another critical thing is to do the validation of data set and in addition finding the right attributes for the system to process. To do this we used a tool named “WEKA”. This tool gave all the needed information regarding the data by executing the algorithm of attribute selection and provides us with facts like how much of our data

is unique, how many missing values are there and are all the entries in data distinct or not. This is a vital step to execute as our outcomes are subject to it and in case the data is forged our results would not be accurate. Fig. 14 depicts the results that “WEKA” produced after running the attribute selection algorithm on the given data set.

Selected attribute	
Name: Final consumption expenditure	Type: Numeric
Missing: 0 (0%)	Distinct: 47
	Unique: 47 (100%)
Statistic	Value
Minimum	55091486717
Maximum	27205529000000
Mean	5012639541342.257
StdDev	7335235756779.33

Fig. 14. WEKA Attribute Selection Details.

B. Experimental Setup

Data and pre-processing: The experiment is executed by reading the data in .csv format by Pandas that reads and parses it. Then the dataset is splitted into two parts one for the training and another one for the testing. Now before we fit a machine learning algorithm or the LSTM model over it. In order to achieve this first we need to transform the data into a supervised learning problem with having an input x and output y in our time series case $t-1$ and t respectively. Then the stationary transformation is required to make model result with more skillful forecast. Lastly, we scale it as the model processes the input and output in range of $(-1, 1)$ range that normalizes the data by using minmax scalar.

1) **Model:** After data pre-processing the optimizer provided by the Keras is configured by hit and trial method and agreed to keep the Adamax optimizer with a flexible learning rate. By default, LSTM has a tanh activation function but we tend to override it with various different functions like sigmoid, SELU and Softmax. The model is tested based on various epochs, neuron populations and learning rates.

2) **Results:** The predicted values are displayed in comparison with the expected values. The results from the model are fed to the graph plotting function the matplotlib. In the process the accuracy of the model and the RMSE are also calculated to measure the accuracy of the proposed model.

C. Final Outcome

Based on selected dataset attributes the experiment is performed and the results are detailed in Table IX. The results produced by IBM SPSS and ANN (LSTM) are compared in

terms of accuracy. The results predicted by Long Short-Term Recurrent Neural Network are more accurate as compared to the IBM SPSS.

The RMSE value calculated during experimentation is 1221190424306.566.

The results in Table IX reflect the six years of testing data (Initial 3 years, Final 3 years). It is observed that for the year 1994 there was an unexpected change in the trend but still the proposed LSTM model predicted closer to the following trend. Another observation from the experiment is that SPSS only produced one promising result for the year 1996 out of six years. In contrast to the proposed LSTM it is observed that in Table IX LSTM model presented 5 promising results out of total six entries.

The conventional LSTM model uses Tanh as a default activation function, these settings did show promising results but the model used with SELU through research had better training curve and performed better as shown in Table X.

Clearly RMSE value of LSTM with default function is much higher than that of LSTM with SELU function. The function with lesser RMSE value is the one to be preferred. The difference between RMSE of both the functions is:

$$\text{Precise difference} = 38071328299.673$$

The difference shows how much closer results to actual value are produced by the SELU function when compared with the default function.

TABLE IX. TABLE OF EXPERIMENT RESULTS

Year	Expected "Final consumption expenditure"	IBM SPSS	ANN(LSTM)
1994	1490000000000	1677776293937	1619476432991
1995	1710000000000	1863005590810	1780559280565
1996	2070000000000	2048234887683	1993555488109
-	-	-	-
2014	2310000000000	5382362231395	20837874049091
2015	2500000000000	5567591528268	23337874049091
2016	2720000000000	5752820825141	25237874049091

TABLE X. ACCURACY OF TANH AND SELU

Functions of LSTM	Historic Data Requirement	RMSE	Average Accuracy
Tanh (Default)	Yes	1241633196117.760	90.94%
SELU	Yes	1203561867818.087	92.34%

VII. CONCLUSION

The impetus of the study was to construct and develop an artificially intelligent expense forecasting system that could grasp over a trend inside the data using artificial neural networks and machine learning techniques. After thorough study of the available algorithms and mathematical models, Long Short-Term Memory (LSTM) was used. Root Mean Square Error (RMSE) was used to calculate the error and accuracy was obtained by the difference between actual and predicted values. The proposed model had produced accurate result up to 91% average accuracy. The base model was further tweaked with variation of different activation function for testing the efficiency. The system can be used to anticipate the future trend of numeric financial data and that it can help in more refined budget definitions, spending criteria and crises avoidance.

ACKNOWLEDGEMENT

Special thanks to Army Public College of Management & Sciences, Rawalpindi and University of Engineering and Technology, Taxila in order to provide resources and support this research. Special thanks to all other contributors.

REFERENCES

- [1] G. Chan, "Forecasting the S&P 500 index using time series analysis and simulation methods," Massachusetts Institute of Technology, 2009.
- [2] C. S. Vui, et al., "A review of stock market prediction with Artificial neural network (ANN)," in Control System, Computing and Engineering (ICCSCE), 2013 IEEE International Conference on, 2013, pp. 477-482.
- [3] N. Nazir and M. Dmutto, "Stock Market Prediction Using Artificial Neural Network," International Journal of Advanced Engineering, Management and Science, vol. 2, 2006.
- [4] T. Kimoto, et al., "Stock market prediction system with modular neural networks," in Neural Networks, 1990., 1990 IJCNN International Joint Conference on, 1990, pp. 1-6.
- [5] Y. Zhang and L. Wu, "Stock market prediction of S&P 500 via combination of improved BCO approach and BP neural network," Expert Systems with Applications, vol. 36, pp. 8849-8854, 2009.
- [6] H. S. Hippert, et al., "Neural networks for short-term load forecasting: A review and evaluation," IEEE Transactions on power systems, vol. 16, pp. 44-55, 2001.
- [7] D. Wang and Z. Sun, "Big data analysis and parallel load forecasting of electric power user side," Proceedings of the CSEE, vol. 35, pp. 527-537, 2015.
- [8] R. Hu, et al., "A short-term power load forecasting model based on the generalized regression neural network with decreasing step fruit fly optimization algorithm," Neurocomputing, vol. 221, pp. 24-31, 2017.
- [9] K. G. Borojeni, et al., "A novel multi-time-scale modeling for electric power demand forecasting: From short-term to medium-term horizon," Electric Power Systems Research, vol. 142, pp. 58-73, 2017.
- [10] K. Amasyali and N. M. El-Gohary, "A review of data-driven building energy consumption prediction studies," Renewable and Sustainable Energy Reviews, vol. 81, pp. 1192-1205, 2018.
- [11] U. Berardi, "A cross-country comparison of the building energy consumptions and their trends," Resources, Conservation and Recycling, vol. 123, pp. 230-241, 2017.
- [12] S. Singh and A. Yassine, "Big data mining of energy time series for behavioral analytics and energy consumption forecasting," Energies, vol. 11, p. 452, 2018.
- [13] A. R. Gollou and N. Ghadimi, "A new feature selection and hybrid forecast engine for day-ahead price forecasting of electricity markets," Journal of Intelligent & Fuzzy Systems, vol. 32, pp. 4031-4045, 2017.
- [14] J. Nowotarski and R. Weron, "Recent advances in electricity price forecasting: A review of probabilistic forecasting," Renewable and Sustainable Energy Reviews, 2017.
- [15] J. Saez-Gallego and J. M. Morales, "Short-term forecasting of price-responsive loads using inverse optimization," IEEE Transactions on Smart Grid, 2017.
- [16] A. Mirakyan, et al., "Composite forecasting approach, application for next-day electricity price forecasting," Energy Economics, vol. 66, pp. 228-237, 2017.
- [17] W. Y. Cheng, et al., "Short-term wind forecast of a data assimilation/weather forecasting system with wind turbine anemometer measurement assimilation," Renewable Energy, vol. 107, pp. 340-351, 2017.
- [18] C. Feng, et al., "A data-driven multi-model methodology with deep feature selection for short-term wind forecasting," Applied Energy, vol. 190, pp. 1245-1257, 2017.
- [19] R. L. Wilson and R. Sharda, "Bankruptcy prediction using neural networks," Decision support systems, vol. 11, pp. 545-557, 1994.
- [20] L. Wilkenson, "SYSTAT: the system for statistics. SYSTAT," Inc., Evanston. 638p, 1989.
- [21] J. Stanley, Introduction to neural networks: California Scientific Software, 1990.
- [22] C. A. Casas, "Parallelization of artificial neural network training algorithms: A financial forecasting application," in Computational Intelligence for Financial Engineering & Economics (CIFEr), 2012 IEEE Conference on, 2012, pp. 1-6.
- [23] R. I. Rasel, et al., "Financial instability analysis using ANN and feature selection technique: application to stock market price prediction," in Innovations in Science, Engineering and Technology (ICISSET), International Conference on, 2016, pp. 1-4.
- [24] A. D. G. Reddy and L. T. Varma, "Wind power forecasting without using historical data," in Proceedings of the International Conference on Advances in Electrical Engineering (ICAEE), 2014, pp. 1-3.
- [25] K. K. Nargale and S. Patil, "Day Ahead Price Forecasting in deregulated electricity market using artificial neural network," in Energy Efficient Technologies for Sustainability (ICEETS), 2016 International Conference on, 2016, pp. 527-532.
- [26] S. Ferlito, et al., "Predictive models for building's energy consumption: An Artificial Neural Network (ANN) approach," in AISEM Annual Conference, 2015 XVIII, 2015, pp. 1-4.
- [27] A. Ahmadi, et al., "Hybrid model for weather forecasting using ensemble of neural networks and mutual information," in Geoscience and Remote Sensing Symposium (IGARSS), 2014 IEEE International, 2014, pp. 3774-3777.
- [28] S. S. Baboo and I. K. Shereef, "An efficient weather forecasting system using artificial neural network," International journal of environmental science and development, vol. 1, p. 321, 2010.
- [29] R. Nayak, et al., "An artificial neural network model for weather forecasting in Bhopal," in Advances in Engineering, Science and Management (ICAESM), 2012 International Conference on, 2012, pp. 747-749.
- [30] K. L. M. D. Sobrevilla, et al., "Daily weather forecast in Tiwi, Albay, Philippines using Artificial Neural Network with missing values Imputation," in Region 10 Conference (TENCON), 2016 IEEE, 2016, pp. 2981-2985.
- [31] D. M. Nelson, et al., "Stock market's price movement prediction with LSTM neural networks," in Neural Networks (IJCNN), 2017 International Joint Conference on, 2017, pp. 1419-1426.
- [32] D. Kang, et al., "Short-term traffic flow prediction with LSTM recurrent neural network," in Intelligent Transportation Systems (ITSC), 2017 IEEE 20th International Conference on, 2017, pp. 1-6.
- [33] W. Kong, et al., "Short-term residential load forecasting based on LSTM recurrent neural network," IEEE Transactions on Smart Grid, 2017.
- [34] Y. Zhang, et al., "Long short-term memory recurrent neural network for remaining useful life prediction of lithium-ion batteries," IEEE Transactions on Vehicular Technology, 2018.
- [35] Quandl. (2016, 04/06/2018). Pakistan GDP by Type of Expenditure at current prices-national currency. Available: https://www.quandl.com/data/UNAE/GDPCN_PAK-GDP-Current-Prices-National-Currency-Pakistan

Software Artefacts Consistency Management towards Continuous Integration: A Roadmap

D. A. Meedeniya¹, I. D. Rubasinghe², I. Perera³

Department of Computer Science and Engineering, University of Moratuwa, Sri Lanka

Abstract—Software development in DevOps practices has become popular with the collaborative intersection between development and operations teams. The notion of DevOps practices drives the software artefacts changes towards continuous integration and continuous delivery pipeline. Subsequently, traceability management is essential to handle frequent changes with rapid software evolution. This study explores the process and approaches to manage traceability ensuring the artefact consistency towards CICD in DevOps practice. We address the key notions in traceability management process including artefact change detection, change impact analysis, consistency management, change propagation and visualization. Consequently, we assess the applicability of existing change impact analysis models in DevOps practice. This study identifies the conceptualization of the traceability management process, explores the state-of-art solutions and suggests possible research directions. This study shows that the lack of support in heterogeneous artefact consistency management with well-defined techniques. Most of the related models are limited with the industry-level applicability in DevOps practice. Accordingly, there is inadequate tool support to manage traceability between heterogeneous artefacts. This study identifies the challenges in managing software artefact consistency and suggests possible research directions that can be applied to manage the traceability in the process of software development in DevOps practice.

Keywords—Consistency management; traceability; continuous integration; DevOps; comparative study

I. INTRODUCTION

Software systems perform in a dynamic context, where changes arise due to different factors such as a change in business goals, performance improvements, fault corrections and change of technology. DevOps (Development-Operations) practice is an emerging software development approach that encourages collaborative nature over traditional software development [1]. DevOps practice addresses the frequent artefact changes during the Software Development Life Cycle (SDLC) enabling a Continuous Integrations and Continuous Delivery (CICD) pipeline. Consequently, maintaining software evolution is essential, although it is challenging to manage the artefacts change consistency management [2]. For instance, a software artefact barely exists in isolation as it is associated with other artefacts in the process. Thus, a change in a requirement may have a considerable effect on the entire system. Hence, artefact consistency management plays a major role in achieving software traceability [3].

A software system consists of both homogeneous and heterogeneous artefacts in different formats, making consistency management a complex task. For example, the

requirement artefact can be in a natural language, while the source code artefact in Java programming language. Therefore, a change occurred in one artefact does not directly reflect in other artefacts due to the type and format mismatches. The artefact traceability is significant in consistency management [4]. Generally, an artefact change appears as a request for a change without direct action of alteration. Thus, a semi-automated or manual process of maintaining the artefact traceability may subject to errors.

In traceability established system, it is essential to detect artefact changes and identify their impact. The Change Impact Analysis (CIA) process identifies the affected artefacts by following the trace paths using different techniques such as traceability graphs [5], Information Retrieval (IR) and Machine Learning (ML) [6][7]. In graph-based traceability, the artefact changes are mapped to the nodes and the change are propagated via the connected links. However, all the endpoints of the links may not be subjected to changes. Therefore, the impact of the propagated changes at the linked endpoints needs to be measured to identify the actual impacted set of a change. Thus, a CIA approach should be selected based on the artefact types that are used to measure the impact [8][9].

Additionally, the properties of the initial change may highly affect the impact calculation, since the linked endpoints are compared with the initial change. Several studies have used IR techniques to identify the properties of the initial change such as the scope and keywords [10][11]. Moreover, CIA techniques based on probabilistic methods such as association rules, Bayes theorem and Change History have used to measure the impact of a change [12][13][14]. However, it is challenging to address the change ripple effects after the initial impacted endpoint identification, as the changes can propagate continuously.

The main components of the traceability management process include trace-link creation, change detection, CIA, consistency management, change propagation and collaboration. This survey paper addresses the traceability management process in DevOps practice. Section II states an overview of DevOps and the traceability management process. Section III discusses the artefact change detection methods, which is the first step in the CICD process. Section IV elaborates CIA with its terminology, approaches and related studies. Section V describes the existing change propagation and consistency management techniques. Related work on the continuous integration in DevOps practice is presented in Section VI. Section VII states the limitations and challenges of achieving traceability in DevOps practice and the possible future research directions. Section VIII concludes the paper.

II. BACKGROUND

A. Concepts of DevOps

DevOps practice broadens the view of software engineering paradigm by improving the collaboration across teams, sharing resources, tools and increasing the project performance. This is based on a maturity model that integrates the development and operations teams [15]. There are stages of a DevOps cycle with respect to SDLC phases that include continuous planning, integration, testing, delivery, deployment and monitoring [1][15][16]. As shown in Fig. 1, in DevOps practice the developers implement the project by enforcing the deployment process and the operations team monitors the progress and faults during the deployment, adhering to CICD process [1]. Mainly the development team is responsible to plan, code, build, test and the operations team is responsible for the project release, deploy, operate and monitor.

The coordination of human resources in a DevOps environment is important to maintain the manageability of collaborative nature. DevOps engineer, that can be an individual or a team, plays a major role by managing the tool support including automation, version control, configuration, maintenance [1]. Consequently, the level of automation in the CICD pipeline is controlled by the DevOps engineer. In this study, we have mainly explored the Continuous Integration (CI) aspects such as change detection, change impact analysis, change propagation and consistency management along with the identification of DevOps tool support and challenges.

B. Traceability Management Process

In a software product, it is essential to maintain artefact consistency whenever a change occurs. Software traceability is required to handle changes during the process of CICD, that integrates the work frequently between the development and operations teams leading to multiple integrations per day [2]. Software traceability follows the life cycle of an artefact both forward and backward and overcomes the inconsistencies during the software development [17]. Thus, each alteration occurs in an artefact is traced among other artefacts and change accordingly based on the impact. The relationship links among artefacts must be updated and maintained consistently. Fig. 2 shows a traceability process model within a collaborative environment. The artefacts with changes in various levels are usually included in each CI task. Thus, the initially established traceability links in the project must be incorporated according to the changes included in each integration. This process consists of change detection, CIA, consistency management and change propagation. Visualization of the traceability links is used to understand the dependencies between the artefacts. It is challenging and costly to manage the consistency of a larger set of artefact relationships whenever a change occurs. Also, the effort of maintaining artefact relations is considerably high though the number of artefacts is minimal [18]. Thus, the accuracy of traceability establishment is important.

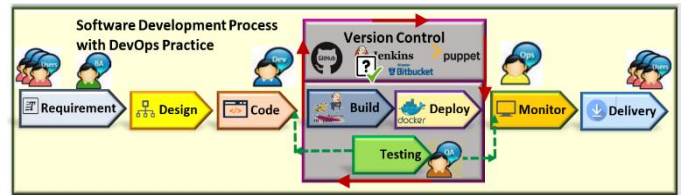


Fig. 1. Software Development Process with DevOps practice.

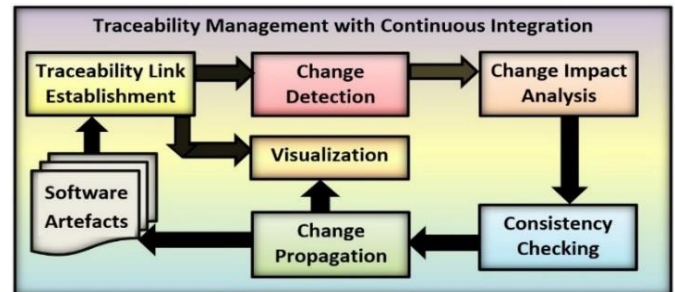


Fig. 2. Traceability Management Process Model.

III. CHANGE DETECTION

A. Types of Artefact Changes

Change is inevitable in any software development process and should be handled properly to improve product quality while avoiding unnecessary cost [19]. Artefacts in each phase of the SDLC are subjected to change at different frequencies due to change of requirement, technology, managerial decision and fault tolerance. A change in a phase of the SDLC can evolve through the phases based on their dependencies.

Mainly three types of changes can occur during software development. (1) edit changes, that alter the existing elements or sub-elements of the artefacts. For example, changing the name of an attribute in a design class diagram or renaming a source code method name is considered as an edit change; (2) delete changes, that removes one or more existing artefact elements or sub-elements from a traceability model such as removing attributes from a source code class or deleting a class in a design class diagram is considered as a deletion change; (3) add changes, that include new artefact elements or sub-elements to the existing project. The change detection process identifies whether a change has occurred and detect the details of change such as change type and artefact type.

B. Change Detection Techniques

Among many techniques, edit history approach keeps track of the alterations or the edits as a history [20]. Here, each change is considered as an item for the history and records as another edit. This is already in use with most of the software and non-software related tools and methodologies such as text editors, mainly the 'Undo', 'Redo' and 'Restore' operators [20][21]. However, this technique is mostly used for the change detection of the source code artefact.

Tree differencing is another main change detection technique that represents elements as Abstract Syntax Tree (AST) and calculates the differences to extract detailed change information [22]. AST is a tree representation method of the syntactic structure in the source code, where every node denotes a construct occurrence in the code. This is a well-defined method, for instance, the study done in [19], has transformed a tree to another in hierarchically structured data based on the idea of matching and minimum cost edit scripts. Here, the authors have separated the change detection problem as ‘good matching’ and ‘minimum conforming edit script’. However, it is required the data to be in a tree format. The approach of calculating differences between ASTs is widely used for source code artefacts [22][23].

The customized differencing algorithm is another technique for software artefact change detection. It is used in software maintenance aspects such as program-profile estimation (stale profile propagation). A software artefact type can be taken as the input for a differencing algorithm [22]. However, the implementation of a general algorithm for all types of software artefacts is identified to be impractical rather than having a set of differencing algorithms for each type of software artefacts.

IV. CHANGE IMPACT ANALYSIS

A. Terminology of Change Impact Analysis

Each change in a single artefact may affect one or more other related artefacts in different degrees. The goal of the CIA is to detect the consequences of an artefact alteration to other artefacts in the software system [12]. Traceability is a key notion to identify the affected artefacts and decide whether evolution is sustainable [24]. Generally, the impact is analyzed before or after a change implementation. The prior analysis of the impact results in better program understandability, change impact prediction and cost estimations. Correspondingly, conducting impact analysis after implementation of a change can be beneficial in tracing ripple effects, selecting test cases and in performing change propagation [1]. Fig. 3 shows the iterative CIA process in software development [25].

Initially, the process analyses a change request to determine the set of changes in which the artefacts can be affected. It is referred to as feature location, with the aim of finding a place that requires the initial change. Then, the CIA is performed to estimate the effects in changes resulting in an Estimated Impact Set (EIS). Afterwards, the change is implemented and the elements in the Actual Impact Set (AIS) are altered. The AIS is not considered to be unique for a given change request as a change can be implemented in different ways.

Fig. 4 shows the types of change impact sets. The Starting Impact Set (SIS) denotes the set of entities initially affected by the change. Then, a subset of it called Candidate or Estimated Impact Set (CIS or EIS) is a subset of SIS, includes the identified potential impact entities that are traced from SIS. The AIS is required to be identified from the EIS. Discovered Impact Set (DIS) are the artefacts that are impacted by the change but have not identified by CIS due to the challenging effect of artefact type mismatches, development mistakes and inconsistencies in artefact naming. These hidden dependencies of the artefacts can be identified manually or using a

knowledge-based technique [26][27]. The False Positive Impact Set (FPIS) denotes the artefacts that are overestimated as belong to the CIS, but which are not actually impacted yet.

B. Change Impact Analysis Techniques

One category of change impact analysis approach is a traceability-based and dependence-based technique to identify the effect of a change [25]. Traceability-based CIA is narrowed in recovering the traceability links among software artefacts. Dependence-based CIA evaluates the impact of a proposed change. This technique is biased towards in analyzing program syntax relations and performing CIA of artefacts in the same level of abstraction such as in the level of software design or within the level of source code. The higher-level Unified Modeling Language (UML) models and use case maps are mainly involved in requirement and design level impact analysis. In addition, the source code-based CIA techniques are more capable to determine change impacts of the final software product with improved precision as they analyze the implementation details directly. Table I explores different CIA techniques with their advantages and limitations.

Another categorization of CIA technique is static and dynamic impact analysis [9][28][29]. Static CIA techniques consider all the possible behaviours and inputs. It analyzes the syntax and semantic dependencies of source code and constructs intermediate representations using call graphs and program dependence graphs [9]. Then, the CIA is conducted based on the representations resulting in large impact sets that are difficult to use in practice. Thus, lower precision is a major drawback in static CIA techniques. Besides, dynamic CIA techniques overcome this drawback by considering only a part of the inputs. Hence, their impact sets are identified to be highly precise though lower in safety. Furthermore, dynamic CIA depends on the analysis of the data obtained during the execution such as trace information, relation and coverage information to assess the impact sets.

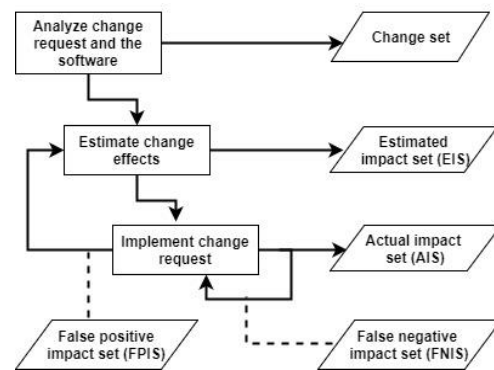


Fig. 3. Change Impact Analysis Process [25].

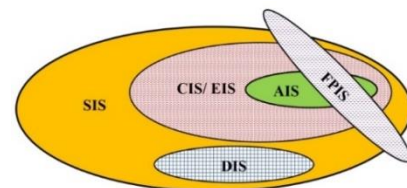


Fig. 4. Change Impact Analysis Categorization.

TABLE I. COMPARISON OF CHANGE IMPACT ANALYSIS TECHNIQUES

Category	Technique	Description
Statistical analysis	Data flow analysis, relational language, program slicing, static call graphs [30]	Has identified that the string analysis is not precise for schema CIA. There is a precision versus computational cost trade-off in this analysis.
	Comparative analysis: Study on impact analysis algorithms, techniques using Precision, Recall and Harmonic mean [11][26][31][32][33][34].	Results certify that existing algorithms require enhancements and effective mechanisms to facilitate automated tools for the CIA. Have identified required characteristics in impact analysis. Discovered the possibility of transferring impact analysis tools in academia to industry to help developers during maintenance and evolution activities.
Probabilistic-based	Change history and Bayes' theorem [26]	Maintenance of object-oriented critical systems is addressed. Limited for object-oriented software.
	Call graphs, Entity Dependency Graph [35][30][36][37][38][39][38]	Explain the concept of two dependency states; namely, persistent relationship state and immediate relationship state in change propagation. Better program understanding and debugging.
	Formal Semantics [40] Logical dependencies and classification [39][41]	Removal of false positive impacts and consistency checking. Adds valuable information. Restricted for particular change and relation types.
	Rule-based [36][41][42]	Allows developers to smoothly retrace the changes.
	Data mining, Apriori algorithm [6]	Useful in change predictions.
History-based	Historical co-change analysis, change history [6][43][44]	Use version histories to identify logical/ evolutionary couplings between entities. Predict impact files after a change.
	Machine learning [7][10][26]	Classification models to predict the validity of the candidate links. Use unsupervised learning to identify hidden dependencies. Less human involvement
	Logical coupling [27]	Use logical coupling with a Markov model. Better accuracy.

Acharya and Robinson [28] have presented a static CIA framework that is developed as a tool named Imp, to analyse the impact of source code artefacts during the frequent builds.

This mathematical model is used forward slicing consists of three criteria such as range, dependences and summary edges to assess the impact sets. Additionally, this work has used Andersen's algorithm with pointer analysis. This methodology consists of two variations one for high setting impact analysis which is expensive and another for low setting impact analysis which can be performed frequently and faster at a low cost.

Another static impact analysis technique is addressed in [29], that have created clusters of associated source codes based on their co-modification history. Here, dimensionality reduction approaches have used to reduce complexity and perform the impact analysis efficiently. Initially, they have mined the changed repository to find co-occurring source files and developed a matrix containing a degree of closeness in each pair of files. Then, an intrinsic dimensionality method based on eigenvalues has conducted to estimate the lower dimensional representation of the matrix and Principle Component Analysis (PCA) was used to reduce the matrix. Finally, the matrix rows were taken as coordinates of the files; the distance between each pair of files was measured and passed to five clustering methods. However, quantitative measures have not used to evaluate the model impact.

In dynamic CIA approach, the main techniques are path impact and coverage impact [30][35]. Path impact performs at the method level with the use of compressed execution traces to determine impact sets. It processes forward and backward traces to identify the impact of the changes. The forward traces determine all the methods called after the altered methods,

while the backward traces find methods into which the execution can return. The coverage impact technique uses the coverage information to identify the executions that traverse at least one method in the change set and it marks the covered methods in each execution. Next, it assesses a static forward trace from each change from the marked methods. Thus, the methods in computed traces become the impact set. Moreover, it is analytically identified that the path impact technique is more precise compared to the coverage impact technique as it makes use of traces instead of the coverage [35]. However, the time and space overhead of the path impact technique is high. The required time in path impact tends to depend on the size of the analyzed trace, though the coverage impact needs a constant time in updating bit vectors at each of the method entries. Besides, the space complexity of coverage impact technique is linear over the size of the program, while it is also proportional to the size of the traces in the path impact technique. The use of dependency network measures such as centrality measures have also used for the CIA. The work by Nguyen et al. [45] has shown the applicability of dependency network analysis measures in practical applications.

Mainly the CIA techniques can be categorized into a graph, formal, historical and scope-based. The comparative and classification-based approaches are used in most related work while some have developed a specific tool. Among the used CIA techniques, call graphs and dependence graphs are widely used to handle the changes that enable the backtracking ability to debug easily. Most of the artefact types including design, code and test cases are influenced by these call graphs related techniques and IR based: Latent Semantic Indexing (LSI), Frequency-Inverse Document Frequency (TF-IDF) and Vector Space Model (VSM) techniques. In contrast, the work in [46] has shown the drawbacks of dependence graphs and proposed a

modular-based approach for large-scale product lines. The formal semantics, First Order Logic (FOL) and review-based analysis have addressed the requirement artefact type solely. While most of these techniques are semi-automatic, the use of data mining and ML in impact analysis has become a newer trend that tries to completely avoid the human effort with full automation. However, in terms of the scope-based CIA related work, there is a lack of support for later phases of SDLC in particular testing and maintenance phases as the majority are restricted for requirements artefact or source code [17][47][48]. Thus, that limits the applicability of these CIA approaches and related works into a DevOps environment.

C. Change Impact Analysis Models

A change type classification method for code revision has presented in [21]. The authors have proposed a taxonomy for change types and defined code changes in the form of tree edit operations on the AST of a program. The changes are classified based on the significance level such as low, where local changes to have a minor significance, medium, high or crucial, where interface changes are critical. This work has extended with a tool called ChangeDistiller in [49]. This model assigns a label to every code entity in the AST that denotes the type of each entity and adds a textual named value, covering the actual code. Additionally, they have extracted change couplings from their release history database which have an identical total significance level. These changes have weighted based on the number of transactions they occurred in. Accordingly, the remaining change couplings were the most likely candidates for being affected by changes to coupled entities. This model is shown in Fig. 5, and implemented as the ChangeDistiller [49] plug-in for Eclipse. However it is limited for small projects.

Another model for the CIA for Java programs has presented in [38]. Fig. 6 shows the architecture of a Java source code impact analysis tool called 'Chianti', which is implemented as a plugin in Eclipse IDE.

There are three main submodules in this tool. The initial one is to derive atomic changes from two Java source code versions which are done via pairwise AST comparisons. One other module is responsible for reading test call graphs to detect the original and edited codes. Also, it assesses impacted tests and impacting changes. The other module visualizes the change impact details to the user. Accordingly, this plugin model is mainly based on the call graphs and does not involve calculations for each impact in a quantitative value.

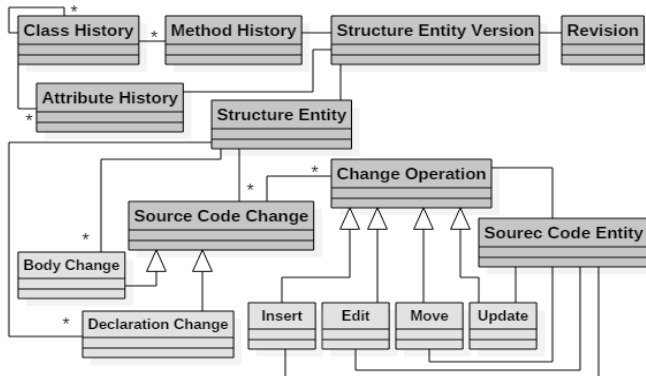


Fig. 5. ChangeDistiller Model [49].

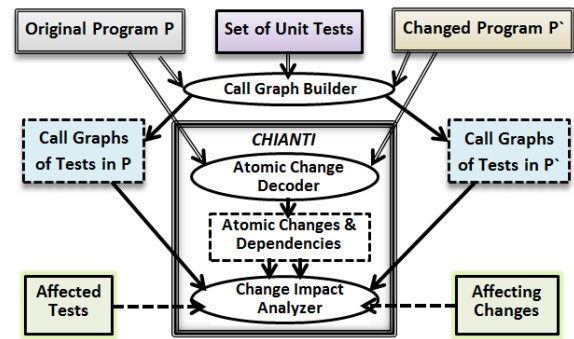


Fig. 6. Chianti Tool Architecture [38].

Wong and Cai [50], have proposed a model to extract the logical models from UML class diagram. This is based on a logical framework named Augmented Constraint Network (ACN). Fig. 7 depicts the structure of an ACN translated class. The classes are weighted based on their number of augmented constraint networks to determine impacted elements. A higher rank is assigned, if there are more sub augmented constraint networks. The distance between the two classes also affects the weight and closely related classes get a higher ranking. The weights are then multiplied with the co-change frequency of entities that are mined from version histories. Accordingly, ten of the highest ranked elements are output to the user.

One of the earliest CIA models [8], has calculated the transitive closure to identify the impacted elements using conceptual models. The concept of intra-method and inter-method data dependency graphs are used to calculate impacts on entities in method bodies and change dependencies between methods, respectively. Object-oriented dependency graphs are used to compute the change impact at the system level. Additionally, they have declared four types of impacts between every two related entities including contaminated (both are impacted), clean (both are not impacted), semi-contaminated (the source does not impact the target though the source can be impacted) and semi-clean (the source is not impacted, but it propagates changes to the target). These types are used to assign weights to relationships among entities, based on their impact relation type. Then the total change impact weight is assessed as the sum of all weights, which are assigned to the relations between two entities. Finally, the total change impact weight is assigned to all graphs to enable impact calculation.

A CIA approach for architectural models using OCL4 to express explicit rules has proposed in [51]. They have searched the impacted elements and a distance measure is used to control the propagation of changes to the indirectly related software entities. It either cancels the change propagation or weights the impact paths based on their nesting depth. Also, they have presented a taxonomy of change types that provide three elemental change types such as add, remove and change. The impact analysis model presented in [52], has extracted changes from a repository and compiled into a matrix. The authors have computed association clusters using singular value decomposition. Every file in a cluster was assigned a weight based on its degree of participation in that cluster. High singular values have denoted that a file was subjected to be impacted by changes P to other files of the same cluster.

```
Constraint Network:  
  A_interface : {orig, other}  
  A_impl : {orig, other}  
  A_impl = orig => A_interface = orig  
Dominance Relation:  
  (A_impl, A_interface)
```

Fig. 7. ACN Translation of a Class [50].

Hattori et al. [53], have proposed another approach to estimate the possible impact elements using a dependency graph that represents the source code and a reachability analysis over the graph. They have extracted the change sets and analysed the impacted entities using a probabilistic algorithm based on Bayes' theorem that removes the false-positives. Apriori and Disjunctive association rule algorithms were used to weight and sort the impacts based on their likelihood. Another change impact analysis model is presented by Arnold and Bohner in the area of traceability [54]. They have considered the changes occurred in documentation and source codes to identify the SIS. Then, dependency graphs were used to obtain CIS based on direct impacts. Moreover, the reachability graph visualizations were used to identify the indirect impacts. They have applied this process incrementally to identify the CIS to minimize the false positive rate. A source code artefact CIA approach based on the change requests provided in natural language document such as bug reports is presented in [55]. They have IR technique to estimate the impact set; LSI to analyze textual change requests, dynamic analysis to evaluate the execution information and data mining to examine the evolutionary information. This work has shown that the accuracy improves regarding the metrics; precision, recall and f-measure by combining these multiple approaches.

Although there are several CIA studies, the majority has been limited only up to design level or source code artefact in considering the artefact types while operational level artefacts like build scripts are not addressed.

V. CONSISTENCY MANAGEMENT

During SDLC, various artefacts process through different stages and it is essential to maintain the consistency between all the artefacts, whenever an artefact change occurs. After predicting the artefact change effects during the CIA, consistency management and change propagation are performed to trace the ripple effects [25]. Thus, maintaining consistency plays a major role in managing artefact consistency during the CICD process in a DevOps environment.

A. Change Propagation Techniques

Heuristic rules are one of the techniques that can be used to aggregate the detected changes to propagate the changes. This enables to obtain the optimal solution of the change propagation path with higher performance irrespective of the completeness of the information [56]. Source code artefact change propagation is addressed in [20] using an aggregation algorithm with heuristic rules.

The distance-based technique is mainly based on temporal and spatial distance. For the change propagation, this method considers the time taken between changes and the location

distance among two modifications. These distances are measured using AST and the graph-based representations associated with graph traversal algorithms [20][51].

B. Consistency Management Approaches

Artefact changes or refinements happen at any time. Their consequences may not result in a uniform pattern, where some refinements may reflect and impact on other artefacts. Thus, the stability among artefacts can be inconsistent and can fail in representing the expected software solution with stakeholder dissatisfaction. Therefore, consistency management, the ability to preserve the synchronization among software artefacts along with the occurring changes, is essential to minimize efforts in software system maintenance [57]. Hence, an artefact alteration or the presence of outdated artefacts should consistently reflect on the other affected artefacts.

Several studies have addressed consistency management and change propagation with CIA [36][40][42]. A predictive model is presented in [14] to predict the change propagation. The approach does not require access to the source code. It derives information from expert knowledge, user manuals and maps them in a weighted dependency graph. Reachability analysis is done on that weighted graph to reason the change propagation. The tool 'JTracker' is popular for assisting change propagation and CIA in such that when a programmer changes a class, this tool creates the potentially impacted neighbouring classes. The propagation is terminated if the changes in neighbouring classes are not necessary. 'JRipples' is another significant tool to support change propagation during the incremental changes [12][25].

In an earlier related study, Lee [58] has addressed impact analysis algorithms and evaluation metrics, which have been developed in a tool called 'ChaT' tool leading path to research on CIA for object-oriented programs. That algorithm relies on the computation of the transitive closure of object-oriented data dependency graphs. Those graphs based on control and data flow information extracted from the code program. The algorithms analyze the relationships between components and weight them according to the type of relation. It is expressed as a set of impact propagation rules.

VI. CONTINUOUS INTEGRATION AND DEVOPS TOOLS

Continuous Integration is the repetitive integration process of developing and testing during a software development process [2][16]. It elaborates the frequent merging of the sole components of a software system to a shared branch by preserving the healthiness of the code. The automation of the CI process is significant to reduce the risks associated with software development such as lack of deployable software, late discovery of defects and lower project visibility [2].

In CI, the code commits to the version control repositories are frequently pushed to the CI servers and generate build scripts to integrate the new changes to the software. For instance, the concept of a single source point is encouraged using version control repositories such as CVS, Subversion, Perforce and Visual SourceSafe that allows accessing all the source codes from a single primary location. After each build script execution by the CI servers, the feedback mechanism notifies the status of the build. It is recommended to fix the

discovered pipeline failures at the earliest possible way to preserve CI. Moreover, CI and testing are intricately linked together [16][59]. In order to trace the software artefacts, this method uses scripts based on version controlling to control the code rather than the individual commands. The ‘Echo’ approach is an evolving tool-based solution that addresses traceability in requirements, as it is impractical to use static documents to track the requirement artefacts in an Agile environment [60].

DevOps enables efficient deliverables by speeding-up the customer query processing using tool support [15]. The tool support in a DevOps environment, such as Jenkins, Travis, Ansible, Docker, Sonar, Maven and OpenStack helps to maintain CI and traceability. For instance, the existing high-level plugins such as Hudson post-build scripts enable automated analysis of CI operations in Jenkins. However, many supportive tools have mainly considered the source code artefact integrations regardless of other artefact combinations such as a modification in requirements, design and test cases. Further, the consequences of changes in integrations have not analyzed in terms of CIA and change propagation aspects. This section explores the main features of DevOps supportive tools.

Jenkins is a prominent opensource DevOps support tool that monitors frequently executed jobs. It is a rapid CI server with error detection. Jenkins server performs a set of tasks supported by a trigger, that can be a change in a version management system [61]. The main tasks of the workflow are acquiring Git source code, trigger the job, build the source project and notify the results. The list of tasks includes performing a software build with Apache Maven, executing a shell script, archiving the build results and starting the

integration tests. Jenkins builds and tests software systems continuously and supervises the job executions even though it is running on a remote machine. Further, Jenkins configuration is simple, deployable in large scale environments and call slaves from the cloud by adhering to a slave topology [62].

Puppet is another configuration tool in DevOps, based on deploying microservices efficiently [59]. The configurations are described using a set of scripts defined in a Domain Specific Language (DSL). Puppet provides a unified interface for activities such as starting system services that require different tasks in the various Operating Systems. Travis is another distributed CI service that supports building and testing open source software projects. It encourages teamwork by tightly coupling to DevOps practices [63]. It can perform automatically scheduled tests with GitHub repositories. Docker is an open platform to build, ship and execute distributed software applications even on a virtual machine or a cloud environment [59]. The existence of microservices has enriched by tools including Docker. It has made the containers or objects that hold and transport data accessible easily.

Table II summarizes the features of the related studies in artefact traceability management in terms of change detection, CIA, consistency management, change propagation and CI. For instance, Zhang et al. [64], have addressed the change detection and impact analysis with a framework implemented in AspectJ programs and [65] is an architectural level artefact specific work. The workspace awareness tool in [66] has involved all the phases in continuous integration in an event-based approach, but it lacks automation. The tool Echo based on agile practice presented by [60], has addressed requirements and design related artefacts.

TABLE II. COMPARISON OF RELATED WORK ON TRACEABILITY MANAGEMENT

Rated studies	Traceability establishment	Change detection	Change impact analysis	Consistency management	Change propagation	Continuous integration
Impact propagation approach based on artefact change types [42].	A rule-based approach to detect dependency	-	Rule-based approach. Multi-level modelling.	Multi-perspective	Analyze dependency relations recursively	-
Requirements traceability tool for Agile methodologies [60].	Text annotations. Conversation-centric model.	Visualization.	Manually via visualization. Forward, backward traceability.	-	Use of elaboration activities.	Versioning.
CIA to locate failure reasons in AspectJ programs [64].		Use syntactic dependency.	Static AspectJ call graphs.	-	-	-
Architectural decisions change management to demystify architecture [65].	A template-based approach using architectural decision.	Decision-based approach.	Manual analysis.	-	Decision-based approach with manual monitoring.	-
Tool solution for early change detection and resolution on code conflicts [66].	Event-based approach.	Visualization.	Event-based approach. Binary measurements.	Manual visualizations.	YANCEES notification service.	Use a tool for workspace awareness
Artefact change management based on a feature-oriented hypothesis. [67].	Feature-oriented approach.	Feature-oriented manner.	Calculate artefact feature dependencies.	-	-	-
An artefact management tool to assess IR capabilities in traceability recovery [68].	Information retrieval methods.	Matrix-based using VSM.	Rule-based approach.	Traceability recovery using LSI.	-	-
Semi-automated traceability creation on requirements, design decisions and architecture [69].		An integrative approach by using LISA tool.	An integrative approach by integrating tool AREL.	-	-	-
Traceability based on event notifications in distributed development environments [70].	Event-based approach.	Publisher-subscriber technique.	Event-based approach. Event logs for artefacts.	-	Update artefact event logs.	-

VII. DISCUSSION

A. Limitations in Existing Studies

One major limitation in the current state-of-art and research-level solutions for change detection, CIA, consistency management, change propagation and CI is being solely addressing the source code artefact [22][28][55][64]. Therefore, tracing heterogeneous artefacts corresponding to all the stages of SDLC with CIA remains challenging with respect to rapid changes. Otherwise, adapting to multiple separate tools or frameworks is one way out which leads to a higher traceability management cost. Another challenge in CI is identified as having continuous prioritization for integrations.

The influence of the CIA is important in the traceability management process in a DevOps practice as consistency management and change propagation depend on it. However, many studies have not addressed all the relevant artefacts and consider only a few numbers of CIA approaches, due to the heterogeneity nature of the artefacts. Thus, related studies are limited to either requirement and design level artefacts or entirely on source code artefact [17][47][48]. There is a lack of research in adequate successful attempts that addresses both development and operations level artefacts covering the entire SDLC. The existing research-level outcomes lack proper user interface and visualization features that are essential for a collaborative development environment such as DevOps for fast decision making. Moreover, some studies are domain specific such as for product line environments, modular software, safety critical context. [24][46][34]. Consequently, being dependent on a specific tool environment and integration incompatibilities with existing tools limits the practical usage of traceability tools in a wider range [49][69]. The rule-based techniques can resolve the heterogeneity nature of the artefacts,

but requires human involvement to define newer rules [40]. Thus, automation becomes problematic that eventually increases the traceability cost. Table III summarizes the feature considerations of some of the existing tools.

The lack of automation capabilities and the need for adapting to multiple tool-chains have limited the adaptation of traceability in DevOps practice. Some of the existing solutions are limited to semi-automation, which is not sufficient to reduce the traceability cost in large-scale solutions. Thus, achieving automation for complete traceability management process model is important for a DevOps environment to cope with the frequent change integrations.

B. Future Research Directions

Addressing the heterogeneity of artefacts in change detection, CIA, consistency management, change propagation and CI is one prominent active research directions. This will help to reduce the traceability management cost in practice and encourage practical traceability adaptation. Machine learning and probabilistic methodologies are becoming a promising solution stack as well [7]. Thus, a possible suggestion is to incorporate machine learning based algorithms to establish traceability links, so that the human involvement in defining rules and monitoring can be avoided to cope with the new formats of artefacts. In addition, it will enable the transformation from semi-automation to automation.

Moreover, different methodologies can be integrated into a common platform to reduce the overhead of adapting to multiple tools or frameworks. This will reduce the cost associated with the tool-chain management and the inconsistencies among tools. Further, maintaining the research outcomes of the traceability management in the context of DevOps would be helpful to approach for stable solutions.

TABLE III. FEATURE COMPARISON OF EXISTING TRACEABILITY MANAGEMENT TOOLS

Tools	TraceME [71]	IBM DOORS [72]	TraceAnalyzer [73]	LDRA-TBmanager [74]	ArchEvol [75]	ReqView [76]	ArchStudio [77]
Features							
Requirement traceability	√	√		√		√	
Design level traceability	√		√		√		√
Heterogeneous artefacts	√		√	√			
Traceability visualization		√	√		√		√
Traceability validation							
CI/ scheduling/ versioning		√		√	√	√	
Change detection							
Change impact analysis	√	√					
CIA validation							
Change propagation visualization							
Consistency management, PM		√				√	√
DevOps tools stack supportability							
IDE independence						√	√
Performance analysis							

VIII. CONCLUSION

This survey explores the current approaches and techniques for achieving software artefact traceability in a DevOps environment. This paper mainly considered the tasks such as change detection, change impact analysis, consistency management and change propagation with continuous integrations in DevOps practice, that accommodate for feasible traceability management. Moreover, software artefacts traceability management can be implemented as a supportive tool in DevOps practice. Traceability links are generated by considering the dependencies among artefacts. In order to support the CICD pipeline, change detection is performed for each CI task that contains artefact changes in the forms of an edit, addition or removal. The main associated techniques are edit-history, tree-differencing and differencing algorithms. Then, the impact of a given changed is identified with different approaches such as call graphs, dependence graphs, program slicing, formal semantics, logical coupling, IR and rule-based approaches. Further, mathematical weight-based approaches are used for the CIA process. Heuristic rules and distance-based techniques are discussed in the change propagation that follows the impacted artefacts based on the CIA results.

However, most of the related studies have limitations that restrict their suitability for traceability management in a collaborative DevOps environment. Most of the existing methodologies have not addressed artefacts in all stages of SDLC and considered only the requirement, design level or source code artefacts. Although some studies have addressed a fully-automation process considering specific artefact types, there are limitations such as high traceability cost and efforts in a DevOps environment due to the frequent CI tasks. Thus, automated tool support for traceability management that addresses the overall SDLC in a DevOps environment is a need in practice. Accordingly, the requirement of having a generalized traceability solution to cope with the maximum types of artefacts, with a minimum cost and maximum level of automation is identified as a future research direction for an efficient traceability management process in DevOps practice.

ACKNOWLEDGMENT

The authors acknowledge the support received from the Senate Research Committee Grant SRC/LT/2017/12, University of Moratuwa, Sri Lanka in publishing this paper.

REFERENCES

- [1] L. J. Bass, I. M. Weber, and L. Zhu, *DevOps : A Software Architect's Perspective*, 1st ed. Addison-Wesley Professional, 2015.
- [2] P. M. Duvall, S. Matyas, and A. Glover, *Continuous Integration: Improving Software Quality and Reducing Risk*, 1st ed. Addison-Wesley Professional, 2007.
- [3] S. A. Bohner and R. S. Arnold, *Software change impact analysis*. Wiley-IEEE Computer Society, 1996.
- [4] I. Sommerville, *Software Engineering*, 10th ed. New York: Addison-Wesley Professional, 2010.
- [5] W.T. Lee, W.Y. Deng, J. Lee, and S.J. Lee, "Change impact analysis with a goal-driven traceability-based approach," *Int. J. Intell. Syst.*, vol. 25, no. 8, pp. 878–908, 2010.
- [6] T. Zimmermann, A. Zeller, P. Weissgerber, and S. Diehl, "Mining version histories to guide software changes," *IEEE Trans. Softw. Eng.*, vol. 31, no. 6, pp. 429–445, 2005.
- [7] C. Mills, "Towards the automatic classification of traceability links," in *32nd IEEE/ACM International Conference on Automated Software Engineering-ASE 2017*, 2017, pp. 1018–1021.
- [8] M. Lee and A. J. Offutt, "Algorithmic analysis of the impacts of changes to object-oriented software," in *Technology of Object-Oriented Languages and Systems*, 2002, pp. 61–70.
- [9] G. Tóth, P. Hegedűs, Á. Beszédes, T. Gyimóthy, and J. Jász, "Comparison of different impact analysis methods and programmer's opinion: an empirical study," in *8th International Conference on the Principles and Practice of Programming in Java - PPPJ '10*, 2010, pp. 109–118.
- [10] W. Wang, Y. He, T. Li, J. Zhu, and J. Liu, "An Integrated Model for Information Retrieval Based Change Impact Analysis," *Sci. Program.*, vol. 2018, no. Article ID 5913634, pp. 1–13, 2018.
- [11] Y. Zhang, C. Wan, and B. Jin, "An empirical study on recovering requirement-to-code links," in *17th IEEE/ACIS International Conference on Software Engineering, Artificial Intelligence, Networking and Parallel/Distributed Computing - SNPD*, 2016, pp. 121–126.
- [12] S. Lehnert, "A taxonomy for software change impact analysis," in *12th International Workshop and the 7th Annual ERCIM Workshop on Principles on Software Evolution and Software Evolution - IWPSE-EVOL '11*, 2011, pp. 41–50.
- [13] T. Mens, J. Buckley, M. Zenger, and A. Rashid, "Towards a Taxonomy of Software Evolution," *Journal of Software Maintenance and Evolution*, vol. 17, no. 5, pp. 309–332, 2005.
- [14] A. Aryani, I. D. Peake, and M. Hamilton, "Domain-based change propagation analysis: An enterprise system case study," in *2010 IEEE International Conference on Software Maintenance*, 2010, pp. 1–9.
- [15] F. M. A. Erich, C. Amrit, and M. Daneva, "A qualitative study of DevOps usage in practice," *Journal of Software Evolution and Process*, vol. 29, no. 6, p. e1885, 2017.
- [16] A. Eck, F. Uebornickel, and W. Brenner, "Fit for continuous integration: how organizations assimilate an agile practice," in *20th Americas Conference on Information Systems - AMCIS '14*, 2014, pp. 1–11.
- [17] M. Rath, D. Lo, and P. Mäder, "Analyzing requirements and traceability information to improve bug localization," *Proc. 15th Int. Conf. Min. Softw. Repos. - MSR '18*, pp. 442–453, 2018.
- [18] J. Cleland-Huang, A. Zisman, and O. Gotel, *Software and Systems Traceability*, 1st ed. London: Springer-Verlag London, 2012.
- [19] S. S. Chawathe, A. Rajaraman, H. Garcia-Molina, and J. Widom, "Change detection in hierarchically structured information," *ACM SIGMOD Rec.*, vol. 25, no. 2, pp. 493–504, 1996.
- [20] E. Kitsu, T. Omori, and K. Maruyama, "Detecting Program Changes from Edit History of Source Code," in *20th Asia-Pacific Software Engineering Conference (APSEC)*, 2013, pp. 299–306.
- [21] B. Fluri and H. C. Gall, "Classifying Change Types for Qualifying Change Couplings," in *14th IEEE International Conference on Program Comprehension (ICPC'06)*, 2006, vol. 2006, pp. 35–45.
- [22] J.-R. Falleri, F. Morandat, X. Blanc, M. Martinez, and M. Montperrus, "Fine-grained and accurate source code differencing," in *29th ACM/IEEE International Conference on Automated Software Engineering - ASE '14*, 2014, pp. 313–324.
- [23] T. Sager, A. Bernstein, M. Pinzger, and C. Kiefer, "Detecting similar Java classes using tree algorithms," in *International Workshop on Mining Software Repositories - MSR '06*, 2006, pp. 65–71.
- [24] H. Cho, J. Gray, Y. Cai, S. Wong, and T. Xie, "Model-Driven Impact Analysis of Software Product Lines," in *Model-Driven Domain Analysis and Software Development*, IGI Global, 2011, pp. 275–303.
- [25] B. Li, X. Sun, H. Leung, and S. Zhang, "A survey of code-based change impact analysis techniques," *Softw. Test. Verif. Reliab.*, vol. 23, no. 8, pp. 613–646, Dec. 2013.
- [26] I. G. Czibula, G. Czibula, D. L. Miholca, and Z. Marian, "Identifying Hidden Dependencies in Software Systems," *Stud. Univ. Babeş-Bolyai Inform.*, vol. 62, no. 1, pp. 90–106, 2017.
- [27] S. Wong, Y. Cai, and M. Dalton, "Change Impact Analysis with Stochastic Dependencies," PA, USA, 2011.

- [28] M. Acharya and B. Robinson, "Practical change impact analysis based on static program slicing for industrial software systems," in 33rd International Conference on Software Engineering - ICSE '11, 2011, pp. 746–755.
- [29] M.-A. Jashki, R. Zafarani, and E. Bagheri, "Towards a more efficient static software change impact analysis method," in 8th ACM SIGPLAN-SIGSOFT Workshop on Program Analysis for Software Tools and Engineering - PASTE '08, 2008, pp. 84–90.
- [30] G. A. Oliva, M. A. Gerosa, D. Milojicic, and V. Smith, "A change impact analysis approach for workflow repository management," in IEEE 20th International Conference on Web Services, ICWS 2013, 2013, pp. 308–315.
- [31] S. J. Kabeer, M. Nayebe, G. Ruhe, C. Carlson, and F. Chew, "Predicting the Vector Impact of Change - An Industrial Case Study at Brightsquad," in ACM/IEEE International Symposium on Empirical Software Engineering and Measurement (ESEM), 2017, pp. 131–140.
- [32] M. Shahid and S. Ibrahim, "Change impact analysis with a software traceability approach to support software maintenance," in 13th International Bhurban Conference on Applied Sciences and Technology (IBCAST), 2016, pp. 391–396.
- [33] F. Déhoulé, L. Badri, and M. Badri, "A Change Impact Analysis Model for Aspect Oriented Programs," in 12th International Conference on Evaluation of Novel Approaches to Software Engineering, 2017, pp. 144–157.
- [34] M. Borg, K. Wnuk, B. Regnell, and P. Runeson, "Supporting Change Impact Analysis Using a Recommendation System: An Industrial Case Study in a Safety-Critical Context," IEEE Trans. Softw. Eng., vol. 43, no. 7, pp. 675–700, 2017.
- [35] T. Apiwattanapong, A. Orso, and M. J. Harrold, "Efficient and precise dynamic impact analysis using execute-after sequences," in 27th International Conference on Software Engineering - ICSE '05, 2005, pp. 432–441.
- [36] Y. Wang, J. Zhang, and Y. Fu, "Rule-Based Change Impact Analysis Method in Software Development," in 2nd International Conference on Computer Engineering, Information Science & Application Technology - ICCIA, 2017, vol. 74, pp. 396–403.
- [37] D. Kchaou, N. Bouassida, and H. Ben-Abdallah, "UML models change impact analysis using a text similarity technique," IET Softw., vol. 11, no. 1, pp. 27–37, 2017.
- [38] X. Ren, B. G. Ryder, M. Stoerzer, and F. Tip, "Chianti: a change impact analysis tool for Java programs," in 27th International Conference on Software Engineering - ICSE '05, 2005, pp. 664–665.
- [39] A. M. D. Duarte, D. Duarte, and M. Thiry, "TraceBoK: Toward a Software Requirements Traceability Body of Knowledge," in 24th International Requirements Engineering Conference, 2016, pp. 236–245.
- [40] A. Goknil, I. Kurtev, and K. van den Berg, "A Rule-Based Change Impact Analysis Approach in Software Architecture for Requirements Changes," eprint arXiv:1608.02757, pp. 1–44, 2016.
- [41] S. Lehnert, "Multiperspective Change Impact Analysis to Support Software Maintenance and Reengineering," University of Hamburg, 2015.
- [42] S. Lehnert, Q. U. A. Farooq, and M. Riebisch, "Rule-based impact analysis for heterogeneous software artifacts," in European Conference on Software Maintenance and Reengineering - CSMR, 2013, pp. 209–218.
- [43] H. Kagdi, "Improving change prediction with fine-grained source code mining," in 22nd IEEE/ACM International Conference on Automated Software Engineering - ASE '07, 2007, pp. 559–562.
- [44] A. R. Sharafat and L. Tahvildari, "A Probabilistic Approach to Predict Changes in Object-Oriented Software Systems," in 11th European Conference on Software Maintenance and Reengineering - CSMR'07, 2007, pp. 27–38.
- [45] T. H. D. Nguyen, B. Adams, and A. E. Hassan, "Studying the impact of dependency network measures on software quality," in 2010 IEEE International Conference on Software Maintenance, 2010, pp. 1–10.
- [46] F. Angerer, H. Prafhofer, and P. Grunbacher, "Modular Change Impact Analysis for Configurable Software," in 2016 IEEE International Conference on Software Maintenance and Evolution - ICSME, 2016, pp. 468–472.
- [47] B. Dit et al., "ImpactMiner: a tool for change impact analysis," in 36th International Conference on Software Engineering - ICSE Companion 2014, 2014, pp. 540–543.
- [48] L. Zhang, M. Kim, and S. Khurshid, "FaultTracer: a change impact and regression fault analysis tool for evolving Java programs," in ACM SIGSOFT 20th International Symposium on the Foundations of Software Engineering - FSE '12, 2012, pp. 40:1-40:4.
- [49] H. C. Gall, B. Fluri, and M. Pinzger, "Change Analysis with Evolizer and ChangeDistiller," IEEE Softw., vol. 26, no. 1, pp. 26–33, 2009.
- [50] S. Wong and Y. Cai, "Predicting change impact from logical models," in IEEE International Conference on Software Maintenance, ICSM, 2009, pp. 467–470.
- [51] L. C. Briand, Y. Labiche, and L. O'Sullivan, "Impact analysis and change management of UML models," in International Conference on Software Maintenance, ICSM 2003, 2003, pp. 256–265.
- [52] M. Sherriff and L. Williams, "Empirical software change impact analysis using singular value decomposition," in 1st International Conference on Software Testing, Verification and Validation, ICST, 2008, pp. 268–277.
- [53] L. Hattori, G. dos Santos Jr, F. Cardoso, and M. Sampaio, "Mining software repositories for software change impact analysis: a case study," in SBDD '08 23rd Brazilian symposium on Databases, 2008, pp. 210–223.
- [54] A. De Lucia, F. Fasano, and R. Oliveto, "Traceability management for impact analysis," in Frontiers of Software Maintenance, 2008, pp. 21–30.
- [55] M. Gethers, B. Dit, H. Kagdi, and D. Poshvanyk, "Integrated impact analysis for managing software changes," in 2012 34th International Conference on Software Engineering - ICSE, 2012, pp. 430–440.
- [56] J. Cleland-Huang, O. C. Z. Gotel, J. H. Hayes, P. Mäder, and A. Zisman, "Software traceability: trends and future directions," in Future of Software Engineering - FOSE 2014, 2014, pp. 55–69.
- [57] I. Pete and D. Balasubramaniam, "Handling the differential evolution of software artefacts: A framework for consistency management," in IEEE 22nd International Conference on Software Analysis, Evolution, and Reengineering - SANER, 2015, pp. 599–600.
- [58] M. L. Lee, "Change impact analysis of object-oriented software," George Mason University, Virginia, 1998.
- [59] V. Farcic, The DevOps 2.0 Toolkit: Automating the Continuous Deployment Pipeline with Containerized Microservices, 1st ed. CreateSpace Independent Publishing Platform, 2016.
- [60] C. Lee, L. Guadagno, and X. Jia, "An agile approach to capturing requirements and traceability," in 2nd International Workshop on Traceability in Emerging Forms of Software Engineering, 2003, pp. 1–7.
- [61] J. Hembrink and P.-G. Stenberg, "Continuous integration with Jenkins," Coach. Program. Teams - EDA 270, pp. 1–8, 2013.
- [62] A. M. Berg, Jenkins Continuous Integration Cookbook, 2nd ed. Packt Publishing, 2015.
- [63] "Travis CI," Travis CI, 2018. [Online]. Available: <https://travis-ci.org/>. [Accessed: 05-Jul-2017].
- [64] S. Zhang, Z. Gu, Y. Lin, and J. Zhao, "Change impact analysis for AspectJ programs," in IEEE International Conference on Software Maintenance, 2008, pp. 87–96.
- [65] J. Tyree and A. Akerman, "Architecture decisions: Demystifying architecture," IEEE Softw., vol. 22, no. 2, pp. 19–27, 2005.
- [66] A. Sarma, D. F. Redmiles, and A. Van Der Hoek, "Palantir: Early detection of development conflicts arising from parallel code changes," IEEE Trans. Softw. Eng., vol. 38, no. 4, pp. 889–908, 2012.
- [67] L. Passos, S. Apel, C. Kästner, K. Czarnecki, A. Wasowski, and J. Guo, "Feature Oriented Software Evolution," in 7th International Workshop on Variability Modelling of Software-intensive Systems - VaMoS '13, 2013, pp. 17:1-17:8.
- [68] A. De Lucia, F. Fasano, R. Oliveto, and G. Tortora, "Recovering traceability links in software artifact management systems using information retrieval methods," ACM Trans. Softw. Eng. Methodol., vol. 16, no. 4, pp. 13:1-13:50, 2007.

- [69] G. Buchgeher and R. Weinreich, "Automatic Tracing of Decisions to Architecture and Implementation," in 9th Working IEEE/IFIP Conference on Software Architecture, 2011, pp. 46–55.
- [70] J. Cleland-Huang, C. K. Chang, and M. Christensen, "Event-based traceability for managing evolutionary change," *IEEE Trans. Softw. Eng.*, vol. 29, no. 9, pp. 796–810, 2003.
- [71] G. Bavota, L. Colangelo, A. De Lucia, S. Fusco, R. Oliveto and A. Panichella, "TraceME: Traceability Management in Eclipse", In 28th IEEE International Conference on Software Maintenance - ICSM, 2012, pp. 642–645.
- [72] IBM, "IBM-Rational DOORS", Available <https://www.ibm.com/us-en/marketplace/rational-doors>, [October 14, 2018].
- [73] A. Egyed, "A scenario-driven approach to traceability", In 23rd International Conference on Software Engineering, ICSE, 2001, pp. 123–132.
- [74] LDRA, "TBmanager", Available <https://ldra.com/industrial-energy/products/tbmanager/tbmanager/>, [January, 10, 2019].
- [75] E. C. Nistor, J. R. Erenkrantz, S. A. Hendrickson and A. van der Hoek, "ArchEvol: versioning architectural-implementation relationships", In 12th International Workshop on Software Configuration Management, SCM, 2005, pp. 99–111.
- [76] "ReqView," 2018. [Online]. Available: <https://www.reqview.com/>. [Accessed: 07-May-2018].
- [77] E. Dashofy, H. Asuncion, S. Hendrickson, G. Suryanarayana, J. Georgas, and R. Taylor, "ArchStudio 4: An Architecture-Based Meta-Modeling Environment," In 29th International Conference on Software Engineering - ICSE, 2007, pp. 67–68.

A GRASP-based Solution Construction Approach for the Multi-Vehicle Profitable Pickup and Delivery Problem

Abeer I. Alhujaylan¹, Manar I. Hosny²

Computer Science Department
College of Computer and Information Sciences (CCIS)
King Saud University (KSU)
Riyadh, Saudi Arabia

Abstract—With the advancement of e-commerce and Internet shopping, the high competition between carriers has made many companies rethink their service mechanisms to customers, in order to ensure that they stay competitive in the market. Therefore, companies with limited resources focus on serving only customers who provide high profits at the lowest possible cost. The Multi-Vehicle Profitable Pickup and Delivery Problem (MVPPDP) is a vehicle routing problem and one variant of the Selective Pickup and Delivery Problem (SPDP) that is considered to plan the services for these types of companies. The MVPPDP aims to serve only the profitable customers, where the products are transformed from a selection of pickup customers to the corresponding delivery customers, within a given travel time limit. In this paper, we utilize the construction phase of the well-known Greedy Randomized Adaptive Search Procedure (GRASP) to build initial solutions for the MVPPDP. The performance of the proposed method is compared with two greedy construction heuristics that were previously used in the literature to build the initial solutions of the MVPPDP. The results proved the effectiveness of the proposed method, where eight new initial solutions are obtained for the problem. Our approach is especially beneficial for building a population of solutions that combine both diversity and quality, which can help to obtain good solutions in the improvement phase of the problem.

Keywords—*Selective pickup and delivery problem; multi-vehicle profitable pickup and delivery problem; greedy randomized adaptive search procedure; metaheuristic algorithms*

I. INTRODUCTION

Transportation management is considered one of the most difficult problems facing people and governments in different countries all over the world. In our daily life, millions of people use land, sea, or air transport means to commute from one place to another, raising the need to optimize the planning of these services, in order to reduce their cost as well as their negative environmental impacts. Therefore, a lot of research has been conducted recently to address these problems in the fields of computer science, operations research, and industrial engineering. Land transport, in particular, has received a great interest from researchers, due to its huge volume. Research efforts try to optimize the daily use of the means of transportation, such as cars, buses, trucks, trains, motorcycles, trams, etc. Among the most known land transport problems

are: vehicle routing problems [1], pickup and delivery problems [2], bus scheduling problems [3], truck routing problems [4], cash transportation problems [5], railroad blocking problems [6], and others [7][8][9].

Researchers in this field generally aim at minimizing congestion and the environmental damage of the transportation services, caused by harmful emissions, such as carbon dioxide and other greenhouse gases, which cause pollution and global warming, and have a negative effect on people's health. In the shipment sector, for instance, the average fleet emission for delivery trucks and vans is 10.17 kg of CO₂ per gallon of diesel consumed [10]. Furthermore, many trucks are not exploited to their full capacity, where statistics indicate that 15% to 30% of pollution, traffic congestion, and accidents are caused by empty trucks [11]. Besides the environmental damage, the inefficient regulation of the trucks' paths and the non-exploitation of their full capacity has an economic effect on the companies that work in the transport sector. In order for these companies to remain and continue its activities in the market, many solutions are suggested to increase the companies' profits, as well as to reduce their costs.

The Vehicle Routing Problem (VRP) is a well-known combinatorial optimization problem that deals with transportation network management and the scheduling and distribution of vehicles and goods. The VRP is concerned with planning and organizing the distribution of goods to find the appropriate routes to transfer the customers' demands by using one or more homogeneous fleet of vehicles. Each vehicle has a limited capacity and it starts its tour from a distribution center (depot), then it transfers goods to customers, and returns to the distribution center. In the literature, several types of the VRP with different complex constraints have been presented and solved over the last 50 years which-contributed to minimizing a lot of road transportation problems, such as, pollution and congestion[12].

The Pickup and Delivery Problem (PDP) is an important variant of the VRP, which aims to minimize the total transportation cost when distributing goods or people from one location (pickup node) to another location (delivery node). The PDP also has several important variants and applications, such as the transportation of raw materials from suppliers to

factories, the distribution of beverages and the collection of empty bottles and cans, shipping cargos, etc. One relatively new variant of the PDP is the Selective Pickup and Delivery Problem (SPDP), which has recently started to receive interest in the academic literature. The SPDP can be distinguished from the standard PDPs by relaxing the constraint that all nodes must be visited. The SPDP helps companies that have limited resources and wish to provide high level services to customers with minimum possible cost, by finding the best routes to deliver their products and pick up some of them. Also, the SPDP contributes positively to environmental and economic considerations; specifically, it helps to reduce the harmful impacts of transportation that result from pollution and congestion, by selecting only a subset of customers to be visited. As such, solving the SPDP helps to achieve the goals of green supply chain management [13][14][15]. There are two types of SPDPs: (1) SPDPs subject to minimizing the travelling cost only (e.g. [16][17][18]), and (2) SPDPs subject to minimizing the travelling cost and maximizing the profits collection (e.g. [19] [20][21]).

The Multi-Vehicle Profitable Pickup and Delivery Problem (MVPPDP), which has been presented by Gansterer et al. [22], belongs to the second type of the SPDP. It considers both travel cost and profit's collection in the planning process. The MVPPDP is a static problem with a central distribution (depot), predefined number of homogenous fleet of vehicles and a set of requests. Each request has a predefined pair of customers, a pickup customer and a delivery customer. Moreover, these requests include transferring a number of homogenous products from pickup customers (origins) to their corresponding delivery customers (destinations) with certain associated profits. The MVPPDP aims to plan perfect routs to serve some of the customers in a one-day planning horizon, with the aim of maximizing the total collected profits minus the total travel costs. Some real-life applications of this problem include: food delivery mobile apps, delivery companies that transfer goods from factories to related shops, etc.

The MVPPDP is an NP-hard problem [22], which means that exact algorithms can find an optimal solution for only a small number of input data. Therefore, metaheuristic algorithms have been often used to find good solutions that are not necessarily optimal, in a reasonable processing time.

In this paper, we present a new approach to construct initial solutions for the MVPPDP. We adapt the construction phase of the well-known Greedy Randomized Adaptive Search Procedure (GRASP) to the underlying problem. GRASP is a multi-start metaheuristic that is commonly applied to solve different combinatorial optimization problems. It was first introduced by Feo and Resende [23]. It consists of two phases: construction and improvement phase. The construction phase is used to build an initial feasible solution, while the second phase is a local search used to improve the initial solution found in the construction phase to get a local optimum [24]. There are several advantages of GRASP compared to other popular metaheuristics, like Genetic Algorithms, Simulated Annealing and Tabu Search. These include combining the advantages of random and greedy search, which helps the GRASP to be fast, competitive

and able to find good solutions in a reasonable time. Furthermore, the number of parameters that need to be tuned is small, which is another advantage that makes the GRASP preferred over other metaheuristics [25]. Also, GRASP has successfully contributed to solving different variants of VRP [26] [27] [28].

The rest of this paper is organized as follows. In Section 2, a review of some related work is presented. The definition and mathematical formulation of the tackled problem is given in Section 3. In Section 4, the proposed method is described in detail. Experimental results are discussed in Section 5. Finally, conclusions and future work are presented in Section 6.

II. LITERATURE REVIEW

The MVPPDP belongs to the type of SPDP that is subject to minimizing the travelling costs and maximizing the profits collection. The MVPPDP aims to visit only the profitable customer pairs, in order to make the gathering operation as profitable as possible. Thus, the MVPPDP can be considered as a combination of two types of problems: the feature of selecting a subset of customers belongs to the SPDP, while the feature of selecting customers that have maximum revenue belongs to the Profitable Tour Problem (PTP). Therefore, the literature review of the MVPPDP will be classified into three parts: The MVRPPDP, the SPDP and the PTP.

A. The Multi-Vehicle Profitable Pickup and Delivery Problem (MVPPDP)

The MVPPDP was presented by Gansterer et al. [22]. Two versions of the General Variable Neighborhood Search (GVNS) were used to solve it: a sequential one (GVNSseq), and a self-adaptive one (GVNSsa). The initial solution was built by using a Greedy Construction Heuristic (C1) and a Two-Stage Cheapest Insertion Heuristic (C2). Then, one of three strategies had been selected randomly to make some changes on the initial solution. After that, 11 neighborhoods operators were used to improve the solution. They tested the performance of proposed algorithms against Guided Local Search (GLS) on a newly created dataset that is divided into three sizes: small, medium, and large. The performance of the C2 heuristic was found to be better than C1 for most instances. Also, the results indicated that both variants of GVNS with the C2 heuristic outperform GLS for all sizes of test data in terms of solution quality. However, GLS had an advantage regarding the average runtimes in both medium and large sized instances.

Haddad [29] presented a new method for the MVPPDP. The proposed algorithm combined Iterated Local Search (ILS) and Random Variable Neighborhood Descent (RVND). Also, the algorithm is not limited to accept only the feasible solutions during the search. The same greedy constructive heuristic that was used in [22] was adopted to construct the initial solution. In order to improve the solution, several neighborhood moves were applied. The proposed algorithm was tested on the benchmark instances proposed by [22]. It proved its efficiency in addressing the small and medium sized instances, where it was able to find new best solutions on 6 instances. However, the performance of the proposed algorithm was not good enough for large sized instances.

B. The Selective Pickup and Delivery Problem (SPDP) Subject to Travelling Cost and Profits Collection

The work in [13] is an application of the SPDP, where three heuristics were proposed to solve a complex real-life problem appearing in the soft drinks distribution and recyclable containers collection in a Quebec based company. The algorithms are the Nearest Neighbor Heuristic (NNH), First Petal Heuristic (FPH), and Second Petal Heuristic (SPH). The results on real-life instances showed a reduction in distance by 23%. The authors in [15] proposed a Mixed Integer Linear Programming (MILP) and a Tabu Search (TS) to solve the Single Vehicle Routing Problem with Deliveries and Selective Pickups (SVRPDSP). Also, three heuristics were developed: shifting pickups (SP), optimization of the sequence of customers in the route (RC), and reducing the number of second visits (RV). The empirical results indicated that the proposed heuristics gave near-optimal solutions for 68 instances that were derived from the VRP library¹. In [14], the Selective Multi-Depot Vehicle Routing Problem with Pricing (SMDVRPP) was introduced to tackle the reverse logistics problem of companies that aim to collect cores of durable goods from its merchants after re-buying or trade-in by customers to encourage them to buy. Two MILPs models and a Rich Neighborhood Tabu Search (TS-RN) were used to solve this problem. The proposed heuristic was tested on 40 randomly generated instances, showing promising results in terms of both accuracy and efficiency. In [20][21], two Hybrid metaheuristics were presented to solve the SVRPDSP: Hybrid General Variable Neighborhood Search (HGVNS) and a hybrid metaheuristic based on an Evolutionary Algorithm (EA). Both metaheuristics were tested on the same instances as in [15], where the experimental results proved the effectiveness and robustness of the proposed metaheuristics. For the interested readers, other applications of the SPDP can be found in [19] [30] [31] [32] and [33].

C. The Profitable Tour Problem (PTP)

The Profitable Tour Problem (PTP) shares with the SPDP the same goal of finding a route that maximizes the difference between the total gained profit and the total cost of traveling. The difference between them is that in the PTP no restrictions are imposed on the vehicle route (i.e., the vehicle's capacity, maximum time of trip and precedence constraints are not considered) [34]. The studies that address the PTP are so rare in the literature [35]. In [36], a new neighborhood search is used to solve the standard VRP. Then, an algorithm that relies on resource constrained shortest paths is used to find the optimal subsequence of visits. To evaluate the proposed method, three metaheuristics were used: local improvement method, a hybrid genetic search and an iterated local search. The proposed strategy performed well, where it contributed to finding new 52 best solutions. In [37] [38], an exact approach and three metaheuristics were proposed to solve the capacitated team orienteering and profitable tour problems: a VNS algorithm and two versions of Tabu Search (TS). The first version of TS explored only feasible solutions, while the other one explored the infeasible solutions as well. All proposed methods succeeded to find the optimal solution

when compared on instances that were solved by a branch-and-price algorithm. In [39], a hybrid VNS was proposed to solve a rich variant of the PTP (RPTP). Instances of the Orienteering Problem with Time Windows (OPTW) were used to test the efficiency of the proposed algorithm, where it was able to get good solutions in a reasonable time.

III. PROBLEM DEFINITION AND MATHEMATICAL FORMULATION

The MVPPDP is a static problem, where all problem constituents are known in advance. The problem is characterized by having a central distribution location (depot), a predefined number of homogenous vehicles and a set of customers' requests. Each request has a predefined pair of customers: a pickup customer and a delivery customer. Moreover, these requests include transferring a number of homogenous products (i.e., they have the same characteristics and quality) from pickup customers (origins) to their corresponding delivery customers (destinations) to get profits. Fig. 1 represents a simple example of the problem, where there are three vehicles that serve only the profitable customer pairs (i.e., those who make high revenues at the lowest possible cost) among 50 customers [22].

Several constraints should be taken into consideration when solving the MVPPDP:

- *Pair constraint:* Each product has a predefined pair of pickup and delivery customers.
- *Precedence constraint:* the pickup customer should be visited before its related delivery customer.
- *Time constraint:* Each vehicle has a certain daily travel time that should not be exceeded during serving the customers.
- *Capacity constraint:* The total amount of products gathered at any point in time should not exceed the capacity of the vehicle.
- Each vehicle journey should start and end from/at the depot with empty load.
- Each customer pair cannot be visited more than once.

The objective is to select a set of customer pairs to serve such that the revenue is maximized and its total cost is minimized.

The MVPPDP can be formally defined as follows [40]: Let $G = (V, A)$ be a graph in which $V = \{0, \dots, 2n + 1\}$ defines the vertex set, where the vertex $(0, 2n + 1)$ represents a central depot, while the remaining vertices represent the pickup customers $P = \{1, \dots, n\}$, and delivery customers $D = \{n + 1, \dots, 2n\}$. $A = \{(i, j) : i, j \in V, i \neq j\}$ defines the arc set, where each arc is associated with a non-negative routing cost c_{ij} . Each delivery vertex i has a revenue r_i to be gained when visiting it. Also, each vertex i has a supply q_i (pickup, $q_i > 0$) or demand (delivery, $q_{n+i} = -q_i$). At start, there is no supply or demand in the depot ($q_0 = 0$). In addition, each vertex i has service duration d_i . There is a set of vehicles $K = \{1, \dots, m\}$, each vehicle has a load capacity C and maximum tour time T .

¹ <http://or.dei.unibo.it/library/vrplib-vehicle-routing-problem-library>

Some notations used in the following mathematical model are described as follows: n : number of pickup customers and number of delivery customers, m : number of vehicles, P : set of pickup customers, $P = \{1, \dots, n\}$, D : set of delivery vertices, $D = \{n + 1, \dots, 2n\}$, V : set of all vertices including the depot (starting point= 0 and ending point= $2n + 1$), $V = P \cup D \cup \{0, 2n + 1\}$, K : set of available vehicles, $K = \{1, \dots, m\}$, r_i : revenue gained by serving a delivery customer at vertex i , q_i : supply (pickup : $q_i > 0$) or demand (delivery: $q_{n+i} = -q_i$) at vertex i , d_i : duration of service at vertex i , c_{ij} : transportation cost when traveling from i to j , t_{ij} : travel time between vertex i and vertex j , C : loading capacity of a vehicle, T : maximum travel time of a vehicle, x_{ijk} : binary decision variable equal to one if and only if arc ij is used by vehicle k , Q_{ik} : decision variable giving the loading amount of vehicle k after visiting vertex i , B_{ik} : decision variable for the beginning of service time of vehicle k at vertex i .

The mathematical model can be formulated as in [22] as follows:

$$\text{Maximize } \sum_{i \in V} \sum_{j \in V} \sum_{k \in K} (r_i - c_{ij}) x_{ijk} \quad (1)$$

The constraints are

$$\sum_{i \in V} \sum_{k \in K} x_{ijk} \leq 1 \quad j \in V \quad (2)$$

$$\sum_{j \in V} \sum_{k \in K} x_{ijk} \leq 1 \quad i \in V \quad (3)$$

$$x_{i0k} = 0 \quad i \in V, k \in K \quad (4)$$

$$x_{2n+1,jk} = 0 \quad j \in V, k \in K \quad (5)$$

$$\sum_{i \in V} (x_{ijk} - x_{jik}) = 0 \quad j \in V \setminus \{0, 2n + 1\}, k \in K \quad (6)$$

$$\sum_{j \in V} (x_{ijk} - x_{n+i,jk}) = 0 \quad i \in P, k \in K \quad (7)$$

$$\sum_{j \in V} x_{0jk} = \sum_{i \in V} x_{i,2n+1,k} = 1 \quad k \in K \quad (8)$$

$$(x_{ijk} = 1) \Rightarrow Q_{jk} = Q_{ik} + q_j \quad i \in V, j \in V \setminus \{0\}, k \in K \quad (9)$$

$$Q_{ik} \leq C \quad i \in V, k \in K \quad (10)$$

$$Q_{0k} = 0 \quad k \in K \quad (11)$$

$$B_{ik} \leq B_{n+i,k} \quad i \in P, k \in K \quad (12)$$

$$B_{jk} \geq x_{ijk} (B_{ik} + d_i + t_{ij}) \quad i \in V, j \in V, k \in K \quad (13)$$

$$B_{2n+1,k} \leq T \quad k \in K \quad (14)$$

$$B_{0k} = 0 \quad k \in K \quad (15)$$

$$x_{ijk} \in 0, 1 \quad i \in V, j \in V, k \in K \quad (16)$$

$$Q_{ik}, B_{ik} \geq 0 \quad i \in V, k \in K \quad (17)$$

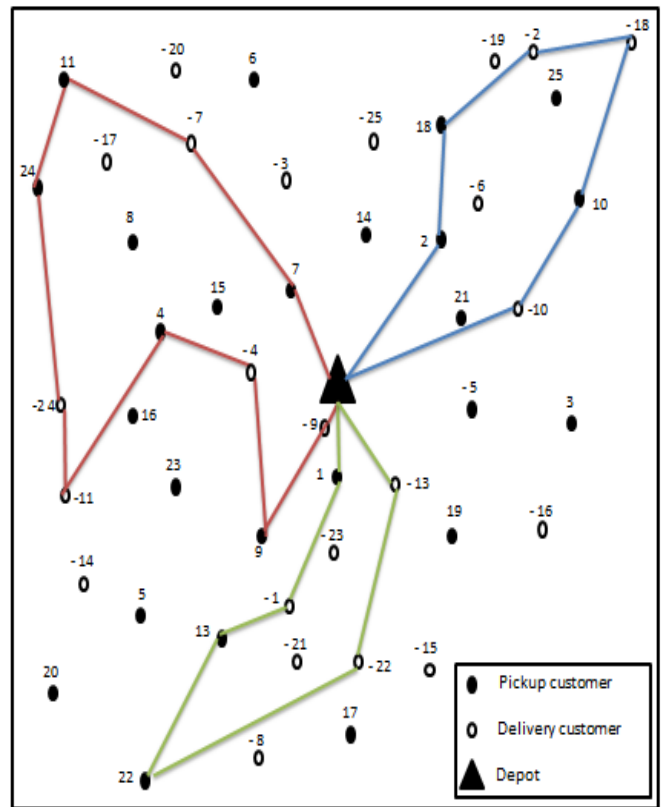


Fig. 1. An Example of the MVPPDP.

The objective function (1) tries to maximize the total profit by subtracting the total travel costs from the total revenues. Constraints (2) and (3) mean that each vertex is visited at most once. Constraints (4) and (5) mean that the origin depot (starting point) cannot be entered, and the destination depot (end point) cannot be departed by any vehicle k . Constraint (6) means flow conservation. Constraint (7) means that each customer pair (pickup customer and delivery customer) has to be served by the same vehicle. Constraint (8) means all vehicles must start from the depot and return to the depot. Constraint (9) means exceeding the vehicle capacity is not allowed. Constraint (10) means that the load of a vehicle is bounded by C . Constraint (11) means that all the vehicles start with empty load. Constraint (12) means that the delivery customer cannot be visited before its corresponding pickup customer. Constraint (13) means that the earliest time to start the service at vertex j is given by the beginning of service time at vertex i plus the service time at i and the travel time between i and j . Constraint (14) means that the maximum time for each vehicle is restricted by T . Constraint (15) means each vehicle starts at the depot at time 0. Finally, decision variables are defined by (16) and (17).

IV. PROPOSED METHOD

Most metaheuristic algorithms start solving a problem by generating one or more initial solutions and then they improve them using some local search method. The type of method used in generating the initial solution(s) plays an important role in the efficiency and effectiveness of those algorithms, regardless of the improvement method used. There are two main approaches that can be used to construct initial solutions: random and greedy. The random approach is simple, fast, and can create diverse solutions. However, the produced random solutions maybe of very low quality, which makes the job of the improvement procedure harder. In contrast, the greedy approach, which takes the objective function into consideration while constructing a solution, is often complicated and needs more computation time. In addition, although it overcomes the other approach with respect to the quality of solution, it risks getting stuck in local optima mainly due to lack of diversity [24]. To combine the advantages of the random and greedy approaches, Greedy-Randomized (GR) procedures can be used. The main idea behind these procedures in general is to select at random one of the best (greedy) decisions (instead of the absolute best as done in pure greedy methods). This helps in diversifying the search and is especially beneficial for use within population-based metaheuristics.

In our proposed method, we use a greedy-randomized procedure that is based on the well-known GRASP (Greedy Randomized Adaptive Search Procedure) to generate initial solutions for the MVPPDP. As previously mentioned, the GRASP consists of a construction phase (greedy-randomized) and an improvement phase (local search). In this paper we only utilize the construction phase to generate the initial solutions for the MVPPDP. Any local search method (e.g. hill climbing, simulated annealing, genetic algorithm, etc.) can be used later to improve the constructed solution quality. The framework of the greedy randomized procedure is shown in Algorithm 1 [24]. We adapted the GR procedure to our problem as explained next.

First, we select seed customers for each route based on a greedy approach. Then, we fill up the routes with the rest of the customers, based on combining two criteria: greediness and randomness.

Because of the importance of selecting seed customers and their clear impact on the performance of the algorithm in general, several heuristics have been proposed. The seed vertex is usually selected according to a specific criterion, often in relation to the depot (e.g., nearest, farthest, related, ..., etc.). In our method, we select the seed customer pairs for each route according to a certain measure that we call the *Customer Benefit (CB)*. The CB is calculated based on the revenue gained after delivering the demand to the delivery customer, with respect to the distance between the customer pair. Using the notations of Section 3, the customer benefit of a customer pair $(i, n + i)$ is calculated as shown in Equation (18):

$$CB_{i,n+i} = \frac{r_{i,n+i}}{c_{i,n+i}} \quad (18)$$

Algorithm 1: The greedy-randomized procedure[24]

```

S = {}; //Initialize the current solution to empty
Evaluate the fitness values of all candidate elements ;
Repeat
Construct the Restricted Candidate List RCL based on the fitness
values of the candidate elements
// select one element randomly from the RCL
e = SelectAtRandom(RCL);
If s ∪ e is feasible then
s ← s ∪ e ;
Reevaluate the fitness values of candidate elements;
Until Complete solution is constructed
    
```

Where $r_{i,n+i}$ is the revenue gained after delivering the goods to the delivery customer, and $c_{i,n+i}$ is the cost of travelling from the pickup node to the delivery node. Thus, the CB tries to rank customers based on their relative benefit versus cost with respect to the operating company. The customer pair that has the highest benefit is selected to be a seed customer.

After selecting the seed customer in the route, several candidate sub-routes will be generated for each vehicle. The following steps will be repeated to fill up each vehicle until either the final allowed time of the vehicle has been reached or no more customer pairs need to be served. Firstly, insert all customer pairs that are not served yet, where each pair of customers is inserted individually into a route in the best possible position. That is, the position that leads to the lowest possible total distance. While doing this, in order to achieve the precedence constraint, the best position for the delivery customer will be selected after adding the pickup customer.

After that, we calculate what we call the *Insertion Ratio (IR)* for each candidate pair [40]. For example, suppose we have the nodes $(a, -a, b, -b, 0)$, where $a, b \in P$ (pickup) and $-a, -b \in D$ (delivery), and 0 represents the depot. Also assume that the current route is $\{0, a, -a, 0\}$, where $(a, -a)$ is a seed customer pair, while $(b, -b)$ is the candidate customer pair to be added in the route. After determining the best position of $(b, -b)$, assume that the route will be $\{0, b, a, -b, -a, 0\}$. Thus, the insertion ratio of $(b, -b)$ is computed by dividing its revenue by its insertion cost (in its best position) in the route, as shown in Equation 19:

$$IR_{b,-b} = \frac{r_{b,-b}}{(c_{0,b}+c_{b,a}-c_{0,a}) + (c_{a,-b}+c_{-b,-a}-c_{a,-a})} \quad (19)$$

Thus, the IR represents the greedy property of selecting the next customer to be inserted in the route. Then, all the candidate customer pairs will be sorted in descending order with respect to their IR values and assigned to the Candidate Solution Set (CSS). After this, the first half of the candidate solution set is assigned to the Restricted Candidate List (RCL), so that the opportunity of selecting a good pair of customers increases. Thus, the random property lies in choosing one customer pair randomly from the RCL. The previous process will be repeated to add the rest of the un-served pairs of customers, while considering the time limit and the vehicle capacity constraint. Once the time limit of the vehicle has been exhausted, a new route (vehicle) will be initiated. At the end, we will have an initial solution for the MVPPDP which contains a number of routs equal to the number of vehicles.

To increase the opportunity of getting better solutions, we decided to use the concept of the population-based metaheuristics, where a number of solutions are generated at the same time and then we select the best one according to a certain evaluation criterion. Therefore, the previous method of generating the initial solution will be repeated several times according to the population size to generate a number of candidate solutions. The quality of each candidate solution is evaluated in terms of the value of the objective function (OF). This objective function is defined as maximizing the total profit by subtracting the total travel cost from the revenues collected, as shown in Equation (1). After that, the best solution that has the highest OF value is saved in a matrix to compare it with other best solutions that are selected from different iterations. Finally, we select the best overall solution which represents the initial solution for the MVPPDP.

The outline of the construction phase of our GRASP is presented in Algorithm 2, where the meaning of each notation is as follows: **Pop_Size**: the size of the population, **Max_Iter**: maximum number of iterations, **Num_Vehicles**: number of vehicles, **CSS**: Candidate Solutions Set, **RCL**: Restricted Candidate List, **US**: Un-Served pairs of customers and **SM**: Solutions Matrix that contains the best solutions in the population for each iteration.

V. COMPUTATIONAL EXPERIMENTS

The computational experiments aim to compare the performance of our proposed algorithm with the construction heuristics used in [40]: the Greedy Construction Heuristic and the Two-Stage Cheapest Insertion Heuristic. Before we present the results of the experiments, we describe the dataset that was used to test the algorithm and the values chosen for each parameter.

A. Test Instances

We used the same instances that are proposed in [22] and [40]². The data instances are 36 instances, which are classified into three groups: small size, which contains 20 and 50 customers, medium size, which contains 100 and 250 customers and large size which contains 500 and 1000 customers. The number of instances in each group is 12 instances. The customers are set to be pickup customers and delivery customers. There is only one central depot, There are at most 8 vehicles which are organized as follows: 2 vehicles to serve 20 customers, 3 vehicles to serve 50 customers, 4 vehicles to serve 100 customers, 5 vehicles to serve 250 customers, 6 vehicles to serve 500 customers and 8 vehicles to serve 1000 customers. The capacity of the vehicle is between [50, 120]. Each pickup customer has an integer demand value between [1, 50], which is transported from a pickup customer and delivered to the related delivery customer to get the associated revenue. The revenue amounts are set to be either fixed for all customers, proportional to the demands, or randomly. Also, the total time limit is set to be either small or large, where the range is within [2500, 15000] to generate short and long routes.

B. Parameter Tuning

Few number of parameters that needs to be tuned is one of the reasons that encouraged us to choose the GRASP metaheuristic. There are only three parameters: the size of the Candidate Solutions Set (CSS), the size of the Restricted Candidate List (RCL), and the number of iterations (Max_Iter). In our method, we added a fourth parameter which is the size of the population (Pop_size); that is the number of solutions that were generated using the greedy-randomized approach, and the best one is selected before moving to the next iteration. Empirical experiments were performed to select the suitable value for each parameter. Six medium-sized data instances have been used to tune the parameters. These are the data instances containing 100 customers that are served by 4 vehicles. All three revenue states were considered in the instances namely fixed revenue for all customers, proportional revenue to demand and randomly selected revenues. Also, each revenue case has been tested twice: when the vehicle capacity is 80 units and the total time limit is 6000 to generate a long route, and when the vehicle capacity is 50 and a total time limit is 4000 to generate a short route. The details of testing each parameter are as follow:

1) *The size of the Restricted Candidate List (RCL)*: To increase the diversity of solutions, half of the solutions that are found in the CSS were assigned to the RCL; i.e., if the number of solutions in $CSS = n$, then $\lfloor (n)/2 \rfloor$ solutions are assigned to the RCL. This value has been chosen by trial, since choosing a smaller size for the RCL resulted in solutions that are similar to each other and thus lack diversity.

2) *The number of iterations*: Table I shows the objective function values after testing six datasets: 100 customers with fixed revenue to generate short route (100-F-S), 100 customers with fixed revenue to generate long route (100-F-L), 100 customers with proportional revenue to generate short route (100-P-S), 100 customers with proportional revenue to generate long route (100-P-L), 100 customers with random revenue to generate short route (100-R-S), 100 customers with random revenue to generate long route (100-R-L). Each data instance was tested with different numbers of iterations: 10, 50, 100 and 500. The results of testing show that there is no enhancement in the objective function values after 100 iterations. Thus, the maximum number of iterations was taken to be 100.

3) *The size of the population*: The same previous dataset instances were tested again to select the appropriate number of solutions in the population. The population size was increased from 10 to 20 solutions. Table II presents the values of the objective function after setting the number of iterations to 100. The results showed that increasing the population size did not lead to an improvement in the objective function value. Thus, the population size was taken to be 10.

² We note that [22] is the published paper of the thesis in [40].

Algorithm 2: The pseudocode of the construction phase of GRASP

```

For  $i=1$  to Max_Iter
  For  $S=1$  to Pop_Size
    For  $k=1$  to Num_Vehicles
      Phase 1: Seed Vertex Selection
      Step 1: Compute the Customer Benefit (CB) for all pairs of customers
      Step 2: Select the customer pair that has the highest CB and insert it in
        the route as a seed customer
      Phase 2: Route Construction
      While Maximum Route Time is not violated
        Step 3: For each customer pair  $\in US$ , insert it in the best position in the route after checking the precedence,
          time, and capacity constraints
        Step 4: Compute the insertion Ratio (IR) for all candidate customer pairs, based on their best insertion
          position calculated in Step 3.
        Step 5: Put all the candidate customer pairs in the CSS in descending order of IR
        Step 6: Assign half of the candidate customer pairs in the CSS to the RCL
        Step 7: Pick one customer pair randomly from the RCL and insert it in its best position in the route, as
          calculated in Step 3.
      End While
    End For
    Step 8: Compute the objective function for the solution and assign the solution to the SM
  End For
  Step 9: Select the best solution that has the highest objective function in SM and assign it to Final-Best-Solutions matrix
End For
Step 10: Select the best solution that has the highest objective function in the Final-Best-Solutions matrix to be the initial solution for the MVPPDP
  
```

TABLE I. RESULTS OF TUNING THE NUMBER ITERATIONS

Number of Iterations	Dataset Instances					
	100-F-S	100-F-L	100-P-S	100-P-L	100-R-S	100-R-L
10	12826.14	25948.13	48647.27	80966.13	4336.17	74177.33
50	14053.64	29000.17	49305.84	80966.13	47310.47	75913.21
100	14053.64	29000.17	51323.10	80966.13	47310.47	76031.08
500	14053.64	29000.17	51323.10	80966.13	47310.47	76031.08

TABLE II. RESULTS OF TUNING THE POPULATION SIZE

Dataset instances	Population size	
	10	20
100-F-S	14053.64	14053.64
100-F-L	29000.17	29000.17
100-P-S	51323.10	51323.10
100-P-L	80966.13	80966.13
100-R-S	47310.47	47310.47
100-R-L	76031.08	76031.08

$$SR_{i,n+i} = \frac{r_{i,n+i}}{c_{x,i} + c_{i,n+i} + c_{n+i,0}} \quad (20)$$

Where $r_{i,n+i}$ is a revenue of the candidate pair, $c_{x,i}$ is the distance from the last vertex (x) in the route to the candidate pickup customer, $c_{i,n+i}$ is the distance between the candidate customer pair nodes, and $c_{n+i,0}$ is the distance from the candidate delivery customer to the depot. Then, the customer pair that has the highest selection ratio is inserted into the route. This procedure is repeated until either the allowed time is consumed or no more customer pairs need to be served. In the C1 heuristic, there is no need to check the precedence and capacity constraints, because each delivery customer is added directly after the related pickup customer.

The *Two-Stage Cheapest Insertion Heuristic (C2)* works as follow: In the first stage, select the seed customer pair for each route, based on the Idle Distance (ID), which is computed for each candidate pair ($i, n + i$) as follows:

$$ID_{i,n+i} = c_{0,i} + c_{n+i,0} \quad (21)$$

Where $c_{0,i}$ is the distance from the depot to the candidate pickup customer, and $c_{n+i,0}$ is the distance from the candidate delivery customer to the depot. The pair with the shortest ID is selected to be a seed customer for the route. Then, the routes are constructed with the rest of unvisited customers by computing the Insertion Ration (IR) for each customer pair as

C. Experimental Results

In this experiment, the proposed algorithm was run 5 times for every dataset. The stopping criterion is the number of iterations which is 100 for all datasets except the large-sized data instances which was set to 20 iterations only, due to time limitation. Before presenting the results of our method, we describe briefly the main construction heuristics that were used in [40], since we are comparing our results with them.

In the *Greedy Construction Heuristic (C1)*, the customer pairs are added sequentially to the route based on the value of the Selection Ratio (SR). In each iteration, the SR is calculated for all candidate customer pairs ($i, n + i$) as follows:

done in Equation (19). The customer pair with the highest IR is inserted in the route with respect to the precedence and capacity constraints. The second stage of the algorithm, tries to insert all customers that have not been inserted in the first stage, due to capacity violation.

Table III presents the results of constructing initial solutions for the MVRPPDP using our GRASP method. The results are calculated in terms of the objective function (OF) of the solution (i.e., the gained profit), which is equal to total

revenue – total cost, as previously shown in Equation (1). Thus, the larger the OF value, the better is the solution obtained. The results of our GRASP were compared with the results of C1 and C2. In Table III, the first column presents the instance name. The following two columns show the results of GRASP in terms of the average and best objective value of 5 runs respectively. The third and fourth columns represent the results of C1 and C2 algorithms in terms of the best objective value. For each group of instances of a particular size, the average results are shown in the highlighted row.

TABLE III. COMPARISON OF THE RESULTS THE GRASP WITH C1 AND C2 IN TERMS OF PROFIT

Instance Name	GRASP (AVG)	GRASP (Best)	C1 (Best)	C2 (Best)
20-F-S	18097.3	<u>18097.3</u>	16185.4	21400
20-F-L	37937.2	37937.3	22006.2	32400.1
20-P-S	39957.7	<u>39957.7</u>	39646.5	43528
20-P-L	57763.9	57763.9	54849.9	55775.5
20-R-S	30039.9	30039.9	22954.4	26884
20-R-L	42845.9	42845.8	30486.7	41933
Average_20	37773.65	37773.65	31021.5167	36986.7667
50-F-S	18396.2	18443.6	15000.5	17958.2
50-F-L	32686.3	33259.2	34988.2	43008.3
50-P-S	53631.8	<u>53631.8</u>	53694.8	38796.9
50-P-L	91164.1	<u>92502.1</u>	99109	62731.2
50-R-S	24364.4	<u>24364.5</u>	19789.7	24619.2
50-R-L	52889.2	54712.1	45326.9	51723.3
Average_50	45522	46152.21667	44651.5167	39806.1833
100-F-S	13369.3	13749.3	19033.1	28818.1
100-F-L	27336.9	28692.9	31825.6	55322.2
100-P-S	51218.1	54475.1	44329.1	46547.4
100-P-L	80299.3	86141.8	69459.3	79541.3
100-R-S	46160.4	46450.7	49912.7	70214.6
100-R-L	76019.9	<u>77136.6</u>	63116.1	91663.1
Average_100	49067.3167	51107.73333	45552.64	62017.7833
250-F-S	10831.9	11231.9	27676.1	40906.1
250-F-L	49193.5	<u>50980.9</u>	44456	67845.1
250-P-S	33041.9	34606.8	63930	43247.3
250-P-L	102591	<u>107171.1</u>	112471	94126.8
250-R-S	40446.5	41914	79486.1	102873
250-R-L	128304.5	129344.6	130371	143886
Average_250	60734.8833	62541.55	71898.3667	83647.3833
500-F-S	21758.3	24012.2	49210	78580.2
500-F-L	84616.4	<u>85889.1</u>	73299.8	135652
500-P-S	49864.8	51297.9	124075	84513.6
500-P-L	138057.2	142740.2	179001	169098
500-R-S	54859.3	56901.7	108049	116568
500-R-L	163822.4	166232.5	170205	218965
Average_500	85496.4	87845.6	117306.633	133896.133
1000-F-S	9132.4	11045.9	27655.6	66345.3
1000-F-L	56276.1	<u>58068.2</u>	32078.4	112840
1000-P-S	134015.9	141167.4	264997	152307
1000-P-L	325103.1	<u>340418.4</u>	380514	318268
1000-R-S	99173.9	102051	193390	197083
1000-R-L	268887.4	271613.1	275805	362266
Average_1000	148764.8	154060.6667	195740	201518.217

D. Results and Discussion

Observing the results in Table III, the proposed algorithm demonstrated good performance on average in solving the small and some medium-sized data instances, where we got new best solutions for 8 data instances (bold values). Also, we got 8 solutions that were better than either C1 or C2 (underlined values). However, the proposed algorithm was not the best one for the large instances on average, but its performance was acceptable in some cases where we got two solutions that are better than one of the other two heuristics. This is probably due to decreasing the number of iterations for the large instances due to extensive time consumption. Also, we observed that when the GRASP was better than one of the other heuristics, its performance was better than C1 for instances with fixed and random profits (except 20-P-S). On the other hand, it was better than C2 on instances with proportional profits to its demand. Overall, we believe that our method is comparable with the other two methods and has the advantage of being able to construct a number of solutions (a population) that are characterized with the greedy-randomized feature, rather than just one greedy solution as done in the other two construction methods.

VI. CONCLUSION

In this paper, the construction phase of a Greedy Randomized Adaptive Search Procedure (GRASP) was used to build initial solutions for the Multi-Vehicle Profitable Pickup and Delivery Problem (MVPPDP). The algorithm uses the concept of a Restricted Candidate List (RCL) to combine between random and greedy properties, which can help in the diversification of the search, and is especially beneficial for population-based metaheuristics. The performance of our algorithm was compared with two construction heuristics that were previously used to build the initial solutions of the MVPPDP. The results proved the effectiveness of the proposed method on small-medium sized instances, where eight new solutions were obtained for the MVPPDP. Also, the GRASP method had a better performance than one of the other construction heuristics on 11 test instances. Nevertheless, the proposed method is not currently able to produce good results on large-sized instances (500 and 1000 customers). This is possibly due to decreasing the number of iterations because of time limitations. Future work will try to improve the performance of the algorithm by optimizing its runtime. In addition, a second phase may be added to try to insert un-visited customers to increase the profit of the company and improve the quality of the initial solutions. Finally, an improvement phase, using a selected population-based metaheuristic, will be added to improve the initial constructed solutions by the GRASP based method.

REFERENCES

- [1] Toth, Paolo and Vigo, The vehicle routing problem. SIAM, 2002.
- [2] R. F. Parragh, Sophie N and Doerner, Karl F and Hartl, "A survey on pickup and delivery problems," J. für Betriebswirtschaft, vol. 58, no. 1, pp. 21–51, 2008.
- [3] J. Saha, "An algorithm for bus scheduling problems," J. Oper. Res. Soc., vol. 21, no. 4, pp. 463–474, 1970.
- [4] U. Y. "uceer and A. " O. " ,a, "A truck loading problem," Comput. Ind. Eng., vol. 58, no. 4, pp. 766–773, 2010.
- [5] M.-W. Yan, Shangyao and Wang, Sin-Siang and Wu, "A model with a solution algorithm for the cash transportation vehicle routing and scheduling problem," Comput. Ind. Eng., vol. 63, no. 2, pp. 464–473, 2012.
- [6] P. H. Barnhart, Cynthia and Jin, Hong and Vance, "Railroad blocking: A network design application," Oper. Res., vol. 48, no. 4, pp. 603–614, 2000.
- [7] R. A. Díaz-Parra, O., Ruiz-Vanoye, J. A., Bernábe Loranca, B., Fuentes-Penna, A., & Barrera-Cámara, "A survey of transportation problems," J. Appl. Math., vol. 2014, 2014.
- [8] J. R. F. Cornillier, F. F. Boctor, G. Laporte, "An exact algorithm for the petrol station replenishment problem," J. Oper. Res. Soc., vol. 59, no. 5, pp. 607–615, 2008.
- [9] R. C. C. Zhu, J. Q. Hu, F. Wang, Y. Xu, "On the tour planning problem," Ann. Oper. Res., vol. 192, pp. 67–86, 2012.
- [10] D. Kodjak, "Policy discussion--heavy-duty truck fuel economy," 10th Diesel Engine Emiss. Reduct., 2004.
- [11] M. Gansterer, R. F. Hartl, and R. Vetschera, "The cost of incentive compatibility in auction-based mechanisms for carrier collaboration," Networks, Jun. 2018.
- [12] C. Lin, K. L. Choy, G. T. S. Ho, S. H. Chung, and H. Y. Lam, "Survey of Green Vehicle Routing Problem: Past and future trends," Expert Syst. Appl., vol. 41, no. 4, pp. 1118–1138, Mar. 2014.
- [13] J. Privé, J. Renaud, F. Boctor, and G. Laporte, "Solving a vehicle-routing problem arising in soft-drink distribution," J. Oper. Res. Soc., vol. 57, no. 9, pp. 1045–1052, Sep. 2006.
- [14] N. Aras, D. Aksen, and M. Tuğrul Tekin, "Selective multi-depot vehicle routing problem with pricing," Transp. Res. Part C Emerg. Technol., vol. 19, no. 5, pp. 866–884, Aug. 2011.
- [15] I. Gribkovskaia, G. Laporte, and A. Shyshou, "The single vehicle routing problem with deliveries and selective pickups," Comput. Oper. Res., vol. 35, no. 9, pp. 2908–2924, Sep. 2008.
- [16] C.-K. Ting and X.-L. Liao, "The selective pickup and delivery problem: Formulation and a memetic algorithm," Int. J. Prod. Econ., vol. 141, no. 1, pp. 199–211, Jan. 2013.
- [17] X.-L. Liao and C.-K. Ting, "An evolutionary approach for the selective pickup and delivery problem," in Evolutionary Computation (CEC), 2010 IEEE Congress on, IEEE, 2010, pp. 1–8.
- [18] W. Y. Ho, Sin C and Szeto, "GRASP with path relinking for the selective pickup and delivery problem," Expert Syst. Appl., vol. 51, pp. 14–25, Jun. 2016.
- [19] I. M. Coelho, P. L. A. Munhoz, L. S. Ochi, M. J. F. Souza, C. Bentes, and R. Farias, "An integrated CPU–GPU heuristic inspired on variable neighbourhood search for the single vehicle routing problem with deliveries and selective pickups," Int. J. Prod. Res., vol. 54, no. 4, pp. 945–962, Feb. 2016.
- [20] I. M. Coelho, P. L. A. Munhoz, M. N. Haddad, M. J. F. Souza, and L. S. Ochi, "A hybrid heuristic based on General Variable Neighborhood Search for the Single Vehicle Routing Problem with Deliveries and Selective Pickups," Electron. Notes Discret. Math., vol. 39, pp. 99–106, Dec. 2012.
- [21] B. P. Bruck, A. G. dos Santos, and J. E. C. Arroyo, "Hybrid metaheuristic for the single vehicle routing problem with deliveries and selective pickups," in Evolutionary Computation (CEC), 2012 IEEE Congress on, IEEE, 2012, pp. 1–8.
- [22] M. Gansterer, M. Küçüktepe, and R. F. Hartl, "The multi-vehicle profitable pickup and delivery problem," OR Spectr., vol. 39, no. 1, pp. 303–319, Jan. 2017.
- [23] M. G. Feo, Thomas A and Resende, "Greedy randomized adaptive search procedures," J. Glob. Optim., vol. 6, no. 2, pp. 109–133, 1995.
- [24] E.-G. Talbi, Metaheuristics: from design to implementation. John Wiley & Sons, 2009.
- [25] P. Priore-Moreno, R. Pino-Diez, C. Martínez-Carcedo, V. Villanueva-Madrileño, and I. Fernández-Quesada, "Application of GRASP methodology to vehicle routing problem," in Proceedings on the International Conference on Artificial Intelligence (ICAI), 2012, p. 1.

- [26] A. Layeb, M. Ammi, and S. Chikhi, "A GRASP algorithm based on new randomized heuristic for vehicle routing problem," *J. Comput. Inf. Technol.*, vol. 21, no. 1, pp. 35–46, 2013.
- [27] C. Duhamel, Christophe and Lacomme, Philippe and Prins, Christian and Prodhon, "A GRASP×ELS approach for the capacitated location-routing problem," *Comput. Oper. Res.*, vol. 37, no. 11, pp. 1912–1923, Nov. 2010.
- [28] Y. Marinakis, "Multiple Phase Neighborhood Search-GRASP for the Capacitated Vehicle Routing Problem," *Expert Syst. Appl.*, vol. 39, no. 8, pp. 6807–6815, Jun. 2012.
- [29] M. HADDAD, "AN EFFICIENT HEURISTIC FOR ONE-TO-ONE PICKUP AND DELIVERY PROBLEMS," Fluminense Federal University, 2017.
- [30] G. Gutiérrez-Jarpa, G. Desaulniers, G. Laporte, and V. Marianov, "A branch-and-price algorithm for the Vehicle Routing Problem with Deliveries, Selective Pickups and Time Windows," *Eur. J. Oper. Res.*, vol. 206, no. 2, pp. 341–349, Oct. 2010.
- [31] S. Qiu, Xiaoqiu and Feuerriegel, "A MULTI-VEHICLE PROFIT-MAXIMIZING PICKUP AND DELIVERY SELECTION PROBLEM WITH TIME WINDOWS."
- [32] A. Baniamerian, M. Bashiri, and R. Tavakkoli-Moghaddam, "Modified variable neighborhood search and genetic algorithm for profitable heterogeneous vehicle routing problem with cross-docking," *Appl. Soft Comput.*, vol. 75, pp. 441–460, 2019.
- [33] M. Wen, J. Larsen, J. Clausen, J. Cordeau, and G. Laporte, "Vehicle routing with cross-docking," *J. Oper. Res. Soc.*, vol. 60, no. 12, pp. 1708–1718, 2009.
- [34] C. Archetti, M. G. Speranza, and D. Vigo, "Chapter 10: Vehicle Routing Problems with Profits," in *Vehicle Routing: Problems, Methods, and Applications*, Second Edition, 2014, pp. 273–297.
- [35] D. Toth, Paolo and Vigo, *Vehicle routing: problems, methods, and applications*. Society for Industrial and Applied Mathematics, 2014.
- [36] P. H. Vidal, Thibaut and Maculan, Nelson and Ochi, Luiz Satoru and Vaz Penna, "Large neighborhoods with implicit customer selection for vehicle routing problems with profits," *Transp. Sci.*, vol. 50, no. 2, pp. 720–734, 2015.
- [37] C. Archetti, N. Bianchessi, and M. G. Speranza, "Optimal solutions for routing problems with profits," *Discret. Appl. Math.*, vol. 161, no. 4–5, pp. 547–557, Mar. 2013.
- [38] M. G. Archetti, Claudia and Feillet, Dominique and Hertz, Alain and Speranza, "The capacitated team orienteering and profitable tour problems," *J. Oper. Res. Soc.*, vol. 60, no. 6, pp. 831–842, 2009.
- [39] R. Lahyani, M. Khemakhem, and F. Semet, "Heuristics for rich profitable tour problems," in *Modeling, Simulation and Applied Optimization*, 2013 5th International Conference on, 2013, pp. 1–3.
- [40] M. Küçüktepe, "A General Variable Neighbourhood Search Algorithm for the Multi-Vehicle Profitable Pickup and Delivery Problem," University of Vienna, 2014.

Secured Multi-Hop Clustering Protocol for Location-based Routing in VANETs

K. Sushma Eunice¹, I. Juvanna²

IT. HITS, Hindustan Institute of Technology and Science
Chennai, India

Abstract—In today's world, with the rise in the count of vehicles and lack of proper navigation, the congestion has become a major problem. In this scenario, VANETs play a very important part in improving the traffic condition and also in providing proper navigation. Improved navigation system reduces congestion thereby reducing the possibility of occurrence of accidents. In this research work, we have used a position-based routing protocol i.e., GPSR (Greedy Perimeter Stateless Routing Protocol) to effectively analyze the geographical position of the vehicles in the network and to provide updated navigation information. In this system, we have used a security mechanism to identify valid and invalid messages for secure V2V and V2I communications. This mechanism drops all the invalid messages thereby keeping the VANET secure. It also reduces the possibility of attacks on wireless communications in the VANET. This system has better safety features and network performance compared to other hybrid schemes via NS2 simulation.

Keywords—*Vanet; tamper-proof device; location-based routing protocols; intelligent transportation system; gpsr algorithm; trusted authority; roadside unit; routing protocols*

I. INTRODUCTION

Advancements in the automobile industry and rise in the economy standards have led to a significant upsurge in the number of vehicles. However, with the increased vehicle count, traffic congestion also rises. Increased traffic congestion may lead to frequent accidents. The major problem that exists in today's transportation system is congestion. Congestion needs to be handled well to prevent road accidents. Therefore, the need of the hour calls out for reliable experience in driving and improved safety for drivers. All these circumstances have paved a way for research in VANETs with the aim of improving the safety of the drivers through inter-vehicle communication (V2V) and communications between a vehicle and public infrastructure (V2I) [2]. The VANET architecture comprises of three main parts. The architecture of VANET is shown in Fig. 1.

A. System Architecture

- **Trusted Authority (TA):** The major role of trusted authority is to register every vehicle and to issue secret keys. Trusted authority acts as a trusted management center. The communication link between trusted authority and RSU is wired. The channel connecting the trusted authority and the RSU is very efficient. As it is a strong wired network, it acts as a very good channel for proper transmission of data. TA acts as a central system, which issues secret keys and necessary

parameters of the system. This information is needed for RSUs and vehicles to verify the authenticity of the messages. TA is responsible for delivering these keys to RSUs and vehicles through secure channels. It is also responsible for locating and finding the vehicles which have sent malicious messages to create problem in the network. In this process, it identifies the malicious message sender and helps to resolve the dispute.

- **Road Side Unit (RSU):** The RSU is placed along the roads and it serves as a link between the trusted authority and the vehicles (ordinary vehicles or edge computing vehicles) [3], [4]. Roadside units are stationary, and they help the vehicles to connect to different vehicles outside the network. RSU can authenticate the messages as well as it can assign the task to edge computing vehicles (ECV) [7]. Edge computing vehicles (ECVs) share the load of the RSUs by verifying the messages that are being transmitted. ECVs need to report to the RSU with the verification result within a stipulated time T. If the RSUs does not receive any response from ECV in the prescribed time, it simply assigns that verification task to other ECV.
- **On-Board Unit (OBU):** Vehicles in network is equipped with an OBU. OBU is responsible for inter-vehicle communication (V2V) and communication between vehicle and public infrastructure [3], [4]. As V2V and V2I communication are wireless, they are prone to more attacks. It is important to secure these wireless communications in order to stay out of the attacker's hands. Attackers always keep an eye on the weak wireless communications to take advantage at any point in time. Hence it is always important to provide enough security to the messages that are transmitted. Sender and receiver both need to be aware of fraudulent messages. Additionally, the vehicles will have a tamper-proof device (TPD) that stores the keys issued by the Trusted Authority (TA). Tamper-proof devices help to achieve physical level security [3].

The main objective of this system is to efficiently utilize the intelligent transportation system for secure communication and better navigation. This system analyses attacks on wireless communications i.e., V2V and V2I. The cars can no longer be considered as mechanical machines. They are loaded with software to make them intelligent systems rather than just being a mechanical machine. These intelligent systems are now used for secure communication with other

vehicles and to pave a way for the efficient and enhanced driving experience. It provides up-to-date routing information by using the GPSR protocol and also validates the messages being transmitted by using a security mechanism. It drops all the invalid messages by enhancing the security in VANET.

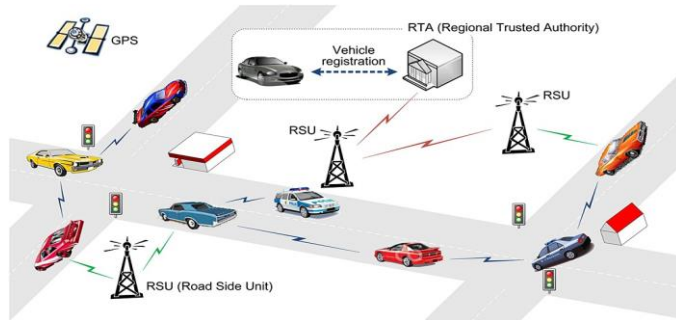


Fig. 1. The Architecture of VANET.

II. RELATED WORKS

J. Cheng, J. Cheng, M. Zhou, F. Liu, S. Gao, and C. Liu, S. Gao and C. Liu [1] proposed a review on routing protocols. From this research work, we can infer the pros and cons of different routing protocols and can analyze efficient routing protocols. The key technology in vehicular ad-hoc networks is the routing protocols and this paper gives a clear picture of the importance of routing protocols.

Y. Xie, L. Wu, Y. Zhang and J. Shen [2] proposed a scheme for secure authentication with conditional privacy. This paper focuses on challenges that we come across while designing the authentication for VANETs to achieve security and preserving conditional privacy. From this work, we can be well prepared for all the issues that we come across while designing the authentication procedures in the vehicular ad-hoc network.

S. Jiang, X. Zhu, and L. Wang [3] proposed an efficient scheme based on HMAC. In this research work, the vehicles are managed by the RSUs in localized order. From this, we can make the RSUs deal with authentication of vehicles in its range to improve the efficiency of the system.

S. Zeadally, R. Hunt, Y.-S. Chen, A. Irwin and A. Hassan [4] proposed a paper on challenges, results, and status of VANETs. From this research work, we can infer various challenges that we face while dealing with VANETs. This provides an insight into the proper working of VANETS.

Y. Sun, R. Lu, X. Lin, X. Shen and J. Su [5] proposed a scheme on pseudonymous authentication with secure privacy preservation. From this research work, we can conclude that pseudonymous authentication scheme with good privacy protection provides very strong protection of privacy of the vehicles and it also does not let adversaries trace the vehicle even if the RSU gets compromised.

C.-C. Lee and Y.-M. Lai [6] proposed a batch verification scheme with group testing. In this research work, group testing is performed to lower the time taken and to boost the efficiency of the system. VANET being intelligent transportation system has a huge number of vehicles and hence transmits a huge number of messages. Authenticating

these messages one by one is a time taking process, hence from this paper we have known that group testing can handle huge traffic which is proved to be efficient.

D. He, S. Zeadally, B. Xu and X. Huang [7] proposed an efficient scheme on preserving privacy in the authentication process. In this scheme, security and the problems that exist in preserving privacy are addressed. It takes care of both privacy protection and mutual authentication. It has relatively good performance in terms of computational cost and communicational cost. This scheme can be adapted to lower the communicational and computational cost.

V. Miller [8] proposed a paper on elliptic curves in cryptography. The author used the elliptic curve in cryptography for the first time to enhance security. From this research work, we can imply that we can use the elliptic curve in cryptography.

Jie Cui, Lu Wei, Jing Zhang, Yan Xu and Hong Zhong [9] proposed a paper on a message-authentication scheme using edge computing. This research work validates the messages being transmitted between different vehicles in the network. This system helps us to verify the messages exchanged in the network to keep the VANET secure.

Brad Karp and H. T. Kung [10] proposed a paper on GPSR protocol. It provides complete working of the protocol. This information can be used to adopt the GPSR protocol and to enhance it.

III. IDENTIFICATION OF VALID AND INVALID MESSAGES

This system deals with the identification of valid and invalid messages in VANET. In this system, there are six different phases [9].

A. Initializing the System

Trusted authority is the central system which oversees issuing necessary parameters of the system and secret keys. These secret keys and system parameters are necessary for identifying each vehicle in the network. Trusted authority traces the vehicles based on these system parameters and keys that are stored in the vehicles. Trusted authority loads all the parameters of the system into the vehicle's TPD and the memory of RSU in advance. Trusted authority and RSU are connected via a wired network for transmission of data. The significant steps involved in this phase are as follows.

- Trusted authority (TA) uses two prime numbers and an elliptic curve E which is non-singular where it is defined as $y^2 = x^3 + ax + b \pmod{q}$.
- Trusted authority selects the system private key randomly and based on that it calculates the public key of the system.
- Trusted authority selects the roadside unit's private key and based on that it calculates the public key of the roadside unit (RSU).
- A trusted authority is responsible for assigning true-identity and password to all the vehicles. It loads all the vehicle's tamper-proof devices with the vehicle's real identity, password, and the system private key.

- A trusted authority is the sole in charge of producing all the public parameters of the system to all the vehicles and RSUs.

B. Generation of Vehicle's Signature and Pseudo-Identity

All the vehicle's need to produce the signature of the message before sending the message to ensure its authenticity. By producing the signature, the sender vehicle proves its authenticity. Tamper-proof device (TPD) issues pseudo identity, signature, and key for all the ordinary and edge computing vehicles.

- Every vehicle will have a TPD, which maintains the vehicle's real identity, password and the system's private key to connect to the system when it comes within the range of that system. The vehicle cross-checks its real identity and the password by matching its value with the values stored in the TPD by sending its value to the TPD.
- TPD hides the true identity of the vehicle from other vehicles and systems apart from the TA. TPD hides the true identity of the system by generating pseudo-identity which is calculated by using randomly selected number.
- Every vehicle needs a signature to ensure the authenticity of the message. The message's signature is calculated by combining the message M and time stamp T [9].

C. Election Strategy of Edge Computing Vehicle (ECV)

Edge computing vehicle (ECV) helps the RSU to authenticate the message signature as much as possible. ECV is elected based on two factors.

- Shortest distance to RSU
- Enough available computation power

Shortest distance to RSU can be calculated by using the distance membership function and enough available computational power can be calculated by using the available performance metric membership function [9]. All the above calculations can be performed using fuzzy logic.

$$DM(x) = 1, d(x) \leq (R/2) \quad (1)$$

$$DM(x) = (R - d(x)) / (\frac{R}{2}) \text{ for } (R/2) < d(x) \leq R \quad (2)$$

$$DM(x) = 0, d(x) > R. \quad (3)$$

Where

DM(x) denotes the distance membership function.

R denotes maximum transmission range of RSU.

d(x) denotes space between the vehicle and the RSU

$$APM(x) = (MCL(x) - UCR(x)) / (MCL(x)) \quad (4)$$

Where

APM(x) denotes the available computational power

MCL(x) denotes maximum computational load on the vehicle

UCR(x) denotes the used computational resource of the vehicle.

D. ECV Authenticates the Batch here, there are Two Phases.

- Phase determining the task: Here, the pseudo identity list is allocated to the edge computing vehicle (ECV) by RSU to authenticate the message. After allocating the list to ECV, RSU then updates ECV by sending a message to it.
- Batch authentication and Result feedback stage: ECV carries out the task of verifying the messages sent by RSU by using the preloaded key of RSU. ECV verifies the message and rejects the message if it is invalid and proceeds to the next step if the message is valid.

E. RSU Verifies the Authentication Result of ECV

Loss of packets and delay always exist in VANETs to some extent. So RSU shares its load with ECV to perform message authentication in an efficient way. RSU waits for the verification result from ECV for a prescribed amount of time and if it doesn't receive the message within that time, then it assigns the verification task to another ECV [9]. In this way, RSU lowers the delay in VANETs. Otherwise, if the RSU receives the verification result from ECV within time T, then it checks the result and proceeds to the next step if the message is valid else rejects the message.

F. Authenticating the Ordinary Vehicle's Messages

The ordinary vehicles don't have to verify the messages separately. It is taken over by ECVs and RSUs.

1) *Drawbacks of this system:* this system only verifies the valid and invalid messages that are being transmitted in the VANET. It does not address the routing issues to provide an enhanced driving experience to the users. The user needs to check for an alternative solution if he needs routing information.

IV. SECURED MULTI-HOP CLUSTERING PROTOCOL WITH LOCATION-BASED ROUTING

The proposed system deals with the congestion issue in a very effective way. We are using the GPSR routing protocol which is very efficient among other position-based routing protocols. It provides better routing as it uses the buffer of the vehicles to provide an updated route to deal with the frequently changing network. In addition, we have integrated a mechanism to identify valid and invalid messages in the VANET.

A. Greedy Perimeter Stateless Routing Protocol (GPSR)

VANETs are considered as intelligent transportation systems. There are many protocols to provide proper routing in VANETs but position-based routing protocols are the efficient ones. In VANETs routing protocols play a very important role. A routing protocol is a key technology that determines the performance of vehicular communication like inter-vehicle communication (V2V) and communication between vehicle and public infrastructures (V2I). The major problem that exists in the VANET is the frequently changing network. The network comprises of various nodes which are

not stationary. Hence the network topology changes and the relation among the nodes becomes unstable. Focussing on the major problem that exists in most of the routing protocols, we have proposed an enhanced Greedy Perimeter Stateless Routing protocol (GPSR) which has better performance as it depends on the buffer of the nodes for routing.

Greedy perimeter stateless routing (GPSR) functions in two different ways.

- Greedy Forwarding
- Perimeter Forwarding

GPSR protocol uses greedy forwarding method or perimeter forwarding method to route the packet to the destination. GPSR packet stores five values, which help the start node to route the packet to the destination node without any mix-up. GPSR Packet is shown in Fig. 2.

GPSR packet consists of five different fields, where D denotes Destination.

Lp denotes the place where the data packet enters into the chosen mode (Eg: Perimeter mode).

Lf denotes the initial node it started within the face of the graph (planar).

e0 denotes the traversal of the first edge on the current face.

M denotes the mode of the packet: GREEDY MODE / PERIMETER MODE.

1) *Greedy forwarding*: In this mode, every node broadcasts its IP address and position (IP, (X, Y)) periodically. Every node maintains a table and stores the position of its one-hop neighbors [10]. With respect to the data maintained in the table, the packet is routed to its destination. As every node broadcasts its IP address and position information, all the nodes will have a piece of up-to-date information about all the routes. This reduces the delay in delivering the packets and paves a way for efficient routing. Congestion issue is also handled very efficiently as there is effective communication between the nodes. There are few cases where greedy forwarding fails and in such case, we go for perimeter forwarding. Greedy forwarding fails when a node that has the packet does not have any one-hop neighbor.

In the below figure there are 12 nodes where node S is a source node, node D is the destination node and all the other nodes are considered as intermediate nodes. Now lets assume that node S has a packet and it has to deliver the packet to the destination D. So node S checks its one-hop neighbor which is closest to the destination i.e., node C and routes the packet to its one-hop neighbor node C. Similarly node C using its table finds its one-hop neighbor which is nearest to the destination D and routes the packet to that node to reach the destined node. In this process, if a node come across a situation where it does not have anyone hop neighbor then greedy forwarding method fails and it switches to perimeter forwarding method.

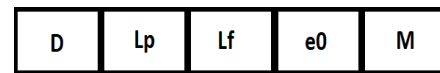


Fig. 2. GPRS Packet.

From Fig. 3, the path that is obtained by following the greedy forwarding method to reach the destination node is S-C-L-N-P-D. This sequence is selected based on the information stored in the table that each node stores.

2) *Perimeter forwarding*: The network contains certain regions where the greedy path does not exist (i.e., absence of one hop neighbors), in such case GPSR uses perimeter forwarding method to recover from that situation. In the perimeter forwarding method, the right-hand rule is used to calculate the perimeters to transmit the data packet to the destined node.

Perimeter forwarding method follows the right-hand rule to route the data packet to the destined node [10]. From Fig. 4, we see that a packet is forwarded from start node S to end node D in the direction of arrows i.e., by following the right-hand rule.

B. Identification of Valid and Invalid Messages

This module verifies all the messages that are being transmitted between the vehicles and the RSU/TA. The verification process is conducted in the following way.

- All the vehicles are equipped with a tamper-proof device (TPD) which log the necessary vehicle information like vehicle true-identity, vehicle password and the private key of the system.
- Trusted authority generates all the necessary parameters that are required for identifying vehicles and the roadside units (RSUs).
- Trusted authority and the RSUs are connected via a wired network for secure and efficient communication. It uses an efficient protocol like Transport Layer Security (TLS) for secure communication.
- A trusted authority is the central system which controls RSUs and the vehicles in the VANET. It is responsible for taking necessary action like tracing the suspect vehicle in case of any dispute/accident.
- There are few vehicles which are elected as edge computing vehicles (ECVs) based on the closeness to RSU and available computational resource. These vehicles work as both producers and consumers. They take care of the work-load on RSU in verifying the messages thereby reducing the load on the RSU.
- The advantage of using ECVs is that it reduces the RSU's overhead thereby enhancing its efficiency.
- RSUs and ECVs identify valid and invalid messages. If any message is identified as invalid, it is rejected.
- Ordinary vehicles no longer need to authenticate the messages received. This task is done by RSUs and the ECVs.

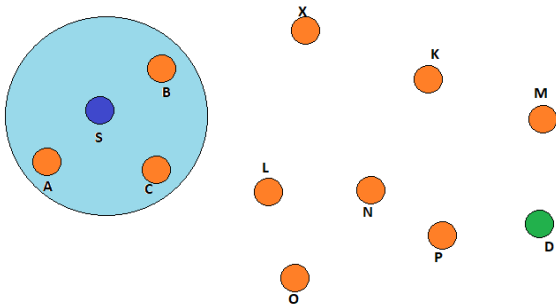


Fig. 3. Greedy Forwarding.

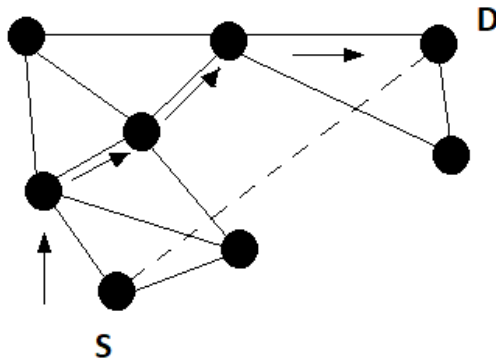


Fig. 4. Perimeter Forwarding.

So all the valid messages are forwarded to the intended vehicles and all the invalid messages are rejected thereby leaving no scope for malicious activities in the VANET.

V. SIMULATION AND ANALYSIS

The results of the simulation are shown here to illustrate the presentation and behavior of the algorithm used.

NS2 is used to show the nodes which represent the vehicles and the transmission of data between them. From Fig. 5, we see that eight nodes are used to represent eight cars moving on the road, four cars moving on the left side of the divider and the other four cars moving on the right side of the divider. The leftover nodes are used to mark the road corners.

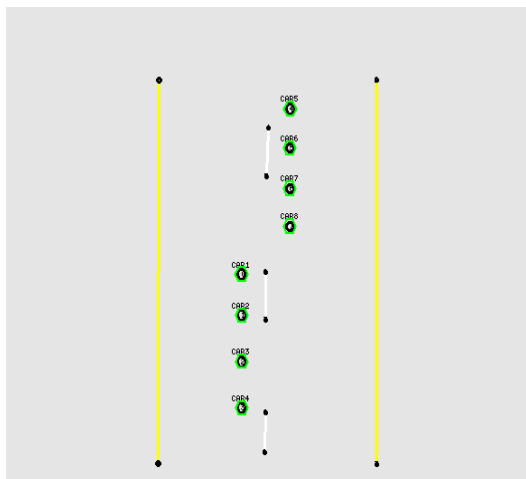


Fig. 5. Nodes Moving on the Road.

In Fig. 6, car 2 has stopped for some reason and broadcasted a message with its location and IP to update the nearby vehicles to change their route to avoid an accident. After receiving the message, the vehicles coming behind car 2 will change its route to avoid an accident. By communicating successfully and securely, vehicles can avoid accidents and can have a better and safe driving experience and navigation. By this, we can say that vehicles can no longer be considered as just mechanical machines. They have improved to a great extent contributing to the intelligent transportation system.

Energy is estimated based on the simulation results obtained using NS2. Fig. 7 depicts the energy. RSUs verify and validate the transmitted messages and hence the energy is calculated based on the count of messages transmitted to the count of messages validated by RSU.

Throughput is estimated based on the simulation results obtained. Fig. 8, depicts Throughput. Throughput is estimated by taking in to account, the quantity of data/messages transmitted with respect to time.

Packet delivery ratio is assessed by analyzing the obtained simulation results. Fig. 9, depicts packet Delivery Ration. Packet delivery ratio is analyzed by noting down the count of vehicles and distance covered.

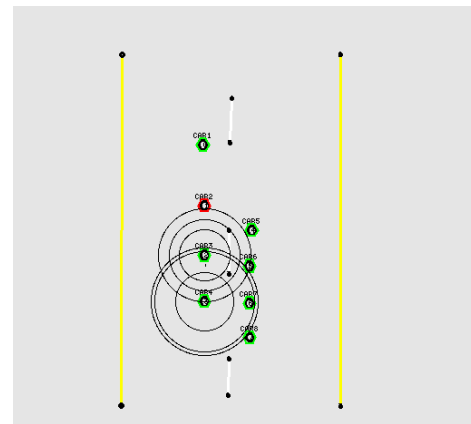


Fig. 6. Nodes Communicating with Each Other.

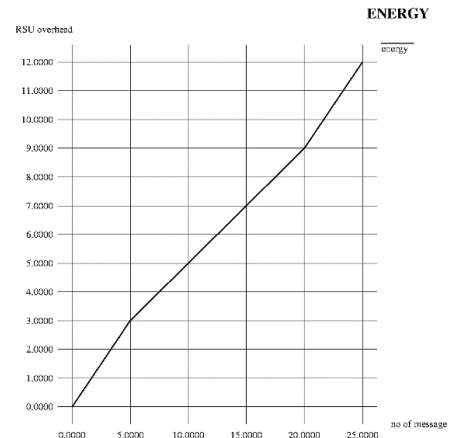


Fig. 7. The Relation between RSU Overhead and the Number of Messages Transmitted.

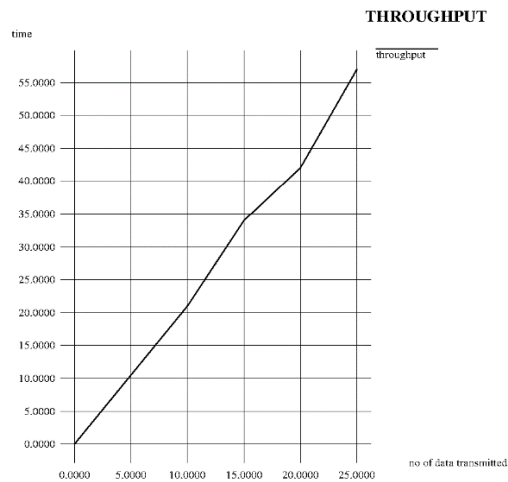


Fig. 8. Relationship between Time and the Amount of Data Transmitted.

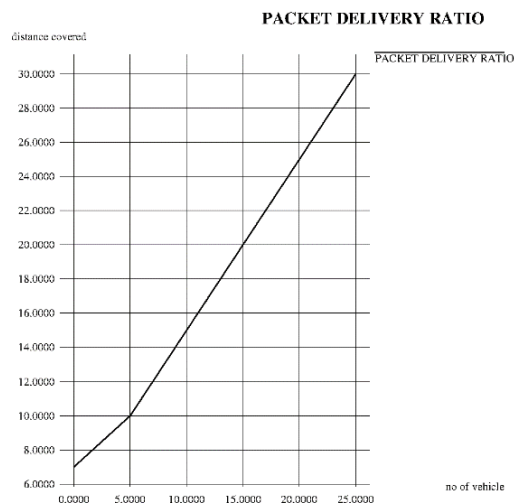


Fig. 9. Relationship between the Number of Vehicles and Distance Covered.

VI. CONCLUSION

From this study, we can conclude that congestion can be reduced and at the same time malicious messages can be avoided in the VANET thereby reducing the scope of attacks

over the vehicular ad-hoc network (VANET). The throughput and the packet delivery ratio are enhanced with this system. The overhead on the RSU is also reduced by electing edge computing vehicle (ECV) which shares the load on the RSU by verifying the valid and invalid messages. Two-way behavior of ECV i.e., both as producer and consumer is beneficial for the RSU and at the same time for the ordinary vehicles in the VANET.

ACKNOWLEDGMENT

We are very grateful to each and everyone who guided us in each and every step and special thanks to the institution for providing the support.

REFERENCES

- [1] J. Cheng, J. Cheng, M. Zhou, F. Liu, S. Gao, and C. Liu, "Routing on the Internet of vehicles: A review," *IEEE Trans. Intell. Transp. Syst.*, vol. 16, no. 5, pp. 2339–2352, Oct. 2015.
- [2] Y. Xie, L. Wu, Y. Zhang, and J. Shen, "Efficient and secure authentication scheme with conditional privacy-preserving for VANETs," *Chin. J. Electron.*, vol. 25, no. 5, pp. 950–956, 2016.
- [3] S. Jiang, X. Zhu, and L. Wang, "An efficient anonymous batch authentication scheme based on HMAC for VANETs," *IEEE Trans. Intell. Transp. Syst.*, vol. 17, no. 8, pp. 2193–2204, Aug. 2016.
- [4] S. Zeadally, R. Hunt, Y.-S. Chen, A. Irwin, and A. Hassan, "Vehicular ad hoc networks (VANETs): Status, results, and challenges," *Telecommun. Syst.*, vol. 50, no. 4, pp. 217–241, 2012.
- [5] Y. Sun, R. Lu, X. Lin, X. Shen, and J. Su, "An efficient pseudonymous authentication scheme with strong privacy preservation for vehicular communications," *IEEE Trans. Veh. Technol.*, vol. 59, no. 7, pp. 3589–3603, Sep. 2010.
- [6] C.-C. Lee and Y.-M. Lai, "Toward a secure batch verification with group testing for VANET," *Wireless Netw.*, vol. 19, no. 6, pp. 1441–1449, 2013.
- [7] D. He, S. Zeadally, B. Xu, and X. Huang, "An efficient identity-based conditional privacy-preserving authentication scheme for vehicular ad hoc networks," *IEEE Trans. Inf. Forensics Security*, vol. 10, no. 12, pp. 2681–2691, Dec. 2015.
- [8] V. Miller, "Use of elliptic curves in cryptography," in *Proc. Adv. Cryptology—CRYPTO*. New York, NY, USA: Springer, 1986, pp. 417–426.
- [9] Jie Cui, Lu Wei, Jing Zhang, Yan Xu, and Hong Zhong, "An Efficient Message-Authentication Scheme Based on Edge Computing for Vehicular Ad Hoc Networks", *IEEE Trans. Intell. Transp. Syst.*, pp. 1524-9050, Early Access.
- [10] Brad Karp and H.T. Kung, "GPSR: greedy perimeter stateless routing in wireless networks", in *Proc. 6th Annual Int. Conf. Mobile computing and networking*, 2000, pp. 243-254.

Compound Mapping and Filter Algorithm for Hybrid SSD Structure

Jin-Young Kim¹

Department of Computer Engineering
Kangwon National University
Samcheok, South Korea

Se Jin Kwon^{2*}

Department of Computer, Media, Industry Engineering
Kangwon National University
Samcheok, South Korea

Abstract—With the recent development of byte-unit non-volatile random access memory (RAM), various methods utilizing quad level cell (QLC) not-AND (NAND) flash memory with non-volatile RAM have been proposed. However, tests have shown that these hybrid structures lead to a reduction in the performance of a hybrid solid state disk (SSD) owing to issues regarding space efficiency. This study proposes a compound address method and filter algorithm suitable for the next generation of NAND flash, called hybrid storage media, where QLCs and phase-change memory (PCM) are used together. The filter-mapping algorithm includes a management method that stores data in phase-change memory or flash memory according to the next command, which is accessed when a write command that is half or less than half a page in length is received from the file system. Tests have shown that the compound mapping and filter algorithm reduces the wasted pages by more than half and the number of merge operations is also significantly decreased. This leads to a decrease in the number of delete operations and improves the overall processing speed of the hardware.

Keywords—Pram; hybrid architecture; QLC NAND flash memory; algorithm

I. INTRODUCTION

There have been rapid changes affecting the memory layer in recent years with the development of byte-unit non-volatile (NV) RAM (phase-change memory). Phase-change memory (PCM) is similar to not-AND (NAND) flash memory, but also includes fast read and write operations, which are characteristics of main memory units. Moreover, its lifespan is approximately 10 times higher than that of NAND flash memory. Key examples of NVRAM include ferroelectric RAM (FeRAM), phase-change memory, and resistive RAM (ReRAM). A hybrid solid state drive (SSD) includes a flash translation layer (FTL), which is a software layer used to efficiently exchange information between hardware components by considering the hardware properties of the phase-change memory and NAND flash memory [1].

The existing hybrid SSD [2, 3] categorizes data into hot and cold data depending on the reading and writing frequency, and then stores high-frequency hot data and metadata into phase-change memory and stores low-frequency cold data into flash memory. When commands are given in duplicate locations it is possible to overwrite the phase-change memory and thus, reduce the number of merge operations in the flash memory to achieve the ultimate goal of improving overall performance.

These existing hybrid SSD structures have the disadvantage of a reduction in overall space utilization efficiency because if a write operation delivers less than one page (a write unit) of data from the file system, the entire page will not be filled. To resolve the above issue, this paper proposes a compound mapping and filter algorithm for a hybrid SSD structure. Hybrid filtering refers to an algorithm that differentiates and stores data in the proper memory unit using two types of chips. This filter can be implemented through a buffer, such as a DRAM or resistor. The algorithm conducts two major functions; first, it gathers short write commands and stores them on a single page to improve the space efficiency. When a write command is one half of 8 KB or less (namely, 4 KB or less), where 8 KB is the standard page size in QLC NAND flash memory, the write command information is stored in a hybrid filter to await the next command. If the next command is 4 KB or less and would be written on a different page, both the existing command in the filter and the new command are stored in the phase-change memory. Second, the number of merge operations is reduced through the hybrid filter, which improves the overall performance. When a command is present in the same sector as the command stored in the filter, so that the data must be overwritten, there is no need for a separate operation because the command information is immediately overwritten in the filter, unlike a log block system, in which free blocks must be allocated to the log block to merge the commands. This reduces the number of merge operations, thereby improving the overall performance.

Section 2 analyzes existing studies and analyzes limitations. Section 3 describes the newly proposed filter algorithm and its implementation examples. Finally, Section 4 analyzes the test results and presents future research directions.

II. PREVIOUS STUDIES

A. Information Update Connection

Existing FTL algorithms are categorized into 1:1 [4], 1:N [5, 6], and M:N [7, 8, 9] depending on the number of data blocks that are connected to a single logic block. A data block is where the data are first written, and a log block delays the merge operations as long as possible by recording the overwritten data in different locations according to each algorithm in the event of a store command involving overlapping pages. In the 1:1 connection, if a write command occurs on overlapping pages, a new log block is allocated

* Corresponding author

from the free blocks, and a duplicate sector is recorded in that block to delay the merge operation. However, because only one data block is linked to a single log block, if repeated write commands occur in the same page, merge operations occur much more frequently, thereby reducing the overall performance of the flash memory. In the 1:N connection, a total of N data blocks are linked to one log block. In other words, several data blocks can share a single log block. In addition, because they are generally used an "out-of-place" method that fills the space in any order, the space utilization efficiency is extremely high. However, in the worst-case scenario, data blocks equaling the number of a page will be connected to a single log block, and a significant delay will occur when conducting merge operations. In the M:N connection, this architecture attempts to overcome the disadvantages of a 1:N connection. The main concept is to limit the number of data blocks that can be linked to a single log block.

B. Limitations of Previous Studies

The algorithms for the connection schemes mentioned in Section II.A are difficult to implement in hybrid SSDs, or do not provide optimum efficiency when implemented. Regardless of the algorithm applied, if the size of a write command is eight sectors (4 KB) or less, at least half of the 16 sectors, which is the standard number for a QLC NAND flash memory page, will inevitably be wasted. If a sector mapping method is applied to resolve this phenomenon using only the NAND flash memory, it will require an extremely large memory volume in the main memory device. However, if a hybrid structure comprised of phase-change memory and NAND flash memory is applied, and a phase-change memory of a certain size is mapped based on sector units, a relatively small volume will be required instead.

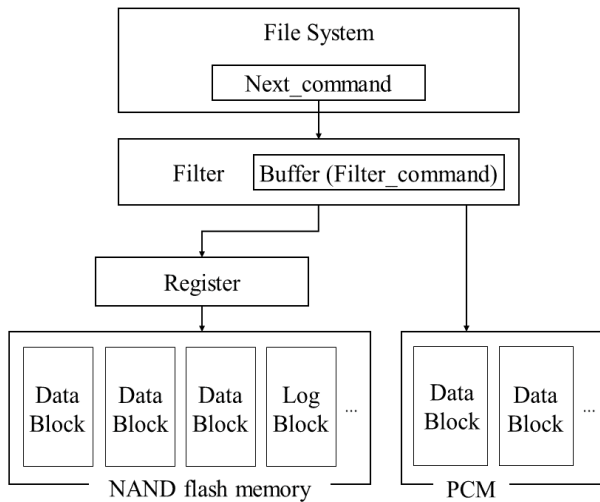


Fig. 1. Overall Structure.

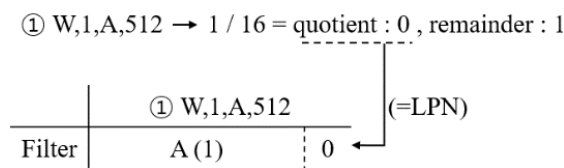


Fig. 2. Command Access and Storage in Filters

Algorithm 1

```

Algorithm 1
1: if 'Next_command' is less than 4KB in size;
2:   if there is a 'Filter_command' in the filter;
3:     if their LPN of the 'Filter_command' and the 'Next_command' are the same;
4:       if the LSN of the 'Filter_command' and the 'Next_command' are the same;
5:         In the filter, overwrite the 'Filter_command' with 'Next_command';
6:       else (=LSNs of two commands are not identical)
7:         'Filter_command' and 'Next_command' are stored in flash memory as one page;
8:     else (=LPN of 'Filter_command' and 'Next_command' are not the same);
9:       if the sector mapping table has the same LSN as 'Filter_command';
10:        overwrites 'Filter_command'
11:        in the data storage location of the same sector in the PCM;
12:       'Next_command' is stored in the filter;
13:     else (=same LSN does not exist in sector mapping table)
14:       the 'Filter_command' is stored in the new space of the PCM;
15:       'Next_command' is stored in the filter;
16:     else (=the filter is empty)
17:       'Next_command' is stored in the filter;
18:   else (=Next_command is larger than 4KB)
19:     'Next_command' is stored in the flase memory;

```

III. PROPOSED METHOD

A. Issue Analysis

Analysis of the traces of existing file system commands available in the UMass Trace Depository [10] indicated that 25% of all traces were not written chronologically. Of these, 24.7% were write commands of one half page size or less. Based on the characteristics of flash memory, if the next page is used after processing a write command, it is impossible to go back to the previously-written page. Pages with wasted sectors after writing fewer than eight sectors (4 KB) accounted for 7% of all write commands. In conclusion, only 26.8% of the volume in all blocks was used, indicating that approximately 73% of the total volume was wasted.

B. Filter Algorithm

To resolve the issues discussed above, a compound mapping and filter algorithm is proposed. The overall structure is shown in Fig. 1. If a command is given to the file system, the command is stored in the appropriate storage space of the PCM and NAND flash memory after passing through the filter algorithm area. The NAND flash memory has data blocks and log blocks. Data passes through the registers before being stored in these blocks. Finally, the PCM contains only data blocks. The general characteristic of flash memory and PCM is that one block consists of four pages and one page consists of sixteen sectors. In this architecture, PCM uses sector mapping and NAND flash memory uses block mapping. The filter algorithm is called a compound mapping because it uses both types of mappings.

For existing 1:N association algorithms, only data blocks and log blocks are used, which places a heavy burden on these two block types. This can result in a significant number of merge operations, shortening a device's lifetime and reducing its performance. To mitigate these issues, we added a new PCM storage space and filter area. The filter area identifies the data according to Algorithm 1 to be described later, and either selects the PCM or flash memory and stores the data in the most suitable device. This will reduce the merging workload and increase storage space efficiency, ultimately improving overall performance.

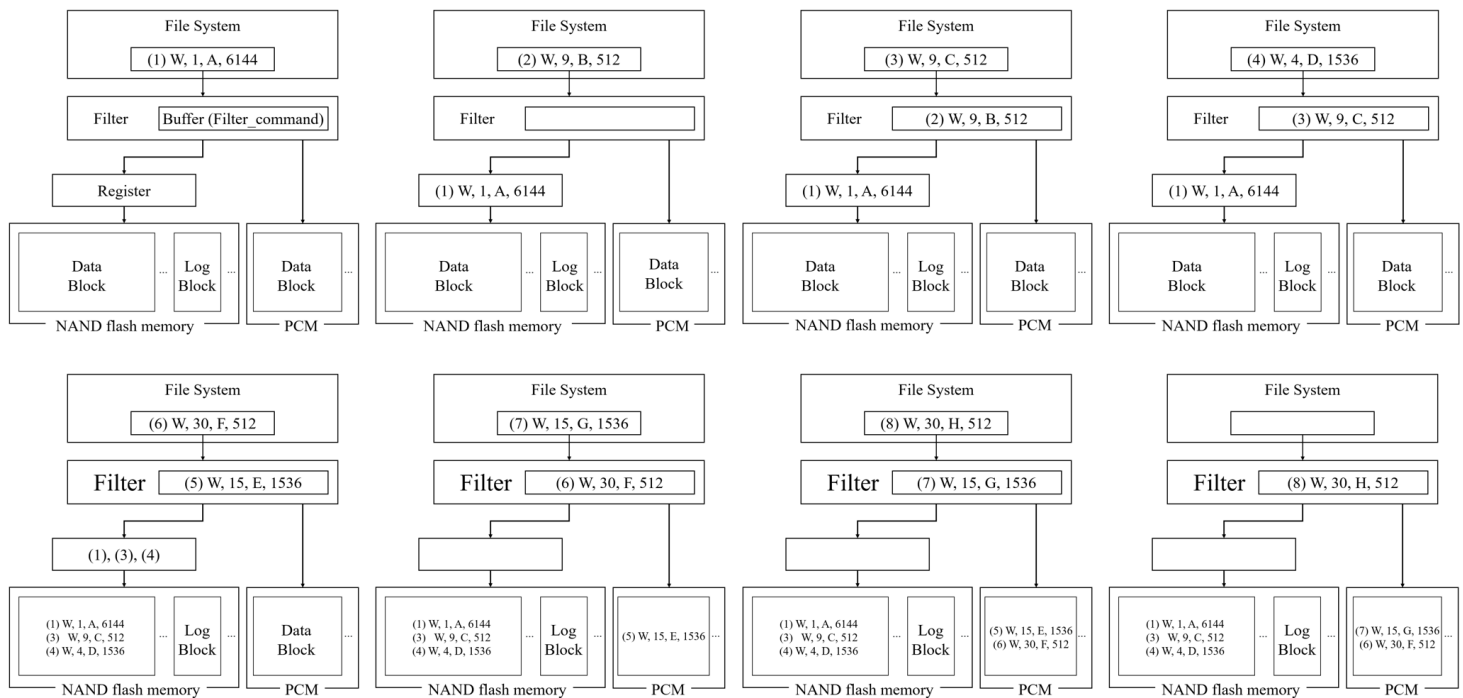


Fig. 3. Algorithm 1 Process with Examples (Proceeding Left to Right on the First Line).

As shown in Fig. 2, a command contains ‘command, logical sector number, data, size’ information. A ‘command’ is a command that runs in the file system as flash memory. ‘W’ means write and ‘R’ means read, but only ‘W’ is used because only write commands are needed. The ‘logical sector number’ is the number of the sector corresponding to the write command. ‘Data’ is the content to be saved and ‘size’ is the capacity of the write command. The unit of size uses bytes by default.

Given the data to process, divide the logical sector number (LSN) by the number of sectors per page to obtain the quotient, where the quotient is called the logical page number (LPN). The LSN and LPN will only reside in the DRAM in the filter area for a short time until the next command is given. The size of the filter in which the instruction can be stored for a short time is equal to the maximum capacity of the filter specified in Algorithm 1.

In order to simplify the filter, it is represented as a single page. In this paper, the LSN is recorded in parentheses for intuitive confirmation. On an actual system, the LSN is not stored in the filter.

For example, in Fig. 2, If LSN 1 is divided by 16, the quotient is 0 and the remainder is 1. Therefore, the LPN is written as 0 and data is written to sector 1 of the filter. This command is the ‘Filter_command’ in Algorithm 1, and a detailed description of this will be provided in the next paragraph. A ‘Filter_command’ will be saved to the PCM or flash memory and stored in the filter as determined by Algorithm 1 when processing the next command.

Algorithm 1 describes the overall processing of the filter and example commands are provided in Fig. 3. We used “OLTP Application I / O”, a collection of I / O command

information given to storage among the traces provided publicly in UMass Trace Repository [10]. In Algorithm 1, a ‘Filter_command’ implies that the command is already stored in the filter and a ‘Next_command’ refers to the command that is currently being processed.

The first item to check when given a command to process is the size of the command. If the size of the ‘Next_command’ is less than or equal to the maximum value that can be stored in the filter, verify that the filter has a ‘Filter_command’ already stored.

In the case of an instruction given as ‘(1) W, 1, A, 6144’ in Fig. 3, the size of the instruction is larger than 4096 B, so it does not go through the filter (Algorithm 1, lines 17–18). This is because when a trace is analyzed, very few consecutive write commands that exceed the maximum size of the filter appear in the same sector.

When a scenario occurs in which a command is to be stored in flash memory, the filter collects as many identical page commands into registers as possible before they are stored in flash memory. If the page currently being collected in the register is equal to the LPN of the command or if the register is empty, the command is stored in this register. This includes the processing of the ‘(3) W, 9, C, 512’ and ‘(4) W, 4, D, 1536’ commands, for example. However, if the page number that is collected in the register differs from the LPN in the next instruction or if the next instruction causes a register overflow, the data of the existing register is stored in the flash memory before the next instruction is stored in the register.

If a scenario occurs that saves a command to a filter, such as processing the ‘(2) W, 9, B, 512’ command, the command can be saved to the filter immediately if the filter is empty (lines 1 and 15–16).

If a 'Next_command' must be saved in the filter (lines 3–7), but the filter is not empty (a 'Filter_command' is already stored in the filter), compare the LPNs of both commands (line 3). If the LPN is the same, the LSNs are compared again. If the LSNs are the same, the filter is overwritten (lines 4–5). In the figure, the command '(3) W, 9, C, 512' would overwrite command '(2) W, 9, B, 512'.

If the LSNs are not the same, two write commands, such as the '(3) W, 9, C, 512' and '(4) W, 4, D, 1536' commands, are stored in the flash memory on the same page and the filter state changes to empty (lines 6–7).

When the '(6) W, 30, F, 512' command is given as the 'Next command', the LPNs of the 'Filter command' and 'Next command' are different (line 8). Therefore, the sector mapping table is referred to and the PCM checks whether this is the same sector as the 'Filter command'. In the current situation, because the PCM is empty, there is no identical sector, so the 'Filter command' is stored in the PCM and the 'Next command' is stored in the filter (lines 12–14).

When the command '(7) W, 15, G, 1536' is given, the PCM is not empty but there is no same sector for the filter command, so data 'F' corresponding to the 'Filter command' is newly saved in the PCM. However, if the '(8) W, 30, H, 512' command is given, the PCM overwrites existing data 'E' with filter command data 'G' because this is the same sector as that of the filter command. If the algorithm used were the 1:N association, it would have already used a significant amount of log block space due to overwriting.

C. Example Execution and Limitations

Fig. 4(a) and (b) show the results of the 1:N algorithm and the proposed filter algorithm performed on the same command. The command is one of the "OLTP Application I / O" commands publicly available from the UMass Trace Repository used for performance evaluations [10].

In the results analysis of Fig. 4, when running the compound mapping and filter algorithm, three pages were used for NAND flash memory and 55 sectors were used for PCM, resulting in 52,682 B. However, using 1:N concatenation, 10 pages were used for the data block and 13 pages for the 188,416 B log block. As a result, the space utilization efficiency of the filter algorithm is three times higher than for the 1:N association algorithm. In addition, the 1:N association algorithm wastes approximately 17 times more space than the filter algorithm.

Compared to the 1:N connection algorithm, not only does the compound mapping algorithm conduct much fewer merge operations, its use of partial sector mapping greatly improves the space utilization. Fig. 4(a) shows the processing of a command by this method. At a glance, the space utilization efficiency and the data storage density are much higher than the conventional 1:N association algorithm shown in Fig. 4(b).

Use of the conventional 1:N association algorithm results in many page allocations, as shown in Fig. 4(b). However, the amount of data that is actually stored in this space is very small, resulting in wasted capacity and lower space utilization efficiency.

The filter algorithm can store data on a sector-by-sector basis, and data of less than half a page (4 KB) can be algorithmically executed in the phase-change memory, where it is possible to overwrite data immediately when a write command occurs for the same position, and data are managed using sector-by-sector mappings. Complex flash memory mapping can be accomplished through a block-mapping application. With this approach, redundant sectors, which account for 79% of all traces, can be effectively managed.

However, from a cost point of view, there is a limit to the capacity of the phase change memory because this memory is expensive. Therefore, a small amount of space should be allocated to maximize the cost efficiency of the phase change memory. A minimum amount of space should also be allocated for the merge operator because if data should be stored in the phase change memory, but its space is not sufficient or the amount of invalid data that can be overwritten is too low, a merge operation will be performed. That is, since the size of the phase change memory is small, the number of merging operations increases. Therefore, the cost of the merge operator should be minimized.

As limitations, the volume used in the sector-mapping table is relatively large, and the cost of the phase-change memory is high. Therefore, a means to reduce the size of the mapping table and at the same time the amount of phase-change memory that provides the greatest efficiency for each NAND flash memory capacity should be sought. It is also necessary to consider a more efficient method of merging and to check detailed conditions on how to exchange information between the flash memory and PCM.

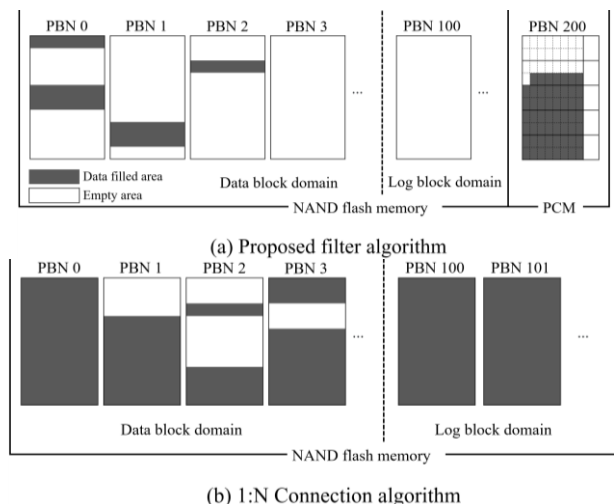


Fig. 4. Comparison of Space Utilization.

TABLE I. ESTABLISHMENT OF TEST HYPOTHESIS

Variable	Value
Number of blocks used in the test	2,048
Number of pages per block	64
Number of sectors per page	16
Sector size (Byte)	512

IV. TEST RESULTS AND DIRECTIONS FOR FUTURE RESEARCH

A. Test Results

This section compares and analyzes the efficiency of the proposed algorithm to a compound mapping filter algorithm that uses 1:N linking sectors based on traces, and measures the number of operations performed and the time needed to achieve the results. The consumed time for flash memory is assumed in the simulation by referring to a technical note provided by Micron Technology [11]. The time required for a random write per sector is 55 μ s, and the time required for a block erasure is 500 μ s. Also, trace analysis indicates that the average size of one write operation is 3584 B.

We used the "OLTP Application I / O", a collection of I / O storage command information for traces provided publicly by the UMass Trace Repository [10]. We analyzed the read / write command and the corresponding sector number and size, and conducted performance evaluations based on this command. Because QLC is still in the development stage, it was not possible to provide a hardware performance evaluation, so the evaluation was performed based on software coding.

As common characteristics for the two algorithms, one block is composed of 64 pages, and each page consists of 16 sectors, as shown in Table I. In both cases, the data block and log block domains use NAND flash memory. The 1:N connection algorithm uses a 1 GB data domain and a 10 MB log block domain; the filter algorithm was set up using a data domain of 1 GB, log block of 5 MB, and filter domain of 5 MB, where the filter domain used dynamic, static, or parameter RAM (DRAM, SRAM, or PRAM).

Table II shows the results of analyzing 378,914 write commands on a single chip. Here, a merge operation refers to merges between the data domain and log blocks in the NAND flash memory. For the 1:N connection algorithm, 1,112,738 write operations were required. This represents approximately 7,789,166 sectors (55 microseconds per sector), or approximately 428.4 seconds in total. On the other hand, the filter algorithm required 200.9 seconds because 522,012 sectors were involved. Therefore, using the filter algorithm, it is possible to reduce the number of write operations and their associated time by 46% compared with the conventional method. Erase operations also yielded significant differences. In the 1:N chain algorithm, 546 block deletion operations and 273 merge operations were performed. However, the filter algorithm applied only 34 block deletions and 17 merge operations. These numbers indicate that when using the filter algorithm, the numbers of delete and merge operations are reduced by 93% compared to the 1:N connections algorithm.

TABLE II. COMPARISON OF ALGORITHM

	Filter Algorithm	1:N Connection Algorithm
Write operations (number)	522,012	1,112,738
Write operations (seconds)	200.9	428.4
Delete operations (number)	34	546
Delete operations (seconds)	0.017	0.273
Merge operations (number)	17	273

B. Directions for Future Research

This study assumed that the filter will use DRAM or SRAM. However, such memory types are relatively expensive compared to PRAM, and hence the memory volume must be reduced as much as possible for greater cost efficiency. Therefore, a method that uses PRAM should be considered. PRAM has a slower access speed compared to DRAM or SRAM, and hence an algorithm that uses a two- or four-step pipeline technique must be designed to improve the speed.

To the two-step pipeline, two filters (Filter 1 and Filter 2) composed of eight connected sectors operate within the phase-change memory. After reading the write command in Filter 1, the write command is also read in Filter 2. Because differences in the delay time may occur depending on the input command, the filter that finishes its operation first will read the new command and process it according to the algorithm.

To further elaborate, if the domain in a phase-change memory uses a filter, and phase-change memory is used for storage, the filter is converted into the data domain immediately, and the eight sectors that are connected out of the extra domains in the phase-change memory will be used as a new filter. The algorithm described in this paper requires two operations when data are stored in the NAND flash memory or phase-change memory because of data passage through the filter. However, when PRAM is used, the filter is incorporated in the phase-change memory architecture, so only one write operation is needed to store data in the phase-change memory.

ACKNOWLEDGMENT

This work was supported by Basic Science Research through the National Research Foundation of Korea (NRF) funded by the Ministry of Education (NRF-2017R1D1A3B04031440). This study was also supported by a 2018 Research Grant from Kangwon National University (No. 000000000).

REFERENCES

- [1] Ahmed Izzat Alsalibi, Sparsh Mittal, Mohammed Azmi Al - Betar, Putra Bin Sumari "A survey of techniques for architecting SLC/MLC/TLC hybrid Flash memory - based SSDs," Practice and Experience, e4420, ISSN 1532-0626, 2018.
- [2] Jung Sik Park, Hi-seok Kim, Ki-Seok Chung, and Tea Hee Han, "PRAM and NAND Flash Hybrid Architecture based on Hot Data

- Detection,” 2nd International Conference on Mechanical and Electronics Engineering ICMEE, 1, pp. 93-97, 2010.
- [3] Jin Kyu Kim, Hyung Gyu Lee, Shinho Choi, and Kyoung Il Bahng, “A PRAM and NAND Flash Hybrid Architecture for High-Performance Embedded Storage Subsystems,” EMSOFT '08 Proceedings of the 8th ACM international conference on Embedded software, pp. 31-40, 2008.
- [4] Jesung Kim, Jong Min Kim, Sam H. Noh, Sang Lyul Min and Yookun Cho, “A space-efficient flash translation layer for CompactFlash systems,” IEEE Transactions on Consumer Electronics, 48(2), pp. 366-375, 2002.
- [5] Sang-Won Lee, Dong-Joo Park, Tae-sun Chung, Dong-Ho Lee, Sangwon Park, and Ha-Joo Song, “A log buffer-based flash translation layer using fully-associative sector translation,” Embedded Computing Systems (TECS), 6(3), pp. 1-27, 2007.
- [6] Usman Anwar, Se Jin Kwon, and Tae-Sun Chung, “SAF: States Aware Fully Associative FTL for Multitasking Environment,” Computer and Information Science 2015, 614, pp. 1-11, (2016)
- [7] Dawoon Jung, Jeong-Uk Kang, Heeseung Jo, Jinsoo Kim, and Joonwon Lee, “Superblock FTL: A superblocK-based flash translation layer with a hybrid address translation scheme.” ACM Transactions on Embedded Computing Systems, 9(4), pp. 40:1-40:41, 2010.
- [8] Jeehong Kim, author Dong Hyun Kang, Byungmin HaHyunjin Cho, and Young Ik Eom, “MAST: Multi-Level Associated Sector Translation for NAND Flash Memory-Based Storage System,” Computer Science and its Applications, 330, pp. 817-822, 2015.
- [9] Hyunjin Cho, Dongkun Shin, and Young Ik Eom, “KAST: K-Associative Sector Translation for NAND flash memory in real-time systems,” DATE '09 Proceedings of the Conference on Design, pp. 507-51, 2009.
- [10] UMass Trace Repository, “OLTP Application I/O” “<http://traces.cs.umass.edu/index.php/storage/storage/>”
- [11] Micron Technology, Inc “NAND Flash 101: An Introduction to NAND Flash and How to Design it into Your Next Product”, “<https://user.eng.umd.edu/~blj/CS-590.26/micron-tm2919.pdf>”

Optimal Compression of Medical Images

Rafi Ullah Habib

Department of Computer Science and Information
College of Science, Majmaah University, Majmaah 11952, Saudi Arabia

Abstract—In today's healthcare system, medical images are playing a vital role in the diagnosis. The challenges arise to the hospital management systems (HMS) are to store and communicate the large volume of medical images generated by various imaging modalities. Efficient compression of medical images is required to reduce the bit rate to increase the storage capacity and speed-up the transmission without affecting its quality. Over the past few decades, several compression standards have been proposed. In this paper, an intelligent JPEG2000 compression scheme is presented to compress the medical images efficiently. Unlike the traditional compression techniques, genetic programming (GP)-based quantization matrices are used to quantize the wavelet coefficients of the input image. Experimental results validate the usefulness of the proposed intelligent compression scheme.

Keywords—Medical images; wavelet transform; JPEG2000; genetic programming; compression; quantization

I. INTRODUCTION

Images can represent many things e.g. medical, military television, satellite or any other computer storage pictures [1]. Sampling and quantization of light intensity for creating the digital images, a massive data is produced and hence its storage and transmission becomes impractical. The solution to this problem is to compress the image and make it more practical for storage and transmission. The redundant information is reduced so that the owners and other contributors can easily increase the storage capacity and speed-up the transmission over a wired/wireless network. Medical imaging has gained immense importance in the last decades. The most appropriate solution to store and transmit medical images is to apply the lossless compression techniques that guarantee the exact reconstruction [2]. Several compression schemes have been proposed to compress digital images [3] [4, 5, 6]. The images contain three different types of redundancies: spatial, coding and psycho-visual redundancies. These redundancies are used in image compression [7]. In [8], the details of spatial, coding and psycho-visual redundancies are given. In spatial redundancy, the intensity of one pixel is calculated by the values of other pixels. In coding redundancy, the variable length code is used to match the statistics of the input image. In psycho-visual redundancy, the focus is on visual perception of the compressed images

Two types of image compression techniques are used: 1) lossless compression, 2) lossy compression. In lossless compression, the original digital image can be obtained back without any loss of information. There are many applications e.g. medical, business, and military where any loss of information is not acceptable. Medical images are more critical and loss of information may lead to incorrect diagnosis and can

be life-threatening [9, 10, 5, 11]. In 2002, in North America, an annual meeting held by the Radiology Society, Digital Imaging and Communications in Medicine (DICOM) working group-4-compression, where they announced an extension to the JPEG (Joint Photographic Expert Group) compression named as JPEG2000. The JPEG2000 compression is an extension to the JPEG compression to overcome its shortcomings. JPEG2000 is a wavelet-based compression that can highly compress images with less distortion [12]. Lossy compression used for general-purpose images where a minor loss of information is acceptable [13]. In lossy compression, the original image can be obtained from the encoded image with the loss of information where the quantization losses occur during the encoding stage [14, 15, 16]. The ratio of the original image and compressed image referred to as compression ratio (CR). The compression ratio is given in Equation 1.

$$CR = \frac{\text{Uncompressed}_{\text{Image}}(\text{Bytes})}{\text{Compressed}_{\text{Image}}(\text{Bytes})} \quad (1)$$

The performance of the compression is measured by the difference between the input image and the reconstructed image and this difference is referred to as distortion [3]. High fidelity of the reconstructed image means the difference between the original and reconstructed image is small and vice versa. Mean square error (MSE) is the most popular method to calculate the difference between the input image and the reconstructed image [3, 17]. MSE is given in Equation 2.

$$MSE = \frac{1}{M \times N} \sum_{i=1}^M \sum_{j=1}^N (f(x,y) - g(x,y))^2 \quad (2)$$

where $M \times N$ is the size of the image, $f(x,y)$ is the original/input image and $g(x,y)$ is the reconstructed image. The MSE is sometimes called quantization error variance. The images with the same type of degradation are highly observed by the human eye when the MSE is smaller [18]. However, in some applications, smaller MSE does not work when different types of degradation are compared. Mostly, the researchers use PSNR (peak signal to noise ration) that is based on MSE [19]. The SNR is expressed in Equation 3.

$$PSNR = 10 \log_{10} \left[\frac{\frac{1}{M \times N} \sum_{i=1}^M \sum_{j=1}^N (f(x,y))^2}{\frac{1}{M \times N} \sum_{i=1}^M \sum_{j=1}^N (f(x,y) - g(x,y))^2} \right] \quad (3)$$

The PSNR is measured in dB and show better indication of degradation in the compressed image. In this paper, an intelligent compression of medical images has been proposed. The GP based module is applied to the JPEG2000. JPEG 2000, developed in 2002 is a wavelet-based efficient compression method as compared to the DCT based JPEG compression. It was initiated in 1996 where some compression algorithms were emerged to improve the compression performance. After introducing some verification models and some other technical

contributions, JPEG2000 become an international standard [20]. A fast approach of the wavelet transform, which is also called a second-generation transform, is used. It is an integer wavelet transform (iWT), using a lifting scheme [21]. Integer discrete cosine transform (iDCT) based JPEG lossless compression of medical images. In iDCT-based compression, Watson's standard quantization matrix of size 8×8 is used to quantize the iDCT coefficients [22, 23]. Fig. 1 shows the Watsons' perceptual quantization matrix. iDCT is a fast and efficient transformation where we do not lose any of the information. Watson's quantization matrix although good enough for quantizing the image blocks and gives us imperceptible alteration. However, it does not provide optimum results. In the proposed work, the featured based quantization matrices are used that are generated by using the GP module. GP module is discussed in detail in Section 4.

16	11	10	16	24	40	51	61
12	12	14	19	26	58	60	55
14	13	16	24	40	57	69	56
14	17	22	29	51	87	80	62
18	22	37	56	68	109	103	77
24	35	55	64	81	104	113	92
49	64	78	87	103	121	120	101
72	92	95	98	112	100	103	99

Fig. 1. Watsons' 8×8 Standard Quantization Matrix.

Rest of the paper is summarized as follow: Literature survey is presented in Section II. In Sections III and IV, the Image file formats and GP module are discussed respectively. The proposed method and experimental results are discussed in Sections V and VI respectively. Conclusion and future directions are presented in Section VII.

II. LITERATURE SURVEY

In 2014, SVD (Singular Value Decomposition) and wavelet-based lossy compression have been proposed [24]. Low singular values are neglected by using SVD and then restore the image. The restored image is then compressed again by applying the WDR (wavelet difference reduction) and an improved result in terms of visual perception, are obtained.

In 2016, Kozhemiakin et al. proposed a lossy compression of Landsat multispectral images [25]. Two facts, degree of correlation and the inherent noise along with its properties have been taken into account to compress the image. Similarly, in [26, 27], the DTT (Discrete Tchebichef Transform) based lossy compression is proposed under the JPEG standard. It provides similar performance for lossy compression like DCT based JPEG compression but it does not work for lossless. This issue has been raised by Xiao et al. in [28].

Several lossless image compression schemes have been proposed especially for medical image applications. Unlike DCT that is used in JPEG lossy compression, a fast transformation, integer DCT (iDCT) has been used to reconstruct the original image without any loss of information [29]. In [28], a lossless image compression based on DTT has been proposed that reduce the computational complexity and improve the compression rate.

In [30], a lossless compression based on segmentation-based compression is introduced. Instead of compressing the whole image, the regions of interest (ROI) zone is extracted from the image and then apply the lossless compression. This improves the compression rate without losing much information. Lossless compression of medical images has been proposed in [31]. The scheme is based on HEVC (High-Efficiency Video Coding) intra coding. The anatomical medical images are characterized by large-scale edges. HEVC intra coding compression scheme is applied to different types of medical image like CT, MRI, X-Ray images.

A compression technique for telemedicine images using the DICOM format has been proposed by [32]. The delimiter based lossless compression is applied to telemedicine images. In the encoding side, an image is converted to a row vector where the number of continuous unique elements with repetitions is evaluated. The same process is reversed and a better quality reconstructed image is obtained. They compare their proposed scheme with [33, 34], in terms of compression ratio.

Compression of CT and MRI images is proposed in [35]. The author evaluates the perceptual quality of the compressed image. In image-based diagnosis, it is very important to understand the human perception of medical image quality. The authors are focusing on the measurement of the visual perception of the compressed CT and MRI images. Similarly, a block-based lossless compression for medical images has been introduced [36]. Before applying the Huffman encoder on the coefficient to compress the medical image, the authors applied DCP (DC prediction), effective NTB (Non-transformed block) validation and truncation method.

Wavelet-Based medical image compression has been proposed [37]. The authors investigate the improvement in the JPEG2000 for volumetric medical image compression. The authors tested their technique on CT scan, MRI and ultrasound images. They develop a generic codec framework, which supports the JPEG2000 compression with its volumetric extension.

A block-based lossless compression of medical images has been proposed [38]. After decomposing the image using integer wavelet transform (IWT), the low level i.e. approximation subband is passed through the lossless Hadamard transform. Correlations inside the blocks are removed by using the Hadamard transformations. The compression ratio of medical images, as well as general-purpose images, is improved. Similarly, several schemes have been proposed in the last decade for the lossless compression of medical images [39, 40, 41].

III. IMAGE FILE TYPES

Image formats are the standards for organizing and storing images in a computer system. Images contain digital data that can be rasterized for display on the computer or any other digital display. The format specifies how the information is encoded to be stored in the storage devices. The images may store information in compressed, uncompressed or vector format. The images can be stored in so many formats. Each image file type has a specific, yet different purpose and has

advantages and disadvantages. Details of some of the most popular file formats that are used in different areas are given in Table II. The general description, proc, cons, and some of the features are explained in [42, 43].

IV. GP MODULE

Genetic programming is an intelligent search technique that is used in numerous applications. GP is a machine learning technique based on natural selection and genetics [44]. It is based on the stochastic method, where randomness plays an important role in searching and learning [45]. The quantization step in JPEG2000 compression, GP based matrices that are based on Watsons’ standard quantization matrix, are used to quantize the wavelet coefficients of the image to be compressed. These matrices are referred to as Genetic Quantization Matrices (GQMs). Compression measurement has been used in the fitness function. The focus is on the compression ratio using GP based JPEG2000 compression for the most sensitive images i.e. medical images. An initial random population is evaluated. The best individuals are reserved and all others are deleted. The retained children make a new generation and the process continues until the termination criterion is satisfied. The block diagram for the GQM is given in Fig. 2. Different functions of the GP module used in the proposed method are as follows:

A. GP Function Set

It is the set of operators to be used in the GP module. In the proposed work, plus, minus, kozadivide, mylog, sin, and some constants are used. The matrix Wat_St is used as one of the operands. The generated GP-based matrices are based on the Watsons’ standard quantization matrix.

B. Fitness Function

The individuals are evolved by using the fitness function. The performance is evaluated by the compression ratio i.e. bits per pixel (bpp), PSNR and SSIM. The PSNR is the visual perception of the compressed image. In addition, the structural similarity index module (SSIM) has been used as a perceptual measurement where the structural similarity is measured. The bit rate is the bits produced by the encoder. Feedback is provided to the GP module that represents the fitness of the individual. The best score of the individual is indicating the best performance. Four basic arithmetic operators along with the Log and exponent are used in the fitness function. The measurement used to evaluate the performance of the proposed approach is given in the fitness function. The formula for the fitness function is given in Equation 4.

$$\text{fitness} = \alpha_1 \times \text{bpp} + \alpha_2 \times \frac{\text{PSNR}}{50} + \alpha_3 \times \text{SSIM} \quad (4)$$

The constants α_1 , α_2 , α_3 are the weighting parameters that are decided according to the application. The compression ratio is measured by bpp. This measurement means how many bits are required for each pixel in the compressed image. In grayscale images, one byte (8 bits) is required to store each pixel. After compression, the bits per pixel are highly reduced to improve the storage cost and transmission time. For example, $\text{bpp} = 0.50$ means that only 0.5 bits are required for each pixel of a compression image. Although, in medical image applications, the focus is on visual perception so the

constants associated with PSNR and SSIM are given a high weight. PSNR is divided by a constant number in order to scale its value.

C. Population Initialization

In GP random population of the individuals are generated. The most commonly used methods for initializing the population are “full – and – grow” and “ramped half – and – half” methods. In the proposed scheme, the “ramped half – and – half” method is used.

D. Termination Criteria

After fulfilling one of the following criteria, the simulation is terminated.

- The fitness/target score is achieved. The fitness score is application dependent. In medical image application, the fitness score must be high.
- The fitness value repeats.
- The number of generations completed.
- The error becomes less than a pre-defined threshold. Same as fitness score, this termination criterion is also critical. In this research work, the error parameter is not used as a part of the fitness function.

E. GP Operators

In the proposed GP module, the most common GP operators, Crossover, mutation and replication are used to produce the new generation. Crossover creates the offspring by exchanging the genetic material of two individual parents. It searches for the best solution. Rapid exchanges in populations are introduced by mutation. In replication, the individual in a population is copied to the next generation. Generally, the crossover operator is kept with a high ratio. Table I shows all of the GP module settings.

TABLE I. CGP PARAMETER SETTING

Objectives	Evolving optimum output
Fitness	bpp, PSNR and SSIM
Operators	plus, minus, myLog, times, kozadivide, cos, exp
GP Operators	Crossover, Mutation, Replication
Operands	Wat_st, wavelet_coeff, constants
Selection	Generational
Expected Offspring	rank89
Initial Population	Ramped half-and-half
Termination Criteria	The fitness score achieved The fitness score repeats The number of generations reaches the pre-defined number. The error becomes less than a pre-defined threshold
Sampling	Tournament
Survival	Keep the best

TABLE II. COMPARISON OF DIFFERENT IMAGES FORMATS

	BMP	JPEG	JPEG2000	TIFF	GIF	RAW	PNG	DICOM
Short Description	It is very common and is widely used on the Windows platform. Can be compressed but not supported by all the image viewers.	Generally, digital cameras are using the JPEG format. This is a very common compressed format used in storage and communication through the internet.	It is an extension of the JPEG standard. Able to store lossless data. Have better compression level (CL). Several browsers do not support this format.	Used for storing images losslessly. It is mostly supported by image-manipulation applications, scanning, faxing, etc.	Lossless compression is allowed to reduce the colour range to 256 levels. Replaced by PNG after fearing over patent issues, Used for animation and is supported by browsers.	Since each camera manufacturer has one or several formats, it relates to several image formats. It contains the data acquired by unprocessed sensors.	It is an extension to the GIF. 256 colour limitation is removed in this format	DICOM is used for communication and management of medical imaging information and related data. The most commonly used to store and transmit medical images. Most of the hospital adopted this format
Lossless	Yes	No	Yes (Lossless & Lossy)	Yes	Yes	Yes	Yes	Lossless
Animation	No	No	Yes	No	Yes	No	Yes	No
Developed by	Microsoft	Joint Photographic Experts Group	Joint Photographic Experts Group	Adobe	CompuServe	Camera manufacturer	W3C (donated by PNG, Development Group)	ACRNCMA (American College of Radiology and National Electrical Manufacturer Association)
Common use	Image editing	Camera, photography, Web commutations.	JPEG replacement, HD imaging	Scanned images, HD imaging. Photographs without quality loss	Animation Simple web graphics	HDR photography, Archiving	Logos, Icons, web graphics, illustrations, text rendering etc.	Storing and transmitting medical images.
Proc	An uncompressed format and perfect, near to the real universal compatibility	Small file size Widely supported format Compatibility Good colour range	Small file size	Lossless, Compatible with PCs and Macs, Multiple images can be saved in one file	Lossless compression, Smaller file sizes, Simple animations video clips, Widely supported the format	Lossless	Widely accepted format, Lossless Transparency support	Developing time consumption is very low. The speed improve the efficiency in terms of the care patient and other healthcare processes
Cons	Large file size	Lossy compression It is not good for text, graphics and other illustrations	Processor intensive	s/w compatibility issues, Not good for web graphics, Large file size	Limited to 256 colours Web colours only No transparency	Large file size	Complex and larger, Only supports web colours (RGB), Limited compatibility	Too many optional fields are to be entered. Therefore, incorrect data is entered and some are incomplete.

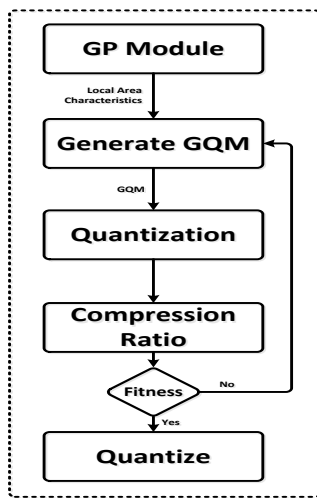


Fig. 2. Block Diagram for GQM.

V. PROPOSED ALGORITHM

In this paper, an intelligent JPEG2000 compression has been introduced to compress medical images. In digital image compression, either DCT based JPEG compression or wavelet-based JPEG2000 compression; the coefficients are quantized by using Watson’s standard perceptual quantization matrix of size 8×8 . This standard quantization matrix provides much better results for all types of images but not the optimum one. In the proposed work, the featured based quantization matrices are generated using genetic programming according to the required compression ratio. The block diagram of the GP based JPEG2000 compression scheme (encoding and decoding) are shown in Fig. 3.

In JPEG2000, to avoid the artefacts appeared in the compressed image, lifting based integer wavelet transform is used to transform the image before quantization [21].

The input image is pre-processed before decomposition. The pre-processing is image tiling, DC level shifting and colour transformation if it is a coloured image. The colour is transformed from RGB channels to Y Cb Cr channels. The input image is decomposed by using lifting based integer wavelet transform. By wavelet decomposition, both the approximation and frequency details of the image are obtained. The frequency details are horizontal, vertical and diagonal details. A reversible biorthogonal CDF 5/3 wavelet transform is used where only integer coefficients are used to avoid the quantization noise. Fig. 4 shows a two-level wavelet decomposition of an image.

The coefficients obtained by decomposing the input image, are quantized similar to the JPEG lossy compression. In this step, instead of using Watson’s perceptual quantization matrix, GP based generated matrices (GQMs) are used to quantize the coefficients. These matrices are featured based and provide the best results in terms of compression ration without affecting the perceptual; quality of the compressed image. The input parameters were tuned For example, the maximum tree level is 31, the maximum The PSNR, bpp and SSIM were also set to the maximum values. Some of the parameters were used with their default values. The numerical pre-fix expression has been

generated while generating GQM. The quantization step is repeated until a fitness criterion is fulfilled. Once, GQM is generated and checked by using the fitness function, it is selected for quantizing the corresponding block of wavelet coefficients. The quantization function is to map the floating-point values to integer values that are efficiently processed by the entropy encoder.

For entropy encoding, code-blocks are the fundamental objects. After decomposition of the image, all of the subbands are divided into rectangular blocks called the precinct and then further divided into non-overlapping blocks called code blocks. Each block is then entered to the entropy encoder that encodes the blocks independently.

In entropy encoding, the coefficients in the code-block are separated into bit-planes. An example entropy encoder is shown in Fig. 5.

The contextual information of the bit-plane data is collected by coding passes. The arithmetic encoder then receives the collected data to generate compressed bit-stream. There are three types of coding passes 1) Significance propagation pass, 2) Magnitude refinement pass, 3) Clean-up pass. For each code block, a separate bit-stream in packet form is generated. If multiple layers are used to encode, the code-block bit-streams are distributed across different packets corresponding to different layers. Therefore, each layer consists of a number of bit-plane coding passes from each code-block in the tile.

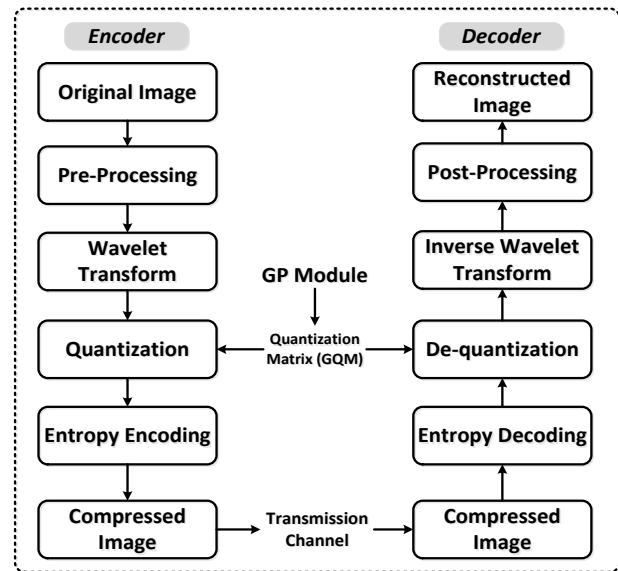


Fig. 3. Block Diagram of Compression and Reconstruction of the Image using a GP-Based JPEG2000 Scheme.

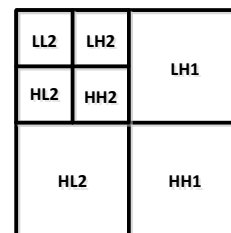


Fig. 4. Two Level Wavelet Decomposition of an Image.

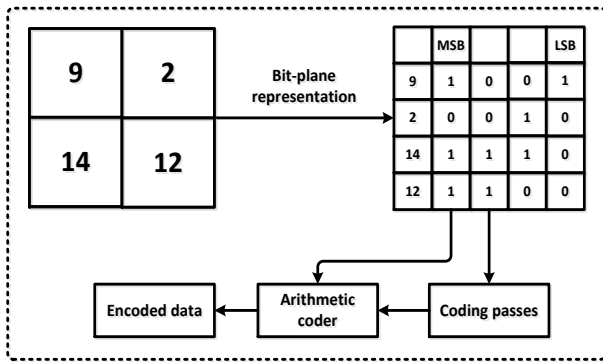


Fig. 5. Entropy Encoder.

Once the image is compressed, it can be stored and transmitted any without perceptual degradation. The reconstruction process is the inverse of the compression encoding process. The input image to the decoding side is the compressed image. First entropy decoding is applied and then de-quantized. For de-quantization, the function expression is used that was generated on the encoding side. The function expression is given before the conclusion section. The same GQMs are generated to de-quantize the coefficients. Further, the inverse lifting based integer wavelet transform is applied. The coefficients are then post-processed to get the reconstructed image.

VI. EXPERIMENTAL RESULTS

MRI image for brain tumours of size 256×256 has been used to test the proposed scheme [46]. The algorithm is also tested on the CT and Ultrasound scan. Experimental work has been carried in a MATLAB environment. For the GP simulation, GPLAB toolkit has been used [47, 48]. As compared to the other proposed lossless compression schemes, the proposed technique provides better results in terms of visual perception and compression ratio. The performance comparison of the proposed approach in terms of PSNR and SSIM values with [32, 33, 37] is shown in Table III. The algorithm provides a high compression ratio without affecting the perceptual similarity of images. The compression percentage is considerably increased as compared to others. The PSNR and the compression percentage depend on the compression ratio (bpp). When the bit rate is improved then PSNR, SSIM and compression percentage is degraded accordingly. The compression percentage is calculated in Equation 5.

$$CL = \left(1 - \frac{\text{CompressedFileSize}}{\text{OriginalFileSize}}\right) \times 100 \quad (5)$$

The sample MRI, CT and ultrasound images used in the experimental work are given in Fig. 6.



Fig. 6. The Sample Medical Images: Brain MRI, Brain CT and Liver Ultrasound Images.

TABLE III. PERFORMANCE COMPARISON WITH DELIMITER BASED COMPRESSION [32], OBJECT-BASED DPCM [33], AND VOLUMETRIC-BASED COMPRESSION [37]

Measures	Images	[32]	[33]	[37]	Proposed
PSNR	CT:			≈ 58	≈ 60
	MRI:	×	×	≈ 57	≈ 62
	Ultrasound:			≈ 38	≈ 47
SSIM	CT:				.97
	MRI:	×	×	×	.98
	Ultrasound:				.93
CR	CT:	1.509	1.815	1.45	1.21
	MRI:	1.536	1.727	1.58	1.23
	Ultrasound:	1.525	Nil	1.84	1.39
CL	CT:			×	
	MRI:	×	×	×	≈ 55%
	Ultrasound:				

Quantization matrices generated through GP module gives the optimum compression ratio. After applying the techniques on the selected set of images, the compression ratio is calculated. Decomposition of one of the images using lifting based integer wavelet transform is given as:

```
waveName = liftwave('cdf5.3','Int2Int')
```

```
[LL1,HL1,LH1,HH1] = lwt2(double(CT_Image), waveName)
```

```
[LL2,HL2,LH2,HH2] = lwt2(double(HH1), waveName)
```

```
[LL3,HL3,LH3,HH3] = lwt2(double(VV1), waveName)
```

Where LL is the approximation subband and others are frequency subbands.

Normally, the performance of the compression technique is measured by the compression ratio. However, other measurements like perceptual similarity and compression level are also measured in the proposed approach. In Table III, it can be seen the performance of the proposed approach with the compression schemes. The available measurements with previous techniques are considered. The CL i.e. the percentage of the compression is much better as compared to [32]. The average CL of JPEG2000 compression for CT, MRI and ultrasound images is 50%. In [33], the compression is object-based, therefore, the compression rate varied according to the size of the object i.e. region of interest (ROI). SSIM, which is the structured similarity measurement, is given only in the proposed technique.

VII. CONCLUSIONS

The standard JPEG compression scheme uses a DCT transformation to describe the image. This transformation has a disadvantage non-locality that is overcome in the JPEG2000 compression scheme. JPEG2000 is wavelet-based compression where the fast approach of discrete wavelet transform has been used. The standard JPEG2000 uses the Watsons' perceptual quantization matrix to quantize the wavelet coefficients. This standard matrix provides reasonably good results but not the optimum one. Hence in this paper, a GP based quantization matrices (GQMs) are generated before quantization. These matrices are featured based matrices where the quantization

values vary according to the input image block (region). The compression is totally application dependent where the requirements can be set as a fitness function. Usually, in medical image application, the focus is on the visual perception of the compressed image. The proposed approach can be used for any other sensitive application i.e. military application.

An exemplary numerical expression in prefix form, developed by GP, is given as:

```
'minus(kozadivide(Wat_st,0.13117),kozadivide(kozadivide  
(minus(kozadivide(Wat_st,0.13117),kozadivide(kozadivide(0.8  
2031,0.70212),kozadivide(Wat_st,mylog(sin(0.34645))))),0.70  
212),kozadivide(Wat_st,minus(kozadivide(Wat_st,0.13117),ko  
zadivide(kozadivide(minus(kozadivide(Wat_st,0.13117),kozad  
ivide(kozadivide(0.82031,0.70212),kozadivide(Wat_st,mylog(  
sin(0.34645))))),0.70212),kozadivide(Wat_st,mylog(sin(0.3464  
5))))))')
```

ACKNOWLEDGMENT

The author would like to thank Deanship of Scientific Research at Majmaah University for supporting this work under Project No. 1440-92.

REFERENCES

- [1] H. Schwarz, D. Marpe and T. Wiegand, "Overview of scalable video coding extension of the H. 264/AVC standard," *IEEE Transaction on Circuits Systems Video Technology*, vol. 17, no. 9, pp. 1103-1120, 2007.
- [2] V. Sanchez. and J. Bartrina-Rapesta., "Lossless compression of medical images based on hevcc intra coding," in 2014 IEEE International Conference on Acoustics, Speech and Signal Processing, Florence, Italy, 2014.
- [3] K. Sayood, Introduction to data compression, 3rd ed., Academic Press, Morgan Kaufmann, 2006.
- [4] S. Park, "Lossless video compression," School of Electrical and Computer Engineering, Purdue University, West Lafayette, 2003.
- [5] R. W. R.C. Gonzalez, Digital Image Processing., Engle wood Cliffs: Pearson Education., 2002.
- [6] G. X. Yu and T. Vladimirova, "Image compression systems on board satellite," *Acta Astronaut*, vol. 64, pp. 988-1005, 2009.
- [7] A. Avramovic, "Lossless compression of medical images based on gradient edge detection," in 19th Telecommunications Forum Tel, Serbia, 2011.
- [8] M. G. B. Z.-C. S. Grgic, "Performance analysis of image compression using wavelets," *IEEE Transactions on Industrial Electronics*, vol. 48, no. 3, pp. 682-695, 2001.
- [9] L. R. Lucas, N. M. Rodrigues, L. D. S. Cruz. and S. M. M. d. Faria., "Lossless Compression of Medical Images Using 3-D Predictors," *IEEE Transactions on Medical Imaging*, vol. 36, no. 11, pp. 2250-2260, 2017.
- [10] C. Narmatha, M. P and M. S, "A Lossless Compression Scheme for Grayscale Medical Images Using a P2-Bit Short Technique," *Journal of Medical Imaging and Health Informatics*, vol. 7, no. 6, pp. 1196-1204, 2017.
- [11] H. M. A. Nyeem, "A digital watermarking framework with application to medical," Queensland University of Technology, Brisbane, Australia, 2014.
- [12] D. Clunie, "DICOM Supplement 61: JPEG 2000 Transfer Syntaxes," 14 January 2002. [Online]. Available: http://dicom.nema.org/dicom/supps/sup61_05.pdf. [Accessed 11 September 2006].
- [13] Y. K. R Loganathan, "An improved active contour medical image compression technique with lossless region of interest," in IEEE-3rd International Conference on Trendz in Information Sciences & Computing, India, 2011.
- [14] X. P. Alaitz Zabala, "Impact of lossy compression on mapping crop areas from remote sensing," *International Journal of Remote Sensing*, vol. 34, no. 8, pp. 2796-2813, 2013.
- [15] V. V. L. O. E. L. L. Nikolay N. Ponomarenko, "Adaptive visually lossless JPEG-based colour image compression," *Signal, Image and Video Processing*, vol. 7, no. 3, pp. 437-452, 2013.
- [16] X. Zhang, "Lossy Compression and Iterative Reconstruction for Encrypted Image," *IEEE Transactions on Information Forensics and Security*, vol. 6, no. 1, pp. 53-58, 2010.
- [17] K. O. E. R. R. G. P.C. Cosman, "Using vector quantization for image processing," *Proceedings of the IEEE*, vol. 81, no. 9, pp. 1326-1341, September 1993.
- [18] D.-S. Huang, "Radial basis probabilistic neural networks: model and application," *International Journal of Pattern Recognition and Artificial Intelligence*, vol. 13, no. 7, pp. 1083-1101, 1999.
- [19] A. A.-F. N. R. A.J. Hussain, "Image compression techniques: A survey in lossless and lossy," *Neurocomputing*, vol. 300, pp. 44-69, 2018.
- [20] J. J. B. Ramis, "The JPEG 2000 Compression Standard," Universitat de Barcelona, Barcelona, 2015.
- [21] W. Sweldens, "The Lifting Scheme: A Construction of Second Generation Wavelets," *SIAM Journal on Mathematical Analysis*, vol. 29, no. 2, pp. 511-546, 1998.
- [22] A. B. Watson, "DCT quantization matrices visually optimized for individual images," in *Proc. SPIE 1913 Human Vision, Visual Processing, and Digital Display*, San Jose, USA, 1993.
- [23] G. Y. J. S. J. V. A.B. Watson, "Visibility of wavelet quantization noise," *IEEE Transactions on Image Processing*, vol. 6, no. 8, pp. 1164-1175, August 1997.
- [24] A. M. Rufai, G. Anbarjafari and H. Demirel, "Lossy image compression using singular value decomposition and wavelet difference reduction," *Digital Signal Processing*, vol. 24, pp. 117-123, 2014.
- [25] S. A. e. a. Ruslan Kozhemiakin, "Lossy compression of Landsat multispectral images," in 5th Mediterranean Conference on Embedded Computing (MECO), Bar, Montenegro, 2016.
- [26] P. Soni, S. Ishwar, M. S. Swamy and P. K. Meher, "A fast 8x8 integer Tchebichef transform and comparison with integer cosine transform for image compression," in 56th International Midwest Symposium on Circuits and Systems (MWSCAS), Columbus USA, 2013.
- [27] P. Soni and P. M. Swamy, "A variable quantization technique for image compression using integer Tchebichef transform," in 9th International Conference on Information, Communications & Signal Processing, Tainan, Taiwan, 2013.
- [28] B. Xiao, G. Lu, Y. Zhang, W. Li and G. Wang., "Lossless image compression based on integer Discrete Tchebichef Transform," *Neurocomputing*, vol. 214, pp. 587-593, 22 June 2016.
- [29] T. D. Tran, "The binDCT: fast multiplierless approximation of the DCT," *IEEE Signal Processing Letters*, vol. 7, no. 6, pp. 141-144, 2000.
- [30] B. Fan, "Selective Compression of Medical Images via Intelligent Segmentation and 3D-SPIHT Coding," University of Wisconsin-Milwaukee, Milwaukee, Wisconsin, USA, 2018.
- [31] S. Victor and Bartrina-Rapesta., "Lossless compression of medical images based on hevcc intra coding," in IEEE International Conference on Acoustic, Speech and Signal Processing (ICASSP), Florence, Italy, 2014.
- [32] P. R. M, V. R. R. B and S. B. C, "The Lossless Medical Image Compression for Telemedicine Applications with Delimiter," *Journal of Advanced Research in Dynamical & Control Systems*, vol. 10, no. 3, pp. 74-79, February 2018.
- [33] M. Cyriac and Chellamuthu., "An object-based lossless compression approach for medical images using DPCM," *International Journal of Bioinformatics Research and Applications*, vol. 12, no. 1, pp. 59-71, 2016.
- [34] Z. Zuo, X. Lan, L. Deng, Y. S. and X. Wang, "An improved medical image compression technique with lossless region of interest," *Optik-International Journal for Light and Electron Optics*, vol. 126, no. 21, pp. 2825-2831, 2015.
- [35] H. Wang and Z. Liu, "Perceptual Quality Assessment of Medical Images," in *Encyclopedia of Biomedical Engineering*, Elsevier, 2018.
- [36] D. Venugopala, S. Mohana and R. Sivanantha, "An efficient block based lossless compression of medical images," *Optik*, vol. 127, no. 2, pp. 754-758, January 2016.

- [37] T. Bruylants, A. Munteanu and S. Peter, "Wavelet based volumetric medical image compression," *Signal Processing: Image Communication*, vol. 31, pp. 112-133, 2015.
- [38] S. D. Venugopal and S. R. Mohan, "An efficient block based lossless compression of medical images," *Optik*, vol. 127, pp. 754-758, 2016.
- [39] L. E. G. Ghadah Al-Khafaji, "International Journal of Computer Applications (," *Fast Lossless Compression of Medical Images based on Polynomial*, vol. 70, no. 15, pp. 28-32, May 2013.
- [40] B. Brindha and G. Raghuraman, "Region Based Lossless Compression for Digital Images in Telemedicine Application," in *International Conference on Communication and Signal Processing, India, 2013*.
- [41] V. Manpreet Kaur, "ROI based medical image compression for telemedicine application," *Procedia Computer Science*, vol. 70, pp. 579-585, 2015.
- [42] "Common image file formats," *Social Compare (Beta)*, 2017. [Online]. Available: <http://socialcompare.com/en/comparison/image-file-formats>.
- [43] L. M. Michele Larobina, "Medical Image File Formats," *Journal of Digital Imaging*, vol. 27, no. 2, pp. 200-206, April 2014.
- [44] W. Banzhaf, D. F. Frank, E. K. Robert and P. Nordin., *Genetic programming: an introduction: on the automatic evolution of computer programs and its applications*, San Francisco, CA, USA: Morgan Kaufmann Publishers Inc, 1998.
- [45] R. O. Duda, P. E. Hart and D. G. Stork, *Pattern Classification*, Second ed., New York, NY: Wiley-Interscience, 2000.
- [46] S. K. staff, "Magnetic resonance imaging (MRI) for brain tumours," *About Kids Health*, [Online]. Available: <https://www.aboutkidshealth.ca/Article?contentid=1334&language=English>.
- [47] S. Sara and S. A. Jonas, "Dynamic Maximum Tree Depth : A Simple Technique for Avoiding Bloat," in *LNCS - Genetic and Evolutionary Computation Conference (GECCO-2003)*, 2003.
- [48] S. Silva, "GPLAB - a Genetic Programming toolbox for MATLAB," 2015.

Protection of Ultrasound Image Sequence: Employing Motion Vector Reversible Watermarking

Rafi Ullah Habib¹, Fayez Al-Fayez²

Department of Computer Science and Information
College of Science, Majmaah University
Majmaah 11952, Saudi Arabia

Abstract—In healthcare information systems, medical data is very important for diagnosis. Most of the health institutions store their patients' data on third-party servers. Therefore, its security is very important, since the advent of advanced multimedia and communication technology, whereby digital contents are manipulated, copied, and duplicated without leaving any trace. In this paper, a reversible watermarking technique is applied to the patients' data (ultrasound image sequence). Since the traditional watermarking schemes can experience some permanent distortions that are not acceptable in the medical application. Thus, a reversible watermarking technique has been used, which can not only secure the ultrasound image sequence but also restore the original sequence back. For watermark embedding, the magnitude and phase angles of motion vectors of the image sequence are used that are obtained by using Full-Search block-based motion estimation algorithm. Before applying the motion estimation algorithm and watermark embedding, the histogram pre-processing is performed to avoid underflow/overflow. Unlike other state-of-the-art watermarking schemes that are reported in the last decades, the experimental results show that the proposed algorithm is simple, provides a much larger embedding capacity and better quality of the watermarked image sequence.

Keywords—Reversible watermarking; ultrasound sequence; full-search; motion vectors; side information

I. INTRODUCTION

Due to advances in the generation, communication and storage of the digital data, its security has gained the immense importance in multimedia applications and services. Medical images are more critical, where the use of manipulated images are more dangerous and can be life-threatening [1, 2]. Thus, the reliability of digital image/sequences, especially medical image/sequences is an open challenge for the researchers and Hospital Information Management Systems (HIMS). HIMS demands secure storage and transmission of the patient data where the end-user cannot tolerate a risk to get the distorted information. In such a scenario, simple watermarking methods are not feasible and hence a reversible watermarking is much needed, where the original content can be restored and the doctors can evaluate the unmodified data. In this paper, a motion vector reversible watermarking scheme has been introduced that is able to secure the ultrasound image sequence with improved imperceptibility and capacity. Although, reversible watermarks contain a large number of bits. However, in the proposed work, it does not affect the visual perception of the video.

The ultrasound videos have a vital role in the medical diagnostic system. For example, in [3], the authors have proposed an accurate classification model for stratification of liver disease in ultrasound. Watermarking using machine learning and bio-inspired algorithms are also used for the security of the digital contents [4]. Several critical parameters like visual perception, capacity, robustness, and security level, are to be considered while using the idealized watermarking system. For still images, the watermark(s) can be embedded in the spatial and frequency domain. For, images sequence, the temporal domain can be used, where the watermark(s) can be embedded in the estimated motion (motion vectors). The basic requirements for medical image watermarking are fidelity, robustness, imperceptibility, security, capacity, computational complexity, reliability, and reversibility [5]. Usually the distortion is visible but still, it is not acceptable when the exact genuine content is critical like the military and medical applications. To avoid such type of problem, a reversible watermarking has been used since last two decades, which have the ability to not only protect the digital content by embedding an assigned watermark but also recover the original content back. There are three major categories of reversible watermarking schemes as presented in [1]: compression-based reversible watermarking, histogram-based reversible watermarking and difference-expansion (DE) based reversible watermarking. In the above-mentioned categories, the compression based reversible watermarking is computationally complex and has limited embedding capacity. However, the remaining two methods are simple and provide high capacity for embedding the reversible watermark, which contains some side information along with the watermark bits. Several reversible watermarking algorithms have been developed in the last decade for protecting the images as well as videos [6 - 9].

Rest of the paper is organized as follow: Details of the current work about reversible watermarking are discussed in Section II. Short descriptions of motion estimation algorithms are discussed in Section III. The proposed watermark embedding and extraction procedures are presented in Section IV. Experimental and conclusions are presented in Section V and Section VI respectively. In Section VII, the research contributions and limitations are discussed.

II. LITERATURE REVIEW

Since the last three decades, digital watermarking has been used for protecting all types of media content like images, audio, videos and other printed materials, and documents.

Digital watermarking is used in many applications like military, medical, remote sensing, surveillance etc. Several reversible watermarking schemes have been designed for different applications.

In 2011, a reversible video watermarking scheme using motion vectors and prediction error expansion has been proposed by X. Zeng et.al [10]. The relationship between neighbouring frames and prediction errors are explored that significantly sharpen the distribution of prediction errors. Then histogram-modification is utilized for expanding the prediction errors. Due to the minor modification of pixel values, the video quality is preserved. In the phase angles of motion vectors and histogram modification, a little side information is generated that is combined with the pure watermark and then embedded in the video. The algorithm is tested on four different normal videos like Salesman, Foreman, Grandmother, Trevor, where unlike the normal videos, the medical image sequence has more capacity for embedding.

In [11], Diljit et al. proposed a reversible watermarking based on shifting histogram. The authors proposed a method to improve the imperceptibility and mitigate the capacity control problem. They also proposed the reversible watermark embedding based on prediction-error expansion. Similarly, Caldelli et al. present an overview of the reversible watermarking that is appeared in five years duration (from 2005 to 2010) [12].

In [13], a bi-directional video watermarking has been proposed. The authors have multiple scan images as watermarks and the same are trained by bi-directional associative memory (BAM) neural network. Its performance is evaluated with different kind of geometric and video processing attacks. The imperceptibility is about 50dB and the robustness is 1.0 in terms of normalized cross-correlation (NCC).

Loganathana and Kaliyaperumal proposed an HVS based video watermarking using BAM neural network and fuzzy inference system [14]. They are focusing on the robustness of the video for secure transmission over communication channels. The weight matrix is generated and embedded in the wavelet coefficients of all components of all frames. Fuzzy inference system takes the HVS characteristics as an input in the wavelet transform. Imperceptibility is 60 dB and the robustness is 1.0 in terms of NCC. Similarly, Agilandeewari and Ganesan proposed an optimal quaternion curvelet transform (QCT) based video watermarking [15]. They improve the three contradictory properties of watermarking; imperceptibility, robustness and security to the most notable attacks i.e. geometric attacks and image and video processing attacks.

In [16], DWT (discrete wavelet transform) based intravascular ultrasound video watermarking has been proposed. The ultrasound sequence is split into frames and applications of DWT; DCT (discrete cosine transforms) followed by Singular Value Decomposition (SVD) composes the watermark embedding technique and obtain an imperceptible watermarked video. The inverse of the above transformations is applied to the extraction side.

In 2014, an intelligent reversible watermarking technique in medical images using Genetic Algorithms (GA) and Particle Swarm Optimization (PSO) has been proposed by Naheed et.al. [17]. In this scheme, the authors have focused on the applications where the high embedding capacity and imperceptibility is required to maintain the reliability of the host content as well as embedded information. In this scheme, the authors are focusing on improving the imperceptibility and embedding capacity. The authors study the Luo's [8] additive interpolation error expansion scheme and enhanced it by incorporating with two popular intelligent techniques: GA and PSO. The better estimation of neighbouring pixel values is obtained by applying GA, exploiting the correlation of image pixel values, which results in an optimal balance between and imperceptibility and embedding capacity.

In 2014, B. Lie et.al [18] proposed a reversible watermarking algorithm for protecting medical images. The authors used differential evolution (DE) based watermarking. After applying the wavelet transformation and singular value decomposition (SVD), the textual data and signature information are embedded in the original medical images using recursive dither modulation (RDM) method. In addition, the strength of the watermark is optimally controlled by applying DE to design the quantization steps (QSs). This scheme is able to get better results in terms of the contradicting properties of watermarking i.e. imperceptibility and robustness.

In 2014, S. Acharjee et.al [19] proposed the watermarking scheme to protect medical image sequences based on motion estimation. The original image is watermarked inside the motion estimation of two consecutive frames of an echocardiograph video/image-sequence. The ultrasound images sequence has been used as test data. The correlation between the original and cover work has been calculated. In addition, SSIM (structural similarity index measure) and (PSNR (peak signal to noise ratio) are used to check the distortion and structural similarity between the original and the watermarked frame respectively.

In 2014, H. Yeh et.al, [20] proposed the watermarking algorithm for videos using the neighbouring similarity. Prediction encoding has been employed to compute the prediction errors and then all of the prediction errors are explored to develop a histogram-based reversible video watermarking algorithm. This algorithm has been tested on many images. Capacity and PSNR are calculated. For different block sizes, it gives different capacities and PSNRs. The PSNRs are around 51dB, which is much better for normal images and applications.

Reversible watermarking scheme for videos using motion vectors has been proposed in 2017 [21]. An efficient reversible watermark embedding method, based on the histogram based shifting, has been proposed. By designating, specific decoded reference frames, the distortion accumulation effects due to modification of the motion vectors have been overcome. All the extracted information can be recovered without loss of the original compressed video carrier.

In 2017, Arsalan et al. [22] has proposed the intelligent reversible watermarking scheme for protecting medical images. In this scheme, the embedding distortion has been reduced by

exploiting the concept of companding function. An integer wavelet transform has been used as an embedding domain for achieving reversibility of the host images. To avoid underflow and/or overflow, histogram processing is employed. In addition, for selecting the suitable coefficients for embedding watermark bits, the learning capabilities of genetic programming (GP) has been utilized. GP model is evolved that not only make an optimal tradeoff between the contradicting properties of watermarking i.e. imperceptibility and capacity but also exploit the wavelet coefficient hidden dependencies and information related to the type of subband.

A recursive histogram-based reversible video watermarking has been proposed by Vural and Yildirim in 2017 [23]. The algorithms are based on motion compensated interpolation or prediction error expansion. A recently developed recursive-histogram based reversible watermarking has been utilized for embedding the watermark bits in the motion compensated interpolation. In reversible video watermarking, the recursive histogram modification cannot be applied directly. Because ensuring the reversibility of each frame and distribution of total capacity among frames are encountered.

III. MOTION ESTIMATION ALGORITHMS

In literature, several block-matching algorithms for extracting the motion vectors are discussed in detail. Short descriptions of some of them are as follows.

A. Exhaustive Search/Full Search (ES/FS)

FS has a high computational cost because of its point selection in the selected window. In this BMA, for each non-overlapping blocks of the current frame, the reference frame is searched within the whole search space to find out the closest match. As the accuracy of motion vectors is focused, the FS method is used for obtaining the motion vectors [24].

B. Three-Step Search (TSS)

It is simple, robust, and near to optimality but its disadvantage is the uniform allocation of checkpoint patterns in the first step, where eight blocks around the centre block with fixed step size are selected for comparison. TSS is not efficient for small motions in a video [25].

C. New Three-Step Search (NTSS)

NTSS overcome the problem of small motion. It employs the centre-biased checkpoint pattern in the first step. NTSS yields better results than TSS and computational complexity is reduced by halfway search. NTSS is normally used for MPEG-1 and H.261 [26].

D. Four-Step Search (FSS)

In four-step search, a nine-point comparison is introduced, that starts with a step size of two and the selection of nine points around the search window. The distortion is calculated at each point and the points having the smallest distortion are selected [27].

E. Diamond Search (DS)

This BMA is similar to FSS, but the search point pattern is diamond-shaped rather than square. DS has two variants: large

and small DS patterns. The performance of DS is the same as that of NTSS, but its computational cost is lower [28].

F. Two-Dimensional Logarithmic Search (TDLS)

TDLS requires more steps than TSS but is more accurate with the large search window. It selects an initial step size and examines the central block and the four blocks at some predefined distance from the central block. If the best match is found, the step size is halved. This process continues until the step size reaches one [29].

G. Orthogonal Search Algorithm (OSA)

It is a combination of TSS and TDLS. The two points at a predefined distance from the centre of the search space in a horizontal direction are examined to determine for least distortion [30].

Comparative analysis of the performance of the BMAs discussed in this section, are given in Table I. The worst-case complexity is given in the second column, where the symbol p represents the search point. It is important to compare BMAs in order to identify which is most suitable for a given application.

IV. PROPOSED METHOD

A reversible watermarking approach has been developed for the security of ultrasound image sequence. Motion estimation is employed to process the ultrasound sequence to improve the capacity, imperceptibility and robustness. MATLAB environment is used for the experimental work. All the results are obtained by using MATLAB (2016a) running on Intel core i5, with 4GB RAM. The details of the ultrasound sequence are given in Table VII [31].

TABLE I. COMPARATIVE PERFORMANCE OF COMMON BMAS

BMA	Computational Complexity	Advantages	Disadvantages
ES/FS	$(2 * p + 1)^2$	Gives the best frame match and highest PSNR.	Computational cost is high.
TSS	$[1 + 8 \log 2(p + 1)]$	Low complexity and optimal performance. Best for MPEG2.	Cannot detect small motions.
NTSS	$[1 + 8 \log 2(p + 1)] + 8$	Efficient for small motions compared to TSS in terms of complexity.	More complex than TSS for large motion vectors.
FSS	$(18 \log 2[(p + 1) / 4] + 9)$	Efficient for small motions by reducing the initial step size.	More complex than TSS.
DS		Better than FSS in terms of MSE and search points.	Similar to NTSS.
TDLS	$[1 + 6 \log 2(p + 1)]$	Fewer complexes than TSS. uses MSE distance criterion.	Only suitable for texture-dominated pictures.
OSA	$[1 + 4 \log 2(p + 1)]$	Performs efficiently in terms of complexity as compared to TSS.	Very inefficient for small motions. Higher MSE than TSS.

- A Full-search block-matching algorithm (BMA) is applied to the input ultrasound sequence to obtain the temporal information in the form of motion vectors. As compared to all other block-based motion estimation algorithms, a drawback of Full Search is its time-consumption. Full Search BMA is used because it is more efficient in terms of accuracy. Full-Search calculates the cost function at each point in the selected window and produces accurate motion vectors as compared to other BMAs. In this work, the accuracy is focused rather than computational cost.
- As compared to the common videos, medical image sequences like EEG topo-maps have more embedding capacity, thus it is easy to make a tradeoff between the contradictory parameters i.e. robustness, imperceptibility and embedding capacity.
- A binary watermark is generated first and then embedded in the motion vectors of the ultrasound sequence. The watermark carries the patient information along with the side information. By using the patient information as a watermark, a risk of a mismatch between the patient information and the associated image/video can be tackled easily. The side information is used to recover the original content back. The details of side information are given in Section 3.2.
- Based on the magnitude and phase angle, the suitable motion vectors are selected for watermark embedding. The selected motion vectors are called candidate motion vectors (CMVs). Although, it is not necessary that motion vectors having large magnitude are suitable for watermark embedding. However, it depends on the associated macroblock. We cannot rely directly on the magnitude of the vector and thus, the associated macroblock are focused parallelly.
- The effect of watermark embedding is checked by using PSNR and SSIM.

A. Watermark Embedding

To overcome the potential problem of overflow and underflow, histogram pre-processing is performed before embedding the watermark bits into the host data. A very simple example of histogram modification is explained in Fig. 1 [17]. The figure shows the original image and the modified image obtained after modifying the histogram. The range of the gray levels is 0–255, and following the histogram modification, the gray level range becomes 1–254. This is because after modification, the grayscale value 0 is replaced by grayscale value 1 and grayscale 1 is replaced by the grayscale value 2 and so on. Similarly, grayscale 255 is replaced by gray scale 254 and grayscale 254 is replaced by 253, and so on.

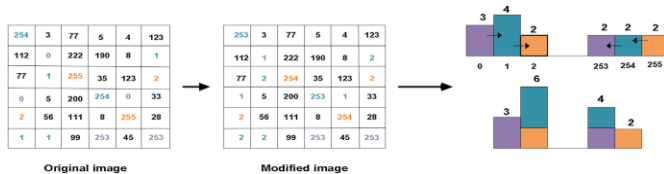


Fig. 1. Histogram of Original and Modified Images.

For reversibility, the frames of the ultrasound image sequence are embedded in the reverse order one-by-one. As shown in Fig. 3, the last frame is embedded first; the second last frame is embedded in next and so on until the first frame is embedded in the last. In the last frame, the only generated watermark bits are embedded where there is no information for reversibility. After this, some information used for extracting and recovering are recorded, such as motion vector and boundary map and is called side information. The details about the side information are given in Section 3.2. The side information is then combined with the watermark and embedded into the previous frame i.e. second last frame. This process continues until watermark bits along with the side information are embedded in the first frame [23]. The size of the side information is small and hence it will not affect the imperceptibility of the watermarked image sequence. The following procedure is followed for embedding the reversible watermark bits.

- 1) After performing the histogram pre-processing, the motion vectors are generated. Watermark is also generated and is ready for embedding in the suitable motion vectors.
- 2) Let we have the motion vector $MV_{i,j}$, where i is the i th frame and j is the j th motion vectors of the i th frame.
- 3) The horizontal and vertical components i.e. MV_x and MV_y are used for watermark embedding in the following manner.
- 4) The algorithm embeds the information in the ultrasound image sequence (video) in which reference frames is specified.
- 5) The vectors having greater magnitude from the selected threshold T , mean that it has fast moved other object. Assume that $S = \{MV_0, MV_1, MV_2, \dots, MV_{n-1}, \}$, $|S| = n$, where $|MV_i| \geq T, 0 \leq i < n$.
- 6) For each motion vector in S , the phase angle is computed $\theta = \tan^{-1}(MV_{iV}/MV_{iH})$, where $(MV_{iV}$ and MV_{iH} are the vertical and horizontal components of motion vectors, respectively.
- 7) Instead of embedding watermark bits in the magnitudes of the candidate motion vectors, Instead of embedding the data bit in the magnitude of motion vectors, the phase angle of two motion vectors is used for embedding watermark bits. The rule of embedding bits in the phases of motion vectors MV_2 and $MV_{2\pm 1}$, are written as follows:

The watermark bits are embedded in the following way:

If the embedding bit is 0, we need to have MV_2 , and $MV_{2\pm 1}$, such that:

$$0^\circ < |\theta_{2i} - \theta_{2i+1}| \leq 180^\circ, \text{ where } 0 \leq i \leq \lfloor \frac{n}{2} \rfloor \quad (1)$$

If the embedding bit is 1, we need to have MV_2 , and $MV_{2\pm 1}$, such that:

$$180^\circ < |\theta_{2i} - \theta_{2i+1}| \leq 360^\circ, \text{ where } 0 \leq i \leq \lfloor \frac{n}{2} \rfloor \quad (2)$$

If both the equations are not satisfied, then try the new motion vectors and continue until the entire watermark bits are embedded. The total angle i.e. $0^\circ - 360^\circ$ is divided into regions. These regions are defined in Tables II, III, and IV.

1 – bit – 2 regions area is used for watermark bit embedding as shown in Table II and Fig. 2. The 1 – bit – 2 region embedding can be extended to other multi-regions as shown in Tables III and IV. The whole range of 360° is divided into two regions where each region has range 180°. The watermark bits are embedded in the following way:

8) Compute the magnitude the motion vectors (MV) of the current frame that are obtained by using the Full-Search method.

9) Based on the pre-defined threshold T, select the set S for the candidate motion vectors (CMVs). $s = \{MV_0, MV_1, MV_2, \dots, MV_{n-1}\}, |S| = n$, where $(MV_{iV}^2 + MV_{iH}^2) \geq T, 0 \leq i < n$

10) Compute the phase angle of the CMV as: $\theta = \tan^{-1}(MV_{iV}/MV_{iH})$.

11) Select the pair of CMVs, MV_{2i} and $MV_{2i+1}, 0 \leq i < \lfloor \frac{n}{2} \rfloor$.

12) If the embedding bit is 0, then there are have two conditions.

a) If $0^\circ < |\theta_{2i} - \theta_{2i+1}| \leq 180^\circ$ then both the motion vectors will not be changed

b) If $180^\circ < |\theta_{2i} - \theta_{2i+1}| \leq 360^\circ$, then we will search for the new CMVs, MV'_{2i} and MV'_{2i+1} such that $|MV'_{2i}| \geq T$ and $0^\circ < |\theta'_{2i} - \theta_{2i+1}| \leq 180^\circ$ and $|MV'_{2i+1}| \geq T$ and $0^\circ < |\theta_{2i} - \theta'_{2i+1}| \leq 180^\circ$.

c) MSE_{2i} and MSE_{2i+1} are calculated. If $(MSE_{2i} < MSE_{2i+1})$, then replace MV_{2i} with MV'_{2i} , otherwise, replace MV_{2i+1} with MV'_{2i+1} .

13) If the embedding bit is 1, then there are two conditions again.

a) If $0^\circ < |\theta_{2i} - \theta_{2i+1}| \leq 180^\circ$ then both the motion vectors will not be changed.

b) If $180^\circ < |\theta_{2i} - \theta_{2i+1}| \leq 360^\circ$, then we will search for the new CMVs, MV'_{2i} and MV'_{2i+1} such that $|MV'_{2i}| \geq T$ and $180^\circ < |\theta'_{2i} - \theta_{2i+1}| \leq 360^\circ$ and $|MV'_{2i+1}| \geq T$ and $180^\circ < |\theta_{2i} - \theta'_{2i+1}| \leq 360^\circ$.

c) MSE_{2i} and MSE_{2i+1} are calculated. If $(MSE_{2i} < MSE_{2i+1})$, then replace MV_{2i} with MV'_{2i} , otherwise, replace MV_{2i+1} with MV'_{2i+1} .

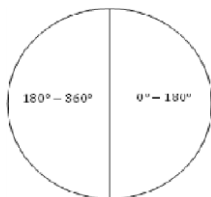


Fig. 2. 1 – bit – 2 Regions Embedding.

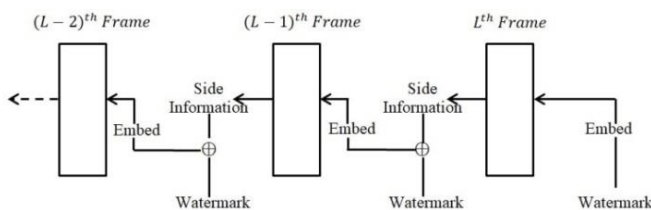


Fig. 3. Embedding Watermark Bits in the Motion Vectors of the Sequence Frames in the Reverse Order.

TABLE II. 1 – BIT – 2 REGIONS EMBEDDING

	Phase Angle Range	Embedded Data
Region 1	0°~180°	0
Region 2	180°~360°	1

TABLE III. 1 – BIT – 4 REGIONS EMBEDDING

	Phase Angle Range	Embedded Data
Region 1	0°~90°	0
Region 2	90°~180°	1
Region 3	180°~270°	0
Region 4	270°~360°	1

TABLE IV. 1 – BIT – 8 REGIONS EMBEDDING

	Phase Angle Range	Embedded Data
Region 1	0°~45°	0
Region 2	45°~90°	1
Region 3	90°~135°	0
Region 4	135°~180°	1
Region 5	180°~225°	0
Region 6	225°~270°	1
Region 7	270°~315°	0
Region 8	315°~360°	1

The embedding mechanism can be extended to *muti bit – multi Regions* embedding as shown in Table V.

TABLE V. 2 – BIT – 4 REGIONS EMBEDDING

	Phase Angle Range	Embedded Data
Region 1	0°~90°	00
Region 2	90°~180°	01
Region 3	180°~270°	11
Region 4	270°~360°	10

B. Side Information

For the exact recovery of the original frame on the extraction/verification side, side information along with the watermark bits are embedded. The side information is obtained during motion estimation and histogram modification steps. Motion vectors, boundary map and peak & zero point pairs are included in the side information. The number of motion vectors of a frame is

$$N(MV) = \frac{M \times N}{w \times h} \quad (3)$$

More motion vectors are recorded for the smaller blocks and vice versa. In the proposed scheme, the (16 × 16) block has been used. The other sizes of the block will be tested in the experiment. Overflow and underflow of the watermarked pixels are considered because of its use in the reconstruction of the frame. For example, the range of the pixel is (0 to 255) that can be modified to (-1 to 256). To avoid this issue, the authors in [10], proposed a pre-processing method where they find the zero point that is closed to the boundary i.e. (0 or 255), and the boundary pixels are removed and the pixels between the boundary pixels and zero points are

removed by modifying the histogram of the original frame. For histogram generating, the boundary pixels are not used and after embedding the watermark, new boundary pixels appear. Thus, the correct histogram can be obtained, while extracting the watermark on the verification side. In the proposed scheme, a binary vector is formulated to record all original boundary pixels that are assigned as 1, and pseudo boundary pixels that are assigned as 0. For most images or video frames, the length of the boundary map is very short or even zero. Side information along with the watermark bits are embedded in the previous frame. Similarly, the again the side information is generated and from the current frame and is combined with the watermark bits for embedding. The same procedure continues until we reach the first frame (embedding in the reverse order). The actually embedded data of a frame is given in Equation 4.

$$F'_i = \begin{cases} w_i, & i = L \\ si_i + w_i & 1 \leq i < L \end{cases} \quad (4)$$

where si represent side information and w represent original watermark bits. The ratio between the side information and the pure watermark capacity is shown in Table VI. As the block size is increased, then the side information decreased and vice versa. If the block size is decreased up to 4×4 , then a lot of side information is recorded and consequently, the imperceptibility will be highly affected. The block having size 16×16 have been used, where the side information is very low and increases the watermark strength by a maximum of four per cent. The threshold T is used while embedding the watermark that makes a tradeoff between the embedding capacity and imperceptibility.

C. Watermark Extraction

While extracting the embedded watermark from the frame, it must be ensured that the original frame and the corresponding reference frames are obtained. The extracting procedure along with recovering side information is shown in Fig. 4, which is the reverse of the order of the embedding procedure. All necessary information (reference frame and side information) for the extraction of embedded data can be prepared. Extracting the embedded watermark and recovering of the first frame employs the intra-frame approach, whereas all the other frames are processed by the inter-frame approach. After extracting the embedded information from the first frame i.e. F_1 , parse it to obtain pure watermark along with the side information that is used for extracting the embedded information from the frame F_2 . Similarly, after parsing the extracted data from F_2 , obtain the pure watermark and side information are obtained that are used for extracting the embedded information from the frame F_3 . This procedure continues until we reach the last frame.

TABLE VI. SIDE INFORMATION LENGTH FOR FRAMES

Number of motion vectors (One Frame)	8100
Total Frames	168
Boundary Map (average)	2
Side Information (Total)	1856
Watermark Capacity (Total)	112224
The ratio of side Information with watermark	1.65%

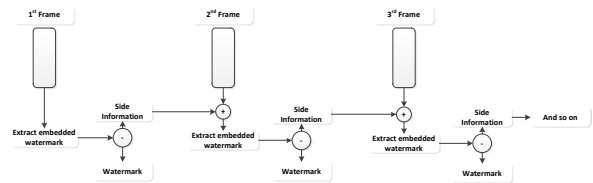


Fig. 4. Extraction of Watermark and Recovery of Side Information in the Order of Video Sequence.

Block diagram for extracting and restoring procedure for the original frame is shown in Fig. 5. Before extracting the F_i frame, we extract and restore the frame F_{i-1} to its original status. We continue the same procedure for all the frames to be extracted.

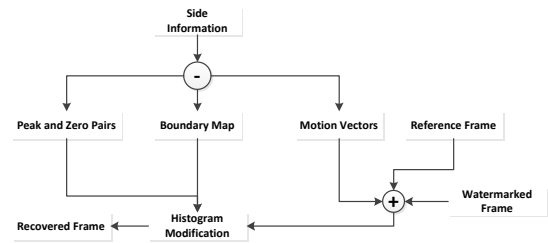


Fig. 5. Extracting and Restoring Procedure for the Original Frame.

V. EXPERIMENTAL RESULTS

MATLAB (2016a) environment has been used for the experimental results. The proposed method is applied to the ultrasound video. Watermark bits that contain the patient information are embedded. First, 1-bit-2 regions embedding is used and the results in terms of payload and PSNR are calculated as shown in Table VII. The payload varies according to the block size. In the experiments, 16×16 block is used and the watermark capacity is 112224. When the block size is reduced, i.e. 4×4 , then, the side information increased and hence the embedding watermark (Pure watermark and side information) strength increased. The payload mentioned in Table VII, is for four frames (frames number 7, 8, 9, 10). The capacity is measured in bits per block. In this work the capacity is $(8100 \times 4) \div 112220 = 0.29$.

TABLE VII. EXPERIMENTAL RESULTS, USING 1 – BIT – 2 REGIONS EMBEDDING

Features	Details
Image sequence/video	Ultrasound video
Total Frames	168
Size	1920 × 1080
Aspect Ratio	16:9
Bits per Pixel	24
Frame Rate	25 fps
Duration	6.72 Seconds
Block Size	16 × 16
Total MVs (One Frame)	8100
T (Threshold)	3
Average CMVs (One Frame)	668
Payload	112224 (For four Frames)
PSNR (Average)	41dB
SSIM (Average)	0.92

MATLAB environment has been used for the experimental results. A 6.72 seconds ultrasound sequence is chosen to test the proposed algorithm that contains 168 frames. Full-Search block-based motion estimation algorithm has been used to extract the motion vectors and then calculate the magnitude and phase angles of CMVs for embedding watermark bits. The four extracted frames (frame number 7, 8, 9, 10) are shown in Fig. 6.

As compared to the normal videos, the ultrasound image sequences have thousands of motion vectors as shown in Fig. 7. However, the highest magnitude of the motion vectors is 4.243, which is very low. The reason is that in the ultrasound video, the movement behaves like shrinking and expansion. The motion vectors of the four frames are shown in Fig. 7 and the corresponding watermarked motion vectors are shown in Fig. 8. As shown in Fig. 7, unlike the normal videos, the medical image sequences are more complex and are having thousands of motion vectors. Thus, the embedding capacity for watermark embedding is high and hence the reversible watermark that has high strength because of additional side information for reversibility can be embedded. The selection of suitable motion vectors is too easy because of many options.

In this paper, the ROI and RONI are not focused while embedding the watermark. Thus, for watermark embedding, it is too easy to select the high magnitude and phase angle in the motion vectors. Tackling of ROI and RONI is not easy without consulting the medical doctors and hospital management system.

Fig. 9 shows the watermarked frames (for frame number 7, 8, 9, and 10). In medical image applications, visual perception is very important, based on which the medical doctors decide. In the proposed scheme, the perceptual similarity (PSNR and SSIM) between the original and watermarked frames is much better and there is no problem for a doctor in diagnosis.

Performance comparison of the proposed technique with [6, 7, 32, 33] has been given in Table VIII. The comparison has been made with respect to several features like imperceptibility, watermark capacity, reversibility and ratio of extra side information with the pure watermark. In literature, several algorithms have been proposed to protect the ultrasound and other medical images but the reversible watermarking algorithms that specifically target the ultrasound image sequence were not found. For example, in [32], the authors have proposed to authenticate the ultrasound images using a compressed watermark. They are authenticating the images individually and they have not proposed the reversibility of the original image. Similarly, in [33], the authors have developed an algorithm for the security enhancement of medical videos. They are using motion vectors for watermark embedding but they are not targeting the ultrasound videos and have not mentioned anything for the reversibility of the original content. In this paper, the proposed approach is compared with the previous approaches [6, 7, 32, 33], where the authors are using normal/medical videos for embedding the watermarks /reversible-watermark(s). The experimental comparison shows that the proposed approach validates the usefulness of the reversible watermarking in

motion vectors for the protection of an ultrasound image sequence.

Fig. 10 shows the similarity of the watermarked image before transmission and the watermarked image received on the verification side. For this purpose, a Matlab function 'isequal' is used. It gives us the result logical 1 (True), because of the exact similarity. The similarity is checked by using the PSNR using Matlab function 'psnr'. The resultant show the Inf, which means the watermarked images on both the embedding and verification sides are identical. The watermarked frames number 7 and 8, before and after transmission are shown in Fig. 10, where the watermarked images are not attacked / tampered during the transmission. If the image is attacked, then the PSNR varies according to the strength of tampering or any other attack.

The table shows that the target is ultrasound image sequence/video for reversible watermarking, where the watermark bits are embedded in the motion compensation of the video. It can be seen that some of the papers did not provide the SSIM and hence it is difficult to analyze the structural similarity of the original and watermarked images properly. Just PSNR is not enough to measure the embedding distortion. The structural similarity of the watermarked images and videos must be checked.

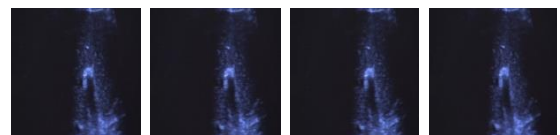


Fig. 6. Four Extracted Frames (Frames Number 7, 8, 9, 10) of the Ultrasound Video.

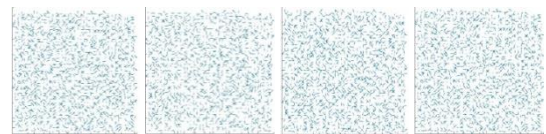


Fig. 7. The Motion Vectors of the Frames Given in Fig. 6.

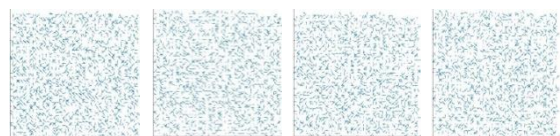


Fig. 8. The Watermark Embedded in the Motion Vectors of Fig. 3.

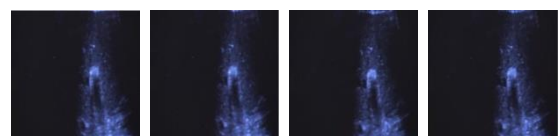


Fig. 9. Watermarked Frames (Frames Number 7, 8, 9, 10).

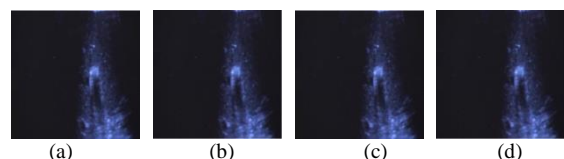


Fig. 10. (a~b) The Watermarked Frames before Transmission. (c~d) the Watermarked Frames after Transmission.

TABLE VIII. PERFORMANCE COMPARISON OF THE PROPOSED APPROACH WITH PREVIOUS APPROACHES

Features	Vural <i>et al.</i> Ref. [6]	Vural <i>et al.</i> Ref. [7]	Badshah <i>et al.</i> Ref. [32]	Acharjee <i>et al.</i> Ref. [33]	Proposed
Video	Normal	Normal	Ultrasound Images	Medical Videos	Ultrasound video
Watermark				Random	Patient Information
Watermark payload/capacity	High	High	Using Compressed watermark	Average	High
Side information	Yes	Yes	No	No	Yes
The ratio of side information with pure watermark	Not provided	2.3% to 3.04 %	No	No	≈ 1.65 %
Avoiding overflow/underflow	Do not tackle	Histogram modification	No	No	Histogram pre-processing
<i>Embedding in</i> motion vectors / spatial domain / frequency domain	Motion vectors	Motion vectors	Spatial domain	Motion Vectors	Motion vectors
Reversibility	Yes	Yes	No	No	Yes
PSNR between watermarked images on sender and receiver side	Not calculated	Not calculated	≈ 50 dB (Highly compressed watermark)	≈ 120	Inf
PSNR between original and watermarked image	Better but decreases when watermark bit increases	Better but decreases when watermark bit increases	Not calculated	Not calculated	≈ 41 db
SSIM	Not calculated	Not calculated	Not calculated	≈ 0.97	≈ 0.92
Robustness	Focusing on capacity and PSNR	Focusing on capacity and PSNR	Focusing on authentication and watermark recovery	Focusing on the recovered watermark	Semi-fragile

In Table VIII, the second and third columns show that the PSNR is much better but when the authors increase the watermark capacity, the PSNR decrease to 30dB. Similarly in the PSNR and SSIM in the second last column are very high. The authors have calculated PSNR and SSIM between the watermarked images on the embedding and receiving side. In the proposed approach, the PSNR between the watermarked image before and after the transmission is Inf, which means that the images before and after transmission are identical. They did not measure the distortion of the original image after embedding the watermark bits. All other PSNRs and SSIMs, given in Table VIII are used to measure the performance of watermark strength and its embedding.

VI. CONCLUSIONS

In this paper, a reversible watermarking scheme has been proposed to secure the sequence of ultrasound video, wherein the original video can be retrieved. For reversibility, side information along with pure watermark is embedded. The side information is obtained from the motion vectors, boundary map and peak-and-zero point pairs. Watermark is embedded by modifying the magnitude and phase angles of the selected motion vectors, which ensures the low embedding distortion.

Extracting and recovering of the first frame employs the intra-frame approach, whereas all the other frames are processed by the inter-frame approach. After extracting from F1, the extracted data can be parsed to get pure watermark as well as side information used for extracting process of F2 and the procedure continues until we reach the last frame. Experimental results demonstrated that the proposed approach provides higher capacity and imperceptibility.

In future, an intelligent system can be used to select the most suitable motion vectors, which will enhance the security and visual quality of ultrasound videos.

VII. RESEARCH CONTRIBUTIONS AND LIMITATIONS

In the last two decades, several numbers of watermarking techniques have been proposed trying to come up with an efficient solution for securing the digital content especially medical data. The proposed scheme is able to protect the ultrasound sequence along with the recovery of the original sequence back. The proposed scheme is able to hide patient information as a watermark without affecting the visual perception of the watermarked sequence. In addition, the scheme is able to avoid the risk of a mismatch between patient information and its associated image/video.

Some limitations can be considered in future work. For example, if the block size is reduced, then a lot of side information is recorded and consequently, the imperceptibility will be highly affected. Similarly, in reversible watermarking, once the original image/sequence is restored then there will be no legal or ethical claim for the restored image. In addition, once the watermark is removed then the security of the image/sequence discontinues.

ACKNOWLEDGMENT

The author would like to thank Deanship of Scientific Research at Majmaah University for supporting this work under Project No. 1440-94.

REFERENCES

- [1] Nyeem, HMA., 2014. A digital watermarking framework with application to medical image security, PhD thesis, Queensland University of Technology.
- [2] Shih, F. Y., Zhong, X., Cheng, I., Satoh, CS., 2018. An adjustable-purpose image watermarking technique by particle swarm optimization, *Multimedia Tools and Applications*, 77, 1623–1642.
- [3] Saba, L., et al., 2016. Automated stratification of liver disease in ultrasound: An online accurate feature classification paradigm, *Computer Methods and Programs in Biomedicine*, Elsevier, 130, 118-134.
- [4] Borra et al. 2018. *Digital Image Watermarking: Theoretical and Computational Advances*, CRC Book.
- [5] Qasim, AF., Meziane, F., and Aspin, R., 2017. Digital watermarking: Applicability for developing trust in medical imaging workflows state of the art review, *Computer Science Review*, Elsevier, 27, 45-60.
- [6] Vural, C., and Barak, B., 2016. Adaptive reversible video watermarking based on motion-compensated prediction error expansion with pixel selection, *Signal, Image and Video Processing*, Springer, 10(7), 1225–1232.
- [7] Vural, C., and Barak, B., 2015. Reversible video watermarking using motion-compensated frame interpolation error expansion. *Signal, Image and Video Processing*, Springer, 9(7), 1613-1623.
- [8] Zhao, Z., Yu, N., and Li, X., 2003. A novel video watermarking scheme in compression domain based on fast motion estimation, *International Conference on Communication Technology*.
- [9] Li, Z., Zhao, J., Hu, J., and Tu, H., 2015. A reversible video steganography algorithm for MVC based on motion vector, *Multimedia Tools Applications*, 74(11), 3759–3782.
- [10] Zeng, X., Chen, Z-Y., Chen, M., and Xiong, Z., 2011. Reversible video watermarking using motion estimation and prediction error expansion, *Journal of Information Science and Engineering*, 27, 465-479.
- [11] Diljith M. T., and Jeffrey J. R., 2007. Expansion Embedding Techniques for Reversible Watermarking, *IEEE Transactions on Image Processing*, 16(3), 721-730.
- [12] Caldelli, R., Filippini, F., and Becarelli, R., 2010. Reversible Watermarking Techniques: An Overview and a Classification, *EURASIP Journal on Information Security*, 2010, 1-19.
- [13] Agilandeeswari, L., and Ganesan, K., 2016. A bi-directional associative memory based multiple image watermarking on cover video, *Multimedia Tools and Applications*, 75(12), 7211-7256.
- [14] Loganathan, A., and Kaliyaperumal, G., 2016. An adaptive HVS based video watermarking scheme for multiple watermarks using BAM neural networks and fuzzy inference system, *Expert Systems with Applications*, 63, 412-434.
- [15] Agilandeeswari, L., Ganesan, K., 2018. RST invariant robust video watermarking algorithm using quaternion curvelet transform, *Multimedia Tools and Applications*, 77(19), 25431-25474.
- [16] Dey, N., et al. 2013. DWT-DCT-SVD based intravascular ultrasound video watermarking, *World Congress on Information and Communication Technologies*, India.
- [17] Naheed, T., Usman, I., Khan, TM., Dar, AH., and Shafique, MF., 2014. Intelligent reversible watermarking technique in medical images using GA and PSO, *Optik - International Journal for Light and Electron Optics*, Elsevier, 125, 2515-2525.
- [18] Lei, B., Tan, E-L., Chen, S., Ni, D., Wanga, T., and Lei, H., 2014. Reversible watermarking scheme for medical image based on differential evolution, *Expert Systems with Applications*, Elsevier, 41, 3178-3188.
- [19] Acharjee, S., Chakraborty, S., Ray, R., and Nath, S., 2014. Watermarking in motion vector for security enhancement of medical videos, *International Conference on Control, Instrumentation, Communication and Computational Technologies*, 589-594.
- [20] Yeh, H-L., Gue, S-T., Tsai, P., and Shih, W-K., 2014. Reversible video data hiding using neighbouring similarity, *IET Signal Processing*, 8(6), 579-587.
- [21] Niu, K., Yang, X., Zhang, and Y., 2017. Novel Video Reversible Data Hiding Algorithm Using Motion Vector for H.264/AVC, in *Tsinghua Science and Technology*, 22(5), 489-498.
- [22] Arsalan, M., Qureshi, AS, Khan, A., and Rajarajan, M., 2017. Protection of medical images and patient-related information in health care: Using an intelligent and reversible watermarking technique, *Applied Soft Computing*, Elsevier, 51, 168-179.
- [23] Vural, C., and Yıldırım, I., 2017. Reversible video watermarking through recursive histogram modification, *Multimedia Tools and Applications*, 76, 15513-15534.
- [24] H.-Y. Ding, Y. Zhou, Y. Yang and R. Zhang, "Robust blind video watermark algorithm in transform domain combining with 3D video correlation," *Journal of Multimedia*, vol. 8, no. 2, pp. 161-167, 2013.
- [25] O. S.Faragallah, "Efficient video watermarking based on singular value decomposition in the discrete wavelet transform domain," *AEU: International Journal of Electronics and Communication*, vol. 67, no. 3, pp. 189-196, March 2013.
- [26] W. Yu, D. Hu, N. Tian and Z. Zhou, "A novel search method based on artificial bee colony algorithm for block motion estimation," *EURASIP Journal on Image and Video Processing*, vol. 2017, no. 66, pp. 1-14, 2017.
- [27] M. S. A. K. and A. Ali, "Multiresolution video watermarking algorithm exploiting the block-based motion estimation,," *Journal of Information Security*, vol. 7, no. 4, pp. 260-268, July 2016.
- [28] T. Bernatin and G. Sundari, "Comparative analysis of different diamond search algorithms for block matching in motion estimation,," *ARNP Journal of Engineering and Applied Sciences*, vol. 12, no. 11, pp. 3550-3553, 2017.
- [29] M. Jakubowski and G. Pastuszek, "Block-based motion estimation algorithms—a survey,," *OPTO–Electronics Review*, vol. 21, no. 1, pp. 86-102, 2013.
- [30] S. P. Metkar and S. N. Talbar, "Fast motion estimation using modified orthogonal search algorithm for video compression,," *Signal, Image and Video Processing*, vol. 4, no. 1, pp. 123-128, 2010.
- [31] Gunnarsson, E, <https://www.videvo.net/video/ultrasoundscan-5/3306/>.
- [32] Badshah, G., Liew, S-C., Zain, J M., and Ali, M., 2016. Watermarking of ultrasound medical images in teleradiology using compressed watermark, *Journal of Medical Imaging, SPIE*, 3(1), 170011-170019.
- [33] Acharjee, S., Ray, R., Chakraborty, S., Nath, S., Dey, N., 2014. Watermarking in Motion Vector for Security Enhancement of Medical Videos, *International Conference on Control, Instrumentation, Communication and Computational Technologies (ICCICCT)*, 589-594.

Extended Fuzzy Analytical Hierarchy Process Approach in Determinants of Employees' Competencies in the Fourth Industrial Revolution

Phuc Van Nguyen¹

Rector, Ho Chi Minh City Open University (HCMCOU)
Ho Chi Minh City
Vietnam

Quyên Lê Hoàng Thủy Tô Nguyễn³

Office of Cooperation and Research Management
Ho Chi Minh City Open University (HCMCOU)
Vietnam

Phong Thanh Nguyễn²

Department of Project Management
Ho Chi Minh City Open University (HCMCOU)
Ho Chi Minh City, Vietnam

Vy Dang Bích Huỳnh⁴

Department of Learning Material
Ho Chi Minh City Open University (HCMCOU)
Ho Chi Minh City, Vietnam

Abstract—This paper explored the education factors and ranked their impacts on the employees' competencies development in Vietnam. Factors contributing to the employees' competencies in the Vietnamese context are proposed based on the literature review under the justification of experts' interviews. Then, the extended fuzzy analytical hierarchy process (EFAHP) approach was used to prioritize the importance of the factors affecting the employees' competency. The research finding confirmed the decisive role of teachers with the greatest weight of impact on the employees' competency, though there was a shift of teacher's role to that of facilitator in the Fourth Industrial Revolution education.

Keywords—Employees' competency; fuzzy logic; Extended Fuzzy Analytical Hierarchy Process (EFAHP)

I. INTRODUCTION

Competency is a multi-dimensional concept developed with two major descriptions, e.g., input approach (American school) and output approach (British school). In general, it refers to the ability to mobilize individual resources including knowledge, skills, and attitudes to successfully fulfill complex demands [1]. Competency is considered as a driver for any achievement, either at the micro or macro level [2]. A competency-based approach is beneficial for both the employer and employee. The employees can have a clear picture of labor market requirements for prior preparation during their school time. From the employer's perspective, a selection of the right staff with adequate competency has a significant impact on the organization's productivity and profitability. However, the gap competencies between supply and demand become more prominent—and Vietnam is no exception.

Vietnam is now encountering an increasing percentage of undergraduate unemployment while employers compete for recruitment of skilled workforces [3]. Furthermore, Vietnam ranked in the bottom percentile in human capital (70%) and qualified workforce (81%) despite impressive scores on the PISA test [4]. Education plays a decisive role in developing the

labor force competency. [5]. Bloch [6] provided empirical evidence for the purpose of improving education to meet the labor market demand. However, employment-oriented competency education in Vietnam was virtually ignored [7]. Trung and Swierczek [8] further identified the drawbacks in higher education such as weak research skills and academic knowledge of lecturers, dominant lecturing and note-learning, and minimal interaction between students and teachers.

This paper aims at ranking the education factors that determine employee competency. The findings are expected to help inform Vietnam's human resources allocation in higher education to suit the needs of the labor market, especially in the Fourth Industrial Revolution.

II. LITERATURE REVIEW

Various researchers identified competencies shortages as the primary cause of the high unemployment rate of university graduates. The problem becomes even more severe when the degree is not a credential but a social decoration. Higher education is responsible for the misalignment between the competencies provided by the university and the ones demanded by the labor market. Several institutional factors are reviewed as the main contributors to the employee competencies: teacher, information and communication technologies (ICT), competency-based approach education (CBA), university and industry partnership, competency-based curriculum (CBC), and competency-based curriculum.

The teacher is one of the critical components in the educational process and significantly impacts on the student's performance in the following categories: (1) instructional delivery, (2) classroom management, and (3) students' competency [9-11]. In the context of Industry 4.0 with rapid technology development, teachers must prepare students to deal with the jobs, technologies, and problems that have not been previously taught [12]. Therefore, lifelong learning is critical and the teacher becomes a facilitator whose major role is to inspire the students. An inspirational teacher can

encourage students' learning interest, motivate them to fulfill tasks they never thought that they could do, and encourage them to be creative in planning and organization of activities. This leads to their competency improvement [13, 14]. According to Hattie [15], the lesson mastery of students increased 17% with the teacher as a facilitator compared to 4% when instruction is student-centered. As a result, better employee competency can be found in the setting where the teacher actively guides the study method instead of merely transmitting the lesson content. Teachers also play an important role in managing a class; this role was ranked as one of the top five factors contributing to student achievement and positive attitudes. In fact, Oliver, et al. [11] found a reduction of 22% negative behavior in classrooms systematically managed by the teacher.

Various studies considered the role of ICT in improving learning outcomes and subsequently learners' competency by providing them the tool for lifelong learning [16-18]. In fact, it is an essential educational resource in the context of Industry 4.0 for both teachers and students. With ICT, the traditional teacher's role in knowledge delivery is challenged. Thus, the facilitator role should be directed. In addition, teachers can understand and address students' different learning styles thanks to the support of ICT. The learning process can be customized to adapt to each individual characteristics. Also, distance learning is allowed, thus maximizing the learner's performance. Soparat, et al. [19] found that five key competencies of students, including communication, critical thinking, problem-solving, life skill and technological applications, can be developed with the use of ICT in education. In summary, ICT is valuable for competency development by supporting online collaboration, networking, differentiation and customization [20].

Competency-based approach education (CBA) is considered as an innovation in higher education because it awards students credits based on competency rather than time spent in class. It clearly indicates the required competencies mastered by learners. As a result, students have opportunities to decide their learning process and either shorten or lengthen the time to complete a degree. Also, students know well the gap between what they know and what they are able to do. With this approach, rigid lesson plans and conveyed content are not a primary focus. Desired outcomes should be defined before preparing the course content. The learners are expected to achieve capacity for actions as a result of mobilizing all resources [21]. Therefore, the ability to apply mastered class knowledge to the working environment is assessed instead of just theoretical knowledge. CBA is found as a solution to mismatching between a professional's education and labor market requirements [20]. However, the credibility of CBA greatly depends on assessment quality [22].

According to Guimón [23], skills development for students is one of the benefits of academia and industry collaboration. Slotte and Tynjälä [24] found a significant improvement in workforce professionals from this partnership. Nowadays, a growing competency gap between education and market demand has pushed the exchange between university and industry. The curriculum development process is evidence of the advantage of firm and university linkage [25]. Under the

circumstances of technology development in the economy, education providers may successfully train the workforce if they closely align the curriculum in accordance with industry feedback. The contribution of industry to curriculum improvement can be diversified under various forms. Industry participation on the university academic board, in internships, and via adjunct faculty positions are potential activities provided by the firm to the university to promote student competency [26].

The development of students' core competencies is contemporarily the final goal of a university in designing a curriculum. It can solve the problem of the competency gap between the education and labor market demand once it mirrors the social and economic needs. A practical curriculum also motivates students and helps them realize their knowledge, skill and attitudes. Anastasiu, et al. [27] proposed a competency-based curriculum with three major parts of education including (1) professional courses and applications, (2) internship and apprenticeship, and (3) soft skills courses and application. The first part of this curriculum aims at providing major knowledge while the two latter ones emphasize the knowledge application together with various skills such as teamwork, organizational culture, project management and entrepreneurship.

III. RESEARCH METHODOLOGY

Analytical Hierachy Process (AHP), a modern structural analysis method invented by Saaty in 1980, is used to identify the factor weights [28-30]. This method is a combination of both qualitative and quantitative data in a logical hierarchy [31-34]. This method is flexible, visual, and helpful in criteria conflict-solving and for complex multi-criteria issues [35, 36]. As a result, the subjective and prejudiced attitude toward decision-making is alleviated [37, 38]. The main contribution of the fuzzy set theory is the ability to express ambiguous data [39]. The fuzzy theory also allows mathematical operators and programmers to apply to the fuzzy domain [40]. Fuzzy set theory consists of a special set of mathematical tools that are particularly suited to handle incomplete information or the ambiguity of object classes or situations in the most flexible way [41]. The steps of the extended fuzzy analytic hierarchy process method (EFAHP) are as follows [28, 41-45]:

Let $X = \{x_1, x_2, \dots, x_n\}$ be an object set, and $U = \{u_1, u_2, \dots, u_m\}$ be a objective set. Then, the m extent analysis values for each i^{th} object for m goals are obtained and shown as follows [46-49]:

$$\tilde{M}_{s_i}^j \text{ where } i = 1, 2, \dots, n; j = 1, 2, \dots, m$$

All the $\tilde{M}_{s_i}^j$ are triangular fuzzy numbers (TFNs).

Step 1: Obtain priority weights

The value of fuzzy synthetic extent on the i^{th} object is represented as Duru, et al. [50], [51]:

$$S_i = \left(\sum_{i=1}^m l_i, \sum_{i=1}^m m_i, \sum_{i=1}^m u_i \right) \otimes \left(\frac{1}{\sum_{i=1}^n u_i}, \frac{1}{\sum_{i=1}^n m_i}, \frac{1}{\sum_{i=1}^n l_i} \right)$$

Step 2: Comparing degrees of possibility

The degree of possibility of $M_2 = (l_2, m_2, u_2) \geq M_1 = (l_1, m_1, u_1)$ is defined as $V(M_2 \geq M_1)$ and can be equivalently expressed as follows [52]:

$$V(M_2 \geq M_1) = \text{hgt}(M_1 \cap M_2) = \mu_{M_2}(d)$$

$$= \begin{cases} 1 & \text{if } m_2 \geq m_1 \\ 0 & \text{if } l_1 \geq u_2 \\ \frac{l_1 - u_2}{(m_2 - u_2) - (m_1 - l_1)} & \text{otherwise} \end{cases}$$

where d is the ordinate of the highest intersection point D between μ_{M_1} and μ_{M_2} , as shown in Fig. 1.

Step 3: Obtaining the weight vector

The degree possibility for a convex fuzzy number to be greater than k convex fuzzy numbers M_i ($i = 1, 2, \dots, k$) can be defined by Duru, et al. [50]:

$$V(M \geq M_1, M_2, \dots, M_k) = V[(M \geq M_1) \text{ and } (M \geq M_2) \text{ and } \dots (M \geq M_k)] = \min V(M \geq M_i), i = 1, 2, \dots, k.$$

Assume that

$$d'(A_i) = \min V(S_i \geq S_k)$$

for $k = 1, 2, \dots, n; k \neq i$.

Then, the weight vector is given by:

$$W' = (d'(A_1), d'(A_2), \dots, d'(A_n))^T$$

where A_i ($i = 1, 2, \dots, n$) are n elements.

Step 4: Calculate the normalized weight vector

Via normalization, the normalized weight vectors are:

$$W = (d(A_1), d(A_2), \dots, d(A_n))^T$$

W is a nonfuzzy number.

Step 5. Ranking of the factors

After getting the weights of the factors, the ranking of all factors is determined.

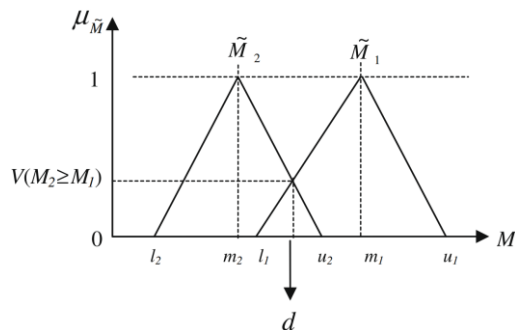


Fig. 1. The Intersection between M1 and M2.

IV. RESULTS AND DISCUSSION

In general, the factors which determine employees' competency in Vietnam were developed with a combination of both literature review and expert interviews by using the extended fuzzy analytic hierarchy process (EFAHP) technique. The ranking of factors influencing on the employees' competency are in Table I.

Vietnam is a country governed by Confucian philosophy in the teacher-student relationship. The teacher's role is evaluated as the most significant factor in the student's competency. Traditionally, the teacher was the tank of knowledge. Nowadays, knowledge is a lifelong learning process. Therefore, a great teacher is the one who can inspire the lifelong learner. The research findings do confirm the theory and provide empirical evidence on the role of the teacher. It is the first target for policy intervention to improve students' competencies. In order to reach the goal, guidelines and tools are two important contributors. The teacher can be considered as a guideline while ICT is a tool for students to realize their goals. The authors found that ICT is a driver for the adoption of e-learning in Vietnam, which is also a means of lifelong learning. Therefore, it is ranked second among the determinants of employees' competency.

The collaboration between university and industry is not so strong in Vietnam. It has caused a major bottleneck to obtaining a skilled workforce. Knowledge cannot be transformed to competency without practice. Therefore, a process should be established to get firms involved in education such as curriculum development, internship, and joint supervision of Ph.D students to conduct research. This also leads to a change to the Competency-Based Approach from traditional Content-Based Approach. The research findings also revealed a lesser role of the curriculum in employee competency in the context of the Fourth Industrial Revolution. The gap between employees' competency and market demand will only widen with technology changes. According to Lin [53], about 9% of world jobs in 2030 will be in new occupations. Transdisciplinary curricula have to be prepared to tackle the global change. Therefore, the education curriculum should be geared toward training students how to learn instead of what to learn and thus flexibly equip them with sufficient competency for future jobs [54].

TABLE I. RANKING OF FACTORS INFLUENCING ON THE EMPLOYEES' COMPETENCY MODEL

Factors	Rank
Teacher	1
University and industry partnership	3
Competency-based curriculum	5
Competency-based approach education (CBA)	4
Information and communication technologies (ICT)	2

V. CONCLUSION

This paper analyzed the contribution of each educational factor to employee competency by using the extended fuzzy analytic hierarchy process (EFAHP) technique. The findings confirmed the teacher's role, even in the context of the Fourth Industrial Revolution. Moreover, the finding found that method is more important than content. In the technology-driven economy, learners should be trained in methodology in order to quickly adapt to labor market demand. In addition, education should be treated and tailored to the markets' need in order to maximize the work benefit from individuals' competences. Educational factors should be well implemented in order to have a positive effect on employees' competency.

ACKNOWLEDGMENT

The authors gratefully acknowledge the Ho Chi Minh City Peoples Committee and Ho Chi Minh City Open University, Vietnam for supporting this research.

REFERENCES

- [1] D. S. Rychen and L. H. Salganik, *Key competencies for a successful life and well-functioning society*. Hogrefe Publishing, 2003.
- [2] D. C. McClelland, "Testing for competence rather than for intelligence.," *American psychologist*, vol. 28, no. 1, p. 1, 1973.
- [3] C. Bodewig and R. Badiani-Magnusson, *Skilling up Vietnam: Preparing the workforce for a modern market economy*. The World Bank, 2014.
- [4] WEF, "Readiness for the Future of Production Report 2018," in "World Economic Forum's System Initiative on Shaping the Future of Production," 2018.
- [5] S. Alainati, S. Alshawi, and W. Al-Karaghoul, "The effect of education and training on competency," 2010.
- [6] M. Bloch, "Situated learning: Legitimate peripheral participation," *Man*, vol. 29, no. 2, pp. 487-489, 1994.
- [7] D. Oliver, "The US Community College Model and Vietnam's Higher Education System," 2002.
- [8] T. Q. Trung and F. W. Swierczek, "Skills development in higher education in Vietnam," *Asia Pacific Business Review*, vol. 15, no. 4, pp. 565-586, 2009.
- [9] I. Arnold, "John Hattie: Visible learning: A synthesis of over 800 meta-analyses relating to achievement," *International Review of Education*, journal article vol. 57, no. 1, p. 219, May 02 2011.
- [10] C. M. Evertson and C. S. Weinstein, *Handbook of classroom management: Research, practice, and contemporary issues*. Routledge, 2013.
- [11] R. M. Oliver, J. H. Wehby, and D. J. Reschly, "Teacher classroom management practices: Effects on disruptive or aggressive student behavior," *Society for Research on Educational Effectiveness*, 2011.
- [12] T. A. Nguyen, P. T. Nguyen, and V. Peansupap, "Explaining model for supervisor's behavior on safety action based on their perceptions," *ARPN Journal of Engineering and Applied Sciences*, Article vol. 10, no. 20, pp. 9562-9572, 2015.
- [13] J. Cornelius-White, "Learner-centered teacher-student relationships are effective: A meta-analysis," *Review of educational research*, vol. 77, no. 1, pp. 113-143, 2007.
- [14] P. Van Nguyen, P. T. Nguyen, V. D. B. Huynh, and Q. L. H. T. T. Nguyen, "Critical factors affecting the happiness: A Vietnamese perspective," *International Journal of Economic Research*, Article vol. 14, no. 4, pp. 145-152, 2017.
- [15] J. Hattie, *Visible learning: A synthesis of over 800 meta-analyses relating to achievement*. routledge, 2008.
- [16] F. O. Pineida, "Competencies for the 21st century: integrating ICT to life, school and economical development," *Procedia-Social and Behavioral Sciences*, vol. 28, pp. 54-57, 2011.
- [17] P. T. Nguyen et al., "Construction project quality management using building information modeling 360 field," *International Journal of Advanced Computer Science and Applications*, Article vol. 9, no. 10, pp. 228-233, 2018.
- [18] P. T. Nguyen, T. A. Nguyen, Q. L. H. T. T. Nguyen, and V. D. B. Huynh, "Application of SWOT for construction company quality management using building information modelling," *Journal of Mechanics of Continua and Mathematical Sciences*, vol. 13, no. 05, pp. 25-33, 2018.
- [19] S. Soparat, S. R. Arnold, and S. Klayson, "The development of Thai learners' key competencies by project-based learning using ICT," *International Journal of Research in Education and Science*, vol. 1, no. 1, pp. 11-22, 2015.
- [20] O. Gavrishina and Y. Zaharov, "Competency-Based Approach in Training Mathematicians: Challenges of Time," *Procedia-Social and Behavioral Sciences*, vol. 214, pp. 212-221, 2015.
- [21] N. Hirtt, "L'approche par compétences: une mystification pédagogique," *L'école démocratique*, vol. 39, pp. 1-34, 2009.
- [22] K. L. McClarty and M. N. Gaertner, "Measuring mastery: Best practices for assessment in competency-based education," *AEI Series on Competency-Based Higher Education*, 2015.
- [23] J. Guimón, "Promoting university-industry collaboration in developing countries," *World Bank*, vol. 3, 2013.
- [24] V. Slotte and P. Tynjälä, "Industry-university collaboration for continuing professional development," *Journal of Education and Work*, vol. 16, no. 4, pp. 445-464, 2003.
- [25] P. Matkovic, P. Tumbas, M. Sakal, and V. Pavlicevic, "Curriculum Development Process Redesign Based on University-Industry Cooperation," in *Proceedings of the 6th International Conference on Education and New Learning Technologies (EDULEARN)*, 2014, pp. 4113-4123.
- [26] M. Perkmann and K. Walsh, "University-industry relationships and open innovation: Towards a research agenda," *International Journal of Management Reviews*, vol. 9, no. 4, pp. 259-280, 2007.
- [27] L. Anastasiu, A. Anastasiu, M. Dumitran, C. Crizboi, A. Holmaghi, and M. Roman, "How to Align the University Curricula with the Market Demands by Developing Employability Skills in the Civil Engineering Sector," *Education Sciences*, vol. 7, no. 3, p. 74, 2017.
- [28] V. D. B. Huynh, P. V. Nguyen, Q. L. H. T. T. Nguyen, and P. T. Nguyen, "Application of Fuzzy Analytical Hierarchy Process based on Geometric Mean Method to Prioritize Social Capital Network Indicators," *International Journal of Advanced Computer Science and Applications*, vol. 9, no. 12, pp. 182-186, 2018.
- [29] C. Meidiana, I. D. Nurfitriya, and K. E. Sari, "Multi-criteria evaluation for determination of anaerobic di-gester location in rural area," *International Journal of Recent Technology and Engineering*, Article vol. 7, no. 4, pp. 153-157, 2018.
- [30] V. D. B. Huynh, P. Van Nguyen, Q. H. T. T. Nguyen, and P. T. Nguyen, "Application of Fuzzy Analytical Hierarchy Process based on Geometric Mean Method to prioritize social capital network indicators," *International Journal of Advanced Computer Science and Applications*, Article vol. 9, no. 12, pp. 182-186, 2018.
- [31] P. Choudhary and U. Singh, "Ranking terrorist organizations network in India using combined Sna-Ahp approach," *International Journal of Recent Technology and Engineering*, Article vol. 7, no. 4, pp. 168-172, 2018.
- [32] P. Van Nguyen, P. T. Nguyen, Q. L. H. Thuy, T. Nguyen, and V. D. B. Huynh, "Calculating Weights of Social Capital Index Using Analytic Hierarchy Process," *International Journal of Economics and Financial Issues*, vol. 6, no. 3, pp. 1189-1193, 2016.
- [33] P. Van Nguyen, P. T. Nguyen, Q. L. H. T. T. Nguyen, and V. D. B. Huynh, "Calculating weights of social capital index using analytic hierarchy process," *International Journal of Economics and Financial Issues*, Article vol. 6, no. 3, pp. 1189-1193, 2016.
- [34] D. L. Luong, D. H. Tran, and P. T. Nguyen, "Optimizing multi-mode time-cost-quality trade-off of construction project using opposition multiple objective difference evolution," *International Journal of Construction Management*, Article in Press 2018.

- [35] P. T. Nguyen, P. Van Nguyen, Q. L. H. T. To Nguyen, and V. D. B. Huynh, "Project success evaluation using TOPSIS algorithm," *Journal of Engineering and Applied Sciences*, Article vol. 11, no. 8, pp. 1876-1879, 2016.
- [36] P. T. Nguyen and V. Likhitrungsilp, "Identification risk factors affecting concession period length for public-private partnership infrastructure projects," *International Journal of Civil Engineering and Technology*, Article vol. 8, no. 6, pp. 342-348, 2017.
- [37] A. L. Ode, L. Samang, and I. Ramli, "Analysis of the priority of the improvement of the provincial road status in mamminasata region at south sulawesi based on analytic hierarchy process," *International Journal of Innovative Technology and Exploring Engineering*, Article vol. 8, no. 4S, pp. 13-17, 2019.
- [38] K. Madhuvanthi, M. K. Nallakaruppan, N. C. Senthilkumar, and S. Siva Rama Krishnan, "Car sales prediction using machine learning algorithms," *International Journal of Innovative Technology and Exploring Engineering*, Article vol. 8, no. 5, pp. 1039-1050, 2019.
- [39] P. T. Nguyen, N. B. Vu, L. Van Nguyen, L. P. Le, and K. D. Vo, "The Application of Fuzzy Analytic Hierarchy Process (F-AHP) in Engineering Project Management," in *2018 IEEE 5th International Conference on Engineering Technologies and Applied Sciences, ICETAS 2018*, 2019.
- [40] N. Geetha Lakshmi and D. Shanmuga Priyaa, "Handling of indeterminacy for trust aware energy consumption using adaptive intuitionistic fuzzy environment in wireless sensor networks," *International Journal of Recent Technology and Engineering*, Article vol. 7, no. 4, pp. 239-247, 2018.
- [41] N. T. Phong and N. L. H. T. T. Quyen, "Application fuzzy multi-attribute decision analysis method to prioritize project success criteria," *AIP Conference Proceedings*, vol. 1903, no. 1, p. 070011, 2017.
- [42] P. T. Nguyen, V. Likhitrungsilp, and M. Onishi, "Prioritizing factors affecting traffic volume of public-private partnership infrastructure projects," *International Journal of Engineering & Technology*, vol. 7, no. 04, pp. 2988-2991, 2018.
- [43] N. T. Phong, V. N. Phuc, and T. T. H. L. N. Quyen, "Application of Fuzzy Analytic Network Process and TOPSIS Method for Material Supplier Selection," *Key Engineering Materials*, vol. 728, pp. 411-415, 2017.
- [44] N. T. Phong and N. L. H. T. T. Quyen, "Application fuzzy multi-attribute decision analysis method to prioritize project success criteria," in *AIP Conference Proceedings*, 2017, vol. 1903.
- [45] T. N. Phong, V. N. Phuc, and T. T. H. L. N. Quyen, "Application of fuzzy analytic network process and TOPSIS method for material supplier selection," in *Key Engineering Materials* vol. 728, ed, 2017, pp. 411-415.
- [46] M. K. Moghadam, A. R. M. Jahromi, and A. S. Nooramin, "A fuzzy AHP decision support system for selecting yard cranes in marine container terminals," *WMU Journal of Maritime Affairs*, vol. 10, no. 2, pp. 227-240, 2011.
- [47] İ. Ertuğrul and N. Karakaşoğlu, "Comparison of fuzzy AHP and fuzzy TOPSIS methods for facility location selection," *The International Journal of Advanced Manufacturing Technology*, vol. 39, no. 7, pp. 783-795, 2008.
- [48] N. T. Phong, V. Likhitrungsilp, and M. Onishi, "Developing a stochastic traffic volume prediction model for public-private partnership projects," in *AIP Conference Proceedings*, 2017, vol. 1903.
- [49] P. T. Nguyen, V. Likhitrungsilp, and M. Onishi, "Prioritizing factors affecting traffic volume of public-private partnership infrastructure projects," *International Journal of Engineering and Technology(UAE)*, vol. 7, no. 4, pp. 2988-2991, 2018.
- [50] O. Duru, S. T. Huang, E. Bulut, and S. Yoshida, "Multi-layer quality function deployment (QFD) approach for improving the compromised quality satisfaction under the agency problem: A 3D QFD design for the asset selection problem in the shipping industry," *Quality & Quantity*, pp. 1-22, 2013.
- [51] J. R. S. C. Mateo, "FAHP," *Multi Criteria Analysis in the Renewable Energy Industry*, pp. 77-93, 2012.
- [52] U. Cebeci and D. Ruan, "A multi-attribute comparison of Turkish quality consultants by fuzzy AHP," *International Journal of Information Technology & Decision Making*, vol. 6, no. 01, pp. 191-207, 2007.
- [53] J. Lin, "Technological adaptation, cities, and new work," *Review of Economics and Statistics*, vol. 93, no. 2, pp. 554-574, 2011.
- [54] V. D. B. Huynh, Q. L. H. T. T. Nguyen, P. Van Nguyen, and P. T. Nguyen, "Application Partial Least Square Structural Equation To Develop A Job Search Success Measurement Model," *Journal of Mechanics of Continua and Mathematical Sciences*, vol. 13, no. 5, 2018.

A Recurrent Neural Network and a Discrete Wavelet Transform to Predict the Saudi Stock Price Trends

Mutasem Jarrah¹, Naomie Salim²

School of Computing, Faculty of Engineering
Universiti Teknologi Malaysia – UTM, Johor Bahru, Malaysia

Abstract—Stock markets can be characterised as being complex, dynamic and chaotic environments, making the prediction of stock prices very tough. In this research work, we attempt to predict the Saudi stock price trends with regards to its earlier price history by combining a discrete wavelet transform (DWT) and a recurrent neural network (RNN). The DWT technique helped to remove the noises pertaining to the data gathered from the Saudi stock market based on a few chosen samples of companies. Then, a designed RNN has trained via the Back Propagation Through Time (BPTT) method to aid in predicting the Saudi market's stock prices for the next seven days' closing price pertaining to the chosen sample of companies. Then, analysis of the obtained results was carried out to make a comparison with the results from those employing the traditional prediction algorithms like the auto regressive integrated moving average (ARIMA). Based on the comparison, it was found that the put forward method (DWT+RNN) allowed more accurate prediction of the day's closing price versus the ARIMA method employing the mean squared error (MSE), mean absolute error (MAE) and root mean squared error (RMSE) criterion.

Keywords—Recurrent Neural Network (RNN); Discrete Wavelet Transform (DWT); deep learning; prediction; stock market

I. INTRODUCTION

Can time series analysis be utilised for estimating stock trends? The short answer is yes. Time series analysis can surely be utilised for estimating stock trends [1]. However, the caveat here is that it is not possible to predict with 100% accuracy; the idea here to remain profitable is to be correct for more than 50% of the time. Time series prediction is important and has been overlooked often in the field of machine learning. It is noteworthy as various prediction problems are associated with a time component. These problems are overlooked as this component of time creates the issues regarding time series making them more complex to deal with [2].

Evaluation of time series includes developing models that encompass or explain an observed time series that help to understand the primary causes. In this study domain, the question 'why' is sought for a dataset of time series. It often involves making assumptions regarding the data form and breaking down time series into its representative elements. The time series evaluation provides a group of methods that help to better understand the dataset in an efficient way, and breaking down of the time series into 4 constituent elements could perhaps be the most helpful amongst these [3]. An example pertaining to the time series' components of Alinma Bank is shown in Fig. 1:

- Level or Observed. The time series' baseline value if they were to be a straight line.
- Trend. The series' voluntary and often linearly increasing or decreasing behaviour that is gradual.
- Seasonality. The series' optional repetitive patterns of behaviour or cycles over time.
- Residual or Noise. The optional changes pertaining to the observations that could not be described by the model.

Each of these time series is associated with an observation or a level. Most of these include noise or residual, while the trend and seasonality are optional. In a time series to determine the stock closing price each day, a key role is played by the stock exchanges for the development of main economic sectors. Thus, these have a considerable impact on people and nations worldwide. Predicting the stock market has been an interesting topic sparking interest amongst numerous experts that hail from different domains [4]. To keep a track on the stock market movement, various algorithms and methods have been used, such as Deep Neural Networks and Support Vector Machines [5, 6]. By assessing the historical information, these techniques can be applied to determine trends of the stock market. However, predicting the stock market is not an easy task due to non-stationary, non-linear, volatility and chaotic nature pertaining to the information [7, 8]. With the rise in trading, many experts have attempted to develop methods and techniques to assess and forecast future stock prices.

This study evaluates the application of the recurrent neural network to predict the stock market by employing real-time and experimental data pertaining to the Saudi stock market. This research plays a key part in the following manner:

- The development of an innovative stock price estimation model that can use the RNN and DWT techniques.
- Employing real-time data sourced from the Saudi stock market to analyse and train the recommended model.

The research paper is structured as follows: Section II presents an overview of works pertaining to the estimation of stock markets. Section III explains the recommended model and its attributes, while Section IV presents and discusses the experimental results. Section V offers the conclusion and recommendations for prospective works.

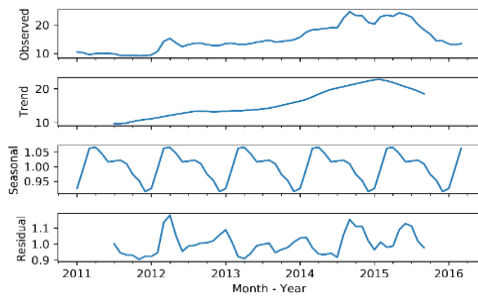


Fig. 1. Time Series Parts.

II. RELATED WORK

This section provides an overview regarding related studies that were focused on estimating and predicting the trends pertaining to the stock market. Presentation of various studies was done aimed at predicting the stock market's behaviour for decades. Nevertheless, this effort turned out to be much difficult than anticipated since the stock market is characterised by its chaotic, complex and dynamic nature [9]. Various data sources and parameters that include insignificant signal-to-noise ratio (SNR) need to be considered [10]. Such parameters only increase the complexity of predicting the trends of the stock market. Even though numerous scholars have developed and proposed many different estimation models to forecast the stock market prices, they did not give accurate results [11].

The economic time series models derived based on economic theories are the key foundation in predicting a series of insightful information in the 20th century. However, these hypotheses cannot be applied directly to estimate and forecast market prices that cause an external impact. Due to the development of the multi-layer concept, artificial neural networks (ANN) are being opted as a tool to perform prediction. Apart from other techniques, researchers have employed different models for predicting the series of market prices by using deep learning methods. A paper has recently been published on estimating stock market prices by deploying ANN. Various other studies used different techniques to predict trends in the stock market. Tools that were employed for technology prediction were brought in for economic prediction, which offered extensive success. Lee, Lee, and Oh (2005) employed the Lotka-Volterra model that was actually derived by observing the relationship between the predator and prey. It is employed to predict the diffusion pertaining to rival technologies. They had employed this to predict the Korea stock market [12]. Yu and Huarng (2008) used bivariate neural networks (BNN), BNN-based model of fuzzy time series with substitutes and BNN-based fuzzy time series by employing neural networks to predict fuzzy time series. The best results were obtained with the BNN-based model of fuzzy time series along with substitutes [13]. Zhu, Wang, Xu, and Li (2008) used the improved and basic neural network models to show that trading volume can improve the performance of neural networks predicting [14]. Zhang and Wu (2009) employed BPNN (back propagation neural network) and BCO (bacterial chemotaxis optimisation) on S&P 500 index and discovered that the put forward fusion model (IBCO-BP) gave superior prediction accuracy, lesser computational complexity as well as a lesser training time [15].

Majhi, Panda, and Sahoo (2009) assessed CFLANN (cascaded functional link artificial neural network), and the LMS model and found the CFLANN model to work the best, followed by FLANN and LMS models [16]. When ANN and ARIMA were assessed by Hamzacebi, Akay, and Kutay (2009), they observed that employing ANN for direct prediction gave superior result and also suggested to perform other studies before standardising the findings [17]. Liao and Wang (2010) used the model stochastic time that was for the effective neural network to demonstrate that few of the predicting results pertaining to the worldwide stock indices as well as the model gave the predicted results [18]. Patel et al. (2015) combined the machine learning models to forecast the trends for the stock market. The research emphasises on forecasting the future values for stock index. Few indices, such as CNX Nifty and S&P Bombay Stock Exchange (BSE) Sensex from Indian stock exchanges, were employed for assessing the experiment. The conclusions mentioned below have been deduced from the literature survey.

The current prediction models make use of the past data of the stock market for predicting the definite features for stock prices. The data need to be prepared to forecast the stock market prices post obtaining the descriptive factors by observing the changing average pertaining to the distinct block length, which provided balanced results in 20-100 days, and the current systems do not perform these functions [3, 19] Qiu, M., & Song, Y. Two basic types of input variables (2016) were employed to forecast the trend pertaining to the daily stock market index. An optimised artificial neural network (ANN) model is employed in this study that contributes to the prediction of the trend pertaining to the next day's price for the Japanese stock market index. This enhances the accuracy of the prediction for the stock market index trend in the future. Genetic algorithms (GA) were employed to optimise the ANN model [20].

Chen W. et al. (2017) applied a model based on RNN (Recurrent Neural Networks) with GRU (Gated Recurrent Units) for the prediction of stock volatility pertaining to the stock markets in China [21]. Wei Bao, Jun Yue and Yulei Rao (2017) put forward a novel deep learning framework in which combination of stacked autoencoders (SAEs), wavelet transforms (WT) and long-short term memory (LSTM) was done to forecast stock price. When predicting for the first time, introduction of SAEs for hierarchically extracted deep features into the stock price is done [22].

Pang, X. et al. (2018) employed a novel neural network approach to obtain a better prediction of the stock market. Data were obtained via the running stock market to analyse in real-time and off-line as well as findings from the analytics and visualisations to demonstrate Internet of Multimedia of Things to perform stock market analysis. Based on the deep learning of word vector, the notion of 'stock vector' was demonstrated. Now one index or one stock index cannot be characterised with the input, but rather the historical data that include multiple stocks along with high dimensions [23]. As a high-tech technique, Fischer, T. and C. Krauss (2018) used LSTM (long short-term memory) networks for sequence learning. These networks are not often used in prediction of economic time series, yet these are apt for this field [24].

III. PROPOSED MODEL

In this study, a two stages model is recommended for estimating the stock market price as depicted in Fig. 2. The first stage makes use of DWT to break down the stock price time series to remove noise, while in the second stage; a RNN is used to produce output that is seven steps ahead. The following shows the used methods for each stage in more detail.

A. Discrete Wavelet Transform

DWT finds application in numerous fields like financial time series and signal processing due to its strong feature extraction capacity. The main characteristic of the wavelet transform is that the frequency components of financial time series along with time can be analysed concurrently versus the Fourier transform. Consequently, a wavelet is helpful in dealing with financial time series that are highly irregular.

This research work employs the Haar function as the basis function for wavelet since it not only break downs the financial time series into frequency and time domain but also decreases the processing time considerably [25, 29-30]. The time complexity of $O(n)$ is associated with the wavelet transform considering the Haar function as the basis, where n signifies the size pertaining to the time series. The wavelet function pertaining to continuous wavelet transform (CWT) can be represented as:

$$\phi_{-}(a, \tau)(t) = 1/\sqrt{a} \phi((t - \tau)/a) \quad (1)$$

Where a signifies the scale factor, τ denotes the translation factor and $\phi(t)$ forms the basis wavelet.

B. Recurrent Neural Network

A class of artificial neural network is the recurrent neural network (RNN) in which connections exist amongst nodes form a directed graph in a sequence. This facilitates exhibiting the behaviour of temporal dynamic for a time sequence. In contrast to feedforward neural networks, RNNs can process sequences of inputs by employing their internal state (memory) [9, 26].

In general, two different operations are associated with the hidden and output layers. First, the inputs coming from all the sources are added by the net operation. The out operation is involved in the second operation, which allows achieving a nonlinearity pertaining to its sigmoid function as well as calculated values $\tanh(\text{net}(S_1))$ or $\text{SoftMax}(\text{net}(S_1))$ is employed [27].

$$S_1 = f(U_1 X_1 + W_{01}) \quad (2)$$

$$S_1 = \tanh(U_1 X_1 + W_{01}) \quad (3)$$

$$(y_1)^\wedge = \text{softmax}(V_1 S_1) \quad (4)$$

Where

S_1 denotes the input for the current step. The function f represents the nonlinearity like \tanh or SoftMax as presented in Eqs. 2 and 3, which is required for estimation of the 1st hidden state and is initialised to 0 s.

U_1 represents the weight at input x_1 .

x_1 signifies the input at time step t .

W_{01} denotes the weight from a previous step.

V_1 refers to the weight that was obtained from the hidden layers.

A common term employed to represent the calculation procedure is ‘Forward pass’ that is used to compute prediction scores. Moreover, these values are amended via the backward back-propagation process. In this research work, employing of the Back Propagation Through Time (BPTT) algorithm was done as it allowed updating the weights by gathering the input values at various time intervals via RNNs training and efficiently frame the sequence prediction issues for RNNs [26]. In the put forward DRNN model, which was developed to forecast the stock prices, allocation of a sequence for the sequential collection was done for a daily dataset of a single stock that fell within a fixed time frame (N days). The daily dataset employs sequence learning characteristics like the day’s closing in N days, which helps to explain the different stock performances.

The earning rate was employed to determine the sequence performance. The rate was determined by averaging the closing prices pertaining to the stock market for three days post sequence generation and then making a comparison with the final day of the present sequence. The put forward model includes a single input layer analogous to the one described earlier, including sequence learning characteristics. To calculate the hidden vector sequence, i.e. $h = (h_1, \dots, h_t)$, the researchers employed the input sequence, i.e. $x = (x_1, \dots, x_t)$, by making use of standard RNN. The output vector sequence, i.e. $y = (y_1, \dots, y_T)$, was calculated based on the put forward DRNN model.

$$h_t = H(W_{xh} X_t + W_{hh} [h])_{(t-1)} + b_h \quad (5)$$

$$y_t = [(W)_{hy} h_t] + b_y \quad (6)$$

In Eq. 5 and 6, the W terms signifies the weight matrices (e.g. W_{xh} refers to the input-hidden weight matrix), whereas the b terms represent the bias vectors (e.g. b_h exemplifies the hidden bias vector), and H signifies the hidden layer functions. Generally, H pertains to the elementwise application of sigmoid functions, which might be utilised for feeding the output layer [28].

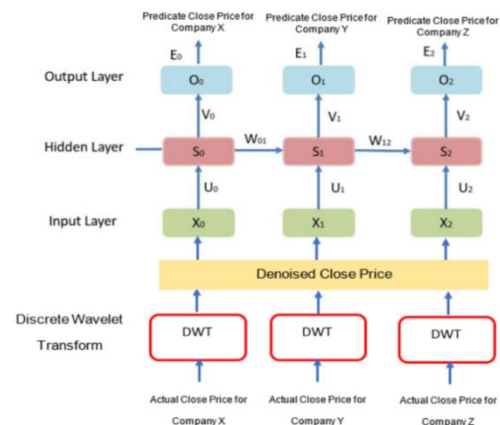


Fig. 2. Proposed Model (DRNN).

IV. EXPERIMENTAL SETUP

This section is divided into three sections; the first section describes the dataset used in the experiments, the second section describes the method of prediction applied and measuring the accuracy. The last section shows the results obtained.

A. Data Description

This study employs past data related to stocks from the stock market of Saudi (Tadawul). It was a body functional in KSA and it was approved to operate as the Securities Exchange (also called the Exchange) and it also kept a record of open/close/low/high/volume daily. Tadawul consisted of 1300 data records for each company with 146 stocks which were launched in the duration from 2011/01/01 to 2016/03/31. About 190,000 series were gathered in total, from which 130,000 were used for training purpose while the remaining were utilised for validation procedures. In this research, for the recommended model, the scholars preferred the close price to serve as input for 6 separate firms belonging to various domains. All the firms had a considerable deviation in their outcomes. The data gathered from these firms displayed a smaller rate of error and was regarded as errorless.

B. Prediction Procedure

In this research, several tests were carried out to tune the parameters to get accurate outcomes. The initial RNN variable we will tune is the number of training periods. Another variable is the size of the batch which controls at what frequency the updating of the network weights takes place. The third variable is the number of neurons, which impacts the network's learning ability. Moreover, the Adam optimisation technique is employed in RNN since it extends stochastic gradient descent which has seen widespread acceptance for its implementation in deep learning. Usually, the more the neurons, the greater the capability to learn the problem structure, though it takes a longer time for training. More capability for learning also raises the potential problem of training data overfitting. The below-given Table I explains the tests with parameters and prediction accuracy average (MAE, MSE, RMSE) for every case.

In the table, we observe that test 3 is the best. Table I displays details of the chosen sample that consists of 10 firms from the market of Saudi and S&P 500 index. Also, we acquired the past stock data from the website: https://macrotrends.dpdcart.com/cart/deliver?purchase_id=12487241&salt=4526fab69067075ba5560b21f1850513b192ef77, in which the models applied were ARIMA and DRNN on the given sample. The outcomes of the S&P 500 tests are given in Fig. 9 and Table IV.

In this research, the sample contained six firms selected arbitrarily. In the process of prediction, the stock market closing price was regarded as a significant parameter due to the fact that it signifies the next day's opening price. In the process of prediction, for each firm, the dataset of the stock market of Saudi is divided into two parts: a training set and testing set, for which the initial 1306 entries are used for training dataset while the remaining will be utilised for the testing set. Moreover, the dataset of S&P500 is divided into two segments:

testing and training datasets. Here, the initial 1313 data entries are used as training dataset while the other remaining is applied for the testing dataset. By making use of the training dataset, models will be developed, while testing dataset will be used to make predictions.

Every testing dataset's time step will walk one by one. A model is utilised to predict the time step, then the expected value from testing dataset will be considered and made accessible for the model to predict the next time step. It serves as a replica for the real-world situations in which new stock market views would be accessible every day and which can be utilised to predict the following day situation. At last, all the predictions made on the basis of the testing dataset are gathered and an error value is computed to determine the model's skill. The Mean Squared Error (MSE), Mean Absolute Error (MAE) and Root Mean Squared Error (RMSE) will be used as it punishes large errors and results in a score that is in the same units as the predict data.

C. Numerical Results

Here, the experts utilised a Windows 10 OS for testing of the model, in which all the tests were carried out by using Python 3.6 which contained these libraries: firstNumpy in which the homogenous array with multiple dimensions is the primary object. It can be regarded as an element table (generally numeric values), all having the same type. Another is Pandas which is a package of Python that offers flexible, fast, and expressive structures which are devised to facilitate intuitive and easily operational "labelled" or "relational" data. Another library is the Sklearnit which is efficient and simple for assessment of data. Then, there is Keras which is able to run on Theano, MS Cognitive Toolkit or TensorFlow. Designed to facilitate fast testing with deep NN, it emphasises modularity, extensibility, and user-friendliness. Lastly, there is the Matplotlib which is a library for plotting for Python language and its mathematical extension NumPy. Fig. 3, 4, 5, 6, 7 and 8, as well as Table II, show a sample firm in which this model was tested for the next 7 days. They also display all the predicted and actual prices of stocks with their accuracy of prediction which is obtained by computing MSE, MAE and RMSE as Table III below. Moreover, Fig. 9 illustrates the summary of the accuracy outcomes of the samples, applied through the proposed DRNN model.

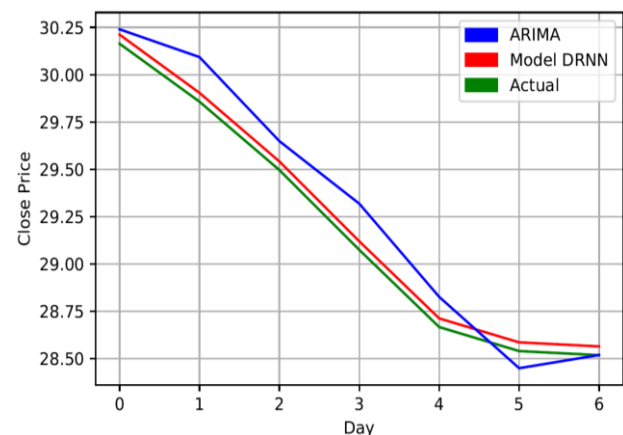


Fig. 3. Prediction for Saudi Mining Co.

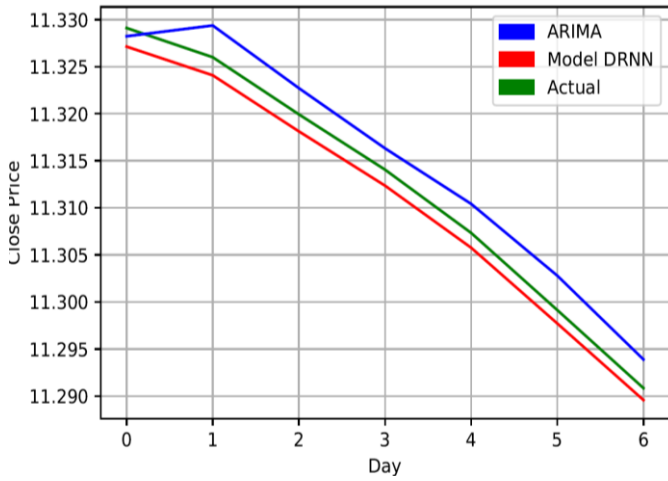


Fig. 4. Prediction for Riyadh Bank.

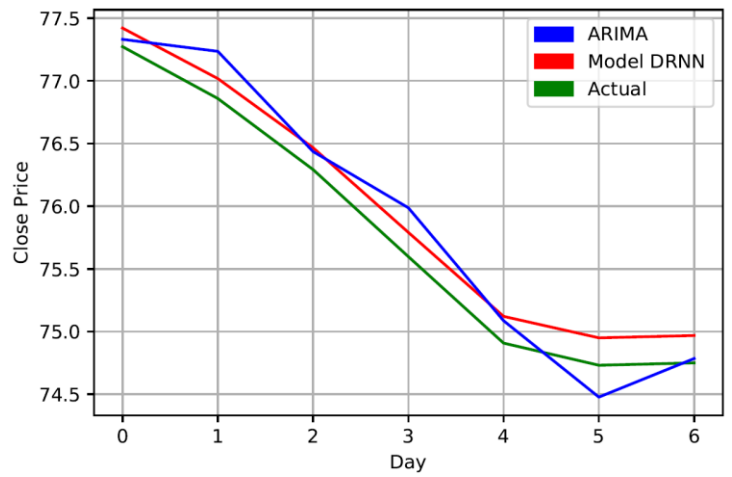


Fig. 7. Prediction for Rajhi Bank.

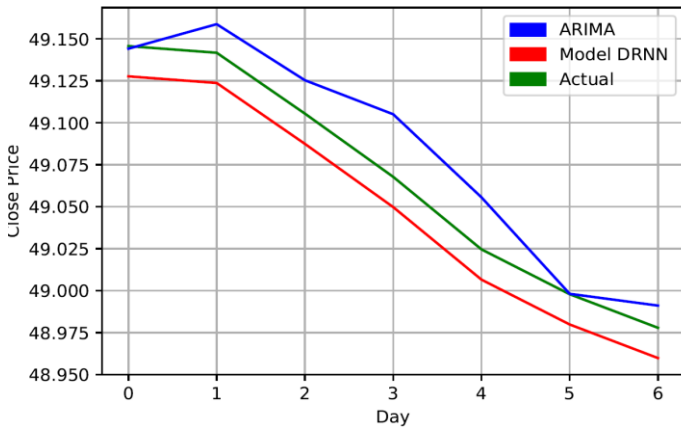


Fig. 5. Prediction for Yanbu Cement Co.

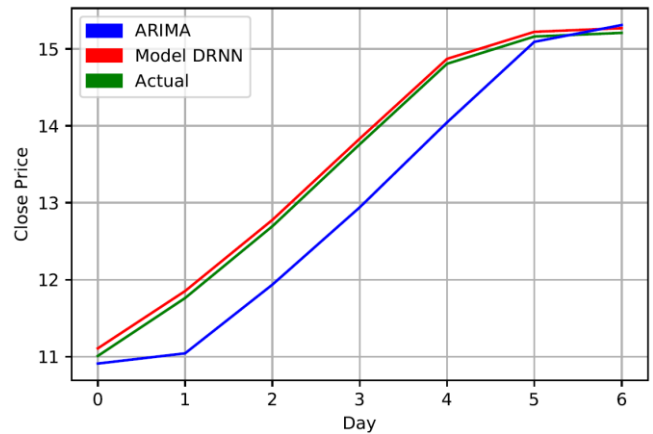


Fig. 8. Prediction for Saudi Indian.

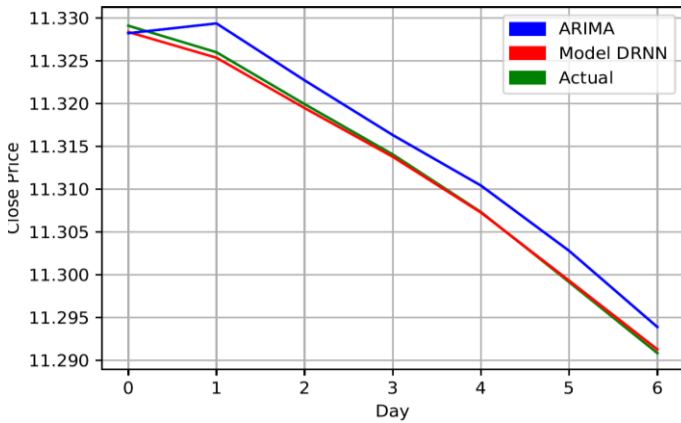


Fig. 6. Prediction for Sabic.

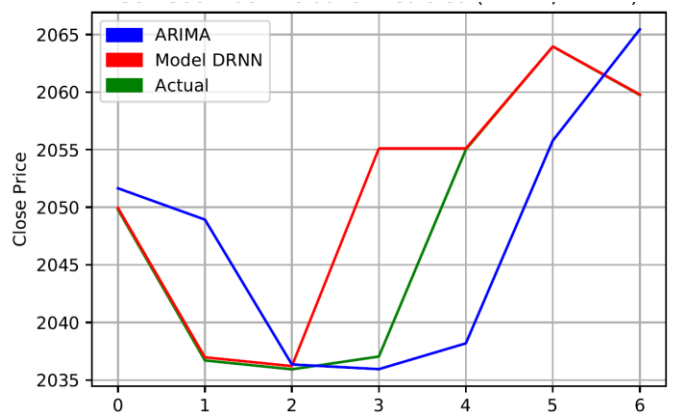


Fig. 9. Summary for Prediction Next 7 Days (S & P Index).

TABLE I. EXPERIMENTS DETAILS

Experiment	Epochs	Batch size	Neurons	MAE	MSE	RMSE
1	100	8	4	0.458	0.257	0.5073
2	100	4	6	0.386	0.234	0.4834
3	100	4	4	0.055	0.008	0.0552
4	150	2	6	5.506	31.23	5.5886
5	150	4	4	0.284	0.091	0.3009
6	150	4	5	2.13	5.788	2.4059
7	150	4	3	1.508	2.538	1.5933
8	200	4	6	2.29	5.859	2.4206
9	200	1	6	2.154	5.82	2.4125
10	200	4	4	2.508	6.847	2.6167

TABLE II. PREDICTIONS RESULT FOR THE NEXT 7 DAYS

Comp.		Day 1	Day 2	Day 3	Day 4	Day 5	Day 6	Day 7
Saudi Arabian Mining Co.	Actual	30.2	29.9	29.5	29.1	28.7	28.5	28.5
	DRNN	30.2	29.9	29.5	29.1	28.7	28.6	28.6
	ARIMA	30.2	30.1	29.6	29.3	28.8	28.4	28.5
Riyad Bank	Actual	11.3	11.3	11.3	11.3	11.3	11.3	11.3
	DRNN	11.3	11.3	11.3	11.3	11.3	11.3	11.3
	ARIMA	11.3	11.3	11.3	11.3	11.3	11.3	11.3
Yanbu Cement Co.	Actual	49.1	49.1	49.1	49.1	49.0	49.0	49.0
	DRNN	49.1	49.1	49.1	49.0	49.0	49.0	49.0
	ARIMA	49.1	49.2	49.1	49.1	49.1	49.0	49.0
Sabic	Actual	77.3	76.9	76.3	75.6	74.9	74.7	74.8
	DRNN	77.4	77.0	76.5	75.8	75.1	75.0	75.0
	ARIMA	77.3	77.2	76.4	76.0	75.1	74.5	74.8
Rajhi Bank	Actual	11.3	11.3	11.3	11.3	11.3	11.3	11.3
	DRNN	11.3	11.3	11.3	11.3	11.3	11.3	11.3
	ARIMA	11.3	11.3	11.3	11.3	11.3	11.3	11.3
Saudi Indian	Actual	11.0	11.8	12.7	13.8	14.8	15.2	15.2
	DRNN	11.1	11.9	12.8	13.8	14.9	15.2	15.3
	ARIMA	10.9	11.0	11.9	12.9	14.0	15.1	15.3

TABLE III. ACCURACY FOR EACH COMPANY

Comp.	Model	MAE	MSE	RMSE
Saudi Arabian Mining Co.	DRNN	0.05	0.00	0.05
	ARIMA	0.14	0.03	0.16
Riyad Bank	DRNN	0.00	0.00	0.00
	ARIMA	0.00	0.00	0.00
Yanbu Cement Co.	DRNN	0.02	0.00	0.02
	ARIMA	0.02	0.00	0.02
Sabic	DRNN	0.19	0.04	0.19
	ARIMA	0.20	0.06	0.24
Rajhi Bank	DRNN	0.00	0.00	0.00
	ARIMA	0.00	0.00	0.00
Saudi Indian	DRNN	0.08	0.01	0.08
	ARIMA	0.48	0.34	0.58

TABLE IV. PREDICTIONS RESULT FOR THE NEXT 7 DAYS (S & P INDEX)

	Day 1	Day 2	Day 3	Day 4	Day 5	Day 6	Day 7
Actual	2049.80	2036.71	2035.94	2037.05	2055.01	2063.95	2059.74
DRNN	2049.95	2036.98	2036.22	2055.11	2055.11	2063.95	2059.79
ARIMA	2051.65	2048.93	2036.36	2035.95	2038.19	2055.79	2065.44

Further, we carry out the last test by using the dataset of S&P500 on the ARIMA and DRNN models. Table IV and Fig. 9 depict the outcomes of this experiment for the next 7 days.

Then we are computing the MSE, MAE, and RMSE as Table V below.

TABLE V. ACCURACY FOR EACH MODEL

	MAE	MSE	RMSE
DRNN	0.15996	0.03701	0.19237
ARIMA	6.60949	76.5758	8.75076

V. CONCLUSIONS AND FUTURE WORK

Many researchers have investigated the problem of prediction in the stock market and developed two prediction systems. The first system addressed the issue of predicting the direction of the motion of the stock market index along with the stock prices. On the other hand, the second system predicted the future value of the stock market index. The predictions by these systems offered financial services to the

users, which could help the users make proper decisions when they aim to invest in the stock markets. In this study, a novel hybrid model is proposed, which uses the DWT and RNN technique along with a technical dataset for predicting the stock prices. The proposed model could combine the data obtained from the stock markets with the DWT then to RNN and create a novel and simple optimization technique. Furthermore, this integration method could be used for determining and formulating better and improved techniques for reducing the risks and assisting the investors.

In future studies, the researchers must consider various additional factors for increasing the prediction accuracy, such as the Hajj period and Umrah, as well as the Islamic month of Ramadan as Ramadan is a globally celebrated Islamic religious tradition. These factors must be investigated for determining their effect on the prediction accuracy of the Saudi stock market.

ACKNOWLEDGMENT

I would like to acknowledge the Saudi stock market (Tadawul) since it provided all the necessary data for the research. I also wish to thank Mr. Ahmed A. Alsowaygh,

Reference Data Chief Specialist, for providing all the help during data collection.

REFERENCES

- [1] Sengupta and S. Chaudhury, "Stock Market Prediction Using Time Series Analysis," 2018.
- [2] S. Bouktif, A. Fiaz, A. Ouni, and M. Serhani, "Optimal deep learning lstm model for electric load forecasting using feature selection and genetic algorithm: Comparison with machine learning approaches," *Energies*, vol. 11, no. 7, p. 1636, 2018.
- [3] W. Xu, H. Peng, X. Zeng, F. Zhou, X. Tian, and X. Peng, "Deep belief network-based AR model for nonlinear time series forecasting," *Applied Soft Computing*, vol. 77, pp. 605-621, 2019.
- [4] D. Pradeepkumar and V. Ravi, "Soft computing hybrids for FOREX rate prediction: A comprehensive review," *Computers & Operations Research*, 2018.
- [5] A. Atkins, M. Niranjani, and E. Gerding, "Financial news predicts stock market volatility better than close price," *The Journal of Finance and Data Science*, vol. 4, no. 2, pp. 120-137, 2018.
- [6] H. Y. Kim and C. H. Won, "Forecasting the volatility of stock price index: A hybrid model integrating LSTM with multiple GARCH-type models," *Expert Systems with Applications*, vol. 103, pp. 25-37, 2018.
- [7] V. Rajput and S. Bobde, "Stock market forecasting techniques: literature survey," *Int J Comput Sci Mob Comput*, vol. 5, no. 6, pp. 500-506, 2016.
- [8] Y. Baek and H. Y. Kim, "ModAugNet: A new forecasting framework for stock market index value with an overfitting prevention LSTM module and a prediction LSTM module," *Expert Systems with Applications*, vol. 113, pp. 457-480, 2018.
- [9] J. Schmidhuber, "Deep learning in neural networks: An overview," *Neural networks*, vol. 61, pp. 85-117, 2015.
- [10] Z. Chen, Y. Luo, and N. Mesgarani, "Deep attractor network for single-microphone speaker separation," in *2017 IEEE International Conference on Acoustics, Speech and Signal Processing (ICASSP)*, 2017, pp. 246-250: IEEE.
- [11] Y. S. Abu-Mostafa and A. F. Atiya, "Introduction to financial forecasting," *Applied Intelligence*, vol. 6, no. 3, pp. 205-213, 1996.
- [12] S.-J. Lee, D.-J. Lee, and H.-S. Oh, "Technological forecasting at the Korean stock market: A dynamic competition analysis using Lotka-Volterra model," *Technological Forecasting and Social Change*, vol. 72, no. 8, pp. 1044-1057, 2005.
- [13] T. H.-K. Yu and K.-H. Hwang, "A bivariate fuzzy time series model to forecast the TAIEX," *Expert Systems with Applications*, vol. 34, no. 4, pp. 2945-2952, 2008.
- [14] X. Zhu, H. Wang, L. Xu, and H. Li, "Predicting stock index increments by neural networks: The role of trading volume under different horizons," *Expert Systems with Applications*, vol. 34, no. 4, pp. 3043-3054, 2008.
- [15] Y. Zhang and L. Wu, "Stock market prediction of S&P 500 via combination of improved BCO approach and BP neural network," *Expert systems with applications*, vol. 36, no. 5, pp. 8849-8854, 2009.
- [16] R. Majhi, G. Panda, and G. Sahoo, "Efficient prediction of exchange rates with low complexity artificial neural network models," *Expert systems with applications*, vol. 36, no. 1, pp. 181-189, 2009.
- [17] C. Hamzaçebi, D. Akay, and F. Kutay, "Comparison of direct and iterative artificial neural network forecast approaches in multi-periodic time series forecasting," *Expert Systems with Applications*, vol. 36, no. 2, pp. 3839-3844, 2009.
- [18] Z. Liao and J. Wang, "Forecasting model of global stock index by stochastic time effective neural network," *Expert Systems with Applications*, vol. 37, no. 1, pp. 834-841, 2010.
- [19] J. Patel, S. Shah, P. Thakkar, and K. Kotecha, "Predicting stock market index using fusion of machine learning techniques," *Expert Systems with Applications*, vol. 42, no. 4, pp. 2162-2172, 2015.
- [20] M. Qiu and Y. Song, "Predicting the direction of stock market index movement using an optimized artificial neural network model," *PloS one*, vol. 11, no. 5, p. e0155133, 2016.
- [21] W. Chen, Y. Zhang, C. K. Yeo, C. T. Lau, and B. S. Lee, "Stock market prediction using neural network through news on online social networks," in *2017 International Smart Cities Conference (ISC2)*, 2017, pp. 1-6: IEEE.
- [22] W. Bao, J. Yue, and Y. Rao, "A deep learning framework for financial time series using stacked autoencoders and long-short term memory," *PloS one*, vol. 12, no. 7, p. e0180944, 2017.
- [23] X. Pang, Y. Zhou, P. Wang, W. Lin, and V. Chang, "An innovative neural network approach for stock market prediction," *The Journal of Supercomputing*, pp. 1-21, 2018.
- [24] T. Fischer and C. Krauss, "Deep learning with long short-term memory networks for financial market predictions," *European Journal of Operational Research*, vol. 270, no. 2, pp. 654-669, 2018.
- [25] D. M. Nelson, A. C. Pereira, and R. A. de Oliveira, "Stock market's price movement prediction with LSTM neural networks," in *2017 International Joint Conference on Neural Networks (IJCNN)*, 2017, pp. 1419-1426: IEEE.
- [26] S. Makridakis, E. Spiliotis, and V. Assimakopoulos, "Statistical and Machine Learning forecasting methods: Concerns and ways forward," *PloS one*, vol. 13, no. 3, p. e0194889, 2018.
- [27] S. Hochreiter and J. Schmidhuber, "Long short-term memory," *Neural computation*, vol. 9, no. 8, pp. 1735-1780, 1997.
- [28] C. Olcan and E. Mahmudov, "Hybrid Fuzzy Time Series Methods Applied to Solar Radiation Forecasting," *Journal of Multiple-Valued Logic & Soft Computing*, vol. 27, no. 1, 2016.
- [29] E. Ahmed et al., "Recent advances and challenges in mobile big data," *IEEE Communications Magazine*, vol. 56, no. 2, pp. 102-108, 2018.
- [30] S. T. Bakhsh, B. Shahzad, and S. Tahir, "Risk Management Approaches for Large Scale Software Development," *Journal of Information Science and Engineering*, vol. 33, no. 6, pp. 1547-1560, 2017.

Medical Image(s) Watermarking and its Optimization using Genetic Programming

Rafi Ullah Habib¹, Hani Ali Alquhayz²

Department of Computer Science and Information
College of Science, Majmaah University, Majmaah 11952, Saudi Arabia

Abstract—In this paper, an medical image watermarking technique has been proposed, where intelligence has been incorporated into the encoding and decoding structure. The motion vectors of the medical image sequence are used for embedding the watermark. Instead of a manual selection of the candidate motion vectors, a generalized approach is used to select the most suitable motion vectors for embedding the watermark. Genetic programming (GP) module has been employed to develop a function in accordance with imperceptibility and watermarking capacity. Employment of intelligence in the system improves its imperceptibility, capacity, and resistance toward different attacks that can occur during communication and storing. The motion vectors are generated by applying a block-based motion estimation algorithm. In this work, Full-Search method has been used for its better performance as compared to the other methods. Experimental results show marked improvement in capacity and visual similarity as compared to the conventional approaches.

Keywords—Capacity; imperceptibility; genetic programming; image sequence; watermarking

I. INTRODUCTION

The exponential growth of internet speed wherewith the information is made available turned the internet into a place. About a third of the total world population has internet access [1], and consequently, with this development, the spread of multimedia data significantly aroused. Copying, distribution, and manipulation of digital content are very easy by using advanced multimedia and communication tools. Thus, before storing and transmission of digital content, its security is a major concern. Authentication of multimedia applications, especially for sensitive data likes medical and military applications is the challenge of today's research.

For the security of digital content, watermarking is one of the best solutions. There are three main contradictory watermarking properties: robustness, capacity, and imperceptibility [2]. The researchers must make a tradeoff between these properties accordingly. Imperceptibility, robustness, security, and efficient technique(s) are the basic requirements while securing digital data [3]. Watermarking is the well-established solution to many problems like copyright protection, copy control, authentication, ownership, broadcast monitoring etc. [4-6]. In this paper, the secure transmission and storage of medical image sequence like Ultrasound images are ensured by employing the generalized watermarking algorithm using genetic programming. The capacity and imperceptibility are the contradicting parameters and it is difficult to improve any of the parameters without affecting the other one.

However, in this paper, an intelligent approach is employed, where the optimal motion vectors are selected for watermark embedding. Before embedding the watermark bit, the motion vectors are extracted. For this purpose, several block-based motion estimation algorithms are used. Some of them are Full-Search Block-Based Motion-estimation Algorithm (BMA), three-step search, new three-step search, four-step search, diamond search, small diamond search pattern etc. In the proposed technique, Full-Search BMA is used for extracting the motion vectors. Full-Search is more efficient in terms of accuracy as compared to all other BMAs [7]. The computational time of Full-Search BMA is high, but its accuracy is better than all other BMAs. Full-Search BMA searches all of the probabilistic similarity. The magnitude and phase angle between the consecutive motion vectors have been used for watermark embedding. It is not necessary that the motion vectors having large magnitude are suitable for watermark embedding. It depends on the associated macroblock. We cannot rely directly on the magnitude of the vector and thus, we will focus on the associated macroblock parallelly. GP is used to select the most suitable motion vectors for embedding purpose, where imperceptibility, security, and embedding capacity are focused.

The storing and distant transmission of medical images/sequences demands high security and especially medical imaging with mobile transmission needs careful handling. Thus, in this paper, a blind generalized semi-fragile watermarking scheme is used to protect the medical image and/or image sequence. The primary objectives of this paper are:

- Unlike traditional blocked-based security, efficient micro-level security is achieved by applying the Full-Search BMA.
- The temporal information of the input medical image sequence is used for watermark embedding. The embedding capacity is increased as compared to the convention embedding in spatial regions of the images.
- Enhancing the important contradicting properties i.e. imperceptibility, robustness, and capacity is a challenge for today's researchers. In this paper, an efficient tradeoff between these contradicting properties has been made. For this purpose, these parameters are used in the GP fitness function. Details about the GP fitness function are given in Section 3.

- For imperceptibility, peak signal to noise ratio (PSNR) and structural similarity index measure (SSIM) are used. Determining the capacity of the watermark is to find how much watermark bits are embedded in the image/video without any perceptual distortion [8]. For watermarking capacity (WC), a number of embedded bits per frame (EBPF) are considered and this measurement is used in the fitness function. By the end of all frames embedding, an average of the embedded bits per frame is taken.

II. LITERATURE SURVEY

Since the last three decades, the researchers are working on the security of medical images. Most of the researchers are using watermarking methods based on error correcting code, multiple watermarking, hybrid watermarking, intelligent watermarking, biometric watermarking, joint compression based watermarking, etc. Some of the proposed techniques are discussed as follow.

In [9], the motion vector watermarking was proposed where the authors have used the motion vectors having large values and less change in phase angle. The experimental results in their work indicate that the visual similarity of the watermarked image is not highly affected. The MPEG compression speed is not affected and has the capability to embed the high capacity watermark in a short video.

Medical image watermarking technique has been proposed in Singh et al. [10], in which the image is decomposed by using discrete wavelet transform (DWT) and the medical text watermark is embedded in the sub-bands of the wavelet domain using spread spectrum technique. Third level decomposition is made and based on threshold criteria, three different watermarks have been embedded in the selected vertical and horizontal wavelet subbands.

In [11], Giakoumaki *et al.* have proposed wavelet-based watermarking algorithms, where the authors address the issues related to medical confidentiality. The input image is decomposed by using wavelet transform and the watermark is embedded in the wavelet coefficients. The authors have utilized two watermarking approaches for medical images. The detailed coefficients of the cover image are used for watermark embedding. Quantization function has been applied to each of the marked coefficients for extracting the multiple watermark bits. By using this hybrid algorithm, robustness, reliability, efficiency, and imperceptibility have been improved. The only disadvantage of this method is higher computational complexity.

In [12], Ouhsein *et al.* proposed a discrete fractional Fourier and DWT based watermarking system. After first level wavelet decomposition, the input image is divided into four subbands. Multiple parameters discrete fractional Fourier (MPDFRF) is applied to each subband and the watermark is embedded into each block.

A blind optimal watermarking method has been proposed by Peng *et al.* [13]. This method is based on the multi-wavelet transformation and support vector machine (SVM). After first level wavelet decomposition, the lower frequency sub-band of

the cover image is used for watermark embedding. The reference information and logo have been used as a watermark to be embedded.

A biometric-based medical image watermarking method has been proposed by Wioletta [14]. The author is using DWT to embed a biometric watermark into the cover work. This method is robust against both legitimate and illegitimate manipulations.

Lin and Ching proposed a blind wavelet-based digital image watermarking scheme that has high capacity and able to hide more than one image inside the cover work without affecting the imperceptibility of the watermarked image [15]. The watermark is permuted before embedding to ensure the robustness and security of the watermark simultaneously.

In 2009, I. Usman *et al.*, have proposed an intelligent watermarking technique [16]. The authors intelligently select the coefficient for watermark embedding. The embedding coefficients are selected using genetic programming. The authors are exploiting the amplitude of the wavelet coefficient. GP has been employed for evolving the mathematical function, which is based on visual similarity and watermarking capacity. The results are effective in terms of imperceptibility and payload.

S. Acharjee *et al.* have proposed a watermarking technique that enhances the security of medical videos [17]. Motion vectors of the electrocardiogram (ECG) videos are used for watermark embedding. A binary image is used as a watermark. The authors are using a threshold to select the motion vectors. In addition, they have tried to reduce the calculation and speed up the authentication process.

III. GENETIC PROGRAMMING (GP) MODULE

Genetic programming is an evolutionary computation technique that is used in many applications. GP is a machine learning technique based on natural selection and genetics [18]. GP is based on the stochastic method, where randomness plays an important role in searching and learning [19]. The most suitable motion vectors, in terms of visual similarity and capacity, are selected for embedding watermark bits. Initially, a random population is evaluated using a fitness function according to the application. The individuals in the population are computer programs. In the proposed scheme, the fitness function that is based on imperceptibility and capacity is focused. In the initial population, the best individual is reserved and all of the others are deleted and replaced by the children of the best individuals. The reserved children make a new generation, where so of the children may have the best score than their parents in the previous generation. This process is repeated until one of the termination criterions is satisfied. Block diagram for developing GP module is shown in Fig. 1.

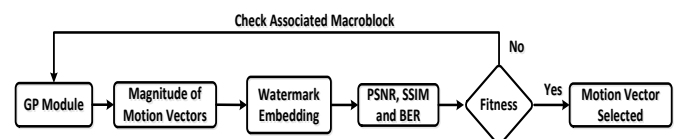


Fig. 1. Basic GP Architecture.

Fitness criteria, suitable functions, and terminals are defined that represent the possible solutions in the form of a complex numerical function. GP module has the following different functions.

A. GP Function Set

The function set used in GP is based in the nature of the problem. The available mathematical function in GP module collectively makes the GP function set. In the simulations, four basic binary functions have been +, -, ×, ÷, log, exponent are used.

B. Fitness Function

Each individual of the population is graded. In the proposed scheme, the PSNR, SSIM, and capacity are used to assess the fitness function. This function provides the feedback to the GP module representing the fitness of the individual. A higher individual fitness score indicates higher performance. GP fitness function contains four basic arithmetic operators and the operands like magnitude and phase angle of motion vectors, macroblock index. The performance evaluation of the fitness function is measured by the PSNR, SSIM and watermarking capacity. The following fitness function is used:

$$\text{fitness} = \alpha_1 \times \frac{\text{PSNR}}{50} + \alpha_2 \times \text{SSIM} + \alpha_3 \times \text{WC} \quad (1)$$

The watermarking capacity is $\text{WC} = \text{EBPF}/(\text{M} \times \text{N})$, where $\text{M} \times \text{N}$ is the size of the frame. The constants α_1 , α_2 and α_3 are the weighting parameters that are decided according to the application. For applications requiring more capacity/payload, some sacrifice can be made in terms of imperceptibility, i.e. the parameter α_3 should be given more weight. Similarly, for the applications, where high imperceptibility is required, the parameters α_1 and α_2 should be given more weight. PSNR and SSIM are calculated between the original image and the watermarked image. PSNR is divided by 50 in order to scale its value, such that equal weight could be given to all of the objective measures.

C. Population Initialization

The individuals in the initial population are generated randomly. The most common methods that are used for the initialization of population are "ramped half – and – half" and "full – and – grow" methods. By using any of the above-mentioned methods, the pre-defined maximum tree depth does not be exceeded [20]. In the proposed scheme, the "Ramped half – and – half" method is used for generating the initial population.

D. Termination Criteria

The simulation is terminated when one of the following becomes true.

- When the fitness score is exceeded i.e. $\text{fitness} > 50$
- When the fitness score repeats
- When the number of generations reaches the pre-defined maximum number of generations
- When the error becomes less than a pre-defined threshold

E. GP Operators

The most common operators used in genetic programming are crossover, replication and mutation. In the proposed scheme, crossover, mutation and replication are used to produce the next generation. In a crossover, the two individual parents exchange genetic materials to create a child. It tries to mimic recombination and reproduction. Optimal and/or near to optimal solution comes with the help of crossover operator. In mutation, the genome is changed in a minor way for the next generation. In replication, the individual is copied to the new generation. In the proposed GP run, a crossover has a higher ratio as compared to the mutation and replication. All of the necessary settings of the GP module are given in Table I.

TABLE I. GP PARAMETERS SETTINGS

Objectives	To evolve the best result
Function Operators	Log, Exponent, +, -, ×, ÷
Function Operands	The magnitude and the Phase angle of motion vectors
Fitness	PSNR, SSIM and watermarking capacity
Expected children	rank89
Selection	General
Initial Population	ramped half – and – half
Termination	Score exceed, Number of generations, error
Sampling	Tournament
Survival	Keep the best
GP Operators	Mutation, Crossover, Replication

IV. PROPOSED ALGORITHM

A generalized watermarking algorithm for the ultrasound image sequence has been presented. The temporal space is acquired by using a Full Search block-based motion estimation algorithm. As compared to all other block-based motion estimation algorithms, Full Search is time-consuming but it is more efficient. The intelligent selection is carried out while choosing the candidate motion vectors. For this purpose, genetic programming is used to select the efficient motion vectors where the watermark bits are embedded. This will increase the visual similarity, capacity and the robustness of the watermarking system.

MATLAB environment has been used for the experimental results. For GP simulation, the Matlab based GPLAB toolbox has been used [21].

A. Watermark Embedding

- A key-based random binary sequence is generated that is used as a watermark in the proposed system. The watermark is quadruplicated and then scrambled before embedding in the motion vectors. $b = \text{rand}(i)$, where i is the number of watermark bits quarter to the required bits. The randomly generated bits are then quadruplicated to make a vector V i.e. $V = (b_1, b_2, \dots, b_n, b_1, b_2, \dots, b_n, b_1, b_2, \dots, b_n, b_1, b_2, \dots, b_n)$ where n is the number of generated bits. The quadruplicated bits are then permuted by using a secret

key to make it more secure [22]. Thus the final watermark to be embedded is: $W_{\text{final}} = V_{\text{permuted}}$.

- We are applying a full-search block-based motion estimation algorithm to the ultrasound image sequence to generate motion vectors.
- The genetic programming module (GP) is introduced, where the initial population, generations and fitness function, termination criteria etc. are decided. In this paper, the fitness function is based on the PSNR and SSIM along with the watermarking capacity.
- For embedding the watermark, the most suitable candidate motion vectors are selected by using the above-mentioned genetic programming module.
- The watermark bits are embedded in the motion vectors and run generation by generation until the termination criteria achieved. The termination criteria can fitness score, a number of generation, execution time or repetition of the fitness values. The numerical fitness expressions are evaluated while embedding the watermark bits in the ultrasound frames. These expressions are used in the watermark extraction. This is to be discussed in detail in Section 4.2.
- Once the motion vector is selected, its magnitude and the phase angle are modified. The magnitude of the motion vector is given in Equation 2.

$$\text{Mag}_{\text{mv}}(i) = \sqrt{h_i^2 + v_i^2}, \quad 0 < i \leq \text{MB} \quad (2)$$

Where MB is the macroblock, h and v are the horizontal and vertical values of the motion vector respectively. Calculate the phase angle to embed the watermark bit. The phase angle is given in Equation 3.

$$\theta(j) = \tan^{-1} mv(v)_i / mv(h)_i \quad (3)$$

where $mv(v)_i$ and $mv(h)_i$ are the vertical and horizontal components respectively.

- If the watermark bit is 1 then we chose the coordinate sectors I and II, otherwise, we chose the coordinate sectors III and IV for embedding. If the $0 \leq \theta \leq 90$, then modify the horizontal component of the selected vector and if $90 < \theta \leq 180$ then the vertical component of the motion vectors is modified [23]. The coordinate regions are shown in Fig. 2.

The effect of watermark embedding is measured by PSNR and SSIM as given in Equation 4 and Equation 5.

$$\text{PSNR} = 20 \log_{10} \left(\frac{255^2}{\text{MSE}} \right) \quad (4)$$

where MSE is the mean square error.

$$\text{SSIM}(x, y) = \frac{(2\mu_x\mu_y + c_1)(2\sigma_{xy} + c_2)}{(\mu_x^2 + \mu_y^2 + c_1)(\sigma_x^2 + \sigma_y^2 + c_2)} \quad (5)$$

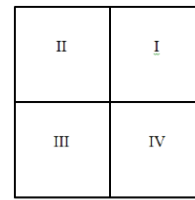


Fig. 2. The Coordinate System.

where x and y are two windows of size $N \times N$, μ_x and μ_y are the averages of x and y, and σ_x^2 and σ_y^2 are the variances of x and y respectively. $c_1 = (K_1L)^2$ and $c_2 = (K_2L)^2$ where L is the maximum value i.e. $2^{\#\text{bits}}$ and $k_1 = 0.01$ and $k_2 = 0.03$ by default.

Normally, the watermark capacity is calculated as bits per pixel (bpp), when the spatial domain is used for watermark embedding. However, in the proposed scheme, the capacity is calculated by the embedded bits in the frame.

When the fitness criteria, which are PSNR, SSIM and capacity are fulfilled, the system will move on to the next frame for watermark embedding and continue until embedding all the frames of the sequence.

B. Watermark Extraction

Once the ultrasound image sequence watermarking is finished and shared through a wired or wireless communication channel, then verification is required on the receiving side.

- On the receiving side, motion vectors of the watermarked image sequence are generated. Then we select those motion vectors, which were used for watermark embedding. For a selection of the marked candidate motion vectors, the fitness numerical expression is used. The same fitness function equation is used to select the motion vectors.
- The watermark bits are then extracted from the selected motion vectors and compared to the same watermark bits that can be generated on the verification side by using the same key.
- If the extracted watermark bits and the generated watermark bits are same, then the image sequence is authentic, otherwise tampered.

The watermark embedding and extraction are shown in Fig. 3 and 4, respectively.

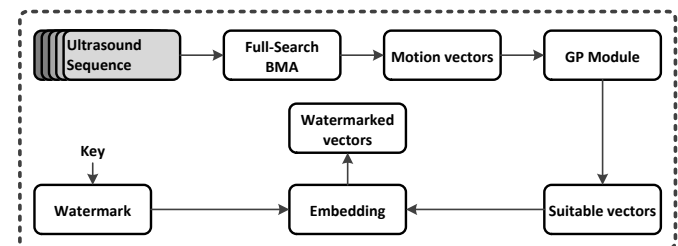


Fig. 3. Watermark Embedding Process.

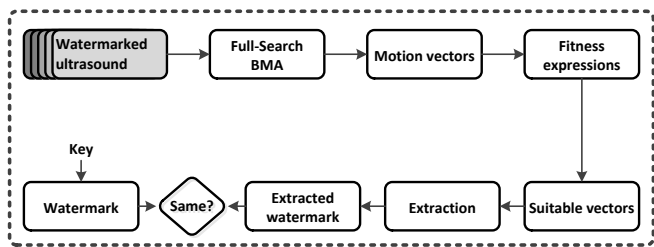


Fig. 4. Watermark Extraction Process.

In the extraction process, the to-be-checked-sequence is used as an input and the motion vectors are selected where the watermarks bits were embedded on the embedding side. For the selection of the motion vectors, the fitness function expressions are used that were evaluated by GP module. The watermark is generated by using the same key and then the generated and extracted watermarks are compared. If both the watermarks are same, the sequence is authentic otherwise tampered. The location(s) of tampering is then analyzed and detected that which frame(s) tampers and how much. For normal videos, it is decided that the tampering is acceptable or not. However, for medical videos, a tiny distortion cannot be accepted. For this reason, the legitimate and illegitimate tampering is not differentiated in this paper.

V. EXPERIMENTAL RESULTS

An ultrasound sequence has been chosen for the experimental work [24]. After applying the Full-Search BMA, lots of motion vectors are obtained. Thus, a high strength watermark can be embedded without affecting the imperceptibility. Although, it is not necessary that large magnitude vectors are suitable for watermark embedding. It depends on the associated macroblock. We cannot rely directly on the magnitude of the vector and thus, the associated macroblock is focused parallelly. Any fixed threshold is not assigned to the magnitude of the motion vectors for the embedding selection. For this purpose, an intelligent system is employed, where the GP module will decide the most suitable motion vector for embedding the watermark bits. The details of the ultrasound sequence before and after Full-search BMA are given in Table II.

TABLE II. DETAIL OF THE ULTRASOUND IMAGE SEQUENCE BEFORE AND AFTER FULL-SEARCH BMA

Features	Details
Image sequence / video	Ultrasound video
Resolution	1920x1080
Size	97 MB
Aspect Ratio	16: 9
Frame rate	25.00 fps
Duration	00: 06
Total frames	168
BMA	Full-Search
Macroblock size	16 × 16
Number of motion vectors/frame	8100
Motion vector threshold for selection	GP based

Fig. 5 and 6 show some of the frames extracted from the video and the corresponding motion vectors respectively. The structures of medical images/videos are much different from normal videos. Hence it is difficult to compare any watermarking algorithm that is designed for normal videos i.e. .bmp, .tiff, .jpeg etc.

The watermarked motion vectors are shown in Fig. 7. In Fig. 5 and 6, it can be seen that there are hundreds of motion vectors even if the size of the macroblock is 16×16 . Hence, the embedding capacity is too high as compared to the regular images. In the proposed method, the motion vectors are intelligently selected for embedding the watermark bits; therefore, the visual similarity can be easily maintained after embedding a high strength watermark. If the motion vectors on the boundary are selected for embedding then it may create some problem of overflow and underflow. To avoid the overflow/underflow, a histogram modification is used before embedding the watermark. The phenomenon used in [25] has been utilized where the authors have proposed a preprocessing method for fixing the issue of overflow and underflow. They find the zero point that is closed to the boundary i.e. (0 or 255), and the boundary pixels are removed and the pixels between the boundary pixels and zero points are removed by modifying the histogram of the original frame. For histogram generating, the boundary pixels are not used and after embedding the watermark, new boundary pixels appear. Thus, a correct histogram can be obtained, while extracting the watermark on the verification side.

It is not easy to compare medical images with normal images like bmp, jpeg, and tiff images. The dicom image contains the details about the image and has patient information in the same file. It contains the header and other information that are structured differently from the other formats. Little Endian or Big Endian byte orders are used to encode the dicom image file format. Dicom formats are converted to bmp because the main interest is the security of the image rather than the patient and machine information associated with the images. The converted images are viewable on the common image viewing system with small size [26].

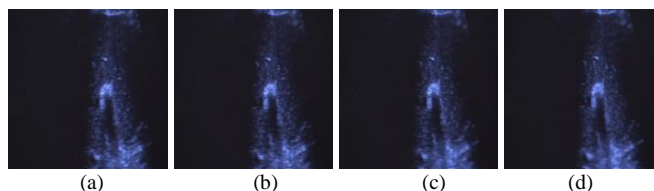


Fig. 5. From a ~ d, the Frames Number 7, 8, 9 and 10 of the Ultrasound Sequence.

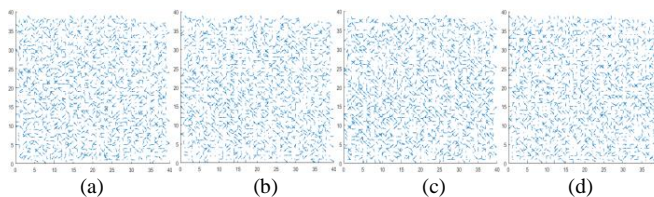


Fig. 6. From a ~ d, the Extracted Motion Vectors.

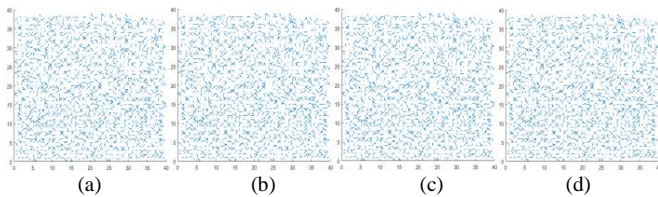


Fig. 7. From a ~ d, the Watermarked Motion Vectors.

Table III shows the embedding distortion that is measured by PSNR and SSIM along with the embedding capacity. The main objective of the proposed approach is to increase the embedding capacity with minimum effect on imperceptibility and vice versa. The results of the proposed algorithm have been compared with the three latest schemes. It can be seen that the proposed approach provide an optimal solution to the contradicting properties of watermarking. As compared to other regular video frames, in medical images, there are more motion vectors. In addition, optimal motion vectors are selected for embedding the watermark bits.

In Table III, it can be seen that the PSNR and SSIM in the second column are very high. The SSIM i.e. 0.99 has been calculated for the original and the extracted watermark and it should be one if the watermarked content is not attacked/tampered. Similarly, the SSIM i.e. 0.97 is calculated for the watermarked image and received the watermarked image. All others SSIMs and PSNRs, shown in Table III are used to measure the embedding distortion.

TABLE III. PROMINENT FEATURES AND PERFORMANCE COMPARISON WITH THE PREVIOUS APPROACHES

Features	[17]	[25]	[27]	Proposed
Embedding domain	Temporal	Spatial	Transformed	Temporal
PSNR	~120dB	~50dB (compressed watermark)	35dB – 36dB (Depending on the gain factor, α)	~43dB (Average)
SSIM	0.99 & 0.97	Not calculated	Not calculated	0.95 (Average)
Capacity	Not mentioned	Using Compressed watermark	High	High, i.e. ~ 50 bits for (16 × 16) block

VI. CONCLUSIONS AND FUTURE DIRECTIONS

An intelligent watermarking in motion vectors is proposed for protecting the medical videos. Medical images/video is very sensitive and small distortion may not be acceptable. Hence, the selection of pixels and motion vectors for embedding the watermark is a challenge for the researchers and hospital management systems. In this paper, a genetic programming module has been designed to select the most suitable motion vectors for watermark embedding that reduced the perceptual distortion and improve the watermarking capacity. Distortion measurements like PSNR and SSIM along with the watermarking capacity have been used to set the

fitness function. The watermark bits are embedded using the magnitude and phase angle of the motion vectors. The imperceptibility and the watermarking capacity have been improved. Random permutation and quadruplicating improve the security of the up to satisfactory level. The experimental results show that the proposed watermarking approach is more efficient in terms of visual similarity and capacity.

Cyber-attacks like data injection, stealing patient information, ransomware, image disruption etc. threat the medical images. In future, an intelligent watermarking system can be employed to increase the security of medical images and to protect the information related to the patient. The watermark that is to be used will contain all of the patient information. A highly compressed version of the patient picture can also be used as a watermark.

ACKNOWLEDGEMENT

The authors would like to thank Deanship of Scientific Research at Majmaah University for supporting this work under Project No. 38/75.

REFERENCES

- [1] Boneh D, Shaw J. "Collusion-secure fingerprinting for digital data" IEEE Transactions on Information Theory, vol. 44(5), pp. 1897-1905, 1998.
- [2] Khan A, Mirza A M. "Genetic perceptual shaping: Utilizing cover image and conceivable attack information during watermark embedding. Information Fusion, " Elsevier, vol. 8 (4), pp. 354–365, 2007.
- [3] Chamlawi R, Khan A, Idris A. "Wavelet based image authentication and recovery," Journal of Computer Science and Technology, vol. 22 (6), pp. 795– 804, 2007.
- [4] Chang C C, Fan Y H, Tai W L. "Four-scanning attack on hierarchical digital watermarking method for image tamper detection and recovery," Pattern Recognition, Elsevier, vol. 41, pp. 654–661, 2008.
- [5] Shih F Y, Wu Y T. "Robust watermarking and compression for medical images based on genetic algorithms. Information Sciences," Elsevier, vol. 175, pp. 200–216, 2005.
- [6] Suhail M A, Obaidat M S, Ipson S S, Aadoun B. "A comparative study of digital watermarking in JPEG and JPEG2000 environment," Information Sciences, Elsevier, vol. 151, pp. 93–105, 2003.
- [7] Yaakob R, Aryanfar A, Halim A A, Sulaiman N. "A Comparison of Different Block Matching Algorithms for Motion Estimation," Procedia Technology, Elsevier, vol, 11, pp. 199-205, 2013.
- [8] Yaghmaee F, Jamzad M. "Estimating Watermarking Capacity in Gray Scale Images Based on Image Complexity, EURASIP Journal on Advances in Signal Processing, vol. 2010, pp. 1-9, 2010.
- [9] Zhang J, Li J, Hang L. "Video Watermark Technique in Motion Vector," In Proceedings Brazilian Symposium on Computer Graphics and Image Processing, pp. 179-182, 2001.
- [10] Singh A K, Kumar B, Dave B, Mohan A. "Robust and imperceptible spread-spectrum watermarking for telemedicine applications," In Proc. Natl. Acad. Sci., India, vol. 85(2), pp. 295–301, 2015.
- [11] Giakoumaki, Pavlopoulos S, Koutsouris D. "A medical image watermarking scheme based on wavelet transform," in Proceedings of 25th Annual International Conference of IEEE-EMBS, San Francisco. 2004, 1541–1544.
- [12] Ouhsein M, Abdallah E, Hamza A B. "An image watermarking scheme based on wavelet and multiple-parameter fractional Fourier transform," in IEEE Int Conf on Signal Processing and Communication, UAE, pp. 1375–1378, 2007.
- [13] Peng H, Wang J, Wang W. Image watermarking method in multiwavelet domain based on support vector machines. Journal of Systems and Software, vol. 83, pp. 1470–1477, 2010.
- [14] Wioletta W. "Biometric watermarking for medical images-example of Iris code," Tech. Trans, vol. 1-M(5), pp. 409–416, 2013.

- [15] Lin C Y, Tai C Y. "A robust image hiding method using wavelet technique," *Journal of Information Science and Engineering*, vol. 22, pp. 163-174, 2006.
- [16] Usman I, Khan A, Ali A, Choi T S. "Reversible watermarking based on intelligent Coefficient selection and integer wavelet transform," *International Journal of Innovative Computing, Information and Control*, vol. 5(12), pp. 1-8, 2009.
- [17] Acharjee S, et al. "Watermarking in Motion Vector for Security Enhancement of Medical Videos," *Int Conf on Control, Instrumentation, Comm and Computational Tech*, pp. 589-594, 2014.
- [18] Banzhaf W, Francone F D, Keller R E, Nordin P, "Genetic programming: an introduction: on the automatic evolution of computer programs and its applications," Morgan Kaufmann Publishers Inc. San Francisco, CA, USA, 1998.
- [19] Duda R O, Hart P E, Stork D G. "Pattern Classification," 2nd Edition, New York: John Wiley & Sons, Inc, 2001.
- [20] Koza J. "Genetic programming: on the programming of computers by means of natural selection," Cambridge, USA: MIT Press, 1992.
- [21] Silva S. "GPLAB–MATLAB programming based toolbox for GP simulation," 2015.
- [22] Piva A, Bartolini F, Caldelli R. "Self-recovery authentication of images in the DWT domain," *International Journal of Image and Graphics*, vol. 5(1), pp. 149-166, 2005.
- [23] Ullah R, Alquhayz H A. "Authentication of Topographic EEG: Employing Transform Based Watermarking," *International Journal of Computer Science and Network Security*, vol. 17(3), pp. 43-54, 2017.
- [24] <https://www.videvo.net/video/ultrasound-scan-5/3306/>.
- [25] Badshah G, Liew S C, Zain J M, Ali M. "Watermarking of ultrasound medical images in teleradiology using compressed watermark," *Journal of Medical Imaging, SPIE*, vol. 3(1), pp. 170011-170019, 2016.
- [26] Ujjare N S, Baviskar S P. "Conversion of DICOM Image in to JPEG, BMP and PNG Image Format," *Int Journal of Computer Applications*, vol. 62(11), pp. 22-26, 2013.
- [27] Sing K, Kumar B, Singh G, Mohan A. "Robust and imperceptible hybrid watermarking techniques for medical images," *Medical Image Watermarking*, Springer, pp. 61-93, 2017.

Voltage Variation Signals Source Identification and Diagnosis Method

Weihown Tee¹, Mohd Rahimi Yusoff², Abdul Rahim Abdullah³, Muhamad Faizal Yaakub⁴

Fakulti Kejuruteraan Elektrik, Universiti Teknikal Malaysia Melaka, Melaka, Malaysia^{1,3}

Fakulti Teknologi Kejuruteraan Elektrik dan Elektronik, Universiti Teknikal Malaysia Melaka, Melaka, Malaysia^{2,4}

Abstract—Power Quality (PQ) problem has become an important issue for generating bad impact to the users nowadays. It is important to detect and identify the source of the PQ problem. This paper presents a voltage variation signals source identification and diagnosis method by determining the average time frequency representation (TFR) phase power of the impedance. The signals focused in this study are the voltage variation signals, which include voltage sag, swell and interruption. The voltage variation signals from different source location (upstream, downstream as well as up and downstream) according to the IEEE Standard 1159 by using the mathematical models. The signals are first analyzed by using the Spectrograms which act as the feature producing tool. Then, the average power TFR of phase domain of each signal is calculated and tabulated. Finally, the performance of the method is identified by using support vector machine (SVM) and k -nearest neighbor (kNN). The results show that this method is an effective and suitable technique for identifying the source of voltage variation.

Keywords—Power quality; voltage variation; spectrogram; source identification; average time frequency representation phase power

I. INTRODUCTION

This Nowadays, electrical power supply quality problem is becoming great and major concern for both the industries and customers due to the increased use of electrical and electronics equipment [1]. Power quality (PQ) problem is explained as the variation in term of frequency or amplitude of the voltage or current waveform flow within a power distribution system. PQ problems are getting deliberated [2] owing to the pervasive use of switching devices within the electrical power distribution systems. PQ problem is related to the discrepancy of current and voltage from their standard pure sinusoidal waveforms. It covers a diversity of electromagnetic incident which may be transient or steady-state in nature. The incidents or phenomenon include the voltage sag, swell, interruption, harmonics, spikes, unbalance, flicker and so on [3]. Indigent quality of power may bring system failures, malfunction of equipment, reduced accuracy and efficiency of the equipment, ageing of the equipment as well as overheating of lines within the power distribution system. PQ improvement action is required to identify the source of the PQ disturbances. The improvement can be accomplished by proper detection, analysis and source identification of PQ events signals.

Studies have been done by researchers to investigate the characteristics of PQ events signals. One of the most popular PQ signals characteristics is the time-frequency characteristic [4], [5]. In the literature, there are diverse of signal processing

methods have been applied in analyzing PQ disturbance signals. The Fourier Transform (FT) and short time FT (STFT) are being applied to detect PQ signals. FT has advantages of compelling less amount of calculation as well as deep suitability, yet it has limitation for detecting steady state signals only. STFT divulges the frequency characteristics of the signals in time interval but it is difficult to reach equilibrium between time resolution and frequency resolution due to its fixed time window. From [6]–[9], these methods may bring poor efficiency of signal recognition. They are incapable to analyze transient signals due to their fixed window size. A Wavelet transform (WT) has then been used to overcome the limitation of STFT which able to improve classification accuracy due to its fluctuating window size. However, WT method [10]–[13] is time consuming and can be easily affected by noises. From the literature, spectrogram has been proposed by researchers to analyze PQ signals. It provides information [14]–[16] of signal energy with respect to time and frequency in three-dimensional form with squared modulus of STFT. This algorithm is popular and simple to be used.

Most of the researchers focus on detection and classification of PQ disturbances by using various time frequency algorithms but not much on diagnosis of disturbances. Some studies [17]–[20] have been done on PQ disturbances which involve identification of source and classification of PQ events with the implementation of automated software approach analysis. From the literature, there is no much information regarding source identification of the PQ events. In [21], the author implemented a network based PQ diagnostic system (PQDS) which has the functions to detect PQ signals, analyze PQ signals and identify the cause of the event as well as the location of the event. However, this PQDS is only applicable on voltage sag by analyzing the power system topography.

In recent days, signal processing methods and machine learning techniques are becoming the attention of the researchers. The k -nearest neighbor (kNN) has been commonly used as the choice of classification method. The kNN algorithm shows a promising classification results with low computation costs [22], [23]. Besides that, support vector machine (SVM) with Gaussian Radial Basis based kernel [24], [25] is widely used in the classification analysis of the PQ disturbances due to its excellent performance in PQ analysis studies.

The aim of this study is to explore the area of PQ events source identification and diagnosis method. The diagnosis method is developed by using the frequency and phase of

spectrogram algorithm on the impedance of the signals. In this study, the PQ events focused will be the voltage variation which includes voltage sag, swell and interruption. Then, the optimal window size in spectrogram is selected based from the literature [26], [27]. The PQ signals from upstream, downstream and both upstream and downstream will be generated according to IEEE Standard 1159 and then be analyzed with the spectrogram. Next, the phase of the impedance of the PQ events will be used to identify the source of the event. SVM and kNN are employed to classify the performance of the diagnosis method. It is important to find out the source of the PQ problem for reducing of the PQ problem towards the equipment. Source from upstream is the power source utility while downstream source is the source in the consumer's side. However, the noise evaluation is not included in this study.

The rest of paper is organized as follows. Section 2 introduces the methodology of the PQ event (voltage variation) analysis and diagnosis method. Section 3 reports the results of the study. Section 4 discusses the results showed in Section 3. Last but not least, the conclusion is presented in Section 5.

II. METHODS AND MATERIALS

A. Voltage Variation Signal Types

PQ disturbances that may appear in a power system are different in their characteristics. To differentiate the characteristics of each specific PQ event, IEEE Standard 1159-2009 explains the categories and specific threshold value of PQ disturbances. The PQ event data can be obtained through repeatedly monitoring of power signal at various plants for a long period of time. However, the uncertainty in occurrence of PQ events in power distribution system result in inadequacy of real time data [28]. To avoid time lose due to the scarcity of real time data collection, the researchers have employed the mathematical model given in IEEE Standard 1159 for generating the PQ disturbances signals, for their analysis work.

In this paper, the type of PQ disturbance focused is voltage variation which is voltage sag, swell and interruption. Mathematical models in MATLAB are modelled to simulate the signals of 50Hz of the PQ events (voltage variation) according to IEEE Standard 1159 [29]. Table I presented the voltage variation types focused in this paper. Each disturbance is presented and tabulated with equation along with the parameters. They are defined accordingly based on the IEEE standard 1159 [29].

B. Frequency Spectrogram

Short duration PQ disturbances can be easily detected and analyzed by using signal processing technique such as the time frequency distributions which give the representation of the signal in term of time frequency. STFT is the most fundamental time frequency analysis technique. It is known to be the simplest and fastest, without much computation time. While spectrogram is formulated from squared modulus of STFT. STFT and spectrogram can be mathematically written as follows [15]:

$$STFT_a(\tau, f) = \int_{-\infty}^{\infty} x(t)\omega(\tau-t)e^{-j2\pi f\tau} dt \quad (1)$$

$$S_x(\tau, f) = |STFT_a(\tau, f)|^2 \quad (2)$$

where $x(t)$ is the input signal and $\omega(\tau-t)$ is the observation window. The observation window used is Hanning window according to the literature, with window size of 1024 samples. Generally, the spectrogram exhibits a three-dimensional observant perceptive of the signal interested with respect to time and frequency. As a result, the input signal is presented in both time and frequency domains.

C. Phase Spectrogram

To obtain phase spectrogram, the signal will be processed with STFT. It can be expressed as follows:

$$STFT_b(\tau, f) = \int_{-\infty}^{\infty} x(t)\omega(\tau-t)e^{-j2\pi f\tau} dt \quad (3)$$

where $x(t)$ is the input signal and $\omega(\tau-t)$ is the observation window. The observation window here used is rectangular window. The parameter t in the observation window in (3) is defined as:

$$t = \frac{1}{FF} \quad (4)$$

where FF is the fundamental frequency of the signal. The result of STFT is a complex-valued function which grants the representation in both magnitude and phase parts of the signal. In this study, the average power time frequency representation (TFR) of the phase domain can be represented by:

$$Power_{TFR, phase}(\tau, f) = \frac{1}{T} \int_{t=0}^T \text{Imag}(STFT_b(\tau, f)) dt \quad (5)$$

where the imaginary part or phase part of the TFR is used. The phase angle of the signal input can be obtained by applying trigonometry function onto the $STFT_b$. It is calculated as follows:

$$\phi_{STFT_b}(\tau, f) = A \tan \left(\frac{\text{Imag}(STFT_b(\tau, f))}{\text{Real}(STFT_b(\tau, f))} \right) \quad (6)$$

where the calculated phase angle of $STFT_b$ is in a line of numbers which is equal to the length of the signal. The average phase angle of $STFT_b$ can be expressed as follows:

$$\theta(\tau, f) = \frac{(\sum \phi_{STFT_b}(\tau, f))}{n} \quad (7)$$

where n is length of the input signal.

TABLE I. MATHEMATICAL MODEL OF VOLTAGE VARIATION

PQ Disturbance	Equations	Parameters
Pure Sine Wave	$y(t) = A \sin(\omega t)$	$\omega = 2\pi f$ $A = 1 \text{ pu}, f = 50 \text{ Hz}$
Swell	$y(t) = A(1 + \alpha(u(t-t_1) - u(t-t_2)))\sin(\omega t)$	$0.1 \leq \alpha \leq 0.9;$ $T \leq t_2 - t_1 \leq 9T;$ $\alpha=0.3, t_1=0.05, t_2=0.15$
Sag	$y(t) = A(1 - \alpha(u(t-t_1) - u(t-t_2)))\sin(\omega t)$	$0.1 \leq \alpha \leq 0.9;$ $T \leq t_2 - t_1 \leq 9T;$ $\alpha=0.3, t_1=0.05, t_2=0.15$
Interruption	$y(t) = A(1 - \alpha(u(t-t_1) - u(t-t_2)))\sin(\omega t)$	$0.1 \leq \alpha \leq 0.9;$ $T \leq t_2 - t_1 \leq 9T;$ $\alpha=0.3, t_1=0.05, t_2=0.15$

D. Impedance Analysis

The impedance of the system is difficult to be simulated by using equation as the impedance varies to the power system itself. But in this study, the impedance of TFR of the event signal is used to perform source identification of the voltage variation. The alternative for obtaining the impedance of the event is by applying the Ohm's law. The equation of the impedance can be written as:

$$Z_{TFR}(\tau, f) = \frac{V_{TFR}(\tau, f)}{I_{TFR}(\tau, f)} \quad (8)$$

E. Machine Learning Method

Support vector machines (SVM) is a supervised machine learning method using computer science in classification. There is a method that expands the concept of hyperplane separation to the data is proposed in SVM to discriminate the data sets that unable to detach linearly according to the literature. In this study, SVM the Gaussian kernel function is implemented. The kernel function is applied in the hyperplane which takes role as the idea product of the nonlinear function. The Gaussian kernel can be expressed as follows:

$$k(x, y) = \exp\left(-\frac{\|x - y\|^2}{2\sigma^2}\right) \quad (9)$$

where x - y is the Euclidean distance between the feature vectors and σ is the kernel parameter. On the other hand, the k -nearest neighbor (kNN) has been commonly used as the choice of classification method due to its simplicity and speed. From the literature, the k values of kNN must be chosen carefully according to the specification of the model employed. In this study, the weight is utilized instead of the k value. The weight can be written as follows:

$$weight = \frac{1}{(d_{st})^2} \quad (10)$$

where d_{st} is the Euclidean distance. The Euclidean distance in (8) can be expressed as:

$$d_{st} = \sqrt{(x_s - y_t)(x_s - y_t)} \quad (11)$$

where x_s and x_y are the vectors.

III. RESULTS AND DISCUSSION

The voltage variation signals which consist of voltage sag, swell and interruption from different source location (upstream, downstream, upstream and downstream) are generated in MATLAB. The number of signals generated are 50 for each event in each source location. In total, 450 signals (50 signals x 3 events x 3 locations) are simulated. The spectrogram transforms the voltage variation signals into time frequency representations with sampling frequency of 12 kHz and fundamental frequency of 50 Hz. The TFRs for each event at each source location will be presented in this section. In this study, kNN with $k = 1$ is used in the algorithm, due to its speed and simplicity [27]. From the literature, the 2nd and 5th

repetitions will be used for the testing set, then the remaining will be applied as training set. The classification accuracy and precision [30], [31] will be presented as the performance evaluation. The classification accuracy is calculated as follows:

$$Classification Accuracy = \frac{No. of correct classified samples}{Total number of samples} \times 100 \quad (12)$$

$$Precision = \frac{TP}{TP + FP} \quad (13)$$

where TP and FP are the true positive and false positive which can be obtained from the confusion matrix. All the analysis is performed in MATLAB R2016a using computer with i7-4790 3.6 Ghz processing Intel(R) Core(TM) and 16 GB random access memory (RAM). The simulation of normal signal or pure sine wave is showed in Fig. 1(a) while the signals processed by spectrogram are presented in Fig. 1(b).

A. Source Location at Downstream

Fig. 2(a) demonstrates the simulated sag signals. As can be seen, the sag situation is set at time in between 0.05s to 0.15s. The signals are then analyzed by spectrogram and presented in Fig. 2(b). The signals are being captured in 50 Hz. The lighter areas exhibit higher amplitude. In turn, the darker areas display lower amplitude. During voltage sag in time period between 0.05s to 0.15s, there is a decline in voltage amplitude where the yellowish contour changes to blue contour when time approaching 0.05s and changes back to yellowish contour when approaching 0.15s. The TFR of magnitude and phase of the impedance is showed in Fig. 2(c). The TFR contour of the impedance is affected between the period of 0.05s and 0.15s. The TFR phase contour of impedance is captured at 50 Hz. The TFR power spectrum for the voltage, current, impedance and impedance TFR phase is plotted in Fig. 2(d). The value of the average power of impedance TFR phase obtained is -25.1.

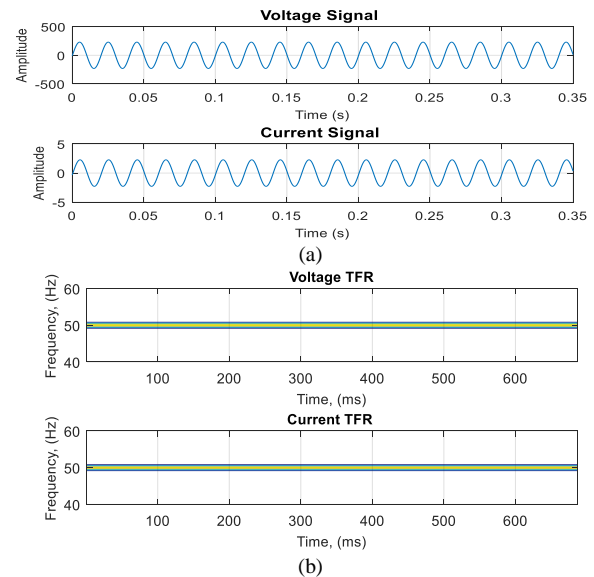


Fig. 1. Normal Voltage and Current Signal, (b) TFR of the Normal Voltage and Current Signal.

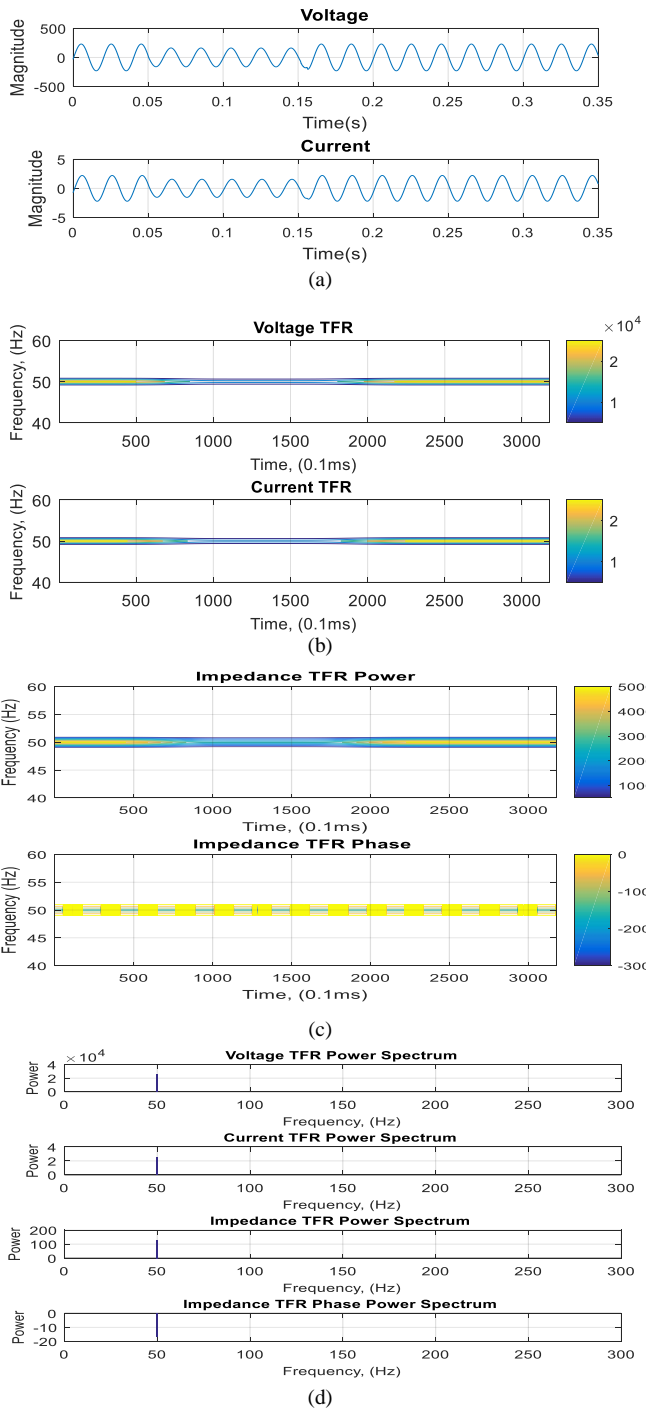


Fig. 2. (a) Voltage and Current Sag Signal, (b) TFR of the Voltage and Current Sag Signal, (c) TFR Power and Phase of Sag Impedance, (d) Power Spectrum.

Fig. 3(a) shows the swell signals. The swell situation is set at time in between 0.05s to 0.15s as well. The simulated voltage has an increase of magnitude within the time set. Fig. 3(b) shows the signals analyzed by spectrogram. The signals are being captured in 50 Hz. During voltage swell in time period between 0.05s to 0.15s, there is an increase in voltage amplitude where the yellowish contour appears between the duration 0.05s to 0.15s which indicates the

amplitude of the signal is higher within the duration. The TFR of magnitude and phase of the impedance is showed in Fig. 3(c). The TFR contour of the impedance is affected between the period of 0.05s and 0.15s where the impedance has higher amplitude within that 0.05s duration. The TFR phase contour of impedance is captured at 50 Hz. The TFR power spectrum for the voltage, current, impedance and impedance TFR phase is plotted in Fig. 3(d). The value of the average power of impedance TFR phase obtained is -90.54.

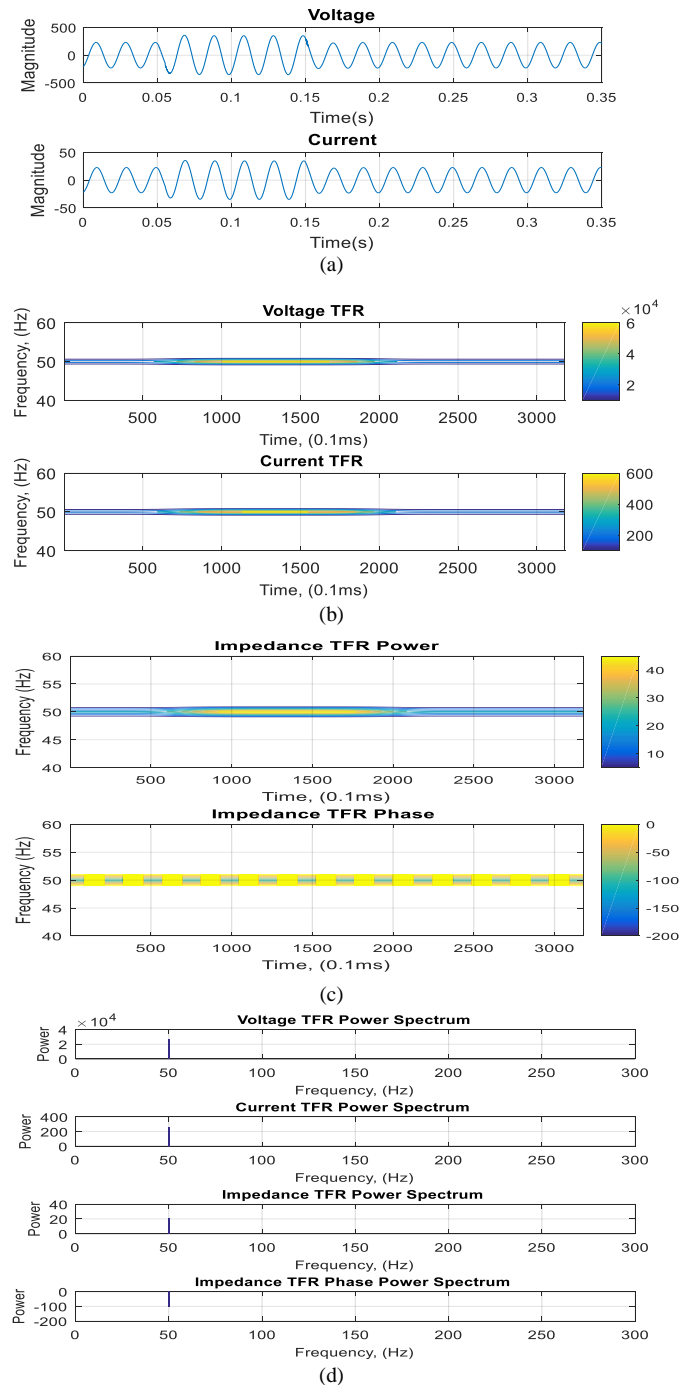


Fig. 3. Voltage and Current Swell Signal, (b) TFR of the Voltage and Current Swell Signal, (c) TFR Power and Phase of Swell Impedance, (d) Power Spectrum.

Fig. 4(a) shows the interruption signals. The interrupted situation is set at time in between 0.05s to 0.15s where the voltage signal is starting to drop to value approximately zero during the period. Fig. 4(b) shows the signals analyzed by spectrogram. The signals are being captured in 50 Hz. During voltage interruption in time period between 0.05s to 0.15s, no contour is plotted as the amplitude of the voltage is dropping near to zero. The TFR of magnitude and phase of the impedance is showed in Fig. 4(c). The TFR contour of the impedance is affected between the period of 0.05s and 0.15s where the impedance has no value within that 0.05s duration. The TFR phase contour of impedance is captured at 50 Hz. The TFR power spectrum for the voltage, current, impedance and impedance TFR phase is plotted in Fig. 4(d). The value of the average power of impedance TFR phase obtained is -102.4.

B. Source Location at Upstream

Fig. 5(a) shows the sag signal. The sag occurs between 0.05s and 0.15s. The signals are then analyzed by spectrogram and presented in Fig. 5(b). The signals are being captured in 50 Hz. During voltage sag in time period between 0.05s to 0.15s, a decrease in voltage amplitude can be seen where the yellowish contour changes to blue contour when time approaching 0.05s and changes back to yellowish contour when approaching 0.15s. The TFR of magnitude and phase of the impedance is showed in Fig. 5(c). The TFR contour of the impedance is affected between the period of 0.05s and 0.15s. The TFR phase contour of impedance is captured at 50 Hz. The TFR power spectrum for the voltage, current, impedance and impedance TFR phase is plotted in Fig. 5(d). The value of the average power of impedance TFR phase obtained is 20.95.

Fig. 6(a) shows the swell signals. The swell situation is set at time in between 0.05s to 0.15s as well. The simulated voltage has an increase of magnitude more than its nominal value within the time set. Fig. 6(b) shows the signals analyzed by spectrogram. The signals are being captured in 50 Hz. During voltage swell in time period between 0.05s to 0.15s, there is an increase in voltage amplitude where the yellowish contour appears between the duration 0.05s to 0.15s which indicates the amplitude of the signal is higher within the duration. The TFR of magnitude and phase of the impedance is showed in Fig. 6(c). The TFR contour of the impedance changes between the period of 0.05s and 0.15s where the impedance has higher amplitude within that 0.05s duration. The TFR phase contour of impedance is captured at 50 Hz. The TFR power spectrum for the voltage, current, impedance and impedance TFR phase is plotted in Fig. 6(d). The value of the average power of impedance TFR phase obtained is 114.5.

Fig. 7(a) shows the interruption signals. The interrupted situation is set at time in between 0.05s to 0.15s where the voltage signal decreases to value approximately zero during the period. Fig. 7(b) shows the signals analyzed by spectrogram. The signals are being captured in 50 Hz. During voltage interruption in time period between 0.05s to 0.15s, no contour can be seen due to the dropping of the amplitude of the voltage approximately to zero. The TFR of magnitude and phase of the impedance is showed in Fig. 7(c). The TFR contour of the

impedance is affected between the period of 0.05s and 0.15s where the impedance has no value within that 0.05s duration. The TFR phase contour of impedance is captured at 50 Hz. The TFR power spectrum for the voltage, current, impedance and impedance TFR phase is plotted in Fig. 7(d). The value of the average power of impedance TFR phase obtained is 38.87.

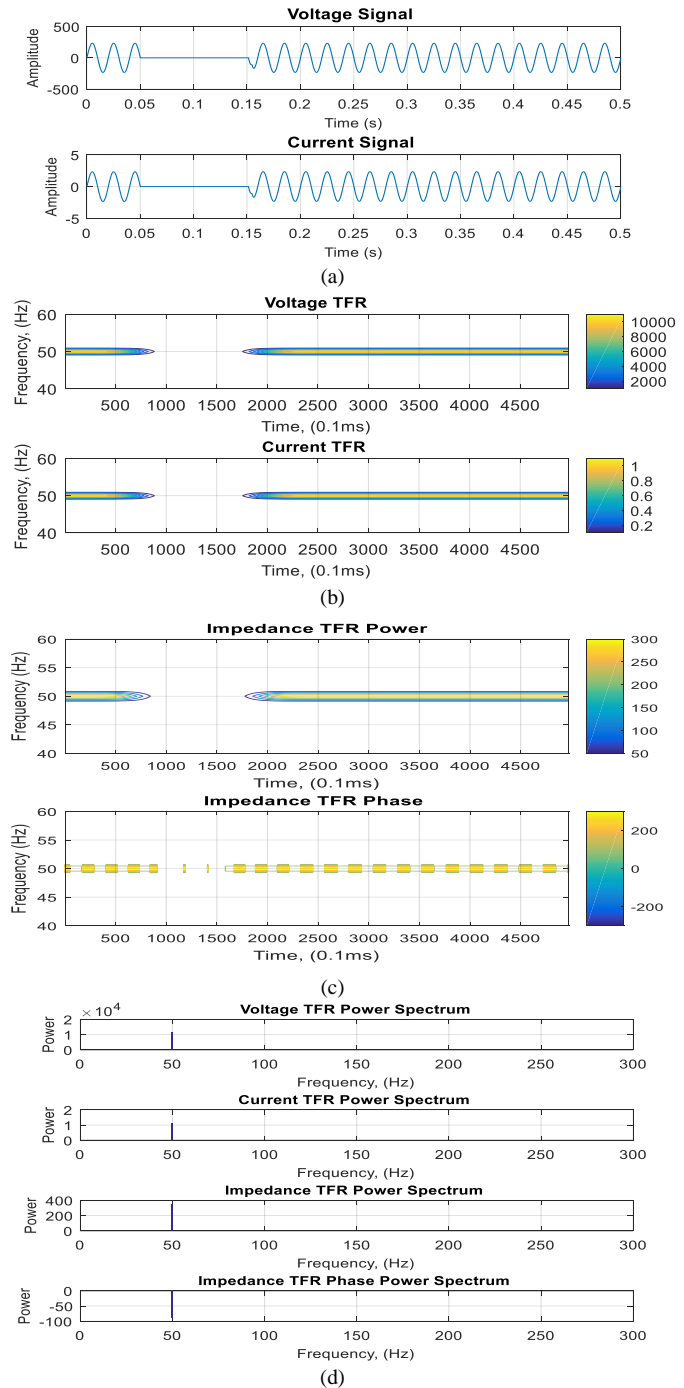


Fig. 4. Voltage and Current Interruption Signal, (b) TFR of the Voltage and Current Interruption Signal, (c) TFR Power and Phase of Interruption Impedance, (d) Power Spectrum.

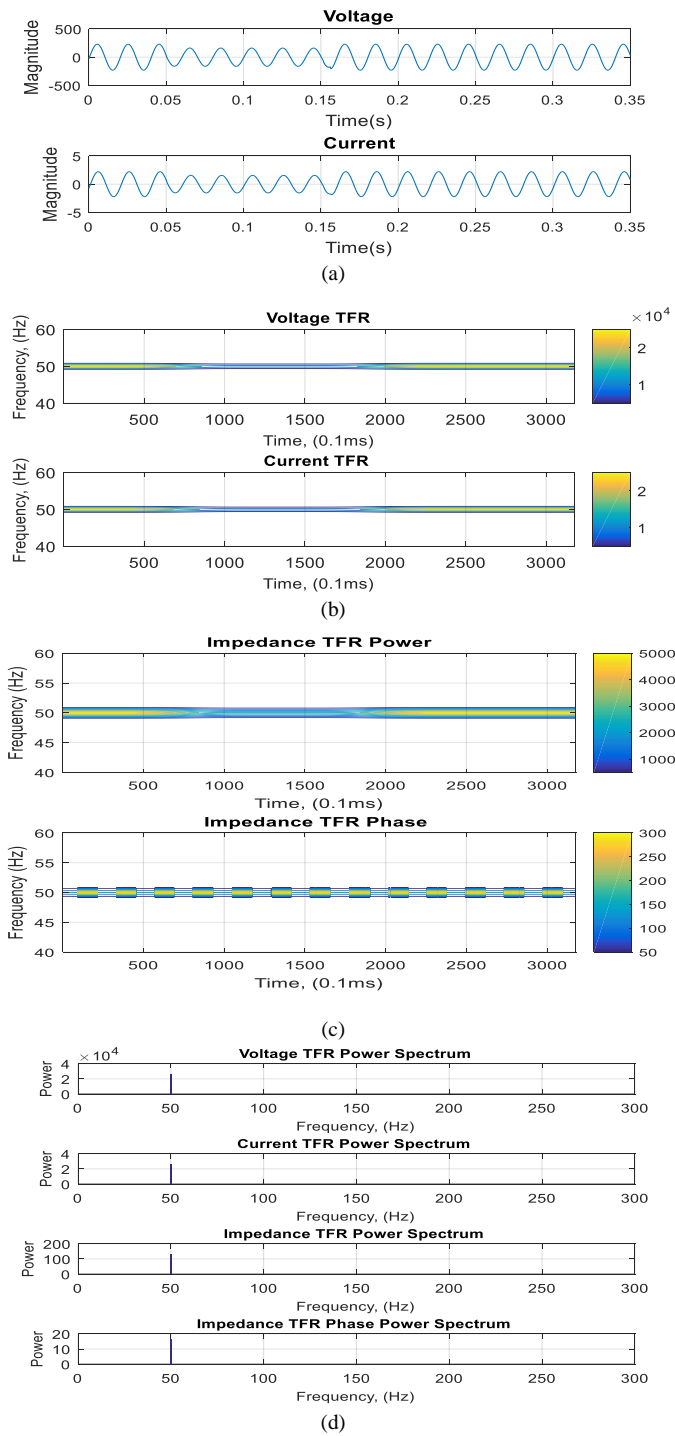


Fig. 5. (a) Voltage and Current Sag Signal, (b) TFR of the Voltage and Current Sag Signal, (c) TFR Power and Phase of Sag Impedance, (d) Power Spectrum.

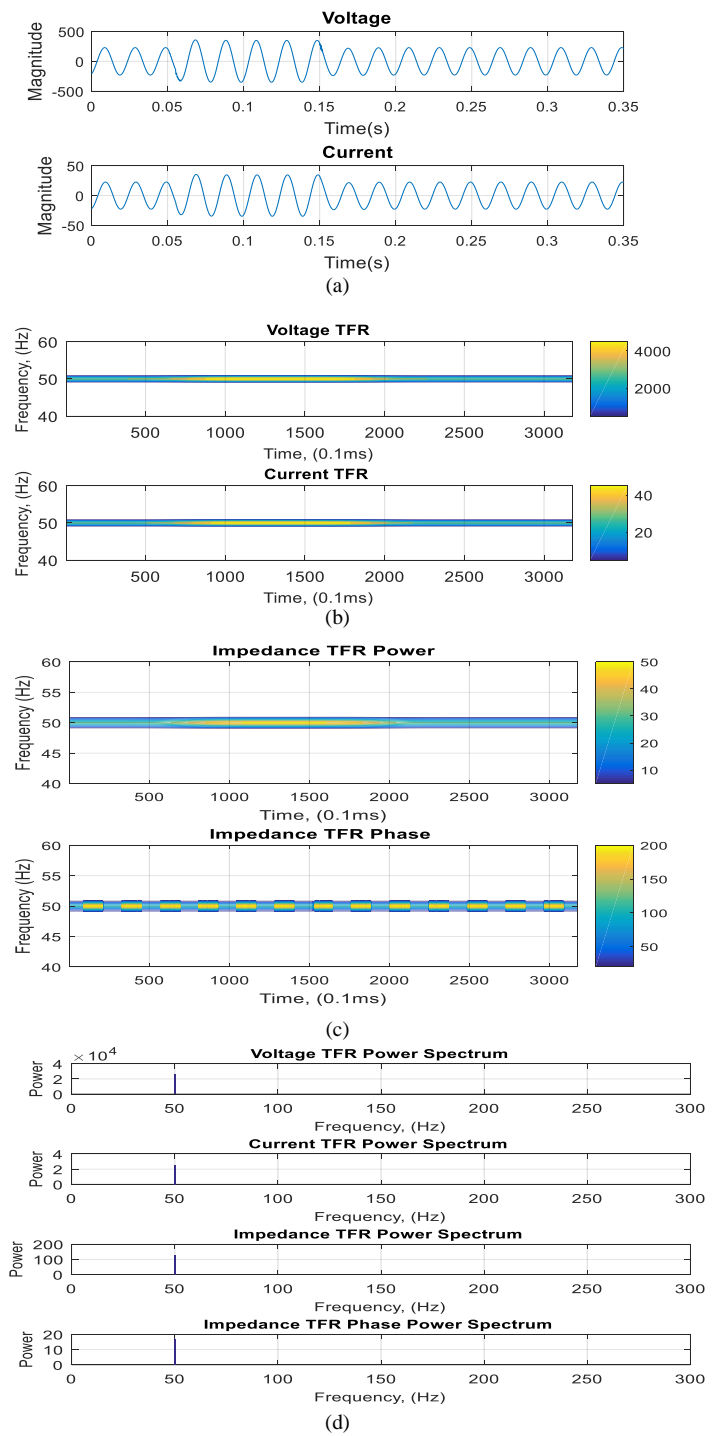


Fig. 6. (a) Voltage and Current Swell Signal, (b) TFR of the Voltage and Current Swell Signal, (c) TFR Power and Phase of Swell Impedance, (d) Power Spectrum.

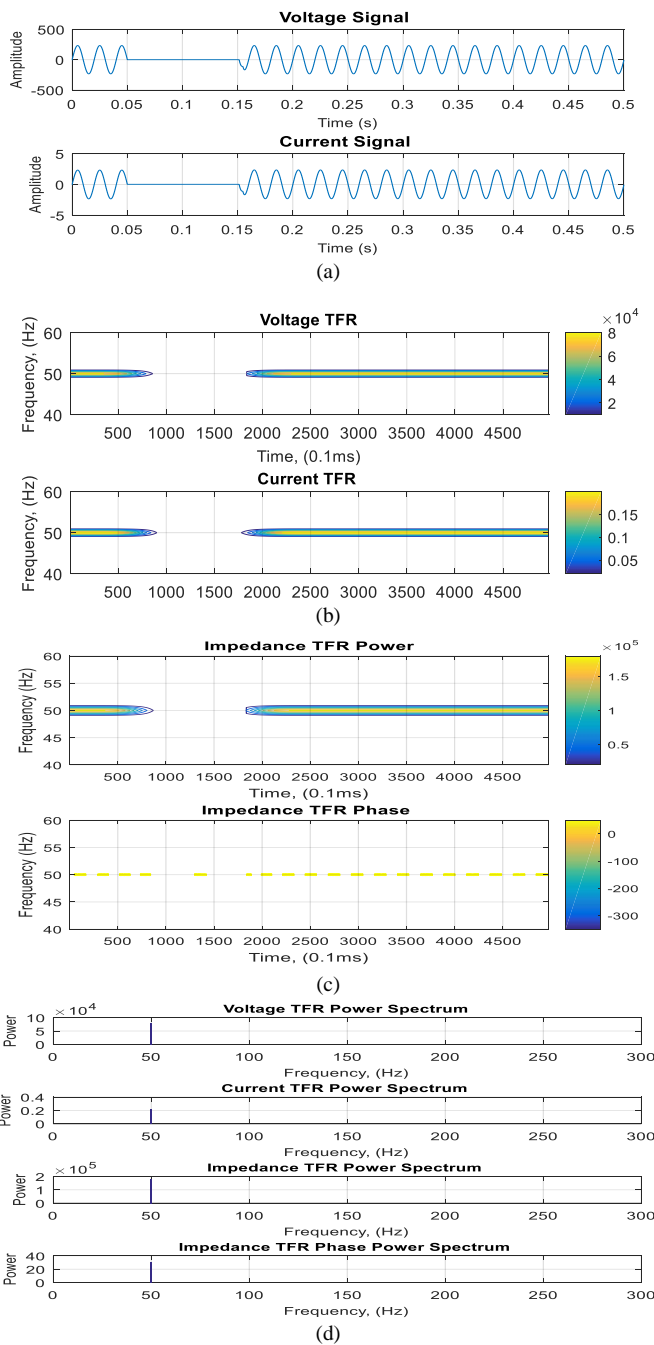


Fig. 7. (a) Voltage and Current Interruption Signal, (b) TFR of the Voltage and Current Interruption Signal, (c) TFR Power and Phase of Interruption Impedance, (d) Power Spectrum.

C. Source Location at both Upstream and Downstream

Fig. 8(a) shows the sag signal. The sag duration is between 0.05s and 0.15s. The signals are then analyzed by spectrogram and presented in Fig. 8(b). The signals are being captured in 50 Hz. During voltage sag in time period between 0.05s to 0.15s, the voltage amplitude drops from yellowish to blue contour. The TFR of magnitude and phase of the impedance is showed in Fig. 8(c). The TFR contour of the impedance is affected between the period of 0.05s and 0.15s. The TFR phase contour of impedance is captured at 50 Hz. The TFR power spectrum

for the voltage, current, impedance and impedance TFR phase is plotted in Fig. 8(d). The value of the average power of impedance TFR phase obtained is 5001.12.

Fig. 9(a) shows the swell signals. The swell happens in between 0.05s to 0.15s. The simulated voltage has an increment of magnitude more than its nominal value within the time set. Fig. 9(b) shows the signals analyzed by spectrogram. The signals are being captured in 50 Hz. During voltage swell in time period between 0.05s to 0.15s, there is an increment in voltage amplitude where the yellowish contour appears between the duration 0.05s to 0.15s which indicates the amplitude of the signal is higher within the duration and changes back to blue contour. The TFR of magnitude and phase of the impedance is showed in Fig. 9(c). The TFR contour of the impedance changes between the period of 0.05s and 0.15s. The TFR phase contour of impedance is captured at 50 Hz. The TFR power spectrum for the voltage, current, impedance and impedance TFR phase is plotted in Fig. 9(d). The value of the average power of impedance TFR phase obtained is 397.43.

Fig. 10(a) shows the interruption signals. The interrupted situation is set at time in between 0.05s to 0.15s where the voltage signal drastically drops to value approximately zero during the period. Fig. 10(b) shows the signals processed by spectrogram. The signals are detected in 50 Hz. During voltage interruption in time period between 0.05s to 0.15s, the contour comes to a halt where no contour plot can be seen. The TFR of magnitude and phase of the impedance is showed in Fig. 10(c). The TFR contour of the impedance is affected between the period of 0.05s and 0.15s where the impedance has no value within that 0.05s duration. The TFR phase contour of impedance is captured at 50 Hz. The TFR power spectrum for the voltage, current, impedance and impedance TFR phase is plotted in Fig. 10(d). The value of the average power of impedance TFR phase obtained is 999.81.

D. Experimental Results

In this study, there are two simulated signals (voltage and current) for each event from each source location are used to determine their phase angle. The signals are named as Downstream Voltage Sag (DVSG), Downstream Current Sag (DCSG), Downstream Voltage Swell (DVSL), Downstream Current Swell (DCSL), Downstream Voltage Interruption (DVI), Downstream Current Interruption (DCI), Upstream Voltage Sag (UVSG), Upstream Current Sag (UCSG), Upstream Voltage Swell (UVSL), Upstream Current Swell (UCSL), Upstream Voltage Interruption (UVI), Upstream Current Interruption (UCI), Up and Downstream Voltage Sag (UDVSG), Up and Downstream Current Sag (UDCSG), Up and Downstream Voltage Swell (UDVSL), Up and Downstream Current Swell (UDCSL), Up and Downstream Voltage Interruption (UDVI) as well as Up and Downstream Current Interruption (UDCI). Table II shows the phase angles of voltage signals calculated for all events along with the precision. The signals are simulated with fundamental angle of 20° for voltage signal and 90° for current signal. The phase angles of both the voltage and current signals showed an overall value which is not differ much from the original input angle. The phase angles of current signals calculated are tabulated in Table III.

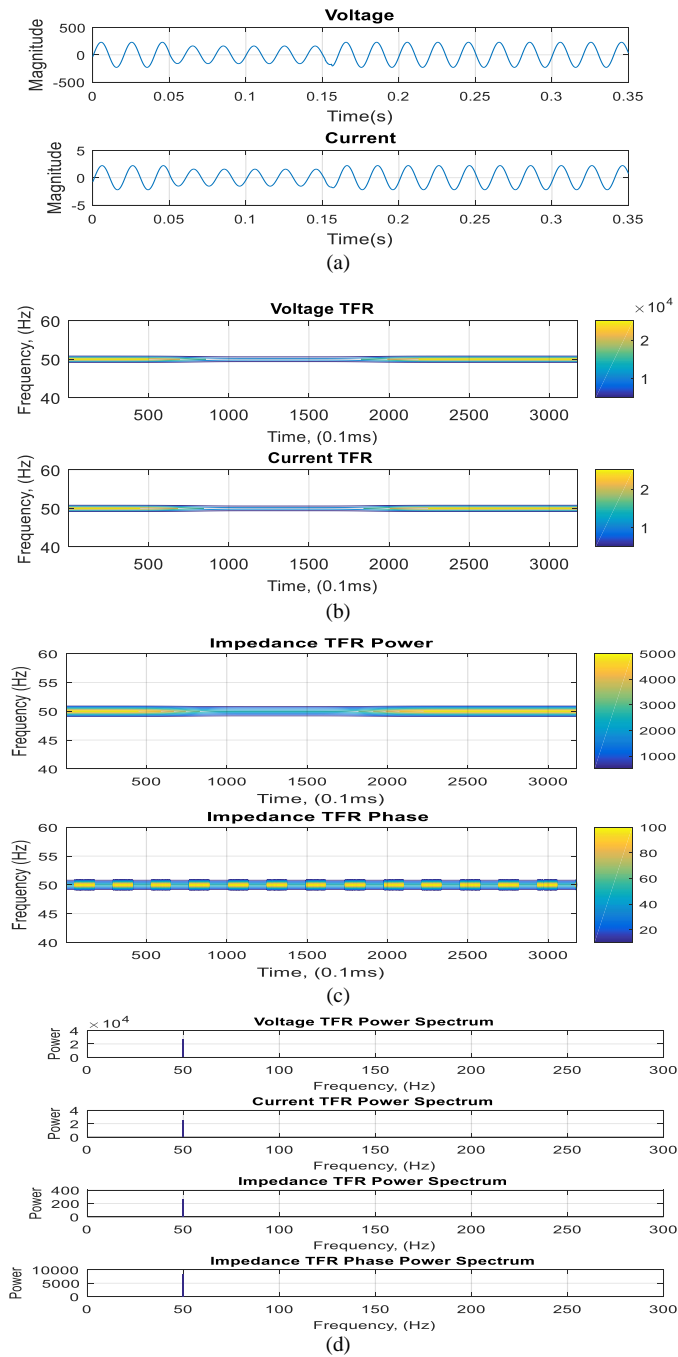


Fig. 8. (a) Voltage and Current Sag Signal, (b) TFR of the Voltage and Current Sag Signal, (c) TFR Power and Phase of Sag Impedance, (d) Power Spectrum.

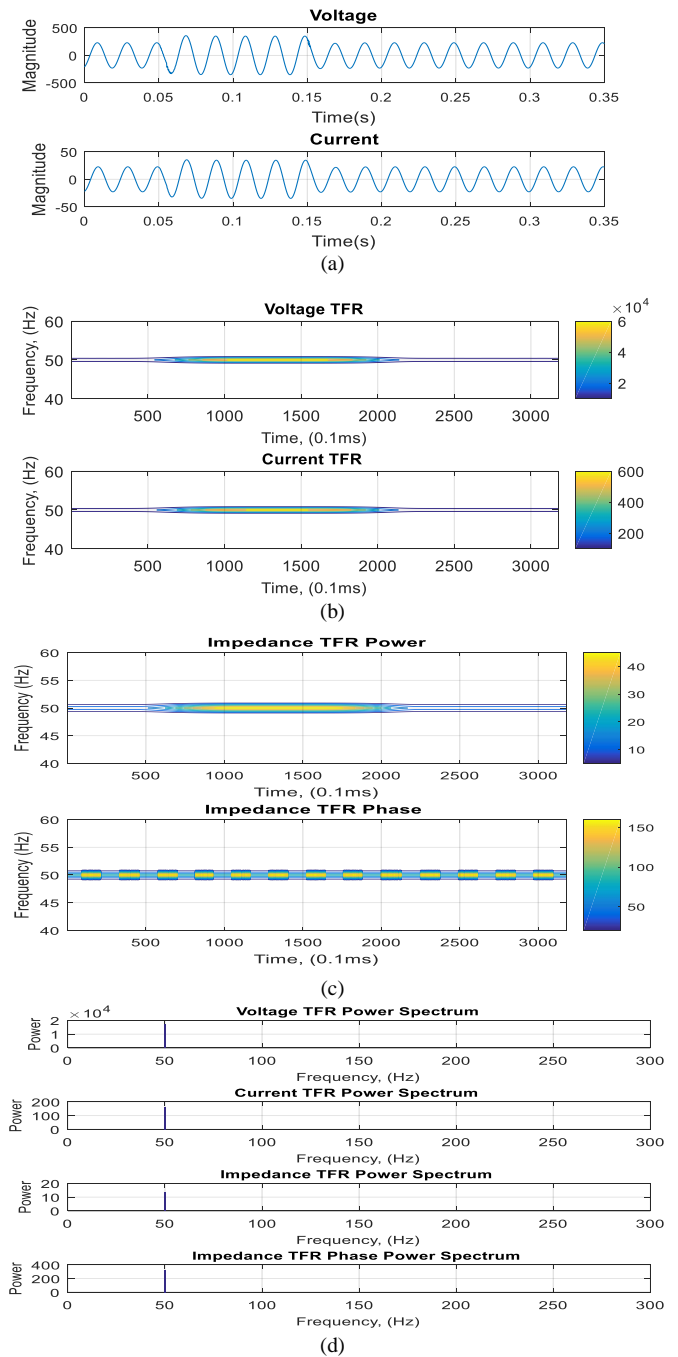


Fig. 9. (a) Voltage and Current Swell Signal, (b) TFR of the Voltage and Current Swell Signal, (c) TFR Power and Phase of Swell Impedance, (d) Power Spectrum.

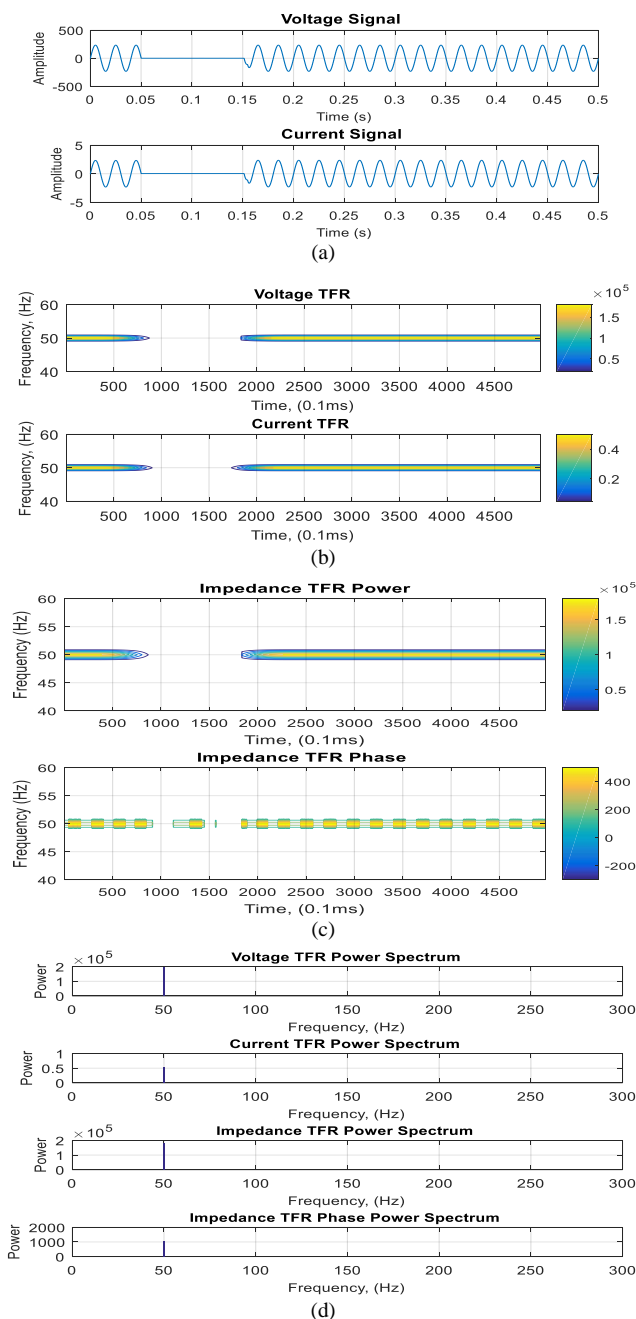


Fig. 10. (a) Voltage and Current Interruption Signal, (b) TFR of the Voltage and Current Interruption Signal, (c) TFR Power and Phase of Interruption Impedance, (d) Power Spectrum.

Table IV shows the average power of impedance TFR phase for each case. As can be seen, case DVSG, DVSL and DVI has negative magnitude of average power. This shows that cases occurred in downstream have low average power of impedance TFR phase. Case UDVSG, UDVSL and UDVI has higher magnitude of average power compared to case UVSG, UVSL and UVI. The mean values for each case have showed similar trend. From this point of view, downstream voltage signals have lowest average impedance TFR phase power while up and downstream signals have highest average impedance TFR phase power.

Table V demonstrates the confusion matrix for each case by using SVM. The confusion matrix for each case with the kNN classifier is tabulated in Table VI. As can be seen, the classification accuracy of SVM is 94.2222%, which is higher than kNN which has classification accuracy of 93.5556%. From this point of view, SVM has better performance in classifying the voltage variation with different location compared to kNN.

TABLE II. PHASE ANGLES OF VOLTAGE SIGNALS

Voltage Signal	Original Input Phase Angle (°)	Phase Angle Obtained (°), (single signal)	Precision (single signal)	Phase Angle (°), (mean of 50 signals)	Precision (mean of 50 signals)
DVSG	20	20.62	0.9751	20.21	0.9735
DVSL	20	20.74	0.9659	20.18	0.9652
DVI	20	20.73	0.9611	20.52	0.9600
UVSG	20	21.0	0.9812	21.2	0.9817
UVSL	20	20.8	0.9745	19.9	0.9656
UVI	20	19.6	0.9700	19.32	0.9653
UDVSG	20	19.34	0.9875	19.01	0.9691
UDVSL	20	20.1	0.9704	20.43	0.9800
UDVI	20	19.26	0.9653	19.12	0.9648

TABLE III. PHASE ANGLES OF CURRENT SIGNALS

Current Signal	Original Input Phase Angle (°)	Phase Angle Obtained (°), (single signal)	Precision (single signal)	Phase Angle (°), (mean of 50 signals)	Precision (mean of 50 signals)
DCSG	90	88.9	0.9501	89.51	0.9610
DCSL	90	90.7	0.9619	89.42	0.9491
DCI	90	89.34	0.9691	89.03	0.9554
UCSG	90	89.2	0.9782	88.96	0.9643
UCSL	90	90.2	0.9915	89.5	0.9548
UCI	90	90.13	0.9630	89.59	0.9594
UDCSG	90	91.1	0.9719	89.15	0.9499
UDCSL	90	90.58	0.9851	89.50	0.9646
UDCI	90	87.53	0.9570	88.09	0.9504

TABLE IV. AVERAGE IMPEDANCE TFR PHASE POWER

Case	Average Impedance TFR Phase Power (single signal)	Average Impedance TFR Phase Power (mean of 50 signals)
DVSG	-25.1	-29.56
DVSL	-90.54	-92.84
DVI	-102.4	-105.53
UVSG	20.95	23.51
UVSL	114.5	113.97
UVI	38.87	39.16
UDVSG	5001.12	5008.73
UDVSL	397.43	401.5
UDVI	999.81	1003.88

TABLE V. CONFUSION MATRIX AND CLASSIFICATION ACCURACY BY USING SVM FOR VOLTAGE SIGNALS

	DVSG	DVSL	DVI	UVSG	UVSL	UVI	UDVSG	UDVSL	UDVI
DVSG	88	12	0	0	0	0	0	0	0
DVSL	0	100	0	0	0	0	0	0	0
DVI	0	4	96	0	0	0	0	0	0
UVSG	0	0	0	94	6	0	0	0	0
UVSL	0	0	0	0	90	10	0	0	0
UVI	0	0	0	0	0	100	0	0	0
UDVSG	0	0	0	0	0	6	94	0	0
UDVSL	0	0	0	0	0	0	6	86	8
UDVI	0	0	0	0	0	0	0	0	100
Overall Classification Accuracy: 94.2222%									

TABLE VI. CONFUSION MATRIX AND CLASSIFICATION ACCURACY BY USING KNN FOR VOLTAGE SIGNALS

	DVSG	DVSL	DVI	UVSG	UVSL	UVI	UDVSG	UDVSL	UDVI
DVSG	96	4	0	0	0	0	0	0	0
DVSL	0	96	4	0	0	0	0	0	0
DVI	0	2	94	4	0	0	0	0	0
UVSG	0	0	0	94	6	0	0	0	0
UVSL	0	0	0	2	98	0	0	0	0
UVI	0	0	0	0	2	96	2	0	0
UDVSG	0	0	0	0	0	2	86	12	0
UDVSL	0	0	0	0	0	0	4	88	8
UDVI	0	0	0	0	0	0	0	6	94
Overall Classification Accuracy: 93.5556%									

According to the literature, the diagnosis method used in this study has different way of approach compared to other diagnosis methods. The performance of this method is analyzed by using the 450 sets of voltage variation data simulated according to the IEEE Standard 1159. Firstly, the signals generated can be analyzed by frequency and phase spectrogram to obtain the necessary parameters as mentioned in the methodology. The signals analyzed are captured at the frequency of 50 Hz and the differ in contour for each voltage variation can be observed from the contour plot. Secondly, the phase angle of the signals can be calculated according to the equation stated in the methodology. The obtained values are close to the actual input value. Secondly, the average power of the impedance TFR phase for the three cases (problem source from downstream, upstream as well as up and downstream) can be obtained by the equation stated. The results are able to categorize the signals into the three cases stated due to the differ values of each case. In addition, the classification accuracy for each type of case has been presented and SVM shows the better performance compared to kNN in this study.

Through the analysis, we found that the problem source of the voltage variation can be identified by the average power of impedance TFR phase. The average power for problem source at downstream has the lowest value while problem source at both up and downstream has the highest value. The range in

between them is the range for problem source at upstream. In sum, this method is useful in identifying the problem source of the voltage variation.

IV. CONCLUSION

A method of diagnosis of source identification by implementing the imaginary part of the impedance of voltage variation is used in this study. The experimental results revealed that voltage variation occurs at both up and downstream has the highest value of average power, followed by the voltage variation occurs at upstream. The average power is lowest for downstream case. In summary, this source identification and diagnosis method is easy to be implemented and performed. As for future works, the implementation of hardware can be proposed in order to provide an online and real-time monitoring tool. On top of that, the source identification and diagnosis method used in this study can be improved and applying it on more type of PQ disturbances other than voltage variation. The analysis of using time frequency distributions can be explored too for getting more parameters and features for classification.

ACKNOWLEDGMENT

The authors would like to thank Universiti Teknikal Malaysia Melaka (UTeM) for providing the research grant GLuar/STEVIA/2016/FKE-CeRIA/100009.

REFERENCES

- [1] S. Khokhar, A. A. B. Mohd Zin, A. S. B. Mokhtar, and M. Pesaran, "A comprehensive overview on signal processing and artificial intelligence techniques applications in classification of power quality disturbances," *Renew. Sustain. Energy Rev.*, 2015.
- [2] M. Uyar, S. Yildirim, and M. T. Gencoglu, "An expert system based on S-transform and neural network for automatic classification of power quality disturbances," *Expert Syst. Appl.*, vol. 36, no. 3 PART 2, pp. 5962–5975, 2009.
- [3] B. Alsayyed Ahmad, H. H. ElSheikh, and A. Fadoun, "Review of power quality monitoring systems," 2015 Int. Conf. Ind. Eng. Oper. Manag., pp. 1–8, 2015.
- [4] O. P. Mahela, A. G. Shaik, and N. Gupta, "A critical review of detection and classification of power quality events," *Renewable and Sustainable Energy Reviews*. 2015.
- [5] D. Granados-Lieberman, R. J. Romero-Troncoso, R. A. Osornio-Rios, A. Garcia-Perez, and E. Cabal-Yepez, "Techniques and methodologies for power quality analysis and disturbances classification in power systems: a review," *IET Gener. Transm. Distrib.*, vol. 5, no. 4, p. 519, 2011.
- [6] J. Han, W. Kim, J.-W. Lee, and C.-H. Kim, "Fault type classification in transmission line using STFT," 11th IET Int. Conf. Dev. Power Syst. Prot. (DPSP 2012), 2012.
- [7] S. a. Deokar and L. M. Waghmare, "Integrated DWT-FFT approach for detection and classification of power quality disturbances," *Int. J. Electr. Power Energy Syst.*, vol. 61, pp. 594–605, 2014.
- [8] M. S. Azam, F. Tu, K. R. Pattipati, and R. Karanam, "A Dependency Model-Based Approach for Identifying and Evaluating Power Quality Problems," *IEEE Trans. Power Deliv.*, vol. 19, no. 3, pp. 1154–1166, 2004.
- [9] A. I. Saichev and W. Woyczynski, "Fourier transform," in *Applied and Numerical Harmonic Analysis*, 2018.
- [10] M. V. Reddy and R. Sodhi, "A rule-based S-Transform and AdaBoost based approach for power quality assessment," *Electr. Power Syst. Res.*, 2016.
- [11] Y. Gu and M. H. J. Bollen, "Time-frequency and time-scale domain analysis of voltage disturbances," *IEEE Trans. Power Deliv.*, 2000.
- [12] S. Mishra, C. N. Bhende, and B. K. Panigrahi, "Detection and Classification of Power Quality Disturbances Using S-Transform and Probabilistic Neural Network," *IEEE Trans. Power Deliv.*, vol. 23, no. 1, pp. 280–287, 2008.
- [13] C. N. Bhende, S. Mishra, and B. K. Panigrahi, "Detection and classification of power quality disturbances using S-transform and modular neural network," *Electr. Power Syst. Res.*, vol. 78, no. 1, pp. 122–128, 2008.
- [14] A. R. Abdullah, N. a. Abidullah, N. H. Shamsudin, N. H. H. Ahmad, and M. H. Jopri, "Power Quality Signals Classification System Using Time-Frequency Distribution," *Appl. Mech. Mater.*, 2014.
- [15] F. Léonard, "Phase spectrogram and frequency spectrogram as new diagnostic tools," *Mech. Syst. Signal Process.*, 2007.
- [16] W. K. Lu and Q. Zhang, "Deconvolutive short-time fourier transform spectrogram," *IEEE Signal Process. Lett.*, 2009.
- [17] J. Zhu, D. L. Lubkeman, and A. A. Girgis, "Automated fault location and diagnosis on electric power distribution feeders," *IEEE Trans. Power Deliv.*, 1997.
- [18] M. J. Santofimia, X. Del Toro, P. Roncero-Sánchez, F. Moya, M. A. Martinez, and J. C. Lopez, "A qualitative agent-based approach to power quality monitoring and diagnosis," *Integr. Comput. Aided. Eng.*, 2010.
- [19] M. Faisal, A. Mohamed, H. Shareef, and A. Hussain, "Power quality diagnosis using time frequency analysis and rule based techniques," *Expert Syst. Appl.*, 2011.
- [20] E. J. Powers et al., "Time-frequency diagnosis, condition monitoring, and fault detection," in *Time-Frequency Signal Analysis and Processing: A Comprehensive Reference*, 2015.
- [21] M. S. Azam, F. Tu, K. R. Pattipati, and R. Karanam, "A dependency model-based approach for identifying and evaluating power quality problems," *IEEE Trans. Power Deliv.*, vol. 19, no. 3, pp. 1154–1166, 2004.
- [22] S. Tan, "Neighbor-weighted K-nearest neighbor for unbalanced text corpus," *Expert Syst. Appl.*, 2005.
- [23] S. Karasu and S. Başkan, "Classification of power quality disturbances by using ensemble technique," in 2016 24th Signal Processing and Communication Application Conference, SIU 2016 - Proceedings, 2016.
- [24] S. Naderian and A. Salemnia, "Detection and classification of power-quality events using discrete Gabor transform and Support Vector Machine," in 6th Annual International Power Electronics, Drive Systems, and Technologies Conference, PEDSTC 2015, 2015, pp. 544–549.
- [25] D. Srinivasan, W. S. Ng, and A. C. Liew, "Neural-network-based signature recognition for harmonic source identification," *IEEE Trans. Power Deliv.*, vol. 21, no. 1, pp. 398–405, 2006.
- [26] M. H. W. Tee., Abdullah, A. R., Sutikno, T., Jopri, "A Comparative Modeling and Analysis of Voltage Variation by Using Spectrogram."
- [27] N. Mohd Ali, A. Abdullah, N. Mohd Saad, J. Too, and W. Tee, "A New Competitive Binary Grey Wolf Optimizer to Solve the Feature Selection Problem in EMG Signals Classification," *Computers*, 2018.
- [28] S. Das, A. K. Pradhan, A. Kedia, S. Dalai, B. Chatterjee, and S. Chakravorti, "Diagnosis of Power Quality Events Based on Detrended Fluctuation Analysis," *IEEE Trans. Ind. Electron.*, 2018.
- [29] IEEE and Institute of Electrical and Electronic Engineers, *IEEE Std 1159 - IEEE Recommended Practice for Monitoring Electric Power Quality*. 2009.
- [30] R. Kumar, B. Singh, D. T. Shahani, A. Chandra, and K. Al-Haddad, "Recognition of Power-Quality Disturbances Using S-Transform-Based ANN Classifier and Rule-Based Decision Tree," *IEEE Trans. Ind. Appl.*, 2015.
- [31] J. Too, A. Abdullah, N. Mohd Saad, and W. Tee, "EMG Feature Selection and Classification Using a Pbest-Guide Binary Particle Swarm Optimization," *Computation*, vol. 7, no. 1, p. 12, 2019.

Reliability and Connectivity Analysis of Vehicular Ad Hoc Networks for a Highway Tunnel

Saajid Hussain¹, Di Wu^{*2}, Wang Xin³, Sheeba Memon⁴, Naadiya Khuda Bux⁵, Arshad Saleem⁶

School of Computer Science and Engineering, Dalian University of Technology Liaoning, Dalian 116024, China^{1,2}

School of Mechanical Engineering, Dalian University of Technology Liaoning, Dalian 116024, China³

School of Information Science and Engineering, Central South University, Hunan, Changsha 410083, China^{4,5}

Shaheed Benazir Bhutto University, Shaheed Benazirabad, Landhi-Nawabshah 67450, Pakistan⁶

Abstract—Vehicular ad-hoc network (VANET) uses ‘mobile internet’ to facilitate the communication between vehicles and with the goal to ensure road safety and achieve secure communication. Thus the reliability of this type of networks is of paramount significance. The safety-related messages are disseminated in VANETs, on the wireless medium through vehicle to vehicle (V2V) and Vehicle to roadside (V2R) communications. Hence, the Reliability of network is an essential requirement. This paper considers the effect of vehicle transmission range R_{tran} and vehicle density ρ on the connectivity probability. In addition, a reliability model which takes into account minimal safe headway S_h among nearby vehicles at highway tunnel is specified. The reason is that under the tunnel Global Positioning System (GPS), a component of onboard unit (OBU) needs a rich line of sight for perfect services, because due to signal interference, the GPS does not work properly. Though, in the case of a fully connected network, there are chances of danger between vehicles which are close to each other. Therefore, the network is not safe, as accidents and collision can happen at any time. Hence, maintaining the minimal safe headway distance under the tunnel is interesting and useful for VANET. The obtained results show that the little difference of the minimal safe headway under the tunnel can cause a serious change in the entire network reliability. Suggesting that while designing the network reliability models the safe headway S_h cannot be ignored.

Keywords—Minimal safe headway; reliability; highway tunnel; vehicular ad hoc networks; connectivity probability

I. INTRODUCTION

Several studies [1- 4], have been conducted to examine the reliability of networks in terms of connectivity, according to the network topology. The reliability of networks is gaining importance day by day particularly safety-sensitive networks like Vehicular ad hoc Networks. In networks, reliability refers to the probability that there prevail no less than one possible connection amongst two vehicles under the specified condition. Reliability issues appear increasingly essential as advance networks turn to be increasingly unpredictable. This encouraged the research on the reliability of networks, which drew much attention during previous decades. In the work of [5], the authors have analyzed vehicle to vehicle wireless connectivity by using mathematical models of mobility and its relation with time. The effect of headway distance, acceleration, association time (i.e. connection setup time), relative speed of vehicles, transmission range and message/data

size in short range based V2V communications in the models were analyzed. The authors in [6], presented a fluid dynamic model to study dynamism of VANET under various traffic conditions, connectivity between OBUs was analyzed. The authors in [7], proposed an analytical model in which the traffic congestion was avoided by reducing vehicles speed instead of blocking the flow of traffic.

VANETs offer an appropriate environment regarding road-safety applications. VANET can support two kinds of applications: 1) to support road safety, and 2) to support non-safety applications. Safety-related applications share necessary information amongst vehicles such as weather conditions, road accident information and propagate emergency messages. Non-safety related applications provide entertainment to passengers, such as onboard media. These applications are supported by vehicle to vehicle (V2V) and vehicle to roadside (V2R) communications. Unfortunately, the links between these two communications are not stable enough to achieve optimal performance of these applications. However, because of the dynamic nature of VANETs, the links can live for a short time. The vehicles high mobility causes quick distinctions in the network topology that leads to dynamic changes of the link connectivity. Similarly, the deviation in number of vehicles and the rapid moving vehicles both causes change in the topology, which degrades the network reliability. That is why the network reliability is necessary for both of the communications V2V and V2R and its applications as it is challenging to communicate with each other once the link is unstable.

Several researchers were focusing on the issues of network connectivity in VANETs. For measuring the impacts of network connectivity, the authors in [8], presented empirical research on various speed models and for better estimation of connectivity, Gaussian distribution of the speed perform well. The authors in [9-10], proposed a connectivity probability model based on platoons considering MAC protocols. The proposed model separated the vehicles into two groups, normal and vehicles with platoons and the model was employed to design MAC protocol. The research conducted in [11-12] presented an infrastructure supported network connectivity considering two-channel models: log-normal shadowing and unit disk communication model. The authors in [11] analyzed the uplink and downlink connectivity probabilities.

Besides, it has been proved by the authors in [13], that the probability of having no isolated node and the probability of having a connected network asymptotically meets a similar value. The results of the study in [14], suggested that a slight change in communication range results in a major difference in connectivity probability in the case of high vehicle density. Further, to maintain the connectivity of vehicles transmission range R plays an essential role [15-16]. Mostly, a larger range of communication results in a large area covered within transmission range which helps to enhance link connectivity performance as compared to small transmission range.

The studies discussed above are interesting. Especially the research conducted by the authors in [17], vehicles are supposed to work with vehicular cloud networks in which videos and pictures for certain vehicles are taken by its neighboring vehicles and transferred via cloud to centralized cloud server. The recommended vehicular cloud network could not include roadside units (RSUs) since their availability is not possible in road tunnels. Hence, messages takes more than two hops in this network resulting in an increasing localization delay.

Though the researchers above did not consider the minimum safe distance under the highway tunnel among nearby vehicles, and only focused on the network connectivity. The reliability of the network plays an essential role in message dissemination on the road regarding entertainment and safety applications. Though, in the case of a fully connected network, there are chances of danger between vehicles which are close to each other. Therefore, the network is not safe, as accidents and collision can happen at any time. Thus, for the analysis of network reliability problems, the minimal safe distance amongst vehicles under the highway tunnel was considered in this study.

In this paper, a network reliability model based on safe distance under the tunnel has been proposed, which provide a possible method to overcome the issues in existing schemes.

The rest of the paper is organized as follows. Section 2 give details of the derived reliability model under the tunnel, which consider the impact of minimum safe headway amongst adjacent vehicles. Section 3 provides the performance evaluation and Section 4 concludes the paper.

II. SAFE HEADWAY BASED RELIABILITY MODEL

A. System Design

In VANETs, due to the dynamic movement of vehicles, the links can live for a short time because of the short association time between vehicles. Moreover, because of the road design the links are also restricted. Hence, the message propagation is mostly transmitted over V2V and V2R multi-hop communications. Therefore, the topology of the links plays an essential role in propagating messages successfully. Instead, we can say, a vehicle connection can have a direct impact on message dissemination. The arrival time of vehicles in VANETs follows exponential distribution with parameter λ with a flow of traffic λ veh/sec [18]. Consider an L km of tunnel with two-lane segment of road for the analysis perspective, where every vehicle arriving the tunnel with a random speed v_i at 0, and exits at L , as given in the Fig. 1.

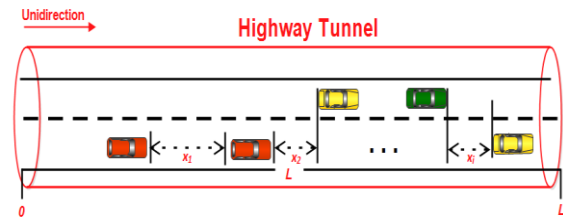


Fig. 1. Tunnel Model.

Evaluation of distance between vehicles in a transit system is called headway [19], represented as $x_i, i = 1, 2, \dots, N$ refer to Fig. 1. According to the literature, the headway distance is exponentially distributed i, i, d with parameter β Therefore, the CDF of headway is $X = x$

$$F_X(x) = 1 - e^{-\beta x} \quad (1)$$

It should be noted that in free flow state the various speed of vehicles is a Gaussian distribution [20]. For safe driving in the tunnel, the two limits are defined for speed $v_i \in [v_{min}, v_{max}]$. Hence, a truncated Gaussian (PDF) could be defined as

$$g(v) = \frac{f(v)}{\int_{v_{min}}^{v_{max}} f(v) dv} \quad (2)$$

Where $f(v) = \frac{1}{\delta\sqrt{2\pi}} e^{-\frac{(v-\mu)^2}{2\delta^2}}$ is a Gaussian PDF with the standard deviation δ and mean speed μ . As the area under the normal curve of the speeds in range $(\mu - 3\delta, \mu + 3\delta)$ is 99.74% of the whole area [19]. Hence, it is adequate to assign $v_{min} = \mu - 3\delta$ and $v_{max} = \mu + 3\delta$ as min and max speed of the vehicle's.

Therefore $g(v)$ could be written as

$$g(v) = \frac{2f(v)}{erf\left(\frac{v_{max}-\mu}{\delta\sqrt{2}}\right) - erf\left(\frac{v_{min}-\mu}{\delta\sqrt{2}}\right)} \quad (3)$$

In the above equation $erf(\cdot)$ represents the error function. Therefore, the values of expected speed could be calculated as

$$E(V) = \int_{v_{min}}^{v_{max}} vg(v) dv \quad (4)$$

Where the average density of vehicles in the tunnel is defined as

$$\rho = \frac{1}{E[V]} = \lambda E\left[\frac{1}{v}\right] \quad (5)$$

Finally, the number of average vehicles traveling in a tunnel segment L is calculated as

$$N_e = L\rho \quad (6)$$

The number of maximum vehicles that could be available on a given segment of tunnel with length L is defined as [12]

$$N_t = \frac{L}{S_h} N_{Ln} \quad (7)$$

Where S_h represents the minimal safe headway distance among vehicles, and N_{Ln} is the total number of tunnel lanes. Hence, the normalized vehicle density can be estimated as

$$K_e = \frac{N_e}{N_t} \quad (8)$$

B. Reliability based on Safe Headway Distance

The two vehicles could be considered connected if the transmission range is greater than the distance between them. Based on traffic theory, the $\beta = \rho$. As stated in eq. (1), it can be written as reliability of two connected vehicles.

$$R_{v2v} = 1 - e^{-\rho R_{tran}} \quad (9)$$

In the above equation, R_{tran} represents the transmission range for all vehicles. In order to guarantee the safety between vehicles, the minimal headway distance would be considered. By setting S_h as a safe minimal headway distance amongst vehicle, the reliability amongst every two vehicles could be defined as

$$R_{v2v} = 1 - e^{-\rho(R_{tran}-S_h)} \quad (10)$$

To guarantee the safety for all the vehicles N_e in the tunnel segment L , it is required that $x_i \leq R_{tran} - S_h$ for $i = 1, 2, \dots, N_e - 1$. As stated earlier, x_i are *i. i. d.*, so the reliability of the network is connected within the tunnel segment L could be defined as

$$R_{net} = (1 - e^{-\rho(R_{tran}-S_h)})^{(N_e-1)} \quad (11)$$

The equation given above is used to compute the network reliability within one-hop communication. Hence, R_{tran} which is the one-hop transmission range could be achieved from Eq. (11), as given below

$$R_{tran} = S_h - \frac{1}{\rho} \log_e(1 - N_e^{-1} \sqrt{R_{net}}) \quad (12)$$

Let the minimum value of R_{net} be 95%, with no loss of generality, R_{min} which is the minimum one-hop transmission range is defined as

$$R_{min} = S_h - \frac{1}{\rho} \log_e(1 - N_e^{-1} \sqrt{0.95}) \quad (13)$$

III. EXPERIMENTAL RESULTS AND ANALYSIS

Considering the above analysis, the reliability performance is discussed, by taking into account the minimal safe headway distance in the tunnel. The numerical results are discussed in this section. The MATLAB is used to perform the simulations. The simulated scenario is given in Fig.1, which is based on a one-way two-lane road segment tunnel with 10 km length.

A. The Average Density of Vehicles against Arrival Rate

The relation amongst the average density of vehicles and the arrival rate under various μ with constant $\delta = 5m/s$ is given in Fig. 2 and 3. The speed of all vehicles follows a truncated Gaussian distribution, in the simulation as defined in eq. (2) and (3). The interrelation amongst the average density of vehicles and arrival rate of vehicles under various μ while constant $\delta = 5m/s$ is given in Fig. 2.

Fig. 3 shows the interrelation of Average density of vehicles and the arrival rate under various δ with constant $\mu = 35m/s$.

Obviously, with the increasing arrival rate λ the average density of vehicles is increased when the rate of the μ and δ are constant. Moreover, with the same arrival rate of vehicles, the higher average speed μ will cause higher density of

vehicles, where, higher standard deviation value δ results in low density. It is clear that, higher density of vehicles enhance network reliability in terms of connectivity. So as a conclusion by considering Fig. 2 and 3, it can be written as: by increasing μ the average density of vehicles will be improved and decreased by the increase in δ .

B. Reliability against Transmission Range

Fig. 4 shows the interrelation amongst reliability and transmission range R_{tran} .

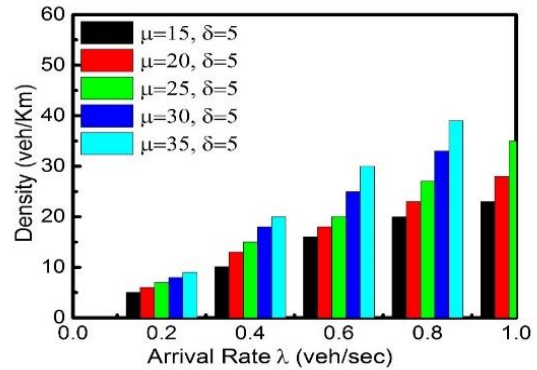


Fig. 2. Average density of vehicles against vehicle arrival rate with $\delta = 5m/s$.

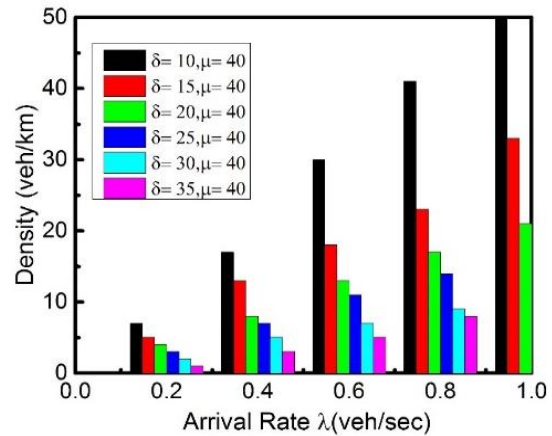


Fig. 3. Average density of vehicles against vehicle arrival rate when $\mu = 35m/s$.

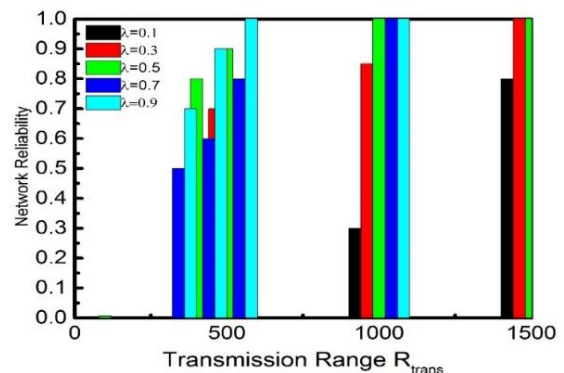


Fig. 4. Reliability against transmission range R_{tran} ($\mu = 20 m/s, \delta = 5 m/s$).

When μ and δ values are constant, the decrease in reliability is observed with the increasing transmission range R_{tran} . In the scenario where transmission range is larger, there are more chances for vehicles to successfully establish links to propagate messages as compared to a smaller range. Moreover, in a given constant R_{tran} , the reliability increases with the increasing arrival rate of vehicles λ . The higher λ shows the more vehicles will enter the desired tunnel segment, and leads to a high density of vehicles. Same as the density of vehicles which were presented in Fig. 2 and 3, surely the reliability in terms of connectivity would be enhanced.

C. Reliability against Average Density

Fig. 5 shows the interrelation amongst the reliability and the vehicles average density ρ . In a specified transmission range R_{tran} , it is observed that with the increasing density of vehicles reliability increased. In a stated density of vehicles, the reliability increases with the increasing transmission range R_{tran} .

It is clear in Fig. 5, the reliability touches to 1 when R_{tran} approach to 500 m or larger, If the density of vehicles is greater than 0.01 veh/km (which shows 100 vehicles in the segment of 10000 m tunnel). That could be said, that the aim is achieved and network becomes fully reliable, also with high successful probability, the message could be propagated. However, a substantial variation in the reliability has been observed when $R_{tran} = 100m$ or $< 100m$. The reliability remained zero, even the density of vehicles reached to 0.04 veh/Km.

The analysis conducted above shows that when transmission range R_{tran} is small such as 100m, even a trivial change in R_{tran} results in a worst performance of entire network reliability. Where, in VANETs, network reliability is an important factor which affects the network performances. Next, we highlight the point that the minimal headway distance amongst vehicle as well results in a great effect on the entire network reliability while transmission range is small.

D. The Minimal Safe Headway S_h and its Effect on the Network Reliability

Here, setting the minimal distance amongst vehicle as the safe headway S_h . In Fig. 6 and 7 effects of S_h on the network reliability is shown.

It is observed from Fig. 6 and 7 that, a little deviation such as 5m in the R_{tran} , can cause serious variations in the network reliability with various S_h values. When $R_{tran} = 90m$ and $R_{tran} = 95m$, the reliability variations are arisen when the density of vehicles ranging from 0.07 to 0.15 veh/km. The changes in the reliability are appeared when $R_{tran} = 100m$ and the density of vehicles ranging from 0.05 to 0.14 veh/Km. When $R_{tran} = 150m$, the changes in the reliability are observed when density of vehicles ranging from 0.03 veh/Km to 0.07 veh/Km.

As observed, when the $R_{tran} = 150m$, the change in the reliability is not as important as when $R_{tran} < 150m$. As an example we took $R_{tran} = 200m$ in Fig. 7, under various S_h the bars remained almost same. Hence, when R_{tran} reaching to more than 150m, the variation in S_h would not

seriously affect the network reliability, which is shown in Fig. 7.

E. Discussions

As Global Positioning System (GPS), which is the component of onboard unit (OBU) needs a rich line of sight for perfect services because of the signal interference the GPS do not work properly. Though, in the case of a fully connected network, there are chances of danger between vehicles which are close to each other. Therefore, the network is not safe, as accidents and collision can happen at any time. Hence, maintaining the minimal safe headway distance under the tunnel is interesting and useful for VANET. It can be observed from the Fig. 6 and 7 the impact of S_h on the network reliability when the vehicles communication range is small, specifically when $R_{tran} < 150m$.

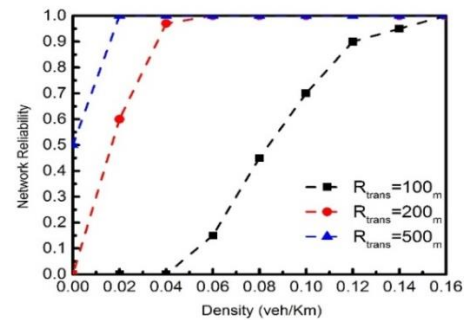


Fig. 5. Reliability Against Average Density of Vehicles.

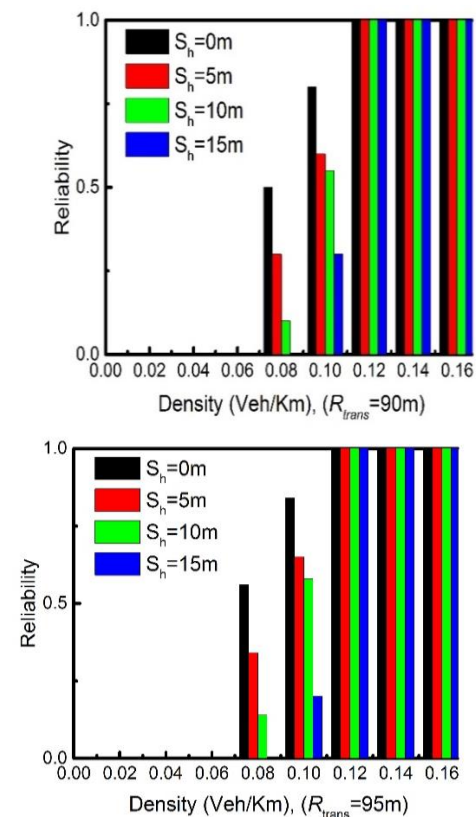


Fig. 6. The Impacts of S_h on the Reliability While $R_{tran} = 90m$ and $95m$.

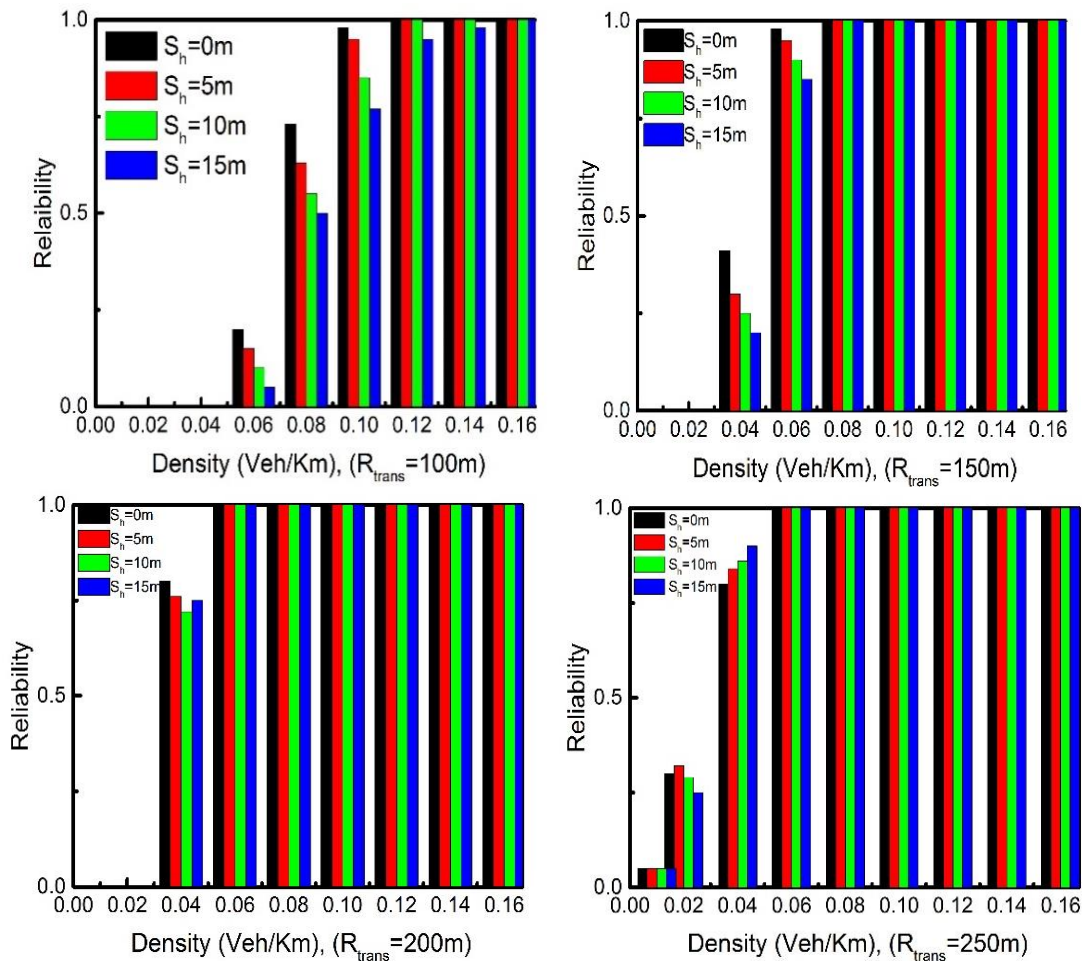


Fig. 7. The Impacts of S_h on the Reliability While $R_{tran} = 100m, 150m, 200m$ and $250m$.

IV. CONCLUSION

Vehicular ad hoc networks support two kinds of communications V2V and V2R, which are mainly used to propagate messages of entertainment and safety applications. Hence, the main feature for the successful propagation of message is link connectivity. Generally, the transmission range, density of vehicles, and the arrival rate of vehicles will affect the network reliability performance. In this paper, we design a reliability calculation scheme which considers the influence of the minimal safe distance amongst nearby vehicles under the tunnel. The results obtained by simulations prove that the deviation of the safe distance will bring substantial changes in the network reliability when transmission range of vehicles is less than 150m. Hence, while designing the network reliability models, the safe headway cannot be ignored.

ACKNOWLEDGMENT

This work was supported by the National Natural Science Foundation of China (no. 61370201) and the Open Research Found from the Key Laboratory for Computer Network and Information Integration (Southeast University, Ministry of Education, China).

REFERENCES

- [1] Dharmaraja, Selvamuthu, Resham Vinayak, and Kishor S. Trivedi. "Reliability and survivability of vehicular ad hoc networks: An analytical approach." *Reliability Engineering & System Safety* 153 (2016): 28-38.
- [2] Zhao, Tong, et al. "A Link Reliability Model of Metropolitan VANETs for Data Dissemination." *Vehicular Technology Conference (VTC-Fall), 2016 IEEE 84th. IEEE*, 2016.
- [3] Ahmed, Waqar, et al. "Reliability modeling and analysis of communication networks." *Journal of Network and Computer Applications* 78 (2017): 191-215.
- [4] Ma, Xiaomin, and Kishor S. Trivedi. "Reliability and performance of general two-dimensional broadcast wireless network." *Performance Evaluation* 95 (2016): 41-59.
- [5] Yan, Gongjun, and Danda B. Rawat. "Vehicle-to-vehicle connectivity analysis for vehicular ad-hoc networks." *Ad Hoc Networks* 58 (2017): 25-35.
- [6] Umer, Tariq, et al. "Modeling vehicles mobility for connectivity analysis in vanet." *Intelligent Transportation Systems*. Springer International Publishing, 2016.
- [7] Hussain, S.; Wu, D.; Memon, S.; Bux, N.K. *Vehicular Ad Hoc Network (VANET) Connectivity Analysis of a Highway Toll Plaza*. Data 2019, 4, 28.
- [8] S. M. Abuelenin, A. Y. Abul-Magd, "Empirical study of traffic velocity distribution and its effect on VANETs connectivity", *Proc. of 2014 ICCVE*, pp. 391-395, 2014.

- [9] C. Shao, S. Leng, B. Fan, Y. Zhang, A. Vinel, M. Jonsson, "Connectivity-aware Medium Access Control in platoon-based Vehicular Ad Hoc Networks", *Proce. of 2015 IEEE ICC*, pp. 3305-3310, 2015.
- [10] C. Shao, S. Leng, Y. Zhang, A. Vinel, M. Jonsson, "Performance Analysis of Connectivity Probability and Connectivity-Aware MAC Protocol Design for Platoon-Based VANETs", *IEEE Trans. on Vehicu. Tech.*, vol. 64, no. 12, pp. 5596-5609, Dec. 2015.
- [11] S. C. Ng, W. Zhang, Y. Zhang, Y. Yang, G. Mao, "Analysis of Access and Connectivity Probabilities in Vehicular Relay Networks", *IEEE Journal on Selected Areas in Communications*, vol. 29, no. 1, pp. 140-150, January 2011.
- [12] S. C. Ng, and G. Mao, "Analysis of k-hop Connectivity Probabilities in 2-D Wireless networks with Infrastructure support", in *Proc. of 2010 IEEE Globecom*.
- [13] X. Ta, G. Mao, Y. Zhang, B. D. O. Anderson, "On the connectivity of wireless Multi-hop Networks with arbitrary wireless channel models", *IEEE Communications Letters*, vol. 13, no. 3, pp. 181-183, March 2009.
- [14] J. Wu, "Connectivity Analysis of a Mobile Vehicular Ad Hoc Network with Dynamic Node Population", *Proc. of 2008 IEEE Globecom Workshops*, pp. 1-8, 2008.
- [15] X Luo, G Liu, H Huang, "Buffer Capacity-Constrained Epidemic Routing Model in Mobile Ad-Hoc Networks", *proc. of IEEE International Conference on Computational Science and Engineering*, pp. 1443-1448, 2014.
- [16] H Yao, H Huang, Q Liang et al., "The Effect of Critical Transmission Range in Epidemic Data Propagation for Mobile Ad-hoc Social Network" in *Pervasive Computing and the Networked World*, Berlin Heidelberg:Springer, pp. 743-756, 2013.
- [17] Agarwal, Y. , Jain, K. , Kumar, S. , & Bhardwaj, G. N. . (2016). TLST: Time of Arrival Based Localization and Smart Tunnel concept in VANETs. 2016 3rd International Conference on Signal Processing and Integrated Networks (SPIN). IEEE.
- [18] S. Yousefi, E. Altman, R. El-Azouzi, and M. Fathy, "Improving connectivity in vehicular ad hoc networks: An analytical study," *Computer communications*, vol. 31, no. 9, pp. 1653-1659, 2008.
- [19] Yousefi S, Altman E, El-Azouzi R, et al. "Analytical model for connectivity in vehicular ad hoc networks," *IEEE Trans. Veh. Technol.*, vol. 57, no. 6, pp. 3341-3356, Nov 2008.
- [20] R. Roess, E. Prassas, and W. McShane, *Traffic Engineering*, 2010.

Instrument Development for Measuring the Acceptance of UC&C: A Content Validity Study

Emy Salfarina Alias¹, Muriati Mukhtar², Ruzzakiah Jenal³

Faculty of Information Science and Technology
Universiti Kebangsaan Malaysia (UKM), Bangi, Selangor

Abstract—Studies on the acceptance of Unified Communications and Collaboration (UC&C) tools such as instant messaging and video conferencing have been around for some time. Adoption and acceptance of UC&C tools and services has boosted productivity and improved communications by integrating voice, video and data into one platform. UC&C also allows collaboration by enabling users to interact with each other in different media. However, their acceptance rate by individual in developing nations has been low. It is hypothesized that the factors that contribute to acceptance are developed based on two underlying theories. The first is that of diffusion of innovation and the other is that of service dominant logic. Items is constructed based on eight constructs which are relative advantage, compatibility, ease of use, trialability, observability, improved service, value co-creation capacity, and coordination efficiency. In order to validate the items, content validity ratios are calculated on a set of questionnaire. The ratios will determine which items should be included or removed from the questionnaire. The paper concludes with a discussion on the implications of the findings from the experts' evaluation and also from the content validity ratios. The new items are used in designing the survey instrument to measure the acceptance of UC&C.

Keywords—Acceptance model; content validity; diffusion of innovation; service science; unified communications and collaboration

I. INTRODUCTION

Unified Communication and Collaboration (UC&C) which has been introduced in over a decade is a popular new technology used by organizations for communications purposes. Previous studies [1]–[3] state that UC&C services are used in organizations to ease user involvement in communication activities. However, organizations still lack knowledge about the availability of UC&C in providing effective communications [4], [5]. Pérez et al. [3] also have pointed out that practitioners and scholars need to develop more understanding of the factors which can contribute or hampers successful adoption of UC&C.

According to Amily and Zaidi [6], the marketing strategies of communication technology should be focused on understanding the needs, trends and lifestyles of their potential users. Besides, the involvement of customer in the technology-based service is important for successful service delivery [7]. Therefore, there is a need to discover factors that influence the acceptance of UC&C in organizations. In a previous study by Emy Salfarina Alias et al. [8], eight constructs that influence the acceptance of UC&C services has been identified. Items

derived from these constructs are then developed into an assessment instrument for UC&C services users. Prior to administering the instrument, it has to go through a validation process. There are various ways to do this, one of which is via feedbacks from expert panels [9]. Accordingly, in this paper, the content validity of the assessment instrument of the UC&C services is evaluated by using by Lawshe's technique.

This paper is structured as follows: In Section II, a discussion of the related works is given. Section III describes the research method followed by results and analysis in Section IV. Section V discusses the findings and the limitations of the study. Section VI concludes the paper with suggestions for future research.

II. RELATED WORKS

Content validity refers to the ability of selected survey instruments to adequately reflect the characteristics of the measured constructs [10]. Also, the purpose of content validity is to determine the extent to which dimensions and concept elements are clearly explained [11]. Item verification function, on the other hand, examines whether it is sufficient to measure each construct [12]. According to Saunders et al. [13] comments and suggestions from experts would help establish content validity in order to make necessary amendments before pilot testing.

The development of the instrument needs to go through the validity process of the content to ensure that constructed constructions are legitimate, clear and reflect its contents [14]. Content validity can be implemented qualitatively or quantitatively as shown in Table I.

According to Nor'ashikin Ali et al. [17], qualitative analysis is difficult to interpret and the results obtained are less accurate because the questionnaire usually involves a large number of items. Meanwhile, Allahyari et al. [14] believes quantitative analysis is a better solution for content validity. Quantitative methods using Lawshe techniques are selected for this study because of its practical method. Based on the research conducted by Tojib and Sugianto [18], the content validity ratio (CVR) calculated using Lawshe techniques is more practical, convenient and saves time especially during the evaluation process. The CVR uses binomial distribution and also prepares tables to determine the values to be followed in calculations based on the number of experts involved [19]. In addition, CVR calculations are also suitable for use in studies involving a small number of experts.

TABLE I. CONTENT VALIDITY METHOD

No.	Method	Description
Qualitative		
1.	Intensive literature review	Construct is measured by adapting questions from previous researchers. This method only refers to existing instruments, without going through an evaluation process by an expert panel.
2	Content validity assessment by the expert panel	Constructs are measured based on expert panel evaluation analysis through comments, ideas, and feedback submitted.
Quantitative		
1.	Content validity ratio (CVR) [15]	This method involves questionnaires assessed by a group of experts using a three points Likert scale to assess every construct. Comment space is provided so that expert panels can provide their additional views. The number of experts is not determined and usually depends on the suitability of the study. The CVR calculation is based on acceptance criteria set by Lawshe [15].
2	Content validity ratio (CVR) [14]	This method is similar with the Lawshe method; it used a five Likert scale to assess each construct. The CVR calculation is based on acceptance criteria set by Allahyari et al. [14].
3	Content validity index (CVI) [16]	This method involves the assessment of constructs by experts panel based on the scale of four which is "1 = irrelevant", "2 = somewhat relevant", "3 = relevant", and "4 = very relevant". The number of expert panels is between three and ten.

The content validity index (CVI) is not considered in this study because the scale 4 is not universal and can cause doubt [18]. According to Nor'ashikin Ali et al. [17] CVI uses normal distribution that can cause inconsistencies and is less suitable for a small number of expert panels. Hence, this paper discusses step by step the process involved in the development of the instrument and subsequently validates the content by adapting the steps proposed by Nor'ashikin Ali et al. [17] using the CVR technique introduced by Lawshe [15].

III. RESEARCH METHOD

A. Research Design

Questionnaire is an effective data collection tool or mechanism for researchers when conducting a survey [20]. The data collected must be up-to-date, uniform and adhere to prescribed sampling procedures [11]. Prior to the questionnaire development process, a thorough understanding of the important concepts in the study must be acquired via an in depth literature review [22].

The development of a questionnaire in this study adapted the procedure introduced by Mackenzie et al. [23] which originally contained 10 steps, but summarized by combining several steps into only six steps to suit the three key processes conceptualization, development process, and validity as shown in Fig. 1.

This study uses a structured and closed questionnaire that respondents are required to read questions/statements and choose the answers available. This type of questionnaire is chosen because it is easy to administer because the questions and answers are available to enable respondents to respond easily and accurately. The questionnaire should facilitate the respondents to answer questions. The approach to the questionnaire of this study is fundamental to the guidelines proposed by Creswell [24] which is from public-shaped questions to special forms, does not involve sensitive issues and not burden respondents. The physical design of a good question can help to increase the understanding of the respondents and then increase the rate of return and the accuracy of the answers. As suggested by Fallis [25], question designs need to be clear, easy to read and not confusing format. The questionnaire administration method should be established early either by correspondence, email, telephone or face-to-face interview.

B. Research Procedure

The research procedure can be broken into six steps. The steps are explained as follows

Step 1: Develop a conceptual definition of the constructs.

Previous study has identified the conceptual framework in evaluating UC&C services through literature review. The conceptual model was developed for measuring the factors that could influence the acceptance of UC&C [8]. The framework has identified eight factors that could contribute to the acceptance of UC&C services. They are relative advantage, compatibility, ease of use, trialability, observability, improved service, value co-created capacity and coordination efficiency. All of these factors have been identified through the literature by combining two theories which are diffusion of innovation theory (DOI) and service dominant logic (SDL) from service science. DOI is chosen because UC&C services is seen to be an evolving technology that is progressing to meet current demand in communication and collaboration. It is thus interesting to view UC&C as a diffusion, hence the use of DOI. Complementing the use of DOI, SDL has been chosen because, SDL encompass the concepts of value in use and value co-creation which are crucial concepts that enable users to extract the value from UC&C services. Using these two theories as the basis, a conceptual framework for the acceptance of UC&C was developed. The framework is made up of eight factors or constructs. Each of the constructs are then elaborated into items. Here, a total of 49 items were identified.

Generating concept definitions for the involved constructs is important to ensure that constructs can represent the concepts being studied and the constructs are unique [26]. Development of the questionnaire can be done through the re-use of existing constructs obtained from past studies, but amendments need to be made to conform to the context of the study [21], [27]. According to Kitchenham and Pfleeger [28], the advantages of reapplying existing constructs are: (i) existing constructs have undergone validity and reliability tests; and (ii) comparison of findings of current and past studies can be done. Table II shows the list of definitions for the eight constructs involved in the study.

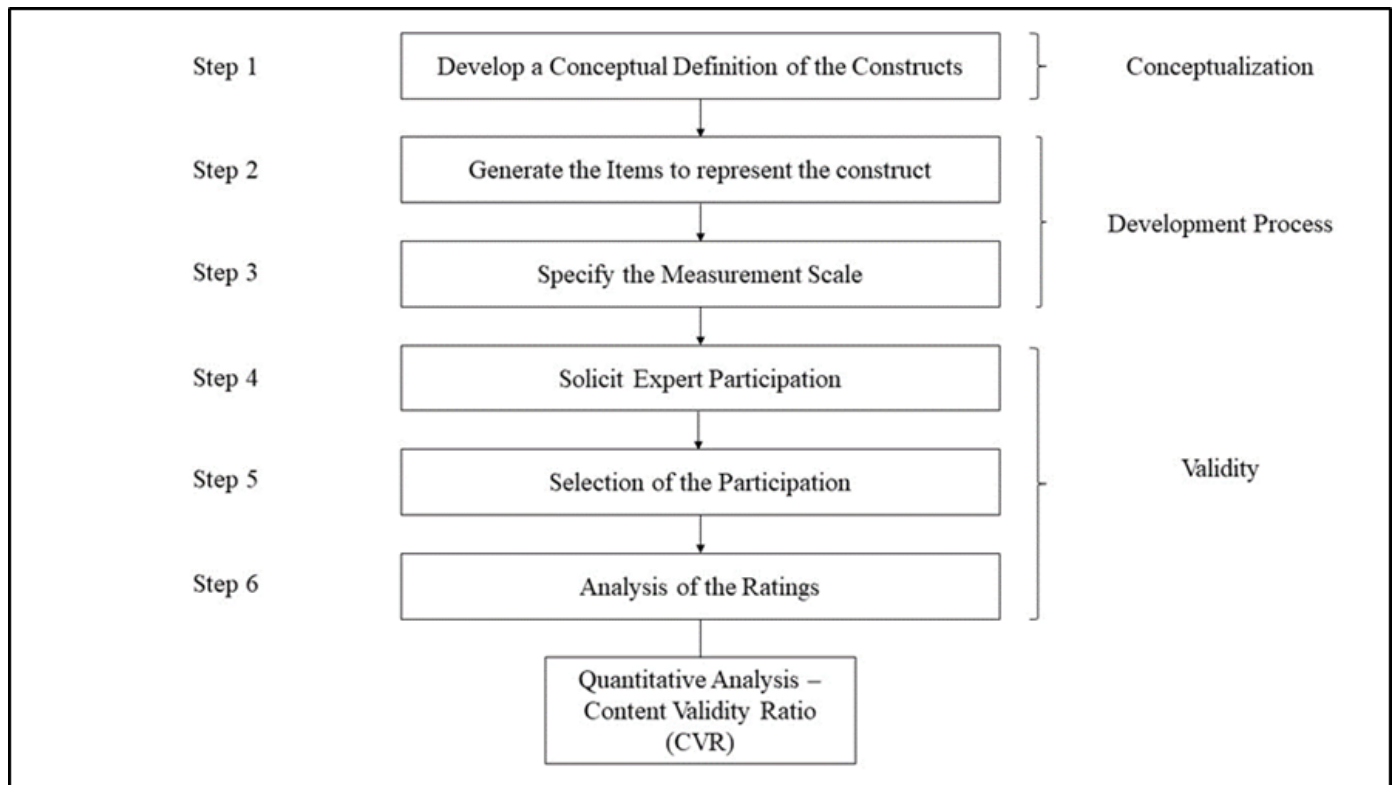


Fig. 1. Process of Instrument Development.

TABLE II. THE DEFINITION OF CONSTRUCT

No.	Factor	Definition	Source
1.	Relative advantage	The degree to which an innovation is Perceived as better than the idea it supersedes.	[29]
2.	Compatible	The degree to which an innovation is perceived As being consistent with the existing values, past experiences, and needs of potential adopters.	[29]
3.	Ease of use	The degree to which an innovation is perceived as Easy to understand and use.	[29]
4.	Trialability	The degree to which an innovation may be experimented with on a limited basis.	[29]
5.	Observability	The degree to which the results of an innovation Are visible to others.	[29]
6.	Improved Service	The degree to which service is improved or new service is created from the introduced innovation.	[8]
7.	Value Co-Created Capacity	The degree to which value co-creation is enabled or allowed in the organizations.	[8]
8.	Coordination Efficiency	The degree to which the institutions or institutional arrangements coordinates value co-creation in the organizations.	[8]

Step 2: Generate the Items to Represent the Construct

Podsakoff et al. [30] asserts that the selection of indicators is necessarily based on indicators with high weighting value in a construct because, low weighting value indicates that the construct is not correctly measured (no validity exists). Hair et al. [31] states that in order to provide stability to the constructs, each construct should have at least three indicators. Overall, this study involved 49 indicators (initial recommendation) to measure eight constructs as shown in Table III.

Step 3: Specify the Measurement Scale

There are various opinions on the number of optimal measurement scales such as even numbers (2, 4, 6, 8 or 10) or odd (3, 5, 7 or 9). For an odd numbered scale, the numbers in the middle represent the neutral, uncertain, unknown or irrelevant choices. Whereas the even numbered scale shows the respondents are forced to choose the answer either positive or negative [28]. An odd numbered scale (scale 3 and 5) can match the model accurately over the even numbered scale. Hence, the survey questionnaire uses three Likert scale which are (1) not necessary, (2) useful but not essential and (3) essential.

Step 4: Solicit Expert Participation

Experts expressing the desire to participate were sent a package that contains: a) cover letter, b) a content review form. Participants are given 20 days to complete the form and send it back to the researcher. The cover letter explains the rationale for conducting the research and also indicates the confidentiality of the responses.

TABLE III. THE CONSTRUCTION OF MEASUREMENT INDICATOR

Construct	Code Item	In the UC&C Context	Adaptation from
Relative advantage	RA1 – RA6	Describes acceptance of the benefits offered by UC&C services among employees in your organization.	[32]–[35]
Compatibility	COM1 – COM6	Describes your acceptance of the suitability of UC&C services within your organization.	[32]–[35]
Ease of use	EU1 – EU4	Describe your acceptance of UC&C service capabilities that are easy to use and understand.	[32]–[34]
Trialability	TRIAL1 – TRIAL7	Describing your acceptance with UC&C service trials helps users become more knowledgeable about their use.	[33], [35]–[37]
Observability	OB1 – OB2	Describes your acceptance of UC & C services that emphasize the provision of experience to users.	[35], [38]
Improved service	IS1 – IS5	Describes the perception of UC&C service could improve and combine the services to create new service.	[39]
Value co-created capacity	VCC1 – VCC5	Describes the perception of the organization is allowed value co-creation to extract the value of UC&C.	[40]–[43]
Coordination efficiency	COOR1 – COOR5	Describes the perception of UC&C services are allowed your organization to coordinate value co-creation.	[34], [37], [42], [44]
Acceptance of UC&C	ACC1 – ACC6	Describes the perception of the UC&C adoption in your organizations.	[45], [46]

Invitation to the panel of experts for the purpose of obtaining consent engagement in content validity sessions is performed individually via official email and telephone. Email is accompanied by an official letter. Once the expert agrees to be involved, a date is set for the interview sessions. The validity session content by all experts takes two to three weeks to be completed and transcribed.

Step 5: Selection of the Participation

1) *Expert Panel Selection:* Nor’ashikin Ali et al. [17] recommends the selected panel of experts to be involved and who are experienced in the same domain and have expertise in the development of the instrument (whether from academic or professional). There are some opinions in determining the number of experts. Lawshe [15] suggested that the panel of experts be composed of at least four people while Allahyari et al. [14] suggested 8 to 16 people. Nor’ashikin Ali et al. [17] on the contrary think that the expert panel should consist of 2 to 20 people.

In this study, seven experts were identified for content validity sessions. The selected specialist consists of academics, experienced professionals in the implementation of UC&C and consultants from industry sectors and Public Sector agencies. Table IV indicates the profiles of experts. Selection criteria are based on panel experience and involvement in relevant areas and fulfilling one or more of the following criteria:

- Knowledgeable and experienced in the field of service science.
- Experienced in the development and implementation of UC&C in the private or public sector.
- Knowledgeable in theory, statistical or construct measurement.

TABLE IV. PROFILES OF EXPERTS

Expert ID	Organization	Year of experience	Expertise/Experience
Expert 1	Industry	6	UC&C
Expert 2	Industry	8	UC&C
Expert 3	Industry	2 and half	UC&C
Expert 4	Academic	10	Service Science
Expert 5	Academic	21	Service Science
Expert 6	Academic	10	Service Science
Expert 7	Academic	14	Service Science

IV. RESULT AND ANALYSIS

Validity means the extent to which the measurements (indicators) used are able to represent the concept correctly and also the extent to which the selected indicators correspond to the construct [47]. Content validity is also known as expert confirmation as it is performed by a group of professional panels or experts in the related field [21]. The validity study described in this paper adapts the process introduced by Lawshe [15] and is also used in the study of [14], [17], [48]. It is based on quantitative methods using Likert 3 scale which is (1) not necessary, (2) useful but not essential and (3) essential. Expert panel is required to evaluate and validate the significance of the indicators based these given scales of 1 to 3.

Based on the feedback from the expert panel, the consensus among experts is measured by the calculation of CVR [15], which is analyzed using Microsoft Excel software. Table V shows that the minimum Lawshe’s CVR value. While, in this study, the calculation of CVR is adapted from Nor’ashikin Ali et al. [17], the answers "2" and "3" are considered relevant while the answers "1" are irrelevant. The formula used is:

$$CVR \text{ value} = (2Ne / N) - 1$$

- Ne = The number of experts who gave the relevant answer "2 = Agree" and "3 = Strongly Agree"
- N = Total number of experts

This equation is described below:

- If everyone on the panel of experts indicated the answer “3 = essential”, then, the CVR value is 1.00 (all agreed).
- If more than half (> 50%), but less than everyone (<100%) on the panel of experts indicated the answer “3 = essential”, then, the CVR value is positive, ranging between 0.00 and 0.99.
- If less than half (< 50%) of the panel of experts indicated the answer “3 = essential”, then, the CVR value is negative:

TABLE V. THE MINIMUM LAWSHE’S CVR VALUE

Number of Panelist	Minimum Acceptable CVR Value
5	0.99
6	0.99
7	0.99
8	0.78
9	0.75
10	0.62
15	0.49
20	0.42
25	0.37
30	0.33

Table VI shows the final results of CVR calculations. Based on the calculation, there are two indicators that are rejected because they returned the value of 0.71. Hence, 47 indicators will be included in the final questionnaire.

TABLE VI. CVR CALCULATION RESULT FOR EACH INDICATOR

Construct	Code	Total essential	CVR	Result
Relative advantage	RA1	7	1.00	Accepted
	RA2	7	1.00	Accepted
	RA3	7	1.00	Accepted
	RA4	7	1.00	Accepted
	RA5	7	1.00	Accepted
	RA6	6	0.71	Rejected
Compatibility	COM1	7	1.00	Accepted
	COM2	7	1.00	Accepted
	COM3	7	1.00	Accepted
	COM4	7	1.00	Accepted
	COM5	7	1.00	Accepted
	COM6	7	1.00	Accepted
Ease of use	EU1	7	1.00	Accepted
	EU2	7	1.00	Accepted
	EU3	7	1.00	Accepted

	EU4	7	1.00	Accepted
Trialability	TRIAL1	7	1.00	Accepted
	TRIAL2	7	1.00	Accepted
	TRIAL3	7	1.00	Accepted
	TRIAL4	7	1.00	Accepted
	TRIAL5	7	1.00	Accepted
	TRIAL6	7	1.00	Accepted
	TRIAL7	7	1.00	Accepted
Observability	OB1	7	1.00	Accepted
	OB2	7	1.00	Accepted
	OB3	7	1.00	Accepted
	OB4	7	1.00	Accepted
	OB5	7	1.00	Accepted
Improved service	IS1	7	1.00	Accepted
	IS2	7	1.00	Accepted
	IS3	7	1.00	Accepted
	IS4	7	1.00	Accepted
	IS5	7	1.00	Accepted
Value co-created capacity	VCC1	7	1.00	Accepted
	VCC2	7	1.00	Accepted
	VCC3	7	1.00	Accepted
	VCC4	7	1.00	Accepted
	VCC5	7	1.00	Accepted
Coordination efficiency	COOR1	7	1.00	Accepted
	COOR2	7	1.00	Accepted
	COOR3	6	0.71	Rejected
	COOR4	7	1.00	Accepted
	COOR5	7	1.00	Accepted
Acceptance of UC&C	ACC1	7	1.00	Accepted
	ACC2	7	1.00	Accepted
	ACC3	7	1.00	Accepted
	ACC4	7	1.00	Accepted
	ACC5	7	1.00	Accepted
	ACC6	7	1.00	Accepted

V. DISCUSSION

The process of developing a detailed instrument (step by step) can be improved by understanding of the researcher and can be used as a guide to build a questionnaire instrument. It can also serve as a guide for future researchers in their specific fields. The development of a complete and orderly instrument can improve the quality of research management while producing good and reliable results. Thus, weak instruments are not capable of generating high quality outputs, thus

generating dubious findings. The valid and reliable questionnaire can be used to assess the level of acceptance of UC&C services in organizations. The results from the panel of experts yielded the following results. A total of 47 items fulfilled the condition of CVR. After the CVR calculations were done, two items were marked up for deletion as they failed to meet the set criteria. Item RA6 was rejected because one of the experts commented that the item has the same meaning with item RA3. Item COOR3 was rejected because it is irrelevant based on the comment from an IT service provider expert. The item is related to the provision of UC&C training for users. Since not all respondents for a future survey will come from IT related fields, the item is still considered important, and it is possible, after further investigation to still retain the item code COOR3. Besides this, three experts suggested minor revisions regarding the clarity or wording of the items, and those revisions were incorporated into the instrument.

Even though the study had carefully selected its experts, more insights can be obtained and the study can be further improved by including more experts from more diverse fields.

VI. CONCLUSION

This paper has highlighted a method that can be used to validate the contents of a survey instrument that was constructed to investigate the factors that drives the adoption of UC&C. A total of 49 items were evaluated which resulted in two items being rejected. In this study, it is shown that the CVR approach is able to differentiate the opinion of experts clearly and easily. All the 47 items that were refined would proceed to a pilot testing by distributing the questionnaire to the targeted respondents. Through the pilot study, the items will then be subjected to more statistical tests in order to confirm that they are reliable and valid to be used in the main study.

ACKNOWLEDGMENT

The researchers would like to thank the expert panels for participating in this study. They would also like to thank UKM Zamalah Research Scheme and FRGS/2/2014/ICT01/UKM/02/ research grant.

REFERENCES

- [1] Bolton, M. Murray, and J. Fluker, "Transforming the Workplace: Unified Communications & Collaboration Usage Patterns in a Large Automotive Manufacturer," in 50th Hawaii International Conference on System Sciences, 2017, pp. 5470–5479.
- [2] C. Meske, T. Kissmer, and S. Stieglitz, "Global adoption of unified communication technologies as part of digital transformation in organizations: A cross-cultural perspective," in Multikonferenz Wirtschaftsinformatik (MKWI 2018), 2018.
- [3] J. Pérez, M. Murray, J. Fluker, D. Fluker, and Z. Bailes, "Connectivity and Continuity: New Fronts in the Platform War," Communications of the Association for Information Systems, vol. 40, no. 1, pp. 167–180, 2017.
- [4] J. Palonka and T. Porębska-Miąc, "Cloud Computing and Mobility as the Main Trends in Unified Communications," Studia Ekonomiczne, vol. 188, no. 119–134, 2014.
- [5] J. Yahaya, M. M. Basir, and A. Deraman, "Unified Communication and Collaboration Model for Virtual Distributed Team Work: A Study in Malaysia," International Journal of Software Engineering and Its Applications, vol. 9, no. 2, pp. 125–142, 2015.
- [6] F. Amily and A. G. @ M. Zaidi, "Unified communication: it's all between you and me," Business Strategy Series, vol. 13, no. 4, pp. 168–172, 2012.
- [7] S. H. M. Handrich, "Adoption of technology-based services: the role of customers' willingness to co-create," Journal of Service Management, vol. 26, no. 1, 2015.
- [8] Emy Salfarina Alias, Muriati Mukhtar, and Ruzzakiah Jenal, "Adoption of Unified Communications and Collaboration from the Perspective of Diffusion of Innovation and Service-Dominant Logic: A Preliminary View," International Journal on Advanced Science Engineering Information Technology, vol. 8, no. 5, pp. 1882–1889, 2018.
- [9] V. K. Shrotryia and U. Dhanda, "Content Validity of Assessment Instrument for Employee Engagement," SAGE Open, 2019.
- [10] M. H. Imani-Nasab, B. Yazdizadeh, M. Salehi, H. Seyedin, and R. Majdzadeh, "Validity and reliability of the Evidence Utilisation in Policymaking Measurement Tool (EUPMT)," Health Research Policy and Systems, vol. 15, no. 1, pp. 1–11, 2017.
- [11] U. Sekaran, Research Methods for Business, 4th ed. New York: John Wiley & Sons, Inc, 2003.
- [12] N. K. Agarwal, "Verifying survey items for construct validity: A two-stage sorting procedure for questionnaire design in information behavior research," in Proceedings of the ASIST, 2011.
- [13] M. Saunders, P. Lewis, and A. Thornhill, Research Methods for Business Students, 5th ed. Edinburgh Gate: Pearson Education Limited, 2009.
- [14] T. Allahyari, N. H. Rangi, Y. Khosravi, and F. Zayeri, "Development and evaluation of a new questionnaire for rating of cognitive failures at work," International Journal of Occupational Hygiene, vol. 3, no. 1, pp. 6–11, 2011.
- [15] C. H. Lawshe, "A quantitative approach to content validity," Personnel Psychology, vol. 28, no. 4, pp. 563–575, 1975.
- [16] M. R. Lynn, "Determination and Quantification of Content Validity," Nursing Research, vol. 35, no. 6, pp. 382–385, 1986.
- [17] Nor'ashikin Ali, A. Tretiakov, and D. Whiddett, "A Content Validity Study for a Knowledge Management Systems Success Model in Healthcare A Content Validity Study for a Knowledge Management Systems Success Model in Healthcare," Jitta, vol. 15, no. 2, pp. 21–36, 2014.
- [18] D. R. Tojib and L. F. Sugianto, "Content Validity of Instruments in IS Research," Journal of Information Technology Theory and Application (JITTA), vol. 8, no. 3, pp. 31–56, 2006.
- [19] R. S. Rai, "Innovating in Practice: A Practice-Theoretical Exploration of Discontinuous Service Innovations," 2016.
- [20] M. Wook, Z. M. Yusof, and M. Z. A. Nazri, "Educational data mining acceptance among undergraduate students," Education and Information Technologies, vol. 22, no. 3, pp. 1195–1216, 2016.
- [21] Muslihah Wook, "Model Penerimaan Perlombongan Data Pendidikan Dalam Kalangan Pelajar Universiti Awam Di Malaysia," Universiti Kebangsaan Malaysia, 2017.
- [22] A. A. Aziz, Z. M. Yusof, U. A. Mokhtar, and D. I. Jambari, "Penerimgunaan Sistem Pengurusan Dokumen dan Rekod Elektronik: Protokol Pembangunan Instrumen dan Kesahan Kandungan Menggunakan Nilai Ketetapan Kandungan," Jurnal Pengurusan, vol. 53, 2018.
- [23] S. B. Mackenzie, P. M. Podsakoff, and N. P. Podsakoff, "Construct Measurement and Validation Procedures in MIS and Behavioral Research: Integrating New and Existing Techniques," MIS Quarterly, vol. 35, no. 2, pp. 293–334, 2011.
- [24] J. W. Creswell, Research Design Qualitative, Quantitative and Mixed Methods Approaches, 4th ed. 2014.
- [25] A. . Fallis, Case Study Methodology in Business Research, vol. 53, no. 9, 2013.
- [26] S. B. Mackenzie and P. M. Podsakoff, "Common Method Bias in Marketing: Causes, Mechanisms, and Procedural Remedies," Journal of Retailing, vol. 88, no. 4, pp. 542–555, 2012.
- [27] U. Sekaran and R. Bougie, Research Methods for Business: A Skill Building Approach, 5th ed. Wiley, 2010.

- [28] B. A. Kitchenham and S. L. Pfleeger, "Principles of Survey Research Part 3: Constructing a Survey Instrument," vol. 27, no. 2, pp. 20–24, 2002.
- [29] E. M. Rogers, *Diffusion of Innovation*, 4th ed. 1995.
- [30] P. M. Podsakoff, S. B. Mackenzie, and N. P. Podsakoff, "Sources of Method Bias in Social Science Research and Recommendations on How to Control It," 2012.
- [31] J. F. Hair, M. Sarstedt, T. M. Pieper, and C. M. Ringle, "The Use of Partial Least Squares Structural Equation Modeling in Strategic Management Research: A Review of Past Practices and Recommendations for Future Applications," *Long Range Planning*, vol. 45, no. 5–6, pp. 320–340, 2012.
- [32] I. M. Al-Jabri and M. S. Sohail, "Mobile banking adoption: application of diffusion of innovation theory," *Journal of Electronic Commerce Research*, vol. 13, no. 4, pp. 379–391, 2012.
- [33] A. Peslak, W. Ceccucci, and P. Sendall, "An Empirical Study of Social Networking Behavior Using Diffusion of Innovation Theory," *Conference on Information Systems Applied Research*, 2010.
- [34] L. Carter and F. Bélanger, "The utilization of e-government services: Citizen trust, innovation and acceptance factors," *Information Systems Journal*, vol. 15, no. 1, pp. 5–25, 2005.
- [35] T. J. Ntemana and W. Olatokun, "Analyzing the Influence of Diffusion of Innovation Attributes on Lecturers' Attitudes Toward Information and Communication Technologies," *Journal on Humans in ICT Environments*, vol. 8, no. 2, pp. 179–197, 2012.
- [36] E. Mao, M. Srite, J. B. Thatcher, and O. Yaprak, "A research model for mobile phone service behaviors: Empirical validation in the U.S. and Turkey," *Journal of Global Information Technology Management*, vol. 8, no. 4, pp. 7–28, 2005.
- [37] Hasimi Sallehudin, "Factors Influencing the Assimilation of Cloud Computing Services and Its Effect on Operational Effectiveness in the Malaysian Public Sector," *University Malaysia Kelantan*, 2017.
- [38] P. Verdergem and L. De Marez, "Rethinking Determinants of ICT Acceptance: Towards An Integrated and Comprehensive Overview," *Technovation*, vol. 31, no. 8, pp. 411–423, 2011.
- [39] A. Ordanini and A. Parasuraman, "Service innovation viewed through a service-dominant logic lens: A conceptual framework and empirical analysis," *Journal of Service Research*, vol. 14, no. 1, pp. 3–23, 2011.
- [40] C. Morosan and A. DeFranco, "Co-creating value in hotels using mobile devices: A conceptual model with empirical validation," *International Journal of Hospitality Management*, vol. 52, pp. 131–142, 2016.
- [41] I. O. Karpen, L. L. Bove, B. A. Lukas, and M. J. Zyphur, "Service-dominant orientation: Measurement and impact on performance outcomes," *Journal of Retailing*, vol. 91, no. 1, pp. 89–108, 2014.
- [42] K. T. Yip, "The Attributes of Value Co-creation in Service and its Impact on Customers Willingness to Pay. Observations from Three Service Industries," *University of Exeter*, 2011.
- [43] K. R. Ranjan and S. Read, "Value co-creation: concept and measurement," *Journal of the Academy of Marketing Science*, vol. 44, no. 3, pp. 290–315, 2016.
- [44] L. Gao and X. Bai, "A unified perspective on the factors influencing consumer acceptance of internet of things technology," *Asia Pacific Journal of Marketing and Logistics*, vol. 26, no. 2, pp. 211–231, 2014.
- [45] H. Ahmadi, M. Nilashi, L. Shahmoradi, and O. Ibrahim, "Computers in Human Behavior Hospital Information System adoption: Expert perspectives on an adoption framework for Malaysian public hospitals," *Computers in Human Behavior*, 2016.
- [46] B. Pinnock, "Environmental and Organisational Drivers Influencing the Adoption of Unified Communications Technology in South Africa," *University of Cape Town*, 2011.
- [47] J. F. Hair, C. M. Ringle, and M. Sarstedt, "Editorial Partial Least Squares Structural Equation Modeling: Rigorous Applications, Better Results and Higher Acceptance," *Long Range Planning*, vol. 46, no. 1–2, pp. 1–12, 2013.
- [48] W. A. Z. Wan Ahmad, M. Mukhtar, and Y. Yahya, "Validating the Contents of a Social Content Management Framework," in *The 2017 6th International Conference on Electrical Engineering and Informatics (ICEEI)*, 2017.

Congestion Control Techniques in WSNs: A Review

Babar Nawaz¹, Khalid Mahmood^{*,2}, Jahangir Khan³, Mahmood ul Hassan⁴, Ansar Munir Shah⁵,
Muhammad Kashif Saeed⁶

Department of Computer Science, IIC University of Technology, Phnom Penh, Kingdom of Cambodia^{1, 2, 3, 4, 5, 6}
Department of Computer Science, University College of Alwajh, University of Tabuk, Kingdom of Saudi Arabia⁴
Department of Computer Science & IT, Institute of Southern Punjab (ISP) Multan, Pakistan⁵

Abstract—Congestion control has a great importance in wireless sensor network (WSN), where efficient application of congestion control mechanisms can prolong the network lifetime. Thus, proper examination is needed to improve more refine way to address the congestion occurrence and resolution. While designing congestion control techniques, the maximum output can be achieved by efficient utilization of required resources within WSN. From last few years several approaches have been brought in, that consist of routing protocols which provide support with congestion control, congestion prevention, and reliable data routing. In old schemes the topology reset and extent traffic drop take place because sink node executes the congestion avoidance. Therefore, node level congestion avoidance, detection, congestion preventing, and resolution mechanisms have been proposed during past few years. Our paper provides a brief overview and performance comparison of centralized and distributed congestion control algorithms in WSN.

Keywords—WSNs; congestion control; congestion preventing; reliable data

I. INTRODUCTION

Wireless sensor network (WSN) consists of very small wireless devices deployed in a huge geographical area to examine the surrounding environment. Through, multi-hop routing protocols the oversee information is transmitted from sensor to sensor towards sink. Information collection and examination takes place at sink node. The sensor nodes have limited power, energy, and communication resources [1] [2] [3]. Different routing schemes are used to efficiently handle the WSN's resources in order to achieve the better performance. Congestion control is the prominent area for the researchers as network traffic is increasing rapidly with frequent changes in buffering mechanisms [5].

The main task of WSNs is to provide transport and network protocols functionalities for reliable data transfer over the unreliable channels and nodes and also deals with fault tolerance [7]. Usually for network level, the cause of node failure is due to the changes in path and topology that must be treated properly to reduce the relative packet loss and energy exhaustion [8]. At transport level, congestion should be managed to prevent the data loss by fair distribution of the bandwidth for all the network nodes especially for the distant nodes [8].

Congestion control helps in avoiding extent traffic drop that is why congestion control is of demanding concern. Congestion

control comprises of three phases. The first phase is congestion detection in which congestion is detected at sensor nodes while in notification phase; a problematic sensor node has been notified of congestion after the detection of congestion. Lastly, in congestion mitigation phase; the congestion is checked and suitable data rate is applied. There are three stages for congestion control; congestion detection, prevention, and congestion control. While designing WSNs, the main focus should be on congestion control to carry out the maximum life of network by efficient use of the resources [1].

Current congestion control approaches have some difficulties, such as the onward traffic management does not consider the traffic estimation on the substitute paths [4]. From source sensor node to sink, the priority is set on hop count instead of actual packet delay [4-6]. Moreover, the distribution of traffic loads at congested and substitute paths are not handled properly.

This survey paper provides a brief overview on congestion control mechanisms by graphically illustrating the working of some of the congestion control algorithms. Moreover, we have provided the performance comparison by examining the parameters mentioned in each of the congestion control algorithm discussed in this survey paper. Moreover, this paper also highlights the shortcomings of the existing congestion control mechanisms.

II. LITERATURE REVIEW

Congestion control algorithms for WSN are extensively discussed in recent past years [8] [9]. In WSNs, congestion occurs at two levels i-e node and link level congestion. Fig. 1 illustrates the congestion levels in WSN.

Congestion occurs when the amount of received data at particular node is higher than its transmitted data which subsequently causes the drop of packets. Generally, congestion occurs at the nodes that are very close to the sink node.

Node-level congestion badly affects the performance of the affected node in WSN. It causes the loss of energy due to the higher packet loss ratio and consequently disconnects the affected node from the network causing certain route unavailability. Energy depletion and poor routing have negative impact on the performance of the network and badly reduce the overall reliability and lifespan of the network.

*Corresponding Author.

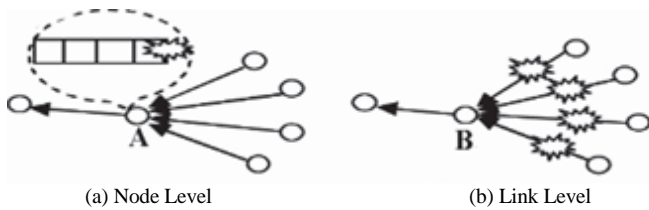


Fig. 1. Congestion Level in WSNs.

Collision, competition and bit error are the reasons for link level congestion occurrence. In Fig. 1 node level congestion occurs at node A. A suitable congestion control scheme can efficiently manage the transmission of data in order to prevent from loss of energy or it can change the route of surplus packets. It will increase the sink node output and frequently assists the WSN application by efficiently monitoring the environment. The minimum packet loss also increases the reliability of the WSN application. Therefore, preventing routing holes, frequently and on time data delivery will increase the life span of the network.

Link level congestion occurs at node B in Fig. 1 where node B receives few packets despite its neighbor sends with full data rate. The reliability of the WSN is badly affected when sink receives fewer packets. In such kind of situation MAC layer should be managed by a congestion control algorithm that helps coordinates to access the medium and prevents form collision.

Mainly, congestion control algorithms are distributed in three types namely congestion mitigation, congestion detection, and reliable data transmission algorithms as shown in Fig. 2. Congestion mitigation algorithms are reactive in nature which react and control the congestion whenever network suffers from congestion. Mostly, these algorithms are working with MAC and network layer operations, and in few circumstances transport layer operations are performed by them.

Congestion detection algorithms are employed to prevent the network from congestion occurrence. MAC and network layer operations are usually handled by such kind of algorithms.

Reliable data transmission algorithms are used to control the congestion in a network in such a way that these algorithms try to get back all the lost information or some part of it. Usually, these algorithms are used at the time when whole information is necessary for application. The transport layer approaches are involved in these algorithms.

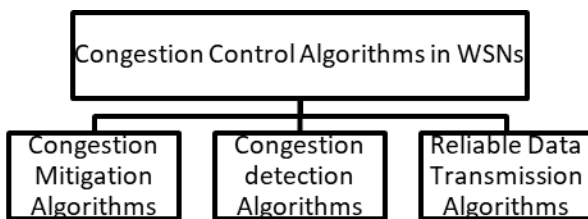


Fig. 2. Congestion Control Algorithms.

III. CONGESTION CONTROL TECHNIQUES

A. RCRT

RCRT is a transport protocol that determines and allocates the data rate to resolve the congestion [7]. The sink node performs congestion detection, rate control, and allocation. This scheme has some limitations like, the slow convergence rate and fails to figure out the flow constrained in congestion area. The operational scheme of RCRT is illustrated in Fig. 3.

B. I2MR

I2MR is a routing protocol aided with the congestion control mechanism [8]. To remove congestion, the I2MR protocol keeps multiple substitute paths for routing information. Experimental weighted moving averages are used to detect the congestion by spotting source node's single buffer. The protocol informs the source node to decrease the transmission rate for controlling congestion. The transmission rate is decreased by the source node through redirecting the traffic to the substitute routes. The I2MR protocol has some restrictions like a massive data loss is unavoidable if the substitute's routes are not available. The rate balancing comprises on one-fourth, one-sixth or one-eighth of the data link rate instead of comprising the predicted traffic that consequence the faulty channel.

C. TADR

The TADR protocol illustrates a hybrid scalar potential area that consists of queue length and depth area [8]. Initially TADR routes the packets to the sink from the shortest paths. Later on the functionality of traffic awareness is developed in it. If congestion occurs, TADR sends the packets to the substitute route that comprises of less-loaded or idle nodes. To prevent hot spots, a bypassing hot-spot rule is brought in. The main drawback of TADR is to find out the time variant potential area that leads to the traffic diversion [8]. The operations of TADR algorithm are shown in Fig. 4.

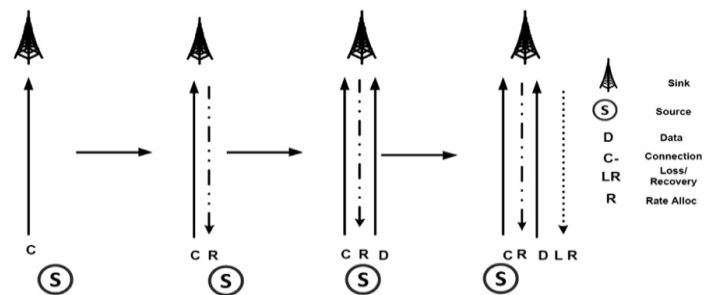


Fig. 3. RCRT Setup Phase [6].

D. Buffer-Based Congestion Avoidance Scheme

Buffer-based congestion avoidance scheme is checked against several MAC protocols, like TDMA with unchanged scheduling and CSMA with implicit ACKs, as illustrated in Fig. 5 [10]. A 1/k buffer solution addresses the hidden terminal problem. In this scheme the fairness for load balancing and buffer access on various routes is assured. The scheme is illustrated in Fig. 5.

E. DAIPaS

The DAIPaS protocol detects the congestion by including the channel interference, buffer occupancy and residual energy of a single node [11]. The nature of selection of shortest routes for traffic is dynamic that prevent it from the congested nodes. In setup phase, DAIPaS broadcasts a HELLO beacon in the vicinity of the network by setting the head nodes level ID to 0. When nodes receive the HELLO message, they further broadcast the message by increasing the ID value by 1. This method continues as far as a unique level ID is assigned to each node in the network. Each node maintains an ID to discover substitute paths or manipulate shortest path towards the sink. The shortest path is determined by examining the flow from the highest to the lowest value. The comparative analysis between incoming and transmission flow along with buffer occupancy determines the congestion. The packet sequence number in the receiving node's header is set to FALSE when DAIPaS goes into the soft stage and the packet is transmitted to the further node. The sending selects the substitute paths on receiving the value and will carry on sending the data on it. The DAIPaS protocol sets the minimum threshold for buffer occupancy and it moves into the hard phase if the buffer size surpasses the minimum threshold or the inward data flow exceed the transmission rate. Consequently, DAIPaS redirects the packets on new route. The DAIPaS rearranges the topology by eliminating the node from the current route.

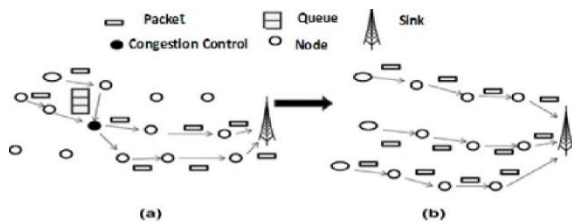


Fig. 4. Illustration of TADR Operations.

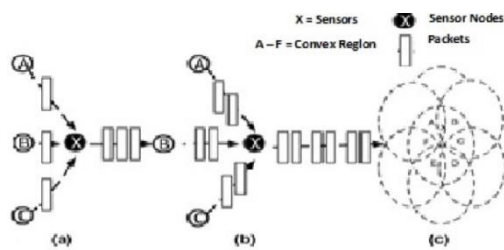


Fig. 5. Illustration of Buffer-Based Congestion Avoidance Scheme.

F. Fusion

Fusion is a method for checking the congestion on queue length [12]. Additionally, to handle the congestion, fusion relies on hop-by-hop flow control, prioritized MAC approaches and rate control. Insufficient buffer spaces occur whenever packets are dropped downstream and packet transmission is stopped. During the comparison with other non-congested sensor nodes, it is noticed that this priority is managed by congested sensor nodes through reducing random back-off timer. Lack of balance in data transfer happen towards the nodes that are situated far from the sink node. To prevent this problem, the rate limitation metrics of traffic are accepted. A prioritized CSMA-based MAC manages congestion in congested sensors by reducing random back-off timer. Accordingly, fusion optimizes fairness and maintains effective output.

G. WRCP (Wireless Rate Control Protocol)

WRCP (Wireless Rate Control Protocol) is a Wireless Sensor Network protocol that is used to improve convergence time of rate control [13]. It is designed by using a receiver capacity model that is a novel interference model. This model enables each receiver to find out the accurate available capacity which is used by WRCP to get a fair rate allocation. WRCP shares this capacity information in between competing flows in a neighborhood. By using explicit capacity information, WRCP shows fast convergence time that result in small end-to-end delays.

H. TRCCIT (Tunable Reliability with Congestion Control for Information Transport)

TRCCIT protocol ensures the appropriate reliability level of the hybrid acknowledgement (HACK) approach [14]. The forwarder overhears the retransmission of sender's packets by setting a hop-by-hop control.

In the situation when the required reliability level is beforehand achieved, the receiver depresses the received packet and sends a simple acknowledgment to the sender to prevent from packet retransmission after the completion of timeout. At the time of congestion detection the TRCCIT addresses to control congestion through multipath forwarding. But utilization of multiple paths forwarding is not continually possible and accordingly TRCCIT congestion control approach is not sufficient.

I. DPCC (Decentralized Predictive Congestion Control)

DPCC is a WSN protocol that comprises an adaptive flow and back-off interval selection approaches that get the job through distributed power control (DPC) and energy efficiency [15]. Initially, DPCC detects the congestion with the help of queue utilization and the embedded channel quality. The adaptive back off interval selection approach applies a rate whereas the adoptive flow control approach selects that suitable rate. Fig. 6 shows the rate selection process. To assure the weight fairness during congestion, the associated weight of

each packet is updated by an optional scheduling approach. Simulation outcome shows that the DPCC increases performance and decreases the congestion through congestion detection and congestion prevention process.

J. GMCAR (Grid-based Multipath with Congestion Avoidance Routing)

GMCAR protocol is an effective QoS routing protocol used in gridded sensor networks [16]. It uses the concept of splitting the wireless sensor network region into grids. In each grid, one master node is selected from associated sensor nodes. All master nodes from each grid collaborate with each other and also responsible to process and route the data of associated sensor nodes. In the routing table of each master node, multiple diagonal paths as routing entries are stored that link master node to the sink. In case of congestion occurrence, a congestion control approach is suggested to reduce the congested areas. When compared to other QoS protocols, the outcome of simulation shows that GMCAR protocol has the potential to achieve the delay reduced to 24.7%, network output increased by 8.5% and 19.5% energy saving. Moreover, it shows superiority in accomplishing better available storage usage.

K. TASA (Traffic Aware Scheduling Algorithm)

TASA (Traffic Aware Scheduling Algorithm) [17] is based on TSCH behavior and it is a centralized scheduling approach. The TASA build a tree-based schedule at sink that has nodes traffic load information. While using the edge of frequency diversity and resources, TASA provides a better output. In graph theory methods, TASA uses matching and coloring for accomplishing the specified objectives. Fig. 7 shows the working of TASA algorithm.

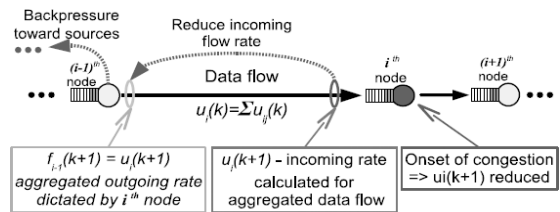


Fig. 6. Rate Selection Overview.

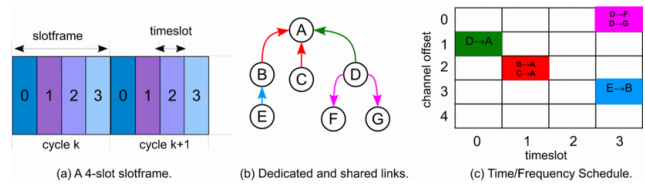


Fig. 7. Traffic Aware Scheduling Algorithm.

L. OTF (On-the-Fly Scheduling)

OTF (On-the-Fly Scheduling) presents a distributed schedule approach. This approach uses slots to prevent interferences and ensures reliability [18]. As per the network need, OTF adjusts the slot number of the nodes with respect to the traffic load. For schedule adaptation, the resources that are added or removed are sent to the sub-layer for schedule adoption.

IV. PERFORMANCE COMPARISON

The performance comparison of aforementioned congestion control schemes is based on their operational strategy, congestion detection criteria, congestion notification, congestion control, priority criteria, and control patterns. The comparison is shown in Table I.

TABLE I. CONGESTION CONTROL PROTOCOLS COMPARISON

References	Congestion Routing Protocols						
	Protocols	Operational scheme	Congestion detection models	Congestion notification	Congestion control	Priority criteria	Control Patterns
[11]	RCRT	Congestion detection, rate adoption and allocation	Buffer Overflow	New Rate in NACK header, or Feedback Rate message	AIMED rate control	NO	End to End
[12]	12MR	Routing support through congestion control	Buffer occupancy and exponential weighted moving average	Feedback Message	Rate control	NO	Hope by Hope
[13]	TADR	Routing with congestion control	Buffer and Rate hybrid scalar positional field		Resources control	NO	Hope by Hope
[14]	Buffer-based congestion avoidance scheme	Congestion control	Buffer Occupancy	Information in header	Stop sending	NA	Hope by Hope
[15]	DAIPaS	Dynamic Alternative path selection	Buffer occupancy and channel load	Information in header	Resources control	NO	Hope by Hope

[16]	Fusion	Flow control, Rate limiting and prioritized MAC	Buffer and rate	Bit in header	Stop sending prioritized MAC	NA	Hope by Hope
[17]	WRCP	Helps in the network to conclude the accurate available capacity at each receiver	NO	Information header	Rate control	NO	Hope by Hope
[18]	TRCCIT	Hop-by-hop control to overhear the retransmission of packets	When congestion detection the TRCCIT address to control congestion through multipath forwarding	Send ACK to sender	Traffic control	NO	Hope by Hope
[19]	DPCC	Dynamic and fair management of traffic broadcast.	Queue Utilization and Channel Quality	Information in ACK header	Rate control adaptive back off	Pre-defined rules	Hope by Hope
[20]	GMCAR	Splitting the sensor network region into grid	Use a congestion control mechanism	Information header	Resources control	NO	Hope by Hope
[21]	TASA	At sink build a tree-based schedule	Build tree base schedule	Average single hope delay	Traffic control	NO	Hope by Hope
[22]	OTF	use slots to prevent interferences and ensures reliability	As per the network need OTF adjust the slot number of the nodes with respect to the traffic load	Information header	Resources control	NO	Hope by Hope

V. CONCLUSION

In WSN, congestion control is an important area of research. It is a challenging task to develop congestion control techniques with limited resource. This paper gives an inclusive review on the current congestion control techniques. The aim of all the techniques is to increase the life time of the WSNs by using available limited resources. We compared different metrics for congestion detection and controlling. Fast feedback, high transmission, inexpensiveness, low power consumption, fault tolerance, consistency, wear-ability, and complexity of the WSN are the important areas which are addressed in congestion control schemes.

For the future work, we will propose an energy efficient congestion control technique that will overcome the shortcomings of the aforementioned techniques.

ACKNOWLEDGMENT

We would like to express our gratitude to IIC University of Technology, Kingdom of Cambodia for providing us good research environment.

REFERENCES

[1] Omidvar, M., Ayatollahitafti, V., & Farahmand, M. (2017). A Congestion-Aware Routing Algorithms Based on Traffic Priority in Wireless Sensor Networks. *Journal of Soft Computing and Decision Support Systems*, 4(1), 1-6.

[2] Khalid Mahmood, Muhammad Amir Khan, Mahmood ul Hassan, Ansar Munir Shah, Shahzad Ali, and Muhammad Kashif Saeed, "Intelligent On-Demand Connectivity Restoration for Wireless Sensor

Networks," *Wireless Communications and Mobile Computing*, vol. 2018, Article ID 9702650, 10 pages, 2018. <https://doi.org/10.1155/2018/9702650>.

[3] Randhawa, S., & Jain, S. (2017). Data Aggregation in Wireless Sensor Networks: Previous Research, Current Status and Future Directions. *Wireless Personal Communications*, 97(3), 3355-3425.

[4] Gholipour, M., Haghighat, A. T., & Meybodi, M. R. (2017). Hop - by - Hop Congestion Avoidance in wireless sensor networks based on genetic support vector machine. *Neurocomputing*, 223, 63-76.

[5] Zhu, L., Zhang, Z., & Xu, C. (2017). Secure data aggregation in wireless sensor networks. In *Secure and Privacy-Preserving Data Communication in Internet of Things* (pp. 3-31). Springer Singapore.

[6] Chen, H. M., Cui, L., & Zhou, G. (2017). A Light-Weight Opportunistic Forwarding Protocol with Optimized Preamble Length for Low-Duty-Cycle Wireless Sensor Networks. *Journal of Computer Science and Technology*, 32(1), 168-180.

[7] Felemban, E. (2017, August). Quality of Information for Wireless Body Area Networks. In *Quality, Reliability, Security and Robustness in Heterogeneous Networks: 12th International Conference, QShine 2016, Seoul, Korea, July 7-8, 2016, Proceedings* (Vol. 199, p. 171). Springer. Chicago.

[8] Kafi, M. A., Othman, J. B., & Badache, N. (2017). A Survey on Reliability Protocols in Wireless Sensor Networks. *ACM Computing Surveys (CSUR)*, 50(2), 31.

[9] Li, X., Li, D., Wan, J., Vasilakos, A. V., Lai, C. F., & Wang, S. (2017). A review of industrial wireless networks in the context of industry 4.0. *Wireless networks*, 23(1), 23-41.

[10] Shah, S. A., Nazir, B., & Khan, I. A. (2016). Congestion control algorithms in wireless sensor networks: Trends and opportunities. *Journal of King Saud University-Computer and Information Sciences*.

[11] J. Paek, R. Govindan, "RCRT: Rate-Controlled Reliable Transport for Wireless Sensor Networks" in *ACM SenSys'07, Sydney, Australia*, Nov. 2007.

- [12] Teo, Jenn-Yue, Ha, Yajun, Tham, Chen-Khong, 2008. Interference-minimized multipath routing with congestion control in WSN for high-rate streaming. *IEEE Trans. Mobile Comput.* 7 (9).
- [13] Ren, Fengyuan, Das, Sajal K., Lin, Chuang, 2011. Traffic-aware dynamic routing to alleviate congestion in WSN. *IEEE Trans. Parallel Distrib. Syst.* 22 (9).
- [14] Chen, Yang, 2006. Congestion avoidance based on lightweight buffer management in sensor networks. *IEEE Trans. Parallel Distrib. Syst.* 17 (9), 934–946.
- [15] Charalambos, Vasosu, 2011. DAIPaS: a performance aware congestion control algorithm in WSN. In: *Proceeding of the IEEE 18th International Conference on Telecommunications*.
- [16] Hull, Jamieson, Balakrishnan, 2004. Mitigating congestion in WSN. In: *Proceedings of the 5th ACM Conference on Embedded Networked Sensor Systems (SenSys)*.
- [17] SRIDHARAN, A. AND KRISHNAMACHARI, B. 2009. Explicit and precise rate control for wireless sensor networks. In *Proceedings of the 7th ACM International Conference on Embedded Networked Sensor Systems (SenSys09)*.
- [18] F. K. Shaikh, A. Khelil, and N. Suri. 2009. AREIT: Adaptable reliable information transport for service availability in wireless sensor networks. In *Proceedings of International Conference on Wireless Networks (ICWN'09)*. 75–81.
- [19] Heikalabad, S. R., Ghaffari, A., Hadian, M. A., & Rasouli, H. (2011). DPCC: Dynamic Predictive Congestion Control in wireless sensor networks. *IJCSI International Journal of Computer Science Issues*, 8(1).
- [20] Banimelhem, O., & Khasawneh, S. (2012). GMCAR: Grid-based multipath with congestion avoidance routing protocol in wireless sensor networks. *Ad Hoc Networks*, 10, 1346–1361.
- [21] M. R. Palattella, N. Accettura, M. Dohler, L. A. Grieco, and G. Boggia. 2012. Traffic aware scheduling algorithm for reliable low-power multi-hop IEEE 802.15.4e networks. In *Proceedings of the 2012 IEEE 23rd International Symposium on Personal, Indoor and Mobile Radio Communications (PIMRC'12)*. 327–332.
- [22] M. R. Palattella, T. Watteyne, Q. Wang, K. Muraoka, N. Accettura, D. Dujovne, L. A. Grieco, and T. Engel. 2016. On-the-fly bandwidth reservation for 6TiSCH wireless industrial networks. *IEEE Sensors Journal* 16, 2 (Jan. 2016), 550–560.

Convolutional Neural Network based for Automatic Text Summarization

Wajdi Homaid Alquliti¹, Norjihani Binti Abdul Ghani²
Faculty of Computer Science and Information Technology
University of Malaya
Malaysia

Abstract—In recent times, the apps for the processing of a natural language has been formed and generated through the use of intelligent and soft computing methods that allow computer systems to practically mimic practices related to the process of human texts like the detection of plagiarism, determination of the pattern as well as machine translation. Thereafter, Text summarization serves as the procedure of abridging writing within consolidated structures. ‘Automatic text summarization’ or the ATS is when a computer system is used to create a text summarization. In this study, the researchers have introduced a novel ATS system, i.e., CNN-ATS, which is a convolutional neural network that enables to Automatic text summarization using a text matrix representation. CNN-ATS is a deep learning system that was used to evaluate the improvements resulting from the increase in the depth to determine the better CNN configurations, assess the sentences, and determine the most informative one. Sentences deemed important are extracted for document summarization. The researchers have investigated this novel convolutional network depth for determining its accuracy during the informative sentences selection for each input text document. The experiment findings of the proposed method are based on the Convolutional Neural Network that uses 26 different configurations. It demonstrates that the resulting summaries have the potential to be better compared to other summaries. DUC 2002 served as the data warehouse. Some of the news articles were used as input in this experiment. Through this method, a new matrix representation was utilized for every sentence. The system summaries were examined by using the ROUGE tool kit at 95% confidence intervals, in which results were extracted by employing average recall, F-measure and precision from ROUGE-1, 2, and L.

Keywords—Automatic text summarization; extracts summarization; information retrieval; deep learning; convolutional neural network

I. INTRODUCTION

Recently, the formation and generation of apps for the processing of a natural language have taken place by using soft and intelligent computing methods that make it possible for computer systems to practically imitate practices associated with processing human texts, such as machine translation, detection of plagiarism, and identification of patterns. Intelligence methods such as genetic-based algorithm, evolution-based algorithm, swarm-based intelligence, fuzzy logic, and neural network are often involved. Thus, a main reason for enabling the mimicking is the utilisation of a precise computer system that performs quicker compared to the performance of individuals. So, automatically summarising

texts is one type of natural language application that presumably makes use of such methods to optimise performance.

Literature has a fairly large amount of systems for automatic summarisation. Most of these systems manage the summarisation problem based on the desired kind of summaries. Numerous methods have been formulated to generate single-document summaries. Various methods were also presented, with machine learning being considered as the most visible. In numerous approaches, there is an assumption that the numerical representation of the text and the extracted features are demonstrations of how designing a method that is equipped with a powerful feature can produce a high-quality text summary. Scoring of the features for each sentence is performed in order to produce a summary for the input document. As a result, those chosen features affect the quality of the summary generated. Thus, there is a need to develop a mechanism to automatically obtain and calculate the feature.

The feature extraction stage is vital for data analysis in the NLP and machine learning processes. This step is helpful in identifying the interpretable representation of data for the machines that can enhance the performance of such learning algorithms. Applying unsuitable features could hinder the performance of even the best algorithms. On the other hand, simple techniques can have very good performance if appropriate features are implemented. The feature extraction stage is performed in a manual or unsupervised manner.

In the past few years, the deep learning technology has experienced massive developments. Empirical results have revealed that this is a better technique compared to other ML algorithms. This could be a result of the fact that this technique, like the brain model, copies the functioning of the brain and stacks several neural network layers on top of each other. According to [1], deep learning machines perform better than traditional machine learning tools since the feature extraction method is included. However, the deep learning methods get to know feature hierarchies by utilising features obtained from the higher hierarchical levels as a result of the organisation of low-level features. The learning features found at different levels of abstraction make it possible for the system to learn the complex functions. These complex functions are then responsible for using data to map the input and the resultant output without relying on human-developed features [1].

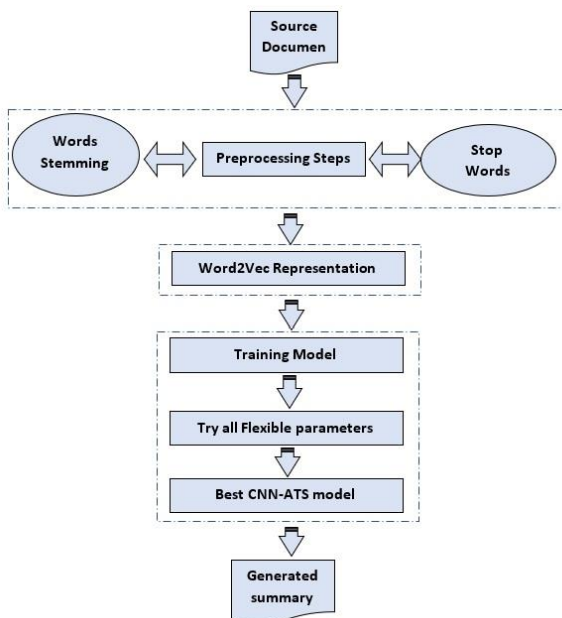


Fig. 1. Depicts the Exhaustive Framework of CNN-ATS Model.

Using deep learning for automatic text summarisation requires high investigation in the text representation. The texts are re-represented in such a way that they correspond with the basics of deep learning convolutional neural network, like the utilisation of the matrix format as a representation of the text structures in CNN architecture. In texts, the informative sentence is an adverse property that influences its capacity of being chosen for summarisation. The sentence’s importance is determined based on their words, which have been identified as ontology and mining. Distributed representation makes it possible to build abstract features, which are helpful in choosing and measuring the informative sentence. Here, new sentences patterns that facilitate text mining interpretation were determined by the researchers. The new matrix representation of sentence demonstrated a similarity to the images that the deep learning technique represented. Fig. 1 depicts the exhaustive framework of the CNN-ATS model.

II. DEFINITION AND RELATED WORK

A. Related Work

In the past few years, many new natural language processing applications were designed which applied intelligent and soft-computing methods. These applications can help the computational systems mimic all human text-based processing activities like pattern recognition, plagiarism detection and machine translation. Many intelligence techniques like swarm intelligence, genetic algorithms, evolutionary algorithms, neural networks and fuzzy logic have been used. These imitating techniques were used because the computer systems are often more precise than human performance. The automated text summarisation was a natural language application which applied these techniques for optimising its performance.

The text summarisation process includes summarising all texts into their condensed form [2]. The text summarisation conducted by a person is known as “manual text summarisation”, however, a computer-assisted text summarisation process is known as “Automatic Text Summarisation” (ATS). In this study, the researchers have investigated the ATS techniques, and have discussed the various ATS processes, input sizes, styles and evaluation processes. The need for text summarisation has been described in Fig. 2.

Many studies used two approaches for investigating the ATS processes, i.e., the abstraction-based and extraction-based summarised techniques. The extraction-based technique generated a summary by choosing (copy-pasting) the significant sentences. All these sentences were later assessed using a scoring mechanism known as “features”, wherein every sentence was assigned a different score. The high-scored sentences were then selected as the candidate summarised sentences. On the other hand, the abstraction-based technique summarised the texts by editing the significant text units (phrases or sentences) by appending, removing, segmenting or paraphrasing a few parts of the text units. This technique is more complex than the extraction-based approach [3].

The target text summary could be used and written in the following styles [4]: “indicative summary” or the “informative summary”. The indicative summary offers brief information regarding what is present in the primary document which focuses on a specific topic. The summary that is generated is compressed between 5-10% of the primary text. On the other hand, the informative summary assesses a majority of the topics present in the primary text. This type of generated summary comprises of 20-30% of the original document. Furthermore, the ATS researchers have investigated two forms of document input sizes, i.e., a single document and a multi-document summarisation process.



Fig. 2. The Need to use a Text Summarisation Technique.

Based on every document's processing level, all summarisation techniques have been categorised into 3 approaches, surface, entity and discourse [2], [5]. A surface level technique applies a shallow feature set for extracting the relevant sentences from the document and including them in a text summary. The entity level process extracts the entities and derives their relationship in the text document, and models their extraction. For identifying the vital entity-entity relationship, many techniques could be used like the vector space model and the graph-based representation. A Discourse-Level process is based on the modelling of the global text structure and its correlation like the rhetorical text structure (e.g., narrative and argumentation structure), a document format (i.e., hypertext mark-ups or document outlines) and the various topics threads (as and when they get exposed in a text).

Some of the earlier proposed techniques that could be used for summarising the texts included the surface level (i.e., feature-scoring) approaches [6]–[8]. In one study, [6] proposed a novel term-frequency process for highlighting the term-importance in the context, while [7] proposed the sentence position technique for helping the summarizer identify the significance of a sentence in the text document. After 10 years, [8] investigated 2 processes and proposed the feature of some pragmatic words (including cue words like “key”, “significant”, “idea”, etc.

As the feature scoring process helped in deriving significant results, the researchers have proposed many additional features for enhancing the text summarisation quality. Earlier literature showed that the text features process played a vital role in generating many qualified summaries [9], [10]. Hence, many studies enclosed the feature weighting technique for adjusting the feature scores in all summarisation-based issues [11]–[13]. This feature selection technique generated a higher solution quality. Also, the text summary quality was sensitive to the features which determined how the sentences were scored and weighted. Hence, there is a higher need for developing a mechanism which can differentiate the low and high significance features. As a result, several feature selection techniques were developed and proposed, however, there is a need to develop better mechanisms for obtaining good-quality results.

One other issue which must be addressed is related to the investigation of a majority of the text document subtopics. This helped in generating a summary, which can cover many themes in the document. For solving this issue, a cluster-based (or diversity) process can be used for diversifying the sentence selection technique, wherein the selected sentences can cover many topics in the text document. Several processes can be used for implementing the diversity-based approach for text summarisation [14]–[19]. This diversity during summarisation helps in controlling the sentence redundancy, which improves the summary quality.

Therefore, it is important to select a good similarity measure for adjusting the data clustering [20]. In their study, [21] estimated the sentence centrality score by sentence clustering. However, computing this score prevents any technique from determining the relationship between all sentences.

B. Deep learning

Deep learning is believed to drastically enhance the advanced artificial intelligent tasks such as object detection, speech recognition, and machine translation [22]. This technique's deep architectural nature can be used to solve complex artificial intelligence-related problems[23]. Thus, researchers have utilised this method in modern domains for numerous tasks such as object detection and face recognition. Application of this method to numerous language models has also been done. For example, [24] Using spiking deep belief network for Real-time classification and sensor fusion. [22] the recurrent neural networks has been used to denoise the speech signals and [25] stacked autoencoders have been used to determine the cluster pattern during gene expression. Also, they using deep learning methods for toxicity prediction [26]. Another study [27] utilised the neural model to produce images with varying styles. Furthermore, [28] the deep learning technology was used to simultaneously analyse sentiments from several modalities.

The deep learning technology went through massive developments in the past few years. Based on empirical results, it was determined that this technique was better compared to other ML algorithms. This could be a result of the fact that this technique, like the brain model, copies the functioning of the brain and stacks multiple neural network layers on top of each other. The author in [1] stated that the deep learning machines perform better than the conventional ML tools since they also utilise the feature extraction method. However, until now, there is no theoretical background for the deep learning technology. Feature hierarchies are learned by deep learning techniques using features obtained from the higher hierarchical levels, which have been formed through the organisation of the low-level features. The learning features found at the different abstraction levels make it possible for the system to gain an awareness of the complex functions that utilise the data to map the input and the resultant output without relying on the human-developed features [1]. For image recognition systems, the handcrafted features are extracted by the conventional setup extract and fed to the SVM. However, the deep learning technology performs better since it also conducts an optimisation of all the extracted features.

The main difference between deep learning technologies and ML is the difference in their performance when the volume of data increases. When the dataset is smaller, the deep learning method has an inefficient performance since it needs large data volume for proper comprehension [28].

C. Convolutional Neural Network

The convolutional neural network (CNN) is a kind of deep feed-forward network that can be generalised and trained easily compared to other networks that possess connectivity between adjacent layers [29], [30]. CNN has had successful usage when other neural networks were not as popular. Presently, it is being utilised in the computer vision community.

CNNs are formulated for data processing in the form of multiple arrays, such as a grey-scale image composed of $3 \times 2D$ arrays with varying pixel intensities. Different data modalities are demonstrated as multiple arrays, such as 1D for signals and sequences, including language; 2D for image or audio

spectrograms; and 3D for the video or volumetric images. The 4 main ideas that allow CNNs to utilise the features of the natural signals are shared weights, pooling, local connections, and use of multiple layers [29]–[31].

Numerous stages are included in a classic CNN architecture (Fig. 3). The initial stages consist of 2 kinds of layers: i.e. pooling and convolutional layers. Within the convolutional layer, one can organise the layers in the feature maps, where every unit is connected to the feature maps' local patches, which originate from the previous layers, through weights called as the filter bank. The result of the local weighted sum goes through the non-linearity, such as the ReLU [32]. All the units found in the feature map are observed to be sharing one filter bank. The different feature maps found in the layer utilise varying filter banks. This architecture was constructed for 2 purposes. Initially, for array data like images, it was considered that the local groups of values are highly correlated. They also form unique and easily noticeable local motifs. Secondly, the local statistics of other signals or images are considered invariant to the location. Thus, if the motif is observed within a certain section of the image, one may also find it elsewhere. This network therefore depends on the fact that the units found at various locations share the same weights and can therefore be detected through the utilisation of similar patterns from the other segments in the array. Mathematically, discrete convolution is considered as the primary filtering operation that is implemented in the feature maps; therefore, it is named so.

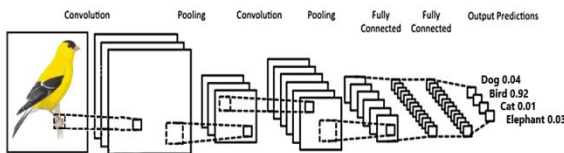


Fig. 3. Architecture of the CNN for Image Classification.

While the convolutional layer uses the earlier layer as the basis for detecting the local combination of the features, the pooling layer combines the semantically similar features into one feature. As a result of these features' relative position, there can be variations in the motif formation. Furthermore, reliably detecting the motif is possible by coarse-graining its position in each feature. The general pooling unit has the ability to calculate a maximal amount of the local patch of units into one feature map [33].

The CNN technique detects the edges based on the raw pixels in Layer 1. Afterwards, it utilises the edges to detect the simple shapes in Layer 2. Then, these shapes are used to detect the simpler shapes in Layer 2. These shapes are also used to determine high-level features, such as the face shape in the higher layers. The last layer is the classifier, which utilises these high-level features [34].

Over the years, a new automatic text summarisation technique possessing a higher degree of accuracy and the ability to automatically summarise any text is being perfected, when compared with the existing one. Developing a new automatic text summarisation technique has gained wide popularity because of its role in text mining for data mining

programs. Much evolution is needed for the use of deep learning in automatic text summarisation in representation as text. Re-represented of the text is done that corresponds to the fundamentals pertaining to deep learning convolutional neural network like the utilisation of the matrix format for representing the text structures in the CNN architecture. In text, the informative sentence is regarded as an adverse property, which can impact its potential to be selected for summarisation. The significance of a sentence is determined based on the words, which are identified as ontology and mining. The ability of constructing abstract features is associated with distributed representation, which helps in the measurement and selection of the informative sentence. Here, the researchers have found out new sentence patterns that allow text mining interpretation. A similar representation was demonstrated by the new matrix representation of sentence when compared with the images seen with the deep learning technique.

III. MATERIALS AND METHODS

Primarily, researchers provided a description of the construction of different experimental benchmarks that were utilized to test the system. Afterwards, they provided a description of the input representation and data encoding system, as well as the design of the deep convolutional network.

A. Data Gathering and Preparation

1) *Data gathering:* Another important part in this research phase is data gathering. Data gathering involves selection of data sets to be used for the purpose of research evaluation. There are important main data sets which we will require for these study for the evaluation our proposed summarization models. To test our summarization methods, we use the Document Understanding Conference (DUC) [15], [35] data collection. The DUC data collection which was created by the National Institute of Standards and Technology (NIST) of U.S. is a standard data set used by most researchers in the area of text summarization. Among the different data collections available in DUC, we have selected the DUC2002 data since it comes with summary extracts/abstracts for multi document articles. The segregation in DUC 2002 document collection is given Table I. For this study, in particular, we will use the document sets reporting on natural disaster events; which includes the document sets: D061j, D062j, D073b, D077b, D079a, D083a, D085d, D089d, D091c, D092c, D097e, D103g, D109h and D115i comprising.

TABLE I. STATISTIC OF DUC 2002 DATA SET

Category	Document Category
1	Single Natural disaster
2	Single event in any domain
3	Multiple distinct events of single type
4	Bibliographical information about a single individual

2) *Data preparation:* The step on pre-processing is essential in the range of computational phonetics, since the nature of the acquired outline relies on upon how proficient is the representation of content. In this proposition, few examinations will contain the preprocessing stage. For the most part, this stage will incorporate just two stages: dispensing with stop words and applying stemming as defined in [2].

B. Input Representation

Audio and image processing systems manage rich, high-dimensional datasets that are inputted as vectors of each raw pixel-intensity for image data, such as the power spectral density coefficients that correspond to the audio data. For tasks similar to speech or object recognition, we are aware that all the information needed for the successful performance of the task is encoded within the data (because these tasks can be performed by humans from the raw data). Nevertheless, natural language processing systems customarily consider words to be discrete atomic symbols. Thus, one can represent 'dog' as Id143 and 'cat' as Id537. These are arbitrary encodings, and they do not offer the system any useful information about the possible existing relationships between the individual symbols. This signifies that the model has the ability to leverage a very small portion of what it has gleaned about 'cats' when it is handling data about 'dogs' (i.e. they are both four-legged, animals, pets, etc.). Furthermore, representing words as discrete or unique results in data sparsity. This also typically means that more data may be needed in order to train statistical models successfully. Some of these obstacles can be overcome using vector representations.

Vector space models (VSMs) stand for (embed) words within a continuous vector space. In this space, mapping of semantically similar words is done to nearby points ('are embedded near each other'). VSMs are believed to have a long and rich NLP history. However, all methods rely on the Distributional Hypothesis in one way or another, which states that words share a semantic meaning when they appear in the same contexts.

This distinction is expounded on in greater detail by [36]. In a nutshell, it states that count-based methods calculate the statistics of how frequent a word will co-occur with its neighbor words within a large text. Then, these count-statistics are mapped down to a small, dense vector for every word. Predictive models directly attempt to predict a word from its neighbors based on learned dense and small embedding vectors (considered as the model's parameters).

In particular, Word2vec is a computationally-efficient predictive model that can be used to learn word embeddings from raw text. There are two flavours, the Skip-Gram model and the Continuous Bag-of-Words model (CBOW). Algorithmically, a declarative example for an input document into the process of Word2vec is demonstrated in Fig. 4.

C. Network Architecture

After all the data are collected, the researchers examined the different model architectures. They considered the default architecture as the convolutional architecture having fully

linked layers. Such architecture is suitable for the high-and multi-dimensional data, such as genomic data or 2D images. For evaluating the enhancement resulting from the increase in the depth of CNN-ATS, the researchers used the Krizhevsky principles to design the CNN-ATS layer configurations [29] that can view the source code [37].

In this study, all the CNN-ATS configurations examined are presented in Tables II to V, with one in each column. All further references made towards the configurations will be created depending on their names (A–Z). The configurations adhered to the generic design that was previously described in [29]. They also varied in depth ranged from 1 weight convolutional layer within the A network to 9 weight convolutional layers within the Z network. Both tables gave descriptions of the configurations. Here, the source text document traverses the stack of numerous convolutional (conv.) layers. The researchers utilised 2 different feature map sizes for use in the conv. layer of (3×3) and (5×5) (this is considered a good size for the up/down, left/right, centre) and different amounts of pooling and conv. layers.

Table II provides a description of the combinations of two stacks of pooling and convolutional layers. Table III illustrates the combination of three stacks of pooling and convolutional layers. This combination is helpful for the models since they can benefit from each other and enhance the CNN-ATS configurations' performance, producing the best selection of sentences for the automatic text summary approach.

The flatten layer comes after the conv. layer (with architectures possessing various depths) and helps turn the 2D matrix data into a vector. This makes it possible to conduct output processing using the fully connected layers, referred to as dense. In the regularisation layer, dropout is used and is configured for the random exclusion of 50% neurons for the decrease in overfitting. The last layer is formed by the soft-max layer [1], [29], [38]. All networks utilise the same fully linked layers configuration.

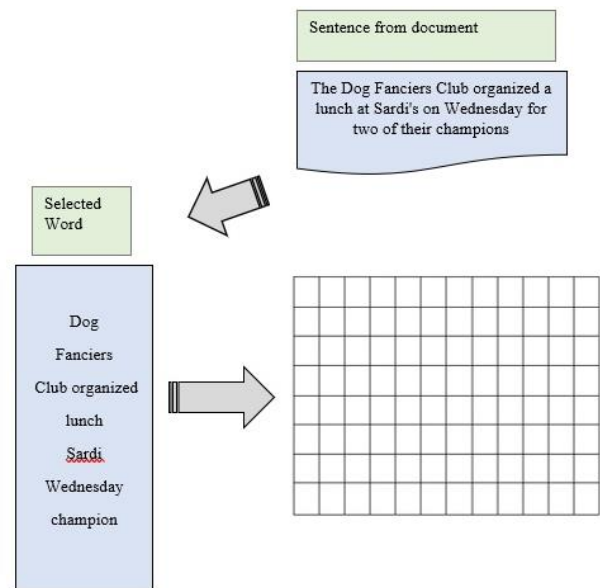


Fig. 4. A Declarative Example of an input Document into Word2vec Process.

For Tables IV and V, the “Best 2 layers” is considered as the best CNN-ATS configurations among the C to F in Table II. On the other hand, the “Best 3 layers” in Table III is considered the best CNN-ATS configurations from G to N.

Generally, one can conduct target prediction as follows.

The problem involves choosing the best Sentences that can be used for the automatic text summary method. If one can find the given sentence, i , in the document, t , one can encode this information in the binary form, y_{it} , wherein $y_{it} = 0$, for an unimportant sentence, and $y_{it} = 1$, for an important sentence, simultaneously. The training stage uses a standard back-propagation algorithm to determine the CNN and minimise the output layer activation and the cross-entropy of the targets.

D. Summarized Text Generation

The chosen sentence is obtained. Only sentences that possess 1 value of CNN-ATS output were chosen for consideration. Sentences deemed important are extracted for

document summarisation. It has been demonstrated that a compression or an extraction rate near 20% of the core textual content is instructive of the contents as the complete text of the document [39]. In the last stage, one can organise the summarising sentences in the order of their conceptual occurrences as observed in the initial text.

E. The Benchmark Methods

The selected methods are standard benchmark methods that have been widely used [15], [35]. They are chosen for comparison purposes at each chapter and classified into five methods:

- Microsoft Word Summarizer.
- Copernic Summarizer (commercial products currently run in the market).
- Best System at DUC2002 Competition.
- Worst System at DUC2002 Competition.
- H2-H1: Human to human Summary.

TABLE II. CNN-ATS CONFIGURATION FOR A-F COLUMNS FOR THE 2 WEIGHT CONVOLUTIONAL LAYERS

CNN-ATS Configuration					
A	B	C	D	E	F
1 Weight Conv Layers	1 Weight Conv Layers	2 Weight Conv Layers	2 Weight Conv Layers	2 Weight Conv Layers	2 Weight Conv Layers
Input Text matrix					
Conv Layer (3X3)	Conv Layer (5X5)	Conv Layer (3X3) Conv Layer (3X3)	Conv Layer (5X5) Conv Layer (5X5)	Conv Layer (3X3) Conv Layer (5X5)	Conv Layer (5X5) Conv Layer (3X3)
Max Pooling (2X2)					
Flatten					
Dense					
Dropout (0.5)					
Dense					
Softmax					

TABLE III. CNN-ATS CONFIGURATION FOR G-N (COLUMNS) FOR THE 3 WEIGHT CONVOLUTIONAL LAYERS

CNN-ATS Configuration							
G	H	I	J	K	L	M	N
3 Weight Layers	3 Weight Layers	3 Weight Layers	3 Weight Layers	3 Weight Layers	3 Weight Layers	3 Weight Layers	3 Weight Layers
Input Text matrix							
Conv Layer (5X5)	Conv Layer (5X5)	Conv Layer (5X5)	Conv Layer (5X5)	Conv Layer (3X3)	Conv Layer (3X3)	Conv Layer (3X3)	Conv Layer (3X3)
Conv Layer (5X5)	Conv Layer (5X5)	Conv Layer (3X3)	Conv Layer (3X3)	Conv Layer (5X5)	Conv Layer (5X5)	Conv Layer (3X3)	Conv Layer (3X3)
Conv Layer (5X5)	Conv Layer (3X3)	Conv Layer (5X5)	Conv Layer (3X3)	Conv Layer (5X5)	Conv Layer (3X3)	Conv Layer (5X5)	Conv Layer (3X3)
Max Pooling (2X2)							
Flatten							
Dense							
Dropout (0.5)							
Dense							
Softmax							

TABLE IV. CNN-ATS CONFIGURATION FOR O-R COLUMNS FOR THE 4-6 WEIGHT CONVOLUTIONAL LAYERS

CNN-ATS Configuration			
O	P	Q	R
4 Weight Layers	5 Weight Layers	5 Weight Layers	6 Weight Layers
Input Text matrix			
Best 2 layers	Best 2 layers	Best 3 layers	Best 3 layers
Max Pooling (2X2)			
Best 2 layers	Best 3 layers	Best 2 layers	Best 3 layers
Max Pooling (2X2)			
Flatten			
Dense			
Dropout (0.5)			
Dense			
Softmax			

TABLE V. CNN-ATS CONFIGURATION FOR S-Z COLUMNS FOR THE 6-9 WEIGHT CONVOLUTIONAL LAYERS

CNN-ATS Configuration							
S	T	U	V	W	X	Y	Z
6 Weight Layers	7 Weight Layers	7 Weight Layers	8 Weight Layers	7 Weight Layers	8 Weight Layers	8 Weight Layers	9 Weight Layers
Input Text matrix							
Best 2 layers	Best 2 layers	Best 2 layers	Best 2 layers	Best 3 layers	Best 3 layers	Best 3 layers	Best 3 layers
Max Pooling (2X2)							
Best 2 layers	Best 2 layers	Best 3 layers	Best 3 layers	Best 2 layers	Best 2 layers	Best 3 layers	Best 3 layers
Max Pooling (2X2)							
Best 2 layers	Best 3 layers	Best 2 layers	Best 3 layers	Best 2 layers	Best 3 layers	Best 2 layers	Best 3 layers
Max Pooling (2X2)							
Flatten							
Dense							
Dropout (0.5)							
Dense							
Softmax							

IV. RESULTS AND DISCUSSION

To test the application of the suggested CNN-ATS based approach for single-document extractive summarisation, 100 articles/documents were taken from the DUC dataset (DUC, 2002) [15], [35]. The standard corpus is used widely in text summarisation studies, which has documents and human model summaries. Firstly, pre-processing is conducted on the collection of documents. In this step, sentence splitting, stop words elimination, tokenisation, and word stemming are all involved. Once the documents complete the pre-processing process, word2vec input representation is applied in order for every sentence to be presented as matrix. Then, the CNN-ATS model is applied for testing and training. Sentences with value 1 were chosen for the output prediction in the suggested model. Lastly, the chosen sentences were chosen as a summary of the main text with the compression rate (20%) as the basis. We used three pyramid assessment measures –precision, mean coverage score (recall), and F-measure to assess our proposed approach. This metric evaluates the system summary’s quality

by making a comparison with human model summaries and other systems for benchmark summarisation.

To make a comparison of the proposed approach’s performance, various comparison configurations models were set up. First, the results for the configurations that are presented in Tables II and III are compared by making a comparison of the F-measure value taken by ROUGE-1. The Best 2 and Best 3 configurations were also selected. Then, the results between the various configurations presented in Tables IV and V were compared by comparing the F-measure value obtained by ROUGE-1. They indicate that the configurations can generate a better summary.

Afterwards, the best configurations results were compared with five benchmark summarisers using three evaluation measures as the basis - Precision, Recall, and F-measure. The five benchmark summarisers were best automatic summarisation system in DUC2002, Copernic summariser, worst automatic systems in DUC2002, Microsoft Word 2007 summariser, and the average of human model summaries (Models) H1:H2.

The proposed code was applied in the Theano [40], which refers to a public deep learning software that uses the Keras as the basis [41]. All layers within the deep network went through simultaneous initialisation with the ADADELTA[42]. Training of the complete network was done using the Dell Precision T1700 CPU system equipped with a 6 GB memory. Two weeks were needed to test and train the deep network.

F. Evaluation Measures

When creating and updating a system for summarisation, it is important to have a method or a tool to monitor the system performance and the modifications therein. For the summarisation process, there are two primary types of assessments: intrinsic as well as extrinsic. Intrinsic evaluations are utilised for assessing the summaries' quality. They may be helpful in answering queries regarding a summary like its grammar, coherence and whether it indicates incorrect knowledge deductions with reference to the original text, or repeated information within its summary itself. Alternatively, extrinsic assessment can be helpful in answering if the summary fulfils its designated purpose. For example, it helps determine if a summary replaces the original text well and conveys the most significant information.

The judgments of the intrinsic assessments are based on the summary output. Human intrinsic assessments measure a summary's cohesion, clarity and informativeness [43]. Automatic intrinsic assessments compare the summaries produced by the systems with those produced by humans. BLEU, ROUGE, Precision/Recall and Pyramid are some of the primary intrinsic tools. The Pyramid needs manual annotation of system-generated summaries and human-generated summaries prior to their comparison. BLEU, Precision/Recall and ROUGE, conversely, are completely automated and only need reference summaries.

F-Measure, Precision and Recall are some of the simplest assessment techniques present that measure the summary relevance with reference to the significance of the sentences it contains. Precision (P) is the quantity of sentences occurring in both the human and the system generated summaries divided by the quantity of sentences present in the system generated summary. Recall (R) is the quantity of sentences present in both the human and system summaries divided by the quantity of the sentences in the human summary. F-Score is a combination integrating both P and R [5]. The F-Score can be calculated with the following formula:

$$F = \frac{(1 + \beta^2)PR}{\beta^2 P + R}$$

Where β represents a weighting variable, which is adjustable to influence precision and recall.

The ROUGE (Recall Oriented Understudy for Gisting Evaluation) was introduced in 2004 [44] in order to solve the drawbacks of BLEU at ISI (Information Science Institute). It is approximately based on BLEU; however, it focuses instead on recall. Moreover, it quantifies overlapping of words in sequences and was discovered to correlate in a better way with human assessments compared to several other systems.

Many variants of ROUGE have been recommended [10]:

- ROUGE-N: counts contiguous n-gram. N ranges from 1 to 4.
- ROUGE-L: Longest Common Subsequence (LCS) based metric.

G. Results

In this research, CNN-ATS was proposed by the researchers. This is a novel-based approach that can be used for single-document extractive summarisation. CNN-ATS is considered a convolutional neural network, which has a new text matrix representation. It is also utilised for automatic text summarisation. It is also a deep learning system that integrates the information about the words and the concept about them. Hence, a comparison of the proposed CNN-ATS technique and 5 other benchmark summarisers was done.

This new deep learning system was evaluated in terms of its computing F-measure obtained through ROUGE-1 for all the different CNN-ATS configurations using the procedure stated in the Subsection 3.5. All results gathered from the A, B, C, D, E and F models have undergone comparison using the boxplot technique. Then, the models that demonstrated the best configurations were referred to as the Best 2 layer models. Then, the analysis results that were gathered from the G, H, I, J, K, L, M and N models were compared in terms of their boxplot data. The best 3-layer model was then chosen. This refers to Stage 1 of the result analysis. A more complete description is given below. Meanwhile, the researchers in Stage 2 evaluated the results' prediction accuracy for the CNN-ATS configuration models corresponding to O, P, Q, R, S, T, U, V, W, X, Y and Z. Their boxplot results were then compared to determine the best CNN-ATS architecture. During Stage 3, the researchers conducted a comparison of the results for best configurations that were gathered from the previous 2 stages with the 5 standard benchmark summarisers.

1) Stage 1: During Stage 1, the researchers conducted an evaluation and a comparison of the F-measure values for 100 documents summaries found in the DUC 2002 dataset. Fig. 5 contains the values for the comparison of F-measure during the Stage 1 experiments that included the CNN-ATS A to N configurations.

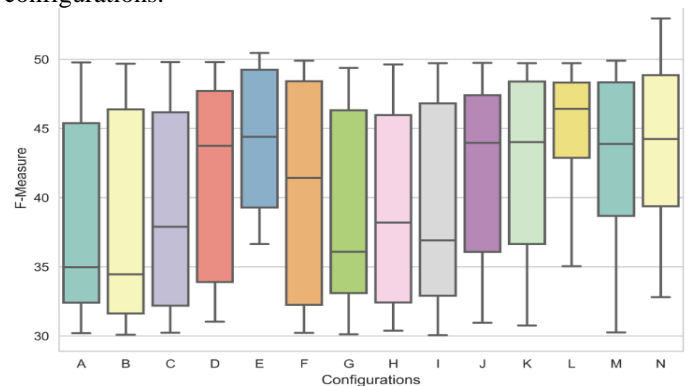


Fig. 5. Comparison of F-Measure Values for the CNN-ATS A to N Configurations Model using Boxplot.

As demonstrated in the figure, the 14 models exhibited a distinct difference in their mean values. Furthermore, the E configuration model gives a mean value of 43.85, while the L model has the best accuracy value of 46.52 (in Stage 1). A smaller variance value of 13.81 was observed in the E model. Therefore, it is considered better compared to the A, B, C, D and F models. The results are also indicative of the fact that E can be considered the best 2-layer model and may be utilised in the CNN-ATS O to Z model configurations to enhance the outcomes of the comprehensive convolutional neural network. The L model was found to have a variance value of 14.67, which indicates that L is the best among the 3-layered models and that it can be utilised further in the CNN-ATS O to Z model configurations to enhance the results of the comprehensive convolutional neural network.

2) Stage 2: During Stage 2, the researchers conducted an analysis of the values of the F-measure for the O, P, Q, R, S, T, U, V, X, Y and Z models of the configurations given in Tables IV and V. Table IV gives the combinations for the 2 stacks of the pooling and convolutional layers. Here, the results from Stages 1 and 2 were utilised by the researchers, where it was seen that the E model had the best 2-layer configuration. On the other hand, the L model was discovered to have the best 3 layered configuration. Table V offers a description of the combination of 3 stacks of the pooling and convolutional layers using the same best configuration models that were gathered for the 2 and 3 layers. Fig. 6 illustrates the comparison of the values of the F-measure using Boxplot for the 11 configurations.

Based on the Boxplot results, one can observe that the O, P, Q models had the best F-measure values equal to 35.07, 36.25 and 36.98, respectively. These values are indicators that the models having 2 stacks of pooling and convolutional layers performed better than the models that have 3 stacks of pooling and convolutional layers. Moreover, the O, P, and Q models exhibited the lowest variance in comparison to the other models. This fact emphasises that the O, P, and Q models can be considered as the combination models in Stage 2.

3) Stage 3: During the final Stage 3, the researchers conducted a comparison of all the best 6 configuration

outcomes that were gathered from the earlier 2 stages in order to determine the best CNN-ATS architecture. Moreover, the researchers made a comparison of the best CNN-ATS architecture with the 5-standard and the 3-standard benchmark summarisers – Copernic summariser, Microsoft Word 2007 summariser, the best automatic summarisation system in DUC 2002, the average of human model summaries (Models) H1:H2, and the worst automatic systems in DUC 2002. The basis of the comparison was the three evaluation measures - precision, recall, and F-measure based on the three types: ROUGE-1, ROUGE-2 and ROUGE-L. Fig. 7 shows the outcomes of the comparison performed with the E, L, N, P and Q configuration models. It was observed that model L performed the best and had a corresponding F-measure with a value of 46.52. Moreover, the E N, P and Q models had a larger variance, which indicates that L can be considered the best combination model based on the various experiments.

As is apparent from all figures and stages in the earlier experiment, a CNN-ATS model L is considered as the best model configuration for generating an improved summary. For comparative evaluation, Table VI presents the average precision, mean coverage score (recall), and average F-measure gathered from the DUC 2002 dataset for the proposed approach using five benchmark summarisers: Copernic summariser, Microsoft Word 2007 summariser, the best automatic summarisation system in DUC, the average of human model summaries (Models), and the worst automatic systems in DUC 2002 using ROUGE-1, ROUGE-2 and ROUGE-L, respectively.

As presented in Fig. 8, 9 and 10, the researchers gave the outcome of the boxplot test after a comparison of the F-Measure, precision and Recall values, respectively was performed for the CNN-ATS, Copernics, MS Word, worst system, best system, and human model summaries H2:H1. Furthermore, one can observe that the CNN-ATS algorithm exhibited a good recall value and F-Measure precision. They also noted a larger variance between the other methods compared to the CNN-ATS algorithm. This emphasises the superiority in the F-Measure values that were observed in the algorithms.

TABLE VI. COMPARISON OF SINGLE EXTRACTIVE DOCUMENT SUMMARIZATION USING ROUGE-1, ROUGE-1 AND ROUGE-L RESULT AT THE %95 CONFIDENCE INTERVAL

ROUGE Model	Evaluation Measure	MS-Word	Copernic	Best-System	Worst-System	H2:H1	CNN-ATS
ROUGE-1	precision	0.47705	0.46144	0.50244	0.06705	0.51656	0.50325
	Recall	0.40325	0.41969	0.40259	0.68331	0.51642	0.50492
	F-Measure	0.42888	0.43611	0.43642	0.1209	0.51627	0.50379
ROUGE-2	precision	0.22138	0.19336	0.24516	0.38344	0.23417	0.28718
	Recall	0.17441	0.17084	0.1842	0.03417	0.23394	0.28896
	F-Measure	0.19041	0.17947	0.20417	0.06204	0.23395	0.28862
ROUGE-L	precision	0.44709	0.29031	0.46677	0.66374	0.484	0.48465
	Recall	0.36368	0.25986	0.37233	0.06536	0.48389	0.48397
	F-Measure	0.39263	0.27177	0.40416	0.11781	0.48374	0.48423

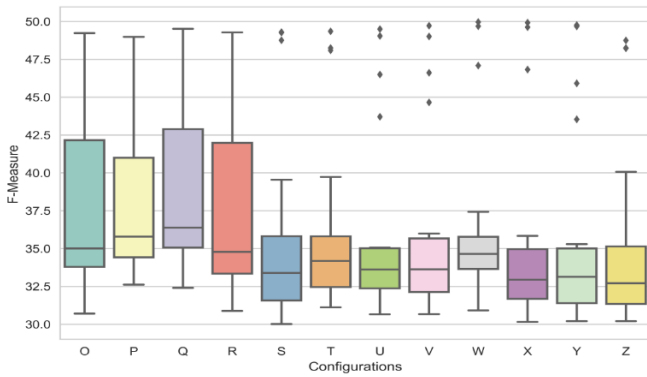


Fig. 6. Comparison of F-Measure Values for the CNN-ATS Models: O, P, Q, R, S, T, U, V, X, Y and Z Models Configurations Model using Boxplot.

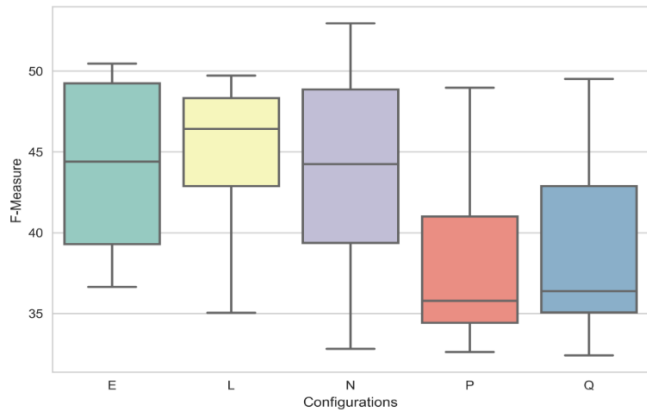


Fig. 7. Comparison of F-Measure Values for the CNN-ATS Models: E, L, N, P and Q Models Configurations Model using Boxplot.

The experiment findings of the proposed method are based on the Convolutional Neural Network that uses 26 different configurations. It demonstrates that the resulting summaries have the potential to be better compared to other summaries. DUC 2002 served as the data warehouse. Some of the news articles were used as input in this experiment. It utilised three pyramid evaluation metrics (average precision, mean coverage score (recall), and average F-measure) to comparatively evaluate the proposed approach as well as other summarisation systems. Through this method, a new matrix representation was utilised for every sentence. It was also used to evaluate the improvements resulting from the increase in the CNN-ATS depth to determine the better CNN configurations, assess the sentences, and determine the most informative one. The chosen sentences were then utilised to establish the summary. The sentences' scoring process was done based on the prediction output values of the CNN network for every sentence.

Based on the results given in Fig. 8, one can observe that F-Measure that uses configuration L produces better summarisation results compared to other configurations. Based on the experimental results of the proposed approach, it can be said that determining a good CNN configuration for text summarisation and utilising the word2vec techniques generates a good summary. Furthermore, CNN-ATS can be considered as the best automatic text summarisation among the six benchmarked methods. This can then be used to create the ideal summary and compare it to the human summary.

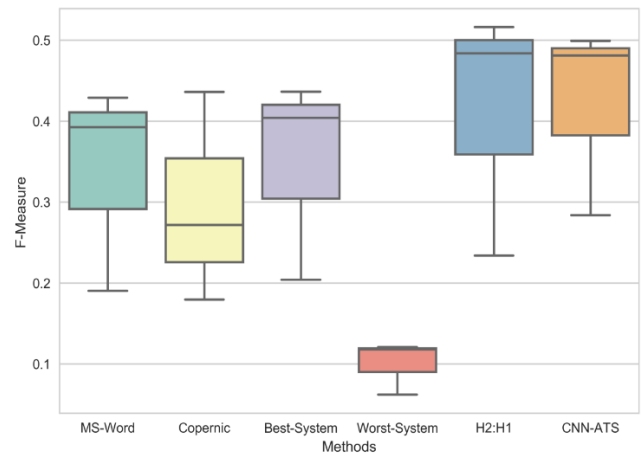


Fig. 8. Comparison of F-Measure Values for the CNN-ATS, MS Word, Copernics, Best System, Worst-System and Human Model Summaries H2:H1.

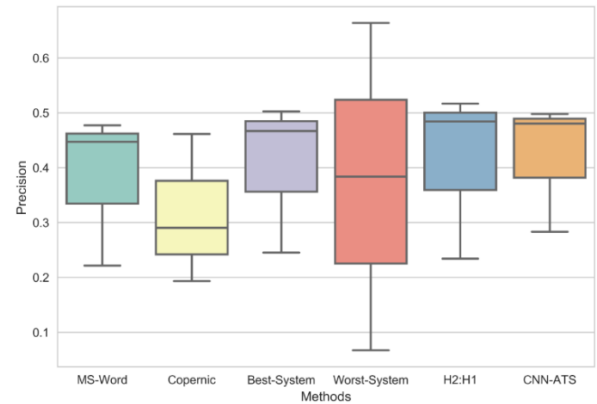


Fig. 9. Comparison of Precision Values for the CNN-ATS, MS Word, Copernics, Best System, Worst System and Human Model Summaries H2:H1.

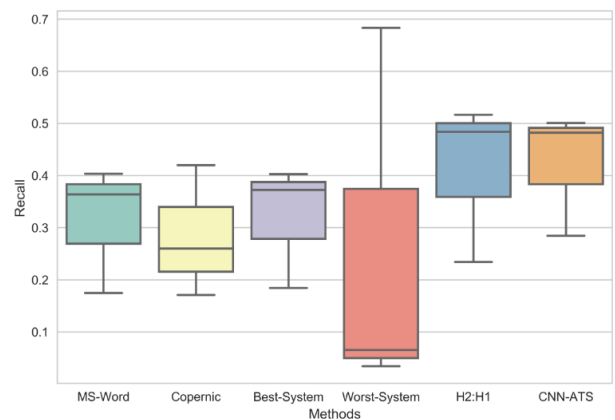


Fig. 10. Comparison of Recall Values for the CNN-ATS, MS Word, Copernics, Best System, Worst System and Human Model Summaries H2:H1.

V. CONCLUSION

To summarise, this chapter presented the utilisation of word2vec for building matrix representations that can be used to determine the summary of the single documents. The convolutional neural network will be the basis. Training and testing of this model was performed using a collection of 100

documents obtained from the DUC2002 dataset. A total of 26 different CNN configurations were used to identify the best architecture that will predict the informative sentences. The researchers examined the deep convolutional networks (possessing up to 9 weight layers) that will predict the informative sentences. They showed that for better selection accuracy, there is a corresponding lower representation depth. The influence that CNN depth has on the summarisation task is investigated. The study then used the selected sentences to group and create text summaries. The outcomes of the proposed summariser in this research were compared with various summarisers, such as Copernic summariser, Microsoft Word 2007 summariser, worst system, and best system. The ROUGE tool kit was then utilised for assessing the system summaries at 95% confidence intervals. The results were extracted using average recall, precision, and F-measure from ROUGE-1, 2, and L, respectively. The F-measure served as a selection criterion since it is a balance of the precision and the recall for the results of the system. The results indicate that the best average precision, recall and F-Measure are generated by our proposed methodology.

VI. AVAILABILITY OF DATA AND MATERIALS

The dataset is available for download [45]. ROUGE Library [44]. NLP Library [46]. Boxplot library [47]. Convolutional Neural Networks [48].

ACKNOWLEDGMENT

This research was supported by the University of Malaya (UM). I'm thankful to my supervisor Prof. Norjihhan Binti Abdul Ghani who provided expertise that greatly assisted the research, although they may not agree with all of the interpretations provided in this paper.

REFERENCES

- [1] Wang and B. Raj, "On the Origin of Deep Learning," Arxiv, pp. 1–72, 2017.
- [2] H. Saggion and T. Poibeau, "Automatic Text Summarization: Past, Present and Future," Multi-source, Multiling. Inf. Extr. Summ. Springer, pp.3-13, pp. 3–13, 2016.
- [3] G. Armano, A. Giuliani, and E. Vargiu, "Studying the impact of text summarization on contextual advertising," Proc. - Int. Work. Database Expert Syst. Appl. DEXA, pp. 172–176, 2011.
- [4] S. Gholamrezazadeh, M. A. Salehi, and B. Gholamzadeh, "A comprehensive survey on text summarization systems," Proc. 2009 2nd Int. Conf. Comput. Sci. Its Appl. CSA 2009, 2009.
- [5] I. Mani, M. T. Maybury, and M. Sanderson, "Advances in Automatic Text Summarization," Comput. Linguist., vol. 26, no. 2, pp. 280–281, 1999.
- [6] H. P. Luhn, "The Automatic Creation of Literature Abstracts," IBM J. Res. Dev., vol. 2, no. 2, pp. 159–165, 1958.
- [7] P. B. Baxendale, "Man-made index for technical literature - an experiment," I.B.M. J. Res. Dev., vol. 2, no. 4, pp. 354–361, 1958.
- [8] H. P. Edmundson, "New methods in automatic extracting," J. Assoc. Comput. Mach., vol. 16, no. 2, pp. 264–285, 1969.
- [9] R. Ferreira et al., "Assessing sentence scoring techniques for extractive text summarization," Expert Syst. Appl., vol. 40, no. 14, pp. 5755–5764, 2013.
- [10] M. M. Haque, S. Pervin, and Z. Begum, "Literature Review of Automatic Single Document Text Summarization Using NLP," Int. J. Innov. Appl. Stud., vol. 3, no. 3, pp. 857–865, 2013.
- [11] M. A. Fattah and F. Ren, "GA, MR, FFNN, PNN and GMM based models for automatic text summarization," Comput. Speech Lang., vol. 23, no. 1, pp. 126–144, 2009.
- [12] M. S. Binwahlan, N. Salim, and L. Suanmali, "Swarm Based Features Selection for Text Summarization," IJCSNS Int. J. Comput. Sci. Netw. Secur., vol. 9, no. 1, pp. 175–179, 2009.
- [13] L. Suanmali, N. Salim, and M. S. Binwahlan, "Genetic algorithm based sentence extraction for text summarization," 2011.
- [14] J. Carbonell and J. Goldstein, "The use of MMR, diversity-based reranking for reordering documents and producing summaries," Proc. 21st Annu. Int. ACM SIGIR Conf. Res. Dev. Inf. Retr. - SIGIR '98, pp. 335–336, 1998.
- [15] K. Filippova, M. Mieskes, and V. Nastase, "Cascaded Filtering for Topic-Driven Multi-Document Summarization," Proc. Doc. Underst. Conf., pp. 30–35, 2007.
- [16] Y. Gong and X. Liu, "Generic Text Summarization Using Relevance Measure and Latent Semantic Analysis," SIGIR'01, Sept. 9–12, 2001, New Orleans, Louisiana, USA, 2001.
- [17] W. Kraaij, M. Spitters, and M. H. der Van, "Combining a mixture language model and naive bayes for multi-document summarisation," SIGIR2001 Work. Text Summ., pp. 1–10, 2001.
- [18] J. Steinberger and K. Ježek, "Text Summarization: An Old Challenge and New Approaches," Found. Comput. Intell., vol. 206, pp. 127–149, 2009.
- [19] M. S. Binwahlan, N. Salim, and L. Suanmali, "Swarm Diversity Based Text Summarization," ICONIP 2009, pp. 216–225, 2009.
- [20] R. L. Cilibrasi and P. M. B. Vitányi, "The Google similarity distance," IEEE Trans. Knowl. Data Eng., vol. 19, no. 3, pp. 370–383, 2007.
- [21] R. M. Alguliev, R. M. Aliguliyev, and N. R. Isazade, "Multiple documents summarization based on evolutionary optimization algorithm," Expert Syst. Appl., vol. 40, no. 5, 2013.
- [22] Y. LeCun, B. Yoshua, and H. Geoffrey, "Deep learning," Nature, vol. 521, no. 7553, pp. 436–444, 2015.
- [23] Y. Bengio, Learning Deep Architectures for AI, vol. 2, no. 1. 2009.
- [24] P. O'Connor, D. Neil, S. C. Liu, T. Delbruck, and M. Pfeiffer, "Real-time classification and sensor fusion with a spiking deep belief network," Front. Neurosci., vol. 7, no. 7 OCT, pp. 1–13, 2013.
- [25] A. Gupta, H. Wang, and M. Ganapathiraju, "Learning structure in gene expression data using deep architectures, with an application to gene clustering," 2015 IEEE Int. Conf. Bioinforma. Biomed., pp. 1328–1335, 2015.
- [26] T. Unterthiner, A. Mayr, G. Klambauer, and S. Hochreiter, "Toxicity Prediction using Deep Learning," Front. Environ. Sci., vol. 3, no. February, 2015.
- [27] L. a. Gatys, A. S. Ecker, and M. Bethge, "A Neural Algorithm of Artistic Style," arXiv Prepr., pp. 1–16, 2015.
- [28] H. Wang, A. Meghawat, L.-P. Morency, and E. P. Xing, "Select-Additive Learning: Improving Cross-individual Generalization in Multimodal Sentiment Analysis," vol. 1, 2016.
- [29] A. Krizhevsky, I. Sutskever, and G. E. Hinton, "ImageNet Classification with Deep Convolutional Neural Networks," Adv. Neural Inf. Process. Syst., pp. 1–9, 2012.
- [30] T. Sainath, A. R. Mohamed, B. Kingsbury, and B. Ramabhadran, "Deep convolutional neural networks for LVCSR," Proc. IEEE Int. Conf. Acoust. Speech Signal Process., pp. 8614–8618, 2013.
- [31] M. Atzori, M. Cognolato, and H. Müller, "Deep learning with convolutional neural networks applied to electromyography data: A resource for the classification of movements for prosthetic hands," Front. Neurobot., vol. 10, no. SEP, pp. 1–10, 2016.
- [32] V. Nair and G. E. Hinton, "Rectified Linear Units Improve Restricted Boltzmann Machines," Proc. 27th Int. Conf. Mach. Learn., no. 3, pp. 807–814, 2010.
- [33] S. P. Mohanty, D. P. Hughes, and M. Salathé, "Using Deep Learning for Image-Based Plant Disease Detection," Front. Plant Sci., vol. 7, no. September, pp. 1–10, 2016.

- [34] Chen, Yu-Hsin and Krishna, Tushar and Emer, Joel and Sze, Vivienne, "Eyeriss: An Energy-Efficient Reconfigurable Accelerator for Deep Convolutional Neural Networks," in IEEE International Solid-State Circuits Conference, ISSCC 2016, Digest of Technical Papers, 2016, pp. 262–263.
- [35] W. Kraaij, M. Spitters, and A. Hulth, "Headline extraction based on a combination of uni-and multidocument summarization techniques," in Proceedings of the ACL workshop on Automatic Summarization/Document Understanding Conference (DUC 2002). ACL, 2002.
- [36] M. Baroni, G. Dinu, and G. Kruszewski, "Don't count, predict! A systematic comparison of context-counting vs. context-predicting semantic vectors," Proc. 52nd Annu. Meet. Assoc. Comput. Linguist. (Volume 1 Long Pap., pp. 238–247, 2014.
- [37] V. GUPTA, "Image Classification using Convolutional Neural Networks in Keras," 2017. [Online]. Available: <https://www.learnopencv.com/image-classification-using-convolutional-neural-networks-in-keras/>.
- [38] C. Angermueller, T. Pärnamaa, L. Parts, and O. Stegle, "Deep learning for computational biology," Mol. Syst. Biol., vol. 12, no. 7, pp. 1–16, 2016.
- [39] A. H. Morris, G. M. Kasper, and D. A. Adams, "The effect and limitations of automatic text condensing on reading comprehension performance," Inf. Syst. Res., vol. 3, no. 1, pp. 17–35, 1992.
- [40] F. Bastien et al., "Theano: new features and speed improvements," pp. 1–10, 2012.
- [41] F. Chollet, "Keras Documentation," Keras.io, 2015.
- [42] M. D. Zeiler, "ADADELTA: An Adaptive Learning Rate Method," 2012.
- [43] U. Hahn and I. Mani, "Challenges of automatic summarization," Computer (Long. Beach. Calif.), vol. 33, no. 11, pp. 29–36, 2000.
- [44] C. Y. Lin, "Rouge: A package for automatic evaluation of summaries," Proc. Work. text Summ. branches out (WAS 2004), no. 1, pp. 25–26, 2004.
- [45] "Document Understanding Conferences DUC 2002 Dataset." [Online]. Available: <https://duc.nist.gov/data.html>.
- [46] R. Rehurek and P. Sojka, "Gensim - Statistical Semantics in Python," EuroScipy, vol. 6611, no. May 2010, p. 25.–28. 8. 2011, 2011.
- [47] "boxplot python library." [Online]. Available: <https://seaborn.pydata.org/generated/seaborn.boxplot.html>.
- [48] "Convolutional_neural_network." [Online]. Available: https://github.com/lISourcell/Convolutional_neural_network/blob/master/convolutional_network_tutorial.ipynb.

Hospital Readmission Prediction using Machine Learning Techniques

A Comparative Study

Samah Alajmani¹

Computer Science Department
Faculty of Computing & Information Technology
King Abdulaziz University
Jeddah, Saudi Arabia

Hanan Elazhary²

College of Computer Science & Engineering
University of Jeddah, Jeddah, Saudi Arabia
Computers & Systems Department
Electronics Research Institute, Cairo, Egypt

Abstract—One of the most critical problems in healthcare is predicting the likelihood of hospital readmission in case of chronic diseases such as diabetes to be able to allocate necessary resources such as beds, rooms, specialists, and medical staff, for an acceptable quality of service. Unfortunately relatively few research studies in the literature attempted to tackle this problem; the majority of the research studies are concerned with predicting the likelihood of the diseases themselves. Numerous machine learning techniques are suitable for prediction. Nevertheless, there is also shortage in adequate comparative studies that specify the most suitable techniques for the prediction process. Towards this goal, this paper presents a comparative study among five common techniques in the literature for predicting the likelihood of hospital readmission in case of diabetic patients. Those techniques are logistic regression (LR) analysis, multi-layer perceptron (MLP), Naïve Bayesian (NB) classifier, decision tree, and support vector machine (SVM). The comparative study is based on realistic data gathered from a number of hospitals in the United States. The comparative study revealed that SVM showed best performance, while the NB classifier and LR analysis were the worst.

Keywords—Decision tree; hospital readmission; logistic regression; machine learning; multi-layer perceptron; Naïve Bayesian classifier; support vector machines

I. INTRODUCTION

Nowadays, numerous chronic diseases, such as diabetes, are widespread in the world; and the number of patients is increasing continuously. The estimated number of diabetic adults in 2014 was 422 million versus 108 million in 1980 [1]. Such patients visit hospitals frequently, requiring continuous preparation for ensuring the availability of required resources including hospital beds, rooms, and enough medical staff for an acceptable quality of service. Accordingly, predicting the likelihood of readmission of a given patient is of ultimate importance. In fact readmission during a one month period (30 days) of discharge indicates "a high-priority healthcare quality measure" and the goal is to address this problem [2].

Machine learning, which is one of the most important branches of artificial intelligence, provides methods and techniques for learning from experience [3]. Researchers often use it for complex statistical analysis tasks [4]. It is a wide multidisciplinary domain which is based on numerous

disciplines including, but not limited to, data processing, statistics, algebra, knowledge analytics, information theory, control theory, biology, statistics, cognitive science, philosophy, and complexity of computations. This field plays an important role in term of discovering valuable knowledge from databases which could contain records of supply maintenance, medical records, financial transactions, applications of loans, etc. [5].

As indicated in Fig. 1, machine learning techniques can be broadly classified into three main categories [3]. Supervised learning techniques involve learning from training data, guided by the data scientist. There are two basic types of learning missions: classification and regression. Models of classification attempt to predict distinguished classes, such as blood groups, while models of regression prognosticate numerical values [3]. In unsupervised learning, on the other hand, the system could attempt to find hidden data patterns, associations among features or variables, or data trends [3], [4]. The main objective of unsupervised learning is the ability to specify hidden structures or data distributions without being subject to supervision or the prior categorization of the training data [6]. Finally, in reinforcement learning the system attempts to learn through interactions (trial and error) with a dynamic environment. During this learning mode, the computer program provides access to a dynamic environment in order to perform a specific objective. It is worth noting that in this case, the system does not have prior knowledge regarding the environment's behavior, and the only way to figure it out is through trial and error [3], [7], [8].

According to Kaelbling et al., the term healthcare informatics refers to the combination between machine learning and healthcare with the purpose of specifying interest patterns [9]. In addition to this, it has the potential for establishing a good relationship between patients and doctors, and minimizing the increasing cost of healthcare [10]. The goal of this paper is to apply machine learning techniques, and specifically prediction techniques, for predicting the likelihood of readmission of patients to hospitals. This problem hasn't been adequately addressed in the literature. In fact most research efforts are oriented towards prediction of diseases. Machine learning includes numerous analytic techniques for prediction and the literature lacks adequate comparative studies

that assist in selecting a suitable technique for this purpose. Our research is based on a large data set collected by numerous United States hospitals [11], [12]. In short, this paper has two main contributions as follows:

- Analyzing five most common machine learning techniques for prediction and providing a comparative study among them.
- Addressing the problem of patient readmission to hospitals, since it has been rarely addressed by researchers.

Organization of the rest of the paper is as follows: First, we present background about the machine learning techniques considered in this research. This is followed by related work to highlight the contributions of the paper. We then present our methodology and discuss the results of the experiments. Finally, we sum up this work via a conclusion and discussion of possible future work.

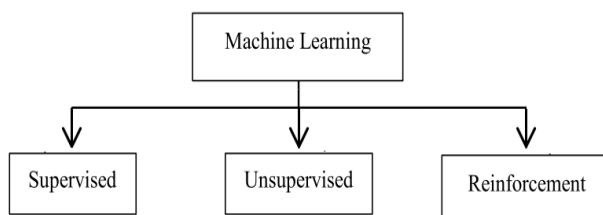


Fig. 1. Classification of Machine Learning Techniques.

II. BACKGROUND

This section discusses the five basic machine learning techniques employed in this research study.

A. Logistic Regression Analysis

Regression is a statistical notion that can be used to identify the relationship weight between one variable called the dependent variable and a group of other changeable variables denoted as the independent variables. Logistic regression (LR) is a non-linear regression model, used to estimate the likelihood that an event will occur as a function of others [13].

B. Artificial Neural Network

An Artificial Neural Network (ANN) is a computational model which attempts to emulate the human brain parallel processing nature. An ANN is a network of strongly interconnected processing elements (neurons), which operate in parallel [14] inspired by the biological nervous systems [15]. ANNs are broadly used in many researches because they are capable of modeling non-linear systems, where relationships among variables are either unknown or quite complicated [14]. An example of an ANN is the Multi-Layer Perceptron (MLP), which is typically formed of three layers of neurons (input layer, output layer, and hidden layer) and its neurons use non-linear functions for data processing [16].

C. Naïve Bayesian Classifier

Naïve Bayesian (NB) classifier relies on applying Bayes' theorem to estimate the most probable membership of a given event in one of a set of possible classes. It is described as being

naïve, since it assumes independence among variables used in the classification process [15], [17], [18].

D. Support Vector Machine

Support vector machines (SVMs) are supervised learning models, which can be applied for classification analysis and regression analysis. They have been proposed by Vapnik in 1995. They can perform both linear and non-linear classification tasks [5], [12], [17], [19].

E. Decision Tree

Decision trees are one of the most famous techniques in machine learning. A decision tree relies on classification by using attribute values for making decisions. In general, a decision tree is a group of nodes, leaves, a root and branches [20]. Many algorithms have been proposed in the literature for implementing decision trees. One important algorithm is CART (Classification and Regression Tree). It is used for dealing with continuous and categorical variables [8], [21].

III. RELATED WORK

Many researchers attempted to use machine learning techniques in healthcare problems other than hospital readmission likelihood prediction. For example, Arun and Sittidech used K-Nearest Neighbor (KNN), NB, and decision trees with boosting, bagging, and ensemble learning in diabetes classification. Their experiments confirmed that the highest accuracy is obtained by applying bagging with decision trees [22]. On the other hand, Perveen et al. attempted to improve the performance of such algorithms using AdaBoost. The evaluation of experimental outcomes showed that AdaBoost had better performance in comparison to bagging [23]. Orabi et al. [24] suggested integrating regression with randomization for predicting diabetes cases according to age, with an accuracy of 84%. Other researchers proposed building a predictive model using three machine learning techniques, which are random forests (RFs), LR, and SVMs; for predicting diabetes in Indians females, in addition to the factors causing diabetes. Their comparative study concluded that RFs had the best performance among the others [25].

Relatively few research studies addressed the problem of hospital readmission likelihood prediction. For example, Strack et al. used statistical models for this purpose [12]. Other researchers focused on comparing different machine learning techniques for addressing this problem. For example, Kerexeta [26] proposed two approaches. In the first, they combined supervised and unsupervised classification techniques, while in the latter, they combined NB and decision trees. They showed that the former approach had a better performance in comparison to the latter in terms of readmission prediction.

To sum up, relatively few research efforts in healthcare are concerned with the problem of prediction of hospital readmission likelihood. Additionally, there is a shortage of adequate comparative studies for comparing machine learning techniques used for prediction. Hence, this paper attempts to tackle those two problems by comparing five common machine learning techniques for tackling the problem of hospital readmission likelihood prediction based on real data.

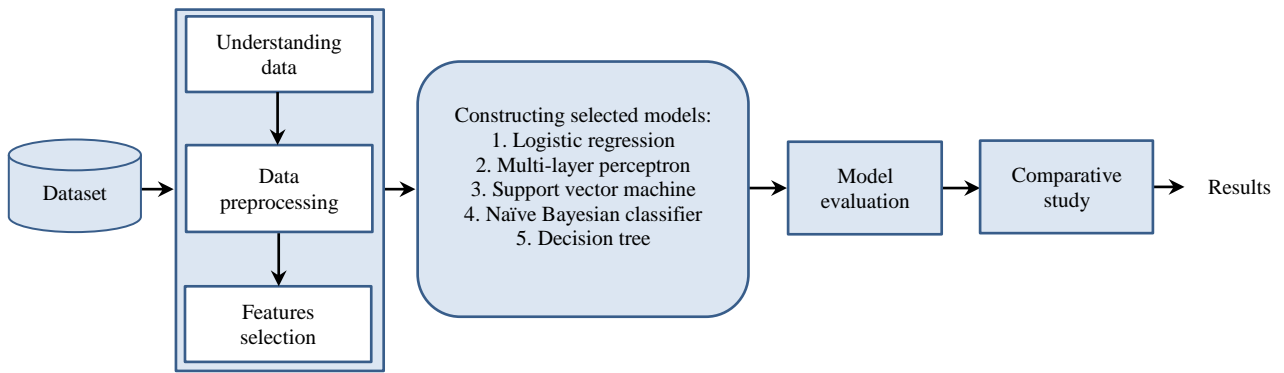


Fig. 2. Proposed Methodology.

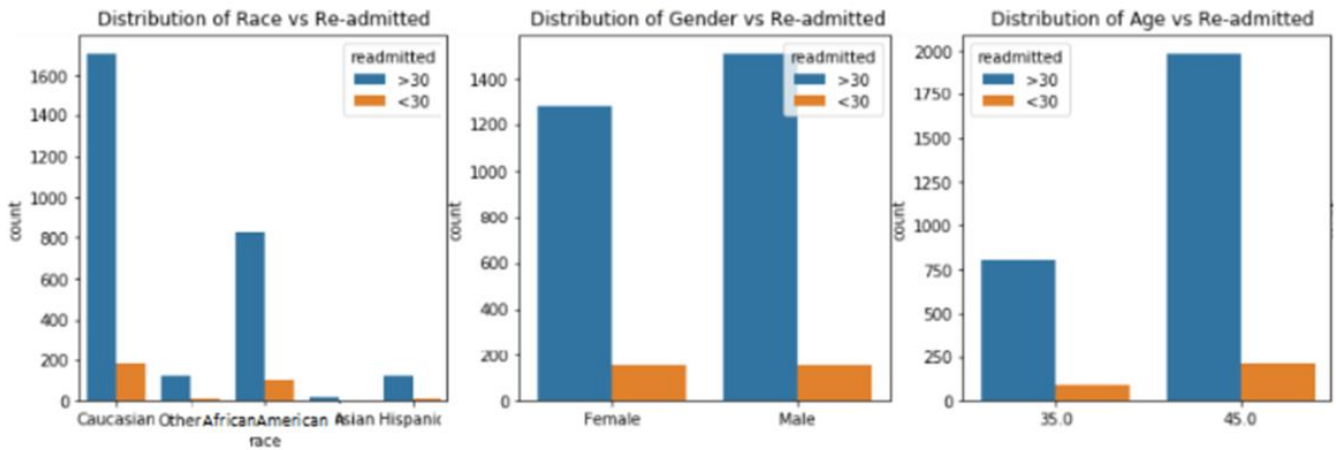


Fig. 3. Analysis of Variables.

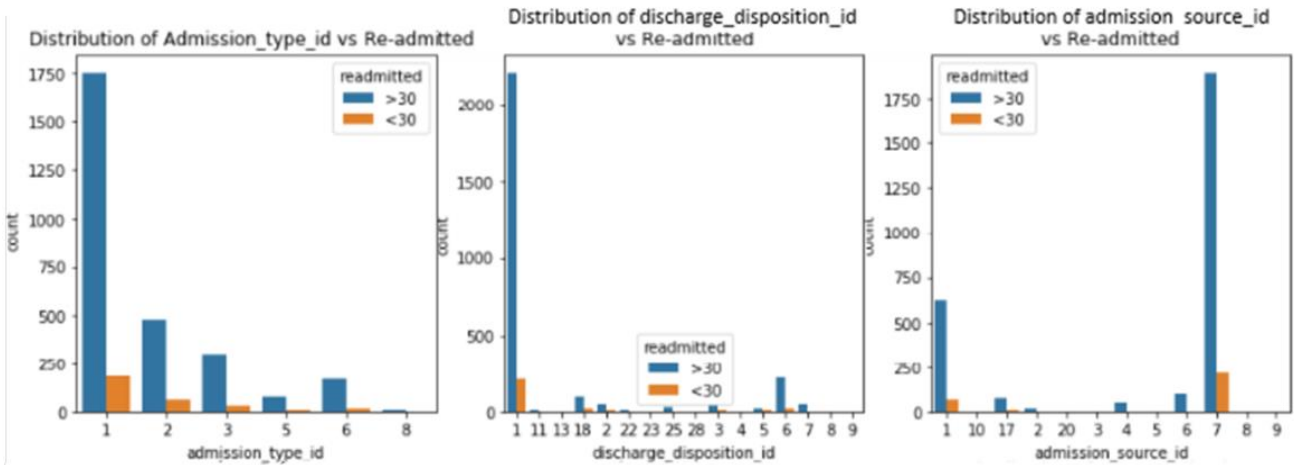


Fig. 4. Analysis of Variables (cont.).

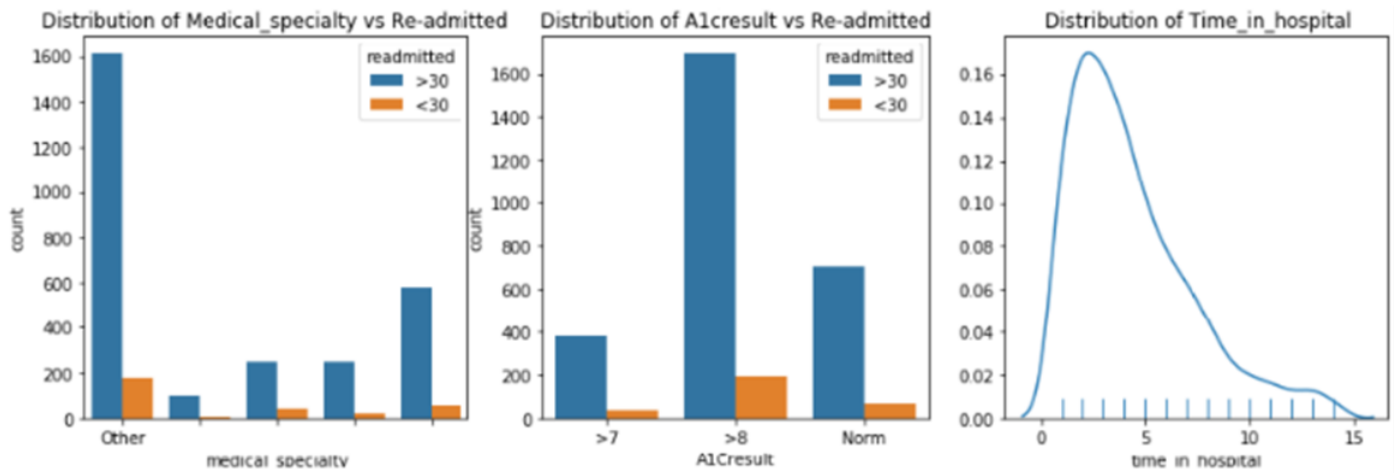


Fig. 5. Analysis of Variables (Cont.).

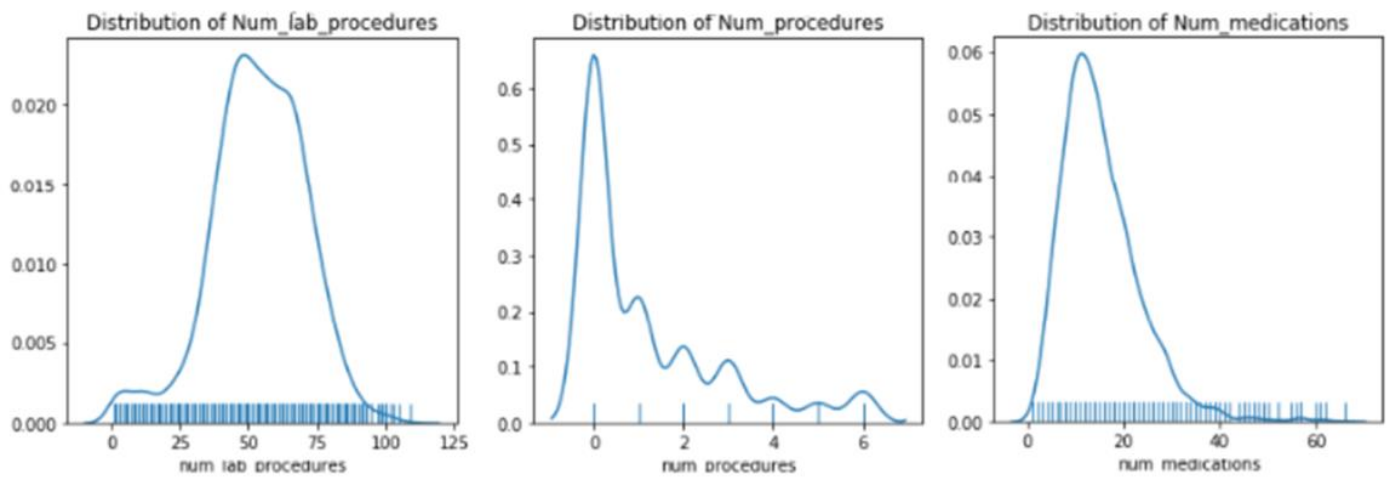


Fig. 6. Analysis of Variables (Cont.).

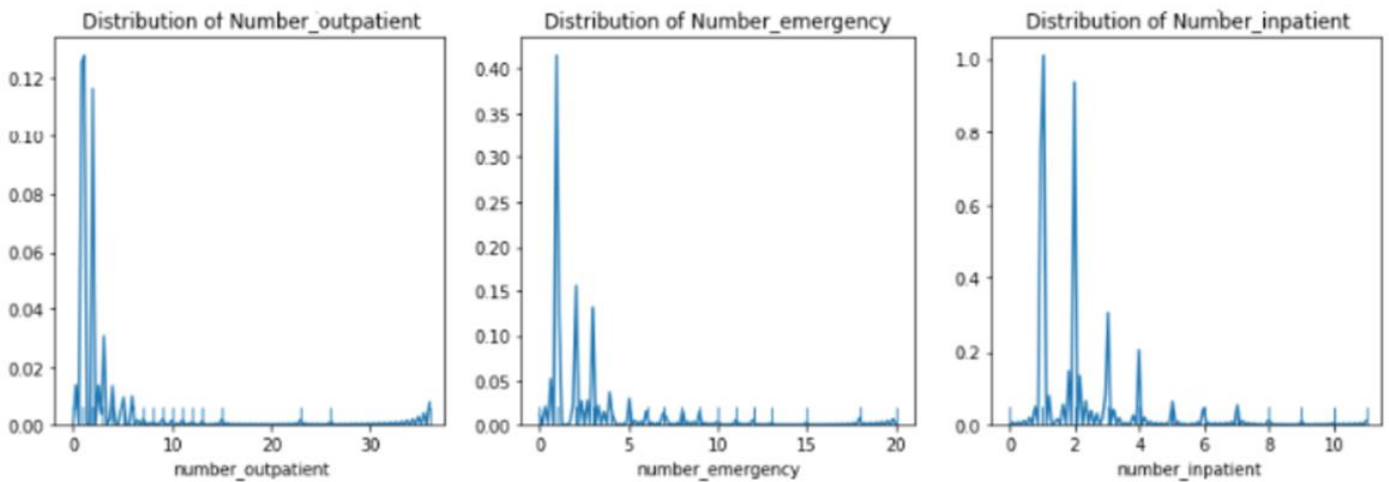


Fig. 7. Analysis of Variables (Cont.).

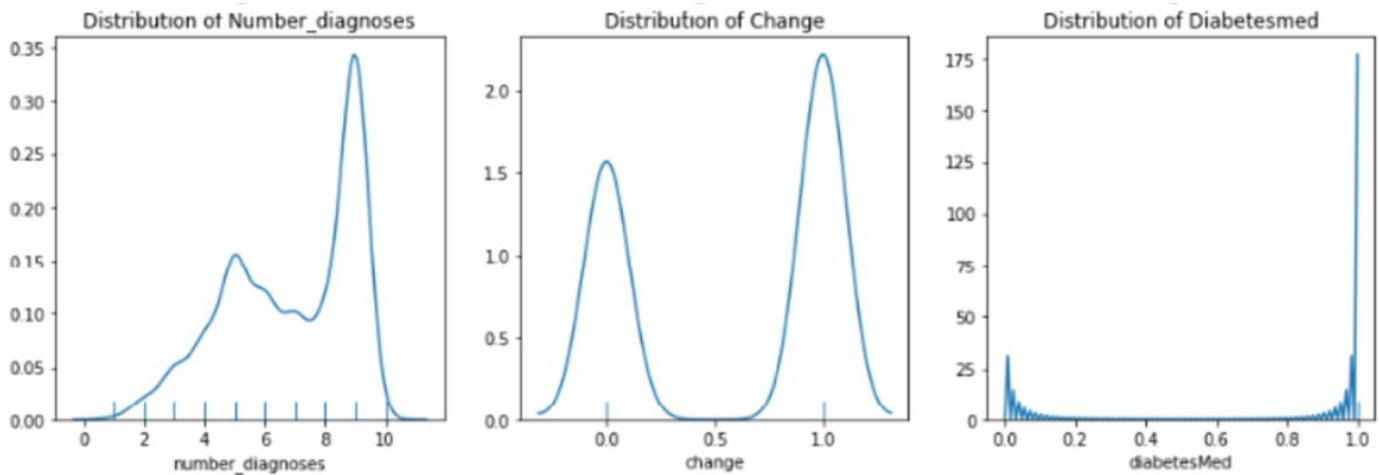


Fig. 8. Analysis of Variables (Cont).

IV. METHODOLOGY

Before starting the comparative study, it is important to understand the data, perform preprocessing if necessary, and select features appropriate for the experiments as depicted in Fig. 2. Those tasks are explained below. It is worth noting that all the experiments were conducted using Python.

A. Data Preparation

1) *Understanding data*: In this study, we exploited a sample of a diabetes patients' dataset, which has been extracted from many hospitals in the United States [11], [12]. This dataset includes 3090 instances in the age range of 30-50 and with 18 attributes. Table I depicts the variables of the dataset together with their descriptions. The scientific meanings of those variables are beyond the scope of this paper. Fig. 3 through 8 depict the distribution of those features.

2) *Data pre-processing*: This is a very important stage which includes data transformation and cleaning. In data transformation, some variables were transformed from categorical to binary (0/1) such as (Change, DM, G, and A). Some other variables were transformed from integer to string such as AS, DI, and AS. In data cleaning, some values of categorical data were missing and had to be accounted for. For this purpose, we employed imputation (substitution) via the mode of the categorical data.

3) *Feature Selection*: In this step, we perform feature selection for dimensionality reduction. In other words, we select the most relevant features. In this study, towards this goal, we assessed the impact of variables on our target. This helped us eliminate variables with low importance. Features which have high influence on accuracy are the most important [27]. We used the Gradient Boosting technique [28] for categorical features. Table II demonstrates the average

weights of the variables. We then utilized a threshold of 0.014 to obtain our feature set [29], [30]. Accordingly, the features A, AS, and DM were rejected since their weights were lower than 0.014. All the other features depicted in Fig. 9 were selected.

TABLE I. DIABETES PATIENTS' DATA

Variable	Variables Abbreviation	Data type
Race	R	Categorical
Gender	G	Categorical
Age	A	Categorical
Admission type Id	AT	Integer
Discharge disposition Id	DI	Integer
Admission source Id	AS	Integer
Medical specialty	MS	Categorical
A1Cresult	A1Cresult	Categorical
Time in hospital	TH	Integer
Number of lab procedures	NL	Integer
Number of procedures	NP	Integer
Number of medications	NM	Integer
Number of outpatient	NO	Integer
Number of emergency	NE	Integer
Number of inpatient	NI	Integer
Number of diagnosis	ND	Integer
Change	Change	Categorical
DiabetesMed	DM	Categorical
DM	0.008867	Rejected

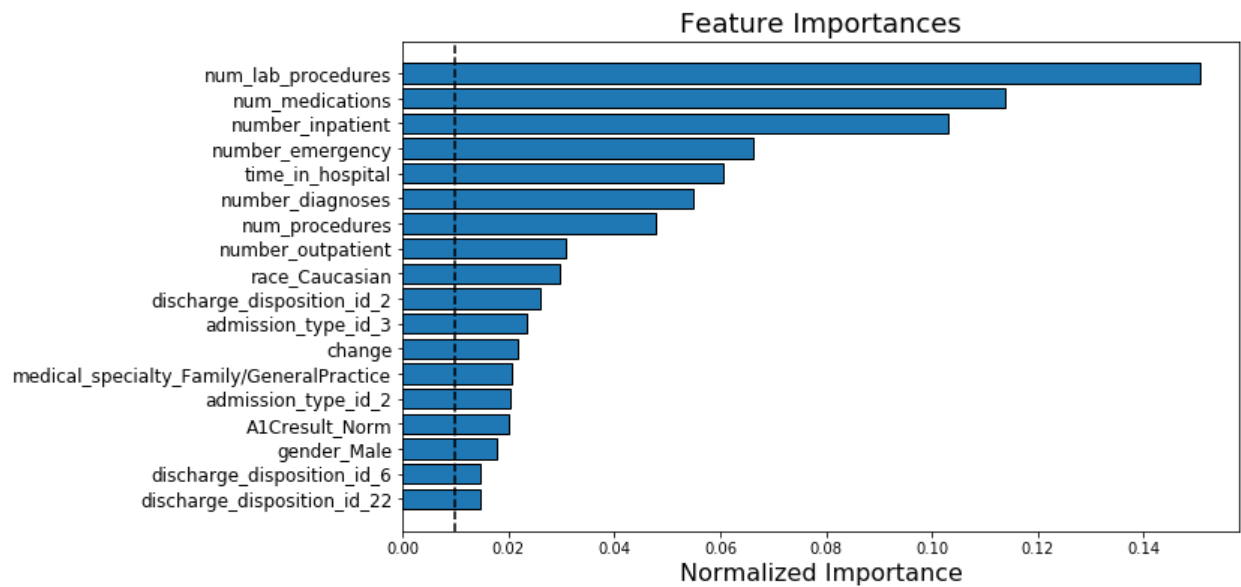


Fig. 9. Importance of Variables.

TABLE II. FEATURES IMPORTANCE

Variable	Importance (average)	Decision
R	0.029016	Confirmed
G	0.020294	Confirmed
A	0.010165	Rejected
AT	0.023854	Confirmed
DI	0.027554	Confirmed
AS	0.008961	Rejected
MS	0.019117	Confirmed
AlCresult	0.020177	Confirmed
TH	0.062025	Confirmed
NL	0.149317	Confirmed
NP	0.046521	Confirmed
NM	0.111058	Confirmed
NO	0.030696	Confirmed
NE	0.066718	Confirmed
NI	0.104099	Confirmed
ND	0.055811	Confirmed
Change	0.023027	Confirmed

B. Constructing Machine Learning Techniques Models

In this comparative study, the selected models included one output/target with two values (True or False) regarding hospital readmission during a period of 30 days. In other words, the value of the readmission parameter is true if readmission is done during a period of 30 days. Otherwise, in case of no readmission or in case readmission is done after 30 days, its value is false. The set of drivers for the prediction was comprised of the selected features as discussed above. The training dataset and the testing dataset were selected randomly. Additionally, 10-fold cross validation was applied by selecting 40% of the data for testing and the rest for training. The settings of the various models are discussed below.

1) *Logistic regression*: This model was built by importing the Logistic regression module and using it to generate the classifier. Grid search was employed to detect the optimal accuracy and the best hyper-parameters.

2) *Support vector machine*: Kernel SVM was trained using the training set. A support vector classification (SVC) task was used. In this technique, there are many parameters such as C, kernel, and gamma; where C represents the error term penalty parameter, kernel determines the kernel type which can be utilized in the algorithm (in our case it is 'rbf'), and gamma indicates the coefficient of the kernel, such that a high value of gamma attempts to completely fit the set of training data. Grid search was employed to determine the optimal parameters and accuracy. Table III illustrates that the optimal accuracy for C is 10. On the other hand, the optimal accuracy for gamma was 0.3.

TABLE III. SVM ACCURACY

C	Accuracy
0.1	0.8169582
1.00	0.9102736
10.00	0.9246298

3) *Decision tree*: This model was generated using the 'gini' function to evaluate the split quality of the tree. In our study, the min_samples_split = 30 is the minimal number of samples needed for splitting an internal node, and max_depth is the maximal tree depth. Grid search was conducted and the best accuracy for max_depth was 15 as depicted in Table IV.

TABLE IV. DECISION TREE ACCURACY

max_depth	Accuracy
5	0.8326603
10	0.8627187
15	0.8788694

TABLE V. MLP WEIGHT MATRIX RESULTS

	Hidden2.1	Hidden2.2	Hidden2.3	Hidden2.4	Hidden2.5	Readmitted<30	Readmitted>30
num_lab_procedures	-0.0021	0.0263	-0.2052	0.2031	-0.0536	0.0000	0.0000
num_medications	0.0055	-0.1040	2.1573	1.3116	0.0572	0.0000	0.0000
number_inpatient	-0.0141	-0.0330	-3.7337	3.9118	0.0097	0.0000	0.0000
num_emergency	-0.0105	-0.0008	0.1937	-0.2044	0.0118	0.0000	0.0000
time_in_hospital	0.0113	0.0307	-1.0520	1.3083	-0.0158	0.0000	0.0000
number_diagnosis	-0.0064	0.0004	-0.8371	-0.0016	0.0135	0.0000	0.0000
num_procedures	0.0005	-0.0362	1.3875	0.0360	0.0034	0.0000	0.0000
number_oupatient	0.0096	-0.0106	0.0029	0.7529	0.0561	0.0000	0.0000
race_caucasian	-0.0238	-0.1076	-0.0529	-1.2512	4.5722	0.0000	0.0000
discharge_disposition_id_2	-0.7015	-3.2359	3.0491	1.3420	-0.8454	0.0000	0.0000
admission_type_id_3	-0.0043	0.0155	2.0813	1.5240	-2.4905	0.0000	0.0000
change	0.0019	0.0294	-0.5155	-0.9567	-0.0422	0.0000	0.0000
medical_speciality_Family/GeneralPractice	-0.0643	-2.8393	5.2166	0.8710	-0.0294	0.0000	0.0000
admission_type_id_2	0.0163	0.0751	0.1518	0.1636	-2.2760	0.0000	0.0000
A1Cresult_Norm	4.1982	-5.7995	-1.5765	-1.0361	-0.0567	0.0000	0.0000
gender_Male	-0.0045	0.0313	-0.7745	-1.3289	-0.0169	0.0000	0.0000
discharge_disposition_id_6	0.0011	-0.0197	0.4592	0.6655	0.0107	0.0000	0.0000
discharge_disposition_id_22	-0.0233	-2.7176	-0.0397	2.7966	2.1024	0.0000	0.0000
Hidden2.1	0.0000	0.0000	0.0000	0.0000	0.0000	-2.4213	0.3857
Hidden2.2	0.0000	0.0000	0.0000	0.0000	0.0000	-1.0671	1.4849
Hidden2.3	0.0000	0.0000	0.0000	0.0000	0.0000	1.0464	1.0589
Hidden2.4	0.0000	0.0000	0.0000	0.0000	0.0000	0.0924	0.6212
Hidden2.5	0.0000	0.0000	0.0000	0.0000	0.0000	-4.5618	-0.0239

4) *Naïve bayesian classifier*: A NB model was created using Gaussian Naive Bayes, which assumes that the attributes follow a natural distribution.

5) *Multi-Layer perceptron*: We built a MLP network using 18 inputs. The number of neurons in a hidden layer was 5. The function of the neurons was stochastic gradient descent. The maximum number of iterations was 300, and the two outputs were (readmitted < 30 and readmitted > 30). Table V illustrates that result of MLP weight matrix after training.

V. RESULTS AND DISCUSSION

This work utilized various performance measures to compare the studied techniques [31]. Specifically, we relied on accuracy, recall, precision, and F1 scores for this purpose. Those parameters are defined in terms of the true positives (TP), true negatives (TN), false positives (FP), and false negatives (FN) as indicated in equations (1) through (4). TPs are cases in which we predicted yes (they will be readmitted in a month period), and they were really readmitted. TNs are cases in which we predicted no, and they were not readmitted. On the other hand, FPs are cases in which we predicted yes, but they were not actually readmitted; Type I error. Finally, FNs are cases in which we predicted no, but they were actually readmitted; Type II error.

$$\text{Accuracy} = (\text{TP}+\text{TN})/(\text{TP}+\text{FP}+\text{FN}+\text{TN}) \quad (1)$$

$$\text{Recall} = \text{TP}/(\text{TP}+\text{FN}) \quad (2)$$

$$\text{Precision} = \text{TP}/(\text{TP}+\text{FP}) \quad (3)$$

$$\text{F1_score} = 2 * (\text{Recall} * \text{Precision}) / (\text{Recall} + \text{Precision}) \quad (4)$$

Accuracy indicates how often the classifier is correct. The recall is a sensitivity measure (ratio of TPs to the sum of TPs and FNs). It indicates the rate of cases the model predicted the patient will be readmitted in a month period (relative to the number of cases the patient was actually readmitted). The precision measures the rate of cases that the model predicts the patient will be readmitted in a month period correctly compared to total number of cases in which the model predicts the patients will be readmitted. Table VI depicts the values of the performance measures.

As previously noted, we used 10-fold cross validation for the models. Table VII and Fig. 10 depict the training and testing accuracy for each model under 10-fold cross validation.

Finally, Table VIII illustrates the minimum, maximum and mean accuracy for every model. It is clear that SVM achieved the highest accuracy of 0.9522. It was followed by DT, with accuracy of 0.9251, and then MLP with accuracy of 0.8358. The lowest performance was detected for NB classifier and LR analysis, which achieved respectively 0.69069 and 0.6865.

TABLE VI. PERFORMANCE MEASURES FOR THE EMPLOYED TECHNIQUES

Model/ Measures	Accuracy	Recall	Precision	F1_score
Decision Tree	0.878869	0.854745	0.908571	0.876033
Logistic Regression	0.641095	0.626773	0.651013	0.638663
Naïve Bayes	0.638852	0.433511	0.746565	0.548514
Support Vector Machine	0.294630	0.942376	0.911664	0.926765
Multi-Layer Perceptron	0.799910	0.781028	0.815741	0.798007

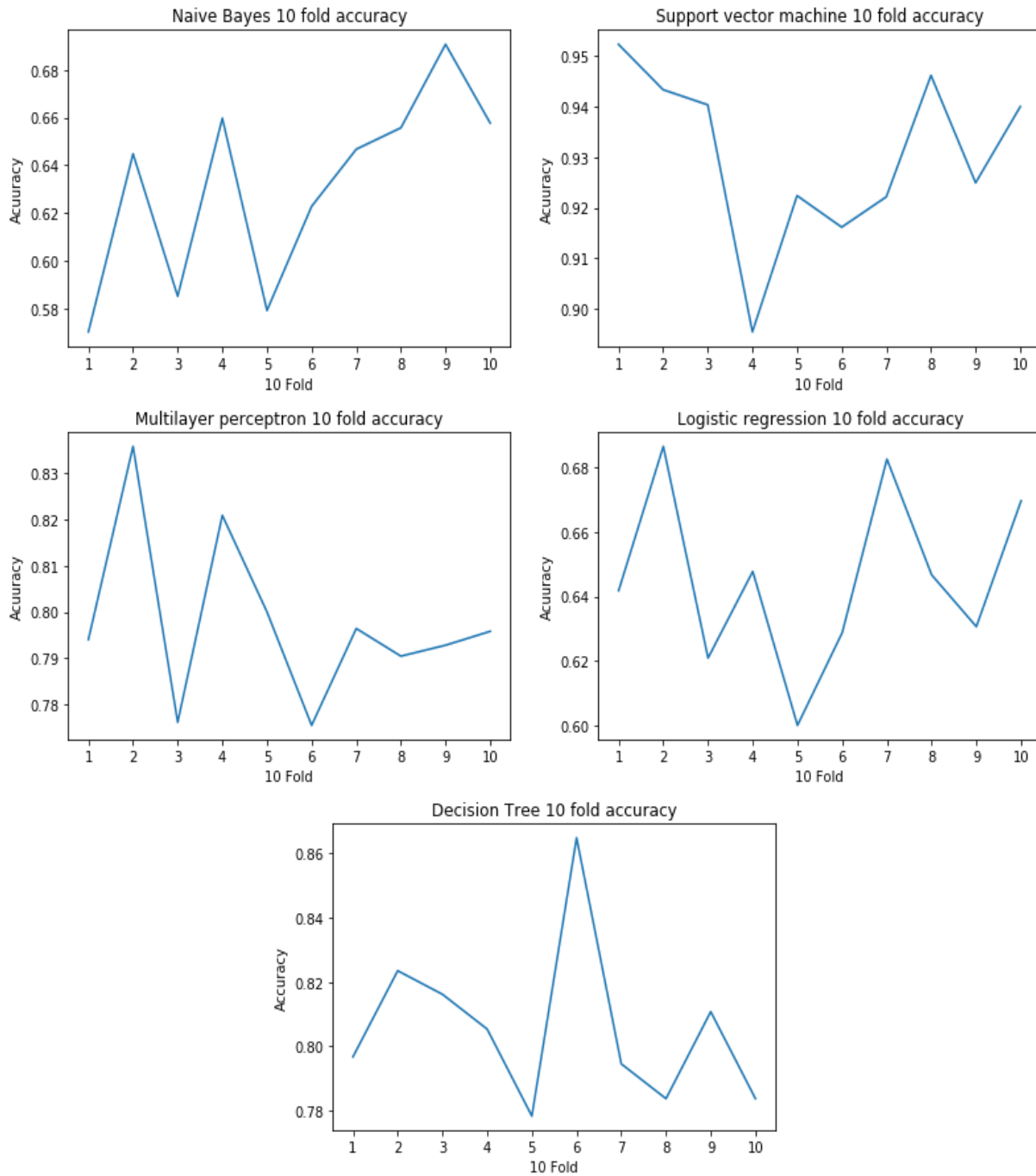


Fig. 10. 10-Fold Cross Validation for Models.

TABLE VII. 10-FOLD CROSS VALIDATION FOR EMPLOYED TECHNIQUES

SVM	CART	NB	LR	MLP
0.952239	0.898507	0.570149	0.641791	0.794030
0.943284	0.901493	0.644776	0.686567	0.835821
0.940299	0.886567	0.585075	0.620896	0.776119
0.895522	0.907463	0.659701	0.647761	0.820896
0.922388	0.853731	0.579104	0.600000	0.800000
0.916168	0.883234	0.622754	0.628743	0.775449
0.922156	0.865269	0.646707	0.682635	0.796407
0.946108	0.925150	0.655689	0.646707	0.790419
0.924925	0.906907	0.690691	0.630631	0.792793
0.939940	0.906907	0.657658	0.669670	0.795796

TABLE VIII. ACCURACY OF EMPLOYED TECHNIQUES

No	Model	Min	Max	Mean
1	Support Vector Machine	0.895522	0.952239	0.930303
2	Decision Tree	0.853731	0.925150	0.893523
3	Multi-Layer Perceptron	0.775449	0.835821	0.797773
4	Naïve Bayes	0.570149	0.690691	0.631230
5	Logistic Regression	0.600000	0.686567	0.645540

VI. CONCLUSION AND FUTURE WORK

This paper presented a comparative study among five machine learning techniques; namely LR, MLP, NB classifier, decision trees, and SVMs; for predicting the likelihood of hospital readmission of diabetes patients. The study relied on real data collected from hospitals in the United States. Based on the study, the SVM provided the best performance. Nevertheless, the study will be extended to compare additional techniques and larger datasets will be considered as well.

REFERENCES

[1] G. Roglic, "Global report on diabetes.," World Heal. Organ., vol. 58, no. 12, pp. 1-88, 2016.

[2] D. Rubin, K. Donnell-Jackson, R. Jhingan, S. Golden, and A. Paranjape, "Early readmission among patients with diabetes: A qualitative assessment of contributing factors," J. Diabetes Complications, vol. 28, no. 6, pp. 869-873, 2014.

[3] I. Kavakiotis, O. Tsave, A. Salifoglou, N. Maglaveras, I. Vlahavas, and I. Chouvarda, "Machine Learning and Data Mining Methods in Diabetes Research," Comput. Struct. Biotechnol. J., vol. 15, pp. 104-116, 2017.

[4] P. Chowriappa, S. Dua, and Y. Todorov, "Machine Learning in Healthcare Informatics," vol. 56, pp. 1-23, 2014.

[5] T. Mitchell, "Machine learning (mcgraw-hill international editions computer science series)," 1997.

[6] E. Bose and K. Radhakrishnan, "Using Unsupervised Machine Learning to Identify Subgroups among Home Health Patients with Heart Failure Using Telehealth," CIN - Comput. Informatics Nurs., vol. 36, no. 5, pp. 242-248, 2018.

[7] L. Kaelbling, A. Littman, and A. Moore, "Reinforcement learning: A survey," J. Artif. Intell. Res., vol. 4, pp. 237-285, 1996.

[8] K. Shailaja, B. Seetharamulu, and M. Jabbar, "Machine Learning in Healthcare: A Review," 2018 Second Int. Conf. Electron. Commun. Aersp. Technol., no. Iceca, pp. 910-914, 2018.

[9] J. Davies and J. Gibbons, "Machine Learning and Software Engineering in Health Informatics," in Proceedings of the First International

Workshop on Realizing AI Synergies in Software Engineering, 2012, pp. 37-41.

[10] R. Bhardwaj, A. Nambiar, and D. Dutta, "A Study of Machine Learning in Healthcare," Proc. - Int. Comput. Softw. Appl. Conf., vol. 2, pp. 236-241, 2017.

[11] A. Asuncion and D. Newman, "UCI Machine Learning Repository," 2007. [Online]. Available: <https://archive.ics.uci.edu/ml/index.php>.

[12] S. B. et al., "Impact of HbA1c measurement on hospital readmission rates: Analysis of 70,000 clinical database patient records," Biomed Res. Int., vol. 2014, 2014.

[13] A. H. Karp, "Using logistic regression to predict customer retention," Proc. Elev. Northeast SAS Users Gr. Conf. <http://www.lexjansen.com/nesug/nesug98/solu/p095.pdf>, 1998.

[14] F. Amato, A. López, E. M. Peña-Méndez, P. Va?hara, A. Hampl, and J. Havel, "Artificial neural networks in medical diagnosis," J. Appl. Biomed., vol. 11, no. 2, pp. 47-58, 2013.

[15] S. F., "Machine-Learning Techniques for Customer Retention: A Comparative Study," Int. J. Adv. Comput. Sci. Appl., vol. 9, no. 2, pp. 273-281, 2018.

[16] N. Jothi, N. Rashid, and W. Husain, "Data Mining in Healthcare - A Review," Procedia Comput. Sci., vol. 72, pp. 306-313, 2015.

[17] D. Sisodia and D. Sisodia, "Prediction of Diabetes using Classification Algorithms," Procedia Comput. Sci., vol. 132, no. Iccids, pp. 1578-1585, 2018.

[18] A. Hazra, S. Kumar, and A. Gupta, "Study and Analysis of Breast Cancer Cell Detection using Naïve Bayes, SVM and Ensemble Algorithms," Int. J. Comput. Appl., vol. 145, no. 2, pp. 39-45, 2016.

[19] E. Holzschuh, "A Decision-Theoretic Generalization of On-Line Learning and an Application to Boosting*," Reports Prog. Phys., vol. 55, no. 7, pp. 1035-1091, 1992.

[20] R. Sharma, V. Sugumaran, H. Kumar, and M. Amarnath, "A comparative study of naive Bayes classifier and Bayes net classifier for fault diagnosis of roller bearing using sound signal," Int. J. Decis. Support Syst., vol. 1, no. 1, p. 115, 2015.

[21] S. Mandal, A. Gupta, A. Mukherjee, and A. Mukherjee, "Heart Disease Diagnosis and Prediction Using Machine Learning and Data Mining Techniques?: A Review," vol. 10, no. 7, pp. 2137-2159, 2017.

[22] N. Nai-Arun and P. Sittidech, "Ensemble Learning Model for Diabetes Classification," Adv. Mater. Res., vol. 931-932, pp. 1427-1431, 2014.

[23] S. Perveen, M. Shahbaz, A. Guergachi, and K. Keshavjee, "Performance Analysis of Data Mining Classification Techniques to Predict Diabetes," Procedia Comput. Sci., vol. 82, no. March, pp. 115-121, 2016.

[24] K. Orabi, Y. Kamal, and T. Rabah, "Early Predictive System for Diabetes Mellitus Disease," vol. 1, pp. 420-427, 2016.

[25] D. Paul, "Analysing Feature Importances for Diabetes Prediction using Machine Learning Debadri," 2018 IEEE 9th Annu. Inf. Technol. Electron. Mob. Commun. Conf., pp. 924-928, 2018.

[26] J. Kerexeta, A. Artetxe, V. Escolar, A. Lozano, and N. Larburu, "Predicting 30-day Readmission in Heart Failure using Machine Learning Techniques," Proc. 11th Int. Jt. Conf. Biomed. Eng. Syst. Technol., vol. 5, no. Biostec, pp. 308-315, 2018.

[27] S. F., "Machine-Learning Techniques for Customer Retention: A Comparative Study," Int. J. Adv. Comput. Sci. Appl., vol. 9, no. 2, pp. 273-281, 2018.

[28] K. Kira and L. A. Rendell, A Practical Approach to Feature Selection. Morgan Kaufmann Publishers, Inc., 1992.

[29] D. W. Opitz, "Feature selection for ensembles," Proc. 16th Natl. Conf. Artif. Intell. AAAI, vol. 16, no. 3, pp. 379-384, 1999.

[30] I. Guyon and A. Elisseeff, "An Introduction to Variable and Feature Selection 1 Introduction," An Introd. to Var. Featur. Sel., vol. 3, pp. 1157-1182, 2003.

[31] M. Sokolova and G. Lapalme, "A systematic analysis of performance measures for classification tasks," Information Processing and Managemet, vol. 45, 2009, pp. 427-437.

A Comparative Analysis of Wavelet Families for the Classification of Finger Motions

Jingwei Too¹, Abdul Rahim Abdullah², Norhashimah Mohd Saad³

Fakulti Kejuruteraan Elektrik, Universiti Teknikal Malaysia Melaka, Melaka, Malaysia^{1,2}

Fakulti Kejuruteraan Elektronik dan Kejuruteraan Komputer
Universiti Teknikal Malaysia Melaka, Melaka, Malaysia³

Abstract—Wavelet transform (WT) has been widely used in biomedical, rehabilitation and engineering applications. Due to the natural characteristic of WT, its performance is mostly depending on the selection of mother wavelet function. A proper mother wavelet ensures the optimum performance; however, the selection of mother wavelet is mostly empirical and varies according to dataset. Hence, this paper aims to investigate the best mother wavelet of discrete wavelet transform (DWT) and wavelet packet transform (WPT) in the classification of different finger motions. In this study, twelve mother wavelets are evaluated for both DWT and WPT. The electromyography (EMG) data of 12 finger motions are acquired from online database. Four useful features are extracted from each recorded EMG signal via DWT and WPT transformation. Afterward, support vector machine (SVM) and linear discriminate analysis (LDA) are employed for performance evaluation. Our experimental results demonstrate Bior3.3 to be the most suitable mother wavelet in DWT. On the other hand, WPT with Bior2.2 overtakes other mother wavelets in the classification of finger motions. The results obtained suggest that Biorthogonal families are more suitable for accurate EMG signals classification.

Keywords—Mother wavelet; discrete wavelet transform; wavelet packet transform; electromyography; classification

I. INTRODUCTION

Electromyography (EMG) has becoming one of the major interest in the rehabilitation areas due to its usefulness in clinical and human machine interface (HMI) applications [1], [2] Advance in HMI raises the efficiency of control system in myoelectric prosthetic control [3]. By using the surface EMG signals recorded from the skin surface, the myoelectric interface based on EMG pattern recognition allows the amputee and patient to gain control on the artificial hand.

The techniques such as signal processing, feature extraction and classification are usually involving in the EMG pattern recognition. One of the methods that have been widely applied in biomedical signal processing is wavelet transform (WT). From the previous works, WT was found to be the best time-frequency method since it often gave promising results in the classification of EMG signals [4], [5]. Unlike short time Fourier transform (STFT), WT offers flexible time and frequency resolution, which leads to high quality signal information. However, the performance of WT differs from the selection of mother wavelet [6]. In one study, Omari et al. [7] classified eight hand motions using discrete wavelet transform (DWT). The authors reported DWT with Symlet 4 achieved the highest accuracy of 95%. For instance, Phinyomark et al. [8]

studied the performance of several mother wavelets in DWT. The authors found that DWT with Daubechies 7 ensured better classification result. On one side, Hariharan et al. [9] made a comparative study of different wavelet families for the classification of wrist motions. The results obtained indicated that wavelet packet transform (WPT) with Coiflet and Biorthogonal families offered superior performance. Another study reported that Daubechies 6 to be the optimal mother wavelet of DWT in EMG pattern recognition [10].

According to literature, it can be inferred that different mother wavelets in WT offered different kind of responses in EMG pattern recognition system. Thus, it is believed that the selection of mother wavelet in WT is remaining insufficient and unclear. In addition, most of the wavelet studies made use of smaller number of motions (less than 10 motions) in the process of evaluations. In fact, a greater number of motion types offers multifunctional myoelectric prosthetic control, which is more preferred by the users [11]. Therefore, in this work, the best mother wavelet of DWT and WPT when discriminating many finger motions are investigated.

In this study, the EMG data of 12 different finger motions are collected form online database. Twelve types of mother wavelets in both DWT and WPT are carefully examined. To obtain the hidden and useful information from the EMG signal, several useful features are extracted from the wavelet coefficients. Finally, the extracting features are fed into the classifiers for performance evaluation, and the best mother wavelet for both DWT and WPT are pointed.

II. MATERIAL AND METHOD

A. EMG Data

In this work, the fourth version of Non-Invasive Adaptive Prosthetic (NinaPro) project is employed [12]. NinaPro project is a publicity access EMG database, which records a huge number of EMG data from multiple subjects. The fourth version of NinaPro database (DB4) comprises of the surface EMG signals recorded from 10 healthy subjects. In DB4, twelve bipolar electrodes were used in the process of recording. Eight electrodes were placed equally around the forearm. Two electrodes were placed on the biceps and triceps brachii muscles. Another two electrodes were placed on the extensor digitorum superficialis and flexor digitorum superficialis muscles. In this study, the surface EMG signals of 12 different finger motions (Exercise A) are utilized. Table I outlines the listed finger motions. In the experiment, each motion was

performed for 5 seconds, followed by a resting state of 3 seconds. Additionally, each motion was repeated for six times, and the EMG signals were sampled at 2 kHz [12]. Furthermore, all the resting phases are removed.

B. System Overview

Fig. 1 demonstrates the flow diagram of proposed EMG pattern recognition system. In the first step, DWT and WPT with 12 different mother wavelets are employed to transform the EMG signals into multiresolution coefficients. Then, four useful features are extracted from each wavelet coefficient to form the feature set. Next, two machine learning algorithms namely support vector machine (SVM) and linear discriminate analysis (LDA) are applied for classification. At the end of the experiment, the best mother wavelet in both DWT and WPT are pointed.

C. Discrete Wavelet Transform

In recent days, discrete wavelet transform (DWT) has becomes popular in rehabilitation and clinical areas. Correspondingly, DWT offers good frequency resolution at low frequency components. On the contrary, good time resolution can be obtained at high frequency components [13]. In wavelet decomposition, DWT decomposes the EMG signal into multiresolution coefficients. The decomposition of DWT involves two digital filters, which are low-pass and high-pass filters. The first decomposition of DWT can be defined as:

$$D[n] = \sum_n x[k] \cdot h[2n - k] \tag{1}$$

$$A[n] = \sum_n x[k] \cdot g[2n - k] \tag{2}$$

where $x[k]$ is the signal, $D[n]$ is the detail and $A[n]$ is referred to approximation. The wavelet decomposition is repeated until the desired level is reached. Within each decomposition, the signal is down-sampled by a factor of 2 [13], [14]. In the past studies, the best DWT wavelet decomposition level to analyze the EMG signals was mostly falling at fourth decomposition level [5], [8], [15]. In this regard, the DWT with fourth decomposition level is used in this work. The sample of DWT with Biorthogonal 3.3 at fourth decomposition level is shown in Fig. 2.

TABLE I. LISTED FINGER MOTIONS

Label	Finger motion task
F1	Index flexion
F2	Index extension
F3	Middle flexion
F4	Middle extension
F5	Ring flexion
F6	Ring extension
F7	Little finger flexion
F8	Little finger extension
F9	Thumb adduction
F10	Thumb abduction
F11	Thumb flexion
F12	Thumb extension

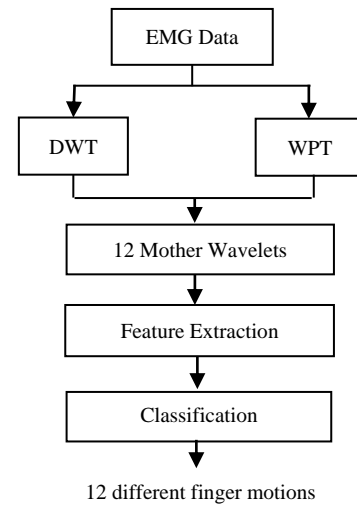


Fig. 1. Proposed Recognition System.

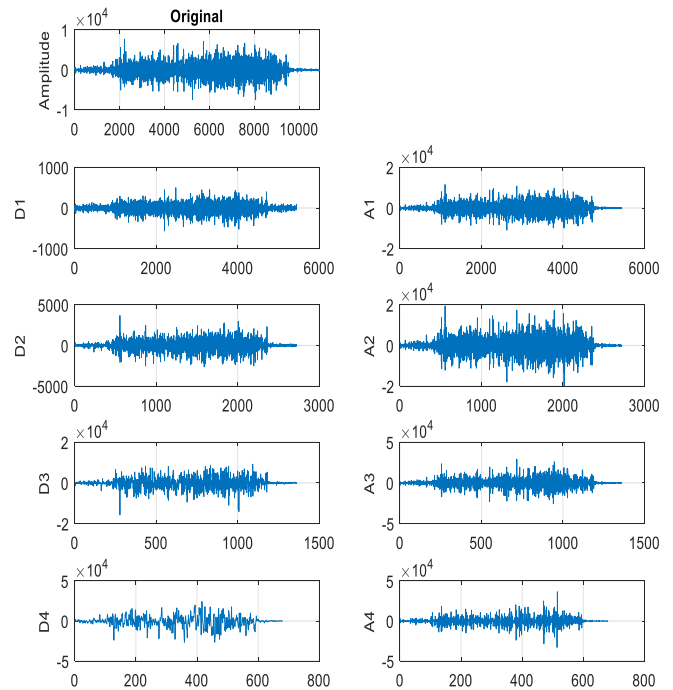


Fig. 2. Wavelet Decomposition of DWT with Biorthogonal 3.3 at Fourth Decomposition Level.

D. Wavelet Packet Transform

Wavelet packet transform (WPT) is one of the powerful pre-processing tools in biomedical signal processing [16]. In WPT, higher frequency component has better time resolution, whereas lower frequency component offers better frequency resolution.

Generally, WPT is also known as a tree of sub-spaces that decomposes the signal into two orthogonal bases [17]. Based on previous works, the best decomposition level is found to be 3 [9], [17]. Fig. 3 demonstrates the wavelet decomposition tree at third decomposition level. At each decomposition level, WPT decomposes the signal into two sub-bands involving the

high and low frequency bands. In decomposition tree, the number of subspaces denotes as j and each of the subspace has its depth i . The wavelet packet decomposition of the parent node (i, j) can be expressed as:

$$\psi_{i+1}^{2^{j+1}}(k) = \sum_n h[n] \cdot \psi_i^j(k - 2^i n) \tag{3}$$

$$\psi_{i+1}^{2^j}(k) = \sum_n g[n] \cdot \psi_i^j(k - 2^i n) \tag{4}$$

where $h[n]$ and $g[n]$ are referred to the high pass and low pass filters, respectively. In this work, WPT at third decomposition level is utilized.

E. Mother Wavelet Selection

Mother wavelet selection is the most critical problem in both DWT and WPT. According to literature, different mother wavelet offers difference performance in different dataset [18], [19]. In fact, a mother wavelet might work properly in dataset A, but not to the dataset B. In this paper, the performance of 12 different mother wavelets for both DWT and WPT are examined. Table II shows the utilized 12 mother wavelets.

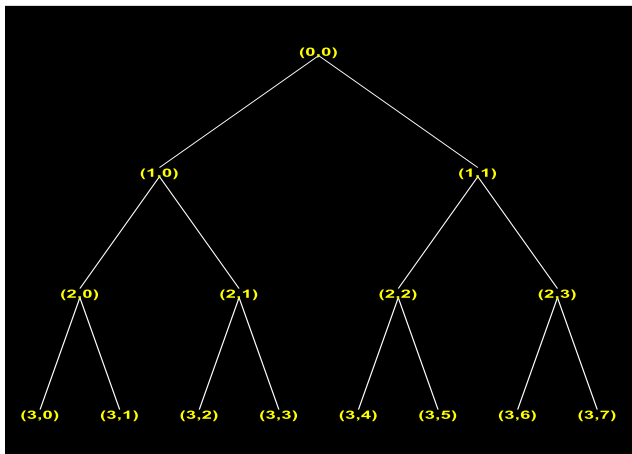


Fig. 3. Wavelet Packet Decomposition Tree at Third Decomposition Level.

TABLE II. TWELVE MOTHER WAVELETS

No.	Mother wavelet	No.	Mother wavelet
1	Biorthogonal 2.2 (Bior2.2)	7	Daubechies 4 (Db4)
2	Biorthogonal 3.3 (Bior3.3)	8	Daubechies 6 (Db6)
3	Biorthogonal 4.4 (Bior4.4)	9	Daubechies 8 (Db8)
4	Coiflet 3 (Coif3)	10	Symlet 4 (Sym4)
5	Coiflet 4 (Coif4)	11	Symlet 6 (Sym6)
6	Coiflet 5 (Coif5)	12	Symlet 8 (Sym8)

F. Feature Extraction

In this study, four popular EMG features namely mean absolute value (MAV), root mean square (RMS), maximum fractal length (MFL) and wavelet energy (E) are utilized.

Mean absolute value (MAV) is a popular feature in the classification of EMG signals. In short, MAV is an average of

the summation of absolute value of EMG signals [5], [20]. Mathematically, MAV can be calculated as:

$$MAV_i = \frac{1}{L} \sum_{n=1}^L |D_{i,n}| \tag{5}$$

where D_i is the coefficient at i frequency band and L is referred to the length of coefficient.

Root mean square (RMS) is one of the famous features that describes the information related to muscle force and activation [21], [22]. RMS can be expressed as:

$$RMS_i = \sqrt{\frac{1}{L} \sum_{n=1}^L D_{i,n}^2} \tag{6}$$

where D_i is the coefficient at i frequency band and L is referred to the length of coefficient.

Maximum fractal length (MFL) measures the low-level muscle activation and it is modified from wavelength and RMS features [23]. In mathematics, MFL can be represented as follows:

$$MFL_i = \log \left(\sqrt{\sum_{n=1}^{L-1} (D_{i,n+1} - D_{i,n})^2} \right) \tag{7}$$

where D_i is the coefficient at i frequency band and L is referred to the length of coefficient.

Wavelet energy (E) of the coefficients in each sub-band represents the energy distribution of EMG signal, and it can be written as [13]:

$$E_i = \frac{1}{L} \sum_{n=1}^L (D_{i,n})^2 \tag{8}$$

where L is the length of the coefficient and D_i is the coefficient at i frequency band.

III. RESULTS AND DISCUSSIONS

In this paper, 12 different mother wavelets in both DWT and WPT are investigated. Remarkably, DWT and WPT transformed the EMG signals into multiresolution coefficients. The features are then extracted from each coefficient to form the feature vector. It is worth noting that the number of extracting features is based on the wavelet decomposition level. DWT at fourth decomposition results in 8 coefficients, thus 384 features (4 features \times 8 coefficients \times 12 channels) are extracted. On the contrary, WPT at third decomposition level produces 14 coefficients. In total, 672 features (4 features \times 14 coefficients \times 12 channels) are extracted from each movement from each subject. Before performance evaluation, the features are normalized in the range between 0 and 1 in order to prevent numerical problem.

Two machine learning algorithms (classifier) namely linear discriminate analysis (LDA) and support vector machine (SVM) with radial basis function are used in performance evaluation. LDA and SVM are chosen due to their promising performances in previous works [24], [25]. For performance evaluation, Ten-fold cross-validation is applied. The data set is

randomly divided into 10 equal parts. Each part is used for testing in succession, while the remaining part is used in training session. The classification results of ten folds are then averaged and recorded.

A. Best Mother Wavelet in DWT

Table III outlines the average class-wise accuracy (classification accuracy of 12 finger motions) of 12 mother wavelets of DWT across 10 subjects. Obviously, LDA showed better average class-wise performance as compared to SVM. Considering the optimal performance, the analysis of mother wavelet in LDA has served as prior. From the results, it can be inferred that the analysis of mother wavelet in DWT is significant important. As can be seen in Table III, each wavelet family offered different kind of classification performance. By using SVM, the best class-wise accuracy is achieved by Coif5 (88.8%). Successively, Bior3.3 achieved the overall best mean class-wise accuracy, 95.23%, followed by Bior2.2, 94.97%. By contrast, the worst performance is obtained by Sym4, 92.99%, followed by Db6, 93.82%. In term of consistency, it is observed that Bior3.3 provided the most consistent and robust result due to smallest standard deviation (SD), 4.11%. On the whole, Bior3.3 is found to be the most suitable mother wavelet function for the classification of 12 different finger motions. In short, Bior3.3 not only offers the best classification performance, but also provides highly consistent result. Hence,

it can be concluded that DWT with Bior3.3 contributes the optimum performance in the classification of finger motions.

B. Best Mother Wavelet in WPT

The experimental results of WPT with 12 different mother wavelets are shown in Table IV. Based on the results obtained, it can be inferred that LDA outperformed SVM in this work. The possible reason might be the normalization of features, thus increasing the linearity of the feature model. From Table IV, each mother wavelet function provided different kind of responses in this work. This phenomenon indicates that the selection of mother wavelet is critically important. By applying SVM, the best mother wavelet in WPT is found to be Coif4, 87.04%, followed by Sym6 and Sym8, 86.78%. By employing LDA, all mother wavelets had their mean class-wise accuracy above 94%. This implies that 12 finger motions have been classified very well. As can be seen in Table IV, Bior2.2 achieved the best recognition rate of 95.64% when LDA is utilized. Sym6 and Sym8 ranked the second best mother wavelets with mean class-wise accuracy of 95.63%. On the other hand, Bior3.3 offered the most consistent result with the smallest standard deviation value, 3.68%. Overall, it is observed that Bior2.2 not only provided the optimum results, but also afforded the consistent performance. Evidently, Bior2.2 is known to be the most suitable mother wavelet in WPT for the classification of finger motions.

TABLE III. AVERAGE CLASS-WISE ACCURACY OF 12 DIFFERENT MOTHER WAVELETS OF DWT ACROSS 10 SUBJECTS

Mother wavelet	Types of classifier	Class-wise accuracy (%)													
		F1	F2	F3	F4	F5	F6	F7	F8	F9	F10	F11	F12	Mean	SD
Bior2.2	LDA	94.05	95.48	95.71	98.33	98.57	98.57	98.33	93.39	84.76	98.33	88.65	95.48	94.97	4.35
	SVM	83.05	88.71	90.65	93.71	92.05	89.76	87.90	91.55	78.52	85.95	76.52	93.21	87.63	5.63
Bior3.3	LDA	95.48	94.29	97.14	98.57	98.57	97.14	100	95.71	86.33	93.57	88.48	97.50	95.23	4.11
	SVM	82.55	89.31	89.23	95.48	92.05	85.83	87.57	93.21	77.56	85.95	77.52	92.14	87.37	5.82
Bior4.4	LDA	96.90	94.40	94.29	98.33	98.57	100	98.33	95.48	80.12	95.24	89.58	95.71	94.75	5.35
	SVM	84.95	91.81	90.65	93.71	94.90	88.69	88.24	92.98	79.71	85.95	76.52	93.21	88.45	5.77
Coif3	LDA	97.14	93.57	97.14	98.33	97.50	100	96.90	95.48	84.75	97.14	83.93	95.71	94.80	5.13
	SVM	83.29	89.81	90.65	93.71	94.90	89.76	88.14	92.98	79.05	85.95	75.33	93.21	88.07	6.13
Coif4	LDA	90.86	93.21	98.57	100	96.90	98.57	98.57	93.15	81.93	95.48	84.62	95.71	93.97	5.70
	SVM	84.71	90.38	92.08	93.71	94.90	88.69	89.67	89.29	78.46	86.95	77.52	92.14	88.21	5.53
Coif5	LDA	95.48	95.48	93.21	100	94.64	98.33	97.14	94.29	81.55	98.57	86.95	97.14	94.40	5.25
	SVM	83.52	91.81	90.65	93.71	94.90	89.76	88.48	92.98	82.25	85.95	78.38	93.21	88.80	5.22
Db4	LDA	94.05	91.79	94.64	98.33	96.90	98.33	95.71	95.71	87.38	96.90	85.74	98.57	94.51	4.22
	SVM	84.71	91.81	92.08	93.71	93.48	88.93	89.90	89.29	78.33	85.95	75.69	92.14	88.00	5.86
Db6	LDA	95.14	90.95	93.71	98.33	96.07	97.14	96.90	94.05	82.54	97.14	86.73	97.14	93.82	4.82
	SVM	86.14	90.38	92.08	93.71	94.90	87.26	90.67	90.71	79.79	86.95	77.52	92.64	88.57	5.37
Db8	LDA	95.14	93.81	100	100	96.07	97.14	97.14	92.86	86.48	98.57	83.36	96.90	94.79	5.14
	SVM	84.29	90.38	89.23	95.14	93.48	87.26	89.57	92.98	81.58	85.95	77.19	92.14	88.27	5.29
Sym4	LDA	92.62	92.14	92.38	96.90	98.57	98.57	98.57	93.39	80.13	95.48	81.83	95.24	92.99	6.11
	SVM	86.14	90.38	92.08	93.71	93.48	87.26	90.33	90.71	79.79	86.95	77.52	92.64	88.42	5.22
Sym6	LDA	96.90	92.64	93.71	96.9	98.57	98.57	98.57	94.82	81.80	98.57	84.73	95.24	94.25	5.55
	SVM	88.14	90.62	92.08	93.71	94.90	87.26	89.24	90.71	79.56	86.95	77.52	92.64	88.61	5.33
Sym8	LDA	96.90	92.64	93.71	96.9	98.57	98.57	98.57	94.82	81.8	98.57	84.73	95.24	94.25	5.55
	SVM	88.14	90.62	92.08	93.71	94.9	87.26	89.24	90.71	79.56	86.95	77.52	92.64	88.61	5.33

TABLE IV. AVERAGE CLASS-WISE ACCURACY OF 12 DIFFERENT MOTHER WAVELETS OF WPT ACROSS 10 SUBJECTS

Mother wavelet	Types of classifier	Class-wise accuracy (%)													
		F1	F2	F3	F4	F5	F6	F7	F8	F9	F10	F11	F12	Average	SD
Bior2.2	LDA	98.57	96.90	94.05	100	98.57	98.57	94.05	94.64	83.63	98.57	91.55	98.57	95.64	4.58
	SVM	83.62	88.98	84.52	92.38	83.48	88.69	85.89	92.38	74.63	85.05	75.17	88.57	85.28	5.72
Bior3.3	LDA	94.90	95.24	96.90	100	94.29	94.82	94.05	100	92.05	95.48	85.80	95.24	94.90	3.68
	SVM	77.86	87.17	85.88	92.05	87.14	90.71	80.48	94.05	71.60	82.96	75.54	86.14	84.30	6.84
Bior4.4	LDA	96.90	95.00	94.05	100	97.14	98.57	97.14	97.14	86.48	98.33	87.29	98.57	95.55	4.35
	SVM	80.14	83.15	83.10	92.38	85.29	90.30	85.48	93.21	86.22	83.86	74.55	91.00	85.72	5.42
Coif3	LDA	90.62	92.38	94.29	100	96.07	98.57	98.57	96.07	88.95	98.57	88.71	98.57	95.12	4.05
	SVM	77.33	84.90	80.46	92.40	87.31	92.62	86.55	92.86	72.03	85.36	74.05	94.40	85.02	7.62
Coif4	LDA	96.90	91.31	95.48	100	98.57	100	94.29	97.14	85.37	98.57	83.26	98.57	94.96	5.57
	SVM	84.81	90.32	81.56	92.74	89.64	91.19	88.71	94.64	83.08	86.31	72.95	88.57	87.04	5.88
Coif5	LDA	98.57	94.05	96.90	100	98.57	97.50	98.57	97.14	88.39	95.48	83.12	98.57	95.57	4.98
	SVM	85.05	88.50	80.13	92.38	89.79	92.62	85.83	93.21	74.92	82.86	75.64	88.98	85.83	6.33
Db4	LDA	92.86	91.90	94.64	100	96.07	100	96.90	98.33	90.83	98.57	85.71	98.57	95.37	4.34
	SVM	83.81	89.21	83.32	92.05	88.81	90.12	89.07	89.29	76.22	82.80	72.13	86.83	85.31	6.01
Db6	LDA	94.90	88.81	94.40	100	96.07	98.57	100	97.14	89.19	97.14	84.93	98.57	94.98	4.86
	SVM	81.07	91.15	82.23	92.40	89.31	91.19	86.50	93.21	84.06	84.88	74.04	89.57	86.63	5.66
Db8	LDA	96.90	93.81	94.40	100	98.57	98.33	94.29	95.71	89.23	98.57	85.26	100	95.42	4.46
	SVM	85.64	88.65	82.46	93.81	92.40	89.23	83.83	93.21	73.03	83.69	77.11	86.67	85.81	6.33
Sym4	LDA	93.71	94.05	97.14	98.00	98.57	98.57	98.57	96.07	92.62	98.33	83.12	98.33	95.59	4.48
	SVM	81.95	88.48	79.89	92.74	89.64	88.93	92.33	94.64	77.46	85.95	75.68	91.07	86.56	6.35
Sym6	LDA	92.98	95.24	97.14	100	97.14	98.57	97.14	97.50	92.62	96.90	83.95	98.33	95.63	4.26
	SVM	84.36	87.58	79.56	92.74	91.31	90.12	89.48	94.64	82.56	84.76	74.64	89.57	86.78	5.81
Sym8	LDA	92.98	95.24	97.14	100	97.14	98.57	97.14	97.50	92.62	96.90	83.95	98.33	95.63	4.26
	SVM	84.36	87.58	79.56	92.74	91.31	90.12	89.48	94.64	82.56	84.76	74.64	89.57	86.78	5.81

IV. CONCLUSION

In this study, the best mother wavelet for DWT and WPT for EMG signals classification is presented. Ultimately, WT with the most suitable mother wavelet affirms the optimum classification performance, which strengthens the recognition rate for the classification of 12 different finger motions. The experimental results illustrated DWT with Bior3.3 was able to provide the highest class-wise accuracy in DB4. On the other side, Bior2.2 is found to be the most suitable mother wavelet in WPT due to its discriminate power in the classification of EMG signals. According to these findings, the best mother wavelet of DWT and WPP were coming from the Biorthogonal families. For such reason, we recommend that Biorthogonal families to be used in WT for the clinical and HMI applications. Future work will be focused on the selection of features in the process of mother wavelet selection, in which the best mother wavelet with the smallest number of features is guaranteed.

ACKNOWLEDGMENT

The authors would like to thank Skim Zamalah UTeM and Ministry of Higher Education (MOHE), Malaysia for funding research under grant GLuar/STEVIA/2016/FKE-CeRIA/100009.

REFERENCES

- [1] N. Nazmi, M. A. Abdul Rahman, S.-I. Yamamoto, S. A. Ahmad, H. Zamzuri, and S. A. Mazlan, "A Review of Classification Techniques of EMG Signals during Isotonic and Isometric Contractions," *Sensors*, vol. 16, no. 8, p. 1304, Aug. 2016.
- [2] M. N. M. Nor, R. Jailani, N. M. Tahir, I. M. Yassin, Z. I. Rizman, and R. Hidayat, "EMG Signals Analysis of BF and RF Muscles In Autism Spectrum Disorder (ASD) During Walking," *Int. J. Adv. Sci. Eng. Inf. Technol.*, vol. 6, no. 5, pp. 793–798, Oct. 2016.
- [3] R. N. Khushaba, A. Al-Timemy, S. Kodagoda, and K. Nazarpour, "Combined influence of forearm orientation and muscular contraction on EMG pattern recognition," *Expert Syst. Appl.*, vol. 61, pp. 154–161, Nov. 2016.
- [4] A. Subasi, "Classification of EMG signals using PSO optimized SVM for diagnosis of neuromuscular disorders," *Comput. Biol. Med.*, vol. 43, no. 5, pp. 576–586, Jun. 2013.

- [5] A. Phinyomark, C. Limsakul, and P. Phukpattaranont, "Application of Wavelet Analysis in EMG Feature Extraction for Pattern Classification," *Meas. Sci. Rev.*, vol. 11, no. 2, pp. 45–52, 2011.
- [6] J. Too, A. R. Abdullah, N. M. Saad, N. M. Ali, and H. Musa, "A Detail Study of Wavelet Families for EMG Pattern Recognition," *Int. J. Electr. Comput. Eng. IJECE*, vol. 8, no. 6, pp. 4221–4229, Dec. 2018.
- [7] F. A. Omari, J. Hui, C. Mei, and G. Liu, "Pattern Recognition of Eight Hand Motions Using Feature Extraction of Forearm EMG Signal," *Proc. Natl. Acad. Sci. India Sect. Phys. Sci.*, vol. 84, no. 3, pp. 473–480, Sep. 2014.
- [8] A. Phinyomark, A. Nuidod, P. Phukpattaranont, and C. Limsakul, "Feature Extraction and Reduction of Wavelet Transform Coefficients for EMG Pattern Classification," *Elektron. Ir Elektrotehnika*, vol. 122, no. 6, pp. 27–32, Jul. 2012.
- [9] M. Hariharan, C. Y. Fook, R. Sindhu, B. Ilias, and S. Yaacob, "A comparative study of wavelet families for classification of wrist motions," *Comput. Electr. Eng.*, vol. 38, no. 6, pp. 1798–1807, Nov. 2012.
- [10] J. Too, A. R. Abdullah, N. Mohd Saad, and W. Tee, "EMG Feature Selection and Classification Using a Pbest-Guide Binary Particle Swarm Optimization," *Computation*, vol. 7, no. 1, p. 12, Mar. 2019.
- [11] M. Atzori et al., "Effect of clinical parameters on the control of myoelectric robotic prosthetic hands," *J. Rehabil. Res. Dev.*, vol. 53, no. 3, pp. 345–358, 2016.
- [12] S. Pizzolato, L. Tagliapietra, M. Cognolato, M. Reggiani, H. Müller, and M. Atzori, "Comparison of six electromyography acquisition setups on hand movement classification tasks," *PLOS ONE*, vol. 12, no. 10, p. e0186132, Oct. 2017.
- [13] E. Gokgoz and A. Subasi, "Comparison of decision tree algorithms for EMG signal classification using DWT," *Biomed. Signal Process. Control*, vol. 18, pp. 138–144, Apr. 2015.
- [14] A. B. M. S. U. Doulah, S. A. Fattah, W. P. Zhu, and M. O. Ahmad, "Wavelet Domain Feature Extraction Scheme Based on Dominant Motor Unit Action Potential of EMG Signal for Neuromuscular Disease Classification," *IEEE Trans. Biomed. Circuits Syst.*, vol. 8, no. 2, pp. 155–164, Apr. 2014.
- [15] R. H. Chowdhury, M. B. I. Reaz, M. A. B. M. Ali, A. A. A. Bakar, K. Chellappan, and T. G. Chang, "Surface electromyography signal processing and classification techniques," *Sensors*, vol. 13, no. 9, pp. 12431–12466, 2013.
- [16] A. Subasi, "Classification of EMG signals using combined features and soft computing techniques," *Appl. Soft Comput.*, vol. 12, no. 8, pp. 2188–2198, Aug. 2012.
- [17] R. N. Khushaba, S. Kodagoda, S. Lal, and G. Dissanayake, "Driver Drowsiness Classification Using Fuzzy Wavelet-Packet-Based Feature-Extraction Algorithm," *IEEE Trans. Biomed. Eng.*, vol. 58, no. 1, pp. 121–131, Jan. 2011.
- [18] J. Rafiee, M. A. Rafiee, N. Prause, and M. P. Schoen, "Wavelet basis functions in biomedical signal processing," *Expert Syst. Appl.*, vol. 38, no. 5, pp. 6190–6201, May 2011.
- [19] N. M. Kakoty, A. Saikia, and S. M. Hazarika, "Exploring a family of wavelet transforms for EMG-based grasp recognition," *Signal Image Video Process.*, vol. 9, no. 3, pp. 553–559, Mar. 2015.
- [20] G. Purushothaman and R. Vikas, "Identification of a feature selection based pattern recognition scheme for finger movement recognition from multichannel EMG signals," *Australas. Phys. Eng. Sci. Med.*, vol. 41, no. 2, pp. 549–559, Jun. 2018.
- [21] K. S. Kim, H. H. Choi, C. S. Moon, and C. W. Mun, "Comparison of k-nearest neighbor, quadratic discriminant and linear discriminant analysis in classification of electromyogram signals based on the wrist-motion directions," *Curr. Appl. Phys.*, vol. 11, no. 3, pp. 740–745, May 2011.
- [22] O. S. Powar, K. Chemmangat, and S. Figarado, "A novel pre-processing procedure for enhanced feature extraction and characterization of electromyogram signals," *Biomed. Signal Process. Control*, vol. 42, pp. 277–286, Apr. 2018.
- [23] A. Phinyomark, P. Phukpattaranont, and C. Limsakul, "Fractal analysis features for weak and single-channel upper-limb EMG signals," *Expert Syst. Appl.*, vol. 39, no. 12, pp. 11156–11163, Sep. 2012.
- [24] P. A. Karthick, D. M. Ghosh, and S. Ramakrishnan, "Surface electromyography based muscle fatigue detection using high-resolution time-frequency methods and machine learning algorithms," *Comput. Methods Programs Biomed.*, vol. 154, no. Supplement C, pp. 45–56, Feb. 2018.
- [25] X. Jiang, L.-K. Merhi, Z. G. Xiao, and C. Menon, "Exploration of Force Myography and surface Electromyography in hand gesture classification," *Med. Eng. Phys.*, vol. 41, pp. 63–73, Mar. 2017.

Comparative Analysis of Cow Disease Diagnosis Expert System using Bayesian Network and Dempster-Shafer Method

Aristoteles¹, Kusuma Adhianto², Rico Andrian³, Yeni Nuhricha Sari⁴
Department of Computer Science^{1,3,4}, Department of Animal Husbandry²
Lampung University, Lampung, Indonesia^{1,2,3,4}

Abstract—Livestock is a source of animal protein that contains essential acids that improve human intelligence and health. Popular livestock in Indonesia is cow. Consumption of meat per capita is increased by 0.1% kg / capita / year. The high demand for beef in Indonesia is due to the increasing of population in Indonesia by 1.49% per year. More than 90% of cows are reared by rural communities with less of knowledge about livestock and have low economic capabilities. In addition, the number of experts or veterinarians are also limited. One of the solutions that can be done to socialize the knowledge of experts or veterinarians is by using expert system. Some methods that can be used in expert systems are Bayesian network and Dempster-Shafer method. The purpose of this research is to analyze the comparison of cow disease diagnosis with bayesian network and Dempster-Shafer method. In order to know which method is better in diagnosing cow disease. The data used is 21 cow diseases with 77 symptoms. Each method is tested with the same 10 cases. The conclusions obtained by Bayesian network and Dempster-Shafer method. Both of methods give the same diagnosis results but with different percentage. The mean value of diagnosis percentage by Dempster-Shafer method is 87,2% while bayesian network method is 75,3%. Thus, it can be said that the Dempster-Shafer method is better at diagnosing cow disease.

Keywords—Expert system; Bayesian network; Dempster-Shafer; cow disease

I. INTRODUCTION

Livestock is a source of animal protein containing essential amino acids that can help improve the degree of intelligence and human health. Also, Livestock have a high selling price. There are many animals that can be used in livestock, such as cows, goats, rabbits and poultry. The quite popular livestock in Indonesia is cow. Because not only beef, but also skin, milk, and cow dung are beneficial to humans.

The high demand for beef in Indonesia is due to the increasing population of Indonesia at 1.49% per year and the consumption of meat per capita increased by 0.1% kg / capita / year. The rate of increase in cow population can not keep pace with population growth and consumption needs [1]. This forced Indonesia to import, both in the form of live cow and meat and offal of cow.

One of the obstacles that can be faced by breeders is cow disease. Disease attacks can disrupt the growth of livestock that will impact on livestock yields [2]. Over 90% of cow are

reared by rural communities with little knowledge of livestock and relatively low economic capabilities [1]. Breeders usually do not examine the diseases that attack livestock thoroughly and handle drug using only by estimates and habits [3]. The process of diagnosing a disease needs an expert experience to get the right conclusions [4]. But, the expert is limited. This is a serious problem for breeders, if they want to cultivate good quality livestock. A solution is needed for these problems.

The One way that can be done to popularize the knowledge of experts or veterinarians is by using an expert system [5]. Expert systems are computer-based applications that adopt knowledge, facts and reasoning techniques obtained from experts in order to solve existing problems [6]. Some methods that can be used in expert systems are the Bayesian network method and the Dempster-Shafer method.

Bayesian Network is a method that shows the probability of relationships between related and unrelated events. The Bayesian network method is built from probabilistic theory and graph theory [7]. Whereas, Dempster-Shafer is a mathematical theory for proof based on belief function and plausible reasoning that is a function of trust and reasonable thinking to combine separate pieces of information or evidence and calculate the likelihood of an event [8]. In expert system development, the Bayesian network and Dempster-Shafer methods are used to calculate the value or percentage of the probability of an event based on the available evidence.

Bayesian network method has been implemented in web-based expert system for diagnosing cow disease. There are 3 diseases that can be diagnosed based on 11 symptoms [9]. Then in 2018 the Dempster-Shafer method is implemented in web-based expert system for diagnosing cow disease with 21 diseases can be diagnosed based on 77 symptoms [10].

In this research, will be built an android-based expert system to diagnose cow disease using Bayesian network method with 21 diseases can be diagnosed based on 77 symptoms. The authors compare cow disease diagnosis expert system using Bayesian Network and Dempster-Shafer method to know which method is better in diagnosing cow disease.

II. LITERATURE REVIEW

A. Expert System

Expert systems are computer-based applications that adopt knowledge, facts, and reasoning techniques obtained from

experts to solve existing problems [6]. In the expert system there is a Knowledge Based and an inference engine. Knowledge Based is a collection of knowledge, facts and rules obtained from experts. Whereas, the inference engine is a method of knowledge-based approach, to study and solve *problems*. So that, conclusions can be drawn based on the data that has been collected [11]. The basic concept of the expert system is shown in Fig. 1, that the user can submit facts to the expert system that consist of knowledge base and inference engine. Facts obtained from users will be matched with knowledge base. After that, the inference engine will give a response to the user in the form of a decision or conclusion [12].

The expert system consists of two parts: the development environment which is used to incorporate knowledge into the expert system and the consultation environment which is used by the user to gain expert knowledge [12]. The structure and components of the expert system are shown in Fig. 2 [13] in [4].

The characteristic of expert system are have a reliable information facility, easy to modify, can be used in various types of computers, have the ability to learn to adapt [13] in [4].

The main objective of expert development is to distribute expert's knowledge and experience into computer systems [14]. Expert systems are applied to support various issues. The function of the expert system is as a clever assistant who can represent the expertise of experts in solving problems [15]. So, it is expected to increase productivity and ease of access to expert knowledge.

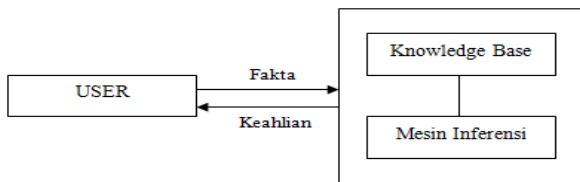


Fig. 1. Basic Concepts of Expert Systems.

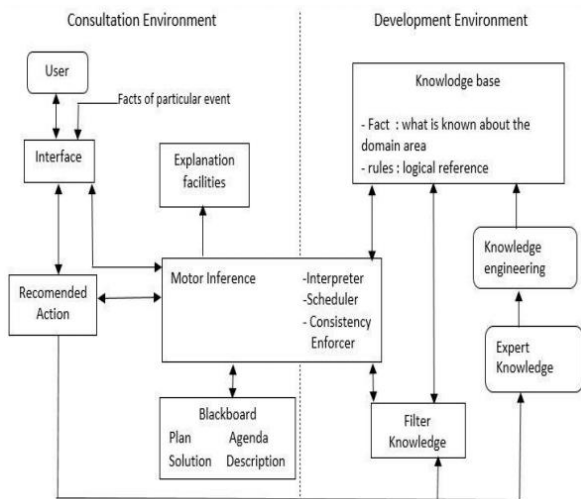


Fig. 2. The Structure and Components of the Expert System.

B. Bayes Theorem

The approach used in bayesian networks is the Bayes theorem which is an approach to uncertainty measured by probability. Bayes theorem is a conditional probability denoted by $P(H | E)$ as for Bayes's theorem formula [6], namely:

$$P(H|E) = \frac{P(E|H)P(H)}{P(E)} \quad (1)$$

Description:

- $P(H)$: probability of hypothesis H
- $P(E)$: probability of evidence E
- $P(H \cap E)$: probability of occurrence of H and E simultaneously
- $P(H | E)$: probability H hypothesis occurs when evidence E occurs
- $P(E | H)$: the probability of the appearance of evidence E, if the hypothesis H occurs.

C. Bayesian Network

Bayesian networks is method that used to connect interrelated and unrelated events or variables. The Bayesian network method is built from probabilistic theory and graph theory. There are two main parts of the bayesian network namely the graph structure and set parameters. Structural time represent qualitatively knowledge or data. Graph structure is called Directed Acyclic Graph (DAG) which consists of nodes and edges. Nodes is used to represent random variable and edge is used to represent caused-effect relationships between connected variables. Whereas, the set parameter is the number of prior probably or the degree of trust of each variable. The set of parameters to represent knowledge quantitatively [7] in [16]. An example of a DAG is shown in Fig. 3 [17].

Fig. 3 is an overview of the bayesian network structure consisting of nodes $(N) = \{A, B, C\}$ and edge $(E) = \{(B, A), (B, C)\}$. Nodes A and C are children that are given a condition. Whereas, node B is the parent that is used as a condition. Steps for implementing the bayesian network are:

1) *Building bayesian network structure*: The bayesian network structure consists of symptom and cow disease data which is represented by graph structure.

2) *Determine parameters*: Parameter value is the prior probability value given by the expert based on the likelihood of the occurrence of the disease based on the symptoms that appear.

3) *Making Conditional Probability Table (CPT)*: CPT is probability of an event B if it is known that event A has occurred. So, it is denoted by $P(B | A)$. CPT is also an opportunity form of various symptoms and forms in the form of tables with positive and negative values. Example of CPT is shown in Table I.

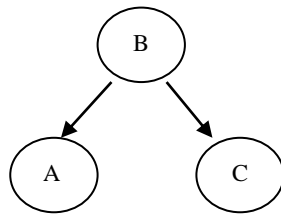


Fig. 3. Directed Acyclic Graph Example.

TABLE I. EXAMPLE OF CPT

Symptoms		Anthrax	
		Positive	Negative
Fever	Positive		
	Negative		

The following is an explanation of each possibility of CPT:

- Positive symptoms and positive disease, for example cow fever and anthrax. This value is called the present value.
- Negative symptoms and positive disease, meaning not cow fever but anthrax. This value is called the present2 value.
- Positive symptoms and negative disease, meaning cow fever but not anthrax. This value is called the absent value.
- Negative symptoms and negative illness, meaning that the cow does not have fever and is not affected by anthrax. This value is called the absent2 value.

4) *Making Join Probability Distribution (JPD)*: JPD is the value of the chance of occurrence that occurs simultaneously for all combinations of values contained in each of the symptoms caused. JPD can be calculated by multiplying the CPT value by the prior value. So the equation is:

$$JPD \text{ present} = P(A \cap B) = P(B|A)P(A) \quad (2)$$

$$JPD \text{ absent} = P(B|A)P(A) \quad (3)$$

JPD present is the result of the multiplication between the present value and the prior value. And, JPD absent is the result of multiplying the absent values with the prior value.

5) *Calculate posterior probability*: Posterior Value Probability is used to calculate the probability value of a symptom occurrence. Posterior values are calculated using the JPD value previously obtained. The form of the equation is:

$$P(A|B) = \frac{P(A \cap B)}{P(B)} \quad (4)$$

$$P(A|B) = \frac{P(B|A)P(A)}{P(B|A)P(A) + P(B|A)P(A)} \quad (5)$$

Or with the following formula:

$$P(\text{Posterior symptoms}) = \frac{JPD_{\text{present}}}{JPD_{\text{present}} + JPD_{\text{absent}}} \quad (6)$$

6) *Probability inference*: Probability inference is to calculate the posterior probability value of each symptom that

is adjusted to the bayesian network structure and the inference method. The result value from probability inference is the value used to indicate the percentage of possible diseases that attack cow. The form of the equation is:

$$P(\text{Disease} | \text{Symptoms of disease}) = \frac{\sum_{i=1}^n P(\text{Posterior gejala})}{n} \times 100\% \quad (7)$$

Where n is the number of symptoms and n Symptoms 0 [14] in [16].

D. Dempster-Shafer

Dempster-Shafer is introduced for the first time by Arthur P. Dempster and in 1976 Glenn Shafer published the Dempster theory in a book entitled Mathematical Theory Of Evident. Dempster-Shafer is a mathematical theory for proof based on belief function and plausible reasoning, which is a function of trust and thought that makes sense, to combine separate pieces of information or evidence, to calculate the probability of an event [8]. The rules used to overcome a number of evidence or evidence are known as Dempster's Rule of Combination. The form of the equation is:

$$(m_1 \oplus m_2)(A) = 0 \quad (8)$$

$$(m_1 \oplus m_2)(A) = \frac{1}{1-K} \sum_{B \cap C = A} m_1(B)m_2(C) \quad (9)$$

where

$$K = \sum_{B \cap C = \emptyset} m_1(B)m_2(C) \quad (10)$$

$$m(A), m_1(B), m_2(C) \rightarrow [0, 1] A \neq \emptyset \quad (11)$$

Description

m = Density Value (Belief)

ABC = Evidence Set

\emptyset = Empty Set

E. Cow Diseases

Cow disease can be caused by virus, bacteria, Parasitees and mycorrhea. In this study 21 diseases that can be diagnosed are caused by bacteria, Parasitees, and mycorrhea. The number of symptoms in the expert system application are 77 symptoms which are divided into ten categories: Body Condition, Behavior, Udder or Milk Bag, Milk, Skin, Eyes, Urine, Stool, and Swelling. The list of cow diseases is shown in Table II. Following is a list of symptoms by category [18]:

- Body condition, consisting of 19 symptoms: fever (G001), paralysis (G002), weakness (G003), weight loss or being thin (G004), uneven body heat (G005), trembling thighs (G006), no rumination (mastication) (G007), flatulence (G008), blood coming out of the anus, mouth, and nostrils (G009), anus temperature rise (G010), shortness of breath (G011), stiffness around the infection (G012), difficulty swallowing (G013), experiencing spasms (G014), dehydration (G015), breath with butyric acid (wry) (G016), inhibited calf growth (G017), rapid fatigue (G018) and discharge from the nose and eyes (G019).

- Behavior, consisting of 11 symptoms namely depression or lethargy (G020), restlessness when chewing (G021), gore hard objects around it (G022), decreased or lost appetite (G023), increased appetite G024, anxiety (G025), cough (G026), cow standing with the distance of the back hind widened (G027), breathing fast (G028), animal walking not stiff (staggering) (G029) and circling (G030).
- Milk bag (udder), consisting of 5 symptoms: decreased or stopped milk production (G031), dry milk bag (G032), swelling of the udder and putting (G033), pain arises when milk is milked (G034) and inflammation in the bag milk (G035).
- Milk, consisting of 3 symptoms: yellow milk and lumpy milk (G036), red milk (G037) and grayish white milk to yellow, opaque and thickened (G038).
- Skin, consisting of 16 symptoms, which are dry, thick, hard scab or scab (scab) with irregular edges and itching (G039), skin abnormalities occur on the face and neck (G040), broken hair or fall out (G041) , visible thick, round, protruding lesions with clear boundaries, grayish white color (G042), hair standing and looking dull (G043), thin and yellowing skin (G044), baldness in the skin (G045), reddish skin (G046), crusty skin (G047), skin feels more oily (G048), skin abnormalities in the nose and mouth snout, around the eyes, ears, lower body, base of the tail, neck along the back and legs (G049), animals always cuddle and rub against other objects or biting the itchy body parts (G050), sores on the skin covered by scab and looks thick (G051), skin blisters in the form of small blisters then become large wounds (G052), these wounds are often found in the upper part of the neck, area hump, waving, shoulder, seki tar eyes and feet (G053) and hives (G054).
- Eyes, consisting of 6 symptoms: red eyes (G055), moist eyes (G056), eyes often closed (G057), tears (G058), pupil narrowing (G059) and turbidity in the cornea (G060).
- Urine, consisting of 3 symptoms: urine becomes dark red or almost black (G061), blood mixed urine (G062) and blood red urine (G063).
- Feces, consisting of 3 symptoms, soft and dilute stool (G064), diarrhea (G065) and worm eggs in feces (G066).
- Swelling, consisting of 8 symptoms, namely swelling in the neck, chest, side of the stomach, waist and external genitals (G067), swelling in the muscles of the shoulder and thighs (G068), swollen or enlarged lymph nodes (G069) , in the swollen part it feels soft, contains fluid, heat and sounds crackling (G070), swelling is seen on the head, lower chest and legs or base of the tail (G071), swollen lymph glands (G072), stomach enlargement and pain (G073), and swelling between the angle of the chin and lower abdomen (G074).

- Fertility, consisting of 3 symptoms: miscarriage up to 3 times at 5-8 months of gestation (G075), fetal fluid that comes out during a murky miscarriage (G076) and temporary or permanent infertility (G077).

TABLE II. COW DISEASE LIST

No.	Disease Name	Disease Code	Cause
1	Anthraks	P001	Bacteri
2	Black Leg	P002	Bacteri
3	Brucellosis	P003	Bacteri
4	Dermatophilosis	P004	Bacteri
5	Leptospirosis	P005	Bacteri
6	Mastitis	P006	Bacteri
7	Paratuberkulosis	P007	Bacteri
8	Pink Eye	P008	Bacteri
9	Salmonellosis	P009	Bacteri
10	Septicemia epizootica	P010	Bacteri
11	Tetanus	P011	Bacteri
12	Tuberculosis	P012	Bacteri
13	Mastitis Mikotik	P013	Fungi
14	Ringworm	P014	Fungi
15	Ascariasis	P015	Parasite
16	Babesiosi	P016	Parasite
17	Demodecosis	P017	Parasite
18	Fasciolosis	P018	Parasite
19	Kaskado	P019	Parasite
20	Myasis	P020	Parasite
21	Surra	P021	Parasite

III. SYSTEM DESIGN

A. Use Case Diagram

Use case diagram is used to interpret the user interface functions. Use case diagram of expert system diagnosis of cow disease consists of 6 activities shown in Fig. 4.

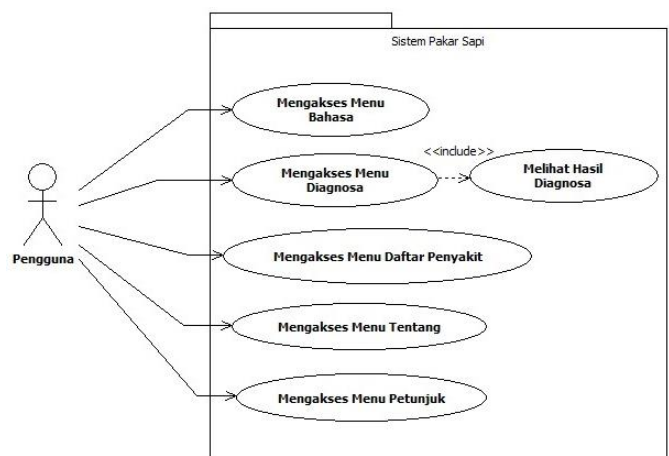


Fig. 4. Use Case Diagram of Cow Expert System.

Fig. 4 illustrates that the actor that is user has five activities that can be done, such as accessing the language menu, diagnosing the disease and seeing the results of the diagnosis, viewing the disease list information, accessing the menu and the instructions menu.

B. Diagnosis and Calculation of Bayesian Network Method

The first diagnosis and calculation is using the Bayesian network method. The following is an example of the calculation.

Known, a cow experiences the following Symptoms:

- Having stiffness around the infection (G012)
- Experience spasms (G014)
- Restless(G025)

Based on these symptoms, it is known that diseases that might attack cattle are Tetanus, Surra and Myasis. The calculation process is as follows:

1) *Disease 1:* Disease 1 is Tetanus. From the symptoms that are known, the three namely G012, G014, and G025 are symptoms of Tetanus. Following are the values of each Symptoms:

Table III is a list of prior Symptoms of cow disease. After the prior value is determined, then making CPT as shown in Table IV.

Table IV is a list of present and absent scores for each Symptoms for Tetanus. The present2 value is obtained from the result of a reduction of 1 with the present value. And the absent2 value is obtained from the results of a reduction of 1 with an absent value. After making CPT, then make JPD as shown in Table V.

Table V is a list of JPD values for Tetanus. JPD values are obtained using Equation (2) and Equation (3). The JPD value for present and present2 is obtained by multiplying the present CPT value and the present CPT by the prior value. Likewise, for the absent and JPD absent2 JPD values are obtained by multiplying the absent and CPT absent CPT values by the results of 1- prior values.

Then calculate Posterior Value as shown in Table VI which is a list of Posterior Value Symptoms of Tetanus. Posterior Value is obtained using Equation (6). The final step is to do probability inference by calculating the average Posterior Value Symptoms of Tetanus using Equation (7) as follows:

$$P(\text{Tetanus} | G012, G014, G025)$$

$$= \frac{0,727273 + 0,727273 + 0,724138}{3} \times 100 = 72,62\%$$

So, the possibility of a cow being affected by Tetanus based on the Symptoms of Having stiffness around the infection, Experience spasms, and Restless is 72.62%.

2) *Disease 2:* Disease 2 is Surra's disease. From the symptoms that are known, two of them include Symptoms of Surra disease, G012 and G014. The following is the calculation process:

Table VII is a list of CPT values for Surra disease. Table VIII is a list of values for JPD Surra and Table IX is a list of Posterior Value Symptoms of Surra.

TABLE III. LIST OF PRIOR SYMPTOMS

Symptoms	Prior Value
Having stiffness around the infection	0,4
Experience spasms	0,5
Restless	0,6

TABLE IV. LIST OF CPT DISEASE 1

Symptoms	Tetanus		
	Positive	Negative	
Having stiffness around the infection	Positive	0,8	0,2
	Negative	1-0,8 = 0,2	1-0,2 = 0,8
Experience spasms	Positive	0,8	0,3
	Negative	0,2	0,7
Restless	Positive	0,7	0,4
	Negative	0,3	0,6

TABLE V. LIST OF JPD DISEASES 1

Symptoms	Tetanus		
	Positive	Negative	
Having stiffness around the infection	Positive	0,8x0,4 = 0,32	0,2x0,6 = 0,12
	Negative	0,2x0,4 = 0,08	0,8x0,6 = 0,48
Experience spasms	Positive	0,4	0,15
	Negative	0,1	0,35
Restless	Positive	0,42	0,16
	Negative	0,18	0,24

TABLE VI. LIST OF POSTERIOR SYMPTOMS DISEASE 1

Symptoms	Posterior Value
Having stiffness around the infection	0,32/(0,32+0,12)= 0,727273
Experience spasms	0,727273
Restless	0,724138

TABLE VII. LIST OF CPT DISEASE 2

Symptoms	Surra		
	Positive	Negative	
Having stiffness around the infection	Positive	0,8	0,2
	Negative	0,2	0,8
Experience spasms	Positive	0,7	0,3
	Negative	0,3	0,7

TABLE VIII. LIST OF JPD DISEASE 2

Symptoms	Surra		
	Positive	Negative	
Having stiffness around the infection	Positive	0,32	0,12
	Negative	0,08	0,48
Experience spasms	Positive	0,35	0,15
	Negative	0,15	0,35

The following are probability inferences for Surra Disease:

$$P(\text{Surra}|\text{G012},\text{G014}) = \frac{0,727273+0,7}{2} \times 100 = 71,36\%$$

So, it's possible that a cow with Disease Surra based on Symptoms of Having Stiffness around the infection and Experience spasms is 71.36%.

3) *Disease 3*: Disease 3 is Disease Myasis. From the symptoms that are known to include one of the symptoms of myasis disease, G025. The following is the calculation process:

Table X is a list of CPT Disease Myasis values. Table XI is a list of JPD Disease Myasis and values. Table XII is a list of Myasis Posterior Value Symptoms Disease.

Here is the probability inference for Disease Myasis:

$$P(\text{Myasis}|\text{G025}) = \frac{0,642857}{1} \times 100 = 64,29\%$$

So, the possibility of a cow with Disease Myasis based on Restless cows is 64.29%.

So, if the known symptoms are having stiffness around the infection, experience spasms, and restless then the results will be displayed by the expert system with the Bayesian network method, sequentially from the possibility of a high disease is Tetanus with a probability of 72.62%, Surra 71, 36%, and Myasis 64.29%. The percentage value is influenced by the prior value and the present value of each Symptoms.

C. Diagnosis and Calculation of the Dempster-Shafer Method

The first diagnosis and calculation is using the Dempster-Shafer method. The following is given an example of the calculation. It is known, a cow experiences the following Symptoms:

- Having stiffness around the infection (G012)
- Experience spasms (G014)
- Restless(G025)

1) *Symptoms 1*: Having stiffness around the infection is a symptom of Disease Tetanus (P011) and Disease Surra (P021). With the value "basic probability assignment" (bpa) that is 0.4. Then:

$$m_1\{P011, P021\}=0,4$$

$$m_1\{\theta\}=(1-m_1\{P011, P021\})=1-0,4= 0,6$$

2) *Symptoms 2*: Experience spasms are Symptoms of Disease Tetanus (P011) and Disease Surra (P021) with a value (bpa) of 0.5. Then:

$$m_2\{P011, P021\}=0,5$$

$$m_2\{\theta\}=0,5$$

With these new Symptoms (m2), a new bpa value for several combinations (m3) is calculated. M3 combination rules can be seen in Table XIII.

TABLE IX. LIST OF POSTERIOR SYMPTOMS DISEASE 2

Symptoms	Posterior Value
Having stiffness around the infection	0,727273
Experience spasms	0,7

TABLE X. LIST OF CPT DISEASE 3

Symptoms	Myasis		
	Positive	Negative	
Restless	Positive	0,6	0,5
	Negative	0,4	0,5

TABLE XI. LIST OF JPD DISEASE 3

Symptoms	Myasis		
	Positive	Negative	
Restless	Positive	0,36	0,2
	Negative	0,24	0,2

TABLE XII. LIST OF POSTERIOR SYMPTOMS DISEASE 3

Symptoms	Posterior Value
Restless	0,642857

TABLE XIII. COMBINATION OF SYMPTOMS 1 AND SYMPTOMS 2

	$m_2\{P011, P021\} 0,5$	$m_2\{\theta\} 0,5$
$m_1\{P011, P021\} 0,4$	$m_3\{P011, P021\} 0,2$	$m_3\{P011, P021\} 0,2$
$m_1\{\theta\} 0,6$	$m_3\{P011, P021\} 0,3$	$m_3\{\theta\} 0,3$

Then the combination between m1 and m2 is calculated as follows:

$$m_3\{P011, P021\} = \frac{0,2+0,2+0,3}{1-0} = 0,7$$

$$m_3\{\theta\} = \frac{0,3}{1-0} = 0,3$$

3) *Symptoms 3*: Restless is a Symptoms of Disease Tetanus (P011) and Surra (P020) with bpa which is 0.6 then:

$$m_4\{P011, P020\}=0,6$$

$$m_4\{\theta\}=0,4$$

With these new Symptoms (m4), new bpa values for several combinations (m5) are calculated. The combination rule m5 can be seen in Table XIV.

Then the combination between m3 and m4 is calculated as follows:

$$m_5\{P011\} = \frac{0,42}{1-0} = 0,42$$

$$m_5\{P011, P021\} = \frac{0,28}{1-0} = 0,28$$

$$m_5\{P011, P020\} = \frac{0,18}{1-0} = 0,18$$

$$m_5\{\theta\} = \frac{0,12}{1-0} = 0,12$$

TABLE XIV. COMBINATION OF SYMPTOMS 1, SYMPTOMS 2 AND SYMPTOMS 3

	$m_4 \{P011, P020\} 0,6$	$m_4 \{\theta\} 0,4$
$m_3 \{P011, P021\} 0,7$	$m_5 \{P011\} 0,42$	$m_5 \{P011, P021\} 0,28$
$m_3 \{\theta\} 0,3$	$m_5 \{P011, P020\} 0,18$	$m_5 \{\theta\} 0,12$

TABLE XV. FINAL RESULT

No.	Disease	bpa	bpa in percent
1	Tetanus	0,42	42%
2	Tetanus Surra	0,28	28%
3	Tetanus Myiasis	0,18	18%

The final result can be seen in Table XV. The highest bpa value is $m_5 \{P011\}$ which is 0.42 which means the highest probability of Disease with Symptoms Having stiffness around the infection, Experience spasms, and Restless is Tetanus (P011). So, the percentage value is affected by many symptoms that intersect between other diseases.

IV. TESTING AND RESULTS

Expert system for diagnosing cow disease with the Bayesian network method built on Android. Whereas, the expert system of diagnosing cow disease with the Dempster-Shafer method was built based on the web. The application of cow expert system with bayesian network method is shown in Fig. 5 and 6.

And, the application of cow expert system with the Dempster-Shafer method is shown in Fig. 7 and 8.

Fig. 5 and 7 are pages that list the symptoms of cow disease which can be chosen by checking or symptomatic symptoms. Whereas, Fig 6 is a diagnostic result page with bayesian network (BN) method and Fig. 8 is a diagnosis result page using the Dempster-Shafer (DS) method.

Tests were carried out to compare the diagnosis results of expert systems using the Bayesian network method with the results of expert system diagnostics using the Dempster-Shafer method. Each method will be tested with the same 10 cases. Comparison of diagnostic results is shown in Table XVI.

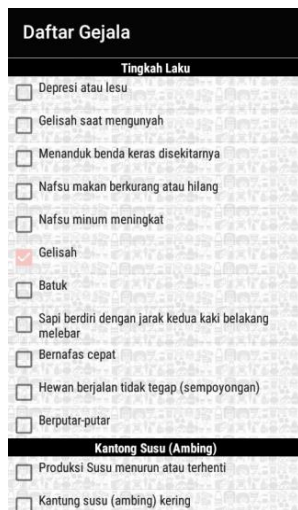


Fig. 5. BN Diagnosis Page.



Fig. 6. BN Diagnosis Result Page.



Fig. 7. DS Diagnosis Page.

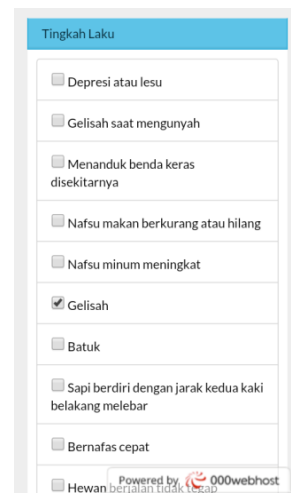


Fig. 8. DS Diagnosis Result Page.

To analyze the percentage of the test results is used the percentage of disease interval obtained from the following equation:

$$I = \frac{100\%}{K} \quad (12)$$

$$I = \frac{100\%}{5} = 20\% \quad (13)$$

Where, I = Interval, K = Kategori Interval.

The percentage interval in this study is 20%. Table of frequency of diseases is shown in Table XVII.

TABLE XVI. COMPARISON OF DIAGNOSIS RESULTS

No.	Case / Symptoms	Bayesian Network Method	Dempster-Shafer Method
1	G001, G004, G020, G023, G039, G069	Dermatophilosis 69,43%	Dermatophilosis 94,22%
2	G001, G003, G020, G023, G032, G036, G055, G061, G065, G075	Leptospirosis 70,50%	Leptospirosis 97,15%
3	G001, G020, G023, G031, G064, G065, G075	Salmonellosis 65,68%	Salmonellosis 59,96%
4	G004, G015, G016, G017, G020, G023, G043, G065, G066	Ascariasis 77,53%	Ascariasis 99,51%
5	G012, G014, G025	Tetanus 72,62%	Tetanus 42%
6	G001, G003, G005, G006, G007, G008, G009, G021, G022, G023, G031, G062, G067	Anthraks 77,91%	Anthraks 99,93%
7	G031, G075, G076, G077	Brucellosis 71,01%	Brucellosis 88%
8	G056, G057, G058, G059, G060	Pink Eye 85,09%	Pink Eye 96,88%
9	G045, G046, G047, G048, G049, G050, G054	Demodecosis 78,38%	Demodecosis 96,22%
10	G002, G010, G020, G068, G070	Black Leg 85,17%	Black Leg 98,08%
Average percentage of diagnosis		75,3%	87,2%

TABLE XVII. DISEASE FREQUENCY

Percentage of disease	Frequency of disease	
	Bayesian Network Method	Dempster-Shafer Method
0% - 19.99%	0	0
20% - 39.99%	0	0
40% - 59.99%	2	0
60% - 79.99%	0	8
80% - 100%	8	2

Results are:

A. Bayesian Network Method

The highest percentage value is 85.17% (Black Leg) and the lowest percentage value is 65.68% (Salmonellosis). The average percentage of diagnoses obtained is 75.3%. At intervals of 60%-79.99% there are 8 diseases. And at intervals of 80%-100% there are 2 diseases namely Pink Eye (85,09%) and Black Leg (85,17%).

B. Dempster-Shafer Method

The highest percentage value is 99.93% (Anthrax) and the lowest percentage value is 42% (Tetanus). The average percentage of diagnoses obtained was 87.2%. At intervals of 40% -59.99% there are 2 diseases, namely, Tetanus (42%) and Salmonellosis (59.96%). And at intervals of 80% -100% there are 8 diseases. Tetanus and Salmonellosis have the lowest percentage because all the symptoms of the disease intersect with other diseases.

V. CONCLUSION

Based on the results of the study, it can be concluded that Bayesian network method and Dempster-Shafer method can be implemented into expert systems. The number of diseases and symptoms that can be diagnosed is more than in previous research, from 3 diseases based on 11 symptoms to 7 diseases based on 77 symptoms. The Bayesian network and Dempster-Shafer methods provide the same disease diagnosis results but with different percentages. The average percentage of diagnosis results with Dempster-Shafer (87.2%) was higher than the percentage of diagnoses with bayesian network (75.3%). So, it can be said that the Dempster-Shafer method is better than the bayesian network method. Based on the 10 cases tested, the results of diagnosis of 8 diseases are higher compared to the percentage value using bayesian network. And 2 other diseases with Dempster-Shafer are smaller than the percentage value with the Bayesian network. The percentage value with bayesian network is influenced by the prior value and the present value of each symptom. Meanwhile, the percentage value with Dempster-Shafer is influenced by the number of symptoms that intersect between other diseases.

REFERENCES

- [1] Rianto Edy and Purbowati Endang, *Complete Guide to Beef Cattle*. Jakarta: Penebar Swadaya, 2011.
- [2] Tallulembang Tatik Melinda and Manggau Fransiskus Xaverius, "Design of Expert System for Diagnosing Cow Disease at The Merauke District Livestock Service Office". *Jurnal Ilmiah Mustek Anim Ha*, Vol.2, No. 2:125-134, 2013.
- [3] Budianto Alexius Endy, "The Application of The Expert System Using Backward Chaining Method for Analyzing Livestock Diseases". *SMARTICS Journal*, Vol.1, No.1:33-35, 2015.
- [4] Aristoteles, Fuljana Mita, Prasetyo Joko, and Muludi Kurnia, "Expert System of Chili Plant Disease Diagnosis using Forward Chaining Method on Android". (IJACSA) International Journal of Advanced Computer Science and Applications, Vol. 8, No. 11, 2017.
- [5] Dewi Indriana Candra, Soebroto Arief Andy and Furqon M. Tanzil, "Expert System of Diagnosing Beef Cattle Disease by Naive Bayes Method". *Journal of Environmental Engineerong & Sustainable Technology*, Vol. 02, No. 2:72-781, 2015.
- [6] Sutojo T, Edy M, and Vincent S, *Artificial Intelligence*. Yogyakarta: Andi, 2011.

- [7] Meigarani Indrayani, Setiawan Wawan, and Riza Lala Setem, "Use of The Bayesian Network Method in Expert System for Diagnosing Leukimia". Jurnal Universitas Pendidikan Indonesia. Bandung, 2010.
- [8] Wahyuni Elyza Gustri and Prijodiproji Widodo, "Prototype Expert System to Detect The Risk Level of Colronary Heart Disease by Dempster-Shafer Method". Jurnal IJCCS, Yogyakarta:UGM, Vol. 7, No. 2:133-144, 2013.
- [9] Tinaliah, "Expert System Application for Diagnosing Cow Disease with Bayesian Network" . Jurnal Ilmiah SISFOTENIKA, Vol. 5, No. 1:13-24, 2015.
- [10] Prasetyo Agung, "Web-Based Cow Disease Diagnosis Expert System Using Dempster-Shafer Method", unpublished.
- [11] Sibagariang Swono, "Android-Based Expert System Diagnoses Cow Disease with Certainty Factor Method". Jurnal TIMES, Vol.IV, No.2 : 35-39, 2015.
- [12] Arhami M, *Basic Concepts of Expert System*. Yogyakarta: Andi, 2005.
- [13] Kusumadewi Sri, *Artificial Intelligence: Techniques and Applications. Edition 1*. Yogyakarta: Graha Ilmu, 2003.
- [14] Supartha, I Kadek Dwi Gandika and Sari Ida Nirmala, "Expert System for Early Diagnosis of Skin Diseases Bali's Cow Using Forward Chaining and Certainty Factor Method". JANAPATU, Vol. 3, No.3: 110-117, 2014.
- [15] Orisa Marisa, Santoso Purnomo Budi and Setyawati Onny, "Web-Based Goat Disease Diagnosing System Using Certainty Factor Method". Jurnal EECCIS, Vol.8, No. 2:151-156, .2014.
- [16] Lestari Lia Septi, "Web-Based Expert System for Early Diagnosing Brain Tumor Using Certainty Factor Method(Essay)". Sultan Syarif Kasim Riau State Islamic University, 2013.
- [17] Purwadi, Ihsan. 2009. Penerapan Bayesian Network Dalam Penetapan Daerah Tertinggal (skripsi). Institut Pertanian Bogor. Directorate General of Animal Husbandry and Animal Health. *Manual For Mammalian Diseases*. Jakarta: Directorate Animal Health, 2014.

Enhanced e-Learning Experience using Case based Reasoning Methodology

Swati Shekapure¹, Dipti D. Patil²

Research Scholar, Sant Gadge Baba Amravati University, Amravati, India¹

Information Technology Department, MKSSS's Cummins College of Engineering for women, Pune, India²

Abstract—In recent year's improvement in innovation includes new limits for verifying data that will incite essential changes in eLearning. The user can see e-learning material subject to the reference given to them and select the best approach to see the resources. This proposed system addresses retrieval, reuse, revise and retain phases of CBR. For building personalized e-Learning, this work identifies different feature set such as learning style, learning object, knowledge level, and problem list. For constructing this model used case-based reasoning along with a k-nearest neighbour. Role of the K-nearest neighbour method is to identify the perfect k factor for better analysis for calculation of accurate retrieval process. There is further addition of new cases based on the simulation of new user history limit to a certain threshold value. This model acquires dynamically incremental dataset for classification. Further, there is time and accuracy comparison on dataset done by K-nearest neighbour, decision tree and support vector machine. Eventually, eLearning spares time, upgrades the learning knowledge and gives scholarly achievement.

Keywords—K-nearest neighbour method; eLearning; learning objects; learning style; case based reasoning

I. INTRODUCTION

The world has changed generously over the most recent 100 years, and instruction needs to change also to guarantee our youngsters are completely arranged Today, a customized learning approach that utilizes innovation in the class room to pace guidance to coordinate student's needs and tailor figuring out how to their interests function for the both students and instructors [4].

Instead of passively accepting and emphasizing data, students' in 21st century customized learning situations play a functioning job in their training and adds to their very own learning. They can work with instructors to set learning objectives [1] for themselves, and can move in the direction of them through mixed getting the hang of, consolidating face to face collaboration with their educator and the utilization of training innovation.

II. CASE BASE SYSTEM

The term case-based reasoning [8] comprises of three words: case, experience, and problem. A case is an experience of previously occurred problems which are stored in a case base. The representation of cases would do in many ways. A case base is nothing but a collection of represented cases. Store cases are a primary foundation for reasoning. The reasoning to be done in a CBR system is different from an

argument in logic and databases. CBR is not based on true rulebooks and accurate decisions. Applying CBR is approximate reasoning. It may happen that the solution in a recorded case was reasonable for its original problem, this would not be the case for a new-fangled problem. This option is created on the universal fact that the condition in the noted knowledge may not be accurate or similar to that in the new-fangled problem. The result of the reuse of similar case depends on the similarity of previous experience to a new challenge.

A. CASE

The evidence documented historical knowledge will be essential, be subject to the area of the inventor, it is called problem space. In the design of a problem-solving a CBR system, the particulars will generally comprise the requirement of the problem and the appropriate characteristics of the situation that are the conditions of the problem. The dynamic part of the case is the explanation that was functional in the previous state. CBR system solution may include facts of the solution or process that are involved in obtaining the solution. It also consists of the attained measure of success in the case explanation, if the cases in the case base have reached different grades of success or failure. When an assessment finished amongst the information stored in a model/rule-based system, and that warehoused in a case base, it seems that the evidence in the case base is of a further detailed nature than that of the model/rule-based system. Although the information in a model/rule-based system has preoccupied so that it related in the broadest diversity of circumstances as possible, the information controlled in case base residues precise to the case in which it is stored. [6] Since the accurate information of a case base, it has been discovered that associated information and knowledge relevant in a particular condition warehoused in neighboring contiguity. Therefore, relatively illustrating information from an extensive net, the information desired to answer a precise unruly instance can establish a cluster. The case base in the CBR structure is the recollection of all earlier warehoused cases [14]. Three broad areas have to consider when creating a case base.

- The construction and illustration of the instances themselves.
- The recollection prototype used for establishing the entire case base.
- The choice of keys which are used to categorize every case.

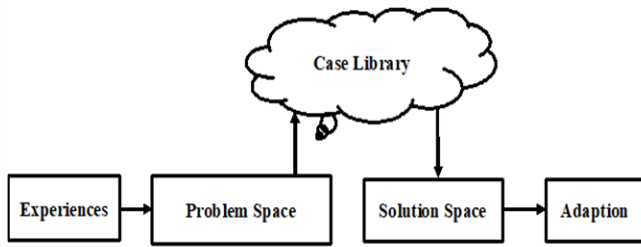


Fig. 1. Solution Space of CBR.

B. Experiences

Experiences are vital for the CBR system. Experiences have documented an event that happened in the prior. Cases can be relatively composite and comprise of entire stories. CBR practices them for answering problems, and these must be in the knowledge base for talks about a problem and its solution. In a simple view, CBR splits a piece of knowledge into two parts shown in Fig. 1.

- a) A problem space (or an explanation of a problem situation).
- b) A solution space that defines in what way one has responded.

Over and over again one limits CBR to a solution that has been positively, but that is by no means essential or satisfactory. An unsuccessful explanation is also a significant part of the evidence that states what one has to circumvent. Positive experiences implement practical solutions and lead to guidance. Negative experiences implement unsuccessful solutions and lead to advise that avoids this case.

Essential experiences take place in:

- a) Classification: Select the class to which an entity be appropriate.
- b) Diagnosis: Select what the analysis of a problem is.
- c) Prediction: Answered what happens in the future.
- d) Planning: select an order of activities to extend a given goal.
- e) Configuration: Select technical features to include.

Although a human can learn through experiences, for computer system experiences are represented in the form of cases and stored in the case library. A new incident occurred then the solution space would retrieve a given solution for adaption.

C. Problems and Solution

The primary purpose of CBR is to solve the problems. The preparation of a challenge from time to time is challenging because it refers to the situation in which it has been specified. So, each problem development involves not the same kind of explanation. It is understandable that one has to identify the condition in which the problem has been specified to discover which answer is suitable. In further, for a detailed report, the situation has to be involved in the problem preparation. Fragment of the case is repeatedly of the fundamental principles. For example, Depending on the values, rules may

have changed in different spaces. Other beliefs provided by diversified fields such as medicine, commercial, industrial, and engineering; even outsized corporations have established their principles. The CBR background has to consider this into interpretation because transmitting justifications across different cultures is challenging. For illustration, every bank has advanced its strategy for giving credits to clients. The same bank possibly will interpret the policy in a different way in each separate nation it activates; this becomes superficial during economic crunches. There are two types of problems in the framework of the CBR method. The issues in the cases verified as familiarities usually denoted as problems in CBR. The facts in the case base can distinguish as contender cases, as they are contenders for reprocess. However, the entire CBR progression has activated by a problem. A new challenge or the concrete problem encourages a user to discover a problem-solving technique [10].

The probable ways of demonstrating an explanation differ: It can be just an explanation in the contracted sense. It can comprise notes, graphics, clarifications and guidance on how to use the statement. The consequence by telling what happened with the solution in the earlier. Comments on the approach with which, the clarification has been obtained. In modest cases, the description comprises a name or small data, for example, an object or an estimated high temperature. Explanations may also have a complex object-oriented configuration as a methodological object. Even more composite solutions for scheduling and those in documentary or image form. In a composite situation, the answer is a conclusion for acting or even a process.

Here one has to differentiate the outcome from the action; the action mentions to execute and run of a plan that may alter states of variables. Whereas the conclusion generally communicated, the result of the work may be indeterminate. Suppose for instance if it has been decided to fly to Mumbai. The execution may fail or be suspended because of numerous unexpected happenings. The latter means that the outcome of using a solution is ambiguous because of unforeseen exterior consequences like bad weather or an earthquake. If these are expected to occur one should extend the explanation by an entry "consequence" for telling what happened. The user who understands the statement does not recognize this. If it is added at that moment, the user might get a clue for specific possible reworking. In conclusion, there are circumstances where the effectiveness of the explanations can only judge if they have implemented in reality [12].

III. NEIGHBOURHOOD FORMATION PROCESS

Proposed work deals into various assignments, for example, a. make a database with the solicitation to perceive learning style b. Adding learning Material and essential KNN for the recommendation c. Adding Test Question and Revise - Retain Algorithm execution d. Checking Comparisons with other ML estimations. This is an adaptable recommendation structure for endorsing learning preferences to the user dependent on CBR and seeing the closest neighbour. This work proposed to fulfil four phases of CBR these are retrieve, reuse, revise and retain as appeared in Fig. 2. It gets understudy's tendencies [2] by finishing express fundamental

outlines, ensuring to examine recommend material. User can use certain learning objects for understanding a specific point. For examining self-execution user attempt the test. Whatever execution of user gets contrasted and the limit esteem. On the off chance that it fulfilling limits, at that point it gets put away for the case library. This work uses case library data as the strategy set. Right when another issue exists proposed structure searches for after case-based reasoning impels. It has point by point differentiating cases, and errand of referencing had done, when the new case exists to get empowered by considering closeness vertex and find the nearest case interfacing with another case.

For identifying new user behavior [11], it has conspired different feature set; these are:

Feature set for the system

1. Problem List = {for, if, if else, while, do while, switch}
2. Learning Styles = {Visual, Auditory, Kinaesthetic}
3. Knowledge Levels = {Beginner, Intermediate, Expert}
4. Learning Objects = {Video, Chart, Audios, Simulation, Highlighted Text}
5. Test Performance = [3, 4, 5, 6, 7]
6. path = {Video->Chart, Audios->Video, Simulation->Highlighted Text}

Related values of input parameters are in Table I.

After conspicuous verification of feature vectors and association between things, the accompanying stage is to make cases for rundown out of abilities by considering historical results. This work has framed diverse cases with id, problem, learning style [9], learning objects, test execution and utilized way. This model had considered preparing a dataset for a finding of proper estimation of K. When the finding of estimation of K had done then KNN is prepared for producing similitude list for new user. On the off chance that the new user didn't get the comparative case, at that point, this work checked new client premium, whatever way embraced for learning and test execution score. In the event that scores gotten by a new user is acceptable according to edge esteem, at that point the particular case gets put away in database with ordering.

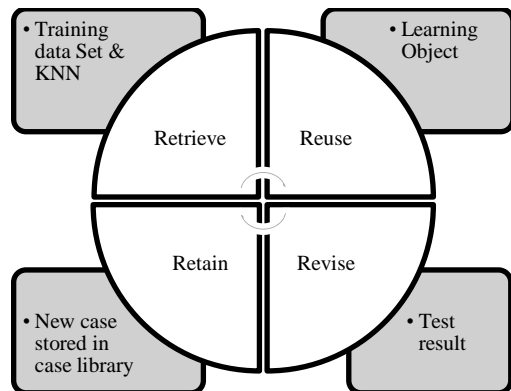


Fig. 2. CBR Phases.

TABLE I. FEATURE SET VALUES

Sr. No.	Input parameter	Feature set	Value
1	Problem	For	1
		If	2
		If-else	3
		while	4
		Do while	5
		switch	6
2	Learning Style	Visual	1
		Auditory	2
		Kinaesthetic	3
3	Knowledge level	Beginner	1
		Intermediate	2
		Expert	3
4	Learning object	Video	1
		Chart	2
		Audios	3
		Simulation	4
		Highlighted text	5
5	Test Performance	Result	Actual Result
6	Path	Video-chart	1
		Audios-video	2
		Simulation-Highlighted Text	3

IV. REVIS-RETAIN ALGORITHM IMPLEMENTATION

Revise and Retain phase of case based reasoning is to add new query with new index value in dataset. This is dynamically incremental phase of CBR whereas assignment of new index value had done by considering test performance of new user. This has finished by simulating result and threshold value set [3]. This phase compromises different work through here presented few algorithms for revise and retain phase implementation. For that initially load training and testing dataset so algorithm represents fetching of input parameters. After loading dataset as training and testing, next step is to check similarity .This research work emphasis on CBR with KNN .So for finding similar case Euclidian distance measures had used. Below presenting how Euclidian distance measure works on input dataset for calculating class of new user. After calculating values of learning style, knowledge level, and test performance the job of retain and revise phase suggest to learning path to new user. So whatever score has established for x value dataset need to normalized obtained weight.

For normalizing input set practice equation 1:

$$Z_i = \frac{x_i - \min(x)}{\max(x) - \min(x)} \tag{1}$$

Where $x=(x_1... x_n)$, Z_i is i^{th} normalized data.

Algorithm for Proposed System:

- 1) Identify training set and test set as well as attribute for prediction
 - i) Load Dataset (trainingset, testset, attr)
 - ii) attr is "Learning Objects"
- 2) For each test element in test set calculate neighbours
 - i) getNeighbors(trainingSet, testset[x], k, attr)
 - ii) Parameters: training Set, single test element x, k, attr= "Learning Object"
- 3) In getNeighbors calculate score one by one with each training element
 - i) For x in trainingSet
 - ii) getScore(x, testInstance, attr)
 - iii) x= training element, test element, attr= "LearningObject"
- 4) In getScore calculate score for each feature in element
 - i) getScore(x, testInstance, attr)
 - ii) LearningStyleScore=calculate(x.learningStyle, testInstance.learningStyle, data.learningstyle)
 - iii) ProblemScore=calculate(x.problem, testInstance.problem, data.problem)
 - iv) KnowledgelevelScore=calculate(x.Klevel, testInstance.Klevel, data.Klevel)
 - v) PathScore=calculate(x.path, testInstance.path, data.path)
- 5) In calculate
 - i) Calculate(xValue, testValue, dictVals)
 - ii) For calculating Learningstyle, xValue=LearningStyle for training element (e.g. Visual),
 - iii) testValue (e.g. Visual),
 - iv) dictVals={"Visual=1", "Auditory=2", "Kinesthetic=3"}
- 6) As per KNN for each feature distance= square(trainingValue - testValue)
 - i) $\text{Pow}(v1, v2)^2$
- 7) As per KNN, Total distance= squareRoot(total)
- 8) Sort all the elements in training set based on distance, as k=4 select first 4 nearest elements
 - i) Neighbours= []
 - ii) For x in sorted (distances)
 - iii) If (k==0)
 - iv) Break;
 - v) Neighbours. Append (distances[x])
 - vi) K=k-1;
 - vii) Return neighbours.
- 9) After getting neighbours, predict feature
 - i) Result=getResponse(neighbors, attr)
 - ii) Attr= "learningObject"
- 10) In get Response, this work find attr=LearningObject value count
 - i) For example
 - ii) first neighbour value=Visual
 - iii) second neighbour value=visual
 - iv) third neighbour value=Visual
 - v) fourth neighbour value=Auditory
 - vi) then,
 - vii) classVotes={ Visual=3, Auditory=1 }
 - viii) Then sorting of above map, to get highest voted value, here "Visual"
- 11) Next step is to check this value with test instance and calculate accuracy

V. RESULT

As a part of result, proposed framework classes' students according to the learning style [7] as visual, Auditory and Kinesthetic. Result introduced for learning style just as the recommendation of learning object to another student. Alongside recommendation, there is learning material benefited to a student. Learning material is as a diagram, graph, notes, simulation, and featured content. Fig. 3 demonstrates identification of learning style of the user.

According to learning style, problem and knowledge level of student (Fig. 4) system shows recommendation to learner as shown in Fig. 5.

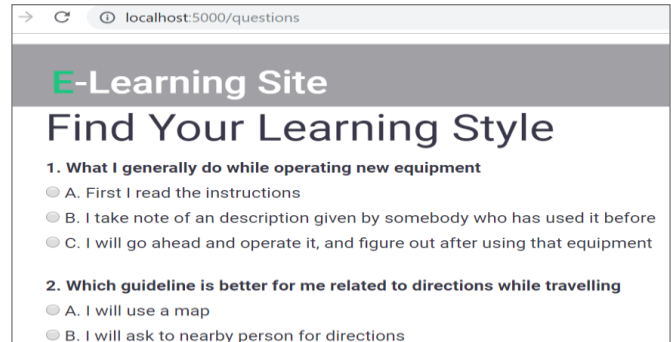


Fig. 3. Questionnaire's Set for Learning Style.

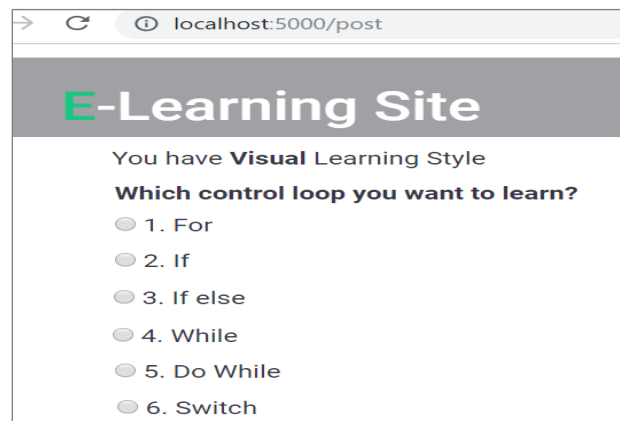


Fig. 4. Generated Learning Style and Input Problem.

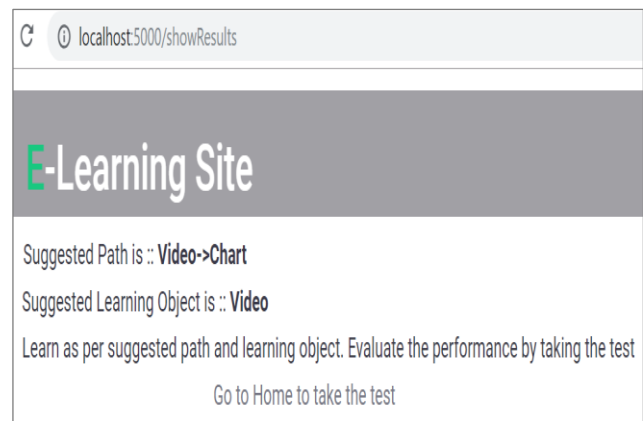


Fig. 5. Recommendation of Learning Objects and Path.

Fig. 6 shows sample set for test performance. The sets depend on input received from user whether learner is beginner, Intermediate or expert in that particular topic. After using different learning objects, student opts for the test.

If the test performance is satisfied then add student path includes learning objects and test performance to a dataset of case based reasoning. Satisfactory performance of student indicates that simulation done in real-world scenario and verified by domain experts. It has retained phase of CBR.

Fig. 7 shows retain phase of CBR

For retrieval phase, similarity check is done on different classification algorithm. These are a k-nearest neighbor, decision tree and support vector machine. For this research work, consideration of dataset size is 200 records, 300 records and 375 records. Table II shows observations for 375 records.

It has been observed that for 200 records decision tree has given results in least amount of time as compared to k-nearest neighbor method and support vector machine.

Fig. 8 shows that average time observations of different learning algorithms. It has been observed that Decision tree takes less time as compared to KNN and SVM, but KNN gives retrieval phase stability which is more as compares to DT and SVM. [15].

Further this work calculated accuracy of decision prediction by above learning algorithm. Fig. 9 shows the observations for 200 records size, 300 records size and 375 record size.

As per the observation it has been found that KNN and decision tree gives maximum accuracy as compared to SVM. But for time comparison KNN timing for retrieval process is stable as compared to Decision tree and Support vector machine. So for this dataset it has better to use KNN than DT and SVM.

TABLE II. OBSERVATIONS FOR 375 RECORDS, TIME IN MILLISECONDS

Sr. No.	KNN	SVM	DT
1	5.23	10	5
2	5.8	10	6
3	7.6	10	5
4	5.6	8	4
5	5.76	7	4
6	5.1	6	4
7	5.23	8	6
8	5.53	7	4
9	4.8	7	4
10	5.53	6	4
11	4.53	7	4
12	5.06	8	7
13	5.2	7	4
14	4.7	7	5
15	4.86	7	4
16	8.1	10	6
17	6.1	7	4
18	4.9	8	4
19	5.46	7	5
20	4.83	7	4
Average	5.49ms	7.7ms	4.65ms

Average Time Comparison

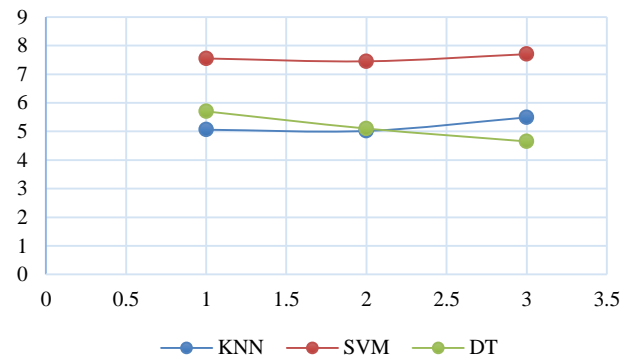


Fig. 8. Average Time Comparison of KNN, SVM and DT.

Accuracy Comparison

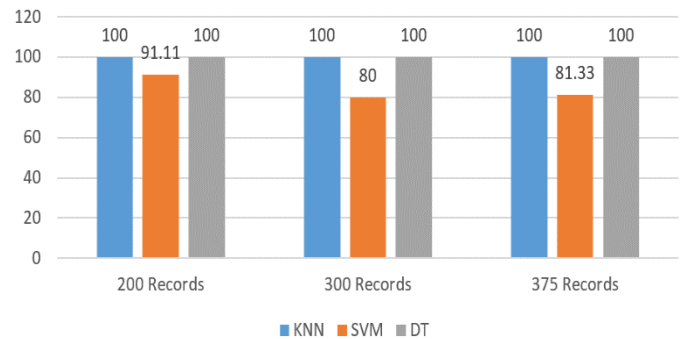


Fig. 9. Accuracy Comparison of KNN, SVM and DT.

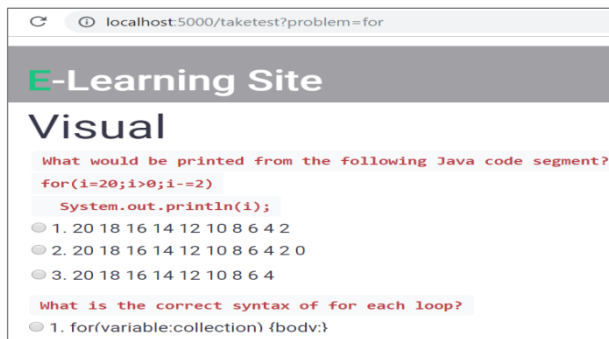


Fig. 6. Set for Test Performance.

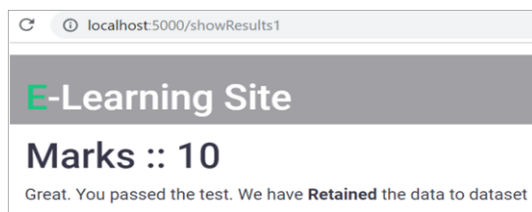


Fig. 7. Retain Phase of CBR.

VI. CONCLUSION

This research paper focuses on the current technology of internet e-learning. This methodology is appropriate for applications in e-learning such as to enhance the website to the personalized facility. Generation of the weblog is dynamic activity so each time our approach generates unambiguous results, that is, key behind this research work to focus on learner's interest as well as their performance. This is Adaptive personalized e-learning system [10] because whatever path used by learner's for specific topic get stored in dataset with new index value. So new user able to check different learning objects and impact of it on performance. Because of this learners way of learning and time automatically hold back for understanding theories. It will definitely be beneficial for younger generations particularly teenagers where they are in position to acquire knowledge[13] in least time with more understanding approach.

In future, the learning solutions and services can be integrated into a new trend which is called mobile learning technology [5] that can help the people who are lack of infrastructure and for the people whose job require to move.

VII. DISCUSSION

In view of student's education to develop students' learning interest and improve performance, a case based personalized eLearning system must know how a different learner learns best. In this innovative framework, work presented for learners modelling through dynamically incremental model of case library. Research have exposed this methodology is able to recommends learning objects , automatically records the path and adjust learner's learning style, based on k-nearest neighbor method for retrieval similar interest.

ACKNOWLEDGMENT

It's with immense gratitude that we acknowledge Dr. V.M. Thakare, Head P. G. Department of Computer Sci. & Technology, Sant Gadge Baba Amravati University, Amravati for sharing his wide knowledge, co-operation from time to time and prestigious guidance during the preparation of this work.

REFERENCES

- [1] Kwok Hung Lau, Tri-Lam, Booi HonKam, Mathews Nkhoma, Joan Richardson, Susan Thomas, " The role of textbook learning resources in e-learning: A taxonomic study, Computers & Education, Elsevier, Volume 118, pp 10-24, March 2018.
- [2] Beulah Christalin LathaChristudas, E.Kirubakaran, P. Ranjit JebaThangaiyah, "An evolutionary approach for personalization of content delivery in e-learning systems based on learner behavior forcing

compatibility of learning materials," Telematics and Informatics, Elsevier, Volume 35, Issue 3, pp. 520-533, June 2018.

- [3] Aleksandra Klasnja-Milicevic, Mirjana Ivanovic, Boban Vesin, Zoran Budimac, "Enhancing e-learning systems with a personalized recommendation based on collaborative tagging techniques," Applied Intelligence, Springer Volume 48, Issue 6, pp. 1519– 1535, 2018.
- [4] Wacharawan Intayoad, Till Becker, Punnarumol Temdee, "Social Context-Aware recommendation for Personalized Online Learning," Wireless Personal Communications, Springer ,Volume 97, pp. 163-179, November 2017.
- [5] Peter Dolog, Michael Sintek, "Personalization in Distributed e-Learning Environments," May 17–22, 2017, New York, USA. ACM 1-58113-912-8/04/0005.
- [6] Khribi, M. K., Jemni, M., & Nasraoui, O. . ." Automatic Recommendations for E-Learning Personalization", Based on Web Usage Mining Techniques and Information Retrieval. Educational Technology & Society, IEEE, pp. 30–42, 2017.
- [7] Kusuma Ayu Laksitowening; Amarilis Putri Yanuarifiani; Yanuar Firdaus Arie Wibowo, "Enhancing e-learning system to support learning style based personalization," IEEE, 16 February 2017.
- [8] Antonio Garrido, Lluvia Morales, Ivan Serina, "On the use of case-based planning for learning personalization," Science Direct, 30 October 2016, Pages 1-15.
- [9] Biroi Ciloglugil, Mustafa Murat Inceoglu, "A Felder and Silverman Learning Styles ModelBased Personalization Approach to Recommend Learning Objects," Springer, 01 July 2016.
- [10] Boban Vesin, Mirjana Ivanović, Zoran Budimac, Lakhmi C. Jain, "Personalization and Adaptation in E-Learning Systems," Springer, 20 July 2016.
- [11] Beulah Christalin, Latha Christudasa, E.Karunakaran, P. Ranjit JebaThangaiyah, "An evolutionary approach for personalization of content delivery in e-learning systems based on learner behavior forcing compatibility of learning materials," Elsevier, 4 Feb 2017.
- [12] Outmane Bourkhouk, Essaid El Bachari, and Mohamed El Adnani, "A Personalized eLearning Based on Recommender System," International Journal of Learning and Teaching, 2016 .
- [13] Fatemeh Roosta; Fattaneh Taghiyareh; Maedeh Mosharraf, "Personalization of gamification-elements in an e-learning environment based on learners' motivation," IEEE, 20 March 2017.
- [14] Shard from Johnson; Xubin Liu; Hui Miao; Jiajin Yuan; Yong Jin; Qin Wei; Zhao Xu, "A Framework of e-Learning Education Clouds to Efficiency and Personalization," IEEE, 3 November 2016.
- [15] Elfa Silfiana Amir; Malikus Sumadyo; Dana Indra Sensuse; Yudho Giri Sucahyo; Harry Budi Santoso, "Automatic detection of learning styles in learning management system by using literature-based method and support vector machine," IEEE, 09 March 2017.

ABBREVIATIONS

1. KNN: K-Nearest Neighbour
2. DT: Decision Tree
3. SVM: Support Vector Method
4. CBR: Case Based Reasoning

Effect of Correlating Image Threshold Values with Image Gradient Field on Damage Detection in Composite Structures

Mahmoud Zaki Iskandarani
Faculty of Engineering
Al-Ahliyya Amman University, Amman-Jordan

Abstract—Effect of image threshold level variation is studied and proved to be a critical factor in damage detection and characterization of impacted composite Reaction Injection Molding ((RIM) structures. The variation of threshold is used as an input to both gradient field algorithm and segmentation algorithm. The choice of optimum threshold for a tested composite type is achieved as a result of correlation between the resulted gradient field images and segmented images. Type and extent of damage is also analyzed using detailed pixel distribution as a function of both impact energy and threshold level variation. The demonstrated cascading based technique is shown to be promising for an accurate testing and classification of damage in composite structures in many critical areas such as medical, aerospace and automotive.

Keywords—Gradient norm; edge detection; gray level mapping; segmentation; threshold; histogram; image processing; composites; impact damage

I. INTRODUCTION

Testing composite structures is one of the most important tasks employed in maintenance and diagnosis of components. Non-Destructive Testing (NDT) techniques are used in the aircraft design, automotive design as well as many other applications. Applications for composite materials has expanded from the use as a non-structural part to the construction of complete frames and body structures due to its toughness, stiffness and high strength to weight ratio.

A composite structure is normally made up of several plies with selected fiber orientation and characteristics. The impact damage of a composite laminate can lead to more damage than it is apparent on the surface. Repetitive impact loading can result in severe damage, which would end in component structural failure. Cracks and debonding (delamination) are common damage cases found in composite structures. Delamination is more critical as it causes reduction the load-carrying capability of a composite component, resulting in catastrophic failure.

Images (Thermal, Ultrasonic, and Visual) for damaged composites will most of time show segmentation. Thus subdivides the composite image into regions. The number of regions formed as a result of segmentation is a function of damage type. The segmented image is a function of both discontinuity and uniformity, which are used to determine similarity and damage magnitude [1-10].

Image segmentation is considered to be vital in analyzing an acquired image in many computer image processing applications such as medical imaging, robotic vision, face recognition applications and many others. Segmentation will partition an image into foreground and background with respect to selected variables. Most of image segmentation techniques are based similarity and discontinuity. In addition to used segmentation methods, thresholding is regarded as a major contributor to achieve accurate image interpretation and subsequent classification, as histogram related thresholding is complex especially for multi-level thresholding [11-15]. It is critical for damage detection in composite structures to implement image enhancement techniques which is essential in image processing with particular consideration to intensity variation of image contents and its effect on segmentation.

II. BACKGROUND

Detecting damage in composite structures is a challenging task owing to the variable appearance and the wide range of shapes and textures that composites can exhibit. The first need is a reliable feature set that allows the damage type to be distinguished clearly, especially in shadowed backgrounds and under difficult illumination. Image segmentation is a critical and challenging problem in image processing and is the initial step for high level analysis. The objective behind image segmentation is to divide an image into different classes based on features, such as color, intensity or histogram, such that pixels are grouped under different classes.

Image segmentation is used to divide an image into multiple segments in order to obtain data that can be used for classification and decision making. The purpose of dividing an image into different region is to enable further image analysis.

Image segmentation has been widely used in many practical applications such as medical imaging, remote sensing, Optical Character Recognition (OCR) and general object detection. Segmentation will transform representation into something that is more representative to study or examine. Image segmentation is mainly used to detect objects and background in images. More specifically, image segmentation is the mechanism of assigning a label to each pixel in an image such that pixels with the same tag share certain characteristics.

The core of image segmentation is thresholding, which can be used to generate binary images by selecting optimum

threshold value for accurate segmentation. Many conventional methods are used in engineering including the k-means clustering, Otsu's method, which employ maximum entropy and maximum variance method. Other related techniques for feature extraction and object recognition, such as Histogram of Gradients (HOG) and wavelet transform are also used [16-19].

Segmentation can be more effective if an optimum level of thresholding is achieved, thus, more accurate interpretation of acquired images and better analysis are obtained, resulting in a well-defined region-based description of images through decomposing them into r spatially coherent regions sharing similar attributes.

In this work, a new approach to damage detection and composite structure analysis is applied to images of impact damaged composites. The technique optimizes and localizes the boundaries of a damaged area as a function of image gradient and threshold values, which is then correlated with impact energies. The approach uses segmentation for both colour and grey images and eliminates histogram intensity variation with image contents by using histogram gradients.

III. MATERIAL AND METHODS

The tested RIM composites subjected to Impact Energies {0, 14J, 28J, 42J, 56J}, hence, increments of 14J. Up to 28J Impact Energy, no evidence of damage was realized. Thus, the considered Impact energies in this work are {28J, 42J, 56J}.

The main objective is to produce an automatic damage characterization and classification through thresholding and image segmentation. Thus, obtaining a region-based description of the damage embedded in an image by dividing the image it into spatially coherent regions with similar attributes.

To achieve the intended purpose of this work, images of damaged structures at various impact energies are tested using MATLAB algorithm as shown in Fig. 1.

Two or more sampling points are considered at non-zero grayscale levels when:

- All of the levels are empty
- All of the levels are full

Sampling stops at the first threshold level where no segmentation is possible. The threshold level just before the one that caused a no segmentation condition is considered the optimum threshold level for a composite type and impact energy level. Any condition outside these is classified as total damage and matrix-fiber failure.

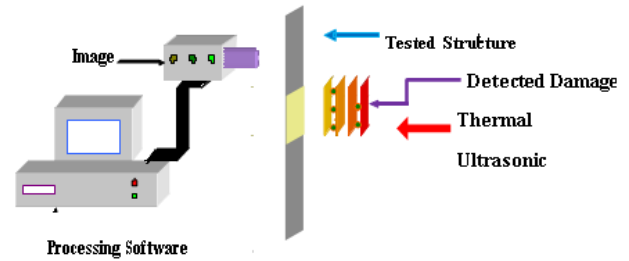


Fig. 1. Experimental Setup.

IV. RESULTS

A. 28J Impact Energy

Table I shows the effect of varying the threshold level on the pixel distribution of an impact damaged RIM composite structure. The structure suffered a 28J of impact energy delivered through a vertically launched load, while Fig. 2-9 shows both Gradient Field and Segmentation images.

TABLE I. PIXEL DISTRIBUTION FOR 28J IMPACT

Threshold	Level 0	Level 128	Level 180	Level 255
0.42	14440	0	0	0
0.43	14396	4	0	0
0.44	14378	18	4	0
0.45	14362	30	8	0
0.46	14328	58	14	0
0.47	14320	60	20	0
0.48	14300	68	32	0
0.49	14290	68	42	0
0.50	14252	92	56	0
0.51	14156	184	60	0
0.52	14096	222	82	0
0.53	14002	272	126	0
0.54	13938	326	136	0
0.55	13854	406	140	0
0.56	13806	424	170	0
0.57	13774	458	168	0
0.58	13794	410	196	0
0.59	13816	432	152	0
0.60	13836	402	162	0
0.61	13810	423	164	3
0.62	13678	528	186	8
0.63	13336	796	254	14
0.64	12794	1211	379	16
0.65	12371	1479	523	27
0.66	11911	1790	680	19
0.67	11867	1802	705	26

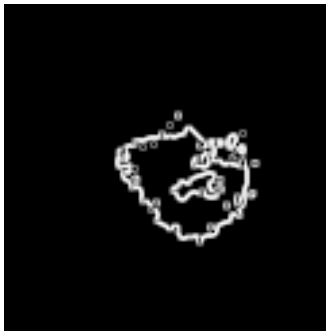


Fig. 2. Gradient Magnitude: 28J Impact, 0.57 Threshold.



Fig. 3. Edge Segmentation: 28J Impact, 0.57 Threshold.

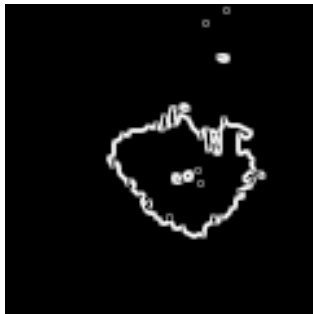


Fig. 4. Gradient Magnitude: 28J Impact, 0.60 Threshold.



Fig. 5. Edge Segmentation: 28J Impact, 0.60 Threshold (Optimum Segmentation).



Fig. 6. Gradient Magnitude: 28J Impact, 0.61 Threshold.



Fig. 7. Edge Segmentation: 28J Impact, 0.61 Threshold (No Segmentation Possible).



Fig. 8. Gradient Magnitude: 28J Impact, 0.67 Threshold.



Fig. 9. Edge Segmentation: 28J Impact, 0.67 Threshold (No Segmentation Possible).

B. 42J Impact Energy

Table II shows effect of varying the threshold level on the pixel distribution of an impact damaged RIM composite structure. The structure suffered a 42J of impact energy delivered through a vertically launched load, while Fig. 10-19 shows both Gradient Field and Segmentation images.

TABLE II. PIXEL DISTRIBUTION FOR 42J IMPACT

Threshold	Level 0	Level 128	Level 180	Level 255
0.29	14400	0	0	0
0.30	14388	12	0	0
0.31	14356	32	12	0
0.32	14290	76	34	0
0.33	14186	158	56	0
0.34	14126	186	88	0
0.35	14134	164	102	0
0.36	14138	166	96	0
0.37	14150	162	88	0
0.38	14132	184	84	0
0.39	14134	170	96	0
0.40	14060	224	116	0
0.41	13990	282	128	0
0.42	14002	260	138	0
0.43	13982	282	128	0
0.44	13984	278	138	0
0.45	13976	292	132	0
0.46	13950	292	158	0
0.47	13912	332	156	0
0.48	13894	344	162	0
0.49	13910	324	166	0
0.50	13912	316	172	0
0.51	13874	338	188	0
0.52	13828	382	190	0
0.53	13758	402	238	2
0.54	13702	465	230	3
0.55	13587	524	283	6
0.56	13445	644	307	4
0.57	13129	850	415	6
0.58	12871	1070	452	7
0.59	12643	1201	533	23
0.60	12583	1275	524	18

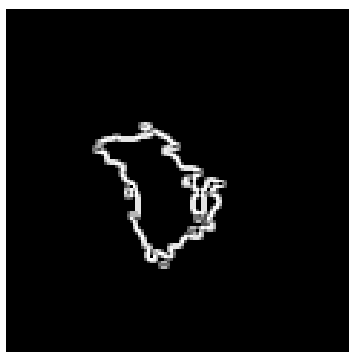


Fig. 10. Gradient Magnitude: 42J Impact, 0.41 Threshold.



Fig. 11. Edge Segmentation: 42J Impact, 0.41 Threshold.

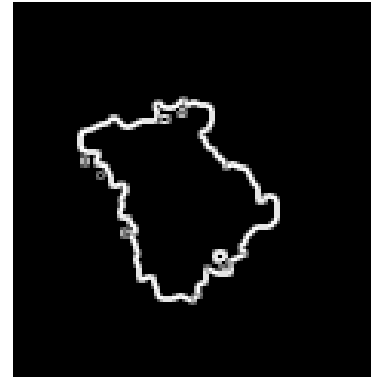


Fig. 12. Gradient Magnitude: 42J Impact, 0.48 Threshold.

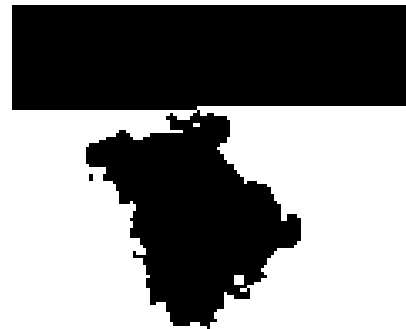


Fig. 13. Edge Segmentation: 42J Impact, 0.48 Threshold.

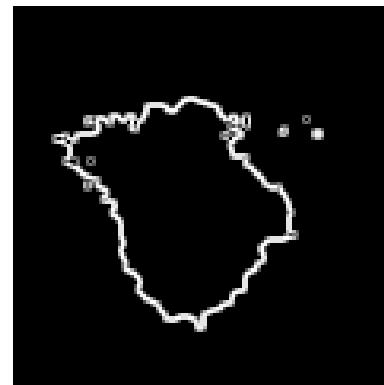


Fig. 14. Gradient Magnitude: 42J Impact, 0.52 Threshold.



Fig. 15. Edge Segmentation: 42J Impact, 0.52 Threshold (Optimum Segmentation).

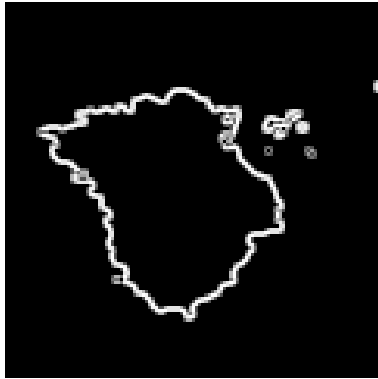


Fig. 16. Gradient Magnitude: 42J Impact, 0.53 Threshold.



Fig. 17. Edge Segmentation 42J Impact, 0.53 Threshold (No Segmentation Possible).

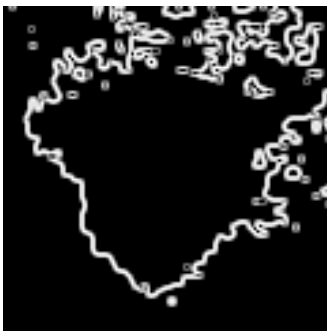


Fig. 18. Gradient Magnitude: 42J Impact, 0.60 Threshold.



Fig. 19. Edge Segmentation 42J Impact, 0.60 Threshold (No Segmentation Possible).

Table III shows effect of varying the threshold level on the pixel distribution of an impact damaged RIM composite structure. The structure suffered a 56J of impact energy delivered through a vertically launched load, while Fig. 20-25 shows both Gradient Field and Segmentation images.

C. 56J Impact Energy

TABLE III. PIXEL DISTRIBUTION FOR 56J IMPACT

Threshold	Level 0	Level 128	Level 180	Level 255
0.18	14400	0	0	0
0.19	14392	7	0	1
0.20	14340	48	3	9
0.21	14226	147	8	19
0.22	13936	365	60	39
0.23	13686	518	161	35
0.24	13360	799	197	44
0.25	13138	961	250	51
0.26	12675	1338	316	71
0.27	12369	1552	407	72
0.28	12063	1742	509	86
0.29	11988	1821	516	75
0.30	11816	2018	504	62
0.31	11752	2062	530	56
0.32	11780	1994	575	51
0.33	11778	2062	523	37
0.34	11766	2131	472	31
0.35	11732	2127	506	35
0.36	11640	2181	536	43
0.37	11544	2200	618	38
0.38	11660	2082	622	36
0.39	11856	1924	581	39
0.40	12202	1710	464	24
0.41	12416	1570	396	18
0.42	12708	1355	328	9
0.43	12877	1188	329	6
0.44	13003	1108	282	7
0.45	13095	1015	288	2
0.46	13165	933	299	3
0.47	13277	884	286	3
0.48	13357	825	216	2
0.49	13507	714	178	1
0.50	13661	564	173	2
0.51	13721	524	155	0
0.52	13757	514	129	0
0.53	13852	464	82	2

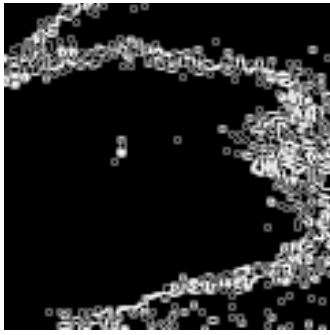


Fig. 20. Gradient Magnitude: 56J Impact, 0.31 Threshold.

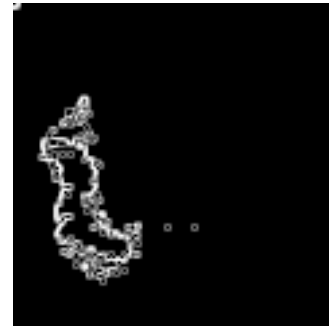


Fig. 24. Gradient Magnitude: 56J Impact, 0.51 Threshold.



Fig. 21. Edge Segmentation 56J Impact, 0.31 Threshold (No Segmentation Possible).



Fig. 25. Edge Segmentation 42J Impact, 0.51 Threshold (No Segmentation Possible).

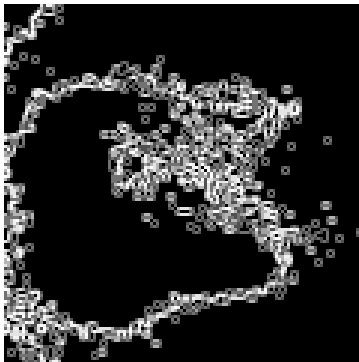


Fig. 22. Gradient Magnitude: 56J Impact, 0.37 Threshold.

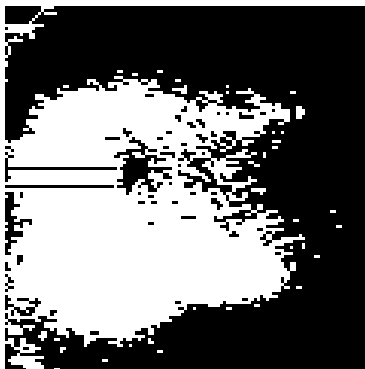


Fig. 23. Edge Segmentation 42J Impact, 0.37 Threshold (No Segmentation Possible).

V. ANALYSIS AND DISCUSSION

Fig. 26 shows the used system for impact damage analysis, while Tables I to III and Fig. 2 to 25 show the resulting gradient and segmented images.

Classification and determination of optimum threshold value that uncover damage in relation to the extent of impact energy, is computed as a result of correlating gradient field images with segmented images. $L=255$ is regarded as the critical Gray level that determines the optimum threshold value.

Three levels of impact energies applied to the RIM composite structure. The results can be interpreted as follows:

A. 28J Impact Energy

Features of the damaged area started to appear at threshold value of 0.43, with optimum features at threshold value of 0.60. The damaged area stated to merge with the surrounded areas at threshold value of 0.61 with total merge at threshold value of 0.67.

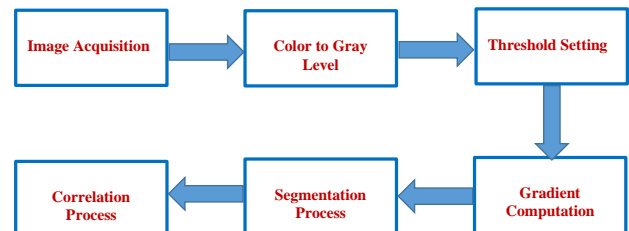


Fig. 26. Image processing system

Four sampled images are presented, which cover two intervals of pixel population:

- Two sampled images: (L=255) empty.
- Two sampled images: (L=255) populated

The sampling resulted in the following pairs of correlated images as shown the respective figures: {(Fig. 2, Fig. 3), (Fig. 4, Fig. 5), (Fig. 6, Fig. 7), Fig. 8, Fig. 9)}.

The correlation resulted in one optimum threshold value for an impact energy of 28J, which is 0.60. The algorithm will take this value as a second parameter and correlate it to the impact energy. Hence, a new pair is resulted, {28J, 0.6}.

From Table I, data string describing the level of damage at 28J is obtained by correlating impact energy level, threshold level and pixel population, thus obtaining: {28J, 0.6, 1, 13836, 402, 162, 0}

A value of 1 is added to indicate that the damage is not severe as segmentation is achieved.

B. 42J Impact Energy

Features of the damaged area started to appear at threshold value of 0.30, with optimum features at threshold value of 0.52. The damaged area stated to merge with the surrounded areas at threshold value of 0.53 with total merge at threshold value of 0.60.

In comparison with the case of 28J impact, it is found (as expected) that the threshold values are lower in as the impact energy is increased from 28J to 42J by a 14J magnitude. This indicates that a larger impact energy requires lower threshold to uncover its extent of damage.

Five sampled images are presented, which cover two intervals of pixel population:

- Three sampled images: (L=255) empty.
- Two sampled images: (L=255) populated

The sampling resulted in the following pairs of correlated images as shown in the respective figures: {(Fig. 10, Fig. 11), (Fig. 12, Fig. 13), (Fig. 14, Fig. 15), Fig. 16, Fig. 17), (Fig. 18, Fig. 19)}.

The correlation resulted in one optimum threshold value for an impact energy of 42J, which is 0.52. This also a lower value compared to the 28J case of 0.6. The algorithm will take this value as a second parameter and correlate it to the impact energy. Hence, a new pair is resulted, {42J, 0.52}.

From Table II, data string describing the level of damage at 28J is obtained by correlating impact energy level, threshold level and pixel population, thus obtaining:

A value of 1 is added to indicate that the damage is not severe as segmentation is achieved {42J, 0.52,1, 13828, 382, 190, 0}.

C. 56J Impact Energy:

At 56J impact energy, the pixel distribution and population characteristics and threshold values did not follow the previous models for both 28J, and 42J impact energies as the

tested composite suffered fiber pull out and fiber extraction, which unbalanced the fiber-matrix relationship in terms of response to external scanning sources.

Three sampled images are presented, but could not confine the samples to the previous set intervals due to the severe damage and fiber breakage. Also, segmentation algorithm failed to isolate damaged region(s) as the whole component suffered total damage.

The sampling resulted in the following pairs of correlated images as shown in the respective figures: {(Fig. 20, Fig. 21), (Fig. 22, Fig. 23), (Fig. 24, Fig. 25)}

The correlation resulted in no single optimum threshold value for an impact energy of 56J possible.

From Table III, data string describing the level of damage at 56J is obtained by correlating impact energy level, threshold level, in this case a 0 is also added (to indicate severe damage) in addition to a selected threshold value (equivalent to optimum threshold in non-severe damage cases) at which most of the damaged area appear (in this case 0.37) as there is no correlation due to no segmentation, thus obtaining: {56J, 0.37, 0, 11544, 2200, 618, 38}

It is clear from the pixel population that the pixel distribution pattern is markedly different when severe damage occurs.

Fig. 27 to 29 show histograms obtained for three impact energies. From the histograms, it is clear that at 56J impact, a dramatic change occurs in the tested composite structure, which is fiber breakage and pull out. Thus affecting pixel values and distribution pattern, and resulting in a unique statistical accumulation.

The obtained histogram results correlates well with gradient contours shown in Fig. 30-32, where at 56J different characteristics are presented with the effect of impact is more marked and no evidence of localized damage as in the cases of 28J and 42J impact energy levels.

Fig. 33-35 illustrate the relationships covering three important factors:

- Impact Energy (IE)
- Affected or Damaged Region(s) (Gradient Field Area) (GFA)
- Threshold Value (TH)

Fig. 33 presents a direct relationship between Impact Energy and Gradient Field Area. This is logical as the higher the impact energy the larger the affected area.

Fig. 34 presents an inverse relationship between the selected Threshold and Gradient Field Area. This is also logical, since the more the affected area, the less of Threshold Value is required to uncover the affected region boundaries. This is also consistent with increasing the Impact Energy.

Fig. 35 establishes the relationship between Impact Energy and Gradient Field Area, which is a direct relationship as deduced from Fig. 34.

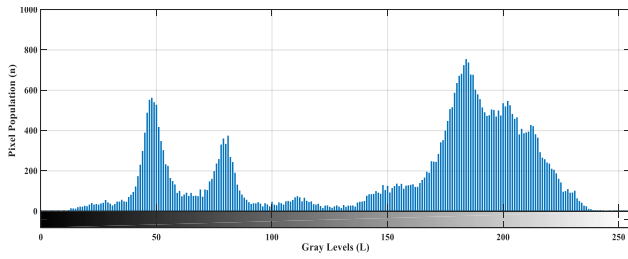


Fig. 27. Image Histogram: 28J Impact, 0.60 Threshold.

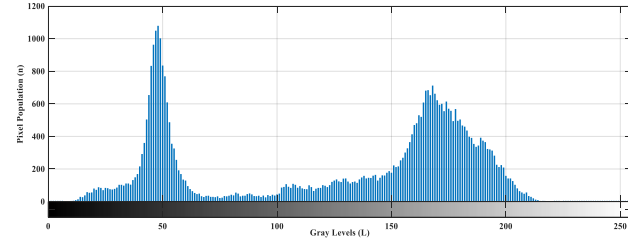


Fig. 28. Image Histogram: 42J Impact, 0.52 Threshold.

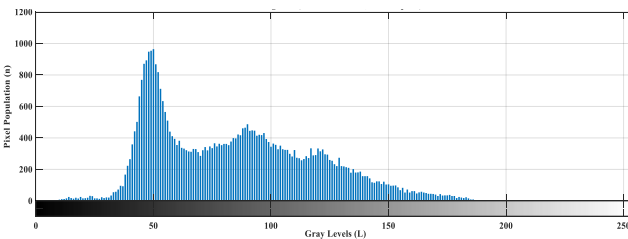


Fig. 29. Image Histogram: 56J Impact, 0.37 Threshold.

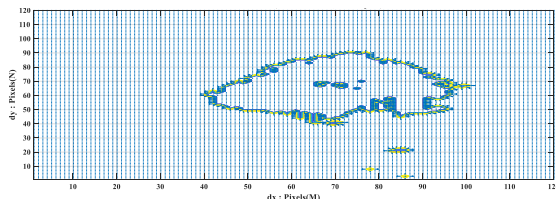


Fig. 30. Gradient Field Contour: 28J Impact, 0.60 Threshold.

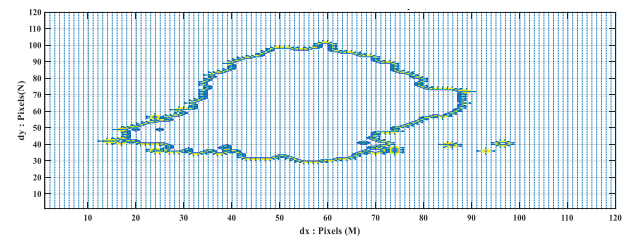


Fig. 31. Gradient Field Contour: 42J Impact, 0.52 Threshold.

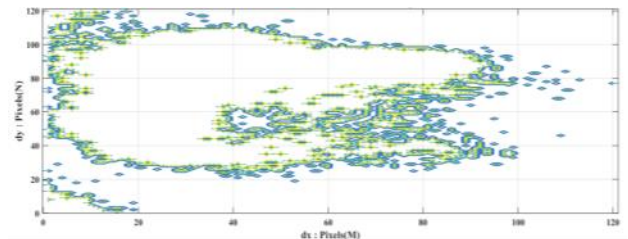


Fig. 32. Gradient Field Contour: 56J Impact, 0.37 Threshold.

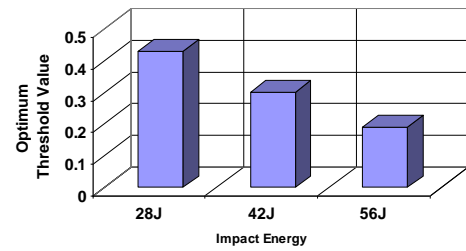


Fig. 33. Relationship between Impact Energy and Selected Threshold.

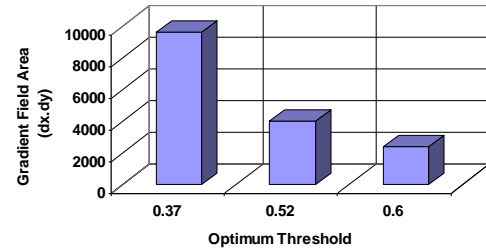


Fig. 34. Relationship between Optimum Threshold and Gradient Field Area.

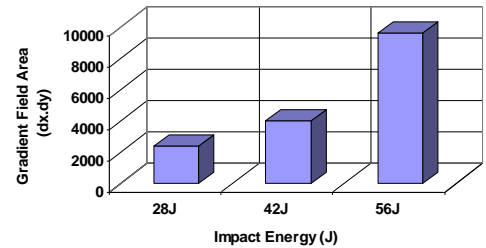


Fig. 35. Relationship between Impact Energy and Gradient Field Area.

The obtained images consist of two parts as shown in equation (1):

$$Image = \sum_{L=0}^{255} Healthy\ Part(Threshold) + \sum_{L=0}^{255} Damaged\ Part(Threshold) \quad (1)$$

Equation (1) can be further represented in relation to threshold values as shown in equation (2), which also applies to undamaged composites

$$Image = \left[\sum_{Threshold=0}^{1.0} (L_0 + L_{128} + L_{180}) \right] + [L_{255}] \quad (2)$$

Applying equation (2) to the tested composites at impact energies of 28J, 42J, and 56J, result in equations (3), (4), and (5).

$$Image(28J) = \left[\sum_{Threshold=0}^{0.6} (L_0 + L_{128} + L_{180}) \right] \quad (3)$$

$$Image(42J) = \left[\sum_{Threshold=0}^{0.52} (L_0 + L_{128} + L_{180}) \right] \quad (4)$$

$$Image(56J) = \left[\sum_{Threshold=0}^{0.37} (L_0 + L_{128} + L_{180}) \right] + [L_{255}] \quad (5)$$

VI. CONCLUSIONS

From the previous observations, we can establish the following:

1) Very Low Impact Energy ($0J \leq IE \leq 28J$)

No observed damage.

2) Lower Impact Energies ($28J \leq IE \leq 42J$):

a) Similar Histogram Characteristics

b) Localized Damage

c) Threshold decreases as Impact Energy Increases

d) Gradient Field Area Increases as Impact Energy Increases.

3) Higher Impact Energies ($IE \geq 56J$)

a) Unique Histogram Characteristics

b) Non-Localized Damage

c) Threshold decreases dramatically as Impact Energy Increases

d) Gradient Field Area Increases markedly as Impact Energy Increases.

The Optimum Threshold level that is used to uncover the extent of damage is related to Impact Energy through expression (6):

$$Th_{Optimum} = K * [\log(IE)]^{-1} \quad (6)$$

$Th_{Optimum}$ is bounded by the following conditions, which are established experimentally and is a function of sample mechanical properties as well as used imaging technique:

a) Very Low Impact Energies ($0J < IE < 28J$): $K=0.5$

b) Lower Impact Energies ($28J \leq IE \leq 42J$): $K=2$

c) Higher Impact Energies ($IE \geq 56J$): $K=1.5$

From Equation (1), we can reproduce a guiding curve describing the relationship between Required Optimum Threshold to uncover damage level and Impact Energy, as shown in Fig. 36.

From the plot, the three main bounding conditions are clear:

1) At very low Impact Energies, the composite sample will have negligible damage, hence, the sample and surface will possess uniform structure and that reduces the Optimum Threshold value to a very low level. Such Levels of Impact Energies can be neglected as it will not affect component safety and reliability.

2) At Lower Impact Energies, there is an evidence of damage and surface deformation as the Optimum Threshold increases.

3) At Higher Impact Energies, most of the tested component is damage as the damage propagates both in depth and breadth. This is a critical case of damage.

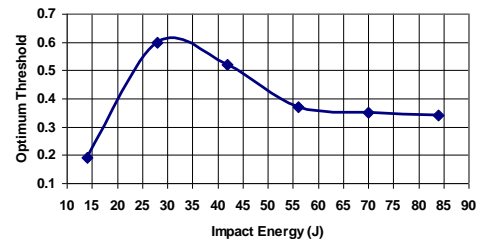


Fig. 36. Relationship between Impact Energy Optimum Threshold.

The proposed approach proved to be simpler, yet very effective approach for separating and segmenting damaged areas in composite structures compared to traditional techniques.

REFERENCES

- [1] Yue El-Hage, Simon Hind, and Francois Robitaille. 2018. Thermal conductivity of textile reinforcements for composites, *Journal of Textiles and Fibrous Materials*, 1 :1-12. DOI: 10.1177/2515221117751154
- [2] Francesco Ciampa, Pooya Mahmoodi, Fulvio Pinto, and Michele Meo. 2018. Recent Advances in Active Infrared Thermography for Non-Destructive Testing of Aerospace Components. *Sensors*, 609: 1-37. DOI: 10.3390/s18020609
- [3] Carlos G Da'vila and Chiara Bisagni. 2018. Fatigue life and damage toleranc of postbuckled composite stiffened structures with indentation damage. *Journal of Composite Materials*, 52(7): 931-943. DOI: 10.1177/0021998317715785.
- [4] L. Ma and D. Liu. 2016. Delamination and fiber-bridging damage analysis of angle-ply laminates subjected to transverse loading. *International Journal of Imaging Systems and Technology*, 50 (22): 3063-3075. DOI: 10.1177/0021998315615647.
- [5] F.Wang, J. Liu, Y. Liu, and Y. Wan. 2016. Research on the fiber lay-up orientation detection of unidirectional CFRP laminates composite using thermal-wave radar imaging. *International Journal of Imaging Systems and Technology*, 84: 54-66. <http://dx.doi.org/10.1016/j.ndteint.2016.08.002>
- [6] T.Liang, W. Ren, G. Tian, M. Elradi, Y. Gao. 2016. Low energy impact damage detection in CFRP using eddy current pulsed thermography. *Composite Structure*, 143: 352-361. DOI: 10.1016/j.compstruct.2016.02.039.
- [7] R.Yang, Y. He, H. Zhang. 2016. Progress and trends in nondestructive testing and evaluation for wind turbine composite blade. *Renewable and Sustainable Energy Reviews*, 60: 1225-1250. DOI: 10.1016/j.rser.2016.02.026.
- [8] L. Ma and D. Liu. 2016. Delamination and fiber-bridging damage analysis of angle-ply laminates subjected to transverse loading. *International Journal of Imaging Systems and Technology*. 50: 3063-3075. DOI: 10.1177/0021998315615647
- [9] F.Wang, J. Liu, Y. Liu, and Y. Wang. 2016. Research on the fiber lay-up orientation detection of unidirectional CFRP laminates composite using thermal-wave radar imaging. *International Journal of Imaging Systems and Technology*. 84: 54-66. DOI: 10.1016/j.ndteint.2016.08.002
- [10] T.Liang, W. Ren, G. Tian, M. Elradi, Y. Gao. 2016. Low energy impact damage detection in CFRP using eddy current pulsed thermography. *Composite Structure*, 143:352-361. DOI: 10.1016/j.compstruct.2016.02.039.
- [11] M. Iskandarani. 2017. Correlating and Modeling of Extracted Features from PVT Images of Composites using Optical Flow Technique and Weight Elimination Algorithm Optimization [OFT-WEA]. *Journal of Computer Science*, 13(9): 371-379. DOI: 10.3844/jcssp.2017.371.379
- [12] F.Peng, J. Li, and M. Long. 2015. Identification of Natural Images and Computer-Generated Graphics Based on Statistical and Textural Features. *Journal of Forensic Sciences*, 60 (2): 435-443. DOI: 10.1111/1556-4029.

- [13] P. Geng, X. Su, T. Xu, J. Liu. 2016. Multi-modal Medical Image Fusion Based on the Multiwavelet and Non sub sampled Direction Filter Bank. International Journal of Signal Processing, Image Processing and Pattern Recognition, 8(11):75-84. DOI: 10.14257/ijcip.2015.8.11.08
- [14] K. Santhi, R. WahidaBanu. 2015. Adaptive contrast enhancement using modified histogram equalization. Optik - International Journal for Light and Electron Optics. Elsevier, 126: 1809–1814. DOI: 10.1016/j.ijleo.2015.05.023
- [15] L. Huang, W. Zhao, Z. Sun and J. Wang. 2015. An advanced gradient histogram and its application for contrast and gradient enhancement. Optik - International Journal for Light and Electron Optics. Elsevier, 31: 86 – 100. DOI: 10.1016/j.jycir.2015.06.007
- [16] H. Xu, Q. Chen, C. Zuo, C. Yang and N. Liu. 2015. Range limited double-thresholds multi-histogram equalization for image contrast enhancement. Optical Review. Springer, 22: 246 – 255. DOI: 10.1016/j.ijleo.2011.12.057
- [17] B. Ashwini, B. Yuvaraju. 2016. Feature Extraction Techniques for Video Processing in MATLAB. International Journal of Innovative Research in Computer and Communication Engineering, 4 (4): 5292–5296. DOI: 10.15680/IJIRCCCE.2016.0404223.
- [18] M. Iskandarani. 2018. Characterization of Composite Structure Surface Uniformity using Interval Based Gradient Field Histogram Analysis of Thermographic Images (IGF-HA). Journal of Computer Science, 14(6): 816-828. DOI: 10.3844/jcssp.2018.819.828.
- [19] M. Iskandarani. 2018. Modelling of Thermal Storage in Damaged Composite Structures using Time Displaced Gradient Field Technique (TDGF). (IJACSA) International Journal of Advanced Computer Science and Applications, 9(6): 55-59. DOI: 10.14569/IJACSA.2018.090608

Images Steganography Approach Supporting Chaotic Map Technique for the Security of Online Transfer

Yasser Mohammad Al-Sharo
Faculty of Information Technology
Ajloun National University, Jordan

Abstract—One of the most important issue in this domain is the security concern of the transfer data. The online transfer data may access illegally through attack the communication gate between the servers and the users. The main aim of this study is to enhance the security level of the online data transfer using two integrated methods; images steganography to hide the transfer data in image media, and chaotic map to remap the original format of the transfer data. The integration between these two methods is effective to secure the data in several format such as text, audio, and images. The proposed algorithm is the prototyped using JAVA programming, 20 images and text messages of usable sizes (plain data) were tested on the dataset using the developed programming. The simulation using local server is accomplished to analyze the security performance based on two factors; the plain data size and the data transfer distance. Many attacking attempts are performed on the simulation test using known attacking techniques such as observe the stego images quality. The experiment results show that about 85% of the attacking attempts fail to catch the stego images. 95% of the attacks fail in remap meaningful parts of the chaotic data. The results indicate the very good level of the propose security methods to secure the online transfer data. The contribution of this study is the effective integration between the steganography and chaotic map approaches to assure high security level of online data transfer.

Keywords—Security; steganography; chaotic map; encryption; network data

I. INTRODUCTION

The era of the globalization increase the importance of online data/information transfer as one of the most important success keys of the businesses competitive advantages [1]. Through the online gathering of the data, the businesses gain many advantages such as: (i) reduce the operational costs of gather the data between the organization branches, department, and users; (ii) improve the products quality based on real time services; (iii) assure the availability and accessibility of the services in anytime and from anywhere. However, several security threats such as viruses, worms, and hacking are concerns of the online data transfer [2,3,4]. These threats could damage or stole the transfer data via the internet gate, which may lead to the fail of the technology of online data transfer. Thus it is important to assure the high security level of the online data transfer to allow the originations to gain the expected business benefits without high risks.

The security of online data transfer is not simple due to many factors like the volume of the transfer data, the format of the transfer data, and the transfer distance [5]. These factors

effect on the selection of the security methods that could be applied to secure the online transfer data. For example, the symmetric or asymmetric encryption techniques are not suitable to encrypt large volume of data, especially the data of images, video, or audio format [6,7]. Hence, the selection of applicable security methods would be decided based on many factors that related to online data transfer.

The Steganography is effective approach that would be used to hide the online gathered data using the embedding images [8]. Steganography is effective due to many reasons such as ability to hide the data of various formats, ability to hide large volume of plain data, and the effectiveness of transfer hidden data over large transfer distance [8]. According to [9], The Steganography is more effective than the cryptography approaches due to difficulty of catch the plain data by the attacker and tries to decrypt it using many attacking techniques such as automatic decryption keys.

Kumar and Pooja [10] mentioned that although steganography is effective security approach, there plain data is hide as its original form, which make it simple for extract the plain data in case of catch the embedded data by the attacker. Therefore, it is more useful to support the steganography by other encryption or security techniques in order to hide encrypted data in the embedded image rather than hide the plain data as it is. For this purpose the chaotic map technique could be applied. In security systems, the chaotic scheme is used to create random swapping of plain information to increase the difficulty of stole the original information by attacker (Khan, & Shah, 2014). Technically, some elements positions of plain information are swapped using random sub situation key. The original values of swapped elements are updated to include the real value of the element plus the value of original element position [11]. This increases the difficulty of access the real value of plain information. The chaotic map is applicable to secure the various formats and volume of online transfer data.

Consequently, the steganography and chaotic map methods could be integrated effectively to secure the online transfer data. The plain data can be secured using chaotic map technique before hide the secured data in embedded file or image (steganography). Thus, it is complex to extract and remap the hidden and secured data due to necessity of accomplish two hacking stages on two effective security methods of online transfer data. The attackers need to know and catch the stego data, then remap the chaotic data, which expected to be so hard.

Keep in mind the above discussion, the main aim of this study is to enhance the security level of the online transfer data using two integrated methods (steganography and chaotic map). In this study, the algorithm of the proposed methods would be suggested, the prototype of the algorithm will explain, and the experiments tests would be conducted. The next section discusses the related works in order to construct the propose algorithm, the third section will explain the details of the research methods, section 4.0 discusses the findings, and lastly, Section V provides the study conclusion and the future works.

II. RELATED WORKS

Mollah et al. [6] explain the three junctions of the security of online data transfer; security of the users' devices, server security, and the security of communication paths. Most of data attacks are happen at the communication path [12], which represents the wire or wireless connection between the server and the users' devices.

The researchers propose several security methods to improve the security level of the transfer data via the online connections. The symmetric and asymmetric data encryption methods are effective to secure the textual plain data [6, 7, 13]. Although the data encryption is not expensive earthier in time or money, the symmetric and asymmetric is not effective for the large volume data such as images, audio or video.

Other researchers propose the load balancing method to assure that the transfer data is not holding in the connection paths due network traffic [14-17]. The load balancing technique aims to analyze the free connection paths and estimate the transfer paths of the whole data or blocks of data. This technique is helpful to reduce the opportunity of attack the hold data in the connection paths. The main drawback of load balancing is the possibility of rapid change in the network traffic, which require costly requirements of pre-paths booking. On other hand, the balancing technique is based on transfer the data as its plain form without encryption processes. Therefore, the risk of attack the data will be high.

Furthermore, the offloading transfer techniques is security methods that proposed by many researchers [12, 18- 21]. The offloading is based on reduce the online processes of data transfer as possible as can. The online connections are for the purpose of data transfer between the organization server and the online server. Hence, the data via offline mode can be gathered between the organization server and the users. Although, the offloading technique reduce the number of online connections, the organization need to have expansive network requirements such as offline servers and offline connections based on wire technology.

Additionally, the researchers suggested the devices signatures to improve the security level of online connections [22-24]. The signatures of users' devices can be defined in advance to access the services of online data transfer. The strange signature will be prevented from access the network services. Device signature is effective in case of small number of users or specific network services in the organizations. It is

not possible to define the large number of signatures of users' devices, especially when the online services are global for all possible users such as yahoo email.

The steganography is proposed by many researches as effective security method to hide the plain data in embedding files such as images [25- 27]. Hence, it is difficult to detect the embedding files and extract the plain data from these files. Mahajan and Kaur [5] surveyed the main factors that could improve the steganography effectiveness. The main analyzed factors are the plain data characteristics (such as format and size), embedding files characteristics, and the data transfer distance. The selection of the embedding files is affected by the plain data characteristics and the transfer distance. The speed of data transfer is important to minimize the data attacking that may cause due to data holding/waiting in the transfer paths. Hence, it is not recommended to use large size of embedding files for steganography. Hence, the steganography effectiveness can be assured through use supporting techniques to strength the plain data security using suitable size of embedding files.

Sedighi et al. [26] discuss the steganography processes and calculations as Fig. 1 illustrates. The most useful embedding file that could use in the steganography is the image type. In order to assure effective stego processes, the candidate embedding image should be analyze (like variance estimation and detectably calculation) to deicide the most suitable part to hide the plain data. The main purpose here is the hide the plain data in embedding image that hard to be observed by the attackers. Thus, the plain data would code in a manner that not-effect on the quality of the embedding image.

Sedighi et al. [26] founded that it is effective to hide the plain data in a part of embedding image based on two main processes. Firstly, analyze the quality and variance of the embedding image based on the following equation:

$$R(\beta) = \sum H(\beta_n), \text{ Where } R(\beta) \text{ is the lightness volume of the image parts.} \quad (1)$$

Based on the above equation it is useful to hide the plain data in the most lightness part. The second process is to decide what the pixels that can be replaced by the plain data with minimum effect on the selected part quality, and this can be obtained using the following equation:

$$D(x,y) = \sum \rho_n [x_n \neq y_n], \quad (2)$$

Where $\rho_n \geq 0$ is the cost of changing pixel x_n tied to β_n via: $\beta_n = e^{-\lambda \rho_n / 1 + 2 e^{-\lambda \rho_n}}$, with $\lambda > 0$ determined from the payload constrain of the Equation #1

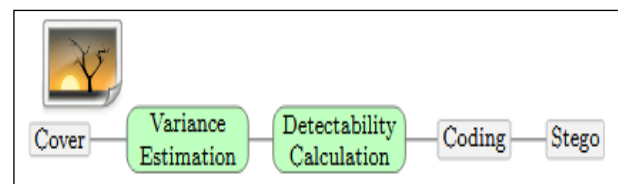


Fig. 1. Steganography Processes (Sedighi et al., 2016).

Another effective security technique is the chaotic scheme, which is used to create random swapping of plain data to increase the difficulty of stealing the original information by an attacker [23]. The chaotic scheme can be described in four main points which are: (1) permutation, where the values of the selected bits/pixels in the plain data are updated as the value of the pixel/bit plus the value of the position. Here it is necessary to work based on permutation to simplify the remapping of the updated data; (2) substitution, whereby the position of each updated bit/pixel is swapped with other bit/pixel. The De-substitution key is necessary to be known by the destination. The permutation and substitution rounds depend on the data size; (3) De-substitution data using the key that owned by the destination; (4) De-permutation the data using the key that owned by the destination [11]. The main advantage of the chaotic map is the possibility to deal with plain data of various sizes and different format. However, the drawback of this technique is the possibility to attack the data through trying to know the De-permutation and De-substitution keys.

Table I summarizes the advantages and disadvantages of the reviewed security methods and techniques. It can be concluded that the most useful integration could happen between the steganography method and the chaotic map technique.

III. RESEARCH METHODS

As concluded from the above section the integration between the steganography and the chaotic map could conduct

effective security level of the online transfer data. The scope of this study is the protection of online transfer data of text and image format due to wide using of these formats in the transferring processes. Fig. 2 illustrates the proposed integration processes. Firstly, the plain data will be protected using chaotic map technique through the permutation and substitution phases. The de-fusion key in each phase will be produced to simplify the remapping of the plain data. The suggested permutation rounds are 200 due to size of the plain data, which will explain in the dataset features in this section. The substitution rounds are 100 (half of permutation rounds). Each two permutation bits/pixels (two permutation rounds) will substitute in one round.

As illustrated in Fig. 2, after conducting the chaotic map processes, the produced data will be processed by the steganography method. The format of the embedding file is images due to the effectiveness of hiding the data in images with low effects on the image quality. Thus, the attacker will find it difficult to detect the embedding images. The steganography processes are: (i) detect the most lightness parts in the embedding images using equation 1; and (ii) replace the detected parts by the data that has already been processed by the chaotic map. In total, the chaotic technique will remap the plain data to increase the difficulty of getting meaningful data, and the steganography will hide the chaotic data to increase the difficulty of catching the online transfer data. Hence, it is hard to attack the protected images using two effective and integrated security approaches (steganography and the chaotic map).

TABLE I. SUMMARY OF SECURITY METHODS AND TECHNIQUES

Source	Security technique	Advantages	Disadvantages	Conclusion
[6, 7, 13]	Data encryption	-Not expensive -fast processes	- Used for textual plain data only. - challenges in handling the large data volume.	Can be used for online data transfer of texts. However, it is not recommended for the large data sizes.
[14, 15, 16, 17]	Load balancing	-Avoid the data holding in the online connections.	- The data not encrypted. - The unexpected traffic may happen when transferring the data.	Can be used as a supportive technique alongside other data security methods.
[12, 18, 19, 20, 21]	Offloading Transfer	-Reduce the online connections between the users and the online server.	- Require extensive requirements.	Can be used for local services of the organizations.
[22, 23, 24]	Device signature	- prevent strange devices from accessing the network services.	- not possible for open access services of undefined users such as yahoo email.	Used to limit services of online data transfer.
[25, 26, 27]	Steganography	- Difficulty of detecting the embedding files.	- The plain data is hidden as its original form.	Need to be supported by other techniques.
[11, 23]	Chaotic Map	- Deal with data of various sizes and formats.	Ability to handle the De-permutation and De-substitution keys.	Can be used as a supportive technique rather than a main technique.

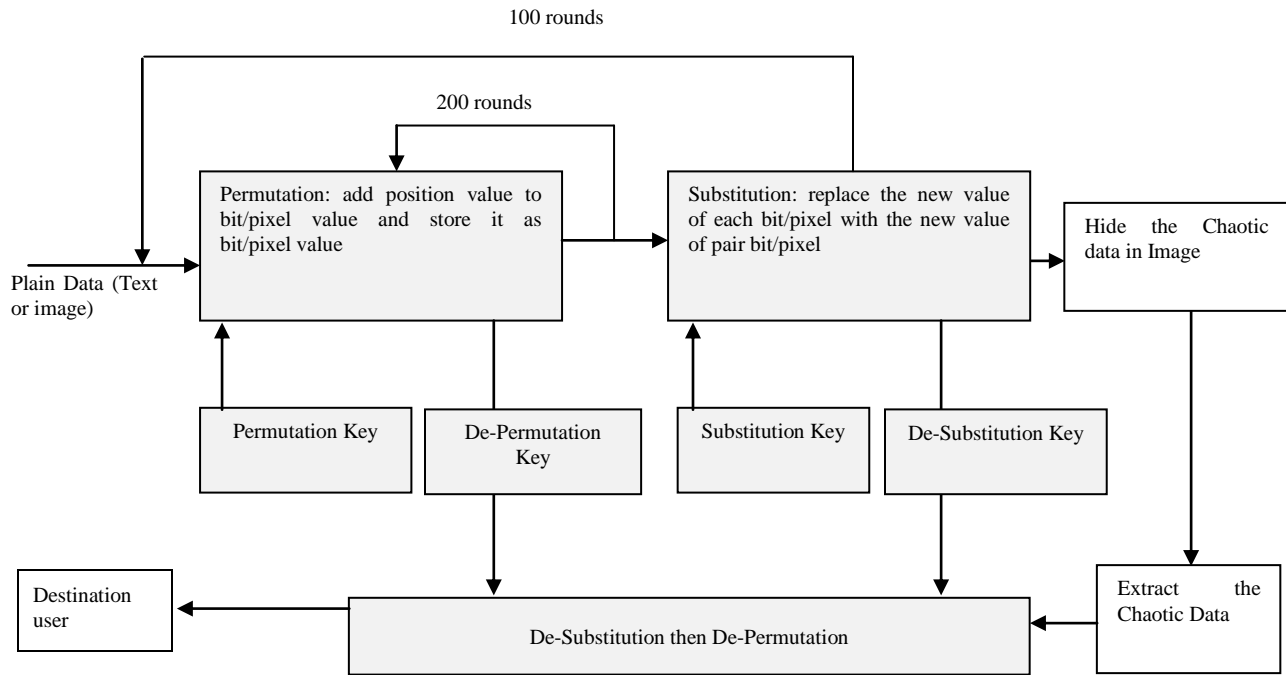


Fig. 2. Methods Design.

Based on the proposed methods in this study, a prototyping using Java programming language is developed to handle the following algorithm:

1. Get plain data (text or image).
2. Select 200 bits/pixels randomly.
3. The value of each selected bit/pixel= the value of the bit/pixel + the value of the current position.
4. Store the permutation key that used in previous step.
5. Randomly swap each bit/pixel in step 3 and with pair bit/pixel.
6. Store the permutation key that used in previous step.
7. Store the produced data
8. Detected the lightness of the embedding image: $R(\beta) = \sum H(\beta_n)$
9. Hide the data in step 7 in the detected part in step 8: $D(x,y) = \sum p_n[x_n \neq y_n]$.
10. Save the embedding image that contains the swapped plain data.

The dataset of this study is composed of the embedding image for the purpose of steganography, and this dataset is adopted by Mahajan & Kaur (2012) study for purpose such as steganography. The dataset is called Kodak which consists of 12 testing images of different features. The main features in dataset images are the quality (PSNR) and images dimensions. These features play important role in increase the steganography effectiveness. Table II summarizes the features of the steganography dataset.

In order to test the algorithm prototyping based on the experimental database, a network simulation is conducted using MATLAB distributed toolbox. Through this toolbox the online data transfer is simulated between two users over large transfer distance i.e. 5000 KM. The simulation includes many attacks techniques that produced at the connection paths of the simulation while transfer the data. The steps of the used attacking techniques are adopted from da Silva et al. [29] and Van Den et al. [30]. The adopted steps are programmed and simulated using MATLAB, and the main attacks techniques are as the following [31]: (1) Traffic analysis: this technique work on detect the embedding files of sizes over the usual or standard sizes i.e. image of size in MBs. This technique can be used to detect the embedding images of steganography. (2) Eavesdropping: this technique is usually used to capture the security keys between the sender and receiver (such as de-permutation key in chaotic map) before trying to resolve the plain data using the captured keys.

TABLE II. FEATURES OF THE STEGANOGRAPHY DATASET

Image Name	Image Type	Image Size	Image Dimensions	Image Quality (PSNR)	Images Color Type
House	PNG	30.6 KB	256*256	25	Grayscale
House	PNG	28.3 KB	256*256	28	Grayscale
House	PNG	25.6 KB	256*256	33	Grayscale
House	PNG	26.4 KB	256*256	39	Grayscale
Lena	PNG	129 KB	512*512	25	Grayscale
Lena	PNG	250 KB	512*512	28	Grayscale
Lena	PNG	370 KB	512*512	33	Grayscale
Lena	PNG	400 KB	512*512	39	Grayscale
Kodak	PNG	511 KB	768*512	28	Color
Kodak	PNG	730 KB	768*512	30	Color
Kodak	PNG	802 KB	768*512	33	Color
Kodak	PNG	818 KB	768*512	43	Color

IV. DISCUSSION AND FINDINGS

As mentioned in the previous section, the proposed algorithm (in integration between steganography and chaotic map) was tested on dataset of 12 embedding images and simulated based on large distance of online data transfer.

The observation of the steganography processes indicates that the colored images of high PSNR (i.e. $PSNR > 40$) would be effective in hide the plain data of image type more than the gray-scale images of $PSNR < 30$; The size of plain images is up to 500 KB. Fig. 3 show embedding image quality before and after hide the plain data of image type. Thus, it is better to secure the plain data of images type using colored plain images.

On the other hand, it is effective to secure textual plain data of size up to 300 KB using gray-scale embedding image of $PSNR > 30$. Fig. 4 shows the quality affection of embedding image after hide text plain data up to 300KB size. Hence, the gray-scale embedding images of $PSNR \geq 30$ is used to hide the plain data of text type.

The effective embedding images are selected to hide the plain data of images and texts. These images are used to apply the proposed algorithm of this study based on the following experimental processes:

- The chaotic map is conducted on the plain data before complete the steganography processes.
- The network simulation is constructed using MATLAB distributed system.
- The embedding images that contain the plan data are transfer over large distances (i.e. 1000, 2000, and 5000 KM).
- The transfer data are attacked using two techniques; traffic analysis and eavesdropping.

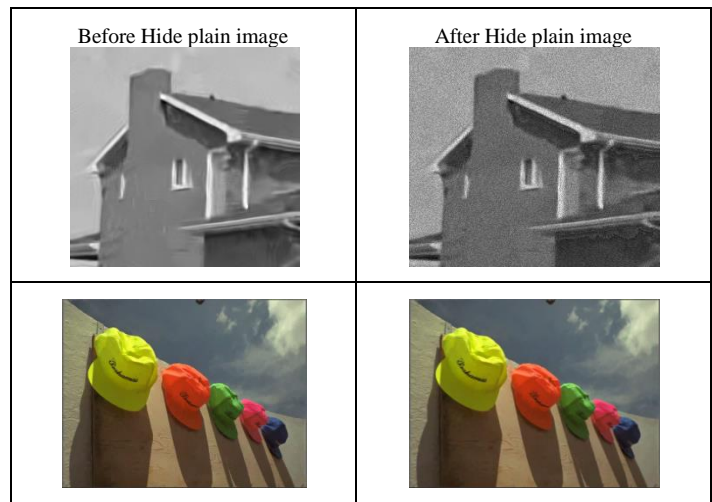


Fig. 3. Embedding Image Quality to Hide the Plain Images.



Fig. 4. Embedding Image Quality to Hide the Plain Texts.

The experimental processes conducted on 20 plain data; 10 image messages and 10 texts messages. The sizes of the images messages are between 400-500 KB, and the sizes of the text messages are between 100-300 KB. Fig. 5 shows the analysis of attacking techniques on the embedding files that contain the plain images. The traffic analysis technique fail in detect 8/10 embedding images. Consequently, the eavesdropping attacking technique fails in remap any plain data of the two detected embedding images.

On the other hand, Fig. 6 shows the analysis of attacking techniques on the embedding files that contain the plain texts. The traffic analysis technique fail in detect 9/10 embedding images. Consequently, the eavesdropping attacking technique success on remap meaningful parts of the plain text in the detected embedding image due to success of resolve the remapping keys.

Based on the experimental tests, it can be concluded that the proposed integration between the steganography and chaotic map techniques is effective. 17 out 20 embedding images (85% of all embedding images) are not detected by the attacks. On the other hand, 19 out 20 plain data (95% of the transfer data) are not resolved by the attacks. It is necessary to mentioned that the steganography represent the first defending stage in the proposed security algorithm, and the second defending stage is represented by the chaotic map.

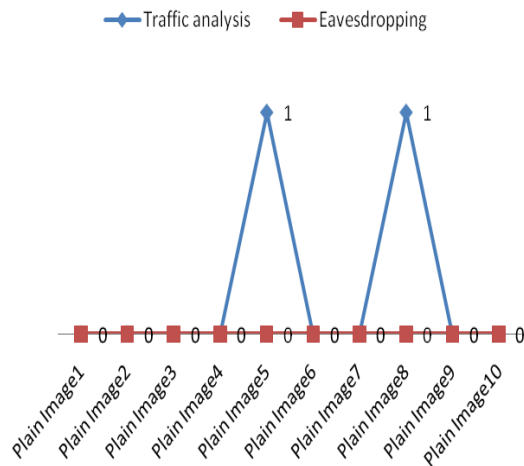


Fig. 5. Attacking on Plain Images.

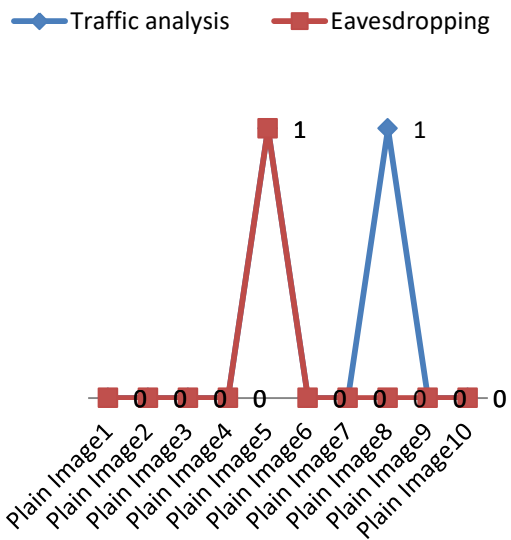


Fig. 6. Attacking on Plain Texts.

V. CONCLUSION AND FUTURE WORKS

The various businesses are gain benefit from the online transfer data. Hence, the security of the online transfer data is very important to assure the safety of businesses data. Several security approaches and techniques are reviewed in this study. The objective of this study is to perform the integration between the steganography and chaotic map techniques in order to secure the online data transfer. The proposed algorithm, prototyping, and simulation of the proposed techniques are conducted. The experimental results show the difficulty of attack and resolve the plain data due to difficulty of attack the two integrated security stage in this study. In the future, more experimental tests will be conducted based on different features of the embedding images, different selections of chaotic map, and different sizes of the plain data.

REFERENCES

- [1] Grabara, J., Kolcun, M., & Kot, S. (2014). The role of information systems in transport logistics. *International Journal of Education and Research*, 2(2), 1-8.
- [2] Masala, G. L., Ruiu, P., & Grosso, E. (2018). Biometric authentication and data security in cloud computing. In *Computer and Network Security Essentials* (pp. 337-353). Springer, Cham.
- [3] Haager, J., Sandwith, C., Terrano, J., & Saripalli, P. (2018). U.S. Patent No. 9,990,502. Washington, DC: U.S. Patent and Trademark Office.
- [4] Kulkarni, M. P., Ghumare, S. A., & Kulkarni, A. (2016). Electronic Fund Transfer: A study of security control in selected banks of Pune Region. *International Journal on Recent and Innovation Trends in Computing and Communication*, 4(5), 486-489.
- [5] Mahajan, M., & Kaur, N. (2012). Adaptive steganography: a survey of recent statistical aware steganography techniques. *International Journal of Computer Network and Information Security*, 4(10), 76.
- [6] Mollah, M. B., Azad, M. A. K., & Vasilakos, A. (2017). Security and privacy challenges in mobile cloud computing: Survey and way ahead. *Journal of Network and Computer Applications*, 84, 38-54.
- [7] Liaqat, M., Chang, V., Gani, A., Ab Hamid, S. H., Toseef, M., Shoaib, U., & Ali, R. L. (2017). Federated cloud resource management: Review and discussion. *Journal of Network and Computer Applications*, 77, 87-105.
- [8] Hamid, N., Yahya, A., Ahmad, R. B. & Al-Qersh, O. M. 2012. Image Steganography Techniques: An Overview. *International Journal of Computer Science and Security (IJCSS)* 6(3): 168.
- [9] Nameer, N. & Eman, E. 2007. Hiding a Large Amount of Data with High Security using Steganography Algorithm. *Journal of Computer sciences* 223-232.
- [10] Kumar, A. & Pooja, K. 2010. Steganography-a Data Hiding Technique. *International Journal of Computer Applications IJCA* 9(7): 24-28.
- [11] Mishra, M., Singh, P. and Garg, C., 2014. A New algorithm of encryption and decryption of images using chaotic mapping. *International Journal of Information & Computation Technology*. ISSN, pp.0974-2239.
- [12] Akherfi, K., Gerndt, M., & Harroud, H. (2016). Mobile cloud computing for computation offloading: Issues and challenges. *Applied Computing and Informatics*.
- [13] Anwar, S., Inayat, Z., Zolkipli, M. F., Zain, J. M., Gani, A., Anuar, N. B., & Chang, V. (2017). Cross-VM cache-based side channel attacks and proposed prevention mechanisms: A survey. *Journal of Network and Computer Applications*, 93, 259-279.
- [14] Ghomi, E. J., Rahmani, A. M., & Qader, N. N. (2017). Load-balancing algorithms in cloud computing: A survey. *Journal of Network and Computer Applications*, 88, 50-71.
- [15] Aslam, S., ul Islam, S., Khan, A., Ahmed, M., Akhundzada, A., & Khan, M. K. (2017). Information collection centric techniques for cloud resource management: Taxonomy, analysis and challenges. *Journal of Network and Computer Applications*.
- [16] Madni, S. H. H., Latiff, M. S. A., & Coulibaly, Y. (2016). Resource scheduling for infrastructure as a service (IaaS) in cloud computing: Challenges and opportunities. *Journal of Network and Computer Applications*, 68, 173-200.
- [17] Gani, A., Nayeem, G. M., Shiraz, M., Sookhak, M., Whaiduzzaman, M., & Khan, S. (2014). A review on interworking and mobility techniques for seamless connectivity in mobile cloud computing. *Journal of Network and Computer Applications*, 43, 84-102.
- [18] Bhattacharya, A., & De, P. (2017). A survey of adaptation techniques in computation offloading. *Journal of Network and Computer Applications*, 78, 97-115.
- [19] Vaezpour, S. Y., Zhang, R., Wu, K., Wang, J., & Shoja, G. C. (2016). A new approach to mitigating security risks of phone clone co-location over mobile clouds. *Journal of Network and Computer Applications*, 62, 171-184.

- [20] Shaukat, U., Ahmed, E., Anwar, Z., & Xia, F. (2016). Cloudlet deployment in local wireless networks: Motivation, architectures, applications, and open challenges. *Journal of Network and Computer Applications*, 62, 18-40.
- [21] Shuja, J., Gani, A., ur Rehman, M. H., Ahmed, E., Madani, S. A., Khan, M. K., & Ko, K. (2016). Towards native code offloading based MCC frameworks for multimedia applications: A survey. *Journal of Network and Computer Applications*, 75, 335-354.
- [22] Singh, A., & Chatterjee, K. (2017). Cloud security issues and challenges: A survey. *Journal of Network and Computer Applications*, 79, 88-115.
- [23] Khan, M. and Shah, T., 2014. A novel image encryption technique based on Hénon chaotic map and S8 symmetric group. *Neural Computing and Applications*, 25(7-8), pp.1717-1722.
- [24] Khan, S., Shiraz, M., Boroumand, L., Gani, A., & Khan, M. K. (2017). Towards port-knocking authentication methods for mobile cloud computing. *Journal of Network and Computer Applications*, 97, 66-78.
- [25] Douglas, M., Bailey, K., Leeney, M., & Curran, K. (2018). An overview of steganography techniques applied to the protection of biometric data. *Multimedia Tools and Applications*, 77(13), 17333-17373.
- [26] Sedighi, V., Cogramne, R., & Fridrich, J. (2016). Content-adaptive steganography by minimizing statistical detectability. *IEEE Transactions on Information Forensics and Security*, 11(2), 221-234.
- [27] Rani, M., & Bedi, C. S. (2015). Review of Various Image Steganography Techniques and Different Type For Data Hiding Scheme. *ZENITH International Journal of Multidisciplinary Research*, 5(9), 19-23.
- [28] Liu, J., Ahmed, E., Shiraz, M., Gani, A., Buyya, R., & Qureshi, A. (2015). Application partitioning algorithms in mobile cloud computing: Taxonomy, review and future directions. *Journal of Network and Computer Applications*, 48, 99-117.
- [29] da Silva, E. G., Knob, L. A. D., Wickboldt, J. A., Gaspar, L. P., Granville, L. Z., & Schaeffer-Filho, A. (2015, May). Capitalizing on SDN-based SCADA systems: An anti-eavesdropping case-study. In *Integrated Network Management (IM), 2015 IFIP/IEEE International Symposium on* (pp. 165-173). IEEE.
- [30] Van Den Hooff, J., Lazar, D., Zaharia, M., & Zeldovich, N. (2015, October). Vuvuzela: Scalable private messaging resistant to traffic analysis. In *Proceedings of the 25th Symposium on Operating Systems +Principles* (pp. 137-152). ACM.
- [31] Pawar, M. V., & Anuradha, J. (2015). Network security and types of attacks in network. *Procedia Computer Science*, 48, 503-506.

ABCVS: An Artificial Bee Colony for Generating Variable T-Way Test Sets

Ammar K Alazzawi¹, Helmi Md Rais², Shuib Basri³

Department of Computer and Information Sciences, Faculty of Science and Information Technology
Universiti Teknologi Petronas, Bandar Seri Iskandar 32610, Perak, Malaysia

Abstract—To achieve acceptable quality and performance of any software product, it is crucial to assess various software components in the application. There exist various software-testing techniques such as combinatorial testing and covering array. However, problems such as t -way combinatorial explosion is still challenging in any combinatorial testing strategy, as it takes into consideration the entire combinations of input variables. Therefore, to overcome this problem, several optimizations and metaheuristic strategies have been suggested. One of the most effective optimization algorithms based techniques is the Artificial Bee Colony (ABC) algorithm. This paper presents t -way generation strategy for both a uniform and variable strength test suite by applying the ABC strategy (ABCVS) to reduce the size of the test suite and to subsequently enhance the test suite generation interaction. To assess both the effectiveness and performance of the presented ABCVS, several experiments were conducted applying various sets of benchmarks. The results revealed that the proposed ABCVS outweigh the existing based strategies and demonstrated wider interaction between components as opposed to AI-search based and computational based strategies. The results also revealed higher prospect of ABCVS in the aspect of its effectiveness and performance as observed in the majority of case studies.

Keywords— T -way testing; variable-strength interaction; combinatorial testing; covering array; test suite generation; artificial bee colony algorithm

I. INTRODUCTION

For investigate acceptable quality and performance for any software product, it is important to assess the various software components in the application. Software testing is afforded with many techniques and tools, divided into two major categories; Black box and White box testing. The inner components of the system under test (SUT) in performing white-box testing, are considered during the generation of the test case, while the input variables and how they interact as a significant function in black-box testing, occurs during test suite production [1]. Due to the complexity of the most software systems, therefore, all-inclusive testing taking the entire configurations and interactions into consideration is not feasible due to computational constraints as well as the need for sampling strategies [2]. From several of the techniques available for black box software, both combinatorial testing (CT) in addition to covering array (CA) are suitable approaches used for testing purposes. In fact, some studies of t -way interaction testing have indicated this form of testing to be effective in identifying nearly all of the flaws in a typical software system [3]. Notably, various uniform and variable

strength t -way techniques are documented throughout the literature in this domain.

However, combinatorial explosion in a combinatorial testing strategy such as a t -way is a problem. Moreover, while it is not feasible to generate the entire combination of variables in this case, it is necessary that a CA of minimum size be generated. Generally, the minimum size of a CA is an unspecified priori. Therefore, it is advisable to generate as much CA as possible with several test cases within an acceptable amount of time. Various strategies have been found in the literature to produce the test suite size with uniform and variable strength interaction. Accordingly, to assess such a strategy, three features are required, namely; 1) the array size of the test suites that denote the effectiveness, 2) speed of the strategy, which refers to performance, and 3) portability of the strategy to support adequate high interaction strength. Different approaches have been adopted using numerous strategies, such as; Artificial Intelligence (AI) based and Pure Computational-based approaches [4]. These strategies are based on pure computational-based approaches which are characterized by their high performance but having worst efficiency, for instance; In-Parameter-Order-General (IPOG-D) [5] and Intelligent Test Case Handler (ITCH) [6]. While ITCH generates test suites of small array sizes, the IPOG D strategy, on the other hand, has a fast-paced approach. Previous studies have suggested that when a small interaction strength is considered (i.e. $t \leq 3$), it can cover most flaws in a typical software system [7-12]. Subsequent research studies although, have proposed the need to support the higher strength interaction, particularly for complex systems [2, 4, 13-15].

The appropriate solution to address the problems associated with the computation of the minimal test suite is by employing a search-based software engineering (SBSE) technique [16-19]. By drawing inspiration from the SBSE technique, various strategies have already been suggested towards the problem of uniform and variable strength interaction (e.g. Simulated Annealing (SA) [9-11, 20, 21], Genetic Algorithm (GA) [12, 21-27], Practice Swarm Optimization (PSO) [7, 28-30], Ant Colony Algorithm (ACA) [8, 12], Harmony Search Algorithm (HS) [4, 31, 32], Cuckoo Search (CS) [3, 33, 34], and the Bat Algorithm (BA) [35-39]). Even though relevant strategies have been found to be useful based on AI, they are noted in the literature as being slow due to costly computations [3, 4, 7]. Another challenge encountered for some AI-based strategies that are considered to be slow is support for small interaction strengths (i.e. $t \leq 4$) for generating test suites. Therefore, in this paper, the ABC algorithm is proposed as an efficient and

acceptable strategy, known as the Artificial Bee Colony Strategy (ABCVS) continuous to our previous research [40, 41] for uniform and variable strength interaction t -way minimal test suite production. It is anticipated that ABCVS will address this problem. In fact, experimental results have revealed that the proposed ABCVS is able to support higher interaction strengths up to $t = 6$ compared to other Artificial Intelligence (AI)-based strategies. Furthermore, ABCVS it can compete against these other strategies in the majority of the case studies examined in the literature regarding efficiency (test suite generation) and performance (speed) and against other AI-based strategies having higher interaction strengths.

The remainder of this paper is structured accordingly. Section II presents the background to this study, (i.e. CA and MCA concepts) which is followed by Section III which surveys 'state of the art' testing strategies in this area. Section IV provides an overview of an ABC which is then followed by Section V describing the proposed strategy, consisting of two parts: (1) construction of the covering matrix, and (2) the proposed ABCVS. Section VI illustrates the tuning of the ABCVS parameters. Section VII evaluates the ABCVS by conducting several benchmark experiments in terms of efficiency and performance alongside with statistical analysis evaluation by using Wilcoxon signed-rank test in Section VIII. Section IX discusses the advantages, limitations and threats to the validity of the approach, which followed by Section X providing overall conclusions to the study and presenting recommendations for future work.

II. COVERING ARRAY WITH PROBLEM DEFINITION MODEL

The strategy of a t -way testing is one of the most minimization criteria used regarding the number of test cases list. The t -way testing is a combinatorial approach, and " t " indicates the interaction strength [12], and one of the input parameters. For example, assume that the (SUT) behavior is represented by user input then the external and internal events or the modes of the system parameters are controlled by separate parameters (P). In this case, each separate value V_i has a parameter, X_i . These V_i are selected from a fixed set of values, consisting of value members. Each p -tuple...(X_1, X_2, \dots, X_p) shows a test case where $X_i \in V_i$ and $1 \leq i \leq P$ [29].

Using a practical software example, let us consider a web configurable software system. This system is consists of five-components, namely; a device, a processor, the operating system (OS), browser, and a display. Fig. 1 illustrates their relationships. This system has employed as a simple illustration of the main idea in t -way testing regarding variable strength, and uniform strength. Each component of this system is known as a separate parameter, and each parameter has one or more values. Table I displays the parameters of the system and their values. In this example, the number of parameters is five, consisting of 3-parameters with 2-values and 2-parameters with 2-values.

To produce different software settings of the system, the software should be tested to identify any existing defects. In this case, a test case can be used to determine particular settings of the software. The total number of test cases are called the test suite, where the test suite must identify existing defects. For instance, assuming device 1 (Phone) is not able to use OS 2

(Windows). Therefore, the system will fail because the operating system (OS) is Windows based and the device parameter is the phone. Therefore, to detect faults, using 2-way schema (Phone,-, Windows,-,-) at least one occurrence time must be covered by the generated test suite.

To obtain 'perfect' software that performs with no defects, it is important to test all software components to cover all possible parameters. In this example, 72 test cases (i.e. $2 \times 2 \times 3 \times 3 \times 2$) are required to cover all cases. Nowadays, software-testing costs are rising due to the evolution and complexity of the software and an increasing the number of parameters and software levels. Since the failure of a limited number of parameters is mainly caused by the interaction of the parameters [12], it is not efficient to produce a comprehensive test case. Therefore, to solve this problem, a particular technique should be used such as a t -way testing approach as an alternative to a more comprehensive test, where $2 \leq t \leq p$. In addition, it is worth noting that the " t " value denotes that the final test suite consists of all possible t -way combinations as an alternative to the p -way. However, it cannot identify the interactions that are responsible for the software failure caused if the " t " value is low.

All possible interaction combinations of the parameters are covered by the combinatorial test, called the t -way CA for the test that generates the test suite. In addition, the " t " value defines the covering depth as well as the strength, and it is considered an important factor that must be determined by the tester. Overall, mathematically both the t -way approach and CA have a direct relationship. Therefore, to define the t -way approach, the following concept is used where CA is an array size $N \times p$, where N contains test cases, consisting of two features:

Each column i contains some members of set V_i , $|V_i| = v_i$. The rows of each sub-array of size $N \times t$, cover all combinations $|V_{k_1}| \times |V_{k_2}| \times \dots \times |V_{k_t}|$ of t at least once [29]; and if $v_1 = v_2 = \dots = v_p = v$, then all possible cases are obtained as given in Eq. (1)

$$\text{FullCoverage} = \binom{p}{t} \times v^t \quad (1)$$

The CA is denoted by $CA(N; t, p, v_1, v_2, \dots, v_p)$, and if $v_1 = v_2 = \dots = v^p = v$, then it is denoted by $CA(N; t, p, v)$ or $CA(N; t, v^p)$ [29]. In some research references, if v_i is different, it is called a Mixed Covering Array (MCA) [38, 42-44].

In the earlier section, it was mentioned that the possible number of test cases of a web configurable software system was 72. In this case, 2-way (pairwise interaction) is used where the total number of test cases has been reduced to nine as shown in Table II, which displays all possible combinations for available parameters. For example, both the parameters, device and the OS, have six (i.e. 2×3) different 2-way cases including (Pc, -, Android, -, -), (Pc, -, IOS, -, -), (Phone, -, Android, -, -), (Phone, -, IOS, -, -), (Phone, -, Windows, -, -) and (Pc, -, Windows, -, -), (see Table II).

The interactions between the parameters are important given that most software is unstable, due to some of these interactions having less impact. Some others interactions are more likely related to system failure. In this case, CA along

with the variable strength is used effectively to determine the various interactions. Various covering strengths exist in this structure between the various sets of parameters. The VS Covering Array (VSCA) is denoted by $VSCA(N; t, p, v, \{C\})$ where $\{C\}$, is consists of one or more CA (t', p', v) and p' is a subset of p . A web configurable software system example is next shown to understand VSCA. In the web configurable software assumes that all parameter combinations require 2-way and a device, processor and OS that requires 3-way

interaction. In this case, the configuration system is indicated as $VSCA(N; 2, 2^3 3^2, CA(3, 2^2 3^1))$. Table III displays the complete test suite to cover this configuration. Three more test cases as shown in Table III, are added to Table II in order to construct $VSCA(12; 2, 2^3 3^2, CA(3, 2^2 3^1))$. For this reason, using VSCA not only covers all 2-way interactions of complete parameters, but also covers all 3-way interactions of the specified parameters.

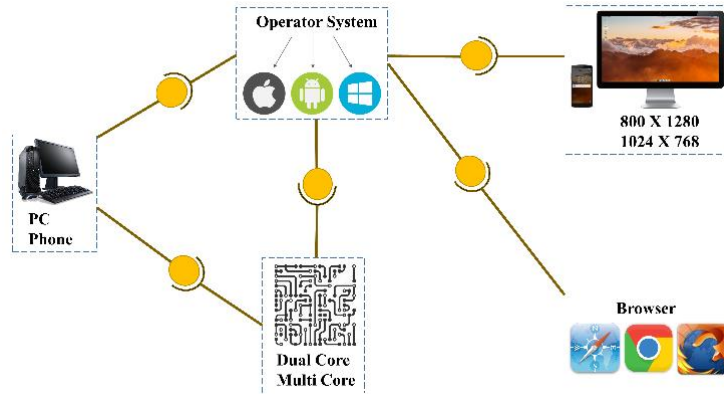


Fig. 1. A Web Configurable Software System..

TABLE I. A WEB CONFIGURABLE SOFTWARE SYSTEM

Parameters				
Device	Processor	OS	Browser	Display
PC (0)	Dual core (0)	Android (0)	Firefox (0)	720 x 1280 (0)
Phone (1)	Multi core (1)	IOS (1)	Chrome (1)	1024 x 768 (1)
		Windows (2)	Safari (2)	

TABLE II. TEST SUITE FOR CA (N; 2, 2³ 3²)

NO	Device	Processor	OS	Browser	Display
1	PC (0)	Dual core (0)	IOS (1)	Firefox (0)	720 x 1280 (0)
2	Phone (1)	Multi core (1)	Android (0)	Firefox (0)	1024 x 768 (1)
3	Phone (1)	Multi core (1)	Windows (2)	Chrome (1)	720 x 1280 (0)
4	PC (0)	Dual core (0)	Windows (2)	Safari (2)	1024 x 768 (1)
5	PC (0)	Dual core (0)	Android (0)	Chrome (1)	1024 x 768 (1)
6	Phone (1)	Multi core (1)	IOS (1)	Safari (2)	1024 x 768 (1)
7	PC (0)	Multi core (1)	Android (0)	Safari (2)	720 x 1280 (0)
8	Phone (1)	Dual core (0)	Windows (2)	Firefox (0)	1024 x 768 (1)
9	Phone (1)	Dual core (0)	IOS (1)	Chrome (1)	1024 x 768 (1)

TABLE III. TEST SUITE FOR VSCA (N; 2, 2³ 3², CA (N; 3, 2² 3¹))

NO	Device	Processor	OS	Browser	Display
1	PC (0)	Dual core (0)	IOS (1)	Firefox (0)	800 x 1280 (0)
2	Phone (1)	Multi core (1)	Android (0)	Firefox (0)	1024 x 768 (1)
3	Phone (1)	Multi core (1)	Windows (2)	Chrome (1)	800 x 1280 (0)
4	PC (0)	Dual core (0)	Windows (2)	Safari (2)	1024 x 768 (1)
5	PC (0)	Dual core (0)	Android (0)	Chrome (1)	1024 x 768 (1)
6	Phone (1)	Multi core (1)	IOS (1)	Safari (2)	1024 x 768 (1)
7	PC (0)	Multi core (1)	Android (0)	Safari (2)	800 x 1280 (0)
8	Phone (1)	Dual core (0)	Windows (2)	Firefox (0)	1024 x 768 (1)
9	Phone (1)	Dual core (0)	IOS (1)	Chrome (1)	1024 x 768 (1)
10	PC (0)	Dual core (0)	Android (0)	Firefox (0)	1024 x 768 (1)
11	PC (0)	Multi core (1)	IOS (1)	Chrome (1)	800 x 1280 (0)
12	Phone (1)	Dual core (0)	Windows (2)	Firefox (0)	800 x 1280 (0)

III. RELATED WORK

Throughout Over the last few decades, there have been many studies in the literature that grouped into four main sets to solve the CA problem [45]: (A) mathematic methods, (B) greedy algorithms, (C) heuristic search algorithms, and (D) random methods.

A. Mathematic Methods

The mathematician researcher uses mathematic methods derived from the extensions of mathematical functions like the Orthogonal Array (OA). To generate CA for optimal mathematics, it is only available for specific configurations (i.e. the parameters and values are required to be uniform) [12]. Notably, there are several strategies designed based on this approach such as TConfig [46] and Combinatorial Test Service (CTS) [47] strategies for the generalisation of an OA. However, a major problem exists for the OA (i.e. as the solution is only available for small configurations because of the restriction).

B. Greedy Algorithms

Most greedy algorithm (GA) solutions initially begin to generate all possible combinations (i.e. solutions) based on the input variables; then, generate one test at a time until all uncovered combinations are covered. A greedy algorithm is different in this case compared to the other strategies for generating test cases. In order to produce a test case using greedy algorithms [3], there are two main approaches; (1) One-test-at-a-time (one-line-at-time) and (2) One parameter-at-a-time.

In each iteration, the one-test-at-a-time (OTAT) approach adds a line (test case) to the test suite. The strategies that adopted the one-test-at-time approach are; Pairwise Independent Combinatorial Testing (PICT) [48], Automatic Efficient Test Generator (AETG) [49], Deterministic Density Algorithm (DDA) [50, 51], Test Vector Generator (TVG) [52, 53], Classification-Tree action-Tree Editor eXtended Logics (CTE-XL) [54, 55], Jenny [56], ITCH [6], GTWay [2] and Density algorithm, which is part of the DDA algorithm (extension) that authorised the DDA to support the variable strength CA. In this case, all the mentioned strategies belong to pure computational-based strategies.

The AETG was the first type of strategy using the OTAT approach to generate the test suite. AETG attempts to select a number of test case candidates in every single cycle covering most of the interactions and adds the selected test case to the final test suite in a 'greedy' fashion. Another greedy strategy was used for many years, where mAETG [9] and mAETG-sat [57] were extended to support the constraints. PICT [48] helps in the generation of all interactions and randomly chooses the required test cases by using the OTAT approach. Because of its random attitude, this strategy tends to offer a non-optimal test size. In addition, PICT has been able to generate test suite sizes up to $t > 6$.

As a variant of the AETG, TVG [52] produced the best results based on the three algorithms, namely; Random, Plus-one, and T-reduced sets. However, given the limited literature available, the details relating to the use of each algorithm remains indistinct. Nevertheless, based on our experience

relative to the implementation of TVG, T-reduce usually generates the most optimal outcome, unlike the other related algorithms. In fact, TVG supported the interaction strength (i.e., $t < 10$) to produce the test suite.

Another strategy showing good results regarding efficiency for most configuration systems, as well as having good speed using the OTAT approach, is the Jenny strategy [56]. This strategy initially produces the test suite in order to cover one-way interaction only and was then further developed to extend the test suite to cover every 2-way interaction. This process, pending all t -way interactions, tends to be covered. The major competitor of Jenny is the Intelligent Test Case Handler, known as ITCH [6] which depends entirely on an exhaustive search algorithm for the producers of the interaction test suite. However, it is considered to be one of the slowest strategies compared to the other computational strategies regarding its efficiency to produce good results for some configuration systems. CTE_XL [54, 55] is another strategy based on the Classification-Tree Method (CTM) that utilises the OTAT approach called Classification-Tree Editor eXtended Logics (CTE_XL). The fundamental idea behind this strategy is based on several features that produce test suites by receiving the input data which is then divided into the two subsets being entirely different, and then gathering these subsets to produce the test case which is then added to the final test suite. However, the CTE-XL strategy underpins low interaction strength for producing the test suites (i.e., $t \leq 3$). The most reliable strategy in the computational technique that uses three algorithms for producing the test suite is GTWay [2]. In this strategy, the utilised algorithms are the t -way pair generation, the parser algorithm, as well as the backtracking algorithm. In the first instance, the parser algorithm helps to ensure that the system configuration parameters are guided in order to be utilised by the algorithm of the t -way pair generation. Then, the algorithm of the t -way pair generation helps in the generation of the required t -way parameter interaction based on a symbolic representation that is defined based on the parser algorithm. Finally, the backtracking algorithm needs to iteratively go through the t -way pair sets to add up the values of the t -way parameter's interactions for the generation of a complete test t -way suite. Although, addressing the strength of the high interaction in this instance is necessary (i.e. $t \leq 12$).

Compared to the OTAT approach, the OPAT approach is where the algorithm begins initially by choosing two parameters. Then, the test suite is horizontally extended by adding the rows one-by-one until the interaction parameters have been covered, starting with a vertical extension to choose more parameters, of which the process continues until the end. One of the strategies that utilised the OPAT approach is IPO. Other strategies based on the IPO include; IPOG [58], IPOG-D [5], IPOG-F [59], IPO-s [60], and ParaOrder [61]. However, ParaOrder and IPOG strategies can support a variable strength-covering array.

C. Heuristic Search Algorithm

Nowadays, significant attention has been concentrated on the Heuristic search (HS) or Artificial Intelligence (AI) algorithms as part of the research interest in SBSE to solve combinatorial interaction problems. HS is a potent technique to produce the minimum array size for the test suite, although it is

slow. Some of the most important heuristic search algorithms include SA [9-11, 20, 21], GA [11, 12, 22-27, 62], ACA [8, 12], PSO [7, 28-30], Cuckoo Search [3, 33, 34], Tabu Search (TS) [11, 63] and Harmony Search (HS) [4, 31, 32]. Initially, most algorithms were implemented in order to produce pairwise interaction (2-way), as by Stardom [8] such as; SA, GA and TS. The literature also shows that these strategies produce a weak result regarding efficiency given their complex structure. However, later, SA [9], GA and ACA [12] were extended to support the interaction strength (3-way). Nevertheless, the efficiency of SA is much better compared to TS and GA, and the efficiency of TS is better compared to GA.

In addition, SA, GA and TS are 'grand' strategies that support and only produce a test suite in CA. The results of the SA strategy have indicated that it is stronger compared to both, GA and ACA. Furthermore, both SA [10] and ACA [8] algorithms were extended to support the variable strength interaction up to (i.e. 3-way), where ACA is called, Ant Colony System (ACS). Searching the large space using SA to find the best test case utilised the Binary Search Algorithm (BSA). Meanwhile, ACA tried to find the best path (i.e. where every path represents a test case) until selecting the best path. In this case, the best path was selected based on the calculated weight. In GA, it begins randomly by selecting the test case after initialising the population, where each test case represented one chromosome. Then, through a fitness function, the chromosome's weight is calculated, after changing the functions (mutation and crossover) and at the end of the process, the best test case (i.e. best chromosome) is added to the final test suite. All these procedures continue until the required coverage is met. Another strategy that supports CA in by generating the test suites based on the PSO algorithm and fuzzy techniques called Fuzzy Self-Adaptive PSO (FSAPSO) [29]. FSAPSO is better compared to CS and DPSO regarding efficiency, but the performance is weak due to the Fuzzy computations. However, in this case, the strategy supported the interaction strength up to $t = 4$ to produce the final test suite.

In addition to SA and ACA [12], other strategies also are based on the GA algorithm with less modification in the structure which produces a good result regarding efficiency. These strategies are PWiesGen [25], PWiesGenPM [22], tuned Genetic (GS) [62] and Genetic Algorithm for Pairwise Test Sets (GAPTS) [26]. Notably, PWiesGenPM is better compared to GAPTS and GS is stronger than PWiesGenPM, GAPTS and PWiesGen. In order to address the variable strength problem, PWiesGen was extended [23] [to overcome this problem] with interaction strength (i.e. $t = 6$). This strategy is called PWiesGen-VSCA.

According to the literature, the first HS or AI that supports the interaction strength (i.e. $t = 6$) is the PSTG [7] strategy based on the PSO algorithm. Further, this strategy shows good performance, but weak efficiency for the strength less than $t = 3$ against the available strategies found in the literature. Calculating the weight to select the best test case to be stored needs big data by using a new approach. Accordingly, this strategy was extended to support the variable strength called VS-PSTG. Another strategy like PSTG that produces the test suite up to (i.e. $t = 6$) is the CS strategy [3], which is precisely

like PSTG but is faster by using the utilised Cuckoo algorithm to reduce the search space.

One of the most efficient strategies used to produce strong results and also supports strengths (i.e. $t = 15$) is HSS [4] which is based on the Harmony Search Algorithm. Either this is where the algorithm imitates the musicians behavior, which endeavors to compose enthralling music from random sampling or from improvisations (that is, adjusting a tune from their memory). In this strategy, it adds the test case in each iteration to the test suite and then goes on until the required coverage is met. Another efficient strategy used to produce a strong result, but having less support compared to HSS regarding strengths (i.e. $t = 6$), is HHH [63]. This strategy is characterised by using High-Level Hyper-Heuristic (HHH) as the first strategy [based on literature], where it uses four algorithms (i.e. meta-heuristic algorithm) instead of one. The four algorithms are; Teaching-Learning based Optimization (TLBO), PSO, Global Neighborhood Algorithm (GNA) and the Cuckoo Search algorithm. This strategy employs Tabu Search as the high-level search, then selects one of the four algorithms in each step, and depends highly on three explicit operators, on the basis of improvement, diversification, and intensification to adaptively choose the best meta-heuristic at any point in time to produce test cases.

The test suite is also produced using the PSO family [28] according to the following strategies; DPSO, DMS-PSO, APSO, TVAC, CLPSO and CPSO. As any AI algorithm has disadvantages and advantages due to randomisation, PSO as one of the algorithms also has inherent weaknesses regarding efficiency, which is the velocity function. To address this problem, DPSO was used to produce a good result by generating the best solution. This strategy supports the interaction strength of more than 6, but the published result [28] is up to 4.

D. Random Methods

This method is an ad hoc approach where a random test case is selected by utilising input distribution [45]. Section 3.2 mentioned that TVG utilised three methods to test case generation. One of these methods is a random method.

IV. OVERVIEW OF ARTIFICIAL BEE COLONY

The ABC algorithm is designed to trigger the honeybee colony foraging manner. A quintessential honeybee swarm comprised of three basic constituents e.g. source of food / employed foragers/failed recruits (onlookers and scout bees) [64]. The employed bees linked to a specific food source. They transmit important information such as (location, navigation and the profitability) of the food source and convey the data with the rest of the standby bees at the hive. The onlooker bees are responsible for food source discovery utilizing the information provided by employed bees. The scout bees assigned to random hunt the new food source. It is presumed that, the employed bees who are lacking of food source transformed into scout bees and begin a new search for the food source. It is inferred that the number of food source equates to the number of employed bees in the colony. In conclusion, the solution to the optimization problem is represented by the food source stand; meanwhile, the quality

(fitness) of the mentioned solution coincides with the quantity of food source [65].

ABC initiated a random population distribution of SN solutions (food source positions) in the search space, where SN signify the size of employed or onlooker bees. Each solution X_i ($i = 1, 2, \dots, SN$) will essentially be a D -dimensional vector provided that the number of optimization parameters to be D . All solutions generated at this stage can be obtained from Eq. (2).

$$x_{ij} = x_{min,j} + \text{rand}(0,1)(x_{max,j} - x_{min,j}) \quad (2)$$

Here, X_{min} and X_{max} are respectively the lower and upper boundary parameters for solution x_i in dimension j ($j = 1, 2 \dots D$), and $\text{rand}[0,1]$ is a scaling factor representing a random number between $[0,1]$. The D -dimensional solutions (food source positions) generated in the initialization step ($C = 0$) are subject to repeated cycles ($C = 1, 2 \dots, MCN$), until a termination criterion is satisfied. One ABC cycle required both implementation of global and local probabilistic search/selection. Every cycle demands various task performance by various bee types as illustrated in the flowchart (Fig. 2). The operations are initially independent and can be justified in distinct manner as below for clearer vision of the ABC methodology.

1) *Employed bee step*: After the employed bees convey the information to onlooker bees post evaluation of their sources fitness (solutions). Each employed bee agitated the old solution (X_{ij}) in its memory to create a potential solution using the Eq (3) below:

$$V_{ij} = X_{i,j} + \text{rand}[-1, 1](X_{ij} - X_{kj}) \quad (3)$$

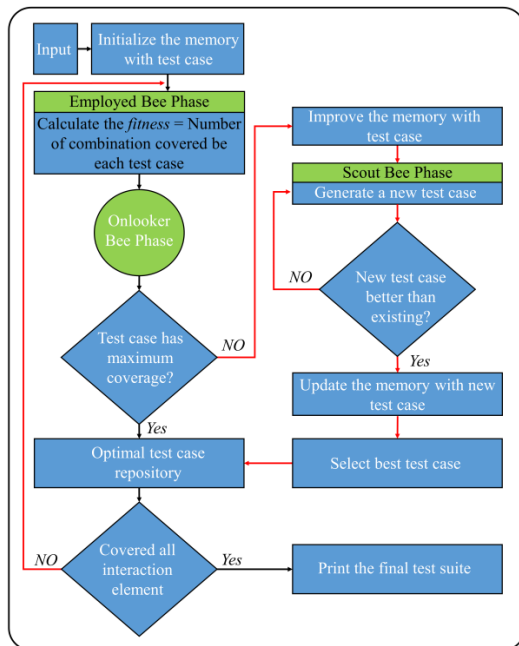


Fig. 2. The ABC Algorithm Flowchart.

Here, $K\{1, 2, \dots, D\}$ and $j\{1, 2, \dots, SN\}$ ($k \neq i$) are randomly chosen indexes, and $\text{rand}[-1,+1]$ is a random number between $[-1,1]$, which works as a scaling factor. Evidently, the

perturbation on solution is inversely proportional to optimum solution approached in the search space. The employed bee will also evaluate the fitness of the new (perturbed) solution and according to greedy-selection scheme, supposing the fitness value is better, it will replace the old one from employed bee memory.

2) *Onlooker bee step*: The duty of onlooker bee is to search for food source (solution), in reference to the association of probability value and food source P_i . The calculation of P_i is as the expression below in Eq. 4:

$$P_i = \frac{fit_i}{\sum_{n=1}^{SN} fit_n} \quad (4)$$

The fitness value of certain solution is signified by fit and solution number is referred to the subscript index. By comparing P_i against a randomly picked number ranging between $[0, 1]$, the probabilistic selection is applied. The selection will be only be accepted if the random number generated is less than or equal to P_i . The approval of probabilistic selection will determine the authorization of an onlooker bee assignment to a given solution. Normally, the calculation of fitness value of solutions in problems minimization is carried as the following in Eq. 5:

$$fit_i = \begin{cases} \frac{1}{1+f_i}, & \text{if } f_i \geq 0 \\ 1 + |f_i|, & \text{if } f_i < 0 \end{cases} \quad (5)$$

The objective function for solution i is signified by f_i . Assuming the selected food source matches with P_i probability, with Eq. (3) the onlooker bee will select a better food source (solution) in the area of the previous one in her memory. Suppose the fitness value of the solution is better, the onlooker bee will auto update the latest solution in her mind, disregarding the old one, which is akin to employed bees.

3) *Scout bee step*: The scout bees are assigned to search random food source in order to discover better solution for the global optimization problem. The scout bees are different from employed/onlooker bees as they are not committed to old solution in order to create trial solution. They obtained their samples from a broad set of D dimensional vectors, in condition it is still within the search space zone. In ABC, the solution will be disregarded if the (non-global) solution cannot be improvised post a pre-evaluated cycle's number. This will affect the assigned employed bee and transformed it to scout bee with limited scout type behavior. The limit also known as the value of this pre-evaluated cycle numbers is a crucial control factor of this algorithm. The limit is expressed as below.

$$\text{Limit} = c.n_e .D$$

Where, N_e signify the number of unemployed bees, while c is constant coefficient with a recommended value of 0.5 or 1. ABC application minimum requirement is one scout bee implementation. Scout-type operations hypothetical searches in the completely D -dimensional space provide exceptional effectiveness to the ABC method in searching the best global solution. Scout bees are independent when it comes to global optimum solution discovery in comparison to other bee types.

Both (employed/onlooker) concurrently check on their local candidate solutions for the global best. Thus, it is impossible for ABC to be trapped in local optima [64].

V. PROPOSED STRATEGY

In this study, to fulfil the optimal test suite, a new strategy is proposed. The proposed strategy uses ABC algorithm as the backbone algorithm to generate the test suites. Generally, the ABCVS strategy undergoes three phases during the construction of the uniform and variable t -way test suite generation using; (1) ABCVS input analysis algorithm, (2) ABCVS interaction generation algorithm and (3) generating the test suite using ABC algorithm as shown in Fig. 3. In Section 5.1, it discusses how to set up the input for the next phase and describes the generating of the interaction tuples by using the interaction generation algorithm. The ABCVS test suite construction is described in Section 5.2.

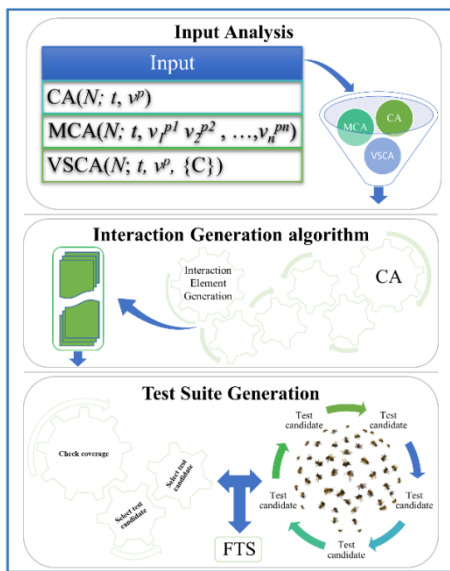


Fig. 3. ABCVS Strategy Design.

A. Input Analysis & Interaction Generation Element Algorithm

This section illustrates how the strategy receiving the CA, MCA and VSCA (inputs) and generation of the interaction parameter (P) combinations, compute and store the interaction element for each of the parameters to be used later for the test case coverage evaluation; based on the values (v) and the specified interaction strengths (t). To clarify the input analysis and the interaction generation elements, Fig. 4 shows a small VSCA configuration as an example illustrated by using a flowchart.

The value interaction elements of each parameter are then constructed based on the parameter interactions. As shown in the previous example ($N; 2, 2^3 3^1, \{CA (3, 2^3)\}$), the main configuration has four parameters, where the first three parameters have two values (0 and 1), and the fourth parameter has three values (0, 1, and 2) with interaction strength $t_m = 2$. The sub-configuration has three parameters, each having two values (0 and 1) with interaction strength $t_s = 3$. As illustrated in Fig. 4, the generation approach for the main configuration

($t_m = 2$) has six possible combinations of the interaction's parameters. For example, the possibility of the interaction elements for combinations (0 B2 0 B4) is 2×3 for both the second and fourth parameters, and the possibility of the interaction elements for combinations (B1 0 B3 0) is 2×2 between the first and third parameters. In order to check the availability of the parameters, the algorithm scans the binary digit of the combination, where each value of the other parameters is included in the interaction element. Regards to the rest of the values (i.e., replaced with "X") indicates "don't care" is the excluded value in the interaction element. The interaction elements of the sub-configuration were produced similarly to that as depicted in Fig. 4. Generating the interaction elements for each test case continues until creating the final test suite. This method is illustrated in the next section.

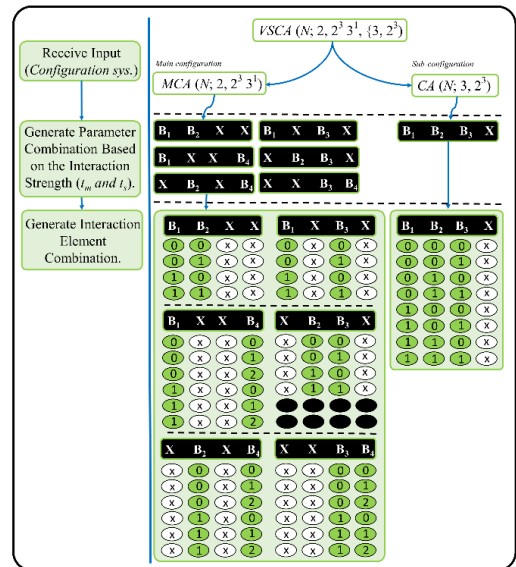


Fig. 4. An Illustration Example for the ABCVS Strategy.

B. The Test Suite Generation Algorithm

According to Fig. 3 that showed the responsible algorithm for the parameter combination generator, and the interaction elements combination generator based on the interaction strength, this will generate the possible interaction elements. In this strategy, a unique answer is produced in each step of the algorithm, which has no effect on the next test case selection. Selecting a test case is the most challenging problem in test suite generation, to achieve the test objective with a minimum number of test cases. In ABCVS, each procedure in this algorithm generates the best solution, which does not affect the next test case selection. For example, at every stage, the first of each bee (employed and onlooker) is randomly valued by the scout bee to the number of food source (which represents a test case) within a particular area. Following the valuation, the quality of food source is called the fitness value (coverage or weight) which is calculated based on the fitness function, and the results are presented to the employed bees. The employed bees optimise the solutions (food source position), calculate their qualities again, and present the results to the onlooker bees. The onlooker bees calculate the probability of selecting the solutions. Then, these values are normalised, and the food

source with higher quality (fitness) are greedily selected, and the proposed solutions are optimised again by the random values and the values of neighbors. The quality of the proposed solutions based on the fitness function is again specified. The onlooker bees investigate the solutions and select the best solution for storing. If it is an obsolete solution, the scout bee generates a new one. Otherwise, if the algorithm is finished, the final solution is registered as the output of the first stage, if not the algorithm should repeat. For instance, in Fig. 5, the test case is selected based on the maximum fitness (coverage or weight). The test case (1000) has the maximum weight of coverage, which is seven. Therefore, this test case (1000) adds to the final test suite by the test suite generation algorithm. Regarding the test case (1001) that does not reach the maximum coverage of fitness, the algorithm updates the population (food source) search space randomly to obtain the best fitness.

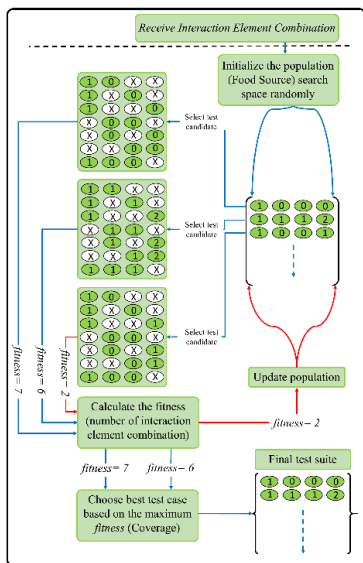


Fig. 5. An Illustration Example for Selection Test Case based on the Maximum Coverage.

VI. TUNING PARAMETER SETTING OF ABCVS

There are three important control parameters in the proposed ABCVS strategy. These control parameters are the colony size number (employed bee and onlooker bee

(population size)) equal to the number of food source, the value of *Limit* and the maximum cycle number (MCN). Growing the population size improves the outcome regarding both the generation time and the array size. In ABCVS, generating the final test suite plays a critical role based on the employed and onlooker phase. It is worth mentioning that these two phases are different in determining the value of configurations. In other words, both of *t*, *p* and *v* affect the number of iterations for the employed and onlooker phase.

An experiment were conducted on CA (N; 2, 5⁷) with a variable number of the bee to determine this value. As shown in Fig. 6 conducted, the best value of this configuration for the number of bees is 1 (i.e. food source = population /2) when the number of cycles (70) is a test suite of size 38 test cases, and when the number of bees is 2, the number of cycles (100) is 37. Increasing the value of bees up to 3 and 4, when the number of cycles is (100) and (90), respectively, the algorithm achieves a test case of size 36 test cases. In these experiments, the *Limit* is kept constant = 100. Therefore, the value increasing does not affect the size, only increasing in the generation time. In Fig. 6, different colours that depend on the number of cycles show the size of the test cases.

Fig. 7 illustrates the effects of the colony size (population size) on the array size in the same configuration CA (N; 2, 5⁷), and shows the best average test suite size for CA (N; 2, 5⁷). The population of size is variable from 1 to 10, and 20 to 100, when the number of cycles also is variable from 10 to 100 and *Limit* = 100 is considered. Regarding the test suite array size analysis, Meta-heuristic is a non-deterministic algorithm based on randomisation. Therefore, this analysis has two values. First, the best value as illustrated in Fig. 6, and the second value is the average of five independent runs. The best average is shown in Fig. 7 for the configuration CA (N; 2, 5⁷), where the best value for this configuration is 36 test cases.

The analysis, in this case, is aimed at determining the suitable value for the colony size (population size) that depends on changing the values of *p*, *t* and *v* of the configuration. Each configuration then determines the suitable experiments. Therefore, the best average value is selected when the population size is 50, and the maximum number of cycles is 80. Note that this value is related to the configurations in the tables of this paper.

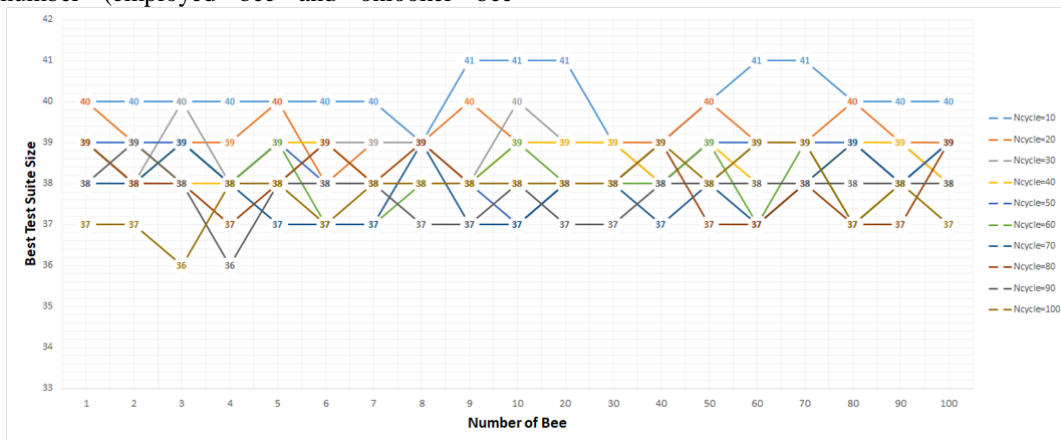


Fig. 6. The Best Test Suite Size with Variant Number of Bee for CA (N; 2, 5⁷).

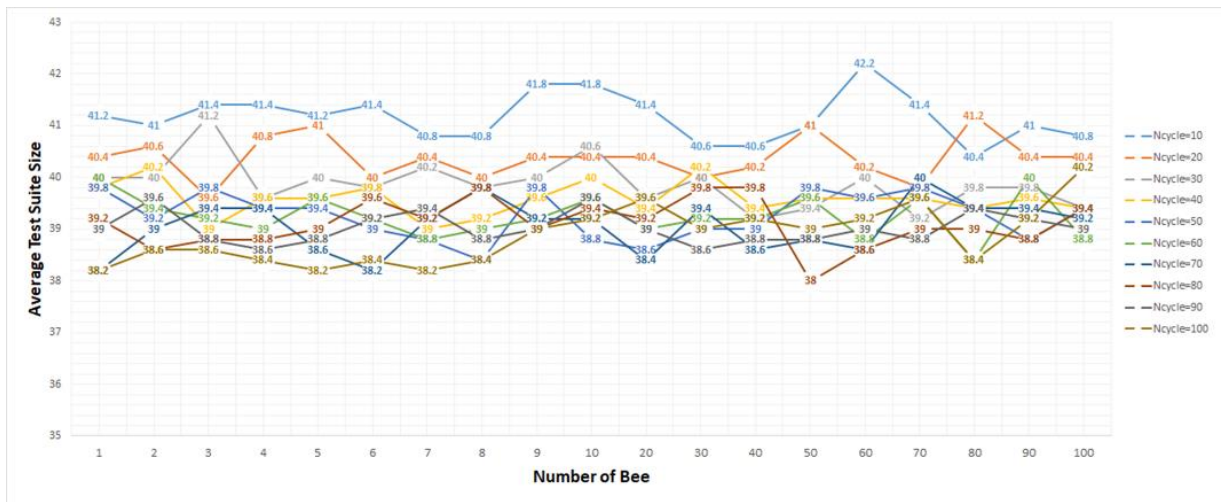


Fig. 7. The Best Average Test Suite Size with Variant Number of Bee for CA (N; 2, 5⁷).

VII. EVALUATION

In this section, there are two parts in the evaluation of the test suite generation strategies; (1) the efficiency evaluation (i.e. test suite size) and (2) the performance evaluation (i.e. the time of test suite generation) [62]. The test suite size and the interaction strength are not affected by the operating system and hardware but depend on the steps of the algorithm's running. Different strategies are selected in different tables based on the criterion; Tables IV-VIII are divided into two categories. In the first category, the available strategies that can be implemented in our system are included regarding efficiency; ABCVS is compared with these strategies. The second category contains unavailable strategies as discussed regarding efficiency and performance by other researchers. The comparison of these strategies has been conducted based on efficiency and performance. Therefore, it implements some of the AI strategies since many are unavailable in the same conditions of the proposed strategy (i.e. hardware and software). Regarding the Tables IV-VIII of configurations, the mentioned strategy's values are available, and used the same value as that published in the papers; otherwise, implementing the strategies on the system is used to obtain the result.

The characteristics of the hardware system for conducting the experiments of the proposed strategy consisted of a Windows 7 (OS) desktop computer with 3.40 GHz Xeon (R) CPU E3 and 8GB RAM. The Java language JDK 1.8. was used to code and implement the ABCVS. In this paper, the best outcome in the tables is shown in bold and in dark cells. Also, "NA" (Not Available) means not publishing, and "NS" (Not Supported) means does not support the corresponding configuration.

A. Evaluation of the Efficiency

In Table IV, the array size evaluation is divided into five parts; the interaction strength $2 \leq t \leq 6$ and parameter $3 \leq p \leq 12$ and value and $V = 3$ for configuration CA (N; t, p, v). The outcome of IPOD-D and IPOG are adopted from the Advanced Combinatorial Testing System (ACTS) [66]. These strategies do not normally generate good results as well as for PICT, TConfig and Jenny. Whereas, IPOG-D, IPOG and TConfig

support generation of the interaction strength up to $t = 6$. As shown in Table VII, other AI-based strategies are studied. The results of CS and PSTG are unavailable and are obtained from the papers. CS and PSTG generate similar results. The strongest strategy in terms of producing the best result is DPSO, where it showed results for $t \leq 4$ obtained from [24], for each configuration of 30 separate runs. Regarding the weak performance of DPSO (i.e. speed), it is impossible to implement each configuration of 30 runs because in CA (2512; 6, 3¹²) 23,620 s are required, thus will take more than 7 days. Other results are available from [67]. The result for $t > 4$ is obtained with 3 runs only. CS another AI-based strategy has generated a good result. In this case, the obtained result for $t > 4$ is adopted in 3 runs only because of the low performance of this strategy. To be fair, the ABCVS strategy is adopted in 5 runs for $t > 4$, and 20 runs for the value $t \leq 4$.

The values in Tables V, VI and VII, are adopted from the corresponding paper [7]. Regarding the configuration system VSCA (N; 2, 3¹⁵, {C}) in Table V, where the PICT and WHITCH strategy produces undesirable results, these strategies have the capability to generate a test suite to $t = 6$. However, WHITCH produced better results. Another computational-based strategy is ParaOrder that had a better result compared to PICT and WHITCH up to $t = 3$ but does not support in generating a test suite for $t \geq 4$. As shown in this table, AI-based strategies are considered the strongest strategies. The strongest strategies that generate the best results are SA and ACS when the strength is 3. However, these strategies are not able to produce a test suite of more than 3. Regarding the strategies such as PwiseGen-VSCA, ABCVS, GS and PSTG, these are better than the other strategies in terms of support strength of more than 3 and less than 6. IPOG and GS have the support strength more than 6.

Table VI shows the configuration VSCA (N; 3, 3¹⁵, {C}), where PSTG, GS and ABCVS strategies generate good results for strength up to $t = 6$, but IPOG and GS produce a better test suite for strength more than 6. However, ACS and SA are not able to generate a result due to not having support strength of more than 3. Also, the results for Density and ParaOrder are not available.

Regarding the configuration system VSCA (N, 2, 4³ 5³ 6², {C}) in Table VII, the results of PwiseGen-VSCA and GS strategies are not available as well as for the ParaOrder and Density strategies for most subsets ({C}), but not all. Furthermore, WHITCH and PICT have support strength up to

6, but these strategies do not generate a good result. ABCVS, TVG and PSTG strategies have the capability to generate better results for strength $t = 6$, and ACS and SA produced a better result for strength $t = 3$.

TABLE IV. A TEST SUITE SIZE FOR CA (N; T, 3^P) WITH 2 ≤ T ≤ 11 AND 3 ≤ P ≤ 12

t	P	Pure computation strategies					AI-based strategies						
		Jenny Best	TConfig Best	PICT Best	IPOG-D Best	IPOG Best	DPSO Best	PSTG Best	CS Best	GS Best	ABCVS Best	ABCVS Avg.	
2	3	9	10	10	15	9	9	9	9	9	9	9.95	
	4	13	10	13	15	9	9	9	9	9	9	10.70	
	5	14	14	13	15	15	11	12	11	11	11	12.75	
	6	15	15	14	15	15	14	13	13	13	13	14.75	
	7	16	15	16	15	15	14	15	14	14	15	15.50	
	8	17	17	16	15	15	15	15	15	15	15	15	15.90
	9	18	17	17	15	15	15	17	16	15	16	17.25	
	10	19	17	18	21	15	16	17	17	16	17	17.70	
	11	17	20	18	21	17	17	17	18	16	17	18.45	
	12	19	20	19	21	21	16	18	18	16	18	19.25	
	3	4	34	32	34	27	32	27	27	28	27	27	33.50
		5	40	40	43	45	41	41	39	38	38	38	41.45
6		51	48	48	45	46	33	45	43	43	44	46.85	
7		51	55	51	50	55	48	50	48	49	49	51.90	
8		58	58	59	50	56	52	54	53	54	54	55.85	
9		62	64	63	71	63	56	58	58	58	58	59.80	
10		65	68	65	71	66	59	62	62	61	62	64.25	
11		65	72	70	76	70	63	64	66	63	66	68.15	
4	5	109	97	100	162	97	81	96	94	90	98	103.65	
	6	140	141	142	162	141	131	133	132	129	135	138.75	
	7	169	166	168	226	167	150	155	154	153	157	161.45	
	8	187	190	189	226	192	171	175	173	173	179	182.05	
	9	206	213	211	260	210	187	195	195	194	197	200.95	
	10	221	235	231	278	233	206	210	211	209	215	217.90	
	11	236	258	249	332	251	221	222	229	223	234	236.50	
	12	252	272	269	332	272	237	244	253	236	251	254.20	
5	6	348	305	310	386	305	244	312	304	301	274	317.70	
	7	458	477	452	678	466	438	441	434	432	442	449.95	
	8	548	583	555	756	575	517	515	515	515	530	534.20	
	9	633	684	637	1043	667	591	598	590	594	609	613.50	
	10	714	773	735	1118	761	667	667	682	672	688	690.60	
	11	791	858	822	1372	851	735	747	778	741	762	765.50	
	12	850	938	900	1449	929	802	809	880	806	814	817.71	
6	7	1089	921	1015	1201	921	729	977	973	963	944	984.35	
	8	1466	1515	1455	1763	1493	1409	1402	1401	1399	1424	1438.6	
	9	1840	1931	1818	2526	1889	1682	1684	1689	1681	1756	1767.0	
	10	2160	>day	2165	2834	2262	1972	1980	2027	1980	2055	2060.1	
	11	2459	>day	2496	3886	2607	2250	2255	2298	2258	2261	2269.2	
	12	2757	>day	2815	4087	3649	2512	2528	2638	2558	2571	2576.5	

TABLE V. TEST SUITE SIZE FOR VSCA (N, 2, 3¹⁵, {C})

{C}	Pure computation strategies						AI-based strategies						
	WHITCH Best	IPOG Best	ParaOrder Best	Density Best	TVG Best	PICT Best	SA Best	ACS Best	PSTG Best	GS Best	PwiseGen Best	ABCVS Best	ABCVAvg.
∅	31	21	33	21	22	35	16	19	19	19	16	20	21.3
CA (3, 3 ³)	48	27	27	28	27	81	27	27	27	28	27	27	27.85
CA (3, 3 ⁴)	59	39	27	32	35	105	27	27	30	29	27	32	35.1
CA (3, 3 ⁵)	62	39	45	40	41	131	33	38	38	38	33	41	42.9
CA (4, 3 ⁴)	103	81	NA	NA	81	245	NA	NA	81	81	81	81	81.2
CA (4, 3 ⁵)	118	122	NA	NA	103	301	NA	NA	97	92	91	90*	100.35
CA (4, 3 ⁷)	189	181	NA	NA	168	505	NA	NA	158	155	158	154*	160.2
CA (5, 3 ⁵)	261	243	NA	NA	243	730	NA	NA	243	243	243	243	243.1
CA (5, 3 ⁷)	481	581	NA	NA	462	1356	NA	NA	441	441	441	446	449.2
CA (6, 3 ⁶)	745	729	NA	NA	729	2187	NA	NA	729	729	729	729	729
CA (6, 3 ⁷)	1050	967	NA	NA	1028	3045	NA	NA	966	960	NA	956	961.1
CA (3, 3 ⁴) CA (3, 3 ⁵) CA (3, 3 ⁶)	114	51	44	46	53	1376	34	40	45	NA	NA	82	85.1
CA (3, 3 ⁶)	61	53	49	46	48	146	34	45	45	46	40	45	46.7
CA (3, 3 ⁷)	68	58	54	53	54	154	41	48	49	50	47	50	51.85
CA (3, 3 ⁹)	94	65	62	60	62	177	50	57	57	57	57	58	60.1
CA (3, 1 ⁵)	132	NS	82	70	81	83	67	76	74	75	74	81	83.2

TABLE VI. TEST SUITE SIZE FOR VSCA (N, 3, 3¹⁵, {C})

{C}	Pure computation strategies						AI-based strategies						
	WHITCH Best	IPOG Best	ParaOrder Best	Density Best	TVG Best	PICT Best	SA Best	ACS Best	PSTG Best	GS Best	PwiseGen Best	ABCVS Best	ABVCS Avg.
∅	75	82	NA	NA	84	83	NS	NS	75	74	NA	81	83.25
CA(4, 3 ⁴)	129	87	NA	NA	93	1507	NS	NS	91	88	NA	93	96.1
CA(5, 3 ⁵)	273	243	NA	NA	244	5366	NS	NS	243	243	NA	243	246.2
CA(6, 3 ⁶)	759	729	NA	NA	729	12,609	NS	NS	729	729	NA	729	729
CA(4, 3 ⁵)	151	119	NA	NA	118	1793	NS	NS	114	111	NA	115	118.6
CA(5, 3 ⁶)	387	337	NA	NA	323	5387	NS	NS	314	308	NA	316	329.15
CA(6, 3 ⁷)	1441	1215	NA	NA	1018	16,792	NS	NS	1002	959	NA	949*	956.6
CA(4, 3 ⁷)	219	183	NA	NA	168	2781	NS	NS	159	158	NA	157*	161.9
CA(4, 3 ⁹)	289	227	NA	NA	214	3095	NS	NS	195	194	NA	196	199.9
CA(4, 1 ¹)	354	259	NA	NA	256	2824	NS	NS	226	226	NA	333	237.0
CA(4, 1 ⁵)	498	498	NA	NA	327	NA	NS	NS	284	282	NA	308	441
CA(5, 3 ⁷)	481	713	NA	NA	471	7475	NS	NS	437	437	NA	439	448.7
CA(5, 3 ⁸)	620	714	NA	NA	556	8690	NS	NS	516	516	NA	527	535.65
CA(6, 3 ⁸)	1513	2108	NA	NA	1479	22,833	NS	NS	1396	1397	NA	1424	1436
CA(6, 3 ⁹)	1964	2124	NA	NA	1840	26,729	NS	NS	1690	1687	NA	1752	1763

TABLE VII. TEST SUITE SIZE FOR VSCA (N, 2, 4³ 5³ 6², {C})

{C}	Pure computation strategies						AI-based strategies						
	WHITCH Best	IPOG Best	ParaOrder Best	Density Best	TVG Best	PICT Best	SA Best	ACS Best	PSTG Best	GS Best	PwiseGen Best	ABCVS Best	ABCVS Avg.
∅	48	43	49	41	44	43	36	41	42	NA	NA	44	44
CA (3, 4 ³)	97	83	64	64	67	384	64	64	64	NA	NA	64	64
CA (3, 4 ³ 5 ²)	164	147	141	131	132	781	100	104	124	NA	NA	128	128
CA (3, 5 ³)	145	136	126	125	125	750	125	125	125	NA	NA	125	125
CA (4, 4 ³ 5 ¹)	354	329	NA	NA	320	1920	NS	NS	320	NA	NA	320	320
CA (5, 4 ³ 5 ²)	1639	1602	NA	NA	1600	9600	NS	NS	1600	NA	NA	1600	1600
CA (3, 4 ³) CA (3, 5 ³)	194	136	129	125	125	8000	125	125	125	NA	NA	125	125
CA (4, 4 ³ 5 ¹) CA (4, 5 ² 6 ²)	1220	900	NA	NA	900	288,000	NS	NS	900	NA	NA	900	900
CA (3, 4 ³) CA (4, 5 ³ 6 ¹)	819	750	NA	NA	750	48,000	NS	NS	750	NA	NA	750	750
CA (3, 4 ³) CA (5, 5 ³ 6 ²)	4569	4500	NA	NA	4500	288,000	NS	NS	4500	NA	NA	4500	4500
CA (4, 4 ³ 5 ²)	510	512	NA	NA	496	2874	NS	NS	472	NA	NA	463*	463
CA (5, 4 ³ 5 ³)	2520	2763	NA	NA	2592	15,048	NS	NS	2430	NA	NA	2403*	2403
CA (3, 4 ³ 5 ³ 6 ¹)	254	215	247	207	237	1266	171	201	206	NA	NA	213	213
CA (3, 5 ¹ 6 ²)	188	180	180	180	180	900	180	180	180	NA	NA	180	180
CA (3, 4 ³ 5 ³ 6 ²)	312	NS	307	256	302	261	214	255	260	NA	NA	266	266

TABLE VIII. TEST SUITE SIZE AND TIME FOR CA (N; T, 7, 3^T) WITH 2 ≤ T ≤ 7

t	Pure computation strategies					AI-based strategies					
	Jenny N/Time	TConfig N/Time	PICT N/Time	IPOG-D N/Time	IPOG N/Time	DPSO N/Time	HSS N/Time	PSO N/Time	CS N/Time	GS N/Time	ABCVS N/Time
2	16/0.04	15/0.08	16/0.01	18/ 0.001	15/ 0.001	14 -Mar	14 /0.92	15/2.2	15/0.28	14 /0.22	14 /2.1
3	51/0.09	55/0.43	51/0.04	50/ 0.001	55/ 0.001	48 /23	50/4.02	50/8.2	50/3.1	49/0.78	49/23.07
4	169/0.3	166/8.24	168/0.09	226/ 0.001	167/ 0.001	150 /156	154/23.1	157/33.2	156/6.2	153/3.01	157/148.7
5	458/0.72	477/72.96	452/0.7	678/0.062	466/ 0.001	438/191	438/70.8	439/113	436/19.1	432 /8.85	439/457.9
6	1087/1.10	921/425.52	1015/1.20	1201/0.062	921/ 0.001	729 /147	926/107.8	981/382	973/31	963/16.98	862/343.5

TABLE IX. TEST SUITE SIZE AND TIME FOR CA (N; 3, 3^P) WITH 4 ≤ P ≤ 20

P	Pure computation strategies					AI-based strategies					
	Jenny N/Time	TConfig N/Time	PICT N/Time	IPOG-D N/Time	IPOG N/Time	DPSO N/Time	HSS N/Time	PSO N/Time	CS N/Time	GS N/Time	ABCVS N/Time
4	34/0.01	32/0.07	34/0.04	27 / 0.001	32 / 0.001	27 -Feb	30/1.9	28/4.2	27 /1.30	27 /0.40	31/1.1
5	40/0.03	40/0.10	43/0.09	45/ 0.001	41/ 0.001	41/7	39/2.7	39/6.1	38 /2.09	38 /0.63	40/3.2
6	51/0.09	48/0.31	48/0.13	45/ 0.001	46/ 0.001	33 /10	44/3.2	45/7.5	45/2.63	43/0.73	45/9.6
7	51/0.07	55/0.43	51/0.23	50/ 0.001	55/ 0.001	48 /23	50/4.02	50/8.2	50/3.12	49/0.78	49/24.7
8	58/0.07	58/1.23	59/0.36	50 / 0.001	56/ 0.001	52/36	54/4.8	54/9.3	55/4.04	54/0.86	55/55.3
9	62/0.08	64/1.72	63/0.57	71/ 0.001	63/ 0.001	56 /55	59/6.01	58/10.5	60/4.69	58/1.11	59/117.8
10	65/0.10	68/2.84	65/0.64	71/ 0.001	66/ 0.001	59 /81	62/7.3	62/11.3	64/5.60	61/1.24	63/248.2
11	65/0.12	72/3.93	70/0.70	76/ 0.001	70/ 0.001	63 /115	66/9.6	64/12.8	66/7.12	63 /1.28	67/534.4
12	68/0.18	77/5.24	72/0.79	76/ 0.001	73/ 0.001	65 /157	67/11.5	67/13.6	70/8.41	67/1.53	71/702.7

TABLE X. TEST SUITE SIZE AND TIME FOR CA (N; 3, v⁷) WITH 2 ≤ v ≤ 6

v	Pure computation strategies					AI-based strategies					
	Jenny N/Time	TConfig N/Time	PICT N/Time	IPOG-D N/Time	IPOG N/Time	DPSO N/Time	HSS N/Time	PSO N/Time	CS N/Time	GS N/Time	ABCVS N/Time
2	14/0.04	16/0.03	15/0.09	14/ 0.001	16/ 0.001	15-Jun	12 /0.9	12 /1.7	13/0.82	12 /0.19	12 /3.9
3	51/0.09	55/0.43	51/0.19	50/ 0.001	55/ 0.001	48 /24	50/4.02	50/8.2	50/2.1	50/0.78	49/23.3
4	124/0.12	112 /2.57	124/0.53	112 / 0.001	124/ 0.001	112 /54	121/5.9	118/21.7	119/6.6	117/1.83	119/97.1
5	236/0.61	239/03.18	241/0.78	252/ 0.001	237/ 0.001	216 /172	233/18.5	226/43.2	233/14.4	231/3.63	230/368.6
6	400/1.00	423/13.15	413/1.00	470/ 0.001	420/ 0.001	365 /188	411/31.3	420/88.6	403/18.2	397/6.48	394/1076.2

B. Evaluation of the Performance

In Table VIII, the configuration CA (N; t, 3⁷) for 2 ≤ t ≤ 6 is used in terms of array size and time. TConfig strategy speed relies on t, where by increasing the t time will increase exponentially. IPOG-D and IPOG are fastest computational-based strategies, where the test suite generation time almost near to zero that indicates the high performance. ABCVS and DPSO performance are very slowly. PICT, Jenny and GS are faster than ABCVS, but these strategies are not able to generate the final test suite in a less than day. Therefore, the proposed strategy it's better in terms of performance than PICT, Jenny and TConfig. The result of the proposed strategy shows the generation time of a test suite does not really rely on increasing t.

Table IX displays the results in terms of array size and time of the strategies. The configuration CA (N; 3, 3^p) is used to evaluate the variable of p on time generation. The growth of p has shown an impact on the proposed strategy in terms of time generation, but has less impact on TConfig performance.

The last evaluation in terms of time generation, the configuration CA (N; 3, 7, v) for 2 ≤ v ≤ 10 is used in Table X. In this evaluation will test the impact of increasing the values on time generation. IPOG and IPOG-D are the fastest strategies in terms of the performance and DPSO is strongest on terms of array size. ABCVS generates close results to DPSO and GS.

VIII. STATISTICALLY EVALUATION

In order to evaluate the strategy regarding array size (i.e. effectiveness), a statistical method is another way to assess the significance of strategy. In this case, the Wilcoxon signed-rank test is used between ABCVS and each strategy in the experimental tables 95% confidence level (i.e. α = 0.05). The reason for adopting this method is that the Wilcoxon signed-rank test takes into account the difference between two sets. To study the difference of the two sets, this test is ideal. In other words, this test is measured from a subject group and can be rated.

Due to the multiple comparisons, we need to control the error rate. Bonferroni-Holm correction was adopted to adjusting α value (i.e. in other words, based on Holm's sequentially rejective step down procedure [26]) depending on the first stored p-value (Asymp. Sig. (2-tailed)) in scaling in ascending order. Therefore, α Holm is adjusted based on:

$$\alpha \text{ Holm} = \frac{\alpha}{M-i+1}$$

Note: Where M indicates the overall number of paired comparison and i indicates the test number.

The test is executed using a software tool called SPSS, where if the value is less than α Holm of the Asymp. Sig. (2-tailed), it indicates a significant difference between the two sets. There are four values to evaluate ABCVS; Ranks ABCVS>, ABCVS<, and ABCVS= are used. In other words, the results of the proposed strategy are greater, smaller or equal to the other existing strategies. Two values have a Statistical Test part; Asymp. Sig. (2-tailed) and Z. The value of Asymp. Sig. (2-tailed) indicates the significant difference between the two sets and that the value does not exceed α Holm. Regarding the value Z, it is out of the scope of this paper (i.e. not important). The strategies with N/A and N/S results are considered incomplete and ignored samples, as there is no available result for the specified test configuration.

Tables XI–XIV present a statistical test for the Tables IV–VII and Table XI presents the result of Table IV for the Wilcoxon test. ABCVS shows there is a significant difference with other strategies in column Asymp. Sig. (2-tailed), except for CS, which has a significant difference from ABCVS.

Table XII presents the test results of Table V. IPOG, ParaOrder, Density, TVG, GS, SA, ACS and PwiseGenVSCA produce a test suite for strength less than 3 for t > 3 and the results are considered “missing”. For this reason, the IPOG, ParaOrder, Density, TVG, PSTG and GS results are better than ABCVS. Whereas, ABCVS performs better than WHITCH, PICT, SA, ACS and PwiseGen-VSCA in this table.

Table XIII presents the test results of Table VI, where ABCVS excelled compared to WHITCH and GS strategies. Table XIV presents the test results of Table VII. TVG and PSTG are shown to have a significant difference compared to ABCVS. However, ABCVS excelled with the WHITCH, and PICT strategies.

IX. DISCUSSION

AI-based strategies are characterised by producing a strong result, although, not without having a complex structure and repetition of which the complex structure of the strategy is inversely correlated with the strategy's strength. For instance, ACO, GA and SA can produce a test suite with t ≤ 3. While CS and PSTG reduce complexity by changing the structure and raising the performance speed to support strengths up to t = 6. Notably, GS supports strengths up to t = 15.

IPOG, PICT and Jenny are computational based strategies having the capability to produce a test suite for $t > 6$ like AI-based strategies. However, computational strategies do not produce good results but instead, do have good performance. Therefore, it is impossible to obtain a strategy that can support high interaction strength with perfect performance and efficiency. The ABCVS indicates that its efficiency regarding generating a test suite with $t = 6$ competes well compared to the other existing strategies. Further, ABCVS is better as compared to computational ones and can compete with AI-based strategies regarding performance and efficiency.

Although, ABCVS like any other strategy have limitations; for example, its contribution towards supporting variable strengths interaction. The ABCVS efficiency for strengths (i.e. $t \leq 3$) is slightly lower compared to others. Given the limited literature in this field, many of these strategies are not available publicly and therefore, in this study, the configurations reported and available in publications have been used. Therefore, further experiments need to be conducted in order to obtain a precise evaluation of the proposed strategy.

TABLE XI. WILCOXON SIGNED RANK SUM TEST FOR TABLE IV.

Pairs	Ranks			Test statistics			Conclusion
	ABCVS >	ABCVS <	ABCVS =	Z	Asymp. Sig. (2-tailed)	α holm	
ABCVS- Jenny	2	36	2	-5.199269	0.00000020	0.00625000	Reject
ABCVS- PICT	0	40	0	-5.522230	0.00000003	0.00714286	Reject
ABCVS- IPOG-D	3	34	3	-5.107580	0.00000032	0.00833333	Reject
ABCVS- IPOG	4	31	5	-4.662525	0.00000300	0.01000000	Reject
ABCVS- DPSO	34	2	4	-4.999589	0.00000057	0.01250000	Reject
ABCVS- PSTG	22	5	13	-3.236855	0.00120900	0.01666667	Reject
ABCVS- CS	20	8	12	-1.071752	0.28383200	0.02500000	Retain
ABCVS- GS	31	2	7	-3.966042	0.00007300	0.05000000	Reject

TABLE XII. TWILCOXON SIGNED RANK SUM TEST FOR TABLE V.

Pairs	Ranks			Test statistics			Conclusion
	ABCVS >	ABCVS <	ABCVS =	Z	Asymp. Sig. (2-tailed)	α holm	
ABCVS- WHITCH	0	16	0	-3.518549	0.000434	0.01250000	Reject
ABCVS- TVG	1	9	6	-1.888148	0.059006	0.01666667	Retain
ABCVS- PICT	0	16	0	-3.516196	0.000438	0.02500000	Reject
ABCVS- PSTG	8	3	5	-0.757616	0.448681	0.05000000	Retain

TABLE XIII. WILCOXON SIGNED RANK SUM TEST FOR TABLE VI.

Pairs	Ranks			Test statistics			Conclusion
	ABCVS >	ABCVS <	ABCVS =	Z	Asymp. Sig. (2-tailed)	α holm	
ABCVS- WHITCH	1	14	0	-3.353003	0.000799	0.01000000	Reject
ABCVS- IPOG	2	11	2	-2.480941	0.013104	0.01250000	Retain
ABCVS- TVG	1	12	2	-2.341884	0.019187	0.01666667	Retain
ABCVS- PSTG	11	2	2	-2.103645	0.035409	0.02500000	Retain
ABCVS- GS	11	2	2	2.551605	0.010723	0.05000000	Reject

TABLE XIV. WILCOXON SIGNED RANK SUM TEST FOR TABLE VII.

Pairs	Ranks			Test statistics			Conclusion
	ABCVS >	ABCVS <	ABCVS =	Z	Asymp. Sig. (2-tailed)	α holm	
ABCVS- WHITCH	0	15	0	-3.410523	0.000648	0.01250000	Reject
ABCVS- TVG	0	6	9	-2.201398	0.027708	0.01666667	Retain
ABCVS- PICT	2	13	0	-3.237382	0.001206	0.02500000	Reject
ABCVS- PSTG	4	2	9	-0.104828	0.916512	0.05000000	Retain

X. CONCLUSION

This paper proposes an efficient strategy called ABCVS, based on the ABC algorithm for both uniform and variable CAs. Supporting variable strength is the main contribution of ABCVS. In addition to the supporting variable strength, ABCVS can generate a test suite up to $t = 6$ and can produce a good result with suitable performance. To study the impact of parameters like population size or a number of cycles, different experiments have been conducted. The suitable tuning parameters of the proposed ABCVS strategy results in better ABCVS, regarding higher interaction, performance and efficiency. Furthermore, different experiments have been conducted on different configurations to compare ABCVS with existing strategies, where ABCVS shows it can compete against the other strategies regarding both efficiency and performance. As part of our future work, we want to study other metaheuristic approaches to hybrid these with ABC to increase efficiency. This hybridisation should be performed in a way that does not decrease performance and can increase the support for test suite generation for $t > 6$.

REFERENCES

- [1] Kalae, A. and V. Rafe, An optimal solution for test case generation using ROBDD graph and PSO algorithm. *Quality and Reliability Engineering International*, 2016. 32(7): p. 2263-2279.
- [2] Zamli, K.Z., et al., Design and implementation of a t-way test data generation strategy with automated execution tool support. *Information Sciences*, 2011. 181(9): p. 1741-1758.
- [3] Ahmed, B.S., T.S. Abdulsamad, and M.Y. Potrus, Achievement of minimized combinatorial test suite for configuration-aware software functional testing using the Cuckoo Search algorithm. *Information and Software Technology*, 2015. 66: p. 13-29.
- [4] Alsewari, A.R.A. and K.Z. Zamli, Design and implementation of a harmony-search-based variable-strength t-way testing strategy with constraints support. *Information and Software Technology*, 2012. 54(6): p. 553-568.
- [5] Lei, Y., et al., IPOG/IPOG - D: efficient test generation for multi - way combinatorial testing. *Software Testing, Verification and Reliability*, 2008. 18(3): p. 125-148.
- [6] Hartman, A., T. Klinger, and L. Raskin, IBM intelligent test case handler. <http://www.alpha-works.ibm.com/tech/whitch>, 2016. 284(1): p. 149-156.
- [7] Ahmed, B.S., K.Z. Zamli, and C.P. Lim, Application of particle swarm optimization to uniform and variable strength covering array construction. *Applied Soft Computing*, 2012. 12(4): p. 1330-1347.
- [8] Chen, X., et al., Variable strength interaction testing with an ant colony system approach, in *Software Engineering Conference, 2009. APSEC'09. Asia-Pacific. 2009, IEEE*. p. 160-167.
- [9] Cohen, M.B., *Designing Test Suites for Software Interactions Testing*. 2004, *Designing Test Suites for Software Interactions Testing: Department of Computer Science*.
- [10] Cohen, M.B., et al. A variable strength interaction testing of components. in *Computer Software and Applications Conference. COMPSAC 2003. Proceedings. 27th Annual International. 2003. IEEE*.
- [11] Stardom, J., *Metaheuristics and the search for covering and packing arrays*. 2001, Simon Fraser University.
- [12] Shiba, T., T. Tsuchiya, and T. Kikuno. Using artificial life techniques to generate test cases for combinatorial testing. in *Computer Software and Applications Conference, 2004. COMPSAC 2004. Proceedings of the 28th Annual International. 2004. IEEE*.
- [13] Kacker, R.N. and J.T. Jimenez, *Tower of Covering Arrays*. 2015.
- [14] HOMAID, A.B., et al., Adapting the Elitism on the Greedy Algorithm for Variable Strength Combinatorial Test Cases Generation. *IET Software*, 2018.
- [15] Homaid, A.A.B., et al., A Kidney Algorithm for Pairwise Test Suite Generation. *Advanced Science Letters*, 2018. 24(10): p. 7284-7289.
- [16] Afzal, W., R. Torkar, and R. Feldt, A systematic review of search-based testing for non-functional system properties. *Information and Software Technology*, 2009. 51(6): p. 957-976.
- [17] Bryce, R.C. and C.J. Colbourn. One-test-at-a-time heuristic search for interaction test suites. in *Proceedings of the 9th annual conference on Genetic and evolutionary computation. 2007. ACM*.
- [18] Maity, S. and A. Nayak. Improved test generation algorithms for pairwise testing. in *Software Reliability Engineering, 2005. ISSRE 2005. 16th IEEE International Symposium on. 2005. IEEE*.
- [19] Yilmaz, C., M.B. Cohen, and A. Porter. Covering arrays for efficient fault characterization in complex configuration spaces. in *ACM SIGSOFT Software Engineering Notes. 2004. ACM*.
- [20] Zamli, K.Z., M.H.M. Hassin, and B. Al-Kazemi. tReductSA-Test Redundancy Reduction Strategy Based on Simulated Annealing. in *International Conference on Intelligent Software Methodologies, Tools, and Techniques. 2014. Springer*.
- [21] Cohen, M.B., C.J. Colbourn, and A.C. Ling, Constructing strength three covering arrays with augmented annealing. *Discrete Mathematics*, 2008. 308(13): p. 2709-2722.
- [22] Sabharwal, S., et al., Construction of mixed covering arrays for pairwise testing using probabilistic approach in genetic algorithm. *Arabian Journal for Science and Engineering*, 2016. 41(8): p. 2821-2835.
- [23] Bansal, P., et al., Construction of variable strength covering array for combinatorial testing using a greedy approach to genetic algorithm. *e-Infomatica Software Engineering Journal*, 2015. 9(1).
- [24] Bansal, P., et al. An approach to test set generation for pair-wise testing using genetic algorithms. in *International Symposium on Search Based Software Engineering. 2013. Springer*.
- [25] Flores, P. and Y. Cheon. PWISEGen: Generating test cases for pairwise testing using genetic algorithms. in *Computer Science and Automation Engineering (CSAE), 2011 IEEE International Conference on. 2011. IEEE*.
- [26] McCaffrey, J.D. An empirical study of pairwise test set generation using a genetic algorithm. in the *2010 Seventh International Conference on Information Technology: New Generations (ITNG). 2010. IEEE*.
- [27] Sthamer, H.-H., *The automatic generation of software test data using genetic algorithms*. 1995, University of Glamorgan.
- [28] Wu, H., et al., A discrete particle swarm optimization for covering array generation. *IEEE Transactions on Evolutionary Computation*, 2015. 19(4): p. 575-591.
- [29] Mahmoud, T. and B.S. Ahmed, An efficient strategy for covering array construction with fuzzy logic-based adaptive swarm optimization for software testing use. *Expert Systems with Applications*, 2015. 42(22): p. 8753-8765.
- [30] Ahmed, B.S. and K.Z. Zamli, A variable strength interaction test suites generation strategy using Particle Swarm Optimization. *Journal of Systems and Software*, 2011. 84(12): p. 2171-2185.
- [31] Zamli, K.Z., A.A. Al-Sewari, and M.H.M. Hassin, On Test Case Generation Satisfying the MC/DC Criterion. *International Journal of Advances in Soft Computing & Its Applications*, 2013. 5(3).
- [32] AbdulRahman A. Alsewari, K.Z.Z., *Interaction Test Data Generation Using Harmony Search Algorithm*. 2011.
- [33] Nasser, A.B., et al., A cuckoo search based pairwise strategy for combinatorial testing problem. *Journal of Theoretical and Applied Information Technology*, 2015. 82(1): p. 154.
- [34] Nasser, A.B., A.R.A. Alsewari, and K.Z. Zamli. Tuning of cuckoo search based strategy For T-Way testing. in *International Conference on Electrical and Electronic Engineering. 2015*.
- [35] Alsariera, Y.A., A. Nasser, and K.Z. Zamli, Benchmarking of Bat-inspired interaction testing strategy. *International Journal of Computer Science and Information Engineering (IJSIE)*, 2016. 7: p. 71-79.
- [36] Alsariera, Y.A. and K.Z. Zamli, A bat-inspired strategy for t-way interaction testing. *Advanced Science Letters*, 2015. 21(7): p. 2281-2284.

- [37] Alsariera, Y.A., M.A. Majid, and K.Z. Zamli, Adopting the bat-inspired algorithm for interaction testing, in The 8th edition of annual conference for software testing. 2015. p. 14.
- [38] Alsariera, Y.A., M.A. Majid, and K.Z. Zamli, SPLBA: An interaction strategy for testing software product lines using the Bat-inspired algorithm, in 4th International Conference on Software Engineering and Computer Systems (ICSECS). 2015, IEEE. p. 148-153.
- [39] Alsariera, Y.A., M.A. Majid, and K.Z. Zamli, A bat-inspired Strategy for Pairwise Testing. ARPN Journal of Engineering and Applied Sciences, 2015. 10: p. 8500-8506.
- [40] Alsewari, A.A., et al., ABC Algorithm for Combinatorial Testing Problem. Journal of Telecommunication, Electronic and Computer Engineering (JTEC), 2017. 9(3-3): p. 85-88.
- [41] Alazzawi, A.K., et al., Artificial Bee Colony Algorithm for Pairwise Test Generation. Journal of Telecommunication, Electronic and Computer Engineering (JTEC), 2017. 9(1-2): p. 103-108.
- [42] Nasser, A.B., et al. Assessing optimization based strategies for t-way test suite generation: the case for flower-based strategy. in Control System, Computing and Engineering (ICCSCE), 2015 IEEE International Conference on. 2015. IEEE.
- [43] Nasser, A.B., et al. Sequence and sequence-less T-way test suite generation strategy based on flower pollination algorithm. in Research and Development (SCORED), 2015 IEEE Student Conference on. 2015. IEEE.
- [44] Nasser, A., et al., Late acceptance hill climbing based strategy for addressing constraints within combinatorial test data generation. 2014.
- [45] Nie, C. and H. Leung, A survey of combinatorial testing. ACM Computing Surveys (CSUR), 2011. 43(2): p. 11.
- [46] Williams, A.W., Determination of test configurations for pair-wise interaction coverage, in Testing of Communicating Systems. 2000, Springer. p. 59-74.
- [47] Hartman, A., Software and hardware testing using combinatorial covering suites, in Graph theory, combinatorics and algorithms. 2005, Springer. p. 237-266.
- [48] Czerwonka, J. Pairwise testing in the real world: Practical extensions to test-case scenarios. in Proceedings of 24th Pacific Northwest Software Quality Conference, Citeseer. 2006.
- [49] Cohen, D.M., et al., The AETG system: An approach to testing based on combinatorial design. Software Engineering, IEEE Transactions on, 1997. 23(7): p. 437-444.
- [50] Bryce, R.C. and C.J. Colbourn, A density - based greedy algorithm for higher strength covering arrays. Software Testing, Verification and Reliability, 2009. 19(1): p. 37-53.
- [51] Bryce, R.C. and C.J. Colbourn, The density algorithm for pairwise interaction testing. Software Testing, Verification and Reliability, 2007. 17(3): p. 159-182.
- [52] Arshem, J., TVG. <http://sourceforge.net/projects/tvg/>, 2010.
- [53] Tung, Y.-W. and W.S. Aldiwan. Automating test case generation for the new generation mission software system. in Aerospace Conference Proceedings, 2000 IEEE. 2000. IEEE.
- [54] Yu, Y., S.P. Ng, and E.Y. Chan. Generating, selecting and prioritizing test cases from specifications with tool support. in Quality Software, 2003. Proceedings. Third International Conference on. 2003. IEEE.
- [55] Lehmann, E. and J. Wegener, Test case design by means of the CTE XL, in Proceedings of the 8th European International Conference on Software Testing, Analysis & Review (EuroSTAR 2000), Copenhagen, Denmark. 2000.
- [56] Jenkins, Jenny. <http://www.burtleburtle.net/bob/math/>, 2003.
- [57] Cohen, M.B., M.B. Dwyer, and J. Shi. Interaction testing of highly-configurable systems in the presence of constraints. in Proceedings of the 2007 international symposium on Software testing and analysis. 2007. ACM.
- [58] Lei, Y., et al., IPOG: A general strategy for t-way software testing, in Engineering of Computer-Based Systems, 2007. ECBS'07. 14th Annual IEEE International Conference and Workshops on the. 2007, IEEE. p. 549-556.
- [59] Forbes, M., et al., Refining the in-parameter-order strategy for constructing covering arrays. Journal of Research of the National Institute of Standards and Technology, 2008. 113(5): p. 287.
- [60] Calvagna, A. and A. Gargantini. IPO-s: incremental generation of combinatorial interaction test data based on symmetries of covering arrays. in Software Testing, Verification and Validation Workshops, 2009. ICSTW'09. International Conference on. 2009. IEEE.
- [61] Wang, Z., B. Xu, and C. Nie. Greedy heuristic algorithms to generate variable strength combinatorial test suite. in Quality Software, 2008. QSIC'08. The Eighth International Conference on. 2008. IEEE.
- [62] Esfandyari, S. and V. Rafe, A tuned version of genetic algorithm for efficient test suite generation in interactive t-way testing strategy. Information and Software Technology, 2018. 94: p. 165-185.
- [63] Zamli, K.Z., B.Y. Alkazemi, and G. Kendall, A Tabu Search hyper-heuristic strategy for t-way test suite generation. Applied Soft Computing, 2016. 44: p. 57-74.
- [64] Karaboga, D., An idea based on honey bee swarm for numerical optimization. 2005, Technical report-tr06, Erciyes university, engineering faculty, computer engineering department.
- [65] Karaboga, D. and B. Akay, A comparative study of artificial bee colony algorithm. Applied mathematics and computation, 2009. 214(1): p. 108-132.
- [66] Kuhn, R. ACTS download page. [cited 2018 2018]; Available from: http://csrc.nist.gov/groups/SNS/acts/download_tools.html
- [67] Wu, H., et al. DPSO download page. [cited 2018 2018]; Available from: <https://github.com/waynedd/DPSO>.

Improving the Performance of $\{0,1,3\}$ -NAF Recoding Algorithm for Elliptic Curve Scalar Multiplication

Waleed K. AbdulRaheem¹, Sharifah Bte Md Yasin², Nur Izura Binti Udzir³, Muhammad Rezal bin Kamel Ariffin⁴
Faculty of Computer Science and Information Technology, University Putra Malaysia, Selangor, Malaysia^{1,2,3}
Institute for Mathematical Research, University Putra Malaysia, Selangor, Malaysia⁴

Abstract—Although scalar multiplication is highly fundamental to elliptic curve cryptography (ECC), it is the most time-consuming operation. The performance of such scalar multiplication depends on the performance of its scalar recoding which can be measured in terms of the time and memory consumed, as well as its level of security. This paper focuses on the conversion of binary scalar key representation into $\{0, 1, 3\}$ -NAF non-adjacent form. Thus, we propose an improved $\{0, 1, 3\}$ -NAF lookup table and mathematical formula algorithm which improves the performance of $\{0, 1, 3\}$ -NAF algorithm. This is achieved by reducing the number of rows from 15 rows to 6 rows, and reading two (instead of three) digits to produce one. Furthermore, the improved lookup table reduces the recoding time of the algorithm by over 60% with a significant reduction in memory consumption even with an increase in key size. Specifically, the improved lookup table reduces the memory consumption by as much as 75% for the big key, which shows its higher level of resilience to side channel attacks.

Keywords—*Elliptic Curve Cryptosystem (ECC); scalar multiplication algorithm; $\{0, 1, 3\}$ -NAF method; Non-Adjacent Form (NAF)*

I. INTRODUCTION

Elliptic curves cryptosystem (ECC) was proposed by Neal Koblitz and Victor Miller independently in 1985 to design the public-key cryptographic system [1]. Similar to other public key cryptographic algorithms, elliptic curve cryptosystem deploys a public key and private key. The public key is used for encryption to provide data confidentiality during communication. ECC is implemented in smart card because of its smaller key size and less computational complexity relative to RSA cryptosystem [2]. This makes it attractive and suitable for such applications.

Scalar multiplication is a fundamental and time-consuming operation in ECC [3]. The scalar multiplication involves computing $Q = kP$ where k is an integer and P, Q are points on an elliptic curve. It is performed by repeating point addition/subtraction and point doubling operations. The representation of scalar k plays an important role in improving the performance of this operation. Hamming weight of scalar involves the number of the non-zero digits. As such, it determines the number of the required point addition/subtraction operation. Therefore, hamming weight is one of the performance factor for the scalar multiplication operation. Many researchers have tried to improve the performance of the scalar multiplication by representing k in other forms with minimal hamming weight [4]. However, these works does not improve the hamming weight for the

$\{0,1,3\}$ method, but improving the timing, memory consuming and security for the previous method since it is working on existing lookup table.

In literature, it is proven that reducing the Hamming weight of the scalar k can improve the performance of scalar multiplication [5],[6] and [7]. Additionally, the scalar k can be represented in base 2 or otherwise or by using combination of different bases. In base 2, k is in binary, NAF or w -NAF. In bases other than 2, k can be represented in r -NAF [8] or g -NAF[9]. Examples of combination of different bases include mixed ternary/binary[10], DBNS [11], [12], and mbNAF [13]. Various recoding algorithms used in the literature include complement recoding technique [14], hybrid complementary and 1's complement recoding technique [15].

In the aforementioned methods, the hamming weight and its effect on the performance of the scalar multiplication were well discussed. For example, width w -NAF is more efficient. However, it increases the w value [6], which implies more time and memory is consumed as it requires more operation during pre-computation. It is important to make a trade-off between the performances categories according to the target objective for implementation [16].

The contributions of this paper are as follows: The $\{0, 1, 3\}$ -NAF method is introduced to convert the binary digit $\{0, 1\}$ using a proposed lookup table or mathematical formula. The existing lookup table is of size 15 rows and 6 columns and contains special cases, which reads three digits during the recoding to produce one. In this paper, a new lookup table of size 6 rows and 5 columns is proposed to recode the scalar. The proposed lookup table reads two digits to produce one and contains no special cases. The proposed is better than the original in terms of time, memory and security. The remainder of this paper is organized as follows: Section 2 discusses the related work, while Section 3 introduces the $\{0, 1, 3\}$ -NAF method. The proposed method and the performance analysis are presented in Section 4 and Section 5, respectively. Finally, conclusion and the future works are presented in Section 6.

II. RELATED WORKS

In literature, recoding algorithm is used to change the representation of k to another form without changing the magnitude of the scalar. There are two types of recoding algorithm [17]: left-to-right (L2R) and right-to-left (R2L). L2R recoding is done by scanning digit of k from the most significant bit (MSB) and the latter is by scanning digit k from Least Significant Bit (LSB). L2R recoding saves memory and

is mostly preferred for memory constrained devices [18]. It depends on the number of rows of the lookup table and number of required digits read while recoding.

However, the performance of recoding algorithms depends on the hardware system implementation and memory storage [16] and [19]. Efficient recoding must have recoding rules that are efficient, simple, and consumes less memory [20]. An optimal recoding strategy must provide a trade-off between high nonzero density and low memory consumption [6]. Selection of radix or digit set for a scalar must also satisfy the characteristics of the scalar multiplication algorithm or implementation technology. According to [21], proper selection of radix and digit set for the scalar can promote an increase of the frequency of useful digits such as zero and a reduction in the total number of nonzero digits to represent a number.

Reitwiesner (1960) proposed a R2L with non-adjacent form (NAF) recoding which converts a binary number $\{0,1\}$ into NAF with digit $\{-1,0,1\}$ -NAF [22] as shown in Algorithm 1. A non-adjacent form means that there is no consecutive non-zero digit in the scalar k . In $\{-1, 0, 1\}$ -NAF recoding, a binary number of form $K = (K_{m-1}, \dots, K_0)_2$ with $K_i \in \{0, 1\}$ converted into a canonical form $Y = (Y_m, Y_{m-1}, \dots, Y_0)$ with $Y_m \in \{-1, 0, -1\}$ using Algorithm 1. The average hamming weight of NAF is $n/3$.

Algorithm 1: R2L NAF Recoding

```

Input:  $X = (X_{m-1}, \dots, X_0)_2$ 
Output:  $Y = (Y_m, Y_{m-2}, \dots, Y_0)_{NAF}$ 
1    $C_0 \leftarrow 0; X_{m+1} \leftarrow 0; Y_m \leftarrow 0$ 
2   For  $i$  from 0 to  $m$  do
3      $C_{i+1} \leftarrow \lfloor (C_i + X_i + X_{i-1})/2 \rfloor$ 
4      $Y_i \leftarrow C_i + Y_i + 2.C_{i+1}$ 
5   Return  $Y = (Y_m, Y_{m-2}, \dots, Y_0)_{NAF}$ 

```

Example 1: Convert the binary number $k = (11111)_2$ into NAF method using the Algorithm 1.

Solution: $(11111)_2 = (10000 - 1)_{NAF}$

It is worthy of note that the hamming weight (number of non-zeroes) reduced from 5 into 2.

Joye and Yen [23] proposed an optimal L2R recoding algorithm for the binary number, The recoding however does not have NAF property as shown in Algorithm 2. They also use the lookup table to convert the binary to $\{-1, 0, 1\}$ form as shown in Table I.

TABLE I. L2R SIGNED-DIGIT RECODING ($x = 0$ OR 1)

bi	X_i	X_{i-1}	X_{i-2}	b_{i-1}	Y_i
0	0	0	x	0	0
0	0	1	0	0	0
0	0	1	1	1	1
0	1	0	x	0	1
1	0	1	x	1	-1
1	1	0	0	0	-1
1	1	0	1	1	0
1	1	1	x	1	0

Algorithm 2: L2R Signed Digit Recoding

```

Input:  $X = (X_{m-1}, \dots, X_0)_2$ 
Output:  $Y = (Y_m, Y_{m-1}, \dots, Y_0)_2$ 
1    $b_m \leftarrow 0; X_m \leftarrow 0; X_{-1} \leftarrow 0; X_{-2} \leftarrow 0$ 
2   For  $i$  from  $m$  down to 0 do
3      $b_{i-1} \leftarrow \lfloor (b_m + X_{i-1} + X_{i-2})/2 \rfloor$ 
4      $Y_i \leftarrow -2b_i + X_i + b_{i-1}$ 
5   Return  $Y$ 

```

Note that in Example 1, using Algorithm 1, 2 or the lookup Table I will give the same result $(10000-1)$, but there is a considered difference in the time and memory consumed.

Rezai et.al [24] proposed an L2R recoding algorithm while deploying Markov chain to measure the hamming weight. They identified that their L2R method has a hamming weight of $3n/13$.

III. EXISTING $\{0, 1, 3\}$ -NAF RECODING ALGORITHM

Yasin [25] proposed a recoding algorithm based on the idea from Reitwiesner's (R2L) [22] and Joye and Yen (L2R) [23]. The algorithm is also an L2R recoding and it converts a binary into a non-adjacent form in base 2 with digit $\{0, 1, 3\}$ using Table II. The author has been proven that the representation follows the non-adjacent form (NAF) property. Algorithm 3 is used to convert the binary into $\{0, 1, 3\}$ -NAF

Table II is a lookup table used together with Algorithm 3. Table II consists of 15 rows, and the algorithm starts with scanning three digits L2R. There are also special cases for certain conditions.

Algorithm 3: L2R $\{0,1,3\}$ -NAF Recoding

```

Input:  $r = (r_{m-1}, \dots, r_0)_2$ 
Output:  $r' = (r'_m, r'_{m-1}, \dots, r'_0)_{\{0,1,3\}-NAF}$ 
1    $b_m \leftarrow 0; r_m \leftarrow 0; r_{-1} \leftarrow 0; r_{-2} \leftarrow 0; r'_{-1} \leftarrow 0$ 
2   For  $i$  from  $m-1$  down to 0 do
3     scan two digits  $r$  from MSB i.e.  $r_i$  and  $r_{i+1}$ 
4     Compute  $b_i \leftarrow \lfloor (b_{i+1} + r_i + r_{i-1})/2 \rfloor$ 
5     Compare  $(b_{i+1}, r_{i+1}, r_i, r_{i-1}, b_i)$  with values from lookup table row by row:
6     If  $[(b_{i+1}, r_{i+1}, r_i, r_{i-1}, b_i) \equiv \{(\text{row1}) \text{ or } (\text{row3}) \text{ or } (\text{row5}) \text{ or } (\text{row6}) \text{ or } (\text{row8}) \text{ or } (\text{row9}) \text{ or } (\text{row10}) \text{ or } (\text{row13}) \text{ or } (\text{row15})\}]$  then  $r'_i = 0$ 
7     If  $[(b_{i+1}, r_{i+1}, r_i, r_{i-1}, b_i) \equiv \{(\text{row2}) \text{ or } (\text{row4}) \text{ or } (\text{row7})\}]$  then  $r'_i = 1$ 
8     if  $[(b_{i+1}, r_{i+1}, r_i, r_{i-1}, b_i) \equiv \{(\text{row11}) \text{ or } (\text{row12}) \text{ or } (\text{row14})\}]$  then  $r'_i = 3$ 
8   return  $(r'_m, r'_{m-1}, \dots, r'_0)$ 

```

Example 2: Convert the number (1101101101) from binary into $\{0,1,3\}$ -NAF method.

Solution: applying the lookup Table II or Algorithm 3 by reading 3 digits from L2R will give the result $(0300300301)_{\{0,1,3\}-NAF}$, which reduce the hamming weight from 7 into 4.

TABLE II. L2R {0,1,3}-NAF RECODING (X=0 OR 1)

No	b_{i+1}	r_{i-1}	r_i	r_{i+1}	Special Case	r'_i	b_i
1	0	0	0	x		0	0
2	0	0	1	0		1	0
3	0	0	1	1	if consecutive #1's is even	0	1
4	0	0	1	1	if consecutive #1's is odd	1	1
5	0	1	0	x		0	0
6	0	1	1	1	If $r'_{i+1}=1$ OR 3	0	1
7	1	0	1	0		1	1
8	1	0	1	1		1	1
9	1	1	0	0		0	0
10	1	1	0	1	If $r'_{i+1}=1$ OR 3	0	1
11	1	1	0	1	If $r'_{i+1}=0$	3	1
12	1	1	1	0	If $r'_{i+1}=0$	3	1
13	1	1	1	0	If $r'_{i+1}=1$	0	1
14	1	1	1	1	If $r'_{i+1}=0$	3	1
15	1	1	1	1	If $r'_{i+1}=1$ OR 3	0	1

IV. PROPOSED ALGORITHM

So we proposed Table III which converts a binary into {0,1,3}-NAF with high performance. Table III consists of 6 rows and it is used together with Algorithm 4. The algorithm starts with scanning two digits from R2L

Table III is an improved version of Table II. The table size is reduced from 15 rows to 6 rows. Algorithm 4 is used together with Table III to converts a binary into {0,1,3}-NAF.

Algorithm 4: Improved R2L {0,1,3}-NAF Recoding

Input: $X = (X_{m-1}, \dots, X_0)_2$

Output: $Y = (Y_m, Y_{m-1}, \dots, Y_0)_{\{0,1,3\}\text{-NAF}}$

- 1 $C_0 \leftarrow 0; X_m \leftarrow 0$
- 2 For i from 0 to m do
- 3 Scan two digit X from LSB (X_{i+1}, X_i)
- 4 Use lookup table, find Y_i that match (C_i, X_{i+1}, X_i)
- 5 Use lookup table, find C_{i+1}
- 6 Return Y

In Algorithm 3, line 4 computes b_i for each iteration. Also, line 5 do comparison of function $f(b_{i+1}, r_{i+1}, r_i, r_{i-1}) = (r'_i, b_i)$ with the values in a row in the lookup table. In Algorithm 4, comparison of function $f(C_i, X_{i+1}, X_i) = (Y_i, C_{i+1})$ is done in line 4. It is worthy of note that number of comparison is minimal than the one in Algorithm 3, since size of lookup table for Algorithm 3 is bigger than the size of lookup table used in Algorithm 4.

TABLE III. IMPROVED LOOKUP TABLE OF {0,1,3}-NAF RECODING

No	C_i	X_{i+1}	X_i	Y_i	C_{i+1}
1	0	0	0	0	0
2	0	1	0	0	0
3	0	0	1	1	0
4	0	1	1	3	1
5	1	0	1	0	0
6	1	1	1	0	0

In Table III, a new mathematical formula can be introduced to recode the digit without using the lookup table as presented in Algorithm 5.

Algorithm 5: Improved {0,1,3} –NAF Recoding R2L.

Input: $x = (x_{m-1}, \dots, x_0)_2$

Output: $y = (y_m, y_{m-1}, \dots, y_0)_{\{0,1,3\}\text{-NAF}}$

1. $C_0 \rightarrow 0, x_m \rightarrow 0$
2. For $i = 0$ to m do
3. $y_i = x_i * x_{i+1} + (x_{i+1} - C_i) - C_i$
4. $C_{i+1} = (y_i + x_i + C_i)/2$
5. return $y = (y_m, y_{m-1}, \dots, y_0)_{\{0,1,3\}\text{-NAF}}$

In the proposed Algorithm 5, the value of y_i can be calculated using the values of (x_{i+1}, x_i, C_i) mathematically as in step 3, while the value of C_{i+1} can be computed using the values of (y_i, x_i, C_i) mathematically as in step 4.

In general, lookup table is more efficient in terms of time and memory since lookup table contains no mathematical operations such as multiplication and division as in Algorithm 5.

V. PERFORMANCE ANALYSIS

In terms of performance, we will compare between the proposed lookup table and the original lookup table [25] in terms of response time, memory usage and security. We implemented the two tables in JAVA (NetBeans IDE 8.0.2). The conversion from binary expansion to a new {0,1,3}-NAF representation is run successfully.

Table IV shows the time in seconds for different bit sizes of 24, 28, 32, and 36 bits. As the bit sizes decreases, the level of reduction in percentage is also decreases.

It is clear that the proposed lookup table is faster than current lookup table. The conversion processes also consume less time. Fig. 1 shows the reduction time between the two lookup tables.

Fig. 1 shows that our proposed lookup table is more efficient for larger bit size due to its higher reduction percentage.

In terms of the memory performance, the proposed algorithm consumes less memory with higher percentage for large bit key sizes as shown in Table V and Fig. 2.

In Fig. 1 and Fig. 2, the performance achieved due the small lookup table size. While recoding, two digits only need to scan so as to produce one digits. Also this can be more efficient with key of big size.

TABLE IV. CONVERSION TIME FROM BINARY TO {0,1,3}-NAF FOR L2R AND MODIFIED R2L {0,1,3}-NAF ALGORITHMS

Size of bits	L2R {0,1,3}-NAF Recoding(Seconds)	Proposed R2L {0,1,3}-NAF Recoding (Seconds)	Reduction Percentage
36	123650	49918	60%
32	6839	2897	58%
28	389	173	56%
24	22	11	50%

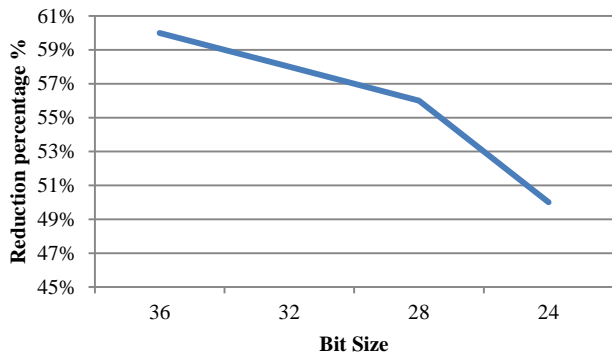


Fig. 1. Reduction Percentage of Time Related to Bit Size for the Proposed Lookup Table.

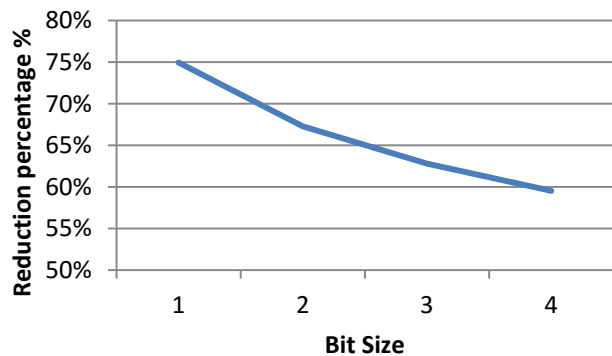


Fig. 2. Reduction Percentage of Time Related to Bit Size for the Proposed Lookup Table.

TABLE V. CONVERSION MEMORY BY KBYTES FROM BINARY TO {0,1,3}-NAF FOR L2R AND MODIFIED R2L {0,1,3}-NAF ALGORITHMS

Size of bits	L2R {0,1,3}-NAF Recoding (Kbytes)	Proposed R2L {0,1,3}-NAF Recoding (Kbytes)	Reduction Percentage
36	75416	18897	75%
32	41837	13691	67%
28	30937	11511	63%
24	25112	10164	60%

So, it is clear that the proposed is better than the original {0, 1, 3}-NAF algorithm.

To achieve better ECC security, a larger bit size is desired which makes the proposed lookup table more efficient in terms of time and the memory usage. It is thus more suitable for implementation in ECC.

In term of security, the original lookup table is vulnerable to side channel attack such as simple power attack SPA and timing attack TA due to its non-constant time execution [26]. The original lookup has two exceptional cases to the count number of 1's in line 4 & 5 in Table II. While using the lookup table, if there is a consecutive 1's it consumes more memory and time while recoding the original lookup table which makes it vulnerable to attacks. For instance, a hacker can guess that there is a consequent 1's at a part of the key [27].

VI. CONCLUSION AND FUTURE WORKS

In this paper, a new lookup table and mathematical formula have been proposed to improve the {0, 1, 3}-NAF method. The proposed method shows improvement in terms of time, memory and security aspects compared to the original {0, 1, 3}-NAF method, since it reduces the lookup table size from 15 rows into 6, and reads two digits during the recoding to produce one instead of three. Time and memory are reduced while recoding execution with a percentage up to 60% and 75% respectively. The performance of the proposed lookup is more efficient while key size is bigger.

We suggest that this scalar recoding is applied in scalar multiplication either using Montgomery Ladder to achieve better security or using τ NAF with Koblitz curves for higher efficiency. The digit 3 can be precomputed using different coordinates such as projective and affine over different curves such as binary, Edward and prime curves.

ACKNOWLEDGMENT

This work was supported by Ministry of Higher Education under FRGS Grant no. 5524822.

REFERENCES

- [1] K. E. Abdullah and N. H. M. Ali, "Security Improvement in Elliptic Curve Cryptography," *Int. J. Adv. Comput. Sci. Appl.*, vol. 9, no. 5, pp. 122–131, 2018.
- [2] Z. U. A. Khan and M. Benaissa, "High Speed and Low Latency ECC Processor Implementation over GF (2^m) on FPGA," *IEEE Trans. Very Large Scale Integr. Syst.*, vol. 25, no. 1, p. 165–176., 2017.
- [3] N. Thangarasu and A. A. L. Selvakumar, "Improved elliptical curve cryptography and Abelian group theory to resolve linear system problem in sensor-cloud cluster computing," *Cluster Comput.*, pp. 1–10, 2018.
- [4] M. M. Ahmad, S. M. Yasin, R. Mahmud, and M. A. Mohamed, "X-Tract Recoding Algorithm for Minimal Hamming Weight Digit Set Conversion," *J. Theor. Appl. Inf. Technol.*, vol. 75, no. 1, pp. 109–114, 2015.
- [5] O. Ugus, D. Westhoff, R. Laue, A. Shoufan, and S. A. Huss, "Optimized Implementation of Elliptic Curve Based Additive Homomorphic Encryption for Wireless Sensor Networks," *arXiv Prepr. arXiv0903.3900.*, 2009.
- [6] K. Okeya and T. Takagi, "The Width- w NAF Method Provides Small Memory and Fast Elliptic Scalar Multiplications," pp. 328–343, 2003.
- [7] A. Rezai and P. Keshavarzi, "CCS Representation : A new non-adjacent form and its application in ECC," *J. Basic Appl. Sci. Res.*, vol. 2, no. 5, pp. 4577–4586, 2016.
- [8] T. Takagi, S. Yen, and B. Wu, "Radix- r Non-adjacent Form," *Springer-Verlag Berlin Heidelb.*, pp. 99–100, 2004.
- [9] M. Joye and S. Yen, "New Minimal Modified Radix- r Representation with Applications to Smart Cards," in *International Workshop on Public Key Cryptography*, 2002, pp. 375–383.
- [10] M. Joye, "Trading Inversions for Multiplications in Elliptic," *Des. codes Cryptogr.*, pp. 189–206, 2006.
- [11] V. Dimitrov, L. Imbert, and P. K. Mishra, "The double-base number system and its application to elliptic curve cryptography," *Math. Comput.*, vol. 77, no. 262, pp. 1075–1104, 2008.
- [12] C. Doche and L. Habsieger, "A Tree-Based Approach for Computing Double-Base Chains A Tree-Based Approach for Computing Double-Base Chains," *Australas. Conf. Inf. Secur. Priv.* (pp. 433-446). Springer, Berlin, Heidelberg., no. June 2008, 2016.
- [13] P. Longa and C. Gebotys, "Setting Speed Records with the (Fractional) Multibase Non-Adjacent Form Method for Efficient Elliptic Curve Scalar Multiplication . Setting Speed Records with the (Fractional) Multibase Non-Adjacent Form Method for Efficient Elliptic Curve Scalar Mult," *IACR Cryptol. ePrint Arch.*, no. February, 2015.

- [14] P. Balasubramaniam and E. Karthikeyan, "Elliptic curve scalar multiplication algorithm using complementary recoding," *Appl. Math. Comput.*, vol. 190, pp. 51–56, 2007.
- [15] X. Huang, P. G. Shah, and D. Sharma, "Minimizing Hamming Weight Based on 1's Complement of Binary Numbers Over $GF(2^m)$," in *Advanced Communication Technology (ICACT), 2010 The 12th International Conference on (Vol. 2, pp. 1226-1230)*. IEEE., 2010, pp. 1226–1230.
- [16] M. Bafandehkar, S. M. Yasin, R. Mahmood, and Z. M. Hanapi, "Comparison of ECC and RSA algorithm in resource constrained devices," *2013 Int. Conf. IT Converg. Secur. ICITCS 2013*, pp. 0–2, 2013.
- [17] H. Cohen, G. Frey, and R. Avanzi, *Handbook of Elliptic and Hyperelliptic Curve Cryptography*. 2006.
- [18] M. Khabbazian, T. A. Gulliver, S. Member, and V. K. Bhargava, "A New Minimal Average Weight Representation for Left-to-Right Point Multiplication Methods," *IEEE Trans. Comput.* 54(11), 1454-1459., pp. 1–7, 2005.
- [19] W. K. A. Abdullaheem, "Comparative Analysis of the Performance for Cloud Computing Hypervisors with Encrypted Algorithms," 2014.
- [20] D. F. Aranha and K. Karabina, "Efficient Software Implementation of Laddering Algorithms Over Binary Elliptic Curves Efficient software implementation of laddering algorithms over binary elliptic curves," *Int. Conf. Secur. Privacy, Appl. Cryptogr. Eng.* (pp. 74-92). Springer, Cham, no. December, 2017.
- [21] E. Guerrini, L. Imbert, and T. Winterhalter, "Randomized Mixed-Radix Scalar Multiplication," *IEEE Trans. Comput.*, vol. 67, no. 3, pp. 418–431, 2018.
- [22] G. W. Reitwiesner, "The Determination of Carry Propagation Length for Binary Addition *," *IRE Trans. Electron. Comput.* (1), 35-38., vol. 0, pp. 35–38, 1960.
- [23] M. Joye and S. Yen, "Optimal Left-to-right Binary Signed-Digit Recoding," vol. 49, no. 7, pp. 1–8, 2000.
- [24] A. Rezaei and P. Keshavarzi, "A New Left-to-Right Scalar Multiplication Algorithm Using a New Recoding A New Left-to-Right Scalar Multiplication Algorithm Using a New Recoding Technique," *Int. J. Secur. its Appl.*, vol. 8, no. 3, pp. 31–38, 2015.
- [25] S. M. Yasin, "New signed-digit {0, 1, 3}-NAF scalar multiplication algorithm for elliptic curve over binary field.," 2011.
- [26] N. Tuveri, S. ul Hassan, C. P. Garcia, and B. B. Brumley, "Side-Channel Analysis of SM2: A Late-Stage Featurization Case Study," in *Proceedings of the 34th Annual Computer Security Applications Conference on - ACSAC '18, 2018*, pp. 147–160.
- [27] J. Fan, X. Guo, E. De Mulder, P. Schaumont, B. Preneel, and I. Verbauwhede, "State-of-the-art of secure ECC implementations: a survey on known side-channel attacks and countermeasures," in *Hardware-Oriented Security and Trust (HOST), IEEE International Symposium on, 2010*, pp. 76–87.

Novel Software-Defined Network Approach of Flexible Network Adaptive for VPN MPLS Traffic Engineering

Faycal Bensalah¹, Najib El Kamoun²

Lab STIC, FS El Jadida, University Chouaib Doukkali, El Jadida, Morocco

Abstract—Multi-Protocol Label Switching VPN (MPLS-VPN) is a technology for connecting multiple remote sites across the operator's private infrastructure. MPLS VPN offers advantages that traditional solutions cannot guarantee, in terms of security and quality of service. However, this technology is becoming more prevalent among businesses, banks or even public institutions. With this strong trend, the management of the paths on which these tunnels can be deployed has become a necessity is a priority need for Internet access providers (ISPs). Through the principle of controller orchestration, ISPs can overcome this difficulty. Software-defined network is a paradigm allowing through the principle of orchestration to manage the entire network infrastructure. In this paper, we propose a new approach called FNA-TE "Flexible Network Adaptive - Traffic Engineering", this approach allows to manage MPLS VPN tunnels to meet the QoS requirements of those with the highest priority.

Keywords—SDN; QoS; VPN; MPLS; Adaptive network

I. INTRODUCTION

Multi-Protocol Label Switching "MPLS" is a transfer protocol that uses tags for routing data [1][2]. This technology brings more flexibility, speed, and security compared to the Internet Protocol "IP". The MPLS technology provides advantageous applications, among them we quote virtual private network "VPN" [3][4][5], quality of service "QoS"[6][7], security[8], all transport on MPLS "AToM".

Among the strengths of the MPLS technology, traffic engineering (TE) is used to optimize the use of network resources to avoid congestion. It is the consideration of the bandwidth available on a link during routing decisions that makes this optimization possible. MPLS-TE allows the establishment of MPLS tunnels routed explicitly according to the constraints of the transported traffic (bandwidth, delay ...) and the resources available in the network. MPLS-TE creates a connected mode in IP networks, optimizing the use of resources and maximizing the traffic load that can flow over the network while preserving the quality of service.

In order to overcome the complexities of implementing traffic engineering policies across multiple routers, software-defined network (SDN) [9][10][11] technology can be used. SDN de-couples the data plane from the control plane by centralizing it on a device called a controller. SDN can be used to solve a variety of problems related to the complexity and the high number of equipment. SDN is mainly based on three logical layers: the given layer, the control layer, and the

application layer. The application layer provides the set of services and applications used by the end user. The given layer contains the physical equipment responsible for conveying the information. The control layer contains all the operations and instructions that manage the entire network.

The rest of the paper is organized as follows: in Section 2 we will discuss the strengths of our contributions. In Section 3 we will detail the architecture of our solution. Section 4 will focus on performance evaluation. And we will conclude in Section 5.

II. FLEXIBLE NETWORK ADAPTIVE – TRAFFIC ENGINEERING

To understand the motivation behind our approach, we will briefly describe the existing issues in MPLS VPN technology:

- A customer may have one or more VPNs with the same or different destinations.
- These VPN tunnels can have different priorities.
- Multiple MPLS VPNs can follow the same path.
- Paths can have asymmetric performance, in terms of effective bandwidth and unused bandwidth.

A. Strengths

- 1) Detect VPN tunnels in the establishment phase or already established.
- 2) Draw the architecture of the intermediate network.
- 3) Detect for each tunnel the associated LSP.
- 4) Classify tunnels by priority.
- 5) Decide on the shortest LSP to assign to the VPN.
- 6) Check that the remaining bandwidth meets the QoS requirements of the tunnel.
- 7) Treat tunnels fairly; that is to say, not necessarily to route the tunnel with the highest priority by the short path having sufficient bandwidth, to the detriment of the lowest priority tunnels. A higher priority tunnel can be routed through the second or nth best path if this degrades the performance of the lower priority tunnels already deployed.

B. Proof

- Let G be a graph (V, E) with V are the vertex routers and E are links. $E(u, v)$ are the ends of a link.
- Let w be a neighbor vertex.

- Let B_a be the available bandwidth.
- The bandwidth of the first link to the source:

$$B_a^S = \text{Min} |\bar{B}_{au} - \bar{B}_{av}|$$

The bandwidth beyond the neighbor:

$$B_a^w = \text{Min} |\bar{B}_{au+1} - \bar{B}_{av+1}|$$

$U + 1$ and $v + 1$ to avoid a closed path.

The most optimal segment S is therefore defined by the following function:

$$S_i = \text{Max} |B_a^{si} - B_a^{wi}| ; \forall i \in V(G)$$

Since the segments are determined; they must be sorted by available bandwidth from the highest (h) to the lowest (l).

The path with the highest available bandwidth is defined by the following equation:

$$\rho^h = \sum_{u \in V(G)} S_i^h ; \forall S_i > B_{requested}$$

Consider MPLS VPN tunnels already established on an S-segment: either V_c the number of VPN tunnels and V_p the priority of a tunnel.

Suppose that the available bandwidth of the shortest path is not sufficient, our algorithm can move to the next path:

$$\rho^{h-1}, \rho^{h-2}, \dots, \rho^{h-n}, \text{ where } n \text{ is the variance.}$$

The variance is relative to the priority. A non-priority VPN can traverse the longest path with restricted bandwidth.

$$\rho^h \left(\sum_{i=1}^{V_c} V_{pi} \right) > V_{p req} ; \rho = \rho^{h-1}$$

Until this phase we were able to determine the shortest path having the available bandwidth meeting the QoS requirements of the source. But, is it necessary to move the other tunnels to another path in favor of the tunnel with the highest priority? In some cases we can find the nth best way for the tunnel with the highest priority:

Case 1: It is possible that several lower priority tunnels coexist in ρ .

Case 2: Moving several non-priority tunnels to another ρ can jeopardize their quality of service.

Case 3: Sometimes routing the highest priority VPN by the nth best path does not degrade the quality of its exchanges as this path meets the customer's QoS requirements.

The following formula is used to define the closest path ρ^{h-i} to the best ρ^h , meeting the Breq requirements.

$$\sum_{i=1}^{V_c} V_{pi} < V_{p req} ; \forall V_c \in [2, +\infty[$$

III. FNA-TE ARCHITECTURE

The proposed approach is based on three layers: application, control and data. Fig. 1 illustrates the proposed architecture.

The application layer is responsible for defining VPN tunnels and their priorities. Fig. 2 illustrates an example of the GUI interface for customizing tunnels.

The control layer can act on the path on which to deploy MPLS VPN tunnels based on the available bandwidth and the shortest route. This layer consists of five modules:

A. Network Discover

This module is responsible for detecting the network topology, V-vertex and E-links. In a hybrid network where routers do not support the OpenFlow protocol, additional protocols can be used as CDP for Cisco devices and LLDP for non-Cisco equipment. The controller verifies the network topology based on these protocols. For SDN devices, OFDP messages can be used for topology detection. In the case of the Moroccan university, specifically Chouaib Doukkali University, the routers set up do not support SDN. The topology detected automatically by our controller is shown in Fig. 3.

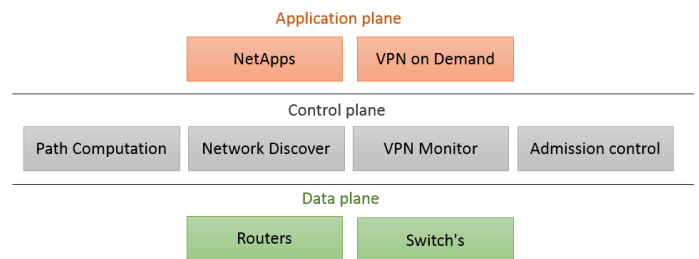


Fig. 1. The Architecture of the Proposed Approach.

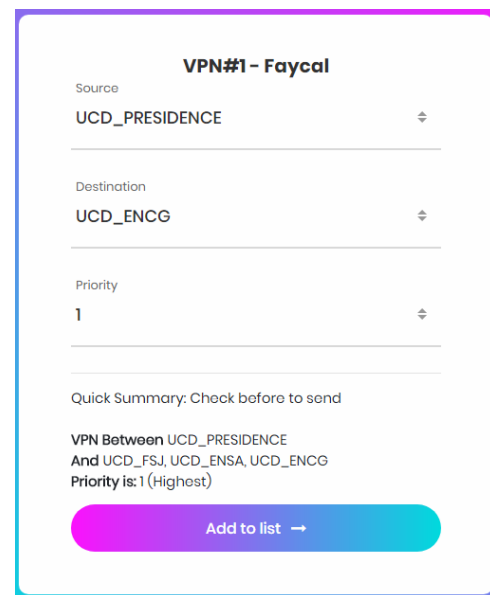


Fig. 2. The GUI Interface of the Application Layer.



Fig. 3. The Network Architecture Detected Automatically.

Algorithm 1: Path Computation

```
1 Load Ba : Available bandwidth;  
2 Load Breq : Requested bandwidth;  
3 Load  $\rho^h$  : Most optimal path;  
4 Load Vc : Number of tunnels on a path ;  
5 if ( $Ba < Breq \ \& \ Vc > 2 \ \& \ Vp > Vreq$ ) then  
6 |  $\rho = \rho^{(h-1)}$  ;  
7 end  
8 for each  $\rho = \rho^{(h-n)}$  ;  $n < 2$  do  
9 | if ( $Ba < Breq \ \& \ Vc > 2 \ \& \ Vp < Vreq$ ) then  
10 | |  $\rho = \rho^{(h-n)}$  ;  
11 | end  
12 end
```

Fig. 4. The Operating Algorithm of the Path Computation Module.

B. Path Computation

As soon as the topology is discovered, this module makes it possible to calculate the most optimal path on which to deploy / route the MPLS VPN tunnel. The processing performed by this module is described in the previous section. However, the algorithm 1 illustrated in Fig. 4 describes the main operating phases of this module.

C. VPN Monitor

This module is used to check the MPLS VPN already deployed on a router. The controller can verify the VPN instances already open on a device by querying the SNMP MIB object: 1.3.6.1.4.1.9.9.711 or launch the "Show ip vrf" or "display ip vpn instance" commands for routers such as Cisco, Juniper, and HP. Recall that the priority of a tunnel can be detected at the base of the initial declaration by the administrator during the first phase (please refer to Fig. 2).

D. Admission Control

This module allows authorizing or not:

- 1) The establishment of a tunnel.
- 2) Routing a higher priority VPN.

- 3) Destruction of a lower priority VPN if all paths are overloaded.
 - 4) The data plan contains all routers of the network architecture consisting of P, PE and CE equipment.
- In the next section we will evaluate the performance of our approach.

IV. PERFORMANCE EVALUATION

A. Network Testbed

In order to evaluate the performances of our approach, we set up a network testbed consists of several routers and tens of clients (Fig. 5). Used applications for the evaluation are Voice over IP [12][13][14], Video streaming, and Database traffic. Evaluation criteria are:

- 1) VoIP latency: Delay it takes for one endpoint to send a packet to another.
- 2) VoIP jitter: Delay between submission of two packets.
- 3) VoIP MOS: Quality imperceptible of the call.
- 4) VoIP loss rate: Quantity of VoIP non-received traffic.
- 5) Video loss rate: Amount of non-received video traffic.
- 6) Delay of database query.

B. Obtained Results

Fig. 6 illustrates the overall results obtained. Fig. 6(a) illustrates the VoIP loss rate obtained by our FNA approach compared to the RSVP-TE protocol. The results obtained showed the effectiveness of our approach compared to FNA-TE, we find that both models offered an acceptable rate up to the scenario of 80 clients, however, from the scenario of 90 clients we found that RSVP-TE exceeded the tolerable threshold of 3%, our model has shown its effectiveness even in the scenario of 200 customers. The VoIP latency results (Fig. 6(b)) thus showed the efficiency of our approach, a latency not exceeding 50 milliseconds was measured by FNA-TE against 150 RSVP-TE. Fig. 6(c) illustrates the VoIP jitter, the results obtained showed that the delay variation of our approach is the smallest not exceeding a value of 19 milliseconds against 50 of RSVP-TE. The same results are observed for Video Traffic Fig. 6(f) and Fig. 6(g).

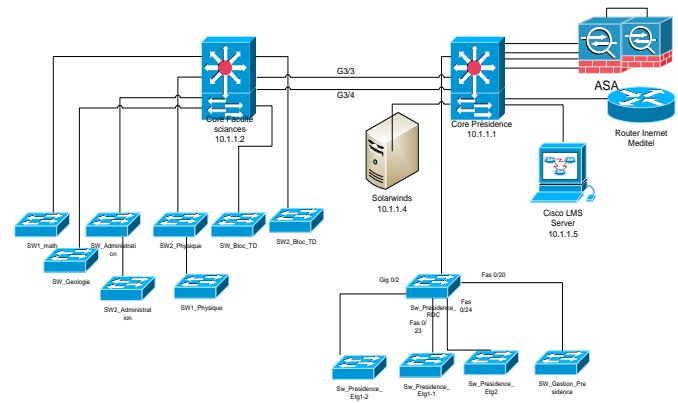


Fig. 5. The Operating Algorithm of the Path Computation Module.

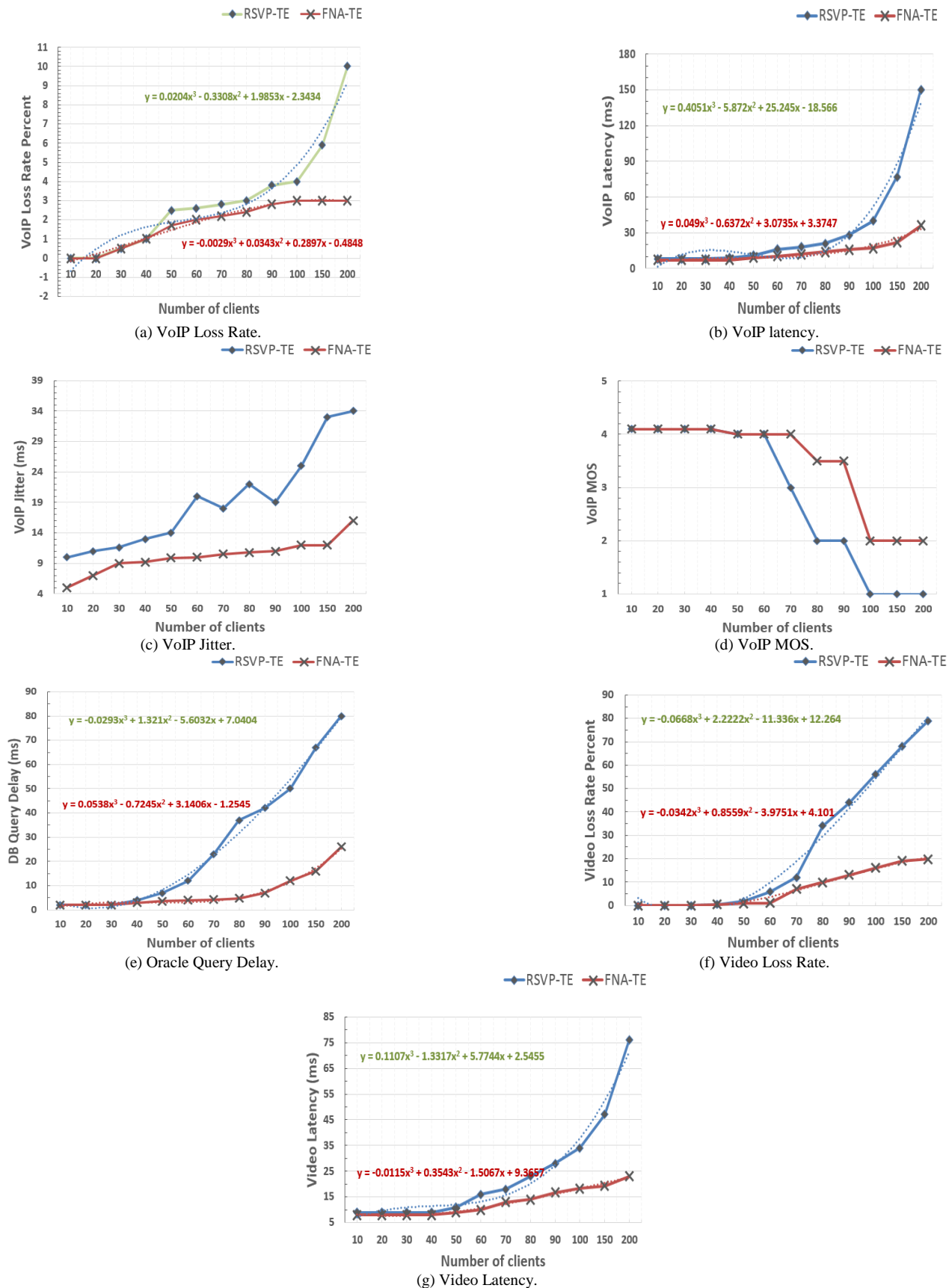


Fig. 6. Obtained Results from Performances Evaluation: (a) VoIP Loss Rate (b) VoIP Latency (c) VoIP Jitter (d) VoIP MOS (e) Oracle Query Delay (f) Video Loss Rate (g) Video Latency.

V. CONCLUSION

In this paper we dealt with a problem of traffic engineering in MPLS-VPN tunnels. Our FNA-TE contribution is to guarantee MPLS-VPN tunnels the least short path guaranteeing the bandwidth necessary for a good level of the quality of service of the transported traffic. Our contribution allows through fair treatment not to compromise the lowest priority tunnels. Our approach was tested in a network consistent with that of Chouaib Doukkali University, in which we evaluated the performance of real-time, streaming and transactional traffic by increasing the load and the number of users. The results obtained showed the effectiveness of our approach compared to the protocol commonly used RSVP-TE.

ACKNOWLEDGMENT

The authors would like to thank editor and referee for providing valuable comments to improve our manuscript.

REFERENCES

- [1] Bensalah, F., El Hamzaoui, M., & Bahnasse, A. (2018). Behavior study of SIP on IP multimedia subsystem architecture MPLS as transport layer. *International Journal of Information Technology*, 10(2), 113-121.
- [2] Bensalah, F., El Kamoun, N., & Bahnasse, A. (2017). Evaluation of tunnel layer impact on VOIP performances (IP-MPLS-MPLS VPN-MPLS VPN IPsec). *International Journal of Computer Science and Network Security (IJCSNS)*, 17(3), 87.
- [3] Khiat, A., Bahnasse, A., Bakkoury, J., & El Khaili, M. (2017). Study, evaluation and measurement of IEEE 802.16 e secured by dynamic and multipoint VPN IPsec. *International Journal of Computer Science and Information Security*, 15(1), 276.
- [4] Bahnasse, A., Louhab, F. E., Talea, M., Oulahyane, H. A., Harbi, A., & Khiat, A. (2017, November). Towards a new approach for adaptive security management in new generation virtual private networks. In 2017 International Conference on Wireless Networks and Mobile Communications (WINCOM) (pp. 1-6). IEEE.
- [5] Bahnasse, A., & El Kamoun, N. (2016). A policy based management of a smart adaptive QoS for the dynamic and multipoint virtual private network. *International Journal of Control and Automation*, 9(5), 185-198.
- [6] Bahnasse, A., Badri, A., Talea, M., Louhab, F. E., & Khiat, A. (2018). Towards a New approach for automating the simulation of QoS mechanisms in a smart digital environment. *Procedia computer science*, 134, 227-234.
- [7] Khiat, A., Bahnasse, A., El Khaili, M., & Bakkoury, J. (2017). SAQ-2HN: A Novel SDN-Based Architecture for the Management of Quality of Service in Homogeneous and Heterogeneous Wireless Networks. *International Journal of Computer Science and Network Security (IJCSNS)*, 17(3), 55.
- [8] Alouneh, S., Al-Hawari, F., Hababeh, I., & Ghinea, G. (2018). An Effective Classification Approach for Big Data Security Based on GMPLS/MPLS Networks. *Security and Communication Networks*, 2018.
- [9] Bahnasse, A., Louhab, F. E., Oulahyane, H. A., Talea, M., & Bakali, A. (2018). Novel SDN architecture for smart MPLS Traffic Engineering-DiffServ Aware management. *Future Generation Computer Systems*, 87, 115-126.
- [10] Bahnasse, A., Louhab, F. E., Oulahyane, H. A., Talea, M., & Bakali, A. (2018). Smart bandwidth allocation for next generation networks adopting software-defined network approach. *Data in brief*, 20, 840-845.
- [11] Alharbi, A., Bahnasse, A., Talea, M., Oulahyane, H. A., & Louhab, F. E. (2017, October). Smart SDN Policy Management Based VPN Multipoint. In *First International Conference on Real Time Intelligent Systems* (pp. 250-263). Springer, Cham.
- [12] BAHNASSE, A., BADRI, A., LOUHAB, F. E., TALEA, M., KHIAT, A., & PANDEY, B. (2018). Behavior analysis of VoIP performances in next-generation networks. *International Journal of Engineering & Technology*, 7(3.15), 353-359.
- [13] Bensalah, F., El Kamoun, N., & Bahnasse, A. (2017). Analytical performance and evaluation of the scalability of layer 3 tunneling protocols: case of voice traffic over IP. *IJCNS International Journal of Computer Science and Network Security*, 17(4), 361-369.
- [14] Bensalah, F., El Kamoun, N., & Bahnasse, A. (2017). Scalability evaluation of VOIP over various MPLS tunneling under OPNET modeler. *Indian Journal of Science and Technology*, 10(29), 1-8.

Big Data Strategy

Alicia Valdez¹, Griselda Cortes², Sergio Castaneda³, Laura Vazquez⁴, Angel Zarate⁵, Yadira Salas⁶,
Gerardo Haces Atondo⁷

Research Center, Autonomous University of Coahuila, Coahuila, Mexico^{1, 2, 3, 4, 5, 6}

Research Center, Autonomous University of Tamaulipas, Tamaulipas, Mexico⁷

Abstract—The importance of data analysis in companies grows every day, with a global market that generates large amounts of transactions. Industry 4.0 is one of the technological trends, which is a set of diverse technologies whose objective is the digitalization and technological connectivity of the entire value chain of organizations. Data analysis and decision making in real time have a positive impact on efficiency. One of the technologies that support this concept is big data, which can support companies to use and manage large volumes of data as support in decision making. In this research project, the computational environment of Apache Hadoop software has been analyzed to create a technological strategy that supports companies in creating a roadmap to know and implement big data technology; as a result, a computer laboratory for big data has been created at the Autonomous University of Coahuila, Mexico to support medium-sized manufacturing companies in their data analysis strategy for decision making.

Keywords—Technological strategy; big data; Hadoop; data analysis

I. INTRODUCTION

The global economy is in a phase that is characterized by digitalization and connectivity, the trend towards the automation of processes in the manufacturing industry.

Technologies such as the internet of things, cloud computing, big data, artificial intelligence and 3D printing, among others; emphasizing the importance of the manufacture of personalized and intelligent products [1]. The analysis of data, the exchange of information and decision making in real time have a positive impact on the efficiency of the entire value chain.

These technologies can support companies to reduce costs, as well as, other factors linked to competitiveness, such as infrastructure, logistics and the digital connectivity system, the cost of energy and the talent of the people.

The digitalization of the economy allows companies to have more information about their customers, at the same time as the entry of new competitors; therefore they face the challenge of increasing and escalating competition, and of making decisions on a large amount of data that they sometimes do not have the capacity to interpret; four main effects are identified in business in all industries: customers' expectations are changing, products are improving with data, new forms of collaboration between companies, and business models are being transformed into digital models [2].

Concepts such as data science and data scientist have emerged as a growing need for data analysis, combining the knowledge of statistics with the design of information and communication technologies, mathematics, operations research and applied sciences in order to extract knowledge derived from the processing, analysis and interpretation of data [3].

Some universities have incorporated the study of data science into their programs, as a need to train students with data science and analytics (DSA) competencies, so that they can successfully face the challenges of the future that require people with critical thinking [4]; because when organizations increase their ability to store data, having staff that can extract valuable information from these data, will be the differentiator of the organization.

Purdue University considers the study of data science in all its careers to be essential, through an initiative called "Integrative Data Science Initiative" [5], they are working in establishing an educational ecosystem of data fluency to prepare students for data-driven knowledge economy, developing infrastructure support for data science research and teaching.

A report elaborated by the Business Higher Education Forum (BHEF), mentions that by the year 2020, 2.72 million new jobs will require information analysis and data management skills; so they are looking to create academic strategies to align the needs of the industry with the development of DSA skills in students, and thus not affect economic growth [6].

Therefore, it is necessary to create technological strategies for companies and universities that allow them to investigate and assimilate new technologies based on Industry 4.0, especially in the analysis of data for the improvement of their processes and decision making; coupled with a college education that provides students and teachers with the foundation for data science competition.

In this project was developed a computational strategy for big data based on the Apache Hadoop Framework, limited to medium sized manufacturing companies.

The software was used as a tool in a computer lab for students and teachers at the Faculty of Mechanical and Electrical Engineering at Autonomous University of Coahuila and tested with real data from a manufacturing company in the raw material inventory processes.

Basically, this study has four sections.

In Section I, the introduction was shown. In Section II, the fundamental concepts are described. Also, the strategy elements such as the framework for big data was also stated. Thus, Section III describes the methodology, and Section IV describes the principal findings of the project.

II. FUNDAMENTAL CONCEPTS

A. Big Data

The increasing availability of data and information in organizations, because of the use of new services such as cloud computing, internet of things, and social network among others; it has meant the learning and use of new technologies for the storage and handling of large amounts of data. Among these technologies, big data stands out.

Watson quoting Mills mentions: “Big data is a term that is used to describe data that is high volume, high velocity, and/or high variety; requires new technologies to capture, store, and analyze it; and is used to enhance decision making, provide insight and discovery, and support and optimized processes” [7].

Russom [8], define a perspective for characterize big data, named the three V's:

- High volume: the amount or quantity of data.
- High velocity: the rate at which, big data is created.
- High variety: the different types of data, structured and unstructured.

This data can be reported by machines, equipment, sensors, cameras, microphones, mobile phones, production software, among others; and can come from different sources such as companies, suppliers, customers and social networks.

The analysis of these data is key to making decisions in real time [9], allows to achieve better quality standards in products and processes, in addition to facilitating access to new markets.

Big data is creating a new generation of decision support data management, other factors has been considered for a successful big data project as: organizational culture, data architecture, analytical tools, and personnel issues.

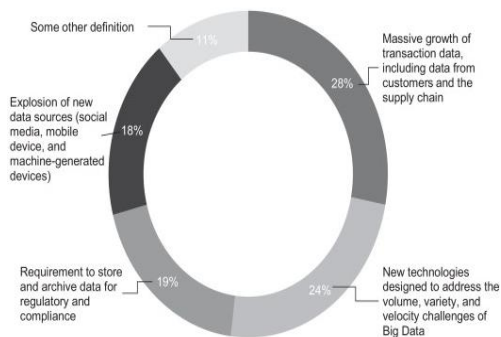


Fig. 1. Definitions of Big Data based on Executive Online Survey, Source [10].

The term big data is not yet fully understood by technology executives, a study that shows the application of an online survey to 154 global executives in April 2012 [10], mentions a variety of concepts and technologies, shown in Fig. 1.

The figure shows different understandings of big data, some definitions were focused on what is it, while others tried to answer what it does; focused on large volumes and varieties of data.

Some of the relevant techniques for structured and unstructured data analysis include [11]:

- Text analytics: extract information from textual data as corporate documents, emails, among others.
- Audio analytics: Analyses and extract information from unstructured audio data as human spoke language.
- Video analytics: involves a variety of techniques to monitor, analyze, and extract meaningful information from video streams.
- Social media analytics: Analysis of structured and unstructured data from social media channels.
- Predictive analytics: Techniques that predict future outcomes based on historical and current data.

Once the big data concept is understood, the related work and the software components are carried out.

B. Related Work

Sivarajah et al., [12] have analyzed the impact of the big data technology, defined as the new raw material of the 21st century; appropriate data processing and management could expose new knowledge, and facilitate in responding to emerging opportunities and challenges in a timely manner. Database and data warehouse technologies are becoming inadequate to manage the amount of data that the world is generating; advanced big data analyzing technologies (e.g. NoSQL Databases, BigQuery, MapReduce, Hadoop, WibiData and Skytree) can be better attained to enable in improving business strategies and the decision-making process in critical sectors such as healthcare, economic productivity, energy futures, among others.

Elgendy and Elragal [13], have investigated the question about how to integrate the big data analytics into the decision making process; they proposed the “B-DAD framework” or Big Data, Analytics and Decision framework for organizations who want to manage the big data technology. The framework has four stages: Intelligence, design, choice, and implementation. The intelligence stage has the activities for identifying big data sources and technologies to manage it; design has model planning, data analytics and analysis; the choice evaluate and decide activities; and the implementation activities are monitoring and feedback.

C. Hadoop Framework

Hadoop is an open source software framework that supports data intensive for distributed storage and distributed

processing of very large data sets on computer clusters; the base Apache Hadoop¹ framework is composed of several modules as: Apache Hadoop MapReduce application tool for the programming aspect and Hadoop Distributed File System (HDFS) for an infrastructural point of view, the Fig. 2 shows the components of the framework.

Hadoop has an ability to move the processing or computing logic to the data where it resides as opposed to traditional systems, which focus on single server [14]. The core of Hadoop is its storage systems and its distributed computing model with its basic components:

- Name node: Head node or master node of the cluster, contains the metadata for HDFS during processing of data, which is
- Data node: These are the systems across the cluster which store the actual HDFS data blocks, these blocks are replicated on multiple nodes to provide high solutions.
- Job tracker: Service running on the Name node, which manages MapReduce jobs and distributed individual tasks.
- Task tracker: Service running in the Data nodes, which monitors individual MapReduce tasks that are submitted.
- Distributed across the nodes.

There are supporting projects for Hadoop, having different roles in the system, these are:

- Apache Hive: is a data-warehouse software that facilitates reading, writing, and managing large datasets residing in distributed storage using structured query languages (SQL) through a Java Data Base Connectivity (JDBC) driver [15], allow users to query the data without developing MapReduce applications.
- Apache HBase: Is the Hadoop database, a distributed, scalable, big data store, hosting of very large tables [16].
- Apache Mahout: Is a distributed linear algebra framework designed to implement algorithms [17].
- Apache Sqoop: Is a tool designed for efficiently transferring data between Hadoop and relational databases management systems (RDBMS) [18]; is a command line tool that controls the allocation between the tables and the data storage layer, translates the tables into a configurable combination for HDMS or Hive [19].

Fig. 3 shows the supporting software for Hadoop.

D. Strategy

The strategy is composed of five phases that involve different activities, being these:

1) Analysis of the hardware that is required for the installation of the software and the data to be analyzed, recommending a data server with a large storage capacity.

2) Selection of the processes of the company that will be analyzed can be customer sales processes, production data, equipment failures, among others; this process selection collects the necessary information and data that will be the raw material for the subsequent activities.

3) Installation and configuration of the Hadoop platform for distributed data processing, as well as the software to support the Hadoop System.

4) Extraction, Transformation and Loading (ETL) activities with analysis services.

5) Big data analytics, tools for analyzing reports (reporting), queries and visualization (dashboards) that will lead to data analytics. Fig. 4 shows the proposed strategy.

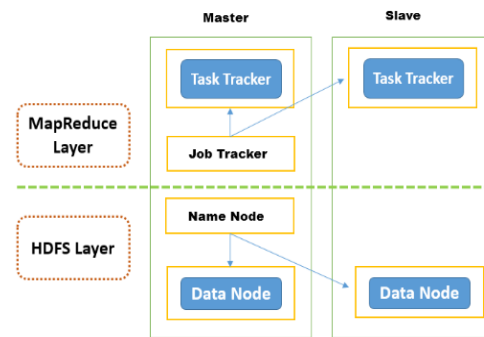


Fig. 2. Hadoop Framework Components, Source [14].

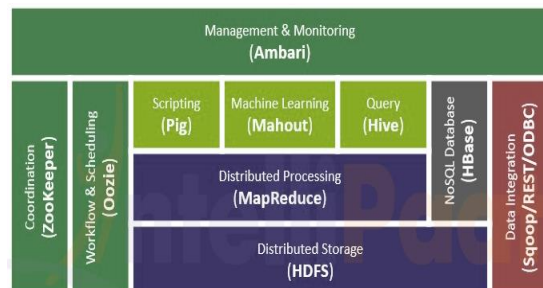


Fig. 3. Supporting Software Projects for Hadoop, Source [14].



Fig. 4. Strategy for Big Data.

¹ <https://hadoop.apache.org>

For the strategy development, a computer laboratory has been installed and configured at the Faculty of Mechanical and Electrical Engineering; for testing before its later use in a medium-sized company in the metalworking sector of the industrial region.

III. METHODOLOGY

The methodology phases were: Analysis of big data technology where a relevant importance has been found to this technology, which forming part of Industry 4.0; with the information of the technology, the software options for its management were found; defining the analysis for the software components and the strategy components. Subsequently, the Hadoop environment was downloaded, installed and configured at the data lab; this phase was the one that took most time; finally testing and implementation with real data. Fig. 5 displays the methodology phases.

The execution mode of Hadoop was a semi-distributed cluster to simulate a cluster of several nodes running on the same machine with its environment variables configured. Fig. 6 shows the execution of Hadoop.

The biggest challenge was the installation and configuration of the Hadoop environment as Hive, Pig and Sqoop software projects for the data analysis, point 3 of the strategy.

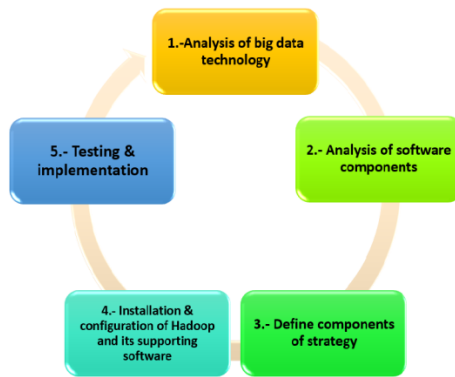


Fig. 5. Methodology Phases.

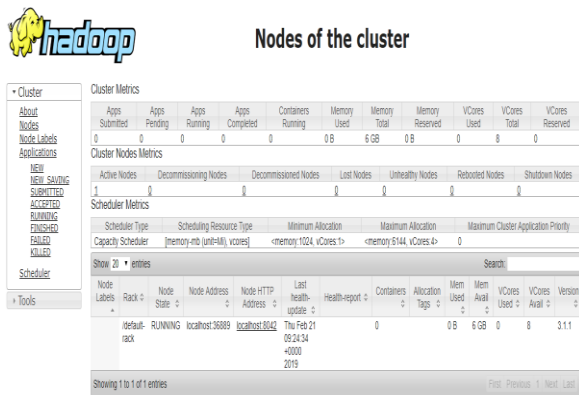


Fig. 6. Hadoop Execution.

A. Technological Architecture

For this project was acquired an HP Proliant server 10th generation with 6TB of storage and three computers functioning as clients, localized at data lab in university. The Linux Red Hat operative system was installed as virtual machine, because the Windows Server is main operating system in the server.

B. Selection of Processes to be Analyzed

Several studies, including IBM, have analyzed the large number of applications for big data; the study shows five preferred orientations to apply big data in organizations in which 49% prefer apply it to focus on the customer, 18% in operational optimization, 15% in financial and risk management, 14% in the new business model and 4% in business collaboration [20].

The client centered processes of manufacturing companies can be considered as: Sales, distribution, market analysis, digital marketing, among others. For this project we have analyzed the processes of inventories management of raw material to produce harnesses and air bags for the automotive industry of a metal-mechanical company.

C. Installation and Configuration of Hadoop Platform

The process began with the installation and configuration of the Hadoop platform as virtual machine using Linux Red Hat version 2.6.18.

The installation and configuration of the software that is required for handling the data in Hadoop is very complex, especially in that each software must install and configure the environment variables separately, to give the user an integral management of the solution; so, this step has been the one that has consumed more time and resources.

The high complexity of the configuration of each software environment as Java, Hadoop, MapRed, Hive, and Scoop has required training to start the operation of the Linux operating system, so training in the management of this operating system will be included in the recommendations.

D. Installation and Configuration of ETL Activities

The activities of extraction, transformation and loading of the data have been made from a relational database (RDBMS) of MS SQL Server, being the data of a medium-sized company of the metalworking industry, belonging to the processes of material inventory management premium for the manufacture of harnesses, armchairs and air bags for the automotive industry of northern Mexico.

E. Data Analysis and Visualization of Results

A part of the design of the database is shown in Fig. 7, where the main entities that are represented were: articles, orders, providers, among others. The visualization of the results has been made with Excel's Power Pivot software for data processing indicator boards.

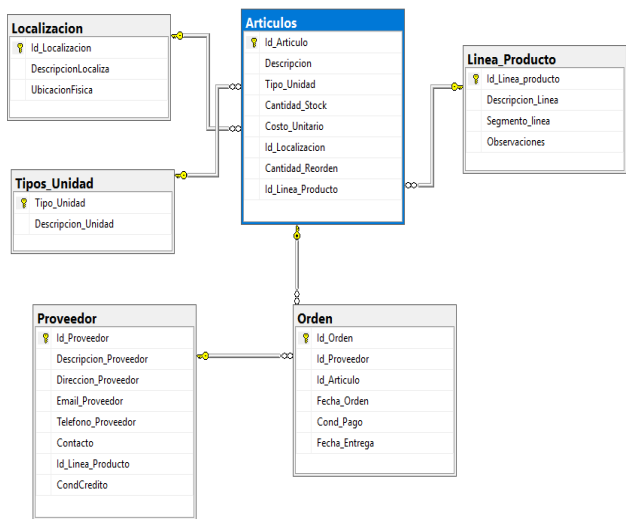


Fig. 7. Database Diagram for Inventory.

With these activities, the development of the strategy is presented, so the findings will be discussed in the results section.

IV. RESULTS

The development of the proposed strategy has resulted in the following findings, also recommended as best practices [21]:

- Assess the true need for a big data processing, depending on the size of the company, real-time data management, types of analysis of the information required and the processes that support the data.
- Consider that the firm can have both types of processing on servers, RDBMS and big data.
- Identify the big data sources and map the big data types into workflow data types.
- Ensure the hardware for processing speed and storage.
- The operational data in companies are stored mostly in RDBMS.
- Consider interfaces for the different data sources that may exist in the company.
- Design an architecture for big data, considering the needs for this technology.
- Consider training in the operation of the Linux operating system and all the software of the Hadoop environment to obtain a real benefit.
- Some companies consider big data technology for the storage of non-SQL data.
- The software to perform the ETL activities is not integrated in the Hadoop platform, it is required to install and configure another type of software for these activities.

The results obtained have shown that developing and implementing a strategy based on big data involves several software, hardware and training activities; mentioning as principals: Emphasize the true need to have a big data processing in the company or use solutions with business intelligence techniques and relational databases.

The RDBMS still have a large proportion of the business operation, so it is recommended to have both types of big data processing and RDBMS if necessary; there are several solutions in the market for big data, finding in the Hadoop platform an open source software that can be installed from a virtual machine for tests and implementations; training in the operative Linux system and all the software that forms the Hadoop environment for communication between the RDBMS and the distributed processing of Hadoop.

Storing large volumes of data may require purchasing extra space or storage in the cloud. It is also important to identify the sources of big data such as social networks, geolocation, GitHub, market data, among others.

The results show the processing of the physical inventory at Monclova plant for the month of July 2018, making a comparative physical analysis against theoretical, divided into 4 reports, Fig. 8 shows the report 1 results where, the company has lost money for almost \$8,000.00 USD in that month.

RESULTADOS INVENTARIO FISICO - Planta Monclova - Julio 2018					
TOOLCRIB					
Reporte 1	CMH TEORICO	CMH FISICO	VARIACION	RESULTADO	
	\$ 80,498,736.08	M3 \$ 80,338,574.74	M3N (\$160,221.32)	M3N	PERDIDA
	200,634.50	QTY 197,267.20	QTY -4,337.30	QTY	99.80% Contabilidad/Neto 0.20% Diferencia/Neto
Absolute OVER		1,583.00	QTY \$ 19,919.99	M3N	
Absolute UNDER		9,802.00	QTY \$ 609,444.74	M3N	
Absolute TOTAL		11,855.00	QTY \$ 629,363.72	M3N	0.78% Diferencia Absoluta 99.22% Contabilidad Absoluta

Fig. 8. Results, Report1.

Hardware resources have also been obtained to have a small computation laboratory for big data in the Faculty of Mechanical and Electrical Engineering as part of the Autonomous University of Coahuila, where students of computer systems in the specialty of data management can learn from the development of this project.

V. CONCLUSION

In this project, a strategy for big data technology has been designed for support data analysis in the medium sized companies, in inventory processes of raw materials to produce various goods for the automotive industry of northern Mexico.

Several states of the strategy propose different goals, each of which involves an important number of activities such as: analysis of the technological architecture, selection of processes of the company to be analyzed, installation and configuration of the Hadoop platform software; installation and configuration of the activities of extraction, transformation and loading of the data, and the final data analysis and visualization of results in Excel Power Pivot.

REFERENCES

Managing different operating systems may require training activities for the company's data administrator.

Developing a strategy for big data in a medium company is a difficult task for all the activities involved to develop successfully.

The tendency of managing large volumes of data, speed and variety of data, may imply an opportunity area for big data technology.

A lot of theoretical contribution was found on the subject.

As future work at the University, include students training for learn DSA skills, as mentioned in the educational trends of higher education.

This project has been a great learning experience for students, authors and teachers in the database area and granted by the PRODEP authority in Mexico.

VI. DISCUSSION

In this project, a technological strategy was developed to manage big data in medium sized companies, was a large set of activities to get the objective. The main activities were: Install and configure the ethernet network with 1 server and 3 nodes, virtualization in Windows or Linux environment, to avoid configuration and implementation failures to create the virtualized environment, a bootable pen drive with Linux operating system was elaborated, and from there the operating system was taken to work with the implementation of the node.

The Java JDK software was installed to be able to operate the tools needed by Hadoop and Hadoop itself.

It has been a great technical challenge of hardware and software for the team responsible of the project.

The evaluation of the project has been successful in the first place for the configuration and installation of the hardware, the network, the server, and the nodes; second, the configuration and installation of the Hadoop software and the environment that works with Hadoop, as well as the administration and management of the data of the Hadoop nodes.

- [1] A. Basco, G. Beliz, D. Coatz and P. Garnero , *Industria 4.0 Fabricando el futuro*, 2018, Buenos Aires, Argentina: BID, pp. 14-18.
- [2] K. Schwab, *The Fourth Industrial Revolution*, 2016, Switzerland: The World Economic Forum, pp. 52-55.
- [3] C. Weihs and K. Ickstadt, "Data Science: The impact of statistics". *International Journal of Data Science and Analytics*, 2018. 6(3): p.189-194.
- [4] T. Chamorro, "3 Ways to Build a Data Driven Team". *Harvard Business Review*, 2018. 10(3): p.1-4.
- [5] J. Akridge, "Purdue University launches robust collaborative Integrative Data Science Initiative", 2018.
- [6] BHEF, *Investing in America's data science and analytics talent*, 2017, Business Higher Education Forum: U.S.A.
- [7] H. Watson, "Tutorial: Big Data Analytics: Concepts, Technologies, and Applications". *Communications of the Association for Information Systems*, 2014 34(65): p. 1247-1268.
- [8] P. Russom, "Big Data Analytics", TDWI Best Practices Report, TDWI, Editor 2011, The Data Warehousing Institute: Seattle, U.S.A.
- [9] C. Ynzunza, J. Izar, J. Bocarando, F. Aguilar and M. Larios, *The environment of Industry 4.0: Implications and future perspectives*. *Conciencia Tecnologica*, 2017. 54(1): p. 1-8.
- [10] A. Gandomi and M. Haider, "Beyond the hype: Big data concepts, methods, and analytics". *International Journal of Information Management*, 2015. 35(2): p. 137-144.
- [11] S. Erevelles, N. Fukawa, and L. Swayne, "Big Data consumer analytics and the transformation of marketing", *Journal of Business Research*, 2016. 69(2): p. 897-904.
- [12] U. Sivarajah, et al., "Critical analysis of big data challenges and analytical methods", *Journal of Business Research*, 2017. 70: p. 263-286.
- [13] N. Elgendy and A. Elragal, "Big data analytics in support of the decision making process", *Procedia Computer Science*, 2016. 100(1071): p. 1071-1084.
- [14] D. Sarkar, *Microsoft SQL Server 2012 with Hadoop*, 2013, Mumbai, India: Packt Publishing.
- [15] Apache Software Foundation. *Apache Hive TM*. 2019 [cited 2019 10/01/2019]; Available form: <https://hive.apache.org>
- [16] Apache Software Foundation. *Apache Hbase TM*. 2019 [cited 2019 10/01/2019]; Available form: <https://hbase.apache.org>
- [17] Apache Software Foundation. *Apache Mahout TM*. 2019 [cited 2019 10/01/2019]; Available form: <https://mahout.apache.org>
- [18] Apache Software Foundation. *Apache Sqoop TM*. 2019 [cited 2019 10/01/2019]; Available form: <https://scoop.apache.org>
- [19] T. White, *Hadoop: The Definitive Guide*, 4th Edition, 2015, U.S.A.: O'Reilly Media Inc.
- [20] D. Lopez, *Análisis de las posibilidades de uso de Big Data en las organizaciones, Negocios y tecnologías de la información*, 2012, Universidad de Cantabria: España, p.73.
- [21] M. Nathan and W. James, *Big data: principles and best practices of scalable real-time data systems*, 2015, U.S.A.: New York; Manning Publications Co.

Performance Analysis of Security Mechanism for Automotive Controller Area Network

Mabrouka Gmiden¹, Mohamed Hedi Gmiden², Hafedh Trabelsi³
Computer and Embedded System Lab (CES), National Engineers
School of Sfax-Tunisia^{1,2,3}

Abstract—Connectivity of modern cars has led to security issues. A number of contributions have proposed the use of cryptographic algorithms in order to provide automotive Controller Area Network (CAN) security. However, due to CAN protocol characteristics, real time requirements within cryptographic schemes are not guaranteed. In this work, effects of implementing cryptographic approaches have been investigated by proposing a performance analysis methodology of cryptographic algorithm. Until get implanting the proposed method in a real vehicle, a platform based on STMicroelectronics'32F407 (STM32F407) microcontroller board has been deployed to test the proposed methodology. The experiments show that the implementation of a cryptographic algorithm has an impact on clock cycles number and therefore, on real-time performances.

Keywords—Automotive CAN security; cryptographic algorithms; analysis methodology; real-time performances

I. INTRODUCTION

New vehicles are becoming more and more connected machines. In fact, a modern car is able to communicate with the outside via various interfaces like USB, MP3, Bluetooth, etc. Furthermore, CAN protocol is today the most used in automotive networks [1]. However, CAN bus cannot guarantee security because of a lack of authenticity [2] [3]. Therefore, CAN networks are vulnerable to cyber-attacks, which threats in-vehicle subsystems even lives of passengers [4]. Then, security problem is added to the automotive issues [5] [6]. Hence, it is crucial to find solutions that guarantee automotive security.

In order to protect the safety of the system within a modern car, many methods have been developed, such as cryptographic protocols, Intrusion Detection Systems (IDSs), etc. Although, several researches have been oriented towards IDSs, they have been still not 100% robust, and they could not prevent all types of attacks. To exceed limitations of detective measures, many researches aim to adopt cryptographic strategies as they have been improved, in internet networks, their efficiency in thwarting attacks.

Applications in CAN network are characterized, unlike traditional computer systems, by real-time constraints. That is why data encryption or signature mechanisms should not impact real-time performances. In the literature, although the diversity of the proposed solutions, serious performance measures are still limited.

In this paper a tool, that allows the analysis of real-time performances resulting from the implementation of cryptographic algorithms, is designed. The method is based on the analysis of the time intervals of CAN frames.

The main contributions of this work are:

- A general literature review about CAN bus security issues along with proposed solutions for this accomplish.
- A practical methodology to secure CAN bus communication based on analyzing and measuring of real-time performances.
- An efficient experimental platform for analyzing, implementing a securing CAN bus communication and injecting spoofed message.

The rest of the paper is organized as follows. Section 2 provides the necessary background of the security issues and related work. Next, the proposed method is described. Section 4 presents the evaluation result of the proposed method. Finally, Section 5 summarizes this work.

II. BACKGROUND

A. CAN Bus Security Issues

The objectives provided by a security system are called security services which they are summarized as confidentiality, authenticity, availability, integrity, and non-repudiation. CAN bus cannot guarantee these properties since its characteristics:

- Broadcasted nature: a CAN message sent by a node will be received by all nodes connected to the bus. So, an attacker can connect to the network traffic and read data frame easily. Then, the CAN bus cannot guarantee confidentiality.
- CAN messages have not any authenticator fields. Thus, an attacker connected to the bus could use the identifier (ID) of any node to send a fake message.
- Arbitration scheme: a frame consists, mainly, as Fig. 1 shows, of: the ID, which represents the priority of the message, Data Length Code (DLC), Data, and Cyclic Redundancy Check (CRC). The identifier of the CAN frame is unique. So, the CAN message with the highest priority wins the arbitration and transmits the first. Thus, any node can put the bus in a dominant state and prevent others from sending messages resulting Denial of Service (DoS) attacks.

- CAN protocol uses CRC to verify whether a message has been modified. However, this latter cannot prevent an attacker from modifying a legitimate message. In fact, she could make a correct CRC for a forged message.
- Possibility of repudiation: in CAN protocol, it is impossible for a legitimate ECU to prove that it has sent or received a given message.
- CAN message contain between 1 and 8 bytes. So, the security protocol cannot transmit any extra authenticated data inside the classic data field (Fig. 1).
- In automotive networks, the primary focus is on real-time capabilities, which are needed to respond within a given short time. So, predictability and reliability are the dominating factors.

B. Requirements of CAN Bus Security Solutions

Since Electronic Control Units (ECUs) are very limited in computing power and memory space, heavy cryptographic functions are difficult to be performed by these calculators. So, proposed solutions should be as lightweight as possible. Moreover, almost CAN networks applications are hard-real time. Therefore, embedded real time performances should not be impacted by the implementation of security mechanisms.

In addition, the proposed mechanism should provide retro-compatibility, i.e. be compatible with used technologies and interoperability, i.e. external communications should not be prevented by the security system. Furthermore, a CAN data frames are easy to be eavesdropping by an attacker. Thus, a method of encryption should be employed in order to provide confidentiality. On otherwise, a Hash-based Message Authentication Code (HMAC) must be generated and transmitted along with CAN messages to guarantee authentication of transmitted data,

C. Related Work

As a countermeasure against various types of vehicle cyber-attacks, there have been two main groups of security solutions: Intrusion Detection Systems and cryptographic mechanisms

1) *Intrusion detection*: To defend attacks against in-vehicle networks, many solutions based on IDS Systems have been proposed.

Studnia et al. proposed an intrusion detection approach for embedded automotive network [7]. The presented solution based on the definition of a formal language. This proposal is dedicated to generate a set of signature for attacks that aim to detect. In [8], authors presented a novel intrusion detection algorithm which aims to identify malicious CAN messages injected by attackers. By against, an intrusion detection algorithm, which is based on the analysis of time intervals of messages, was proposed [9]. The algorithm did not require any hardware modification, but it could not detect irregular message in coming.

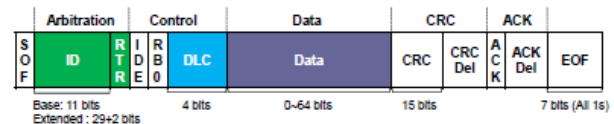


Fig. 1. CAN Format Frame.

2) *Message authentication*: Although, several researches have been oriented towards IDS system, significant increase of cryptographic schemes have been shown during last years.

Woo et al. in [10] proposed the use of HMAC and Advanced Encryption Standard-128 (AES-128) for encryption. The proposed protocol used 16 bits, in the extended ID field, and the 16-bit CRC field for transmission of 32 bits code. The implementation of the protocol kept the bus load under 50%; hence it provided acceptable overhead. Nurnberger et al. introduced VatiCAN which enabled sender and receiver ECUs to exchange authenticated data using the Keccak algorithm [11]. By contrast to other authentication mechanisms, VatiCAN used individual keys per ECU. So, each calculator should store the key of each ECU exchanges authenticated messages with. In their protocol [12], Bulck et al inspired the idea of VulCAN from the two protocols VatiCAN and Leia. In VulCAN, each authenticated CAN identifier should be associated with a symmetric 128-bit cryptographic key. As in VatiCAN, VulCAN allowed multiple IDs to distribute the same key. While valid ECUs use the key to compute a 64-bit MAC, the value of counter (which prevents re-play attack) increases. Like VatiCAN, authors addressed nonce initialization challenge by the use of short-term session keys and (re-)synchronized counters by a global Nonce Generator (NG).

In [13] a method based on adapting traditional encryption schemes was presented. The proposed system required that the hardware modules installed on each ECU, which made the implementation more difficult. The proposed method differentiated itself from other competitive tools; by not only supporting cryptography mechanism; but also allowing the measure of real-time parameters. Also, in [14], authors used the same platform to implement an IDS. The main contribution in this paper is the design of a platform which allowed the implementation of an IDS. So, the same tool is deployed in this paper to measure real-time performances resulting from the implementation of cryptographic mechanisms. The method is based on the analysis of the time intervals of the CAN message.

III. EVALUATION OF CRYPTOGRAPHIC ALGORITHMS

The system proposed in this paper, aims at analyze the security requirements on CAN bus network after implementing a cryptographic mechanism. This section is devoted to the detailed presentation of the proposed system: subsection A introduces the system model, subsection B gives phases of methodology process and subsection C provides algorithms process.

A. System Model

In this section, the system model, which is adopted for implementing the proposed method, is introduced. As shown in Fig. 2, the system model is composed of 2 CAN nodes connected to a CAN bus to form a network.

Assume that Node 1 sends messages to Node 2 with ID =0x1 every 2ms. Likewise, Node 2 send messages to Node 1 with ID =0x2 every 5ms.

B. Fundamental Idea

The Main problem, on the communication side, is the overhead caused by the additional data in combination with possible additional latency. Both are especially challenging when dealing with short signals requiring real time operation and low latencies. The goal of this work is to develop a system which can be deployed for implanting a cryptographic mechanism along with analyzing real-time performances and injecting spoofed message. Therefore, a platform based on STM32F4 board, is deployed. The proposed method enables to determine effects of implementing security mechanism on CAN bus performances.

The fundamental idea is to apply a cryptographic mechanism on a given message in Node 1 and send it to Node 2. After the transmission of a message frame, performances of the related algorithm is measured according to a method will be detailed later.

C. Phases of Methodology Process

Since the proposed approach is designed to be implemented in the standard version of CAN protocol, the transmission process of CAN messages will be different from the classic one. The whole transmission process is summarized in Fig. 2.

When the sender node receives a request from the receiver, it encrypts data; divides it into segments. Then, it sends segments via CAN bus. To guarantee confidentiality and integrity of automotive data network, the encryption of messages is required. The CAN message encryption phase is insured by encryption mechanisms and MAC methods.

1) *Fragmentation technique*: As the maximum payload length of CAN data field is only 8 bytes, the available space, for appending a Message Authentication Code (MAC), is very limited. Rather than appending a MAC in one CAN frame's data field, dividing data into segments is suggested; and, then, each segment is transmitted.

2) *CAN message transmission phase*: The transmission of CAN frame is carried out from the sender to the receiver according to CAN protocol and via CAN bus.

3) *CAN message reconstitution phase*: Arrival messages need to be reconstituted for obtaining the complete message.

4) *CAN message decryption phase*: The resulted message is decrypted to obtain the original message.

5) *Calculating clock cycle*: The last step of the methodology is to calculate the clock cycle needed to perform a CAN data transmission.

IV. TEST AND EVALUATION

Testing the proposed method on a real car, with the same requirements and conditions, is very difficult. For that, the authors tried to establish a platform which can resemble same conditions of automotive network. Subsection A details different components of the system and results of experimental tests are assessed in subsection B.

A. System Implementation

1) *Experimental setup*: In order to design the model system, several solutions are possible (PIC microcontroller, ARDUINO board, Raspberry PI board...). In this paper, STM32F407 microcontroller board, with a 32 bit ARM Cortex-M4 core clocked at 16 MHz and an adaptive real-time accelerator is used¹. The high-speed CAN transceiver MCP 2551 is used as a transceiver. In this work, the two nodes connected with an oscillator clock of 16MHz. Node 1, which is connected to the PC, is dedicated to send messages to Node 2 across the CAN bus. The setup is shown in Fig. 3.

2) *Implementation*: For the implementation of algorithms, Keil Microcontroller Development Kit (MDK) 5 is adopted as an integrated development environment (IDE) to program STM32 in C language.

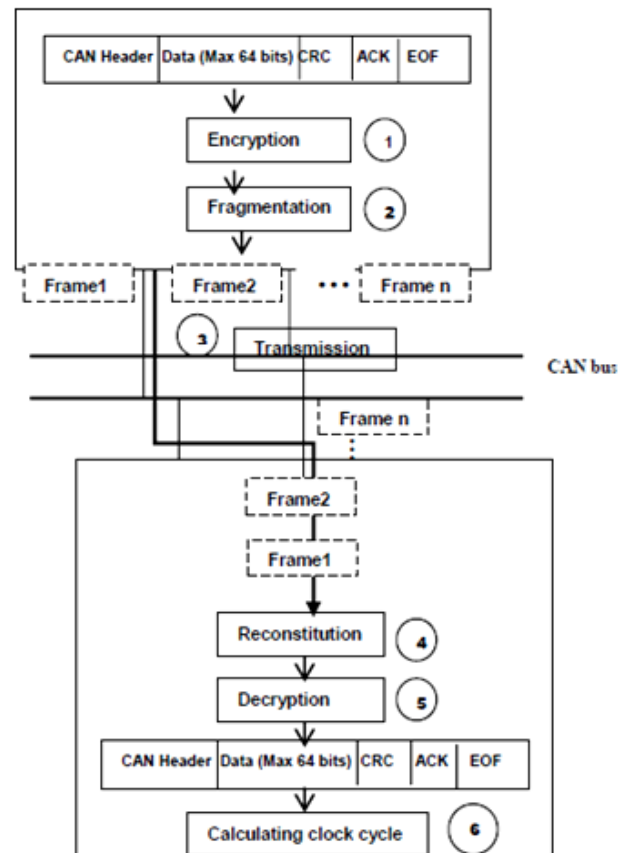


Fig. 2. Overall Process of Analyzing Methodology for a Secure CAN Bus Communication.

¹STM32F407VG, <http://www.st.com/en/microcontrollers/stm32f407vg.html>, 2017.

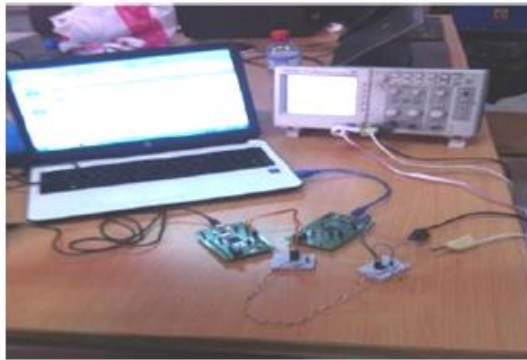


Fig. 3. Test Environment.

On otherwise, STM32CUBEMX is used to configure the STM32 board.

To integrate security into the CAN bus network, authors included the STM32 cryptographic library package (X- CUBE CRYPTOLIB) in particular AES in CMAC mode (AES_CMAC) and HMAC_SHA (Hash-based Message Authentication Code (HMAC) à l' aide de SHA).

3) *Algorithms*: In order to design a secure CAN network, an encryption algorithm block or a hash function is added to CAN network. This algorithm enables to encrypt data sent by the sender and to decrypt data received by the receiver.

The following section focuses on AES_128_CMAC, AES_256_CMAC, HMAC_SHA196 and HMAC_SHA256 algorithms. Due to the complexity in automotive architecture, the implementation of these algorithms, as codes which can be implemented in CAN nodes, is a challenge. For the implementation of this approach, the same platform as well as the same configuration steps as those indicated in [14].

a) *AES_128_CMAC*: AES_128_CMAC has a key with 128 bits and gives a message with 128 bits in output. Since the CAN data message can contain 108 bits in totally, authors chose to append MAC in the data field and truncate it to two segments.

Assuming that node 1 require sending data D0, of 64 bits, to node 2 via a secure CAN bus. In first example, AES_128_CMAC algorithm is applied. The transmission process of the encrypted message is summarized in Fig. 4.

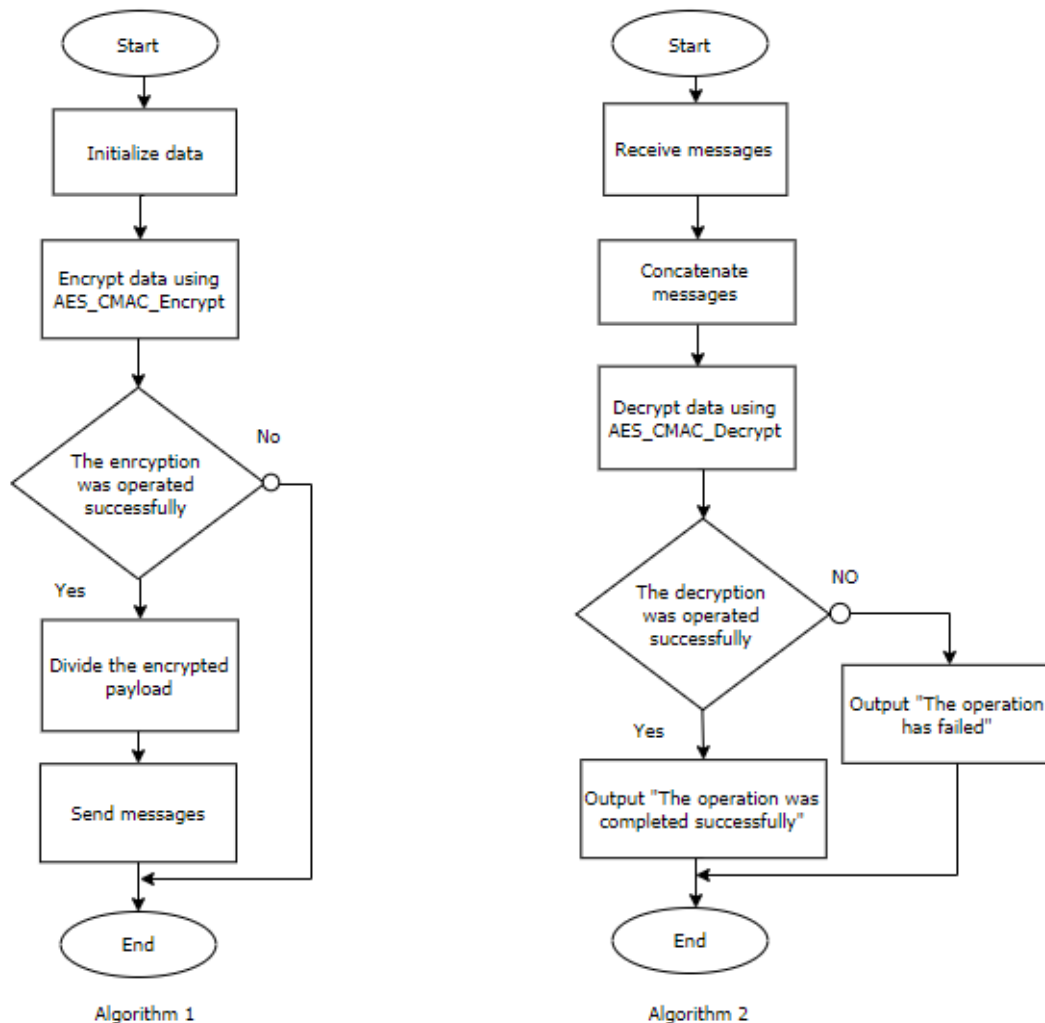


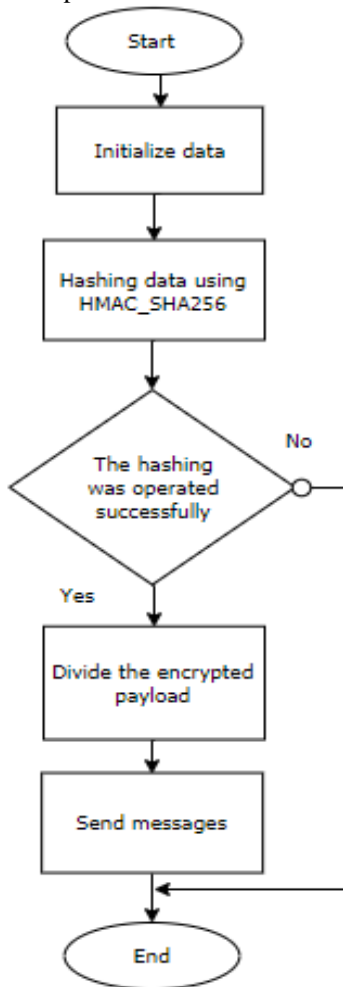
Fig. 4. Transmission Process of a Secure Data.

The process of decrypt frames is summarized in Algorithm 1.

- Step 1: Start.
- Step 2: Initialization.
- Step 3: Encrypt data using AES_CMAC_Encrypt.
- Step 4: Check encryption operation by comparing the encrypted payload by the expected text.
- Step 5: Encryption is failed? Pass to Step7.
- Step 6: Divide the encrypted payload in two segments.
- Step 7: Send the two messages to node 2.
- Step 8: End process.

When node 2 receives messages, it decrypted them as shown in Algorithm 2.

- Step 1: Start
- Step 2: Receive messages.
- Step 3: Concatenate the two messages.
- Step 4: Decrypt data using AES_CMAC_Decrypt
- Step 5: Check decryption operation by comparing the obtained text by the expected text.
- Step 6: Decryption is failed? Pass to Step 7 then Step 9. Else pass to Step 8.



Algorithm 3

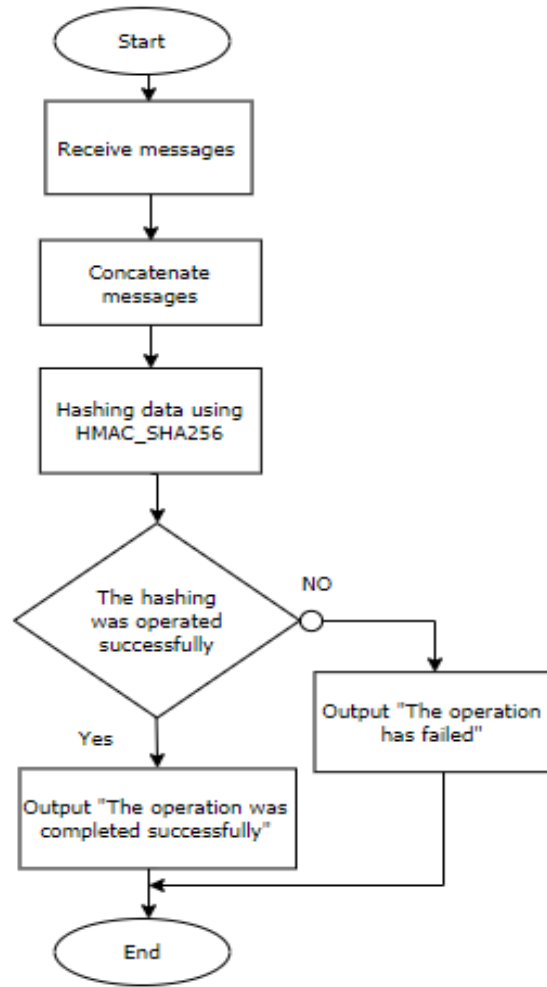
- Step 7: Output "The operation was completed successfully".
- Step 8: Output "The operation has failed".
- Step 9: End process.

b) Algorithm of HMAC_SHA256: As a second example, we applied to the D0 a HMAC SHA256 block. HMAC_SHA256 gives a message with 256 bits in output. In this case, MAC was appended in the data field then truncated to four segments.

The transmission of a secure message using HMAC_SHA256 is summarized in Fig. 5.

Algorithm 3 shows the authentication of the data.

- Step 1: Start.
- Step 2: Initialization.
- Step 3: Hashing data using HMAC_SHA256.
- Step 4: Hashing is failed? Pass to Step7.
- Step 5: Divide the hashed payload in four segments.
- Step 6: Send the four messages to node 2.
- Step 7: End process.



Algorithm 4

Fig. 5. Transmission Process of an Authantecated Data.

Algorithm 4 shows the verification of authentication using HMAC_SHA256.

- Step 1: Start
 - Step 2: Receive messages.
 - Step 3: Concatenate the four messages.
 - Step 4: Operate HMAC_SHA256
 - Step 5: Check hashing function by comparing the obtained text by the expected text.
 - Step 6: Hashing is failed? Pass to Step7 then Step 9. Else pass to Step 8.
 - Step 7: Output “Operation success”.
 - Step 8: Output “Operation fails”.
- End process.

4) Clock cycle calculation: The tests were executed on STM32F4 which their CPU is running at 168MHz.

To determine the impact of using a cryptographic algorithm in CAN bus communication, the number of clock cycles should be calculated. At first, the number of cycles needed to perform each process is defined as follows:

$$Cycles_{CAN} = Init\ key\ cycle + Init\ message\ cycle + Process\ block\ of\ data\ cycle * number\ of\ blocks \quad (1)$$

So, the number of cycles required to transmit a CAN message encrypted by AES_128_CM MAC is calculated as follows:

$$Cycles_{CAN} = Init\ key\ cycle + Init\ message\ cycle + Process\ block\ of\ data\ cycle * number\ of\ blocks + 2 * (min\ of\ CAN\ data\ transmission\ cycle) \quad (2)$$

The number of cycles required to transmit a CAN message encrypted by HMAC_SHA256 is calculated as follows:

$$Cycles_{CAN} = Cycle\ de\ Init_key + Cycle\ de\ Init_message + cycle\ de\ block\ de\ donnée * (nombres\ de\ block) + 4 * (min\ de\ cycle\ de\ transmission\ de\ donnée\ CAN) \quad (3)$$

V. EVALUATION

The size of the code requested by each proposed algorithm is presented in Table 1.

A. Comparison between AES-CMAC

Table 2 shows the number of clock cycles requested by AES_CM MAC.

Referring to Fig. 6, the performances of AES_CM MACs don't much differ when the key size differs. It is because of the change of cycle numbers taken by each algorithm.

TABLE I. CODE SIZE OF EACH ALGORITHM TO PROCESS A BLOCK OF DATA

Algorithm Mode	Code Size (Byte)	Constant Data Size (Byte)
AES (128, 192, 256) CMAC	5 796	6 040
HMAC_SHA256 ,128	3485	6040

TABLE II. PERFORMANCE OF AES-CMAC ALGORITHMS

Algorithm Mode	Operation	Init key	Init message	Data block processing
AES_128_CM MAC	Decryption	636	639	1628
	Encryption	618	525	1628
AES_192_CM MAC	Decryption	632	719	1859
	Encryption	616	608	1859
AES_256_CM MAC	Decryption	840	758	2141
	Encryption	816	649	2141

The difference between the numbers of clock cycles, used by the three algorithms, is relatively little. However, AES_256_CM MAC requires more clock cycles than AES_128_CM MAC and AES_192_CM MAC; hence it is the slowest one. On the other hand, AES_128_CM MAC is the least secure since it has the shortest key. However, this latter is considered faster than the others. It takes the least number of clock cycles; hence it has better performance than AES_192_CM MAC and AES_256_CM MAC.

Therefore, the variation of key size affects the number of clock cycles and subsequently the performances of algorithm. On the one hand, the key of AES_256_CM MAC is longer than the key of AES_128_CM MAC. Thus, AES_256 is more secure. But the AES_256 is slower than AES_128.

B. Comparison between HMAC_SHA

Table 3 shows the number of clock cycles requested by HMAC_SHA.

Referring to Fig. 7, the performances of HMAC_SHA don't much differ when the key size differs. It is because of the change of cycle numbers taken by each algorithm. The difference between the numbers of clock cycles, used by the three algorithms, is relatively little. However, HMAC_SHA256 requires more clock cycles than HMAC_SHA224; hence it is the slowest one. On the other hand, HMAC_SHA224 is the least secure since it has the shortest key. However, this latter is considered faster than HMAC_SHA256; hence it has better performances. Therefore, the variation of key size affects the number of clock cycles and subsequently the performances of algorithm.

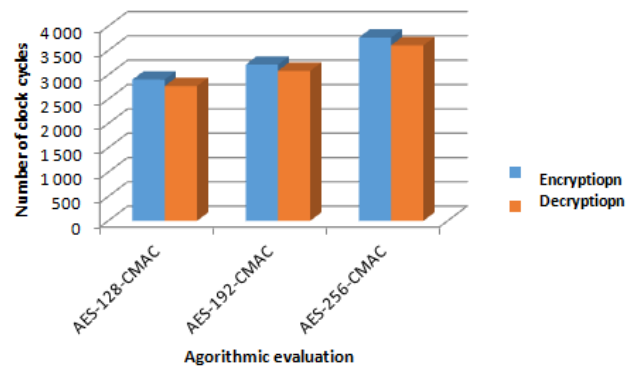


Fig. 6. Comparison between AES_CM MAC.

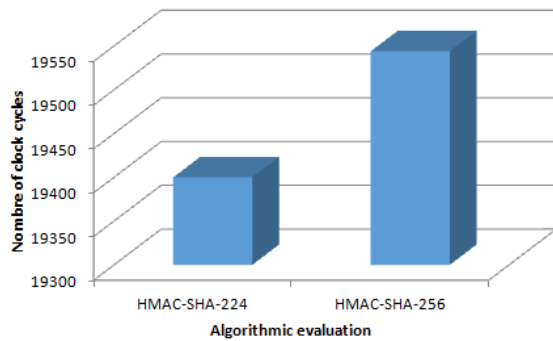


Fig. 7. Comparison between HMAC_SHA.

TABLE III. PERFORMANCE OF HMAC_SHA ALGORITHMS

Algorithm Mod	Init key	Init message	Finalization
HMAC_SHA224	4 708	3 352	11 340
HMAC_SHA256	4 789	3 352	11 403

C. Comparison between HMAC_SHA256 and AES_256_CMAC

The comparison between number of clock cycles of HMAC_SHA256 and AES_256_CMAC is shown in Fig. 8, since they have the same key size. The difference between the numbers of clock cycles, taken by the two algorithms, is not large. However, the HMAC_SHA requires more of number of clock cycles than the AES_CMAC; hence this latter is faster. Therefore, AES_CMAC algorithm requires has better performances than the HMAC_SHA.

As can be seen, the effectiveness of the algorithm for providing security depends on the key length and the protocol mode. These parameters can have an impact on the speed execution of algorithm. In addition, the security mechanism has an impact on system bus load and message latencies.

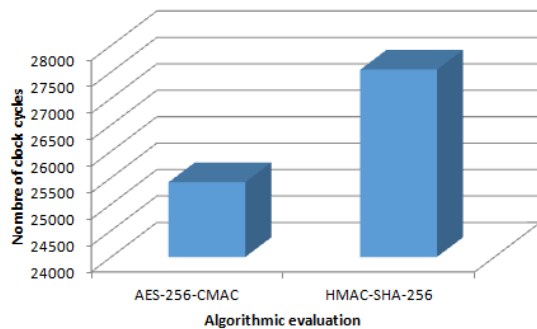


Fig. 8. Comparison between HMAC_SHA_256 and AES_256_CMAC.

VI. CONCLUSIONS

To defend against vehicle attacks, many approaches have been proposed in the literature. However, the greater part did not address real-time requirements in CAN bus communication. In this paper, effects of implementing

cryptographic approaches have been investigated by proposing a performance analysis methodology of cryptographic algorithm. In this paper, after describing the fundamental idea, a description of the proposed system was given. The advantage of the presented method is that addresses safety and security of CAN bus by calculating the performances of cryptographic algorithm.

In this manuscript, it has been proved that the CAN network has limitations and it will not be able to meet requirements. Car manufacturers and researchers are invited to turn their attention to the recent protocols such as: Ethernet and VANET. In fact, despite being in progress, they will be very efficient in the future. Future work can include these new protocols to design a secure automotive network in the presence of recent communication interfaces.

REFERENCES

- [1] R.B.GMBH, Bosch Automotive Electrics and Automotive Electronics, 5 ed. Bosch Professional Automotive Information. Springer Vieweg, 2014.
- [2] R. Currie, "Hacking the CAN Bus: Basic Manipulation of a Modern Automobile Through CAN Bus Reverse Engineering", The SANS Institute, 2017.
- [3] Introduction to the Controller Area Network (CAN), TEXAS INSTRUMENTS, Application Report, SLOA101B–August 2002–Revised May 2016, 2016.
- [4] K. Koscher, A. Czeskis, et al., Experimental Security Analysis of a Modern Automobile, IEEE Symposium on Security and Privacy, 2010.
- [5] S. Checkoway, D. McCoy, et al., Comprehensive experimental analyses of automotive attack surfaces, Proc.20th USENIX Security, San Francisco, CA, 2011.
- [6] C. Miller and C. Valasek, Adventures in automotive networks and control units. Last Accessed from http://illmatics.com/-car_hacking.pdf on, 2013. (Cite en pages 37, 38, 76 et 116).
- [7] I. Studnia, E. Alata, et al., A language-based intrusion detection approach for automotive embedded networks, The 21st IEEE Pacific Rim International Symposium on Dependable Computing (PRDC 2015), Nov 2014, Zhangjiajie, China.
- [8] M. J. Kang and J. W. Kang, "A novel intrusion detection method using deep neural network for in-vehicle network security," in 2016 IEEE 83rd Vehicular Technology Conference (VTC Spring), May 2016, pp.
- [9] Song, H. M., Kim, H. R., & Kim, H. K. (2016). Intrusion detection system based on the analysis of time intervals of CAN messages for in-vehicle network. 2016 International Conference on Information Networking (ICOIN). doi:10.1109/icoin.2016.7427089.
- [10] S. Woo, H. J. Jo, and D. H. Lee, "A Practical Wireless Attack on the Connected Car and Security Protocol for In-Vehicle CAN," "In IEEE Transactions On Intelligent Transportation Systems", 2014.
- [11] S. Nurnberger and C. Rossow, "- vatiCAN - vetted, authenticated CAN bus," in Cryptographic Hardware and Embedded Systems: 18th International Conference, Santa Barbara, CA, USA, August 17-19, 2016, Proceedings. Berlin, Heidelberg: Springer Berlin Heidelberg, 2016.
- [12] J.V. Bulck, VulCAN: Efficient Component Authentication and Software Isolation for Automotive Control Networks, ACSAC'17, December 2017, San Juan, Puerto Rico, USA.
- [13] P. Mundhenk, A. Paverd, et al., Security in Automotive Networks: Lightweight Authentication and Authorization, ACM Trans. Design Automation of Electronic Systems, vol. 22, no. 2, 2017.
- [14] M. Gmiden, M.H. Gmiden, H. Trabelsi, An intrusion detection method for securing in-vehicle CAN bus, Conference: 2016 17th International Conference on Sciences and Techniques of Automatic Control and Computer Engineering (STA), IEEE, 2016.

Feature-based Sentiment Analysis for Slang Arabic Text

Emad E. Abdallah¹, Sarah A. Abo-Suaileek²

Department of Computer Information System, Faculty of Prince Al-Hussein Bin Abdallah II for Information Technology
Hashemite University, Zarqa 13115, Jordan

Abstract—The increased number of Arab users on microblogging services who use Arabic language to write and read has triggered several researchers to study the posted data and discover the user's opinion and feelings to support decision making. In this paper, a sentiment analysis framework is presented for slang Arabic text. A new dataset with Jordanian dialect is presented. Numerous specific Arabic features are shown with their impact on slang Arabic Tweets. The new set of features consists of lexicon, writing style, grammatical and emotional features. Several experiments are conducted to test the performance of the proposed scheme. The new proposed scheme produces better results in comparison with others. The experiments show that the system performs well without translating the tweets to English or standard Arabic.

Keywords—Sentiment analysis; Arabic features; opinion mining; emotional features; social media

I. INTRODUCTION

Social media has become a powerful source of information and part of our daily life. Social media with huge volume of data attract more people every day from different cultures, societies and languages. These data could be analyzed to capture valuable information about various topics. Sentiment analysis (SA) has become gradually popular and turns into an excellent source of information for companies, designers and sales representative. Twitter with 500 million users has turn into a great source to discover the user's opinion, emotions and feelings about services, products, political problems, or any other issues and possibly to create a framework to deal with it in future. Twitter gives users the ability to share their opinion in a short-term message with maximum 140 characters [1].

Sentiment analysis for English text has been researched heavily and several public datasets have been created and made publicly available. For example Stanford twitter sentiment corpus (STS), health care reform HCR [2]. Different types of features like lexicon [3, 4], emotional [5], n-grams [6], part of speech tags, semantic features [7] are used. Most of the sentiment analysis datasets have used positive and negative labels, but some datasets study the neutral and mixed labels.

Sentiment analysis for foreign languages received very little attention in comparison with English language. SA for Arabic language has not been researched seriously due to the language nature. It has many difficulties including the complexity of Arabic grammars, multi-meaning of a single word (ex: "عين المي" The word "عين" means eye and the right meaning in this clause is water source), multi-accents different meaning (ex: "مناظر بتجنن" in Jordanian accent the word "بتجنن"

means very beautiful, the same word in Saudi accent is "وايد حلو", in Egyptian accent "جميلة نوي"). Other primary problem is the standard public list. There is no standard list for negative, or positive words. Moreover, the slang text make it harder to analyse or even categorized. Previous research in this area translate the Arabic text to English then apply on of the English SA [8-11] without building any special features for the Arabic language.

The reminder of this article is ordered as follows. In Section II, the related work of sentiment analysis and the motivation of the research is provided. In Section III, the methodology of the proposed approach is presented and the feature extraction process is described. Essential steps for feature extraction and classification process are described in Section IV and Section V, respectively. In Section VI, the experimental results are shown to validate the performance of the proposed approach.

II. RELATED WORK

In this section, several sentiment analysis techniques for Twitter messages in different languages are presented. Numerous features and tools are described. Existing approaches in SA can be gathered into three main categories: knowledge-based, statistical, and hybrid approaches [12]. Knowledge-based techniques categorize text by classes based on the presence of explicit words [13]. Statistical techniques influence on elements from machine learning such as SVM [14]. Hybrid techniques influence on both machine learning and elements from knowledge representation such as semantic networks [15]. One of the early approaches in the field is presented in [16]. The emotions in the tweets was the focus for their automatic classification algorithm. Supervised learning machine and distant supervision is used. The noisy labels are used in training process. The accuracy over different classifiers like Nivea Bayes, Maximum Entropy and SVM was around 80%.

Another approach presented in [17] studied how twitter can be used for opinion mining purposes. Linguistic analyses are performed over automatically collected corpus to discover singularities and to train sentiment classifier. The operators use syntactic structures to define emotions. In [18] the parts of speech (POS) for specific prior polarity features are introduced. The approach uses unigram features as baseline and creates two types of models, tree kernel and feature based models. The best performance achieved with the specific prior polarity and their tags feature. Ensembles classifier with lexicon is proposed

in [19]. The experiments show that the best feature come from bag of words.

Linguistic features in sentiment analysis for English language are studied in [6]. The idea is to present a comparison between POS tags and different linguistic features like lexicons and microblogging features. The experiments show that the POS tags features alone is not powerful enough in comparison with a combination of linguistic features. The impact of semantic features on sentiment analysis area is studied in [8]. Three different sematic features are used for the analysis. The replacement, augmentation and the interpolation. The best results are achieved when interpolating the semantic concept into the unigram language model. The semantic features with the Unigrams and POS sequence are compared and the results show that the semantic feature model outperforms the Unigram and POS.

Two different languages in one application is presented in [20]. The Chinese and English tweets are studied in this approach. The IK Analyzer is employed as a tool for Chinese words segmentation, then the words are trimmed down and select some features using chi-square to modify the model. Comment reviews are collected from very popular movies. English comments are collected from Facebook and tweeter. The accuracy achieved by SVM is higher than N-gram classifier. The accuracy for English comments higher than Chinese comments. The problem of above is that the tweets are not collected based on specific trend hashtag in china or English languages.

Another approach that is built for two languages is presented in [21]. SA application is shown for English and Spanish languages using multilingual hybrid features and machine translated data. One of the interesting results is that the linguistic features is very helpful when moving to other language. However, some linguistic tasks like tokenization and remove stop words may have bad influence on performance. Additional results show that a list of expression that captor strength of polarity in the tweets can reached using unigram and bigram. They showed experimentally that combining the two languages using joint classifiers can assist to increase the performance by removing noisy features.

A language-independent framework is introduced to serve as classifier without giving much care to emotions in text [3]. Semi supervised heuristic labeling and content based features is used. The data set contain tweets in English, German, French and Portuguese languages. The approach achieved good results and it is possible to be applied on new languages.

Sentiment analysis from machine learning perspective for Arabic language is introduced in [10]. The collected dataset consist of 2591 tweet/comment from Twitter and Facebook. Bigram feature is the main feature for their research without creating special features designed for Arabic text. Attention for precision and recall are given special attention. The best results are achieved by SVM classifier.

Motivated by the need for Sentiment analysis approach designed for Arabic Language. We presents the first technique that deals with slang Arabic text in twitter with specific features designed for this purpose. The experiments show that

the system performs well without translating the tweets to English or standard Arabic.

III. METHODOLOGY

The novelty of our work concentrated on building a framework that deals with Arabic slang text that is wildly used on social media. Several specific Arabic features (SAF) categories is presented. Political Jordanian Arabic dataset (PJAD) is collected to be used for training and for simulation experiments. The dataset is collected using a specially developed tool called tweet collection tool (TCT). The performance of the proposed SFA is evaluated using several machine learning algorithms. Fig. 1 shows the main steps of the Arabic sentiment analysis process.

The Arabic special features are based on four categories: lexicon, writing style, grammatical, and emotional features. The PJAD is collected using a political trend hashtags in Jordan. The Dataset consist of 2000 randomly selected tweets with 1000 positive labels and 1000 negative labels.

A. Tweet Collector Tool (TCT)

In this section, the proposed TCT java tool is presented. The goal is create a complete tool that can be used by any language for sentiment analysis purposes. The tool consist of two main phases: tweets collection and features extraction. Tweet collection phase, the application enables the user to search for any specific hashtag or word and retrieve the collected tweets of any size (ex of hashtags: "2016انتخابات_#", "#عمان_#", "#رفع_الاسعار_#"). The twitter API is used and it is optimized to use 4 secret keys, consumer key (API key), consumer secret (API secret), access token and access token secret. Fig. 2 shows a simple data flow of the twitter API. Second phase consist of extracting SAF from the collected dataset.

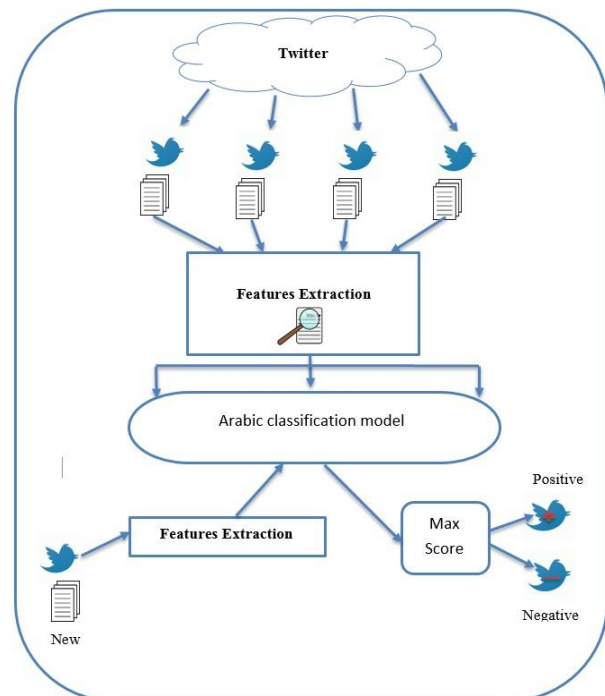


Fig. 1. Arabic Sentiment Analysis Process.

B. Political Jordanian Arabic Dataset (PJAD)

In this section, the PJAD is described; the new dataset topic is the parliamentary elections in Jordan. The tweets contains slang and standard Arabic text. The tweets have political theme and the tweeters use the Jordanian accent in their tweets. Labelling the extracted tweets is done through several volunteers. Table I shows examples of the collected tweets with their labels. The Dataset consist of 2000 randomly selected tweets with 1000 positive labels and 1000 negative labels.

IV. FEATURES EXTRACTION

Features extraction is the process where important properties (features) are mined from the collected tweets. The features are used later for training purposes. Clearly, using the whole tweets is confusing and misleading to be used for training. The extracted features are mainly, a mix set of four categories: lexicon, writing style, grammatical, and emotional features. Combine all the four types of features are proved through experiments that can increase the classification performance.

A. Lexicon Features

Arabic linguistic features are studied by digging deeply in the word-character structure and how it affects the results. The words state in each individual tweet is used [22] to extract five features: word count [23] character count, word length more than 5 characters, word length more than 6 characters and word length more than 9 characters.

B. Writing Style Features

A set of features are used to extract the user mood, user style and may extract a frequent characteristic of negative or positive text. The writing style feature consists of three groups of features: special characters, occurrences of punctuations and occurrences of digits.

C. Emotional Features

Emotion side in tweets is very important factor to classify the tweets whether is it positive or negative. For Arabic language there is no standard lists for negative and positive emotions. Hence, we create our own lists. A special emotional feature is created to describe the main negative and positive words lists. It contains four features, positive words, negative words, combination of positive words, and combination of negative words. Table II shows an example of emotional features.

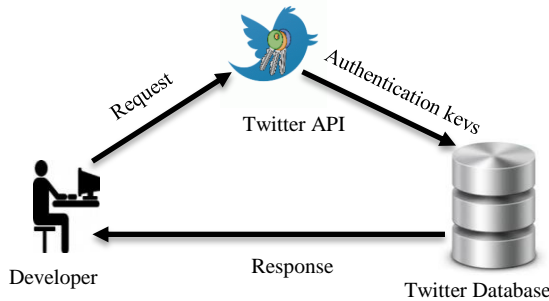


Fig. 2. Twitter API Data Flow.

TABLE I. EXAMPLES OF NEGATIVE AND POSITIVE TWEETS IN PJAD

Polarity	Tweet
Negative	وخلي الحكومة ترفع لحد ما ربنا يرفعهم عنده
Negative	الله يرفع ضغطهم و يدين عليهم يارب
Positive	خير قنوة و خير مثال للعمل الذي يسعى الى رفع مكانه الفرد في مجتمعه
Positive	اطال الله عمرك وابقاك ذخرا للعلم وللاردين مولاي
Positive	أعجز عن وصف يلين بحق هذا الرجل
Negative	مايبجي الفساد غير من اشكالك المواطن الفاسد بنحبس وبنعرف بس انتو مش ميبينين

D. Grammatical Features

Grammatical features describe the grammars that are used in Arabic tweets. It consists of seven grammar roles. The features are Kan and sisters (واخواتها كان), Enna and sisters (ان واخواتها), preposition, Plural Words, preposition, Question words and the exception word feature. In English sentiment analysis, the preposition stop words are removed. On Arabic Language it is not easy to remove preposition stop or deals with them as stop words because it is a primary part of Arabic statement.

V. CLASSIFICATION

Classification refers to extract models that recognize significant data from classes [24]. The models define data category and classes' labels. Classification helps to determine unseen information which yield to better understanding for the data. Classification has two primary steps: Learning step and classification step. In the learning step, the model is built using several training examples from the dataset. The training examples contains two divided entities with their related features and end with the class label. Fig. 3, depicts a simplified example of the training phase. The classifier model produce general rules to be able to classify new tweet to positive or negative in the future. Testing phase evaluate a new set of data using the extracted rules that are defined from the learning phase. The performance of the classifier is evaluated in terms of classification accuracy.

Several machine learning classifiers are employed including Random forest (RF), Regression (CVR), Dagging, Multi-Class-Classifier (MC), Simple Logistic (SL), Naïve-Bayes (NB) and the MultiBoost.

TABLE II. EMOTIONAL FEATURES

Emotional Features	Example
Positive words feature	خير , نشيطة, سعيد , سعيدة , فرح , متفائل , طموح , حلم , مودة , مودة , تعاون , امل ,
Negative words feature	حرام , للاسف , فاتورة , مشاكل اقتصاد , فساد , مش , حرامية , راجعون
Combination of positive words	يحتار عدوك , صادقين مع , معلومه ممتازة , معك حق جميل جدا , الله يبعدنا
Combination of Negative words	يوكل هوى , ارتفاع , والله حرام , حرام عليكم المحروقات , ما يتخافوا , جميلة الدعم

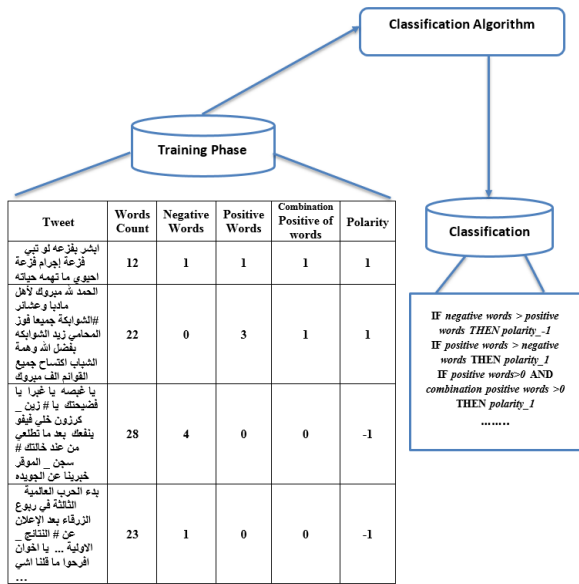


Fig. 3. Example of the Training Phase.

The performance of the classifiers is assessed in terms of classification accuracy, average false positive rate, recall, precision, and f-measurements. Classification accuracy is calculated as the number of correctly classified tweets against the total number of tested tweets.

$$Accuracy = \frac{\text{Number of of correctly classified tweets}}{\text{Total number of tested tweets}}$$

False positive rate (FPR) is calculated as the percentage of all tweets anticipated incorrectly against the sum of the true negatives (TN) and the false positives (FP). The recall or true positive rate (TPR), is the percentage of positives that are correctly identified. It is calculated as the percentage of all tweets anticipated correctly against the sum of the true positive (TP) and the false negative (FN)

$$Recall = TPR = \frac{TP}{TP + FN}$$

Precision is the number of items correctly labeled as to the positive class divided by the total number of elements labeled as belong to the positive class. F-measurements is the average of the recall and precision.

$$Precision = \frac{TP}{TP + FP}$$

VI. EXPERIMENTAL RESULTS

Several experiments were conducted to test the performance of the proposed scheme. Numerous feature selections and classification techniques are shown. We demonstrated the potential and the much-improved performance of the proposed technique. The new proposed PJAD dataset is used for the simulation experiments.

A. Experiment 1: Hold-Out Test

In this test, we partitioned the 2000 tweets into two independent datasets. Nearly 70% of the tweets (1400 tweets)

are used to train the classifiers and build the classification model. The testing tweets (30%) are then used by the classification model. The anticipated tweets are compared with the right class and the accuracy is calculated. Table III show the number of tweets that are correctly classified, not classified correctly classified, true positive rate (TPR) and false positive rate (FPR) for each classifier. Best results are achieved by Simple Logistic classifier (71.5%), TPR (0.715) and low FPR (0.288) due to the given weights for features like liner function tends (see Fig. 4 for accuracy comparisons). Fig. 5, 6 and 7 depict the detailed analysis, we show the F-measurements, recall, and Precision over four classifiers with 70% - 30% hold-out-test.

TABLE III. ACCURACY RESULTS WITH PERCENTAGE SPLIT. (30% OF THE TWEETS ARE USED FOR TESTING)

Classifier	Accuracy	Correctly class.	Miss class.	TPR	FPR
NB	66.5%	400	201	0.665	0.325
AdaBoost M1	69.66%	419	182	0.697	0.303
Simple Logistic	71.5%	430	171	0.715	0.288
SVM	70.66%	425	176	0.707	0.293

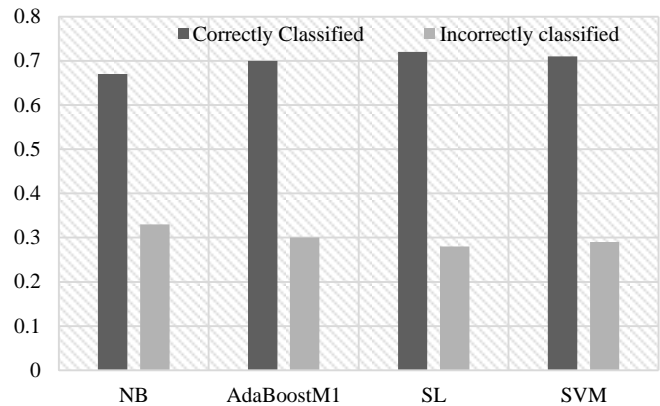


Fig. 4. Correctly and Incorrectly Classified Tweets with 70% SPLIT.

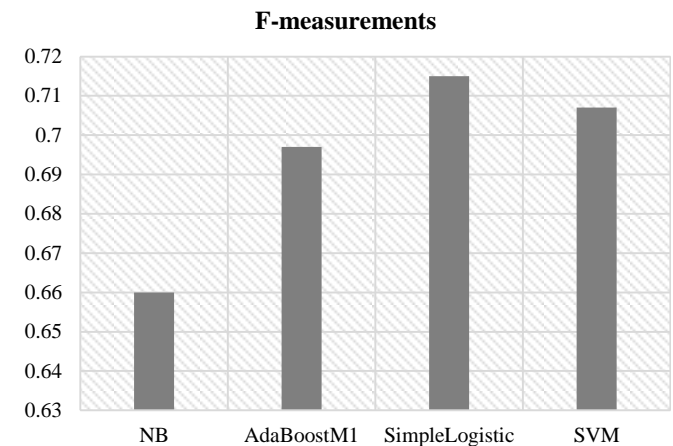


Fig. 5. F-Measurement Results Hold-Out Test (70%-30%).

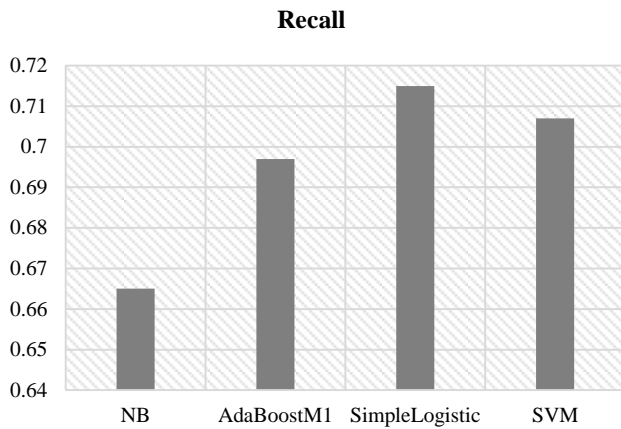


Fig. 6. Recall Results Hold-Out Test (70%-30%).

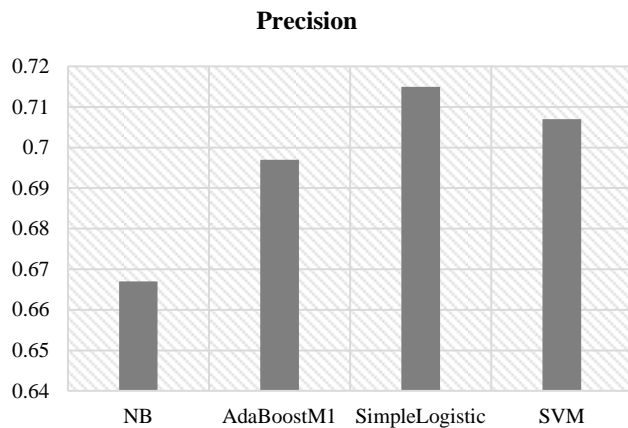


Fig. 7. Precision Results Hold-Out Test (70%-30%).

B. Experiment 2: Cross-Validation Test

For the second experiment, all the 2000 tweets of the dataset are used and divided into ten separate sets where nine of them are used for training and the tenth one is used for testing. The algorithm runs for ten times and the average accuracy across all the folds is calculated.

The accuracy of the correctly and incorrectly classified instances is presented in Fig. 8. Clearly, the results are acceptable for all classifiers taking into consideration that some tweets are confusing where the tweets are neutral. Table IV shows the number of tweets that are correctly classified, not classified correctly, true positive rate (TPR) and false positive rate (FPR) for each classifier. Best results are achieved by Dagging classifier (72.83%), TPR (0.728) and low FPR (0.272) due to it is training over SVM classifier. Several classifiers are presented to prove that the extracted features are effective and the system perform well with any classifier. Fig. 9, 10 and 11 depict the detailed analysis, we show the F-measurements, recall, and precision over several classifiers with 10 cross validation.

The cross-validation test results are often less than the hold-out test as the procedure used with the cross-validation test is to test the datasets ten times rather than one time for hold-out

test. However, the results remain even with small increase. There are no unnatural changes between the two validation tests.

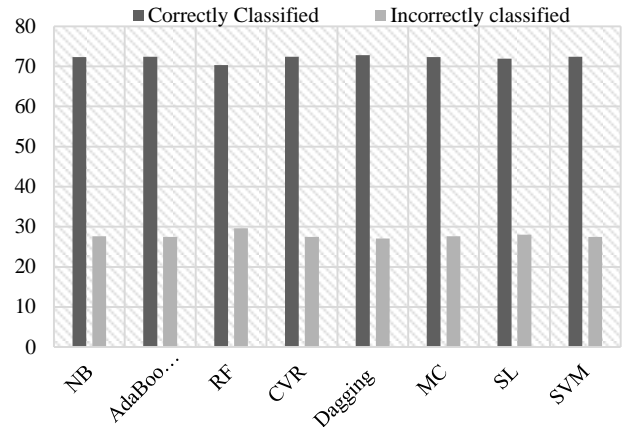


Fig. 8. Correctly and Incorrectly Classified Tweets with Cross Validation (10-Cross)

TABLE IV. ACCURACY RESULTS WITH PERCENTAGE SPLIT. (30% OF THE TWEETS ARE USED FOR TESTING)

Classifier	Accuracy	Correctly classified	Miss classified	TPR	FPR
NB	72.33%	1446	553	0.723	0.277
AdaBoostM1	72.48%	1449	550	0.725	0.275
RF	70.33%	1406	593	70.3	0.297
CVR	72.43%	1448	551	0.724	0.275
Digging	72.83%	14456	553	0.728	0.272
MC	72.33%	1446	553	0.723	0.277
SL	71.93%	1438	553	0.719	0.281
SVM	72.43%	1448	551	0.724	0.276

F-measurement

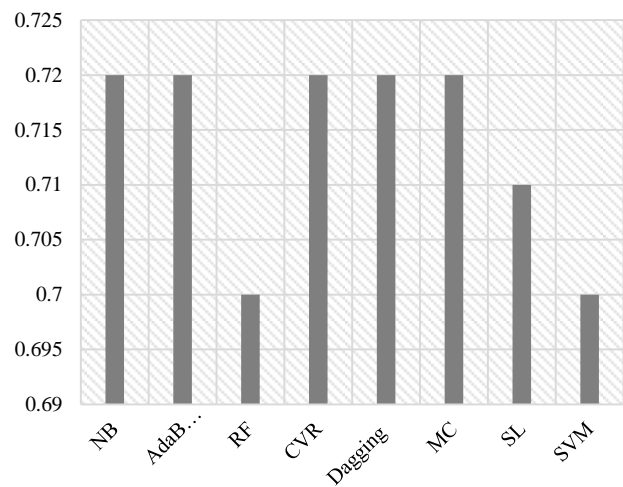


Fig. 9. F-Measurement Performance Over 2000 Tweets (10-Cross).

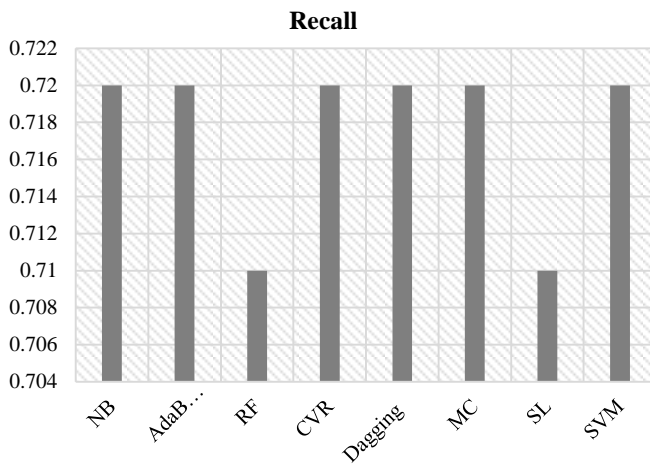


Fig. 10. Recall Performance Over 2000 Tweets (10-Cross).

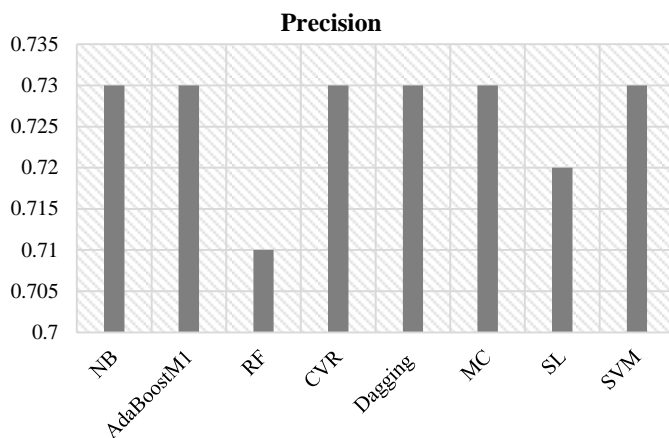


Fig. 11. Precision Performance Over 2000 Tweets (10-Cross).

It is clear from the tables above that the proposed features set is powerful for distinguishing between the positive and negative tweets with a performance accuracy of 72% and low FPR of 2%. In general, the proposed features set is proved to be effective to this problem with acceptable accuracy rate (considered high) taking into consideration, the tweets are randomly chosen and never been filtered. Moreover, the neutral tweets need to be classified as positive or negative tweet and this might confuse any trained classifier. Some Arab tweets authors have positive and negative opinion in the very same tweet, making the tweet classification is quite difficult. Different writing behaviors for each writer and the baffling words in Arabic language makes it a challenging task to recognize whether the tweet is positive or negative.

VII. CONCLUSION

A new sentiment analysis framework for Arabic language is proposed. The main attractive idea of the new schema is the Arabic features that deals with the complexity of the language. Four general features categories are proposed including lexicon, grammatical, writing style, and emotional features. Several numerical experiments were performed to demonstrate the potential and the much-improved performance of the proposed method. The best results achieved by Dagging

classifier for political data set gathered with Jordanian accent. For future work, it would be interesting to analyze the relationship among the number of features used, classification technique and the correctly classified tweets.

REFERENCES

- [1] Fernández-Gavilanes, M., Álvarez-López, T., Juncal-Martínez, J., Costa-Montenegro, E. and González-Castaño, F.J., "Unsupervised method for sentiment analysis in online texts," *Expert Systems with Applications*, 58, 57-75. (2016).
- [2] Saif, H., Fernandez, M., He, Y., & Alani, H. "Evaluation datasets for Twitter sentiment analysis: A survey and a new dataset, the STS-Gold" (2013).
- [3] Xiang, B., Zhou, L., & Reuters, T. "Improving twitter sentiment analysis with topic-based mixture modeling and semi-supervised training." *ACL*, 2, 434-439. (2014).
- [4] Mohammad, S. M., Kiritchenko, S., & Zhu, X. "NRC-Canada: Building the state-of-the-art in sentiment analysis of tweets." *arXiv preprint arXiv:1308.6242*. (2013).
- [5] Kouloumpis, E., Wilson, T., & Moore, J. D. "Twitter sentiment analysis: The good the bad and the omg!" *Icwsn*, 11, 538-541. (2011).
- [6] Pak, A., & Paroubek, P., "Twitter as a corpus for sentiment analysis and opinion mining" In *LREc*, 10, 1320-1326. (2010).
- [7] Saif, H., He, Y., & Alani, H. "Semantic sentiment analysis of twitter." *International Semantic Web Conference Springer Berlin Heidelberg*. 508-524, (2012).
- [8] Nabil, M., Aly, M., & Atiya, A. F. "Astd: Arabic sentiment tweets dataset." *Proceedings of the 2015 Conference on Empirical Methods in Natural Language Processing*. 2515-2519. (2015).
- [9] Al-Kabi, M. N., Gigieh, A. H., Alsmadi, I. M., Wahsheh, H. A., & Haidar, M. M. "Opinion mining and analysis for arabic language." *International Journal of Advanced Computer Science and Applications (IJACSA)*, SAI Publisher. 5(5). (2014).
- [10] Rushdi-Saleh, M., Martín-Valdivia, M. T., Ureña-López, L. A., & Perea-Ortega, J. M. "Bilingual experiments with an arabic-english corpus for opinion mining." *Recent Advances in Natural Language Processing, RANLP*. (2011).
- [11] Hamed, A. R., Qiu, R., & Li, D. "Analysis of the relationship between Saudi twitter posts and the Saudi stock market." *Seventh International Conference on Intelligent Computing and Information Systems (ICICIS)*. 660-665. (2015).
- [12] Cambria, E., Schuller, B., Xia, Y., & Havasi, C. "New avenues in opinion mining and sentiment analysis." *IEEE Intelligent Systems*, 28(2), 15-21. (2013).
- [13] Ortony, A. C., & Collins, G. A. *The cognitive structure of emotions*. 1st edition 1988. Cambridge Univ. Press.
- [14] Kim, S. M., & Hovy, E. "Identifying and analyzing judgment opinions." *Proceedings of the main conference on Human Language Technology Conference of the North American Chapter of the Association of Computational Linguistics*, 200-207. (2006).
- [15] Cambria, E., & Hussain, A. *Sentic computing: Techniques, tools, and applications* 2ed edition 2012. Springer Science & Business Media.
- [16] Go, A., Bhayani, R., & Huang, L. "Twitter sentiment classification using distant supervision." *CS224N Project Report, Stanford*, 1, 12. (2009).
- [17] Narr, S., Hulphenhaus, M., & Albayrak, S. "Language-independent twitter sentiment analysis." *Knowledge Discovery and Machine Learning (KDML)*, LWA, 12-14. (2012).
- [18] Agarwal, A., Xie, B., Vovsha, I., Rambow, O., & Passonneau, R. "Sentiment analysis of twitter data." *Proceedings of the workshop on languages in social media Association for Computational Linguistics*. 30-38, (2011).
- [19] Da Silva, N. F., Hruschka, E. R., & Hruschka, E. R. "Tweet sentiment analysis with classifier ensembles." *Decision Support Systems*, 66, 170-179. (2014).
- [20] Yan, G., He, W., Shen, J., & Tang, C. "A bilingual approach for conducting Chinese and English social media sentiment analysis." *Computer Networks*, 75, 491-503. (2014).

- [21] Balahur, A., & Perea-Ortega, J. M. "Sentiment analysis system adaptation for multilingual processing: The case of tweets." *Information Processing & Management*, 51(4), 547-556. (2015).
- [22] Ootom, A. F., Abdallah, E. E., Hammad, M., Bsoul, M., & Abdallah, A. E. "An intelligent system for author attribution based on a hybrid feature set." *International Journal of Advanced Intelligence Paradigms*, 6(4), 328-345. (2014).
- [23] Abdallah, E. E., Abdallah, A. E., Bsoul, M., Ootom, A. F., & Al-Daoud, E. "Simplified features for email authorship identification." *International Journal of Security and Networks*, 8(2), 72-81. (2013).
- [24] Alpaydin, Ethem "Introduction to Machine Learning." MIT Press. p. 9. ISBN 978-0-262-01243-0. (2010).

Healthcare Management using ICT and IoT based 5G

Vijey Thayanathan

Department of Computer Science

King Abdulaziz University, Jeddah 21589, Saudi Arabia

Abstract—In healthcare management, all patients need to be looked after properly with the latest technology. Although treatment facilities of healthcare management are available wirelessly, many treatments are still pending and delayed because the number of patients is increasing. In this research, 2 problems are focused on they are the availability of treatment facilities and an efficient way of handling healthcare administration records. In healthcare management, e_Health applications focus on medical treatment and administration. However, these applications depend on the Information and Communication Technology (ICT) and Radio Frequency Identification (RFID) systems. Using IoT based 5G and the latest technologies, this research provides an efficient method to solve these problems. In this method, ICT based on 5G networks and IoT based 5G are the major components which include efficient management protocols for treating the patients and elders through the appropriate e_Health applications. Although some patients and older adults visit healthcare homes or hospitals regularly, they never become satisfied people because they always expect better services. Some healthcare management treats these people as customers and maintains customer relationship. Improving the accuracy and quality of healthcare services and customers' satisfaction depends on Customer Relationship Management (CRM) through evolving technologies. As results, ICT based on RFID and other latest technologies enhances the quality of e_Health application and healthcare services with the satisfaction of CRM values. Despite the profits and benefits, these enhancements are the conclusions of the healthcare service and management.

Keywords—Information communication technology; e_Health; customer relationship management; Radio Frequency Identification (RFID); Internet of Things based fifth generation (IoT based 5G)

I. INTRODUCTION

Healthcare industries are divided into two areas; they are such as private services are offered with the competition, and compulsory services are provided to everybody respectively. Even hospitals, which provide compulsory services are also becoming strategic organizations. Most of the hospitals in the world are privately owned because many different types of health issues are increasing with patients' population. These hospitals get profits through CRM values such as quality of service (QoS). Healthcare industries include hospitals, health care homes, elderly homes, etc.

In ICT based e_Health development, RFID was introduced to replace the barcode as the first issue in which CRM achieved first glance of enhancement successfully. The barcode replacement created satisfaction for both customers and organizations, where they gain the extra profit as well as time-saving in a number of ways such as quick changes in price,

quick self-filling, etc. Barcode system is still used in many organizations, but RFID is going to move to the second generation of CRM enhancement, which investigates CRM values against future technologies. The features of ICT depend on the RFID and IoT devices which merge with the latest 5G based technologies.

In this research, healthcare industries are considered profitable organizations. With such organizations, CRM values are encouraged to increase the services as well as sell more medical products, gain more customers, lock the existing customers, and analyses the effectiveness of marketing activities. According to [1], the integration of IoT with 5G and RFID technologies provide a number of benefits in many potential applications such as e_Health, healthcare monitoring.

This research will focus on achieving appropriate CRM values through ICT for improving the quality of the e_Health services and applications. Overall objectives of the research are the improvement of the medical facilities such as efficient treatments on time with a less or manageable medical cost. Specifically, overall objectives focus on the enhancement of CRM through the RFID technologies which are being improved with next-generation technology and standard. With an improvement of CRM, all profitable and unprofitable organizations will achieve a better position of managing customers in all environments.

Although ICT is playing an important role in most of the administrations used in the e_Health applications, the roles of the social cognitive theory, satisfied connectivity, and perceived interactivity motivate us to investigate this research. Despite the RFID and ICT facilities in the e_Health applications, data collected from Facebook users. Here, ICT provides the social cognitive facilities to handle the health information between the users and health service providers. Authors claimed that their proposed model exchanged health information based on the social cognitive theory [2]. Further, their results motivate that human-to-human interaction with IoT, other interactions such as information handlings with human, outcome expectation of IoT based e_Health applications challenged with self-management competence, and outcome expectation of social relationships can be used to enhance the ICT facilities to improve the e_Health applications. Here, motivation is the development of intelligent ICT (IICT) which allows us to design and research new healthcare devices for managing the e_Health applications friendly manner influenced to improve the CRM values.

Although many challenges and possible implementations are urgent to improve the quality, I have focused on CRM values which allow health care providers to improve the safety issues such as medical errors, quick monitoring facilities of

patients' identifications and efficient, caring services. The following contributions have been considered in this paper.

- Studying the existing healthcare issues depended on ICT, IoT, and RFID for managing the patients' healthcare system.
- Based on the study and investigation of current CRM values, management issues of e_Health applications such as patients' monitoring and caring services have been considered for improving the patients' healthcare services.
- Designing a model of generic CRM in healthcare using ICT, CRM values, IoT based 5G for improving the e_Health and healthcare management services.
- Finding the theoretical comparisons of CRM values for improving healthcare management such as QoS.

The rest of the paper is organized as follows. Section II focuses on the literature review and background. In Section III, we provide details of current technologies used in e-healthcare. Section IV explains the proposed model and brief methodology of the proposed scheme for e_Health based on CRM values. Theoretical analysis of the e_Healthcare services obtained from the selected CRM values for e_Health application is considered in Section V. In Section VI, overall conclusions are written based on the CRM values, theoretical analysis, and results.

II. LITERATURE REVIEW AND BACKGROUND

In general, healthcare information system (HIS) based on the RFID network and ICT management supports the Management Information System (MIS) and the Clinical Information System (CIS). To improve the HIS, the CRM values such as satisfaction should influence the administration and clinical requirements [3]. More and more healthcare organizations have started utilizing ICT with RFID to improve their CRM values [4]. Although HIS depends on this new utilization, some organizations face an error of at least 5 percent in their system. To overcome these errors, new organizations employ the IICT as a state of the art which not only increase the quality of e_Health applications and services but also minimize the medical cost.

Although RFID technology reduces the medical cost and offers tremendous benefits to the e_Health applications, employing RFID to analyze the CRM values in e_Health services will be one of the new challenges. Maximum security with minimum energy consumption can be considered through CRM values. Here, medical signal interferences and interactions are causing unnecessary problems such as insecure system during the medical operation when the RFID network is not configured correctly. In this situation, limitation and capacity of the RFID such as range of reader [5] (long or short range) should be employed according to the environment.

Psychological problems based on long-term diseases need some IICT based monitoring facilities. Here, the use of RFID

and CRM values and e_Health services provided by IICT are also significant challenges. There will be plenty of other challenges related to long-term diseases such as diabetes because deceases will transform into new problems which never end. Table I shows the growth of CRM with evolving RFID technology [6] which improves the quality of life to all including patients who stay in the care homes and smart hospitals.

Everywhere, uses of IoT devices, smartphones, wearable tags, etc. increase the facilities of the e-healthcare services. Here, ICT enhances the management issues of e_Health applications such as handling patients' medical information or records. Although Fig. 1 shows the management issues, CRM values influence healthcare industries which provide the basic facilities to all patients. For instance, availability of healthcare service increases the satisfaction which improves the profit of the healthcare industries.

According to the healthcare industries, IoT provides many facilities such as quick feedback, adequate security, etc. which improve not only e_Health applications but also provide excellent services. Using IoT, patients feel the satisfaction with low-cost which is one of the CRM values. Integrating ICT with IoT enhances the healthcare monitoring facilities because RFID tags interact quickly with RFID readers merged with IoT devices. In mobile health, wearable IoT based tags and devices provide quick monitoring facilities which make happy feelings and satisfaction. When CRM values enhance the happy feelings through efficient technologies, e_Health applications based on CRM offer better services to patients and profits to healthcare industries.

According to [8-10], influences of IoT in RFID become identification of things (IDoT). This RFID enables e_Health devices to share their unique identification for monitoring the performance of available devices. IDoT technologies enhance the features of ICT when patients use e_Health applications. Further, IDoT allows healthcare providers to improve CRM values through availability, security, etc. With the growing era of IDoT, the communication between the medical devices which include patients' wearable tags, containers' tags, etc.

TABLE I. HEALTHCARE MANAGEMENT WITH EVOLVING TECHNOLOGY

Years	Evolving technology in healthcare
Before 2010	First, 3 generations had been used with ICT and basic barcode
2010 to 2011	The 3 rd generation had been dominating with the low-cost RFID tags
2011 to 2020	With the 4G, e_Healthcare based on RFID, security, IoT, and ICT is improving with CRM values
After 2020	5G will be dominating the healthcare services with satisfaction, nursing, etc. based on RFID security and privacy [7], ICT and IoT

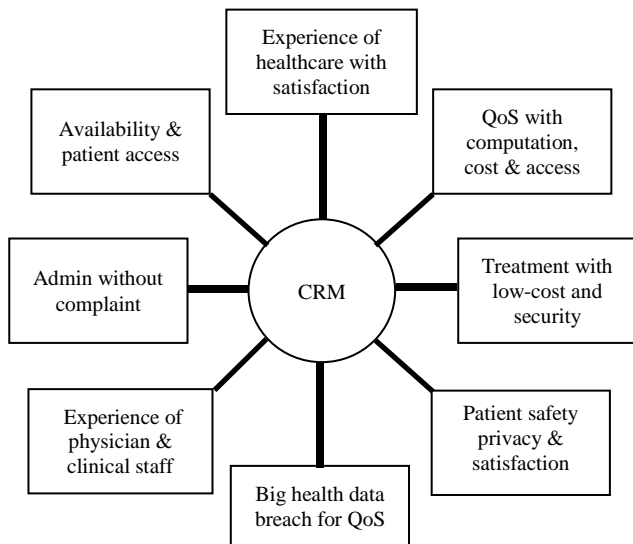


Fig. 1. Healthcare Management with CRM Values.

III. CURRENT TECHNOLOGY ISSUES FOR HEALTHCARE

Healthcare industries are merging with e_Health services and applications. Current technology issues are forcing to merge the e_Health services according to the patients' satisfaction which is one of the CRM values.

The potential e_Health applications have some influences with ICT and RFID for improving the patients' monitoring facilities in many directions [11]. All e_Health applications have to be invoked to treat the patients with their satisfaction which are CRM values [12-14] improve with the use of technologies. Satisfied patients considered as customers are loyal to their medical service providers which include the RFID-based HIS [15], hospitals, healthcare units, etc. Strategic approaches to using CRM values need some limitations according to the services used in the e_Health applications [16, 17]. The ICT implementation based on CRM values could enhance the medical services provided not only in the remote areas [18-22] but also in the war affected places.

According to the references [23, 24], authors have developed and analyzed the evaluating model for verifying the results of some selected e_Health applications. Through this conceptual model, e_Health applications based on ICT and CRM values have been considered to face some challenges [25]: they are remote monitoring in war-affected areas with low-cost RFID, climate changes, polluted air, etc.

A. RFID in e_Health Applications

The use of RFID in the medical system enhances not only the patients' monitoring facilities but also improve the services handled through modern technologies. Here, the authors have used the technology, organization, and environment (TOE) framework [26] to manage the medical care and systems. Despite many frameworks, shortages of medicine and medical systems were impeding the effort to control the e_Health applications such as diseases and administration of the medical care respectively. Hence, enabling or impeding RFID simplifies not only the healthcare asset management but also medical operations. Using TOE within healthcare management,

healthcare providers improve their service through technology such as RFID, ICT, etc., an organization such as hospitals and environments such as remote areas. As far as the results of the TOE are concerned, RFID vendors and healthcare service providers enhanced the implications of the healthcare services and e_Health applications through using and implementing TOE framework. Authors claimed that RFID implementations enhanced the medical facilities using six different cases which include the CRM values indirectly. Table II provides examples of CRM values and ICT involvements in RFID applications.

Although healthcare provides the basic facilities to all patients and elders, CRM enhances healthcare services with maximum benefits. Thus, generic function (1) depends on many inputs to improve the benefits of healthcare.

TABLE II. IDoT APPLICATION BASED ON CRM

Examples of CRM values	Healthcare management with 5G based ICT and IoT
Satisfaction	All ICT based services and IDoT based monitoring facilities will be available for managing personal and confidential medical data with satisfaction
Cost	Low-complex technology, quick treatments, and responses without delay, secure system with IDoT, etc., managing resources and services efficiently
QoS	Managing healthcare data without delay, leak, etc. Regular healthcare with ICT & IDoT, timekeeping, maintaining maximum accuracy, etc.

$$H = f(\text{Inputs to healthcare}) \quad (1)$$

In (2), H is the healthcare function depended on the e_Health applications which involve with some healthcare inputs such as administration, treatments, CRM values, etc. This function may take n, m and r inputs.

$$H = \sum_{i=1}^n A_i + \sum_{j=1}^m T_j + \sum_{k=1}^r C_k \quad (2)$$

Health is the service depended on quality, accuracy, etc. and the managing and maintaining a healthy life with the satisfaction and peaceful mind. Here, the administration of the health service should provide maximum satisfaction with low-cost.

B. Healthcare with CRM

Elderly people are struggling without proper management which influences with CRM values such as satisfaction, QoS, cost, etc. These days, satisfaction not only depending on the human admirations but also electronic tracking devices involved during the services offered by the elderly homes and hospitals [27, 28]. According to Innominato et al. [29], home-based e_Health multifunction and the multiuser platform provides maximum satisfaction when different e_Health applications are handled simultaneously. Daily data collected from the patients are sent to this platform for analyzing the patients' problems with their satisfaction. This platform allows the hospital team to handle the daily data with the efficient ICT concept from the specific server.

C. Healthcare Management with Call Handling

As an example scenario, the healthcare management with call handling can be improved using ICT concepts and latest

technologies. As shown in Fig. 2, call handling provides many benefits to both users and service providers for improving CRM values.

In healthcare management, call handling dominates many issues to open the services between the users and medical service providers including nurses and physicians. Here, users may be patients, elders, others, etc. who expect to register for starting the healthcare services. Despite many online services, source and destinations are linked by wireless channels. Call handling initiates many issues, but some of the following issues in healthcare management are dominating the main medical services. They are the availability of the services, administration details for registrations, treatments strategies, etc.

Availability of service: All calls including online services interacted by users whenever they want. Here, QoS depends on the call handling (accepting, blocking, dropping, etc.).

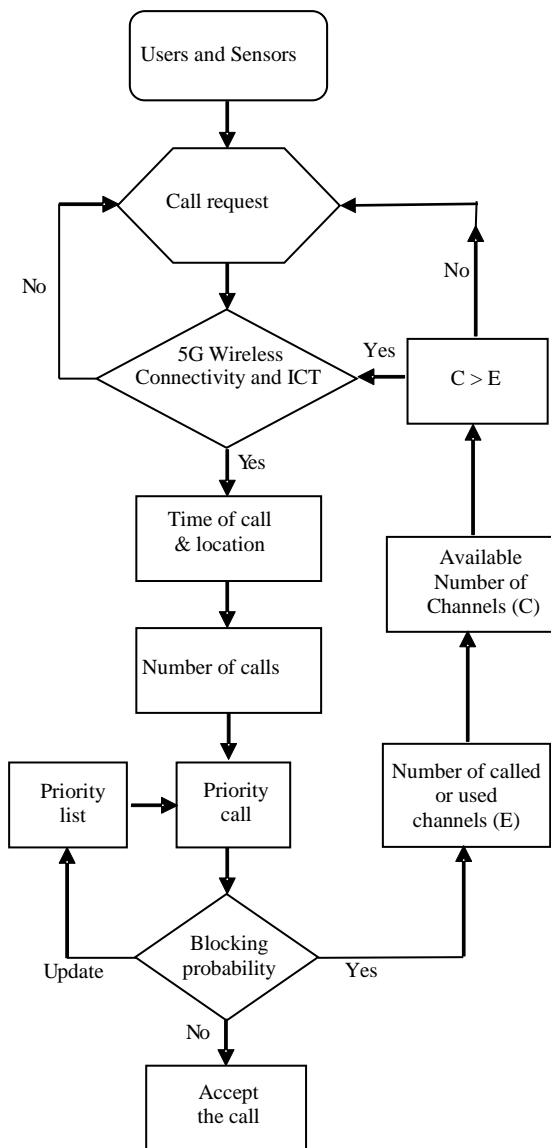


Fig. 2. Call Handling Scenario in Healthcare Management.

Administration details for registrations: All accepted calls should be registered without any data loss and delay influenced to QoS.

Treatment strategies: All registered calls should be allocated for caring or consulting with patients according to their priority and available resources. Here, minimum cost, maximum security, etc. are the key parameters of QoS.

In the call handling, the probability of priority calls can be calculated as $P = 1/e^{\mu t}$. Here, μ is the mean value of calls. When patient's random call x is active during the interval t , the probability p is calculated to compute the expected number of channels and calls.

$$P(x) = \frac{e^{-\lambda} \lambda^x}{x!} \quad (3)$$

Where, $\lambda = \mu t$ represents the new online health enquiry rate. Although call handling represented by Poisson distribution (3), all priority and emergency calls can be considered for managing health services. Most of the CRM values depend on best services used with time keeping, minimum delay, maximum security, etc. When service providers maintain the call handling accurately, QoS of the CRM value enhances the healthcare management.

D. ICT for e_Health Applications

The ICT system is being developed to integrate the health and social for collecting the CRM values which improve the e_Health applications. This integrated approach includes much more robust ICT solutions, along with new e_Health services that healthcare providers will also change the management behaviors. Several types of ICT tools developed to exchange health information (medical and administration) are identified in the e_Health applications. According to [30, 31], authors claimed that Integrated Care for Older Adults with Complex Health Needs (iCOACH) included the ICT facilities.

IV. PROPOSED MODEL

Healthcare management depends on satisfaction, quality, experience, competition, etc. Here, the proposed model employs the generic CRM which enhances the healthcare facilities. The rationale for this model is that the needs of generic CRM can be effectively studied by understanding how CRM value is delivered to the customer (patients and elders). Also, this model shows how ICT based on IoT or 5G technology can be employed to deliver better healthcare such as QoS, cost, and satisfaction. The accuracy of the technology-based treatments can be considered as an overall quality which is given below:

$$Q(\tau) = W_T + W_D + W_J + W_C \quad (4)$$

Here, τ is the time dependent matrix for prioritizing the users' case and situations. To measure the quality, each weight is multiplied as $W_T = a_T \times w_T$, $W_D = a_D \times w_D$, $W_J = a_J \times w_J$, and $W_C = a_C \times w_C$. Where, best throughput (a_T) minimum delay (a_D), minimum jitter (a_J) and quick and best charger (a_C) are the independent parameters. In (4), w_T, w_D, w_J and w_C are weights of the throughput, delay, jitter and charging respectively. Strategically, this model is very useful for the CRM process. It attempts to provide a rationale for applying

RFID technology in the healthcare industries, and it also serves as a healthcare manager for monitoring e_Health applications.

As shown in Fig. 3, a proposed model based on a generic CRM approach can be developed to improve the healthcare service which depends on the quality [33, 34]. Healthcare technology changes are improving daily. Therefore, healthcare industries update their facilities with reasonable changes, which will affect all issues in the business including CRM. Through this model, organizations can identify the opportunities and develop e_Health strategies, payment policies [35], etc. With an appropriate CRM policy, healthcare services can be created and implemented for improving healthcare management. The CRM policies depend on CRM values attracted to the customer (patients or older adults). Despite many CRM values and their updated issues such as technical requirements and policies, patients need quick, low-cost and peaceful service according to e_Health applications. Updating the policies of CRM values enhances the profit and benefits of the healthcare industries. In this research, the role of ICT in the patients' care facilities is important to update the CRM policies. In addition, all CRM values including QoS not only depend on the users' of ICT infrastructure but also available best service of ICT merging with evolving technologies and policies.

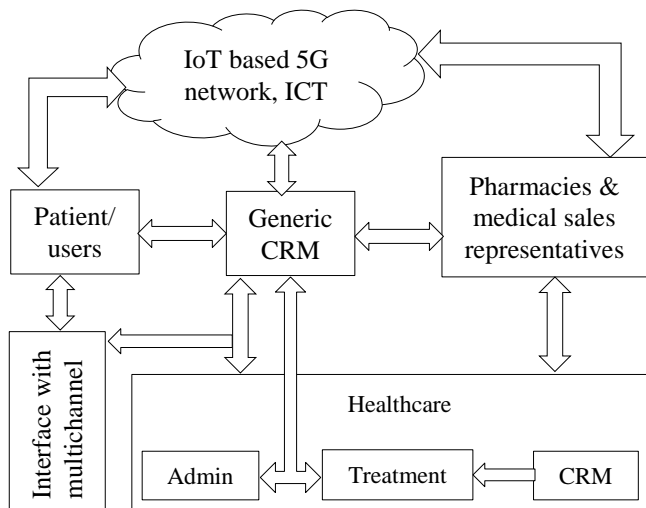


Fig. 3. A Proposed Model of Generic CRM in Healthcare.

Minimizing the medical cost is the ultimate target of all ordinary patients. All CRM values not only improve the overall performance of healthcare management but also provide support to all types of users. Service providers should maintain accuracy when they deploy the latest technologies. Accuracy keeps the satisfying treatment which creates satisfaction when patients use the e_Health applications.

V. ANALYSIS AND DISCUSSIONS

This section describes healthcare services and management prioritized as a QoS which provides the patients' satisfaction. Although healthcare management deals with many issues and services, handling calls and prioritizing calls according to the patients' health condition are considered as QoS.

A. Operational Scenarios and Indicative Results

New healthcare management will have some new resolutions based on the emerging technology of ICT and CRM values. The ICT based CRM policies will help to increase the quality of the healthcare services and industries' benefits (error reduction, quick monitoring, security, etc.). Following scenarios illustrate the CRM values when patients use basic ICT and IoT based ICT. In these scenarios, four types of healthcare and 100 patients are used for recording the patients' opinion of CRM values.

1) *Scenario 1 (Cost with healthcare issues)*: Future of the e_Health services must be error free because still at least 5% error causes many problems in healthcare industries. Fig. 4 shows the average cost of conventional and proposed ICT deployments with the increasing number of patients (users). In this analysis, the percentage of ICT-5G based IoT improves when users are increased. Hence, CRM value (cost) will be better when cost is considered as healthcare measurement during the call handling and patient monitoring. Cost related to a data breach can be reduced when healthcare units or industries provide better services and treatment with new technology.

Although accuracy calculations are dominating to reach the best service, healthcare management allows the service providers to maintain the accuracy for improving the patients' satisfaction.

2) *Scenario 2 (QoS during the treatment)*: Future of the health care services and management will depend on the quick and efficient treatment facilities which maximize the health services and improve the overall quality and profit. Fig. 5 is an expected performance of quality issues during the healthcare services provided by hospitals and healthcare industries. When healthcare service providers increase their services and features involved with latest technologies such as IoT, IDoT, IoT based on 5G, etc., QoS increases. Also, technological issues such as 5G requirements (latency, delay, etc.) increase the QoS. With basic accuracy calculations, service providers can choose the best technology for maintaining healthcare applications. Also implementing IoT based 5G for improving ICT and health-related communication technologies such as call handling depending on the technical requirements. In e_Health application over the wireless communication, accuracy of the treatment is the most important parameter. It not only provides the accuracy of the medical treatment but also increases the QoS. Although medical services are leading to reach high quality and reputation, competition is still challenging with the evolving technology.

Technology is changing, merging and evolving with many new requirements but the percentage of QoS should increase with the implementation according to the service architecture of the 5G environments.

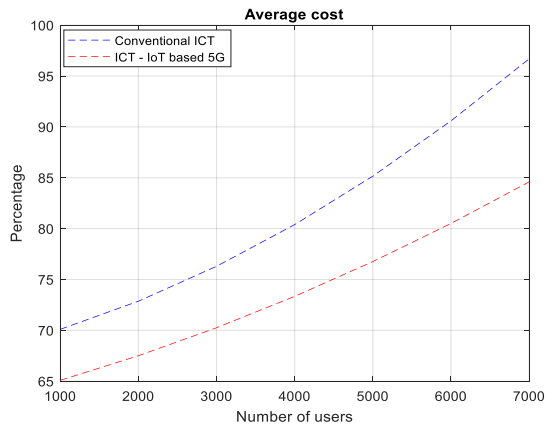


Fig. 4. Cost Improvement through ICT Technologies.

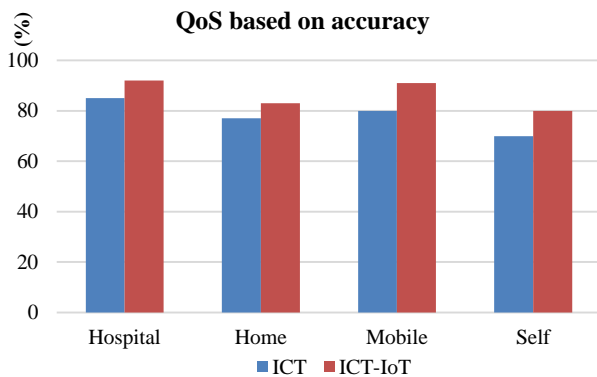


Fig. 5. Comparison of Technology Issues for Improving QoS.

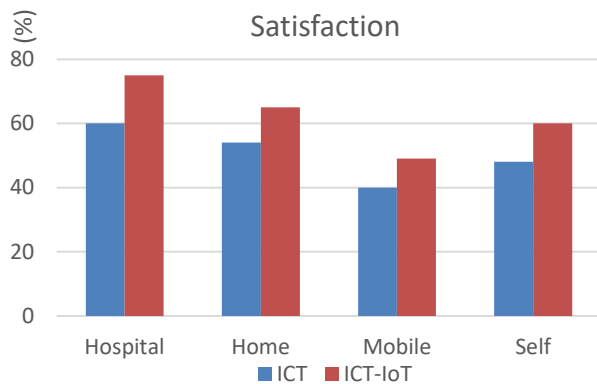


Fig. 6. Comparison of the Best Technology for Improving Satisfaction.

3) Scenario 3 (Satisfaction considered as best service): All medical services must be efficient with the nursing, caring, etc. which provide satisfaction. Regarding medical services, both patients and service providers should satisfy. Patients' satisfaction depended on the best service used through the best technology increase the CRM value of satisfaction as in Fig. 6. Future of healthcare management will be competitive with the best services, low-cost technology, and maximum satisfaction.

Through this research, at least a 10% improvement in e_Health applications over the wireless network will be expected. Not only patients will enjoy the CRM values, but also customers (elders) who use the healthcare industries for their private purposes will enjoy the CRM values with the best and latest technology. Here, patients are like customers because patients not only use health care services but also they buy healthcare products regularly according to the e_Health applications and become happy and satisfied customers.

According to the properties of IoT devices, communication and computation capabilities are limited because IoT devices are very small and work with the low-power. Examples of IoT devices are wearable watches, smart cameras, etc. In CRM, IoT based devices help to improve the quality, accuracy, etc. which provides the satisfaction considered as one of the CRM values. For instance, wearable watches provide quick monitoring of health issues such as sugar levels of blood. This facility reduces the cost and time of the patient and increases the quality which improves the CRM values.

Although many securities are available for protecting data in public and private healthcare organizations, data breaching is damaging the accuracy and quality of the treatment. Currently, 5G provides efficient protection techniques for protecting data breaches. They are secure software-defined networks (SDN) with lightweight cryptographic algorithms; secure SDN based intelligent approach with routing algorithms, non-orthogonal multiple accessing techniques with physical layer security, etc.

Regarding the proposed model, cost and time are the important factors considered in figures 7a and 7b. Using this model, technology not only improves the e_Health applications and healthcare services but also cost ad time which involves with the CRM values. Table III illustrates the admin (call handling) and small treatments considered for measuring satisfaction ratio which increases with evolving technologies.

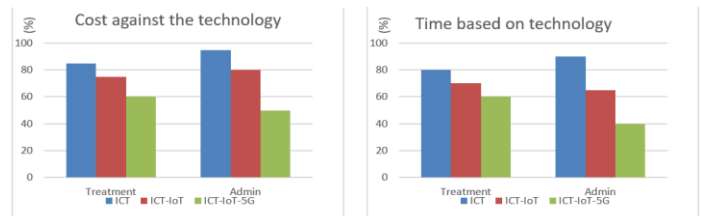


Fig. 7. Expected Improvements a) Cost and b) Time with Technologies.

TABLE III. SATISFACTION RATIO AGAINST THE TECHNOLOGY

Technology	0 < Satisfaction ratio < 1	
	Call handling rate per minute (50 calls)	Treatment per hour (10 treatments)
ICT	0.4 to 0.5	0.45 to 0.55
ICT - IoT	0.5 to 0.6	0.55 to 0.65
ICT IoT - 5G	0.6 to 0.65	0.65 to 0.7

Although many limitations in the healthcare management issues, limitation of this study focuses on QoS during the healthcare services, cost against healthcare services and profit through the CRM values. Healthcare facilities are improved by efficient services, secure technologies, minimum waiting time, etc. Using technology will not only improve profit and CRM values but also reduce the waiting time. When service providers consider all these limitations correctly according to the priority, both users and service providers will get the benefits. According to my opinion, these limitations will open many new research ideas and activities in this field. They are such as minimum waiting time and cost against the QoS, efficient use of technology and services against the cost, etc.

B. Recent Advances in e_Health Systems

Implementation of ICT and IICT should be available within the e_Health system for analyzing all healthcare services influenced by the patients' satisfaction. Here, the recent advance approach is CRM which depends on the ways patients are treated in the hospitals and healthcare units. In this approach, applying CRM values excellently within the healthcare system is one of the recent advances. Following technology, services, application, and facilities are examples of recent improvements in the e_Health system.

According to Newman-Casey et al. [36], experiences with e_Health technology among glaucoma patients and their relationship with medication adherence can be analyzed using CRM values which not only improve the e_Health applications but also simplify the patients' relationships when health providers set and apply medication adherence during the health monitoring and physical observations.

A systematic review of the technology acceptance model (TAM) [37] in health informatics, improve the e_Health services. Further, authors have identified three ICT application areas for implementing TAM in the healthcare services they are telemedicine, electronic health records, and mobile applications respectively. The ICT application area recently investigated using the TAM will be the major challenge for enhancing the healthcare facilities when e_Health applications are integrated with ICT. In addition to this, TAM can be extended to develop dynamic health service environments by the integration of components from CRM values. As discussed in [38], the ICT helps trauma survivors to improve their mental health services considered as e_Health applications. Here, existing treatments and patients' monitoring facilities which support the mental health services can be enhanced with the modern electronic technologies. Further, discussion allows researchers to understand how IICT or different technologies can be used for implementing therapeutic tasks with CRM values. Despite many treatments, trauma survivors need therapeutic processing which not only helps to remove mental disorders and problems but provides satisfaction. Intelligent approaches are minimizing the cost and time through the CRM values and technology enhances the flexibility of available services and capacity for decision making. Here, IICT allows healthcare users and service providers to manage their healthcare devices intelligently. Knowledge management (KM) in long-term care will allow healthcare service providers to set the barriers of health care such as users' knowledge. Furthermore, the authors proposed

long-term care in a TOE framework with KM [32] and IICT concept. Although the framework includes security, complexity, and costs analysis mechanism, it provides CRM concepts to improve management support, nursing leadership, etc. According to [39], the ICT within the health system encourages the citizens which include service providers and users to improve their e_Health facilities. Authors prefer to deploy the ICT because citizens will get not only quick treatment but also they can have an efficient system with a less medical cost. Although the objective of this article is to manage the clinical products within the hospital or medical unit, important of the ICT facilities are considered. In this management, using CRM values will increase healthcare efficiency and economic efficiency.

VI. CONCLUSIONS

The study of CRM values allows healthcare providers to improve the facilities of e_Health applications. Enhancement of the e_Health applications such as quality always increases the profit and benefits when healthcare users and service providers deploy the ICT, RFID, and IoT within the medical systems efficiently. In order to enhance the quality of healthcare and e_Health development using ICT, CRM values and 5G based IoT, the efficient proposed model is introduced in this paper. The CRM values and applications of RFID and IoT enhance the healthcare facilities through the ICT which works with the latest technologies and provides user-friendly features to e_Health users. Also, ICT-5G based IoT technology improve the average healthcare cost. Satisfaction and other CRM values such as QoS depend on the accuracy of the treatments involved with the technology.

Future work is to find low-cost solutions which minimize the overall cost of the medical cost and waiting time through the QoS as CRM value, ICT, RFID, modern technologies, etc. All over the world, the evolution of technology is increasing in many dimensions but the cost and waiting time in hospitals are increasing without proper management. The services with CRM values should be implemented in all actions of the hospital or medical services satisfied by moral and ethical issues. These are the only valuable key terms derived from the CRM values. The objectives of the e_Health application are low-cost medical facilities, minimum waiting time, etc. But, high medical cost and intolerable waiting time are creating low-quality services rather than the best services with maximum moral issues. ICT provides many benefits to users and service providers for delivering efficient services. Further, it simplifies business communication through the available technical capabilities.

ACKNOWLEDGMENT

This work was funded by the Deanship of Scientific Research (DSR), King Abdulaziz University, Jeddah, under grant No. (D1435-362-611). The authors, therefore, acknowledge with thanks, DSR technical and financial support.

REFERENCES

- [1] Sharif, Abubakar, Jun Ouyang, Feng Yang, Hassan T. Chattha, Muhammad Ali Imran, Akram Alomainy, and Qammer H. Abbasi. "Low-cost, Inkjet-printed UHF RFID Tag based System for the Internet of Things Applications using Characteristic Modes." IEEE Internet of Things Journal (2019).

- [2] Lin, Hsien-Cheng, and Chun-Ming Chang. "What motivates health information exchange in social media? The roles of the social cognitive theory and perceived interactivity." *Information & Management* 55, no. 6 (2018): 771-780.
- [3] Alzahrani A, Qureshi MS, Thayanathan V. RFID of next-generation network for enhancing customer relationship management in healthcare industries. *Technology and Health Care*. 2017 Jan 1;25(5):903-16.
- [4] Thayanathan V, Alzahrani A, Qureshi MS. Information and communication technology (ICT) applications for customer relationship management (CRM). In *ICTs and the Millennium Development Goals 2014* (pp. 161-183). Springer, Boston, MA.
- [5] Nordby K. Conceptual designing and technology: Short-range RFID as a design material. *International Journal of Design*. 2010;4(1):29-44.
- [6] Tsai, Meng-Hsiun, Chiu-Shu Pan, Chi-Wei Wang, Jui-Ming Chen, and Cheng-Bang Kuo. "RFID Medical Equipment Tracking System Based on a Location-Based Service Technique." *Journal of Medical and Biological Engineering* 39, no. 1 (2019): 163-169.
- [7] Juels A. RFID security and privacy: A research survey. *IEEE Journal on selected areas in communications*. 2006 Feb;24(2):381-94.
- [8] Chen, Yen-Hung, Rui-Ze Hung, Lin-Kung Chen, Pi-Tzong Jan, and Yin-Rung Su. "Channel-Quality Aware RFID Tag Identification Algorithm to Accommodate the Varying Channel Quality of IoT Environment." *Applied Sciences* 9, no. 2 (2019): 321.
- [9] Amendola, Sara, Rossella Lodato, Sabina Manzari, Cecilia Occhiuzzi, and Gaetano Marrocco. "RFID technology for IoT-based personal healthcare in smart spaces." *IEEE Internet of things journal* 1, no. 2 (2014): 144-152.
- [10] Ciftler, Bekir Sait, Abdullah Kadri, and Ismail Güvenç. "IoT localization for bistatic passive UHF RFID systems with 3-D radiation pattern." *IEEE Internet of Things Journal* 4, no. 4 (2017): 905-916.
- [11] Wang SW, Chen WH, Ong CS, Liu L, Chuang YW. RFID application in hospitals: a case study on a demonstration RFID project in a Taiwan hospital. *Innull 2006 Jan 4* (p. 184a). IEEE, pp. 1-10.
- [12] V Wangenheim F. Situational characteristics as moderators of the satisfaction-loyalty link: an investigation in a business-to-business context. *Journal of Consumer Satisfaction, Dissatisfaction, and Complaining Behavior*. 2003 Jan 1;16, pp. 145-156.
- [13] Weng TS. Using information technology on customer relationship management. In *WSEAS International Conference. Proceedings. Recent Adv. in Comp. Engineering 2009 Mar 23* (No. 10). WSEAS, pp. 271-79.
- [14] Guha S, Harrigan P, Soutar G. Linking social media to customer relationship management (CRM): a qualitative study on SMEs. *Journal of Small Business & Entrepreneurship*. 2018 May 4;30(3):193-214.
- [15] Wu CH, Ip WH, Kwok SK, Ho GT, Chan CY. Design and Development of an RFID-based HIS-A Case Study. *International journal of engineering business management*. 2011 Feb 15;3(1):1-8.
- [16] Leema AA, Hemalatha M. Applying RFID Technology to construct an Elegant Hospital Environment. *International Journal of Computer Science Issues (IJCSI)*. 2011 May 1;8(3):444.
- [17] Yao W, Chu CH, Li Z. The use of RFID in healthcare: Benefits and barriers. In *RFID-Technology and Applications (RFID-TA), 2010 IEEE International Conference on 2010 Jun 17* (pp. 128-134). IEEE.
- [18] Tariq A, Tanwani A, Farooq M. User-centered design of e-health applications for remote patient management. The in10th annual conference of the NZ ACM special interest group on human-computer interaction, CHINZ 2009, Auckland, NZ 2009.
- [19] Tzeng SF, Chen WH, Pai FY. Evaluating the business value of RFID: Evidence from five case studies. *International journal of production economics*. 2008 Apr 1;112(2):601-13.
- [20] Wu NC, Nystrom MA, Lin TR, Yu HC. Challenges to global RFID adoption. In *Technology Management for the Global Future, 2006. PICMET 2006 2006 Jul* (Vol. 2, pp. 618-623). IEEE.
- [21] Roussos G. *Networked RFID: systems, software, and services*. Springer Science & Business Media; 2008 Oct 17.
- [22] Ngai EW, Suk FF, Ng CC. An information system design theory for an RFID-based healthcare management system. *PACIS 2008 Proceedings*. 2008 Jul 3:178.
- [23] Yang S, Zhang R, Liu Z. The AGA is evaluating a model of customer loyalty based on the e-commerce environment. *Journal of Software*. 2009 May;4(3):262-269.
- [24] Cohen TN, Cabrera JS, Litzinger TL, Captain KA, Fabian MA, Miles SG, Reeves ST, Shappell SA, Boquet AJ. Proactive safety management in trauma care: applying the Human Factors Analysis and Classification System. *Journal for Healthcare Quality*. 2018 Mar 1;40(2):89-96.
- [25] Inaba, T. "Realization of SCM and CRM by using RFID-captured consumer behavior information." *Journal of Networks*. 2009 no. 2: 92-9.
- [26] Aboelmaged M, Hashem G. RFID application in patient and medical asset operations management: A technology, organizational and environmental (TOE) perspective into key enablers and impediments. *International journal of medical informatics*. 2018 Oct 1;118:58-64.
- [27] Ruan W, Sheng QZ, Yao L, Li X, Falkner NJ, Yang L. Device-free human localization and tracking with UHF passive RFID tags: A data-driven approach. *Journal of Network and Computer Applications*. 2018 Feb 15;104:78-96.
- [28] Cerlinca TI, Turcu C, Turcu C, Cerlinca M. RFID-based information system for patients and medical staff identification and tracking. In *Sustainable Radio Frequency Identification Solutions 2010*. InTech.
- [29] Innominato P, Komarzynski S, Karaboué A, Ulusakarya A, Bouchahda M, Haydar M, Bossevot-Desmaris R, Mocquery M, Plessis V, Lévi F. Home-based e-health platform for multidimensional telemonitoring of symptoms, body weight, sleep, and circadian activity: relevance for chronomodulated administration of irinotecan, fluorouracil-leucovorin, and oxaliplatin at home—results from a pilot study. *JCO Clinical Cancer Informatics*. 2018 Feb 22;2:1-5.
- [30] Gray CS, Barnsley J, Gagnon D, Belzile L, Kenealy T, Shaw J, Sheridan N, Nji PW, Wodchis WP. Using information communication technology in models of integrated community-based primary health care: learning from the iCOACH case studies. *Implementation of Science*. 2018 Dec;13(1):87.
- [31] Fernández ÖS, Pérez CG, García-Cuyàs F, Giménez NA, Gallego MB, Font AG, Quintana MG, Corbacho SH, Casellas ES. Shared Medical Record, Personal Health Folder and Health and Social Integrated Care in Catalonia: ICT Services for Integrated Care. In *New Perspectives in Medical Records 2017* (pp. 49-64). Springer, Cham.
- [32] Donovan J, Franzel S, Cunha M, Gyau A, Mithöfer D. Guides for value chain development: a comparative review. *Journal of Agribusiness in Developing and Emerging Economies*. 2015 May 18;5(1):2-3.
- [33] Mitchell J, Coles C, Keane J. Upgrading along value chains: strategies for poverty reduction in Latin America. *COPLA Global—Overseas Development Institute, London*. 2009 Dec.
- [34] Carlson JJ, Sullivan SD, Garrison LP, Neumann PJ, Veenstra DL. Linking payment to health outcomes: a taxonomy and examination of performance-based reimbursement schemes between healthcare payers and manufacturers. *Health policy*. 2010 Aug 1;96(3):179-90.
- [35] Newman-Casey PA, Killeen OJ, Renner M, Robin AL, Lee P, Heisler M. Access to and Experiences with e-Health Technology Among Glaucoma Patients and Their Relationship with Medication Adherence. *Telemedicine and e-Health*. 2018 Apr 23.
- [36] Rahimi B, Nadri H, Afshar HL, Timpka T. A Systematic Review of the Technology Acceptance Model in Health Informatics. *Applied clinical informatics*. 2018 Jul;9(03):604-34.
- [37] Azarang A, Pakyurek M, Giroux C, Nordahl TE, Yellowlees P. Information Technologies: An Augmentation to Post-Traumatic Stress Disorder Treatment Among Trauma Survivors. *Telemedicine and e-Health*. 2018 Jul 13.
- [38] Lo MF, Ng PM. Knowledge Management for Health Care and Long-Term Care in the Technology-Organization-Environment Context. In *Sustainable Health and Long-Term Care Solutions for an Aging Population 2018* (pp. 161-186). IGI Global.
- [39] Canha M, Marques CG, Loureiro R. The use of information and communication technologies in the management of clinical products. The Implementation of Advanced Warehouses in a Portuguese hospital center. *Superavit*. 2018 Apr 6;3:103-12.

Towards a Conceptual Model to Evaluate Usability of Digital Government Services in Malaysia

Rini Yudesia Naswir¹

Malaysia Administrative
Modernisation and Management
Planning Unit (MAMPU)
Putrajaya, Malaysia

Mahmudul Hasan³

Department of Information Systems
and Operations Management
The University of Auckland
Auckland, New Zealand

Ganthan Narayana Samy⁵

Razak Faculty of Technology and
Informatics
Universiti Teknologi Malaysia
Kuala Lumpur, Malaysia

Nurazean Maarop²

Razak Faculty of Technology and
Informatics, Universiti Teknologi
Malaysia, Kuala Lumpur, Malaysia

Salwani Daud⁴

Razak Faculty of Technology and
Informatics, Universiti Teknologi
Malaysia, Kuala Lumpur, Malaysia

Pritheega Magalingam⁶

Razak Faculty of Technology and
Informatics, Universiti Teknologi
Malaysia, Kuala Lumpur, Malaysia

Abstract—The Malaysian government is committed to provide comprehensive digital government services and it is reflected in some policies and strategic plans such as 11th Malaysia Plan 2016-2020 (RMKe-11) for digital government transformation. However, though most of the Malaysia government services are online yet they are still inadequate and the majority of users are unhappy with the current services. Usability is a critical aspect in the success of digital government. Thus, this research aims to develop and validate a usability conceptual model of digital government services in Malaysia context to identify key factors that influence the perceived usability that assists to encourage usage and satisfaction of digital government services. This research has applied quantitative-deductive approach and employed PLS-SEM analysis. Empirical results indicate that Effectiveness, Efficiency, Learnability, Satisfaction, Usefulness, and Citizen Centric are key factors of perceived usability of digital government services. The evaluation of the proposed conceptual model yielded that three of the six factors which are Effectiveness, Satisfaction, and Citizen Centric have significant positive influence on perceived usability of digital government in Malaysia context.

Keywords—Digital government; citizen-centric; quantitative; usability

I. INTRODUCTION

Technology can be used by the organisation to permit faster response to customer enquiries and problems, to reduce labour costs, to improve internal efficiency and productivity, and to gain distinctive and differentiating competitive advantages [1, 2]. Digital government generally refers to the use of information and communication technologies (ICTs) in government to improve service delivery and improve relationships with citizens, civil society, and private sector [3]. Digital government services consists of online services, mobile applications, big data, open data, social media, digital media, and cloud computing [4]. Malaysian e-government services have been evolutionised from e-government 1.0 in 1995 with static government websites for accessing information to e-government 2.0 in 2007 where online services are provided for relevant public services transaction among the citizens. In

2015, e-government 3.0 also known as digital government was introduced [5] with dynamic service delivery where government online information services are generating opportunities and innovations through the citizens' participation. The new digital government strategies are stated in the Malaysian Public Sector ICT Strategic Plan (PSISP) 2016-2020 with theme "Citizen Centric Digital Services" and vision "Inclusive Digital Government Drives Citizen Centric Service Delivery". However, Digital Government Satisfaction Survey 2014 by The Boston Consulting Group has reported that only 30% of respondents are satisfied with the Malaysian government services that are provided through Internet and 56% of the respondents rated the quality of the government online services are worse than the private sector and only 4% said that the government online services are much better than private sector [6].

Usability is a critical factor in the success of digital government [7]. Usability is one of the challenges in developing digital government services because usability affects citizens' usage and acceptance of the digital government [8] and may influence their electronic interaction with the government. Usability can improve users' trust in the digital government [7] and affect the credibility of the digital government services [9]. Trust in digital government websites is associated with perceived website quality [10] which means the websites are technically reliable and ease to use. The government needs to concern about usability because it will affect the user experience and users' trust in the digital government services [11]. The digital government services through websites represent their physical office of government agencies. High usability of the digital government services shows that the government is committed to deliver their services to fulfil the citizens' needs and demands. There are some studies have been conducted regarding usability factors of the e-government or digital government where the majority of these services are about election and voting website, local government website [7, 9, 12-13], e-learning [14], and digital library [15-16]. Besides, to our best knowledge, there are only a few studies in Malaysia context reporting on the usability of

higher education agencies' websites [17], and student information system [18]. Therefore, it becomes significant to explore what other potential usability factors affecting perceived usability of the digital government services in Malaysia. To answer this question, this study has embarked a quantitative case study approach to deduce more relevant factors of interest and validate the factors.

The remainder of our paper proceeds as follows. The next section we present the reviews of literature on digital government and usability theories, the design of the conceptual model and the development of the hypotheses. Section III presents the methodology detailing our data collection and analysis procedure. We then discuss our findings in Section IV and this paper end with brief concluding remarks, limitations, and recommendations for future research in Section V.

II. LITERATURE REVIEW

A. Digital Government in Malaysia

Digital government is a way of digitalizing government services to improve the service delivery system in an efficient and effective way to maintain a relationship with the citizens. Digital government leads to improvement of government function, services, and works to provide comprehensive service delivery that will satisfy the citizens. The digital government enables low cost of communication between government and citizens through digital platform such as websites, online services, social media, and mobile application. This effort was expected to improve citizens' views on governments [19], especially in term of efficiency and trust. The government has to concern about trends and rapid changes of technology to ensure the digital government services are meeting citizens's demands. The government faces a challenge to grasp the speed and scope of changes in technologies like some emerging technologies such as the Internet of Things, data analytics, and artificial intelligence which have a great potential for government to improve their service delivery [20]. Besides that, digital communication should offer a faster and efficient response from the government [21] but the government needs to put adequate concern on technological issues such as interoperability, flawed configurations, and misalignment with work processes.

Recently, the Malaysian government has announced a nationwide development plan known as "RMKe-11" for five years' period from 2016 to 2020. The RMKe-11 focuses on rapidly delivering high impact outcomes to both the capital economy and people economy at an affordable cost. RMKe-11 [22], is aimed at transforming public service for productivity through and enhanced ICT and digital government.

In proposing the usability conceptual model of digital government services in Malaysia, we first reviewed usability baseline theories and models to identify usability factors from existing theories and models, coupled with a review of literatures especially in digital government context. Finally, we proposed a conceptual model which are to be validated subsequently. Fig. 1 illustrates our literature review process. We described the overall process and results of literature analysis in the following sections.

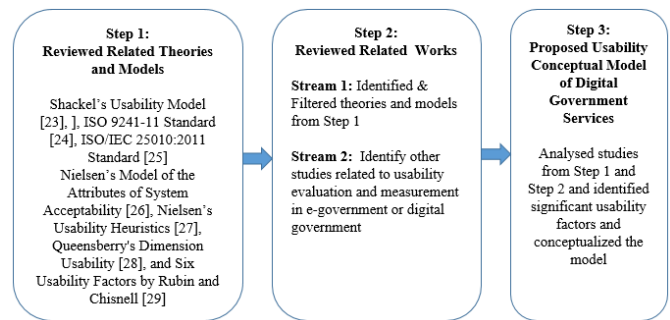


Fig. 1. Literature Review Process.

B. Usability and Related Theories

Usability is one of the critical factors that influence successful system development and implementation. In this study, we define usability as efficiency and effectiveness of a system that meets user needs and expectations, and the system is able to satisfy the user to perform and complete their task.

There are several related theories and models were introduced regarding the usability. Shackel [23] proposed a usability model by integrating the effectiveness of system, learnability, flexibility, and attitude of system users. ISO 9241-11 is standard used to measure usability in term of effectiveness, efficiency, and satisfaction [24]. Indeed, ISO 9241-11 Standard is one of the usability frameworks that were cited widely in usability engineering field. ISO/IEC 25010:2011 [25] is another usability measurement which is a part of System and Software Quality Requirements and Evaluation (SQuARE) series of International Standards. There are five quality characteristics defined by ISO/IEC 25010:2011 which are effectiveness, efficiency, satisfaction, freedom from risk, and context coverage. Nielsen [26] has developed a model of the attributes of system acceptability and listed five factors that affect usability which is easy to learn or learnability, efficient to use, easy to remember, few errors, and subjectively pleasing and Nielsen's Usability Heuristics [27]. Quesenberry [28] defined usability as "quality or characteristic of a usable product". The author introduced the dimension of usability that consists of 5Es which are effective, efficient, engaging, error tolerant, and easy to learn. Recently, Rubin and Chisnell [29] identified six factors such as usefulness, efficiency, effectiveness, learnability, satisfaction, and accessibility that affects usability.

C. Related Works

The existing usability theories and models mentioned in the previous section (section B) have been considered and applied appropriately by several researchers for usability evaluation and measurement in their study. For example one study Brown et al. [30] proposed a usability evaluation model to evaluate mobile health technology. There are eight concepts included in their model and these are error prevention, information needs, memorability, learnability, competency, performance speed, flexibility/customization, and other outcomes. Another study [31] investigated the usability on social media sites' when adopted for business-to-business (B2B) marketing purposes in China. The authors' investigation found that three factors such as learnability, efficiency, and memorability impact the perceived usability. Usability framework was proposed by

another study to evaluate the usability of a smartphone application to indicate prevention and early intervention of anxiety in youth. This evaluation used five dimensions of usability, which are ease of use, ease of learning, quality of support information, satisfaction, and stigma [32]. Other studies conducted usability testing through explorative, descriptive design on Facebook-based obesity prevention program for Korean American adolescents (Health Teens). The usability testing involved one-on-one observation, the think-aloud method, audiotaping, screen activity capture, and survey. The authors [33] applied Technology Acceptance Model (TAM) for usability evaluation of the program.

Some authors also applied or adapted the existing usability theories and models mentioned earlier in the e-government or digital government context. A study evaluated 120 samples of higher education institutions' websites through the Malaysian Ministry of Higher Education's portal. The usability evaluation was conducted on some criteria and these are page size, speed, and broken links [17]. Meanwhile, another study proposed a model of usability measurement for an academic digital library. The authors adopted three major factors from ISO 9241-11 Standard namely efficiency, effectiveness, and satisfaction and one major factor from Nielsen's Model of the Attributes of System Acceptability namely learnability.

Additionally, student information systems usability was analyzed by [18], and factors that affect the system usability are useful information, timely access, interface design, and error recovery. In [14], author used Shackel's Usability Model comprising four usability factors including effectiveness, learnability, flexibility, and attitude to assess the usability of e-learning system. Furthermore, [9] evaluated three local e-government websites using criteria from Nielsen's Usability Heuristic and added three more criteria which are interoperability, support and develop users and pleasurable and respectful interaction with users. [16] used six factors of usability which are usefulness, efficiency, effectiveness, learnability, satisfaction, and accessibility to evaluate the usability of the Central Science Library (CSL) website. Meanwhile, [12] build 15 web usability standards with six general areas which are overall design standards, hypertext, navigational standards, readability, language option, and findability in evaluated 34 websites from the list of Alabama counties which are specifically for voting and elections. Also, [13] used five usability categories which are overall design standards, conventions for hyperlinked text in the main text, navigational standards, findability, and readability. Meanwhile, [34] conducted a study that examined the usability of six different electronic nursing record systems. The usability testing was conducted based on five measurements which are efficiency (relevancy), proficiency (accuracy), competency index, additional entry, and time consumed. [35] used usability guides were derived from ISO 9241-11 Standard namely effectiveness, efficiency, and satisfaction to measure usability of open course ware (OCW) initiative from Universidad Tecnica Particular de Loja, Ecuador.

From the above discussion, there are some common usability factors appeared in various theories and models which also appeared as the measurement in the evaluation of e-government or digital government usability by some

researchers. Thereby, after reviewing baseline theories and related works we identified five factors (effectiveness, efficiency, learnability, satisfaction, and usefulness) that may affect the perceived usability of digital government services in Malaysia. Table I shows the frequency analysis of common usability factors found in prior studies.

TABLE I. FREQUENCY ANALYSIS OF USABILITY FACTORS

No.	Common Usability Factors	Frequency
1	Learnability	20
2	Effectiveness	17
3	Efficiency	16
4	Satisfaction	16
5	Usefulness	10

D. Proposed Conceptual usability Model of Digital Government Services

1) *Effectiveness*: Effectiveness related to the capability of a system or service to meet users' goals or expectations [24, 25]. Effectiveness focuses on process interaction viewpoint with regard to system accuracy and completeness that leads the user to achieve specified goals. Effectiveness is an important factor when providing digital government services as effectiveness can measure how well digital government services meet user expectations.

2) *Efficiency*: Efficiency refers to the resources expended about the quickness, accuracy, and completeness. Efficiency is considered an important factor because efficiency measures the ability of the digital government services to assist the user in performing their task.

3) *Learnability*: Learnability refers to ease of teach and learn where the novice users should be able to use the system after a specific time or specified training, and retention of skills for the casual users. Learnability is considered an important factor as easy to learn of the digital government services may encourage the user to return using digital government services.

4) *Satisfaction*: Satisfaction focuses on positive attitude which includes comfort and acceptability from the user viewpoint. In other words, users are subjectively satisfied when using the system or services. Satisfaction is considered an important factor as satisfaction has the potential to encourage user loyalty which also will increase the usage of digital government services.

5) *Usefulness*: According to usefulness is "the degree to which a product enables a user to achieve his or her goals, and is an assessment of the user's willingness to use the product at all." Usefulness refers to the quality of the information, easily to understand the information, and capability of the information to help the user complete their task. Usefulness is considered an important factor because usefulness may lead to easy of understanding the information in the digital government services which also will assist the user in performing their task.

6) *Citizen centric*: In addition to the five factors identified, we also added Citizens-centric as one of the factors

to be included in the proposed usability conceptual model of digital government in Malaysia environment. The digital government services have transformed from government-centric approach to citizen-centric approach which widely applied in many countries such as United States of America, Canada, England, Australia, Italy, South Korea, and Singapore [36]. Furthermore, [37] stated that citizen-centric evaluation is necessary to improve the usability of digital government services where the government needs to reflect the feedback or opinion from the citizens in redesign or re-engineering of digital government services. In regard to Malaysia context, [38] have proposed citizen empowerment as one of the success factor in digital government implementation. Hence, the citizen-centric approach is essential in the development of sustainable digital government to improve the service delivery. The importance of a citizen-centric approach in digital government services are as follows [39, 40]:

- To deliver services that meet citizens needs, who are the primary user.
- To focus on design and development of effective digital government services to meet the citizens needs.
- To diversify channels to provide a choice and convenience for citizens to access government services.
- To take into account the provisioning of government information to meet the needs of different levels of stakeholders.
- To encourage citizens's e-participation and response.

Based on previous studies related to usability in related domain, many researcher have highlighted the importance of usability features and factors from common usability literature and guidelines. This study found that there is a significant need to consider citizen-centric factor in the proposed usability model.

Fig. 2 shows our proposed usability conceptual model of digital government services. In addition, we proposed six hypotheses for the proposed usability conceptual model of digital government in Malaysia environment.

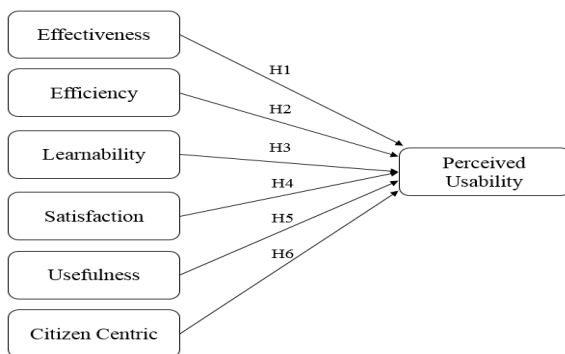


Fig. 2. The Proposed usability Conceptual Model of Digital Government Services in Malaysia.

H1: Effectiveness will have a positive influence on perceived usability of digital government in Malaysia environment.

H2: Efficiency will have a positive influence on perceived usability of digital government in Malaysia environment.

H3: Learnability will have a positive influence on perceived usability of digital government in Malaysia environment.

H4: Satisfaction will have a positive influence on perceived usability of digital government in Malaysia environment.

H5: Usefulness will have a positive influence on perceived usability of digital government in Malaysia environment.

H6: Citizen Centric will have a positive influence on perceived usability of digital government in Malaysia environment.

III. METHODOLOGY

We first conducted a preliminary interview with Deputy Director, Digital Government Division, Malaysian Administrative Modernization & Management Planning Unit (MAMPU) to investigate about the current state of the digital government and to identify how important to have a research on usability of the Malaysian digital government services. We then acknowledged that there is a need to conduct a study related to the usability of digital government services in Malaysia. Therefore, we continued the research by readings on various academic journals using Science Direct, Web of Science, IEEE Xplorer Library, Google Scholar, and Google. We then applied a deductive approach based on quantitative research design. Deductive approach is concerned with the reconstruction of existing theory to create a new one [41]. The deductive approach involved exploring a known theory or phenomenon and tests if the theory is valid in a given circumstance. There are some stages in deductive approach, which are theory review, deducing hypothesis from theory and formulating hypothesis, testing the hypothesis using relevant method, and examining the outcome of the test to confirm or reject the hypothesis [42].

A. Case Selection

Our research focused on digital government services provided through MyGovernment Portal (www.malaysia.gov.my) such as tax and compound payment, business registration, membership registration and renewal, and application of scholarship in Malaysia. We selected MyGovernment because of this portal acts as a single gateway of Malaysian digital government for information, transaction, and communication with the government.

B. Research Instrument Design

Instrument development for survey data collection of this research was based on Google Forms. The instrument design was based on factors shown in Fig. 2 which consists of six independent variables namely Effectiveness (ET), Efficiency (EC), Learnability (L), Satisfaction (S), Usefulness (U), and Citizen Centric (CC), and a dependent variable, namely,

Perceived Usability (PU). The items used in the instrument were designed and adopted from previous digital government studies.

In prior, three experts were involved to review the content of the survey and the analysis was performed using content validity index (CVI). The initial survey instrument consists of two sections with a total of 39 items or questions. Section A collects Demographic Information, consists of eight items using Scale and Category. Meanwhile, Section B represents Usability measures comprises 31 questions and were reviewed in prior by three experts to evaluate the relevancy and reliability of the items by using CVI approach. The expert review analysis applied rating that advocated by [43], which are scaled as Not Relevant (1), Somewhat Relevant (2), Quite Relevant (3), and Highly Relevant (4). A 4-point scale is suggested to avoid having a neutral and ambivalent midpoint [44]. As a result, all items in this study have achieved the CVI of 3 or 4 by the experts and met the CVI criteria as suggested by [45] and [46]. Mean of Item CVI is 0.89 and it is the same value for Mean of Expert Proportion. Subsequently, the actual survey instrument was also improvised based on the comments and suggestions from the experts with a total of 37 items or questions. The actual survey has been revised and improved containing 37 questionnaire items. In particular, Section A consists of 8 items, and Section B consists of 29 questions (see Appendix A for detail).

C. Data Collection and Analysis

This research applied a non-probability sampling namely purposive sampling. Citizens of Malaysia are the target population engaging individual perspective on perceived usability of the Malaysian digital government. Descriptive analysis was adopted in analyzing the quantitative data in the survey. Descriptive analysis answering questions are about who, what, where, when, and to what extent. Descriptive analysis helps to view data in correct context, identify relevant information in the data, assess the quality of the data, and recognize the assumptions, limitations, and generalizability of the findings [47].

We applied PLS-SEM as a statistical tool that supports multivariate analysis and able to simultaneously analyse multiple variables. By following the guidelines by [48], we chose PLS-SEM for four reasons: Firstly, development, exploration, and testing of usability conceptual model of digital government in Malaysia environment which consists of six exogenous constructs which are Effectiveness, Efficiency, Learnability, Satisfaction, Usefulness, and Citizen Centric, and one endogenous construct which is Perceived Usability. Secondly, no identification issues with small sample sizes where the minimum size is 30. Generally, this technique can achieve high levels of statistical power with small sample size. Thirdly, this technique is highly robust as long as the missing value is below a reasonable level. The missing value is impossible because all items and questions in the online survey are set as mandatory. Fourthly, this technique can easily incorporate reflective and formative measurement model to assess the relationship between constructs and their indicators.

IV. RESULTS AND DISCUSSION

A. Demographic Analysis

Demographic profile for this research consists of eight variables and these are gender, age, educational level, field of study, Internet experience, Internet usage per day, digital government experience, and digital government usage. From the survey, 22 (33.8%) of the respondents are male, and 43 (66.2%) respondents are female. The big percentage of respondents' age ranges between 31 to 40 years old which is a total of 52 (80.0%) respondents. In addition, 31 (47.7%) respondents have Bachelor Degree as a highest academic level, while 20 (30.8%) respondents are Master Degree holder. 46 (70.8%) respondents are from IT field, and seven (10.8%) respondents are from the business field. The survey also shows that 60 (92.3%) respondents have experience of using the Internet for more than five years and spending more than three hours using Internet per day. Furthermore, 41 (63.1%) respondents have experience of using digital government for more than five years, and 31 (47.7%) respondents are using digital government daily or almost daily.

PLS-SEM involves two stages of assessment which are the assessment of the measurement model and assessment of structural model. Following sections of this paper describes these two stages in details.

B. Measurement Model

Measurement model describes the relationship between constructs and their corresponding indicator variables. The measurement model of this has six exogenous constructs which are Effectiveness (ET), Efficiency (EC), Learnability (L), Satisfaction (S), Usefulness (U), and Citizen Centric (CC) and one endogenous construct which is Perceived Usability (PU). Each of the variables is measured by multiple indicators using Likert Scale from 1 to 5 (Strongly Disagree to Strongly Agree). In particular, the type of this measurement model is reflective which all the indicators are caused by the same construct [48]. Assessment of reflective measurement model includes composite reliability to evaluate internal consistency, individual indicators reliability and average variance extracted (AVE) to evaluate convergent validity, and Fornell-Larcker criterion and cross loadings to assess discriminant validity.

Internal consistency reliability refers to composite reliability values in which higher value indicates higher level of reliability. All constructs in the measurement model have composite reliability value higher than 0.708 with the highest is Usefulness (0.963). Furthermore, the individual indicators reliability is examined through outer loadings relevance testing. A higher value of outer loadings indicates that the construct has much in common [49]. From the PLS calculation, outer loadings value for all indicators are higher than 0.708 except for B-S3 (0.689) and B-PU1 (0.705).

AVE is used to measure convergent validity on the construct level. AVE value of 0.50 or higher indicates that, on averages, the construct explains more than half of the variance of its indicators. Meanwhile, AVE value below 0.40 indicates

that, on average, more error remains in the items than the variance explained by the construct [48]. From the result, all constructs have AVE value higher than 0.50 with the highest is Usefulness (0.839). Fornell-Larcker criterion and cross-loadings check are used to measure discriminant validity. For Fornell-Larcker criterion, the square root of the AVE of each of the construct should be higher than its correlation with any other construct.

Our results show that all model evaluation criteria have been met except for Efficiency → Perceived Usability, and Satisfaction → Perceived Usability based on Fornell-Larcker

criterion. Furthermore, cross-loadings results show that an item’s loadings on its own construct in all cases are higher than all of its cross loadings with other constructs. Thus, the discriminant validity between all the constructs is based on the cross loadings criterion (see Appendix A for detail). Besides that, outer loadings of B-S3 and B-PU1 are lower than the suggested value. However, the Efficiency and Satisfaction constructs, and the B-S3 and B-PU1 indicators are still retained because the respective composite reliability and AVE are higher than suggested value.

Table II shows the summary of measurement model results.

TABLE II. SUMMARY OF MEASUREMENT MODEL RESULTS

Latent Variable	Indicator	Convergent Validity			Internal Consistency	Discriminant Validity	
		Loadings (>0.708)	Indicator Reliability (>0.50)	AVE (>0.50)	Composite Reliability (>0.708)	Fornell-Larcker Criterion	Cross-Loadings
ET	B-ET1	0.853	0.728	0.755	0.902	Yes	Yes
	B-ET2	0.916	0.839				Yes
	B-ET3	0.836	0.699				Yes
EC	B-EC1	0.831	0.691	0.659	0.885	No	Yes
	B-EC2	0.742	0.551				Yes
	B-EC3	0.829	0.687				Yes
	B-EC4	0.840	0.706				Yes
L	B-L1	0.839	0.704	0.770	0.952	Yes	Yes
	B-L2	0.801	0.642				Yes
	B-L3	0.917	0.841				Yes
	B-L4	0.863	0.745				Yes
	B-L5	0.902	0.814				Yes
	B-L6	0.934	0.872				Yes
S	B-S1	0.875	0.766	0.686	0.896	No	Yes
	B-S2	0.845	0.714				Yes
	B-S3	0.689	0.475				Yes
	B-S4	0.887	0.787				Yes
U	B-U1	0.898	0.806	0.839	0.963	Yes	Yes
	B-U2	0.933	0.870				Yes
	B-U3	0.893	0.797				Yes
	B-U4	0.917	0.841				Yes
	B-U5	0.938	0.880				Yes
CC	B-CC1	0.853	0.728	0.733	0.891	Yes	Yes
	B-CC2	0.887	0.787				Yes
	B-CC3	0.826	0.682				Yes
PU	B-PU1	0.705	0.497	0.667	0.888	Yes	Yes
	B-PU2	0.884	0.781				Yes
	B-PU3	0.850	0.723				Yes
	B-PU4	0.817	0.817				Yes

C. Structural Model

Structural model assessment involves examining the model's predictive capabilities and the relationship between the constructs. We followed rules of thumb for structural model evaluation recommended by [48]. We first assessed structural model for collinearity issues. We then examined the significance of path coefficients to understand the relevance of the structural model relationships followed by measuring R^2 to see predictability of the overall model. In addition, we also assessed the effect size f^2 which allows examining an exogenous construct's contribution to an endogenous latent variable's R^2 value. Finally, we measured predictive relevance (q^2) of the endogenous construct.

Our collinearity assessment is measured based on VIF (variance inflation factor) value where the value should be between 0.20 and 5.00. Table III shows the VIF value for all six constructs. Five of the constructs are between the suggested value, while Efficiency is 5.148 which is higher than 5.00. Hence, the Efficiency is eliminated for the next assessment.

Path coefficients represent the hypothesized relationships among the constructs. The bootstrapping is used to assess the significance of path coefficients where the bootstrap samples are 5,000 [49]. In addition, the critical value (t) applied for this research is 1.96, $p < 0.05$ (significance level=5%). Our results show that Effectiveness, Satisfaction, and Citizen Centric are significant whereby Learnability and Usefulness are not significant ($p > 0.05$). Table IV shows the significance testing results of the structural model path coefficients.

Furthermore, the R^2 value is 0.828 which is higher than 0.75 that indicates as substantial. The f^2 effect size of Citizen Centric is higher (Effectiveness: 0.142, Satisfaction: 0.323, Citizen Centric: 0.376) than the recommended threshold 0.35 which indicates that the exogenous construct has a large effect on the endogenous construct namely Perceived Usability. The q^2 effect size is 0.912 which is higher than 0.35 that indicates the exogenous constructs have a large predictive relevance for the endogenous construct (Perceived Usability).

TABLE III. PATH RESULT OF STRUCTURAL MODEL

Constructs	VIF
Effectiveness (ET)	2.866
Efficiency (EC)	5.148
Learnability (L)	3.192
Satisfaction (S)	2.984
Usefulness (U)	2.179
Citizen Centric (CC)	2.761

TABLE IV. PATH RESULT OF STRUCTURAL MODEL

Paths	Path Coefficients	t Values	p Values	97.5% Confidence Intervals	Significance Level ($p < 0.05$)
ET → PU	0.193	2.183	0.029	0.375	S
L → PU	0.136	1.573	0.116	0.308	NS
S → PU	0.337	3.442	0.001	0.530	S
U → PU	0.028	0.362	0.718	0.167	NS
CC → PU	0.348	3.874	0.000	0.514	S

V. CONCLUSIONS, LIMITATIONS AND FUTURE RESEARCH

Digital government was introduced in Malaysia in 2015 with dynamic service delivery where government online information services are generating opportunities and innovations through citizens' participation. Perceived usability should be emphasized to ensure the success of digital government development and meet the citizens' needs and expectations. The essential contribution of this research is the integration of existing key elements of usability theories and models, and digital government services to propose usability conceptual model of digital government in Malaysia environment. The second contribution is the validation of usability conceptual model of digital government in Malaysia environment. This research has validated that three of the six factors which are Effectiveness, Satisfaction, and Citizen Centric are relevant and significant on the perceived usability of digital government in Malaysia. Meanwhile, Efficiency is eliminated during the assessment to treat collinearity problems, and Learnability and Usefulness are indicated as not significant. Development of this conceptual model is started by conducting the literature review and preliminary study. Then, expert review was conducted for the content validity of the survey instrument. Subsequently, data collection through was conducted through an online survey among citizens as target respondents. Finally, the conceptual model was evaluated and validated using PLS-SEM technique. The conceptual model has three factors that are significant on the perceived usability of digital government in Malaysia environment. The model could become guidance for the Malaysian government to revise and develop a strategy for the sustainable digital government to improve public sector service delivery system and align towards the high-income nation. Although the model is developed in the Malaysian government context, the model may be useful also for industries who involves in the development of digital services.

However, there are some limitations to this research. Firstly, survey instrument design of this research only involved content validation through expert review. Secondly, the data collection process which was conducted in one time due to time and cost constraints. The more accurate data will be collected if data collection is conducted more than one time. Another limitation of this research is regarding the purposive sampling method as the survey questionnaire cannot be spread widely and in a longer time to get more variety of respondents' background. Finally, this research is conducted on citizens perspective on perceived usability of digital government in Malaysia environment which more on non-functionality of system usability. Therefore, this model does not cover much on the functionality of system usability such as interoperability, accessibility, navigational, error prevention/recovery, and speed.

The conceptual model was designed based on usability factors which considered as comprehensive as possible. There are other potential factors that may have significant positive influence to perceived usability of digital government. This research is based on citizens' perspective of digital government services provided through MyGovernment Portal (www.malaysia.gov.my). Therefore, it is advisable to conduct future works on other digital government services which may

involve online payment, mobile application, or life event approach.

ACKNOWLEDGMENT

We would like to thank Universiti Teknologi Malaysia, Malaysia Administrative Modernisation and Management and Ministry of Education Malaysia under the Vote 17H73.

REFERENCES

- [1] R. H. Walker, M. Craig-Lees, R. Hecker, and H. Francis, "Technology-enabled service delivery: An investigation of reasons affecting customer adoption and rejection," *Int. J. Serv. Ind. Manag.*, 2002.
- [2] P. Pitchay Muthu Chelliah, R. Thurasamy, A. I. Alzahrani, O. Alfarraj, and N. Alalwan, "E-Government service delivery by a local government agency: The case of E-Licensing," *Telemat. Informatics*, 2016.
- [3] C. G. Reddick, *Public Administration and Information Technology*. Burlington, MA: Jones & Bartlett Learning, 2012.
- [4] United Nations, "United Nations e-government survey 2014," 2014.
- [5] MAMPU, "Malaysian Administrative Modernisation and Management Planning Unit: Dialog transformasi bersama MAMPU: Arah tuju ICT menjelang 2020.," 2015.
- [6] M. Carraasco and P. Goss, "Digital Government: Turning the Rhetoric into Reality," 2014.
- [7] N. E. Youngblood and J. MacKiewicz, "A usability analysis of municipal government website home pages in Alabama," *Gov. Inf. Q.*, 2012.
- [8] T. Clemmensen and D. Katre, "Adapting e-gov Usability Evaluation to Cultural Contexts," in *Usability in Government Systems User Experience Design for Citizens and Public Servants*, 2012.
- [9] Z. Huang and M. Benyoucef, "Usability and credibility of e-government websites," *Gov. Inf. Q.*, 2014.
- [10] T. S. H. Teo, S. C. Srivastava, and L. Jiang, "Trust and Electronic Government Success: An Empirical Study," *J. Manag. Inf. Syst.*, vol. 25, no. 3, pp. 99–132, Dec. 2008.
- [11] N. Condori-Fernández, J. I. Panach, A. I. Baars, T. Vos, and Ó. Pastor, "An empirical approach for evaluating the usability of model-driven tools," in *Science of Computer Programming*, 2013.
- [12] B. A. King and N. E. Youngblood, "E-government in Alabama: An analysis of county voting and election website content, usability, accessibility, and mobile readiness," *Gov. Inf. Q.*, 2016.
- [13] R. A. Galvez and N. E. Youngblood, "e-Government in Rhode Island: what effects do templates have on usability, accessibility, and mobile readiness?," *Univers. Access Inf. Soc.*, 2016.
- [14] M. H. Thowfeek and M. N. A. Salam, "Students' Assessment on the Usability of E-learning Websites," *Procedia - Soc. Behav. Sci.*, 2014.
- [15] S. Joo and J. Y. Lee, "Measuring the usability of academic digital libraries: Instrument development and validation," *Electron. Libr.*, 2011.
- [16] A. Pant, "Usability evaluation of an academic library website Experience with the Central Science Library, University of Delhi," *Electron. Libr.*, 2015.
- [17] M. A. Aziz, W. A. R. Wan Mohd Isa, and N. Nordin, "Assessing the accessibility and usability of Malaysia higher education website," in *Proceedings - 2010 International Conference on User Science and Engineering, i-USER 2010*, 2010.
- [18] M. R. Nordaliela, H. Suriani, and E. L. Nathaniel, "Usability Analysis of Students Information System in a Public University," *J. Emerg. Trends Eng. Appl. Sci.*, vol. 4, no. 6, pp. 806–810, 2013.
- [19] Y. Kim and J. Zhang, "Digital government and wicked problems," *Gov. Inf. Q.*, vol. 33, no. 4, pp. 769–776, 2016.
- [20] M. Ku, J. R. Gil-García, and J. Zhang, "The emergence and evolution of cross-boundary research collaborations: An explanatory study of social dynamics in a digital government working group," *Gov. Inf. Q.*, 2016.
- [21] J. B. Berger, M. Hertzum, and T. Schreiber, "Does local government staff perceive digital communication with citizens as improved service?," *Gov. Inf. Q.*, 2016.
- [22] EPU, "Economic Planning Unit: Eleventh Malaysia Plan," 2015.
- [23] B. Shackel, "Usability - Context, framework, definition, design and evaluation," *Interact. Comput.*, 2009.
- [24] N. Bevan, J. Carter, and S. Harker, "ISO 9241-11 revised: What have we learnt about usability since 1998?," in *International Conference on Human-Computer Interaction*, 2015, pp. 143–151.
- [25] ISO/IEC, "ISO/IEC 25010:2011 (en) Systems and software engineering - Systems and software Quality Requirements and Evaluation (SQuaRE) - System and software quality models," 2011.
- [26] J. Nielsen, *Usability Engineering*. 1993.
- [27] J. Nielsen, "Enhancing the Explanatory Power of Usability Heuristics," *Proc. ACM CHI'94 Conf. (Boston, MA, April 24-28)*, 1994, 152-158.
- [28] W. Quesenbery, "The five dimensions of usability," in *Content and Complexity: Information Design in Technical Communication*, 2014.
- [29] J. Rubin and D. Chisnell, *Handbook of Usability Testing: How to Plan, Design, and Conduct Effective Tests* 2nd Ed. 2008.
- [30] W. Brown, P. Y. Yen, M. Rojas, and R. Schnall, "Assessment of the Health IT Usability Evaluation Model (Health-ITUEM) for evaluating mobile health (mHealth) technology," *J. Biomed. Inform.*, 2013.
- [31] E. Lacka and A. Chong, "Usability perspective on social media sites' adoption in the B2B context," *Ind. Mark. Manag.*, 2016.
- [32] R. D. Stoll, A. A. Pina, K. Gary, and A. Amresh, "Usability of a Smartphone Application to Support the Prevention and Early Intervention of Anxiety in Youth," *Cogn. Behav. Pract.*, 2017.
- [33] B. K. Park, E. S. Nahm, V. E. Rogers, M. Choi, E. Friedmann, M. Wilson, and G. Koru, "A Facebook-Based Obesity Prevention Program for Korean American Adolescents: Usability Evaluation," *J. Pediatr. Heal. Care*, 2017.
- [34] I. Cho, E. Kim, W. H. Choi, and N. Stagers, "Comparing usability testing outcomes and functions of six electronic nursing record systems," *Int. J. Med. Inform.*, 2016.
- [35] G. Rodríguez, J. Pérez, S. Cueva, and R. Torres, "A framework for improving web accessibility and usability of Open Course Ware sites," *Comput. Educ.*, 2017.
- [36] K. Sorn-in, K. Tuamsuk, and W. Chaopanon, "Factors affecting the development of e-government using a citizen-centric approach," *J. Sci. Technol. Policy Manag.*, vol. 6, no. 3, pp. 206–222, 2015.
- [37] D. Nariman, "Evaluating user expectancy and satisfaction of e-government portals," in *Proceedings of the International Conference on Complex, Intelligent and Software Intensive Systems, CISIS 2011*.
- [38] M. Hasan, N. Maarop, R.Y. Naswir, G.N. Samy, P. Magalingam, S. Yaacob, and S.M. Daud, "A Proposed conceptual success model of citizen-centric digital government in Malaysia," *Journal of Fundamental and Applied Science*, vol. 10, no 2S, 2018
- [39] G. N. Gupta, "Citizen-centric Approach for e-Governance," *Comput. Soc. India*, 2007.
- [40] Y.-C. Chen, "Citizen-Centric E-Government Services: Understanding Integrated Citizens Service Information Systems," *Soc. Sci. Comput. Rev.*, vol. 28, no. 4, pp. 427–442, Nov. 2010.
- [41] P. Khaikleng, S. Wongwanich, and S. Sujiva, "Development of a Program Theory for Evaluating the Success of Education Reform Policy Implementation in Schools by Using Inductive and Deductive Approaches," *Procedia - Soc. Behav. Sci.*, 2014.
- [42] J. Dudovskiy, "Deductive Approach (Deductive Reasoning) - Research-Methodology," *Research Methodology*. 2018.
- [43] L. L. Davis, "Instrument review: Getting the most from a panel of experts," *Appl. Nurs. Res.*, 1992.
- [44] M. R. Lynn, "Determination and Quantification Of Content Validity," *Nurs. Res.*, vol. 35, no. 6, p. 382-386, Nov. 1986.
- [45] C. T. Beck and R. K. Gable, "Ensuring content validity: an illustration of the process.," *J. Nurs. Meas.*, 2001.
- [46] J. S. Grant and L. L. Davis, "Selection and use of content experts for instrument development," *Res. Nurs. Health*, 1997.
- [47] S. Loeb, S. Dynarski, D. McFarland, P. Morris, S. Reardon, and S. Reber, "Descriptive Analysis in Education: A Guide for Researchers," 2017.
- [48] J. F. Hair, G. T. M. Hult, C. Ringle, and M. Sarstedt, "A Primer on Partial Least Squares Structural Equation Modeling (PLS-SEM)," 2016.

[49] J. F. Hair, C. M. Ringle, and M. Sarstedt, "PLS-SEM: Indeed a Silver Bullet," *J. Mark. Theory Pract.*, vol. 19, no. 2, pp. 139–151, 2011.

[50] M. Z. I. Lallmahomed, N. Lallmahomed, and G. M. Lallmahomed, "Factors influencing the adoption of e-Government services in Mauritius," *Telemat. Informatics*, 2017.

[51] S. Wangpipatwong, W. Chutimaskul, and B. Papisratorn, "Factors Influencing the Adoption of Thai eGovernment Websites : Information Quality and System Quality Approach," *Int. J. Comput. Internet Manag.*, 2005.

[52] M. F. Caboral-Stevens, "Theory development and pilot testing of a new survey instrument on usability by older adults," 2015.

[53] D. Stefanovic, U. Marjanovic, M. Delić, D. Culibrk, and B. Lalic, "Assessing the success of e-government systems: An employee perspective," *Inf. Manag.*, vol. 53, no. 6, pp. 717–726, Sep. 2016.

[54] D. Belanche, L. V. Casaló, and M. Guinalú, "Website usability, consumer satisfaction and the intention to use a website: The moderating effect of perceived risk," *J. Retail. Consum. Serv.*, 2012.

[55] S. Z. Ahmad and K. Khalid, "The adoption of M-government services from the user's perspectives: Empirical evidence from the United Arab Emirates," *Int. J. Inf. Manage.*, 2017.

[56] E. A. Abu-Shanab, "E-government familiarity influence on Jordanians' perceptions," *Telemat. Informatics*, 2017.

[57] L. van Velsen, T. van der Geest, M. ter Hedde, and W. Derks, "Requirements engineering for e-Government services: A citizen-centric approach and case study," *Gov. Inf. Q.*, 2009.

[58] P. Sousa, H. Fonseca, P. Gaspar, and F. Gaspar, "Usability of an Internet-based platform (Next.Step) for adolescent weight management," *J. Pediatr. (Rio. J.)*, 2015.

[59] R. De Oliveira, M. Cherubini, and N. Oliver, "Influence of personality on satisfaction with mobile phone services," *ACM Trans. Comput. Interact.*, 2013.

[60] M. Anwar, V. Esichaikul, M. Rehman, and M. Anjum, "E-government services evaluation from citizens satisfaction perspective: A case of Afghanistan," *Transform. Gov. People, Process Policy*, 2016.

APPENDIX A

A. Survey Instruments

Section A: Respondent's Profile		Source	
Gender		[14][50]	
Age			
Educational Level			
Field of Study			
Internet Experience			
Internet Usage per Day			
Digital Government Experience			
Digital Government Usage			
Section B: Malaysian Digital Government Usability Measures			
Factor	Code	Items/Questions	Source
Effectiveness	B-ET1	The digital government services offer fast completion of transactions.	[14]
	B-ET2	No distraction on the digital government services.	
	B-ET3	No errors on the digital government services.	
Efficiency	B-EC1	The digital government services are easy to use by a normal user.	[15], [16],[51]
	B-EC2	The digital government services are well designed.	
	B-EC3	The digital government services can save citizens's time.	
	B-EC4	The digital government services can save citizens's expense.	
Learnability	B-L1	I am quickly becoming good at using the digital government services.	[32], [52]
	B-L2	I learn to use the digital government services quickly.	
	B-L3	I can easily remember how to use the digital government services.	
	B-L4	The information on the digital government services is clear.	
	B-L5	The information on the digital government services is easy to understand.	
	B-L6	In general, it is easy to learn to use the digital government services.	
Satisfaction	B-S1	The digital government services are high quality in term of accuracy or trustworthy.	[32], [53], [54]
	B-S2	I am happy with the digital government services.	
	B-S3	I plan to use the digital government services in the future.	
	B-S4	I am satisfied with the way that the digital government services have carried out transactions.	
Usefulness	B-U1	The digital government services are more convenient than traditional system.	[55], [56]
	B-U2	Using the digital government services enable me to accomplish the required task more quickly.	
	B-U3	The digital government services allow me to accomplish more transactions with the government.	
	B-U4	The digital government services increase my productivity and efficiency.	
	B-U5	In general, the digital government services are useful for me.	
Citizen Centric	B-CC1	The digital government services facilitate citizens via life events approach.	[36], [57]
	B-CC2	The digital government services facilitate convenient communication channels with the government.	
	B-CC3	The digital government services accept citizens's suggestions or complaints.	
Perceived Usability	B-PU1	The digital government services are beneficial for citizens.	[57]–[60]
	B-PU2	I find it is easy to make digital government services do what I need.	
	B-PU3	The digital government services meet my expectations.	
	B-PU4	The digital government services match or fulfil my needs.	

B. Cross-Loadings

	CC	EC	ET	L	PU	S	U
B-CC1	0.853	0.634	0.539	0.574	0.650	0.604	0.477
B-CC2	0.887	0.702	0.606	0.568	0.715	0.565	0.570
B-CC3	0.826	0.601	0.627	0.502	0.744	0.647	0.493
B-EC1	0.641	0.831	0.709	0.728	0.764	0.681	0.543
B-EC2	0.572	0.742	0.556	0.562	0.645	0.662	0.361
B-EC3	0.614	0.829	0.540	0.613	0.676	0.550	0.660
B-EC4	0.620	0.840	0.648	0.705	0.686	0.583	0.705
B-ET1	0.719	0.760	0.853	0.720	0.783	0.659	0.651
B-ET2	0.565	0.689	0.916	0.560	0.707	0.679	0.385
B-ET3	0.479	0.475	0.836	0.462	0.514	0.533	0.356
B-L1	0.595	0.717	0.602	0.839	0.597	0.544	0.728
B-L2	0.589	0.712	0.567	0.801	0.607	0.532	0.679
B-L3	0.550	0.692	0.539	0.917	0.580	0.537	0.559
B-L4	0.553	0.723	0.690	0.863	0.675	0.647	0.546
B-L5	0.531	0.687	0.595	0.902	0.684	0.609	0.501
B-L6	0.553	0.720	0.611	0.934	0.716	0.637	0.525
B-PU1	0.599	0.661	0.585	0.584	0.705	0.528	0.606
B-PU2	0.688	0.812	0.695	0.670	0.884	0.707	0.451
B-PU3	0.665	0.672	0.668	0.600	0.850	0.821	0.470
B-PU4	0.743	0.647	0.626	0.553	0.817	0.633	0.477
B-S1	0.536	0.599	0.543	0.511	0.663	0.875	0.342
B-S2	0.555	0.606	0.616	0.537	0.661	0.845	0.335
B-S3	0.545	0.638	0.556	0.596	0.571	0.689	0.597
B-S4	0.693	0.687	0.683	0.585	0.819	0.887	0.432
B-U1	0.485	0.549	0.489	0.544	0.479	0.391	0.898
B-U2	0.511	0.681	0.533	0.660	0.543	0.438	0.933
B-U3	0.635	0.665	0.521	0.609	0.628	0.497	0.893
B-U4	0.574	0.646	0.500	0.614	0.536	0.459	0.917
B-U5	0.528	0.653	0.486	0.616	0.566	0.514	0.938

A Hybrid of Multiple Linear Regression Clustering Model with Support Vector Machine for Colorectal Cancer Tumor Size Prediction

Muhammad Ammar Shafi¹, Mohd Saifullah Rusiman², Shuhaida Ismail³, Muhamad Ghazali Kamardan⁴

Department of Mathematics and Statistics
Universiti Tun Hussein Onn Malaysia, 86400 Pagoh Muar, Johor, Malaysia

Abstract—This study proposed the new hybrid model of Multiple Linear Regression Clustering (MLRC) combined with Support Vector Machine (SVM) to predict tumor size of colorectal cancer (CRC). Three models: Multiple Linear Regression (MLR), MLRC and hybrid MLRC with SVM model were compared to get the best model in predicting tumor size of colorectal cancer using two measurement statistical errors. The proposed model of hybrid MLRC with SVM have found two significant clusters whereby, each clusters contained 15 and three significant variables for cluster 1 and 2, respectively. The experiments found that the proposed model tend to be the best model with least value of Mean Square Error (MSE) and Root Mean Square Error (RMSE). This finding has shed light to health practitioner in determining the factors that contribute to colorectal cancer.

Keywords—Colorectal cancer; multiple linear regression; support vector machine; fuzzy c- means; clustering; prediction

I. INTRODUCTION

The colon and rectum is the final portion of the human body digestion tube. The food that humans eat will go through the stomach from mouth to anus. In the stomach, the food is grinded into smaller particle and then enters the small intestine in a careful and controlled manner. The small intestine is where the final stage of food digestion and absorption of the nutrients contained in the food take place. The food that is not digested and absorbed will enter the large intestine or colon and finally to the rectum. In addition, some of the undigested foods accumulated through the years produce bacteria and causes cancer and it is called colorectal cancer. Colorectal cancer is a type of cancer that arise from the inner wall of large intestine [1,2].

However, a cause of colorectal cancer is still unclear. It involves many risk factors including family history, colon polyp and long-standing ulcerative colitis. Symptoms of colorectal cancer are also unclear for detection. Moreover, some of the symptoms of colorectal cancer are too common in the society like anemia, weight loss and many more [3].

Furthermore, information and knowledge about risk of colorectal cancer in Malaysia is still lacking compared to the awareness towards cervical cancer [4, 5, 6, 7, 8]. It might have been one of the reasons behind the increasing number of patient suffering colorectal cancer. It was reported that colorectal cancer causes the third highest number of death

among patients after lung cancer and breast cancer by 10.6% [9]. Data in 1995 showed colorectal cancer admission percentage increased from 8.1% to 11.9% [10].

Basically, there are four stages of colorectal cancer. Earlier stages comprise of stage I and II and final stages refer to stage III and IV. According to Malaysian Oncology Society in 2017, stage I refer to the condition where the cancer start to exist in wall of colon or polyp, stage II, III and IV refer to the condition where the cancer has spread through the wall of the colon. There are several methods to reduce the risk of developing colorectal cancer such as treatment, radiotherapy and screening [11, 12, 13]. Nowadays, linear regression and support vector machine model are very popular model among researchers in dealing with various fields [14, 15]. This study plans to find the best model among MLR, MLRC and hybrid model by comparing the value of errors.

II. MATERIALS AND METHODS

The population of this study is based on secondary data from patients aged between 21 until 90 years old who received treatment at a general hospital around Kuala Lumpur in 2012 with the symptoms or suffering from colon cancer of any four stages. The study includes both male and female patients from various ethnics.

A. Multiple Linear Regression Model (MLR)

Regression analysis proposed by Sir Francis Galton in 19th century who study the relation between the heights of parents and the height of their children. The term regression persists to describe statistical relations between variables. Regression analysis is a statistical method that utilizes the relation between two or more quantitative variables toward predicted variables. MLR model is one of statistical methods which is widely used in many disciplines such as business, the social and behavioral sciences and biological sciences [17].

MLR model uses the least squares estimation technique in order to find the coefficient β_i . Before conducting multiple linear regression analysis, regression model should fulfill the classical assumptions as stated below:

- 1) Constant variance of residual
- 2) Residual of normality
- 3) Multicollinearity checking

The MLR model parameter can be stated as follows:

$$Y_i = \beta_0 + \beta_1 X_{i1} + \beta_2 X_{i2} + \dots + \beta_k X_{ik} + \varepsilon_i(\beta), \quad i=1, \dots, N \quad (1)$$

where:

Y_i is the value of response variable

B_0, β_1, β_2 and β_j are unknown constant

X_j is value of predictor variable

ε_i is the random error

Regression model is a linear model with multiple linear predictor variables. It is 'multiple' because there are more than one predictor variables in linear parameter. A model which is linear predictor in the parameters is referred as a first-order model.

B. Fuzzy C-Means Methods

Fuzzy C-Means (FCM) is a method of clustering which allows the data to belong into two or more clusters. This model developed by Dunn (1973) and was improved by Bezdek (1981). A large family of fuzzy clustering algorithms is based on minimization of the fuzzy c-means objective function formulated as:

$$J = \sum_{q=1}^N \sum_{r=1}^C u_{qr}^z d_{qr}^2 \quad (2)$$

where z is any real number greater than 1, μ_{qr} is the membership values, d_{qr} represent as the distance according to Euclidean. N is the number of objects and C is the number of clusters. The index q ($q=1, \dots, N$) correspond to object number q and the index r ($r=1, \dots, C$) correspond to cluster number r . In case of Euclidean distance, the algorithm for minimising J can be summarized by the following steps:

1) Randomly select cluster centers 'c'. Choose the termination tolerance between 0 and 1, then choose fuzziness exponent, $z > 1$.

2) Update distance, d_{qr} for given μ_{qr} by computing the weighted average for each group and the Euclidean distance as:

$$d_{qr}^2 = \|x_q - v_r\|^2, \quad v_r = \frac{\sum_{q=1}^N u_{qr}^z x_q}{\sum_{q=1}^N u_{qr}^z} \quad (3)$$

3) Update membership values as,

$$u_{qr} = \frac{1}{\sum_{k=1}^c \left(\frac{d_{qr}}{d_{qk}} \right)^{\frac{2}{z-1}}}, \quad \text{for } z > 1 \quad (4)$$

4) Calculate the objective or criterion J and make iteration in order to minimize the objective function. The iteration repeated for $k = 1, 2, \dots, \infty$, then stop the iteration, else repeated step 2.

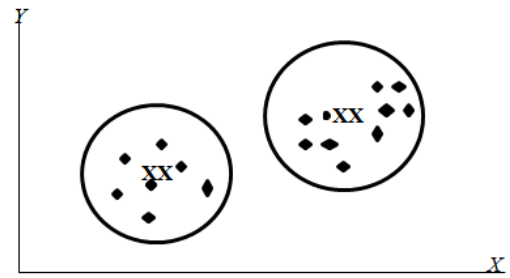


Fig. 1. The FCM Graph with Two Clusters.

The example of FCM cluster is shown in Fig. 1. The clusters have naturally circular shape with the clusters, XX located in the middle for each cluster.

C. Support Vector Machines Model (SVM)

SVM model was proposed by Vapnik in 1963 in order to determine the subtle patterns in complex data sets. An SVM commonly used for classifying objects in prediction or forecasting technique. The advantage of SVM is that it has two classifications types which are linear and non-linear [16].

SVM with linear classification is applied in this study. Linear classifier is used to determine to which group an object belongs to. It is done by dividing the groups with a line called hyperplane. The hyperplane linear classification is shown in Fig. 2.

In addition, equation of kernel functions with polynomial kernel as below [18]:

$$K(x, y) = (x^T y + 1)^d \quad (5)$$

D. Hybrid MLR Clustering with SVM Models

Multiple linear regression clustering is proposed in this study which is combination of MLR and FCM method. While, the hybrid is defined as a combination of both MLR clustering model and SVM model [18]. The steps of hybrid MLR clustering with SVM models is shown in Fig. 3.

This study contains three stages in preparing the new hybrid MLRC and SVM model. The first stage is MLR and SVM model will be applied to colorectal cancer data to determine the MSE and RMSE value of the model. In stage two, Pearson correlation was performed to find the highest correlation among the independent variables. Then, the selected variables are put into fuzzy c-means to find the appropriate clustering.

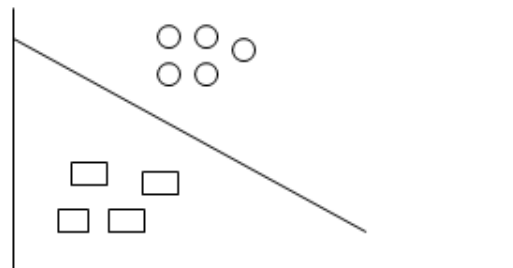


Fig. 2. Linear Classification with a Hyperplane.

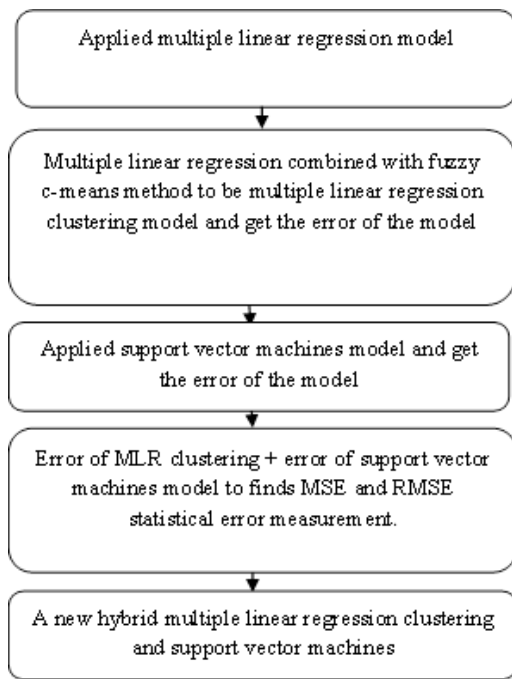


Fig. 3. Steps of Hybrid Model.

Finally, in stage three, the new dataset is obtained based on combination of MLRC and SVM to predict the tumor size of colorectal cancer. The equation for a new dataset as shown is Eq (6).

$$Y = L_t + N_t \tag{6}$$

Where, Y is a new dataset, L_t is the error of linear part (MLR) and N_t is the error of nonlinear part (SVM) of the hybrid model.

The performance for each cluster is evaluated using statistical performances which are MSE and RMSE values. The final equation to find MSE value is as follow:

$$MSE_{final} = \frac{n_1(MSE_1) + N_2(MSE_2)}{n_1 + n_2} \tag{7}$$

Where, n_1 and n_2 are the number of data for cluster 1 and cluster 2 respectively. MSE_1 , MSE_2 is the value of mean square error for cluster 1 and cluster 2, respectively.

III. RESULTS

This study used secondary data of tumor size for colorectal cancer and contains 180 patients as respondents. The dependent variable is tumor size while 25 factors and symptoms variables are chosen as independent variables. The average age of patients facing colorectal cancer and symptoms is 61 years old. While, the average tumor size in diameter (mm) is 53.45.

The comparison among MLR, MLRC and hybrid of MLRC with SVM model are compared using cross validation statistical techniques which are MSE and RMSE. The model

with the lowest of MSE and RMSE value is chosen as the best model to predict the tumor size of colorectal cancer.

A. Multiple Linear Regression Model

The data in this study were tested using three assumptions of MLR which is residual of constant variance, residual of normality and multi-collinearity and all the assumptions were satisfied and fulfilled.

This study applied MLR model in the data of tumor size colorectal cancer with 25 independent variables. Table I shows the parameter of the model.

All the significant variables chosen are important to predict tumor size of colorectal cancer. The estimated multiple linear regression model for colorectal cancer is as follows:

$$\hat{Y} = 76.056 + 0.421 \text{ age} + 3.459 \text{ icd10} + 0.961 \text{ TNM staging} - 16.738 \text{ family history} + 5.035 \text{ Crohn's disease} + 5.557 \text{ history of cancer} - 6.517 \text{ gastric} + 12.865 \text{ ovarian} - 4.350 \text{ intestinal obstruction} - 7.943 \text{ anemia} - 3.994 \text{ abdominal} \tag{8}$$

TABLE I. PARAMETER OF THE MODEL

Independent variables	Beta (β)	Sig. Value
(Constant)	76.056	*0.000
x_1 (Gender)	1.977	0.286
x_2 (Age at Diagnosis (years))	-0.421	*0.000
x_3 (Ethnic Group)	2.231	0.114
x_4 (ICD 10 Site)	3.459	*0.027
x_5 (TNM Staging)	0.961	*0.040
x_6 (Family_History)	-16.738	*0.000
x_7 (Diabetes Mellitus)	0.832	0.679
x_8 (Crohn's Disease)	5.035	*0.012
x_9 (Ulcerative colitis)	1.508	0.432
x_{10} (Polyp)	-1.577	0.396
x_{11} (History of cancer)	5.557	*0.007
x_{12} (Endometrial)	-0.869	0.648
x_{13} (Gastric)	-6.517	*0.001
x_{14} (Small bowel)	-3.33	0.087
x_{15} (Hepatobiliary)	-1.047	0.589
x_{16} (Urinary tract)	2.597	0.176
x_{17} (Ovarian)	12.865	*0.000
x_{18} (Other cancer)	3.248	0.084
x_{19} (Intestinal Obstruction)	-4.35	*0.022
x_{20} (Colorectal)	1.227	0.511
x_{21} (weight_loss)	3.063	0.1
x_{22} (Diarrhoe)	0.75	0.695
x_{23} (Anemia)	-7.943	*0.003
x_{24} (blood_stool)	-2.158	0.233
x_{25} (Abdominal)	-3.994	*0.038

*Significant at 0.05

TABLE II. ANOVA FOR MULTIPLE LINEAR REGRESSION

Sources	Sum of Squares	df	Mean Square	F-Value	P-Value
Regression	21396.590	25	855.864	6.606	0.000
Residual	19951.960	154	129.558 (MSE)		11.3826 (RMSE)
Total	41348.550	179			

In addition, Analysis of Variance (ANOVA) analysis was performed. The result shows that the MSE term is 129.558 and RMSE is 11.3826. The result of ANOVA is shown in Table II.

B. Multiple Linear Regression with Fuzzy C-Means Method

The three assumptions applied for MLR in cluster 1 and cluster 2 models were fulfilled and satisfied. Furthermore, the independent variables x17 (ovarian), x8 (crohn's disease), x5 (TNM staging), x11 (history of cancer) and x1 (gender) were chosen since it has the highest correlation value. The data will be divided into two cluster, cluster 1 and cluster 2. The correlation values among x17, x8, x5, x11 and x1 as shown below in Table III:

Based on Table III, y vs x17 show the best cluster results. The final MSE value is calculated based on equation 6. The amount of respondents in the data taken with 180 patients. The results are in Table IV.

1) Cluster 1 (Y vs X17): Cluster 1 (based on X17) for the clustering model between MLR and FCM used 85 data as respondent in the analysis. The measurement of error MSE and RMSE is shown in Table V. The model for cluster 1 is as follow:

$$\hat{Y}_1 = 64.278 - 0.573 \text{ age} + 4.321 \text{ ethnic} + 5.836 \text{ icd10} + 2.024 \text{ TNM Staging} - 9.670 \text{ family history} + 3.130 \text{ Crohn's disease} + 3.127 \text{ ulcerative colitis} + 4.924 \text{ history of cancer} - 6.784 \text{ small bowel} + 3.414 \text{ urinary tract} + 13.736 \text{ ovarian} + 4.193 \text{ other cancer} - 6.583 \text{ intestinal obstruction} + 4.677 \text{ weight loss} + 5.555 \text{ diarrhea} - 4.315 \text{ blood stool.} \quad (9)$$

TABLE III. CORRELATION VALUES

correlation	value	significant
Y vs x17 (1)	0.246	0.001
Y vs x8 (2)	0.145	0.052
Y vs x5 (3)	0.141	0.058
Y vs x11 (4)	0.117	0.119
Y vs x1 (5)	0.089	0.237

TABLE IV. THE FINAL OF MSE AND RMSE VALUE OF THE MODEL

Correlation	Final MSE
Y vs x17	116.985
Y vs x8	123.560
Y vs x5	116.985
Y vs x11	116.985
Y vs x1	123.560

TABLE V. MSE AND RMSE VALUE OF MODEL CLUSTER 1

Methods	Value
MSE	32.763
RMSE	5.724

TABLE VI. MSE AND RMSE VALUE OF MODEL CLUSTER 2

Methods	Value
MSE	192.341
RMSE	13.868

2) Cluster 2 (Y vs X17): Cluster 2 (based on X17) for the clustering model between MLR and FCM used 95 data as respondent in the analysis. The measurement of error MSE and RMSE is shown in Table VI. The model for cluster 2 is as follow:

$$\hat{Y}_2 = 78.073 - 22.907 \text{ family history} - 13.157 \text{ gastric} + 12.454 \text{ ovarian} \quad (10)$$

C. Hybrid MLR Clustering with SVM Model

A measurement statistical error of MSE and RMSE and coefficient of parameter model was applied in a new model hybrid of MLRC and SVM. The error measurement of MSE and RMSE could be evaluated by sum error of MLRC and SVM model to determine the value of MSE and RMSE. The smallest value of error will be the best model to predict tumor size of colorectal cancer. The final MSE and RMSE of the model show in Table VII.

1) Cluster 1 (Y vs X17): Cluster 1 (based on X17) for the clustering model between MLR clustering and SVM used 85 data as respondent in the analysis. The MSE and RMSE values and error of cluster 1 are shown in Table VIII and Fig. 4, respectively.

TABLE VII. MSE AND RMSE VALUE OF MODEL

Methods	Value
MSE	78.661
RMSE	8.869

TABLE VIII. MEASUREMENT ERROR OF CLUSTER 1

Methods	Value
MSE	44.979
RMSE	6.707

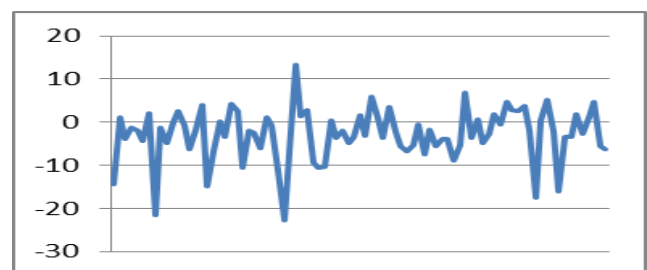


Fig. 4. The Error of Cluster 1.

There are several independent variables of the model which are significant to predict tumor size of colorectal cancer and the MLRC and SVM model in Cluster 1 for the model is as follows:

$$\hat{Y} = 64.278 - 0.573 \text{ age} + 4.321 \text{ ethnic} + 5.836 \text{ icd10} + 2.024 \text{ TNM Staging} - 9.670 \text{ family history} + 3.130 \text{ Crohn's disease} + 3.127 \text{ ulcerative colitis} + 4.924 \text{ history of cancer} - 6.784 \text{ small bowel} + 3.414 \text{ urinary tract} + 13.736 \text{ ovarian} + 4.193 \text{ other cancer} - 6.583 \text{ intestinal obstruction} + 4.677 \text{ weight loss} + 5.555 \text{ diarrhoea} - 4.315 \text{ blood stool} \quad (11)$$

2) Cluster 2 (Y vs X₁₇): Cluster 2 (based on X₁₇) for the clustering model between MLRC and SVM model used 95 data as respondent in the analysis. The three assumptions were fulfilled and satisfied. The MSE and RMSE values and error of cluster 2 are shown in Table IX and Fig. 5, respectively.

TABLE IX. MEASUREMENT ERROR OF CLUSTER 2

Methods	Value
MSE	107.482
RMSE	10.367

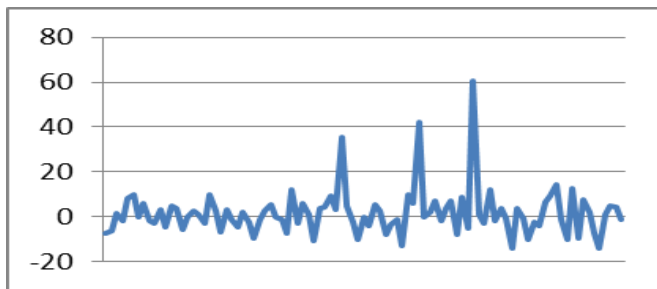


Fig. 5. The Error of Cluster 2.

The MLRC and SVM model for colorectal cancer model in Cluster 2 is then predicted as follows:

$$\hat{Y} = 78.073 - 22.907 \text{ family history} - 13.157 \text{ gastric} + 12.454 \text{ ovarian} \quad (12)$$

IV. CONCLUSION

This study proposed a hybrid of MLRC with SVM model. The MSE and RMSE have been used to measure the effectiveness of the model in predicting tumor size of colorectal cancer based on the factors and symptoms of colorectal cancer.

It was found that the proposed model of MLRC with SVM has yield a good result in predicting the tumor size of colorectal cancer suffered by patients in general hospitals of Kuala Lumpur. The results showed that MSE and RMSE for a new hybrid of MLRC and SVM model are 78.661 and 8.869 respectively.

Based on hybrid MLRC with SVM, there are 16 significant independent variables that are found to be a contributed factors to colorectal cancer which are age, ethnic, icd10, TNM staging, family history, Crohn's disease, ulcerative colitis, history of cancer, small bowel, urinary tract,

ovarian, other cancer, intestinal obstruction, weight loss, diarrhea and blood stool. On the other hand, only three independent variables are significant in cluster 2 which are family history, gastric and ovarian. The summary of the error of the models is shown in the Table X.

TABLE X. SUMMARY ERROR OF MODELS

Model of linear regression	MSE	RMSE
MLR	129.558	11.383
MLR clustering	116.985	10.816
A new hybrid model (MLR clustering and support vector machines model)	78.661	8.869

In future, the new hybrid model of MLRC and SVM model can be applied to various fields especially for vagueness data and complex data. Moreover, the study using hybrid model can be used in order to predict the factors and symptoms of colorectal cancer and hence, can reduce the mortality rate.

ACKNOWLEDGMENT

This research is supported by the Universiti Tun Hussein Onn Malaysia under the TIER 1 grant scheme vot number H232.

REFERENCES

- [1] "Healthline," colon cancer, 2011. Retrieved from healthline.com
- [2] "MedicineNet," colon cancer, 2011. Retrieved from <http://MedicineNet.com>
- [3] Obi, J. C, Imianvan, A. A, "Fuzzy neural approach for colon cancer prediction," Scientia Africana, vol. 11, pp. 65-76, 2012.
- [4] Harny, M.Y, Norwati, D, Norhayati, M.N, Amry, A.R, "Knowledge and attitude of colorectal cancerscreening among moderate risk patients in west Malaysia," Asian Pacific J Cancer prev, vol. 12, pp. 1957-60, 2011.
- [5] Hoffman, R. M., Rhyne, R. L., Helitzer, D. L, "Barriers of colorectal cancer screening: physician and general population perspectives, New mexico, 2006," Preventing Chronic Diseases, vol. 289, pp. 2492-2493, 2011.
- [6] Lim, G.C.C, "Overview of cancer in Malaysia," Jpn Jclin Oncol, vol. 32, pp. s37-42, 2011.
- [7] "Second report of the national cancer registry," 2010.. [<http://www.makna.org.my/NCR/>].
- [8] Vincent, J, Hochhalter, A. K., Broglio, K., Avots-Avotin, A. E., "Surveys respondents planning to have screening colonoscopy report unique barriers," The Permanente Journal, vol. 15, pp. 4-11, 2011.
- [9] World Health Organization Data, "Publications of the World Health Organization," The WHO Web Site, 2010.
- [10] Ministry of Health, Malaysia, "Information and Documentation System Unit. Planning & Development Division," 2010.
- [11] Pereira M. Graca, Ana Paula Figueredo and Frank D. Fincham, "Anxiety, Depression, Traumatic Stress and Quality of Life in Colorectal Cancer after Different Treatments: A Study With Portuguese Patients and Their Partners," European Journal of Oncology Nursing, pp. 1-6, 2011.
- [12] Roslani April Camilla, Taufiq Abdullah and Kulenthran Arumugam, "Screening for Colorectal Neoplasias with Fecal Occult Blood Tests: False-positive Impact of Non-Dietary Restriction," Asian Pacific Journal of Cancer Prevention, vol. 13, pp. 237-241, 2012.

- [13] Yusoff Harmy Mohamed, Norwati Daud, Norhayati Mohd Noor and Amry Abdul Rahim, "Participants and barriers to colorectal cancer screening in Malaysia," *Asian Pacific J Cancer Prev*, vol. 13, pp. 3983-3987, 2012.
- [14] Bin, M.A.S, Bin, M.S.R, Yusof, N.S.H.C, "Determinants Status Of Patient After Receiving Treatment At Intensive Care Unit: A Case Study In Johor Bahru," *Computer, Communications, and Control Technology (I4CT)*, 2014 International Conference on, pp. 80 – 82, 2014.
- [15] Shafi, M.A., Rusiman, M.S, "The Use Of Fuzzy Linear Regression Models For Tumor Size In Colorectal Cancer In Hospital Of Malaysia," *Applied Mathematical Sciences*, vol. 9, no. 56, pp. 2749-2759, 2015.
- [16] Jaon Bell, "Machine learning hands on for developers and technical professionals," John Wiley & Sons, Inc, 2015.
- [17] Michael H. Kutner, Christopher J. Nachtsheim, John Neter, William Li, "Applied linear statistical models," Mc Graw Hill Fifth Edition, 2004.
- [18] Ping Fei Pai, Chih-Sheng Lin, "A Hybrid ARIMA and Support Vector Machines Model in Stock Price Forecasting," *The International Journal of Management Science*, pp. 497-505, 2004.

Intrusion-Miner: A Hybrid Classifier for Intrusion Detection using Data Mining

Samra Zafar¹

School of Electronic Information and
Electrical Engineering
Dalian University of Technology
Dalian 116024, China

Muhammad Kamran²

College of Computer Science and
Engineering
University of Jeddah, Jeddah,
Saudi Arabia

Xiaopeng Hu³

School of Electronic Information and
Electrical Engineering
Dalian University of Technology
Dalian 116024, China

Abstract—With the rapid growth and usage of internet, number of network attacks have increase dramatically within the past few years. The problem facing in nowadays is to observe these attacks efficiently for security concerns because of the value of data. Consequently, it is important to monitor and handle these attacks and intrusion detection system (IDS) has potentially diagnostic ability to handle these attacks to secure the network. Numerous intrusion detection approaches are presented but the main hindrance is their performance which can be improved by increasing detection rate as well as decreasing false positive rates. Optimizing the performance of IDS is very serious issue and challenging fact that gets more attention from the research community. In this paper, we proposed a hybrid classification approach ‘Intrusion-Miner’ with the help of two classifier algorithm for network anomaly detection to get optimum result and make it possible to detect network attacks. Thus, principal component analysis (PCA) and Fisher Discriminant Ratio (FDR) have been implemented for the feature selection and noise removal. This hybrid approach is compared with J48, Bayesnet, JRip, SMO, IBK and evaluate the performance using KDD99 dataset. Experimental result revealed that the precision of the proposed approach is measured as 96.1 % with low false positive and high false negative rate as compare to other state-of-the-art algorithm. The simulation result evaluation shows that perceptible progress and real-time intrusion detection can be attained as we apply the suggested models to identify diverse kinds of network attacks.

Keywords—Intrusion detection system; principal component analysis; intrusion-minor; fisher discriminant ratio

I. INTRODUCTION

The networked computer systems are playing a progressive vital role in our society with hastily increasing adoption of internet. Although, internet brings enormous advantages, it also has increased threats of computer systems connected to the internet becoming target of intrusions by cyber criminals [1, 2]. However, it is impossible to have a safety mechanism without susceptibility. Consequently, they are inadequate to make the infrastructure absolutely secure due to careless layout, malicious attacks and implementation flaws continuously try to escapade system’s weaknesses. It is important to monitor and identify these attacks so, it will become traditional to invent a security mechanism. This security mechanism is known as intrusion detection and it is considered as a crucial part of the present security approaches.

An IDS helps in keeping a track of malicious attacks or breaking of the policy of a system or a network and reports to control room by generating alarms. Fig. 1. clearly illustrates the whole process. Intrusion detection are basically divided into two design approaches, misuse and anomaly detection system based on detection philosophy [1, 3, 4]. For a misuse IDS approach, information gathered from traffic analyzed by the IDS to compare it to large database having signatures of already known attacks. These signature attacks are documented by human experts. It is not effective for unknown and novel attacks for which the signature are not yet available. On the other hand in anomaly detection approach system administrator defined the baseline, breakdown, normal state of traffic load, typical packet size and protocol in advance. Network segments are monitored by a detector to stack up against the normal baseline state and inspect for deviations. It can detect potentially a wide range of novel attacks [5].

An IDS monitors all ingoing and outgoing activities of network. They manage this by collecting information from a number of systems and network resources. It identifies attacks, probes, exploits and other vulnerabilities of the network analyzing the heaped information. An IDS respond to malicious attacks in one of the various ways, for example by generating alarm, creating the event or paging an administrator. An IDS may comprise of software and hardware equipment and sensor devices. These devices can be implemented anywhere in a network. These IDS can be implemented using data target, response and data mining techniques based on IDS.

These are four types of system attacks on network:

- Denial of Service attack (DoS): In these attacks, the attacker prevents a valid user to get access by blocking him. For this, the attacker tries to occupy the resources of the computer system in such a way that they become busy.
- Users-to-Root attack (U2R): In such attacks, the attacker tries to exploit the system weaknesses by locking up a legitimate user and accessing root component of the system. Few examples of U2R attacks are ‘buffer overflow’, ‘load-module’, ‘perl’, and ‘rootkit’.
- Remote-to-Local attack (R2L): In these attacks, vulnerabilities of a machine allow an attacker to get an

access locally a legitimate user account without having his (or her) own account. A few examples of R2L attacks include 'phf', 'ftp write', 'warezmaster', 'warezclient', 'spy', 'imap', 'multihop', and 'guess passwd'.

- Probing attack (PROBE): These attacks involve the bypassing of security by the attacker and collecting the data from the nodes in the network. Few example like 'portsweep', 'ipsweep', and 'nmap' are a few examples of PROBE attacks

Over the deployment of data mining methodologies, systematic IDS are developed to detect intrusion excellently and perform generalizations. Therefore, the installation and implementation of such kind of systems can be obviously complicated. The systems' integral problems can be categorized into discrete problem sets based on proficiency, precision, and availability parameters [5, 7, 8]. Though, data mining techniques IDS generally designed for anomaly detection methodologies that have higher false positive occurrence as compared to other detection techniques that only focus on handcrafted signature. Therefore, previous techniques face difficulty during processing of data, online intrusions detection and require huge amount of data as compare to current methodologies [6, 27, 30].

Hence, constructing the proficient intrusion detection system is dynamic defense in the network system's and it make it possible to detect network attacks. So, a hybrid classification approach Intrusion-Miner proposed to get optimum results. Then, to find best performance yielding classifiers, we will evaluate our proposed classifier intrusion miner on KDD99 dataset. We also evaluate the time taken by the algorithm for training of all the classifiers. Finally, a proposed hybrid approach compared with previous classifiers in-term of TP, FP and average accuracy.

In this paper the work has been organized as follows. In Section II, we discuss about the related work of current study and Section III contains the overview of the proposed methodology. This section provides proposed scheme with detail of its phases and general form of proposed model. In Section IV, we provide the detailed analysis including the result and discussion of relative performance. Finally, in Section V, we conclude the paper and show possible future work.

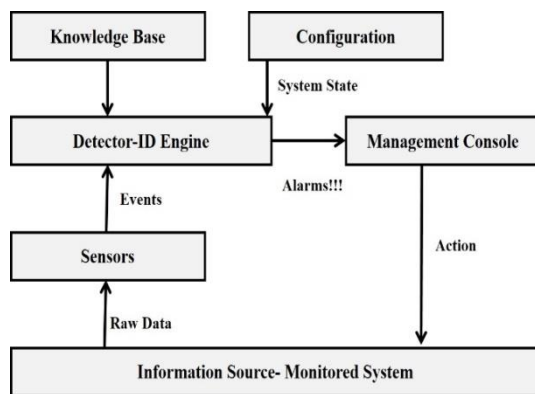


Fig. 1. Intrusion Detection Model.

II. RELATED WORK

The most primitive study regarding to intrusion detection system was first proposed in (1980) [9]. The approach was based on statistic method to analyze and monitor those attackers who get into the system in illegitimate manner. Consequently, the work is led by Dorothy E. Denning [10] in (1987) who build the first prototype of intrusion detection expert system (IDES). In this work, they executed a dual approach that utilized a rule based expert system as well as statistical variance components that has its basis on host system. Subsequently, in (1995) they lead their work and build a new version namely next generation intrusion detection expert system [11]. The description of inclusion of host IDS in to the network IDS namely a hybrid IDS model was proposed in [12]. This new hybrid model contain both misuse and anomaly modes. Then data mining techniques are applied on these features to learn rules that precisely define the actions of intrusions and normal activities. Both known and unknown intrusions can be detected efficiently by using this hybrid IDS [13]. The hybrid approach integrates self-organizing maps and statistical methods to detect the network anomalies proposed in [14]. Feature are selected and noise removal is achieved on the basis of FDR and PCA. In 2015, the progress of this hybrid methodology by combining two data mining approaches implemented in [7]. A novel K-means clustering algorithm is employed to reduce the number of features related with each a data point. Sunil Nilkanth Pawar [15] suggested a genetic algorithm technique that is based on chromosomes having variable length to build network IDS. For the generation of rules chromosome having relevant features were utilized. Fitness of each function is defined by an effective fitness function. Every single chromosome represents one or more than one rules for efficient anomalies detection. The efficiency of the proposed technique is proved by testing it on DARAPA 1998 dataset.

Consequently, to deal with the IDS efficiently a hybrid model namely SVM model that interconnect kernel PCA (KPCA) with upgraded chaotic intelligence scheme namely particle swarm optimization (PSO) proposed in [16]. Preprocessing on support vector machine (SVM) is functionalized by KPCA scheme to increase the SVM performance and decrease the training time. The extracted results shows higher accuracy and precision and shorten the training time. Iftikhar Ahmad [17] exploit PCA to select feature subset in his proposed approach. PCA is conducted on the basis of highest eigenvalues. Rather than using a conventional methodology to select the structures with their highest eigenvalues such as PCA, A genetic principal mechanism are employed to select subsets of features and for sorting purpose SVM is used. The obtained results indicates that it increase the detection rates and decreases the number of features. Chun Guo [18] presented a novel and tractable hybrid learning method for building effective IDS. The suggested model is known as Distance Sum-Based SVM (DSSVM). In this method, the distance sum and the cluster centers are defined along with interconnection among each data samples. Experimental results obtained from this model clearly showed that this hybrid approach shows better results in terms of intrusion detection and computational cost.

Saurabh Mukherjee [19] introduced a technique which utilizes a method based on feature vitality such as correlation based as well as gain ratio and information gain to recognize the anomalies in the selection system. However, the effective classifier namely naïve Bayes also implemented on intrusion detection system. The evaluated results showed better performance of IDS. One of the most common and powerful data mining algorithms called K-Means clustering with the conjunction of Naïve Bayes classification for IDS recommended in [20]. As compare to the separate Naïve Bayes classification, this advance application offers high-reaching detection rate. However, the limitation of this approach is that more false positives are generated.

Zhi [21], came up with a newly proposed model for intrusion detection model which combines two classifiers C4.5 and hybrid neural network. As network attacks are classified into four categories neural network perform well in detecting Probing and DOS attacks whereas, R2L and U2R attacks are detected more accurately with the help of C4.5 classifier. Muniyandi [22] presented a novel hybrid approach which combines C4.5 and k-Means classifiers. The presented hybrid technique provide anomaly detection by cascading the C4.5 decision tree and k-Mean clustering methods. Simulation results show that the proposed technique gives impressive detection rate. Mrutyunjaya Panda [23] implemented Naïve Bayes grouping technique in his work to solve the issue of IDS. He worked for anomaly based network intrusion detection using KDD99 dataset. He also performed a comparison of back propagation neural network based approach with the adopted technique and results clearly showed that the suggested technique accomplishes better in terms of TP rate, TT and cost. Yang Li and Li Guo [24] proposed a network intrusion detection technique dependent on Transductive Confidence Machines for K-Nearest Neighbors (TCM-KNN), by adopting this technique the anomalies can be identify efficiently with high detection rate, less false positive conditions by utilizing fewer nominated data and its features. The results of average TP and FP have in good agreement with values 99.6% and 0.1 % respectively. A method in which SVM used to categorize different types of attack proposed in [25]. This proposed method shows higher accuracy result with RBF and the accuracy value is 98.57%, for the NSL-KDD data set. Dhanabal [26] Analyze NSL-KDD data set and applied on SVM, J48, and Naïve Bayes for classifying attacks. In regarding to this some of experimental result demonstrates that CFS can be used for dimensionally reduction and in this case J48 classifier classifies the data with better accuracy From the literature review it is perceived that some algorithms performs well for a certain attack category while fails for others.

Therefore, we can expect much performance improvement from a multiple classifier selection model instead of using a single classifier in solitary. We take the advantage of information gain to address the data handling issue. Moreover, we used the hybrid of probabilistic algorithm to design the final architecture of our classifier. We evaluate classifiers on KDD99 data set to find optimum performance.

III. PROPOSED APPROACH

This section provides the details about the proposed scheme. The proposed scheme mainly consists of three phase namely: (i) Feature Selection; (ii) Fisher Discriminant Ratio for Eigenvectors; and (iii) Classification. The main architecture of the proposed scheme has been shown as a 2-step engineering approach in Fig. 2 and top level architecture Fig. 3 respectively.

A. Feature Selection

The first step of the proposed approach is to select the features from the input dataset. This step is important because it involves to identifying those features of the data that may trigger an alarm when an intrusion is suspected. Moreover, it also involves excluding those features from the classification step that do not play any vital role in the classification process. Furthermore, the redundant and irrelevant features are also filtered out; as a result, overall computation time of the algorithm is reduced along with the improvement in the classification results in terms of classification accuracy and generalization. The generalization is an important property of classification as it helps the algorithm to avoid over-fitting on a particular data.

The feature selection method is divided into three types that are wrapper, filter and hybrid methods. In filter method, a preprocessing step is performed to select a subset of features on the bases of selected criteria. In this preprocessing step, features are selected without considering their performance of the classifier. In this way, filter method are considered as less time consuming as compare to the wrapper method because; wrapper method evaluate the feature selection method on the bases of the outcomes of the classifiers. Even though wrapper method perform well as compare to filter method in terms of classifier accuracy, but when the classifier is changed the results obtained become not applicable in the same situation. To overcome these limitations of above two mentioned methods, a new approach was proposed that is called hybrid method. This method combines both filter method and wrapper method to support the classifier. This hybrid approach is used in our work with the filter method. In many applications PCA has been used to extract the most relevant information from dataset. It has been already successfully used in applications based on face recognition techniques [28]. In our proposed technique, a unique class of uncorrelated features is derived from a class of correlated features. Hence, PCA reproduce a class of orthogonal basis vectors to express the data as a linear combination of that basis. This method involves some classification task problems when new data is added because it takes more time in processing; similarly, it also lacks the desired property of invariant under a transformation of data.

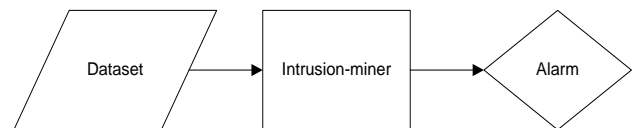


Fig. 2. A Two-Step Engineering Approach of Intrusion-Miner.

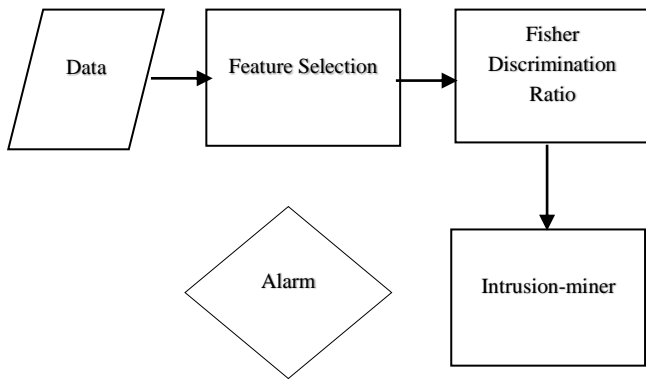


Fig. 3. Top Level Architecture of Intrusion-Miner.

To formally understand this process, consider the following modeling.

Suppose we have $X = \{x_1, x_2, x_3, \dots, x_N\}$ samples (or records) in the training data. By subtracting it from the mean \bar{X} , we obtain the shifted data manifold as $Y = \bar{X} - X$ for $y_i \in R^n$ with $y_i = (y_{i1}, y_{i2}, \dots, y_{in})^T$ and $i = 1, 2, \dots, N_i$. The job of PCA is to search for orthonormal vectors $u_k = (u_{k1}, u_{k2}, \dots, u_{kn})$ for $k = 1, 2, \dots, N_t$ such that

$$\lambda_k = \sum_{r=1}^{N_t} (u_k^T y_r)^2 \quad (1)$$

The goal is to maximize λ_k . The vectors u_k verify that $u_l^T u_k = \delta_{lk}$, where δ_{lk} represents the kronecker data. Moreover, the scalar λ_k and the vectors u_k denote the eigenvalues and eigenvectors respectively and they are used to compute the covariance matrix as $C = YY^T$.

In the proposed Intrusion-miner, the role of the eigenvectors is to form a new feature space for removing the noise and also to reduce the features set. In this way, we project the samples in the training data by utilizing the space as defined by the eigenvectors. As a result, uncorrelated features are generated in the form of a set that can describe the data manifold. The classifiers are then run on these features to generate final result. Before a classifying a test sample v (a data sample from the testing data), the sample needs to be projected onto the space spanned by the eigenvectors. This into the corresponding feature vector represented as:

$$\omega_k = (v - \bar{X}) * u_k \quad (2)$$

In order to regenerate the original data from the principal components, \bar{X} is used as:

$$v_k^{rec} = \bar{X} + \omega_k + u_k^T \quad (3)$$

The above equation shows how that how the eigenvector k is used to follow the reconstruction process u_k^{rec} for the sample v . for ensuring the maximum use discriminative power of the projections, we propose to compute and use the FDR value as follows.

B. Fisher Discriminant Ratio (FDR)

The data preprocessing step is of utmost importance in the classification of real-world datasets because they usually have some noise, missing values, invalid values, redundant values, and irrelevant features. To solve the problems faced by PCA

regarding the selection of eigenvectors with higher values and yet missing the most discriminative ones, we propose to use FDR as:

$$FDR = \sum_{i=1}^M \sum_{j \neq i}^M \frac{(\mu_i - \mu_j)}{(\sigma_i^2 + \sigma_j^2)} \quad (4)$$

Where, μ_i and σ_i represent the mean and variance for the class i respectively.

Algorithm 1. The main FDR algorithm follows.

- Compute $Y = X - \bar{X}$
- Compute the projection s of X to corresponding eigenvectors
- Sort the eigenvectors based on their discriminative power computed using Eq. (4)
- For eigenvectors with lower values FDR values, subtract the projection of training samples from the corresponding eigenvectors.
- The main advantage of using FDR with PCA is that it allows using k most discriminative eigenvectors to make the classification task more efficient.

C. Classification Module

Due to imbalanced nature of the intrusion datasets, a classifier or classification algorithm needs to exploit the local data distribution for making the decisions during classification. The instance based learner k-NN is one such algorithm, so we propose to use this algorithm along with some desired characteristics of using the global data model for classification. Consequently, both the local and the global properties of the data can be used to classify the data efficiently. We used the hybrid of probabilistic algorithm BayesNet with Instance based learner (IBk) to design the final architecture of our classifier–IntrusionMiner. Moreover, the performance of various other classifiers like J48, BayesNet, JRip, SMO, and IBk are also the part of our study for performance comparison.

D. General Form of Proposed Model

In order to find optimum performance yielding classifiers, we evaluate six classifiers on KDD99 dataset. Parameters selected for the performance comparison are FP and TP rate. These parameters could be considered the best point of comparison for classifying the algorithms. Moreover, it is important to record the overall average accuracy (AA). Similarly, the average Training Time (TT) of each algorithm also plays an important role for real world problems. An algorithm should be selected for building the final model if it performs well on all the attack categories. On the basis of performance, the proposed model will use one best classifier to detect network anomaly of each attack category.

IV. EXPERIMENT AND RESULTS

This section describes the experiments and their results using the proposed model for effective intrusion detection. This section is further divided into sub-sections as follows.

A. Data Set Description

The dataset used for this experiment was taken from [29] that was also used in KDD-99 dataset. The original dataset contains about 4,900,000 unique connections. Every connection vector contains 41 features. From these 41 features 7 features are discrete by nature and remaining 34 are continuous. The network activities are labeled as not normal or ‘attacks’ considering the normal network behavior. In our experiments, the following four types of attacks were simulated DoS, U2R, R2L and Probe. In our experiments on the KDD-99 dataset, we take the protocols like TCP, UDP, and ICMP into account. The actual training dataset used in our research work is made up of 494,021 records. Among which 97,277 (19.69%) were normal, 4,107 (0.83%) Probe, 391,458 (79.24%) DoS, 52 (0.01%) are U2R and 1,126 (0.23%) R2L. In the dataset there are 41 attributes associated with each connection and each attribute describes variant features of the connection. Each connection is differentiated by a label (attack type or normal) that is allocated to it.

The imbalance nature of the dataset is presented using Fig. 4. It is quite evident from Fig. 4 that the data is highly imbalanced as there is a huge difference in the number of records for each class. For brevity, in our experiments, we selected the 10% of the samples present in the KDD training dataset. Thus, we selected 9841 records from the ‘Normal’ class, 39072 records from the ‘DoS’ class, 437 records from ‘Probe’ class, 13 records having class of ‘U2R’, and 213 records from ‘R2L’ class making a total of 49,596 (that is 10% of total records).

B. Evaluation Setup

The experiments were performed on a system having a processor of Intel(R) Core(TM) i3 with a 4GB RAM running Microsoft Windows 8.1 Pro. An open source machine learning package Weka was used for simulation. The version of Weka tool used is 3.6.0 which is the Windows version. We used Weka in our research work because it provides numerous data mining and machine learning algorithms. It provides the facility of data preprocessing, clustering, classification, visualization, regression and association rules. However, only a subset of classifiers algorithms is exploited in our proposed work. The classification techniques mentioned in our classification module in Section 3.3 were used through Weka so that all the results can be compared to the performance of the proposed Intrusion-miner.

C. Data Pre-Processing

The actual KDD99 dataset contains large number of records as mentioned above. In our experiments, we divided the dataset into two subsets. The first subset which is training set contains 49,596 instances in total and consists of 9,841 normal instances, 13 U2R instances, 39,092 DoS instances, 213 R2L instances, and 437 Probe instances. In the second subset, we separated 15,437 instances that act as an absolute

testing set. For preprocessing the selected datasets, we followed the approach mentioned in Section 3.1 and 3.2 respectively. After the preprocessing step we can effectively evaluate the performance of selected classifiers by running them on these subsets of the dataset.

D. Classification and Performance Comparison

Evaluation of data mining classifiers having best performing instances mentioned in Section 3.3 was done on KDD99 dataset. Fig. 5(a-d) shows the simulation results of these classifiers. Each classifier was compared on the basis of the parameters like TP-Rate (correctly identified positive cases), FP-Rate (negative cases that have been incorrectly classified as positive), and AA (total correctly classified instances divided by the total number of instances) as shown in Eq. (5), (6) and Eq. (7) and the time taken by the algorithm for training.

$$TP = \frac{d}{c+d} \tag{5}$$

$$FP = \frac{b}{a+b} \tag{6}$$

$$AA = \frac{a+d}{a+b+c+d} \tag{7}$$

Where a is correct predictions when precedent is negative, b is the number of incorrect prediction when precedent is positive, c is number of incorrect predictions when precedent is negative and while d is the incorrect predictions when precedent is positive.

Table I compares the results of the classifiers using the parameters AA, TP-Rate and FP-Rate for various attacks (classes). It is quite evident from Table I that the proposed Intrusion-Miner has better results as compared to other state-of-the-art classifiers. Also note that in most of the cases the Bayesian classifier BayesNet and the Instance based learner IBk performed better than J48, JRip, and SMO.

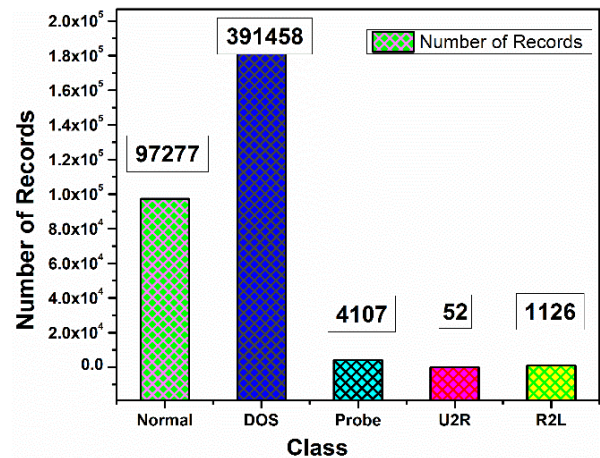


Fig. 4. The Number of Records for Each Class in the Dataset Depicting the Imbalanced Nature of the Dataset.

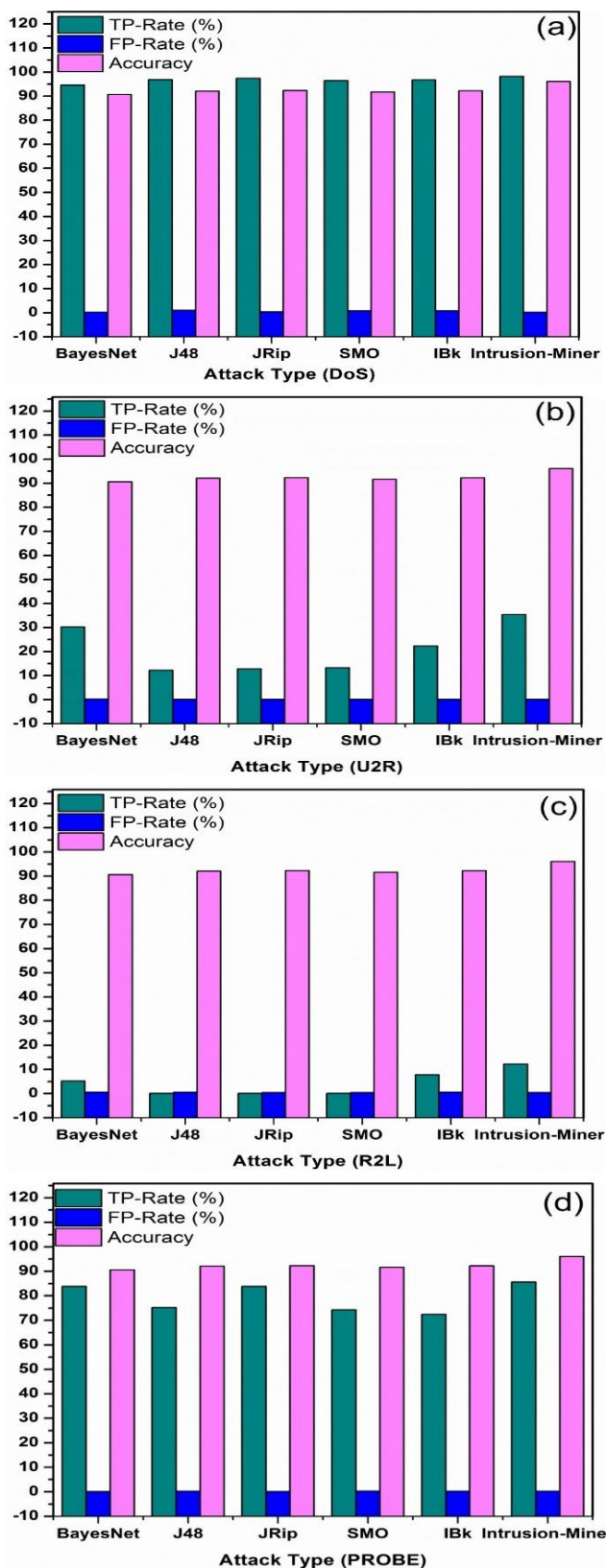


Fig. 5. Classification of Results as a Comparison of State-of-the-Art Classifiers with the Proposed Intrusion-Miner in Term of FP, TP and AA are Shown in (a) DoS, (b) U2R, (c) R2L, (d) Probe Respectively.

This is because of the nature of the dataset being imbalanced. Furthermore, the Intrusion-miner has even better results than BayesNet and IBk alone. We believe this is due to the fact that it exploits the properties of probabilistic nature of Bayesian classifier and learning capabilities of instance based classifiers and then combines both of these desired characteristics of the classifiers to achieve better classification results in terms of TP-Rate, FP-Rate, and AA. We also give the comparison of these algorithms in terms of time taken to build the classification model using the training set in Fig. 6. It is clear that the proposed Intrusion-Miner has also better speed than some of its counterpart. Although, some of the algorithms like BayesNet, J48, and IBk built the model even faster; however, the better accuracy of Intrusion-Miner as evident from Table I is enough to neglect this minor difference of time.

TABLE I. A COMPARISON OF STATE-OF-THE-ART CLASSIFIERS WITH THE PROPOSED INTRUSION-MINER

Attack Type	Algorithm	TP-Rate (%)	FP-Rate (%)	Accuracy
DOS	BayesNet	94.6	0.2	90.62
	J48	96.8	1	92.06
	JRip	97.4	0.3	92.3
	SMO	96.4	0.8	91.65
	IBk	96.7	0.8	92.22
	Intrusion-Miner	98.2	0.2	96.1
U2R	BayesNet	30.3	0.3	90.62
	J48	12.2	0.1	92.06
	JRip	12.8	0.1	92.3
	SMO	13.3	0.1	91.65
	IBk	22.3	0.1	92.22
	Intrusion-Miner	35.4	0.1	96.1
R2L	BayesNet	5.2	0.6	90.62
	J48	0.1	0.5	92.06
	JRip	0.1	0.4	92.3
	SMO	0.1	0.4	91.65
	IBk	7.8	0.6	92.22
	Intrusion-Miner	12.2	0.4	96.1
PROBE	BayesNet	83.8	0.13	90.62
	J48	75.2	0.2	92.06
	JRip	83.8	0.1	92.3
	SMO	74.3	0.3	91.65
	IBk	72.4	0.2	92.22
	Intrusion-Miner	85.6	0.2	96.1

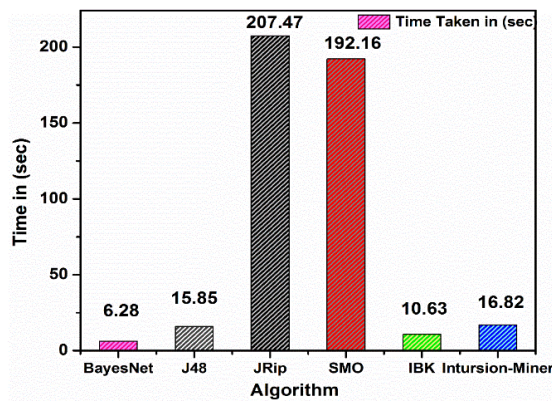


Fig. 6. Time Taken (in seconds) by Various Algorithms to Build the Model.

E. Discussion on Results

It is a general accepted fact that the accuracy of the algorithm, the overall TP-Rate, and FP-Rate are among the most important parameters for measuring the performance of a classification algorithm. However, when dealing with highly imbalanced dataset like the one used in KDD-99, it is also required to note the performance of the classifier for each class individually as well. According to our hypothesis, it is obvious from Table I that it is not possible to detect all attack categories with a single algorithm giving low false alarm rate and high probability of detection. It gives us an idea that for different attack categories different algorithms could be used. Simulation results shown in Table I clearly depict that some algorithms show better performance towards a specific attack category. For instance, most of the algorithms produce significant TP rates—like 95% for DoS category. While for U2R and R2L type of attacks, the accuracy of all the classifiers is significantly lower than other classes of attack. This is because the classifiers generally tend to learn using the majority results; consequently, the records having class having a very small number are often miss-classified. Having said all that, the proposed Intrusion-Miner outperforms all the other algorithms used in this paper in terms of classification results.

While selecting an algorithm, Training Time (TT) of each algorithm is important and needs to be taken into the account. To build real-time network intrusion detection system, it is important to consider because it gives an idea which algorithm is suitable for real time environment. In this respect, the proposed Intrusion-Miner is also able to yield the classification model while taking an acceptable training time to build the model.

V. CONCLUSION

In this paper, a hybrid learning approach called Intrusion-Miner has been proposed with the help of probabilistic BayesNet and IBK for better classification. Final result from the analysis of KDD 99 dataset using weka shown that it gave optimum performance during simulation that shows through tables, figures and graph to have a clear understanding for researchers. Simulation results proved that proposed Intrusion-Miner has better outcome as compared to other state-of-the-art algorithm and each classifier compared in term of AA, FP, TP and TT of algorithm. We also evaluated the speed of building classification model in which Intrusion-Miner has higher

speed. From experimental results, it can be clearly observed that proposed approach not only achieve remarkable improvement in performance but also help in implementation of real time system applications and maximizing detection rate.

For future work, we recommend researchers to investigate other optimizing techniques for IDS that further improve the overall accuracy. In future, we plan to expand our work and use some other datasets as well.

REFERENCES

- [1] M.H. Bhuyan, D.K. Bhattacharyya, J.K. Kalita, Network anomaly detection: methods, systems and tools. IEEE communications surveys & tutorials, vol. 16, no. 1, pp. 303-336, 2014.
- [2] A.K. Ghosh, J. Wanken, F. Charron. Detecting anomalous and unknown intrusions against programs. in Computer Security Applications Conference, 1998. Proceedings. 14th Annual. 1998, IEEE.
- [3] A.A. Ghorbani, W. Lu, M. Tavallaee, Network intrusion detection and prevention: concepts and techniques. Springer Science & Business Media, vol. 47, 2009.
- [4] C. Kreibich, and J. Crowcroft, Honeycomb: creating intrusion detection signatures using honeypots. ACM SIGCOMM computer communication review, vol. 34, no. 1, pp. 51-56, 2004.
- [5] E. De la Hoz, et al. PCA filtering and probabilistic SOM for network intrusion detection. Neurocomputing, vol. 164, pp. 71-81, 2015.
- [6] S. Aljawarneh, M. Aldwairi, M.B. Yassein, Anomaly-based intrusion detection system through feature selection analysis and building hybrid efficient model. Journal of Computational Science, vol. 25: pp. 152-160, 2018.
- [7] U. Ravale, N. Marathe, P. Padiya, Feature selection based hybrid anomaly intrusion detection system using K means and RBF kernel function. Procedia Computer Science, vol. 45: pp. 428-435, 2015.
- [8] S.A. Aljawarneh, R.A. Mofteh, A.M. Maatuk, Investigations of automatic methods for detecting the polymorphic worm's signatures. Future Generation Computer Systems, vol. 60: pp. 67-77, 2016.
- [9] M. Nezakatolhoseini, and M.A. Taherkhani, A Framework for Performance Evaluation of ASIPS in Network-Based IDS. arXiv preprint arXiv:1211.0620, vol. 4, no. 5, 2012.
- [10] D.E. Denning, An intrusion-detection model. IEEE Transactions on software engineering, vol. 2, pp. 222-232, 1987.
- [11] D. Anderson, T. Frivold, A. Valdes, Next-generation intrusion detection expert system (NIDES): A summary. 1995.
- [12] D. Zhao, Q. Xu, Z. Feng. Analysis and design for intrusion detection system based on data mining. in Education Technology and Computer Science (ETCS), 2010 Second International Workshop on. 2010. IEEE.
- [13] G. Nadiammal, M. Hemalatha, Effective approach toward Intrusion Detection System using data mining techniques. Egyptian Informatics Journal, vol. 15, no. 1, pp. 37-50, 2014.
- [14] E. De la Hoz, et al., PCA filtering and probabilistic SOM for network intrusion detection. Neurocomputing, vol. 164, pp. 71-81, 2015.
- [15] S.N. Pawar, R.S. Bichkar, Genetic algorithm with variable length chromosomes for network intrusion detection. International Journal of Automation and Computing, vol. 12, no. 3, pp. 337-342. 2015.
- [16] F. Kuang, et al., A novel SVM by combining kernel principal component analysis and improved chaotic particle swarm optimization for intrusion detection. Soft Computing, vol. 19, no. 5, pp. 1187-1199, 2015.
- [17] I. Ahmad, et al., Enhancing SVM performance in intrusion detection using optimal feature subset selection based on genetic principal components. Neural computing and applications, vol. 24, no. 7-8, pp. 1671-1682, 2014.
- [18] C. Guo, et al., A distance sum-based hybrid method for intrusion detection. Applied intelligence, vol. 40, no. 1, pp. 178-188. 2014.
- [19] S. Mukherjee, N. Sharma, Intrusion detection using naive Bayes classifier with feature reduction. Procedia Technology, vol. 4: pp. 119-128, 2012.

- [20] S.K. Sharma, et al. An improved network intrusion detection technique based on k-means clustering via Naïve bayes classification. in Advances in Engineering, Science and Management (ICAESM), 2012 International Conference on. 2012. IEEE.
- [21] Z.-S. Pan, et al. Hybrid neural network and C4. 5 for misuse detection. in Machine Learning and Cybernetics, 2003 International Conference on. 2003. IEEE.
- [22] A.P. Muniyandi, R. Rajeswari, R. Rajaram, Network anomaly detection by cascading k-Means clustering and C4. 5 decision tree algorithm. Procedia Engineering, vol. 30, pp. 174-182, 2012.
- [23] M. Panda, M.R. Patra, Network intrusion detection using naive bayes. International journal of computer science and network security, vol. 7, no. 12, pp. 258-263, 2007.
- [24] Y. Li, L. Guo, An active learning based TCM-KNN algorithm for supervised network intrusion detection. Computers & security, vol. 26, no.7-8, pp. 459-467, 2007.
- [25] Y.B. Bhavsar, and K.C. Waghmare, Intrusion detection system using data mining technique: Support vector machine. International Journal of Emerging Technology and Advanced Engineering, vol. 3, no. 3, pp. 581-586, 2013.
- [26] L. Dhanabal, S. Shantharajah, A study on NSL-KDD dataset for intrusion detection system based on classification algorithms. International Journal of Advanced Research in Computer and Communication Engineering, vol. 4, no. 6, pp. 446-452, 2015.
- [27] R.K. Kovarasan, and M. Rajkumar, An effective intrusion detection system using flawless feature selection, outlier detection and classification. Progress in Advanced Computing and Intelligent Engineering, vol. 713, pp.203-213, 2019.
- [28] M. Turk, A. Pentland, Eigenfaces for recognition. Journal of cognitive neuroscience, vol. 3, no. 1, pp. 71-86, 1991.
- [29] S. Stolfo, J., et al., Cost-based modeling for fraud and intrusion detection: Results from the JAM project. 2000, COLUMBIA UNIV NEW YORK DEPT OF COMPUTER SCIENCE.
- [30] J. Jabez., S. Gowri, S. Vigneshwari, J. A. Mayan, and S. Srinivasulu. Anomaly Detection by Using CFS Subset and Neural Network with WEKA Tools, Information and Communication Technology for Intelligent Systems, vol 107, pp. 675-682, 2019.

AUTHORS' PROFILE

Samra Zafar received the BS degree in computer science from COMSATA University Islamabad, Pakistan, in 2015. Currently Master student of Computer Science with the School of Computer Science and Technology, Dalian University of Technology. Her research interests include data mining, machine learning, WSN and software defined network.

Muhammad Kamran received the MS and PhD degrees in computer science from the National University of Computer and Emerging Sciences, Islamabad, Pakistan, in 2008 and 2012, respectively. Currently, he is an Assistant Professor with the College of Computer Science and Engineering at University of Jeddah, Jeddah, Saudi Arabia. His research interests include machine learning, evolutionary computation techniques, information security, health-informatics, big data analytics, and decision support systems.

Xiaopeng Hu received the PhD degree in computer science from Imperial College London, U.K., in 2005. He is currently a Professor of Computer Science with the School of Computer Science and Technology, Dalian University of Technology. His research interests include computer vision, machine learning, and sensor fusion.

Gene Optimized Deep Neural Round Robin Workflow Scheduling in Cloud

Shanmugasundaram M¹, Kittur H M³

School of Electronics Engineering
Vellore Institute of Technology
Vellore, India

Kumar R²

Department of Electronics and Instrumentation Engineering
National Institute of Technology
Nagaland

Abstract—Workflow scheduling is a key problem to be solved in the cloud to increase the quality of services. Few research works have been designed for performing workflow scheduling using different techniques. But, scheduling performance of existing techniques was not effective when considering a larger number of user tasks. Besides, the makespan of workflow scheduling was higher. In order to solve such limitations, Gene Optimized Deep Neural Round Robin Scheduling (GODNRRS) Technique is proposed. The designed GODNRRS Technique contains three layers namely input, hidden and output layer to efficiently perform workflow scheduling in the cloud. The GODNRRS Technique initially gets the number of user tasks as input in the input layer and forwards it to the hidden layer. After taking input, GODNRRS Technique initializes gene population with the assist of virtual machines in Amazon cloud server at the first hidden layer. Next, GODNRRS Technique determines fitness function for each virtual machine using their energy, memory, CPU time, bandwidth capacity at the second hidden layer. Afterward, GODNRRS Technique defines a weight for each virtual machine at the third hidden layer depends on their fitness function estimation. Consequently, GODNRRS Technique distributes the user tasks to optimal virtual machines according to their weight value at the fourth hidden layer in a cyclic manner. At last, the output layer renders the scheduled tasks result. Thus, GODNRRS Technique handles workflows in the cloud with improved scheduling efficiency and lower energy and makespan. The GODNRRS Technique conduct the experimental evaluation using metrics such as scheduling efficiency, makespan, and energy consumption with respect to a different number of user tasks from LIGO, Montage and cybershake real-time applications. The experimental result show that the GODNRRS Technique is able to increase the efficiency and also reduces the makespan of workflows scheduling in the cloud as compared to state-of-the-art works.

Keywords—Bandwidth capacity; processor time; energy; fitness function; memory; user task; virtual machine

I. INTRODUCTION

Cloud computing is promising with increasing popularity in workflow scheduling. Workflow scheduling plays an imperative part in cloud computing where it assigns tasks to suitable resources to execute. Effective task scheduling is required for obtaining high performance in a cloud environment. Many workflows scheduling method has been designed in the existing works. But, scheduling performance of conventional techniques was not efficient. Therefore,

GODNRRS Technique is proposed in this work to increase the workflow scheduling efficiency in the cloud.

Genetic-based algorithm (GA) was designed in [1] with aiming at optimizing the workflow scheduling performance in the cloud. However, scheduling efficiency was poor. A dynamic cost-effective deadline-constrained heuristic algorithm was introduced in [2] for scheduling a scientific workflow in a public cloud. But, the makespan of scheduling was higher.

A Dynamic Priority-Based Approach was presented in [3] for efficient workflow scheduling in a cloud computing system. However, handling multiple workflows and dynamic workflow scheduling was not considered. Particle swarm optimization (PSO) was intended in [4] to reduce the overall workflow execution cost while meeting deadline constraints. But, the energy of the virtual machine was not considered in this method.

The chemical reaction optimization (CRO) and ant colony optimization (ACO) algorithms were combined in [5] to resolve the workflow-scheduling problem in Cloud. However, scheduling performance was lower. Multi-Objective Game Theoretic Scheduling of Bag-of-Tasks Workflows was presented in [6] to reduce the execution time and economic cost. But, energy utilized by the virtual machine was higher.

Multi-objective workflow scheduling was introduced in [7] with the application of a heuristic algorithm depends on the task's completion time. However, the false positive rate of workflow scheduling was more. An evolutionary multi-objective optimization (EMO)-based algorithm was developed in [8] in order to address the workflow scheduling issues in infrastructure as a service (IaaS) platform. But, the time complexity of scheduling was more.

Pareto-based multi-objective workflow scheduling algorithm was designed in [9] in order to lessen makespan and to increase energy efficiency in the cloud. However, workflow-scheduling was not improved. A multi-swarm multi-objective optimization algorithm (MSMOOA) was designed in [10] to perform workflow scheduling in the cloud. But, energy and makespan of scheduling remained an open issue.

In order to address the above mentioned existing drawbacks in cloud workflow scheduling, GODNRRS Technique is developed in this research work. The main contributions of GODNRRS technique are described in below.

- To increase the workflow scheduling performance in a cloud environment with a minimal makespan when compared to state-of-the-art works, GODNRRS technique is proposed. By using the deep neural learning, GODNRRS Technique handles the larger number of workflows in the cloud with lower time complexity. Further, round-robin scheduling helps for GODNRRS Technique distributes a number of user tasks to optimal virtual machines in a cycle manner.
- To reduces the energy usage in the cloud as compared to conventional works, a genetic algorithm is applied in GODNRRS technique where it finds optimal virtual machines using fitness evaluation (i.e. energy, memory, CPU time, bandwidth capacity) to carry out user tasks on a cloud server.

The rest of the paper structure is formulated as follows: Section II reviews the related works. In Section III, the proposed GODNRRS Technique is explained with assists of architecture diagram. In Section IV, Simulation settings are described and the result discussion is presented in Section V. Section VI presents the conclusion of the paper.

II. RELATED WORKS

Budget Deadline Aware Scheduling (BDAS) was introduced in [11] to increase the task parallelism through partitioning tasks. A service-oriented scheduler planner was developed in [12] to get resource efficiency, overall controlled performance and task prioritization for continuous data processing workflows.

A cloud workflow scheduling problem was solved in [13] with the help of a hybrid resource provisioning method to lessen the total renting cost. A Completion Time Driven Hyper-Heuristic (CTDHH) approach was presented in [14] for cost optimization in Scientific Workflow Applications.

A novel scheduling algorithm was designed in [15] for cloud computing using the driver of the dynamic essential path (DDEP) by considering actual computation cost and communication cost of task node in the scheduling process. A Hybrid GA-PSO algorithm was intended in [16] to decrease the makespan and the cost and balance the load of the dependent tasks over the heterogonous resources in the cloud.

A workflow task scheduling algorithm based on the resources fuzzy clustering was introduced in [17] to minimize makespan of the precedence constrained applications. Cost-Time Efficient Scheduling Plan was implemented in [18] for executing workflows in the cloud.

A Deadline-constrained Cost Optimization Approaches was designed in [19] with the application of ant colony optimization for workflow scheduling in clouds. A fuzzy dominance sort based heterogeneous earliest-finish-time (FDHEFT) algorithm was presented in [20] to diminish cost and makespan for workflow scheduling in the cloud. An improved round robin (IRR) algorithm was presented in [21] for workflow scheduling in cloud.

III. GENE OPTIMIZED DEEP NEURAL NETWORK ROUND ROBIN SCHEDULING TECHNIQUE

Cloud computing technology uses the internet to render scalable services for its users. Besides, cloud employs a huge amount of heterogeneously distributed resources to provide countless different services to its users with quality of service (QoS) requirements. Workflow scheduling is one of the considerable problems to be resolved in cloud computing. A lot of workflow scheduling schemes has been intended in the existing works. However, scheduling performance of conventional techniques was not effectual. Furthermore, the makespan of workflow scheduling was more. In order to overcome the above drawbacks, Gene Optimized Deep Neural Round Robin Scheduling (GODNRRS) Technique is developed. The GODNRRS Technique improves the workflow scheduling performance in a cloud environment. The GODNRRS Technique is designed to reduce the execution time of workflow and reduce energy utilization. The GODNRRS Technique is proposed by combining the genetic algorithm, round-robin scheduling in deep neural learning on the contrary to state-of-the-art works.

The deep neural learning is used in GODNRRS Technique on the contrary to existing scheduling algorithm as it helps for efficient workflow scheduling with minimal time when the number of user tasks to the cloud server is more. Deep neural learning depends on artificial neural networks (ANNs). Besides to that, a genetic algorithm is employed in GODNRRS Technique as it assists for finding optimal virtual machines based on fitness evaluation (i.e. energy, memory, CPU time, bandwidth capacity) to perform tasks. Moreover, round-robin scheduling is applied in GODNRRS Technique to schedule the user tasks to optimal virtual machines in a cycle manner based on their weight value. This supports for GODNRRS Technique to significantly carry out workflow scheduling process in the cloud with higher efficiency. Thus, GODNRRS Technique also balances the workloads of virtual machines in the cloud. The architecture diagram of GODNRRS technique is depicted in Fig. 1.

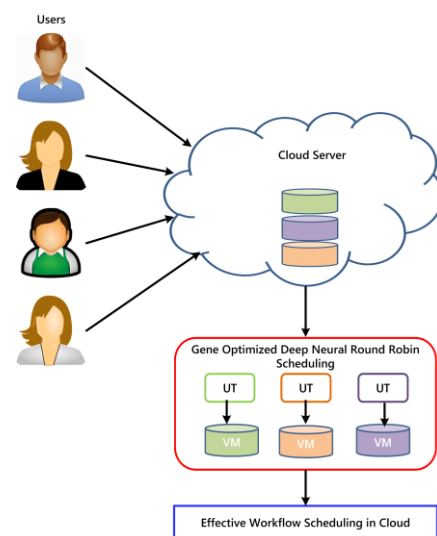


Fig. 1. Architecture of GODNRRS Technique for Workflow Scheduling.

Fig. 1 presents the overall processes of GODNRRS technique to attain improved efficiency for scheduling the workflows in the cloud. Let us consider a Cybershake, LIGO and Montage real-time applications where the users request numerous numbers of tasks to the cloud server.

As demonstrated in the above figure, GODNRRS Technique takes a number of user tasks ‘ $UT_i = UT_1, UT_2, UT_3 \dots UT_n$ ’ from Cybershake, LIGO and Montage real time applications as input. Then, Gene Optimized Deep Neural Round Robin Scheduling is applied with the aim of scheduling the tasks to best virtual machines ‘ $VM_i = VM_1, VM_2, VM_3, \dots, VM_n$ ’ and thereby minimizing the makespan and energy in cloud. The detailed processes of GODNRRS Technique are described in below.

The GODNRRS technique is an artificial neural network (ANN) with many layers between the input and output layers. The GODNRRS Technique is a feed-forward network where data flows from the input layer to the output layer without looping back. Fig. 2 demonstrates the structure of GODNRRS Technique.

Fig. 2 shows the flow processes of GODNRRS Technique to manage the workflows on a cloud server. As presented in the below figure, the GODNRRS structure contains three layers such as input, hidden, output layer. These three layers are interconnected to each other. The first layer contains input neurons that get a number of incoming user tasks to the cloud server as input and transmit taken input to the second layer known as the hidden layer. In GODNRRS Technique, four hidden layers are used where the initial population, fitness evaluation, weight determination, and round-robin scheduling is carried out to assign tasks to optimal virtual machines (VMs) and thereby managing the workflows among diverse virtual machines. At last, the output layer returns the scheduled user tasks result with higher efficiency.

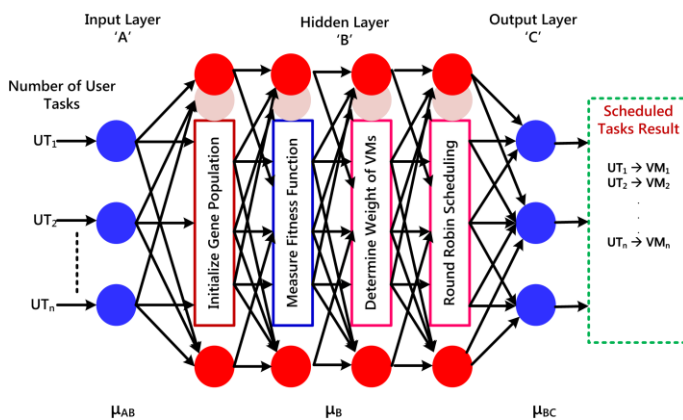


Fig. 2. Structure of GODNRRS Technique.

Let us consider a number of user tasks are ‘ $UT_1, UT_2, UT_3, \dots, UT_n$ ’ to cloud server (CS). This cloud server renders multiple services to users by assigning the tasks to virtual machines. Let us assume a cloud server includes of number of virtual machines represented as ‘ $VM_1, VM_2, VM_3, \dots, VM_n$ ’ . The GODNRRS technique acquires user tasks ‘ UT_i ’ as input. After obtaining the input, the input layer ‘A’ in GODNRRS technique unites the user tasks ‘ UT_i ’ with weights μ_{AB} and bias

term x_j . Hence, the neurons process in the input layer ‘(A)’ obtained mathematically as,

$$A(t) = \sum UT_i \mu_{AB} + x_j \tag{1}$$

From equation (1), ‘ $A(t)$ ’ refers action of a neuron in input layer at a time ‘ t ’. Here, ‘ UT_i ’ denotes a user tasks to amazon cloud server and ‘ μ_{AB} ’ represents the weight between the input and hidden layer and ‘ x_j ’ is a bias term. After obtaining the input, the input layer forwards the user tasks to hidden layer. The first hidden layers in GODNRRS Technique initialize the gene population with help of diverse number of virtual machines in cloud server. Therefore, neurons action in first hidden layer ‘ $B_1(t)$ ’ is determined mathematically as,

$$B_1(t) = \sum A(t) \mu_{B1}, IGP_{VM_i} \tag{2}$$

From equation (2), ‘ $B_1(t)$ ’ point outs the outcome of first hidden layer at time ‘ t ’ whereas ‘ $A(t)$ ’ indicates the input get from the input layer (i.e. number of user tasks ‘ $UT_i = UT_1, UT_2, UT_3 \dots UT_n$ ’ and ‘ μ_{B1} ’ refers weight of first hidden layers. Here, ‘ IGP_{VM_i} ’ represents the initial population of genes with virtual machines for an incoming user tasks at the time which is mathematically formulated as:

$$IGP_{VM_i} = VM_1, VM_2, \dots, \dots, VM_n \tag{3}$$

From (3), ‘ n ’ designates a number of virtual machines in cloud server. After completing initialization process, GODNRRS technique determines the fitness function for each virtual machine based on energy, memory, CPU time, bandwidth capacity. Thus, neurons action in second hidden layer ‘ $B_2(t)$ ’ at a time ‘ t ’ is mathematically expressed as,

$$B_2(t) = \sum B_1(t) \mu_{B2}, F_{VM_i} \tag{4}$$

From equation (4), ‘ $B_2(t)$ ’ signify the result of second hidden layer and ‘ $B_1(t)$ ’ denotes the input obtained from the first hidden layer i.e. initial population of genes with VMs. Here ‘ μ_{B2} ’ is weight of second hidden layers and ‘ F_{VM_i} ’ point outs the fitness function of each virtual machine in cloud server. From that, fitness function of VMs is mathematically calculated as:

$$F_{VM_i} = [e_{VM_i}, m_{VM_i}, c_{VM_i}, b_{VM_i}] \tag{5}$$

From equation (5), fitness function of each virtual machine ‘ F_{VM_i} ’ is measured by considering energy ‘ (e_{VM_i}) ’, memory ‘ (m_{VM_i}) ’, CPU time ‘ (c_{VM_i}) ’, bandwidth ‘ (b_{VM_i}) ’ capacity. In GODNRRS Technique, energy estimates an amount of remaining power available in virtual machine to perform arrival tasks and to provide the required services to user in cloud. Accordingly, energy is determined as difference between the total energy ‘ e_T ’ and the energy used ‘ e_U ’ by virtual machine using below,

$$e_{VM_i} = e_T - e_U \tag{6}$$

From equation (6), the residual energy capacity of each virtual machine ‘ e_{VM_i} ’ is determined. The energy is estimated in terms of a joule (J). Followed by, memory calculates the amount of storage space available in virtual machine to carry out the user tasks. From that, memory is measured as

differentiation between the total memory ‘ m_T ’ and the memory utilized ‘ m_U ’ by virtual machine using below,

$$m_{VM_i} = m_T - m_U \quad (7)$$

From equation (7), the remaining memory capacity of all virtual machine ‘ m_{VM_i} ’ is obtained. Then, CPU time is measured as difference between total CPU time ‘ c_T ’ and the amount of CPU time utilized by users ‘ c_U ’ using below:

$$c_{VM_i} = c_T - c_U \quad (8)$$

From equation (8), the residual CPU capacity of all virtual machine ‘ c_{VM_i} ’ is determined. Afterward, Bandwidth is estimated as differentiation between the total bandwidth ‘ b_T ’ and bandwidth utilized by virtual machine ‘ b_U ’ using below,

$$b_{VM_i} = b_T - b_U \quad (9)$$

From equation (9), the residual bandwidth capacity of each virtual machine ‘ b_{VM_i} ’ is obtained. Based on the estimated fitness functions (i.e. available energy, memory, CPU time, bandwidth capacity), third hidden layer in GODNRRS Technique assigns weight to each virtual machine. Hence, neurons process in third hidden layer ‘ $B_3(t)$ ’ is obtained mathematically as,

$$B_3(t) = \sum B_2(t) \mu_{B_3}, W_i (VM_i) \quad (10)$$

From equation (10), ‘ $B_3(t)$ ’ is a result of third hidden layer at a time ‘ t ’. Here, ‘ $B_2(t)$ ’ indicates the input get from the second hidden layer (i.e. determined fitness function) and Here, ‘ μ_{B_3} ’ point outs weight of third hidden layers and ‘ $W_i (VM_i)$ ’ refers the weight value of virtual machine. In GODNRRS Technique, weight is determined for each virtual machine in cloud server by considering fitness function where weight is an integer value. The GODNRRS Technique assigns weight value based on the residual processing capacity of virtual machine i.e. energy, memory, CPU time, and bandwidth capacity. Subsequently, weight of virtual machine is computed mathematically as:

$$W_i(VM_i) \rightarrow \sum_{i=1}^n F_{VM_i} \quad (11)$$

From equation (11), the weight value is discovered for each virtual machine. Thus, GODNRRS Technique schedules the user tasks first to a virtual machine with higher weight than those with a minimal weight value. In the fourth hidden layer, GODNRRS Technique accomplishes round-robin scheduling where user tasks are allocated to an optimal virtual machine according to their weight value. As a result, neurons activity in fourth hidden layer ‘ $B_4(t)$ ’ is mathematically determined as,

$$B_4(t) = \sum B_3(t) \mu_{B_4}, RRS (UT_i \rightarrow VM_i) \quad (12)$$

From equation (12), ‘ $B_4(t)$ ’ indicates the fourth hidden layer output at a time ‘ t ’ and ‘ $B_3(t)$ ’ is the input taken from the three hidden layer (i.e. weight value of virtual machine) and ‘ μ_{B_4} ’ represents weight of fourth hidden layers. Here, ‘ $RRS (UT_i \rightarrow VM_i)$ ’ denotes the scheduling of user tasks to optimal virtual machines according to their weight values in round robin manner. For instance, if weight of ‘ $\llbracket VM_1$ ’ is 5 and ‘ VM_2 ’ is 8, the GODNRRS Technique schedule 3 user tasks to ‘ VM_1 ’ and 5 user tasks to ‘ VM_2 ’ in a cyclic manner.

This supports for GODNRRS Technique to effectively distribute the user tasks to the best virtual machines in cloud server as compared to state-of-the-art works. The scheduled tasks result is then sent to output layer. The process in output layer ‘ $C(t)$ ’ at time ‘ t ’ is formulated mathematically as:

$$C(t) = Y \mu_{BC} B_4(t) \quad (13)$$

From equation (13), ‘ μ_{BC} ’ is a weight between the hidden and output layer and ‘ Y ’ is an activation function. The output layer in GODNRRS Technique gives scheduled result of tasks to optimal virtual machines. By using the above processes, the GODNRRS Technique efficiently handle the workflows in cloud with minimal energy and makespan.

The algorithmic process of GODNRRS technique is explained in below,

Algorithm: GODNRRS Algorithm

Input:	Number of cloud tasks ‘ $UT_1, UT_2, UT_3, \dots, UT_n$ ’; Cloud server ‘ CS ’; Number Of Virtual Machines ‘ $VM_1, VM_2, VM_3, \dots, VM_n$ ’
Output:	Improved efficiency for workflow scheduling in cloud
Step 1:	Begin
Step 2:	For ‘ $UT_i \in ACS$ ’
Step 3:	Takes a number of tasks as input using (1) // Input Layer
Step 4:	Forwards incoming ‘ UT_i ’ to hidden layer
Step 5:	Initialize gene populations with VMs using (2), (3) // First Hidden Layer
Step 6:	For each ‘VM_i’ // Second Hidden Layer
Step 7:	Measure ‘ e_{VM_i} ’, ‘ m_{VM_i} ’, ‘ c_{VM_i} ’, ‘ b_{VM_i} ’ using (6), (7), (8), (9)
Step 8:	Calculate ‘ F_{VM} ’ using (4) and (5)
Step 9:	End for
Step 10:	Determine weight of each ‘ F_{VM} ’ using (10), (11) // Third Hidden Layer
Step 11:	Schedule ‘ UT_i ’ to optimal VM based on weight using (12) // Fourth hidden layer
Step 12:	Returns scheduled tasks result using (13) // Output layer
Step 13:	Endif
Step 14:	End

The above algorithm describes the step by step process of GODNRRS technique to get better workflow scheduling performance in the cloud. As shown in the above algorithmic process, the number of tasks to the cloud server is obtained as input in the input layer. Then, the gene population is initialized with the help of a number of virtual machines at the first hidden layer. After that, fitness function is evaluated for each virtual machine depends on energy, memory, CPU time, bandwidth capacity at the second hidden layer. Followed by, the weight value is defined for each virtual machine by considering their fitness function at the third hidden layer. Subsequently, assignment of user tasks to best virtual machines is carried in a cyclic way based on their weight value at the fourth hidden layer. Finally, the output layer provides the scheduled tasks result. By using the above algorithmic process, GODNRRS Technique efficiently handles workflows in the

cloud with higher efficiency and minimal energy and makespan as compared to existing works.

IV. EXPERIMENTAL SETUP

In order to evaluate the performance of proposed, GODNRRS Technique is implemented in Eclipse IDE Java Language in Cloudsim simulator using Cybershake, LIGO and Montage real-time applications. The GODNRRS Technique considers the various number of user tasks in the range of 100-1000 from LIGO and Montage real-time applications for conducting the experimental process. These the workflows are run on Amazon's cloud computing platform EC2 to get required services. Montage is an astronomical application which is employed to create custom mosaics of the sky based on a set of images. Most of its tasks are represented as I/O intensive which does not need much processing capacity. Besides, LIGO workflow is utilized in gravitational physics for identifying gravitational waves generated by different events in the universe. This workflow is represented as having CPU intensive tasks. The Cybershake is employed in earthquake science to indicate earthquake hazards in a region through generating synthetic seismograms. The Amazon EC2 comprises of attributes such as Name, API Name, Memory, Compute Units (ECU), Cores, Storage, Arch, Network Performance, Max Bandwidth (MB/s), Max IPs, Linux cost and Windows cost. With the help of the Cloudsim simulator, GODNRRS technique renders demanded services to cloud users with the available resources through efficient workflow scheduling. The system configuration is shown in below Table I.

TABLE I. SYSTEM CONFIGURATION

Parameters	Quantity
Number of users	1
Number of virtual machine	20
Number of Data centers	1
RAM size	2 GB
Processor Speed	3.40 GHz
Number of processors	1
Bandwidth	20 MB
Architecture	X86

The performance of GODNRRS technique is estimated in terms of scheduling efficiency, makespan, and energy consumption. The experimental result of proposed technique is compared against two conventional methods namely Multi-Population Genetic Algorithm (MPGA) [1] and Just-in-time (JIT) Workflow Scheduling [2] and Improved Round Robin (IRR) [21].

V. RESULTS AND DISCUSSIONS

In this section, the performance result of GODNRRS technique is discussed. The simulation result of proposed technique is compared with Multi-Population Genetic Algorithm (MPGA) and Just-in-time (JIT) Workflow Scheduling and Improved Round Robin (IRR) respectively using below parameters with the assist of tables and graphs.

A. Scheduling Efficiency

Scheduling efficiency '(SE)' evaluates the ratio of number of user tasks that correctly scheduled to the best virtual machine to the total number of user tasks. The scheduling efficiency is mathematically formulated as,

$$SE = \frac{CS_{UR_i}}{N} * 100 \quad (14)$$

From equation (14), 'N' point outs a number of user tasks and 'CS_{UR_i}' refers the number of user task that accurately scheduled. The scheduling efficiency is determined in percentage (%).

Sample Mathematical Calculation for Scheduling Efficiency using LIGO Workflow:

- Existing MPGA: the number of user tasks exactly scheduled is 65 and total number of user tasks is 100. Then, scheduling efficiency is obtained as,

$$SE = \frac{88}{100} * 100 = 88\%$$

- Existing JIT Workflow Scheduling: the number of user tasks precisely scheduled is 70 and total number of user tasks is 100. Then, scheduling efficiency is determined as,

$$SE = \frac{89}{100} * 100 = 89\%$$

- Existing IRR: the number of user tasks accurately scheduled is 79 and total number of user tasks is 100. Then, scheduling efficiency is determined as,

$$SE = \frac{92}{100} * 100 = 92\%$$

- Proposed GODNRRS Technique: the number of user tasks correctly scheduled is 90 and total number of user tasks is 100. Then, scheduling efficiency is measured as,

$$SE = \frac{99}{100} * 100 = 99\%$$

The GODNRRS technique is implemented in Eclipse IDE Java Language using Cloudsim simulator by considering the real application workflows namely Cybershake, LIGO and Montage in order to estimate the scheduling efficiency. The GODNRRS Technique takes a different number of user tasks in the range of 100-1000 from above real-time application to conduct experimental process. When performing the experimental evaluation using 500 user tasks from Montage real-time application, GODNRRS Technique gets 96 % scheduling efficiency whereas existing MPGA, JIT Workflow Scheduling and IRR obtains 84%, 86 % and 86 % respectively. From that, it is significant that the scheduling efficiency using proposed GODNRRS technique is higher than other conventional works. The tabulation result analysis of scheduling efficiency for LIGO and Montage, cybershake workflows is presented in below Table II.

Fig. 3(a, b, c) demonstrates the experimental results of scheduling efficiency for Cybershake, LIGO and Montage real-time applications with respect to a dissimilar number of user tasks using three methods namely MPGA, JIT Workflow Scheduling, IRR and GODNRRS technique. As presented in Fig. 3, proposed GODNRRS technique achieves higher scheduling efficiency for handling workflows in Cybershake, LIGO and Montage real-time applications when compared to MPGA, JIT Workflow Scheduling and IRR. This is due to the integration of genetic algorithm, round-robin scheduling and deep neural learning in proposed GODNRRS technique on the contrary to state-of-the-art works. By using the algorithmic processes of GODNRRS, proposed technique increases the workflows scheduling performance in the cloud for the above real-time applications by assigning tasks to optimal VMs based on their weight. This supports for proposed technique to increase the ratio of number of user tasks that correctly scheduled to the optimal virtual machines as compared to existing works. Hence, the proposed GODNRRS technique improves the workflow scheduling efficiency of LIGO application by 16%, 12.5% and 8 % as compared to compared to MPGA, JIT Workflow Scheduling and IRR respectively. In the same way, proposed GODNRRS technique enhances the workflow scheduling efficiency of Montage application by 19%, 13 % and 9 % as compared to compared to MPGA, JIT Workflow Scheduling and IRR respectively. Likewise, this technique increases the workflow scheduling efficiency of Cybershake application by 18%, 14 % and 8 % as compared to compared to MPGA, JIT Workflow Scheduling and IRR respectively.

B. Makespan

The makespan ‘M’ represents the total length of the schedule. Thus, the makespan determines the amount of time

taken to schedule all user tasks to the optimal virtual machines. The makespan is mathematically computed using below,

$$M = N * t(SS_{UT}) \tag{15}$$

From equation (15), ‘N’ indicates a number of user tasks considered for experimental work and ‘t(SS_{UT})’ denotes the time employed for scheduling the single user tasks. The makespan is estimated in milliseconds (ms).

Sample Mathematical Calculation for Makespan using LIGO Workflow:

- Existing MPGA: the time employed to schedule the single user task is 0.35 ms and total number of tasks is 100. Then, makespan is estimated as,

$$M = 100 * 0.35 = 35ms$$

- Existing MPGA: the amount of time utilized to schedule the single user task is 0.33 ms and total number of user tasks is 100. Then, makespan is calculated as,

$$M = 100 * 0.33 = 33ms$$

- Existing IRR: the amount of time used to schedule the single user task is 0.30 ms and total number of user tasks is 100. Then, makespan is obtained as,

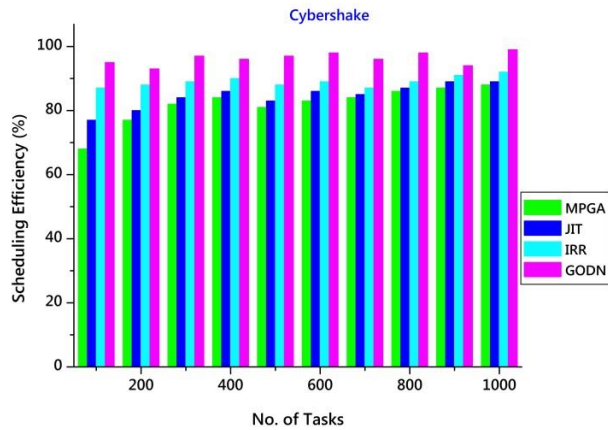
$$M = 100 * 0.30 = 30ms$$

- Proposed GODNRRS Technique: the amount of time needed to schedule the single user task is 0.28 ms and total number of user tasks is 100. Then, makespan is determined as,

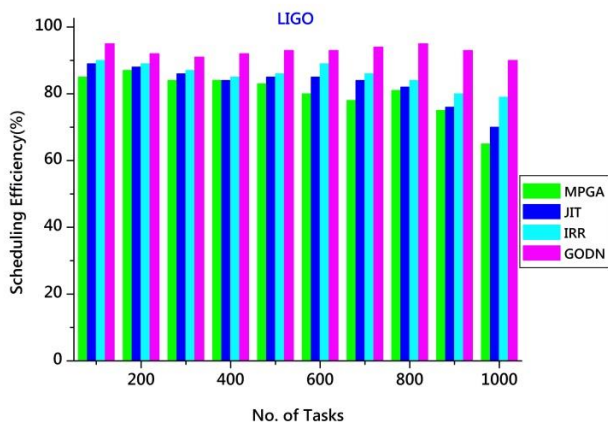
$$M = 100 * 0.28 = 28ms$$

TABLE II. TABULATION FOR SCHEDULING EFFICIENCY

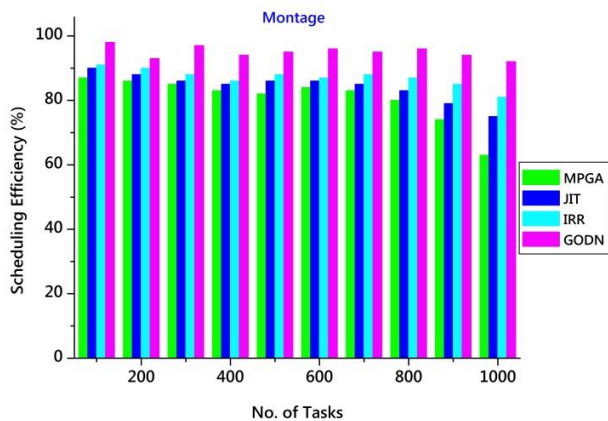
Number of user tasks (N)	Scheduling Efficiency (%)											
	Cybershake Workflow				LIGO Workflow				Montage Workflow			
	MPGA	JIT	IRR	GODNRRS	MPGA	JIT	IRR	GODNRRS	MPGA	JIT	IRR	GODNRRS
100	88	89	92	99	85	89	90	95	87	90	91	98
200	87	89	91	94	87	88	89	92	86	88	90	93
300	86	87	89	98	84	86	87	91	85	86	88	97
400	84	85	87	96	84	84	85	92	83	85	86	94
500	83	86	89	98	83	85	86	93	82	86	88	95
600	81	83	88	97	80	85	89	93	84	86	87	96
700	84	86	90	96	78	84	86	94	83	85	88	95
800	82	84	89	97	81	82	84	95	80	83	87	96
900	87	89	91	94	87	88	89	92	86	88	90	93
1000	88	89	92	99	85	89	90	95	87	90	91	98



(a) Scheduling Efficiency Analysis for Cybershake Workflow.



(b) Scheduling Efficiency Analysis for LIGO Workflow.



(c) Scheduling Efficiency Analysis for Montage Workflow.

To determine the makespan involved during processes of cloud workflow scheduling, the GODNRRS technique is implemented in Eclipse IDE Java Language using Cloudsim

simulator with two real application workflows namely cybershake, LIGO and Montage. This technique considers a varied number of user tasks in the range of 100-1000 from cybershake, LIGO and Montage real-time application to accomplish experimental work. When taking 700 user tasks from LIGO application to accomplish the experimental process, the proposed technique acquires 70 ms makespan whereas conventional works MPGA and JIT Workflow Scheduling and IRR gets 105 ms, 98 ms and 84 ms respectively.

From that it is important that the makespan using proposed GODNRRS technique is lower than other state-of-the-art works. The comparative result analysis of makespan for LIGO and Montage, cybershake workflows is depicted in below Table III.

Fig. 4(a, b, c) shows the experimental results of Makespan for both LIGO and Montage real-time applications versus a various number of user tasks using three methods namely MPGA, JIT Workflow Scheduling, IRR and GODNRRS technique. As depicted in Fig. 4, proposed GODNRRS technique attains minimal Makespan to schedule all workflows in Cybershake, LIGO and Montage real-time applications when compared to MPGA, JIT Workflow Scheduling and IRR. This is owing to a combination of genetic algorithm, round-robin scheduling and deep neural learning in proposed technique on the contrary to conventional works. With the support of the algorithmic steps of GODNRRS, proposed technique schedules all tasks in Cybershake, LIGO and Montage real-time applications to best VMs according to their weight value with a minimal amount of time. This helps for proposed GODNRRS technique to minimize the amount of time taken to effectively schedule all user tasks in the considered real-time applications as compared to existing works. Thus, the proposed technique decreases the Makespan of LIGO workflow scheduling by 28%, 22 % and 11 % when compared to MPGA, JIT Workflow Scheduling, and IRR respectively. Likewise, it also reduces the Makespan of Montage workflow scheduling by 46%, 33 % and 25 % as compared to compared to MPGA, JIT Workflow Scheduling, and IRR respectively. Similarly, the proposed GODNRRS technique minimizes the Makespan of Cybershake workflow scheduling by 45%, 43 % and 22 % as compared to compared to MPGA, JIT Workflow Scheduling, and IRR respectively.

C. Energy Consumption

Energy consumption 'EC' calculates an amount of energy utilized by the virtual machine to carry out user task. The energy consumption is calculated using below,

$$EC = N * e(S_{UT_i}) \quad (16)$$

From equation (16), ' $e(S_{UT_i})$ ' is the energy used to accomplish the single user task and 'N' refers to a number of user tasks considered during the experimental process. The energy consumption is estimated in terms of a joule '(J)' .

TABLE III. TABULATION FOR MAKESPAN

Number of user tasks (N)	Makespan (ms)											
	Cybershake Workflow				LIGO Workflow				Montage Workflow			
	MPGA	JIT	IRR	GODNRRS	MPGA	JIT	IRR	GODNRRS	MPGA	JIT	IRR	GODNRRS
100	34	32	27	23	35	33	30	28	36	31	29	25
200	46	42	32	26	48	44	38	34	50	40	36	28
300	66	60	45	36	69	63	54	48	72	57	51	39
400	76	72	52	40	80	76	64	56	84	68	60	44
500	85	80	55	40	90	85	70	60	95	75	65	45
600	96	90	60	42	102	96	78	66	108	84	72	48
700	98	91	63	46	105	98	84	70	112	84	77	49
800	112	104	72	56	120	112	96	88	128	96	88	64
900	117	108	77	59	126	108	99	90	135	99	90	63
1000	100	120	90	82	110	100	97	95	120	110	100	92

Sample Mathematical Calculation for Energy Consumption using LIGO Workflow:

- Existing MPGA: the amount of energy required to perform a single user task is 0.54 J and the total number of user tasks is 100. Then energy consumption is determined as,

$$EC = 100 * 0.54 = 54J$$

- Existing JIT Workflow Scheduling: the amount of energy desired to complete a single user task is 0.53 J and the total number of user requests is 100. Then energy consumption is calculated as,

$$EC = 100 * 0.53 = 53J$$

- Existing IRR: the amount of energy used to complete a single user task is 0.51 J and the total number of user requests is 100. Then energy consumption is formulated as,

$$EC = 100 * 0.51 = 51J$$

- Proposed GODNRRS Technique: the amount of energy utilized to carry out a single user task is 0.46 J and the total number of user tasks is 100. Then energy consumption is measured as,

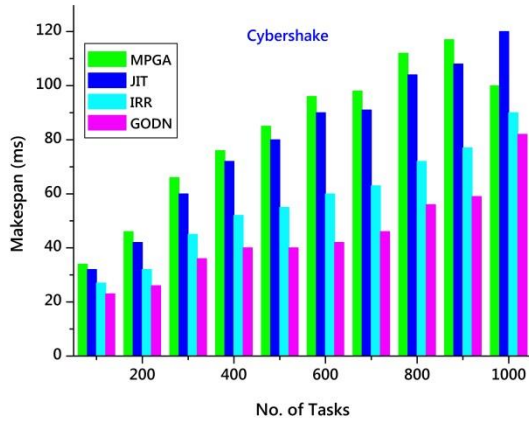
$$EC = 100 * 0.46 = 46J$$

In order to calculate the amount of energy taken for accomplishing the user tasks in the cloud, the GODNRRS technique is implemented in Eclipse IDE Java Language with Cloudsim simulator by using the two real application workflows namely LIGO and Montage. This technique employs a diverse number of user tasks in the range of 100-1000 from Cybershake, LIGO and Montage real-time application to accomplish experimental evaluation. When using 800 user tasks from cybershake application as input, this technique obtains 72J energy consumption whereas state-of-the-art works MPGA and JIT Workflow Scheduling and IRR acquires 152J, 104J, and 80 J respectively. From that, it is clear that the energy consumption using proposed technique is lower than other state-of-the-art works. The performance result analysis of energy consumption for LIGO and Montage, cybershake workflows is portrayed in below Table IV. Fig. 5 (a, b, c) describes the experimental results of energy consumption for Cybershake, LIGO and Montage real-time applications based on different number of user tasks using three methods namely MPGA, JIT Workflow Scheduling, IRR and GODNRRS technique.

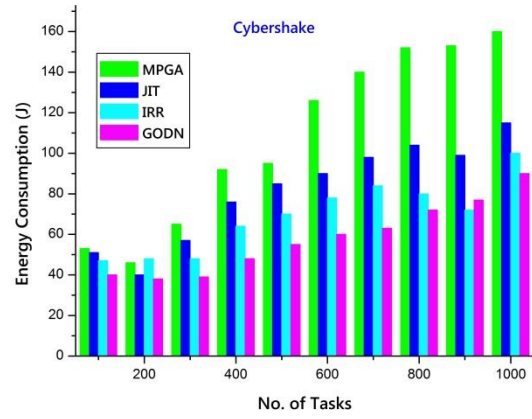
As shown in Fig. 5, proposed technique obtains lower energy consumption to perform tasks in the considered real-time applications when compared to MPGA, JIT Workflow Scheduling and IRR.

TABLE IV. TABULATION FOR ENERGY CONSUMPTION

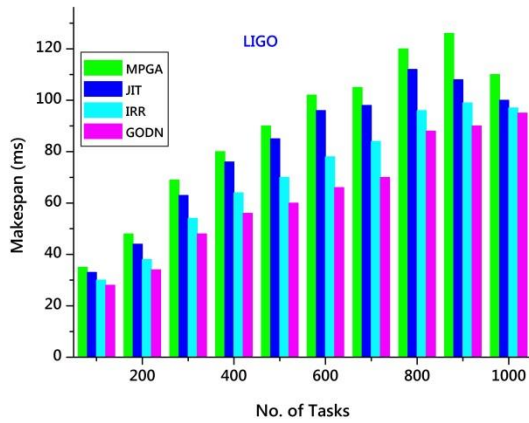
Number of user tasks (N)	Energy consumption (J)											
	Cybershake Workflow				LIGO Workflow				Montage Workflow			
	MPGA	JIT	IRR	GODNRRS	MPGA	JIT	IRR	GODNRRS	MPGA	JIT	IRR	GODNRRS
100	53	51	47	40	54	53	51	46	55	52	49	43
200	46	40	48	38	48	46	42	50	50	42	52	44
300	65	57	48	39	69	66	60	57	72	60	54	48
400	92	76	64	48	92	88	80	72	96	80	72	60
500	95	85	70	55	105	100	90	85	110	90	80	70
600	126	90	78	60	114	108	102	96	120	96	90	78
700	140	98	84	63	119	112	105	98	126	105	91	77
800	152	104	80	72	136	128	112	104	144	112	96	80
900	153	99	72	77	135	126	117	108	144	108	99	81
1000	160	115	100	90	140	130	120	115	150	121	118	112



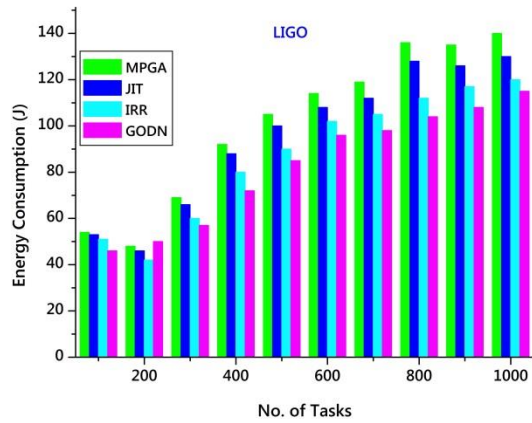
(a) Makespan Analysis for Cybershake Workflow



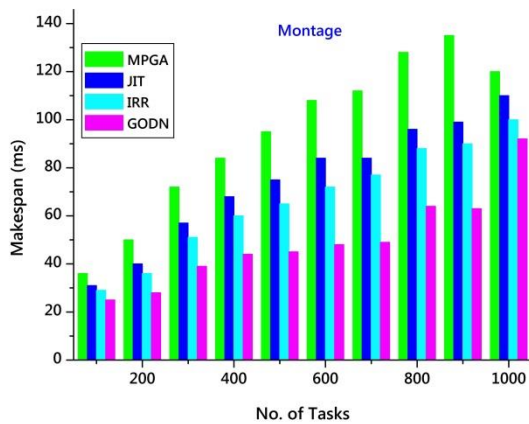
(a) Energy Analysis for Cybershake Workflow.



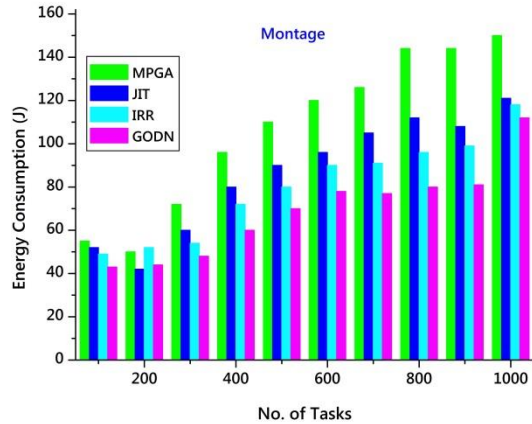
(b) Makespan Analysis for LIGO Workflow



(b) Energy Analysis for LIGO Workflow.



(c) Makespan Analysis for Montage Workflow.



(c) Energy Analysis for Montage Workflow.

This is because of the application of the genetic algorithm, round-robin scheduling and deep neural learning in proposed GODNRRS technique on the contrary to existing works. With the concepts of GODNRRS, proposed technique identifies optimal virtual machines based on fitness measurement (i.e. energy, memory, CPU time, bandwidth capacity) to carry out

user tasks in the cloud. This assists for proposed GODNRRS technique to minimize the amount of energy taken to effectively perform Cybershake, LIGO and Montage workflows in Cloud as compared to existing works. Therefore, the proposed GODNRRS technique minimizes the energy utilization by 16%, 12 % and 4 % as compared to MPGA, JIT

Workflow Scheduling and IRR respectively when considering LIGO real-time applications. Similarly, the proposed GODNRRS Technique decreases the energy consumption by 33 %, 19 % and 14% as compared to compared to MPGA, JIT Workflow Scheduling and IRR respectively when taking Montage real-time applications. Likewise, the proposed GODNRRS technique reduces the energy consumption by 43 %, 27 % and 16% as compared to compared to MPGA, JIT Workflow Scheduling and IRR respectively when taking cybershake real-time applications.

VI. CONCLUSION AND FUTURE WORK

The GODNRRS technique is designed with the goal of increasing the scheduling performance of workflows in the cloud environment when employing a huge number of user tasks as input. The goal of GODNRRS technique is obtained with aid of a genetic algorithm, round-robin scheduling in deep neural learning on the contrary to existing works. The designed technique achieves enhanced scheduling efficiency while increasing the number of user tasks as input as compared to conventional works. Further, the proposed GODNRRS Technique attains lower makespan for scheduling all the workflows in the cloud environment as compared to state-of-the-art works. In addition to that, this technique obtains minimal energy, memory, CPU time, bandwidth utilization to perform the user jobs on cloud server as compared to existing works. The efficiency of proposed technique is estimated in terms of scheduling efficiency and makespan and energy utilization for both LIGO, Montage and cybershake real-time applications and compared with two existing works. The experimental result shows that GODNRRS technique presents a better performance with an improvement of scheduling efficiency and minimization of makespan when compared to state-of-the-art works. In future work, we are planning to deal with various workflows from different regions by considering different data centers. Finally our aim is to implement our proposed technique in a real time cloud environment.

REFERENCES

- [1] Henrique Yoshikazu Shishido, Julio Cezar Estrella, Claudio Fabiano Motta Toledo, and Marcio Silva Arantes, "Genetic-based algorithms applied to a workflow scheduling algorithm with security and deadline constraints in clouds", *Computers & Electrical Engineering*, Vol. 69, Pages 378-394, 2018.
- [2] J. Sahni and D. P. Vidyarthi, "A Cost-Effective Deadline-Constrained Dynamic Scheduling Algorithm for Scientific Workflows in a Cloud Environment," in *IEEE Transactions on Cloud Computing*, vol. 6, no. 1, pp. 2-18, 1, March 2018.
- [3] Indrajeet Gupta, Madhu Sudan Kumar, and Prasanta K. Jana, "Efficient Workflow Scheduling Algorithm for Cloud Computing System: A Dynamic Priority-Based Approach", *Arabian Journal for Science and Engineering*, Springer, Vol. 43, Issue 12, pp. 7945–7960, December 2018.
- [4] Maria Alejandra Rodriguez, and Rajkumar Buyya, "Deadline Based Resource Provisioning and Scheduling Algorithm for Scientific Workflows on Clouds", *IEEE Transactions on Cloud Computing*, Vol. 2, Issue 2, pp. 222 – 235, June 2014.
- [5] Aida A. Nasr, Nirmeen A. El-Bahnasawy, Gamal Attiya, and Ayman El-Sayed, "Cost-Effective Algorithm for Workflow Scheduling in Cloud Computing Under Deadline Constraint", *Arabian Journal for Science and Engineering*, Springer, vol. 44, Issue 4, pp. 3765–3780, April 2019.
- [6] R. Duan, R. Prodan and X. Li, "Multi-Objective Game Theoretic Scheduling of Bag-of-Tasks Workflows on Hybrid Clouds," in *IEEE Transactions on Cloud Computing*, vol. 2, no. 1, pp. 29-42, January 2014.
- [7] Farzaneh Abazari, Morteza Analoui, Hassan Takabi, Song Fu, "MOWS: Multi-objective workflow scheduling in cloud computing based on heuristic algorithm", *Simulation Modelling Practice and Theory*, Vol. 93, pp. 119-132, May 2019.
- [8] Z. Zhu, G. Zhang, M. Li and X. Liu, "Evolutionary Multi-Objective Workflow Scheduling in Cloud," in *IEEE Transactions on Parallel and Distributed Systems*, vol. 27, no. 5, pp. 1344-1357, 1 May 2016.
- [9] Juan J. Durillo, Vlad Nae, and Radu Prodan, "Multi-objective energy-efficient workflow scheduling using list-based heuristics", *Future Generation Computer Systems*, Vol. 36, pp. 221-236, July 2014.
- [10] Uang-shun Yao, Yong-sheng Ding, and Kuang-rong Hao, "Multi-objective workflow scheduling in cloud system based on cooperative multi-swarm optimization algorithm", *Journal of Central South University*, Springer, Vol. 24, Issue 5, pp. 1050–1062, May 2017.
- [11] V. Arabnejad, K. Bubendorfer and B. Ng, "Budget and Deadline Aware e-Science Workflow Scheduling in Clouds," in *IEEE Transactions on Parallel and Distributed Systems*, vol. 30, no. 1, pp. 29-44, 1 Jan. 2019.
- [12] S. Esteves and L. Veiga, "WaaS: Workflow-as-a-Service for the Cloud with Scheduling of Continuous and Data-Intensive Workflows," in *The Computer Journal*, vol. 59, no. 3, pp. 371-383, March 2016.
- [13] Long Chen, and Xiaoping Li, "Cloud workflow scheduling with hybrid resource provisioning", *The Journal of Supercomputing*, Springer, Vol. 74, Issue 12, pp. 6529–6553, December 2018
- [14] Ehab Nabil Alkhanak, and Sai Peck Lee, "A hyper-heuristic cost optimisation approach for Scientific Workflow Scheduling in cloud computing", *Future Generation Computer Systems*, Vol. 86, pp. 480-506, September 2018.
- [15] Zhiqiang Xie, Xia Shao, and Yu Xin, "A Scheduling Algorithm for Cloud Computing System Based on the Driver of Dynamic Essential Path", *PLOS ONE*, Vol. 11, Issue 8, pp. 1-19, August 2016.
- [16] Ahmad M. Manasrah and Hanan Ba Ali, "Workflow Scheduling Using Hybrid GA-PSO Algorithm in Cloud Computing," *Wireless Communications and Mobile Computing*, vol. 2018, pp. 1-17, January 2018.
- [17] Fengyu Guo, Long Yu, Shengwei Tian, and Jiong Yu, "A workflow task scheduling algorithm based on the resources fuzzy clustering in cloud computing environment", *International Journal Of Communication Systems*, Vol. 28, Issue 6, pp.1053-1067, April 2015.
- [18] Amandeep Verma, and Sakshi Kaushal, "Cost-Time Efficient Scheduling Plan for Executing Workflows in the Cloud", *Journal of Grid Computing*, Springer, Vol. 13, Issue 4, pp. 495–506, December 2015.
- [19] Q. Wu, F. Ishikawa, Q. Zhu, Y. Xia and J. Wen, "Deadline-Constrained Cost Optimization Approaches for Workflow Scheduling in Clouds," in *IEEE Transactions on Parallel and Distributed Systems*, vol. 28, no. 12, pp. 3401-3412, 1 December 2017.
- [20] Xiumin Zhou, Gongxuan Zhang, Jin Sun, Junlong Zhou, Tongquan Wei, and Shiyan Hu, "Minimizing cost and makespan for workflow scheduling in cloud using fuzzy dominance sort based HEFT", *Future Generation Computer Systems*, Vol. 93, pp. 278-289, April 2019.
- [21] D. Chitra Devi and V. Rhymend Uthariaraj, "Load Balancing in Cloud Computing Environment Using Improved Weighted Round Robin Algorithm for Nonpreemptive Dependent Tasks," *The Scientific World Journal*, vol. 2016, pp. 1-14, December 2016.

Multi-criteria Intelligent Algorithm for Supply Chain Management

Mahdi Jemmali¹, Loai Kayed B.Melhim², Mafawez Alharbi³

Department of Computer Science and Information,
College of Science in Zulfi, Majmaah University,
Al-Majmaah 11952, Saudi Arabia

Abstract—In most societies, supply chain management and e-procurement processes, are one of the cornerstones of any economy and a primary influencer on people's lives. Providing these communities with their different commodity needs depends on a wide range of suppliers. Due to supplier's variety and diversity; the process of choosing the suitable supplier is considered the difficult and critical process, especially if this process is performed traditionally then decision making will be time and effort consuming to reach the desired results. To solve the problem of choosing the suitable supplier, this research suggests an intelligent algorithm, based on a given determinants that are specified by the decision maker or the customer. The proposed algorithm employs a set of intelligent formulas that will convert the predefined preferences into quantitative measurements. Quantitative measurements will be used to differentiate between different suppliers or between the set of given offers. The experimental results showed that *D3S* model employed the given preferences and succeeded in selecting the most appropriate offer among the many presented offers by the available suppliers.

Keywords—Decision making; supplier; scoring; algorithms, supply chain management

I. INTRODUCTION

Supply chain performance is critical part of any supply chain process either in advanced or in emerging economies. The continuously developing technologies all over the globe can be part of the solutions that can enhance the supply chain performance. Governments have to employ these technologies by making some decisions in its public procurement system to increase its effectiveness; since supply chain performance is a key role in the development of socio-economics for any country [1]. The next main issue in supply chain management is the market itself. Recent markets are changeable and characterized as unpredictable and volatile. While customers and organizations requests may vary, changed or even canceled, there are a set of limitations that have to be considered such as reliable vs unreliable suppliers, product model varieties and the time-consuming supply processes [1], [2]. These parameters would make decisions for supplier evaluation and selection a challenging task.

For governments or supply chain organizations, choosing a suitable supplier is affected by a set of different factors, such as cost and reliability. Supplier evaluation and selection is not performed by reviewing a list of prices; the process of selection requires analyzing and considering many factors. Besides, the supplier selection process should consider the environmental and the socio-economic issues in order to perform the selection and evaluation process; to reach the best sustainable supplier,

one that can enhance supply chain performance. Outsourcing initiatives create new challenges to the markets, the supply chain process in many countries is suppliers dependent; making it more critical when evaluating the performance of those suppliers. Supplier selection and evaluation requires the consideration of many factors that include multiple objectives and criteria [3].

II. RELATED WORK

Many research types have been performed in the field of supplier selection and evaluation, such as: adopting different approaches with different implementations and employing a lot of applied mathematics and methodologies [3]. Different researches resulted in many decision support tools that are based on multi-criteria, which is been presented as a decisions supporting tools [4], [5], [6] and [7].

Governments or organizations that are in charge of the supplier evaluation and selection process must present a set of specific requirements that should be met during the selection or the evaluation process. This problem has been addressed by [8], where the authors integrates fuzzy Analytic Hierarchy Process (AHP) for discriminant analysis and fuzzy goal programming to support decision making process. However, the separation of highly capable suppliers from less-capable ones are completely specified by the quality and the quantity of the data used to trained the proposed model. For the same field, [9] presented a fuzzy (AHP), a decision-making knowledge that can recognize or change the rules of order allocations. The presented approach was implemented to adapt with group of multi-criteria supplier selection problems, which groups order allocation with supplier selection for dynamic supply chains to deal with market variations. While in [10] the authors explored the literature review to initiate a decision support model that specifies the supplier main criteria (delivery, price, service and quality), then exploits experts' opinions to perform the ranking process and finally applies analytic hierarchy process (AHP) for the supplier selection process.

In the process of decision making, decision makers must consider many factors and criteria. The diversity and differences of these factors and criteria, may complicate the decision-making process. Such difficulties is the balance between the cost and the quality of the required product or service. In such a case, multiple criteria decision-making (MCDM) has to be used by the decision makers and many different criteria must be used to facilitate decision-making by the decision-maker, as well as, to be capable of measuring different aspects of the problem considered, besides

the ability to distinguish between other available alternatives. The *MCDM* method is very useful for decision makers to choose among alternative options when multiple criteria decision methods are applied. The usage of *MCDM* can help to reduce the effort of users resulting from dealing with the huge amount of information that is integrated to create solutions to complex problems [11]. Different approach was presented by [12] that combines threat perception and decision support systems. The authors presented a design overview of existing decision support system approaches to highlight their features/merits then to incorporate the missing parameters in the existing decision support systems to enhance these systems.

Using fuzzy and multiple criteria decision-making techniques was adopted by many researchers as shown in the reviews [13], [14]. For example [2] deployed two-stage fuzzy approach subjective measures to deal with order allocation and supplier selection problem. While [15] found that it is possible to choose a set of suited alternatives based on hybrid fuzzy decision making approach. Author in [16] presented decision-making problems based on fuzzy group and experts opinions, to present a solution that can adapt with conflicting quantitative and non-quantitative criteria of evaluation to determine the best alternative solution. In [17], authors presented organizational and technological perspective, to support the management of automated industry supply chain operations. The supplier selection process was performed based on the experts opinion to specify the important criteria by matching between subsidiary criteria and principal criteria to recognize the sub-criteria and relate them to the basic criteria.

Researches of the multi-criteria decision approaches was treated in [18]. In this review, the authors presented the studies that appeared in international journals in the years from 2000 to 2008. The reviewed paper focused on multi-criteria supplier and selection decision approaches. The presented approaches were analyzed to find the limitations by a critical study of the given approaches and then to determine which is the most widely used and adopted approaches in the supplier evaluation and selection problem. recently, authors in [7] presented an intelligent *DMPA* model based on a set of multi-criteria preferences that can be adopted by decision makers, in supply chain management and e-procurement processes, to select the appropriate offer among the presented offers from many suppliers.

In different approach [19] implemented a framework for *ERP* system selection with a set of thirty related features, and then evaluate the weight of each criterion by stepwise weight assessment ratio analysis (*SWARA*). While the ranking of all the alternatives was performed by preference ranking organisation method for enrichment of evaluations (*PROMETHEE*).

To realize the impact of the barriers and benefits on the e-procurement adoption decision for e-procurement systems the authors in [20] used Interpretive Structural Modeling (*ISM*) to describe any relations between the barriers and benefits of the barriers and benefits on the e-procurement selection process, then validate these relations by using Structural Equation Modeling (*SEM*).

In a sophisticated decision support system, it is difficult to select and evaluate offers given by different suppliers. Because of the variant constraints and the contradictory variables

that decision makers (governments or organizations) should consider before any decision is taken; an intelligent algorithm will be proposed to exploit a set of pre-selected determinants to evaluate and select the given offers to give decision makers the ability to choose the most offer that meet the selected determinants. The evaluation process will be performed based on multi-criteria determinants, given by the manager or by the customer, as it will be proven by the given experimental results.

The rest of this paper is structured as follows. The research problem definition is presented in Section 2, while the proposed decision support system model is explained by example in Section 3. In Section 4, the scoring of the *D3S* algorithm will be presented. Section 5 presents experimental results and finally, conclusion will be presented in Section 6.

III. PROBLEM DEFINITION

Decision making and supply chain management considered as important and critical tasks for any government and for any economic power. Given the importance of this topic, the presented research will highlight this problem by introducing a model that will deploy an intelligent algorithm based on a set of determinants selected in advance by the decision maker or the customer, the presented model will evaluate the supplier based on the given determinants by implementing these determinants into a group of variables. Each variable represents a certain criterion regarding the suppliers and the offers they present. The presented intelligent algorithm, the Decision Support and Selection System (*D3S*) adapt with all the preselected determinants (cost, after sale service, compatibility, etc.) to derive the best supplier with the best offer among many presented suppliers and offers.

The manager is the only responsible who decide the limit of his requirements of each constraint. For this reason, we fix a threshold variable evaluated by the manager to measure the distance between offer and demand for each variable. The pre-selected determinants will be represented by a set of variables represented by vector X where $X = \langle X_1, \dots, X_{15} \rangle$. The vector X is described by the following 15 elements:

- X_1 : Item name
- X_2 : Item maker
- X_3 : Item model
- X_4 : Required quantity
- X_5 : Number of trainees to use the item
- X_6 : Time required for training (Hours)
- X_7 : Max Budget (Dollar)
- X_8 : The time required to deliver the product (Days)
- X_9 : Warranty (Years)
- X_{10} : After sale services (Years)
- X_{11} : Available maintenance time (Days)
- X_{12} : Available maintenance time (Hours)
- X_{13} : Certificate of Origin (*yes, no, NA*).
- X_{14} : Size of company (*M, L, S, NA*)
- X_{15} : Company experience in the field of supply (Years).

Where,
Variables X_1, \dots, X_6 implement products determinants specified by the customer and the variable X_7 represents

budget limit. The variables X_8, \dots, X_{12} represent the services provided by the company. The variables X_{13}, \dots, X_{15} hold company details.

For the variable X_{14} , S, M, L refers to small, medium company and large companies respectively. While for the variables X_{13} and X_{14} the value NA represents “not applicable”. For the variables X_{13} and X_{14} , if the user chooses NA then the corresponding variable will not have any preferred value i.e. will not be considered when applying the evaluation process.

Example 1: For a given company, the *IT* section needs to buy 20 printers with some preferences which are fixed as follows: Item name is printer, Item maker is HP, Item model is “Laser Jet Pro 400”, Required quantity is 20, Number of trainees to use the item 3, Time required for training is 6 hours, Max Budget is 7000\$, The time required to deliver the product is 21 days, Warranty is 3 years, After sale services is 2 years, Available maintenance time 5 days and 8 hours, the Item must have Certificate of Origin, Size of company presenting the offer is not fixed as preference and the Company experience in the field of supply must be at least 4 years.

Based on the preferences given above for the customer, the variable X is modeled as follows: $X_1 = Printer$, $X_2 = HP$, $X_3 = Laser\ Jet\ Pro\ 400$, $X_4 = 50$, $X_5 = 3$, $X_6 = 6$, $X_7 = 7000$, $X_8 = 21$, $X_9 = 3$, $X_{10} = 2$, $X_{11} = 5$, $X_{12} = 8$, $X_{13} = yes$, $X_{14} = NA$ and $X_{15} = 4$.

The variables described in the vector X are classified into four categories. Each category will be denoted by a vector as follows:

- Item: $X^1 = \langle X_1, \dots, X_6 \rangle$
- Budget: $X^2 = \langle X_7 \rangle$
- Services: $X^3 = \langle X_8, \dots, X_{12} \rangle$
- Company: $X^4 = \langle X_{13}, \dots, X_{15} \rangle$

Thus, $X = \langle X^1, X^2, X^3, X^4 \rangle$.

We denoted by:

- j is the index offer
- $Y(j)$ the offer with j index.
- n the total number of presented offers.
- k the index representing the given determinants.

The presented offer j (before evaluation) will be denoted by $Y(j) = \langle Y_k(j), \text{with } k \in \{1, \dots, 15\} \rangle$. The vector $Y(j)$ can be written also based on the previous classification as $Y(j) = \langle Y^1(j), Y^2(j), Y^3(j), Y^4(j) \rangle$.

IV. DECISION SUPPORT SYSTEM MODEL

This section presents the mathematical model of the (*D3S*) by focusing on the decision variables which will form the basis of the evaluation process which will determine whether to continue evaluating or to reject the given offer.

A. Decisive Variables

The system must choose intelligently (considering the decisive variables) the best offer based on the given preferences specified by the customer. In this research only

X_1, X_2 and X_3 will be decisive variables, which means the first evaluation of the given offer j will be executed based on these variables (X_1, X_2 and X_3). Indeed, the first evaluation test will be: ($X_1 = Y_1(j)$ and $X_2 = Y_2(j)$ and $X_3 = Y_3(j)$) is true. Else, reject this offer with no more evaluations on the remaining variables.

Fig. 1 below shows the preliminary evaluation process based on decisive variables.

B. Decision Process

The preliminary process of *D3S* is given in Fig. 1. Several components is presented to show the steps of the proposed algorithm to determine the best offer among an amount of offers obtained after research.

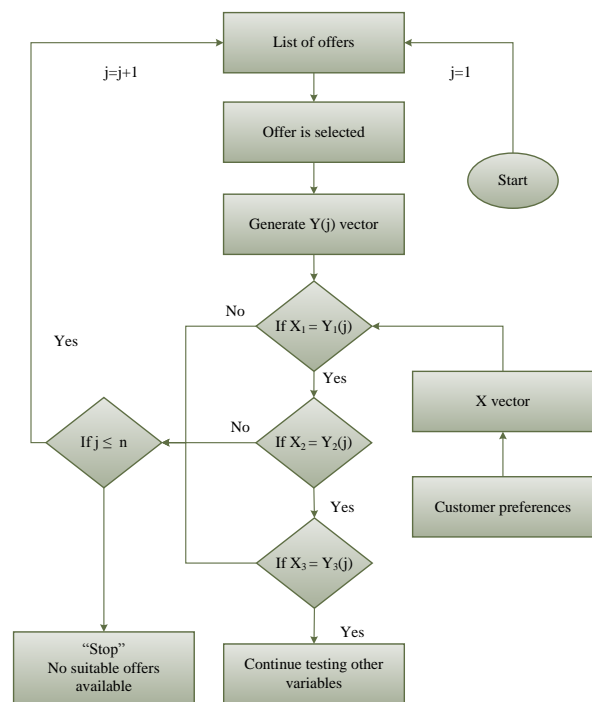


Fig. 1. The *D3S* preliminary model

Fig. 1 consists of the following components:

- List of offers: the offers have been inserted and stored in the database and can be used to create the offers list.
- Offer is selected: after having the offers list in “list of offers” component, the system select the offer number.
- Generate $Y(j)$ vector: all vector element values of $Y_i(j)$ will be retrieved from the list of offers.
- Customer preference: this component present the pre-selected determinants.
- X vector: the system generate a list contain all values of X_i corresponding elements. This list will be presented in the vector X .
- If $X_1 = Y_1(j)$: This component examine the equality between X_1 and $Y_1(j)$.

- If $X_2 = Y_2(j)$: This component examine the equality between X_2 and $Y_2(j)$.
- If $X_3 = Y_3(j)$: This component examine the equality between X_3 and $Y_3(j)$.
- If $i < n$: This component test if the number of the total offers have been reached. If $i < n$ the system must increment the value of i and restarted from the component “list of offers” with the new value of i .
- Continue test: If the decisive variables were tested and returned true, the system continue testing the remaining variables from X_4 to X_{15}
- Stop: if the total number of all offers have been reached, that mean there is no offer to test and the system must exit and returned the message “no offers are suitable based on the available determinants”.

V. SCORING AND ALGORITHMS OF THE D3S

This section explains how to define and derive the distance between a given offer and the specified threshold that will be determined based on the given determinants. the distance will be derived for all the variables from x_4 to x_{15} . After that the final calculated score of an offer will be explained. Finally, the D3S algorithms will be presented.

A. Distance Formulation

After finalizing decisive variables, we can separate these variables from the rest of the remaining variables. Thus, we will have a new sub-problem with 12 variables: $\{Y_4(j), \dots, Y_{15}(j)\}$. The question is How to create a model that deploys X_4 and X_{15} variables and can be used to derive the value of any given offer?

The first step is to specify any existing correlations between these 12 variables. This is can be performed by the application of t-students tests from SPSS software. The resulted values of t-students tests will be saved into w_i variables, which will be the weight w_i corresponding to each associated variable X_i with $i \in I = \{4, \dots, 15\}$. To measure the customer satisfaction rate a threshold for each I variables must be determined this threshold represents a bound measuring the customer satisfaction for each variables. The defined threshold will be denoted by Th_i the threshold of variable X_i with $i \in I$.

Now after defining the threshold for all the variables, it is primordial to give the distance between the threshold and the given values of each offer j variables with $i \in I$. The corresponding distance value will be in the interval of $[0-10]$. This distance will be denoted by d_i^j .

Proposition 1:

$$d_i^j = \frac{Y_i(j)}{Th_i} \times 10 \quad (1)$$

For special case when $Y_i(j) > Th_i$, when the distance exceeds 10. In this case we force d_i^j to be 10. This to guarantee that the best value is 10. Therefore, using Equation (1), the calculation of d_i^j will be as follows:

$$d_i^j = \begin{cases} \frac{Y_i(j)}{Th_i} \times 10 & \text{if } Y_i(j) \leq Th_i \\ 10 & \text{otherwise} \end{cases} \quad (2)$$

Example 2: Assume that $j = 20$ in this example. For the variable X_4 , the user requires $th_4 = 50$, however the company offer is $Y_4(20) = 30$. In this case the distance based on Equation 2 will be $d_4^{20} = \frac{Y_4(20)}{Th_4} \times 10 = \frac{30}{50} \times 10 = 6$, so the evaluation of the offer for the variable X_4 is 6 out of 10.

All distances d_i^j will be calculated by the D3S model. For the variable x_7 distance d_7^j and the variable x_{14} distance d_{14}^j , there are some extra calculations and will be explained in the subsections below.

1) *Budget distance:* For the variable $Y_7(j)$, we proceed with inverse evaluation. This means that when the budget will be more higher, the evaluation will be more lower and vice versa. For the budget calculations, specify the special evaluation based on the sign of T_B^j in the following equation of budget test, and defined as:

$$T_B^j = 1 - \frac{Y_7(j)}{Th_7}. \quad (3)$$

To specify weather the offer is expensive or meet the specifications determined by the customer, this will be derived from T_B^j as explained in Remark 4.

Remark 1:

$$T_B^j \begin{cases} > 0 & \text{is good than preferences} \\ = 0 & \text{exactly equal to preferences} \\ < 0 & \text{expensive than preferences} \end{cases} \quad (4)$$

Example 3: For offer 20, assume that the maximum budget $Y_7(20) = 40,000$ and the threshold Th_7 determined by the head manger is 30,000. In this case the presented offer exceeds the available budget by 10,000. Applying Equation 3 we have: $T_B^{20} = 1 - \frac{Y_7(20)}{Th_7} = 1 - \frac{40,000}{30,000} = 1 - 1.333 = -0.333$. Since $T_B^{20} = -0.333 < 0$ and referring to Equation 4 the system can deduce that the offer does not meet the given preferences.

Besides the weight factor in the model, we can add an other parameter related essentially to the budget because of the importance of this variable. To provide the customer with more options regarding the budget, so that to increase the effectiveness of the budget variable. we propose to introduce the multiplicity factor denoted by M as given by the following proposition.

Proposition 2: $d_7^j = M \times T_B^j$, with $M \in]0,10[$.

Indeed, the multiplicity factor is a real number that is determined by the customer to determine the degree of impact of the price in the model. In certain situations, the customer don't care about price, he just give importance to other variables. In these situations, the customer specify small value to multiplicity factor. On the other hand, if the customer is limited to a certain budget and price is a must to him, for this case the customer specify a high value of the multiplicity factor.

2) *Size of company distance*: The value of d_{14}^j is in $[0 - 10]$. For this reason, we propose the following measuring of corresponding distance d_{14}^j for the variable "Size of company".

The distances of the variable x_{14} will be presented in the Tables I, II, III and IV

TABLE I. SIZE OF COMPANY DISTANCE WHEN $X_{14} = M$

X_{14}	$Y_{14}(j)$	d_{14}^j
M	M	10
	L	10
	S	0
	NA	0

TABLE II. SIZE OF COMPANY DISTANCE WHEN $X_{14} = L$

X_{14}	$Y_{14}(j)$	d_{14}^j
M	M	0
	L	10
	S	0
	NA	0

TABLE III. SIZE OF COMPANY DISTANCE WHEN $X_{14} = S$

X_{14}	$Y_{14}(j)$	d_{14}^j
M	M	10
	L	10
	S	10
	NA	0

TABLE IV. SIZE OF COMPANY DISTANCE WHEN $X_{14} = NA$

X_{14}	$Y_{14}(j)$	d_{14}^j
M	M	10
	L	10
	S	10
	NA	10

B. Weights Calculation

Due to the relative importance of the budget, variables related to price will be given more weights. The weights values will be calculated based on the econometric model by the SPSS based on the previous offers calculations to specify the required t-student values for the specified variables.

C. Scoring Formulation

To help decision-makers, the offers are ranked for easier calculations. The previously defined weights and distances will be used to determine offers scoring values, these values will be in the range $[0 - 100]$. For each Y element the distance d_i^j between $Y_i(j)$ and the threshold value Th_i must be calculated where $i \in \{4, \dots, 15\}$. The customer (decision maker) specifies the threshold for each given offer j . Calculations of the distance are related to $\langle Y_4(j), \dots, Y_{15}(j) \rangle$.

The following proposition explain the score for every given offer j denoted by Sc_j and is as follows:

Proposition 3:

$$Sc_j = \frac{\sum_{i=4}^{15} (w_i \times d_i^j)}{\sum_{i=4}^{15} w_i} \times 10 \quad (5)$$

Proof: Each d_i^j is in the interval of $[0 - 10]$. the multiplication of each d_i^j by the corresponding weight w_i for all $i \in \{4, \dots, 15\}$ will be defined as the total weighted distance (TWD). The resulted TWD will be divided by $\sum_{i=4}^{15} w_i$ to obtain a value, multiplying this value by 10 will obtain Sc_j . ■

Table VII, shows interval values descriptions:

TABLE V. INTERVAL SCORE VALUE DESCRIPTION

Num	Rank interval	Description
1	$[0 - 20[$	Rejected
2	$[20 - 40[$	Not considered
3	$[40 - 50[$	Below preferences
4	$[50 - 60[$	Acceptable
5	$[60 - 70[$	Good offer
6	$[70 - 80[$	Very good
7	$[80 - 85[$	Excellent
8	$[85 - 90[$	Very excellent
9	$[90 - 95[$	Exceptional
10	$[95 - 100]$	Very exceptional

Example 4: Assume that the weights of each variable is given following:

$w_4 = 17.8; w_5 = 1.1; w_6 = 1.3; w_7 = 4.6; w_8 = 1.9; w_9 = 1.6; w_{10} = 2.1; w_{11} = 1.9; w_{12} = 3.1; w_{13} = 1.2; w_{14} = 1.4; w_{15} = 2.1$ For offer number 6, assume we have the following calculated distances:

$d_4^6 = 9.8; d_5^6 = 3.3; d_6^6 = 10; d_7^6 = 0; d_8^6 = 7.8; d_9^6 = 10; d_{10}^6 = 10; d_{11}^6 = 8; d_{12}^6 = 6.3; d_{13}^6 = 0; d_{14}^6 = 0; d_{15}^6 = 8.$
 $Sc_6 = \frac{\sum_{i=4}^{15} (w_i \times d_i^6)}{\sum_{i=4}^{15} w_i} \times 10 = \frac{294.3}{40.1} \times 10 = 73.4.$ Refer to Table V, the 6th offer is a "Very good offer".

D. D3S Algorithms

that will be used by the this section presents 4 algorithms D3S model. The first algorithm is devoted for the calculations of Sc_j score. while the second algorithm will be used to select the best offer. The evaluation of the best score determined by the manager will be calculated by the third algorithm. The last algorithm accurate all the previous algorithms to formulate D3S.

The next algorithm will be used to calculate all the distances d_i^j and the vector weights W in order to find the score Sc_j of the certain offer j

Algorithm 1 *Scoring*($Y(j)$) algorithm for calculation of the Sc_j score

- 1: **for** $i = 4$ to 15 **do**
- 2: Calculate d_i^j
- 3: **end for**
- 4: $W = SPSS(X)$
- 5: $Sc_j = \frac{\sum_{i=4}^{15} w_i \times d_i^j}{\sum_{i=4}^{15} w_i}$
- 6: **Stop.** Return Sc_j .

After defining Sc_j , we move to calculate the best score of the given n offers as the next algorithm shows.

Algorithm 2 Best offer selection algorithm: $Best(j)$

```

1: Initialize  $X, Th$ .
2: for  $j = 1$  to  $n$  do
3:   if  $(X_1 = Y_1(j) \text{ and } X_2 = Y_2(j) \text{ and } X_3 = Y_3(j))$ 
   then
4:     Calculate  $Sc_j = Scoring(Y(j))$ .
5:   else
6:     Stop. "Rejected offer".
7:   end if
8: end for
9:  $Sc = \max(Sc_j)$ .
10:  $best = j$  where  $Sc = Sc_j$ 
11: Stop. Return  $best$ .

```

After getting the best scores for the given n offers. The next step is to evaluate the description of the offer referring to the Table VII. Suppose that the latter table is saved in a pointer table named $Desc$. We denote by $Desc(Sc_j)$ (Description of the obtained score) the function that devoted to return the description of the score given as an input of the function refereeing to the table pointer $Desc_s.c$.

Algorithm 3 Evaluation algorithm of the best score: $Evaluation()$

```

1:  $desc = Desc(best)$ 
2: Print  $desc$  to the manager
3: Print cases to the manager (1) or :
4: case (1)
5:   "Accept the best offer"
6: case (2)
7:   "Refuse the best offer"
8: if (1) is selected then
9:   send the best offer to the financial department
10: else
11:   Reminder with fixed date and time to search another time.
12: end if

```

Now we use the previous algorithms to generate the $D3S$ final algorithm as follows:

Algorithm 4 $D3S$ scoring algorithm

```

1: for  $j = 1$  to  $n$  do
2:    $best = Best(j)$ 
3: end for
4:  $Evaluation(best)$ 
5: Stop.

```

VI. EXPERIMENTAL RESULTS

For more explanations the given algorithms were implemented by Microsoft Visual C++ (Version 2012). The implemented algorithms were executed by 8GB RAM i5 PC. Decisive variables in these experiments are as follows: $X_1 = PC$; $X_2 = HP$; $X_3 = xa03nf$. We received a total of 55 offers. 28 of the received offers were rejected after applying decisive variables leaving 27 offers for evaluation.

The customer specifies the maximum budget by 4,000\$. Due to this limitation 17 out of the remaining 27 offers will be dropped leaving only 10 offers to be considered. the values regarding vector X and $Y(j)$ elements with $j \in \{1, \dots, 10\}$ are shown in Table VI below. The 10 offers weight and distances are shown in Table VII. Finally, Table VIII represents the 10 pre-selected offers derived scores.

TABLE VI. OFFER AND PREFERENCES

	Preferences		Offer				
			1	2	3	4	5
TH	1	PC	PC	PC	PC	PC	PC
	2	HP	HP	HP	HP	HP	HP
	3	xa03nf	xa03nf	xa03nf	xa03nf	xa03nf	xa03nf
	4	50	54	43	52	30	50
	5	3	2	1	2	3	4
	6	2	1	2	3	1	2
	7	3354	3100	3210	3258	3548	3344
	8	9	8	7	9	10	11
	9	3	2	1	3	3	2
	10	1	1	1	1	1	2
	11	5	5	4	3	5	3
	12	8	8	7	8	4	4
	13	yes	yes	yes	No	NA	NA
	14	M	M	L	S	S	NA
	15	5	5	8	2	3	2

	Preferences		Offer				
			6	7	8	9	10
TH	1	PC	PC	PC	PC	PC	PC
	2	HP	HP	HP	HP	HP	HP
	3	xa03nf	xa03nf	xa03nf	xa03nf	xa03nf	xa03nf
	4	50	49	52	50	53	22
	5	3	1	2	3	1	4
	6	2	3	4	3	2	1
	7	3354	3351	3245	3158	3111	3987
	8	9	7	9	8	12	4
	9	3	3	2	1	2	2
	10	1	2	1	2	1	1
	11	5	4	5	3	4	4
	12	8	5	6	7	7	7
	13	yes	No	yes	NA	No	NA
	14	M	S	L	M	NA	L
	15	5	4	20	10	0	1

TABLE VII. WEIGHTS AND DISTANCES

	w_i	d_i^j				
		1	2	3	4	5
4	17.8	10.0	8.6	10.0	6.0	10.0
5	1.1	6.7	3.3	6.7	10.0	10.0
6	1.3	5.0	10.0	10.0	5.0	10.0
7	4.6	0.8	0.4	0.3	-0.6	0.0
8	1.9	8.9	7.8	10.0	10.0	10.0
9	1.6	6.7	3.3	10.0	10.0	6.7
10	2.1	10.0	10.0	10.0	10.0	10.0
11	1.9	10.0	8.0	6.0	10.0	6.0
12	3.1	10.0	8.8	10.0	5.0	5.0
13	1.2	10.0	10.0	0.0	0.0	0.0
14	1.4	10.0	10.0	0.0	0.0	0.0
15	2.1	10.0	10.0	4.0	6.0	4.0

	w_i	d_i^j				
		6	7	8	9	10
4	17.8	9.8	10.0	10.0	10.0	4.4
5	1.1	3.3	6.7	10.0	3.3	10.0
6	1.3	10.0	10.0	10.0	10.0	5.0
7	4.6	0.0	0.3	0.6	0.7	-1.9
8	1.9	7.8	10.0	8.9	13.3	4.4
9	1.6	10.0	6.7	3.3	6.7	6.7
10	2.1	10.0	10.0	10.0	10.0	10.0
11	1.9	8.0	10.0	6.0	8.0	8.0
12	3.1	6.3	7.5	8.8	8.8	8.8
13	1.2	0.0	10.0	0.0	0.0	0.0
14	1.4	0.0	10.0	10.0	0.0	10.0
15	2.1	8.0	10.0	10.0	0.0	2.0

TABLE VIII. SCORING OFFERS

	Index	Sc_i
Offer	1	85.0
	2	75.4
	3	76.4
	4	56.0
	5	71.8
	6	73.4
	7	84.7
	8	80.2
	9	74.1
	10	46.8

The description of each offer will be presented by Table V:

- Offer 1: Very excellent
- Offer 2: Very good
- Offer 3: Very good
- Offer 4: Acceptable
- Offer 5: Very good
- Offer 6: Very good
- Offer 7: Exceptional
- Offer 8: Excellent
- Offer 9: Very good
- Offer 10: Below preferences

Based on the given valued the chosen offer (the best offer) is offer 7.

VII. CONCLUSION

In order to cope with the technological, economical and political challenges, in the case of supply chain management and e-procurement; decision makers should consider all these limitations when evaluating or selecting a given offer. To highlight this challenge, this paper presented an intelligent *D3S* model, which consists of 4 developed algorithms and preliminary *D3S* model. The developed *D3S* model is based on multi-criteria evaluation and selection intended to be used as a decision support system, that can be utilized by the decision makers in their evaluation during the supply chain management or the e-procurement processes. Experimental results showed that the deployment of the *D3S* derived the best offer among a set of presented offers while considering a given determinants specified by the customer.

ACKNOWLEDGMENT

The authors would like to thank the Deanship of Scientific Research at Majmaah University for supporting this work under Project Number No. 1440-88

REFERENCES

[1] A. Aalaei and H. Davoudpour, "Revised multi-choice goal programming for incorporated dynamic virtual cellular manufacturing into supply chain management: A case study," *Engineering Applications of Artificial Intelligence*, vol. 47, pp. 3–15, 2016.

[2] F. Çebi and İ. Otay, "A two-stage fuzzy approach for supplier evaluation and order allocation problem with quantity discounts and lead time," *Information Sciences*, vol. 339, pp. 143–157, 2016.

[3] A. Gunasekaran, Z. Irani, K.-L. Choy, L. Filippi, and T. Papadopoulos, "Performance measures and metrics in outsourcing decisions: A review for research and applications," *International Journal of Production Economics*, vol. 161, pp. 153–166, 2015.

[4] K. Govindan, S. Rajendran, J. Sarkis, and P. Murugesan, "Multi criteria decision making approaches for green supplier evaluation and selection: a literature review," *Journal of Cleaner Production*, vol. 98, pp. 66–83, 2015.

[5] F. R. Lima-Junior and L. C. R. Carpinetti, "A multicriteria approach based on fuzzy qfd for choosing criteria for supplier selection," *Computers & Industrial Engineering*, vol. 101, pp. 269–285, 2016.

[6] S. Bali and S. S. Amin, "An analytical framework for supplier evaluation and selection: a multi-criteria decision making approach," *International Journal of Advanced Operations Management*, vol. 9, no. 1, pp. 57–72, 2017.

[7] M. Jemmali, M. Alharbi, and L. K. B. Melhim, "Intelligent decision-making algorithm for supplier evaluation based on multi-criteria preferences," in *2018 1st International Conference on Computer Applications & Information Security (ICCAIS)*. IEEE, 2018, pp. 1–5.

[8] A. K. Kar, "Revisiting the supplier selection problem: An integrated approach for group decision support," *Expert systems with applications*, vol. 41, no. 6, pp. 2762–2771, 2014.

[9] A. Zouggar and L. Benyoucef, "Simulation based fuzzy topsis approach for group multi-criteria supplier selection problem," *Engineering Applications of Artificial Intelligence*, vol. 25, no. 3, pp. 507–519, 2012.

[10] F. Dweiri, S. Kumar, S. A. Khan, and V. Jain, "Designing an integrated ahp based decision support system for supplier selection in automotive industry," *Expert Systems with Applications*, vol. 62, pp. 273–283, 2016.

[11] S. Brownlow and S. Watson, "Structuring multi-attribute value hierarchies," *Journal of the Operational Research Society*, vol. 38, no. 4, pp. 309–317, 1987.

[12] A. Naseem, S. T. H. Shah, S. A. Khan, and A. W. Malik, "Decision support system for optimum decision making process in threat evaluation and weapon assignment: Current status, challenges and future directions," *Annual reviews in control*, vol. 43, pp. 169–187, 2017.

[13] A. Mardani, A. Jusoh, and E. K. Zavadskas, "Fuzzy multiple criteria decision-making techniques and applications—two decades review from 1994 to 2014," *Expert systems with Applications*, vol. 42, no. 8, pp. 4126–4148, 2015.

[14] R. M. Rodríguez, Á. Labella, and L. Martínez, "An overview on fuzzy modelling of complex linguistic preferences in decision making," *International Journal of Computational Intelligence Systems*, vol. 9, no. sup1, pp. 81–94, 2016.

[15] L. Ferreira, D. Borenstein, and E. Santi, "Hybrid fuzzy madm ranking procedure for better alternative discrimination," *Engineering Applications of Artificial Intelligence*, vol. 50, pp. 71–82, 2016.

[16] B. Vahdani, S. M. Mousavi, H. Hashemi, M. Mousakhani, and R. Tavakkoli-Moghaddam, "A new compromise solution method for fuzzy group decision-making problems with an application to the contractor selection," *Engineering Applications of Artificial Intelligence*, vol. 26, no. 2, pp. 779–788, 2013.

[17] J. Carvalho, M. L. R. Varela, G. D. Putnik, J. E. Hernández, and R. A. Ribeiro, "A web-based decision support system for supply chain operations management towards an integrated framework," in *Decision Support Systems III-Impact of Decision Support Systems for Global Environments*. Springer, 2013, pp. 104–117.

[18] W. Ho, X. Xu, and P. K. Dey, "Multi-criteria decision making approaches for supplier evaluation and selection: A literature review," *European Journal of operational research*, vol. 202, no. 1, pp. 16–24, 2010.

[19] S. Shukla, P. Mishra, R. Jain, and H. Yadav, "An integrated decision making approach for erp system selection using swara and promethee method," *International Journal of Intelligent Enterprise*, vol. 3, no. 2, pp. 120–147, 2016.

[20] P. Toktaş-Palut, E. Baylav, S. Teoman, and M. Altunbey, "The impact of barriers and benefits of e-procurement on its adoption decision: An empirical analysis," *International Journal of Production Economics*, vol. 158, pp. 77–90, 2014.

Techniques, Tools and Applications of Graph Analytic

Faiza Ameer¹, Muhammad Kashif Hanif², Ramzan Talib³, Muhammad Umer Sarwar⁴,
Zahid Khan⁵, Khawar Zulfiqar⁶, Ahmad Riasat⁷
Department of Computer Science,
Government College University,
Faisalabad, Pakistan

Abstract—Graphs have acute significance because of poly-tropic nature and have wide spread real world big data applications, e.g., search engines, social media, knowledge discovery, network systems, etc. Major challenge is to develop efficient systems to store, process and analyze large graphs generated by these applications. Graph analytic is important research area in big data graphs dealing with efficient extraction of useful knowledge and interesting patterns from rapidly growing big data streams. Tremendously huge and complex data of graph applications requires specially designed graph databases having special data structures and effective features for data modeling and querying. The manipulation of large size of data requires effective scalable and distributed computational techniques for efficient graph partitioning and communication. Researchers have proposed different analytical techniques, storage structures, and processing models. This study provides insight of different graph analytical techniques and compares existing graph storage and computational technologies. This work also assesses the performance, strengths and limitations of various graph databases and processing models.

Keywords—Graph; graph analytic; big data; graph tools; analytical techniques

I. INTRODUCTION

Graphs have astute magnitude due to their versatile and expressive nature. Real world big data problems like weather forecasting, geographical changes, large network systems, social networks, semantic search and knowledge discovery, text mining, IOT, cyber security, etc. all can be viewed and modeled as graphs.

Graphs can be used to represent and analyze big data. Big data is huge volume, high velocity and a large variety of information asset that demands cost effective, and innovative forms of information processing for enhanced insight and decision making [1]. The term huge volume refers to the large size of static or continuously growing data like Facebook, Twitter, Google, etc. High Velocity represents the required speed of data generation, and analysis. Large variety means the use of various types of structured (e.g., data from relational databases), semi-structured (e.g., XML and JSON documents), and unstructured data (e.g., video, audio, images etc.) [1].

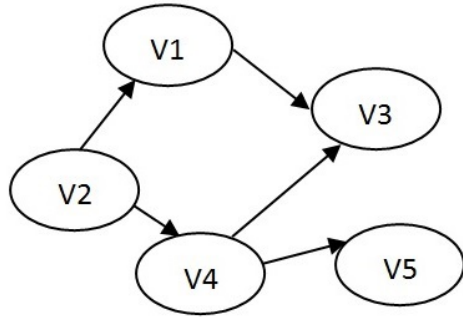
Graph analytic is based on graph theory (a branch of Mathematics). Graph theory was born out of a very practical urban planning problem. The problem started in Königsberg (old city in Russia). The city had two large islands, connected by seven bridges. Back in 1736, the problem was to devise a walkway from one part of city to another by traversing

all seven bridges only once. A mathematician, named Euler, proved mathematically that this problem had no solution due to odd number of bridges. He reformulated the problem and solved it by eliminating all features except land masses (termed as vertex) and the connecting bridges (termed as edge). The resulting mathematical structure was called a graph (Fig. 1). By solving this problem, Euler laid down the foundations of whole field of graph theory [2]. Different operations which can be performed on a graph are add/remove a vertex, add/remove an edge, or find the nearest neighbors (i.e., finding nodes connected to the vertex), etc.

Graph analytic models large and complex data problems as a set of graphs. It expresses relationship patterns of objects by exploiting the mathematical properties of data and statistical modeling techniques to provide efficient algorithmic solutions and discover meaningful patterns [2]. Many organizations are competing with their peers in market using graph analytic by making accurate and timely decisions [2]. There exists variant techniques for graph analytic like path analytic, connectivity analytic, centrality analytic, and community analytic based on solution to different types of problems [2]. Each one of them use different principles and methods to answer divergent analytical questions.

To handle large graphs, new systems incorporate efficient storage and processing technologies. The new database technologies fulfill the growing requirements of current applications and cover the limitations of traditional database models. Modern graph related database management system includes graph databases and graph stores [3]. These databases provide general features for data storage, data modeling, and support for graph queries and query languages. Use of graphs in big data have also generated much interest in the field of large-scale graph data processing. Modern parallel processing systems are based on four different processing models: MPI-Like, Map-Reduce, BSP, and Vertex-Centric Graph Processing. Pregel, Giraph, GPS, Mizan, and GraphLab are important parallel processing models.

The remainder of the paper is organized in different sections. Section II gives a brief overview of the applications of graphs. Section III describes different graph analytic techniques. In Section IV, graph storage techniques are discussed. Section V provides different processing models for large graphs. At the end, we conclude the outcomes.



	V1	V2	V3	V4	V5
V1			1		
V2		1		1	
V3			1		1
V4					
V5					

Fig. 1. Sample graph and its representation using adjacency matrix.

II. SOME APPLICATIONS/USE CASES OF GRAPHS

A. Social Media

A Facebook page contains some elements, e.g., primary users, friends, groups, and posts. The posts may contain text, tags, and media such as images and videos. Some people comment and like posts. The commenter must be a Facebook user. Other people may also like or respond to some of the comments. Many posts have locations associated with them. If all of these are considered together, graph can be made to visualize almost the same types of information. In graphs, everything can be organized in terms of objects and relationship of these objects (Fig. 2).

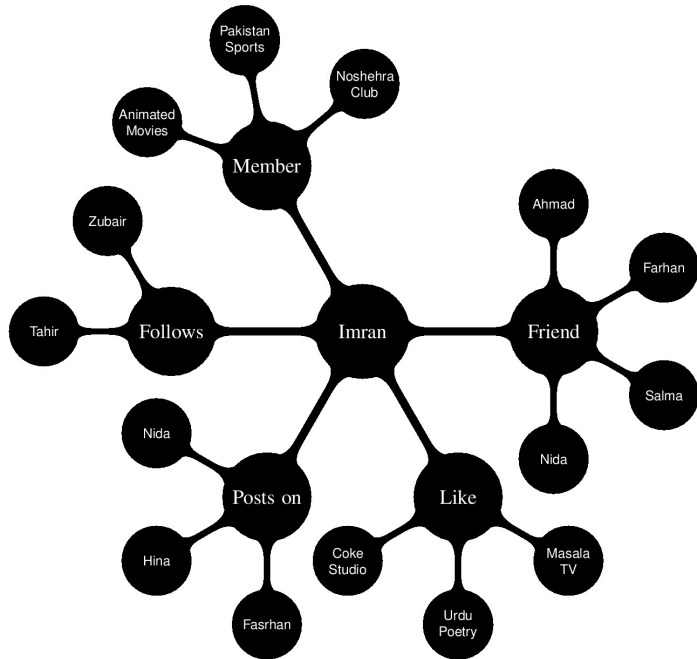


Fig. 2. An example of social media graph.

Graphs can help to answer different questions [2]. For example,

- Behavioral psychologists, want to know, that a war game user or any other violent game user, also shows violent behavior in online fighting or not?
- Following somebody's post over time and applying text mining techniques, it can be investigated that person is addicted to the game or not.
- Are there groups? What are these groups? Who are the most influential users in group? Which people are referred to, listened by everybody? Are the players interacting with other players? Where they belong to? Who are they? Do they form a close community? (Fig. 3).

B. Analysis and Planning of Smart Cities

Cities have multiple interacting networks including transportation networks, water and sewage networks, power transmission networks, broadband IP, and M2M networks. Each network has multiple subtypes, e.g., transportation networks include the bus networks, the subway network, and the railway network, etc. These networks can be represented as graphs where each node has a geographical coordinate (Fig. 4).

A city planner would like to make sure that he covers the entire city with optimized traversal time and plan traffic congestion. To accomplish this, he would need to create a network model. During planning, he needs to make sure that all the right things happen at the same place. For example, people coming out of metro stations will find nearby businesses, IP network, and water supply. Network models also represent congestion, people's behavior, materials behavior, and energy use patterns for network.

C. Fraud Detection

Traditional fraud prevention measures focused on discrete data points such as specific accounts, individuals, devices or IP addresses. Sophisticated fraudsters use stolen and synthetic identities to escape detection. Graph databases (e.g., Neo4j) are used beyond individual data points to the connections that link these fraud rings. They uncover difficult to detect patterns in real time as well as with high accuracy [6]. Taking example of bank, following are some common fraud patterns:

- A group containing two or more people organize a fraud ring.

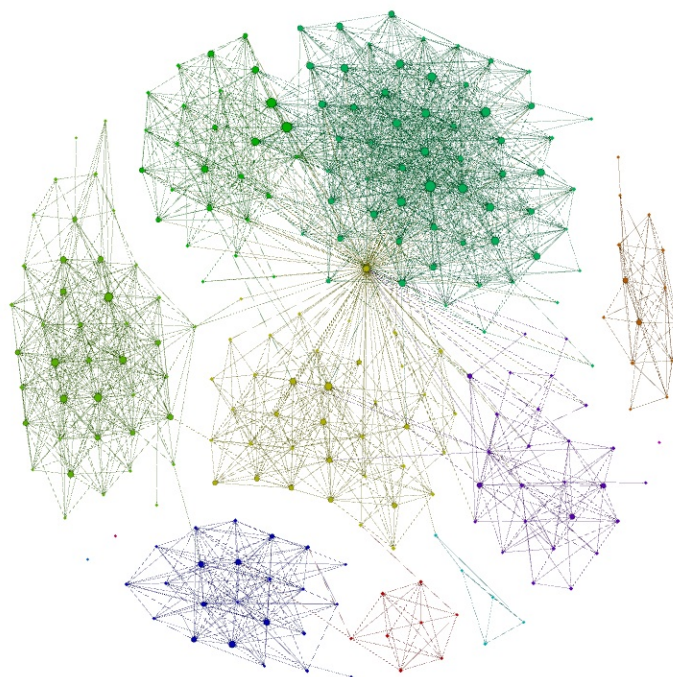


Fig. 3. Visualizing groups in graph [4].

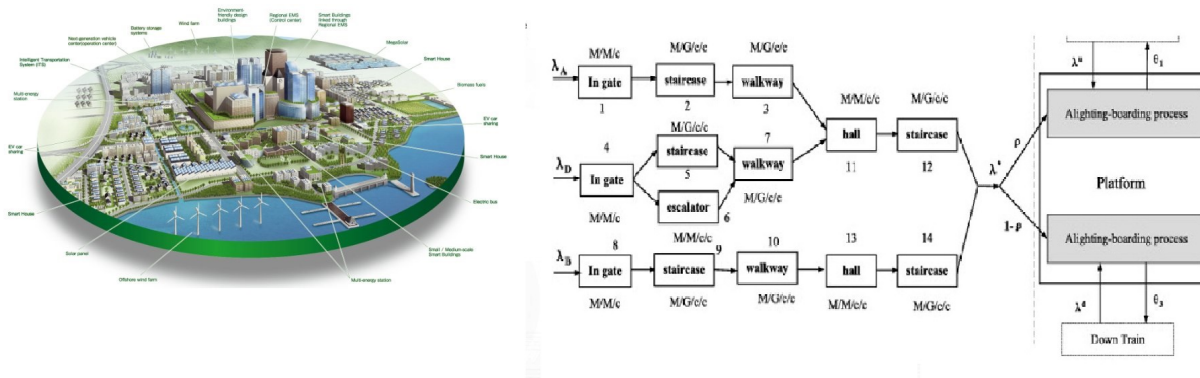


Fig. 4. Graph in planning a smart city [5].

- These people open accounts using fictional identities with subset of shared contact information, i.e., phone numbers and addresses.
- New accounts are added to the original unsecured credit lines, credit cards, overdraft protection, and personal loans.
- When banks increase the revolving credit lines, the ring breaks in, coordinate their activity, max out all of their credit lines, and disappear.
- Sometimes, fraud rings bring all of their balances to zero using fake cheques immediately before the prior step, doubling the damage.
- Even after identification of fraud ring, agents are never able to reach the fraudster in real time.
- The due debt is written off without paying due amount.

Through graph database, bank's existing fraud detection infrastructure can be implied to support ring detection during key stages in the customer and account life cycle. Real time graph analysis can help banks identify probable fraud rings (Fig. 5).

III. GRAPH ANALYTIC TECHNIQUES

The techniques for graph analytic include path analytic, connectivity analytic, community analytic and centrality analytic.

A. Path Analytic

Path analytic deals with finding the best path between two given nodes. Specification of "best" may include optimization of specific function, traversal of certain nodes/edges, avoidance of nodes/edges, and satisfaction of some preferences. For example,

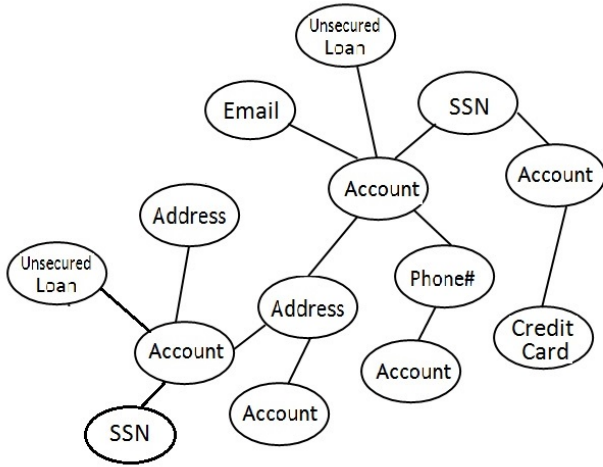


Fig. 5. Graphs in bank fraud detection.

In Google maps, shortest route would change based on weather, traffic, and road conditions.

A standard method for finding least weighted path is Dijkstra's algorithm. Complexity for applying Dijkstra's algorithm for big data is very high. The worst case complexity of Dijkstra is proportional to the number of edges times log (number of nodes). For 1 million nodes and 10 million edges, the worst case complexity is proportional to approximately 14 million [2]. There are several modification of Dijkstra's algorithm to enhance the performance, e.g., Bi-directional Dijkstra Algorithm, Goal-directed Dijkstra Algorithm, etc.

B. Connectivity Analytic

Connectivity analytic explores the connectivity pattern and similarity between structures of graphs based on different features. It also discovers robustness, i.e., which node should be the next target of attacker.

Degree of a node is the number of edges connected to a node. Through degree of nodes, we can specify if a node is more connected than another. Degree of the node can be calculated by adding in-degree (incoming edges) and out-degree (outgoing edges) of the node. Similarity of the graph can be found by comparing degree histogram of the graphs and calculating vector distance of histogram. Degree histogram contains number of nodes against degree value of node. Graph similarity can be calculated by Euclidean distance (Fig. 6) using the vector distance function given in Equation (1).

$$D = \sqrt{\sum_{i=0}^k (h_{1i} - h_{2i})^2} \tag{1}$$

There are many other sophisticated methods/formulas available to compare graph similarities, e.g., Hellinger distance, Histogram intersection etc. A joint, two dimensional colorful histogram of the graph, provides more insight about the graph [2]. For example, in a social networking graph, the

nodes with more incident edges than outgoing edges represent members who are listeners.

Graph 1		Graph 2	
Degree	Count	Degree	Count
0	1	0	1
1	3	1	3
2	0	2	1
3	3	3	2
4	0	4	0
5	4	5	4
6	2	6	3

Euclidian Distance = $\sqrt{3}$

Fig. 6. Using histogram for finding graphs similarity.

For measuring robustness of the network, we have to evaluate how much a structure is affected by an attack. It can be done using Weighted Spectral Distribution (WSD). WSD emphasizes the contribution of eigenvalues believed to be important [7].

C. Community Analytic

A cluster of nodes which are more connected to inside of the cluster than outside of the cluster is called community (Fig. 7). Community analytic deals with detection and behavior pattern of communities. For example, who are member of community? From where they belong to? Is the community stable? Dominant members in the community? Is community evolving, growing, splitting or going to be dead? Internal degree of a sub graph is the summation of edges of all vertices within the cluster. Summation of edges of all vertices outside the sub graph is called external degree of cluster.

Communities are found by comparing internal and external degrees of clusters. A cluster having more internal density (Equation (2)) than external density (Equation (3)) is called community.

$$\delta_{int} = \frac{\# \text{ of internal edges in } C}{n_c(nC - 1)/2} \tag{2}$$

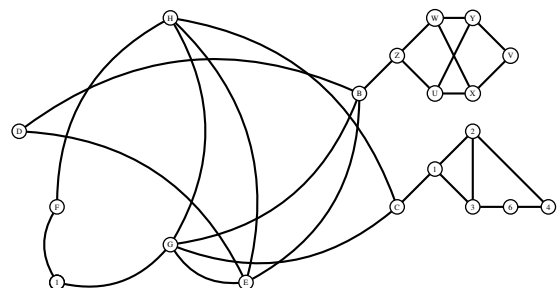


Fig. 7. Communities

$$\delta_{ext} = \frac{\# \text{ of inter cluster edges of } C}{n_c(n - nC)} \quad (3)$$

A community always have higher internal density than external density. A community have different local properties (i.e., clique, n-clique, n-clan, and k-core) and a global property which is called modularity. Modularity is a global property of graph. It estimates the quality of the cluster. Louvain community detection is one of methods of detecting community and finding modularity of network/community. Clique is a perfect community where every vertex is connected to every other vertex in the cluster. Finding cliques is computationally very hard problem as compared to finding k-size cliques (Fig. 8). n-clique and n-clan are distance based measures while k-core is a density based method of finding community. n-clique is a sub graph having distance of length not more than n between each member. n-clan is an n-clique having distance between all nodes not more than n and without involving outsider nodes. k-core is a cluster in which each vertex is directly connected to at least k other vertices of the cluster.

D. Centrality Analytic

Centrality analytic characterizes important nodes (influencers) of a network with respect to a specific analysis problem. Their significance is detected by looking at how central they are in a community. We know that every node does not have equal importance in a network. Some nodes are more important than others in specific perspectives. For example, a central server in a computer network, a junction station in a transport network etc. We need to find the nodes which are maximally connected to other nodes and the nodes if removed would maximally disturb the communication of other nodes. Network centrality has centrality and centralization characteristics. Centrality is the measure of importance of a node (or edge) based on its position in the network. While, centralization is the measure for a network (not just a single node). If more nodes start having higher centrality, then there is less variation in the centrality values of the network. As a result, the centralization of the network drops (Fig. 9).

Network centralization is the sum of the difference between the maximum centrality and the centrality of the node divided by the maximum centrality (Equation (4)).

$$\text{Centralization} = \frac{\sum(c_{max} - c(v_i))}{c_{max}} \quad (4)$$

There are many types of centrality including degree centrality, closeness centrality, betweenness centrality, eigenvector centrality, and katz centrality. There are different principles and methods to calculate centrality values.

IV. GRAPH STORAGE TECHNIQUES

As the size increases, more edges stream into graphs adding more data into database and making real time analysis a challenge. These graphs may be stored both in RDBMS or NoSQL for efficient query processing using supportive query languages. Currently, NoSQL databases are schema less

databases and are getting more attention due to high scalability and fault-tolerance. NoSQL databases can have key/value stores (e.g., Apache Cassandra), document stores (e.g. MongoDB), and graph databases (e.g., AllegroGraph, Neo4J, OpenLink Virtuoso) [8]. There are two types of database management system for graphs, i.e., graph stores and graph databases.

Graph stores provide facilities for storing and querying graphs. G-Store is a storage manager for large vertex-labeled graphs. Redis graph is a Python implementation for storing graphs. VertexDB implements a graph store on top of TokyoCabinet (a B-tree key/value disk store). Filament is a graph storage library with default support for SQL through JDB. Additionally, we can mention CloudGraph, Horton, and Trinity as prototypes of graph stores [3].

Graph databases can have better speedups over relational databases for selected problems. For example, graph queries formulated in terms of paths can be concise and intuitive [8]. Graph databases must provide database languages (for data definition, manipulation and querying), query optimizer, database engine, external interfaces, storage engine transaction engine, management, and operation features (tuning, backup, recovery, etc.). Some databases available according to above criteria are DEX (Sparksee), AllegroGraph, InfiniteGraph, HypergraphDB, Neo4J, and Sones.

DEX (Sparksee) is a high performance graph database management system based on bitmaps and other secondary structures. DEX works efficient for the manipulation of very large graphs. DEX uses a java library for management of graphs [9]. AllegroGraph was initially developed as graph database and meets the semantic web standards (i.e., RDF/S, SPARQL and OW) [3]. AllegroGraph also provides special features for geo-temporal reasoning and social network analysis.

InfiniteGraph is an object-oriented database to support large-scale graphs in a distributed environment [3]. It provides the efficient traversal of relations across massive and distributed data stores. HyperGraphDB is highly customizable system based on hypergraph database model. It represents complex and large scale domain specific knowledge within uniform conceptual framework. It removes usual difficulties while dealing with higher order relationships [10]. It is useful for modeling data of complex applications like artificial intelligence, bio-informatics, and natural language processing. Most graph database models supports different features like graph structures, data definition and manipulation, storage, essential graph queries, basic integrity constraints, and representation of entities and relationships [3].

V. COMPUTATIONAL MODELS FOR GRAPH PROCESSING

A parallel computational model abstractly specifies the way a parallel program will run. In parallel computational model, a program is divided into multiple concurrently running processes. It decides how and when these processes communicate and exchange data. It also observes how parallelism is actually achieved. In shared memory architecture, the memory of multiple machines is virtually considered as a single large memory. While in message passing model, the processes can directly pass messages to and from other processes or they can use a common message carrying pipe. There are also multiple ways for achieving parallelism, e.g., task parallelism,

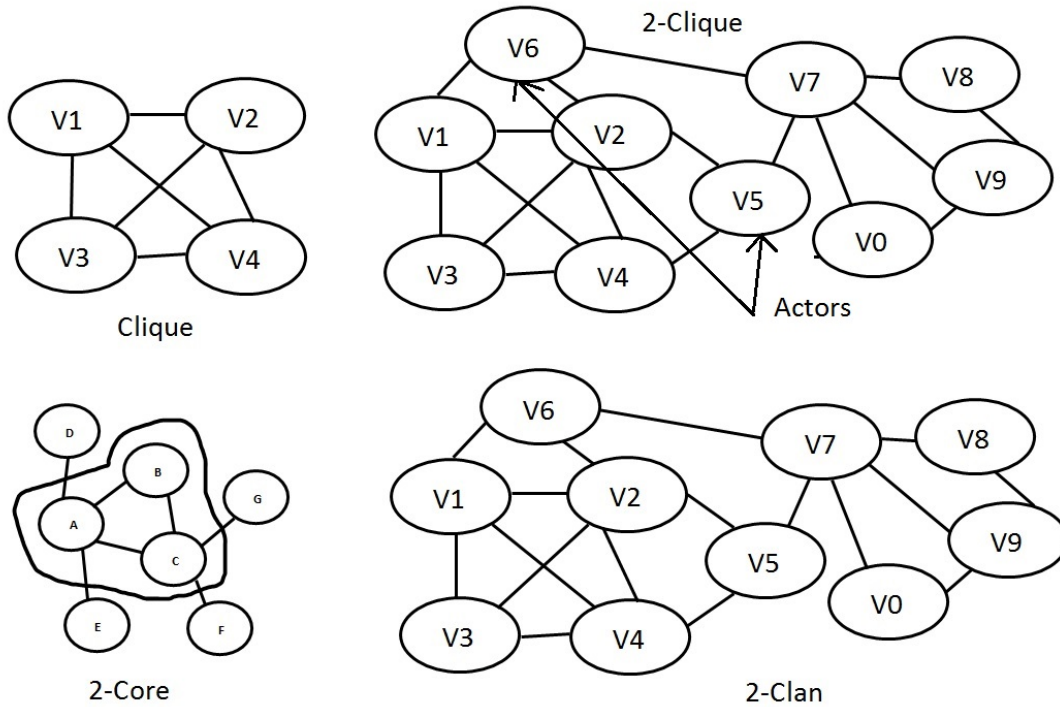


Fig. 8. Clique, n-clique, n-clan, k-core

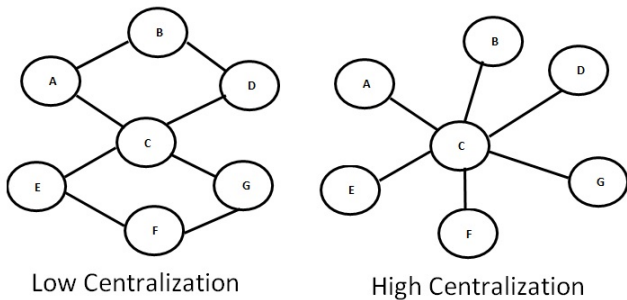


Fig. 9. Centralization of a network

data parallelism. In data parallelism, the data is divided into partitions. While in task parallelism, a single task is divided into multiple sub-tasks. In both cases, the partitions are synchronized and can run independently of each other. A computational model is independent of the programming languages.

Some of widely used techniques for implementation of big graph processing algorithms are:

- A customized distributed infrastructure can be developed [11]. It requires different implementation for different graph and its processing algorithm.
- An existing distributed computing platform can be utilized, like Map-Reduce, or SQL-like queries. However, these structures are often ill suited and lead to suboptimal performance and usability issues for graph

processing [11].

- A single-computer graph algorithm library can also be utilized. JDSL [12], BGL [13], NetworkX [14], LEDA [15], Stanford GraphBase [16], or FGL [17] are example of such libraries. Major issue with libraries is scalability [11].
- An existing parallel graph system such as Parallel BGL [18] and CGMgraph [19] can be deployed. One major issue is of fault tolerance.

Next, some of the most important distributed computational models are described.

A. MPI-like

There are many libraries available that use MPI for distributed graph processing. Some important libraries are Parallel BGL [18] and CGMgraph [19]. As mentioned above, there are some important distributed graph processing issues like no support for fault tolerance [20].

B. MapReduce

MapReduce was developed by Google for processing of big data. MapReduce consists of two phases: map phase and reduce phase. The system have a master node and several of workers. In the map phase, input is divided into smaller jobs by the master node and then these are assigned to all the workers which work independently. In the reduce phase, the workers combine the result for the original problem [20]. MapReduce model did not turn out to be ideal for many different graph algorithms, e.g.

parallel BFS. It can lead to a lot of computational overhead, sub-optimal performance, and poor usability [11].

C. Bulk Synchronous Parallel

Bulk Synchronous Parallel (BSP) is a general parallel processing model which consists of three main attributes, i.e., several concurrently running processes, communication layer, and a synchronization barrier. In communication layer, pairs of processes exchange messages. BSP works in series of super steps. Processes perform computation during supersteps. Before going to next superstep, synchronization barrier maintains consistency by synchronizing processes. Synchronization may either happen periodically after a specific time interval or there may be another specific way. After completing computation assigned in each super step, every process waits for other processes to finish the processing and to receive all the messages destined to it. Once all processes complete, one superstep they get synchronized and then next superstep is executed. When a processor is not needed to compute or exchange data, it becomes inactive. It is activated when it is needed to perform computation or to exchange message. This model is terminated when all the processors become inactive. BSP is a simple, efficient, and scalable model for parallel algorithm design and analysis. It does not take into account the case of heterogeneous clusters [21].

D. Vertex-Centric Graph Processing

To apply BSP on big graphs, Google proposed a model of vertex-centric graph processing [11]. It is especially designed for big graphs. Each vertex is considered as a processor. After each superstep, the messages are synchronized, i.e., each vertex waits for other vertices to finish the processing and also to receive all the messages destined to it. Similarly, next superstep is continued and the process keeps repeating until the algorithm finishes.

The first implementation of this idea is Pregel, which is not available to the general public. Introduction of Pregel inspired many other BSP based graph processing systems like GPS (Graph Processing System) [23], Apache Giraph [24], and GraphLab [24].

1) *Pregel*: Pregel is flexible, scalable, and fault tolerant platform for big graph computation [11]. Similar to BSP, computation is divided into sequence of supersteps, separated by global synchronization points. This system mutates graph topology. Vertex can receive messages from its previous iteration, send/receive messages to/from other vertices, and modify its state and also the state of its outgoing edges.

Pregel system consists of one master and multiple workers. The master coordinates and oversees the activities of worker. The master divides the input directed graph. It uses an abstract API of C++ to uniformly distribute these partitions to the workers. Then signals all the workers to start execution. The worker nodes calls the compute() method for each active vertex with the messages received from the last superstep. After completing its computation; the vertex votes for halt and becomes inactive, and is not called in the next supersteps. If this vertex gets new message then it is activated again. When all vertices become inactive, master marks the end of current job. If a worker fails, Pregel dynamically reassigns

the job to other worker [11]. In this way, Pregel offers a fault tolerant system. In addition to fault tolerance, Pregel offers scalability, efficiency, ease, and simplicity. It also offers additional performance boosters like combiners and aggregators. Combiners are used during message passing (especially to a vertex on another machine). Aggregators are mechanism for global communication and monitoring of data.

2) *Apache Giraph*: Apache Giraph [24] is an open-source system and extends basic BSP model. Yahoo implemented using Java and built it on Hadoop echo system (Fig. 10). Giraph follows message passing model and performs global synchronization without using semaphores.

It uses Hadoop for running workers, HDFS for input and output data storage. Apache ZooKeeper is used for coordination, check pointing, and failure recovery schemes. Usability of Giraph is excellent due to Hadoop web monitoring interface. Giraph also provides shared aggregators to avoid bottlenecks at the master, yield substantial memory savings, and reduced Java garbage collection overheads. It supports different data structures for vertex adjacency lists. By default, it uses byte array for faster input loading times but graph mutation is inefficient. On the other hand, hash map edges efficient for mutation but inefficient for memory. Giraph is massively parallelizable and uses multi-threading which boosts up the speed of graph loading, dumping, and computation. Additionally, global synchronization, debugging, and monitoring progress is easy in Giraph.

3) *Graph Processing System*: A Graph Processing System (GPS) is open source system which is implemented in Java for computation of extremely large graphs. It offers scalability, fault tolerance, and ease of programing to express complex graphs efficiently [23]. It is faster than Giraph [24]. It has extension of the Pregel API, LALP, and DP for performance boosting [26]. It introduced master.compute() function to access, update, and store global aggregated values that are transparent to vertices. LALP divides the adjacency lists of high degree vertices among workers along with a mirror of the vertex. When such vertex broadcasts a message to its neighbors, one copy of message is sent to its mirror at each machine and all neighbors in the partition. During execution, DP dynamically repartitions the graph to balance the workload across workers. GPS minimize the thread synchronization using message buffers per-worker rather than per-vertex. However, overhead of reassigning vertices among workers can exceed the overall benefits.

4) *GraphLab/PowerGraph*: GraphLab is an open source project which is popular for its maturity for graph analytical tasks. Its recent version is called PowerGraph. It is implemented in C/C++. GraphLab adopts a gather, apply, scatter (GAS) data-pulling model and shared memory abstraction [26]. For each vertex a user-defined GAS function is implemented. In gather phase, each active vertex collects information from its neighboring vertices and edges. It then performs a generalized accumulation operation over them. In apply phase, the vertex updates its value based on old value and resultant accumulation. In scatter phase, each active vertex activates its adjacent vertices. In contrast to BSP model, vertices do not receive messages for its neighbors but can directly pull their neighbors data (via Gather). Due to this feature, the communication barriers are no longer required and execution is completely asynchronous. This

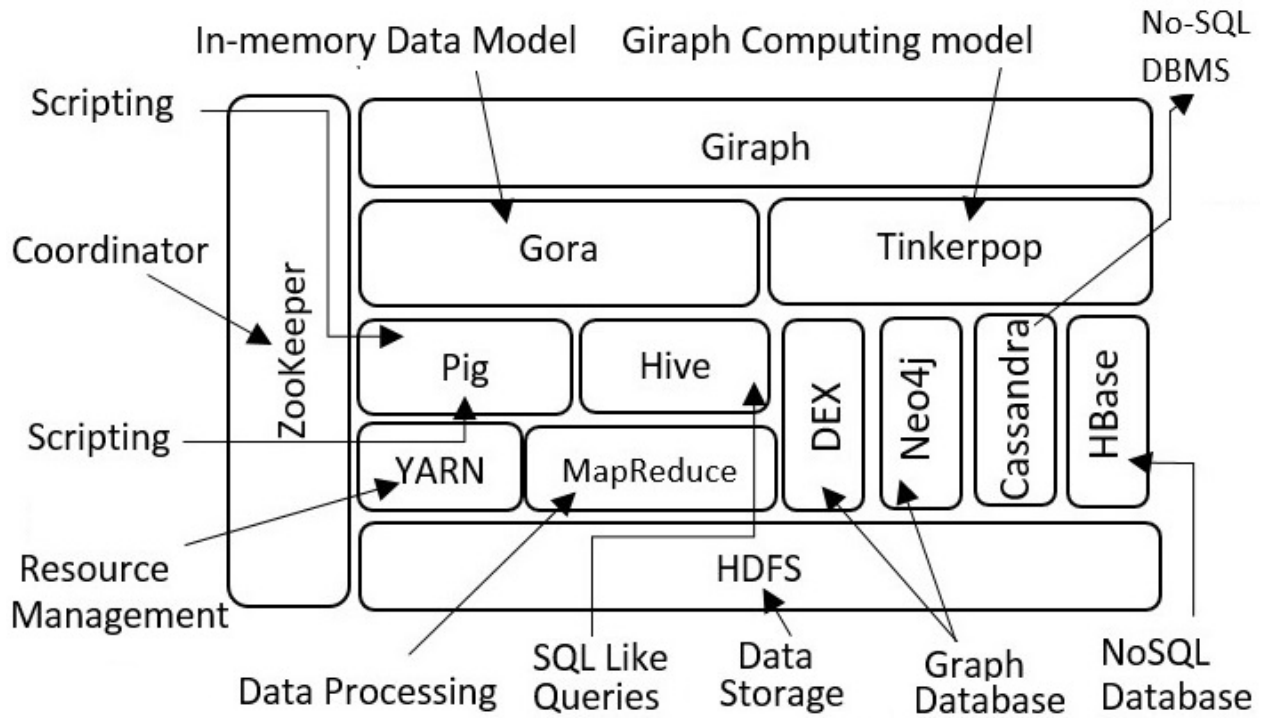


Fig. 10. Giraph and Hadoop Echo System [22].

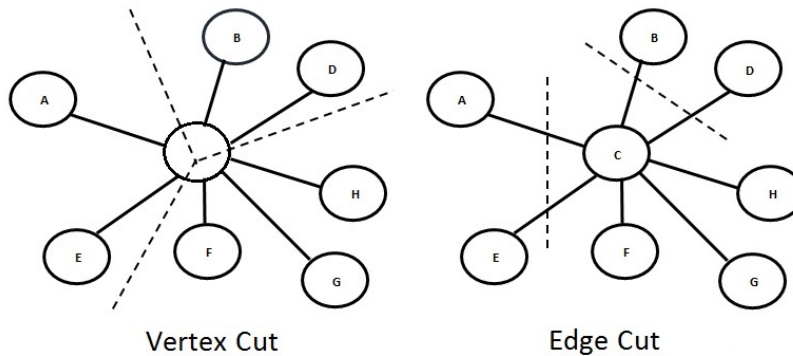


Fig. 11. Vertex Cut vs. Edge Cut.

avoids wasting CPU and network resource [24]. GraphLab also offers an optional synchronous execution mode which requires communication barriers.

GraphLab performs vertex cuts for partitioning graph while Giraph, GPS, and Mizan all perform edge cuts (Fig. 11). It replicates vertices on remote machines and each edge is assigned to a unique machine. This feature results in more balanced workloads for asymmetric degree distributions graphs [24]. In GraphLab graph mutation is partially supported. Vertices and edges can be added but cannot be removed from graphs.

5) *Mizan*: Mizan is a C++ optimized and open source system [26]. It monitors vertices and optimizes the computation by dynamic load balancing and complex vertex migration.

Mizan requires separate pre-partitioning of graph. Due to this overhead, Mizan is not suitable for large graph because it can exceed the overall benefits of the system [24]. Moreover, it has few bugs and many useful features are missing.

6) *GraphX*: GraphX is an embedded graph processing system which supports GraphLab and Pregel abstractions [26]. GraphX framework is built on top of Apache Spark which is a widely used distributed dataflow framework (Fig. 12).

It does not require changes to Spark. It enforces graph computation through a specific join, map, and group by dataflow pattern [27]. GraphX API is modified version of Pregel abstraction and a range of common graph operations. Through this API, graphs can be composed with unstructured and tabular data. The physical data can be represented as a

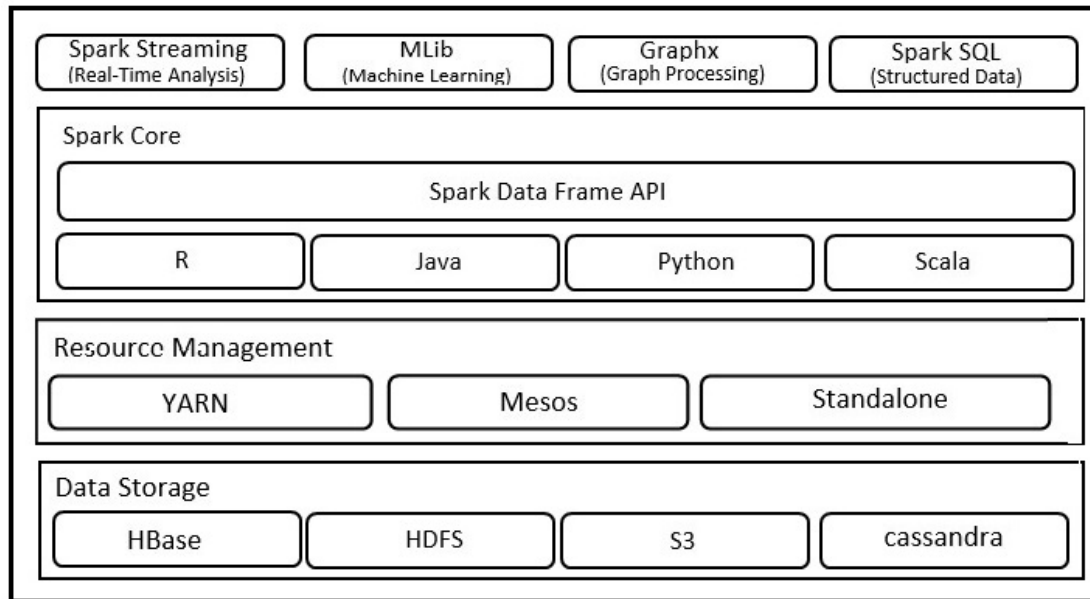


Fig. 12. Apache Spark and Graphx [25].

graph as well as collections without data movement, duplication, and sacrificing performance or flexibility [27].

GraphX optimizes distributed join and materialized view maintenance for better graph processing performance. It provides low-cost fault tolerance [27]. Its performance is comparable with specialized graph processing systems. It provides better end-to-end performance for pipelined jobs. However, it takes longer than GraphLab for actual graph computation [26].

VI. CONCLUSION

This work describes a broad overview of the storage techniques and algorithmic strategies for graph analytics. Moreover, we point out the critical challenges that need to be addressed. Graph databases provide an intrinsic support to data structures, data modeling, querying, and some integrity constraints features that results in faster computation. However, there is still need for further development in the definition of standard graph database languages for computation and querying of graph databases. Moreover, new query languages are needed which should be capable of expressing graph analytical operations. Big graphs requires special and faster parallel computation models which offers different features like fault tolerance, flexibility, simplicity, better usability, optimal performance, scalability, computational efficiency, and better resource utilization. We are working on security requirements of graph analytics.

REFERENCES

- [1] A. Gandomi and M. Haider, "Beyond the hype: Big data concepts, methods, and analytics," *International Journal of Information Management*, vol. 35, no. 2, pp. 137–144, 2015.
- [2] A. Gupta, "Graph Analytics for Big Data," <https://www.coursera.org/learn/big-data-graph-analytics>, [Accessed: 2017-05-22].
- [3] R. Angles, "A comparison of current graph database models," in *Data Engineering Workshops (ICDEW), 2012 IEEE 28th International Conference on*. IEEE, 2012, pp. 171–177.
- [4] "Visualizing groups in graph," <http://allthingsgraphed.com/2014/08/28/facebook-friends-network/>, accessed: 2017-04-15.
- [5] "smart cities," <https://futurism.com/heres-a-look-at-the-smart-cities-of-the-future/>, accessed: 2017-02-12.
- [6] "Financial services and neo4j: fraud detection," <https://neo4j.com/blog/financial-services-neo4j-fraud-detection/?ref=solutions>, accessed: 2017-06-10.
- [7] D. Fay, H. Haddadi, S. Uhlig, A. W. Moore, R. Mortier, and A. Jmakovic, "Weighted spectral distribution," *University of Cambridge, Computer Laboratory, Tech. Rep. UCAM-CL-TR-729*, 2008.
- [8] C. T. Have and L. J. Jensen, "Are graph databases ready for bioinformatics?" *Bioinformatics*, vol. 29, no. 24, pp. 3107–3108, 2013.
- [9] N. Martinez-Bazan, S. Gomez-Villamor, and F. Escala-Claveras, "Dex: A high-performance graph database management system," in *Data Engineering Workshops (ICDEW), 2011 IEEE 27th International Conference on*. IEEE, 2011, pp. 124–127.
- [10] B. Iordanov, "Hypergraphdb: a generalized graph database," in *International Conference on Web-Age Information Management*. Springer, 2010, pp. 25–36.
- [11] G. Malewicz, M. H. Austern, A. J. Bik, J. C. Dehnert, I. Horn, N. Leiser, and G. Czajkowski, "Pregel: a system for large-scale graph processing," in *Proceedings of the 2010 ACM SIGMOD International Conference on Management of data*. ACM, 2010, pp. 135–146.
- [12] M. T. Goodrich and R. Tamassia, *Data structures and algorithms in Java*. John Wiley & Sons, 2008.
- [13] J. G. Siek, L.-Q. Lee, and A. Lumsdaine, *The Boost Graph Library: User Guide and Reference Manual, Portable Documents*. Pearson Education, 2001.
- [14] D. A. Schult and P. Swart, "Exploring network structure, dynamics, and function using networkx," in *Proceedings of the 7th Python in Science Conferences (SciPy 2008)*, vol. 2008, 2008, pp. 11–16.
- [15] K. Mehlhorn and S. Näher, *LEDA: a platform for combinatorial and geometric computing*. Cambridge university press, 1999.
- [16] D. E. Knuth, *The Stanford GraphBase: a platform for combinatorial computing*. Addison-Wesley Reading, 1993, vol. 37.
- [17] M. Erwig, "Inductive graphs and functional graph algorithms," *Journal of Functional Programming*, vol. 11, no. 05, pp. 467–492, 2001.
- [18] D. Gregor and A. Lumsdaine, "The parallel bgl: A generic library for distributed graph computations," *Parallel Object-Oriented Scientific Computing (POOSC)*, vol. 2, pp. 1–18, 2005.

- [19] A. Chan, F. Dehne, and R. Taylor, "Cgmgraph/cgmlib: Implementing and testing cgm graph algorithms on pc clusters and shared memory machines," *The international Journal of High Performance Computing Applications*, vol. 19, no. 1, pp. 81–97, 2005.
- [20] M. U. Nisar, *A Comparison of Techniques for Graph Analytics on Big Data*. uga, 2013.
- [21] L. G. Valiant, "A bridging model for parallel computation," *Communications of the ACM*, vol. 33, no. 8, pp. 103–111, 1990.
- [22] "Giraph and Hadoop Echo System," <https://image.slidesharecdn.com/hadoopsummit2014-140403113102-phpapp02/95/giraph-at-hadoop-summit-2014-19-638.jpg?cb=1396526440>, accessed: 2017-03-12.
- [23] S. Salihoglu and J. Widom, "Gps: A graph processing system," in *Proceedings of the 25th International Conference on Scientific and Statistical Database Management*. ACM, 2013, p. 22.
- [24] M. Han, K. Daudjee, K. Ammar, M. T. Özsu, X. Wang, and T. Jin, "An experimental comparison of pregel-like graph processing systems," *Proceedings of the VLDB Endowment*, vol. 7, no. 12, pp. 1047–1058, 2014.
- [25] "Apache spark and graphx," <https://www.safaribooksonline.com/library/view/learning-spark/9781449359034/ch01.html>, accessed: 2017-06-15.
- [26] Y. Lu, J. Cheng, D. Yan, and H. Wu, "Large-scale distributed graph computing systems: An experimental evaluation," *Proceedings of the VLDB Endowment*, vol. 8, no. 3, pp. 281–292, 2014.
- [27] J. E. Gonzalez, R. S. Xin, A. Dave, D. Crankshaw, M. J. Franklin, and I. Stoica, "Graphx: Graph processing in a distributed dataflow framework."

Dual-Cross-Polarized Antenna Decoupling for 43 GHz Planar Massive MIMO in Full Duplex Single Channel Communications

Muhsin¹

Faculty of Electrical Engineering
Institut Teknologi Telkom Surabaya
Surabaya, Indonesia

Rina Pudji Astuti²

School of Electrical Engineering
Telkom University
Bandung, Indonesia

Abstract—Massive Multiple Input Multiple Output (MIMO) and Full Duplex Single Channel (FDSC) at mm-Wave are key technology of future advanced wireless communications. Self-interference is the main problem in this technique because big number of antennas. This paper proposes dual-cross-polarized configuration to reduce self-interference between antennas. We conduct some computer simulations to design the antenna and to verify self-interference effect of the designed antenna. Computer simulation shows that the proposed design has lower Envelope Correlation Coefficient (ECC). This result is achieved because dual-cross-polarized technique can reduce coupling between antennas. We found that bit-error-rate (BER) performances of the proposed antenna is better than single polarized antenna indicating that the designed antenna is well design to reduce self-interference effect between antennas.

Keywords—Massive MIMO; dual polarized; mm-Wave; coupling; self-interference; full duplex single channel

I. INTRODUCTION

FDSC on massive MIMO at mm-Wave offers better performance compared to conventional communications using FDD or TDD on Single Input Single Output (SISO). Massive MIMO provides high degree of diversity [1]–[3] and FDSC simultaneously which transmit and receive signals in same frequency and time [4]–[8]. Combination of FDSC and massive MIMO is expected having benefits from both techniques.

Self-interference is the main problem of implementing FDSC on massive MIMO. It caused by duplexer's leakage and coupling matrix between antennas. Coupling matrix between antennas become greater with increasing number of antennas. Low coupling is needed to reduce amount of self-interference. Dual-cross-polarized antenna [9], [10] and sectoral antenna [11] are two main methods to achieve low coupling.

Sectoring antenna is potentially the most suitable configuration in base station. Low coupling is achieved by make low intersection between antennas' radiation pattern by sectoring antenna which has high gain. Each sector only served by partial number of antennas, there antennas usually formed as array to achieve high gain. Previous research in [11] use this method for dual band massive MIMO antenna at 28 and 38 GHz.

Planar antenna is the most common antenna for high frequency application. Dual polarized method can be easily applied in planar antenna to minimize coupling effect. It has been

shown in [10], [12] that dual polarized in planar configuration can reduce coupling and improve isolation between antennas. These research has been done in low number of antennas and lower frequency. More massive number of antennas in mm-Wave has been evaluated in [9], [13]. Another technique to improve antenna isolation using absorptive shielding has been proposed in [14]. This technique is not suitable for massive MIMO because of high number of antenna.

This paper proposed dual polarized antenna decoupling for FDSC evaluated at 43 GHz. This technique can reduce self-interference by reducing coupling between antennas. 4×4 planar array MIMO at 43 GHz is used as basic model with single polarized and dual polarized configuration. These antennas are tested in simulation system considering self-interference with and without S-parameter matrix based self-interference cancellation.

Antenna design is presented in Section II starting from single element to full 16 elements MIMO antenna with both single polarized and dual polarized configurations. Simulation model of self-interference is explained in Section III. Antennas are evaluated by ECC and BER performance in Section IV and V, respectively. Finally, conclusion is pretested in Section VI.

II. ANTENNA DESIGN

Basic model of antenna design in microstrip planar antenna with circular disk proximity coupled. This model is chosen due to its flexibility. Both single polarized and dual polarized model are extended from this basic model.

Design process is started with single antenna model using basic model. This basic single antenna then extended into single cluster composed from four single antennas. Finally, final antenna for both single polarized and dual polarized configurations are formed by duplicating single cluster of antenna model. This clustering method is chosen to simplify design process.

A. Single Antenna Design

Single antenna is formed as basic model of MIMO array. Stepping of design is started by this single antenna model. Single antenna is modeled and optimized in order to get its best performance. The performance can be measured by return loss because antenna works at certain value of return loss.

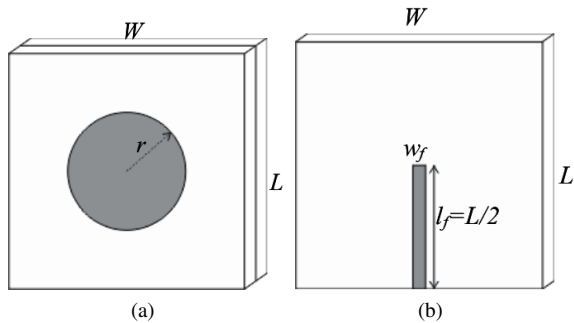


Fig. 1. Geometry of circular disk proximity coupled antenna: (a) top layer, (b) middle layer

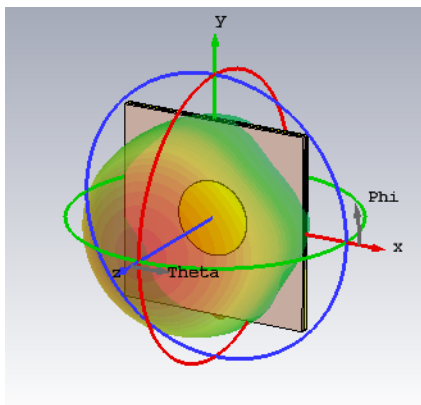


Fig. 2. Radiation pattern of single antenna.

Each single antenna is designed as circular disk proximity coupled antenna as shown in Figs. 1(a) and 1(b). Rogers RT-5880 with $h = 0.127$ mm is used as substrate's material with permittivity $\epsilon_r = 2.2$.

Basic formula in [15] has simplified as

$$r = \frac{F}{\sqrt{1 + \frac{2h}{\pi\epsilon_r F} \left[\ln \left(\frac{\pi F}{2h} + 1.7726 \right) \right]}} \quad (1)$$

with

$$F = \frac{8.791 \times 10^9}{f\sqrt{\epsilon_r}}, \quad (2)$$

where h is depth or height of substrate in cm, f is antenna's resonance frequency, and ϵ_r is substrate's relative permittivity.

Antenna is design and optimized at 43 GHz resonant frequency and 50Ω reference impedance. The result is antenna's width $W = L = \lambda = 6.98$ mm, length of feed $l_f = W/2 = 3.49$ mm, width of feed $w_f = 0.70$ mm, and disk radius $r = 1.30$ mm.

Single antenna model has unidirectional radiation pattern with 7.456 dBi gain with total efficiency of -0.1933 dB as shown in Fig. 2. Formed planar massive MIMO antenna by using this single antenna is also unidirectional. This configuration is suitable for single sector sectoral massive MIMO base station as in [11].

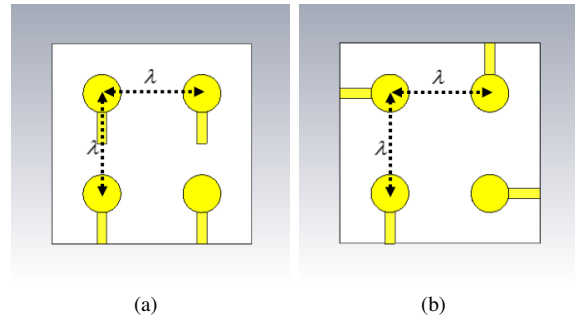


Fig. 3. Single cluster of the antenna: (a) single polarized MIMO antenna, (b) dual polarized MIMO antenna.

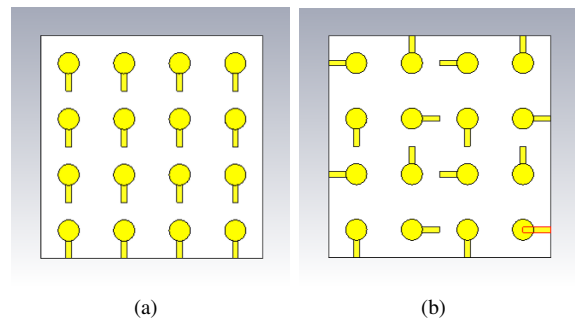


Fig. 4. Final model of the antenna: (a) single polarized MIMO antenna, (b) dual polarized MIMO antenna.

B. Clustering

Clustering method is chosen in order to simplify the design process. A single cluster of each configuration are shown in Fig. 3 using a wavelength spacing between antennas' center horizontally and vertically. Polarization variation is set by different direction of feeding.

Single antenna is set as basis of single cluster using dimensional parameter from Section II-A. This model then optimized to get the best performance in a single cluster. It assured antenna's performance in smaller number of antennas before final model is formed. There is an assumption that significant change only happened in 1 to 4 elements expansion.

C. Final Model of The Antenna

Different feeding is applied to each configuration to get different polarization characteristic. Single polarized antenna is fed with same direction as shown in Fig. 4(a). Dual polarized antenna is fed with cross direction as shown in Fig. 4(b). It is made by extend single cluster to form full 16 elements MIMO antenna.

Designed antenna has 8 sectors in total shown in Fig. 5(a). Each sector has total 16 antennas with 4×4 planar configuration. Antennas are numbered for each single element from left-top to bottom right. This numbering is used to identify each single antenna. Antennas numbering is shown in Fig. 5(b). Clustering is applied for 4 near antennas, for example antenna 1, 2, 5, and 6 are in the same cluster. There are 4 clusters composed massive MIMO antenna for each configuration.

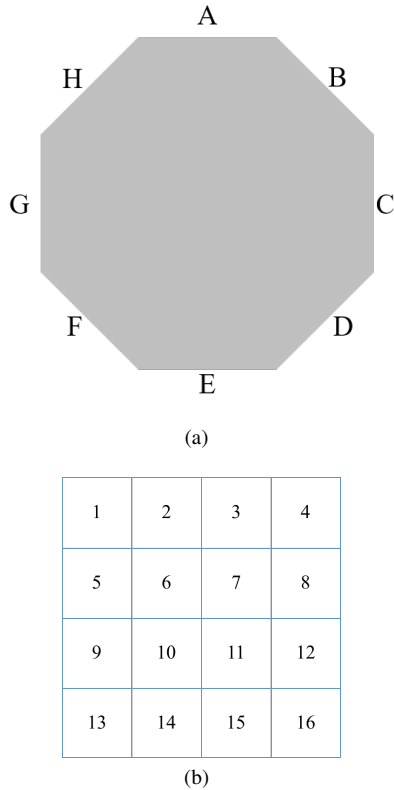


Fig. 5. Antenna's sectoring and numbering: (a) sectoring, (b) numbering.

III. SIMULATION MODEL

There are three parts explained in this section. First part is self-interference model. Quasi-Orthogonal Space Time Block Code (QOSTBC) for full rate massive MIMO is explained in second part of this section. Last part explains self-interference management for massive MIMO FDSC.

A. Self-Interference

Self-Interference is the main problem in FDSC as described in [4]–[8], [16]. Self-interference is interference part caused by the node itself. In this case, self-interference caused by duplexer's leakage and coupling between antennas. It can be modeled as

$$y = Hx + Sw + L_I w + n_0 \quad (3)$$

where y is received signal, x is transmitted information signal, w is transmitted self-interference signal, and n_0 is Additive White Gaussian Noise (AWGN). This model is shown in Fig. 6. Self-interference is caused by S and L_I with

$$S = \begin{pmatrix} s_{11} & s_{12} & \cdots & s_{1N} \\ s_{21} & s_{22} & \cdots & s_{2N} \\ \vdots & \vdots & \ddots & \vdots \\ s_{N1} & s_{N2} & \cdots & s_{NN} \end{pmatrix} \quad (4)$$

and

$$L_I = \begin{pmatrix} L_1 & 0 & 0 & \cdots & 0 \\ 0 & L_2 & 0 & \cdots & 0 \\ 0 & 0 & L_3 & \cdots & 0 \\ \vdots & \vdots & \vdots & \ddots & \vdots \\ 0 & 0 & 0 & \cdots & L_N \end{pmatrix} \quad (5)$$

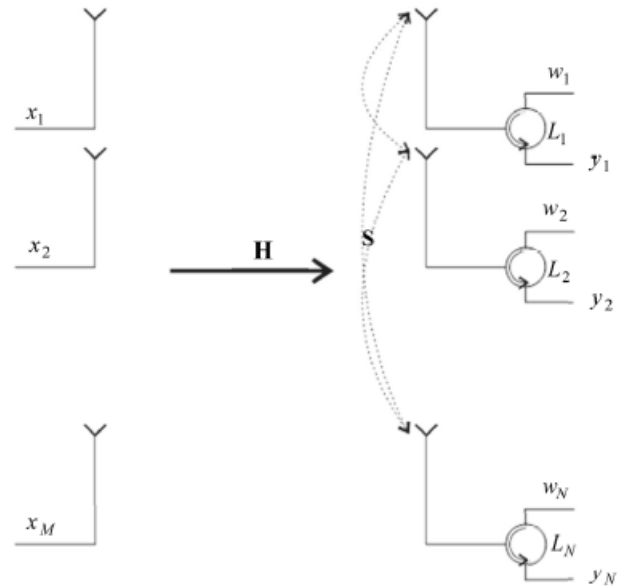


Fig. 6. Model of self-interference by other antennas and duplexer's leakage.

where each element of S represents coupling between antennas and diagonal element of L_I represents duplexer's leakage at each antenna. Both of these matrix's ideal values are 0 which means no coupling and no duplexer's leakage.

B. Quasi Orthogonal Space Time Block Code (QOSTBC)

QOSTBC is used as MIMO coding in this research. QOSTBC can achieve full rate characteristics by making quasi or semi orthogonal on its MIMO coding. It brings rate and orthogonality trade-offs by making full rate Space Time Block Code (STBC) allowing certain acceptable orthogonality value.

There are two types of QOSTBC proposed in [17], [18]. Extended-Alamouti QOSTBC has pattern of

$$C_{EA} = \begin{pmatrix} A & B \\ -B^* & A^* \end{pmatrix} \quad (6)$$

with each of A and B is Alamouti coded signal. If A is Alamouti coded signal of x_1 and x_2 ,

$$A = \begin{pmatrix} x_1 & x_2 \\ -x_2^* & x_1^* \end{pmatrix}. \quad (7)$$

If B is Alamouti coded signal of x_3 and x_4 ,

$$A = \begin{pmatrix} x_3 & x_4 \\ -x_4^* & x_3^* \end{pmatrix}. \quad (8)$$

EA-QOSTBC for 4 coded signal by substituting (7) and (8) to (6) is

$$C_{EA} = \begin{pmatrix} x_1 & x_2 & x_3 & x_4 \\ -x_2^* & x_1^* & -x_4^* & x_3^* \\ -x_3^* & -x_4^* & x_1^* & x_2^* \\ x_4 & -x_3 & -x_2 & x_1 \end{pmatrix}. \quad (9)$$

Another popular typr of QOSTBC is ABBA QOSBC. In ABBA QOSTBC,

$$C_{ABBA} = \begin{pmatrix} A & B \\ -B & A \end{pmatrix}. \quad (10)$$

ABBA QOSTBC by substituting (7) and (8) to (10) is

$$\mathbf{C}_{ABBA} = \begin{pmatrix} x_1 & x_2 & x_3 & x_4 \\ -x_2^* & x_1^* & -x_4^* & x_3^* \\ x_3 & x_4 & x_1 & x_2 \\ -x_4^* & x_3^* & -x_2^* & x_1^* \end{pmatrix}. \quad (11)$$

These pattern of EA-QOSTBC and ABBA QOSTBC can be repeated until $2^n \times 2^n$ matrix is formed with n is number of coded signals or symbols. In this research, we consider ABBA QOSTBC due to its simplicity.

C. Equivalent Virtual Channel Matrix (EVCM)

EVCM take advantages of mathematical property by transform coded signals into coded channel matrix [18] It can simplify simulation and MIMO decoding process by assuming relatively same response of channel in a single period of coded signals.

Let say there is received signal vector for one receive antenna is

$$\mathbf{r} = \mathbf{C}_x \mathbf{h} + \mathbf{v} \quad (12)$$

with \mathbf{C}_x is coded transmit signal, $\mathbf{h} = [h_1 \ h_2 \ \dots \ h_{N_C}]^T$ is a set of independent channel, and $\mathbf{v} = [v_1 \ v_2 \ \dots \ v_{N_C}]^T$ is equivalent additive noise where N_C is length of STBC in time domain. For two antennas case using Alamouti SBTC,

$$\begin{pmatrix} r_1 \\ r_2 \end{pmatrix} = \begin{pmatrix} x_1 & x_2 \\ -x_2^* & x_1^* \end{pmatrix} \begin{pmatrix} h_1 \\ h_2 \end{pmatrix} + \begin{pmatrix} v_1 \\ v_2 \end{pmatrix} \quad (13)$$

$$\begin{pmatrix} r_1 \\ r_2 \end{pmatrix} = \begin{pmatrix} h_1 x_1 & h_2 x_2 \\ h_2 x_1^* & -h_1 x_2^* \end{pmatrix} + \begin{pmatrix} v_1 \\ v_2 \end{pmatrix}. \quad (14)$$

Conjugating second row of (14),

$$\begin{pmatrix} r_1 \\ r_2 \end{pmatrix} = \begin{pmatrix} h_1 x_1 & h_2 x_2 \\ h_2^* x_1 & -h_1^* x_2 \end{pmatrix} + \begin{pmatrix} v_1 \\ v_2^* \end{pmatrix} \quad (15)$$

$$\begin{pmatrix} r_1 \\ r_2^* \end{pmatrix} = \begin{pmatrix} h_1 & h_2 \\ h_2^* & -h_1^* \end{pmatrix} \begin{pmatrix} x_1 \\ x_2 \end{pmatrix} + \begin{pmatrix} v_1 \\ v_2^* \end{pmatrix} \quad (16)$$

which equivalent with

$$\begin{pmatrix} y_1 \\ y_2 \end{pmatrix} = \begin{pmatrix} h_1 & h_2 \\ h_2^* & -h_1^* \end{pmatrix} \begin{pmatrix} x_1 \\ x_2 \end{pmatrix} + \begin{pmatrix} n_1 \\ n_2 \end{pmatrix} \quad (17)$$

D. Self-Interference Management

There are some methods to manage effect of self-interference. In this paper, these methods are categorized into four main methods. All of these methods are focused on reducing or cancelling self-interference in the systems. These four main methods are receiving-transmitting power control, antenna decoupling, isolated duplexer, and cancellation by self-interference cancellation matrix.

Receiving-transmitting power control are focusing on reducing self-interference signal power ratio defined as

$$\alpha_i = \frac{P_{Tx-i}}{P_{Rx-i}} \quad (18)$$

for node, base station, or user i . P_{Tx-i} and P_{Rx-i} are transmitted power and received power on node, base station, or user i . In node i , it is evaluated using (3) by

$$\alpha_i = \frac{\text{pow}(\mathbf{S}\mathbf{w} + \mathbf{L}_I\mathbf{w})}{\text{pow}(\mathbf{H}\mathbf{x})} \quad (19)$$

where $\text{pow}(z)$ represents power of z . Effect of self-interference is decreasing if α can be reduced.

Antenna decoupling are focusing on value of on (3). If this part can be reduced close to zero, receive signal equation become

$$\mathbf{y} = \mathbf{H}\mathbf{x} + \mathbf{L}_I\mathbf{w} + \mathbf{n}_0. \quad (20)$$

If \mathbf{S} is reduced, effect if $\mathbf{S}\mathbf{w}$ in (3) also reduced. This decoupling is realized by modifying S-Parameter of the antenna by some antenna design technique.

Isolated duplexer works by using near-perfect duplexer with leakage near to zero. Assuming duplexer's leakage can be eliminated, receive signal equation become

$$\mathbf{y} = \mathbf{H}\mathbf{x} + \mathbf{S}\mathbf{w} + \mathbf{n}_0 \quad (21)$$

which left $\mathbf{S}\mathbf{w}$ as self-interference part. Effect of $\mathbf{L}_I\mathbf{w}$ is reduced if duplexer's leakage is reduced.

Cancellation by self-interference cancellation matrix works by reducing receive signal (3) by

$$\mathbf{SIC} = \mathbf{S}\mathbf{w} + \mathbf{L}_I\mathbf{w}. \quad (22)$$

Assuming \mathbf{S} and \mathbf{L}_I can be predicted, this self-interference cancellation matrix can be formed.

Each of self-interference managements method have its challenge. In this research, we assume linear deviation on antenna decoupling. Received signal is

$$\mathbf{y} = \mathbf{H}\mathbf{x} + \tilde{\mathbf{S}}\mathbf{w} + \mathbf{L}_I\mathbf{w} + \mathbf{n}_0 \quad (23)$$

with deviated scattering parameter

$$\tilde{\mathbf{S}} = \mathbf{S} + k\mathbf{I}. \quad (24)$$

\mathbf{S} is default-mean scattering parameter, k is normally distributed value with zero mean and σ deviation, and \mathbf{I} is identity matrix. Self-interference cancellation matrix is using mean value in (22).

IV. ENVELOPE CORRELATION COEFFICIENT OF ANTENNA MODEL

In this section, both single polarized and dual polarized configuration are evaluated by ECC. This coefficient represents correlation between antennas. ECC can be calculated from antenna's scattering parameter using [19], [20]

$$\rho_{env} = \frac{|s_{ii}^* s_{ij} + s_{ji}^* s_{jj}|^2}{\left(1 - (|s_{ii}|^2 + |s_{ji}|^2)\right) \left(1 - (|s_{jj}|^2 + |s_{ij}|^2)\right)} \quad (25)$$

with i and j are antenna's index number where $i \neq j$. These ECC show independency between antennas. If two antennas are completely independent, ECC value is 0. If these antennas are completely dependent, ECC value is 1. Requirement for diversity is set at ECC less than 0.5.

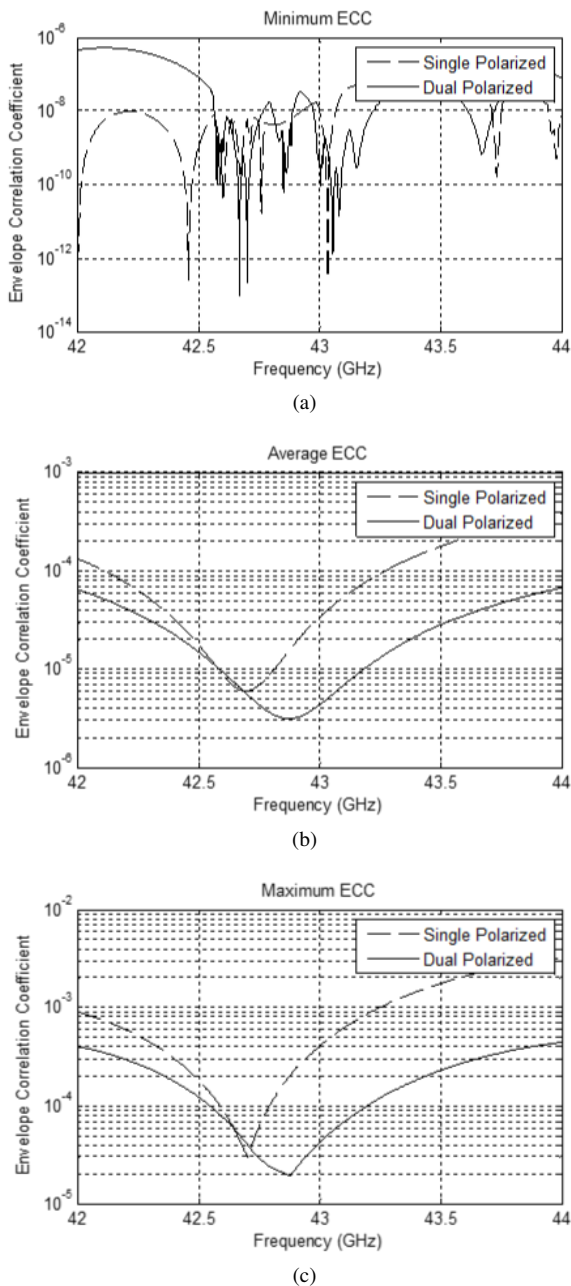


Fig. 7. Envelope correlation statistical value: (a) minimum, (b) average, (c) maximum

There are 120 pairs of ECC for 16 elements antenna. It is simplified to only presents minimum, average, and maximum value of ECC as representations. These statistical value contain range and mean of all ECC values. Fig. 7 shows minimum, average, and maximum value of ECC. Lower ECC is shown by dual polarized configuration. ECC value also has impact on diversity gain. This relation is presented in [21] by

$$G_{div} = 10\sqrt{1 - |\rho_{env}|}. \quad (26)$$

Lower ECC means greater diversity gain at related pair of antennas. Dual polarized configuration also provides polarization diversity. Theoretically, dual polarized configuration has better performance on diversity compared to single polarized configuration.

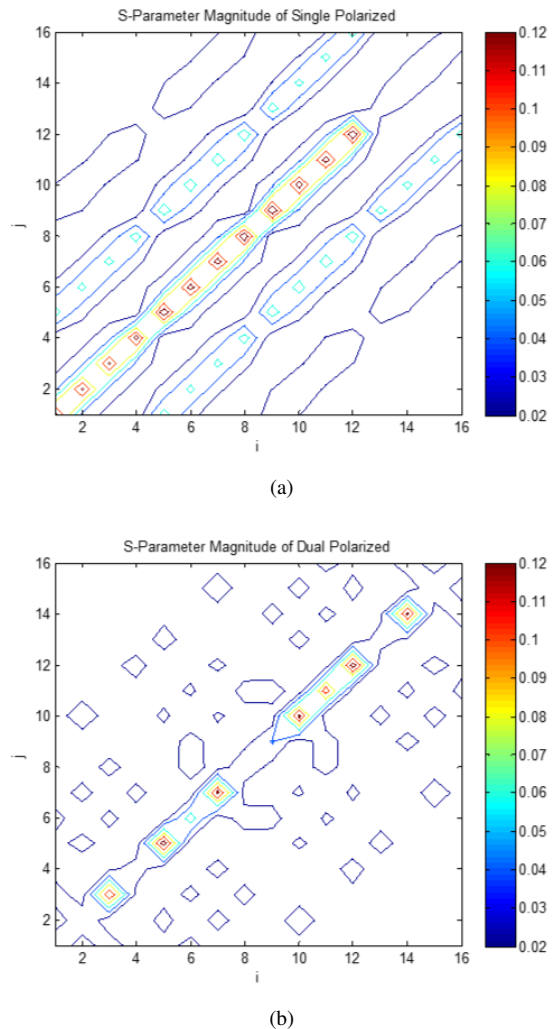


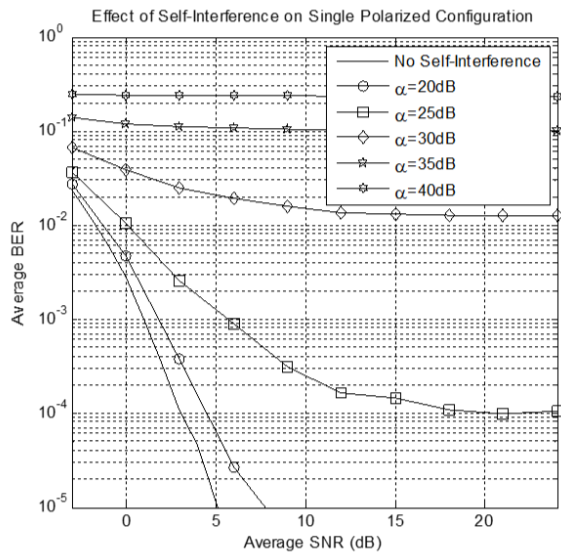
Fig. 8. Scattering parameter magnitude: (a) single polarized, (b) dual polarized.

Both of single polarized and dual polarized configurations has ECC lower than 0.5. It means diversity can be effectively applied on both configurations. Average ECC of both configurations are lower than 10^{-3} which is very small. Antennas correlation is neglected because of very low ECC.

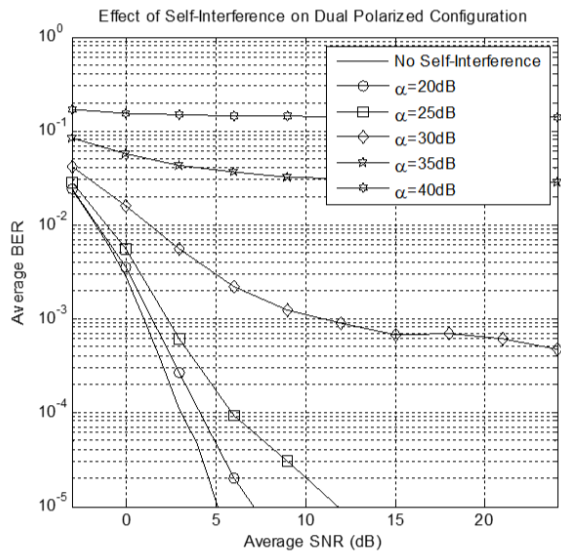
There are two main focuses on lowering ECC. The most popular technique is by reducing coupling between antennas. This coupling is presented by $s_{ij} = s_{ji}$ with $i \neq j$. It mainly can be reached by making orthogonal radiation pattern or polarization. These orthogonality represents relation between related antennas. Designing low return loss antennas also can reduce correlation between antennas.

A. Various α without Deviation

Dual polarized configuration has lower coupling compared to single polarized configuration as shown in Fig. 8. The highest coupling on single polarized and dual polarized configuration is -22.98 dB and -29.29 dB, respectively. The highest return loss on single polarized and dual polarized configuration is -17.18 dB and -17.58 dB, respectively. In this case, lower ECC on dual polarized configuration is more caused by lower



(a)



(b)

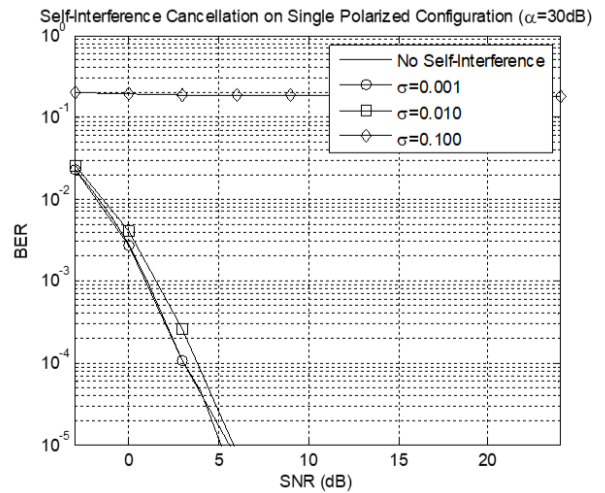
Fig. 9. System performance in various self-interference signal power ratio: (a) single polarized, (b) dual polarized.

coupling rather than lower return loss.

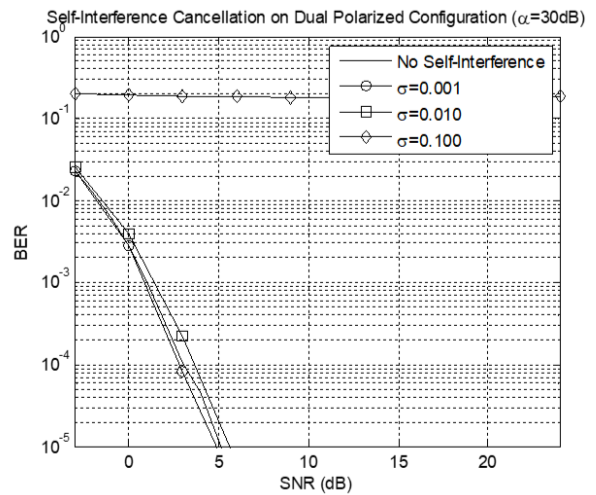
V. SYSTEM PERFORMANCE ON FULL DUPLEX SINGLE CHANNEL

System performances are tested on 16×16 MIMO configuration. Correlation between antennas are neglected because the values of ECC in center frequency are below 10^{-3} . Several self-interference signal power ratio is applied. Full rate QOSTBC with 16 antennas is applied with EVCM representation.

Both single polarized and dual polarized configurations are tested using S-parameter of antennas from antenna simulation. These values at magnitude representation are presented in Fig. 8. These values are used as in the systems simulation.



(a)



(b)

Fig. 10. System performance with $\alpha = 30$ dB with deviation and self-interference cancellation: (a) single polarized, (b) dual polarized.

Experiment results are classified into three categories: good, bad, and very bad. System is classified as good if there is no error floor in the simulation result. Bad classification is made for system with error floor. If total error or flat BER is happened, result is classified as very bad.

System performance of both single polarized and dual polarized configurations are shown in Fig. 9. It has been shown that dual polarized configuration has better performance than single polarized configuration. Lower BER at the same self-interference signal power ratio and SNR has been achieved by dual polarized configuration.

There is critical range at α of 20dB until 35dB for single polarized configuration and 25dB until 40dB for dual polarized configuration. Performance change drastically in critical range region from good to very bad. Critical range of dual polarized configuration is at the larger α compared to single polarized configuration. This critical range shows that dual polarized configuration has better stability by changing of α .

A. Deviated S-Parameter

Based on simulation result without deviation, $\alpha = 30\text{dB}$ is taken for simulation with deviated \mathbf{S} because of its critical range. Both of single polarized and dual polarized are classified as bad in this research's classification.

Results of simulation with self-interference cancellation at $\alpha = 30\text{ dB}$ are presented in Fig. 10. It has been shown that the result of single polarized and dual polarized configuration are relatively similar. It is because self-interference cancellation cancels the self-interference from other antennas. We also found that higher deviation of S-parameter leads to higher error because the deviation makes error on self-interference cancellation using basic (constant) S-parameter.

VI. CONCLUSION

We have proposed dual-cross-polarized antenna decoupling for 43 GHz Planar Massive MIMO in Full Duplex Single Channel Communications. We designed dual-cross polarized antenna such that coupling between antennas can be reduced using different polarization for nearby antenna. The results confirmed that the proposed antenna reduces coupling by average of 37.83% at 43 GHz, reduces ECC by average of 89.69% at 43 GHz, and provide lower BER in self-interference environment compared to single polarized antenna configuration.

REFERENCES

- [1] E. Yaacoub, M. Hussein, and H. Ghaziri, "An overview of research topics and challenges for 5G massive MIMO antennas," in *2016 IEEE Middle East Conference on Antennas and Propagation (MECAP)*. IEEE, 2016, pp. 1–4.
- [2] E. G. Larsson, O. Edfors, F. Tufvesson, and T. L. Marzetta, "Massive mimo for next generation wireless systems," *arXiv preprint arXiv:1304.6690*, 2013.
- [3] L. Lu, G. Y. Li, A. L. Swindlehurst, A. Ashikhmin, and R. Zhang, "An overview of massive mimo: Benefits and challenges," *IEEE journal of selected topics in signal processing*, vol. 8, no. 5, pp. 742–758, 2014.
- [4] J. I. Choi, M. Jain, K. Srinivasan, P. Levis, and S. Katti, "Achieving single channel, full duplex wireless communication," in *Proceedings of the sixteenth annual international conference on Mobile computing and networking*. ACM, 2010, pp. 1–12.
- [5] S. Li and R. D. Murch, "An investigation into baseband techniques for single-channel full-duplex wireless communication systems," *IEEE Transactions on Wireless Communications*, vol. 13, no. 9, pp. 4794–4806, 2014.
- [6] M. Jain, J. I. Choi, T. Kim, D. Bharadia, S. Seth, K. Srinivasan, P. Levis, S. Katti, and P. Sinha, "Practical, real-time, full duplex wireless," in *Proceedings of the 17th annual international conference on Mobile computing and networking*. ACM, 2011, pp. 301–312.
- [7] Y. Hua, P. Liang, Y. Ma, A. C. Cirik, and Q. Gao, "A method for broadband full-duplex mimo radio," *IEEE Signal Processing Letters*, vol. 19, no. 12, pp. 793–796, 2012.
- [8] C. Campolo, A. Molinaro, A. O. Berthet, and A. Vinel, "Full-duplex radios for vehicular communications," *IEEE Communications Magazine*, vol. 55, no. 6, pp. 182–189, 2017.
- [9] Muhsin, R. P. Astuti, and B. S. Nugroho, "Dual polarized antenna decoupling for 60 GHz planar massive mimo," in *2017 International Conference on Signals and Systems (ICSigSys)*. IEEE, 2017, pp. 158–162.
- [10] A. Alfakhri, M. A. Ashraf, A. Alasaad, and S. Alshebeili, "Design and analysis of compact size dual polarised ultra wideband MIMO antennas with simple decoupling structure," in *2016 21st International Conference on Microwave, Radar and Wireless Communications (MIKON)*. IEEE, 2016, pp. 1–4.
- [11] M. M. M. Ali and A.-R. Sebak, "Design of compact millimeter wave massive MIMO dual-band (28/38 GHz) antenna array for future 5g communication systems," in *2016 17th International Symposium on Antenna Technology and Applied Electromagnetics (ANTEM)*. IEEE, 2016, pp. 1–2.
- [12] A. Alfakhri, M. A. Ashraf, A. Alasaad, and S. Alshebeili, "A compact size ultra wideband MIMO antenna with simple decoupling structure," in *2016 17th International Symposium on Antenna Technology and Applied Electromagnetics (ANTEM)*. IEEE, 2016, pp. 1–2.
- [13] Muhsin and K. Anwar, "Abba dual-cross-polarized antenna decoupling for 5g 16-element planar mimo at 28 ghz," in *2018 2nd International Conference on Telematics and Future Generation Networks (TAFGEN)*. IEEE, 2018, pp. 1–6.
- [14] A. Sabharwal, P. Schniter, D. Guo, D. W. Bliss, S. Rangarajan, and R. Wichman, "In-band full-duplex wireless: Challenges and opportunities," *IEEE Journal on selected areas in communications*, vol. 32, no. 9, pp. 1637–1652, 2014.
- [15] R. Garg, *Microstrip antenna design handbook*. Artech house, 2001.
- [16] P. Meerasri, P. Uthansakul, and M. Uthansakul, "Self-interference cancellation-based mutual-coupling model for full-duplex single-channel mimo systems," *International Journal of Antennas and Propagation*, vol. 2014, 2014.
- [17] H. Jafarkhani, "A quasi-orthogonal space-time block code," *IEEE Transactions on Communications*, vol. 49, no. 1, pp. 1–4, 2001.
- [18] P. Marsch, W. Rave, and G. Fettweis, "Quasi-orthogonal stbc using stretched constellations for low detection complexity," in *2007 IEEE Wireless Communications and Networking Conference*. IEEE, 2007, pp. 757–761.
- [19] A. A. Glazunov, "Mean effective gain of user equipment antennas in double directional channels," in *15th IEEE International Symposium on Personal, Indoor and Mobile Radio Communications (PIMRC) 2004*, vol. 1. IEEE, 2004, pp. 432–436.
- [20] S. Blanch, J. Romeu, and I. Corbella, "Exact representation of antenna system diversity performance from input parameter description," *Electronics letters*, vol. 39, no. 9, pp. 705–707, 2003.
- [21] S. K. Dhar and M. S. Sharawi, "A uwb semi-ring mimo antenna with isolation enhancement," *Microwave and Optical Technology Letters*, vol. 57, no. 8, pp. 1941–1946, 2015.

Multimodal Age-Group Recognition for Opinion Video Logs using Ensemble of Neural Networks

Sadam Al-Azani¹, El-Sayed M. El-Alfy²
College of Computer Sciences and Engineering,
King Fahd University of Petroleum and Minerals
Dhahran 31261, Kingdom of Saudi Arabia

Abstract—With the wide spread usage of smartphones and social media platforms, video logging is gaining an increasing popularity, especially after the advent of YouTube in 2005 with hundred millions of views per day. It has attracted interest of many people with immense emerging applications, e.g. filmmakers, journalists, product advertisers, entrepreneurs, educators and many others. Nowadays, people express and share their opinions online on various daily issues using different forms of content including texts, audios, images and videos. This study presents a multimodal approach for recognizing the speaker's age group from social media videos. Several structures of Artificial Neural Networks (ANNs) are presented and evaluated using standalone modalities. Moreover, a two-stage ensemble network is proposed to combine multiple modalities. In addition, a corpus of videos has been collected and prepared for multimodal age-group recognition with focus on Arabic language speakers. The experimental results demonstrated that combining different modalities can mitigate the limitations of unimodal recognition systems and lead to significant improvements in the results.

Keywords—Multimodal recognition; opinion mining; age groups; word embedding; acoustic features; visual features; information fusion; ensemble learning; Arabic speakers

I. INTRODUCTION

Due to the increasing adoption of mobile and web technologies, people tend to share their opinions and interact online on various aspects of their lives through a variety of social media platforms and websites, e.g. reviewing products, rating movies, or evaluating services [1]–[3]. Examples of major social media platforms and blogging websites include Twitter, Facebook, Google+, Instagram, Pinterest and LinkedIn. Over the past years, there has been a growing interest in social media analysis ranging from simple stats dashboards, to more advanced sentiment analysis and topic trending, to more incredible recommendation systems. The aim is transformation of available raw data into insightful information of relations and content to support decision making and guide strategic planning. This plays important role in business intelligence to set up plans and strategies to leverage marketing campaigns and enhance customer satisfaction.

Most of the state-of-the-art techniques for sentiment analysis have focused on textual data analysis of people's comments or feedback. Sentiment analysis is concerned with analyzing, evaluating and understanding the opinions, attitudes, appraisals towards different entities, aspects or features [4]. These techniques are based on using natural language processing, text mining, and computational linguistics to identify subjective information, determine opinions polarities (e.g. positive or negative) or affective states (e.g. happiness, sadness, fear, anger,

surprise or disgust) for a given text, recognize sentiments on different aspects of a product, etc. Lots of work have been carried out in this regard. For a rigorous survey on sentiment analysis, we refer interested reader to [5], which reviews over one hundred articles published from 2002 to 2015 and organizes them based on tasks, approaches and applications. As Twitter has been one of the most prevalent microblogging platforms, several studies have focused on sentiment analysis of tweets. In [6], the authors presented a recent survey of algorithms and sentiment related tasks for Twitter such as tracking sentiments over time, irony detection, emotion detection, and tweet sentiment quantification.

Due to the limitations and challenges facing textual based sentiment analysis, researchers have been more recently attracted to consider other sources of information that are becoming more popular in social media such as voice, images and videos. For instance, there has been a great interest in information fusion for affective computing utilizing more than one modality or information channel [7]. Several factors can negatively affect the unimodal analysis and recognition systems, including noisy sensor data, non-universality, and lack of individuality. Each modality has its own challenges. For example, recognition systems based on voice might be affected by different attributes such as low voice quality, background noise and disposition of voice-recording devices. Text-based recognition systems also suffer from several issues related to morphological analysis, multi-dialects, ambiguity, temporal dependency, domain dependency, etc. This is also true regarding recognition systems based on visual modality, which can also suffer from illumination conditions, posture, cosmetics, resolution, etc. In consequence, this leads to inaccurate and insufficient representation of patterns. So, incorporating different modalities for an entity can overcome such issues because each source of information can replenish each other. This might result in developing more accurate and robust recognition systems. It provides several evidences for the same identity which can lead to significantly improving the performance as compared to unimodal systems.

Several approaches, resources and techniques have been provided, designed and conducted to address sentiment analysis. Current sentiment and opinion mining based approaches evaluate peoples opinions in different analysis levels including document, sentence and aspect/ feature using different approaches: lexicon-based, machine learning based and hybrid based approaches. However, they don't take into account the impact of users' age on the analyzed opinions. Multimodal age recognition systems can be beneficial in such applications

to tune the analysis and decisions towards particular age groups in order to meet their needs. For example, some products are specific for young people and reviews on these products by elder people are biased and may provide incorrect indicators for decision makers. Governments can also benefit from these systems to explore political decisions or services related to their citizens according to their age groups. Adaptive educational systems will be smarter when they consider age of the learner alongside the emotion.

Detecting users' age-groups through emotional modalities makes the problem more interesting and significant, especially with the revolution in social media platforms nowadays. Several social media platforms are being used to support opinion videos such as YouTube, Vimeo, Twitter, Facebook, Instagram, Flickr, etc. Thus, it is highly important to exploit such data for mining significant information and insights. Profiling user identification such as recognizing age group from emotional modalities is a challenging task because it relies on several attributes that are hard to model such as feeling, thought, behavior, mood, temperament [8]. The research of user profiling identification and detection for Arabic language is even more scarce [9], [10]. This is another motivation for this study to build a dataset of multimodal age-group identification for Arabic opinion videos and present a multimodal age-group identification system. To our knowledge this is the first study to present a multimodal age-group identification approach specific from opinion videos. Additionally, it is the first study to present a multimodal for Arabic videos in this concern, in general. It evaluates the capability of audio, textual and visual features individually to detect age-group for the same entity. Then, it presents an ensemble neural network method to fuse different modalities in order to improve the performance of the individual modalities. Several experiments are conducted to evaluate the proposed approach.

The rest of the paper is organized as follows. The most related work is briefly reviewed in Section II. Section III describes the methodology. Section IV presents the experimental work and results. Finally, Section V concludes the paper.

II. RELATED WORK

Age identification is considered as a task of user profiling detection and has received a growing attention in social media and human-computer-interaction systems with rising need for personalized, reliable, and secure systems. In the literature, this problem is addressed in a variety of ways. Some research work considered it as a classification problem to predict age group of a given user, e.g. [11], whereas others addressed it as a regression problem to predict the age in years, e.g. [12], [13]. Most of existing methods have mainly focused on single modalities or single mediums including texts [14], [15], images [16]–[19], voice/speech [11], [20], and meta-data of users on Twitter [21].

Safavi et al. [11] presented a method to detect age-group from children's speech using the OGI Kids dataset. They applied Gaussian Mixture Model-Universal Background Model (GMM-UBM), and Gaussian Mixture-Support Vector Machine (GMM-SVM) with i-vector systems. Regions of the spectrum containing important age information for children are identified by conducting Age-ID experiments over 21 frequency sub-bands. The main findings were the GMM-UBM and i-vector

system significantly performed better than the GMM-SVM system with an accuracy of 85.77%. An approach for age estimation from telephone speech patterns based on i-vectors was also presented in [13]. Each utterance was represented by i-vector and Support Vector Regression (SVR) is applied to estimate the age of speakers. Bocklet et al. [20] present a method to detect a person's age and gender from his/her voice. As acoustic features, they applied Mel Frequency Cepstrum Coefficients (MFCCs), Perceptual Linear Prediction (PLPs) and Temporal Patterns (TRAPS)-based features. Different models were generated and combined at feature level and score level fusion and evaluated using GMM. They reported that combining different acoustic models led to improve the results with minor differences between feature level and score level fusions.

Different age categories were considered in the literature to address the age recognition task. For example, the authors in [14] ran their experiments on three categories: 10s (13-17), 20s (23-27) and 30s (33-42) years old. In Safavi et al. [11], three age groups are considered: (5-9 years old), (9-13 years old), (13-16 years old).

Multimodal recognition systems are still in their early stage and started applying for different tasks as gender detection [22], sentiment analysis [7], [23]. Our work differs from the literature in several aspects. First, it recognizes age-groups from three modalities for the same user and compares the effectiveness of these modalities with each others. It explores different features for representing modalities such as word embedding based features for textual modality, dense optical flows for visual modality and a combination of several types of acoustic features. It builds a corpus for opinions videos of Arabic speakers. Moreover, it explores a novel ensemble of a neural network approach to combine different modalities.

III. METHODOLOGY

In this study, the age-group recognition task is addressed as a classification problem. This can be useful in applications such as targeted marketing which is directed to certain age groups rather than specific ages. For example, companies can tune their products to meet the needs of a specific age-group of people. Fig. 1 depicts the general framework of the proposed multimodal age-group recognition system. Some preprocessing operations are conducted to come up with three modalities for each video: audio, text, and visual. Each audio input is in WAV format with 256 bits, 48000Hz sampling frequency, and a mono channel. This is followed by the transcription task to generate texts corresponding to each video. Each video input is then resized into 240×320 after detecting faces. A feature extractor is constructed for each input source. The acoustic feature extractor constructs feature vectors of 68 features for each input. Moreover, a textual feature extractor is implemented to extract textual features with a dimensionality of 300 features for each instance. The visual feature extractor generates 800 features for each input.

A fusion method based on ensemble neural network is proposed to combine the different modalities. It is based on two levels; the first level is trained using the training dataset and gives a score for each age group from each modality (visual, text and audio). The resulting scores from the first

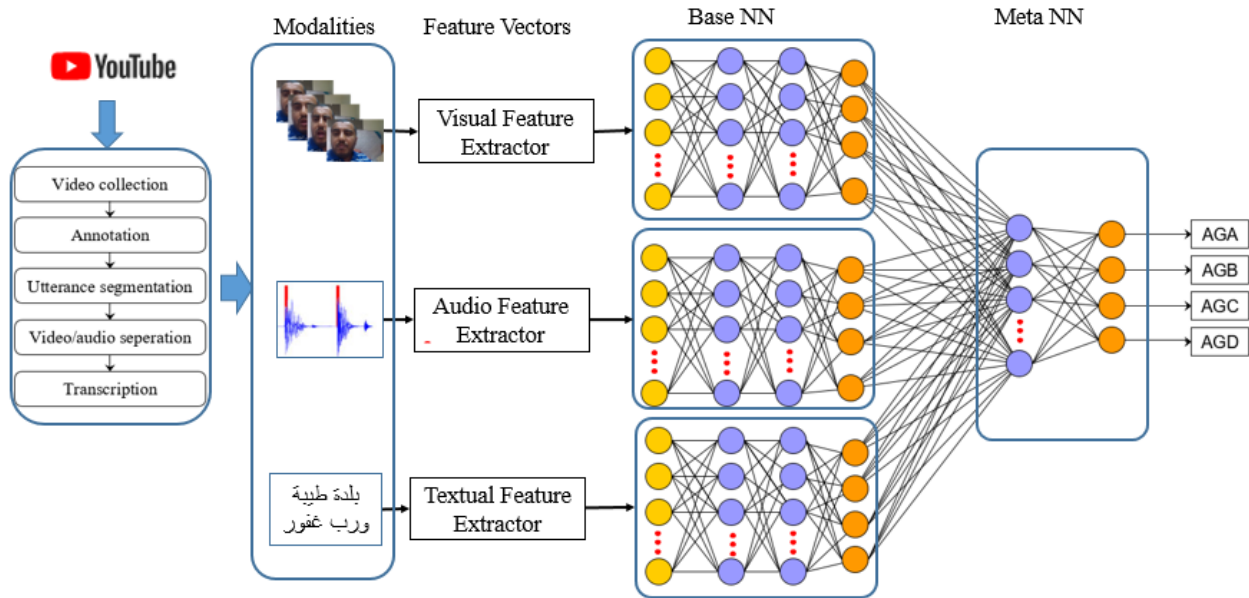


Fig. 1. Multimodal age identification system from opinion videos

level are combined using a meta-learner in the second level to produce the final scores. The predicted age group is determined corresponding to the maximum final score.

A. Multimodal Age-groups Recognition Dataset

A video corpus is collected from YouTube. It is composed of 63 opinion videos expressed from both females and males in different domains including reviews of products, movies, cultural views, etc. Using various settings, the collected videos were recorded by users in real environments including houses, studios, offices, cars or outdoors. Users express their opinions in different periods. The videos are segmented into 524 utterances. The age-groups are specified as four classes as described in Table I. The instances are manually labeled into the considered age-groups carefully and systematically. First, for the well-known speakers, we looked for their ages in their profiles and assigned their age by subtracting date of recording videos from their birthdays. For the remaining speakers who we couldn't find their birthdays, three human annotators were involved to assign their age-group labels, using majority votes to break ties.

B. Feature Extraction

1) *Acoustic features extraction:* The input audio is split into frames with size of 50 millisecond with a frame step of 20 millisecond. For each generated frame, a set of 34 features are computed: (1) ZCR (Zero Crossing Rate), (2) Energy, (3) Entropy of Energy, (4) Spectral Centroid, (5) Spectral Spread, (6) Spectral Entropy, (7) Spectral Flux, (8) Spectral Rolloff, (9-21) MFCCs (22-33) Chroma Vector, and (34) Chroma Deviation. Then statistics are computed from each audio's segment to represent the whole audio using one descriptor; in our study we used the mean and standard deviation. Thus, each input audio is represented by $34 \times 2 = 68$ features. This process of audio feature extraction is illustrated in Fig. 2.

2) *Visual feature extraction:* Two main steps are involved: face detection and visual feature extraction. The general frontal face and eye detectors [24] are utilized to detect the face of the speaker and segment faces from the rest of given frame based on HAAR features [25], which increasingly combines more complex classifiers in a cascade to detect the face. In addition, an eye detector detects eye positions which provide significant and useful values to crop and scale the frontal face to a size of 240×320 pixels in our case.

Then, optical flow is considered to extract the visual features from the videos processed in the previous step. Optical flows are, first, computed for each frame in a video and then used to compute histograms. They measure the motion relative to an observer between two frames at each point of them. At each point in the scene, the magnitude and the direction values are obtained which describe the vector representing the motion between the two frames. This leads to $NoF \times W \times H \times 2$ dimensions to describe each video, where NoF represents the number of frames in a video and the $W \times H$ represents the resolution of the frame. In our case frames are scaled into the resolution of 240×320 . To describe each video as a single feature vector (descriptor), a histogram of the optical flows per video is calculated. The scene is split into a grid of 10×10 with considering eight directions: $\{0 - 45, 46 - 90, 91 - 135, 136 - 180, 181 - 225, 226 - 270, 271 - 315, 316 - 360\}$. Consequently, each scene is represented by 800 features and to represent the whole input video the average of the histograms is calculated. The face detection and visual feature extraction is illustrated in Fig. 3.

3) *Textual features:* The word embedding technique skip-grams word2vec [26], [27] is employed to extract textual features. Embedding techniques are recognized as an efficient method for learning high-quality vector representations of words/terms/phrases from large amounts of unstructured text data. They refer to the process of mapping words, terms or phrases from the vocabulary to real-valued vectors such that

TABLE I. DESCRIPTION OF DATASET

Class	Description	#Samples
AGA	Age-group A: 15-29 years old	128
AGB	Age-group B: 30-39 years old	159
AGC	Age-group C: 40-49 years old	142
AGD	Age-group D: greater than 49 years old	95
Total		524

TABLE II. THE PERFORMANCE OF STANDALONE MODALITIES USING DIFFERENT NETWORKS STRUCTURES; HIGHEST RESULTS ARE MARKED IN BOLD.

	Structure# NN1			Structure#NN2			Structure# NN3			Structure# NN4			Structure# NN5		
	Prc	Rec	F ₁	Prc	Rec	F ₁	Prc	Rec	F ₁	Prc	Rec	F ₁	Prc	Rec	F ₁
Audio (A)															
AGA	0.8235	0.8750	0.8485	0.8077	0.8203	0.8140	0.8400	0.8203	0.8300	0.7197	0.7422	0.7308	0.8739	0.8125	0.8421
AGB	0.8373	0.8742	0.8554	0.8137	0.8239	0.8188	0.8012	0.8616	0.8303	0.7529	0.8050	0.7781	0.7989	0.8994	0.8462
AGC	0.8593	0.8169	0.8375	0.8345	0.8169	0.8256	0.8085	0.8028	0.8057	0.7879	0.7324	0.7591	0.8667	0.8239	0.8448
AGD	0.9080	0.8316	0.8681	0.8404	0.8316	0.8360	0.8851	0.8105	0.8462	0.7889	0.7474	0.7676	0.8791	0.8421	0.8602
Weighted-Avg	0.8527	0.8511	0.8512	0.8227	0.8225	0.8226	0.8279	0.8263	0.8264	0.7608	0.7595	0.7595	0.8501	0.8473	0.8473
Macro-Avg	0.8570	0.8494	0.8524	0.8241	0.8232	0.8236	0.8337	0.8238	0.8280	0.7624	0.7567	0.7589	0.8547	0.8445	0.8483
Textual (T)															
AGA	0.6695	0.6172	0.6423	0.5549	0.7500	0.6379	0.5923	0.6016	0.5969	0.6316	0.5625	0.5950	0.5299	0.5547	0.5420
AGB	0.5054	0.5912	0.5449	0.5105	0.4591	0.4834	0.5290	0.5157	0.5223	0.4945	0.5660	0.5279	0.4535	0.4906	0.4713
AGC	0.5217	0.5070	0.5143	0.4880	0.4296	0.4569	0.4753	0.5423	0.5066	0.5093	0.5775	0.5413	0.4631	0.4859	0.4742
AGD	0.6463	0.5579	0.5989	0.6265	0.5474	0.5843	0.6234	0.5053	0.5581	0.6866	0.4842	0.5679	0.6087	0.4421	0.5122
Weighted-Avg	0.5755	0.5687	0.5702	0.5363	0.5382	0.5323	0.5470	0.5420	0.5428	0.5668	0.5534	0.5552	0.5029	0.4962	0.4968
Macro-Avg	0.5857	0.5683	0.5751	0.5450	0.5465	0.5406	0.5550	0.5412	0.5460	0.5805	0.5476	0.5580	0.5138	0.4933	0.4999
Visual (V)															
AGA	0.5827	0.6328	0.6067	0.6419	0.7422	0.6884	0.5556	0.7422	0.6355	0.5567	0.8438	0.6708	0.6389	0.5391	0.5847
AGB	0.6562	0.5283	0.5854	0.6074	0.6226	0.6149	0.5917	0.4465	0.5090	0.6794	0.5597	0.6138	0.6200	0.5849	0.6019
AGC	0.5279	0.7324	0.6136	0.6452	0.5634	0.6015	0.6230	0.5352	0.5758	0.7080	0.5634	0.6275	0.5492	0.7465	0.6328
AGD	0.8500	0.5368	0.6581	0.6404	0.6000	0.6196	0.5946	0.6947	0.6408	0.6860	0.6211	0.6519	0.7397	0.5684	0.6429
Weighted-Avg	0.6386	0.6107	0.6114	0.6320	0.6317	0.6301	0.5919	0.5878	0.5819	0.6584	0.6412	0.6383	0.6271	0.6145	0.6135
Macro-Avg	0.6542	0.6076	0.6159	0.6337	0.6321	0.6311	0.5912	0.6047	0.5902	0.6575	0.6470	0.6410	0.6370	0.6097	0.6156

TABLE III. BIMODAL AND MULTIMODAL RESULTS USING ENSEMBLE CLASSIFIER

Modalities	A-T			T-V			A-V			A-T-V		
	Prc	Rec	F ₁	Prc	Rec	F ₁	Prc	Rec	F ₁	Prc	Rec	F ₁
AGA	0.8682	0.8750	0.8716	0.7090	0.7422	0.7252	0.8923	0.9062	0.8992	0.9120	0.8906	0.9012
AGB	0.8580	0.8742	0.8660	0.6772	0.6730	0.6751	0.8805	0.8805	0.8805	0.8712	0.8931	0.8820
AGC	0.8493	0.8732	0.8611	0.6739	0.6549	0.6643	0.8750	0.8873	0.8811	0.8611	0.8732	0.8671
AGD	0.9080	0.8316	0.8681	0.7234	0.7158	0.7196	0.9011	0.8632	0.8817	0.8804	0.8526	0.8663
Weighted-Avg	0.8672	0.8664	0.8664	0.6924	0.6927	0.6925	0.8856	0.8855	0.8855	0.8801	0.8798	0.8798
Macro-Avg	0.8709	0.8635	0.8667	0.6959	0.6965	0.6960	0.8872	0.8843	0.8856	0.8812	0.8774	0.8792

elements with similar meaning to have a similar representation.

Word vectors are positioned in the vector space such that words sharing common contexts and having similar semantic are mapped nearby each other. Skip-grams (SG) is a neural network structure trained to predict a context given a word. Word embedding-based features have been adopted for different natural language processing tasks and achieved high results comparing to other traditional features [28]. In our study, a skip-gram model trained from opinions expressed in Twitter with a dimensionality of 300 [29] is used to derive textual features. A feature vector is generated for each sample by averaging the embeddings of that sample [30]. The main steps of textual feature extraction are shown in Fig. 4.

C. Classification Approach

This study deals with a multimodal identification system for three modalities. Therefore, seven different main models can be generated as follows. Three models are generated for audio, textual and visual modalities. Three other models are generated for the bimodal approaches of audio-textual, textual-

visual, and audio-visual modalities. The seventh model is for the trimodal of audio, textual and visual modalities.

Due to the theoretical foundation underlying neural network research and recently-achieved strong practical results on challenging problems, neural networks have recently been rediscovered as a significant alternative to several standard classification techniques [31]. However, the models need to be generated well. Different systematic structures of neural networks are investigated to detect the age group from the considered standalone modality. Three models of feed-forward networks structures, Multilayer Perceptron (MLP) models, are applied. The first model is for visual modality, the second is for the audio modality while the third model is for textual modality. Several factors and decisions should be considered when configuring and setting up the neural network structures including: number of hidden layers to use in the neural network, number of neurons in each hidden layer, etc. Another issue for the multimodal approaches is: should the models be homogeneous or heterogeneous?; the former means using the same structure for each modality while the latter means using different structures. In the case of the heterogeneous models,

TABLE IV. P-VALUES FOR PAIR WISE T-TESTS ON ACCURACY

Methods	P-Value	Conclusion
A vs. AT	0.0303	Reject H0. The accuracy rate of audio-textual modality is significantly higher than the audio modality
A vs. AV	0.00005	Reject H0. The accuracy rate of audio-visual modality is significantly higher than the audio modality
A vs. ATV	0.00001	Reject H0. The accuracy rate of audio-textual-visual modality is significantly higher than the audio modality
T vs. AT	0	Reject H0. The accuracy rate of audio-textual modality is significantly higher than the textual modality
T vs. TV	0	Reject H0. The accuracy rate of textual-visual modality is significantly higher than the textual modality
T vs. ATV	0	Reject H0. The accuracy rate of audio-textual-visual modality is significantly higher than the textual modality
V vs. AV	0	Reject H0. The accuracy rate of audio-visual modality is significantly higher than the visual modality
V vs. TV	0.279427	Accept H0. combining visual modality with textual modality has no effect comparing to visual modality
V vs. ATV	0	Reject H0. The accuracy rate of audio-textual-visual modality is significantly higher than the visual modality
AV vs. ATV	0.010979	Reject H0. The accuracy rate of audio-textual-visual modality is significantly higher than the audio-visual modality

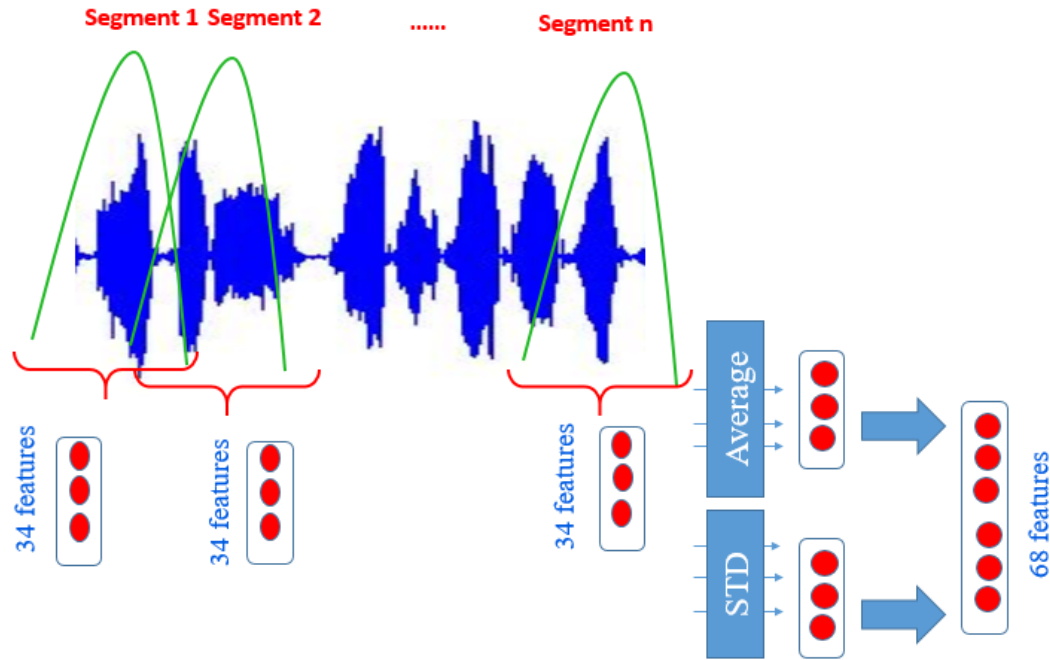


Fig. 2. Audio feature extraction process.

what are the considered attributes. In this study, two hidden layers are considered for each model while several criteria are considered to determine the number of neurons in each layer:

- Same number of neurons in each hidden layer with the same structure.
- Number of neurons is assigned according to the size of inputs for each structure. Several cases are considered including:

- the number of neurons in a hidden layer is calculated using:

$$N_{h1} = i + o \quad (1)$$

where i is the size of input, o is the number of classes

- the number of neurons in a hidden layer is calculated using:

$$N_{h2} = \frac{i + o}{2} \quad (2)$$

- the number of neurons in a hidden layer is calculated using:

$$N_{h3} = i \times 2 \quad (3)$$

Other parameters are selected and remain the same for all structures to be: activation function = “relu”, alpha = 0.0001, batch_size= “auto”, learning-rate = 0.001, tol = 0.0001, momentum = 0.9, epsilon= 10^{-8}).

Consequently, five different structures are defined from the aforementioned criteria. The first structure is denoted as NN1 and uses a constant number of neurons in both hidden layers for all modalities. Since the three modalities are trained and evaluated using the same structure, this type is homogeneous. The second structure is denoted as NN2 and uses a number of neurons equals to N_{h1} in the first hidden layer and equals to N_{h2} for the second hidden layer. The third structure is denoted as NN3 and uses a number of neurons equals to N_{h1} in both hidden layers. The fourth structure is denoted as NN4 and uses a number of hidden layers equals to N_{h2} for both hidden layers. The fifth structure is denoted as NN5 and uses a number of hidden layers equals to N_{h3} for both hidden layers. So, all structures except the first one (NN1) rely on the size of the input and are heterogeneous for all modalities. Those structures are considered as baseline models/classifiers.

Another MLP model is constructed as a meta-classifier to ensemble all modalities base models. In this study, a simple structure of one hidden layer is adopted in the second stage. It

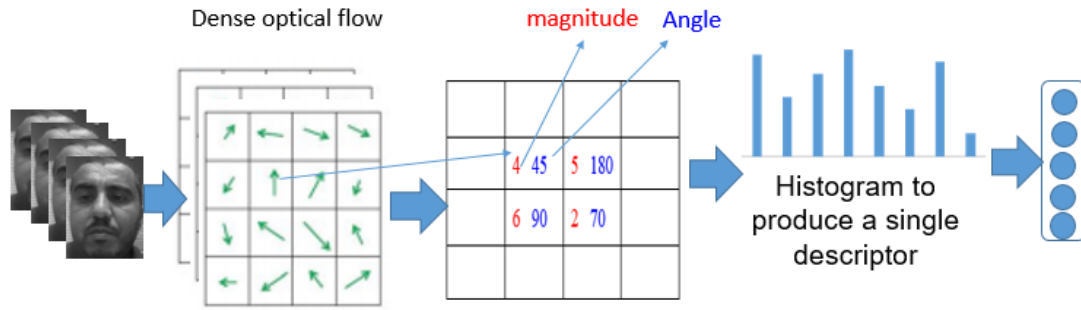


Fig. 3. Face detection and dense optical flow features extraction process.

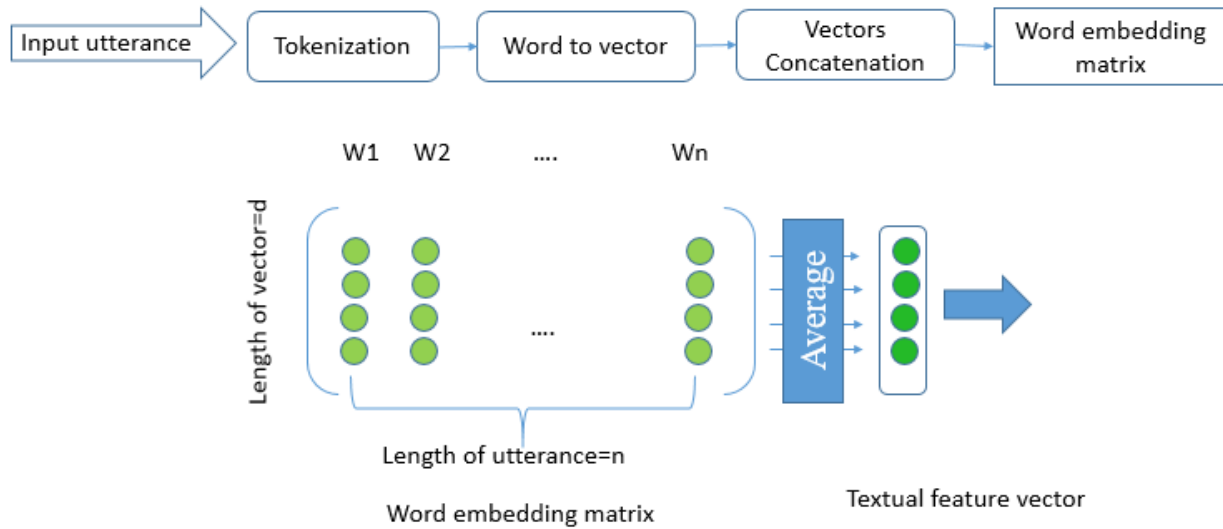


Fig. 4. Textual feature extraction process.

takes as inputs the probabilities of classes produced by the base models. Mathematically, let $Y_V = \{v_1, v_2, v_3, v_4\}$ represents the scores for age groups generated by visual-based model, $Y_A = \{a_1, a_2, a_3, a_4\}$ represents the scores for age groups generated by audio-based model, and $Y_T = \{t_1, t_2, t_3, t_4\}$ represents the scores for age groups generated by textual-based model. These scores are fed into the meta-MLP as input to identify the global age-group of users using the three modalities. So, it takes inputs with size of $M \times N$, where M is the number of modalities and N is the number of classes. As mentioned above, four models can be generated when combining the three different modalities: audio-textual, textual-visual, audio-visual, and audio-textual-visual modalities. In case of bimodal approaches, the size of meta-classifier input is eight while its size is 12 in case of multimodal approach.

IV. EXPERIMENTS AND RESULTS

The proposed models are evaluated using 10-fold cross validation mode. A prototype is implemented and evaluated for each standalone modality and for the ensemble model in Python using the scikit-learn machine learning package [32]. Several well-known measures are reported to evaluate and compare the performance of various models: Precision (Prc), Recall (Rec), and F_1 , which is a weighted average for precision and recall, and is a preferred performance measure for

imbalanced class distributions. These measures are computed as follows for each class c_i :

$$Prc_i = \frac{\# \text{ instances correctly classified as class } c_i}{\# \text{ instances classified as class } c_i} \quad (4)$$

$$Rec_i = \frac{\# \text{ instances correctly classified as class } c_i}{\# \text{ instances actually in class } c_i} \quad (5)$$

$$F_{1i} = 2 \times \frac{Prc_i \times Rec_i}{Prc_i + Rec_i} \quad (6)$$

Besides the per-class performance, we reported the weighted and macro-averages of all classes in each case. The macro-average is unweighted of each class metric without taking class imbalance into account. This measure may overemphasize the low performance of infrequent classes. Hence, we also report weighted average where each class metric is weighted by the support (i.e. the number of true instances for each class).

A. Unimodal Age-group Recognition Results (Baseline)

Table II shows the results for each modality with different base neural network structures for unimodal age-group identification approaches. The results are presented in terms of precision, recall and F_1 for each class as well as weighted and macro averages for all classes. Audio modality achieves the highest results comparing to text and visual modalities in all cases. For audio modality, NN1 achieves the highest results with a weighted F_1 average of 85.12%, followed by NN5 which reports a weighted F_1 average of 84.73%. However, NN4 achieves the lowest results for audio modality. However, the overall lowest results are obtained using the textual modality. The best performance in the case of textual modality is obtained using NN1 with a weighted average of 57.02%. Regarding the visual modality, the highest results are achieved using NN4 with a weighted average of 63.83%.

B. Bimodal and Multimodal Age-group Recognition Results

The best structures evaluated in the first level classification are then used to represent each modality and fed into the second level classifier. For audio modality and textual modality, NN1 is used while for visual modality NN4 is used. NN1 for audio modality, NN1 for text modality and NN4 for visual modality are fused using the meta-structure. Table III shows the results obtained using bimodal and multimodal approaches. The highest results are achieved using audio-visual (A-V) approach with a weighted average of 88.55% and then audio-text-visual (A-T-V) approach with a weighted average of 87.98%. It can be seen that significant improvements are reported over the baseline performance in Table II. For example, in the worst cases, the highest weighted F_1 obtained for baseline textual modality is 57.02% and for visual modality is 63.83% whereas after combining them the results are improved to be 69.25%. In the best cases, the highest weighted F_1 obtained for audio modality is 85.12% and for visual modality is 63.83% while combining them leads to improving the results to be 88.55%

It is important to perform statistical test to provide evidence that the improvement of combining different modalities is significant and not by chance. To do so, we re-run the 10-fold cross-validation 10 times for each model. We then used the pairwise t-test to determine how significant is the improvements. Table IV shows the results for the performed t-tests using 95% confidence interval. The reported p-values are less than 0.05 for all the cases except one. Thus, the null hypothesis is rejected and significant improvement is obtained except when textual modality is combined with visual modality (no statistically significant improvement is observed).

V. CONCLUSION

We have presented a novel multimodal ensemble neural network model for detecting users' age-group from opinion videos. For evaluation purpose, three modalities are extracted, namely: audio, text and visual from videos expressed in Arabic language with different dialects. Various ways are adopted to construct different neural network structures for the unimodal recognition as baseline. Then, all modalities are combined using the proposed ensemble neural network approach. For standalone modalities, the audio-based model has achieved the highest performance with the smallest number of features.

However, text modality reported the lowest results. Combining different modalities has led to significant improvements in the results in nearly all cases. The highest results have been achieved using the bimodal audio-visual and trimodal audio-textual-visual approaches. As future work, the authors are exploring the impact of age knowledge in opinion mining and sentiment analysis.

ACKNOWLEDGMENT

The authors would like to thank King Fahd University of Petroleum and Minerals (KFUPM), Saudi Arabia, for support during this work. The first author also acknowledges the scholarship provided by Thamar University, Yemen, for his higher studies.

REFERENCES

- [1] Z. Xiang and U. Gretzel, "Role of social media in online travel information search," *Tourism management*, vol. 31, no. 2, pp. 179–188, 2010.
- [2] W. He, S. Zha, and L. Li, "Social media competitive analysis and text mining: A case study in the pizza industry," *International Journal of Information Management*, vol. 33, no. 3, pp. 464–472, 2013.
- [3] I. Lee, "Social media analytics for enterprises: Typology, methods, and processes," *Business Horizons*, vol. 61, no. 2, pp. 199–210, 2018.
- [4] B. Liu, "Sentiment analysis and opinion mining," *Synthesis Lectures on Human Language Technologies*, vol. 5, no. 1, pp. 1–167, 2012.
- [5] K. Ravi and V. Ravi, "A survey on opinion mining and sentiment analysis: Tasks, approaches and applications," *Knowledge-Based Systems*, vol. 89, pp. 14–46, 2015.
- [6] A. Giachanou and F. Crestani, "Like it or not: A survey of twitter sentiment analysis methods," *ACM Computing Surveys (CSUR)*, vol. 49, no. 2, p. 28, 2016.
- [7] S. Poria, E. Cambria, R. Bajpai, and A. Hussain, "A review of affective computing: From unimodal analysis to multimodal fusion," *Information Fusion*, vol. 37, pp. 98–125, 2017.
- [8] K. Zvarevashe and O. O. Olugbara, "Gender voice recognition using random forest recursive feature elimination with gradient boosting machines," in *IEEE International Conference on Advances in Big Data, Computing and Data Communication Systems (icABCD)*, 2018, pp. 1–6.
- [9] P. Rosso, F. Rangel, I. H. Farías, L. Cagnina, W. Zaghouni, and A. Charfi, "A survey on author profiling, deception, and irony detection for the arabic language," *Language and Linguistics Compass*, vol. 12, no. 4, p. e12275, 2018.
- [10] F. Rangel, P. Rosso, M. Montes-y Gómez, M. Potthast, and B. Stein, "Overview of the 6th author profiling task at pan 2018: multimodal gender identification in twitter," *Working Notes Papers of the CLEF*, 2018.
- [11] S. Safavi, M. Russell, and P. Jančovič, "Identification of age-group from children's speech by computers and humans," in *Fifteenth Annual Conference of the International Speech Communication Association*, 2014.
- [12] T. Bocklet, A. Maier, and E. Nöth, "Age determination of children in preschool and primary school age with gmm-based supervectors and support vector machines/regression," in *Proceedings of International Conference on Text, Speech and Dialogue*, 2008, pp. 253–260.
- [13] M. H. Bahari, M. McLaren, D. Van Leeuwen *et al.*, "Age estimation from telephone speech using i-vectors," 2012.
- [14] J. Schler, M. Koppel, S. Argamon, and J. W. Pennebaker, "Effects of age and gender on blogging," in *AAAI spring symposium: Computational approaches to analyzing weblogs*, vol. 6, 2006, pp. 199–205.
- [15] M. Potthast, F. Rangel, M. Tschuggnall, E. Stamatatos, P. Rosso, and B. Stein, "Overview of pan'17," in *International Conference of the Cross-Language Evaluation Forum for European Languages*. Springer, 2017, pp. 275–290.
- [16] Y. Fu and T. S. Huang, "Human age estimation with regression on discriminative aging manifold," *IEEE Transactions on Multimedia*, vol. 10, no. 4, pp. 578–584, 2008.

- [17] R. Rothe, R. Timofte, and L. Van Gool, "Dex: Deep expectation of apparent age from a single image," in *Proceedings of the IEEE International Conference on Computer Vision Workshops*, 2015, pp. 10–15.
- [18] X. Wang, R. Guo, and C. Kambhampettu, "Deeply-learned feature for age estimation," in *2015 IEEE Winter Conference on Applications of Computer Vision (WACV)*. IEEE, 2015, pp. 534–541.
- [19] M. T. B. Iqbal, M. Shoyaib, B. Ryu, M. Abdullah-Al-Wadud, and O. Chae, "Directional age-primitive pattern (dapp) for human age group recognition and age estimation," *IEEE Transactions on Information Forensics and Security*, vol. 12, no. 11, pp. 2505–2517, 2017.
- [20] T. Bocklet, G. Stemmer, V. Zeissler, and E. Nöth, "Age and gender recognition based on multiple systems-early vs. late fusion," in *Eleventh Annual Conference of the International Speech Communication Association*, 2010.
- [21] L. Sloan, J. Morgan, P. Burnap, and M. Williams, "Who tweets? deriving the demographic characteristics of age, occupation and social class from twitter user meta-data," *PLoS one*, vol. 10, no. 3, p. e0115545, 2015.
- [22] M. Abouelenien, V. Pérez-Rosas, R. Mihalcea, and M. Burzo, "Multimodal gender detection," in *Proceedings of the 19th ACM International Conference on Multimodal Interaction*, 2017, pp. 302–311.
- [23] L.-P. Morency, R. Mihalcea, and P. Doshi, "Towards multimodal sentiment analysis: Harvesting opinions from the web," in *Proceedings of the 13th International Conference on Multimodal Interfaces*, 2011, pp. 169–176.
- [24] P. Viola and M. J. Jones, "Robust real-time face detection," *International Journal of Computer Vision*, vol. 57, no. 2, pp. 137–154, 2004.
- [25] P. Viola and M. Jones, "Rapid object detection using a boosted cascade of simple features," in *Proceedings of the 2001 IEEE Computer Society Conference on Computer Vision and Pattern Recognition (CVPR 2001)*, vol. 1, pp. 1–1.
- [26] T. Mikolov, K. Chen, G. Corrado, and J. Dean, "Efficient estimation of word representations in vector space," in *Proceedings of Workshop at International Conference on Learning Representations*, 2013.
- [27] T. Mikolov, I. Sutskever, K. Chen, G. S. Corrado, and J. Dean, "Distributed representations of words and phrases and their compositionality," in *Advances in Neural Information Processing Systems*, 2013, pp. 3111–3119.
- [28] S. Al-Azani and E.-S. M. El-Alfy, "Combining emojis with arabic textual features for sentiment classification," in *9th IEEE International Conference on Information and Communication Systems (ICICS)*, 2018, pp. 139–144.
- [29] A. B. Soliman, K. Eissa, and S. R. El-Beltagy, "Aravec: A set of arabic word embedding models for use in arabic nlp," in *Proceedings of the 3rd International Conference on Arabic Computational Linguistics (ACLing 2017)*, vol. 117. Elsevier, 2017, pp. 256–265.
- [30] S. Al-Azani and E.-S. M. El-Alfy, "Using word embedding and ensemble learning for highly imbalanced data sentiment analysis in short arabic text," *Procedia Computer Science*, vol. 109, pp. 359–366, 2017.
- [31] C. C. Aggarwal, *Data classification: algorithms and applications*. CRC press, 2014.
- [32] F. Pedregosa, G. Varoquaux, A. Gramfort, V. Michel, B. Thirion, O. Grisel, M. Blondel, P. Prettenhofer, R. Weiss, V. Dubourg *et al.*, "Scikit-learn: Machine learning in python," *Journal of Machine Learning Research*, vol. 12, pp. 2825–2830, 2011.

Performance Evaluation of Completed Local Ternary Pattern (CLTP) for Face Image Recognition

Sam Yin Yee¹, Taha H. Rassem*², Mohammed Falah Mohammed³
Faculty of Computer Systems and Software Engineering,
Universiti Malaysia Pahang,
26300, Kuantan, Malaysia

Nasrin M. Makbol⁴
College of Computer Science and Engineering
Hodeidah University,
Hodeidah, Yemen

Abstract—Feature extraction is the most important step that affects the recognition accuracy of face recognition. One of these features are the texture descriptors that are playing an important role as local features descriptor in many of the face recognition systems. Recently, many types of texture descriptors had been proposed and used for face recognition task. The Completed Local Ternary Pattern (CLTP) is one of the texture descriptors that has been proposed for texture image classification and had been tested for different image classification tasks. It proposed to overcome the Local Binary Pattern (LBP) drawbacks where the CLTP is more robust to noise as well as shown a good discriminative property than others. In this paper, a comprehensive study on the performance of the CLTP for face recognition task has been done. The aim of this study is to investigate and evaluate the CLTP performance using eight different face datasets and compared with the previous texture descriptors. In the experimental results, the CLTP had been shown good recognition rates and outperformed the other texture descriptors for this task. Several face datasets are used in this paper, such as Georgia Tech Face, Collection Facial Images, Caltech Pedestrian Faces, JAFFE, FEI, YALE, ORL, UMIST datasets.

Keywords—Face recognition; recognition accuracy; Local Binary Pattern (LBP); Completed Local Binary Pattern (CLBP); Completed Local Ternary Pattern (CLTP)

I. INTRODUCTION

Now-a-days, there are several ways for identifying a person. Much-advanced technology to recognize a person are voice recognition, fingerprint system, face recognition, and even iris pattern detection [1]. However, the friendliest and natural, lowest damage to verify a person is to use the face recognition. Moreover, it can be used to detect the facial expression of the person. The human brain has an ability to recognize a person face even she/he is wearing glasses, changing hairstyle or changing a facial expression or recognize the face after several years.

Face recognition is an image analysis that gained attention nowadays [2]. There are many algorithms has been proposed due to the importance of this field to achieve high recognition accuracy rates. Face recognition systems can be used in different fields such as security systems, attending systems, detect the criminal person in public place and checks the criminal record of someone. It would make a huge contribution in computer vision and is a success in the technology field. Face recognition plays an important role for identifying a person in compared with the others identification application. The identity of a person based on physiological characteristics can be recognized by the biometric approach of face recognition.

Since two decades, several feature descriptors are proposed and used face recognition such as texture, shape, color descriptors. Examples of texture descriptors that used for face recognition systems are the Local Binary Pattern (LBP) [3], Local Ternary Pattern (LTP) [4], Completed Local Binary Pattern (CLBP) [5], Colour Completed Local Binary Pattern (CCLBP) [6], Complated and Completed Local Ternary Pattern (CLTP) [7], [8]. The LBP was reported to be initially used for texture descriptors in 2002 [3]. The superiorities of LBP are bound to its invariance to revolution, robustness against monotonic dim level change, and also its low computational complexity. However, it has some disadvantages which high-sensitivity to noise as well as sometimes cannot distinguish different patterns [9]. These two problems have been mentioned in many research papers as the drawbacks of LBP.

In spite of that, the Local Ternary Pattern (LTP) has been proposed to overcome the limitation of LBP which is more robust to noise comparing with LBP. However, the LTP sometimes cannot distinguish different patterns like the LBP. There are many texture descriptors have been proposed afterwards, such as CLBP, and CLTP.

The CLTP is proposed to be more robust to noise as well as more discriminative in comparison with the LBP, LTP and CLBP. For face recognition task, the performance of the CLTP had been evaluated and compared with other texture descriptors. However, only two face datasets were used in that evaluation study [9].

In this paper, we are collecting eight face datasets to evaluate the CLTP performance for face recognition. This is in order to have a deep investigation about the CLTP performance where different face datasets have challenges and different face properties. In this paper, the face recognition performance of CLTP is get evaluated with the different standard dataset. It used to compare with Completed Local Binary Pattern (CLBP) to extract the face image and showed a higher accuracy result than CLBP. In this study, the Georgia Tech Face, Collection Facial Images, Caltech Pedestrian Faces, JAFFE, FEI, YALE, ORL, UMIST datasets are used.

The present paper is organized as follows. Section II describes the related work in detail. Section III explains the proposed system. Section IV describes the experiment setup, Sections V and VI explain the experiment result and conclusions respectively.

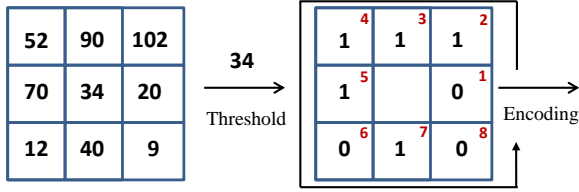


Fig. 1. LBP operator.

II. RELATED WORK

In this section, the LBP, CLBP and CLTP are explained.

A. Local Binary Pattern (LBP)

The initial LBP method proposed by Ojala et al. [3] was used to extract a texture feature. It provides the local measure of image contrast. LBP has initially been defined within the concept of 8 pixels and gray value centre pixel. The grey level variance between the centre pixel and its neighbourhood pixel is calculated. The neighbourhood pixels is set to 1 if the variance is positive or 0 if its negative; then, these values are used to obtain a binary code which is generated later to represent a histogram that describes the image texture. Fig. 1 shows the process of calculation in the original LBP.

The LBP descriptor was developed by Ojala et al. [10] based on the use of differently-sized neighbourhoods with the aid of a symmetric circle neighbourhood defined by R and P . The LBP is defined as:

$$LBP_{P,R} = \sum_{p=0}^{P-1} 2^p s(i_p - i_c), \quad s(x) = \begin{cases} 1, & x \geq 0, \\ 0, & x < 0, \end{cases} \quad (1)$$

where i_c denotes the gray value of the centre pixel in the pattern, $i_p (p = 0, \dots, P - 1)$ denotes the gray values of the neighbour pixel on a circle of radius R . While P denotes the number of neighbours.

In LBP, the bilinear interpolation estimation method is used to identify the neighbours that do not lie in the exact centre of the pixels.

B. Completed Local Binary Pattern (CLBP)

The CLBP is proposed as extension of LBP in 2010 by Guo et al. [5]. The CLBP becomes one of the successful texture descriptors. The CLBP operator is consist of three different parts which are CLBP_S, CLBP_M and CLBP_C.

Firstly, each pattern in the image is decomposed into two complementary components, namely, the sign component s_p and the magnitude component m_p which can be mathematically expressed as follows.

$$s_p = s(i_p - i_c), \quad m_p = |i_p - i_c| \quad (2)$$

Then, the s_p and m_p are used to construct $CLBP_S$ and $CLBP_M$, respectively. The mathematical expression of $CLBP_S$ is as follows:

$$CLBP_S_{P,R} = \sum_{p=0}^{P-1} 2^p s(i_p - i_c), \quad s_p = \begin{cases} 1, & i_p \geq i_c, \\ 0, & i_p < i_c, \end{cases} \quad (3)$$

where i_c , i_p , R , and P are defined in (1), while c denotes the mean value of m_p in the entire image.

The following component is CLBP_M which proceeds with qualities rather than binary values. The neighbourhoods pixel will change to 1 if the difference between their value and mean of the pattern is positive. Otherwise, it will change to 0. CLBP_M is shown in the following equation.

$$CLBP_M_{P,R} = \sum_{p=0}^{P-1} 2^p t(m_p - c), \quad t(m_p, c) = \begin{cases} 1, & |i_p - i_c| \geq c \\ 0, & |i_p - i_c| < c \end{cases} \quad (4)$$

where i_c donates the middle pixel, and P is uniformly dispersed neighbours which is i_p , and m_p is the mean value of the whole image. Example of CLBP extraction is shown in Fig. 2.

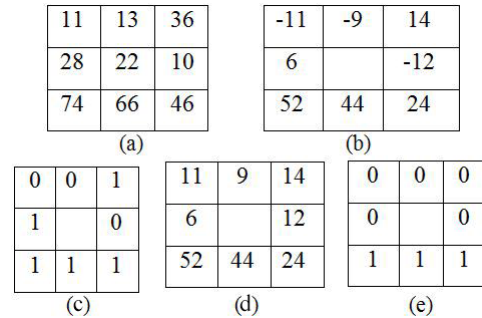


Fig. 2. Difference between sign components and magnitude components. (a) 3*3 sample block, (b) Local differences, (c) Sign components, (d) Magnitude components (mean = 22), (e) Final magnitude components.

Lastly, Guo et al. utilized the estimation of the grey level of the image to build CLBP-Centre (CLBP_C). The CLBP_C can be described scientifically as Equation 5.

$$CLBP_C_{P,R} = t(i_p - c_I) \quad (5)$$

Where c_I is the threshold that can be calculated as the mean of the grey level of the picture. Therefore, the CLBP is very useful in extracting the rotation invariant uniform into a binary pattern which helps in removing the pivot invariant uniform element in the face. Fig. 3 shows the illustration of CLBP_C.

C. Completed Local Ternary Pattern (CLTP)

Completed Local Ternary Pattern (CLTP) had been presented by Rassem and Khoo (2014) for rotation invariant texture classification. CLTP is proposed to overcome the drawbacks of the LBP as well as the CLBP [8]. The CLTP_S

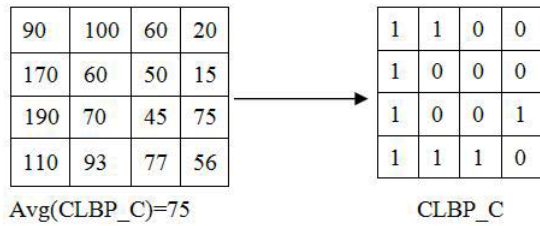


Fig. 3. Encoding method of CLBP_C.

is divided into two signs, namely an upper sign and lower sign similar to the CLTP_M as Equation 6 and 7 as follows:

$$s_{P,R}^{upper} = s(i_p - (i_c + t))$$

$$, s_{P,R}^{lower} = s(i_p - (i_c - t)) \quad (6)$$

$$m_{P,R}^{upper} = |i_p - (i_c + t)|$$

$$, m_{P,R}^{lower} = |i_p - (i_c - t)| \quad (7)$$

Where i_c and i_p are defined in Equation 1.

Firstly, the $s_{P,R}^{upper}$ and $s_{P,R}^{lower}$ components are used to calculate the $CLTP_S_{P,R}^{upper}$ and $CLTP_S_{P,R}^{lower}$, respectively. Then, the $CLTP_S_{P,R}^{upper}$ and $CLTP_S_{P,R}^{lower}$ are combined to get the $CLTP_S$. The mathematical equation of $CLTP_S$ is shown below.

$$CLTP_S_{P,R}^{upper} = \sum_{P=0}^{P-1} 2^P s(i_p - (i_c + t))$$

$$, s_p^{upper} = \begin{cases} 1, & i_p \geq i_c + t \\ 0, & otherwise \end{cases} \quad (8)$$

$$CLTP_S_{P,R}^{lower} = \sum_{P=0}^{P-1} 2^P s(i_p - (i_c - t))$$

$$, s_p^{lower} = \begin{cases} 1, & i_p < i_c - t \\ 0, & otherwise \end{cases} \quad (9)$$

$$CLTP_S_{P,R} = [CLTP_S_{P,R}^{upper} \quad CLTP_S_{P,R}^{lower}] \quad (10)$$

The illustration of $CLTP_S$ process is shown in Figure 4.

$CLTP_M$ is similar to the $CLTP_S$ which needs to add the $CLTP_M_{P,R}^{upper}$ and $CLTP_M_{P,R}^{lower}$ to get the $CLTP_M_{P,R}$. The output of $CLTP_M$ also will be in a binary form same with $CLTP_S$ as shown below:

$$CLTP_C_{P,R}^{upper} = t(i_p^{upper}, c_I) \quad (14)$$

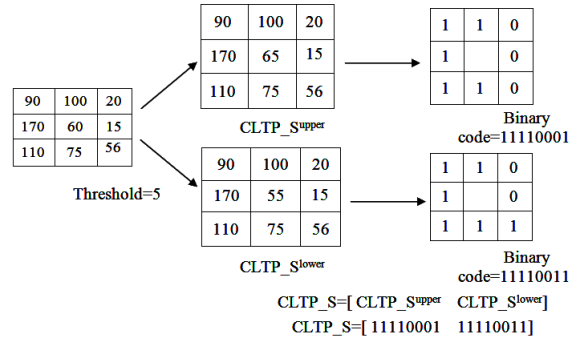


Fig. 4. CLTP_S Operator

$$CLTP_M_{P,R}^{upper} = \sum_{P=0}^{P-1} 2^P (t(m_p^{upper}, c))$$

$$, t(m_p^{upper}, c) = \begin{cases} 1, & |i_p - (i_c + t)| \geq c \\ 0, & |i_p - (i_c + t)| < c \end{cases} \quad (11)$$

$$CLTP_M_{P,R}^{lower} = \sum_{P=0}^{P-1} 2^P (t(m_p^{lower}, c))$$

$$, t(m_p^{lower}, c) = \begin{cases} 1, & |i_p - (i_c - t)| \geq c \\ 0, & |i_p - (i_c - t)| < c \end{cases} \quad (12)$$

$$CLTP_M_{P,R} = [CLTP_M_{P,R}^{upper} \quad CLTP_M_{P,R}^{lower}] \quad (13)$$

Below is the illustration of $CLTP_M$ process in Figure 5.

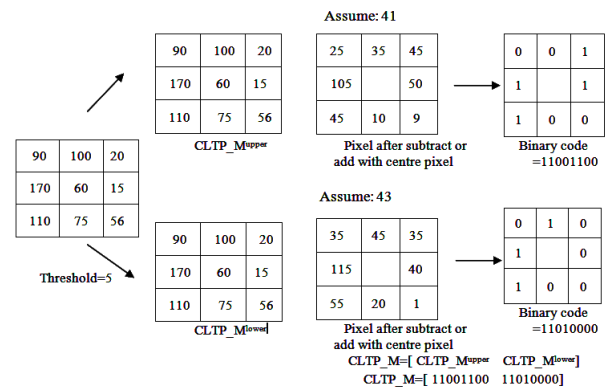


Fig. 5. CLTP_M Operator

The outcome of $CLTP_C$ is a 2D matrix of the binary value. It compares the average pixel number of the original pixel number with the upper and lower of $CLTP_C$ component. Then it comes out with a 2D matrix of binary value of $CLTP_C_{P,R}^{upper}$ and 2D matrix of binary value of $CLTP_C_{P,R}^{lower}$, the mathematical method is shown as Equation 14 and 15 below:

$$CLTP_C_{P,R}^{lower} = t(i_p^{lower}, c_I) \quad (15)$$

The final $CLTP_C_{P,R}$ can be obtained as shown in the following Equation.

$$CLTP_S_{P,R} = [CLTP_S_{P,R}^{upper} \quad CLTP_S_{P,R}^{lower}] \quad (16)$$

The illustrator of $CLTP_C$ as shown in below Fig. 6.

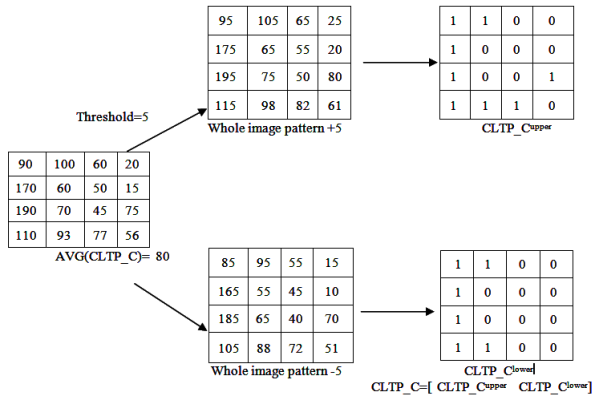


Fig. 6. $CLTP_C$ Operator.

III. PROPOSED SYSTEM

The face recognition has a very complex process and it extremely contrasts from others in different aspects. Thus, the improvement for face recognition system will be a troublesome undertaking in image processing of computer vision. A radius size is allocated to carry out the extraction process in the earlier stage of feature extraction. The ranges of radius sizes have many sets, of which the widely recognized sets used are (1, 8), (2, 16) and (3, 24), These radius sizes can become an arrangement of various outcome as shown in Fig. 7.

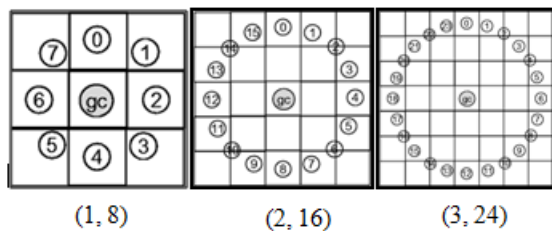


Fig. 7. The illustration of radius sizes.

First, a set of training and testing images are prepared and processed for feature detection. Once the feature of the image is detected, the feature extraction stage applies the CLTP feature descriptor to the image. The feature extraction stage is the process to extract the CLTP texture of each image i.e., training and testing images. After proceeding with the feature extraction, the similarity training images features are grouped together. The familiar image in the testing will be compared with all the extracted features image in training image to find the smallest distance or closest value between the training and testing image features. General face recognition structure is shown in Fig. 8.

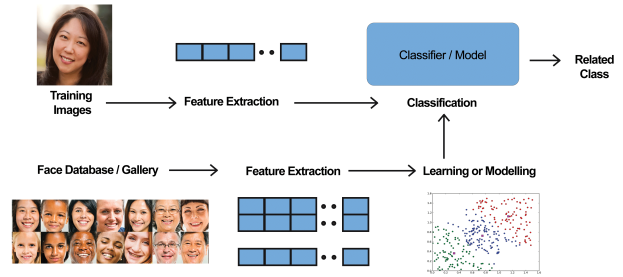


Fig. 8. General face recognition structure.

IV. EXPERIMENT SETUP

In the performance evaluation, to check the effectiveness of the CLBP and CLTP descriptors, different datasets had been used in the experiments with different training images numbers. The training images are select randomly from every individual, and the remaining images will be used for testing images. For different datasets, the step is repeat 100 times to choose different training samples and calculate the average recognition rate. Due to the large dimension of the Caltech Pedestrian Faces 1999 [11] dataset images, they had been cropped to 60 x 60 images size to execute the experiment, while others dataset remains the same sizes. The face recognition performance of CLBP and CLTP on different datasets are tested and recorded. The outcomes are shown in Tables I to VIII for the datasets of JAFFE [12], UMIST [13], ORL [12], YALE [14], Collection Facial Images [15], Georgia Tech Face [16], Caltech Pedestrian Faces Dataset 1999 [11] and FEI [17], respectively.

V. EXPERIMENT RESULT

A. Japanese Female Facial Expressions Dataset (JAFFE)

JAFFE dataset [18] comprised 213 faces images from 10 different classes of Japanese female in Japan. The features extraction of (1, 8), (2, 16) and (3, 24) radius sizes based on 2, 5 and 10 random choose of training images from the classes were used. Each class has 20 JPEG images with a different view of facial expression including angry, smile, sad, worry, nervous, neutral and others. The size of each image is 256 x 256. Example of some images of JAFFE is shown in Fig. 9.



Fig. 9. Some images from JAFFE dataset

As shown in Table I, the classification result of $CLTP$ is higher rate than $CLBP$ with all different pattern sizes using different number of training images. The $CLTP_S/M/C_{3,4}$ achieved highest classification rate, reaches 98.72% while the $CLBP_S/M/C_{3,4}$ achieved 97.53%.

TABLE I. CLASSIFICATION ACCURACY ON JAFFE DATASET (JAFFE)

JAFFE dataset	R=1, P=8			R=2, P=16			R=3, P=24		
	2	5	10	2	5	10	2	5	10
CLBP_S	56.61	63.83	70.13	47.52	52.62	58.46	48.83	56.26	62.8
CLTP_S	71.77	79.09	83.82	77.12	84.21	88.45	81.54	88.25	91.76
CLBP_M	70.38	74.08	76.67	74.6	79.74	83.93	73.29	79.75	83.86
CLTP_M	74.83	82.63	87.02	77.95	83.01	86.15	75.77	81.99	86.63
CLBP_M/C	87.15	91.62	93.39	88.14	92.57	95.33	89.29	93.73	96.42
CLTP_M/C	83.86	90.09	93.49	88.69	93.73	96.55	89.94	94.42	96.84
CLBP_S_M/C	85.88	91.57	94.11	85.89	92.31	95.18	89.96	94.87	96.92
CLTP_S_M/C	85.59	91.29	94.97	89.45	94.55	97	90.57	94.81	96.73
CLBP_S/M	73.51	81.33	86.98	71.89	81.48	87.98	79.31	86.27	91.02
CLTP_S/M	80.52	88.23	92.17	85.94	91.7	94.68	86.07	92.21	95.43
CLBP_S/M/C	86.38	92.27	94.86	88.79	94.05	95.82	92.94	96.8	97.53
CLTP_S/M/C	87.34	93.25	96.12	92.42	96.29	97.73	93.55	97.2	98.72

B. Sheffield Face Dataset (UMIST)

UMIST dataset [13] contains 564 images from 20 individual classes. Each class has a different number of images. The biggest class has 48 images. Different training number has been selected from each class; 8, 13 and 19, while the remaining images are used for testing. Each individual has captured with a different view of the angle of the face. Some images of the UMIST dataset are shown in Fig. 10.



Fig. 10. Some images from UMIST dataset.

The result of UMIST dataset on $N = (8, 13, 19)$ is presented in Table II. The $CLTP_S/M/C_{3,24}$ has showed 99.68% of face recognition classification rate while the $CLBP_S/M/C_{3,4}$ achieved 99.55%. In some cases, the $CLBP$ showed better results than $CLTP$, especially with small pattern size (1, 8) and (2, 16). While with (3, 24), the $CLTP$ was better than $CLBP$ with different number of training images.

C. ORL Face dataset (ORL)

ORL face dataset [12] comprises of 400 pictures of 40 classes, they capture their images under various lighting condition, times, outward appearance and facial points of interest. In each class, $N=(2, 5, 8)$ images are selected randomly for training images, others are used for testing images. Fig. 11 shows some images of ORL datasets.



Fig. 11. Some images from ORL dataset.

In ORL dataset, $CLTP_S/M/C_{3,24}$ achieved the best classification rate result 98.52%. The best results by $CLBP$

was 97.98%. The $CLTP$ outperformed the $CLBP$ with different number of training image as well as with different texture pattern except in (1,8) where the $CLBP_S/M/C_{1,8}$ performed better than $CLTP_S/M/C_{1,8}$. The full experiment results are shown in Table III.

D. YALE Face dataset (YALE)

YALE dataset [14] has captured by 15 people, every people are requested to capture 11 images so that it contains 165 images in the whole dataset. Each image is captured from alternate points of view, with a big difference in brightening and face expression. In this project, each picture in the YALE dataset was physically trimmed follow the face detected point sizes. In each class, $N=(2, 5, 10)$ images are used for training while the remaining for testing. Some images from the dataset are shown in Fig. 12.



Fig. 12. Some images from YALE dataset.

Table IV shows the classification rates using $CLBP$ and $CLTP$. As shown in the table, the $CLTP$ outperformed the $CLBP$ with different pattern texture size as well as using different training images' numbers. The best result is achieved by $CLTP_S/M/C_{3,24}$, reaches 80.47% compared with 77.20% achieved by $CLBP_S/M/C_{3,24}$.

E. Collection Facial Images dataset

Collection Facial Images dataset [15] includes 152 classes. Each class has 20 different images with a size of 180 x 200. This dataset consists of various faces, most of them were undergraduate students between 18 to 20 years old. This dataset only has a slightly different facial expression so that the accuracy of face recognition would be higher than other datasets. In each class, $N = (2, 5, 10)$ images are used for training while the remaining for testing.

In Collection Facial Images dataset, The $CLTP_S/M/C_{3,24}$ achieved 99.84% accuracy rate using 10 training images compared with 99.80% by

TABLE II. CLASSIFICATION ACCURACY ON SHEFFIELD FACE DATASET (UMIST)

UMIST dataset	R=1, P=8			R=2, P=16			R=3, P=24		
	8	13	19	8	13	19	8	13	19
CLBP_S	55.77	61.06	65.4	64.39	72.33	79.36	72.13	80.75	87.44
CLTP_S	69.8	79.06	85.08	78.96	88.42	93.7	85.63	93.29	97.43
CLBP_M	67.6	74.07	79.03	70.65	76.93	82.23	75.91	83.26	87.13
CLTP_M	79.76	86.17	89.85	89.72	93.52	95.78	93.03	97.16	98.31
CLBP_M/C	90.29	94.69	97.01	92.11	96.24	97.76	93.15	96.79	98.19
CLTP_M/C	90.6	94.93	96.68	96.36	98.79	99.41	96.8	99.15	99.24
CLBP_S_M/C	91.49	96.1	98.2	94.42	98.35	99.39	95.5	98.88	99.54
CLTP_S_M/C	92.98	96.71	97.98	96.45	98.88	99.47	96.67	99.32	99.32
CLBP_S/M	88.77	94.4	97.31	93.58	97.49	98.74	95.9	98.43	99.27
CLTP_S/M	90.63	95.09	96.71	94.96	98.2	99.1	95.98	99.05	99.54
CLBP_S/M/C	95.69	98.34	99.08	97.79	99.47	99.54	98.12	99.5	99.55
CLTP_S/M/C	95.36	98.11	98.53	97.73	99.45	99.53	97.88	99.57	99.68

TABLE III. CLASSIFICATION ACCURACY ON ORL FACE DATASET (ORL)

ORL dataset	R=1, P=8			R=2, P=16			R=3, P=24		
	2	5	8	2	5	8	2	5	8
CLBP_S	26.89	31.42	33.74	42.15	52.3	55.49	51.58	63.27	68.71
CLTP_S	53.36	70.19	77.11	65.92	83.21	88.85	71.23	87.74	91.7
CLBP_M	43.43	54.02	59.81	56.55	67.5	70.7	60.45	74.05	79.39
CLTP_M	48.11	65.53	72	63.93	80.68	85.63	70.35	85.68	90.53
CLBP_M/C	64.74	79.92	84.84	69.65	86.29	91.18	70.8	88.1	94.15
CLTP_M/C	65.64	83.39	89.54	76.01	92.83	96.84	79.05	94.35	97.74
CLBP_S_M/C	68.55	83.86	89.1	73.93	89.58	94.35	77.06	91.98	95.7
CLTP_S_M/C	69.2	87.28	92.55	78.46	93.58	97.14	81.34	94.97	98.01
CLBP_S/M	66.87	81.1	86.34	76.39	90.2	94.64	80.22	92.46	95.79
CLTP_S/M	68.53	86.11	91.2	77.9	91.81	96.25	81.75	95.14	98.21
CLBP_S/M/C	79.5	93.37	97.3	83.08	95.34	97.66	84.57	95.98	97.98
CLTP_S/M/C	75.71	92.06	95.85	84.76	95.91	98.31	86.98	97.08	98.52

TABLE IV. CLASSIFICATION ACCURACY ON YALE FACE DATASET (YALE)

YALE dataset	R=1, P=8			R=2, P=16			R=3, P=24		
	2	5	10	2	5	10	2	5	10
CLBP_S	41.4	50.16	53.93	37.24	45.83	54.67	41.24	52.36	62.6
CLTP_S	43.59	54.64	57.67	47.78	58.83	64	53.2	62.32	70.4
CLBP_M	44.36	50.34	56.13	48.22	57.49	64.07	49.9	58.72	63.33
CLTP_M	53.02	60.94	64.73	54.24	66.53	67.13	61.05	70.09	74.07
CLBP_M/C	60.78	68.43	70.8	60.16	69.44	66.93	62.5	70.63	72.47
CLTP_M/C	59.33	67.87	68.93	64.19	73.88	77.87	66.13	72.98	76.4
CLBP_S_M/C	57.25	65.06	69.27	55.02	66.07	69.6	59.68	69	71.4
CLTP_S_M/C	60	67.04	70.73	64.09	72.98	71.6	66.57	73.93	73.73
CLBP_S/M	51.5	61.87	64.93	52.64	65.66	73.6	60.36	69.82	75.4
CLTP_S/M	57.64	67.11	67.87	61.03	72.22	74	64.16	73.52	74.4
CLBP_S/M/C	59.9	71.33	70.33	58.96	70.3	77.07	64.21	75.31	77.2
CLTP_S/M/C	61.81	69.86	74.93	68.99	74.78	76.53	70.49	76.58	80.47

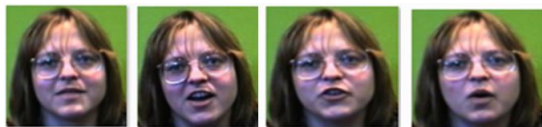


Fig. 13. Some images from Collection Facial Images dataset.

CLBP_S/M/C_{3,24}. Table V shows that the CLTP with better than CLBP with big texture pattern size (3,24) while the performance with (1,8) and (2,16) was depending on the combination of the operators in CLBP and CLTP.

F. Georgia Tech Face dataset

The Georgia Tech Face dataset [16] contains 50 and class contains exactly 15 samples of colour images with a size of 141 x 216 captured in 1999. The images show the front of the face with different expressions, scale and illumination condition. Besides that, some of the faces in this dataset wearing spectacles and some photos in small size and with a low-resolution. In each class, N=(2, 5, 10) images are used for training while the remaining for testing. Fig. 14 shows some examples of Georgia Tech Face images.

CLTP in Table VI has achieved a better result than CLBP

TABLE V. CLASSIFICATION ACCURACY ON COLLECTION FACIAL IMAGES DATASET

Collection Facial Data dataset	R=1, P=8			R=2, P=16			R=3, P=24		
	2	5	10	2	5	10	2	5	10
CLBP_S	51.47	59.25	63.23	68.66	76.11	79.9	81.25	87.31	90.15
CLTP_S	76.47	84.73	87.91	92.47	96.04	97.15	95.82	97.83	98.39
CLBP_M	67.54	76.92	81.68	83.4	89.26	92.06	90.62	94.61	96.11
CLTP_M	76.36	85.23	89.46	88.05	94.06	96.43	95.21	97.79	98.56
CLBP_M/C	89.27	95.04	97.05	95.88	98.58	99.32	96.88	98.93	99.47
CLTP_M/C	87.34	93.61	96.08	95.05	98.18	98.94	97.63	99.22	99.58
CLBP_S_M/C	90.59	95.62	97.21	96.48	98.69	99.27	97.21	99.14	99.54
CLTP_S_M/C	89.31	94.42	96.46	96.32	98.63	99.25	97.84	99.33	99.65
CLBP_S/M	84.13	91.42	94.42	96.38	98.12	98.72	98.08	99.11	99.43
CLTP_S/M	85.8	92.25	95.03	95.08	97.95	98.73	98.08	99.23	99.49
CLBP_S/M/C	92.71	96.71	97.83	98.33	99.5	99.71	99.13	99.67	99.8
CLTP_S/M/C	91.15	95.52	97.04	97.79	99.31	99.64	99.12	99.7	99.84

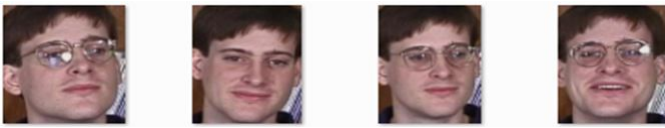


Fig. 14. Some images from Georgia Tech Face dataset.

with 91.63%. CLTP result work better in the larger texture pattern size (R=3, P=24). While, the CLBP achieved better with texture pattern (1,8) with different image training numbers. In (2,16), the CLTP was better in some cases and less than CLBP in another cases.

G. Caltech Pedestrian Faces Dataset 1999

The Caltech Pedestrian Faces Dataset 1999 was downloaded from online sources [11] collected at California Institute of Technology consisting of 380 face images with 19 identities classes were used in this experiment. Every class contains 20 JPEG images with different angle view of the face, face expression background and lighting. This dataset images size is 896 x 592. In each class, N =(2, 5, 10) images are used for training while the remaining for testing. Examples of Caltech Pedestrian Faces images are shown in Fig. 15.



Fig. 15. Some images from Caltech Pedestrian Faces Dataset 1999.

Table VII shows the classification accuracy for CALTECH using CLBP and CLTP. The performance of CLTP is better work in the Caltech Pedestrian Faces Dataset 1999 compare the CLBP. This can see that majority result of CLTP is higher than CLBP on different texture pattern sizes and training images. CLTP achieved 78.78% as the best accuracy results while CLBP achieved 76.57%.

H. FEI Face dataset

The FEI face dataset [17] is a dataset of faces collected at Brazil. This dataset has 200 faces of Brazilian people captured in 2005 and 2006 at Artificial Intelligence Laboratory of FEI

in São Bernardo do Campo, São Paulo, Brazil. FEI face dataset has 2800 face images from students and staffs in the FEI from 19 years old to 40 years old. In 200 classes, there were 14 images from every class which contain different degree view with the profile rotation of almost 180 degrees and with different facial expression. The size of faces image was in 640 x 480 pixels. Examples of some images from FEI face dataset are shown in Fig. 16.



Fig. 16. Some images from FEI Face dataset.

The result classification of FEI face dataset with various radius sizes is shown in Table VIII. The CLTP_S/M/C_{3,24} achieved highest classification rate, reaches 76.38% while 75.48% achieved by CLBP. Table VIII shows the full experiment results of CLBP and CLTP with different training images as well as under texture pattern sizes. The result table shows that the CLTP outperformed the CLBP in many cases.

In general, the summary of the classification accuracy results of all benchmark datasets are shown in Table IX. The results showed the priority of the CLTP performance against the CLBP. The CLTP achieved the best in all datasets compared with CLBP.

VI. CONCLUSION

Completed Local Ternary Pattern (CLTP) is one of the new texture descriptors that is proposed to overcome the drawbacks of the LBP. In this paper, we applied the CLTP for face image classification task. The performances of CLTP as well as CLBP were studied and evaluated using eight different benchmark datasets. The experiment results show that the CLTP achieved the highest classification rates compared with CLBP. The CLTP outperformed CLBP performance under different pattern sizes and using a different number of training images. The CLTP good performance is due to its robustness to noise than CLBP. In addition, CLTP has more discriminating property than CLBP. In future work, the CLTP can be combined with other descriptors such as CLBP. This combination will help

TABLE VI. CLASSIFICATION ACCURACY ON GEORGIA TECH DATASET

Georgia Tech	R=1, P=8			R=2, P=16			R=3, P=24		
dataset	2	5	10	2	5	10	2	5	10
CLBP_S	35.1	44.49	52.5	32.4	42.62	49.89	34.48	45.25	54.47
CLTP_S	28.39	36.45	43.16	36.26	48.29	57.09	40.84	54.48	64.55
CLBP_M	28.57	36.72	42.02	32.39	43.11	49.58	36.89	47.39	56.58
CLTP_M	32.73	44.55	53.12	38.45	51.22	61.06	43.68	57.48	67.62
CLBP_M/C	48.64	61.54	70.5	52.67	66.56	74.7	55.2	69.3	78.17
CLTP_M/C	45.37	60.91	71.04	55.74	70.43	78.95	60.35	75.25	83.08
CLBP_S_M/C	54.06	68.38	76.9	55.98	70.21	79.07	59.25	72.99	81.66
CLTP_S_M/C	45.41	61.28	71.68	55.82	72.15	81.23	61.58	76.47	84.33
CLBP_S/M	47.98	61.54	70.57	54	69.52	78.66	58.14	74.5	83.84
CLTP_S/M	39.79	53.97	64.76	51.42	67.93	78.09	57.51	73.24	82.44
CLBP_S/M/C	62.62	77.07	84.11	66.84	82.2	89.36	69.74	84.85	91.4
CLTP_S/M/C	50.43	67.31	77.75	64.55	79.81	87.71	68.63	84.06	91.63

TABLE VII. CLASSIFICATION ACCURACY ON CALTECH PEDESTRIAN FACES 1999 DATASET

Caltech Pedestrian	R=1, P=8			R=2, P=16			R=3, P=24		
Faces 1999 dataset	2	5	10	2	5	10	2	5	10
CLBP_S	22.69	23.55	23.34	30.82	34.35	36.06	35.65	49.19	59.62
CLTP_S	36.11	41.23	43.52	43.95	52.04	56.3	33.12	43.54	52.36
CLBP_M	25.62	26.58	27.79	35.51	40.49	44.48	43.14	49.84	52.16
CLTP_M	36.85	41.24	44.31	44.38	51.76	57.05	55.34	64.17	68.17
CLBP_M/C	35.52	40.58	42.68	43.19	50.96	55.05	43.66	50.34	54.59
CLTP_M/C	49.35	56.08	59.96	53.67	64.55	70.2	55.98	63.41	68.96
CLBP_S_M/C	43.1	47.71	50.34	51.91	61.22	64.69	51.46	60.39	64.97
CLTP_S_M/C	51.99	59.46	64.32	58.35	68.44	73.03	59.51	69.34	74.69
CLBP_S/M	37.65	42.4	47.97	49.32	57.34	62.16	60.63	69.14	74.06
CLTP_S/M	50.46	55.79	59.86	59.88	69.25	74.23	65.94	73.66	77.53
CLBP_S/M/C	50.09	55.45	61.27	53.1	62.31	69.17	63.06	71.78	76.57
CLTP_S/M/C	56.79	64.95	70.01	57.13	67.26	73.28	65.33	74.15	78.78

TABLE VIII. CLASSIFICATION ACCURACY ON FEI DATASET

FEI dataset	R=1, P=8			R=2, P=16			R=3, P=24		
	2	5	10	2	5	10	2	5	10
CLBP_S	12.38	16.77	20.82	9.02	12.06	14.86	11.99	16.29	20.07
CLTP_S	28.22	36.31	42.37	39.52	51.75	61.03	41.92	56.08	65.8
CLBP_M	19.17	26.29	32.78	23.77	32.59	40.14	26.64	36.8	45.67
CLTP_M	22.98	31.06	37.59	24.51	33.4	40.83	23.16	32.53	41.3
CLBP_M/C	33.04	46.15	55.33	36.8	49.94	58.24	39.23	53.2	64.2
CLTP_M/C	38.28	52.06	60.38	41.23	55.01	63.5	36.77	51.33	63.01
CLBP_S_M/C	32.63	43.96	51.64	37.45	50.22	57.91	43.39	57.05	66.98
CLTP_S_M/C	43.61	57.33	65.67	46.93	61.26	69.33	43.55	58.52	68.83
CLBP_S/M	22.79	33.68	42.89	29.5	41.97	51.77	40.55	55.16	63.62
CLTP_S/M	39.46	54.52	65.01	44.31	59.57	69.39	42.13	57.93	67.52
CLBP_S/M/C	37.2	50.91	60.46	45.98	60.55	70.71	53.88	68.94	75.48
CLTP_S/M/C	50.83	65.34	72.91	53.8	68.65	75.4	51.16	67.4	76.38

TABLE IX. CLASSIFICATION ACCURACY ON BENCHMARK DATASETS

dataset	Reference	Classes	Size	CLBP	CLTP
1 JAFFE	[18]	10	256 x 256	97.53%	98.72%
2 ORL	[12]	20	60 x 60	97.98%	98.52%
3 UMIST	[13]	40	112 x 92	99.55%	99.68%
4 Yale	[14]	15	153 x 153	77.20%	80.47%
5 Collection Facial Images	[15]	152	180 x 200	99.80%	99.84%
6 Georgia Tech Face	[16]	50	141 x 216	91.40%	91.63%
7 Caltech Pedestrian Faces 1999	[11]	19	60 x 60	76.57%	78.78%
8 FEI	[17]	200	640 x 480	75.48%	76.38%

to improve the classification accuracy rates in the face image classification task.

ACKNOWLEDGMENT

This research has been supported by Universiti Malaysia Pahang (UMP) Grant Number RDU180365.

REFERENCES

- [1] I. Nurtanio, E. R. Astuti, I. K. E. Purnama, M. Hariadi, and M. H. Purnomo, "Classifying cyst and tumor lesion using support vector machine based on dental panoramic images texture features," *IAENG International Journal of Computer Science*, vol. 40, no. 1, pp. 29–37, 2013.
- [2] Z. Xia, C. Yuan, X. Sun, D. Sun, and R. Lv, "Combining wavelet transform and LBP related features for fingerprint liveness detection," *IAENG International Journal of Computer Science*, vol. 43, no. 3, pp. 290–298, 2016.
- [3] T. Ojala, M. Pietikäinen, and D. Harwood, "A comparative study of texture measures with classification based on featured distributions," *Pattern recognition*, vol. 29, no. 1, pp. 51–59, 1996.
- [4] X. Tan and B. Triggs, "Enhanced local texture feature sets for face recognition under difficult lighting conditions," *IEEE transactions on image processing*, vol. 19, no. 6, pp. 1635–1650, 2010.
- [5] Z. Guo, L. Zhang, and D. Zhang, "A completed modeling of local binary pattern operator for texture classification," *IEEE Transactions on Image Processing*, vol. 19, no. 6, pp. 1657–1663, 2010.
- [6] T. H. Rassem, B. E. Khoo, N. M. Makbol, and A. A. Alsewari, "Multi-scale colour completed local binary patterns for scene and event sport image categorisation," *IAENG International Journal of Computer Science*, vol. 44, no. 2, 2017.
- [7] T. H. Rassem and B. E. Khoo, "Completed local ternary pattern for rotation invariant texture classification," *The Scientific World Journal*, vol. 2014, 2014.
- [8] T. H. Rassem, M. F. Mohammed, B. E. Khoo, and N. M. Makbol, "Performance evaluation of completed local ternary patterns (CLTP) for medical, scene and event image categorisation," in *2015 4th International Conference on Software Engineering and Computer Systems (ICSECS)*. IEEE, 2015, pp. 33–38.
- [9] T. H. Rassem, N. M. Makbol, and S. Y. Yee, "Face recognition using completed local ternary pattern (CLTP) texture descriptor," *International Journal of Electrical and Computer Engineering (IJECE)*, vol. 7, no. 3, pp. 1594–1601, 2017.
- [10] T. Ojala, M. Pietikainen, and T. Maenpaa, "Multiresolution gray-scale and rotation invariant texture classification with local binary patterns," *IEEE Transactions on Pattern Analysis and Machine Intelligence*, vol. 24, no. 7, pp. 971–987, jul 2002.
- [11] (May 25th, 2018) Caltech face dataset. [Online]. Available: www.vision.caltech.edu/Image_Datasets/faces/faces.tar
- [12] F. S. Samaria and A. C. Harter, "Parameterisation of a stochastic model for human face identification," in *Applications of Computer Vision, 1994., Proceedings of the Second IEEE Workshop on*. IEEE, 1994, pp. 138–142.
- [13] D. B. Graham and N. M. Allinson, "Characterising virtual eigensignatures for general purpose face recognition," in *Face Recognition*. Springer, 1998, pp. 446–456.
- [14] P. N. Belhumeur, J. P. Hespanha, and D. J. Kriegman, "Recognition using class specific linear projection," 1997.
- [15] (2008) Collection of facial images. 2008. [Online]. Available: <http://cswwww.essex.ac.uk/mv/allfaces/index.html>
- [16] A. Nefian and M. H. Hayes III, "A hidden markov model-based approach for face detection and recognition," Ph.D. dissertation, School of Electrical and Computer Engineering, Georgia Institute of Technology, 1999.
- [17] C. E. Thomaz and G. A. Giraldo, "A new ranking method for principal components analysis and its application to face image analysis," *Image and Vision Computing*, vol. 28, no. 6, pp. 902–913, 2010.
- [18] M. J. Lyons, J. Budynek, and S. Akamatsu, "Automatic classification of single facial images," *IEEE transactions on pattern analysis and machine intelligence*, vol. 21, no. 12, pp. 1357–1362, 1999.

Quantitative Analysis of Healthy and Pathological Vocal Fold Vibrations using an Optical Flow based Waveform

Heyfa Ammar

King Abdulaziz University, Jeddah, Kingdom of Saudi Arabia
University of Tunis El Manar, Tunisia

Abstract—The objective assessment of the vocal fold vibrations is important in diagnosing several vocal diseases. Given the high speed of the vibrations, the high speed videoendoscopy is commonly used to capture the vocal fold movements into video recordings. Commonly, two steps are carried out in order to automatically quantify laryngeal parameters and assess the vibrations. The first step aims to map the spatial-temporal information contained in the video recordings into a representation that facilitates the analysis of the vibrations. Numerous techniques are reported in the literature but the majority of them require the segmentation of all the images of the video, which is a complex task. The second step aims to quantify laryngeal parameters in order to assess the vibrations. To this aim, most of the existing approaches require an additional processing to the representation in order to deduce those parameters. Furthermore, for some reported representations, the assessment of the symmetry and the periodicity of the vocal fold dynamics needs setting up parameters that are specific to the representation under consideration; which makes difficult the comparison between the existing techniques. To alleviate these problems, the present study investigates the use of a recently proposed representation named optical flow based waveform, in order to objectively quantify the laryngeal parameters. This waveform is retained in this study as it does not require the segmentation of all the images of the video. Furthermore, it will be shown in the present work that the automatic quantification of the vibrations using this waveform can be carried out without applying any additional processing. Moreover, common laryngeal parameters are exploited; hence, no specific parameters are needed to be defined for the automatic assessment of the vibrations. Experiments conducted on healthy and pathological phonation show the accuracy of the waveform. Besides, it is more sensitive to pathological phonation than the state-of-the-art techniques.

Keywords—Quantification; vocal fold vibrations; optical flow based waveform; pathology

I. INTRODUCTION

Diseases that affect our ability to speak can have disastrous impacts on our lives as our voice remains the most important way to communicate. It is then important to diagnose and treat vocal disorders as soon as signs like hoarseness, difficulty of speaking and many others, take place. To make a sound, the right and left vocal folds (VF) consisting of two membranes located in the larynx, open and close periodically, and their vibrations are symmetric. For the aim of diagnosing their functional behavior, the examination of these high-frequency vibrations is made possible thanks to the analysis of high speed videoendoscopy (HSV) recordings. HSV allows to capture the VF movements at a frequency that could exceed 4000

images/second. However, this high frequency makes it hard to visually assess the vibrations. For this reason, in a first step, the spatial-temporal information contained in the HSV recordings are commonly mapped into representations appropriate for the human visualization and analysis. Then, in the second step, the VF vibrations are assessed either visually based on the shape of the considered representation, or automatically through the quantification of some vibratory parameters. Many efforts are invested by researchers to propose objective techniques for the assessment of the VF vibrations. However, they suffer from one or more of the following limitations:

- 1) In order to be generated, the representation used to reflect the VF vibrations requires the glottal segmentation in all the images of a HSV recording. This is a hard and a complex task as the segmentation of the VF necessitates the user intervention and the number of images in a video is large given the high sampling rate. Furthermore, the segmentation may fail when the VF are completely closed. Examples of such representations are the glottal area waveform (GAW) [1], the digital kymography (DKG) [2], the phonovibrography (PVG) [3], the glottovibrography (GVG) [4] and more [5], [6].
- 2) The objective assessment of the vibrations through a representation, mostly requires a further processing of it in order to be able to derive the laryngeal parameters. For instance, the DKG should be segmented in order to derive parameters like vibration amplitudes, periodicity indices and so on [7]. The same holds for the PVG [3], [8] and the GVG [4].
- 3) The automatic assessment of the vibrations is sometimes based on parameters that are specific to the representation under consideration. Researchers agree on the features to be assessed namely the periodicity and the symmetry of the vibrations; but, different parameters aiming to quantify these features can be found in the literature. Consequently, it becomes difficult to compare between the representations in terms of efficiency and accuracy of the vibration assessment. For instance, parameters specific to PVG are proposed in [3], [8]. A comparative study conducted in [9] investigates the efficiency of parameters derived from different methods like GAW, DKG and the laryngotopography [10].

To alleviate the limitations mentioned above, the present work investigates the use of a recently proposed optical flow based

waveform (OFW) [11] in order to quantify the vibratory characteristics. The exploitation of this waveform is retained in this work for mainly three reasons. First, to generate the OFW, the segmentation of only one image per vibratory cycle is necessary. This allows a remarkably decrease in the amount of images to be segmented. Furthermore, the segmented image corresponds to the one of maximal opening of the glottis in each vibratory cycle; and hence, results of high accuracy could be obtained. Second, the OFW can be directly exploited for the automatic assessment of the vibrations without any further processing. Third, the quantification of the vibratory characteristics can be easily and accurately computed through the OFW based on the most commonly used parameters. The most important and common parameters in the literature are [7], [12], [13]: the fundamental frequency, the left-right phase symmetry, the left-right amplitude symmetry, the time periodicity and the amplitude periodicity. The accuracy of the objective analysis of the OFW is evaluated in comparison to the measures obtained by the analysis of the electroglottographic (EGG) signals [14] and DKG. Experiments show that by using the same parameters, the OFW is more sensitive to a pathological phonation than DKG.

The remainder of this paper is organized as follows. Section II describes the quantification technique and the data used for the evaluation of the obtained measures. The results are depicted in Section III and discussed in Section IV. Finally, some conclusions are drawn in Section V.

II. MATERIALS AND METHODS

A. Materials

Video recordings corresponding to healthy and pathological vibrations of the VF are analyzed in order to evaluate the accuracy of the quantification measures. HSV recordings of healthy phonation are provided by E. Bianco and G. Degottex-IRCAM [15], [16] and contains about 48 videos along with the corresponding EGG and audio signals. Videos corresponding to disordered VF of different pathologies are publicly available online¹.

B. Brief Overview of the OFW Technique

The rOFW (resp. the lOFW) carried out at a level \mathcal{L} from the posterior to the anterior commissure is the trajectory of a point located on the right VF (resp. left VF) at the glottal level \mathcal{L} , during phonation. Typical values of \mathcal{L} are 25%, 50% and 75%. Fig. 1 is an illustration of the OFWs that correspond to healthy vocal folds at the three glottal levels. The amplitudes of the lOFW are displayed in the negative part for more clarity.

To generate the waveforms, the OFW technique proceeds according to the following steps. After sampling the HSV video recording into K images $\{I^{(k)}\}_{k=1,\dots,K}$, the region that includes the glottis and the VF is firstly detected according to the technique described in [4]. All the processing is carried out on this region of interest in order to alleviate the computations. The second step aims to partition the set of K images into \mathcal{C} sets of images $\{\{I_c^{(k')}\}_{k'=1,\dots,K}\}_{c=1,\dots,\mathcal{C}}$ to allow

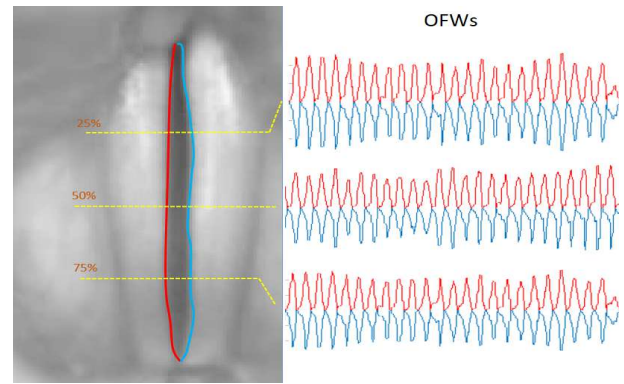


Fig. 1. Optical flow based waveforms at three levels of the glottal area. rOFW in red. -lOFW (in blue) is displayed instead of lOFW for more clarity.

a cycle-to-cycle interpretation of the VF vibratory behavior. Each set $\{I_c^{(k')}\}_{k'}$ consists of K_c images composing the vibratory cycle $c = 1, \dots, \mathcal{C}$ among the \mathcal{C} cycles of the phonation under consideration. K_c is the number of images of the cycle c and k' is a number that defines the temporal location of the image in the cycle. Hence, in a healthy phonation, the set $\{I_c^{(k')}\}_{k'}$ starts by an image of a closed status of the VF which gradually open until reaching the image I_c^{ref} of maximal opening. Then, the VF gradually close during a closing stage until the end of the cycle.

The image I_c^{ref} considered as the *reference image* of the cycle c , is of a particular importance. It allows an accurate detection of the glottal edges and consequently, an accurate localization of the points to be tracked, located on the right and the left vocal folds at the chosen level \mathcal{L} of the glottis. The optical flow (OF) estimation is carried out in the backward and the forward directions from the reference image within the same cycle, in order to better reflect the vibratory behavior of the VF. The displacements of the points of interest along the cycle are cumulated with respect to their positions in I_c^{ref} and constitute the OFW. Further details are given in [11] in which the visual interpretation of the OFW either related to a healthy or a pathological phonation showed its accuracy in assessing the important features of the vibrations such as the periodicity and the symmetry between the two vocal fold dynamics. Despite the efficiency of the visual analysis of the waveforms, an objective and automatic assessment is necessary [17]. In the present study, we investigate the objective and automatic analysis of the OFW by quantifying vibratory parameters as described in the following paragraph.

C. Objective Assessment of the VF Vibrations based on OFW

The diversity of the reported representations aiming to facilitate the visual analysis of the VF vibrations (like the glottal area waveform [1], the phonovibrography [3], the glottovibrography [4], the DKG [2]) implied the appearance of numerous quantification measures. Although most of these measures are closely related to their respective representations, their common objective is to assess important features such as the fundamental frequency, the amplitude/phase symmetry and the periodicity of the vibrations. Additionally to these features,

¹at www.entusa.com

we propose to evaluate the amplitude similarities between the two VF vibrations at each instant.

a) Amplitude Similarity: It is important to know how similar are the amplitudes of the two waveforms over time. For this reason, the one-way ANOVA test is carried out in order to evaluate the similarity between the right and the left vibration amplitudes at all instants.

b) Fundamental frequency: The fundamental frequency F_{0R} (resp. F_{0L}) of the trajectory $rOFW$ (resp. $lOFW$) of the right (resp. the left) vocal fold is estimated using the non linear curve fit model defined by [18]:

$$rOFW(k) = s_0 + a_1 \sin\left(\frac{2\pi}{T_R}k\right) + b_1 \cos\left(\frac{2\pi}{T_R}k\right) + a_2 \sin\left(\frac{4\pi}{T_R}k\right) + b_2 \cos\left(\frac{4\pi}{T_R}k\right). \quad (1)$$

where s_0 is the direct component related to the average value of $rOFW$ over time, a_1, b_1, a_2 and b_2 are coefficients. Hence, the vibration period T_R is estimated and the fundamental frequency F_{0R} related to the trajectory of the right vocal fold is deduced as $F_{0R} = \frac{1}{T_R}$. Analogously, the vibration period T_L related to the trajectory of the left vocal fold is estimated and its fundamental frequency $F_{0L} = \frac{1}{T_L}$ is computed.

c) Symmetry: A large left-right asymmetry can cause voice problems especially when frequency differences between the right and the left vocal folds are significant. This behavior appears when the patient suffers from an unilateral laryngeal paralysis. The symmetrical aspect of the vibrations can be viewed in several ways: amplitude, phase and frequency differences [19]. They can be assessed using the following quantification measures [7].

- **Left-right amplitude symmetry index (ASI):** This indicates the degree of similarity between the amplitudes of the two vocal folds when they are at their maximum value (which corresponds to the maximum closing in the waveform) within a given cycle. It is defined by the difference between the maximum right displacement a_R and the maximum left displacement a_L divided by the sum of them as shown in Fig. 2:

$$ASI = \frac{a_R - a_L}{a_R + a_L} \quad (2)$$

A value of ASI that approaches 0 indicates a perfect symmetry in amplitude between the two vocal folds at the selected level of the glottis.

- **Left-right phase symmetry index (PSI):** When the two vocal folds reach their maximal opening at the same time, their vibrations can be qualified by phase-symmetric. The PSI is defined as the difference between the instants t_R and t_L when respectively the right and the left vocal folds reach their maximal opening, divided by the mean vibration period [7]:

$$PSI = \frac{t_R - t_L}{T_R}. \quad (3)$$

A value of PSI that approaches 0 indicates a perfect symmetry in phase between the vocal folds.

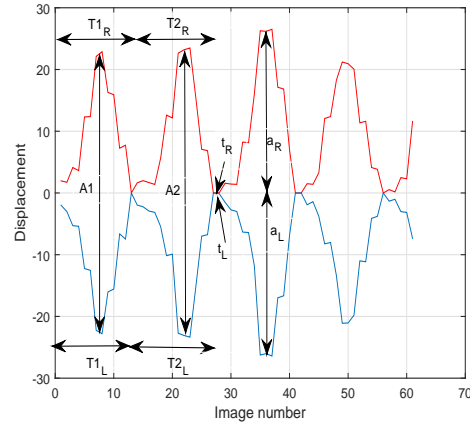


Fig. 2. The waveform parameters. $rOFW$ in red, $(-lOFW)$ in blue. a_R and a_L : maximum displacements within one cycle of the right and left VF. t_R and t_L : instants when the right and the left VF reach their maximal opening. T_{1R}, T_{2R}, T_{1L} and T_{2L} : duration periods of two cycles related to the right and the left vibrations.

d) Periodicity: The periodicity can be defined as the repetition of the same spatial-temporal vibratory behavior along many cycles. It is evaluated by assessing the time and amplitude periodicity.

- **Time periodicity index (TPI):** This is the ratio between the shorter duration of a cycle and the larger duration in two successive cycles [7]. We analyze the time periodicity in the right and the left vocal fold waveforms and determine the respective time periodicity indices TPI_R and TPI_L as follows:

$$TPI_R = \frac{\min(T_{1R}, T_{2R})}{\max(T_{1R}, T_{2R})}, \quad (4)$$

$$TPI_L = \frac{\min(T_{1L}, T_{2L})}{\max(T_{1L}, T_{2L})}.$$

where T_{1R} and T_{2R} (resp. T_{1L} and T_{2L}) the durations of two successive cycles in the right (resp. left) vocal fold waveform. The values range between 0 and 1. A vibration is perfectly periodic when the corresponding time periodicity index approaches 1.

- **Amplitude periodicity index (API):** This is the ratio between the smaller amplitude and the larger one in two consecutive cycles. It is defined by:

$$API = \frac{\min(A_1, A_2)}{\max(A_1, A_2)} \quad (5)$$

where A_1 and A_2 are the sum of the right and the left amplitudes when the vocal folds reach their maximal closing respectively calculated in two successive cycles as illustrated in Fig. 2.

III. RESULTS

In order to evaluate the accuracy of the objective assessment based on the OFW, healthy and pathological phonation are explored.

TABLE I. QUANTIFICATION OF THE GLOTTAL PARAMETERS. RELAXED VOICE (103 CYCLES, 4485 IMAGES). BY USING EGG, $F_0 = 155$

	$\mathcal{L} = 25\%$		$\mathcal{L} = 50\%$		$\mathcal{L} = 75\%$	
	DKG	OFW	DKG	OFW	DKG	OFW
F_0	153	L/R:152	153	L/R:152	153	L/R:152
ASI	-0.04	0.02	0.06	-0.03	0.02	-0.05
PSI	-0.02	L/R:0.001	0.01	L/R:0.0016	0	L/R:0
TPI	0.96	L/R:0.87	0.96	R: 0.9, L: 0.93	0.96	L/R:0.92
API	0.92	0.93	0.92	0.92	0.92	0.82

A. Healthy vocal folds

In healthy phonation, ideally, the waveforms of the left and right vocal folds should be as superimposed as possible ensuring phase and amplitude symmetries. In addition, the same pattern should be observed among many cycles. Quantitatively, the P-values resulting from the ANOVA test should be greater than 0.05, the estimates of the fundamental frequencies of the left and right vibrations should be close to each other, the symmetry indices (such as ASI and PSI) should approach 0 and the periodicity indices (as TPI and API) should approach 1. The quantitative measures obtained by the OFW are compared to those obtained by the analysis of the EGG signals and the DKG. The analysis of the EGG signal is performed according to the technique described in [14] and using the MOQ software².

Tests are conducted on four different types of phonation using several laryngeal mechanisms on healthy vocal folds. The aim is to evaluate the accuracy of the objective measures computed through the analysis of the OFW. The P-values computed through the ANOVA test confirm the similarity in vibrations' amplitudes of the right and the left vocal folds for all the tested mechanisms for 97% of the cycles at the glottal level $\mathcal{L} = 25\%$, 94% of the cycles at the level $\mathcal{L} = 50\%$ and 93% of the cycles at the level $\mathcal{L} = 75\%$ level. As depicted in Tables I, II, III and IV, the fundamental frequency estimated according to the proposed approach is the same for both vocal folds, and within the three glottal levels, in all the sequences related to healthy phonation. Moreover, the estimates are close to the ones estimated by DKG and EGG for all the sequences.

To evaluate the periodicity of the vibrations, the TPI and API are used and their values are found to be above 0.8 for all the sequences. Note that the final decision about how well the vocal folds are healthy is delegated to the clinician based on the provided quantitative measures and his experience. The vibratory parameters measured using DKG in one hand, and using the proposed approach on the other hand, have the same values in 70% of the tested situations including the different glottal levels. In the remaining 30%, the difference between the values ranges between 0.02 and 0.14.

Concerning the symmetry indices, they are 0 for the majority of cases and multiples of 0.001 and 0.01 in some tests.

B. Pathological Vocal Folds

HSVs related to different vocal fold disorders are used to evaluate the efficiency and the reliability of the OFW in assisting clinicians in the diagnosis. The first video is about a right true vocal cord paralysis where the cause of

TABLE II. QUANTIFICATION OF THE GLOTTAL PARAMETERS. (SAMPLE USC2008.02.050.OUV.RENF.50.FRAMES OF THE DATABASE, 130 CYCLES, 7200 IMAGES). BY USING EGG, $F_0 = 115$

	$\mathcal{L} = 25\%$		$\mathcal{L} = 50\%$		$\mathcal{L} = 75\%$	
	DKG	OFW	DKG	OFW	DKG	OFW
F_0	124	L/R: 121	124	L/R:121	124	L/R:121
ASI	-0.04	0.005	-0.03	0.01	-0.05	-0.04
PSI	-0.03	L/R:0	-0.03	L/R: 0	-0.02	L/R:0
TPI	0.8	R: 0.86, L: 0.87	0.8	R: 0.83, L: 0.81	0.8	L/R:0.8
API	0.95	0.9	0.98	0.9	0.96	0.8

TABLE III. QUANTIFICATION OF THE GLOTTAL PARAMETERS (SAMPLE USC2008.02.065.GLISSENDO.65.FRAMES81 CYCLES, 1158 IMAGES). BY USING EGG, $F_0 = 510$

	$\mathcal{L} = 25\%$		$\mathcal{L} = 50\%$		$\mathcal{L} = 75\%$	
	DKG	OFW	DKG	OFW	DKG	OFW
F_0	467	L/R:471	467	L/R:471	467	L/R: 472
ASI	0.01	-0.007	-0.09	0.02	-0.14	0.01
PSI	-0.07	R: 0, L: 0	-0.02	R: 0, L: 0	-0.05	L/R: 0
TPI	0.93	R: 0.91, L: 0.92	0.93	L/R: 0.93	0.93	R: 0.92, L: 0.93
API	0.9	0.8	0.97	0.9	0.98	0.9

the paralysis is unknown or idiopathic. The video is sampled into 940 images corresponding to 9 cycles according to the cycle detection approach proposed in [11]. The waveforms of the right and the left VF are generated and the ANOVA test is carried out. The majority of the P-values are less than the confidence level confirming the vibration asymmetries between the two VF. In addition, the estimated fundamental frequencies of both waveforms related to the left and the right VF are different and have suspicious values especially at 25% of the glottis, as shown in Table V. These values could suspect the presence of an anomaly, precisely in the right cord where the frequency is 0.02 Hz at 25% and 9 Hz at the two other glottal levels, compared to a frequency of 21 Hz at the left vocal cord for the three levels. Even though the fundamental frequency estimated by DKG has a suspicious value compared to the frequency range related to healthy VF, the OFW is found to be more sensitive to a pathologic phonation. Another suspicious value is given by the TPI parameter which is 0.5, expected to approach 1 in a healthy phonation.

The patient of the second video suffers from a cancer in the larynx involving the left vocal fold. The majority of the P-values is less than the confidence level. The values of the TPI and the API parameters in Table VI let suspect an aperiodicity of the VF vibrations. Also, the estimates of the

TABLE IV. QUANTIFICATION OF THE GLOTTAL PARAMETERS (SAMPLE USC2008.02.004.M1.4.FRAMES, 51 CYCLES, 655 IMAGES). BY USING EGG, $F_0 = 590$

	$\mathcal{L} = 25\%$		$\mathcal{L} = 50\%$		$\mathcal{L} = 75\%$	
	DKG	OFW	DKG	OFW	DKG	OFW
F_0	522	L/R:518	522	L/R:517	522	L/R:518
ASI	-0.09	0.09	0.09	-0.04	-0.02	0.04
PSI	-0.08	L/R: 0	-0.05	L/R: 0	0.005	L/R: 0
TPI	0.9	L/R: 0.9	0.92	R: 0.9, L: 0.92	0.92	L/R:0.88
API	0.9	0.8	0.94	0.8	0.94	0.88

²available at <http://voiceresearch.free.fr/egg/>

TABLE V. QUANTIFICATION OF THE GLOTTAL PARAMETERS OF DISORDERED VFS. RIGHT TRUE VOCAL CORD PARALYSIS (9 CYCLES)

	$\mathcal{L} = 25\%$		$\mathcal{L} = 50\%$		$\mathcal{L} = 75\%$	
	DKG	OFW	DKG	OFW	DKG	OFW
F_0	79	R: 0.02 , L: 21	79	R: 9 , L: 21	79	R: 9 , L: 20
ASI	0.003	-0.04	-0.01	-0.01	0.09	0.16
PSI	0.02	L/R:0	0.01	L/R 0	0.12	L/R:0
TPI	0.5	R: 0.58 , L: 0.43	0.5	R: 0.58 , L: 0.47	0.5	L/R: 0.56
API	0.87	0.74	0.91	0.75	0.86	0.76

TABLE VI. QUANTIFICATION OF THE GLOTTAL PARAMETERS OF DISORDERED VFS. CANCER OF THE LEFT TRUE VOCAL CORD (5 CYCLES,552 IMAGES)

	$\mathcal{L} = 25\%$		$\mathcal{L} = 50\%$		$\mathcal{L} = 75\%$	
	DKG	OFW	DKG	OFW	DKG	OFW
F_0	61	R: 30, L: 0.04	61	R: 20, L: 60	61	R: 20, L: 41
ASI	0.17	-0.15	0.01	-0.08	0.04	-0.24
PSI	0.05	L/R:0	0.04	L/R 0	0.008	L/R:0
TPI	0.82	R: 0.43, L: 0.72	0.82	R: 0.46, L: 0.6	0.8	R: 0.58, L: 0.8
API	0.51	0.63	0.67	0.7	0.58	0.48

fundamental frequencies of both waveforms have suspicious values, especially the left vocal fold at 25% of the glottis, leading to conclude an anomaly in that glottal part which is in concordance with the ground truth.

The third video is about a left true vocal cord paralysis from injury to the Vagus Nerve during carotid endarterectomy surgery. The P-values of the ANOVA test are less than the confidence level for more than half of the cycles which confirms the pathological aspect of the vibrations. Besides, the fundamental frequency estimates of the right and the left waveforms are close to each other as shown in Table VII, but their values let suspect an abnormality in the vibrations. Also, the values taken by the periodicity parameters (TPI and API) suspect disordered VF.

IV. DISCUSSION

Numerous techniques are proposed in the literature allowing to map the spatial-temporal information contained in a HSV recording into a representation suitable for the visual and the automatic assessment of the vibrations. Most of the state-of-the-art representations require an additional processing, like applying a segmentation technique, in order to quantify laryngeal parameters. In contrast, it is possible to directly measure these parameters by using the OFW.

TABLE VII. QUANTIFICATION OF THE GLOTTAL PARAMETERS OF DISORDERED VFS. ABDUCTOR PARALYSIS (8CYCLES, 860 IMAGES)

	$\mathcal{L} = 25\%$		$\mathcal{L} = 50\%$		$\mathcal{L} = 75\%$	
	DKG	OFW	DKG	OFW	DKG	OFW
F_0	63	R: 33, L: 34	63	R: 31, L: 33	63	R:31, L: 61
ASI	-0.02	0.01	0.04	0.02	-0.16	0.11
PSI	-0.01	L/R:0	-0.003	L/R 0	-0.04	L/R:0
TPI	0.85	R: 0.62, L: 0.7	0.85	R: 0.68, L: 0.67	0.85	L/R:0.77
API	0.9	0.7	0.91	0.7	0.87	0.66

Moreover, the present study shows that the exploitation of the OFW allows to quantify the most commonly used laryngeal parameters namely the fundamental frequency of the vibrations, the amplitude/phase symmetry parameters and the time/amplitude periodicity without need of dealing with intermediate metrics specific to OFW.

Healthy and pathological vibrations are explored in this study.

Regarding healthy phonation, different mechanisms used by different persons are considered. The quantification accuracy is evaluated in comparison to the measures obtained through the analysis of the corresponding EGG signals (for the evaluation of the fundamental frequency estimate) and the DKG. For all the tested sequences, the fundamental frequency estimated through the OFW is close to those estimated using the EGG signals and DKG. Also, the measures of the symmetry and the periodicity obtained through analyzing the OFW are close to the measures obtained through DKG, for the three glottal levels.

Regarding the assessment of pathological vibrations, tests conducted on sequences of different disorders show the reliability of the OFW in suspecting a vibratory anomaly. Furthermore, it is shown that the OFW is more sensitive to a pathological phonation than DKG.

V. CONCLUSION

The objective assessment of the vocal fold vibrations is the main focus of the present study. To this aim, the optical flow based waveform is retained. Its generation does not require the segmentation of all the images of the HSV. More importantly, the present paper shows that the quantification of the vocal fold vibrations by using OFW does not necessitate an additional processing, contrary to the majority of the state-of-the-art techniques. Furthermore, it is possible to quantify the commonly used laryngeal parameters. The results show the reliability of the OFW in quantifying the VF vibrations. Moreover, it is more sensitive to a pathological phonation.

REFERENCES

- [1] I. R. Titze, "Parameterization of the glottal area, glottal flow, and vocal fold contact area," *The Journal of the Acoustical Society of America*, vol. 75, no. 2, pp. 570–580, 1984.
- [2] T. Wittenberg, M. Tigges, P. Mergell, and U. Eysholdt, "Functional imaging of vocal fold vibration: digital multislice high-speed kymography," *Journal of Voice*, vol. 14, no. 3, pp. 422–442, 2000.
- [3] J. Lohscheller, U. Eysholdt, H. Toy, and M. Dollinger, "Phonovibrography: Mapping high-speed movies of vocal fold vibrations into 2-d diagrams for visualizing and analyzing the underlying laryngeal dynamics," *IEEE transactions on medical imaging*, vol. 27, no. 3, pp. 300–309, 2008.
- [4] S.-Z. Karakozoglou, N. Henrich, C. d'Alessandro, and Y. Stylianou, "Automatic glottal segmentation using local-based active contours and application to glottovibrography," *Speech Communication*, vol. 54, no. 5, pp. 641–654, 2012.
- [5] R. Menon, L. Petropoulakis, J. J. Soraghan, H. Lakany, K. MacKenzie, O. Hilmi, and G. Di Caterina, "Automatic quantification of vocal cord paralysis-an application of fibre-optic endoscopy video processing," 2017.

- [6] J. Lin, E. S. Walsted, V. Backer, J. H. Hull, and D. Elson, "Quantification and analysis of laryngeal closure from endoscopic videos," *IEEE Transactions on Biomedical Engineering*, 2018.
- [7] Q. Qiu, H. Schutte, L. Gu, and Q. Yu, "An automatic method to quantify the vibration properties of human vocal folds via videokymography," *Folia Phoniatrica et Logopaedica*, vol. 55, no. 3, pp. 128–136, 2003.
- [8] J. Unger, D. J. Hecker, M. Kunduk, M. Schuster, B. Schick, and J. Lohscheller, "Quantifying spatiotemporal properties of vocal fold dynamics based on a multiscale analysis of phonovibrograms," *IEEE Transactions on Biomedical Engineering*, vol. 61, no. 9, pp. 2422–2433, 2014.
- [9] A. Yamauchi, H. Yokonishi, H. Imagawa, K.-I. Sakakibara, T. Nito, N. Tayama, and T. Yamasoba, "Quantification of vocal fold vibration in various laryngeal disorders using high-speed digital imaging," *Journal of Voice*, vol. 30, no. 2, pp. 205–214, 2016.
- [10] A. Yamauchi, H. Imagawa, K.-I. Sakakibara, H. Yokonishi, T. Nito, T. Yamasoba, and N. Tayama, "Phase difference of vocally healthy subjects in high-speed digital imaging analyzed with laryngotopography," *Journal of Voice*, vol. 27, no. 1, pp. 39–45, 2013.
- [11] H. Ammar, "Optical flow based waveform for the assessment of the vocal fold vibrations," *Australasian Physical & Engineering Sciences in Medicine*, vol. 42, no. 1, pp. 91–109, 2019.
- [12] H. S. Bonilha, D. D. Deliyski, and T. T. Gerlach, "Phase asymmetries in normophonic speakers: visual judgments and objective findings," *American Journal of Speech-Language Pathology*, vol. 17, no. 4, pp. 367–376, 2008.
- [13] C. R. Krausert, D. Ying, Y. Zhang, and J. J. Jiang, "Quantitative study of vibrational symmetry of injured vocal folds via digital kymography in excised canine larynges," *Journal of Speech, Language, and Hearing Research*, vol. 54, no. 4, pp. 1022–1038, 2011.
- [14] D. M. Howard, G. A. Lindsey, and B. Allen, "Toward the quantification of vocal efficiency," *Journal of Voice*, vol. 4, no. 3, pp. 205–212, 1990.
- [15] G. Degottex, E. Bianco, and X. Rodet, "Usual to particular phonatory situations studied with high-speed videoendoscopy," in *International Conference on Voice Physiology and Biomechanics*, 2008, pp. 19–26.
- [16] G. Degottex, "Glottal source and vocal-tract separation: estimation of glottal parameters, voice transformation and synthesis using a glottal model," Ph.D. dissertation, Paris 6, 2010.
- [17] D. Deliyski, K. Kendall, and R. Leonard, "Laryngeal high-speed videoendoscopy," *Laryngeal evaluation: Indirect laryngoscopy to high-speed digital imaging*, pp. 245–270, 2010.
- [18] J. J. Jiang, C.-I. Chang, J. R. Raviv, S. Gupta, F. M. Banzali, and D. G. Hanson, "Quantitative study of mucosal wave via videokymography in canine larynges," *The Laryngoscope*, vol. 110, no. 9, pp. 1567–1573, 2000.
- [19] J. G. Švec, F. Šram, and H. K. Schutte, "Videokymography in voice disorders: What to look for?" *Annals of Otology, Rhinology & Laryngology*, vol. 116, no. 3, pp. 172–180, 2007.

A Parallel Hybrid-Testing Tool Architecture for a Dual-Programming Model

Ahmed Mohammed Alghamdi¹, Fathy Elbouraey Eassa²
Faculty of Computing and Information Technology^{1,2}
King Abdulaziz University, Jeddah, Saudi Arabia

Abstract—High-Performance Computing (HPC) recently has become important in several sectors, including the scientific and manufacturing fields. The continuous growth in building more powerful super machines has become noticeable, and the Exascale supercomputer will be feasible in the next few years. As a result, building massively parallel systems becomes even more important to keep up with the upcoming Exascale-related technologies. For building such systems, a combination of programming models is needed to increase the system's parallelism, especially dual and tri-level programming models to increase parallelism in heterogeneous systems that include CPUs and GPUs. There are several combinations of the dual-programming model; one of them is MPI+ OpenACC. This combination has several features that increase the application's parallelism concerning heterogeneous architecture and support different platforms with more performance, productivity, and programmability. However, building systems with different programming models are error-prone and difficult and are also hard to test. Also, testing parallel applications is already a difficult task because parallel errors are hard to detect due to the non-determined behavior of the parallel application. Integrating more than one programming model inside the same application makes even it more difficult to test because this integration could come with a new type of errors. Our main contribution is to identify and categorize OpenACC run-time errors and determine their causes with a brief explanation for the first time in research. Also, we proposed a solution for detecting run-time errors in application implemented in the dual-programming model. Our solution based on using hybrid testing techniques to discover real and potential run-time errors. Finally, to the best of our knowledge, there is no parallel testing tool built to test applications programmed by using the dual-programming model MPI + OpenACC or any tri-level programming model or even the OpenACC programming model to detect their run-time errors. Also, OpenACC errors have not been classified or identified before.

Keywords—Software testing; OpenACC run-time error classifications; hybrid testing tool; dual-programming model; OpenACC

I. INTRODUCTION

In the past few years, building Exascale systems based on CPU/GPU heterogeneous architecture has become a hot research topic. Therefore, creating parallel applications with more ability to work with the upcoming Exascale era has also become increasingly important. However, the current parallel programming languages are not satisfying the increasing need for creating parallel applications. Also, parallelism cannot be supported efficiently by the majority of traditional

programming languages. Therefore, programming models, which are a group of directives and operations used to support parallelism, have been used to add parallelism to the traditional programming languages.

There are several programming models with different features and used for various purposes. These programming models include the message passing programming model MPI [1] and the programming model that support the shared-memory parallelism such as OpenMP [2]. In addition, there are programming models that support CPU/GPU heterogeneous systems. The programming models that support heterogeneous parallelism are CUDA [3] and OpenCL [4], as low-level programming models, and OpenACC [5] as a high-level heterogeneous programming model.

Testing parallel applications is a difficult task because they have non-determined behavior, which makes it hard to detect their parallel errors when they occur. Even if these errors have been detected and the source code modified, it is difficult to decide if the errors have been corrected or still but hidden. If the application has integrated different programming models that will make the testing process even harder. Although there are many testing tools dedicated to detecting static and dynamic run-time errors, still not enough especially for detecting errors that occur in applications implemented in high-level programming models and also dual-programming models.

This research aims to identify some of OpenACC's run-time errors and design a suitable hybrid-testing tool architecture for systems implemented in C++ and the dual-programming model MPI+OpenACC. The combination of static and dynamic testing techniques will be used for detecting run-time errors by analyzing the source code before and during run time, which will improve the testing time and cover a wide range of errors.

The rest of this paper is structured as follows. Section 2 briefly gives an overview of the related work. Section 3 will identify OpenACC run-time error classification. The proposed architecture will be discussed in Section 4; the discussion will comprise Section 5, and finally the conclusion in Section 6.

II. RELATED WORKS

In testing parallel applications, there are many studies, which varied for several purposes and different scopes. These variations of testing tools including tools that detect a specific type of errors, the used testing techniques, and the targeted programming models as well as the programming model levels

single, dual, and try level. There are many researches have been done in detecting a specific type of errors such as data race and deadlock, using several testing techniques. There are many tools that used static and dynamic testing for detecting deadlock such as UNDEAD [15]. Other tools are designed to detect race condition like the tool introduced in [14]. Finally, in [9] there are some detection techniques, which proposed for detecting livelock.

Several testing tools have been dedicated to testing the programming models by using different approaches. Some of them focusing in testing single programming models such as testing tools for MPI [16], [17], OpenMP [18], [19], CUDA [20] and OpenCL [21], but other studies tested the dual-programming models including MPI + OpenMP [11], [22]. Another approach is to focus on the testing techniques such as dynamic testing in [9], [10], static testing in [6]–[8], and the hybrid-testing techniques in [11]–[14].

There are many debuggers used for HPC applications include both open-source and commercial versions. ALLINEA DDT [23], is a commercial debugger that supports C++, MPI, and OpenMP designed to work on Petascale. Another commercial debugger is TotalView [24], which supports MPI, OpenMP and CUDA. These debuggers do not help in testing or detecting run-time errors but used to find the causes of these errors. Also, the thread, process, and kernel are needed to be selected for investigation. In terms of open-source testing tools, there are many tools to detect race condition in OpenMP including ARCHER [25], which used hybrid techniques to identify OpenMP data race. Finally, AutomaDeD [26], MEMCHECKER [16] and MUST [27] are used for detecting errors in MPI.

In terms of OpenACC testing, there is a shortage of testing OpenACC for detecting run-time errors. However, there are some studies that related to evaluating different compilers by creating test cases for OpenACC 2.0 as shown in [28]. Another study has been published in [29], also for evaluating CAPS, PGI, and CRAY compilers. Finally, OpenACC 2.5 was evaluated in [30] for validating and verifying the new feature of OpenACC compilers' implementation

Despite efforts made to create and propose software testing tools for parallel application, there is still a lot to be done primarily for GPU-related programming models and for dual- and tri-level programming models for heterogeneous systems. Heterogeneous systems can be hybrid CPUs/GPUs architectures or different architectures of GPUs. We noted that OpenACC has several advantages and benefits and has been used widely in the past few years, but it has not targeted any testing tools covered in our study. Finally, to the best of our knowledge, there is no parallel testing tool built to test applications programmed by using the dual-programming model MPI + OpenACC or any tri-level programming model.

III. CLASSIFICATION OF OPENACC RUN-TIME ERRORS

Many studies have been done in detecting and identifying MPI run-time errors, so we will not cover them in our paper. However, OpenACC errors have not been previously investigated, identified, or classified. Therefore, we investigate and analyze OpenACC documents and specifications as well as

conducting several experiments to identify and classify run-time errors that cannot be detected by the compilers.

Similar to any programming model that supports parallelism, OpenACC has several run-time errors as a result of their parallel nature. Compilers cannot detect these errors, which occur after compilation and cause several issues without developers' awareness. Usually, run-time errors have similar names but with different behavior and causes. For instance, the race condition in any application implemented by using one type of programming model has different causes and behaves differently from race condition in other applications implemented by another programming model. Also, run-time errors in applications implemented by the dual-programming model are different based on the combination between the hybrid programming models, and some errors occur specifically in a specific programming model.

OpenACC directives can be divided into data management directives and compute directives [31]. Compute directives are responsible for determining the blocks of the source code that can distribute the work to multiple threads in the GPU. Data management directives are responsible for avoiding unnecessary data movement between CPU and GPU. We use only compute directives that lead to moving data from and to the GPU each time we use these directives. The data directives determine data lifetime in the GPU, and in this time the GPU essentially owns the data. The data region in OpenACC is divided into a structured data region and unstructured data region [32]. The structured data region must have an explicit start and end points within a single function, and memory exists within the data region. On the other hand, the unstructured data region can have more than one start and end points and can branch across multiple functions, and memory exists until explicitly deallocated.

In the latest version of OpenACC 2.7 document [33], there is an error that appears several times through this document, which will cause run-time errors if not solved. This error is related to the presence of the variable in the GPU when needed to be used, for several OpenACC directives. Basically, it can happen when the variable is deleted from the GPU by a thread while it is needed by another thread. Furthermore, if any variable is not allocated in the GPU when it is needed, a message that indicates that there is a run-time error occurs in different parts of the source code without considering or explaining the cause or the error type. In addition, discovering these types of errors are difficult, even more complicated discovering them in applications developed by dual-programming model. As a result, we detect, identify and classify some of the OpenACC run-time errors into several categories determined by the way that OpenACC directives interact and behave. This classification includes the common run-time errors that occur because of the nature of parallel systems using the OpenACC programming model. Also, we include other errors related to OpenACC programming model and also classify them into the first two categories. In the following, we show our classifications.

A. Device-Based Data Transmission Errors

In this classification, run-time errors could happen as a result of mishandling of data using OpenACC directives and

data clauses. Developers easily make these errors if they do not pay attention to the usage of OpenACC clauses, which leads to wrong results or non-deterministic behavior. These errors happen when developers mistakenly use the following data clauses in structured or unstructured data clauses. The data clauses include copy, copyin, copyout, create, delete, and present. Several cases can be included in this classification.

1) Errors that lead to run-time error messages can occur in unstructured or structured data regions. These errors will issue a run-time error message that indicates an invalid value. In the unstructured data region, there is a variable in a copyout clause in the exit data region without having the same variable in the enter data region, which the compiler cannot detect. In this case, there are several scenarios to demonstrate this error; one of them is the following code in Fig. 1. We noticed that the variable in the copyout clause is the array "a", but the error will happen because the variable "a" is deleted before the copyout clause, so there is nothing to copy back from GPU to the CPU, as in Fig. 1b. Also, in Fig. 1a, the copyin variable is the array "b", but a different array "a" in the copyout clause, which causes the same run-time error. Finally, if the developers forget to write "acc" in the enter or exit data or forget to enter the data directive, this error will occur, and the compiler will not detect it.

In the structured data region, when the developer used the copy, copyout, create, and present clauses and the variable is not present in the current GPU, the run-time error message will be issued. This error cannot be detected by a compiler and will happen only after compilation at run-time.

2) The other class is errors that could lead to wrong results without the developer's awareness as well as that of the compiler, who therefore cannot detect them. There are several scenarios that could lead to these errors, including the structured and unstructured data regions. In the unstructured data region, if the developer uses a create clause instead of a copyin clause when a copy of the variable needs to be copied from the CPU to the GPU, this leads the program to yield wrong results, as is shown in Fig. 2a. Also, the variable is deleted at the exit region when this variable needs to be copied back to the CPU, as shown in Fig. 2b. Finally, this error can also happen when forgetting to write "acc" at the exit data region or not using the exit data region directive.

In the structured data region, some cases can cause wrong results when using a data clause, including using copyin instead of copy when developers want to copy data to the GPU and do some operations and copy back the results to the CPU. This will cause wrong results that cannot be detected by the compiler. This can also happen if a developer forgets to add "acc" to the data region directive.

B. Memory Errors

These errors also can cause wrong results or run-time errors, like the previous classification, but can also affect the GPU memory by keeping variables and matrixes in the GPU memory without using them. The main idea of this error

classification is that it is based on sending variables to the GPU without getting back any variables, or keeping some of them without using or deleting them. Also, this can occur when creating variables in the GPU without deleting or copyout them at the exit of the region. This can cause several issues, including affecting the GPU performance by consuming the GPU memory unnecessarily and can cause further errors in the case of using the same memory location with another variable in another part of the code. This type of error happens in the unstructured data region because the developer must determine the enter data and exit data by himself, while in the structured data region the developer only determines the data clause to use, and the compiler will deal with the internal operations needed at the enter and exit data.

```
#pragma acc enter data create(a[0:n])

#pragma acc kernels loop
for(int i = 0; i < n; i++)
{
    a[i] = (double) i + a[i];
}

#pragma acc exit data copyout(a[0:n])
```

(a) Using Create Clause Instead of Copyin Clause.

```
#pragma acc enter data copyin(a[0:n])

#pragma acc kernels loop
for (int i = 0; i < n; i++)
{
    a[i] = (double) i + a[i];
}

#pragma acc exit data delete (a[0:n])
```

(b) Deleted the Array without Copyout.

Fig. 1. Unstructured Data Region has Errors Leading to Wrong Results.

```
#pragma acc enter data copyin(b[0:n])

#pragma acc kernels loop
for (int i = 0; i < n; i++) {
    a[i] = (double) i + a[i];
}

#pragma acc exit data copyout (a[0:n])
```

(a) Different Copyin and Copyout Arrays.

```
#pragma acc enter data copyin(a[0:n])
#pragma acc exit data delete(a[0:n])

#pragma acc kernels loop
for (int i = 0; i < n; i++)
{
    a[i] = (double) i + a[i];
}

#pragma acc exit data copyout (a[0:n])
```

(b) Deleted the Array before the Copyout.

Fig. 2. Unstructured Data Region has Errors Leading to a Run-Time Error Message.

C. Race Condition

OpenACC race condition has different causes and behaves slightly different from other programming models, because of the nature of OpenACC and how it works in the heterogeneous architecture. Race condition can occur because of multiple threads will execute several processes concurrently and the thread execution sequence makes a difference in the parallel execution results. In addition, by using OpenACC, developers cannot guarantee the threads' execution order [32]. Because of the developers' responsibility to make sure there is no data dependency, OpenACC is more likely to have race conditions, which can happen as a result of several causes and situations, including:

1) The synchronization between host and device or vice versa to keep the data coherence between them. The programmer should be careful when dealing with updating data between host and device and should know when and how to do this updating because sometimes this can cause a race condition. The following example in Fig. 3 shows data race occurring because multiple threads may be updating the same element in the "hist" array, which will cause a race condition. Also, these parallel regions are in the same data region.

2) *Paralyzing for loops*: We paralyze for the loop so the code in the body of the loop can run in parallel using concurrent hardware execution thread. The iteration variable appears to be incremented sequentially, but threads are actually using different values of iteration variable in this, for the loop variable may be running in parallel at the same time. OpenACC makes no guarantee about the execution order of the threads. Moreover, it is possible that the last iteration of the loop may be completed before the zero loop iteration. This will lead to a potential race condition when the order of execution is important and affects the operations executed in the loop body, or when there is a dependency between some variables in the loop block that need to be updated before completing the next statements.

3) *Shared data read and write*: This situation involves creating a shared array or any dataset in a global kernel, and trying to read, write, and update from different threads concurrently—for example, writing a value by a thread in a location and reading the same location by another thread. This may cause a potential race condition.

4) *Asynchronous Directive*: OpenACC supports the asynchronous and wait directives. Programmers are responsible for ensuring their applications synchronization when they use asynchronous and wait directives to avoid a race condition between the host and device. In OpenACC, there is a hidden barrier at the end of each compute region, and the CPU thread execution will not proceed until all GPU threads have arrived at the end of the OpenACC compute region [33]. By default, all OpenACC directives are synchronous, which means that the CPU thread sent the required data and instructions to the GPU; after that, the CPU thread will wait for the GPU to complete its work before continuing execution [31].

```
#pragma acc data copyout(hist[0:B]) copyin(data[0:count])
{
    #pragma acc parallel loop
    for(int i = 0; i < B; i++)
        hist[i] = 0;

    #pragma acc parallel loop
    for(int i = 0; i < count; i++)
    {
        #pragma acc update
        hist[data[i]]++;
    }
}
```

Fig. 3. Race Condition because of Synchronization between Host and Device.

Using asynchronous and wait directives allows the CPU to continue working while the GPU works at the same time, which allows the pipelining execution of the system and enhances performance. However, when developers use these directives without considering their system requirements and miss using them, this can lead to a race condition. The following code in Fig. 4 shows the code that has a race condition because of the misuse of the asynchronous directive. The array "A" will go to asynchronous queue number 1, and "B" will go to queue number 2, and the CPU will continue working without waiting for the previous two queues to be completed and without considering that these arrays are needed before computing array "C". Therefore, array "C" will have a race condition that leads to wrong results.

5) *Reduction clause*: The reduction clause variable copies are generated for each loop iteration, similar to the private clause, reducing all of these private copies into one final result that will be returned from the GPU to the CPU [33]. In OpenACC, a reduction clause can specify the operator on the scalar variables, including summation, multiplication, and maximum and minimum operators. Some compilers will detect reduction on the reduction variable and implicitly insert the reduction clause, but for others, the programmer should always indicate reductions in the code.

Although some data dependency can be avoided by using a reduction clause, misusing the reduction clause in some cases will lead to OpenACC race condition. When there is no reduction clause that will lead also to race condition. Because reduction clause combines the result of each copy of the reduction variable with the original variable at the end of the OpenACC compute region, the variable should be initialized to some value based on the used operator before using the reduction clause. Otherwise, undefined behavior will result.

6) *Independent clause*: When developers use the independent clause, that tells the compiler that this loop is data-independent, which can cause problems if there is a dependency. It is the developers' responsibility to ensure not using independent clause if there is a data dependency because it allows programmers to tell the compiler that the loop iterations are data-independent. These independent loop clauses can be used to tell the compiler that all loop iterations are independent, which means that there is no dependency or relation between any two loop iterations.

D. Deadlock

In OpenACC, one cause of deadlock in the CPU is having livelock in the GPU. This happens because of the nature of the implicit barrier at the end of each compute region. That means the GPU will be busy with the livelock while the CPU is waiting for the GPU to finish its operation. In the usage of the asynchronous directive, the GPU livelock also causes CPU deadlock, but by different behavior in terms of the usage of the wait directive; this will cause the CPU to have deadlock in that statement. In this case, the deadlock behaviors are based on the asynchronous and wait directive interactions. The following Fig. 5 shows deadlock situations that occur in the OpenACC application.

```
#pragma acc data copy(A[:N], B[:N], C[:N])
{
    #pragma acc parallel loop copy(A[:N])
    for(int i = 0; i < N; i++)
    {
        A[i] = i;
    }
    #pragma acc parallel loop copy(B[:N])
    for(int i = 0; i < N; i++)
    {
        B[i] = i;
        if ( i == 3 )
        {
            while ( i == 3 )
            {
                B[i] = 3;
            }
        }
    }
    #pragma acc parallel loop
    for (int i = 0; i < N; i++)
    {
        C[i] = A[i] + B[i];
    }
}
```

(a) Implicit Barrier Deadlock.

```
#pragma acc data copy(A[:N], B[:N], C[:N])
{
    #pragma acc parallel loop copy(A[:N])
    for(int i = 0; i < N; i++)
    {
        A[i] = i;
    }
    #pragma acc parallel loop copy(B[:N]) async
    for(int i = 0; i < N; i++)
    {
        B[i] = i;
        if ( i == 3 )
        {
            while ( i == 3 )
            {
                B[i] = 3;
            }
        }
    }
    #pragma acc parallel loop
    for (int i = 0; i < N; i++)
    {
        C[i] = A[i] + B[i];
    }
}
#pragma acc wait
```

(b) Wait Directive Deadlock.

Fig. 4. Deadlock because of the GPU Livelock.

```
#pragma acc parallel loop copy(A[:N]) async(1)
for(int i = 0; i < N; i++)
{
    A[i] = i;
}
for(int j = 0; j < N; j++)
{
    cout << " A[" << j << "] = " << A[j] << endl;
}
cout << "*****" << endl;
#pragma acc parallel loop copy(B[:N]) async(2)
for(int i = 0; i < N; i++)
{
    B[i] = i;
}
for(int j = 0; j < N; j++)
{
    cout << " B[" << j << "] = " << B[j] << endl;
}
cout << "*****" << endl;
#pragma acc parallel loop copy(C[:N])
for (int i = 0; i < N; i++)
{
    C[i] = A[i] + B[i];
}
for(int j = 0; j < N; j++)
{
    cout << " C[" << j << "] = " << C[j] << endl;
}
```

Fig. 5. Race Condition because of the Miss use of Asynchronous Directive.

IV. PROPOSED ARCHITECTURE

We propose a parallel hybrid-testing tool for applications implemented in the dual-programming model (MPI + OpenACC) and C++ programming language, as shown in Fig. 6. Our design has the ability to detect real and potential runtime errors, with providing the necessary information for programmers to help them fix these errors. Our design has integrated static and dynamic testing techniques for covering a range of errors.

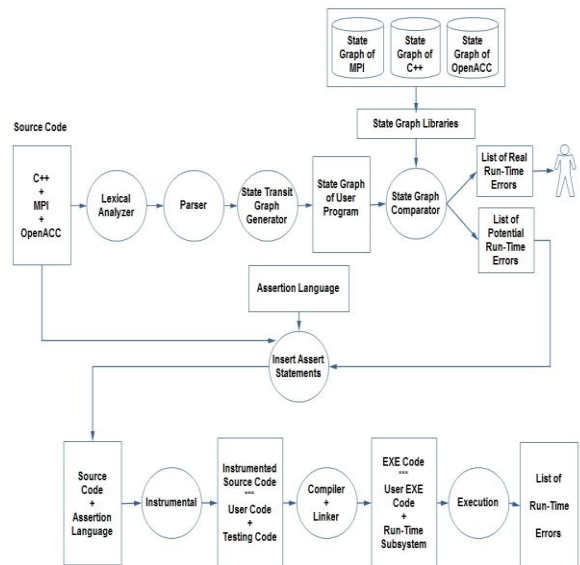


Fig. 6. The Architecture of Parallel Hybrid Testing Tool

The targeted source code will be analyzed in the static phase for discovering both potential and real run-time errors as well as marking the source code for further examination in our dynamic phase of the testing tool. The real errors which will defiantly occur during run time will be sent to the programmers with related information for their action to fix these errors before execution the source code. As a result, static detection helps in enhancing the testing performance by reducing the testing time.

The static part of our architecture includes the following parts:

- Lexical Analyzer; Take the source code as an input and convert it into a table of tokens.
- Parser: Analyze the source code checking for correct syntax in the process and confirming the formal grammar rules.
- State Transit Graph Generator: Generate a state graph for the given source code and represent it in a suitable structure.
- State Graph Comparator: Compare the generated graph with programming language and model graphs.

Any differences in the comparing process will be resulted in a list of run-time errors.

In the dynamic part of our design, the source code and the inserted statements will be taken as an input and pass them to be instrumented. The instrumenter will provide instrumented code that includes both user and testing codes written in C++. The instrumentation has two ways to do include.

- 1) Add the inserted testing codes to the original source code.
- 2) Call API functions to test the targeted part of the source code.

The first method generates larger source code size because it includes both user and testing codes. While the second has a smaller size because only the calling statements will be added to the user source code, and the function will test the user code. Also, when we have similar user code to be tested that will lead to repetitive testing code, in the first method, through the instrumented code which makes it even bigger. However, in the second method, we only write the testing code once and call it multiple times without affecting the instrumented source code size.

V. DISCUSSION

Despite efforts made to detect run-time errors in the parallel application, there is still a lot to be done primarily for GPU-related programming models and for dual- and tri-level programming models for heterogeneous systems. Heterogeneous systems can be hybrid CPUs/GPUs architectures or different architectures of GPUs. We noticed that OpenACC has several advantages and benefits and has been used widely in the past few years by non-computer science specialists, but it has not targeted any testing tools covered in our study. Also, OpenACC has been used in the top

five high-performance computing applications, and the top supercomputer in the World Summit also use OpenACC in five out of 13 applications [34]. As a result, the increase used of OpenACC will come with more errors that possibly occur and need to be discovered.

Furthermore, OpenACC errors have not been identified or classified, which makes it more difficult for us to build our tool. We studied OpenACC and conduct several experiments and build different scenarios to understand the run-time errors behavior in OpenACC as well as their effect when interacting with MPI. Based on these errors we proposed our design and determined the techniques to be used for testing the targeted applications.

In terms of our tool, the hybrid-testing techniques have been considered in our design. The combination of static and dynamic techniques takes advantage of both and reduces testing time by discovering the real errors during static analysis. The first phase is the static analysis approach which analyzes the source code before compilation and sending the resulted report to the programmers with the respective related information that help them to correct these errors. Also, mark the needed part for further dynamic investigation because some errors may or may not occur during run time based on the execution environment and behavior. The second part is the dynamic analysis approach which takes the marked parts from the static analysis, insert suitable testing statements and run them to test the user program.

Dealing with a parallel application is complicated and challenging because of their nature and how they behave, which need more effort to build our tool to cover a wide range of errors and predict scenarios of how the run-time errors will behave in each case. Finally, the used techniques will be determined based on the run-time error type and behavior.

VI. CONCLUSION AND FUTURE WORK

As the Exascale supercomputers will be feasible in a few years, there is an increasing importance of building parallel systems. However, there is a shortfall in testing those systems, especially parallel systems that use heterogeneous programming models including high- and low-level programming models. Creating parallel applications by combining more than one programming model has benefits but also with more complex codes which are difficult to test and debug. That will lead to creating new approaches and techniques to detect run-time errors in such complex parallel applications.

Despite efforts made to create and propose software testing tools for parallel application, there is still a lot to be done primarily for GPU-related programming models and for dual- and tri-level programming models for heterogeneous systems. Heterogeneous systems can be hybrid CPUs/GPUs architectures or different architectures of GPUs. We noted that OpenACC has several advantages and benefits and has been used widely in the past few years, but it has not targeted any testing tools covered in our study.

In this paper, the main contribution that we identify and classify OpenACC run-time errors and their causes has been determined, with a brief explanation. Also, we proposed a

solution for detecting run-time errors in application implemented in the dual-programming model. Based on the number of the application threads, our system will work in parallel creating testing threads for each needed application thread to be tested.

Our design will be implemented, and its ability for detecting run-time errors will be evaluated in our future work. The AZIZ supercomputer, which is one of the top ten supercomputers in Saudi Arabia will be used in our experiments in detecting parallel applications especially with heterogeneous architecture. Finally, to the best of our knowledge, there is no parallel testing tool built to test applications programmed by using the dual-programming model MPI + OpenACC or any tri-level programming model.

REFERENCES

- [1] Message Passing Interface Forum, "MPI Forum," 2017. [Online]. Available: <http://mpi-forum.org/docs/>.
- [2] OpenMP Architecture Review Board, "About OpenMP," OpenMP ARB Corporation, 2018. [Online]. Available: <https://www.openmp.org/about/about-us/>.
- [3] NVIDIA Corporation, "About CUDA," 2015. [Online]. Available: <https://developer.nvidia.com/about-cuda>.
- [4] Khronos Group, "About OpenCL," Khronos Group, 2017. [Online]. Available: <https://www.khronos.org/opencl/>.
- [5] OpenACC-standard.org, "About OpenACC," OpenACC Organization, 2017. [Online]. Available: <https://www.openacc.org/about>.
- [6] E. Saillard, P. Carribault, and D. Barthou, "MPI Thread-Level Checking for MPI+OpenMP Applications," in EuroPar, vol. 9233, 2015, pp. 31–42.
- [7] J. Jaeger, E. Saillard, P. Carribault, and D. Barthou, "Correctness Analysis of MPI-3 Non-Blocking Communications in PARCOACH," in Proceedings of the 22nd European MPI Users' Group Meeting on ZZZ - EuroMPI '15, 2015, pp. 1–2.
- [8] A. Santhiar and A. Kanade, "Static deadlock detection for asynchronous C# programs," in Proceedings of the 38th ACM SIGPLAN Conference on Programming Language Design and Implementation - PLDI 2017, 2017, pp. 292–305.
- [9] M. K. Ganai, "Dynamic Livelock Analysis of Multi-threaded Programs," in Runtime Verification, 2013, pp. 3–18.
- [10] Y. Cai and Q. Lu, "Dynamic Testing for Deadlocks via Constraints," IEEE Trans. Softw. Eng., vol. 42, no. 9, pp. 825–842, 2016.
- [11] E. Saillard, "Static / Dynamic Analyses for Validation and Improvements of Multi-Model HPC Applications . To cite this version: HAL Id: tel-01228072 DOCTEUR DE L ' UNIVERSITÉ DE BORDEAUX Analyse statique / dynamique pour la validation et l ' amélioration des applicat," University of Bordeaux, 2015.
- [12] H. Ma, L. Wang, and K. Krishnamoorthy, "Detecting Thread-Safety Violations in Hybrid OpenMP/MPI Programs," in 2015 IEEE International Conference on Cluster Computing, 2015, pp. 460–463.
- [13] Y. Huang, "An Analyzer for Message Passing Programs," Brigham Young University, 2016.
- [14] R. Surendran, "Debugging, Repair, and Synthesis of Task-Parallel Programs," RICE UNIVERSITY, 2017.
- [15] J. Zhou, S. Silvestro, H. Liu, Y. Cai, and T. Liu, "UNDEAD : Detecting and Preventing Deadlocks in Production Software," in Proceedings of the 32nd IEEE/ACM International Conference on Automated Software Engineering, 2017, pp. 729–740.
- [16] The Open MPI Organization, "Open MPI: Open Source High Performance Computing," 2018. [Online]. Available: <https://www.openmpi.org/>.
- [17] E. Saillard, P. Carribault, and D. Barthou, "PARCOACH: Combining static and dynamic validation of MPI collective communications," Int. J. High Perform. Comput. Appl., vol. 28, no. 4, pp. 425–434, 2014.
- [18] H. Ma, S. R. Diersen, L. Wang, C. Liao, D. Quinlan, and Z. Yang, "Symbolic Analysis of Concurrency Errors in OpenMP Programs," in 2013 42nd International Conference on Parallel Processing, 2013, pp. 510–516.
- [19] P. Chatarasi, J. Shirako, M. Kong, and V. Sarkar, "An Extended Polyhedral Model for SPMD Programs and Its Use in Static Data Race Detection," 2017, pp. 106–120.
- [20] R. Sharma, M. Bauer, and A. Aiken, "Verification of producer-consumer synchronization in GPU programs," ACM SIGPLAN Not., vol. 50, no. 6, pp. 88–98, 2015.
- [21] P. Collingbourne, C. Cadar, and P. H. J. Kelly, "Symbolic Testing of OpenCL Code," in Hardware and Software: Verification and Testing, 2012, pp. 203–218.
- [22] B. Klemme, "Software Testing of Parallel Programming Frameworks," University of New Mexico, 2016.
- [23] Allinea Software Ltd, "ALLINEA DDT," ARM HPC Tools, 2018. [Online]. Available: <https://www.arm.com/products/development-tools/hpc-tools/cross-platform/forge/ddt>.
- [24] R. W. S. Inc., "TotalView for HPC," 2018. [Online]. Available: <https://www.roguewave.com/products-services/totalview>.
- [25] Lawrence Livermore National Laboratory, University of Utah, and RWTH Aachen University, "ARCHER," GitHub, 2018. [Online]. Available: <https://github.com/PRUNERS/archer>.
- [26] G. Bronevetsky, I. Laguna, S. Bagchi, B. R. de Supinski, D. H. Ahn, and M. Schulz, "AutomaDeD: Automata-based debugging for dissimilar parallel tasks," in IFIP International Conference on Dependable Systems & Networks (DSN), 2010, pp. 231–240.
- [27] RWTH Aachen University, "MUST: MPI Runtime Error Detection Tool," 2018.
- [28] J. Yang, "A Validation Suite for High-Level Directive-Based Programming Model for Accelerators a Validation Suite for High-Level Directive-Based Programming Model for," University of Houston, 2015.
- [29] C. Wang, R. Xu, S. Chandrasekaran, B. Chapman, and O. Hernandez, "A validation testsuite for OpenACC 1.0," in Proceedings of the International Parallel and Distributed Processing Symposium, IPDPS, 2014, pp. 1407–1416.
- [30] K. Friedline, S. Chandrasekaran, M. G. Lopez, and O. Hernandez, "OpenACC 2.5 Validation Testsuite Targeting Multiple Architectures," 2017, pp. 557–575.
- [31] S. Chandrasekaran and G. Juckeland, OpenACC for Programmers: Concepts and Strategies, First edit. Addison-Wesley Professional, 2017.
- [32] R. Farber, Parallel Programming with OpenACC. 2016.
- [33] OpenACC Standards, "The OpenACC Application Programming Interface version 2.7," 2018.
- [34] M. McCorkle, "ORNL Launches Summit Supercomputer," The U.S. Department of Energy's Oak Ridge National Laboratory, 2018. [Online]. Available: <https://www.ornl.gov/news/ornl-launches-summit-supercomputer>.

Efficient Mining of Association Rules based on Clustering from Distributed Data

Marwa Bouraoui¹, Amel Grissa Touzi²

Signal, Image and Technology of Information Laboratory
National Engineering School of Tunis, Tunis El Manar University
Tunis, Tunisia

Abstract—Data analysis techniques need to be improved to allow the processing of data. One of the most commonly used techniques is the Association Rule Mining. These rules are used to detect facts that often occur together within a dataset. Unfortunately, existing methods generate a large number of association rules, without accentuation on the relevance and utility of these rules, and hence, complicating the results interpretation task. In this paper, we propose a new approach for mining association rules with an emphasis on easiness of assimilation and exploitation of the carried knowledge. Our approach addresses these shortcomings, while efficiently and intelligently minimizing the rules size. In fact, we propose to optimize the size of the extraction contexts taking advantages of the Clustering techniques. We then extract frequent itemsets and rules in the form of Meta-itemsets and Meta-rules, respectively. Experiments on benchmarking datasets show that our approach leads to a significant reduction of the number of generated rules thereby speeding up the execution time.

Keywords—Distributed data; association rules mining; clustering; meta-items; meta-rules

I. INTRODUCTION

Association rules mining has become one of the core data mining tasks with many real world applications such as selective marketing, fraud detection in web, economic census, and several other applications. It aims to discover associations among transactions encoded in a database. An association rule is a probabilistic rule which implies certain association relationship among a set of objects in the form of “if-then” statement. Association rules mining was introduced by Agrawal et al. [1] and they have described the formal model of this problem as follows. Let $I = \{i_1, i_2, \dots, i_n\}$ be a finite set of items. Let $D = \{T_1, T_2, \dots, T_n\}$ be a finite set of transactions, each transaction T_i consists of a set of items where $T_i \subset I$. Let X be a subset of I . An association rule is a conditional implication of the form $r: X \rightarrow Y$ between two itemsets $X, Y \subset I$ where $X \cap Y = \emptyset$. The basic algorithms for mining association rules are Apriori [2], FP-Growth [3].

Nowadays, most enterprises collect huge amounts of business data from daily transactions and store them in distributed datasets; especially, for security issues and communication overhead. Those distributed datasets are usually not allowed to be transmitted or joined together. Mining association rules from such data has attracted a lot of attention in recent data mining research. Several classes of parallel and distributed algorithms have been developed in this

context [4-11]. Most of them compete in domains like the result accuracy, the execution time, memory consumption, communication cost and so forth. Yet, little attention has been paid to the readability of the outputted results. Indeed, as the dataset size grows, mining association rules activity tends, potentially, to generate a prohibitively large number of rules. Unfortunately, a likewise output adds only inconvenience to data exploitation task from mined rules rely heavily on human interpretation in order to infer their semantic meanings.

To overcome these shortcomings, the solution we consider is to combine clustering and association rules mining technologies, to efficiently mine rules from large distributed data. Indeed, clustering technology helps, inherently, reducing the data context size, bringing into play its segmentation property. We propose a new approach, Clustering based Distributed Association Rules Mining Algorithm (C-DARM), which continues to extract rules from business data, but avoid rendering irrelevant and extensive number of results. More specifically, our aim is refining the output for a better understanding, and an uncomplicated interpretation of the carried knowledge. To do this task efficiently, we propose to introduce a pre-processing step based on clustering to optimize the size of the remote extraction contexts. The main idea is to mine distributed frequent itemsets from a representative set consisting of a collection of classes, called Meta-Itemsets, we then mine rules in the form of Meta Association Rules. In global, our solution provides:

- An efficient distributed process for mining rules from initially distributed data.
- A reduced number of rules when dealing with large datasets while ensuring no loss of information.
- A global view of the rules which boosts the result assimilation and interpretation.
- A pre-processing strategy to exclude not interesting attributes according to type of data and user requirements.

The rest of this paper is organized as follows: Section 2 provides an overview of the common distributed algorithms for mining association rules. Section 3 details our new proposed approach. Performance analysis and experimental results are shown in Section 4. We finally conclude our paper and present our ideas for future work.

II. LITERATURE REVIEW

Apriori is one of the most versatile and effective algorithm for frequent itemsets mining. Various improvements of this algorithm have been proposed to solve several issues such as minimizing database scanning, reducing transaction base size, proposing effective pruning techniques and efficient data structures. We suggest AprioriTid [11], DHP [12], Partition [13], Sampling [14] and DIC [15] for a further detailed explanation of the cited points.

An alternative algorithmic scheme works by mining closed frequent itemsets in the first step. A set is closed if it has no superset with the same frequency. The notion of closed itemsets is strongly connected to the Formal Concept Analysis (FCA) [16] field. The FCA offers a condensed and concise representation allowing the deduction of association rules bearing information [17]. The state-of-the-art algorithm for mining closed frequent itemsets is Close [18]. Others algorithms have been introduced which offer various improvements of this one. We can cite A-Close [19], Close + [20], Charm [21], Titanic [22, 23], and Closet [24].

Modern organizations are geographically distributed and, typically, each site locally stores its amount of data. Challenges are raised due to this data diffusion over nodes, and therefore, researches have been initiated in parallel and distributed algorithms in general, and in mining association rules, in particular. The suggested solutions take advantage of the improvement made on processor speed and network technologies.

The first proposed algorithms are CD (Count Distribution) [25] and DD (Data Distribution) [26] which are, basically, an Apriori parallelization. CD and DD are based on data parallelism and task parallelism, respectively.

In order to reduce the CD communication overhead, the NPA algorithm [27] is suggested. Unlike CD, the computing phase of global supports takes place on a master site, and eventually avoids a redundant and overload calculation. NPA minimizes then the communication cost, reducing it from the order of $O(|C_k| * n^2)$, for the CD algorithm, to the order of $O(|C_k| * n)$ for the NPA algorithm, where $|C_k|$ is the candidates sum of size k , and n is the number of sites.

Based on CD, FDM (Fast Distributed Mining) algorithm was proposed in [28]. It reduces the size of generated candidates, introducing new pruning techniques namely the local pruning and the global pruning.

Another Apriori-based algorithm was presented, the Optimized Distributed Association Rules Mining (ODAM) [6] that derives from FDM and CD as well. It essentially removes infrequent 1-itemsets, merges identical transactions into a single one, and then inserts new transactions into memory. It outperforms CD and FDM because of its downsizing property. Furthermore, it reduces the total message exchange count and the communication cost by forwarding support counts of candidate itemsets to a single site, called "receiver".

In [7] the Efficient Distributed Frequent Itemset Mining (EDFIM) algorithm is implemented which is an extension of the ODAM algorithm. It performs infrequent itemsets pruning

and duplicate transactions merging operations, after every pass. It reduces, therefore, the size of transactions and subsequently the scan iterations count. EDFIM uses local and global pruning actions, and a merger site to reduce the communication overhead.

Here [5], an Apriori-TID based algorithm was proposed for mining distributed association rules, the Distributed Parallel Apriori algorithm (DPA). DPA uses diverse rule interesting measures such that Pearson coefficient, Chi square, etc. It provides also a technique for a faster rate for mining frequent itemsets by handling their sparse matrix.

In [4], Lin and Chung introduced the FLR-mining algorithm. It iteratively estimates the workload based on the number of header items. It is qualified to terminate the number of the carried computing nodes automatically and achieving better load balancing as compared with existing methods.

In [8], the Parallel FP-Growth is implemented. It examines the challenges of the parallelization process and a method to balance the execution efficiently on shared-nothing architecture. In the first place, it evaluates the horizontal subset of data. Then, it parallel constructs local FP-Tree. Finally, mining procedure took place on this FP-Tree.

In [29], the LMatrix algorithm is presented. It minimizes the number of database scans by generating a matrix that models local transactions, from which it calculate the local supports at each iteration.

The IDD (Intelligent Data Distribution) algorithm [30] is an enhanced version of the DD algorithm. To improve performance, local transactions are connected by ring structure rather than all-to-all broadcast, which decrease the communication cost.

Backed by CD and IDD algorithms, HD (Hybrid Distribution) [31] is suggested as a combination of the two. The processors are divided into groups and CD is applied considering one group as one processor.

In [32], ParEclat, ParMaxEclat, ParClique, ParMaxClique are proposed which are parallel versions of Eclat, MaxEclat, Clique and MaxClique algorithms, respectively. Each algorithm consists of three phases; preparation, asynchronous processing, and reduction. Data partition and computation are executed in the preparation phase. Next, each processor generates local frequent itemsets asynchronously. In the final phase, ultimate results are combined together.

These briefly introduced algorithms can be further classified by the following attributes:

- Base Algorithms (Basic sequential algorithm)
- Parallelism (Data, Task, Hybrid)
- Load Balancing (Static, Dynamic, Hybrid)
- Database Layout (Horizontal, Vertical)
- Database Partition (Partitioned, Replicated, Shared)
- Memory System (Distributed, Shared, Hierarchical)

TABLE I. CLASSIFICATION OF PARALLEL AND DISTRIBUTED ALGORITHMS OF MINING ASSOCIATION RULES

Algorithm	Base Algorithm	Parallelism	Load Balancing	Database Layout	Database Partition	Memory System
CD, FDM, NPA	Apriori	Data	Static	Horizontal	Partitioned	Distributed
DD, IDD	Apriori	Task	Static	Horizontal	Partitioned	Distributed
HD	Apriori	Hybrid	Hybrid	Horizontal	Partitioned	Distributed
CD, IDD	Apriori	Data	Static	Horizontal	Partitioned	Distributed
ODAM, EDFIM, LMatrix	Apriori	Data	Static	Horizontal	Partitioned	Distributed
PCCD	Apriori	Task	Static	Horizontal	Partitioned	Shared
Parallel FP-Growth	FP-Growth	Task	Static	Horizontal	Partitioned	Hierarchical
ParEclat, ParMaxEclat, ParClique, ParMaxClique	Eclat, Clique	Task	Static	Vertical	Replicated	Hierarchical

We can summarize the above characteristics in the form of a Table I.

Recently, new approaches involved clustering methods in the association rules mining field. The objective of clustering is to split the heterogeneous set of objects into a number of homogeneous subsets having a similar behavior, called clusters. The similarity of objects is generally measured in terms of geometric distance between objects. The distance function differs depending on the nature of the data.

As clustering breaks up a dataset based on item similarities, it guarantee better semantic results when dealing with association rules. In [9], authors proposed to mine rules based on clustering and soft sets. The idea is to apply the CFSFDP clustering technique to classify the transactions. From the resulting clusters, supports are obtained by considering logical formulas over the soft sets. However, this algorithm mines rules considering items belonging to the same cluster, and consequently misses cross clusters rules. In [10], clustering technique was combined with association rule mining to speed up the extraction of conceptual association rules. Conceptual association rules imply the relationships between concepts generated using Formal Concept Analysis. Unfortunately, the construction of concepts is a too heavy task and it can't suit in memory when dealing with a large dataset.

Note that all these approaches that capitalize on clustering techniques to mine association rules 1) are applied in the sequential environments; 2) lead to an important loss of information; and 3) suffer from high computational cost when dealing with large datasets.

III. MOTIVATION

Nowadays, the volume of data generated in the web, transactional systems, and different other areas continue to increase explosively. Thence, a major problem of association rules discovery methods becomes the large number of results it tend to generate, even for a reasonable size of the extraction context. Above all, when the support threshold drops low, the number of resulted patterns goes up dramatically. Consequently:

- The number of generated rules is very large, so it is difficult to understand and interpret by the user.

- The management of structures for data modeling requires high execution time.
- Generated rules from data are usually redundant.
- The definition of data and data structures requires a large memory space because of the complex modeling algorithms such as trees or graphs.

It emerges from this ascertainment the importance of investigating efficient methods for distributed mining of association rules. In particular, it is crucial that outputted rules are understandable and useful to the user. When mining association rules from this sort of data, we may find thousands of rules. Moreover, the effectiveness degrades because it generates numerous redundant patterns. We may cite a trivial but illustrative example here, for a database having a transaction of length k , it will generate $2^k - 1$ frequent itemsets and even a large number of useless association rules.

In the other hand, clustering technology helps, inherently, reducing the data context size, bringing into play its segmentation property. This data input transformation discloses some interesting relationships between transactions and proposes a useful starting point for other purposes, such as pattern mining, in our case.

The solution we consider is to combine clustering and association rules mining technologies, to efficiently mine rules from large distributed databases. Our aim is to reduce the large number of association rules that are typically computed by existing algorithms, thereby rendering the emerging rules much easier to interpret and visualize.

Our approach takes place in three phases:

- *A data pre-processing phase based on clustering:* it consists on organizing data into groups (using a fuzzy clustering algorithm). Then, to generate, from these classes, a new, more condensed representation of the extraction context in the form of a Cluster-Fuzzy Formal Context. A cleaning step is thus necessary to optimize the size of the extraction contexts by filtering up the unnecessary data. The resultant classes (Meta-Itemset) are therefore used as starting points for the mining of distributed frequent itemsets.

To accomplish this phase, we propose two new concepts:

- 1) A new representation and definition of itemset: Meta-Itemset
- 2) A new representation and definition of the extraction context: Cluster-Fuzzy Formal Context

- *Distributed frequent itemsets mining phase:* it consists on mining frequent itemsets as a set of frequent Meta-Itemsets from the remote Cluster-Fuzzy Formal Contexts. This process is distributed and covers synchronization between local sites and a master site.
- *Generation of association rules phase:* it consists on mining association rules in the form of Meta-Association Rules by applying a rule generation algorithm on the obtained frequent Meta-Itemsets.

IV. NEW APPROACH

In this section, we detail our new approach for mining association rules from distributed data.

A. General Principle

Our contribution in mining association rules is to refine the results for a better understanding, and an uncomplicated interpretation of the carried knowledge, while efficiently and intelligently minimizing the rules size. To meet this challenge, we propose to combine clustering and association rules mining technologies. Thus, we introduce a pre-processing step based on clustering to optimize the size of the remote extraction contexts. The main idea is to mine distributed frequent itemsets from a representative set consisting of a collection of classes, called Meta-Itemsets. Hence, a clustering algorithm is applied to organize the data into classes. We generate, from these classes, a new representation more condensed of the extraction context in the form of a Cluster-Fuzzy Formal Context. A cleaning step is then carried out to remove the non-interesting Meta-Itemsets. From these new remote optimized contexts, we mine frequent Meta-Itemsets through a distributed process that deal with synchronization between remote sites and a receiver site. We finally generate a set of association rules in the form of Meta Association Rules. The number of these rules is much fewer than the number of rules generated by the classical association rules mining algorithms.

For a further explanation, we illustrate by the next figure (Fig. 1) the general process of our approach and with Fig. 2, the global one.

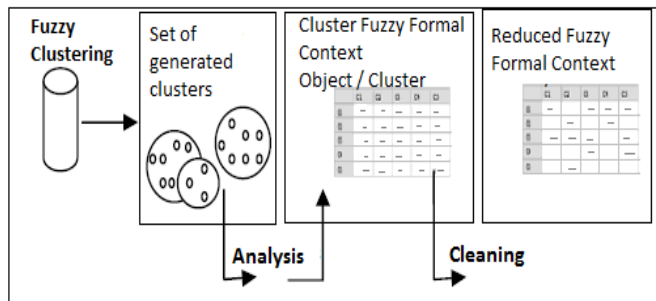


Fig. 1. Process in a Specific Site.

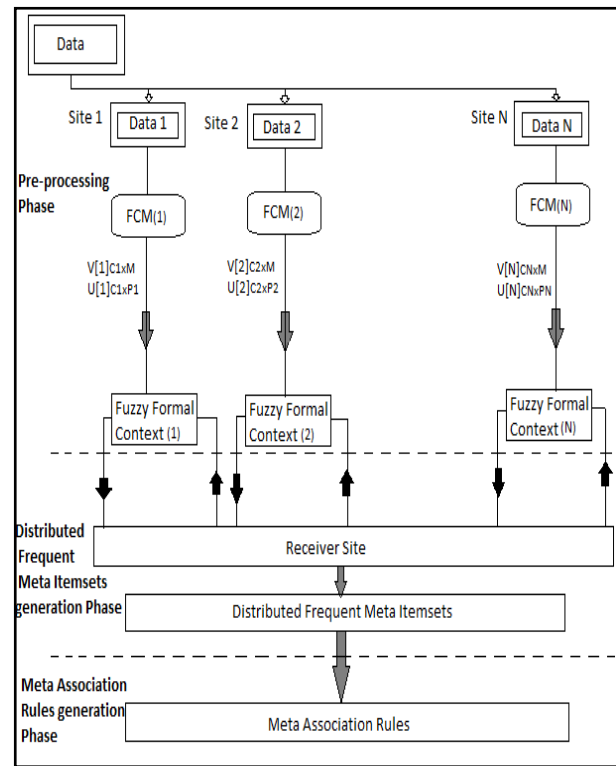


Fig. 2. Global Process.

We present in the following the general principle of our approach:

Input: N sites, $D[n]$ ($n = 1..N$) a set of distributed data through N sites, s local minSupp , S global minSupp , C number of clusters, α accuracy

Step 1: Iterative Pre-processing Phase based on Clustering

For each site ($i = 1, i \leq N, i++$)

Apply a fuzzy clustering algorithm to organize the data into different groups (or clusters). The output is a membership matrix mapping objects to clusters.

Construct the Cluster-Fuzzy Formal Context (Object / Cluster) from the obtained matrix.

Reduce the Cluster-Fuzzy Formal Context according to the accuracy parameter (a cleaning step).

End For

Step 2: Distributed Frequent Meta Itemsets Mining Phase

On the obtained Cluster-Fuzzy Formal Contexts, apply a distributed process to generate the distributed frequent Meta Itemsets.

Step 3: Meta Association Rules Generation Phase

Generate association rules in the form of rules between clusters, called Meta-Rules.

Output: A set of Meta-Association Rules

B. Process of Mining Association Rules

Our process takes place in three main phases, namely the iterative pre-processing phase based on clustering, mining distributed frequent Meta-Itemsets phase and the generation of the Meta Association Rules phase. In the following, we detail these phases.

1) *Iterative pre-processing phase based on clustering:* This phase depicts the clustering-based pre-processing process. Through this phase, we aim to optimize the size of itemsets as well as the extraction contexts, which are used later as starting points for mining distributed frequent itemsets. This process is iterative and runs through all sites.

To express our process, we assume that the data D is horizontally distributed through N sites. Each site $D[n]$ ($n = 1 \dots N$) is composed by P_n objects, where each one is described by a vector $dn[j]$ ($j = 1 \dots P_n$). On each site, we apply locally a fuzzy clustering algorithm such as the FCM algorithm [25]. We get C_n fuzzy clusters where $C_n[i]$ ($i = 1 \dots C_n$) is the i th cluster in the n th site. Each cluster is therefore characterized by its center $V_i[n] \in RM$, that we call a prototype. Each object $dn[j] \in D[n]$ ($n = 1 \dots N$) is characterized by a membership degree to each cluster. For each site $D[n]$, $U[n] = [\mu_{ij}[n]] C_n \times P_n$ is the fuzzy partition, where C_n is the number of clusters, P_n is the number of objects belonging to this site, and μ_{ij} is the membership degree of the i th object to the j th cluster. In order to enlighten these step proceedings, we define, next, two new concepts:

Definition: Meta-Itemset

A Meta-Item is a resulting class of the clustering process on the database. A Meta-Item is represented by its center. A Meta-Itemsets is a set of Meta-Items. A k -Meta-Itemset is a Meta-Itemset that is formed by k Meta-Items.

Definition: Cluster-Fuzzy Formal Context

In Cluster-Fuzzy Formal Context for the site $D[n]$ ($n=1..N$), we link the objects to the clusters by the means of a relation that models the belonging relationship. The Cluster-Fuzzy Formal Context in the site $D[n]$ ($n=1..N$) represents a triple $(X[n], V[n], I[n])$ where $X[n] = \{dj : j = 1.. P_n\} \in RM$ represents the set of objects, $V[n]= \{cj : j = 1..C_n\} \in RM$ represents the centers of the clusters, and $I[n]$ represents the membership degree of $X[n]$ to $V[n]$.

The figure below (Fig. 3) is an illustration of the pre-processing phase:

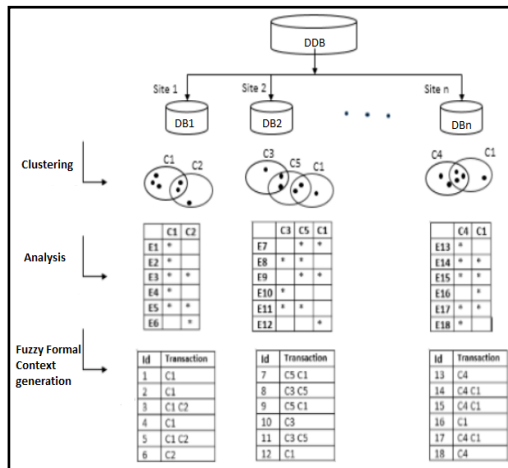


Fig. 3. Pre-Processing Phase.

Example:

Through this example, we explain the pre-processing step which takes place in a specific site. Let $E1, E2, E3, E4, E5, E6, E7, E8$ be a set of student markets in the following modules: Database (DB), Object Oriented Programming (OOP), Operating System (OS), Artificial Intelligence (AI) and Signal Processing (SP), as shown in the Table II.

We apply a fuzzy classification algorithm (FCM) on these data and obtain the membership matrix, mapping objects to clusters (Table III).

At this stage, we perform the polish step on the obtained matrix. We then apply a filtering step to exclude non-interesting entries to optimize the size of the final extraction context. We introduce a parameter of precision α , establishing an edge, below which, the belonging of an object to a class is considered insignificant. The choice of then α parameter depends on the nature of the data and the user requirements. In our example we fixed $\alpha = 0.3$ (Table IV).

TABLE II. SAMPLE OF STUDENTS MARKETS

	BD	OOP	OS	AI	SP
E1	13	14	8	9	9
E2	15	12	1	11	6
E3	6	9	13	11	7
E4	10	6	17	14	13
E5	11	12	9	9	9
E6	16	5	13	14	13
E7	8	9	11	10	9

TABLE III. CLUSTERING RESULTS

	C1	C2	C3
E1	0.095	0.710	0.210
E2	0.049	0.800	0.061
E3	0.072	0.100	0.830
E4	0.836	0.072	0.110
E5	0.091	0.550	0.370
E6	0.820	0.110	0.083
E7	0.037	0.067	0.899

TABLE IV. NEW CONTEXT

	C1	C2	C3
E1	-	0.710	-
E2	-	0.800	-
E3	-	-	0.830
E4	0.836	-	-
E5	-	0.550	0.370
E6	0.820	-	-
E7	-	-	0.899

2) *Distributed frequent meta-itemsets mining phase:* This phase consists of mining distributed frequent Meta-Itemsets from the obtained Cluster-Fuzzy Formal Contexts. This process is a distributed that deal with synchronization between remotes sites and a receiver site. At each iteration, we calculate the local supports of candidates and, hence, select the locally frequent ones. Then, sites forward locally frequent Meta-Itemsets, along to the receiving site, for further processing. In the master site, the calculation of the Global Supports task is executed, and subsequently the deduction of globally frequent k-Meta-Itemsets. From these selected sets, we generate the candidate k+1-Meta-Itemsets, travelling back to local sites as an input for the next iteration. This process repeats until no other candidate can be generated and, subsequently, generate the ultimate global frequent Meta-Itemsets. Intervening a master site reduces the communication cost from the order of $O(|C_k| * n^2)$ to the order of $O(|C_k| * N)$ where $|C_k|$ is the candidate size and n is the site number. For clarity, used notations are listed in Table V.

Definition: Locally and Globally frequent Meta-Itemset

A Meta-Itemset I is called locally frequent if $s \geq \text{minSupp}$. A Meta-Itemset I is called globally frequent if $S \geq \text{minSupp} * T$ (T is the number of transactions).

Process is described below:

Input: N sites, N Cluster-Fuzzy Formal Contexts, s local minSupp, S global minSupp.
 $k = 1$
 Repeat
 For each site ($i = 1, i \leq N, i++$)
Local Sites:
 Calculate the local supports $Li(k)$ of the k-Meta-Items.
 Remove the infrequent ones and then get the locally frequent k-Meta-Itemsets $LLi(k)$.
 Diffuse locally frequent Meta-Itemsets $LLi(k)$ to the receiver site, along with supports of both frequent and infrequent k-Meta-Itemset.
 End For
Receiver site:
 Receive locally frequent k-Meta-Itemsets, calculate the supports sum of homologous, and thus deduce the global support $G(k)$ of the k-Meta-Itemsets.
 Remove the infrequent ones and then get the globally frequent k-Meta-Itemsets $GLL(k)$.
 Generate the candidate set $GA(k+1)$ from $GLL(k)$.
 Disseminate the remaining candidates to local sites.
 $k + 1$
 Until to find all frequent Meta-Itemsets.
Output: Set of frequent Meta-Itemsets

3) *Meta association rules mining phase:* This phase consists in applying an algorithm for generating association rules from the frequent Meta-Itemsets resulting from the previous steps. The output is a set of association rules in the form of Meta Association Rules.

TABLE V. NEW CONTEXT

Notation	Meaning
N	Number of sites
minSupp	Support threshold
s	Local minSupp
S	Global minSupp
Li(k)	Local supports of the k-Meta-Itemsets in site i
LLi(k)	Locally frequent k-Meta-Itemsets in site i
G(k)	Global supports of the k-Meta-Itemsets
GLL(k)	Globally frequent k-Meta-Itemsets
GA(k)	Candidate set generated from GLL(k-1)

Lemma

The Meta Association Rules obtained by running our distributed process on the distributed data obtained from Phase 1, are the same as if the process is applied centrally on each site. This validates the accuracy and compliance of the generated rules.

Theorem 1

Let $C_i [1], C_j [2]$ be two clusters generated by a fuzzy clustering algorithm in the $D [i]$ and $D [j]$ sites, respectively. The meta-rule $C_i [1] \Rightarrow C_j [2]$ with a coefficient (EF) is denoted by $C_i [1] \Rightarrow C_j [2] (EF)$ where $EF = \text{Sum}([\mu_{ij} [n]] C_n \times P_n) ; \mu_{ij} [n] \in [0, 1]; \forall i \in \{1..P_n\}; \forall j \in \{1,2\} \forall n \in \{1..N\}$.

The value EF is in the range] 0...1]. It is called the Exactitude Factor of this meta-rule. This value indicates the importance degree of this Meta-Rule. If the coefficient EF is equal to 1 then the rule is called exact rule. Then the following properties are equivalent:

$$C_i [1] \in C_j [2] (EF) \Leftrightarrow$$

$$\forall \text{Objets } Ob1 \in C_i [1] \Rightarrow Ob1 \in C_j [2] (EF)$$

$$\forall \text{Objets } Ob1 \in C_i [1], Ob1 \text{ verifies the property } p1 \text{ of } C_i [1] \text{ and the property } p2 \text{ of } C_j [2]. (EF)$$

Theorem 2

Let $C_n [1], C_n [2], C_n [3]$ be three clusters generated by a fuzzy clustering algorithm in the $D [i], D [j]$ and $D [k]$ sites, respectively. The meta-rule $C_i [1], C_j [2] \square C_k [3]$ with a coefficient (EF) is denoted by $C_i [1], C_j [2] \square C_k [3] (EF)$ where $EF = \text{Sum}([\mu_{ij} [n]] C_n \times P_n) ; \mu_{ij} [n] \in [0, 1]; \forall i \in \{1..P_n\}; \forall j \in \{1,2,3\} \forall n \in \{1..N\}$.

The value EF is in the range]0...1]. It is called the Exactitude Factor of this meta-rule. This value indicates the importance degree of this Meta-Rule. If the coefficient EF is equal to 1 then the rule is called exact rule. Then the following properties are equivalent:

$C_i[1], C_j[2] \in C_k[3] \text{ (EF)} \Leftrightarrow$

$\forall \text{ Object Ob1} \in C_i[1] \cap C_j[2] \Rightarrow \text{objects Ob1} \in C_k[3] \text{ (EF)}$

$\forall \text{ Object Ob1} \in C_i[1] \cap C_j[2] \text{ Ob1 verifies the property p1, p2 et p3. (EF)}$

V. VALIDATION AND EXPERIMENTAL RESULTS

An in-depth performance study has been performed to compare our method to classical ones. First of all, note that our approach presents these two essential assets:

- The introduction of Meta Association Rules concept: This concept injects a layer of abstraction, which is very crucial and fundamental when we are dealing with a huge size of data. It allows having a more global view on the voluminous dataset. Besides, we define association rules between classes, thus, enabling automatic generation of association rules between data.
- The extensibility and versatility of the procedure: In our approach, the association rules mining step can be performed with any KDD algorithm. In the literature, studies have shown that one KDD algorithm could be more effective than another depending on the used data's domain. Thus, we have the luxury of choosing the most optimal method according to the domain of the used dataset. Even better, the clustering step in our process can be fulfilled with any fuzzy clustering algorithm, in order to classify the starting data.

In the following we discuss our experimental results:

Both the Java platform and the R platform are exploited in order to accomplish the implementation phase. The final program is, for the most part, in Java language, while some specific functionalities were dispatched for the R environment in sake of efficiency. In fact, R, by default, comes with a lot of commands carried out for data mining analysis. To interface between the two platforms, we integrated the rJava library which enables embedding basic R code snippets in Java code. Java is an object-oriented programming language that allows having a well-structured, modular and much more maintainable application. In addition, Java is designed to make easy distributed computing with intrinsically embedded network functionality. However it is not much efficient when it comes to statistical or mathematical modelling. In the other hand, R is a programming language that process and organize datasets in order to apply complex statistical tests. It propounds to organize and process large volumes of data quickly and flexibly. R is a programming language, but its use is strongly oriented towards the analysis of data and statistics. It provides a wide variety of modern and classical statistics (linear and nonlinear modeling, classical statistical tests, classification, clustering). Therefore, we adopted a combination of the two technologies.

In order to assess effectiveness of the proposed approach, we operate thorough tests on three real-life datasets. The first

one is the Mushrooms dataset and it illustrates a set of dense data that depict fungi characteristics (surface, odor, color, edible or poisonous). The second one is the C20d10K dataset, which is a sample of the PUMS90KS file (Public Use Microdata Samples). It contains Census Kansas data carried out in 1990. The 10,000 lines of data (corresponding to the first 10,000 people listed) were selected to include only the first 20 attributes. The third one is the T10I4D100K dataset and it characterizes synthetic data from the marketing basket, generated artificially by the IBM generator.

The following table (Table VI) summarizes the properties of the datasets:

A basic and simple distribution method was to randomly split up horizontally each dataset into two sites. Next, we fixed the minSupport to 30% for Mushrooms, 20% for C20d10K and 0.02% for T10I4D100K. Therewith, The MinConf was varied between 80%, 40%, and 10% for each dataset. Next parameter to fix concerns the cleaning step; we settled the accuracy to 0.1 ($\alpha=0.1$) for Mushrooms and T10I4D100K, and 0.03 for C20d10K. To tune the fuzzy clustering step, we fixed the fuzzy degree to 2 ($m = 2$), and we varied the cluster number between 5, 10, 15 and 20. Note that the mushrooms dataset is non-binary and non-digital, thus, we have run an extra pre-processing step to rewrite its data in digital format.

TABLE VI. THE CHARACTERISTICS OF THE TEST DATASETS

	Number of objects	Average size of objects	Number of items
Mushrooms	8 415	23	128
C20d10K	10 000	20	386
T10I4D100K	100 000	10	1 000

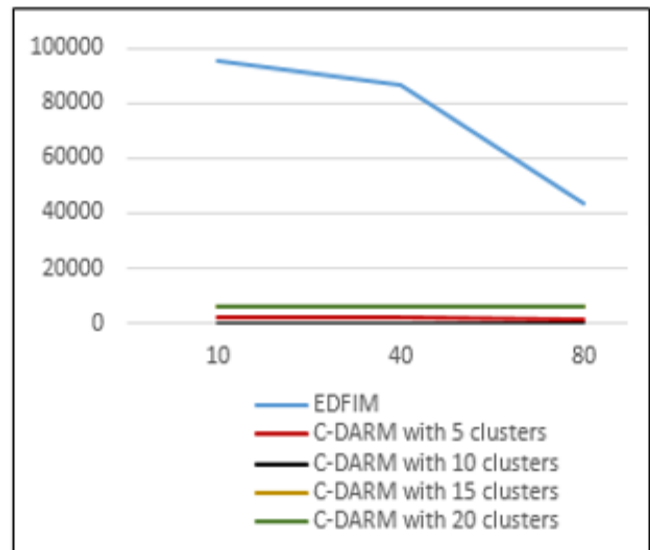


Fig. 4. Number of Generated Rules with Mushrooms.

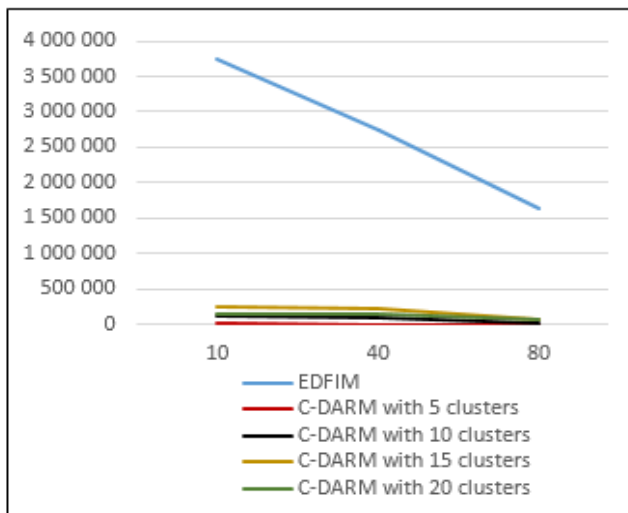


Fig. 5. Number of Generated Rules with C20d10K.

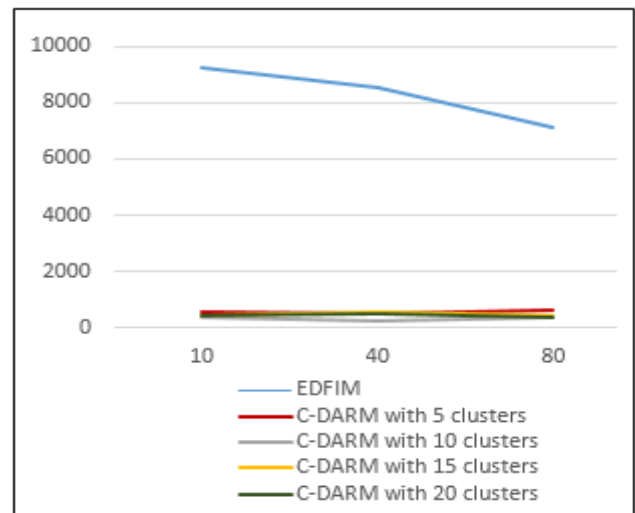


Fig. 7. Execution Time with Mushrooms.

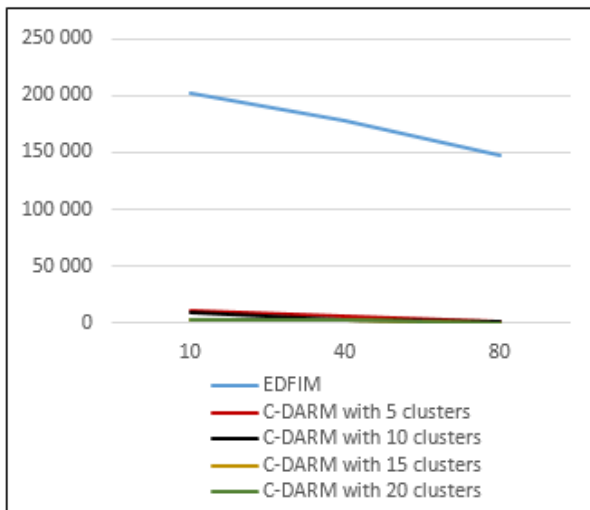


Fig. 6. Number of Generated Rules with T10I4D100K.

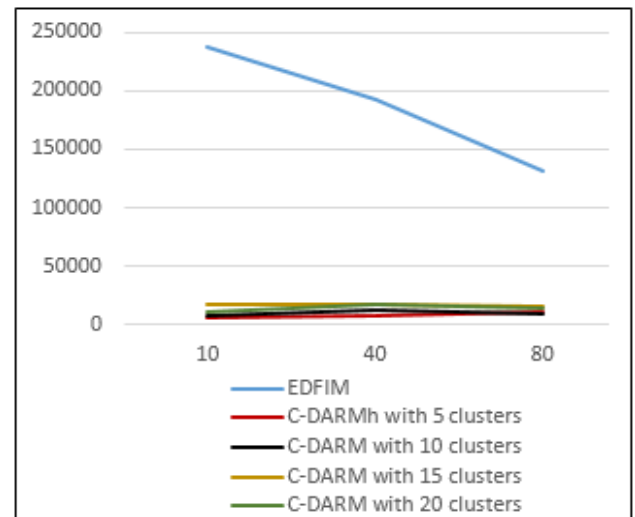


Fig. 8. Execution Time with C20d10K.

We summarize below (Fig. 4-6) our experimental results with emphasis on the number of generated rules, properties of each dataset. It confirms that the clustering phase led to a significant decrease of this number. This reduction is due to the fact that association rules are mined from classes, in contrast to the classical mining process which produces rules from raw data that is very large. Indeed, the number of clusters generated by clustering algorithm is always lower than the number of starting objects on which the clustering algorithm is applied.

Likewise, we notice a significant decrease on the execution time of our process, compared to traditional methods. This reduction could be discerned from the reduced number of generated rules. The main reasons for this are the size optimization of the the itemsets (Meta-Itemsets), as well as of the extraction contexts (Cluster-Fuzzy Formal Contexts). Moreover, such gain leads to an important decrease of the time necessary to scan the input at every pass. We summarize below (Fig. 7-9) our experimental results with emphasis on the execution time, properties of each dataset.

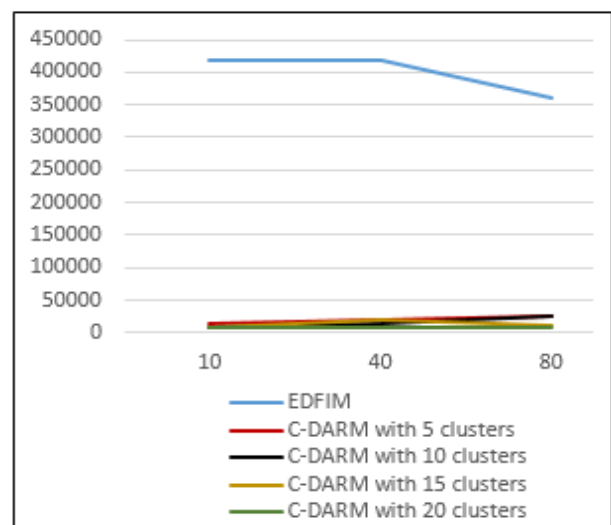


Fig. 9. Execution Time with T10I4D100K.

VI. CONCLUSION

In this paper, we have investigated embedding clustering technology in the association rules mining for the sake of readability and exploitation. The main idea is to mine distributed frequent itemsets from a representative set consisting of a collection of classes, called Meta-Itemsets. We generate from these classes a new representation more condensed and optimized of the extraction context in the form of a Cluster-Fuzzy Formal Context. From these new contexts, we mine distributed frequent Meta-Itemsets through a distributed process. We finally generate rules in the form of Meta-Rules. The number of these Meta-Rules is much fewer than the number of rules generated by the classical association rules mining algorithms. Indeed, the number of clusters generated by a clustering algorithm is always fewer than the number of starting objects on which the clustering algorithm is applied. As summary, our approach presents an essential asset which is the introduction of Meta Association Rules concept. It injects a layer of abstraction and more global view, which is very crucial and fundamental when we are dealing with a huge size of data.

As a perspective, we propose to intervene the Big Data technologies, like MapReduce, which prove their effectiveness for distributed data mining approaches.

REFERENCES

- [1] R. Agrawal, T. Imielinski, and R. Swami, "Database mining: A performance perspective", IEEE Transaction on Knowledge and Data Engineering, 1993.
- [2] R. Agrawal, R. Skirant, "Fast algorithms for mining association rules", Proc. 20th International Conference on Very Large Databases, pp. 478-499, 1994.
- [3] J. Han, J. Pei, and Y. Yin, "Mining Frequent Patterns without Candidate Generation", Proc. ACM International Conference on Management of Data, vol. 29, no. 2, pp. 1-12, 2000.
- [4] K. Lin, & S.-H. Chung, "A fast and resource efficient mining algorithm for discovering frequent patterns in distributed computing environments", Future Generation Computer Systems, vol. 52, pp. 49-58, 2015.
- [5] P. Asha, & S. Srinivasan, "Distributed Association Rule Mining with Load Balancing in Grid", Journal of Computational and Theoretical Nanoscience, vol. 13(1), pp. 33-42, 2016.
- [6] M. Z. Ashrafi, D. Taniar, K. Smith. "An Optimized Distributed Association Rule Mining Algorithm", IEEE Computer Society, Distributed Systems, vol. 5, No. 3, pp. 1541-4922, 2004.
- [7] A. Adelpoor, M. SanieeAbadeh, "An Efficient Frequent ItemSets Mining Algorithm for Distributed Databases", International Journal of Computer Science and Electronics Engineering, Volume 1, Issue 1, ISSN 2320-4028, 2013.
- [8] I. Pramudiono, and M. Kitsuregawa, "Parallel FP-growth on PC cluster", Proc. Advances in Knowledge Discovery and Data Mining, Springer Berlin Heidelberg, pp. 467-473, 2003.
- [9] Li, B., Pei, Z., & Qin, K, "Association Rules Mining Based on Clustering Analysis and Soft Sets", In International Conference on Computer and Information Technology, pp. 675-680, 2015.
- [10] T. T. Quan, L. N. Ngo, & S. C. Hui, "An effective clustering-based approach for conceptual association rules mining", Proc. International Conference on Computing and Communication Technologies, pp. 1-7, 2009.
- [11] R. Agrawal and R. Srikant. "Fast algorithms for mining association rules in large databases." In Proc. Of the 20th Int. Conf. On Very Data Bases (VLDB'94), pages 478-499, September 1994.
- [12] J. S. Park, M.-S. Chen, and P. S. Yu. "An effective hash based algorithm for mining association rules." In Proc. Of the 1995 ACM SIGMOD Int. Conf. (SIGMOD'95), pages 175-186, May 1995.
- [13] A. Savasere, E. Omiecinski, and S. Navathe. "An effective algorithm for mining association rules in large databases." In Proc. Of the 21st VLDB Int. Conf. (VLDB'95), pages 432-444, September 1995.
- [14] H. Toivonen. "Sampling large databases for association rules." In Proc. Of the 22nd VLDB Int. Conf. (VLDB'96), pages 134-145, September 1996.
- [15] S. Brin, R. Motwani, J. D. Ullman, and S. Tsur. "Dynamic itemset counting and implication rules for market basket data." In Proc. Of the 1997 ACM SIGMOD Int. Conf. (SIGMOD'97), pages 255-264, May 1997.
- [16] R. Wille « Restructuring lattice theory: an approach based on hierarchies of concepts ». Ordered sets, pp. 445-470, 1982.
- [17] L. Lakhal, G. Stumme «Efficient Mining of Association Rules Based on Formal Concept Analysis Formal Concept Analysis: Foundations and Applications, pp.180-195, 2005.
- [18] N. Pasquier, « Extraction de Bases pour les Règles d'Association à partir des Itemsets Fermés Fréquents ». Inforsid'2000 Congress, 2000.
- [19] N. Pasquier, « Data mining : algorithmes d'extraction et de réduction des règles d'association dans les bases de données ». Thèse de doctorat, Université de Clermont-Ferrand II, Janvier 2000.
- [20] N. Pasquier, Bastide, Y., R. Taouil, & Lakhal, L. (1999). Discovering frequent itemsets for association rules. Proceeding of the 7th biennial international conference in database theory ('ICDT 1999).
- [21] M. J. Zaki, C. J. Hsiao, « CHARM: An Efficient Algorithm for Closed Itemset Mining », Proceedings of the 2nd SIAM International Conference on Data Mining, Arlington, pp. 34- 43, Avril 2002.
- [22] G. Stumme, R. Taouil, Y. Bastide, N. Pasquier, L. Lakhal, « Fast Computation of Concept Lattices Using Data Mining Techniques », M. Bouzeghoub, M. Klusch, W. Nutt, U. Sattler, Eds., Proceedings of 7th Intl. Workshop on Knowledge Representation Meets Databases (KRDB'00), Berlin, Germany, pp. 129-139, 2000.
- [23] G. Stumme, R. Taouil, Y. Bastide, N. Pasquier, L. Lakhal, « Computing Iceberg Concept Lattices with TITANIC », J. on Knowledge and Data Engineering (KDE), vol. 2, no 42, pp. 189-222, 2002.
- [24] J. Pei, J. Han, R. Mao, S. Nishio, S. Tang, D. Yang, « CLOSET : An efficient algorithm for mining frequent closed itemsets », Proceedings of the ACM SIGMOD DMKD'00, Dallas, TX, pp. 21-30, 2002.
- [25] Agrawal (R.), Shafer (J. C.), "Parallel Mining of Association Rules". IEEE Transactions on Knowledge and Data Engineering, Vol. 8, No. 6, pp. 962-969, December 1996.
- [26] M.J. Zaki. Parallel and Distributed Association Mining: A survey. In IEEE Concurrency, special issue on Parallel Mechanisms for Data Mining, Volume 7, N°4, pages 14-25, December 1999.
- [27] Shintani (T.), Kitsuregawa (M.), "Hash Based Parallel Algorithms for Mining Association Rules". Proc. 4th Int. Conf. Parallel and Distributed Information Systems, IEEE Computer Soc. Press, Los Alamitos, Calif., 1996, pp. 19-30.
- [28] Cheung (D. W.), Han (J.), Vincent (Ng.), Fu (A. W.), Fu (Y.). "A Fast Distributed Algorithm for Mining Association Rules". Proceedings of PDIS, 1996.
- [29] J. ArokiaRenjit, K.L. Shunmuganathan, "Mining the data from distributed database using an improved mining algorithm", (IJCSIS) International Journal of Computer Science and Information Security, Vol. 7, No. 3, March 2010, USA.
- [30] M.J. Zaki. Parallel and Distributed Association Mining: A survey. In IEEE Concurrency, special issue on Parallel Mechanisms for Data Mining, Volume 7, N°4, pages 14-25, December 1999.
- [31] Han E. H., Karypis G., and Kumar V., Scalable Parallel Data Mining for Association Rules, in Proceedings of ACM Conf. on Management of Data, ACM Press, New York, pp. 277-288, 1997.
- [32] Zaki M. J., Parthasarathy S., Ogihara M., and Li W., Parallel algorithms for discovery of association rules, Data mining and knowledge discovery, vol. 1, no. 4, pp. 343-373, 1997c.

Academic Emotions affected by Robot Eye Color: An Investigation of Manipulability and Individual-Adaptability

Kento Koike¹, Yuya Tsuji², Takahito Tomoto³, Daisuke Katagami⁴, Takenori Obo⁵, Yuta Ogai⁶, Junji Sone⁷
Yoshihisa Udagawa⁸

Graduate School of Engineering, Tokyo Polytechnic University, Kanagawa, Japan¹
Faculty of Engineering, Tokyo Polytechnic University, Kanagawa, Japan^{2, 3, 4, 5, 6, 7, 8}

Abstract—We investigate whether academic emotions are affected by the color of a robot’s eyes in lecture behaviors. In conventional human-robot interaction research on robot lecturers, the emphasis has been on robots assisting or replacing human lecturers. We expanded these ideas and examined whether robots could lecture using one’s behaviors that are impossible for humans. Psychological research has shown that color affects emotions. Because emotion is strongly related to learning, and a framework of emotion control is required. Thus, we considered whether emotions related to the learner’s academic work, called “academic emotions,” can be controlled by the color of a robot’s illuminated eye light. In this paper, we found that the robot’s eye light color affects academic emotions and that the effect can be manipulated and adapted to individuals. Furthermore, the manipulability of academic emotions by color was confirmed in a situation mimicking a real lecture.

Keywords—Robot lecturer; academic emotions; lecture behavior; human-robot interaction

I. INTRODUCTION

As science and technology have developed, there have been attempts to replace human educators and lecturers with robots. Kamide et al. [1] reported the behaviors which emphasize key points in the screen and keep the attention of audiences are important as nonverbal behaviors when a humanoid robot gives a presentation. In addition, Ishino et al. [2] suggested that robots that can control own nonverbal behavior can emphasize the area that the learner wants to focus on with gaze, gestures, and paralinguistic, and this behavior can promote the learner’s interest. However, to date there has been no attempt to use the unique nonverbal behavior of robots in lectures.

Colors affect people psychologically (e.g., [3], [4]); people experience different emotions in response to different colors. During teaching, the expression of a human teacher changes naturally; however, robot lecturers can use unique behaviors, such as changing their eye color. What emotions would be evoked in learners if the teacher’s eyes were to turn red? Investigating what kind of emotions this type of behavior evokes may be expected to lead to a wide range of applications in robot-led education.

The importance of responding appropriately to the learner’s mental state has been highlighted in a study [5]. Thus, during

learning, it is necessary to consider not only the material but also the emotion presented to the learner. For example, during classroom teaching, whether the teacher is smiling, angry, or sad can have a strong effect on the emotion evoked in the learner. The learner feels stressed when confronted with an angry teacher and relaxed when learning from a smiling teacher. Emotions that are related directly to learning, teaching, and academic achievement are called “academic emotions” by Pekrun et al. [6]. Therefore, we considered that it is important to investigate how to improve learners’ academic emotions using external factors.

In this paper, to investigate the academic emotions evoked by the color of a robot’s eye lights, the following hypotheses were examined: (A) the learners’ academic emotions can be manipulated; (B) adaptive academic emotions can be produced in learners; and (C) academic emotions can be manipulated by colors in a situation like a real lecture. In the future, not only robot instructors will replace lecturers, but it is also possible to add ideal robot students (i.e., who behave to promote classes, such as asking an ideal question) to the classroom. Therefore, the roles of robots were divided into lecturer robots and learner robots, and the effects of color were investigated. The verification of hypotheses (A), (B), and (C) are described in Sections III, IV, and V, respectively.

II. RELATED WORK

A. Robot in Education

In recent years, robots have gained considerable attention in educational applications. Deublein et al. [7] suggested that robots’ motivational behavior can improve learning outcomes in an educational context. Ishino et al. [2] suggested that the robot can promote the learner’s interest by controlling nonverbal behavior in a presentation lecture.

Jimenez et al. [8] suggested that expressing the robot’s emotions promotes collaborative learning with the learners. In addition, Jimenez et al. [9] examined how robots emotional interact with learners in collaborative learning. Thus, we also know that emotion occurs within human-robot interaction in education. However, the emotions given to learners are not clarified.

B. Intelligent Tutoring System

In recent years, research on Intelligent Tutoring System (ITS) has been increasing in attempts to support not only learner's knowledge state but also mental state. For example, the Intelligent Mentoring System [10], [11] in ITS is an attempt to support knowledge and mental states by acquiring information with different granularity such as answer history and mouse movement from learners. AutoTutor [12] has shown one of the more practical ways ITS can read learners' emotions. However, these studies have been conducted to read the learner's emotions, and not to control the learner's emotions from the ITS output.

III. EXPERIMENT I

A. Summary

We examined the effect of the color function of Pepper (Softbank Robotics) on the academic emotions of learners' learning activities. Participants were 10 graduate and undergraduate students.

B. Purpose

In this experiment we investigated the following hypotheses. (A-1) The academic emotions of the learner are affected by presenting color information as part of the lecture behavior of the robot and (A-2) the students' academic emotions are manipulated by presenting color information.

C. Stimulus

We prepared four utterance patterns as Pepper's lecture behavior. There were two utterance patterns each for the roles of lecturer and learner.

- Important: "The point I will explain now is important." (as Lecturer).
- Warning: "Please stop talking, that is not related to class." (as Lecturer).
- Confused: "I had some difficulties, I do not understand." (as Learner).
- Understanding: "I see, right." (as Learner)

The color representation in this study changed only the LED color in Pepper's eyes, and the color of the other parts of the robot and its posture were unchanged. Because only color representation was used, gestures were not performed. Emotions evoked by color are interpreted subjectively; thus, the following correspondence between the colors and emotions was shown to limit interpretation (Fig. 1).

- Red: Anger or strong feeling.
- Green: Joy or mild feeling.
- White: Apathy.

The 12 combinations of the four utterance patterns and three colors were used as stimuli.

D. Questionnaire

In psychology, emotions that are related to learning, teaching, and academic achievement are called academic

emotions. These emotions are enjoyment, boredom, anger, hope, anxiety, hopelessness, pride, and relief [6], [13]. We prepared seven-point Likert scale questionnaires using these academic emotions as evaluation items.

E. Procedure

In the experiment, all utterance patterns for Pepper were given in order of white, red, and green.

Each utterance pattern was evaluated by a questionnaire with the question "How do you feel when you take a lecture with this robot?"

The procedure is as follows (Fig. 2).

- 1) Participants sit in front of Pepper.
- 2) Participants evaluate Pepper's lecture behavior.
 - a) Pepper says an [Important] utterance while illuminating its eyes (white).
 - b) Participants evaluate the lecture behavior in context with a questionnaire.
 - c) Repeat a) and b) while changing the utterance patterns in [Warning, Confused, and Understanding].
 - d) When all of the utterance patterns have been evaluated, change color in () and repeat a) to c).



Fig. 1. Pepper's different Eye Colors (From Left, White, Red, and Green).

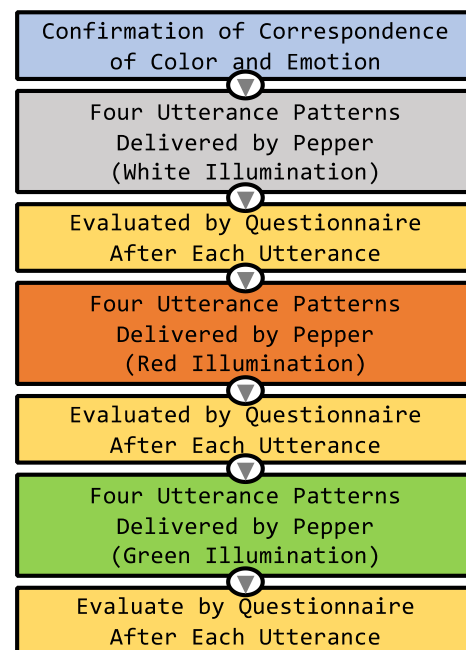


Fig. 2. Procedure for Experiment I.

F. Results

The results are shown in Fig. 3 to 6. The results were subjected to multiple comparisons using Ryan’s method after confirming a significant difference ($p < 0.05$) by Friedman’s test. The significance symbols in the figures indicate the significant difference ($p < 0.05$) calculated by Ryan’s method and the error bars indicate standard errors.

Fig. 3 shows the results for the Important utterance pattern. There were significant differences between white and red and between white and green in boredom, pride, hope, and relief. White enhanced boredom and suppressed pride, enjoyment, hope, and relief. Conversely, red and green suppressed boredom and enhanced pride, enjoyment, hope, and relief. There was also a significant difference in enjoyment between white and green suggesting that white suppressed and green enhanced enjoyment.

Fig. 4 shows the results of the Warning utterance pattern. There was a significant difference between white and red in hope. White suppressed and red enhanced hope. There were many differences in the values themselves, but no other significant differences were found, probably because the Warning context itself depended on the individual learner.

Fig. 5 shows the results for the Confused utterance pattern. There was a significant difference between white and red in hope and relief. White suppressed and red enhanced hope and relief. There was also a significant difference between white and green in enjoyment. White suppressed and green enhanced enjoyment.

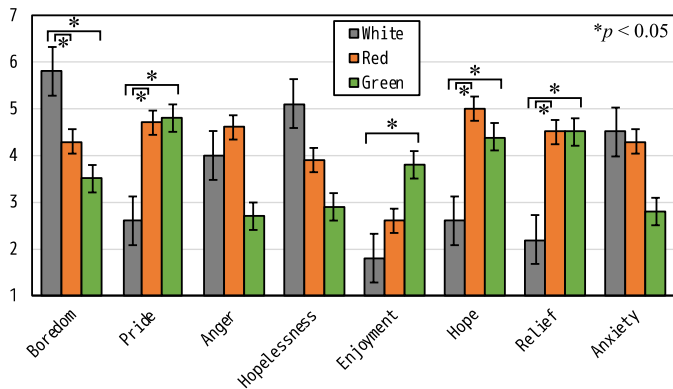


Fig. 3. Results for the Important utterance pattern

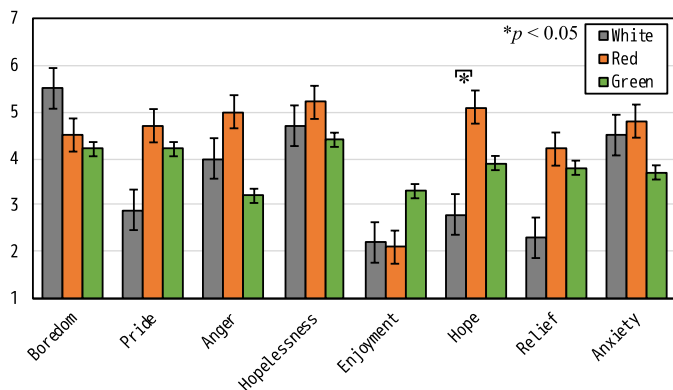


Fig. 4. Results for the Warning utterance pattern

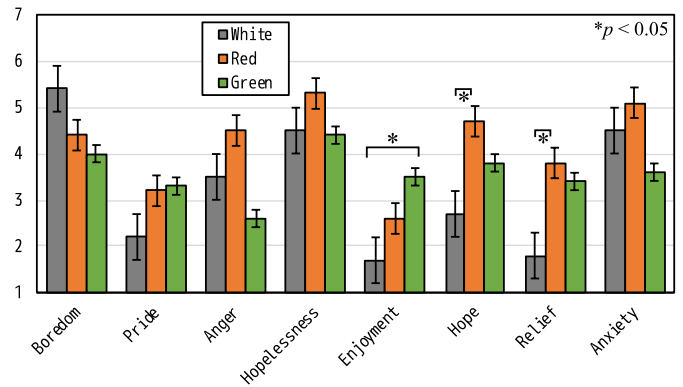


Fig. 5. Results for the Confused utterance pattern

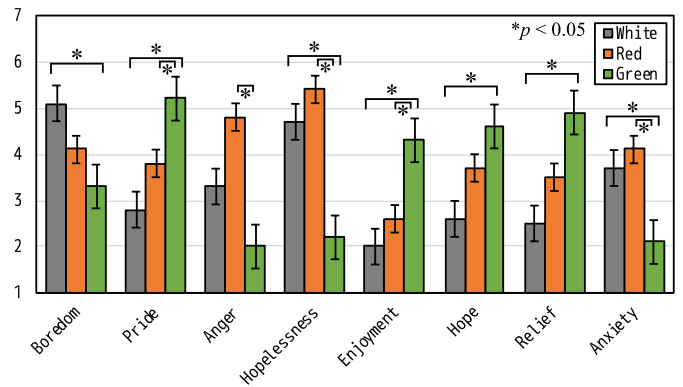


Fig. 6. Results for the Understanding utterance pattern

Fig. 6 shows the results for the Understanding utterance pattern. There were significant differences between white and green and between red and green in pride, hopelessness, enjoyment, and anxiety. Green enhanced pride and enjoyment and suppressed hopelessness and anxiety. Conversely, white and red suppressed pride and enjoyment and enhanced hopelessness and anxiety. There was also a significant difference between white and green in boredom, hope, and relief. White suppressed and green enhanced hope and relief, and white enhanced and green suppressed boredom. There was also a significant difference between red and green in anger. Red enhanced and green suppressed anger. These results show that green had a positive effect on Understanding utterance patterns.

G. Evaluation

These results show that the effects of the combination of utterance and color are different, and that the academic emotions of the learner depended on the color and could be manipulated by changing the color. That is, hypotheses (A-1) and (A-2) were verified.

IV. ANALYSIS BASED ON INDIVIDUALITY OF LEARNERS

In Section III, we found that the learner’s academic emotions were changed and manipulated by changing the color. However, all learner profiles cannot be treated the same, and it is desirable to have a color representation that can respond to the individual characteristics of the learner. Therefore, in this section, we investigated and analyzed the characteristics of the learners using questionnaires on educational psychology.

A. Questionnaire for Investigating Individuality

Nishimura et al. developed the Japanese short version of the Self-Regulation Questionnaire [14], [15] that assesses intrinsic, identified, introjected, and external regulation in self-determination theory. Each type of regulation was measured via five items. The items were rated using a four-point scale (1–strongly disagree to 4–strongly agree). Nishimura et al. [14] reported the validities of this scale by correlation analysis with the original Self-Regulation Questionnaire [16].

The features of each type of regulation are as follows:

- Intrinsic: Learning itself is purposeful; for example, learning itself is interesting or desirable and corresponds to conventional internal motivation.
- Identified: A motivation that represents recognizing the value of doing activities and accepting it as one’s own, such as recognizing that learning shapes one’s future.
- Introjected: A negative but partially internalized feature of the activity’s value, such as self-expansion and maintenance of self-worth by comparison with others.
- External: Influenced by reward acquisition and avoidance of punishment and corresponds to conventional external motivation.

B. Method

To examine the individuality of the learner, we asked the participants in Experiment I to answer the Self-Regulation Questionnaire [14] and the values were calculated for each of the four regulations. By correlating the regulation values with the values of eight academic emotions, we obtained individual profiles for each learner that allowed adaptive interactions to be produced for the learners in advance.

C. Results

Table I shows the results of the correlations for each utterance pattern. Each result was tested for noncorrelation, and significant differences are shown ($^+p < 0.10$, $^*p < 0.05$). A significance of 5% is indicated with a background color (blue, positive; orange, negative).

The results in Table II show that there are places where significant differences occur depending on the combination of utterance pattern, color, academic emotion, and regulation. There were regulations that had significant positive and negative correlations with green (Table Ib). Similar results were observed for pride with white and green (Table Ic). Therefore, regulation and academic emotion are related.

TABLE I. CORRELATION BETWEEN REGULATIONS AND EMOTIONS

(a) Results of the Importance Utterance Pattern									
Color	Regulation	Boredom	Anger	Hopelessness	Anxiety	Pride	Enjoyment	Hope	Relief
White	Intrinsic	0.43	0.13	-0.09	0.30	0.75*	0.18	0.53	0.31
	Identified	-0.06	-0.02	0.74*	0.17	0.04	-0.48	-0.20	-0.16
	Introjected	-0.11	-0.35	0.88*	-0.25	-0.08	-0.31	-0.38	-0.25
	External	0.24	0.33	0.25	0.16	-0.46	0.01	-0.35	-0.14
Red	Intrinsic	-0.11	-0.32	0.35	-0.41	-0.25	0.16	-0.62+	-0.40
	Identified	0.17	0.51	0.17	0.17	-0.1	-0.64*	-0.06	-0.12
	Introjected	0.27	0.43	-0.50	0.28	0.48	-0.54	0.62+	0.37
	External	0.07	0.32	-0.06	0.10	0.08	-0.24	0.54	0.33
Green	Intrinsic	0.26	-0.15	-0.38	0.51	0.04	0.47	0.32	0.16
	Identified	-0.10	-0.20	-0.03	-0.08	0.23	-0.20	0.1	0.25
	Introjected	-0.04	-0.06	0.15	-0.42	0.22	-0.28	-0.11	0.09
	External	-0.43	-0.28	-0.05	-0.22	0.24	-0.38	0.23	0.13
(b) Results of the Warning Utterance Pattern									
Color	Regulation	Boredom	Anger	Hopelessness	Anxiety	Pride	Enjoyment	Hope	Relief
White	Intrinsic	0.16	-0.26	-0.18	0.04	0.10	-0.38	0.34	-0.47
	Identified	0.30	0.33	0.43	0.08	-0.28	-0.10	0.12	-0.44
	Introjected	0.13	0.18	0.42	-0.04	-0.01	0.45	0.34	-0.17
	External	0.25	0.52	0.57+	0.22	-0.57+	-0.17	-0.43	-0.25
Red	Intrinsic	-0.03	-0.27	0.03	-0.19	-0.39	0.26	0.25	-0.61+
	Identified	0.27	-0.33	0.45	0.18	-0.19	-0.43	-0.15	-0.15
	Introjected	0.75*	0.15	0.38	0.24	0.40	-0.40	-0.12	0.46
	External	0.10	-0.19	0.07	-0.10	0.27	-0.34	0.21	0.36
Green	Intrinsic	0.14	0.31	-0.38	0.14	-0.03	0.77*	0.39	0.34
	Identified	-0.32	-0.02	-0.22	-0.34	0.58+	-0.06	0.61+	0.42
	Introjected	-0.08	-0.07	0.23	-0.34	0.50	-0.42	0.17	0.05
	External	-0.20	-0.51	0.19	-0.25	0.43	-0.68*	0.04	0.15

(c) Results of the Confused Utterance Pattern									
Color	Regulation	Boredom	Anger	Hopelessness	Anxiety	Pride	Enjoyment	Hope	Relief
White	Intrinsic	0.39	0.52	0.45	0.48	0.72*	-0.17	0.46	-0.18
	Identified	-0.06	-0.32	0.37	0.31	-0.07	-0.30	-0.25	-0.20
	Introjected	-0.24	-0.45	0.03	-0.04	-0.50	-0.58+	-0.44	-0.33
	External	0.11	-0.66*	0.19	0.16	-0.68*	-0.23	-0.36	-0.11
Red	Intrinsic	-0.31	-0.37	-0.58+	-0.4	-0.57+	0.09	-0.68*	-0.39
	Identified	0.44	0.70*	0.10	0.37	-0.28	-0.70*	-0.12	0.35
	Introjected	0.42	0.72*	0.15	0.44	-0.04	-0.50	0.11	0.54
	External	0.49	0.47	0.58+	0.45	-0.17	-0.25	0.43	0.46
Green	Intrinsic	-0.03	0.39	-0.53	0.32	0.8*	0.52	0.47	0.75*
	Identified	0.08	-0.17	0.49	0.27	-0.23	-0.43	0.08	0.15
	Introjected	-0.26	-0.54	0.54	-0.35	-0.52	-0.52	-0.04	-0.03
	External	0.48	-0.40	0.44	0.00	-0.68*	-0.47	-0.40	-0.33

(d) Results of the understanding Utterance Pattern									
Color	Regulation	Boredom	Anger	Hopelessness	Anxiety	Pride	Enjoyment	Hope	Relief
White	Intrinsic	0.46	0.59+	0.47	0.35	0.04	-0.20	0.03	-0.03
	Identified	0.22	-0.52	0.14	0.11	-0.37	-0.79*	0.44	-0.09
	Introjected	-0.01	-0.41	-0.21	0.11	-0.34	-0.63+	0.13	-0.17
	External	0.15	-0.35	0.13	0.07	-0.22	0.12	0.47	0.12
Red	Intrinsic	-0.24	-0.61+	-0.45	0.12	-0.13	0.8*	0.58+	0.31
	Identified	0.22	-0.02	0.05	0.05	0.41	-0.32	0.23	0.28
	Introjected	0.41	0.23	0.14	-0.35	0.85*	-0.38	-0.06	0.18
	External	0.29	0.18	0.33	-0.04	0.1	-0.49	0.17	0.36
Green	Intrinsic	-0.47	-0.47	0.00	0.04	0.17	0.66*	0.48	0.58+
	Identified	0.39	0.17	0.17	0.43	-0.03	-0.35	0.02	0.06
	Introjected	0.23	0.28	-0.37	-0.19	0.06	-0.39	-0.11	-0.14
	External	0.51	-0.22	-0.44	-0.27	0.55+	-0.46	0.14	0.04

D. Evaluation

Multiple academic emotions may be evoked simultaneously; red was correlated with anger and enjoyment depending on the regulation (Table Ic). Consequently, it was difficult to evoke a single academic emotion alone. Therefore, academic emotion expression was simplified by dividing it into positive emotion and negative emotion, and we examined what kind of interaction caused positive and negative emotions by using an evaluation formula.

We constructed the evaluation formula to evaluate learners' emotions comprehensively. The evaluation of $E_{c,i,s}$ of regulation s , for utterance i , with color c , was 1 for the positive emotions Pride, Enjoyment, Hope, and Relief ($p = 1$ to 4), and -1 for the negative emotions Boredom, Anger, Hopelessness, and Anxiety ($n = 1$ to 4). Each academic emotion and each regulation ($r_{c,i,s,n}$ or $r_{c,i,s,p}$) were multiplied, and then the total value was calculated as

$$E_{c,i,s} = \sum_{n=1}^4 (-1)r_{c,i,s,n} + \sum_{p=1}^4 r_{c,i,s,p} \quad (1)$$

If there is no individual adaptability, the correlation is low and the value of (1) approaches 0. If a certain regulation has a high positive correlation for positive items and a high negative correlation for negative items, (1) takes a positive value, and in the opposite case, (1) takes a negative value. Therefore, when

the value of (1) is high, it indicates good compatibility with a regulation, and when it is low, it indicates poor compatibility. In other words, if you want the learner to have a positive emotion, it is effective to perform an interaction with the combination of the utterance and the color that results in (1) taking a positive value. Conversely, if you want negative emotions, it is effective to perform an interaction that results in (1) taking negative values.

Table II shows the results of (1). Absolute values of 1 or more are shown in bold, and absolute values of two or more are shown with a background color (blue, positive; orange, negative).

The results indicated that green is effective overall, especially for external regulation, to convey that the lecturer robot is presenting important information. Even if the lecturer robot is warning the learner, green is still effective overall, but red is effective when evoking a negative emotion. Green is also effective for intrinsic regulation when a learner robot shows confusion or understanding, but counterproductive for identified regulation.

Analysis of individuality showed that appropriate interactions depend on the learner's self-regulation, and we examined the possibility of an adaptive interaction for each learner. Thus, hypothesis (B) was proved.

TABLE II. RESULTS OF INDIVIDUALITY ANALYSIS

Color	Self-regulation	Utterance Patterns			
		Important	Warning	Confused	Understanding
White	Intrinsic	0.99	-0.16	-1.02	-2.02
	Identified	-1.64	-1.84	-1.11	-0.77
	Introjected	-1.20	-0.08	-1.15	-0.48
	External	-1.92	-2.97	-1.19	0.50
Red	Intrinsic	-0.61	-0.03	0.12	2.74
	Identified	-1.94	-1.48	-2.37	0.30
	Introjected	0.45	-1.17	-1.62	0.16
	External	0.28	0.62	-1.51	-0.62
Green	Intrinsic	0.76	1.26	2.39	2.79
	Identified	0.78	2.46	-1.10	-1.46
	Introjected	0.29	0.55	-0.49	-0.54
	External	1.19	0.71	-2.41	0.70

V. EXPERIMENT II

In Sections III and IV, we used a single utterance and assumed it was similar to a real lecture; however, there was no flow or context. The context of the preceding and following utterances may also affect academic emotions. Therefore, we investigated the influence of continuous utterances on the academic emotions of the learner in the context of a real lecture.

A. Summary

We examined the effect of the color of Pepper's eyes on the emotion of learners' learning activities. The participants were 18 graduate and undergraduate students (nine participants in the experimental group, and nine participants in the control group).

B. Purpose

We investigated whether academic emotions can be manipulated by colors in a real lecture.

C. Stimulus

As in Experiment I, we only changed the color of Pepper's eyes, and the eye color and the corresponding emotion were the same. A real lecture on statistical analysis was divided into 12 utterances (Tables III and IV), and we assigned colors when the utterances contained the intents of Important, Warning, Confused, and Understanding.

D. Questionnaire

As in Experiment I, we prepared seven-point Likert scale questionnaires that used the academic emotions as evaluation items.

E. Procedure

In the experiment, a continuous context was created based on a recording of a real lecture, and the interaction between the Pepper robots was created on a video.

An example of the experimental setup is shown in Fig. 7. The participant was given a laptop and wore headphones. A video of the Pepper was shown (Fig. 8).

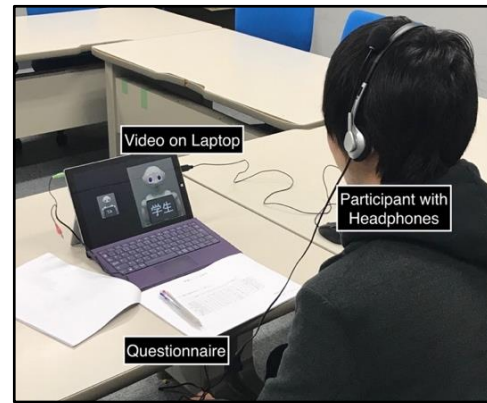


Fig. 7. Experimental setup

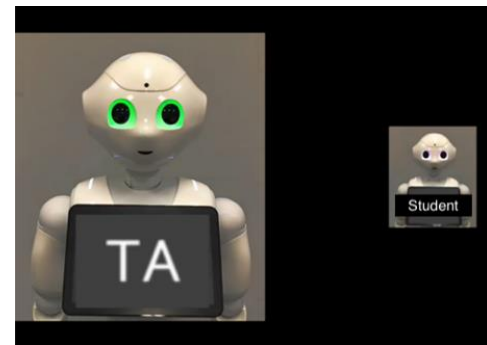


Fig. 8. Image from the stimulus video for the 10th utterance in Table III.

In the video, we gave Pepper the roles of teacher, teaching assistant (TA), and student. We used the utterances that promote Important and Warning for the teacher and the TA roles, and the utterances that represent Confused and Understanding for the student role. Hence, in the video, interactions were performed by Pepper in these three roles.

The participants were instructed to familiarize themselves with the context of the interaction in the video for each utterance in advance, and to assume that they were in the same environment as the three Pepper robots. Then, the emotions felt by the participant when they heard each utterance were recorded with a questionnaire.

The 18 participants were divided into the experimental group (nine participants), who were presented with the colors and the corresponding emotion table, and the control group (nine participants), who were not presented with the colors and the corresponding emotion table.

The procedure was as follows (Fig. 9):

- 1) Participants sit in front of a laptop.
- 2) Participants evaluate Pepper's lecture behavior in a video.
 - a) Pepper speaks Utterance [1], while illuminating its eyes when it has an intent.
 - b) Participants evaluate in context with a questionnaire.
 - c) Repeat a) and b) while changing number in [] from 1–12 corresponding to the utterance.

TABLE III. SCRIPTS FOR UTTERANCES 1–7 FOR EXPERIMENT II

Utterance No.	Intent	Role	Script (areas in [] are presented in the color in (). Otherwise the color is white.)
1	Warning	Teacher	<p>Good morning everybody. I would like to start today's lecture. First of all, here is the question and answer section. One student asked the question "I answered 'Please describe xxx' in the Excel text box. Is this right?" This is "basically, let's output the problem in Excel", so save the contents in Excel. You should write in the text or write directly in the cell. However, among the present submissions, someone wrote in the free description column of Moodle. [(Green) This time, there was a mistake, but everyone should write in Excel from now on; please be careful.]</p>
2	Important	Teacher	<p>Also, I think that "Statistical analysis" is more difficult than in the previous class because it is more specialized. In my lectures, I would like you not just to remember what I have taught you, but to think "where can I use this?" Because we need to get used to difficult things. [(Red) In addition, there is one more important point that applies to study in general: when thinking "where is it difficult," "where is it hard to understand," please carefully think about where you stopped understanding.]</p>
3	Confused	Student	[(White) I did not understand where the interval of 10 to 100 was or how to make a data division in a histogram.]
4	Confused	Student	[(Green) The variance and standard deviation could be determined. However, I investigated the problem of describing the difference between variance and standard deviation, but I don't understand the difference.]
5	Important	Teacher	<p>Thank you, this has been asked a lot. I would like to explain later how to use variance, standard deviation, and their differences. Everyone, you could think about what that meant the words in the histogram and data divisions. In fact, the lecture materials are those of my predecessor, so there is no explanation of the data division. Usually, there is nothing perfect about what you get. So, I would like you to develop skills such as supplementing these materials and examining points that you do not understand. [(Red) Therefore, I think it is very important to do activities that supplement the lecture materials, because it is OK for you to take notes when things that are not in the materials are explained.]</p>
6	Important	Teacher	<p>There was a comment that "the explanation of the composition cumulative ratio and the explanation of the Pareto chart were quite difficult". Pareto charts and cumulative ratios are simple things that you can easily understand if you find easy-to-understand web-pages, but there are many web-pages that are hard to understand. So, I think it would be quite difficult when you use such a web-page. There was also the question, "Do you want a cumulative ratio for the histogram?" This depends on the situation. In most cases, it may not be required up to that point, and it is often good if a histogram can be created, but in some cases it, a cumulative ratio should be shown. [(Green) The important thing here is whether you can do it when someone says "do it because I need it". It is more important whether you can do it when told, rather than whether you always do it.]</p>
7	Important	Teacher	<p>Now, I would like to explain the statement I mentioned earlier, "The difference between variance and standard deviation is difficult to understand." [(Red) The explanation here is important, so please listen carefully.] Simply put, both are used for data dispersion. Both the variance and the standard deviation mean that the smaller the value is, the smaller the variance will be. The difference is that the variance is easier to calculate. Moreover, although the size of the dispersion can be compared, dispersion does not show how large the variation is. Please look at document 1. <About document 1> This is extracted with basic statistics, but dispersion can show that scores in social studies and math are different. However, dispersion does not show how large the variation is. Therefore, using standard deviation is somewhat difficult for mathematical expressions. But how much does the overall score deviate, for example, in the case of an average of about 50 points; is the variation about 5 points or 20 points? It is the standard deviation that is required to determine this. So, basically, standard deviation is more useful. So, in most cases, it is important to keep in mind that the most useful standard deviations are most often used.</p>

TABLE IV. SCENARIO OF UTTERANCE 8 TO 12 FOR EXPERIMENT II.

Utterance No.	Intent	Role	Script (areas in [] are presented with the color in (). Otherwise the color is white.)
8	Important	Teacher	<p>Yes, this is the last review. [(Green) Although the context may change, I want to tell you a very important story that will be useful beyond this lecture.] Please see document 2. <About document 2> This triangle displayed in front of you is called the learning pyramid. This is important information, so I would like you to remember it, but everyone listens to lectures for about a week at university, right? Researchers found that if you just listen to the lecture, the knowledge retention rate is 5%. So even if I try my best and talk about 100 things, you will only remember five. So, I want you to be conscious of this, and stop just listening to the lecture. I think that you will not get anything out of it with this technique. The knowledge retention rate is 10% for reading and 20% for watching videos. In addition, the rate is about 30% if you see someone operating something, such as a demonstration. All of these are passive learning techniques. How is everyone so far? Probably, there are many people engaged in passive learning. In other words, people who think that they are not linked to their own future, who are not conscious of this, or are interested only in the contents of the lecture, tend to have a low level of understanding. Instead, for example, when you assume you will become a CEO in the future, when you think about it in relation to you, or when you perform activities such as teaching people, 75% to 90% of knowledge is retained. So, basically, knowledge is not retained when you input or listen, but when you output. Knowledge can only be absorbed when you use it, so it is very important to think on your own. Among the techniques, teaching people is very effective, so please teach your friends whenever possible.</p>
9	Confused	Student	<p>[(White) Excuse me, when I made a graph with an input range, the Lecturer said "Don't forget to check the label," but I do not know what the label is.]</p>
10	Warning	TA	<p>What is the label...I think that when choosing the input range, you chose from the name of the top subject. But isn't the name of the subject a number? Therefore, saying "the name of the top subject is not a numerical value" is a label check. If you add a label, it will analyze it as a simple character, not the data at the top. [(Green) It is easy to make mistakes when testing, so be careful.]</p>
11	Understanding	Student	<p>[(Red) I see, that's it.]</p>
12	Understanding	Teacher & Student	<p>*Teacher* Next, we will learn how to find the mean, variance, and standard deviation. These three values can be calculated by functions. The average uses the AVERAGE function. In addition, the variance uses the VAR function, and the standard deviation uses the STDEV function. There are several types of variance and standard deviation, such as P and S, but you can use any of them in this lecture. Did you understand? *Learner* [(White) Yes, I understand.]</p>

For the control group, the robots' eyes were always illuminated white in step 2 a).

F. Results

Fig. 10 shows the typical average values for Utterances 2 to 6 in the experiment group, and Fig. 11 shows the corresponding typical average values for the control group.

G. Evaluation

Because the color was always white for the control group, Fig. 11 shows the emotion related to the uttered content itself. There was almost no change in emotion for the continuous utterance in the control group; however, in the experimental group (Fig. 10), there were multiple changes in emotion. For example, in Utterance 3, Boredom in the experimental group is clearly increased, and Anger and Hope are suppressed. Furthermore, in Utterance 5, Pride, Anger, and Hope in the

experimental group are clearly increased. These results confirmed that emotion could be manipulated by color even in a situation similar to a real lecture.

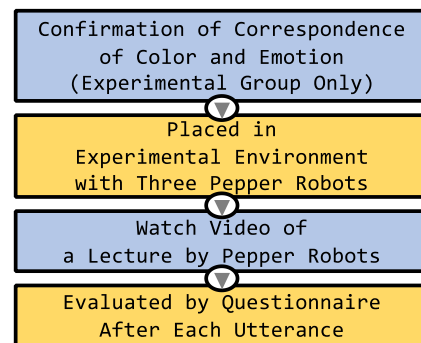


Fig. 9. Procedure for Experiment II

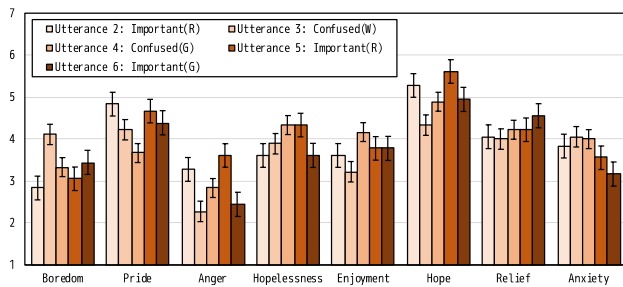


Fig. 10. Results for the experimental group: error bars indicate standard errors

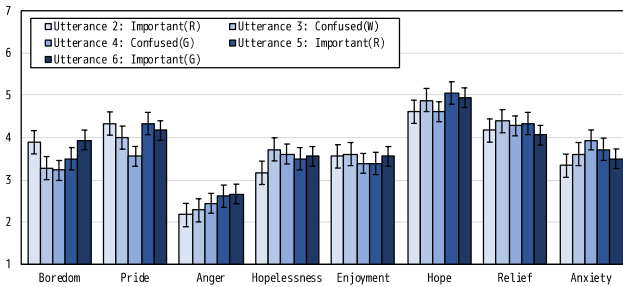


Fig. 11. Results for the control group: error bars indicate standard errors

VI. DISCUSSION

These results suggest that although teaching using nonverbal behavior in robots has been used in a learning context, teaching using color increases the range of options to provide more diverse and individually tailored teaching. Robots affect the mental state of humans, but the reasons why this is so have not been explicitly characterized. In addition, it suggests that color psychology can be applied to robot-led education. Using the relationship between color and emotion, which has long been cultivated in color psychology, in robot-led education is a new method and should help to develop more affect-sensitive robot-led education.

VII. CONCLUSION AND FUTURE WORK

To investigate academic emotions evoked by the color of a robot's eye lights, the following hypotheses were verified. (A) The learners' academic emotions could be manipulated; (B) adaptive academic emotions could be produced in learners; and (C) academic emotions could be manipulated by colors in a situation similar to a real lecture. The verification of hypotheses (A), (B), and (C) were described in Sections II, III, and IV, respectively.

The results indicated that eye color could manipulate the academic emotion, and that adaptive lecture behavior could be produced based on the individuality of the learner. Furthermore, academic emotions were manipulated by the robot's eye color in a situation similar to a real lecture.

However, these results are for limited utterance pattern and color combinations and require more detailed investigation. In addition, these results show that they act on the learner's emotions, not the learning effects. Therefore, future works are

confirmation of reproducibility in the practical field and confirmation of versatility by combining multiple patterns.

ACKNOWLEDGMENT

This work was supported by the "FY2016 MEXT Private University Research Branding Project" and the "Research and Development of Educational and Communicational Robot System" approved by the Council for Promotion of Universal Future Society Project at MEXT.

REFERENCES

- [1] H. Kamide, K. Kawabe, S. Shigemi, and T. Arai, "Nonverbal behaviors toward an audience and a screen for a presentation by a humanoid robot," *Artif. Intell. Res.*, vol.3, no. 2, pp.57–66, 2014.
- [2] T. Ishino, M. Goto, and A. Kashihara, "A Robot for Reconstructing Presentation Behavior in Lecture," *Proceedings of the 6th International Conference on Human-Agent Interaction*, pp.67–75, 2018.
- [3] X. Gao and J. H. Xin, "Investigation of human's emotional responses on colors," *Color Res. Appl.*, vol.31, no. 5, pp.411–417, 2006.
- [4] A. J. Elliot and M. A. Maier, "Color and psychological functioning," *Curr. Dir. Psychol. Sci.*, vol.16, no. 5, pp.250–254, 2007.
- [5] M. Dennis, J. Masthoff, and C. Mellish, "Adapting Progress Feedback and Emotional Support to Learner Personality," *Int. J. Artif. Intell. Educ.*, vol.26, no. 3, pp.877–931, Sep. 2016.
- [6] R. Pekrun, T. Goetz, W. Titz, and R. P. Perry, "Academic emotions in students' self-regulated learning and achievement: A program of qualitative and quantitative research," *Educ. Psychol.*, vol.37, no. 2, pp.91–105, 2002.
- [7] A. Deublein, A. Pfeifer, K. Merbach, K. Bruckner, C. Mengelkamp, and B. Lugin, "Scaffolding of motivation in learning using a social robot," *Comput. Educ.*, vol.125, pp.182–190, 2018.
- [8] F. Jimenez, T. Yoshikawa, T. Furuhashi, and M. Kanoh, "An emotional expression model for educational-support robots," *J. Artif. Intell. Soft Comput. Res.*, vol.5, no. 1, pp.51–57, 2015.
- [9] F. Jimenez, T. Yoshikawa, T. Furuhashi, and M. Kanoh, "Effects of a Novel Sympathy-Expression Method on Collaborative Learning Among Junior High School Students and Robots," *J. Robot. Mechatronics*, vol.30, no. 2, pp.282–291, 2018.
- [10] K. Kojima, K. Muramatsu, and T. Matsui, "Experimental study toward estimation of a learner mental state from processes of solving multiple choice problems based on eye movements," *Proceedings of 20th International Conference on Computers in Education*, pp.81–85, 2012.
- [11] K. Muramatsu, E. Tanaka, K. Watanuki, and T. Matsui, "Framework to describe constructs of academic emotions using ontological descriptions of statistical models," *Res. Pract. Technol. Enhanc. Learn.*, vol.11, no. 1, p.5, 2016.
- [12] S. D'Mello, R. W. Picard, and A. Graesser, "Toward an affect-sensitive AutoTutor," *IEEE Intell. Syst.*, vol.22, no. 4, pp.53–61, 2007.
- [13] R. Pekrun, T. Goetz, A. C. Frenzel, P. Barchfeld, and R. P. Perry, "Measuring emotions in students' learning and performance: The Achievement Emotions Questionnaire (AEQ)," *Contemp. Educ. Psychol.*, vol.36, no. 1, pp.36–48, 2011.
- [14] T. Nishimura, S. Kawamura, and S. Sakurai, "Autonomous Motivation and Meta-Cognitive Strategies as Predictors of Academic Performance: Does Intrinsic Motivation Predict Academic Performance?," *Japanese J. Educ. Psychol.*, vol.59, no. 1, pp.77–87, 2011. (in Japanese).
- [15] T. Nishimura and S. Sakurai, "Longitudinal changes in academic motivation in Japan: Self-determination theory and East Asian cultures," *J. Appl. Dev. Psychol.*, vol.48, pp.42–48, 2017.
- [16] R. M. Ryan and J. P. Connell, "Perceived locus of causality and internalization: Examining reasons for acting in two domains," *J. Pers. Soc. Psychol.*, vol.57, no. 5, p.749, 1989.

Formal Concept Analysis based Framework for Evaluating Information System Success

Ansar Daghour¹, Khalifa Mansouri², Mohammed Qbadou³

Laboratory: Signals, Distributed Systems and Artificial Intelligence (SSDIA) ENSET of Mohammedia
University Hassan II of Casablanca

Abstract—This paper aims to propose a methodology for evaluating information system success. It is based on two main fields, which are formal concept analysis and multi criteria decision-making methods. A framework whose main objective is to visualize the synchronization between company processes and information system indicators via process mapping and formal concept analysis exploited the methodology. Moreover, owing to the application of multi criteria decision-making methods, we can rank the information system among the others system for the purpose to ameliorate system performance. In practice, we apply the steps of this framework on a Moroccan bank by choosing a combination of processes and indicators.

Keywords—Formal concept analysis; process; multi criteria; indicator; evaluation

I. INTRODUCTION

Information system (IS) [1] is an organized system developed to collect, process and distribute information within company. In [2], authors given two views on IS that involves software, hardware, data, people and procedures. Others authors [3] provide different system view that adds company process. The literature is rich with models and methods, which aim to evaluate information system success. IS research is interdisciplinary related with the study of the impact of IS on the behavior of the company and its process [4]. For this purpose, in this work, we choose to evaluate the IS of a company in relation with the business process.

In this paper, we seek to present a framework to evaluate IS regardless the company sector. The proposed framework involves three main steps: data collection; to collect the data of company processes and IS indicators, visualization and calculation to visualize the concept lattice of a combination of process and indicators, then, the application of the two most used multi criteria decision-making (MCDM) methods namely AHP and Topsis. In the final step, results about the information system evaluation are given and possible recommendations to increase the information system success.

The structure of this paper is as follows: section 2 presents a state of art of information system measurement, formal concept analysis (FCA), process mapping and multi criteria decision-making (MCDM) methods. Section 3, presents the main steps of the proposed framework: data collection, visualization and calculation and finally results and recommendations. In section 4, we apply the proposed approach on a real case study of a Moroccan bank. Then, the concluding remarks and perspectives are presented in conclusion.

II. LITERATURE REVIEW

A. IS Success Models

The literature provides many definitions of IS success as evaluation methods. Thereby, the results of the researchers are diverse and sometimes even contradictory. Authors [5] specify that the most appropriate evaluation indicator is the system use, according to them the measure of the IS success through cost or benefit studies is insufficient whereas, Bailey and Pearson [6], express the importance of the users satisfaction which is guarantor of an increase of the productivity of the IS. Other authors [7] explain that the IS effectiveness is related to anything that can bring value to the organization. As for Goodhue and Thompson [8], they share the same vision of DeLone and McLean [9] and define the success of the IS through the individual and organizational impacts.

Regarding the evaluation of IS success, the literature is very rich, we will quote the most known and used models over the years. These models of DeLone and McLean (1992, 2003) are part of the evaluation process and evaluation model of IS that is inspired by the measurement of the Balanced Score Card.

Through this presentation of the state of the art on the evaluation of the IS success, in the rest of this paper, we will use the DeLone and McLean model [10] which is the result of several authors' validation [11].

B. Formal Concept Analysis

Formal conceptual analysis (FCA)[12] is a method of data analysis describing the relationship between a set of objects and a set of attributes. It produces two types of output from the input data. The first is a concept lattice that represents a set of formal concepts in the data that is hierarchically ordered by a sub-concept-super concept relation. The second output of FCA is a collection of so-called attributes implications that describe a very particular dependency.

1) *Concept lattice*: is a mathematical formalism [13] derived from a formal context $K = (G, M, I)$. The formal context K consists of G , a set of objects, of M , a set of attributes and I a binary relation defined on the Cartesian $G \times M$ product. In a binary table representing $I \subseteq G \times M$, the rows correspond to objects and columns to attributes (Table I).

The lattice resulting from the AFC process is composed of formal concepts ordered by a partial order relation. A concept is a pair (A, B) where $A \subseteq G$ and $B \subseteq M$, A is the maximal set

of objects sharing the set of attributes of set B (and vice versa). In a concept (A, B), A is called the extension and B the intension of the concept. The concepts in a lattice of concepts are defined with respect to a Galois connection that relies on two derivation operations:

$$A' = \{m \in M \mid gIm \text{ for all } g \in A\}$$

$$B' = \{g \in G \mid gIm \text{ for all } m \in B\}$$

A concept (A, B) verifies that $A' = B$ and $B' = A$:

A' is the set of all the attributes of B owned by the objects of A and B' is the set of all objects with the attributes of B.

C. Process Mapping

The process approach [14] consists in identifying and managing the processes used in an organization as well as their interactions. It presupposes the representation of the dynamic architecture of what is done in the organism (representation of all the processes, their sequences and their interactions).

The process is a set of correlated or interactive activities that transforms input elements in output elements.

The processes can be classified as follows [15]:

- Realization process, which allows to realize the products / services in order to satisfy the customers;
- Management process, which presents the strategies of a company (priorities, objectives, methods of communication and methods of treatment and control);
- Support processes, which offer the means and the resources necessary to carry out all the processes.

As soon as processes are identified, the process mapping must be carried out, which is an indispensable tool for measuring progress. Process mapping [16] provides a global view of how the organization works and visualizes its processes and interactions. Process mapping makes it possible to communicate identically to a large number of actors involved in a complex activity and to give meaning to the tasks to be more performed (Fig. 1).

D. MCDM Methods

The multi-criteria decision making process is an iterative and non-linear process that generally consists of its stages [17]:

- The reformulation of the decision problem;
- The modeling of local preferences at each point of view;
- The aggregation of preferences to establish one or more systems;
- Exploitation of this aggregation;
- The recommendations.

TABLE I. EXAMPLE OF BINARY TABLE

I	Y ₁	Y ₂	Y ₃	Y ₄
X ₁	1	1	1	1
X ₂	0	0	1	1
X ₃	0	0	1	1
X ₄	0	1	1	0
X ₅	1	1	0	1

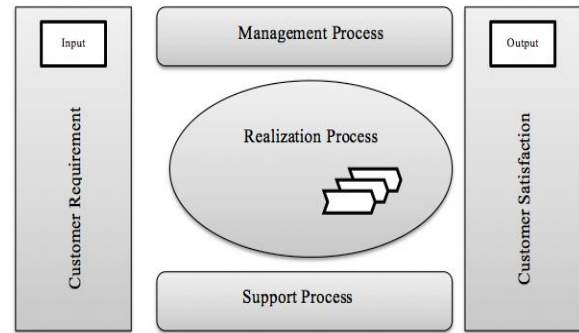


Fig. 1. Global Process Mapping.

Among the MCDM methods, we will use the two most used methods namely AHP and TOPSIS.

1) *Ahp method*: The AHP method developed in 1980[18] has been used successfully in several fields. It starts from matrices of binary comparisons to arrive after several stages to compare the choice of the decision problem. The method consists of representing a problem by a hierarchy structure according to the following steps:

- Construct the matrix U_{ij} of order m if the compared entities are criteria, or of order n if the compared entities are alternatives;
- Construct the comparison matrices whose values are obtained by transforming the judgments into numerical values according to the Saaty scale (Scale of Binary Comparisons), respecting the principle of reciprocity;

$$\left\{ \begin{array}{l} \sum_{j=1}^n U_{ij} W_j = \lambda_{max} W_i \text{ pour } i = 1 \dots n \\ \sum_{i=1}^n W_i \end{array} \right.$$

- Checking this consistency.

2) *Topsis method*: The fundamental idea of this method, which was developed in 1981[19], is to choose a solution that comes closest to the ideal solution (better on all criteria) and to move as far as possible from the worst solution (which degrades all the criteria).

The steps of the TOPSIS method are as follows:

- Normalize performance:

$$e'_{ij} = \frac{g_j(a_i)}{\sqrt{(g_j(a_i))^2}}$$

Where: $i=1 \dots m$ and $j=1 \dots n$

- Calculate the product of normalized performance:

$$e''_{ij} = \pi_j * e'_{ij}$$

$$\sum_{j=1}^n \pi_j = 1$$

Where: $i=1 \dots m$ and $j=1 \dots n$

- Determine the positive and the negative ideal solutions:

$$a^* = \{max_i e''_{ij}, i = 1 \dots m \text{ et } j = 1 \dots n\};$$

$$a^* = \{e_j^*, j = 1 \dots n\} = \{e_1^*, e_2^* \dots e_n^*\};$$

$$e_j^* = max\{e''_{ij}\}$$

$$a^- = \{min_i e''_{ij}, i = 1 \dots m \text{ et } j = 1 \dots n\};$$

$$a^- = \{e_j^-, j = 1 \dots n\} = \{e_1^-, e_2^- \dots e_n^-\};$$

$$e_j^- = min\{e''_{ij}\}$$

- Calculate the separation measures:

$$D_i^* = \sqrt{\sum_{j=1}^n (e''_{ij} - e_j^*)^2} \quad \forall: i = 1 \dots m;$$

$$D_i^- = \sqrt{\sum_{j=1}^n (e''_{ij} - e_j^-)^2} \quad \forall: i = 1 \dots m;$$

- Calculate the relative closeness coefficient to the ideal solution:

$$CC_i^* = \frac{D_i^-}{D_i^* + D_i^-} \quad \forall: i = 1 \dots m \text{ et } 0 \leq CC_i^* \leq 1;$$

- Rank the alternatives.

III. PROPOSED FRAMEWORK

This paper provides a framework to evaluate IS success based on two main fields, which are formal concept analysis and multi criteria decision-making methods. The aim of this work is to give a generic tool, which can be applied in different sectors with the possibility to choose the enterprise processes, and system success indicators, which will be the subject of the study. The framework architecture involves three essential parts: data collection, visualization and calculation and finally results and recommendations (Fig. 2).

A. Data Collection

It represents the basic step that allows the user to enter the data of the study (company processes and indicators of the information system success) after authentication by login and password. To model the processes of the company, we chose to use the mapping process. This technique consists of identifying

as finely as possible all the processes of the company based on its information system and related to the process of the company to present them graphically.

Regarding the identification of the information system success indicators, we used the DeLone and McLean model (2003), which is a reference in the field of information system evaluation. The six model indicators will constitute the key performance indicators of the study and will also serve in the construction of the analytical hierarchy in the next step.

B. Visualization and Calculation

This step is purely technical for the visualization and calculation. It consists of a first sub-part based on concept analysis more specifically concept lattices. The visualization of the binary tables lead to construct concept lattices that give pertinent information based on the studied process and indicators. We can apply this step to each combination of process and indicators that will be store in database for analysis and recommendations.

The second sub-part concerns the application of two famous MCDM methods namely Ahp and Topsis to evaluate the information system performance and even to rank the studied system with others; for the purpose of testing and verifying the proposed framework on others sector. For this reason, we have developed a prototype of software that implements the two methods. It is developed in Java language under Net Beans platform; we will present two principals interfaces (Fig. 3 and 4).

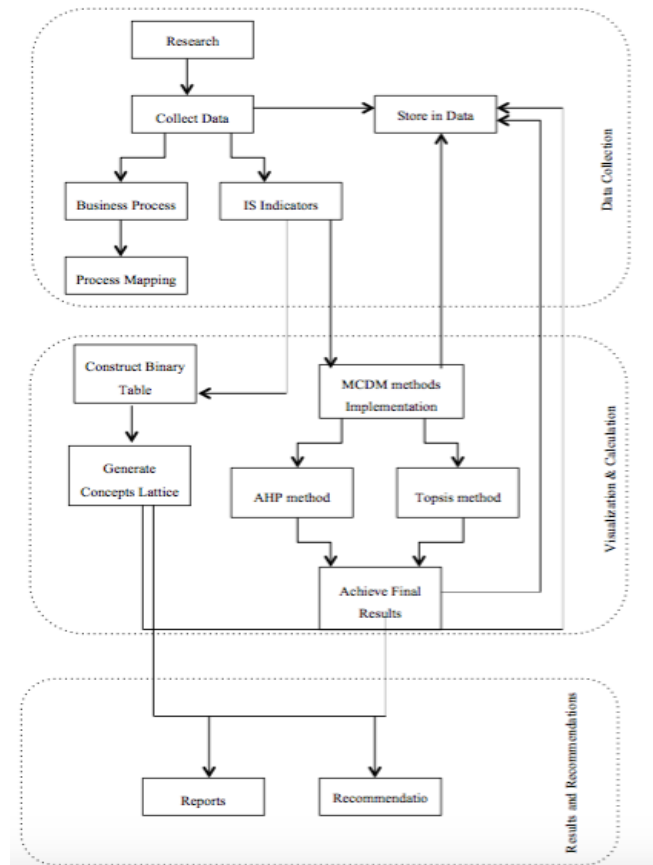


Fig. 2. Proposed Framework Architecture.

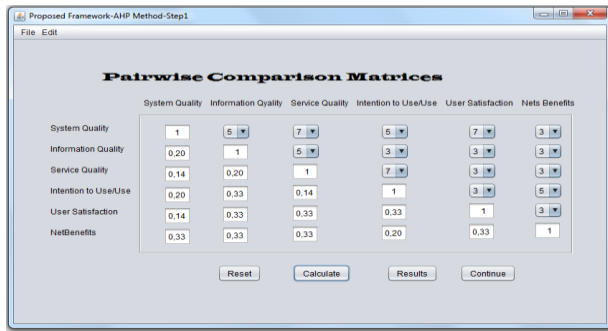


Fig. 3. Implementation of AHP Method.

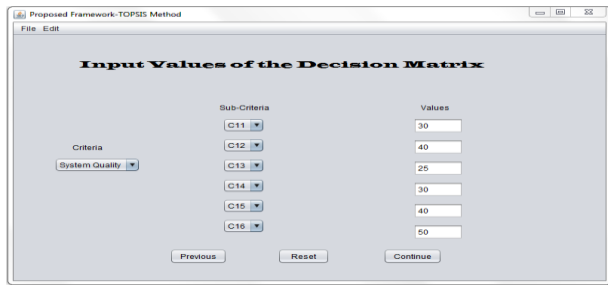


Fig. 4. Implementation of TOPSIS Method.

C. Results and Recommendations

The database stores data that has two main uses. The first is the use of all concept lattice generated of formal concept analysis to evaluate synchronization between different company processes to detect inconsistencies. As for the second, it concerns the results of the application of the MCDM methods, which allow on the one hand evaluating the information system success and the possibility of ranking the studied system with respect to other systems based on the chosen evaluation indicators. This framework can produce recommendations that can help both to better synchronize company processes and evaluate the performance of information systems based on the study of possible combinations between processes and information system success indicators.

IV. CASE STUDY

In this work, we present a case study of an information system belonging to a Moroccan bank. We chose to implement our framework on a company in the banking sector since it is known as the most customer sector of data processing and specifically information systems. Furthermore, the banking example appears as an analytical framework adapted to a study of process mapping. The bank operates through a set of correlated or interacting activities that use inputs to produce a result; these activities are grouped together as a process. In this paper, we apply formal concept analysis to evaluate some processes according to IS success indicators. The same approach can be done iteratively on all the processes of the bank. Subsequently, the MCDM methods will be applied to evaluate the IS success through the chosen indicators. As part of this work, we will just give an example of a process.

A. Implementation

1) *Data Collection*: The first step in our framework is data collection to identify the processes and indicators or evaluation criteria that will be the focus of the study.

It has already been mentioned that our approach can be applied to any combination of processes and indicators that allow the evaluation of these processes, in this case study we have chosen a list of processes (Table II) as well as a set of criteria (Table III) derived mainly from the DeLone and McLean model.

TABLE II. LIST OF INDICATORS OF STUDY

Symbol	Indicator	Signification
I ₁	Information Quality	Refers to the ability of the system to store, deliver and most importantly produce relevant information in terms of: accuracy, completeness, understandability and utility;
I ₂	System Quality	Has multiple dimensions: Access, ease of learning, flexibility, reliability and response time;
I ₃	System Use	It is measured according to the nature of the domain; it can refer to the amount of use, the frequency of use, the range of use and even the nature of use;
I ₄	Reliability	The ability to perform the promised service dependably and accurately;
I ₅	Individual Impact	It mainly measures the productivity and the innovation of the tasks, the customers satisfaction and the control of management;
I ₆	Intention to Use	Designates future intentions to use the system that is related with the use of the system and directly affects the net benefits;
I ₇	Assurance	The knowledge and courtesy of employees and their ability to convey trust and confidence;
I ₈	User Satisfaction	It influences the advantages provided by an information system and indicates whether a user is satisfied or not after using a system;
I ₉	Organizational Impact	It includes three sub-dimensions that are: strategic benefits, information benefits and transactional benefits.

TABLE III. LIST OF PROCESSES OF STUDY

Symbol	Process
P ₁	Manage dynamic data within bank
P ₂	Ensure the exchange of information
P ₃	Achieve the organizational needs
P ₄	Adapt and Integrate applications
P ₅	Analyze technological risks
P ₆	Ensure system security
P ₇	Provide user guides for new systems
P ₈	Manage human resources

2) *Data Collection*: After the data collection, we proceed to the technical step; the first sub-part is based on concepts analysis, more precisely concept lattices.

We consider the set of processes $\{P_1, P_2, P_3, P_4, P_5, P_6, P_7$ and $P_8\}$ that can improve the set of indicators $\{I_1, I_2, I_3, I_4, I_5, I_6, I_7, I_8$ and $P_9\}$. The formal context noted C is represented in the form of a table (in rows processes and in columns the indicators). If the process X_i ameliorates the indicator Y_j then the cell C_{ij} is marked by 1 (in the otherwise 0) as shown in Table IV.

The corresponding formal context $\langle X, Y, I \rangle$ contains the following formal concepts:

$C_0 = \langle \{P_1, P_2, P_3, P_4, P_5, P_6, P_7, P_8\}, \{I_1\} \rangle$; $C_1 = \langle \{P_1, P_2, P_3, P_4\}, \{I_1, I_4\} \rangle$; $C_2 = \langle \{P_2, P_3, P_4\}, \{I_1, I_4, I_7\} \rangle$; $C_3 = \langle \{P_5, P_6, P_7, P_8\}, \{I_1, I_3\} \rangle$; $C_4 = \langle \{P_5, P_6, P_8\}, \{I_1, I_3, I_6\} \rangle$; $C_5 = \langle \{P_3, P_4, P_6, P_7, P_8\}, \{I_1, I_5\} \rangle$; $C_6 = \langle \{P_3, P_4\}, \{I_1, I_5, I_4, I_7\} \rangle$; $C_7 = \langle \{P_4\}, \{I_1, I_5, I_4, I_7, I_9\} \rangle$; $C_8 = \langle \{P_6, P_7, P_8\}, \{I_1, I_5, I_3\} \rangle$; $C_9 = \langle \{P_6, P_8\}, \{I_1, I_5, I_3, I_6\} \rangle$; $C_{10} = \langle \{P_7\}, \{I_1, I_5, I_3, I_8\} \rangle$; $C_{11} = \langle \{P_1, P_2, P_3, P_5, P_6\}, \{I_1, I_2\} \rangle$; $C_{12} = \langle \{P_1, P_2, P_3\}, \{I_1, I_2, I_4\} \rangle$; $C_{13} = \langle \{P_2, P_3\}, \{I_1, I_2, I_4, I_7\} \rangle$; $C_{14} = \langle \{P_5, P_6\}, \{I_1, I_2, I_3, I_7\} \rangle$; $C_{15} = \langle \{P_3, P_6\}, \{I_1, I_2, I_5\} \rangle$; $C_{16} = \langle \{P_3\}, \{I_1, I_2, I_5, I_4, I_7\} \rangle$; $C_{17} = \langle \{P_6\}, \{I_1, I_2, I_5, I_3, I_6\} \rangle$; $C_{18} = \langle \{\}, \{I_1, I_2, I_3, I_4, I_5, I_6, I_7, I_8, I_9\} \rangle$.

The corresponding concept lattice $\beta\langle X, Y, I \rangle$ is displayed as in the following figure:

The second subpart concerns the application of two MCDM methods chosen for this study. We will start with the first method namely the AHP (Analytical Hierarchy Process), and then we apply the TOPSIS (Technique for Order Preference by Similarity to an Ideal Solution).

a) *Ahp method Implementation*: The weights of the indicators (information quality, system quality, system use, reliability, individual impacts, intention to use, assurance, user satisfaction and organizational impacts) are estimated using AHP method. The data of this study are collected by an online questionnaire via the Google docs.

TABLE IV. REPRESENTATION OF THE FORMAL CONTEXT C

	I ₁	I ₂	I ₃	I ₄	I ₅	I ₆	I ₇	I ₈	I ₉
P ₁	1	1	0	0	0	0	1	0	0
P ₂	1	1	0	0	0	0	1	1	0
P ₃	1	1	1	0	0	0	1	1	0
P ₄	1	0	1	0	0	0	1	1	1
P ₅	1	1	0	1	0	1	0	0	0
P ₆	1	1	1	1	0	1	0	0	0
P ₇	1	0	1	1	1	0	0	0	0
P ₈	1	0	1	1	0	1	0	0	0

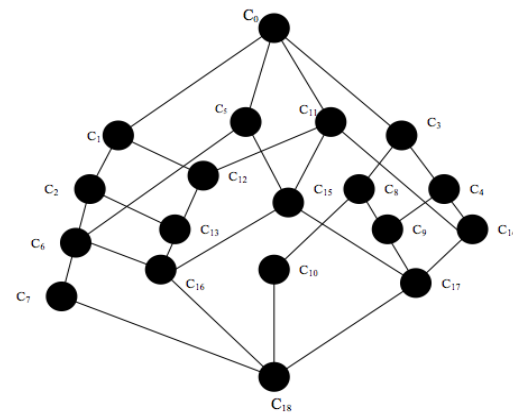


Fig. 5. Concept Lattice of Case Study.

An aggregated pairwise comparison matrix (Table V) was constructed, thereafter; the other steps of the AHP method were calculated using our prototype. The result of this first method is the identification of the weight of each indicator in the evaluation of the studied system.

The priority weights of indicators are as follows:

$I_1= 0,249$; $I_2=0,230$; $I_3= 0,134$; $I_4=0,104$; $I_5=0,079$; $I_6= 0,084$; $I_7= 0,048$; $I_8= 0,039$ and $I_9= 0,030$.

b) *Topsis method Implementation*: In this work, we use the MCDM method named TOPSIS, which uses the weights calculated, by the previous method. The main purpose of this sub-part is to rank the system among others in terms of IS success in order to detect the sources of errors.

We will refer to the previous work [20] that focused on the evaluation of the banking information system in which five banks were compared. The bank of this study is referenced B₅ to differentiate it with the others; the values of the relative closeness to ideal solution are shown in Table VI.

TABLE V. AGGREGATED PAIRWISE COMPARISON MATRIX

	I ₁	I ₂	I ₃	I ₄	I ₅	I ₆	I ₇	I ₈	I ₉
I ₁	1	5	3	5	3	3	5	3	3
I ₂	0,2	1	5	7	3	5	7	7	3
I ₃	0,33	0,2	1	3	5	1	5	3	5
I ₄	0,2	0,14	0,33	1	3	7	1	3	3
I ₅	0,33	0,33	0,2	0,33	1	3	3	3	3
I ₆	0,33	0,2	1	0,14	0,33	1	5	3	5
I ₇	0,2	0,14	0,2	1	0,33	0,2	1	3	3
I ₈	0,33	0,14	0,33	0,33	0,33	0,33	0,33	1	3
I ₉	0,33	0,33	0,2	0,33	0,33	0,2	0,33	0,33	1

TABLE VI. BANKS RANKING

Alternatives	D _i ⁺	D _i ⁻	CC _i	Rank
B ₅	0,216	0,085	0,282	6
B ₁	0,196	0,116	0,372	4
B ₂	0,203	0,164	0,446	2
B ₃	0,209	0,094	0,310	5
B ₄	0,166	0,204	0,551	1
B ₅	0,187	0,130	0,409	3

According to the value of CC_i , the alternative with the lowest closeness coefficient is the bank of the case study with $CC_i = 0,282$.

3) *Results and discussions*: This last part concerns the display of evaluation results as well as the discussions. Visualization of the concept lattice gives a hierarchical representation allowing knowing the relation between the processes of the company and the evaluation indicators of the system. The figure above (Fig. 5) represents the concept lattice of case study; it consists of nodes and segments and contains all the objects and properties of the context, each node corresponds to a formal concept.

The figure can be analyzed as follows: Each process labeled by a set of indicators implies that the descendant objects of this process inherit the same indicators. Even more, in the figure, the intention of the formal concept corresponds to the empty set and the extension corresponds to the set of all the processes.

By analyzing more closely the lattice, we note that three set contained only one process. These are the P_4 , P_6 and P_7 processes that represent: adapt and Integrate applications, ensure system security and provide user guides for new systems. Which implies that the bank has problems in the performance of these processes, which is explained by the concept lattice obtained, and view the domain of the company the first critical problem that it has to handle is the security of the information system.

Regarding the application of MCDM methods and more specifically the AHP method, the bank that represents the case study is more interested in the indicators related to the quality (information quality, system quality, service quality) forgetting the importance of net benefits (individual and organizational), use of the system and user satisfaction.

The weight of the indicators influence directly the ranking of the bank obtained by the Topsis method, we note that the bank of our case study is ranked the last among the others banks belonging to the previous works. This ranking can be explained by several reasons: the concentration on indicators possibly related to the different types of quality (information, system and service), the mismanagement of the resources of the company, the lack of experience and skills for the system use in summarizing what has been said before, the bank must address the problems related to the system security management processes, establish user guides to ensure the proper control of the system and therefore the satisfaction of users and facilitate the steps process of adaptation and integration of new applications.

V. CONCLUSION

The purpose of this article is to propose a framework to evaluate the information system success based on the synchronization between the processes of the company. This work focuses on two main areas: the first is the formal concept analysis in order to identify the level of synchronization

between the processes and the evaluation indicators that can impact these processes. The second is the MCDM methods, which aim to classify the studied system among the others based on the chosen evaluation indicators. In this paper, we have proposed a framework implementing the set of techniques and methods that were used to end up with an approach to evaluate the IS success that has been applied as a case study which can be generalized on any company. In our future work, we will work on other sectors to know if the change of the sector impacts on the relation between processes and evaluation indicators and therefore on the evaluation.

REFERENCES

- [1] G Piccoli and F Pigni, Information systems for managers: with cases, 40th ed.: Prospect Press, 2018.
- [2] M S Silver, M L Markus, and C M Beath, "The Information Technology Interactive Model: A Foundation for the MBA Core Course," MIS Quarterly, pp. 361-390, 1995.
- [3] J Zheng, Informatio system: A system perspective, 2015.
- [4] R D Galliers, M L Markus, and S Newell, Exploring Information Systems Research Approaches. New York, 2006.
- [5] H C Lucas, "Unsuccessful Implementation: the Case of a Computer-based Order Entry System," Decision Sciences, vol. 9, no. 1, pp. 68-79, 1978.
- [6] E J Bailey and S W Pearson, "Development of a Tool for Measuring and Analyzing Computer User Satisfaction," Management Science, vol. 29, no. 5, pp. 530-545, 1983.
- [7] A W Gatian, "Is User Satisfaction a Valid Measure of System Effectiveness?," Information & Management, vol. 26, no. 3, pp. 119-131, 1994.
- [8] D L Goodhule and R L Thompson, "Task-Technology Fit and Individual Performance," MIS Quarterly, vol. 19, no. 2, pp. 213-236, 1995.
- [9] W H DeLone and E R Mclean, "Information Systems Success: The Quest for the Dependent Variable," Information Systems Research, vol. 3, no. 1, pp. 60-95, 1992.
- [10] W H DeLone and E R Mclean, "The DeLone and McLean Model of Information Systems Success: a Ten-Year Update," Journal of Management Information Systems, vol. 19, no. 4, pp. 9-30, 2003.
- [11] P B Seddon, "A Specification and Extension of the DeLone and McLean Model of IS Success," Information Systems Research, vol. 8, no. 3, pp. 240-254.
- [12] R BELOHLAVEK, "Introduction to Formal Concept Analysis," Department of Computer Science, Faculty of Science Palacky University, 2008.
- [13] B Ganter and R Wille, "Formal Concept Analysis," Mathematical Foundations, 1999.
- [14] International Organization for Standardization, "The process approach in ISO 9001:2015," 2015.
- [15] B L Goldense, "The Five Types of Manufacturing Processes," Machine Design Journal, vol. 87, no. 9, p. 88, 2015.
- [16] The University of Sheffield (TUOS), "Process Mapping Guidance and Standards," 2018.
- [17] A Ishizaka and P Nemery, Multi-Criteria Decision Analysis, Methods and Software: Wiley and Sons Ltd.: Chichester, UK, 2013.
- [18] T L Saaty, The analytic hierarchy process: New York: McGraw-Hill , 1980.
- [19] C Hwang and K Yoon, "Multiple Attribute Decision Making: Methods and applications, a state of the art survey," Springer-Verlag, 1981.
- [20] A Daghour, K Mansouri, and M Qbadou, "Assessing Information System Performance in Banks Based on Multi-Criteria Decision Making Techniques ," International Journal of Engineering & Technology , vol. 7, no. 4.32, pp. 101-104, 2018.

Cluster based Hybrid Approach to Task Scheduling in Cloud Environment

Y. Home Prasanna Raju¹
Department of CSE
Acharya Nagarjuna University
Guntur, A.P., India

Nagaraju Devarakonda²
Department of IT
Lakireddy Bali Reddy College of Engineering
Vijayawada, A.P., India

Abstract—Cloud computing technology enables sharing of computer system resources among users through internet. Many numbers of users may request for sharable resources from a cloud. The sharable resources must be effectively distributed among requested users with in a less amount of time. Task scheduling is one of the ways of handling the user requests effectively in a cloud environment. There were many existing biologically inspired optimization techniques worked with task scheduling problems. The proposed paper is aimed at clubbing clustering techniques with biologically inspired optimization algorithms for deriving better results. A new hybrid methodology KPSOW (K-means with PSO using weights) has been proposed in the paper, which makes use of the strengths of both the K-means and PSO algorithms with the inclusion of weights concept. The results have shown that KPSOW has made considerable changes in reducing the makespan and improves the utilization of computing resources in the cloud.

Keywords—Task scheduling; cloud computing; clustering; k-means; particle swarm optimization; makespan

I. INTRODUCTION

In the Computer science and information technology field, usage of internet plays an important role for sharing of resources among many people. Many technologies came for supporting the distribution of resources through a network. Distributed computing is one of the technologies which support the distribution of resources in a network. Task scheduling is the mostly used key factors in distributed system. Simulated annealing techniques [1] can be applied for scheduling tasks in a distributed environment for better results. Cloud computing is one of the distributed technologies which provides a platform for sharing of resources via pay per use model through internet. Cloud provides services [2] to users in three categories. The categories are Platform-as-a-Service (PaaS), Software-as-a-Service (SaaS) and Infrastructure-as-a-Service (IaaS). Cloud can be viewed as a Network-as-a-Service (NaaS) [3] using virtualization process. There are many challenges/issues [4,5] to be faced for a reliable cloud computing environment. Clouds can be of different types like private cloud, public cloud and hybrid cloud which is the combination of both the private and public clouds. To utilize the cloud services effectively, task scheduling can be used in the cloud environment. For effective utilization, the parameters that can be considered are makespan, energy consumption, resource utilization etc. There must be minimum energy consumption while handling the cloud tasks. How energy can be minimized using virtual

machine scheduling [6] in cloud centers was shown by Chaima Ghribi, Makhlouf Hadji and Djamel Zeghlache. Balancing of load in cloud environment [7, 8, 9] is another important aspect to be considered for speedy response from the cloud. If the load is properly balanced, the computing resources can evenly get the cloud tasks from the scheduler which creates a balancing environment, even when high complexity tasks or more tasks enter the cloud. Priyansh Srivastava, Bhavesh Gohil, and Dhiren Patel [10] showed the load balancing model for a cloud using Cloudsim tool. Genetic algorithms [11, 12] can also be useful for task scheduling. Genetic algorithms belong to a class of evolutionary algorithms which are used for generating high quality optimization solutions. They rely on bio-inspired operations like selection, crossover, mutation etc. Another way of giving optimizing solutions to task scheduling is through bio-inspired algorithms like Particle Swarm Optimization (PSO) [13, 14, 15, 16] and Ant Colony Optimization algorithms [17, 18] etc. PSO imitates the behavior of birds searching for food. Birds move to next location where more food is available. The bird's movement is based on its local search criteria. Every time bird's best position and its velocity is considered to meet the global search criteria which is final optimized solution whereas ACO imitates the behavior of ants searching for food. When an ant finds food, it moves to that location by releasing a pheromone on its travelled path. Now the other ants follow the path by smelling that pheromone. The pheromone may evaporate as the time goes on. So the ant's movement during the search path is based on the concentration of pheromone laid on that path. Optimized paths are found using the above ant's behavior.

The tasks to be scheduled are of different types like having different complexity levels. If the similar tasks are taken into groups before allocating them to computational resources, then there is a chance of generating optimizing solutions for a cloud environment. Hence to obtain better makespan results in cloud environment, the proposed paper is made making use of clustering techniques with the help of bio-inspired algorithms for cloud task scheduling problem. A new hybrid algorithm KPSOW has been proposed in the paper. KPSOW combines the strengths of both K-means [19, 20, 21, 22] and PSO algorithms using weights concept.

The rest of the paper is organized as follows. Sections 2, 3 and 4 explain the working nature of K-Means algorithm, FCFS scheduling algorithm and Particle Swarm Optimization algorithm, respectively. The three sections also explain how

these algorithms can be mapped to task scheduling problem in cloud environment. Section 5 explains methodology which gives a complete idea of proposed work. Section 6 describes and depicts the results of proposed work. Finally, conclusions are given in Section 7.

II. K-MEANS CLUSTERING

K-means clustering algorithm is one of the popular used algorithms for clustering. K defines number of clusters to be generated from the process. It collects a set of tasks as input and separates them into clusters by finding distances between mean values of the clusters. Euclidean distance measure is used for finding mean distances. Number of clusters to be generated is to be given as domain knowledge to the algorithm. The algorithm proceeds as follows. Let us assume K value is 2 and there are n tasks. Initially, each cluster is allocated a single task randomly. Now the clusters task length is considered as mean value in the first iteration. Euclidean distances are applied to all the remaining task lengths in the set from the mean values of cluster1 and cluster2. The task lengths which are having minimum mean distance is allocated to those corresponding clusters. Now, new mean values are calculated for the newly generated clusters. Mean squared error value is calculated at each iteration step to find error while forming clusters. Calculation of mean squared error value is shown in the equation (1).

$$e = \sum_{p=1}^K \sum_{t \in C_q} |t - md_q| \quad (1)$$

Where $e \rightarrow$ Mean squared error

$K \rightarrow$ number of clusters to be generated

$C \rightarrow$ represents a cluster

$t \rightarrow$ is a task in the cluster C_q

$md_q \rightarrow$ a mean value in the cluster C_q

Current error value is compared with the previous iteration error value. If the error is converged or there are no more changes in the cluster objects then the algorithm is stopped. The K-means clustering algorithm can be used in cloud environment for grouping similar type of complex tasks.

III. FCFS SCHEDULING ALGORITHM

FCFS is one of the simplest scheduling algorithms used for scheduling tasks from the task ready queue. It is commonly referred to as First-Come-First-Serve scheduling algorithm. FCFS is used when all tasks are given similar priority. The working nature of FCFS algorithm is: it executes the tasks as their arrival order in the ready queue: i.e. as the FCFS name suggests, the task which comes first will get executed. FCFS has the property called FIFO (First-In-First-Out). The same original FCFS algorithm can be used to process the tasks by computational resources in the order of their presence in the cloud environment. Let us assume there are 15 tasks in the ready queue and 3 computational resources (virtual machines) in a cloud environment. By using FCFS algorithm, task1 is assigned to virtual machine1 and task2 is assigned to virtual machine2 and task3 is assigned to virtual machine3. When task1 is executed successfully then task4 is assigned to virtual machine1 and when task2 is executed successfully then task5 is assigned to virtual machine2. The same process is repeated until all tasks get executed. For this scenario, a total of 5 tasks

are assigned to each virtual machine on an average. Non-preemption and not having resources utilization in parallel are the common problems of FCFS. But FCFS is the simplest task scheduling algorithm for optimizing resources. There were papers [23] giving an analysis of scheduling algorithm with priority was done based on FCFS.

IV. PARTICLE SWARM OPTIMIZATION

One of the Bio-Inspired Optimization algorithms is Particle Swarm Optimization (PSO) algorithm. As the name suggests, PSO simulates the behavior of birds in the process of searching for food. The birds follow a certain strategy to search for food. The strategy which takes less time to search for food is called a best strategy. In PSO algorithm, bird strategies are called as particles. Each strategy is assigned a fitness value. Depending upon the application, the particle which has an optimum fitness value is treated as an optimum solution to the given problem. The algorithm starts with a set of particles. Fitness values are calculated for all particles in each iteration. For each iteration, two values are updated. First one is 'pbest' and the second one is 'gbest'. 'pbest' is personal best position of each particle and 'gbest' is global best position of particles so far in all iterations. From the next iteration, particle positions and velocities are updated with the help of previously calculated best values as shown in the equations (2) and (3).

$$UV[] = UV[] + l_1 * rand() * (pbest[] - current[]) + l_2 * rand() * (gbest[] - current[]) \quad (2)$$

$$current[] = current[] + UV[] \quad (3)$$

where

$UV[] \rightarrow$ array of updated velocities of particles

$current[] \rightarrow$ array of current positions of particles

l_1 and $l_2 \rightarrow$ learning factors, usually value 2 is taken to both the factor variables

$rand() \rightarrow$ random function which takes values between 0 and 1

The above process is repeated up to a maximum number of iterations or up to the optimal solution is converged. The same PSO approach can be mapped to cloud task scheduling problem for obtaining an optimal solution. The assignment of cloud tasks to virtual machines is considered as a particle. The time it takes to execute tasks by respective virtual machines is considered as a fitness function. The position of particles is the placement of tasks to the virtual machines. Better optimal solution can be obtained using PSO approach compared to FCFS algorithm.

V. METHODOLOGY

One of the main problems in cloud computing environment is the task-scheduling problem. The task-scheduling problem is mainly concerned about the mapping of application tasks and computing resources in order to achieve the balanced work load and efficient execution of application tasks using the limited resources. There are different task-scheduling algorithms that can be adopted, but suitable to the situation. There were many surveys done on task scheduling

[24, 25, 26]. Selecting the best scheduling policy is the prime concern. Based on this scheduling policy, the application tasks can be mapped to the computing resources and then executed. The scheduling goal assumed in the proposed algorithm KPSOW is the minimization of task completion time. KPSOW makes use of the strengths of both the K-means and PSO algorithms with the inclusion of weights concept. The working behavior of KPSOW is shown in Fig. 1.

The basic idea of proposed work is separating the cloud tasks into low complexity tasks and high complexity tasks and assigning low complexity tasks to low performance computing resources and high complexity tasks to high performance computing resources, thereby makespan of the scheduling tasks can be reduced. Let us consider there are N number of tasks $T_1, T_2, T_3, \dots, T_N$ and M number of computing resources $VM_1, VM_2, VM_3, \dots, VM_M$ in a cloud. Here the tasks can be considered as cloud tasks and computing resources can be considered as virtual machines (VMs). Let the lengths of tasks be $TL_1, TL_2, TL_3, \dots, TL_N$, and performances of virtual machines be $VMP_1, VMP_2, VMP_3, \dots, VMP_M$. By using the length of each task, total cloud tasks are separated into two separate groups by calculating the Euclidian distance between them. K-means algorithm is used for separating the cloud tasks into groups. Let the generated groups be C1 & C2 and number of tasks in each group be $nc1$ and $nc2$. Later find out the weights for each cluster using the equation (4) equation (5).

$$WC1 = \sum_{i=1}^{nc1} TL_i \quad (4)$$

$$WC2 = \sum_{i=1}^{nc2} TL_i \quad (5)$$

where WC1 → weight of cluster1
WC2 → weight of cluster2

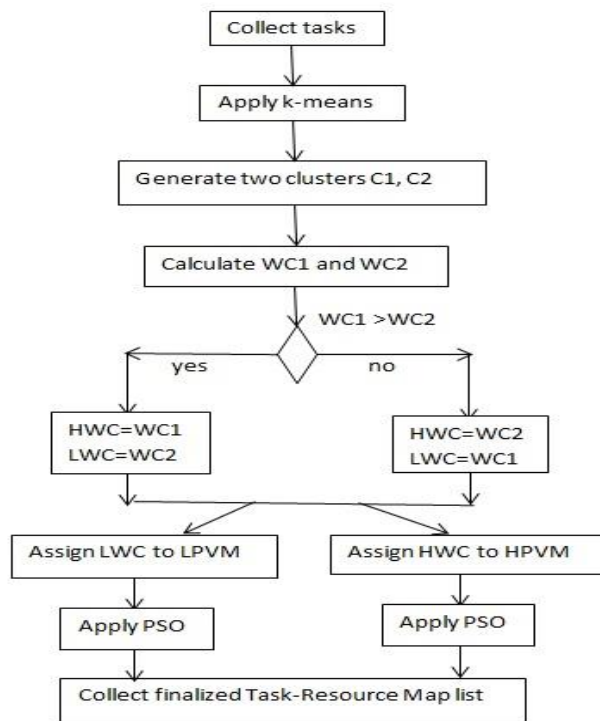


Fig. 1. Working Nature of Proposed KPSOW.

Now compare the weights generated from equation (4) & (5) and assign low weight value to Light Weight Cluster (LWC) variable and high weight value to Heavy Weight Cluster (LWC) variable. LWC represents the low complexity tasks group and HWC represents the high complexity tasks group. Next step is assigning low complexity tasks group to low performance VM (LPVM which are low VMP machines) and high complexity tasks group to high performance VM (HPVM which are high VMP machines). At last, do schedule tasks from LWC group to LPVM and HWC group to HPVM by minimizing the makespan using the algorithm PSO. PSO has been implemented as explained in the section4. After running the PSO algorithm, the final Task-Resource Map list is collected. The final Task-Resource Map list is considered as the best scheduling solution for minimizing the makespan. Makespan is calculated by using the equation (6).

$$makespan = \sum_{TL \in VM_1} \frac{TL}{VMP_1} + \sum_{TL \in VM_2} \frac{TL}{VMP_2} + \dots + \sum_{TL \in VM_M} \frac{TL}{VMP_M} \quad (6)$$

where $VM_1 \rightarrow 1^{st}$ Virtual machine
 $VM_M \rightarrow M^{th}$ Virtual machine
 $VMP_1 \rightarrow 1^{st}$ Virtual machine performance
 $VMP_M \rightarrow M^{th}$ Virtual machine performance

The objective of proposed method is to find out the minimum makespan when cloud tasks are executed by the virtual machines in a cloud.

VI. EXPERIMENTAL RESULTS

Cloudsim simulation tool has been used for evaluating the performance of proposed KPSOW method. Simulation has been performed with a total of 5 virtual machines. These 5 virtual machines are grouped into two categories based on their performances. Assume that first three virtual machines (VM_1, VM_2, VM_3) are considered as low performance VMs and the last two virtual machines (VM_4, VM_5) are considered as high performance VMs. The constraint that is considered for low performance VMs is $VMP_1 < VMP_2 < VMP_3$ and for high performance VMs is $VMP_4 < VMP_5$. The constraint makes sure that less number of tasks is allocated to low performance virtual machines and more number of tasks is allocated to high performance virtual machines. Virtual machine performances have been taken in the range 500 to 600 MIPS and 1100 to 1300 MIPS for low performance VMs and high performance VMs respectively. Cloud task lengths are taken randomly in between 500 to 1000 MIPS. The proposed KPSOW method has been run for 50, 100, 150, 200 cloud tasks separately with all five virtual machines and makespan is compared with the existing methodologies FCFS (First come First Serve) and PSO (Particle Swarm Optimization). Comparison of makespan is shown in Table I and Fig. 2. Results show that KPSOW just took 12.64 sec to schedule 50 cloud tasks where as FCFS and PSO took 15.23 and 13.35 sec respectively. Similarly KPSOW took 23.45 sec to schedule 100 cloud tasks where as FCFS and PSO took 32.07 and 24.33 sec respectively. To schedule 150 cloud tasks, KPSOW took 33.23 sec where as FCFS and PSO took 45.25 and 40.59 sec respectively. At last KPSOW took 38.6 sec to schedule 200 cloud tasks where as FCFS and PSO took 57.47

and 47.81 sec respectively. The results show that KPSOW has done well in reducing the makespan.

The proposed paper has also tested the VM utilization percentage against the above said methodologies for all 50, 100, 150, 200 tasks separately. VM utilization percentage has been calculated using the equation (7).

$$P_{Vi} = \frac{t_{vi}}{T} * 100 \tag{7}$$

Where

P_{Vi} → represents the utilization percentage of i^{th} virtual machine

t_{vi} → represents the total tasks distributed to i^{th} virtual machine.

T → total tasks considered

Comparison of VM utilization in percentages is shown in Tables II to V and Fig. 3 to 6.

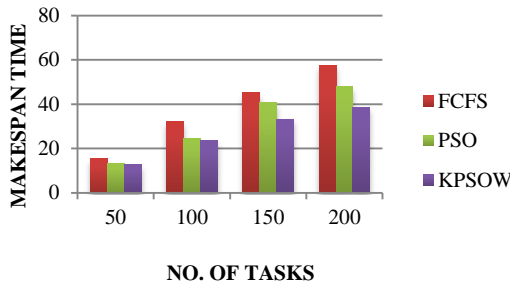


Fig. 2. Comparison of Makespan.

TABLE I. MAKESPAN COMPARISON VALUES

Techniques	No. of Tasks			
	50	100	150	200
FCFS	15.23	32.07	45.25	57.47
PSO	13.35	24.33	40.59	47.81
Proposed KPSOW	12.64	23.45	33.23	38.6

TABLE II. VM UTILIZATION IN % FOR 50 TASKS

Techniques	VIRTUAL MACHINE NUMBER				
	VM1	VM2	VM3	VM4	VM5
FCFS	20.0	20.0	20.0	20.0	20.0
PSO	26.0	16.0	10.0	4.0	44.0
Proposed KPSOW	16.0	28.0	56.0	24.0	76.0

TABLE III. VM UTILIZATION IN % FOR 100 TASKS

Techniques	VIRTUAL MACHINE NUMBER				
	VM1	VM2	VM3	VM4	VM5
FCFS	20.0	20.0	20.0	20.0	20.0
PSO	24.0	8.0	17.0	23.0	28.0
Proposed KPSOW	32.07	30.18	37.77	36.17	63.82

TABLE IV. VM UTILIZATION IN % FOR 150 TASKS

Techniques	VIRTUAL MACHINE NUMBER				
	VM1	VM2	VM3	VM4	VM5
FCFS	20.0	20.0	20.0	20.0	20.0
PSO	26.66	11.33	16	14.66	31.33
Proposed KPSOW	26.25	32.5	41.25	27.14	72.85

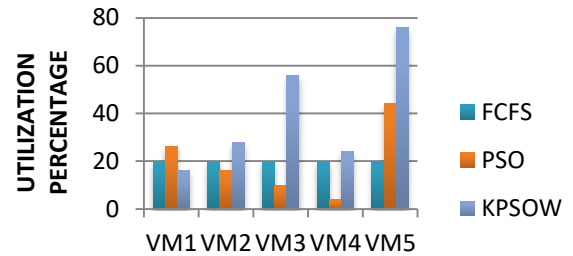


Fig. 3. Comparison of VM Utilization % for 50 Tasks.

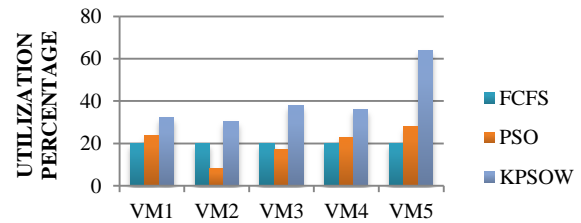


Fig. 4. Comparison of VM Utilization for 100 Tasks.

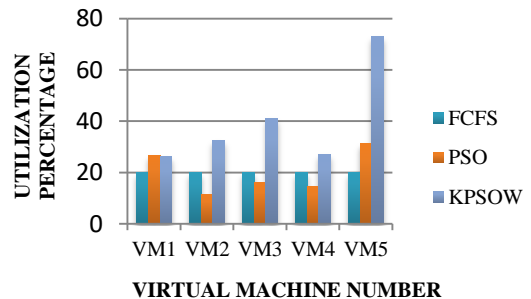


Fig. 5. Comparison of VM Utilization for 150 Tasks.

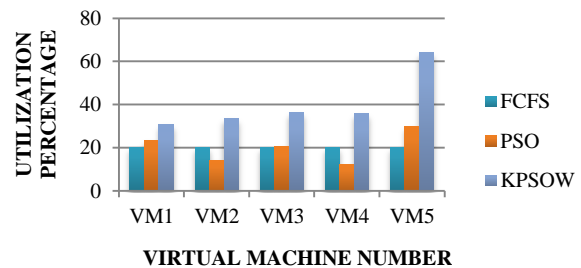


Fig. 6. Comparison of VM Utilization for 200 Tasks.

TABLE V. VM UTILIZATION IN % FOR 200 TASKS

Techniques	VIRTUAL MACHINE NUMBER				
	VM1	VM2	VM3	VM4	VM5
FCFS	20.0	20.0	20.0	20.0	20.0
PSO	23.5	14.0	20.5	12.0	30.0
Proposed KPSOW	30.55	33.33	36.11	35.86	64.13

Utilization figures state that KPSOW algorithm has utilized virtual machines with proper load balancing. The proposed algorithm has followed the initial constraint assumption. Results show that the number of tasks allocated to VM₃ is greater than VM₂ and VM₂ is greater than VM₁ in LPVMs & number of tasks allocated to VM₅ is greater than VM₄ in HPVMs for proposed KPSOW algorithm. PSO has better utilization ratio compared to K-means. So the proposed methodology effectively allocates less number of tasks to low performance virtual machines and more number of tasks to high performance virtual machines. Hence, KPSOW has given better utilization ratio for all virtual machines compared to FCFS and PSO methodologies.

VII. CONCLUSION

Task scheduling is an effective way of scheduling for getting tasks executed faster in cloud environment. Scheduling tasks with a clustering approach is one of the ways of ordering jobs in cloud environment for effective execution. The proposed KPSOW algorithm is the one such method. KPSOW has effectively used cluster weights concept for forming low complexity and high complexity task groups. KPSOW can be used in a cloud when there is more number of cloud tasks with varied complexities. Results are stating that KPSOW has made remarkable changes in reducing the makespan and also improves the utilization of computational resources when compared to the earlier methodologies. KPSOW shows simplicity in executing complex tasks in a speedy way and will be helpful to the society where the reliable cloud environment is required.

REFERENCES

[1] M. Kashani and M. Jahanshahi, "Using simulated annealing for task scheduling in distributed systems," in Computational Intelligence, Modelling and Simulation, 2009. CSSim '09. International Conference on, sept. 2009, pp. 265–269.

[2] C.N. Hoefler and G. Karagianni, "Taxonomy of Cloud Computing Services", IEEE 2010.

[3] F. Baroncelli, B. Martini and P. Castoldi, "Network virtualization for cloud computing", annals of telecommunications-Annales des télécommunications, vol. 65, (2010), pp. 713-721.

[4] T. Dillon, C. Wu, and E. Chang, "Cloud computing: issues and challenges", in Advanced Information Networking and Applications (AINA), 2010 24th IEEE International Conference on, (2010), pp. 27-33.

[5] Maricela-Georgiana Avram (Olaru), "Advantages and Challenges of Adopting Cloud Computing from an Enterprise Perspective," The 7th International Conference Interdisciplinary in Engineering (INTERENG 2013).

[6] Chaima Ghribi, Makhlof Hadji and Djamal Zeghlache, "Energy Efficient VM Scheduling for Cloud Data Centers: Exact Allocation and Migration Algorithms", In 13th IEEE/ACM International Symposium on Cluster, Cloud and Grid Computing (CCGrid), IEEE, pp. 671–678, (2013).

[7] R. Lee and B. Jeng, "Load-balancing tactics in cloud", in Cyber-Enabled Distributed Computing and Knowledge Discovery (CyberC), 2011 International Conference on, (2011), pp. 447-454.

[8] N. J. Kansal and I. Chana, "Cloud load balancing techniques: A step towards green computing", International Journal of Computer Science Issues, vol. 9, no. 1, pp. 238–246, 2012.

[9] Ramezani, F., Lu, J., Hussain, K., "Task-Based System Load Balancing in Cloud Computing Using Particle Swarm Optimization", Journal of Parallel Programming 42, 5, 739-754, 2014.

[10] Priyansh Srivastava, Bhavesh Gohil, and Dhiren Patel, "Load Management Model for Cloud Computing Using Cloudsim", International Journal of Computer Theory and Engineering, Vol. 9, No. 5, October 2017.

[11] Chenhong Zhao, Shanshan Zhang, Qingfeng Liu, Jian Xie, Jicheng Hu, "Independent tasks scheduling based on Genetic Algorithm in Cloud Computing", 978-1-4244-3693-4/09/\$25.00 2009 IEEE.

[12] GAN Guo-ning, HUANG Ting-lei, GAO Shuai, "Genetic Simulated Annealing Algorithm for task scheduling based on Cloud Computing Environment", 978-1-4244-6837-9/10/\$26.00 2010 IEEE.

[13] S. Pandey, L. Wu, S. Mayura Guru, R. Buyya, "A particle swarm optimization-based heuristic for scheduling workflow applications in cloud computing environments," 24th IEEE international conference on advanced information networking and applications, PP 400-407, 2010.

[14] Lizheng Guo, Guojin Shao, Shuguang Zhao, "Multi-Objective Task Assignment in Cloud Computing by Particle Swarm Optimization", 978-1-61284-683-5/12/\$31.00 2012 IEEE.

[15] Ali Al-maamari and Fatma A. Omara, "Task Scheduling Using PSO Algorithm in Cloud Computing Environments", International Journal of Grid Distribution Computing Vol. 8, No.5, (2015), pp.245-256.

[16] Masdari, M., Salehi, F., Jalali, M., Bidaki, M., 2016. "A Survey of PSO-Based Scheduling Algorithms in Cloud Computing", Journal of Network and Systems Management 25, 1, 1-37.

[17] K. Li, G. Xu, G. Zhao, Y. Dong, and D. Wang, "Cloud task scheduling based on load balancing ant colony optimization," in Chinagrid Conference (ChinaGrid), 2011 Sixth Annual, aug. 2011, pp. 3–9.

[18] X. Lu and Z. Gu, "A load-adaptive cloud resource scheduling model based on ant colony algorithm", in Cloud Computing and Intelligence Systems (CCIS), 2011 IEEE International Conference on, (2011), pp. 296-300.

[19] Khan, S., Ahmad, A., "Cluster centre initialization algorithm for kmeans clustering", Pattern Recognition Lett. 25, 1293–1302, 2004.

[20] A M Fahim, A M Salem, F A Torkey, "An efficient enhanced k-means clustering algorithm", Journal of Zhejiang University Science A, vol. 10, pp. 1626-1633, July 2006.

[21] Lloyd, S. P. (1957). "Least square quantization in PCM". Bell Telephone Laboratories Paper. Published in journal much later: Lloyd, S. P. (1982). "Least squares quantization in PCM" (PDF). IEEE Transactions on Information Theory. 28 (2): 129–137.

[22] E.W. Forgy (1965). "Cluster analysis of multivariate data: efficiency versus interpretability of classifications". Biometrics. 21 (3): 768–769. JSTOR 2528559.

[23] Ms. Rukhsar Khan, Mr. Gaurav Kakhani, "Analysis of Priority Scheduling Algorithm on the basis of FCFS & SJF for Similar Priority Jobs", International Journal of Computer Science and Mobile Computing, Vol.4 Issue.9, September- 2015, pg. 324-331.

[24] Raja Manish Singh, Sanchita Paul, Abhishek Kumar, "Task Scheduling in Cloud Computing: Review", (IJCSIT) International Journal of Computer Science and Information Technologies, Vol. 5 (6) , 2014, 7940-7944.

[25] P.Nagendra Babu1, M.Chaitanya Kumari, S.Venkat Mohan, "A Literature Survey on Cloud Computing", International Journal of Engineering Trends and Technology (IJETT) – Volume 21 Number 6 – March 2015.

[26] P. Akilandeswari and H. Srimathi, "Survey and Analysis on Task Scheduling in Cloud Environment", Indian Journal of Science and Technology, Vol 9(37), DOI: 10.17485/ijst/2016/v9i37/102058, October 2016.

How Volunteering affects the Offender's Behavior

Agent-based Modelling and Simulation

Momina Shaheen¹, Tayyaba Anees², Muhammad Imran Manzoor³
School of Systems and Technologies
University of Management and Technology
Lahore, Pakistan

Shuja Akbar⁴, Iqra Obaid⁵
Department of Computer Science
COMSATS University Lahore Campus
Lahore, Pakistan

Aimen Anum⁶
Department of Computer Science
COMSATS University Islamabad, Sahiwal Campus
Sahiwal, Pakistan

Abstract—Agent Based modelling is widely used for presenting and evaluating a social phenomenon. Agent based modelling helps the researcher to analyze and evaluate a social model and its related hypothetical theories by simulating a real situation. This research presents a model for showing the behavior of an offender that is greatly influenced by volunteering of people on the offending tendencies. It is observed that how the offending behavior of someone urges others to do the same criminal act or violation of norms. And how can volunteering make the offender feel shameful of his doings and motivate others to volunteer in likewise situation in future. An agent based Model is presented and simulated to evaluate and validate the conceptualization of presented social dilemma. This model is simulated by asking some questions with exacting focus on the offending behavior of an agent. This study evaluates all the simulated results from the presented model to describe theoretical foundation spreading of offending or criminal behavior. Moreover, it validates the role of volunteering in the decrement of offending tendencies of the people as it presents an understandable situation in which offending of someone increases the offending tendencies of audience. Moreover the results of this research show that the volunteering decreases the offending tendencies of not just offender but also of the audience.

Keywords—Offender's behavior; spreading of criminal behavior; agent-based modelling; simulation; norm violation; criminology

I. INTRODUCTION

ABM (Agent based Modeling) is a computational technique consisting of agents (autonomous decision making entities); communicating with one another in the neighborhood [1]. It directs the interaction between micro-level behavior and heterogeneous agents. Agent behavior is usually a set of rules that you need to follow to make a decision considering their interactions and environmental observations [2].

Agent based Modeling is used to perform pseudo-experiments, representing the mutual interaction and behavior of an agent. It provides the understanding of the reasons, causing the appearance a widespread phenomenon and the emergence of a variety of behavioral aspects in a population, hence validating the hypothetical fundamentals of this.

Considering these uses Agent based Modeling is an accommodating tool to study the surfacing of customs and norms in a society [3]. Agent based Modeling has been implemented in social settings to examine the various perspectives affecting the crimes [4].

In Agent base modeling, criminologist research investigates some vicious crimes like street robbery, civil violence, etc. using ABM approach [5]. To investigate spatial-temporal aspects of crime, Agent based Modeling is exercised with focus on spatial and behavioral aspects of crime. Based on diffusion of status of some places the model showed in [6] investigates the dynamics of crime places. On behavioral point, the relation among the behaviors of targets, offenders and the guardians is simulated through Agent based Modeling.

Offender makes a decision individually which assesses a situation and attempts to maximize the outcome of his actions [7][8].

In [9], the behaviors of offenders and the targets with respect to areas of crime are simulated on the basis of usual actions and theories, the fallouts of simulations are validated against actual facts. The criminologists have examined a variety of aggressive crimes like street robberies [10][11], civil violence [12][13] and gang rivalries [14] with the help of Agent based Modeling. Similarly, various research studies have also been performed on the reaction of society to a criminal activity, which keep up a correspondence to the spreading of norms in society [4]. The bystanders' effect [4], which abstain a person from volunteering against a criminal act which he observes, is another example of such situations. Some possible reasons for such a behavior diffusion of responsibility, social influence, and audience inhibition are illustrated in [4] with reference of [15]. By the presence of audience, person neglects his decision of volunteering owing to possibility of misinterpretation of the condition ensuing into an embarrassment as people do not want to disagree with the whole group [16]. In appendage to that, individuals are changed by others. When she realizes others not interceding, she also organizes alike. The third feature is also associated with the Volunteer's dilemma (VD) shown by Diekmann [17]) as It is considerable that someone volunteers, but it is best if that is not me", therefore, shifting the concern

from own shoulders to the others. Observing these factors, it is habitually discussed that the viewer's inhibition and the social impact are values of diffusion of responsibility.

Hereafter, in some literature, the volunteer's dilemma is grasped as a result of the diffusion of responsibility, in which number of individuals in a bystanders group is inversely proportional to volunteering [18][19]. In practical conditions, the VD does not always assure negative result. People volunteer so frequently. It is proven in [18] that cooperative behavior in humans is obsessed by many characteristics of social communication, including the aspects strongly unified with the cognitive performance of guilt, like reciprocal altruism" and conflict resolution".

Guilt, ultimately, is less destructive and more adaptive [20]. Guilt is a negative value ensuing due to irregularity among the adopted and desired behavior. Hence, to get rid of guilt and act correctly, it may lead to an altruistic volunteering from a person, in conflict situations necessitating a supportive decision making. In fact, responsibility is guilt's function [21][5][22]. In other words, volunteering in the VD can be ensured, if an individual efforts to be accountable to get rid of guilt. Results of a careful investigation of the VD have exposed that 'no-intervention' owed by bystanders' effect frequently approaches to guilt which, as significance, encourages the applicants to volunteer [18]. Analytical model of volunteering is not delivered in study. A model of volunteering, having supporting on three human conduct theories is presented by (Gerritsen, 2015). Though, this model shows a distinguished, but simplistic example of presentation of social theories within agent's behavior, it is limited to two dimensions. First, supports a single volunteer. Second, does not deliver any specification of offender behavior.

A. Problem Statement

Volunteering of a person is very important in the situation of norm violation as it can lead to the public good. The problem that is to be discussed in the study is when the population of people would decide to intervene in the certain situation of norm violation in the presence of the factors of a person's perception (bystanders, cost of intervention, audience inhibition, seriousness of the norm violation) and how the volunteering of a person(s) can accelerate or stop the violation themselves. And if there is a need of multiple people to intervene in a certain condition then how the situation can become. Moreover, there is a need to find the emotional effect on the people witnessing norm violation and on the offender. Does offender get ashamed when people stop him from such act of if no one volunteers and if anyone one volunteer but he is not enough to stop that act then how it will encourage or urge the offender to do that act again in future. Similarly if people who have some tendency to violate the norm or have offending tendency then to which extent they get influenced by the offender or volunteer.

B. Scenario and Motivation

Social dilemmas are the circumstances in which an individual's optimal behavior conflict with the group's optimal decision [23], in other words social dilemma is a condition in

which a person prefers its self-interest unless whole population chooses the selfish option and the whole group loses. Problems occur when the whole population chooses to practice personal profit and instantaneous satisfaction rather than perform in the groups long-term. Repeated interactions which allow punishment, reciprocation and reputation effect are used to be the solution of these social dilemmas [24]. In these situation individuals can either be cooperators or defectors. A cooperator pays cost of participating in public good but defectors desist from doing so.

If a criminal activity is taking place and no one intervene or call the police then the crime won't be stopped hence the witnesses fail the victim and the moral and legal norms. Such a dilemma is called Volunteers Dilemma. The public goods are achieved when a volunteer intervene in a norm violation in order to stop the criminal activity. But if nobody volunteers then it may harm the victim of that situation. These unfortunate situations do not happen just in exercise but also in the reality such as the murder of Kitty Genovese (1964).

There are some other situations where more than one volunteers are needed to resolve a conflict. In that scenario, if there are lesser number of volunteers than needed volunteers, then the situation get totally changed as the offender(s) may feel more powerful or volunteers get disappointed. Another outcome in this scenario can be that number people who are required to volunteer may not be fulfilled but the volunteers are sufficiently enough then the offender will get ashamed over his doing or may not dare to do that again. The worst outcome of this scenario can be that if there are many observers seeing that criminal activity but no one volunteers, then the offender will have no regret or shame, moreover the people in the audience can get inspired from this situation and they can also get involved in similar situations. Hence it could lead to the spreading of dishonesty [25][26][27][6].

C. Research Objectives

The core objective of this research is to study the effect of volunteering on the offender and the emotional guilt in the bystanders mind by incorporating a model of volunteers in a norm violation in the field of Agent-based Modeling (ABM) that will help answer the questions mentioned in Table I.

This study will also discuss the emotional effect on the bystanders, offenders and the volunteer. This would help to understand the whole behavioral model extensively. And how these emotional effect will motivate them to do something for public good in future.

TABLE I. RESEARCH QUESTIONS

No.	Research Questions
RQ1	What if there are not enough volunteers that are required to stop the norm violation?
RQ2	What is the impact lesser volunteer on the offender and people?
RQ3	How can volunteering refrain offenders from violating the norms?
RQ4	What is the emotional impact of volunteering on offenders?

II. LITERATURE REVIEW

On the area of Norm Violation and its spreading, Volunteer Dilemma, Agent-Based models, guilt and offender behavior a lot of literature is available and for this study. In this chapter a selected literature is included for understanding the area and background of the problem.

A. Norm Violation and Offender Behavior in VD

If we want to determine the reasons why norm violations took place then one reason can be that some social norm violations trigger more norm violations. For instance people don't bother to return the shopping carts if they see others doing the same. Similarly if people see an offender beating a person and no one oppose him then they can do the same in future. This reason of spreading of norm violation is also discussed in [25]. They developed an experimental design (dice experiment) to understand the dynamics between information, beliefs and co-evolution of norms by observing prevalence of norms, accuracy of beliefs and offsetting dynamics of traced social behaviors. Diekmann et al. in [28] also use this approach of Dice experiment to determine the spreading of norm violation. But [25] extended the experiment to an extent of 12 dice reports to overcome the weakness of magnitude of latter experiment. And this experiment shows that the stabilization or decay of social norms is based on the subjective beliefs of norm violation in the population.

Hill et. al. performed an empirical experiment to reveal the breaking of norm. The study presents experiment conducted to know that serving non reciprocal behavior influence individual or not. It includes experiment design which consisted of three features. First is studying behavior by iterated trust game. Second is mover's decision of reciprocity. Final is extrinsic changes to see the impact of observed behavior on personal decision making. And the hypotheses that are presented in the paper are: a) detected behavior of others has impact on behavior, b) being observed effects. The conclusion drawn in their paper are foreign shocks to observe people inspiring others to depart, thus, rewarding can benefit reciprocity.

Matthew T et al., investigated the supposition that a person's own self-regulation is a significant internal system that enables people to alter their behavior to follow rules [29]. They performed six studies in [29]. The first study shows whether small self-control would lift the chance that group would violate the ethical norms. It appears believable that self-control allows people to behave ethically. Two studies confirm a relation among low self-control and morally wrong behavior. Entirely, two pilot studies proposed that depleted self-control might influence one to involve in immoral behavior. The purpose was to develop a decision by working and measuring consequent willingness to take moral risks. The results of this study confirmed that the decrement of self-control would result in violation of people towards social norms such that reduction would lift moral risk-taking. In second study a behavioral measure was used to measure the possibility of violating societal norms. Authors expected that small self-control would enhance the propensity to break social norms. Outcomes of this study shows that subjects with low self-control would use more swear words than the subjects with high self-control and the less self-control to the breaking the rules of societal norms. In

third study, subjects finished the identical intersection of these tasks. Then subjects in favor condition received a favor, while those in the no-favor condition did not. Subjects were more expected to do a favor for the researcher when the researcher does a favor for them. They projected that reduction would decrease the chance that members would comply with norms of reciprocation. Depleted subjects failed to obey standards of reciprocity. Depletion decreased reciprocity nevertheless of if the norm was to execute or not. In fourth study the women were focused in self-control reduction condition and the words on screen were ignored. Members in the no reduction state were enquired to lookout a video as they watch usually. At the end definite that reduction would lift the chance that contestants would break up the trial regulation. Thus, self-control reduction leads the participants to disobey a social regulation. In next study they assumed that the members with low self-control would inadequately follow these directions in contrast with those members that are high in trait self-control. Therefore, members with high self-control pursued the speech alteration practices additional realistically than persons with low self-control. In the final study the subjects who perform better in the Study 5 ought to track the exercise directions more devotedly than individuals who do poorer. So the subjects with low self-control practice their exercise directions less devotedly than members great in self-control. Hence, the comparative deficiencies were found self-control was connected to straight cause of breaking the social rules. Authors have recognized that obedience can develop hurtful behavior. Corporations are hard to see without obedience successfully. A weak self-control among members can pay to a weakening of the social fabric.

Another investigation to judge crime activities and lies was done in [30]. The goal of this investigation was to explore behavioral consequences of dark traits. Correlation analyses were used to investigate relation between dark traits and result variables of misconduct and high stakes lying. A sample of 464 undergraduates participants from North America (age: 16-42 yrs., males: 131, female: 333) were selected. Comprehensive Misconduct Inventory (CMI) of 58 items was used to measure tendency to involve in misconduct behaviors. CMI consisted of seven sub-scales such as Hard/Soft drug-abuse Minor/Serious Criminality, Harassing, Driving misconduct, Anti-authority misconduct. Authors used PTQL (Propensity to Lie Questionnaire) to calculate the degree to which people slot in in high stake dishonesty. They collected an online survey and the participants are asked for a self-report. And the result of this study which was collected in one hour shows that men are more engaged in misconduct than women. A positive and significant relation was found between Dark Traid variables and CMI subscales as Misconduct variables were individually regressed on 3 dark Traid variables.

The Goal Firming theory for BWT not only persuades the social rules but all legitimate rules [27]. A controlled experience was conducted to test this theory. All the subjects in experiment were at least 18 years old. For the 1st study, the experiment was conducted in shopping area mostly used to park bicycles. Out of 77 subjects 33% were in order condition while 69% in disorder condition. The 2nd study was conducted to determine the influence of cross norm inhibition on serious

norms. 44 participants were in order while 49 were in disorder condition. In 3rd study, the participants who returned the shopping carts were in order while the others who don't were in disorder. The results of study three shows that 30% were in order and 58% were in disorder condition. 4th study focused on national law of fireworks and the 80% subjects were found in disorder condition. 5th and 6th study were based on stealing an envelope with €5 note was placed in mailbox. 5th study includes 60 participants and the mailbox was not covered but in study six participants were 72 and the mailbox was covered with graffiti. 13% were in order condition in 5th study and 25% in 6th study stole the envelope. Conclusions revealed that the effect was not restricted to social norms.

Gino et al. conducted two experiments to examine how social norms, saliency and cost benefit analysis encourage immoral behavior. In first experiment they examine the influences of confederate's identity [31]. Their laboratory experiment includes four conditions; a) control condition, b) shredder condition, c) in-group identity condition, and d) out-group identity condition. One hundred forty-one (79 male, 62 female) subjects with average age of 22 years participated in the experiment. The results revealed that subjects in the control condition showed the minimum number of properly solved matrices. Cheating in the shredder condition was raised by more than 50%. Cheating raised more in the in-group-identity condition and reduced in the out-group-identity condition. Their second experiment was conducted to determine the effects of saliency. It includes three conditions: a) control condition, b) the shredder condition and c) the saliency condition. Ninety-two pupils (49 male, 43 female) with average age of 20 years took part in this experiment. 15 to 17 subjects were assigned randomly to each of six sessions lasting 15 minutes. Results showed that number of matrices solved was lesser in control condition, greatest in shredder and intermediate in saliency condition. So they reach to the conclusion that effect of social norms can cause higher dishonesty if the saliency were reduced.

B. Use of Agent Based Models for Social Phenomena

Agent based modeling is vastly used technique and it is being popular now a days for computing and Artificial Intelligence (AI) [32]. Agent based modeling is used not only in computing and engineering field but also in a number of fields like Social Sciences, Bio Informatics, Life Sciences, Ecological Sciences, etc. [33][34][35]. In fact, for the scheduling and planning of manufacturing process the agent based techniques are used in [36][37]. Similarly it is used for simulating social actions [38] [39]. Because through ABM the hypothesis related to these fields can be tested empirically [40].

Somehow, the techniques of agent based modeling need some improvements that are discussed by Heath in [41] as well as it faces some challenges [42] [32]. But for the phenomena of social sciences it is quite appropriate to use existing techniques as it has been used since two decades. The complex phenomenon and social patterns are modeled by agent based tools [42]. However the techniques use some implicit methodological protocols and need a refined pattern for simulating social phenomenon. In [43], the authors introduced a three staged process for the establishment of this methodology.

Lemos et al. used Agent based Model of Epstein from civil violence against an authority with the agents "citizen" and "cops" to introduce the legitimacy feedback and to examine its effects [12]. They formulated some functions on the basis of legitimacy measurement to express the legitimacy in terms of variables consumed by the model. Two type of feedbacks they used, homogeneous (all agents have same perception) and heterogeneous (agents have different perceptions) perceived legitimacy. They found that in homogeneous legitimacy distant future performance of the system was unspecified but for diverse the time evolution of the system was initially calm then rebellion and after that successively intermittent peaks of rebellion. Their results represented significant improvement from their previous work in the aspect of soundness, explanatory power and simplicity.

Crime behavior changes with the advancement of technology hence in [44] authors argued that in crime fighting arsenal, mathematical models are valuable weapons. They discussed different techniques for crime fighting such as mathematical models numerical simulations, differential equations and agent based models with some empirical evidences and statistics. They reached to the conclusions that a multi-disciplinary approach is needed to build a model for crime. They proposed that multi-disciplinary approach can be division of work among sociologists, mathematicians and statisticians as the theory would be formulated by sociologists, mathematicians build a mathematical model and the statisticians made tools for the estimation of that model.

On the basis of reviewed literature the enough related information regarding to the area of the problem has been extracted. In the light of the literature it can be seen that there is some space of experimenting the multiple volunteering in the Volunteer's Dilemma, as this topic is always remained unfocused. Moreover, the guilt and shame is also discussed in norm violation and in this area of VD this can be implemented to find the positive outcomes (if any) on the Volunteering. The Offender is the one who offend, it can be seen that the offending and norm violating had bad impact on a society but how these can be controlled and how they affect the people. The spreading of dishonesty and crime are discussed in the literature, it can be find out if the volunteering or volunteering can play a role in this issue.

III. METHODOLOGY

This study aims to present the extended model of bystander effect presented in [4] to support the multiple interventions of the people in a certain situation where multiple interventions are needed. Guilt has a positive effect in the situation of Volunteer Dilemma. The model also incorporate the guilt of an individual that is the result of his/her own past experience as the booster to enhance the threshold so that individual have more tendency to volunteer. This research uses Model methodology in which the norm violation and the volunteer's dilemma (described in [17]) is presented with the help of the model depicting the situation. The model will be created and analyze through the ABM (agent-based modeling). The model will be tested in different scenarios, generated by the variations in the values of the factor affecting the crime situation. Data will be generated from those simulations by changing the

values of variables. These data gathered under different values of variables will be compared to reach some conclusions. This data will enable to find out the behavior and the emotional belief of the bystanders, volunteers and the offender. And we will see if the volunteering would avoid doing the offender from doing such norm violation or not. As long as the literature supports this methodology, testing procedure of this study is influenced by (Gerritsen, 2015). After seeing the effect of guilt on the agent that guilt is a positive factor to increase the volunteering tendency in an agent. There is a thought of seeing that what is the effect of volunteering on offender (norm violator) through embarrassment or realization of wrong doing? This will involve some effects from bystanders if the ratio of number of volunteer required and number of volunteers that actually volunteer is less than 1 it means not enough volunteer participated then number of volunteer will be compared with the number of bystanders. So we can say that either shame or urge of offending will be calculated by comparing the volunteering from two factors of required volunteer and bystanders.

Another model is described in this study that represent the behavior of the offender on volunteering and the effect of offending of someone on the other people who are seeing him doing that norm violation. This model is based on the spreading of criminal activities due to non-volunteering of people over norm violation. It represents a good platform to show that how offending tendency of people increased or decreased.

A. Offender Behavior Model

There are some evidences from the literature that if someone is involved in a criminal activity and no one took any notice against him then he is a source of encouraging others who have a tendency to do criminal activity [25][27][6]. Some field experiments shows that if some people don't return shopping carts or do illegal parking then others also get involved in doing the same activity [18]. This is how the dishonesty and wrong-doings spread with higher ratio among the people if everyone decides to be silent [26].

In this model (shown in Fig. 1) the offending tendencies of agents are calculated. In the start there is only one offender and then population increases gradually. The "Offending Tendency" rate is randomly selected for each agent from 0.1 to 0.9. Another constant is introduced in this model, k-constant; this constant is assigned different values on the basis beliefs and desires of the agents.

At the start the agent will observe the number of bystander (n) and the number of volunteer (m) and the Offending Tendency OT is randomly assigned to every agent. Here 37 the number of required volunteers (v) is also determined to have ratio of actual volunteers and required volunteers (i.e. m/v). There are two cases that will run through this model are:

CASE 1: If the ratio of volunteers and required volunteer is less than 1 (i.e. $m/v < 1$) then;

- a) If Offending Tendency (randomly assigned) is greater or equal to the ratio of volunteers and required volunteers (i.e. $OT \geq m/v$), then that particular agent will have desire to offend more and the value of k-constant will be given as -4 (i.e. $k=-4$).
- b) If Offending Tendency is less than the ratio of volunteers and required volunteers (i.e. $OT < m/v$), then the agent will have a desire to help due to the embarrassment and the k will be assigned the value '4' in this particular situation.

CASE 2: If the ratio of volunteers and required volunteer is greater or equal to 1 (i.e. $m/v \geq 1$) then;

- a) If Offending Tendency is greater or equal to the half of the ratio of volunteers and required volunteers (i.e. $OT \geq \frac{1}{2}(m/v)$), then the agent will have desire to relax some OT and the k-constant will be assigned by the value 2 (i.e. $k = 2$)
- b) If Offending Tendency is lesser than the half of the ratio of volunteers and required volunteers (i.e. $OT < \frac{1}{2}(m/v)$), then the agent will have increased motivation to help the victim and the k-constant will be assigned by the value 2 (i.e. $k = 1$).

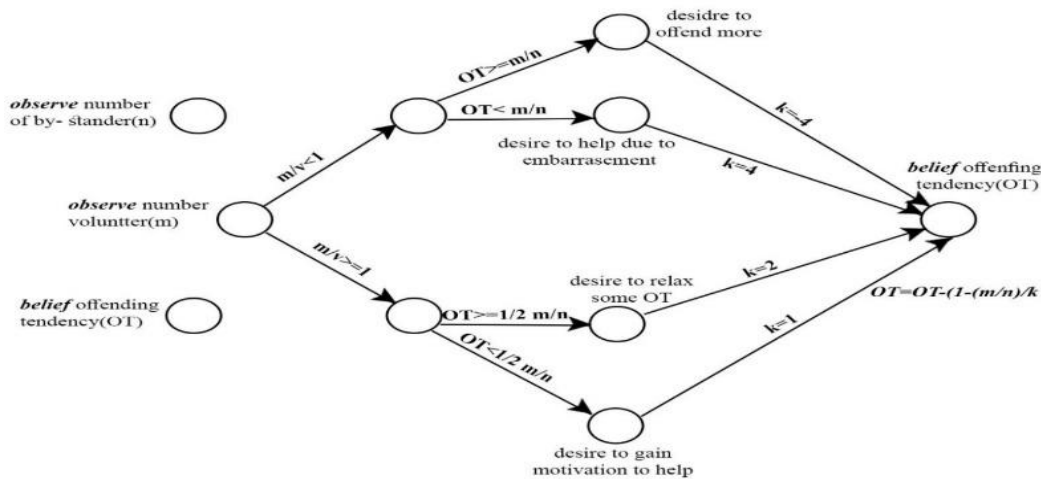


Fig. 1. Offender's Behavior Model.

At the end, for each case the value of Offending tendency is calculated on the basis of the values of 'k' and 'm/v' gained by each case separately through this formula $OT = (OT - (1 - (m/n)/k))$. this will be the solid value of OT, calculated for each agent separately, and this OT will be used for the next iteration.

IV. IMPLEMENTATION

In this study two models are presented in previous chapter the extended bystanders model and the model of offender behavior. These two models are needed to be implemented in some environment to examine the behavior of people. Examining these models there can be some hypotheses that are drawn on the basis of the research questions. Sometimes applying a situation on real environment and real people get a lot of time and attention as well as people perform artificially in such experiments so it lead to inaccurate results. It is nearly impossible to study all the people in the situation individually. Moreover, these types of experiments can lead the participants in real hazards. To get the results of our model with the absence of these issues the simulated environment are used.

A. Hypotheses

The following hypotheses can be drawn from the models on the basis of Research Questions shown in Table I.

H1. If there will be no volunteer or lesser than the required volunteers, which are required to achieve public good then the offending tendency of the offender would be increased.

H2. If there is sufficient volunteering to refrain the offenders from violating the norm then the offending tendency of the offender would be decreased and he will be shameful over his act.

H3. In the case of no-volunteering or minor volunteering the offending tendency of the others will also be increased (seeing that no punishment is given to the offender, the bystander will urge to violate that norm)

H4. If there will be sufficient volunteering then the not only the offender but also the bystanders will decrease their offending tendency.

To testify these hypotheses the model must be implemented on some simulated environment to get the accurate and precise results.

B. Simulation

In this study simulations are used to implement the presented models. Simulations are very appropriate for practicing this model as simulation techniques are used to implement the real environment situation in which getting results and doing analysis is difficult. Simulation is used to avoid expensive prototyping, testing, sensitive systems which are not able to bear extensive tests and performing experiments on real system is not possible because experiments are much time consuming than simulations (Rossetti et al. 2009). These Value, Time, Accuracy, Visibility and Versatility simulate real life without any effect on real objects.

There are many simulations tools that can be used to simulate the environment required for this research. But the model that is used for this study is NetLogo. NetLogo is a tool

used for simulating a real environment of a complex phenomenon with multiple agents. This programmable tool is capable of creating and simulating the behavior of multiple agents, event hundreds of agents can be simulated (Tisue and Wilensky, n.d.). This agent based simulating tool is helpful for simulating phenomenon of social sciences (Madey 2009).

C. Types of Agents

Several types of agents are used to simulate this complex phenomenon. These are the types of agents with descriptions

1) *Observer*: Observer is an agent who is observing the criminal act and thinking about whether he should intervene or not on the basis of his beliefs and desires. Observer agents are distinguished by Green color.

2) *Bystander*: Those agents who are present at the place where a norm violation is happening. These agents are distinguished by Blue color.

3) *Offender*: The agent who is violating a certain norm. Offender is distinguished by color Red and shape of a bug.

4) *Volunteer*: The agent who feels himself personally responsible and capable to do the intervention to stop the offender from violating the norm. Agent who has volunteered is distinguished by the grey color.

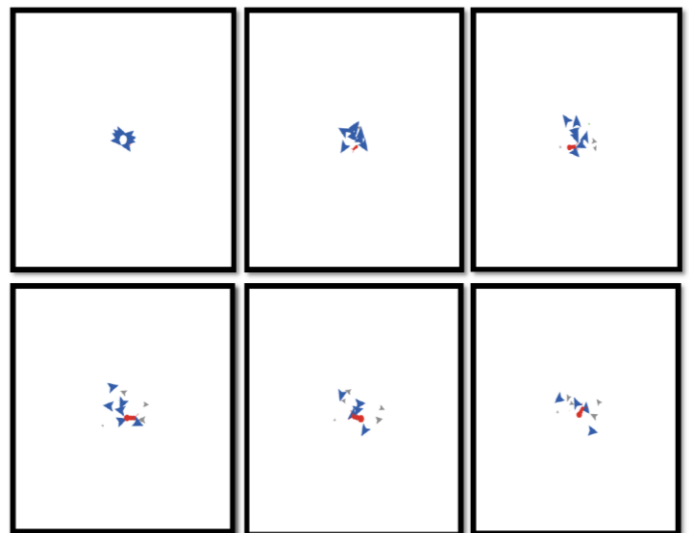


Fig. 2. Simulations Representing the Agents in a Controlled Environment.

D. Scenarios

In this study different scenarios taken for the execution of this model in order to fetch the results required for the validation of these hypothesis. These scenarios are taken on the basis of population with some variables described below:

1) *Offending tendency*: This variable is randomly assigned to each agent from 0.1 to 0.5. The offender is assigned with relatively high offending tendency.

2) *Desire of intervention*: A Boolean variable set true the value of accumulated variable 'x' is greater than the value of norm (normality).

3) *Capability*: A Boolean variable set true if the observer feels himself capable of doing the intervention.

4) *Intention*: A Boolean variable set true if the observer have desire to intervene AND feels himself capable of doing intervention.

5) *K*: is a constant value assigned on the basis of the desire of an agent to offend.

These were the significant variable used to implement this model on NetLogo. The whole model that is implemented in the NetLogo is described in the next chapter through ODD Protocol.

V. AGENT BASED DESCRIPTION USING ODD PROTOCOL

The ODD model (Overview, Design, Detail, described by (J. Gary Polhill 2008)) is used describe a model to enhance its completeness and readability of the model.

A. Overview

This Model is designed to present the volunteers' dilemma along with the offender behavior in which the guilt is incorporated with the multiple interventions of volunteering.

In this section the overview of the model that is implemented in Netlogo is presented by the terms of purpose of the model, state variables and process scheduling.

B. Purpose

The purpose of this model is to find the effect of guilt on the volunteering tendency of the agent and the effect of volunteering on the offending tendency of people and offender. If there are more bystanders the ratio of volunteering would be lesser due to increased audience inhibition and cost of intervention. Hence, the rate of volunteering and the number of bystanders are inversely proportional to each other. The model describes the phenomenon of spreading of norm violation by offending tendencies of people. And how the volunteering can reduce the spreading of these norm violations?

There are some factors in such phenomenon. The thresholds of seriousness (due to abnormality of the situation or the accumulated guilt of the observer from past experiences) then the observer will find him more responsible. The offending tendency of the offender would be increased if the volunteers will be lesser. The offending tendency of the offender would be decreased and he will be shameful over his act due to volunteering. If there will be sufficient volunteering then the not only the offender but also the bystanders will decrease their offending tendency. To testify these hypotheses the model must be implemented on some simulated environment to get the accurate and precise results.

C. State Variables and Scale

This model contains a large number of variables used to implement this model. Those variables with their brief descriptions are enlisted in Table II.

There are certain characteristics owned by the agents who exist in the current phenomenon. These characteristics are variant in the whole phenomenon. The BDI model is used as theoretical framework to describe the change in sensing of the agents. These characteristics are shown in Table III.

As the BDI model is used for this purpose to represent the beliefs, desire and interventions of an agent. The same agent may have different beliefs on how the situation is getting changed. So the various belief variables can be assigned to one agent, which are assigned by their corresponding values, as mentioned in Table IV.

As the belief of an agent get changed. Similarly, the agents have different desires on how the situation is getting changed and the variables of desire can be assigned according to their corresponding values. The properties of Desire of an agent are given in Table V.

All the phenomenon of Offenders bahvior is implemented in Netlogo for the simulation study of given agents (as shown in Fig. 2).

TABLE II. VARIABLE USED IN OFFENDER BEHAVIOR MODEL

<i>Variable</i>	<i>Brief Description</i>
agents{property: bystander}	The agents which will play the role of bystanders in the model.
agents{property: offender}	The agent who is violating a norm.
aggregate-off-tendency	Global variable. It shows the total accumulated offending tendency of the agents existing in the situation.
count-interveners	Global variable. Count the total number of interveners/volunteers
count-performed	Global variable. Count the total number of interventions.
current-intervener	Global variable. The agent who is volunteering currently

TABLE III. CHARACTERISTICS OF AN AGENT

<i>Characteristic Variable</i>	<i>Brief Description</i>
property	Shows the type of the agent whether it's a bystander or offender etc.
state	Describe the state or current action of an agent
observe	Determine what the agent observes.

TABLE IV. BELIEF PROPERTY OF AN AGENT

<i>Belief properties</i>	<i>Brief Description</i>
"Resource"	Boolean variable.
"capable"	Boolean variable.
"opportunity-for"	Boolean variable.

TABLE V. DESIRE PROPERTY OF AND AGENT

<i>Desire Properties</i>	<i>Brief Description</i>
"intervention"	Boolean variable. Set true if the agent has desire to intervene.
"no-need-of-intervention"	Boolean variable. Set true if the agent doesn't have desire to intervene.

```

to apply-rules-m2
  if (not stop-sim)[
    let k 0
    ask current-intervener[
      let n count neighbor-list
      if (n = 0) [set n 1]
      let m count neighbor-list with [perform_intervention = "yes"]
      let v crime-intensity
      ifelse (m / v < 1) [
        ifelse (offending-tendency >= m / n)[ set k -4 ] [ set k 4 ] ]
        [ ifelse (offending-tendency >= 0.5 * (m / n)) [ set k 2 ] [ set k 1 ] ]
        set offending-tendency offending-tendency - ((1 - (m / n)) / k) ]
      set k 0
    ask current-offender [
      let n count neighbor-list
      if (n = 0) [set n 1]
      let m count neighbor-list with [perform_intervention = "yes"]
      let v crime-intensity
      ifelse (m / v < 1) [
        ifelse (offending-tendency >= m / n)[ set k -4 ] [ set k 4 ] ]
        [ ifelse (offending-tendency >= 0.5 * (m / n)) [ set k 2 ] [ set k 1 ] ]
        set offending-tendency offending-tendency - ((1 - (m / n)) / k)
    ]
  ]
end

```

Fig. 3. Applying the Rules of Offender behavior Model in Netlogo.

D. Process Overview and Scheduling

In start the agents are created and the variables are initialized. The roles of the agent are assigned as offender or bystanders along with their random offending tendencies.

Then the seriousness is calculated on the basis of input variables. Then the agents walk and their roles get changed according to their sensing. The bystander agent can or cannot be the observer in next time and update its neighbor list. Then the rules of model 1 and model 2 are implemented. In the end for the refined output the graphs are drawn. This process scheduling of this model is simple and the scheduling and flow of processes in the model can be distinguished by a simple flow chart, given in Fig. 4. A chunk of code in Fig. 3 represents the rules of Offender's Behavior Model applied in NetLogo.

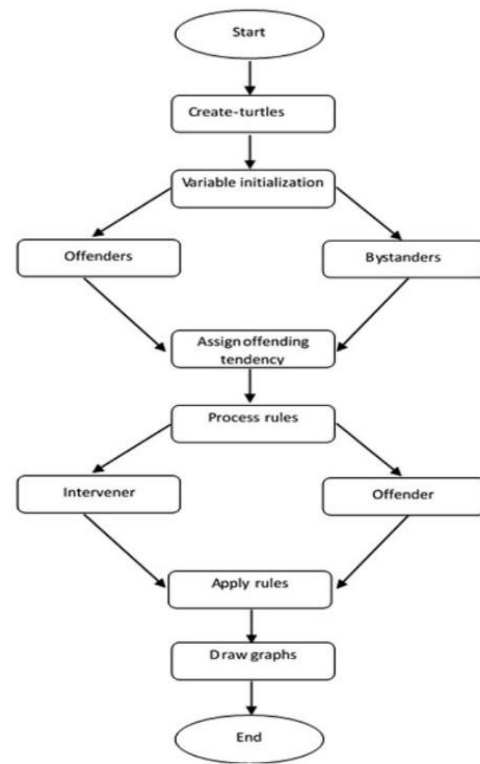


Fig. 4. Process Flow of the Whole Offenders Model used with Bystander's Model.

VI. SIMULATION ANALYSIS AND RESULTS

This Chapter shows the results fetched from the simulations that are run for some scenarios of the models.

A. Simulation Analysis

The implementation of this model is run for the 243 scenarios initially. Some of the interesting scenarios that answer the questions of our hypothesis are listed in Table VI below.

1) *Case 1:* In this case people are volunteering to achieve public good. People have a desire to intervene, so people are volunteering to stop this norm violation and the person who is violating this norm get ashamed over his doing and he can relaxes some offending tendency that is why the offending tendency is gradually decreasing. This case validates the hypotheses **H2**.

2) *Case 2:* More number of agents are required to volunteer and the situation is intense and serious, that's why the people volunteer and it lessen the offending tendency of the offending agent to 1.5 (as shown in Fig. 5(a) and Fig. 5(b)). This case validates the hypotheses **H2 and H4**.

3) *Case 3*: This is an interesting case depicting the effect of volunteering on offender. People are volunteering and we can see that the offending tendency of the agent has decreased to '0' (as shown in Fig. 5(c)) Therefore, he is not offender anymore (as shown in Fig. 5) that the offender has disappeared). This is because of increasing volunteering of the people (shown in Fig. 5(b)). This case testifies the hypotheses H2 and H4.

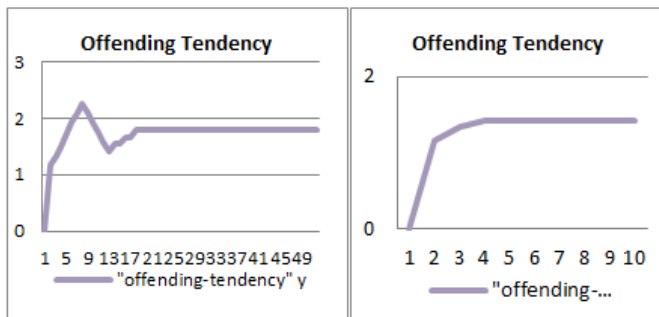
B. Results

After analyzing the cases and running the phenomenon with a large number of scenarios, the analysis of the whole problem can be done. The analyses were enough to answer all the research questions shown in Table I.

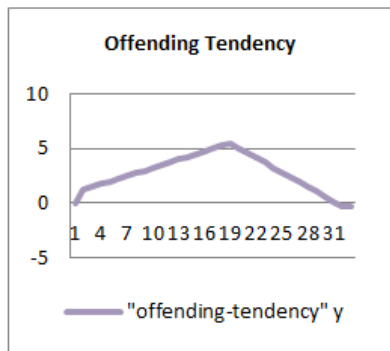
The scenarios, presented in the dissertation, satisfy all the hypotheses. And represent the volunteering can reduce the offending behavior among people. In all the cases where volunteering is performed the ratio of offending tendency decreases. Moreover it can also be seen that in more than 50% cases the offending tendency does not reduce due to no or lesser volunteering.

TABLE VI. SOME INTERESTING CASES

Cases	No of total Agents	Crime Intensity/Required No. of volunteers (v)	Radius
1	4	2	5
2	4	3	5
3	12	1	5



a. Case 1 b. Case 2



c. Case 3

Fig. 5. How Offending Tendency of the Agents Changes for Each Case.

Researcher and scholars have done a lot of work in this area of volunteering dilemma and presented different models of volunteering guilt and offender behavior. Agent-based modeling was also used by the researchers to present the behavior of agents in this situation of volunteering dilemma but the scenario of multiple volunteering was not as much focused as needed. These aspects add some interesting changes in the ratio of volunteering.

Another important contribution of this study is related with the behavior of offender and the effect of offending and non-volunteering on other persons. This study describes that through volunteering, offender get ashamed and its tendency of offending relaxes. But if there is no intervention from the observers of the crime act then he might not get ashamed and he will have urge to offend more. Moreover, this non-volunteering can urge other to do the same norm violation as they get influenced by the offender. In this way this research presents a reason of spreading of norm violation.

In practice, this research will be useful for observing the criminal behavior among people and to define new ways of investigating the ways these violations crimes can be reduced. Some ways have been described in this research such as practicing the ways which are significant to increase volunteering and the others are shame and guilt.

VII. CONCLUSION

The models presented in this research are agent based model representing a) the effect of offender's behavior on the others and on society, b) the volunteering as a factor to reduce offending behavior among people, in a crime situation. The presented model is formulated by using the outcomes of game-theoretic experiments, done on the VD.

The model is an extension of the models presented in (Lemos, Coelho, and Lopes, n.d.) and (Zia et al. 2016), and shares the similar results. It is drawn from results of this repetitive game that if the thresholds of seriousness (guilt is added in this) are increased then the participation of people in volunteering is increased. The observer in crime situation influenced by the audience and does not volunteer either due to the fear of embarrassment or due to diffusion of responsibility. The research study also validates the guilt as positive factor to increase the threshold, hence, increasing the tendency of a person to volunteer. This study elaborates the positive effect of volunteering upon the offending of a person or society. The results shows that the volunteering of people cause embarrassment to the offender and he would avoid offending afterwards.

VIII. CONTRIBUTIONS

Norm Violation, Volunteer Dilemma and Offending behavior are not new in the field of social sciences, a huge literature can be found on this area, presenting the different dimensions of volunteer Dilemma and different aspects of increasing the volunteering. Researchers have also studied the different factors affecting these issues such as, effect of bystanders, diffusion of responsibility, guilt, influence of people etc. (Zia et al. 2016). This research study is an attempt

to represent a model that elaborates how the Volunteering brings good in a society through decreasing the ratio of offending. If the offending ratio is increased then the spreading of the criminal behavior would be initiated and the society could suffer. In this research all the factors that can help to reduce the offending tendency are discussed.

REFERENCES

- [1] G. N. Gilbert and Sage Publications., Agent-based models.
- [2] T. R. Caskey, J. S. Wasek, and A. Y. Franz, "Deter and protect: crime modeling with multi-agent learning," *Complex Intell. Syst.*, pp. 1–15, Oct. 2017.
- [3] A. Diekmann and W. Przepiorka, "'Take One for the Team!' Individual Heterogeneity and the Emergence of Latent Norms in a Volunteer's Dilemma," *Soc. Forces*, vol. 94, no. 3, pp. 1309–1333, Mar. 2016.
- [4] C. Gerritsen et al., "Agent-based modelling as a research tool for criminological research," *Crime Sci.*, vol. 4, no. 1, p. 2, Dec. 2015.
- [5] K. Zia, M. Shaheen, U. Farooq, and S. Nazir, Conditions of depleting offender behavior in volunteering dilemma: An agent-based simulation study, vol. 9825. 2016.
- [6] T. Bosse and C. Gerritsen, "Social Simulation and Analysis of the Dynamics of Criminal Hot Spots," *J. Artif. Soc. Soc. Simul.*, vol. 13, no. 2, p. 5, 2009.
- [7] R. R. Brüngger, C. Kadar, and I. P. Cvijikj, "Design of an Agent-Based Model to Predict Crime (WIP)," *SummerSim-SCSC*, 2016.
- [8] D. B. (Derek B. Cornish and R. V. G. Clarke, The reasoning criminal : rational choice perspectives on offending.
- [9] L. Liu, X. Wang, J. Eck, and J. Liang, "Simulating Crime Events and Crime Patterns in a RA/CA Model," in *Geographic Information Systems and Crime Analysis*, IGI Global, IAD, pp. 197–213.
- [10] E. R. Groff, "Situating? Simulation to Model Human Spatio-Temporal Interactions: An Example Using Crime Events," *Trans. GIS*, vol. 11, no. 4, pp. 507–530, Aug. 2007.
- [11] E. R. Groff, "Simulation for Theory Testing and Experimentation: An Example Using Routine Activity Theory and Street Robbery," *J. Quant. Criminol.*, vol. 23, no. 2, pp. 75–103, Mar. 2007.
- [12] C. Lemos, R. J. Lopes, and H. Coelho, "On Legitimacy Feedback Mechanisms in Agent-Based Modeling of Civil Violence," *Int. J. Intell. Syst.*, vol. 31, no. 2, pp. 106–127, Feb. 2016.
- [13] C. Lemos, H. Coelho, and R. J. Lopes, "Agent-based modeling of social conflict, civil violence and revolution: state-of-the-art-review and further prospects.
- [14] R. A. Hegemann, L. M. Smith, A. B. T. Barbaro, A. L. Bertozzi, S. E. Reid, and G. E. Tita, "Geographical influences of an emerging network of gang rivalries," *Phys. A Stat. Mech. its Appl.*, vol. 390, no. 21–22, pp. 3894–3914, Oct. 2011.
- [15] B. Latan? and S. Nida, "Ten years of research on group size and helping.," *Psychol. Bull.*, vol. 89, no. 2, pp. 308–324, 1981.
- [16] F. Hoffmann, "Disliking to disagree," pp. 1–68, 2017.
- [17] A. Diekmann, "Volunteer's Dilemma," *J. Conflict Resolut.*, vol. 29, no. 4, pp. 605–610, Dec. 1985.
- [18] Guillaume De, "Guilt Aversion in the Volunteer's Dilemma," 1928.
- [19] P. R. Heck and J. I. Krueger, "Running head: SOCIAL PERCEPTION AND OUTCOME BIAS In press.," no. 401.
- [20] J. P. Tangney, J. Stuewig, and L. Hafez, "Shame, guilt, and remorse: implications for offender populations," *J. Forens. Psychiatry Psychol.*, vol. 22, no. 5, pp. 706–723, Oct. 2011.
- [21] "ResearchGate." [Online]. Available: [https://www.researchgate.net/publication/230026124_On_the_relationship_ip_between_responsibility_and_guilt_Antecedent_appraisal_or_elaborated_appraisal](https://www.researchgate.net/publication/230026124_On_the_relationship_between_responsibility_and_guilt_Antecedent_appraisal_or_elaborated_appraisal).
- [22] C. Bellemare, A. Sebald, and S. Suetens, "Heterogeneous guilt aversion and incentive effects," no. August, 2013.
- [23] M. ARCHETTI, "Cooperation as a volunteer's dilemma and the strategy of conflict in public goods games," *J. Evol. Biol.*, vol. 22, no. 11, pp. 2192–2200, Nov. 2009.
- [24] R. Conte, M. Paolucci, and F. Cecconi, "Trends in Social Science: The Impact of Computational and Simulative Models," in *New Frontiers in the Study of Social Phenomena*, Cham: Springer International Publishing, 2016, pp. 145–152.
- [25] H. Rauhut, "Beliefs about lying and spreading of dishonesty: undetected lies and their constructive and destructive social dynamics in dice experiments.," *PLoS One*, vol. 8, no. 11, p. e77878, 2013.
- [26] F. Gino, S. Ayal, and D. Ariely, "Contagion and Differentiation in Unethical Behavior: The Effect of One Bad Apple on the Barrel," *Psychol. Sci.*, vol. 20, no. 3, pp. 393–398, Mar. 2009.
- [27] K. Keizer, S. Lindenberg, and L. Steg, "The Spreading of Disorder," *Science (80-)*, vol. 322, no. 5908, pp. 1681–1685, Dec. 2008.
- [28] A. Diekmann, W. Przepiorka, and H. Rauhut, "Lifting the veil of ignorance: An experiment on the contagiousness of norm violations," *Discuss. Pap.*, 2011.
- [29] M. T. Gailliot, S. A. Gitter, M. D. Baker, and R. F. Baumeister, "Breaking the Rules: Low Trait or State Self-Control Increases Social Norm Violations," *Psychology*, vol. 3, no. 12, pp. 1074–1083, 2012.
- [30] N. Azizli et al., "Lies and crimes: Dark Triad, misconduct, and high-stakes deception," *Pers. Individ. Dif.*, vol. 89, pp. 34–39, Jan. 2016.
- [31] N. J. Raihani and R. Bshary, "The Evolution of Punishment in N-Player Public Goods Games: A Volunteer's Dilemma," *Evolution (N. Y.)*, vol. 65, no. 10, pp. 2725–2728, Oct. 2011.
- [32] M. Wooldridge and N. R. Jennings, "Agent theories, architectures, and languages: A survey," *Springer Berlin Heidelberg*, 1995, pp. 1–39.
- [33] M. Niazi and A. Hussain, "Agent-based computing from multi-agent systems to agent-based Models: a visual survey," *Scientometrics*, pp. 1–21, 2011.
- [34] V. Rai and A. D. Henry, "Agent-based modelling of consumer energy choices," *Nat. Clim. Chang.*, vol. 6, no. 6, pp. 556–562, 2016.
- [35] M. Sajjad, K. Singh, E. Paik, and C.-W. Ahn, "A Data-Driven Approach for Agent-Based Modeling: Simulating the Dynamics of Family Formation," *J. Artif. Soc. Soc. Simul.*, vol. 19, no. 1, 2016.
- [36] Weiming Shen, Lihui Wang, and Qi Hao, "Agent-based distributed manufacturing process planning and scheduling: a state-of-the-art survey," *IEEE Trans. Syst. Man Cybern. Part C (Applications Rev.)*, vol. 36, no. 4, pp. 563–577, Jul. 2006.
- [37] P. Leitão, "Agent-based distributed manufacturing control: A state-of-the-art survey," *Eng. Appl. Artif. Intell.*, vol. 22, no. 7, pp. 979–991, 2009.
- [38] K. Narasimhan, T. Roberts, M. Xenitidou, and N. Gilbert, "Using ABM to clarify and refine social practice theory," *Adv. Intell. Syst. Comput.*, vol. 528, pp. 307–319, 2017.
- [39] C. Castelfranchi, "Modelling social action for AI agents," *Artif. Intell.*, vol. 103, no. 1, pp. 157–182, 1998.
- [40] R. B. and F. Squazzoni, "Does Empirical Embeddedness Matter? Methodological Issues on Agent-Based Models for Analytical Social Science," 2005.
- [41] R. H. and F. C. Brian Heath, "A Survey of Agent-Based Modeling Practices (January 1998 to July 2008)," 2009.
- [42] J. Pavón, M. Arroyo, S. Hassan, and C. Sansores, "Agent-based modelling and simulation for the analysis of social patterns," 2008.
- [43] M. G. Richiardi, R. Leombruni, N. J. Saam, and M. Sonnessa, "A Common Protocol for Agent-Based Social Simulation.
- [44] J. Sooknanan, B. Bhatt FIMA, and D. M. Comissiong, "Another Way of Thinking: A Review of Mathematical Models of Crime," 2013.

Real Time RNA Sequence Edition with Matrix Insertion Deletion for Improved Bio Molecular Computing using Template Match Measure

Kotteeswaran C¹

Research Scholar,

Department of Computer Science and Engineering,
Bharath University, Chennai, Tamilnadu, India

Khanaa V²

Professor and Dean,

Department of Information Technology
Bharath University, Chennai, Tamilnadu, India

Rajesh A³

Principal

C.Abdul Hakeem College of Engineering and Technology
Melvisharam, Tamilnadu, India

Abstract—The RNA sequence editing has become a challenging task in the molecular computing. There are number of approaches that have been discussed earlier for the problem RNA editing in bio molecular computing, but they suffer to achieve higher performance. To improve the performance, an real time approach has been presented which uses sequence depth measure (SDM). The method receives the RNA sequence and estimates the depth measure for different sub sequences generated. Based on the SDM value, a cumulative sequence match measure (SMM) has been measured to classify the sequence towards the different classes available. The matrix insertion and deletion is performed based on the template match measure (TMM) which has been computed based on the matches found in the templates available for different classes. The experimental results of our approach prove to outperform in terms of Accuracy, Risk Detection Accuracy, Time Complexity and False Classification Ratio which in turn increases the performance of bio molecular computing and matrix insertion deletion.

Keywords—Bio Molecular Computing; RNA Sequence; SDM; SMM; Templates; TMM

I. INTRODUCTION

The modern society has higher influence on new type of diseases which cannot be predicted. Every day, the researchers found new type of diseases appear in the human anatomy. There are number of researches on going to identify the solution and cause for the disease identified. However, for any disease to be occur on human body has higher support of their DNA system. The gene present in the human body only supports the arrival of the disease. For example, when you look at the DNA sequence of cancer affected peoples, you can identify the presence of certain sequence in all the patients DNA sequence. So the particular sequence encourages the disease and by identifying the sequence and modifying they would reduce the risk of getting into the disease.

The bio molecular computing is the presence of analyzing the RNA sequence which has been generated from the DNA pattern towards different disease classes. The bio molecular computing has been carried out towards finding the solution for different diseases. In general, the RNA sequence is the collection of chain of proteins and molecules. By analyzing the sequence, first we can identify whether the sequence is complete or not and also it has no restriction for their length. However, the sequence should follow a pattern or template which represents the membership of the set of sequences. In most cases, the RNA sequence has to be identified for their incorrect sequence and has to be removed and modified to produce a new sequence called RNA editing.

To perform RNA editing, there are number of approaches available and the matrix insertion deletion system is one which represent the RNA sequence in form of matrix. On the matrix available, according to certain forms and rules, the new sequence can be added and the existing sequences can be updated or deleted for specific sequence identified as malformed. By adding and removing the sequence from the entire RNA sequence, the sequences belongs to the class can be tuned. Because the sequence has been used to identify the possibility of disease and to identify the sequence which has been encourages the disease, they has to be well classified. To perform such classification there are number of methods and measures available. This paper present a real time approach which uses the sequence match measure which has been measured based on the appearance of the gene sequences in the RNA sequences set of any class available.

To classify the RNA sequence, the sequence depth measure is used which has been computed based on the depth of similarity available between the tiny sequence and the entire sequence set. By computing the SDM measure, the depth of closure can be identified for each class which has been used to perform classification. On the other side, the TDM measure has been used to perform matrix insertion deletion, which has been computed based on the templates of

sequences available for the class. The comprehensive explanation on our approach is presented in Section III.

II. RELATED WORKS

Variety of methods are available for the classification and editing of RNA sequences. This section discusses various techniques that are specifically related to the problem of RNA editing.

The vital measure of insertion deletion system that are widely used in the literature are ambiguity and complexity measures [1]. Typically, we outline the many stages of ambiguity ($i=0,1,2,3,4,5$) for insertion-deletion systems. Then, we attempt to exemplify that there are characteristically i -ambiguous insertion-deletion languages which are j -unambiguous for the various mishmashes $(i, j) \in \{(5,4), (4,2), (3,1), (3,2), (2,1), (0,1)\}$. Further, we prove an important result that the ambiguity problem of insertion-deletion system is undecidable. Finally, we define three new complexity measures TLength – Con, TLength – Ins, TLength – Del for insertion-deletion systems and analyze the trade-off between the newly defined ambiguity levels and complexity measures.

On minimal context-free insertion-deletion systems [2], examine the type of context-free insertion-deletion systems. We know that such systems are common if the size of the inserted/deleted string is minimum three. We indicate that if this size is constrained to two, then the acquired systems are not common. We illustrate the acquired class and we bring together a new complexity measure for insertion-deletion systems which allows a well enlightenment of the acquired results.

Working with cells and atoms, an outline to Quantum [3], tends toward formal models of computability, we shall avoid over much “real” information to do with physics and biochemistry. The common approach we approve is to look to reality (whatever this means; passively, but safely, for us reality is what we can find in books and call such) in search of data supports (hence data structures) and operations on these data structures. With these constituents we can state a process (in the form of an arrangement of moves among configurations describing states of a system) which, provided that an input and an output can be linked with it, is considered a computation. The complete machinery is customized as a computing system.

Structured RNA rephrasing: Modeling RNA editing with guided insertion [4], study a model of string rephrasing based on the refined RNA editing mechanism found in trypanosome kinetoplasts. We establish simple properties of three main alternatives of this model which we indicate to form a strict order in terms of dramatic power. We also present a method and software for simulating real biological RNA editing via this model and apply the theoretical results to suggest real biological constraints on this process.

Grammatical methods in computer vision: An overview [5], examine several approaches and applications that have used grammars for solving inference problems in computer vision and pattern recognition. Grammars have been valuable since they are automatically easy to understand, and have precise sophisticated illustrations. Their ability to model

semantic interpretations of patterns, both spatial and sequential, have ready them extremely popular in the research community. In this paper, we attempt to give an overview of what syntactic methods exist in the literature, and how they have been used as tools for pattern modeling and recognition. We also define numerous real-world applications, which have used them with great success.

Movement modeling and recognition using finite state machines [6], propose a state-based approach to movement learning and recognition. Using spatial grouping and temporal alignment, each movement is defined to be an ordered sequence of states in spatial-temporal space. The 2D image positions of the centers of the head and both hands of the user are used as features; these are located by a color-based tracking method. From training data of a given movement, we first learn the spatial information and then group the data into fragments that are automatically aligned temporally. The temporal information is further integrated to build a finite state machine (FSM) recognizer. Each movement has a FSM corresponding to it. The computational efficiency of the FSM recognizers allows us to achieve real-time on-line performance. We apply this method to construct an experimental system that plays a game of "Simon Says" with the user.

An Minimum Description Length (MDL) method to learning activity grammars [7], recommend a new technique for finding the best subset of non-noise terminal symbols and acquiring the best activity grammar. Our method uses the MDL principle, to evaluate the trade-offs between model complexity and data fit, to compute the difference between the results of each terminal subset. The assessment results are then used to find a class of candidate terminal subsets and grammars that remove the noise and allow the discovery of the basic structure of an activity. In this paper, we present the validity of our proposed method based on experimentations with artificial data.

Recognition of multiple human activities through context-free grammar based representation [8], describes a general approach for automated recognition of complex human activities. The approach uses a context-free grammar (CFG) based representation scheme to exemplify complex actions and interactions. The CFG-based representation enables us to formally define complex human activities based on simple actions or movements. Human actions are categorized into three types: atomic action, composite action, and interaction. Our system is not only able to represent complex human activities formally, but also able to identify represented actions and interactions with high accuracy. Image sequences are processed to extract poses and movements. Based on movements, the system detects actions and interactions occurring in a sequence of image frames. Our results show that the system is able to represent complex actions and interactions naturally. The system was tested to represent and identify eight types of interactions: approach, depart, point, shake-hands, hug, punch, kick, and push.

Identification of visual activities and interactions by stochastic parsing [9], describes a probabilistic syntactic approach to the detection and recognition of temporally

extended activities and interactions between multiple agents. The basic idea is to divide the identification problem into two levels. The lower level detections are performed using standard independent probabilistic event detectors to propose candidate detections of low-level features. The outputs of these detectors provide the input stream for a stochastic context-free grammar parsing mechanism. The grammar and parser provide longer range temporal constraints, disambiguate uncertain low-level detections, and allow the inclusion of a priori knowledge about the structure of sequential events in a given domain.

Homologous recombination by RecBCD and RecF pathways [10], a more immediate function of homologous recombination has been accepted: namely, it is a tool for the maintenance of chromosomal integrity that acts to repair DNA lesions, both double-strand DNA breaks and single-strand DNA gaps, produced during the sequence of DNA replication. The familiar connection between the processes of replication and recombination was initially appreciated in the life cycle of bacteriophage T4(56) and then later accepted as an important determinant of viability in bacteria (39,45). In T4 phage, recombination is linked to replication to generate a high yield of phage DNA; in Escherichia coli, recombination is linked to replication to allow its completion when interrupted by DNA damage, and also to initiate DNA reproduction in the nonexistence of origin function.

A fundamental part for SSB in Escherichia coli RecQ DNA helicase function [11], use an similarity refinement scheme to recognize three heterologous proteins that associate with Escherichia coli RecQ: SSB (single-stranded DNA-binding protein), exonuclease I, and RecJ exonuclease. The RecQ-SSB interaction is direct and is intervened by the RecQ winged helix subdomain and the C terminus of SSB. Interaction with SSB has significant well-designed consequences for RecQ. SSB stimulates RecQ-mediated DNA unwinding, whereas deletion of the C-terminal RecQ-binding site from SSB produces a variant that blocks RecQ DNA binding and unwinding activities, suggesting that RecQ identifies both the SSB C terminus and DNA in SSB.DNA nucleoprotein complexes.

All the above discussed methods suffer to produce efficient results on classification and produces poor accuracy.

III. TMM BASED REAL TIME RNA EDITING SCHEME

The proposed TMM based RNA editing scheme receives the input RNA sequence and generates number of gene sequence tuples from the RNA sequence given. For each sequence tuple generated, the method estimates the sequence depth measure within a class of RNA sequence. Finally a cumulative SMM measure has been assessed to classify the class of RNA sequence given. Second, the method estimates the TMM measure towards each gene tuple generated within the class identified and based on that the method performs the matrix addition and deletion operations. The detailed approach is discussed below:

Fig. 1 shows the architecture of the proposed SDM based matrix insertion deletion system and shows various components in detail.

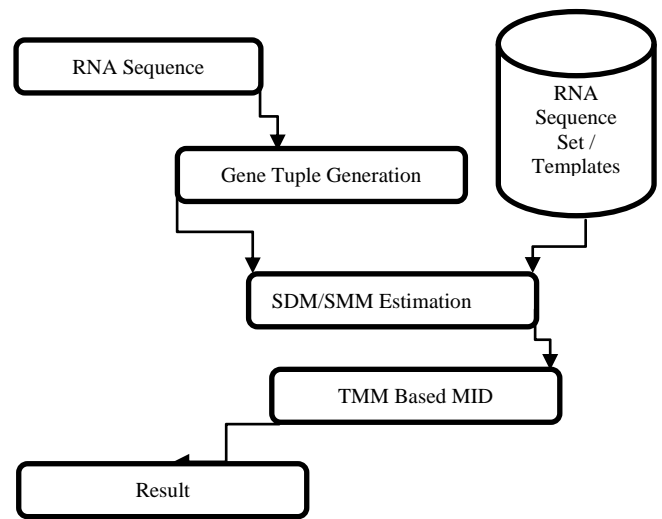


Fig. 1. Architecture of Proposed SDM based Matrix Insertion Deletion System.

A. Gene Tuple Generation:

The RNA sequences are varying in their length and they have no restriction for their size. The input RNA sequence has been read and the entire sequence has been split into number of tiny sequences. The sequences are generated in different length and from different position of the RNA string. The number of position considered is depending on the size of the string available. For each length available, the method generates all possible strings from the RNA sequence. The generated strings are added to the tuple set which has been used to estimate various measures.

Algorithm 1:

Input: RNA sequence S

Output: Tuple set Ts.

Start

Read Rna sequence S.

Compute overall length $l = \text{size}(S)$

Initialize minimum length $ml = 2$.

Initialize starting index $si=1$

For each ml

Generate tuple $Ts = \int_{i=si}^l \sum \text{sub string}(S, i, ml)$

End

Stop

The above algorithm produces the tuple set from the input RNA sequence and has been used estimate different measures.

B. SMM Estimation

In this stage, the tuple set generated in the previous stage has been read. Using the tuple set and the RNA sequence set of different classes, the method estimates the SMM value. First, the method estimates the Sequence Depth measure (SDM) for each tuple available in the tuple set towards the sequence set of RNA. It has been measured based on the number of matches and appearances found in each sequence of the class. Finally, a sequence match measure (SMM) has been computed for the class based on the values of SDM of all tuples in the tuple set. Estimated SMM value has been used to perform classification.

Algorithm 2:

Input: Tuple set Ts, RNA set Rs
Output: SMM
Start
 Read Ts, Rs.
 For each Ti from Ts
 Compute number of entries in each
sequence $Ne = \sum_{i=1}^{size(Rs)} \sum Occurrence(Ti \in Rs(i))$
 Compute number of matches in overall set
 $Nm = \sum_{i=1}^{size(Rs)} \sum Rs(i) \in Ti$
 Compute $SDM = \frac{Ne}{maxlength(\forall Rs(i))} \times \frac{Nm}{size(Rs)}$
 End
 Compute $SMM = \frac{\sum SDM}{Number\ of\ sequences\ of\ Rs}$
Stop

The above algorithm calculates the sequence match ratio for the period being considered and based on the sequence set of the period it has been estimated.

C. TMM Based MID

In this period, first the technique receives the RNA arrangement given. Using the RNA arrangement, the method generates the gene sequences as tuple set. Generated tuple set has been used to estimate the Sequence support ratio for different classes. Based on the arrangement support measure, the method selects a single class. For the selected class, the method estimates the TDM measure with the templates of strings available. Based on the TDM value, the method performs matrix insertion deletion.

Algorithm 3:

Input : RNA sequence R, Template set T, Matrix M, Tuple set Ts.
Output: Matrix M
Start
 Read R, T, M.
 Tuple set Ts =Generate gene sequence (R)
 For each class c
 SSM = Compute SSM(Ts, C)
 End
 Class c = Choose class with higher SSM.
 For each tuple Tk from Ts
 For each template Ti from T
 Compute Number of Total match $Ntm = \sum_{i=1}^{size(T)} \sum T(i) \equiv Tk$
 Compute number of partial match $Npm = \sum_{i=1}^{size(T)} \sum T(i) \approx Tk$
 Compute $TMM = Ntm \times Npm$
 End
 If $TMM > Th$ then
Sequence set ss = Generate possible sequences with Tuple Tk.
 Matrix M = $\sum (sequences \in M) \cup ss$
 Else
 Matrix M = $\sum (sequences \in M) \cap ss$
 End
 End
Stop

The above discussed algorithm estimates TMM measure for different template and based on the value the matrix insertion and deletion is performed.

IV. RESULTS AND DISCUSSION

The proposed TDM based real time matrix insertion and deletion scheme has been implemented and evaluated for its performance. The method has been simulation using Matlab by considering the RNA data set with number of classes. The proposed method has improved the performance of matrix insertion and deletion to support the bio molecular computing. The method has produced the following results. The evaluation has been performed using various RNA data set and gene sequence set.

The accuracy on insertion deletion has been evaluated with different methods and presented in Fig. 2. The results show that the suggested method has generated greater precision than other approaches.

The risk detection accuracy has been evaluated and presented in Fig. 3. The comparative result illustrates that the suggested method has generated greater outcomes on risk detection accuracy.

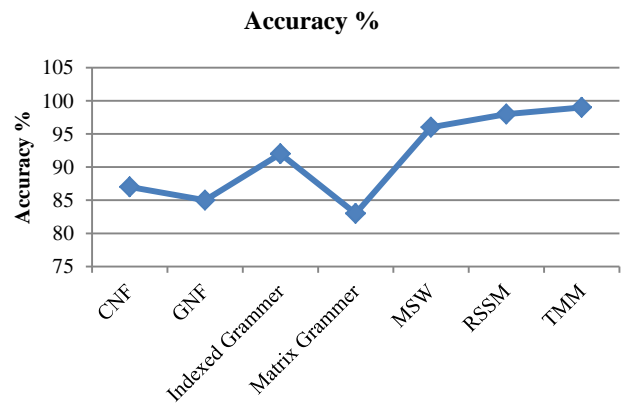


Fig. 2. Assessment on Accuracy.

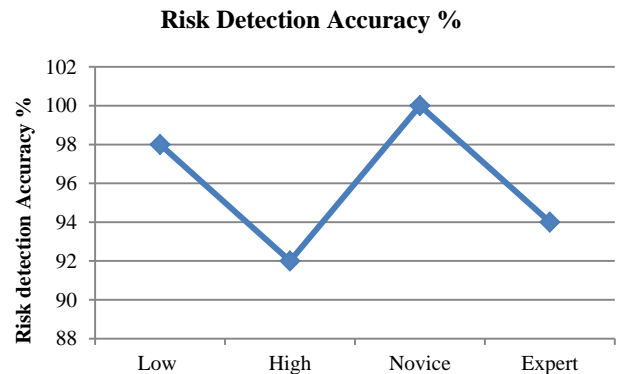


Fig. 3. Assessment on Risk Detection Accuracy.

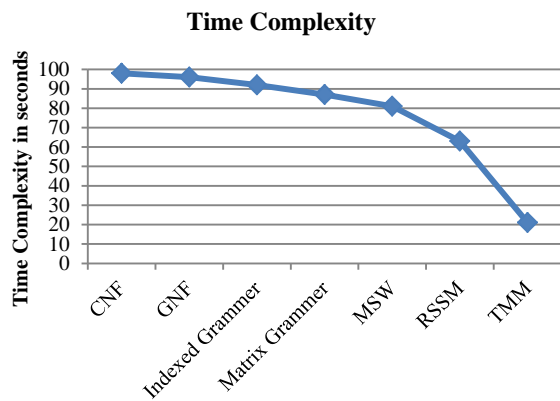


Fig. 4. Assessment on Time Complexity.

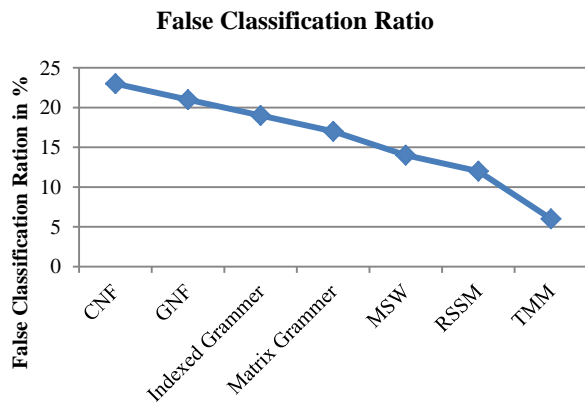


Fig. 5. Assessment on False Classification Ratio.

The time complexity being introduced by different method of insertion deletion systems has been measured and compared with the result of proposed TMM approach. The comparative result has been presented in Fig. 4. The result illustrates that the suggested TMM approach has lower time complexity than other approaches.

The false classification produced by different methods has been measured and compared with the outcome of suggested TMM procedure. The comparative result has been presented in Fig. 5 and shows that the proposed TMM algorithm has reduced the false ratio compared to other methods.

V. CONCLUSION

A real time template match measure based matrix insertion and deletion system is presented. The method reads the input RNA sequence and generates the tuple set based on the size of

the RNA arrangement and the amount of indexes considered. Varying length of RNA sequence has been generated. With the generated tuple set, the method computes the sequence depth measure (SDM) and sequence match measure (SMM). The sequence depth measure represents the similarity of depth the sequence has with other one. Based on the SMM value the method performs classification, the class with higher sequence match measure has been selected and assigned with label. Based on identified class, the method estimates the template match measure (TMM) for different tuples available in the tuple set. Finally, according to the TMM value, the method performs matrix insertion and deletion operations. The matrix insertion is performed according to the TMM value and generates number of RNA sequences. The proposed method improves the performance of the system by improving the accuracy. Also, the method reduces the time complexity and false classification ratio.

REFERENCES

- [1] Kamala Krithivasan., Lakshmanan Kuppusamy., Anand Mahendran., Khalid M. "On the ambiguity and complexity measures in insertion-deletion systems", LNCS, Proceedings of Bionetics, C 1–3, 2010.
- [2] Sergey Verlan. "On minimal context-free insertion-deletion systems", Journal of Automata, Languages and Combinatorics, vol 2. pp. 317–328 (2007).
- [3] Cristian S. Calude., Gheorghe Paun.: "Computing with cells and atoms, An introduction to Quantum", DNA and Membrane Computing. Taylor and Francis, London (2001).
- [4] F. Biegler, M.J. Burrell, and M. Daley "Regulated RNA rewriting: Modelling RNA editing with guided insertion", Theoretical Computer Science, vol.387, issue 2: pp 103-112, 2007.
- [5] Chanda, G., and Dellaert, F. "Grammatical methods in computer vision: An overview", Technical report, Georgia Institute of Technology, 2004.
- [6] Hong, P.; Turk, M.; and Huang, T. S. 2000, "Gesture modeling and recognition using finite state machines", In Automatic Face and Gesture Recognition, 2000. Proceedings. Fourth IEEE International Conference on, pp:410–415. IEEE.
- [7] Kitani, K. M.; Sato, Y.; and Sugimoto, A. "An mdl approach to learning activity grammars", Technical Report 376, IEICE - The Institute of Electronics, Information and Communication Engineers, Tokyo, Japan, 2006.
- [8] Ryoo, M. S., and Aggarwal, J., "Recognition of composite human activities through context-free grammar based representation", In Computer Vision and Pattern Recognition, IEEE Computer Society Conference on, volume 2, pp:1709–1718,2006.
- [9] Ivanov, Y., and Bobick, A. Recognition of visual activities and interactions by stochastic parsing. Pattern Analysis and Machine Intelligence, IEEE Transactions on vol.22, issue8: pp:852–872,2000.
- [10] Spies, M. and Kowalczykowski, S.C. "Homologous recombination by RecBCD and RecF pathways", In The bacterial chromosome , pp. 389–403. ASM Press, Washington, DC, 2005.
- [11] Shereda, R.D., Bernstein, D.A., and Keck, J.L., "A central role for SSB in Escherichia coli RecQ DNA helicase function", J. Biological Chemistry, vol. 282: page: 19247–19258,2007.

CMMI-DEV Implementation Simplified

A Spiral Software Model

Maruthi Rohit Ayyagari¹

College of Business, University of Dallas
Irving, Texas, USA

Issa Atoum²

Department of Software Engineering
The World Islamic Sciences and Education, Jordan

Abstract—With the advance technology and increase in customer requirements, software organizations pursue to reduce cost and increase productivity by using standards and best practices. The Capability Maturity Model Integration (CMMI) is a software process improvement model that enhances productivity and reduces time and cost of running projects. As a reference model, CMMI does not specify systemic steps of how to implement the model practices, leaving a room for organization development approaches. Small organizations with low budgets and those who are not looking for CMMI appraisals cannot cope with the high price of CMMI implementation. However, they need to manage the risk of CMMI implementation under their administration. Therefore, this paper proposes a simplified plan using the spiral model to implement the CMMI to reach level 2. The objective is to make the implementation more straightforward to implement and fit CMMI specification without hiring external experts. Compared to related implementation frameworks, the proposed model is deemed competitive and applicable under organizations' conditions.

Keywords—CMMI; Spiral model; Capability Maturity Model Integration; process improvement; CMMI Implementation

I. INTRODUCTION

Software quality is considered the engine to productivity. Improving software quality will continue to be an open problem in this century [1], [2]. The Capability Maturity Model Integration for Development (CMMI-DEV) is a software process improvement model designed to leverage the level of software products' quality. The CMMI is usually used to develop higher software quality, increasing efficiency, improving customer satisfaction and achieving profit [3]. The CMMI defines the most critical elements that are required to build great products or deliver exceptional services. As a result of using CMMI, several studies have identified the advantages of adopting such model [3]–[6] and several organizations gained various benefits. A survey of 30 organizations reveal the following results from CMMI implementation [7]. The medians from the sample showed a 34% reduction in cost, a 50% reduction in the schedule, a 61% increase in productivity, a 48% increase in product quality, and a 14% increase in customer satisfaction.

Fig. 1 shows the conceptual diagram of the CMMI model which contains four interacting categories. An organization engages process improvement which empowers project management all over the project lifecycle. Consequently, project management employs engineering activities to develop new CMMI practices. As a result, decisions are taken based on

measurements and analysis of the current situation. However, implementing software process improvement models are hinged on achieving business results [8], [9].

Software organizations are highly exposed to an aggressive changing environment [10]; therefore, organizations need to have adequate risk management over time. Although CMMI could help to resolve the problem, the CMMI model is considered a complex model [11]. Therefore, proper implementation of CMMI should take care of the implementation time, cost and scope. The implementation process will affect the current business environment, and the current running products and services. Small organizations often have low budgets; nevertheless, they are willing to improve their practice towards better product delivery. Such organizations could improve their current software process by implementing the CMMI using their existing software's process models. However, often these organizations lack certified CMMI professionals, but they usually have teams of project managers, developers, quality assurance engineers.

The CMMI model is considered a long project that could take 6-8 months, and its implementations are risky on business. Therefore, to solve the abovementioned problems, this paper recommends the spiral model for implementing CMMI for the organizations that are willing to implement CMMI on their own as shown in Fig. 2.

Although some works try to implement CMMI, they are limited. The model proposed by [14] was applied to the KSA and was restricted to the Process and Product Quality Assurance (PPQA) process area. Moreover, commercial software is expensive [19]. Additionally, a small organization cannot cope with CMMI appraisals due to cost, expertise need, and time constraints.

The spiral model is an incremental risk-oriented life cycle model that has four main phases: determine objectives, identify and resolve risks, development, and test, and plan the next iteration. A software project will iteratively go through these four phases. In the context of this paper, the spiral model is employed for CMMI implementation which resolves the above mentioned problems of agility and risk management. In the first place, the requirement will be gathered which includes what business unit to focus on, what level of CMMI to focus on. In the second phase, the risks and the alternative solutions will be identified including resources and time constraints. The third step carries out the CMMI iterative plan. Then, an evaluation is carried out, and the next iteration is planned.

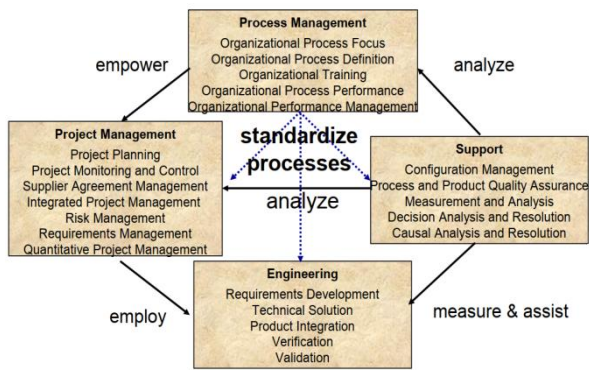


Fig. 1. CMMI Process Area Category.

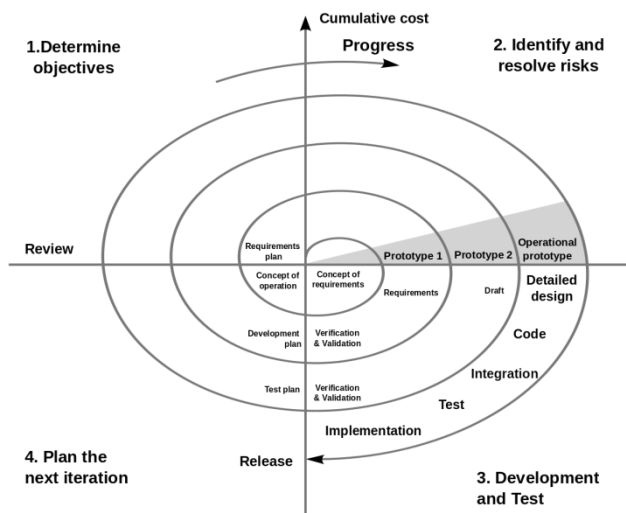


Fig. 2. Bohem Spiral Software Model.

The objective of this paper is to provide a systemic model to implement the CMMI in small organizations iteratively. Consequently, the proposed implementation model could be executed by the organization without hiring certified CMMI practitioners from outside the organization.

This paper is structured as follows. Section 2 provides more information about CMMI and software spiral model. Section 3 provides the related work. Section 4 explains the proposed model. Section 5 evaluates the proposed metric, while Section 6 provides conclusions, with implications and future research.

II. BACKGROUND

A. CMMI Simplified

CMMI came from the software engineering Institute, a US national lab with the mission of maturing the software engineering profession [6]. The CMMI was originated based development of its predecessor, the capability maturity model (CMM) as well as input from engineering practices of quality and management. The CMMI is a reference model of structure description of proven practices in product engineering and engineering management. Although the model is a trailing

edge, its practices are sound, and the model has faced concurrent and construct validity as measured over time. One of its main advantages is that it describes what, not how, thus it leaves much room for innovation exploration and new approaches to product development.

The CMMI has three categories: CMMI for services, CMMI for Acquisition and CMMI-DEV for development. The later, CMMI-DEV is concerned with developing software projects, which is the concern of this paper. There are two ways to represent or view the CMMI-DEV model. The first and the most common way describes how to improve the organization as a series of stages of maturity (shown in Fig. 3), while the second is concerned with the process areas and implement the ones that must address the company needs at the time (Fig. 4). There are five levels of maturity, each of which represents an organizational plateau of the overall capability of the organization. Each level has a predefined set of processes that are assigned to it for cohesive implementation and results. The latest version CMMI-DEV 1.3 model has five maturity levels, each of which has specific process areas. The expectation is that as these process areas are implemented, product productivity and quality increase. At level one (initial) there are no process areas, the processes are usually ad hoc and chaotic. Level two (managed), ensures requirements are systematically converted to quality-accepted products. This level has essential project management and product support practices. At level three (defined), processes are well characterized and understood as described in standards and procedures. At level four (quantitatively managed), processes are continually improving process performance through incremental and state-of-the-art technology. The last level demonstrates the tuning and optimization of organizational processes and practices.

CMMI-DEV is divided into categories of practice called process areas. There are 22 Process Areas or (PAs) that are described in a pure form in a manner that resembles a project lifecycle. PAs are windows through which a developer looks at organization current practices. Requirements Development (RD) and Requirements Management (REQM) process areas handle the elicitation, development, and validation of requirements and validation of demands as well as managing the changes that naturally occur during the project. Project Planning (PP) and Project Management and Control (PMC) deal with essential project management estimating, planning and then managing a project. These two process areas are augmented by Supplier Agreement Management (SAM) when using outsources and by Risk Management (RSKM) for mitigating risk before they occur or managing them when they become issues. Technical Solution (TS) and Product Integration (PI) take care of the design, development and build up a product along with ensuring that the parts of the product fit together when delivered to the customer. Verification (VER) and Validation (VAL) deal with making sure that the product is free of defects. Verification refers to building the product right so that it should work as intended in the customer's environment while validation refers to making the right product.

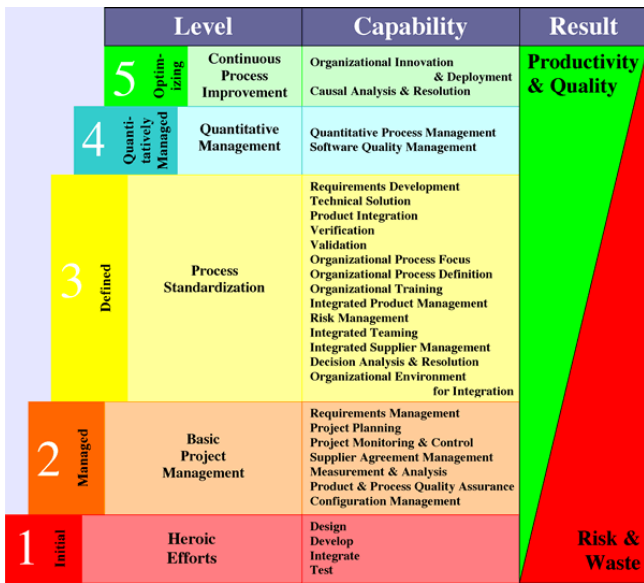


Fig. 3. CMMI Pyramid Staged View.

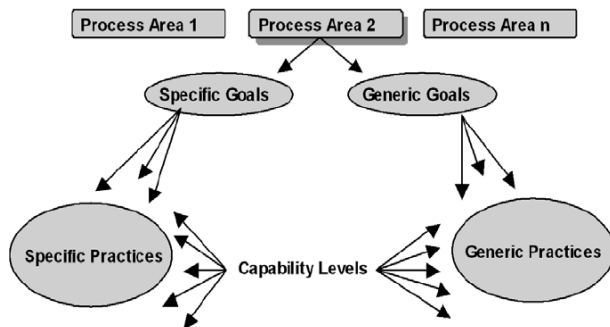


Fig. 4. CMMI Continuous Approach.

Some organizational process areas govern other processes, the organizational process focus (OPF) and organization process definition (OPD). The OPF is designed to fasten process improvement while the OPD provides a repository for standard processes, templates, metrics guidelines, and best practices that are stored for retrieval when desired. When such catalog is in place, a project can draw from these resources to structure the project, work more efficiently and with greater confidence of success, through the process area of Integrated Project Management (IPM). Project Planning (PP) and Project Monitoring and Control (PMC) are all grown up to take advantage of the standard way of working in software projects. People as resources to projects need to know what to do and how to do their work which is managed by the Organizational Training (OT) process group. As an organization collects better and more consistent metrics, it can start to characterize its standard process quantitatively through Organizational Process Performance (OPP) and managed by data rather than by best guess through Quantitative Project Management (QPM). These process areas are further augmented by an increased focus on continuous refinement of the organization standard processes based on business needs and changes as seen in Organizational Performance Management (OPM) and supported by metrics based on root cause analysis that is Causal Analysis and Resolution (CAR) process area.

B. Software Spiral Model

Spiral model as described in Bohem paper [12], is an iterative software development approach that takes into consideration risk management and small development over time. The software life cycle model consists of four main phases.

1) Determine objectives, alternatives, and constraints. Fundamental requirements are gathered aligned with project objectives such as software behavior, availability, and reliability. Based on project constraints (time, cost, scope) the alternatives-buying versus the building, and scoping are identified.

2) Evaluate alternatives and identify and resolve risks for each option. Risks include a lack of experience, fear of new technology, and improper policies or processes.

3) Development and test: The software is developed by writing code and building related artifacts; then they are inspected or tested accordingly.

4) Plan the next iteration. Results are evaluated, and plans are developed for the next iteration: the plans include-scope plans, schedule plan, and test plan.

There are several advantages to using a spiral model. The risk analysis component reduces the chances of project failure. Since the model is an iterative model, functionality can be added at a later phase; therefore, the software is produced early in the software life cycle.

III. RELATED WORK

Although the CMMI-DEV framework was described in detail [13], it is considered a guideline and does not provide operational activities leaving the decision of implementation to the organization. CMMI-DEV perceives complexity; therefore a better visual model (e.g., ArchiMate) should show the concepts and their relationship in a simple way [11]. It is not only the complexity of the CMMI-DEV model, but its implementation is not a direct approach. Organizations need individual experts and guidance from certified CMMI partner to implement the model effectively. In the KSA, [14] collected data about CMMI companies and implemented an abstract-level model for the PPQA process area to increase perceived usefulness and perceived ease of use.

Similarly, [15] proposed a set of activities to implement and evaluate the software process objectively. The implementation of the CMMI-DEV must be carefully taken to save resources especially for cases where other models are implemented simultaneously [16]. In a reference book for software development, [17] proposed the process review report as a typical artifact for implementing CMMI.

A set of tools are commercially available to help in the implementation of CMMI, ManageHub, an integrated process asset library that contains a CMMI compliant infrastructure can reduce implementation time and cost [18]. The CMMI Toolkit is a collection of structured inter-related documentation that has processes, checklists, and templates in a hierarchy form [19]. However, the tools that could work with small organizations depend on business needs. A set of open source

tools that could be used to manage and implement CMMI are available [20]; however, without human guidance the software is useless.

Although many organizations have implemented CMMI-DEV successfully, the implementation plans were not revealed, and certified practitioners executed the implementation most of the time.

IV. PROPOSED SPIRAL METHOD

The research methodology depends on Spiral software model. First, the spiral model is run as a project; then the outcomes are evaluated against a set of criteria extracted from literature and proposed by this research. The criteria include implementation cost, fitness for purpose and use, satisfaction, and usability of the proposed model.

The rationale for the CMMI project improvement program is to improve competitive posture and adapt to organizational changes to achieve and maintain the CMMI level 2. The first step towards implementation is to assign a project manager. Once the project manager is appointed, he first identifies the primary stakeholders. The CMMI implementation is a critical project; therefore, gaining executive support is crucial primarily if the implementation affects more than one business unit simultaneously. Then the project manager will develop the steering committee and a project organization. Ideally, the implementation for the in-house project should include teams of quality, technical, and the engineering process group. Fig. 5 shows a sample CMMI implementation project organization. Table I shows their roles and responsibility in CMMI-DEV 1.3 implementation for Process Improvement (PI).

The set of activities that could be performed to implement the CMMI are shown in Fig. 6. The steps are at high-level, and further detailing will be carried out by the project manager. The activities in Fig. 6 are executed in phases as shown in the CMMI spiral model shown in Table II. If these activities are not performed iteratively, a project failure may occur due to high risk and change management.

Therefore, the proposed setup of the experiment integrates the list of CMMI development activities (shown in Fig. 6) and the list of stories executed by the proposed spiral model presented in Table II.

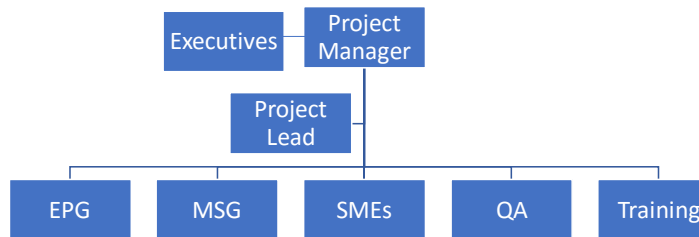


Fig. 5. CMMI Development Project Organization.

TABLE I. ROLES AND RESPONSIBILITIES OF CMMI IMPLEMENTATION TEAMS

Role	Responsibility
EPG	<ul style="list-style-type: none"> • Build sponsorship of PI, • Nurture/sustain improvement activities, • Manage PI effort, and • Ensures PI effort coordination.
Management Steering Group (MSG)	<ul style="list-style-type: none"> • Link organization’s vision/mission to the implementation, • Signifying sponsorship, • Assigning resources, • Monitoring progress, and • Providing guidance and correction.
Subject Matter Experts (SMEs)	<ul style="list-style-type: none"> • Knowledge of organization processes implemented within their business unit, • Work with the process (users), • Affected by the new business unit processes and stakeholders
QA	<ul style="list-style-type: none"> • Testing and peer review • Quality metrics modeling and analysis
Training	<ul style="list-style-type: none"> • Train relative stakeholders to new technology • Training for CMMI core activities • Train users for new practices

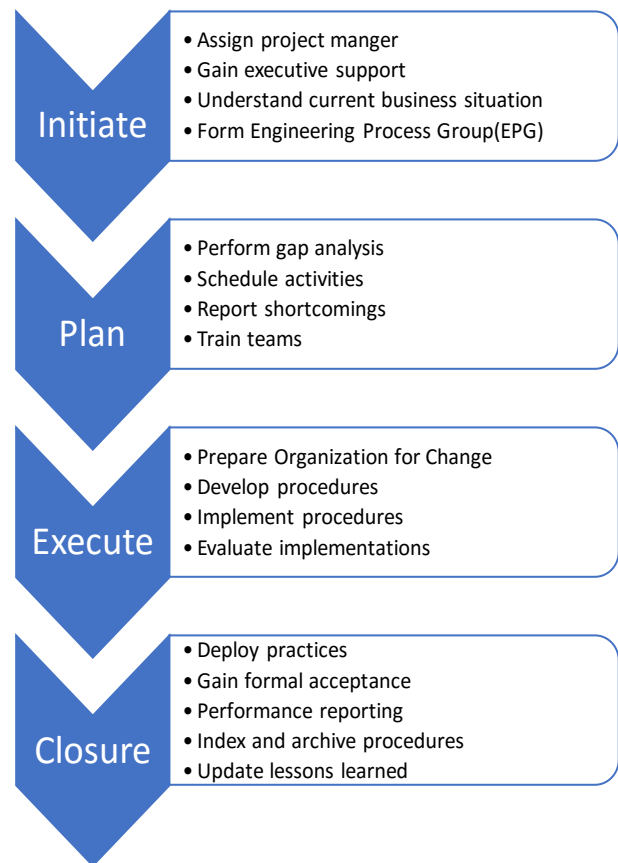


Fig. 6. CMMI Development Project Activities.

TABLE II. SAMPLE ITERATIONS IN CMMI SPIRAL MODEL

Iteration#	Phase1	Phase2	Phase3	Phase4
1	Study current business	Identify the best business unit to cover	Document current development processes	Plan for EPG team
2	Form EPG	Check alternative resources and project constraints (cost, time)	Announce the group and authorize the group to CMMI-DEV	Plan for Gap analysis
3	Run gap analysis	Manage resistance also, gain executive support	Document discrepancies from CMMI practice	Plan for training
4	Train EPG team	Allocate sponsorship and timeframes	Certify members or evaluate their knowledge gain	Plan for development
5	Develop practices	Manage resources, scope and cost	Document new procedures	Plan for practices' implementation
6	Implement procedures (can be more than one iteration)	Identify and control change	Verify new changes on the organization	Plan for deployment
7	Deploy new practices (can be more than one iteration)	Resolve issues related to current practices adopted by the organization	Evaluate and validate the practices	Plan for formal acceptance
8	Gain formal acceptance	Plan for possible rejection (plan B)	Communicate change and formalize the implementations	Plan for closure
9	Run closure activities	Identify alternatives to future change and document ownership.	Communicate closure	Plan for continuous improvement activities
10	Go to activities in iteration 1			

V. EVALUATION AND DISCUSSION

Although many implementations have been carried out to implement CMMI-DEV, most of them are executed by certified CMMI partners. To the authors' knowledge, no implementation methods were reported. The proposed method is an effective tactic envisioned to implement CMMI-DEV using currently available resources on small organizations that target the CMMI level 2.

The proposed method is evaluated against the following evaluation criteria proposed by this paper:

- A. Easy to implement: In small organizations with limited resources, the implementation should be carried out systematically and with ease.
- B. Fit for specification: The goal of the implementation is to transfer the organization to the required level of the CMMI maturity model.
- C. Fit for purpose: The purpose of the implementation is to increase the productivity of the organization and reduce the risk of project failures without adding extra unneeded efforts. Generally, small organizations do not look for CMMI appraisals.
- C. Satisfaction: All related stakeholders should be satisfied with the improvement made in the organization.
- D. Cost: Small organizations with low budgets harvest the opportunity of currently available resources.

E. Table III shows the comparison of the spiral method and a list of carefully chosen works from the literature — the signposts that the criterion is an obtainable while means unavailable criterion.

According to Table III, all methods are fit for specification (Criterion B), that is, their goal is to reach the CMMI best practice at the intended level. Moreover, all compared models are easy to implement (Criterion A), except for the general CMMI-DEV guide as it leaves the implementation details to the developers. Also, compared models are fit for purpose (Criterion C), except the KSA model [14] which is limited to the PPQA process area. The proposed spiral model is competitive to the compared models concerning satisfaction (Criterion D) and cost (Criterion E) perspectives.

Furthermore, the proposed framework has been evaluated by expert judgment of two project managers, three senior managers from three different organizations who are willing to implement the CMMI. Project managers approved and appreciated the proposed spiral model; however, they were concerned with what is going to happen during project progress. The senior managers advocate the approach but were worried about how to manage resistance during the implementation process.

This paper extends previous work on CMMI implementation guidelines and provides operational implementations activities as a project. The proposed approach provides several immediate implications for research and practice; therefore, it should help in the evaluation and CMMI-DEV, and the adoption of the proposed model in small organizations.

TABLE III. COMPARISON OF THE PROPOSED METHOD AND RELATED CMMI IMPLEMENTATION APPROACHES

Criterion	Proposed Spiral method	CMMI Guide [13] [17]	[14] [15]	Certified CMMI Partners	Implementation tools
A	☑	☒	☑	☑	☑
B	☑	☑	☑	☑	☑
C	☑	☑	☒	☑	☑
D	☑	☑	☒	☑	☒
E	☑	☒	☑	☒	☒

Despite the vital contributions of this paper, the spiral approach encompasses limitations that should be well-thought-out when construing the results. First, the model was verified with a set of criteria for small organizations. This limitation may restrain the generalizability of the results on large organizations looking for appraisal certifications. Second, the proposed approach has not been implemented in any organization due to organizations privacy concerns. Therefore, results possibly only imitate the general concept of iterative CMMI implementation. Future work should consider conducting an extensive survey on various small organizations, before proceeding to approve the implementation approach.

VI. CONCLUSION

CMMI is a software process improvement model that improves efficiency, productivity and reduced the implementation cost of organization projects. The CMMI as a reference model does not specify systemic steps of how to implement the model, leaving room for organization development methods. The paper proposed a spiral software model to implement CMM-DEV 1.3 in small software development organizations. The model powers the use of small iteration based on available resources and organization constraints, and risk management to reduce failure. The proposed implementation approach was compared with a set of CMMI implementation approaches. The proposed model was deemed applicable and viable on cost and satisfaction criteria.

REFERENCES

- [1] Atoum, C. H. Bong, and N. Kulathuramaiyer, "Towards Resolving Software Quality-in-Use Measurement Challenges," *Journal of Emerging Trends in Computing and Information Sciences*, vol. 5, no. 11, pp. 877–885, 2014.
- [2] I. Atoum, "A Novel Framework for Measuring Software Quality-in-use based on Semantic Similarity and Sentiment Analysis of Software Reviews," *J. King Saud Univ. - Comput. Inf. Sci.*, p. , 2018.
- [3] J. Samalikova, R. J. Kusters, J. J. M. Trienekens, and A. J. M. M. Weijters, "Process mining support for Capability Maturity Model Integration-based software process assessment, in principle and in practice," *J. Softw. Evol. Process*, vol. 26, no. 7, 2014.
- [4] A. G. A. Saeed, R. S. Afgun Usmani, H. Akram, S. M. Saqlain, "The Impact of Capability Maturity Model Integration on Return on Investment in IT Industry: An Exploratory Case Study," *Eng. Technol. Appl. Sci. Res.*, vol. 7, no. 6, 2017.
- [5] D. Chevers, "Software Process Improvement: Awareness, Use, and Benefits in Canadian Software Development Firms," *Rev. Adm. Empres.*, vol. 57, no. 2, pp. 170–177, Apr. 2017.
- [6] Software Engineering Institute, "CMMI for Development, Version 1.3," Carnegie Mellon University, 2010.
- [7] R. W. Reitzig, D. R. Goldenson, D. Gibson, and M. R. Cavanaugh, "Calculating CMMI-Based ROI: Why, When, What, and How?," 2007.
- [8] C. Ebert, "Technical controlling and software process improvement," *J. Syst. Softw.*, vol. 46, no. 1, pp. 25–39, Apr. 1999.
- [9] S. Bayona, J. A. Calvo-Manzano, and T. San Feliu, "Critical Success Factors in Software Process Improvement: A Systematic Review," in *Software Process Improvement and Capability Determination*, 2012, pp. 1–12.
- [10] K. Lee, Y. Park, and D. Lee, "Measuring efficiency and ICT ecosystem impact: Hardware vs. software industry," *Telecomm. Policy*, 2017.
- [11] L. Valverde, M. M. da Silva, and M. R. Gonçalves, "CMMI-DEV v1.3 Reference Model in ArchiMate," in *OTM Confederated International Conferences "On the Move to Meaningful Internet Systems"*, 2018, pp. 191–208.
- [12] B. W. Boehm, "A spiral model of software development and enhancement," *Computer (Long Beach, Calif.)*, vol. 21, no. 5, pp. 61–72, 1988.
- [13] SEI CMMI Production Team, *CMMI for Development v1.3*. Lulu.com, 2010.
- [14] I. Keshta, M. Niazi, and M. Alshayeb, "Towards Implementation of Process and Product Quality Assurance Process Area for Saudi Arabian Small and Medium Sized Software Development Organizations," *IEEE Access*, vol. 6, pp. 41643–41675, 2018.
- [15] J. Persse, *Project management success with CMMI: seven CMMI process areas*. Upper Saddle River, NJ: Prentice Hall, 2007.
- [16] J. Aguiar, R. Pereira, J. B. Vasconcelos, and I. Bianchi, "An overlapless incident management maturity model for multi-framework assessment (ITIL, COBIT, CMMI-SVC)," *Interdiscip. J. Information, Knowledge, Manag.*, pp. 137–163, 2018.
- [17] R. Nandyal, *CMMI: a framework for building world class software and systems enterprises*. New Delhi: Tata McGraw-Hill, 2004.
- [18] CMMI-Live, "CMMI® Tool That Can Reduce Implementation Time and Cost." [Online]. Available: www.cmmilive.com/cmmi-tool-that-can-reduce-implementation-time-and-cost/. [Accessed: 01-Mar-2019].
- [19] DQS India, "CMMI Process Implementation Toolkit." [Online]. Available: <https://dqsindia.com/cmmi/toolkit/>. [Accessed: 01-Mar-2019].
- [20] SourceForge.net, "CMMI Management and Monitoring Tool download." [Online]. Available: <https://sourceforge.net/projects/cmmi-toolmanager/>. [Accessed: 01-Mar-2019].

Algorithm for Enhancing the QoS of Video Traffic over Wireless Mesh Networks

Abdul Nasser A. Moh¹, Borhanuddin Bin Moh. Ali⁴
Department of Computer and Communication Systems
Engineering, Faculty of Engineering
University Putra Malaysia Serdang 43400, Selangor,
Malaysia

Radhwan Mohamed Abdullah²
Division of Basic Sciences, College of Agriculture and
Forestry, University of Mosul, Mosul, Iraq

Abedallah Zaid Abualkishik³
American University in the Emirates
Dubai, United Arab Emirates

Ali A. Alwan⁵
Department of Computer Science
Kulliyah of Information and Communication Technology
International Islamic University Malaysia
Kuala Lumpur 53100, Malaysia

Abstract—One of the major issues in a wireless mesh networks (WMNs) which needs to be solved is the lack of a viable protocol for medium access control (MAC). In fact, the main concern is to expand the application of limited wireless resources while simultaneously retaining the quality of service (QoS) of all types of traffic. In particular, the video service for real-time variable bit rate (rt-VBR). As such, this study attempts to enhance QoS with regard to packet loss, average delay, and throughput by controlling the transmitted video packets. The packet loss and average delay of QoS for video traffic can be controlled. Results of simulation show that Optimum Dynamic Reservation-Time Division Multiplexing Access (ODR-TDMA) has achieved excellent utilization of resource that improvised the QoS meant for video packets. This study has also proven the adequacy of the proposed algorithm to minimize packet delay and packet loss, in addition to enhancing throughput in comparison to those reported in previous studies.

Keywords—Wireless Mesh Networks (WMNs); Medium Access Control (MAC); Quality of Service (QoS); video traffic

I. INTRODUCTION

The importance of medium access control (MAC) protocol for wireless mesh networks (WMNs) is dependent on several reasons, such as enabling statistical multiplexing for wireless access interface, optimizing the use of limited wireless resources, and ensuring that the required quality of service (QoS) for multimedia packets are fulfilled, particularly for video service with real-time variable bit rate (rt-VBR) [1]. The assignment of dynamic slots is important to ensure that the achievement of statistical multiplexing in various service categories and features are adequate for variable bit rate (VBR) class that coordinates the vast traffic needs for both spatially-dispersed and independent wireless terminals [2–4]. There are several weaknesses in the present protocols for MAC; for instance residual lifetime, excessive overhead for transmission of buffer data, instant queue length, and punctual arrival of packet as an essential threshold. Two types of access schemes can be employed for transmission of data from individually-distributed wireless terminals to contention less and contention-based access points. In the effort to diminish packet

loss as a result of collision, the contention-based system [5-8] requires smaller control packet and lower collision probability. As such, several MAC protocols were developed for application in wireless networks. For instance, a comparative analysis has been carried out which involved two MAC protocols, namely RI_MAC (a contention-based receiver that initiates the asynchronous duty cycle in the MAC protocol) and ATMA (advertisement-based Time Division Multiplexing Access (TDMA) MAC protocol) [9]. A system that is free from any contention [10 -13] was described as being based on either a polling mechanism that assigns an uplink in the slot to transfer the parameters or a piggyback approach where the parameters are piggybacked on uplink data burst. The polling period must be altered to reduce loss of packet while the overhead of the piggyback has to be reduced. An MAC protocol based on TDMA was developed to prevent collision during data transfer in order to maintain QoS in networks with ad-hoc feature [14]. Other researchers have developed procedures for adaptive registration of mobile-to-mobile (M2M) networks with massive Internet of Things (IoT) devices. This was followed by the development of an MAC protocol with hybrid-slotted Carrier Sense Multiple Access/TDMA (CSMA/TDMA) (HSCT), in which the logical frame comprises two parts: the first part is a contention-based CSMA with a collision avoidance (CSMA/CA) period (SCP) that is segregated into many access windows (i.e., C-slot). The second part is a contention-free slotted TDMA period (STP) segregated into many T-slots [15]. Additionally, a hybrid CSMA/TDMA or queue-MAC has been developed to adjust to the varied traffic [16], where the contention-based CSMA was applied for a light load to address any delay due to scattered data transfer. Another MAC protocol based on TDMA was developed for gate-way multi-hop Wi-Fi-based long distance (WiLD) network in the attempt to enhance throughput and deal with the delay in performance [17]. This method was able to substantially reduce the possibility of collision for MAC protocol based on token through the use of synchronized inherent nodes approach. The suggested protocol enhanced the performance of the network by using the (available bandwidth to maximize the overlapping TDMA slots. The improvisation

of MAC protocols was reflected by the average end-to-end delay in the packet for multiple hops, as well as saturated throughput. According to the best of our knowledge Dynamic Reservation (DR-TDMA) is one of the most efficient and comprehensive algorithm used in resource allocation for multimedia traffic in wireless network [18].

In particular, this approach includes the allocation algorithm that is based on an efficient rate of VBR video traffic which integrates algorithm to the control rate in order to ensure the flow of video with the related traffic thresholds. Hence, a 6-bit piggybacking overhead was used to predicate the requirement for video connections in the previous protocols, In the last stage in each frame, DR-TDMA estimates the connection buffer status (with regard to number of packets, packets-guaranteed groups and best-effort) based on received data and parameters on connection, either immediately in control packet or piggybacked to data packet. Packets verified to video traffic threshold are referred as guaranteed packets with high QoS, whereas packets that fail to conform to the function on the basis of best-effort with the absence of QoS. In addition, the algorithm for slot allocation comprises two units, namely best-effort and guaranteed allocations.

The available slots were initially allocated by the scheduler to video connections awaiting guaranteed packets via time-to-expiry algorithm. The remaining slots were then allocated to best-packet video connection in virtue queue based on the algorithm for fair bandwidth allocation.

This study proposed the utilization of ODR-TDMA for video traffic. Hence, the primary aim of the suggested algorithm is to offer fair delay for the delayed video packets by reducing the variance in the delay between the transferred video packets. Since η was modified, the corresponding value was met for each varied number of video user, which the ODR-TDMA attempts to achieve through the creation of each frame. The control of the allocated resources or bandwidth is done in an adaptive manner for video traffic that correspond to the average bit rate as well as the ability to manage QoS with regard to packet loss, average delay and throughput.

This paper is organized as follows. Section II presents the system and traffic model description. Section III explains and discusses the proposed ODR-TDMA mechanism. The performance evaluation and simulation results have been reported in Section IV. Conclusion is presented in the final Section V.

II. SYSTEM AND TRAFFIC MODEL DESCRIPTION

The developed resource allocation algorithm can be utilized for slotted TDMA Wi-Fi, which functions by complying with the standards set in IEEE 802.11. The protocol was developed using Time Division Duplex (TDD). Fig. 1 shows the structure of frame used in the developed resource allocation algorithm.

The size for a frame of air interface was fixed at 2 ms, and the frame was divided into equal-sized slots to moderate date scheduling with each slot having a 48-byte frame body.

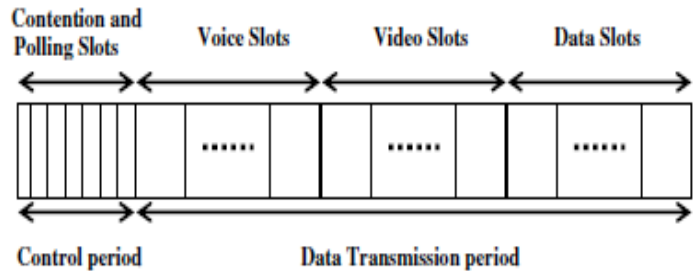


Fig. 1. Uplink Frame Structure.

III. ODR-TDMA MECHANISM

High usage of wireless channel and excellent QoS can be achieved through efficient resource allocation algorithm. In fact, the algorithm for transmission at uplink can also be easily used for the downlink scheduled by TDM. The upper and lower Delay_Thresholds were broadcast by base station to all video users in each frame created and their delay time in transferring packets is indicated by overhead piggybacking based on three categories: first, higher state for packet delay that is higher than upper Delay_Threshold; second, lower state for packet delay that is smaller than lower Delay_Threshold; and finally, In-between state for packet delay that is lower than upper Delay_Threshold but is higher than lower Delay_Threshold.

The latest updated status for packet delay is used by the allocation algorithm to manage slots for users at the end of each frame. This algorithm maximizes the amount of In-between delay state by converting lower and higher delay state into In-between state to obtain a fair delay.

The allocation algorithm depends on three steps. In the first step it assigns higher delay state, and increase number of allocated slots by 1. The second step keep number of allocated slots without change. Finally, the third step assign users with delay lower than low delay threshold and reduce the number of allocated slots by 1.

Since the lower delay state was the least affected by any decrease in the free available slots, it appeared in the final step. When the slot is absent, the user has to wait until an available slot is found. If the waiting required 3 frames, a slot is allocated by the base station in the present frame to deliver a packet and to update its delay state. Step 3 showed that users were distributed based on their wait state, where users with higher waiting time were served with fair allocation efficiently. Both the lower and upper Delay_Threshold were modified by the base station using the following equations [18]:

$$DTH_U = DTH_L + DTH_{VAR} \quad (\text{sec}) \quad (1)$$

The Upper_Delay_Threshold (DTH_U) is the summation of the Lower Delay threshold (DTH_L), and the Variance Threshold (DTH_{VAR}) is fixed at 4 msec.

$$DTH_L = \frac{(Rslot * Tf * EX)}{(Nv * Rv)} \quad (\text{sec}) \quad (2)$$

$Rslot$ is bit rate/slot at uplink channel bit rate for 24 slots/frame; Tf is the duration of the frame and is fixed at 2 ms; EX is the number of additional slot for video traffic that exceeds the product of η and M ; Nv is the number of video user; and Rv is average bit rate/video user.

$$EX = Ex + NoS - (\eta * M) \text{ (slots)} \quad (3)$$

η is the weighting factor for the algorithm proposed in this study, M is the number of slots that is equal to the total mean bit rate for all video users, and NoS is the number of slots allocated for each user.

$$M = (Nv * Rv) / Rslot \text{ (slots)} \quad (4)$$

These equations suggest that the ODR-TDMA is able to modify the average number of slots allocated for video traffic near M by regulating the values of lower and upper delay threshold. The upper and lower delay thresholds that are based on these equations were controlled more strictly by the base station when the EXCESS slot increased. Hence, lower delay state is used more often in comparison to higher delay state, thereby reducing the number of allocated slots. The values of Variance Threshold, which is the average of packet delay variance among the transferred packets, must be small, which is the reason for choosing 4 ms for 2 frames. The upper and lower Delay_Threshold values are equal to the Maximum Transfer Delay (MTD) video packets or 50 ms (maximum) and zero (minimum), respectively. The random value chosen by ODR-TDMA in the initial reading for η was fixed as one the following values: {1.00, 1.01, 1.02, 1.03, 1.04}. It measured both packet delay and loss for each frame, and subsequently compared them with QoS, which was stored in the buffer upon adherence. With regard to the remaining frames, MPP was employed to scan the area and measure Nv . The value of Nv was then compared with the values derived from prior processing to determine the suitable Lower and Upper Delay_Thresholds. With repetition, ODR-TDMA began to learn to identify the optimal value for η which meet the requirements for QoS and adhere to the number of video users. Fig. 2 shows the flowchart for the developed ODR-TDMA for video traffic.

ODR-TDMA is able to obtain data from other wireless networks, therefore causing delay for users. To be precise, when MN failed to gain access to a WLAN network due to limited area of coverage, it can request for data, including the IP address of the Mesh Access Point (MAP) connected, to be sent to another network interface card. This MAP then sends an MN reply information message of neighbouring access networks (e.g. network id and channel numbers) that are within coverage. A list of available channels that operate in the available WLAN network was generated by the MN. If there was no WLAN network channel available within the coverage of the other network, the MN stayed in another network interface card, thereby allowing MPP access to the number of delayed users. All channels were scanned, either passively or actively, when the MN entered the interface card of the WLAN. If no MN was found, the interface card is switched off, but if an MN was found, the MPP will connect it with a new WLAN interface card to communicate data.

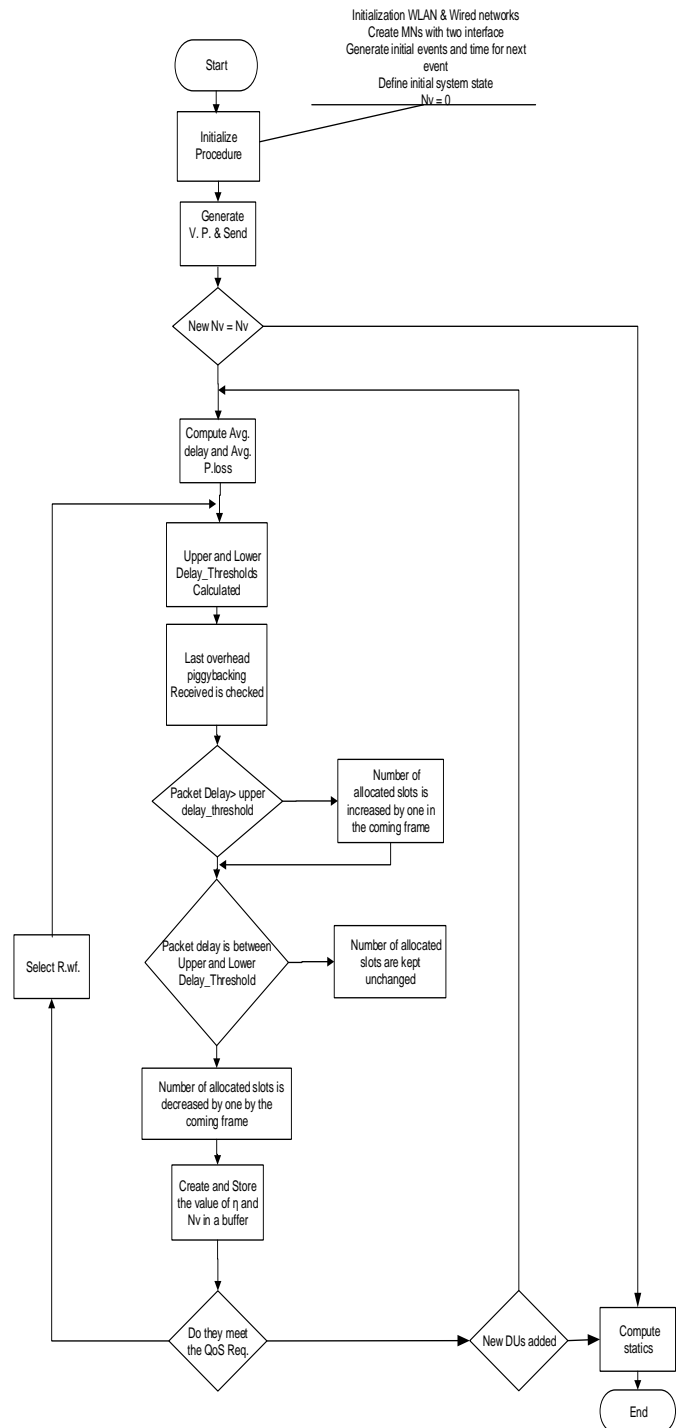


Fig. 2. ODR-TDMA Algorithm.

IV. PERFORMANCE EVALUATION AND SIMULATION RESULTS

Three primary metrics of performance were employed to evaluate the ODR-TDMA algorithm based on the alteration in MNs for the initial case and in η for the second case. The outcomes from packet loss, packet delay, and throughput are presented and compared with the findings made in previous

studies in two parts; the first part presents packet loss, average delay, and throughput when MNs were increased, whereas the second part shows a comparison of the outcomes for performance metrics between ODR-TDMA and Fair Dynamic Reservation- Time Division Multiple Access (FDR-TDMA) when MNs were increased.

A. Effect of Increasing N_v when η is within a Range of {1:1.04}

This section discusses the effect of ODR-TDMA when there was an increase in MN with the value for η fixed at {1: 1.04}. The results for packet loss ratio, average delay, and throughput show the impact of ODR-TDMA in fulfilling the requirements of QoS. Fig. 3 shows that a small increase in η could reduce packet loss that is proportional with the increase in both N_v and η . The expansion reflects the stability of η as the value was gradually increased for N_v . It is interesting to note the small increase in η , as shown in Fig. 4 resulted in a substantial reduction in average packet delay. Efficient use of the allocated bandwidth by ODR-TDMA resulted in a substantial decrease in average packet delay and packet loss due to the change in value of Delay_Threshold. An increase in the MNs enhanced the dominance of η that affects the increase in multiplexing gain, as well as a decrease in total variation rate for video traffic.

High values of η have an impact a small group of users rather than a large group in attaining a similar QoS. Delay_Threshold is frequently influenced by the allocated slots and η . A reduction in allocated slots and an increase in η tend to reduce the availability of free bandwidth, thereby generating higher delay state and reducing average packet delay due to the conversion to in-between state by ODR-TDMA.

Throughput is the average number of slot ratio for a successful transmission of data packet to the total amount of slots per frame. The similarities of the resulting throughput with η are shown in Fig. 5. The second section presents a comparison of ODR-TDMA and FDR-TDMA. The video traffic channel parameters were fixed as recommended by [18].

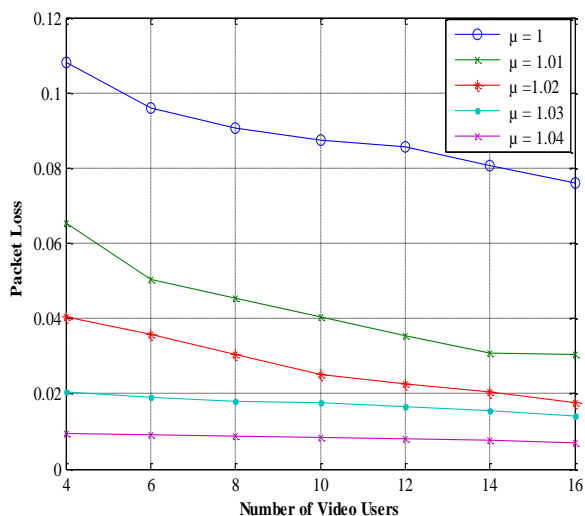


Fig. 3. Packet Loss Ratio as a Function of N_v .

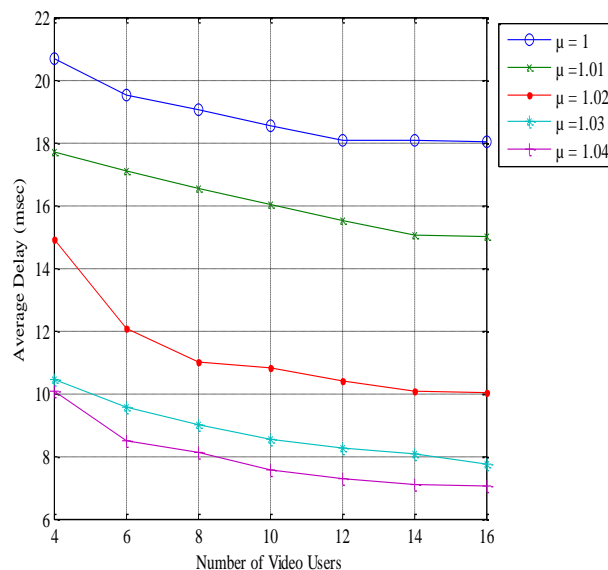


Fig. 4. Average Delay vs. No. of Video users.

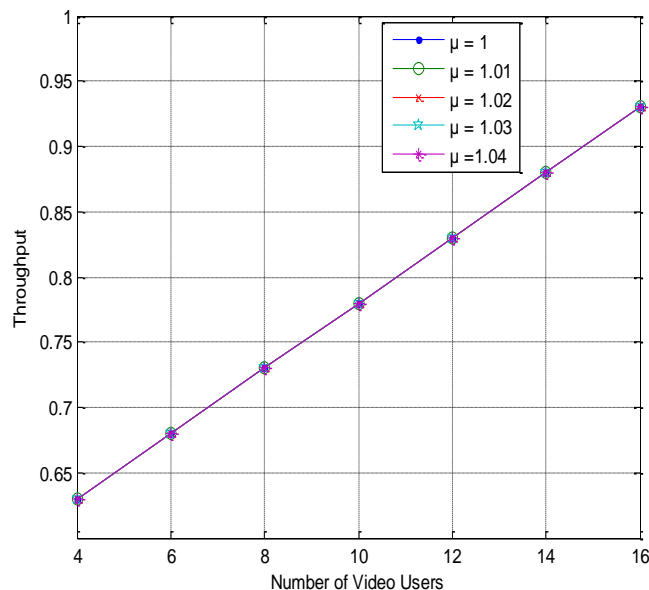


Fig. 5. Throughput vs. No. of Video users.

B. Comparison of ODR-TDMA with Previous Protocols

Channel parameters and users were set as recommended by [18] to compare video traffic simulations. The outcomes of the simulation of the packet loss ratio are shown in Fig. 6 to 9. They show that the average values for throughput and packet delay for a video user are $\eta = 1.04$ and 250 Kbps, respectively. The first factor used to compare ODR-TDMA with other protocols was packet loss ratio. Fig. 6 shows a comparison with FDR-TDMA, which illustrates that ODR-TDMA generated better outcomes by virtue of the reduced packet loss and the achieved consistency, which thereby gives exceptional QoS. The targeted 0.06 ODR-TDMA packet loss ratio supported 29 video users at a packet delay lower than 4 ms, where only 26 users were supported by FDR-TDMA.

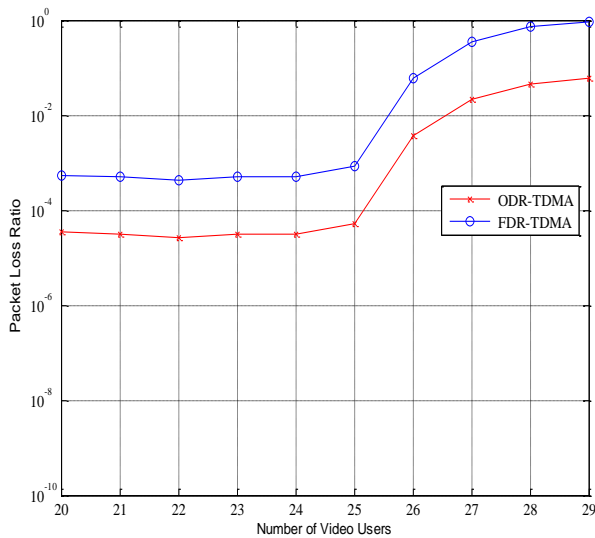


Fig. 6. Comparison of Packet Loss.

Fig. 7 illustrates that ODR-TDMA resulted in lower packet delay in comparison to FDR-TDMA, since it supported 20-23 users with a delay of less than 2 msec whereas the delay in FDR-TDMA was 5 msec. By taking into account throughput and delay, the ODR-TDMA served 29 users with higher throughput, as can be seen in Fig. 8, in which the delay increased by only 3.25 msec in comparison to FDR TDMA that served similar number of users with a delay of up to 19 msec.

Fig. 8 shows that ODR-TDMA exhibited slightly higher throughput when the system was overloaded. Both throughputs started at the same point and resulted in expansion, whereas N_v increased within a similar range up to $N_v = 26$, wherein ODR-TDMA began to achieve higher throughput in comparison to FDR-TDMA.

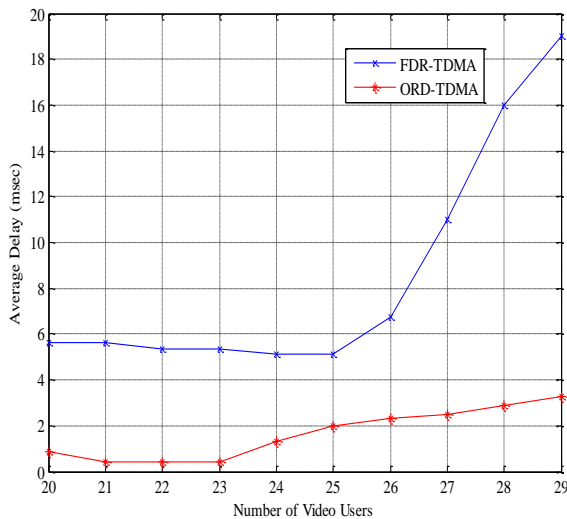


Fig. 7. Comparison of Average Delay.

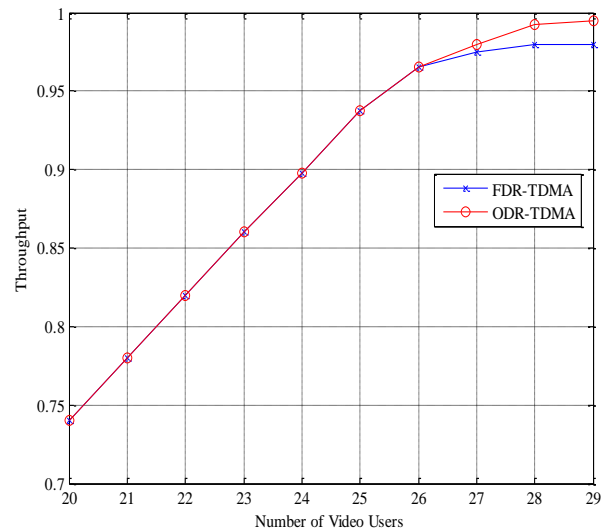


Fig. 8. Comparison on Throughput.

V. CONCLUSION

This study presents a unique resource allocation based on fair delay optimization for video traffic over WMNs system. As such, the recommended allocation algorithm was able to achieve the required QoS by reducing the variance in delay between the transmitted video packets in addition to flexibly controlling the allocated resource (bandwidth) for video traffic approximately the corresponding average bit rate that enhanced efficiency in its usage. The simulation results show an exception resource employment has achieved and offered an almost fair delay for the video packets. Moreover, it has the ability to manage the QoS for video traffic in terms of average delay and packets loss in order to generate exceptional QoS. In conclusion, the algorithm proposed in this study is successful in terms of improving packet loss, packet delay, and throughput in comparison to FDR-TDMA. For future work and as ODR-TDMA only concentrates and works with users who have higher delay than the higher delay threshold, a new algorithm could be developed to concentrate on users who have lower delay than the lower delay threshold and keep them in sleep mode during the waiting time so it can save the total consumption energy.

REFERENCES

- [1] O. Kubbar, H.T. Mouftah, Multiple access control protocols for wireless ATM: problems definition and design objectives, IEEE Communication Magazine, 1997, pp. 93–99.
- [2] Y. Kwok, V.K.N. Lau, A quantitative comparison of multiple access control protocols for wireless ATM, IEEE Transaction on Vehicular Technology, 2001, pp. 796–815.
- [3] I. Akyildiz, J. McNair, L. Carrasco, R. Puigjaner, Medium access controls for multimedia traffic in wireless networks, IEEE Network Magazine, vol. 13, 1999, pp. 39–47.
- [4] J. Wen, J. Lain, Y. lai, Performance simulation of wireless multimedia systems using NC-PRMA/DA and SNC-PRMA/DA protocols, IEEE Transactions on Systems, MAN, AND Cybernetics Part A: Systems and Humans, vol. 32, 2002, pp. 780–787.

- [5] Elnoubi, A.M. Alsayh, A packet reservation multiple access (PRMA)-based algorithm for multimedia wireless system, *IEEE Transaction on Vehicular Technology*, vol. 53, 2004, pp. 215–222.
- [6] J. Kuri, M. Gagnaire, ATM traffic management in an LMDS wireless access network, *IEEE Communication Magazine*, 2001, pp. 128–133.
- [7] N. Passas, S. Paskalis, D. Vali, L. Merakos, Quality-of-service-oriented medium access control for wireless ATM networks, *IEEE Communication Magazine*, 1997, pp. 42–50.
- [8] J.F. Frigon, H.C.B. Chan, V.C.M. leung, Dynamic reservation TDMA protocol for wireless ATM networks, *IEEE Journal of Selected Areas in Communication*, vol. 19, 2001, pp. 370–383.
- [9] Jain, R.. Comparative analysis of contention based and TDMA based MAC protocols for wireless sensor networks. *International Journal of Information Technology*, 2018, pp.1-6.
- [10] C.G. Kang, C.W. Ahn, K.H. Jang, W.S. Kang, Contention-free distributed dynamic reservation MAC protocol with deterministic scheduling (C-FD3 R MAC) for wireless ATM networks, *IEEE Journal of Selected Area Communications*, vol. 18, 2000, pp. 1623–1635.
- [11] L. Musumeci, P. Giacomazzi, L. Fratta, Polling- and contention-based schemes for TDMA-TDD access to wireless ATM networks, *IEEE Journal of Selected Area Communications*, vol. 18, 2000, pp. 1597–1607.
- [12] C.S. Chang, K.C. Chen, M.Y. You, J.-F. Chang, Guaranteed quality-of-service wireless access to ATM networks, *IEEE Journal of Selected Area Communications* vol. 15, 1997, pp. 106–118.
- [13] L. Fratta, P. Giacomazzi, L. Musumeci, PRAS: a Mac protocol for wireless ATM networks, *Globecom'99*, 1999, pp. 2743–2715.
- [14] L. Lei, S. Cai, C. Luo, W. Cai, and J. Zhou, "A dynamic TDMA-based MAC protocol with QoS guarantees for fully connected ad hoc networks," *Telecommunication Systems*, vol. 60, 2015, pp. 43-53.
- [15] Shahin, N., Ali, R. and Kim, Y.T., 2018. Hybrid Slotted-CSMA/CA-TDMA for Efficient Massive Registration of IoT Devices. *IEEE Access*.
- [16] Zhuo, S., Wang, Z., Song, Y.Q., Wang, Z. and Almeida, L., 2016. A traffic adaptive multi-channel MAC protocol with dynamic slot allocation for WSNs. *IEEE Transactions on Mobile Computing*, vol 15, pp.1600-1613.
- [17] Hussain, Md Iftexhar, Zaved Iqbal Ahmed, Nityananda Sarma, and D. K. Saikia. "An efficient TDMA MAC protocol for multi-hop WiFi-based long distance networks." *Wireless Personal Communications*, vol. 86, 2016, pp. 1971-1994.
- [18] Rizk, M.R.and et al., Fair Delay Optimization-based Resource Allocation Algorithm for Video Traffic over Wireless Multimedia System, *Wireless personal communications*, vol. 48, 2009, pp. 551-568.

Cybercrime in Morocco

A Study of the Behaviors of Moroccan Young People Face to the Digital Crime

M. EL Hamzaoui¹

Laboratory of Innovation in Science, Technologies and
Modeling (ISTEM)
Faculty of science, University Chouaib Doukkali
El Jadida, Morocco

Faycal Bensalah²

Lab STIC
Faculty of science, University Chouaib Doukkali
El Jadida, Morocco

Abstract—Cybercrime encompasses all illegal actions and facts that target cyberspaces and cause enormous economic and financial damages to organizations and individuals. A cyberspace is essentially composed of digital information as well as its store and communication instruments/platforms. To remedy this phenomenon, attention has focused particularly on both computer security and legislation in an area where the human behavior is also decisive. Social psychology has well defined the concept of behavior and also studied its relations with the attitude in human action. This paper aims to broaden the scope of cybercrime to also discuss marginal phenomena which do not attract enough attention but could easily be converted to digital criminals once circumstances become appropriate. The main objective of this work is the study of the ‘human’-‘digital world’ interactivity in a specific geographical area or precisely the study of the human behavior towards digital crimes. The proposed study targets young people of a small Moroccan city that is in the south of the country central region and constitutes its global economy barycenter. The study dealt specifically with a sample of Moroccan young living in El Jadida city that coincidentally contains individuals from other Moroccan cities which enriched this study more.

Keywords—Cybercrime; cyberspace; information system; information and communication technologies; social psychology

I INTRODUCTION

Cybercrime is a synonym for digital crime. However, this simplified definition cannot hide the phenomenon dark side; cybercrime is characterized by a variety of dangers able to cause enormous financial and economic damage [1,2].

Cybercrime does not have a definition that specifies its general framework and its dimensions. Since cybercrime is strongly linked to cyberspaces, its definitions [3,4] converge almost completely on this common idea: “Cybercrime is, generally, a phenomenon able to target illegally computer-assisted activities opened on communications’ networks”. In general, cyberspaces are the technologies and platforms used for the storage and communication of digital information.

Practically, organizations (enterprises, administrations, etc.), that adopt a good governance in the management of their digital environments use, on the one hand, Information Systems (IS) to manage, store and manipulate digital information and, on the other hand, Information and Communication Technologies (ICT) to communicate it.

Historically, cybercrime dates back to the 1980s and 1990s. In 1988, Robert Morris released a program onto Internet (worm [5]) to find out how many computers were currently connected to it but a bug in this program caused damage to many computers in US. Legislatively, this act is classified as one of the Digital World (DW) first crimes.

The fight against this phenomenon attracted especially the interest of computer scientists, lawyers and academics [6,7,8,9]. Therefore, computer security and legislation became the main tools to fight against cybercrime but other interesting parameters are still neglected. For example, given its effects on human uses of DW services [10], the parameter of human behavior will be very useful in the fight against cybercrime.

The specialists of people security and installation safety use the “human factor” concept to refer to the men behavior inside work environments [11]. In general, the human factor refers to the contribution of the human being to events and is also involved in the study of relationships between human behavior and environments, in which man can act on actions, undergo effects or make changes.

In this context, the social psychology studies relationships links attitude to behavior in human action and develops theories and models to facilitate the comprehension of the enigmas of human attitude, behavior and action in society. Along with this work, we will respect and adopt the social psychology terminology as well as the scientific perception of behavior defined and used in some research works of this field.

This paper also draws attention to a new issue concerning certain phenomena that could be converted into digital crimes when circumstances permit. Therefore, we have, on the one hand, to re-draw the cyberspace dimensions to include all data that could be used indirectly in digital crime and, on the other hand, to generalize the cybercrime definition in order to consider these dangerous phenomena: “*Cybercrime is a multidimensional phenomenon (legislation, technical, social, societal, etc.) able to target randomly (directly and/or indirectly and at any time), through all illegal means (hacking, destruction, theft, corruption, etc.), cyberspaces composed mainly of information, IS, ICT and any other instrument, platform or electronic/non-electronic device used to store or to communicate information.*”

This work aims to present, through a study on the El Jadida young people behaviors in the face of digital crimes, the role

that the human behavior could play in the fight against cybercrime.

II THEORETICAL FRAMEWORK

A. Fight against Cybercrime between Computer Security and Legislation

The preferred preys of DW criminals are cyberspaces including digital information (mobile and immobile). Digital dangers are all actions that can randomly target digitalized parts of any personal or organizational activity and cause massive damage (e-commerce [12], logistics [13], finance [14,15], marketing [16,17], etc.).

The fight against cybercrime is therefore a complex and multidimensional operation that mainly involves computer security specialists and lawyers:

Concerning the computer security, The OSI 7498-2, second part of the reference model for open systems interconnection (OSI 7498 model), specifies the security architecture through a detailed description of the computer networks security. The computer networks security management is a main functional area of the OSI management [18] that covers the basic digital security objectives (Preventing unauthorized divulgations of data, prohibition of unauthorized modifications of data, prevent unauthorized access to resources, etc.). The digital environments can also be secured in different manner such as electronic certificates, authentication and authorization, Secured communication channels (VPNs), and DMZs.

Concerning the legislation relating to cybercrime, several works were dealing this subject [19,20] but obstacles and constraints were being and are still numerous and complex [21]. Then, the global success of the fight against cybercrime requires the harmonization of legislative efforts undertaken in geographical areas characterized by their territorial sovereignties (countries, unions, etc.) but differ in legislative, cultural and other specificities.

In this context, the most active UN-institution in reaching harmonization on global cybersecurity and cybercrime legislation is the International Telecommunication Union (ITU) in Geneva [20] that has developed a guide to help developing countries understand the legal aspects of cybercrime and to contribute to the harmonization of legal frameworks.

According to Schojolberg [20], the long history of global harmonization on cybercrime legislation was initiated by Donn B. Parker research of computer crime and security from the early 1970ties and it could then evolve through various scientific works and manifestations.

In Morocco, our study geographical zone, since the begin of the 21th century, enormous efforts have been made in this regard (new laws were promulgated, proposition of numeric projects as the “Maroc Numeric 2013” strategy, ratification of the Budapest Convention of 23 November 2001 on cybercrime, etc.).

B. Overview on the Behavior in Social Psychology

This work is intertwined with social psychology, which focuses on relationships that can link attitude to behavior in human action. In this field, several theories and models have been proposed to understand and illustrate the main concepts such as human attitude, behavior and action in society:

The Theory of Reasoned Action (TRA) [22] was developed by Fishbein and Ajzen (1967) to predict how individuals behave according to their pre-existing attitudes and behavioral intentions. Then, in 1985, Ajzen developed 'Theory of Planned Behavior' (TPB) [23], an improved version of the TRA, by adding to its behavioral control. The TPB was developed to predict and explain human social behavior, and to serve as a framework for behavior change interventions.

In Ajzen's research works, behavior is defined as the manifest, observable response in a given situation with respect to a given target and immediately preceded by the intention that expresses the person's readiness to perform a given behavior. According to the TPB, the intention itself is based, on three basis factors; namely the ‘attitude toward a behavior’ that allows to know the degree to which performance of the behavior is positively or negatively valued, the ‘Subjective norm’ that encompasses the perceived social pressure to engage or not in a behavior and the ‘Perceived behavioral control’ that refers to people's perceptions of their ability to perform a given behavior (Fig. 1). Moreover, the ‘behavioral control’ is a main key of the success of a behavior performance.

In short, the TPB states that human behavior is channeled through three mains axes which are behavioral beliefs, normative beliefs and control beliefs.

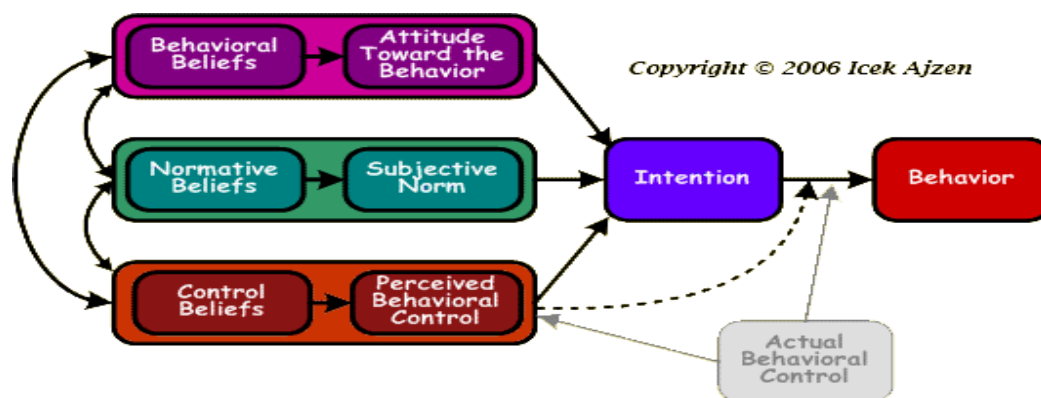


Fig. 1. Schematic Representation of the ‘Theory of Planned Behavior’.

III CONVERTIBLE PHENOMENA TO DIGITAL CRIMES

Cybercrime is the set of classic digital abuses (hacking, interception, destruction, etc.) as well as other digital crimes that could be grow in proportion to the development of digital services on Internet (Frauds with blue card, digital identity theft, etc.).

Unfortunately, the fight against cybercrime had focused on the digital aspect of information and neglected phenomena that are able to touch, with or without bad faith, any type of information (written texts, discussions, etc.) in order to digitize and to use them in digital crimes. Henceforth, these phenomena will be called, along this paper, the Convertible Phenomena to Cybercrimes (CPC).

The CPC constitute a result of both very particular actions and individual or collective behaviors, voluntary or not, which especially related to the individual and/or managerial imprudence within organizations but also in private area (trust to the other, lack of belonging workplace spirit, security vulnerabilities, etc.). The CPC do not attract enough attention from the responsible of their living environments and are also characterized by important properties make them dangerous such as the ability of randomly conversion into digital crimes, the dependence on geographical specificities (traditions of workspaces, social customs, etc.), etc.

For example, in North Africa cities, one can sometimes find easily, in the peanut vendors' shop, personal and organizations archives documents containing extremely sensitive data (financial transactions, commercial actions, etc.). These information leaks can cause damage to organizations and lead to serious social crises for individuals.

Similarly, according the some countries' traditions, the discussions between organization' employees, in public places (cafes, public transport, etc.), could facilitate the disclosure of secrets which are well hidden and clasped in the organization vaults. These verbal data could be digitized (digital texts, voice recordings, etc.) and then misused in the DW. Despite the lack of statistics and studies on the CPCs, they are certainly involved in digital crimes.

Concerning the based bad faith CPCs (aggression, scam, corruption, etc.), we can cite the example of the criminals who illegally remove, in the real world, sensitive digital information (information of a bank account, electronic device password, etc.) for illegal uses in the DW.

IV REALIZED STUDY: YOUNG MOROCCAN PEOPLE AND CYBERCRIME

A. General Framework of the Study

In Morocco, as in any other country, it is difficult to limit to technology and legislation in the fight against cybercrime. In this perspective, to facilitate the discovery of the possible relations between human behavior and digital crime, we conducted a quantitative study on a random, representative and varied sample of young people from a carefully selected Moroccan city.

TABLE I. DIFFERENT AXIS OF OUR QUANTITATIVE STUDY AND THEIR OBJECTIVES

Axis	Objective
1	Collection of respondents' personal data.
2	Measure of the degree of the respondents' familiarization with the digital world.
3	Measure of the vigilance of the respondents in the digital world.
4	Knowledge of the respondents' judgments on computer security.
5	Discovery of the respondents' behaviors towards crimes opportunities.
6	Discovery of the respondents' opinions on both cybercrime in Morocco and its relative legislation.

This quantitative study dealt with six fundamental axes where each one is distinguished by a set of criteria defining its own nature (Table I). The axes' objectives are well arranged in order to facilitate the realization of the entire study objective; the study of human behavior in the face of digital crime.

Moreover, the study axes will allow us to define the respondents' personalities and the necessary components to determine their behaviors in accordance with the social psychology principles. Then, these axes will allow us to know the various factors determining the respondent's intention to choose and adopt a new behavior:

- The degree of the respondent's acceptance of both his future behavior and the potential consequences.
- The influence of the environment on the respondent behavior.
- The beliefs about the respondent's ability to succeed in his future adopted behavior.

B. The Study Results: Data and Statistics

The main data collected in our quantitative study are presented in Tables II, III, IV, V and VI.

Concerning the last criterion of the third axis (Table IV), a rate of 39.53% of the respondents who were never victims of the DW know victims of this world.

C. Synthesis of Obtained Data

Because of quantitative studies aims to give approximate results close to the observed reality, we have chosen to work in the following syntheses on intervals instead of exact values that vary from a study to another. This approach will allow us to define, for each synthesis case, a Logic Interval of its Study and Realization (LISR); an interval where it could really take place.

To facilitate the synthesis of the obtained results, we proceeded to a new repartition of the study six axes in four homogeneous and coherent synthesis operations.

1) *Synthesis 1: Personal data*

We note a strong coherence between age and study level criteria (Table VI) for all respondents. Only 4% of the respondents, aged between 6 and 12, are college students while just 1% of them, aged between 16 and 18, are university students. Then, the respondents are characterized by a certain study level advancement with respect to age, which proves the quality of the studied sample.

TABLE II. RESULTS OF THE CRITERIA OF THE FIRST AXIS OF OUR QUANTITATIVE STUDY

Axis	Criterion	Obtained Result
1	Age	- Between 6 and 12 years: 10% of the respondents global number. - Between 13 and 15 years: 26% of the respondents global number. - Between 16 and 18 years: 33% of the respondents global number. - Plus, then 18 years: 31% of the respondents' global number.
	Study level	32% of the respondents are university students, 32% are high school students, 30% are middle school students and 6% are primary school students.
	Origin city	Majority of the respondents come from El Jadida (55%) followed by Casablanca (31%). Other origin cities (Rabat, Fez, Safi, Settat, Khouribga, Marrakech, etc.) together represent a rate of 14%.

TABLE III. RESULTS OF THE FIRST CRITERION OF THE SECOND AXIS OF OUR QUANTITATIVE STUDY

Axis	Criterion	Obtained Result				
		Very high	Rather high	Medium	Rather weak	Very low
2	Degree of familiarization with Internet	31%	24%	31%	4%	10%

TABLE IV. RESULTS OF THE CRITERIA OF THE AXES 2,3,4 AND 5 OF OUR QUANTITATIVE STUDY

Axis	Criterion	Obtained Result	
		Yes	No
2	Being used to purchase on Internet	51.00%	49.00%
3	Knowledge of risks related to purchase on Internet	58.60%	41.40%
	Being, one day, a victim of the digital world crimes	14.00%	86.00%
	Knowledge of the digital world victims	37.80%	62.20%
4	Effectiveness of computer security tools in the fight against the digital world risks	54.00%	46.00%
	Possibilities of digital attacks in the absence of computer security tools	67.00%	33.00%
5	Being aware of the risks involved in committing a crime	50.00%	50.00%
	Audacity to commit crimes in the face of an excellent opportunity in the real world	11.00%	89.00%
	Audacity to commit crimes in the face of an exceptional opportunity in the digital world	30.00%	70.00%

TABLE V. RESULTS OF THE CRITERIA OF THE SIXTH AXIS OF OUR QUANTITATIVE STUDY

Axis	Criterion	Obtained Result				
		Relevant	Fairly relevant	Medium	Fair weak	Very weak
6	Judgment of the relevance of the Moroccan legislation on cybercrime	11%	12%	33%	17%	11%
	Evaluations of the cybercrime in Morocco	mediocre, a phenomenon with unclear legislation and threatens the DW, an evolving phenomenon against a rigid legislation, etc.				

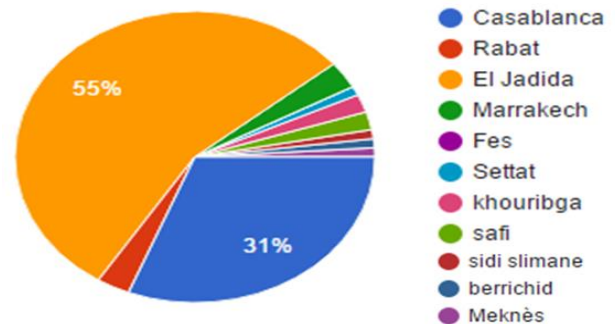
TABLE VI. COHERENCE BETWEEN AGE AND STUDY LEVEL OF THE RESPONDENTS SAMPLE

Age (years)	Interval	Percentage	↔	Percentage	Level	Study level
	≥ 19	[16,18]		31%	32%	
	[13,15]	33%	32%	High School		
	[06,12]	26%	30%	College		
		10%	6%	Primary School		

Basing on these data, we can define two major blocks; namely the Block of the University and High School Students (BUHSS) and the Block of the Middle and Primary Schools Students (BMPSS).



(a). Map Positions of Some Origin Cities of the Studied Sample.



(b). Repartition of the Origin Cities of the Studied Sample.

Fig. 2. Geographical Positions and Repartition of Origin Cities of the Study Respondents.

The Number of the BUHSS (NBUHSS) represents 64% of the Total Number of the Studied Population (TNSSP) while the Number of the BMPSS (NBMPSS) represents a percentage of 36%.

Considering the study role in the determination of the human behavior, we will analysis the criteria of our study axes according to the “Study Level” criterion, especially according to BUHSS and BMPSS.

In this study, the main reason to consider the city criterion (Fig. 2) is that the city is a geographical area where cultural exchange profoundly influences individual behavior.

The chosen sample survey covers almost all main cities of the Moroccan large central region and also extends to reach a few cities on its borders (Fig. 2(a)). This diversity of the origin cities characterizing our studied sample (Fig. 2(b)) will certainly increase our knowledge level about young people in many Moroccan cities where regional cultures intervene strongly. Therefore, this will allow us to easily generalize the study results on all Moroccan young.

2) Synthesis 2: Interactivity with the DW

- Use of Internet network services: A rate of 86% of the respondents is considered familiar with Internet but 14% of them are not (Table III).

The study of this criterion according to the study level criterion gave us:

Relatively to the TNSSP, if V% ($0 \leq V \leq 14$) is the percentage of the BUHSS respondents ‘Non-Familiarized with the Utilization of the Internet Services, NFUIS’, the NFUIS percentages relative to the NBUHSS and the SBMPSS are respectively:

- P1: Number (NFUIS of BUHSS)/NBUHSS = $V/64$
- P2: Number (NFUIS of BMPSS)/NBMPSS = $(14-V)/36$

In principle, the unfamiliarity with the DW decreases with the increase of the study level, which implies that the percentage of the NFUIS inside the BUHSS relative to the NBUHSS must be lower than the percentage of the NFUIS inside the BMPSS relative to NBMPSS.

Therefore, one can define, in Fig. 3, two zones on both sides of the point $V=8.96$ ($P1=P2=14\%$) and deduce that the closest situation to reality must be in the second zone ($V < 8.96$) (Table VII); when the variable X tends to zero.

- Purchase on Internet: A percentage of 51% of the TNSSP make purchases on Internet (Table IV) which represents 59.30% of all the respondents familiar with the DW. In reality, only those familiar with the DW can purchase on the Internet. This situation may be due to the lack of online purchasing services (technical and technological constraints), lack of digital trust, etc.
- Consequences of the Internet services uses: A percentage of 58.6% of the TNSSP knows risks related to the purchase on Internet but 41.40% of them ignore these risks (Table IV).

Relatively to the TNSSP, if W% ($5.4 \leq W \leq 41.40$) is the percentage of the respondents ‘Ignorant of the Internet Purchased Risks, IIPR’, the IIPR percentages relative to the NBUHSS and the NBMPSS are respectively:

- P1: Number (IIPR of BUHSS)/ NBUHSS = $W/64$
- P2: Number (IIPR of BMPSS)/ NBMPSS = $(41.40-W)/36$

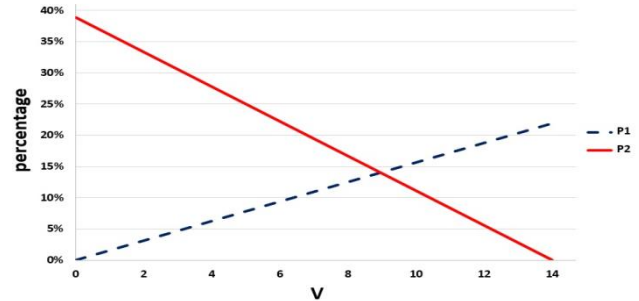


Fig. 3. Percentages of the NFUIS Relative to the BUHSS and the BMPSS.

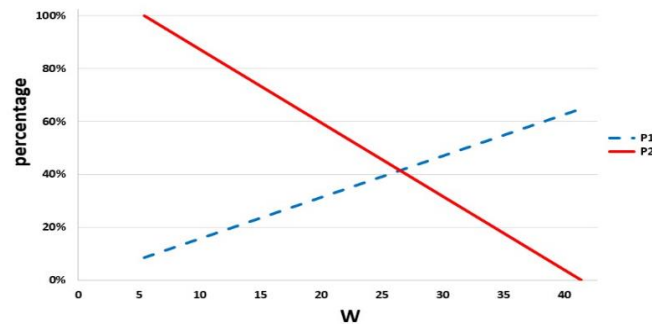


Fig. 4. Percentages of the IIPR Relative to the BUHSS and the BMPSS.

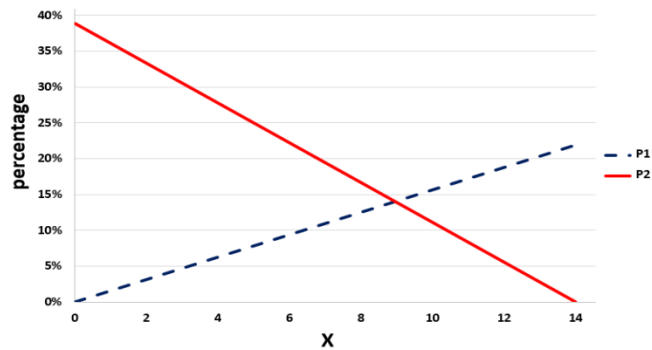


Fig. 5. Percentages of VDWC the Relative to the BUHSS and the BMPSS.

TABLE VII. LISR AND EXTREME CASES OF THE VARIABLE V

Zone	Extreme Cases	LISR
$V > 8.96$	$V=14, P1=21.88\%, P2=0\%$	
$V < 8.96$	$V=0, P1=0\%, P2=38.39\%$	[0,8.96]

TABLE VIII. LISR AND EXTREME CASES OF THE VARIABLE W

Zone	Extreme Cases	LISR
$W > 26.50$	$W=41.40, P1=64.69\%, P2=0\%$	
$W < 26.50$	$W=5.5, P1=8.44\%, P2=100\%$	[0,26.5]

TABLE IX. LISR AND EXTREME CASES OF THE VARIABLE X.

Zone	Extreme cases	LISR
X>8.96	X=14, P1=21.88%, P2=0%	[8.96,21.88]
X<8.96	X=0, P1=0%, P2=38.89%	[0,8.96]

In principle, the knowledge of the risks of purchases on the Internet depends on the level of study and also increases relative to it. Therefore, one can define, on Fig. 4, a study area on each side of the point W=26.50 (P1=P2=41.40%) (Table VIII) and conclude that the interval [0,26.5] may be the LISR of this criterion since the IIPR percentage relative to the middle and high schools students total number exceeds that of the BUHSS.

In this context, the DW risks most known by the respondents are principally scam, late delivery, counterfeiting and piracy.

- Being a victim of the DW crimes: Only 14% of all respondents were victims of the DW and 86% of them are not (Table IV).

Relatively to the TNSSP, if X% ($0 \leq X \leq 14$) is the percentage of the respondents of the BUHSS ‘Victims of the DW Crimes, VDWC’, the percentages of the VDWC relative to the NBUHSS and the NBMPSS are respectively:

- P1: Number (VDWC of BUHSS)/NBUHSS = X/64
- P2: Number (VDWC of BMPSS)/NBMPSS = (14-X)/36

Before interpreting the data and treating these two equalities, we recall that all data on VDWC and NFUIS, including percentages, coincide perfectly. Therefore, the variables X and V behave in the same way, which increases the probability that the NMMV inside the studied sample can be exactly its NFUIS.

The discussion of the extreme cases of this criterion, as illustrated in Fig. 5, led to the definition of two zones on both sides of the point X=8.96 (P1=P2=14%) (Table IX).

On the one hand, if the NBMPSS uses the digital services more correctly than the NBUHSS, the first Zone (X>8.96) may be a LISR of this criterion. In this case, between 14% and 21.88% of the university and high school students of EL Jadida city could be DW victims.

On the other hand, the second Zone (X<8.96) represents an LISR of this criterion if the NBUHSS uses correctly the DW services. In this case, between 24.89% and 38.89% of the primary and middle school students of El Jadida city could be DW victims.

Moreover, we recall that 37.8% of the TNSSP know VDWC but 62.2% of them do not know anyone. In addition, a percentage of 39.53% of the respondents who were never the VDWC know VDWC, but only 3.81% of those who were the VDWC know VDWC. Therefore, it is clear that the knowledge of VDWC increases the level of vigilance in the use of the digital services.

- Effectiveness of Computer Security Tools in the Fight Against Cybercrimes (CSTFAC): The interval of the percentage of NBUHSS individuals who do not trust

the effectiveness of the CSTFAC is [15.64%, 71.88%] while that relative to the BMPSS is [0%,100%]. Consequently, at least 28.31% of the BUHSS trust the CSTFACs but this percentage will never exceed 84.36%.

The percentage of individuals, who believe that machines could be in safe without computer security tools, is 33%, which is a weak percentage. If one considers that only the VDWC who underestimate the computer security importance, one can then deduce that 42.42% of these individuals are the VDWC.

3) *Synthesis 3: Behaviors of the Respondents in the Face of the Crimes Opportunities*

Firstly, we remember that the half of the TNSSP (50%) is aware of the dangers of committing any kind of crimes.

- Behavior in the face of the opportunities for safe crime: A percentage of 11% of the TNSSP has the audacity to perpetrate crimes in the real world if conditions are favorable while 89% of them cannot do.

Because of, as it is already mentioned, the CPC can take place, with or without bad faith, we can conclude that, in this case, 11% of the TNSSP could voluntarily support the CPC while 89% of them could do it accidentally. Concerning the digital crime, a percentage of 30% of the TNSSP has the audacity to perpetrate this kind of crimes while 70% of them do not have it. One notes that the rate of people with the audacity to commit crimes increases by 272.73% from the real world to the DW.

Relatively to the TNSSP, if Y% ($0 \leq Y \leq 30$) is the percentage of the BUHSS respondents ‘Able to Perpetuate Digital Crime, APDC’, the percentages of the APDC relative to the NBUHSS and to the NBMPSS are respectively:

- P1: Number (APDC of BUHSS)/NBUHSS = Y/64.
- P2: Number (APDC of BMPSS)/NBMPSS = (30-Y)/36.

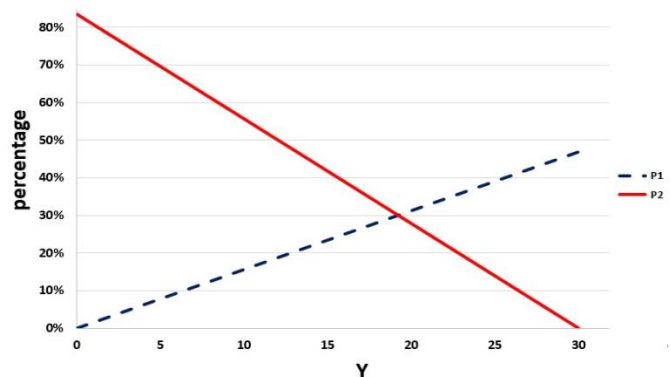


Fig. 6. Percentages of the APDC Relative to the BUHSS and the BMPSS.

TABLE X. LISR AND EXTREME CASES OF THE VARIABLE Y

Zone	Extreme cases	LISR
Y>19.20	Y=30, P1=46.88%, P2=0%	[19.20,30]
Y<19.20	Y=0, P1=0%, P2=83.33%	[0,19.20]

The consideration of the study level allows to define, on Fig. 6, two zones on both sides of the point $Y=19.20$ ($P1=P2=0\%$) (Table X):

The Zone ($Y>19.20$) could be a LISR of this criterion when, on the one hand, the NBUHSS is well familiarized with the DW but without responsibility and, on the other hand, the NBMPPSS is well surrounded and well supervised. We warn that, depending on the circumstances and the entourage, up to 46.88% of the NBMPPSS could become digital thieves.

The Zone ($Y<19.20$) could be a LISR of this criterion when the individuals of the BMPSS are clumsy in the WD but those of the NBUHSS are correct. We warn that up to 83.33% of the SBMPSS could commit crimes in the DW. A dangerous social phenomenon could take place if the parents, education system and responsible will not intervene to anticipate, sensitize and supervise these young people.

4) *Synthesis 4: Cybercrime in Morocco*

- Moroccan legislation on cybercrime: A percentage of 72% of the TNSSP judges positively this legislation while 28% of them judge it negative (Table V).

Relatively to the TNSSP, if $Z\%$ ($36 \leq Z \leq 64$) is the percentage of the BUHSS respondents having ‘Positive Judgments to the Moroccan Legislation Relating to Cybercrime, PJMLRC’, the percentages of the PJMLRC relative to the NBUHSS and the NBMPPSS are respectively:

- $P1$: Number (PJMLRC of BUHSS)/NBUHSS = $Z/64$
- $P2$: Number (PJMLRC of BMPSS)/NBMPPSS = $(72-Z)/36$

The study level is very important in the interpretation of this criterion because in principle the NBUHSS are well placed than the NBMPPSS to judge adequately specific legislations.

As for previous cases, one can defines, as illustrated on Fig. 7, a study area on each side of the line joining the points $P1=P2$ ($=72\%$) and the point $Z=46.08$ and also specifies the criterion LISR (Table XI).

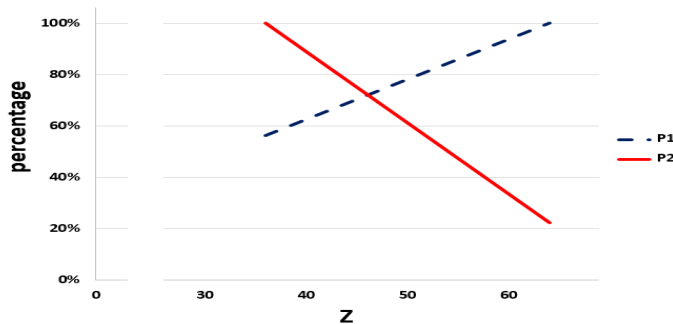


Fig. 7. Percentages of the PJMLRC Relative to the BUHSS and the BMPSS.

TABLE XI. LISR AND EXTREME CASES OF THE VARIABLE Z

Zone	Extreme cases	LISR
$Z>46.08$	$Z=64, P1=100\%, P2=22.22\%$	[46.08,64]
$Z<46.08$	$Z=36, P1=56.25\%, P2=100\%$	

In sum, the majority of the TNSSP judge cybercrime, an evolving phenomenon accompanied by a non-scalable legislation.

V NOTICES AND RECOMMENDATIONS

After having chosen the quantitative study axes and criteria to study the human behavior in the face of digital crimes according to the social psychology, we proceeded directly to the realization phase in three steps (data collection, results presentation, results synthesis). Through this study, we have been able to deduce important remarks concerning the study itself, to discover some bases of the direct and indirect links could relate human behavior to cybercrime and to confirm some impacts of the human factor on the electronic economy:

A. Remarks and Limits of the Adopted Study

- The coherence between some study criteria (for example the study level and age criteria) increases the studied sample quality, which facilitates more the study itself.
- Despite the specific characteristics of the studied geographical area, the fact of meeting within it, during the study, a considerable number of neighboring areas individuals makes it possible to generalize the study results on the immediate geographical neighborhood.
- It is now necessary to perform, in a second phase, a complementary psychological study in the field of cybercrime. This study will allow, on the one hand, discovering the global impact of the human psychological components on the cybercrime study and, on the other hand, discussing the possibility of developing, based on our study, a theoretical and/or practical model that links between social psychology and the cybercrime field.

B. Links between Human Behavior and Cybercrime

- The ignorance is a powerful source of cybercrime: ignorance of the computer security importance, ignorance of the DW risks, ignorance of cybercrime legislation, etc.
- The audacity to perpetrate crimes multiplies from the real world to the DW.
- The victims of the DW are most likely unfamiliar.
- The knowledge of the DW victims increases the level of vigilance when using digital services.
- The increase of the study level leads to the increase of the vigilance degree in the use of the DW services.
- The increase of the study level increases the conviction that the computer security tools, used to counter the DW risks, are necessary but insufficient.
- The increase of the study level means the increase of the individual comprehension level but it does not imply the increase of the degree of the individual consciousness and maturity, especially in the DW.

- The absence of both awareness and responsibility makes the familiarization with the DW, which is strongly linked to the increase in the study level, a real threat to the DW.

C. Impacts of the Human Behavior on the Digital Economy

- The lack of familiarity with the DW has a negative impact on the profitability of digital services such as e-commerce, digital marketing, etc.
- The remarkable increase in the audacity of perpetrating crimes during the transition from the real world to the DW certainly threatens the digital economy.

VI CONCLUSION

Generally, the relationship human factor-cybercrime is multidimensional and its consideration in the cybercrime study is important to clarify the manner to use effectively the human behavior in the fight against digital crimes. In short, it is extremely important to know for each studied population its dominant characteristics (attitude, intention and behavior) in order to decide on its management and control policies/strategies.

To conclude the present study, on the one hand, we extended the human attitude criteria by adding, to these study basic criteria (age, study level and origin city), two new criteria (knowledge and qualification) and, on the other hand, we limited to three dimensions (Fig. 8).

- Vertical dimension (some attitude components and behavior): The attitude criteria all evolve positively from bottom to top. On the one hand, the age and study level criteria increase, in a consistent way, in this direction and, on the other hand, the knowledge

(security, legislation, etc.) and the qualification (computer tools mastery, capacity of e-commerce actions, etc.), which depend on the three basic criteria, also evolve positively upward from ignorance to knowledge and from non-qualification to qualification, respectively. This dimension also illustrates from which study level could start appearing other attitude criteria.

- First horizontal dimension (interactivity Attitude-behavior-cybercrime): This dimension illustrates the links that could relate the human being, based on his attitude and intention, to a specific behavior inside the cybercrime area; namely a digital criminal or a WD victim.
- Second horizontal dimension (fight against cybercrime): The main activities of the fight against cybercrime, that can be undertaken based on the human behavior, begin with the training and sensitization (ethics, deontology, etc.) in academic environments followed by the watch (monitoring, measurement, etc.) to be able to anticipate and develop the adequate action strategies. Finally, we find the action which includes all the possible used tools and/or platforms (technical, legislative, etc.) to, on the one hand, protect the human behaviors victims of the cybercrime and, on the other hand, to fight against the human behaviors constitute digital malefactors (blocking, arrest, etc.).

In the future, we will carry out, in the future second phase of this study, a quantitative psychological study that will enable us to further deepen our knowledge in this psychological aspect of cybercrime and to continue developing this important axis of the cybercrime field.

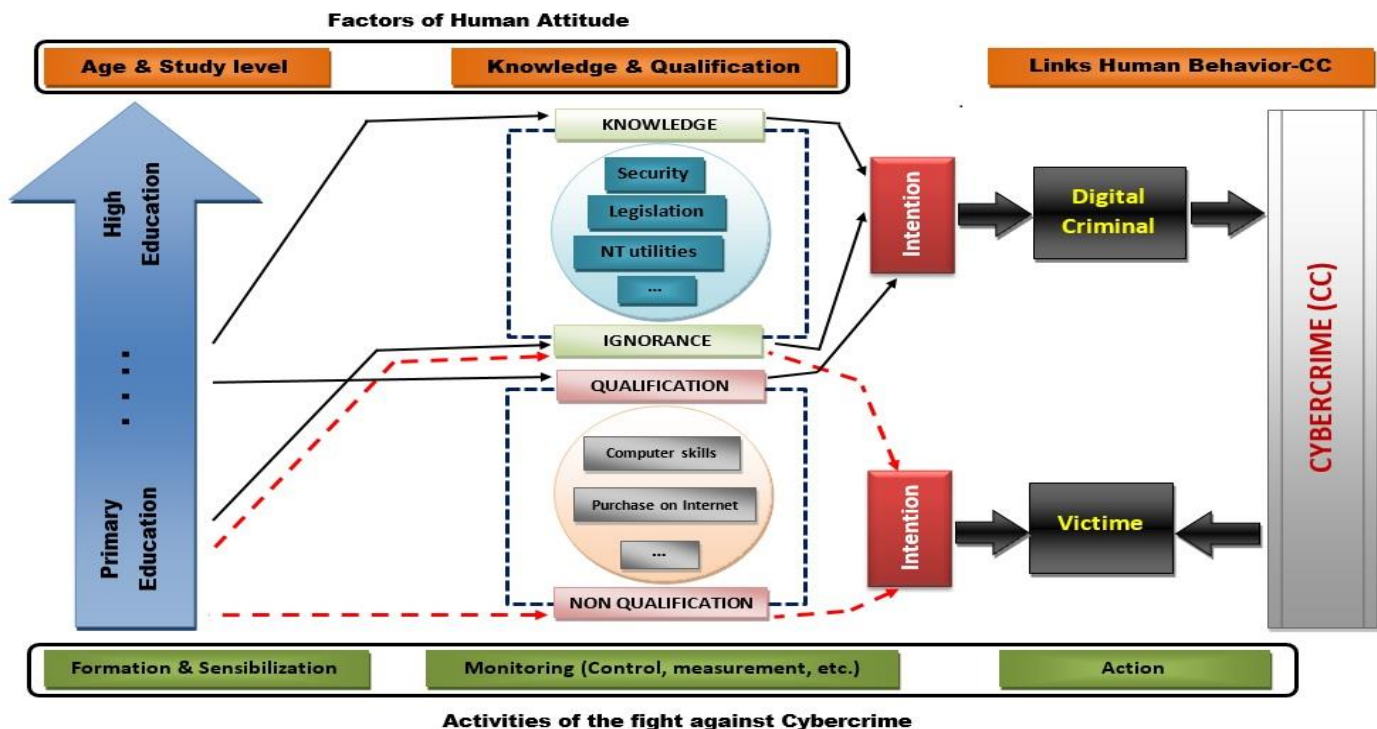


Fig. 8. Schematic Representation of Possible Links between Cybercrime and Human Factor.

ACKNOWLEDGMENT

Our sincere thanks to the ENCG-J students, whose names are listed below in alphabetical order, for their participation in the realization of our field study: ACHIR Chaimaa, BAHRI Hajar, BENIOURI Hamza, BOUZIANE Abdelmounim, MAZOUI Asmae, SABRI Sanaa and RAVELONARIVO Ny Harimirana.

REFERENCES

- [1] M. Lagazio, N. Sherif and M. Cushman, "A multi-level approach to understanding the impact of cyber crime on the financial sector," *Computers & Security*, Elsevier, vol. 45, pp. 58–74, 2014,.
- [2] N. Kshetri, "The simple economics of cybercrimes," *IEEE security & privacy*, vol. 4, issue 1, pp. 33–39, 2006.
- [3] A. Bendovschi, "Cyber-Attacks – Trends, Patterns and Security Countermeasures," *Procedia Economics and Finance*, vol. 28, pp. 24–31, 2015.
- [4] S. Gordon and R. Ford, "On the definition and classification of cybercrime," *Journal in Computer Virology*, vol. 2, issue 1, pp. 13–20, 2006.
- [5] H. Orman, "The Morris worm: a fifteen-year perspective," *IEEE Security & Privacy*, vol.1 , issue 5 , Sept-Oct 2003.
- [6] R. Solms and J. Niekerk, "From information security to cyber security," *Computers & Security*, vol. 38, pp. 97–102, October 2013.
- [7] L. Tabansky, "Critical Infrastructure Protection against Cyber Threats," *Military and Strategic Affaires*, Vol. 3, no. 2, Nov 2011.
- [8] A. Arabo, "Cyber Security Challenges within the Connected Home Ecosystem Futures," *Procedia Computer Science*, vol. 61, pp. 227–232, 2015.
- [9] H. de Bruijn and M. Janssen, "Building Cybersecurity Awareness: The need for evidence-based framing strategies," *Government Information Quarterly*, vol. 34, issue 1, pp. 1-7, January 2017.
- [10] R. Broadhurst, P. Grabosky, M. Alazab and S. Chon, "Organizations and Cyber crime: An Analysis of the Nature of Groups engaged in Cyber Crime," *International Journal of Cyber Criminology*, vol. 8, issue 1, pp.1–20, January - June 2014.
- [11] C. Dejours, "Le facteur humain," *Collection Que sais-je ?*, 6th edition, 2014.
- [12] K. Janssens, N. Nijsten and R. Van Goolen, "Spam and Marketing Communications," *Procedia Economics and Finance*, vol. 12, pp. 265-272, 2014.
- [13] C. Williams, "Security in the cyber supply chain: Is it achievable in a complex, interconnected world?," *Technovation*, vol. 34, issue 7, pp. 382-384, July 2014.
- [14] M. Antonescua and R. Birau, "Financial and non-financial implications of cybercrimes in emerging countries," *Emerging Markets Queries in Finance and Business*, *Procedia Economics and Finance*, N32, pp. 618 – 621, 2015.
- [15] M. Lagazio, N. Sherif and M. Cushman, "A multi-level approach to understanding the impact of cyber crime on the financial sector," *Computers & Security*, vol. 45, pp. 58-74, September 2014.
- [16] Kanich C, Kreibich C, Levchenko K, et al, "Spamalytics: an empirical analysis of spam marketing conversion," *Proceedings of the 15th ACM Conference on Computer and Communications Security (CCS)*, pp.3–14, 2008,
- [17] K.T. Smith, L.M. Smith and J.L. Smith, "Case studies of cybercrime and their impact on marketing activity and shareholder value," *Academy of Marketing Studies Journal*, vol. 15, num. 2, pp. 67-81 ,2011.
- [18] C. Nuangjamnong, S.P. Maj and D.R. Veal, "The OSI Network Management Model - Capacity and performance management," *Proceedings of 4th IEEE International Conference on Management of Innovation and Technology. ICMIT 2008*. Bangkok, Thailand. IEEE, pp. 1266-1270, 2008.
- [19] Marc D. Goodman and Susan W. Brenner, "The Emerging Consensus on Criminal Conduct in Cyberspace," *International Journal of Law and Information Technology*, vol. 10, No. 2, 2002,
- [20] E.F.G. Ajayi, "Challenges to enforcement of cyber-crimes laws and policy," *Journal of Internet and Information, Systems*, vol. 6, num 1, pp. 1-12, August 2016.
- [21] S.M. Young, "Verdugo in Cyberspace: Boundaries of Fourth Amendment Rights for Foreign Nationals in Cybercrime Cases," *10 Mich. Telecomm. & Tech. L. Rev. 139 (MTLR)*, vol. 10, issue 1, 2003.
- [22] M. Fishbein and I. Ajzen, "Attitudes towards objects as predictors of single and multiple behavioral criteria," *Psychological Review*, vol. 81, Num .1, 1974, pp. 59-74, 1974.
- [23] I. Ajzen, "The theory of Planned Behavior," *Organizational behavior and Human Decision Processes*, vol. 50, pp. 179-211, 1991.

A Comprehensive Comparative Analysis of Two Novel Underwater Routing Protocols

Umar Draz¹, Tariq Ali^{* 2}, Khurshid Asghar³, Sana Yasin⁴, Zubair Sharif⁵, Qasim Abbas⁶, Shagufta Aman⁷

CS. Department, (CU) Sahiwal, Pakistan^{1, 2, 4, 5, 6, 7}

CS. Department, UO, Okara, Pakistan³

Abstract—The most unmanned area of this planet is sheltered with water; that is roughly 71.9% of the total area of this planet. A large quantity of marine life is present in this area. That is the reason underwater research is bounded due to unexplored benefits. Due to the addition of sensors and growing interests in the exploration and monitoring of marine life Underwater Wireless Sensor Network (UWSN) can play an important role. A variety of routing protocols has been deployed in order to get information between deployed nodes. Providing stable data transmission, maximum throughput, minimum consumption of the energy and delay are challenging tasks in the UWSN. These routing protocols can be Layer-by-Layer Angle-Based Flooding (L2-ABF) and Diagonal and Vertical Routing Protocol (DVRP). In order to get stable data transmission, the node density plays our role in shallow and deep water. Several parameters are employed to evaluate the output efficiency of these routing protocols. In this paper, like an end to end delay, loss of data packets during transmission and data delivery ratio within communication are considered the major parameters for evaluation. For this, the network simulator is used with the aqua sim package. The results, we have produced during this study; guides us about the best routing protocol for data transmission. It finally reveals that the L2-ABF performs better then DVRP in a different situation, further the tradeoffs relationship is achieved against multiple situations.

Keywords—Data transmission; throughput; end-to-end delay; energy consumption; L2-ABF; DVRP; Delay

I. INTRODUCTION

Providing stable data transmission, maximum throughput, less energy consumption and minimizing the end-to-end delay are challenging tasks in Underwater Wireless Sensor Network (UWSN). Data packets become loss or late delivery due to explosive characteristics of UWSN and continuous flow of water. Different types of systematic strategies and monitoring operations are introduced in this field to resolve these issues like explain in [1]. However; our novel Layer by Layer Angle Based Flooding (L2-ABF) protocol is proposed in [2]. It based on the concept of an angle-based cone that calculates the angle from the region before data flooding. It does not require the configuration and location information of the nodes for data flooding. The exclusivity of this protocol is that it measures the quick changes in the network and resolves the energy consumption and delay issues of the network. Depth-Based Routing (DBR) protocol is also very useful in UWSN, to provide the scalable and efficient routing services. In this approach, inexpensive depth sensors are required that gives the local depth information of the nodes. The similarity

between the L2-ABF and DVRP (another proposed protocol is discussed in [3]) is that both do not require location information for routing. Dynamic Sink Mobility (DSM) that is equipped with DBR is also effective for data transmission in UWSN. It provides smooth routing by moving the sink node towards the source node. The advantage of DSM in comparison to DBR is that it enhances the stability period and network lifetime with smooth data transmission [4]. Comparison study of L2-ABF and DBR is done in [15]. The results concluded that L2-ABF is more efficient then DBR against the performance, implementation and routing techniques. Fig. 1 shows the possible scenario of data transmission in UWSNs.

A sensor cloud like, Swarm Sensor Equipped Aquatic (SEA) uses the L2-ABF protocol as groundwork. It flows with water and permits 4-dimensional screening of the local underwater atmosphere. It measures the pressure level of the water before transmitting the data from the source to the destination that increases the reliability of the UWSN environment. This approach works on the greedy method and selects the subsets of the forwarders that are helpful in the recovery process [13]. After an extensive literature review, a comparative analysis of L2-ABF and DVRP is decided in this paper. Both protocols are compared to the above-mentioned parameters. The major concern is the routing strategies that both protocols used to transmit the data from the source node to the destination node. Rest of the paper is ordered as: related work and comparative analysis are described in Sections 2 and 3, while simulation and performance analysis are discussed in Sections 4 and 5, respectively. At the end Section 6 deals the conclusion.

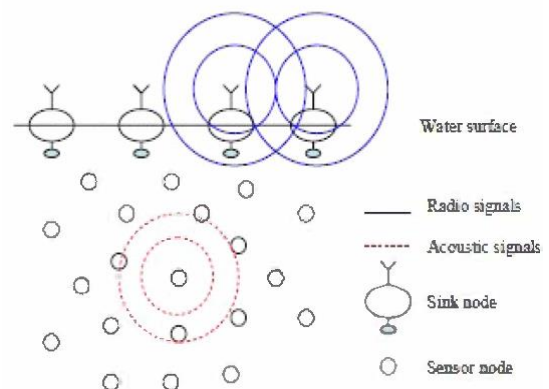


Fig. 1. Possible Scenario of Data Transmission in UWSN.

II. RELATED WORK

UWSNs are recently appeared as a promising field for several underwater applications. Due to the self-motivated structure, high power consumption and latency, designing an energy efficient routing protocol are the challenging tasks. Different researcher put their efforts in this field to resolve the above mentioned issues and to provide the stable data transmission. The energy consumption ratio for underwater environment is analyzed in [4]. Two parameters are under consideration: deep water and shallow water. Primarily energy consumption is calculated for fixed sensor nodes and then for the mobile sensor nodes as well. The results show that the energy consumption ratio is high in the mobile sensor nodes that require highest hope count. Focused Beam Routing (FBR) protocol is proposed in [5] that are based on the cross layer technique. The approach that makes it distinguished between others is its way of data transmission. The distributed nature of the FBR dynamically set the route as the data packets navigate for their target. Survey of different routing protocols is done in [6] in which routing protocols are differentiated in two categories: sender based and receiver based protocols. The differentiation process is done by the route decision maker. A novel underwater routing protocol called AUV-Aided Underwater Routing Protocol (AURP) is proposed in [7]. This protocol not only works for the acoustics communications, but it also controls the mobility of the autonomous underwater vehicle. The novelty of this protocol is that, it reduces the data transmission by replacing the relay nodes with ordinary nodes. These relays gather data from the gateways nodes instead of directly sensor nodes. Depth based multi-hop routing protocol is discussed in [8] based on the Depth Based Routing Protocol (DBRP) that provides the concept of depth for transfer the communication. Self-Organized Rapid Routing Protocol (SORRP) also recreates the radial topology with the gateway nodes. It always transmits the data to shortest path. This algorithm is compatible for both type of 2D and 3D environment. Survey of cross layer, non-cross layer and intelligent routing protocol is done in [10] Dynamic Based Multi Hop Routing Protocol (DBMRP) is proposed that use multi hop method for data transmission. Diagonal and Vertical Routing Protocol (DVRP) [3] proposed for diagonal and vertical communication in underwater moves. In order to discover the cosmic underwater environment, energy proficient localization free routing protocol is invented in [11, 12]. This protocol utilizes the less energy and provides the high data throughput that ultimately reduces the packet loss ratio in the UWSN. Different types of development trends of UWSN routing protocols are also discuss in this paper that provides the future directions to researcher. Role of proactive, reactive and geographical protocols for terrestrial environment are analyzed in [10]. DBFP is very useful to provide the reliability to the UWSN. The individuality of this protocol is that, it reduces the extensive transmission delay, narrow bandwidth and high packet loss. HH-VBF [5] technique uses the vectors from the source to the destination that resolve the energy and robustness issue of the network. Its performance is better than the DBR performance in the sparse network.

Angle based cone concept and its effects on end-to-end delay are introduced in [13, 14] to control the flooding in the UWSN. The use of angle makes the disaster pollution and

submarine detection easier in compare to other techniques in the literature. This approach is familiar in UWSN, for the avidness of ocean accident. L2-ABF protocol is specially designed to control the continuous nodes movement. It reduces the network delay and energy consumption to provide smooth data transmission in the network. It has some advantages on other protocols in the network such that, it can measure the quick changes in the network due to the layer by layer deployment of the nodes [15]. The unique feature of this protocol is that it calculates their flooding zone by using their angle based approach and then transmits the data according to that zone. Position adjustment technique that is based on the location error is also contributed in the UWSN. This protocol works for the void hole avoidance in the network. The point of differentiation of this protocol is that it avoids the extra flooding in the network by using their repositioning ability. The position adjustment policy is works through the angle as described in [16, 24] and other reliable data recovery mechanism for underwater are discussed in our previous article [17, 18]. Furthermore; three hop reliability model [19] and the energy based comparison study of routing protocols [20] are another our achievements. Flood is a major issue in water areas so we have proposed the watchman nodes and flood recovery watchman based algorithm is discussed in [21] and its formal verification in [22]. Our two routing protocols like SMDBRP and AEDGRP are successfully compared in our previous article [23].

A comparison of DBR and L2-ABF is mentioned in [14]. End to end delay, delivery ratio, and energy consumption are the parameters that are under consideration for the comparison. The results conclude that L2-ABF is more efficient than the DBR protocol. Stratification based data collection technique is used in acoustic sensor networks to observe the abnormal ocean environment and to explore the resources in the ocean [9, 10]. This technique is based on the layer by layer approach in which the upper layer is called the ekman layer in the network and bear large water velocity. Message Priority Based Protocols (MPBP) is designed for the aquaculture application in the UWSN. This protocol is capable to handle the emergency and regular packets based on the assigned priority.

III. COMPARATIVE ANALYSIS

This section covers the comparative analysis of two underwater routing protocols like L2-ABF and DVRP. Both protocols are well-known and working great, but no one has compared these two protocols in such detail. These two protocols are performing well for underwater scenarios for better performance in deep water distribution where node density plays a parcel role. To further enhance the performance, we can configure the parameters like packet loss, delay and throughput; these are very effective for evaluation purposes. In this study, we have evaluated the output efficiency by using TCP and UDP connections; also remember about the energy consumption because these networks are very limited to energy so conservation should always be considered on high priority. The distribution of the mobility model is random. The foremost objective for this study is to evaluate the performance of routing protocols by using the NS-2 simulator. The parameters for experiments are

described in Table I, while the formula of throughput and delay is shown below.

$$\text{Throughput} = \frac{\sum (\text{Packets received at receiver})}{\sum (\text{Packets initiated by sender})} * 100$$

The duration of time started from the sender node when it through data and ending at when the data is received by the receiver is called propagation delay.

$$\text{Delay} = \frac{\sum (\text{arrival time packet} - \text{transmit time of packet})}{\sum (\text{Packets at destination caught})} * 100$$

It is observed that both protocols work well in the UWSNs environment and provide a high data transmission rate in comparison to other routing protocols. The major difference between these two protocols is the selection of a path to transmit data to the targeted node. L2-ABF uses the layer by layer approach for routing but DVRP performs with the diagonal and vertical routing-based flooding. The similarity between these two protocols is that both use the location-based local information for data gathering.

TABLE I. SIMULATION PARAMETERS

Simulation Parameters	Value
Type of Channel	Wireless channel
Propagation	Two Ray Ground
Network type	Wireless Phy
Mac type	802_11
Maximum packet in ifq	50
Number of Nodes	50
Number of iterations	25 iterations for each
Packet size	1000 bytes
Traffic Type	CBR, FTP
Agents	TCP and UDP
Routing Protocol	L2-ABF, DVRP
The topography of X dimension	1800
The topography of Y dimension	2000
The topography of Z dimension	2400

IV. SIMULATION USING NS-2

In this section, simulation analysis of L2-ABF and DVRP are done by using the NS-2 simulator. To compare both protocols, initially, 500 numbers of mobile nodes are deployed in the network (with random topology). In order to evaluate the other remaining parameters, the same iterations are repeated. It has been observed that L2-ABF is comparatively better than the DVRP for the above-mentioned parameters.

V. PERFORMANCE ANALYSIS

In performance Analysis, the result for each experiment is explained with their corresponding graph. In each experiment, different variables are considered like throughput, loss of packets, delay, node density etc. The first section covers the effect on the performance in terms of delay, throughput and packet loss for TCP and UDP over L2-ABF, if the thickness of nodes varies.

A. Analysis of DVRP against Throughput, Delay and Packet Loss vs. Node Density

For the DVRP, as it used diagonal and vertical path selection, therefore, the throughput is steadily fast under the TCP as compared to UDP. The middle of the network it deviates through some extent, it is due to insufficient to take the angle between a maximum number of nodes quantity. Therefore, 600 kbps is achieved through TCP while the difference between UDP and TCP is only about 200 kbps as shown in Fig. 2. As node density is increased, the throughput is increased, so directly proportional relation exists between these two terms. Only 40 nodes are under consideration to take the first iteration, by the way, due to the directly proportional relationship this is increased when nodes are increased in our experiment. Fig. 3 illustrates the delay analysis under TCP and UDP, in TCP the delay is maximum because due to three handshake mechanism while the delay is minimum in UDP as UDP does not use such a technique. Due to the increase in the number of nodes in water, the packet loss ratio is also increased. Many reasons for this, as the distance between source and sink, is increased the route length increased. From Fig. 4, it has been found that under UDP the packets are much greater than as compared to TCP, only 40% packets are achieved while the rest of the amount has been lost at sink end.

B. Analysis of DVRP against Throughput, Delay and Packet Loss vs. Node Speed

From Fig. 5, 6 and 7 shows the throughput, delay and packet loss analysis of DVRP under the same traffic agents. It is observed that throughput is increased in TCP while the delay and packet loss are decreased against UDP. The effect of node speed is a concern when the throughput is increased because the simulation time of each node with respect to speed is uniform but due to two-way communication between the source and sink this is possible and it affects the other parameters.

C. Analysis of DVRP against Throughput, Delay and Packet Loss vs. Pause Time

Pause time is the time when communication is disturbed due to some reasons. Many reasons for this, for example, when the node or link failure between the node and the overall pause time is inserted in the network or when the 3D dynamic environment the mobile water also has enough current to create the possible pause between the nodes. In Fig. 8, 9 and

10 the same analysis is conducted against the pause time. The throughput fluctuated against TCP and UDP with pause time while the delay is measured in seconds as UDP effect the overall performance of the routing protocol of DVRP.

D. Analysis of L2-ABF against Throughput, Delay and Packet Loss vs. Node Density

As the name comes layer by layer approach it first computes the layer model of the deployment of the nodes. Properly make the angle to the different numbers of nodes, a large number of nodes are covered when the angle is broadcast. Therefore, the throughput is maximum as compared to our other protocols like DVRP. The figure shows the effect of UDP and TCP both of them are easily copied and no such large difference between these two traffic agents. Fig. 11 shows the throughput analysis of L2-ABF about 500 kbps. In Fig. 12, the delay is measured, no such delay is to be noted. The packet loss analysis of L2-ABF in TCP and UDP is measured against node density is shown in Fig. 13.

E. Analysis of L2-ABF against Throughput, Delay and Packet Loss vs. Node Speed

From Fig. 14, 15 and 16 the same analysis has been performed against node speed. In Fig. 14, the throughput analysis is measured and it shows the deviation for both UDP and TCP agents. While the delay is represented in Fig. 15 against UDP the delay is maximum and for TCP the L2-ABF shows the minimum delay. The packet loss analysis of L2-ABF is measured against both these two traffic agents as UDP has more than packet loss as compared to TCP. The same analysis of DVRP is shown above, it has been seen that the DVRP not as much packet loss as compared to L2-ABF due to its angle-based flooding, while the diagonal and vertical routing scheme also shows its effect when the UDP have large delay analysis.

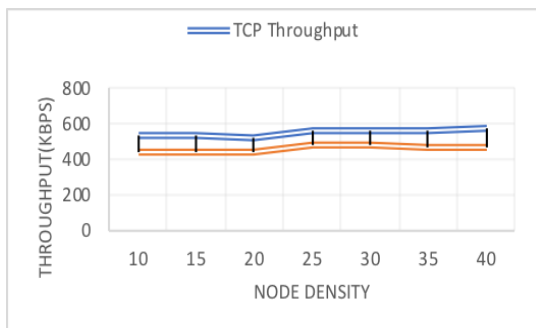


Fig. 2. Analysis of DVRP Throughput for TCP and UDP with Respect to Node Density.

F. Analysis of L2-ABF against Throughput, Delay and Packet Loss vs. Pause Time

From Fig. 17, 18 and 19 shows the detailed analysis of the same parameters against pause time. The pause time is the effect for DVRP so it is bad as L2-ABF. Most of the situations where the angle based approach is not worked as work in DVRP. The delay is minimum for TCP and maximum for UDP, but for the throughput, it takes the reverse situation. When we talk about the packet loss the major window of network simulator is also displayed in which 607 packets ate

sent while the 478 packets are received for both DVRP and L2-ABF in Fig. 20.

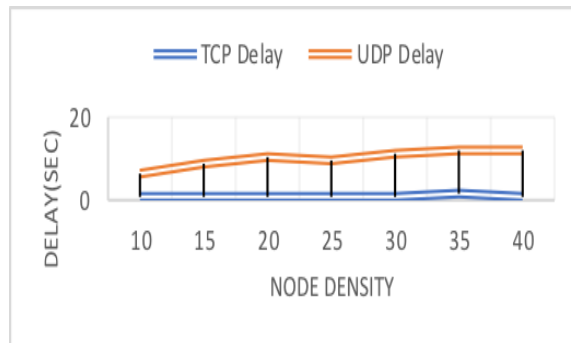


Fig. 3. Analysis of DVRP Delay for TCP and UDP with Respect to Node Density.

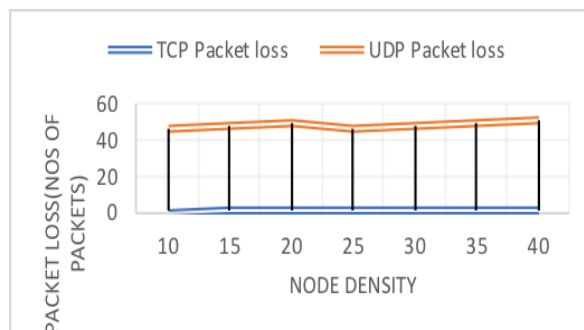


Fig. 4. Analysis of DVRP Packet Loss with Respect to Node Density.

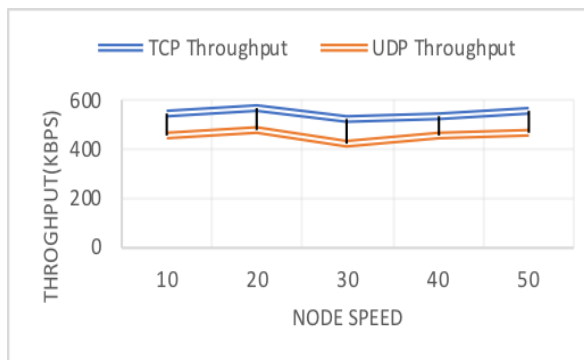


Fig. 5. Analysis of DVRP Throughput for TCP and UDP with Respect to Node Speed.

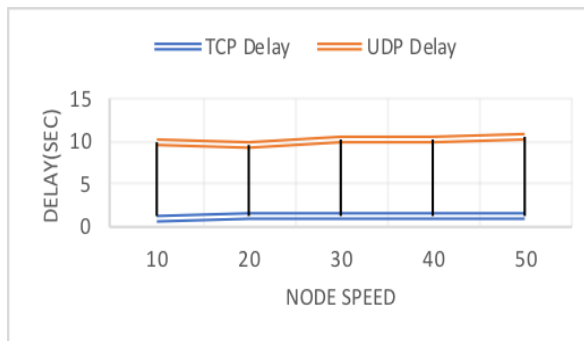


Fig. 6. Analysis of DVRP Delay for TCP and UDP with Respect to Node Speed.

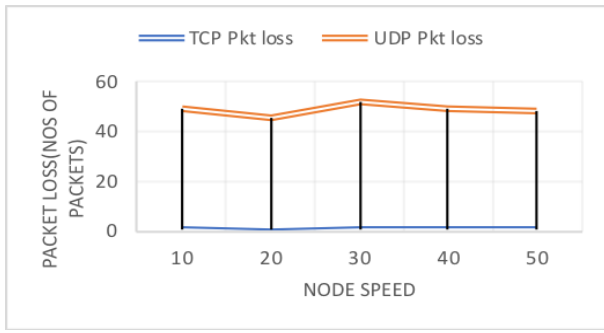


Fig. 7. Analysis of DVRP Packet Loss for TCP and UDP with Respect to Node Speed.

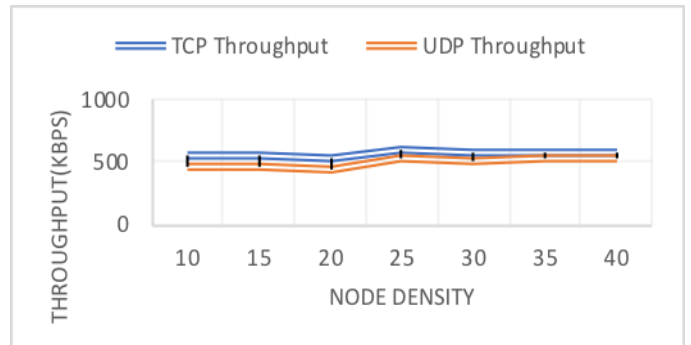


Fig. 11. Throughput of L2-ABF in TCP & UDP Connection using Node Density.

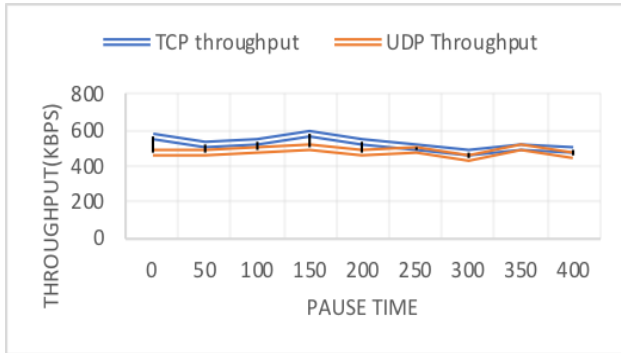


Fig. 8. Analysis of DVRP Throughput for TCP and UDP with Respect to Pause Time.

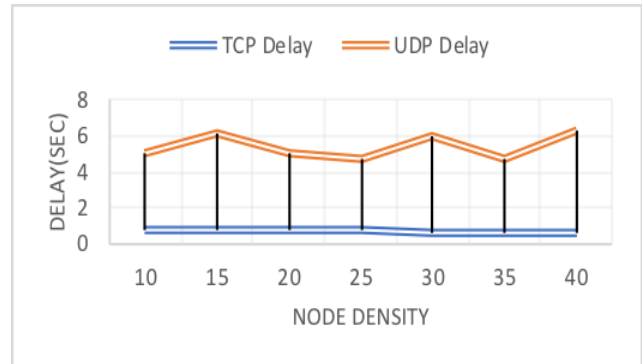


Fig. 12. Delay of L2-ABF in TCP & UDP Connection using Node Density.

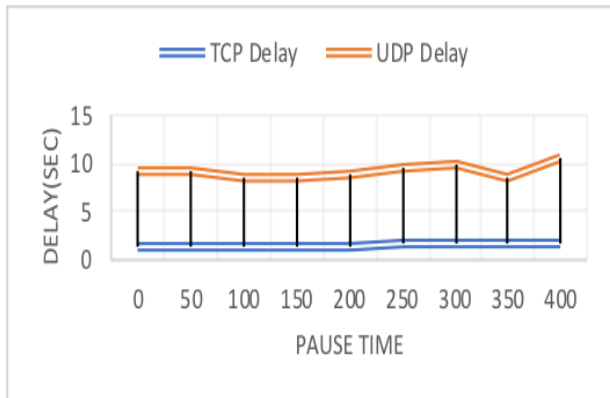


Fig. 9. Analysis of DVRP Delay for TCP and UDP with Respect to Pause Time.

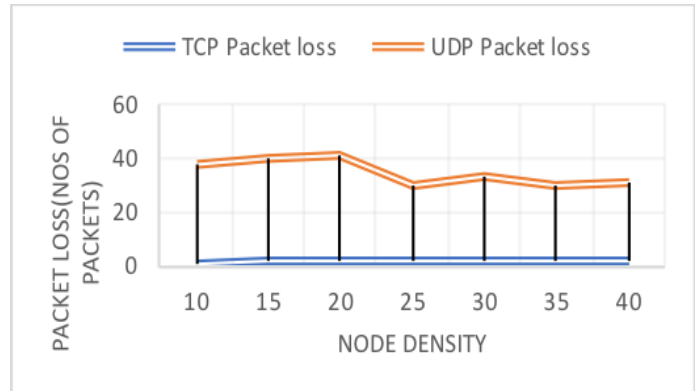


Fig. 13. Packet Loss of L2-ABF in TCP & UDP Connection using Node Density.

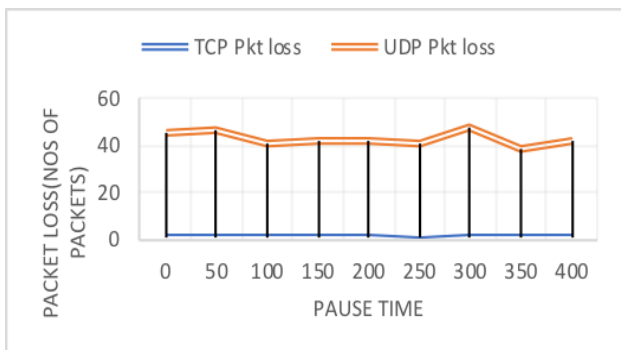


Fig. 10. Analysis of DVRP Packet Loss for TCP and UDP with Respect to Pause Time.

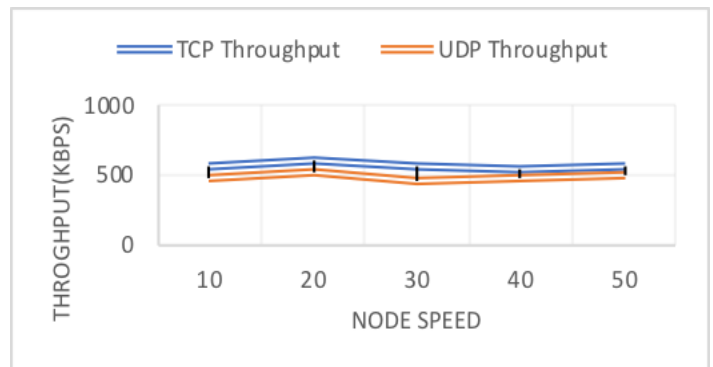


Fig. 14. Throughput of L2-ABF in TCP & UDP.

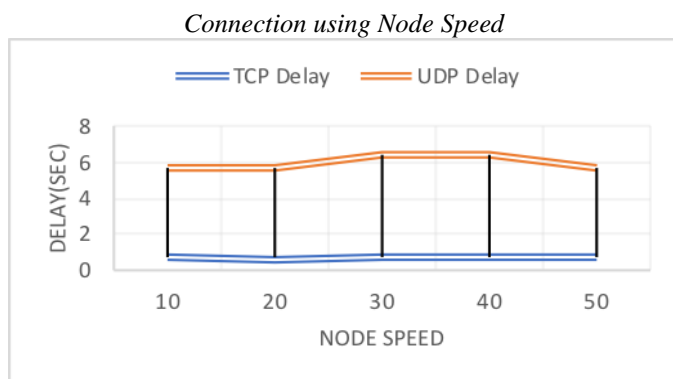


Fig. 15. Delay of L2-ABF over TCP & UDP Connection using Node Speed.

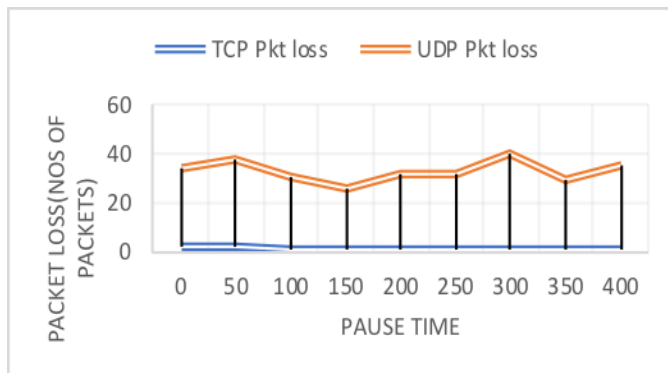


Fig. 19. Packet Loss of L2-ABF in TCP & UDP Connection using Node Speed Time.

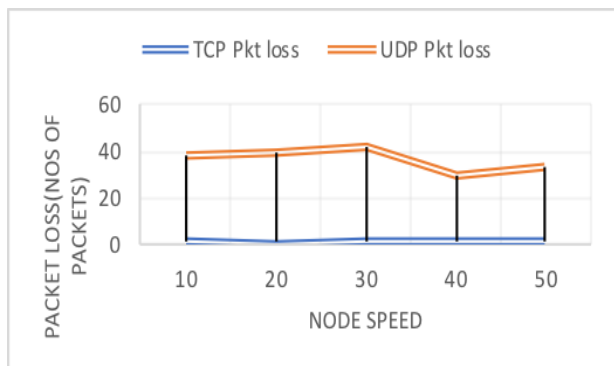


Fig. 16. Packet Loss of L2-ABF in TCP & UDP Connection using Node Speed.

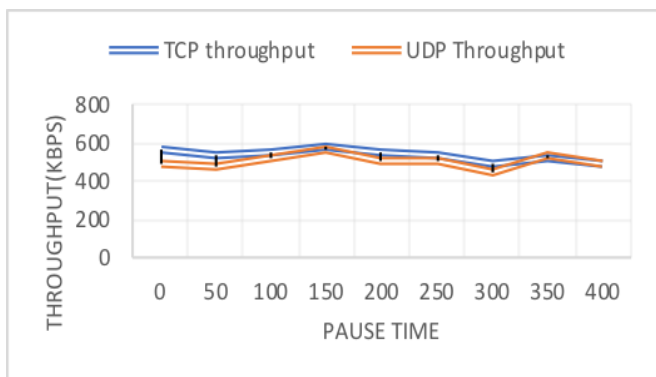


Fig. 17. Throughput of L2-ABF in TCP & UDP.

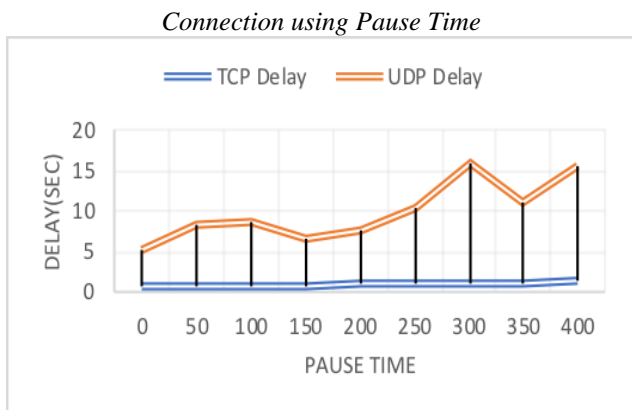


Fig. 18. Delay of L2-ABF over TCP & UDP Connection using Pause Time.

```

test@clit-OptiPlex-9010: ~
1. L2-ABF
2. DVRP
1
num_nodes is set 40
INITIALIZE THE LIST xListHead
Starting Simulation.....
channel.cc:sendUp - Calc highestAntennaZ_ and distCST_
highestAntennaZ_ = 1.5, distCST_ = 1856.3
SORTING LISTS ...DONE!
MAC_802_11: accessing MAC cache_array out of range (src 75, dst 0, size 40)!
MAC_802_11: accessing MAC cache_array out of range (src 72, dst 19, size 40)!
MAC_802_11: accessing MAC cache_array out of range (src 65, dst 15, size 40)!
MAC_802_11: accessing MAC cache_array out of range (src 66, dst 34, size 40)!
MAC_802_11: accessing MAC cache_array out of range (src 68, dst 66, size 40)!
MAC_802_11: accessing MAC cache_array out of range (src 66, dst 19, size 40)!
MAC_802_11: accessing MAC cache_array out of range (src 60, dst 66, size 40)!
MAC_802_11: accessing MAC cache_array out of range (src 66, dst 67, size 40)!
MAC_802_11: accessing MAC cache_array out of range (src 70, dst 67, size 40)!
MAC_802_11: accessing MAC cache_array out of range (src 66, dst 67, size 40)!
[suppressing additional MAC cache_warnings]
test@clit-OptiPlex-9010:~$ gawk -f SMDBRP.awk SMDBRP.tr
Packet Sent:607
Packet Received:478
    
```

Fig. 20. TCL File for Total Packet Analysis and Sent for L2-ABF and DVRP.

VI. CONCLUSION

This study is based on a realistic scenario for the evaluation of UWSN's routing protocols such that L2-ABF and DVRP under traffic agents TCP and UDP. Results for each experiment are available for study in detail, to support our word, the L2-ABF is comparatively better than DVRP against different factors like node density and pause time. Meanwhile; the delay and throughput analysis of DVRP performs better under TCP as compared to L2-ABF. Because of this study including all the experiments, we can say the routing protocol L2-ABF is better than DVRP in most of the situations, and to get maximum output under both traffic agents TCP and UDP. We can also conclude DVRP can be used to carry useful information in UWSN, due to its performance against delay but it might not be used when we need to carry information in a small amount of time because it has propagation delay in maximum.

In our future study, try to simulate the behavior of other different underwater protocols that best suited for the underwater deep and shallow environment.

REFERENCES

- [1] Domingo, M. C., & Prior, R. (2008). Energy analysis of routing protocols for underwater wireless sensor networks. *Computer communications*, 31(6), 1227-1238.
- [2] Ali, T., Jung, L. T., & Faye, I. (2012). Delay efficient Layer by Layer Angle Based Flooding Protocol (L2-ABF) for Underwater Wireless Sensor Networks. In Conference.
- [3] Ali, T., Jung, L. T., & Faye, I. (2014). Diagonal and vertical routing protocol for underwater wireless sensor network. *Procedia-Social and Behavioral Sciences*, 129, 372-379.
- [4] Jornet, J. M., Stojanovic, M., & Zorzi, M. (2008, September). Focused beam routing protocol for underwater acoustic networks. In *Proceedings of the third ACM international workshop on Underwater Networks* (pp. 75-82). ACM.
- [5] Yoon, S., Azad, A. K., Oh, H., & Kim, S. (2012). AURP: An AUV-aided underwater routing protocol for underwater acoustic sensor networks. *Sensors*, 12(2), 1827-1845.
- [6] Guangzhong, L., & Zhibin, L. (2010, May). Depth-based multi-hop routing protocol for underwater sensor network. In *Industrial Mechatronics and Automation (ICIMA), 2010 2nd International Conference on* (Vol. 2, pp. 268-270). IEEE.
- [7] Hyder, W., Poncela, J., Luque, M. A., & Otero, P. (2018). Self-Organized Fast Routing Protocol for Radial Underwater Networks. *Sensors*, 18(12), 4178.
- [8] Li, N., Martínez, J. F., Meneses Chaus, J. M., & Eckert, M. (2016). A survey on underwater acoustic sensor network routing protocols. *Sensors*, 16(3), 414.
- [9] Hwang, D., & Kim, D. (2008, September). DFR: Directional flooding-based routing protocol for underwater sensor networks. In *OCEANS 2008* (pp. 1-7). IEEE.
- [10] Lee, U., Wang, P., Noh, Y., Vieira, L. F., Gerla, M., & Cui, J. H. (2010, March). Pressure routing for underwater sensor networks. In *INFOCOM, 2010 Proceedings IEEE* (pp. 1-9). IEEE.
- [11] Nicolaou, N., See, A., Xie, P., Cui, J. H., & Maggiorini, D. (2007, June). Improving the robustness of location-based routing for underwater sensor networks. In *Oceans 2007-Europe* (pp. 1-6). IEEE.
- [12] Ali, T., Jung, L. T., & Ameer, S. (2012, November). Flooding control by using angle based cone for UWSNs. In *Telecommunication Technologies (ISTT), 2012 International Symposium on* (pp. 112-117). IEEE.
- [13] Ali, T., Jung, L. T., & Faye, I. (2014). End-to-end delay and energy efficient routing protocol for underwater wireless sensor networks. *Wireless Personal Communications*, 79(1), 339-361.
- [14] Shaf, A., Ali, T., Farooq, W., Draz, U., & Yasin, S. (2018, January). Comparison of DBR and L2-ABF routing protocols in underwater wireless sensor network. In *Applied Sciences and Technology (IBCAST), 2018 15th International Bhurban Conference on* (pp. 746-750). IEEE.
- [15] Draz, U., Ali, T., Yasin, S., & Shaf, A. (2018, March). Evaluation based analysis of packet delivery ratio for AODV and DSR under UDP and TCP environment. In *Computing, Mathematics and Engineering Technologies (iCoMET), 2018 International Conference on* (pp. 1-7). IEEE.
- [16] Ali, T., Jung, L. T., & Faye, I. (2014). End-to-end delay and energy efficient routing protocol for underwater wireless sensor networks. *Wireless Personal Communications*, 79(1), 339-361.
- [17] Ali, T., Jung, L. T., & Faye, I. (2014). A Reliable Data Flooding in Underwater Wireless Sensor Network. In *Proceedings of the First International Conference on Advanced Data and Information Engineering (DaEng-2013)* (pp. 499-511). Springer, Singapore.
- [18] Ali, T., Jung, L. T., & Ameer, S. (2012, November). Flooding control by using angle based cone for UWSNs. In *2012 International Symposium on Telecommunication Technologies*(pp. 112-117). IEEE.
- [19] Ali, T., Jung, L. T., & Faye, I. (2014, June). Three hops reliability model for underwater wireless sensor network. In *2014 International Conference on Computer and Information Sciences (ICCOINS)* (pp. 1-6). IEEE.
- [20] Shaf, A., Ali, T., Draz, U., & Yasin, S. (2018). Energy Based Performance analysis of AODV Routing Protocol under TCP and UDP Environments. *EAI Endorsed Trans. Energy Web*, 5(17), e9.
- [21] Draz, U., Ali, T., & Yasin, S. (2018, November). Cloud Based Watchman Inlets for Flood Recovery System Using Wireless Sensor and Actor Networks. In *2018 IEEE 21st International Multi-Topic Conference (INMIC)* (pp. 1-6). IEEE.
- [22] Ali, T., Yasin, S., Draz, U., & Ayaz, M. (2019). Towards Formal Modeling of Subnet Based Hotspot Algorithm in Wireless Sensor Networks. *Wireless Personal Communications*, 1-34.
- [23] Draz, U., Ali, T., Yasin, S., Naseer, N., & Waqas, U. (2018, February). A parametric performance evaluation of SMDBRP and AEDGRP routing protocols in underwater wireless sensor network for data transmission. In *2018 International Conference on Advancements in Computational Sciences (ICACS)* (pp. 1-8). IEEE.
- [24] Ali, T., Ayaz, M., Jung, L. T., Draz, U., & Shaf, A. (2017). Upward and Diagonal Data Packet Forwarding in Underwater Communication.

Extreme Learning Machine and Particle Swarm Optimization for Inflation Forecasting

Adyan Nur Alfiyatin¹, Agung Mustika Rizki², Wayan Firdaus Mahmudy³, Candra Fajri Ananda⁴

Faculty of Computer Science, Brawijaya University, Malang, Indonesia^{1,2,3}
Faculty of Economics and Business, Brawijaya University, Malang, Indonesia⁴

Abstract—Inflation is one indicator to measure the development of a nation. If inflation is not controlled, it will have a lot of negative impacts on people in a country. There are many ways to control inflation, one of them is forecasting. Forecasting is an activity to find out future events based on past data. There are various kinds of artificial intelligence methods for forecasting, one of which is the extreme learning machine (ELM). ELM has weaknesses in determining initial weights using trial and error methods. So, the authors propose an optimization method to overcome the problem of determining initial weights. Based on the testing carried out the proposed method gets an error value of 0.020202758 with computation time of 5 seconds.

Keywords—Extreme learning machine; particle swarm optimization; inflation; prediction

I. INTRODUCTION

The economy of a country is affected by macro variables; they are Gross Domestic Brute (GDP), unemployment, and inflation. From those three components, inflation holds the most important rule [1]. Inflation is an incidence of rising prices of goods and services in general for a long time and continuously influences each other [2]. The economic stability of a country is seen based on the country's inflation rate. In Indonesia, the stability of economics is controlled by the central bank namely Bank Indonesia through monetary policy. Monetary policy is a policy illustration that serves to overcome economic problems with the aim of maintaining the stability of currency values. In this case, the stability of the prices of goods and services reflected in inflation [3]. To achieve low and stable inflation, Bank Indonesia set a framework called the Inflation Target Framework (ITF).

ITF framework has determinations of inflation targets for the next few years. An influential process for determining the inflation target is by using inflation rate forecasting. With the inflation rate forecasting, it can reduce the inflation rate up to 4 – 5 % [3]. The method used by Bank Indonesia for current inflation forecasting is by forward looking. It is better to overcome the inflation shocks that occurred during the set time. Getting information on domestic conditions about the changes occurring in the economic field will serve as one of the important information on policy formulation. In order to obtain accurate information and good influence on the policy, the set required a forecasting. Forecasting will yield accurate information if the variables used are significant and the data used is credible. A forecasting used past data, with the aim to know the pattern of future events based on past data patterns [4].

Some methods used for forecasting are machine learning [5], neural network, regression [6], fuzzy time series [7], and extreme learning machine (ELM) [8]. Based on those methods, ELM has the advantage of speeds in the learning process, the generalization is very good without overtraining, and it can determine the best results according to the input weights used. Therefore, many researchers combine ELM with optimization methods in order to get the best input weight that will be used in the hidden layer, such as hybrid ELM and PSO, ELM and GA, ELM and Regression. The purpose of the optimization method is to define the best weight of input neurons to be implemented in the ELM. So, this research will combine particle swarm optimization and ELM for inflation rate forecasting in Indonesia. The focus is to know the hybrid performance method between particle swarm optimization and ELM.

II. RELATED WORK

Recently, many researchers on forecasting used machine learning method [5] aimed for determining the performance of stock-making forecasting. Methods used are decision tree, neural network, multi-layer perceptron (MLP), support vector machine (SVM) and hybrid methods. Some of the methods tested in the study have their respective advantages in the tree decision method which has simple techniques and capabilities that can be relied upon in predicting values, both by using large and small amounts of data, Neural Networks support is able to accept or model the input relations / non-linear complex output. SVM is a learning strategy that was started and designed to solve problems, but also to solve non-linear regression problems as well. After reviewing some of the advantages and disadvantages of the method, this study proves that with a combination of the methods, the performance is better than the performance of a single method.

The next study was conducted by Semaan [6], to forecast exchange rates with statistical methods (regression) and neural networks (ANN). The purpose of this study is to know the performance of both methods and the value of the accuracy produced to find out the relationship between independent and dependent variables that affect the exchange rate. The results show that the ANN method can increase the value of accuracy for exchange rate forecasting compared with the regression method. The advantage of the ANN method is if there is a complex pattern of data with a large number, the data pattern can be extracted by ANN even though the exact mathematical equation between the relationship between the dependent variable and the independent variable is unknown. Excellence

as well as weakness of ANN can be overcome by the addition of regression methods due to the ability of regression methods that can tell the mathematical equations between the relationship of dependent and independent variables accordingly.

Other research conducted by Huarng and Yu [9] is about the combination of fuzzy time series and backpropagation for stock forecasting. This study aims to compare the performance between conventional fuzzy time series with a combination of fuzzy time series and backpropagation. Fuzzy time series is used for forecasting unidentified patterns while backpropagation is suitable for solving problems which patterns are identified. So that if these two methods are combined, the results will be better than using single method only. And it proved from this study that the combined method can work better for forecasting on known and unknown patterns, therefore this method outperforms the basic model of conventional fuzzy time series.

Research on inflation rate forecasting is also carried out by Sari [10] [11] uses time series data on consumer price index, money supply, BI rate, exchange rate and inflation rate with the backpropagation method shows that the involvement of external factors for forecasting the inflation rate is very influential on the results of the accuracy. Further research is carried out by Anggodo [12] using additional data with the same parameters gets better results because it uses a combined method between neural network and optimization.

Based on some previous researches, it shows that artificial neural network method gets higher accuracy value in comparison with statistical method, and if artificial neural network is combined with other method, then the method performance will be improved. In this research, the proposed method will be hybrid of artificial neural network, namely Extreme Learning Machine (ELM). The optimization using particle swarm optimization to define the forecasting performance is calculated using root mean square error (RMSE). This research highlights the addition of parameters are credit value and asset value to forecast the inflation rate and it is expected that combined neural network and optimization methods will get the best results compared to previous studies [10]–[12].

III. DATA SET

In this study, data were obtained from Bank Indonesia [13] and Badan Pusat Statistics (BPS). Records of data used were from January 2005 to December 2017. The parameters are using historical data with time series analysis (b-1, b-2, b-3). b-1 represents the previous month's parameter, b-2 represents the previous 2 months and b-3 represents the previous three months. This study also used several external factors that influence the inflation rate such as CPI, BI rate, money supply, exchange rate, credit value and asset value. Parameters are used as input variable for inflation rate forecasting while the output variables are the inflation forecasting rate in Indonesia.

IV. PARTICLE SWARM OPTIMIZATION (PSO)

PSO is used to optimize input weights in ELM so that the generation of weight in ELM is not randomly made. The use of Hybrid PSO-Elm aims to obtain optimal weight within minimal time. Particle Swarm Optimization proposed by Kennedy and Eberhart (1995) adopted the behaviour of a flock of birds. The solution to the PSO is called "particle". The PSO stage starts from the position initialization randomly, updates the speed, updates the Pbest value and the Gbest value, and fitness calculation. Pbest (Personal Best) is the optimal value determined by the particle itself while Gbest (Global Best) is the best value of a group from PBest [14]. For more details, it can be seen in Fig. 1 (pseudo code) below:

```
Begin
t=0
initialization position particle (xti,j), velocity (vti,j), Pbestti,j=xti,j,
calculate fitness of particles, Gbestti,j
do
    t = t+1
    update velocity vi,j (t)
    update position xi,j (t)
    calculate fitness of each particles
    update Pbesti,j (t) and Gbesti,j (t)
while (not a stop condition)
end
```

Fig. 1. Pseudo Code of Particle Swarm Optimization.

The equation used to update velocity (1) and update position (2):

$$v_{i,j}^{t+1} = w \cdot v_{i,j}^t + c_1 r_1 (Pbest_{i,j}^t - x_{i,j}^t) + c_2 r_2 (Gbest_{g,j}^t - x_{i,j}^t) \quad (1)$$

$$x_{i,j}^{t+1} = x_{i,j}^t + v_{i,j}^{t+1} \quad (2)$$

V. EXTREME LEARNING MACHINE (ELM)

This method was introduced by Huang, et al. [9]. ELM is feed forward neural network concept that Single Hidden Layer Feedforward Neural Networks (SLFNs) because ELM has only one hidden layer on its network architecture. ELM is designed to overcome the weakness of previous neural networks in the speed learning process. With the selection of parameters such as input, weight and hidden bias randomly so the performance from learning speed at the ELM is faster than another neural network method, ELM gets good generalization performance without overtraining problems. Step by step in the ELM process, there are:

A. Data Normalization

Data normalization was a process of changing the form of data into a more specific value in the limit value 0-1. The aim was to adjust the input data to the output data. Equation (3) showed the normalization of function.

$$v' = \frac{v}{\max v} \quad (3)$$

v[^] = New data

v = Actual data

max v = the maximum value of the actual data of each parameter.

B. Training Process

This process aims to conduct training using train data. With this process, an optimal weight value will be obtained. Steps in the training process are as follows [15]:

- Determine matrix W_{mn} randomly as weight input within range [0,1], in the form of array sizes m (number of hidden neurons) \times n (number of input neurons). Then it makes another random value for the bias matrix b within range [0,1] in size $1 \times$ (number of hidden neurons).
- Calculate the value of the hidden layer matrix output with equation (4). Calculation of b ($\text{ones}(i_{\text{train}},1)$) multiplies the matrix let as much as the amount of training data.

$$H = \frac{1}{1 + \exp(-(x_{\text{train}} w^T + b(\text{ones}(i_{\text{train}},1))))} \quad (4)$$

where:

- H = the hidden layer output matrix
- x_{train} = the input matrix on normalized training data
- w^T = the matrix transpose of weights
- i_{train} = the number of training data
- b = the bias matrix

- Calculate β as the output weights by using the equation (5) that H^+ or Moore-Penrose Pseudo Invers matrix can be calculated by equation (6).

$$\beta = H^+ t \quad (5)$$

$$H^+ = (H^T H)^{-1} H^T \quad (6)$$

where:

- β = the output weight matrix
- H^+ = the Moore-Penrose Pseudo Invers matrix from matrix H
- t = the target matrix
- H = the hidden layer output matrix

- Calculate the output by using the equation (7).

$$Y = H \beta \quad (7)$$

where:

- Y = predicted result
- H = hidden layer output matrix
- β = output weight matrix

C. Testing Process

After the training process, the testing process was done by using the test data. It aims to test the results of training, so it can know the accuracy of the system. Steps are shown as follows [15]:

- Determine W_{mn} , b and β value from training process.
- Calculate the value of the output matrix on the hidden layer using equation (8). The calculation of b ($\text{ones}(i_{\text{test}},1)$) is to multiply the bias matrix by the number of test data.

$$H = \frac{1}{1 + \exp(-(x_{\text{test}} w^T + b(\text{ones}(i_{\text{test}},1))))} \quad (8)$$

where:

- H = hidden layer output matrix
- x_{test} = input matrix on test data that had been normalized
- w^T = matrix transpose of weights
- i_{test} = number of test data
- b = bias matrix

- Calculate the output value by using equation (7).
- Denormalization of predicted results using equation (10).
- Calculate the evaluation value using equation (9).

$$RMSE = \sqrt{\frac{\sum_{i=1}^n (\text{actual data}_i - \text{predicted data}_i)^2}{n}} \quad (9)$$

D. Data Denormalization

This process served to return the normalized value to the original value. Equation (10) shows data denormalization process:

$$v' = \frac{v}{\max v} \quad (10)$$

v' = New data

v = Present data

$\max v$ = the maximum value of the actual data of each parameter

VI. PROPOSED METHOD

The method used for inflation forecasting is PSO-ELM. PSO was used for weight optimization to obtain optimal input values to be used in ELM. Furthermore, the forecasting process will be carried out by the ELM method. The fitness formula that will be used in the equation (11) is as follows:

$$\text{fitness} = \frac{1}{1 + RMSE} \quad (11)$$

The initial process of the system is the initialization of particles at PSO, particles randomly generated between 0-1 in the form of real code numbers. These particles are used as weights from the input layer to the hidden layer. Then calculate the value of fitness based on equation (11). After knowing the fitness value then determined the value of PBest and Gbest, after that updates the velocity, then updates the position and calculates fitness again. After obtaining the optimal weighting value, ELM method testing is done, and the inflation forecasting results were based on the ELM method. For more details, see in Fig. 2.

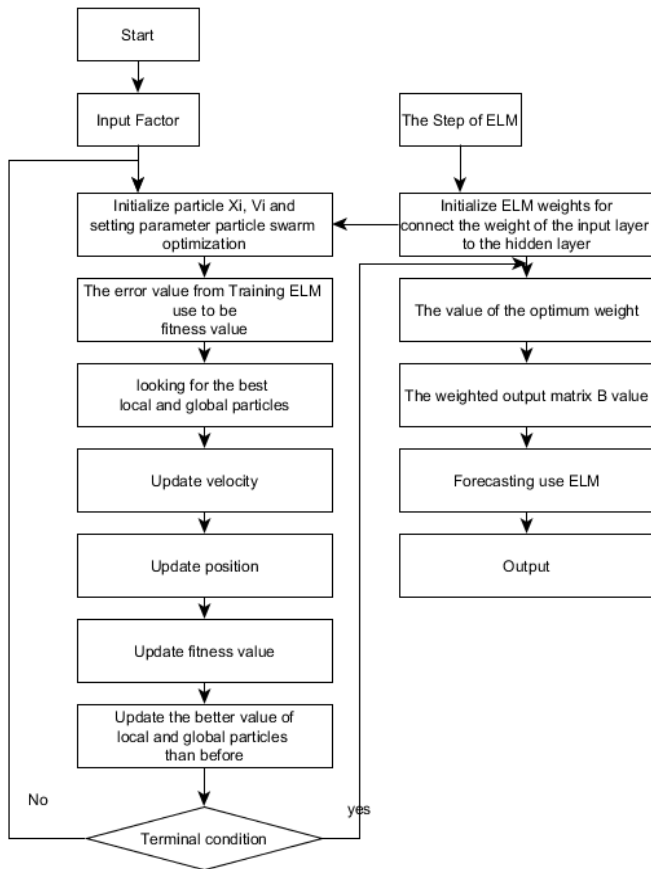


Fig. 2. Process PSO-ELM for Inflation Forecasting.

VII. EXPERIMENT AND RESULT

In forecasting the inflation rate using PSO and ELM, several tests were conducted which included particle testing, iteration testing, inertia weight, and testing the number of neurons in the hidden layer.

First tested object is particles number. It is to determine the optimal number of particles to get the maximum solution. The range of values used starts from 10-150 in multiples of 10. The range used is small because the PSO is good for searching narrow areas [16]. Other parameters use 100 iterations, inertia weight 0.6, and acceleration coefficients ($c_1 = 2$ and $c_2 = 1$).

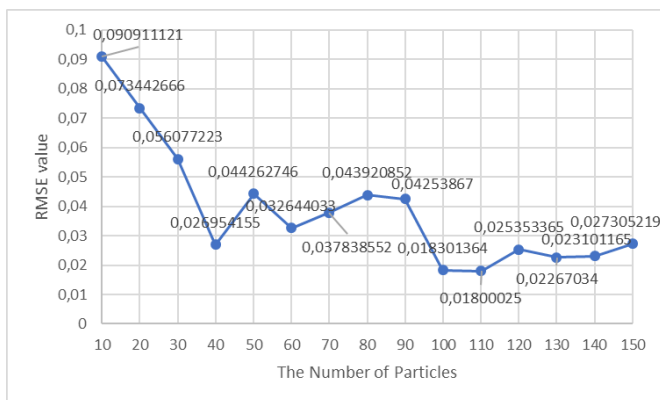


Fig. 3. Particle Chart Test.

In Fig. 3, it shows that there is a significant decrease in fitness value at the number of particles 40, then fluctuates to the number of particles 150. However, the number of particles 100 and 110 get the best fitness value with values of 0.018301364 and 0.01800025 with computation times are 9 and 10 seconds. So that in this test, the best number of particles is set at 110 with a computing value of 10 seconds. This is because the number of particles gives candidates more and varied solutions so that the search for the best solution can be done more thoroughly [16].

The next testing is the number of iterations. It is done to find out the relationship between the number of iterations and fitness values. Values are tested from 10 to 200 in multiples of 10. Other parameters use 110 on the number of particles, inertia weight 0.6, and acceleration coefficients ($c_1 = 2$ and $c_2 = 1$).

Fig. 4 shows that the best fitness value occurs in the number of iterations 110 of 0.023886. After that, between 120 and 200 the number of iterations fluctuates which form the same pattern with the greater fitness value. Therefore, this test sets the number of iterations 110 to be used in the next parameter.

Third testing is the inertia weight testing. It is used to produce the best weight to obtain optimal prediction results. This inertia weight testing starts from 0 to 1 with an addition of 0.1 and is done 6 times [14]. Fig. 5 shows the graph of the test results.

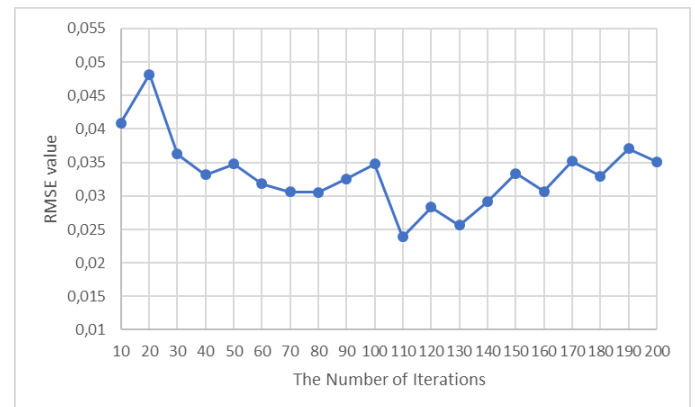


Fig. 4. Iteration Chart Test.

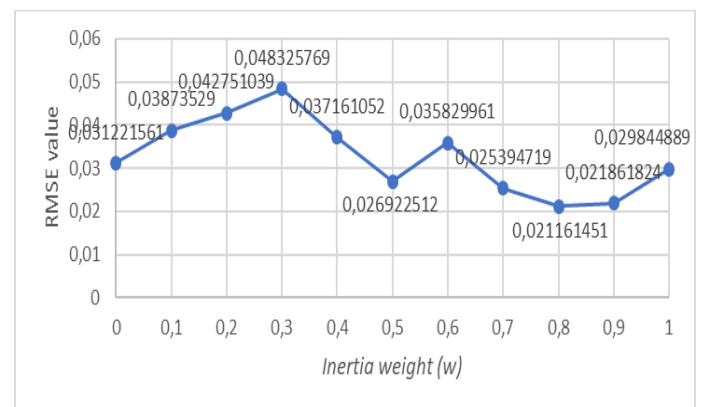


Fig. 5. Inertia Weight Chart of Testing.

Fig. 5 shows that the best fitness value of the value 0.8 with RMSE is 0.021161451. In a research conducted by Ratnavera [17], the best w value is above 0.5 and less than 1, because if w is more than 1, it will cause the particles in the PSO to be unstable due to uncontrolled speed produced. And it is proved in this study that when the value of w is 1 the RMSE value increases and it is higher than the value of 0.9.

Fourth tested object is Acceleration Coefficient. This Acceleration Coefficient test aims to determine the extent to which particles move in one iteration. This test is done by using the same combination of values and different between the range of values 1-4. Based on the book written by Cholissodin & Riyandani [18], the optimal value for the acceleration coefficient is stated in the range of values.

Fig. 6 shows that the best combination acceleration values occur in $c1$ and $c2$ worth 2 with the RMSE value of 0.020203. The values of $c1$ and $c2$ influence the motion direction of a particle whether towards local best or global best. In order to obtain optimal results, the two parameters' values between $c1$ and $c2$ are not dominant or at least close to balance, so that the particle movement route can be in accordance with the right portion to get the optimal solution [17].

The last testing is the number of neurons in the hidden layer. This test used the number of neurons, which is 3, 5 and 7. This amount is based on research [19] assume that the more number of neurons used, the more complex in determining the weight of neurons and the computing requires quite long time.

Fig. 7 shows that the error value decreases and the computing time needed is too long on adding the number of neurons. Hence, in this study, the number of neurons used was 3 neurons.

Based on all tests that have been carried out on each parameter, the authors set the architecture on PSO-ELM for forecasting the inflation rate with optimal results using 100 particles, 110 iterations, inertia weight = 0.8, acceleration coefficient = 2 and the number of neurons in the hidden layer are 3 neurons that took 9 seconds in computing time.

After the architecture is set to obtain optimal results, then the comparison between the other methods is carried out. The other methods are the backpropagation, ELM, and GA-ELM method. Table I shows the results of the comparison method.

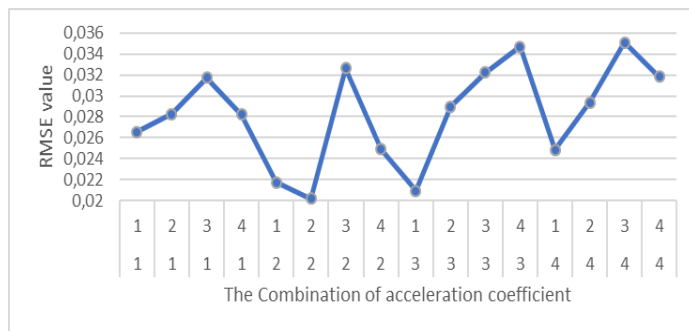


Fig. 6. Acceleration Coefficient Chart of Testing

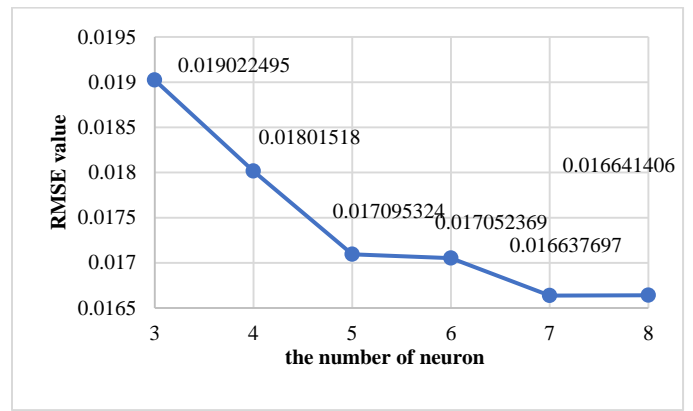


Fig. 7. The Number of Neurons Testing.

TABLE I. COMPARISON OF METHODS

Methods	Number of Hidden	Iteration	RMSE	Computation Time
Backpro	70	900	1.16035821	5 second
ELM	20	1	0.0202008	0 second
GA-ELM	7	300	0.013811	228 minutes 10 seconds
PSO-ELM	3	100	0.020202758	5 second

Table I shows that the results of four methods had very significant computation time between backpropagation, ELM, Hybrid GA-ELM and Hybrid PSO-ELM. The method that has the longest computation time is the hybrid of GA-ELM = 228 minutes 10 seconds, followed by backpropagation and hybrid PSO-ELM = 5 seconds, and the fastest is ELM = 0 seconds computation time.

Although backpropagation and PSO-ELM has the same computational time, backpropagation takes higher error value than hybrid PSO-ELM. Therefore, the PSO method can help the ELM method in decreasing the error value generated for predictions.

The case is different between ELM and PSO-ELM where ELM requires a shorter computational time than the PSO-ELM method (5 seconds). However, it is not a problem in system performance because the resulting error is relatively the same.

VIII. CONCLUSION

Based on the tests that have been executed, it is confirmed that the performance between the single ELM and Hybrid PSO-ELM methods has the same performance, proved by the difference in error values of 0.0000019. Thus, both methods are very relevant for solving forecasting problems.

The performance of the proposed method will be more optimal if the researcher uses more data to solve more complex problems. For further research, it can increase the PSO method to obtain the same time computing value with a single ELM method.

REFERENCES

- [1] N. G. Mankiw, *Macroeconomics* fifth edition, 9 edition. New York: Worth Publishers, 2010.
- [2] M. Anwar and T. Chawaa, "Post-ITF Inflation Expectation Analysis," *Work. Pap.*, vol. 9, no. Bank Indonesia, 2008.
- [3] A. Kadir, P. R. Widodo, and G. R. Suryani, *Implementation of Monetary Policy in the Inflation Targeting Framework in Indonesia.*, no. 21. 2008.
- [4] F. Rachman, "Is Inflation Target Announced by Bank Indonesia the Most Accurate Inflation Forecast?," *Econ. Financ. Indones.*, vol. 62, no. 2, pp. 98–120, 2016.
- [5] S. Kamley, S. Jaloree, and R. S. Thakur, "Performance forecasting of share market using machine learning techniques: A review," *Int. J. Electr. Comput. Eng.*, vol. 6, no. 6, pp. 3196–3204, 2016.
- [6] D. Semaan, A. Harb, and A. Kassem, "Forecasting exchange rates: Artificial neural networks vs regression," *2014 3rd Int. Conf. e-Technologies Networks Dev. ICeND 2014*, vol. 2, pp. 156–161, 2014.
- [7] K. Huang and T. H. K. Yu, "The application of neural networks to forecast fuzzy time series," *Phys. A Elsevier*, vol. 363, no. 2, pp. 481–491, 2006.
- [8] L. Yu, Z. Danning, and C. Hongbing, "Prediction of length-of-day using extreme learning machine," *Geod. Geodyn.*, vol. 6, no. 2, pp. 151–159, 2015.
- [9] G.-B. Huang, Q.-Y. Zhu, and C.-K. Siew, "Extreme learning machine: a new learning scheme of feed forward neural networks," *2004 IEEE Int. Jt. Conf. Neural Networks (IEEE Cat. No.04CH37541)*, vol. 2, pp. 25–29, 2004.
- [10] N. R. Sari, W. F. Mahmudy, and A. P. Wibawa, "Backpropagation on Neural Network Method for Inflation Rate Forecasting in Indonesia," *Int. J. Adv. Soft Comput. Appl.*, vol. 8, no. 3, 2016.
- [11] N. R. Sari, W. F. Mahmudy, A. P. Wibawa, and E. Sonalitha, "Enabling External Factors for Inflation Rate Forecasting using Fuzzy Neural System," *Int. J. Electr. Comput. Eng.*, vol. 7, no. 5, pp. 2746–2756, 2017.
- [12] Y. P. Anggodo and I. Cholissodin, "Improve Interval Optimization of FLR using Auto-Speed Acceleration Algorithm," *Telecommunication, Comput. Electron. Control*, vol. 16, no. 1, pp. 1–12, 2017.
- [13] B. Indonesia, "Laporan Inflasi," 2017. [Online]. Available: <http://www.bi.go.id/id/moneter/inflasi/data/Default.aspx>.
- [14] W. Sun, C. Wang, and C. Zhang, "Factor analysis and forecasting of CO2 emissions in Hebei, using extreme learning machine based on particle swarm optimization," *J. Clean. Prod.*, vol. 162, pp. 1095–1101, 2017.
- [15] G. Bin Huang, Q. Y. Zhu, and C. K. Siew, "Extreme learning machine: Theory and applications," *Neurocomputing*, vol. 70, no. 1–3, pp. 489–501, 2006.
- [16] A. N. Alfiyatin, W. F. Mahmudy, and Y. P. Anggodo, "Modelling Multi Regression with Particle Swarm Optimization Method to Food Production Forecasting," *J. Telecommun. Electron. Comput. Eng.*, vol. 10, no. 3, pp. 91–95, 2018.
- [17] A. Ratnaweera, S. K. Halgamuge, and H. C. Watson, "Self-organizing hierarchical Particle swarm optimizer with time varying acceleration coefficients," *IEEE Trans. Evol. Comput.*, vol. 8, no. 3, p. 240–255, 2004.
- [18] I. Cholissodin and E. Riyandani, *Swarm Intelligence*. Malang: Universitas Brawijaya, 2016.
- [19] M. C. C. Utomo, W. F. Mahmudy, and S. Anam, "Determining the Neuron Weights of Fuzzy Neural Networks Using Multi-Populations Particle Swarm Optimization for Rainfall Forecasting," *J. Telecommun. Electron. Comput. Eng.*, vol. 9, no. 2, pp. 37–42, 2017.

Impact Factors of IT Flexibility within Cloud Technology on Various Aspects of IT Effectiveness

Salameh A. mjlae¹
Department of Computer Science
Balqa Applied University
Salt, Jordan

Zarina Mohamad², Wan Suryani³
Department of Computer Science
University Sultan Zainal Abidin
Besut, Malaysia

Abstract—Cloud computing Adoption has achieved an essential inflection factor; this is affecting IT and business models and strategies all through the industries. There is a lack of empirical evidence how the adoption of cloud technology and a certain power of cloud technology specifically, affect various aspects of information technology effectiveness as IT-helpfulness to users, user satisfaction, and IT-quality of service. The intent of this paper has been added to the main of knowledge that could be used by researchers, companies, and businesses alike to accomplish optimal outcomes with focus on the main useful power of cloud-based services, solutions, and components inside them. The research findings presented that statistical evidence that confirms factors of IT Flexibility inside-cloud computing has a much stronger correlation with several aspects of information technology effectiveness than the remainder. The new awareness gain would improve the decision making procedure for IT executives and IT managers at what time allowing for cloud computing adoption base services and solutions

Keywords—Cloud Computing Adoption (CCA); IT Flexibility (ITF); IT Effectiveness (ITE)

I. INTRODUCTION

Cloud adoption-based services and solutions are nowadays one of the most leading issues that IT companies face [1] Cloud computing get from a extended the past of research and enhancement on a variety of models to IT outsourcing, Cloud technology is a approach to provision and expanding IT abilities on a require and pay-per-use, with reducing costs, storage capacity, high accessibility, and more reliability represents the best advantages [2, 3, 4, 23]. Services and solutions through cloud technology as a consequence from a lot of years of investigation in the several areas include virtualization [5], networking, and software services [6], distributed computing [7], and utility computing [8]. Duncan (1995) exposed technological factors of the ITF constructs as (connectivity, modularity, and compatibility) as a measure of ITF.

These constructs provided as the foundation for subsequent researches performed by Ness (2005), Byrd and Turner (2000), [11], Tallon and Kraemer (2005). In their research, Byrd and Turner (2000) demonstrated ITF as the capability of an organizations to implement processes that be able to increase growth of the organizations. ITF also described as the fast deployment of IT components as facilitated during a company information technology infrastructure. Chebrolu (2010) expanded Ness' (2005) research by appropriately by cloud

computing adoption as a proxy for ITF. As noted by Duncan (1995), an organization's IT-infrastructure could be considered flexible if innovative business processes are enabled. According to Tallon and Kraemer (2003), ITF involved the capability of a company to easily and rapidly offer new source of IT assistance for the business plan.

Fink and Newmann (2009) suggested that organizations IT infrastructures should be elastic as much as necessary to accommodate an increasingly change environments. Cloud technology can be depicted as a modern business computing paradigm extends to information technology Flexibility to improve IT capabilities through pervasive provisioning of IT services [16, 17, 24]. IT effectiveness is often considered in the context of how technology benefits the organization tangibly [18]. Cloud computing may drive ITE rather than efforts creating strategies alignment in IT base services. The failure of researchers and companies to understand cloud computing from an ITE viewpoint appear to stem from the fact that there are few investigations which evaluate the overall benefits that are achieved when the organizations adopts cloud technology base services and solutions.

II. PROBLEM STATEMENT

Increased competitive weights upon companies because of worldwide competition, expanded to all type of business are proceeding to generate, go up they require for productivity and better effectiveness between IT companies. In preparation for global economic recovery from the latest world stagnancy which began in 2007, several IT companies were evaluated their whetting their business models and management practices. IT-budgets will be lower, the business model is more focused.

The act of remove extra costs from the IT-budget and deciding regions of planned business and plan investment are important in a confined business. Come through IT solutions is leading unplanned, rapid, and recurrent change in business model alongside with the resulting demand in the lead information technology for its help essential to attain sustained competitive benefit. While cloud adoption provides some advantage include real-time provisioning and cloud consumer be billed accurately for the actual amount of its IT resource usage that can support business model into IT companies, it has its percentage of complexity in conditions of availability, performance, security, and development. The global cloud services market is expected to rise to \$ 336 billion by 2020

from \$ 175 billion in 2015. The Middle East and North Africa region will see the greatest growth in cloud computing between 2014 and 2019.

Total spending on general cloud computing services in 2018 in the Middle East region will rise to \$ 1.5 billion compared with \$ 727 million estimated in 2014. In 2014, the Hashemite Kingdom of Jordan formed a partnership with Microsoft to implement cloud services in the public sector. Projects of the Hashemite Kingdom of Jordan that between 2014 and 2018, it's to spend on cloud technology up to 26.5 % compound yearly increase rate and exceed \$6 million by 2020 Providing that a wide of services and solution of computing-related as pay-as-you-go base open numerous opportunity for the cloud service providers in that increasing marketplace.

It is not obvious how a number of those IT companies which adopt services and solution on the cloud technology are more successful than what they were before and which solutions or services of CSP, in fact, assist which aspects of those IT companies the majority. Specifically, in light of the literature review, there was a need for empirical proof on the influence of each factor of ITF precise to cloud computing adoption on every aspect of ITF. This research is an try to verify their relationships and to attempt which, if any, factors of ITF precise to cloud technology adoption has a upper correlation with which aspect of ITE.

III. SIGNIFICANCE OF THE STUDY

The relationship between factors of IT flexibility precise to cloud computing adoption and their aspects of information technology effectiveness among IT companies was investigated and evaluated.

In May 2010, Chief information officer of federal government IT companies offered at NIST cloud technology discussion board with a view to the adoption of services and solutions within cloud technology like Google's Earth platform, Amazon's EC2 infrastructure and Salesforce.com's in aspects of system response time, cost savings, scalability, collaboration capabilities, connectivity and consolidation. NIST started a plan to prompt adoption of cloud technology through knowing basic technical standards. The IT companies in different types of business which are prepared to adoption solutions of cloud technology without empirical evidence how factors of ITF precise to cloud technology adoption impact on the aspect of their information technology effectiveness inside IT companies and this paper provides this evidence.

IV. RESEARCH METHODOLOGY

A. Research Design

The aim of this non-experimental quantitative correlational research was to examine and measure the relationship between factors of ITF (Compatibility, Modularity, and Connectivity) precise to cloud technology adoption and aspects of ITE The aim of this study was adding to the main of knowledge that could technically be useful by IT companies, business model, and researchers to attain the best outcome from beginning to adoption services and solutions of cloud technology. This paper was intended to work study the degree to which factors of ITF precise to cloud technology adoption correlate with

different aspects of ITF in conditions of information technology capability to provide services and solutions to the IT companies in global competitions.

B. The Research Work Questions

1) To what extent, if any, is the ITF (Connectivity) specific to cloud technology adoption associated with IT quality of service between IT companies?

2) To what extent, if any, is the factor of ITF (Connectivity) specific to cloud technology adoption associated with User Satisfaction between IT companies?

3) To what extent, if any, is the factor of ITF (Connectivity) specific to cloud technology adoption associated with IT helpfulness to users between IT companies?

4) To what extent, if any, is the factor of ITF (Modularity) specific to cloud technology adoption associated with IT quality of service between IT companies?

5) To what extent, if any, is the factor of ITF (Modularity) specific to cloud technology adoption associated with User Satisfaction between IT companies?

6) To what extent, if any, is the factor of ITF (Modularity) specific to cloud technology adoption associated with IT helpfulness to users between IT companies?

7) To what extent, if any, is the factor of ITF (Compatibility) specific to cloud technology adoption associated with IT quality of service between IT companies?

8) To what extent, if any, is the factor of ITF (Compatibility) specific to cloud technology adoption associated with User Satisfaction between IT companies?

9) To what extent, if any, is the factor ITF (Compatibility) specific to cloud technology adoption associated with IT helpfulness to users between IT companies?

C. Hypotheses Test

H1₀: a factor of ITF (Connectivity) precise to cloud computing adoption was not positively associated with IT QoS, between IT companies.

H1₁: a factor of ITF (Connectivity) precise to cloud computing adoption was positively associated with IT QoS, between IT companies.

H2₀: a factor of ITF (Connectivity) precise to cloud computing adoption was not positively associated with user satisfaction, between IT companies.

H2₁: a factor of ITF (Connectivity) precise to cloud computing adoption was positively associated with user satisfaction, between IT companies.

H3₀: a factor of ITF (Connectivity) precise to cloud computing adoption was not positively associated with information technology helpfulness to users, between IT companies.

H3₁: a factor of ITF (Connectivity) precise to cloud computing adoption was positively associated with information technology helpfulness to users, between IT companies.

H40: a factor of ITF (Modularity) precise to cloud computing adoption was not positively associated with IT QoS, between IT companies.

H4a: a factor of ITF (Modularity) precise to cloud computing adoption was positively associated with IT QoS, between IT companies.

H50: a factor of ITF (Modularity) precise to cloud computing adoption was not positively associated with user satisfaction, between IT companies.

H5a: a factor of ITF (Modularity) precise to cloud computing adoption was positively associated with user satisfaction, between IT companies.

H60: a factor of ITF (Modularity) precise to cloud computing adoption was not positively associated with information technology helpfulness to users, between IT companies.

H6a: a factor of ITF (Modularity) precise to cloud computing adoption was positively associated with information technology helpfulness to users, between IT companies.

H70: a factor of ITF (Compatibility) precise to cloud computing adoption was not positively associated with IT QoS, between IT companies.

H7a: a factor of ITF (Compatibility) precise to cloud computing adoption was positively associated with IT QoS, between IT companies.

H80: a factor of ITF (Compatibility) precise to cloud computing adoption was not positively associated with user satisfaction, between IT companies.

H8a: a factor of ITF (Compatibility) precise to cloud computing adoption was positively associated with user satisfaction, between IT companies.

H9₀: a factor of ITF (Compatibility) precise to cloud computing adoption was not positively associated with information technology helpfulness to users, between IT companies.

H9_a: a factor of ITF (Compatibility) precise to cloud computing adoption was positively associated with information technology helpfulness to users, between companies.

The purpose of this quantitative correlational study, which takes into account some suppleness in evaluated the relationships between the factors. with an end goal to keep the same reliability along with validity from prior investigate instrumentation and methods by Tallon and Kraemer [14], Ness [6], a 7-point Likert-type scale has been used to perform ordinal dataset value. Previous investigate make use of the base for sure construct elements, measures, in the role of methods for determining and measuring the construct's correlation, validity, in addition to reliability. The research from Pierce [9], Tallon and Kraemer [14] and Ness [6], besides their survey formats, utilized as a method toward accomplishing instrumentation and construct measurement.

The analysis of ordinal scale with values was managed during the chi-square test besides linear and bivariate

regression test. The utilize of linear regression test for the ordinal dataset was constant by previous investigate by Pierce [9], Tallon and Kraemer [14] and Ness [6]. The survey questions on ITF by Ness [6], with proper changes to be relevant for services and solution through cloud computing, have been used as part of the whole survey instrument in this research attaining on the whole construct correlation, validity, and reliability between factors of ITF precise to cloud computing adoption and aspects of ITE.

D. Conceptual Model

This research's conceptual model is viewed in Fig. 1. It is an development by Tallon and Kraemer [14], Lawal [19], Ness [10] and Chebrolu [12] research, explore in depth to examine the impact factors of ITF precise to cloud computing adoption and aspects of ITE

E. Operational Definition of Variables

The components from prior investigate by Tallon and Kraemer [14], Ness [10], Chebrolu [12], and Lawal [19], have been used to evaluate the construct of ITE, while the components have been used to evaluate the construct of ITF has been used to assess the construct of factors of ITF within cloud computing and aspects of ITE. This structure of measurement was helped in achieving validity and consistency between this investigate and prior investigate. Adoption of Cloud technology had been many survey questions having already been used to evaluate each factor's power for ITE dependent on a seven-point Likert-type scale. The overall quality of the general construct on ITE was assessment during the average of the means of all construct's factors. The main factors associated to all constructs on this research were as follows: The three factors of ITF within cloud computing adoption: are compatibility (COMP), modularity (MODU) and connectivity (CONN).

- **Compatibility.** Refers to the capability to share, use, or connect to any kind of data across any technical component [9]. Chung, Tang, and Ahmad (2010) suggested that compatibility within organizations refers to whether the new technology will be compatible with current work practice [26].
- **Modularity.** Refers to how rapidly technical components can be added, changed or removed to meet new managerial conditions [9], [21], [25]. Pekkarinen (2008) suggested that modularity is the ability to integrate numerous functions within organizations to reduce service complexity and accomplish improved responsiveness to service diversity.
- **Connectivity.** Refers to how technical components link individuals, functional areas, and applications in organizations to enhance communication and resource sharing throughout an organization. This association could be within or outside of the customary confines of the organization [9], [27].
- **Information technology effectiveness.** Is often considered in the context of how the technology benefits the organization tangibly [22],[28].

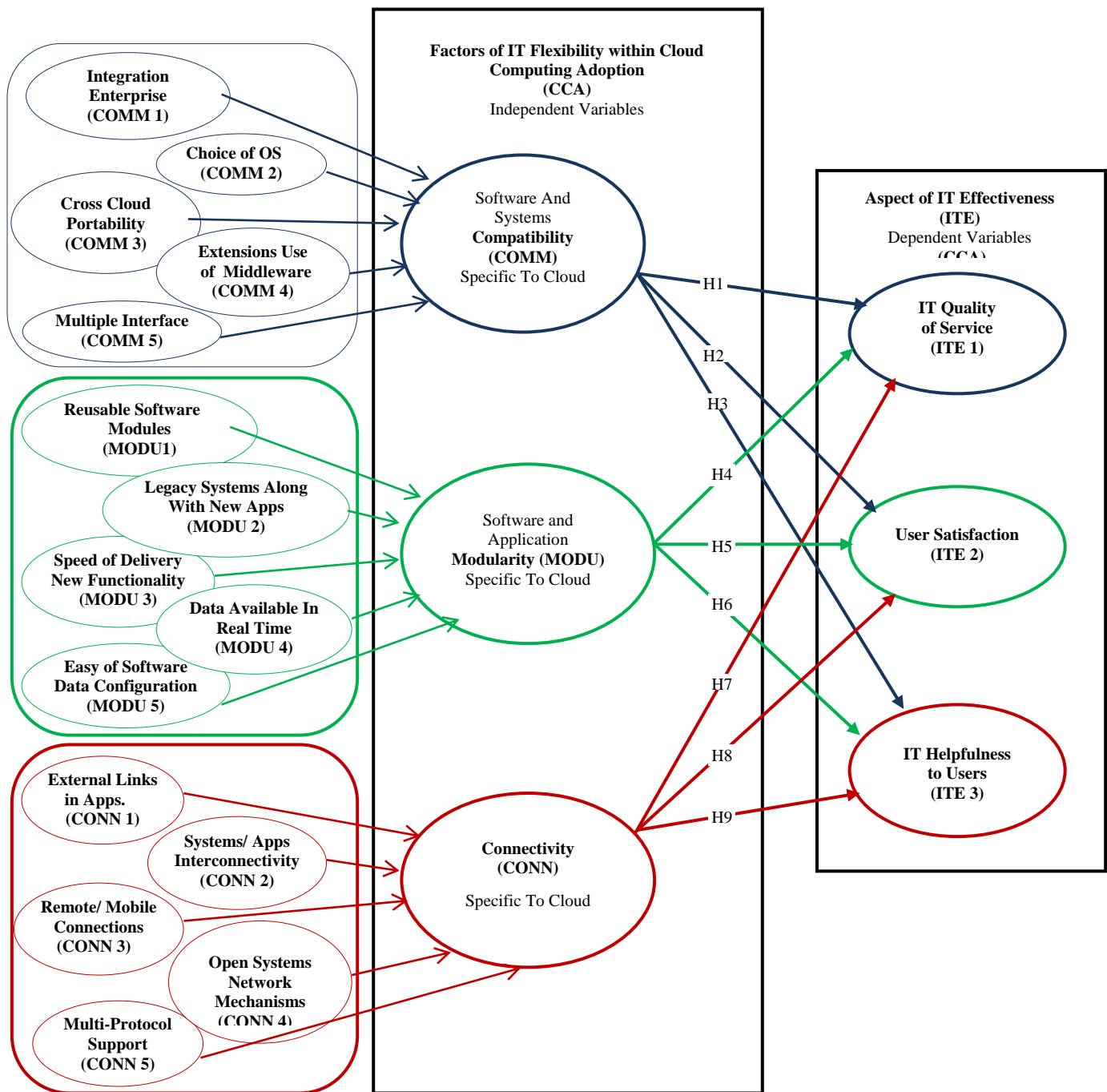


Fig. 1. Shows Conceptual Model.

Information Technology Effectiveness Elements: The main items that were utilized to assess Information Technology effectiveness construct have been taken from previous investigate by Gurbaxani, and Tallon Kraemer, which they utilized to evaluate the model of strategic flexibility. Ness [10] affirmed that aspects had been used to evaluate strategic flexibility appear to be close up associated operationally and provide the good origin to evaluate ITE. These aspects are the overall QoS (ITEF1), user satisfaction with IT (ITEF2) and helpfulness of IT staff to users (ITEF3). This research has been consistency with the previous investigators in concepts of methodology, and so a seven-point Likert-type scale has been

used when data gathering and analyze, which represent dataset elements with a view to measurement convenient to size or quality. In linear regression analyze, it is verified that independent variables (IV) in the gather data had a normal distribution before to test.

F. Sample

The sampling method was used from previous investigators were pursued to some extent probable to do again validity and reliability. The aboard population for this research wants to be those who had a broad knowledge of information technology adds to its business model. Including (CIO, Associate CIO,

Interim CIO, Acting CIO, Global CIO, and Co-CIO). in the position of chief information officer were precise to be content with this population condition. The Survey with Google Forms have been used to draw a random sample of 1221 email addresses of IT staff in a variety of departments within IT companies including sizes (small & medium) from the sampling. A whole of 149 responded were received, in which 132 respondents complete the questionnaire. Seventeen respondents were excluded for not achieving the set conditions. On the 41days, the questionnaire was closed because a appropriate sample was accomplished. Unlike similar studies done by Chebrolu [12], were focused on all size and different business type of IT companies .this research paper is focused on only IT companies within size small and medium only.

G. Instrumentation

The study instrument contains questions that have been proposed to collection data from the participants on IT and cloud technology adoption. The origin of the current research survey instrument has been established on the research done by Lawal [19] and Ness [10], on ITF and ITE. The survey was a mixture of the original survey questions that have been produced by Gurbaxani, Tallon and Kraemer, [13], additionally later have been used by Tallon and Kraemer [14], Chebrolu [12], Ness [10], Lawal [19] and Mjlae[29], for ITF and ITE. The survey questions for ITF have been changed minimally to be appropriate for adoption of cloud computing. In order to recreate the original questionnaire survey, the format and design of the prior questionnaire survey were maintained to add reliability and validity. All questions have been used seven-point Likert-type scale.

H. Data Collection and Analysis

Data has been gathered utilized an online survey instrument. A whole of 149 participants had responded to the survey questionnaire from among 1221 eligible participants list, but only 132 participants provide full answers question. The survey results were downloaded from the Services of Google forms web site. The data has been then moved to IBM SPSS Software version 22. The bi-variate linear regression analysis has been executing as an affirmation to the chi-square outcomes has been obtained. The power of every one relationship between COMP, MODU, CONE, ITEF1, ITEF2, and ITEF3 was evaluate based on the statistical significance value calculated for all factors in addition to the correlation coefficients.

V. FINDINGS

A. Validity and Reliability

As indicated the G*Power 3.1, a sample size of 119 was suggested to accomplish the statistical power needed to build up the validity of this research. The survey sample gathered by docs.google.com/forms was totaled 149. Also, a total of Cronbach's Alpha score of 0.805 has been calculated from standardized items that substantiate the interior consistency of this research. Norusis [20] suggested a Cronbach's Alpha score of minimum 0.5 to set up the reliability of a study's measures. These statistical tests have presented that the data has been used in this research are both reliable and valid. Only 143 participants have been answered all 15 questions as several

participants select to avoid some questions. Norusis [20] suggested that before calculating a correlation coefficient, a test for data outliers ought to be prepared to avoid misleading outcomes. Whisker plot and A box were done using the entire 143 response data. The whisker plot and box identified three response dataset (35, 40, 82) for ITEFs outside of interquartile scope; while it was recognized sex response datasets (35, 40, 82, 97, 101, 131) for CONE and MODU; and identified eleven response datasets (8, 14,19,28, 35, 40, 82, 97, 101, 112, 131) for COMP outside of interquartile scope. Norusis [20] warn that any data outliers the whisker scope in whisker plot and the box is well chosen an extreme value and should be delete from the total replies data set. as a result, the data sets (8, 14,19,28, 35, 40, 82, 97, 101, 112, and 131) were deleted from this research remain 132 answers intended for the test.

B. Analysis and Evaluation

1) *Linear regression analysis and bivariate correlations:* the total answer dataset to 132, an inter level correlation analysis has been executed on every one paired constructs such as CONN-ITEF1, CONN-ITEF2, CONN-ITEF3, MODU-ITEF1, MODU-ITEF2, MODU-ITEF3, COMP-ITEF1, COMP- ITEF2, and CMOP-ITEF3 as shown in table (2). The array of variables in the bi-variate correlations analysis has been made to ITEF1, ITEF2, ITEF3 were the target dependent variables whereas Connectivity (CONN), Modularity (MODU) and Compatibility (COMP) were the independent variables(IV). The outcome of the analysis was depend on Phi/Pearson's value exposed that positive correlations was existed between CONN - ITEF at $r = .758$ ($p < .001$, $r^2 = .574$); MODU - ITFE at $r = .772$ ($p < .001$, $r^2 = .595$), and between COMP - ITEF at $r = .741$ ($p < .001$, $r^2 = .549$). The linear regression analysis was validated the bivariate correlation test outcome by generating the exact calculations.

2) *Pearson's chi-square test:* The Pearson's chi-squared analysis outcome with 132 response data sets as show in table [2], which stand at 335.729, $p < .001$ for CONN -ITEF1; at 352.392, $p < .001$ for CONN -ITEF2; 310.497, $p < .001$ for CONN -ITEF3; 349.114, $p < .001$ for MODU - ITEF1; 428.361, $p < .001$ for MODU -ITEF2; 358.983, $p < .001$ for MODU -ITEF3; 330.701, $p < .001$ for COMP ITEF1; 359.974, $p < .001$ for COMP -ITEF2; 350.377, $p < .001$ for COMP -ITEF3. All the relationships between aspects of ITEF and factors of IT flexibility within cloud computing (CONN, MODU, and COMP) are statistically significant because of p-value $< .001$ in case of all of them

3) *Scatter plot analysis:* According to Norusis [7], the heteroscedasticity or inequality of regressions, represent a sequence of random variables with various variances, and therefore square-root transformations are usually used for positive data when addressing the assumption of heteroscedasticity in linear regression analyses. All the paired constructs of CONN -ITEF1, CONN - ITEF2, CONN -ITEF3, MODU -ITEF1, MODU -ITEF2, MODU -ITEF3, COMP - ITEF1, COMP -ITEF2, and COMP -ITEF3 all found to have positive slopes. The technique of square-root transformation

for the ITEF1, ITEF2, and ITEF3 constructs was used for further analysis. However, the same kinds of slopes with similar r2 linear values are obtained.

4) *Normal P-P plot for $\sqrt{ITEF1}$, $\sqrt{ITEF2}$, $\sqrt{ITEF3}$, *CONN*, *MODU*, and *COMP**: According to Norusis [20], an assumption of hypothesis testing is a normal distribution of values of the dependent variables. To show that $\sqrt{ITEF1}$, $\sqrt{ITEF2}$, and $\sqrt{ITEF3}$ had normal distribution at the reduced response dataset of 132, the observed increasing probability was plotted against the estimated cumulative probability for $\sqrt{ITEF1}$, $\sqrt{ITEF2}$, and $\sqrt{ITEF3}$. It was found that the standardized values represent the normal distribution of the dependent variables and agree with the condition of homoscedasticity for linear regression analysis. Hence, the 132 data sets represent in $\sqrt{ITEF1}$, $\sqrt{ITEF2}$, $\sqrt{ITEF3}$ for this research were convincing and applicable for parametric linear regression test. In the same way, the pragmatic cumulative probability was plotted beside the expected increasing probability for three independent variables (*CONN*, *MODU*, *COMP*) to ensure that the 132 datasets were applicable and suitable for linear regression test.

5) *The chi-square, linear regression, and bivariate correlations analysis with \sqrt{ITEF} (1-3)*: the Chi-square, linear regression, and bivariate correlations analysis were executed by the \sqrt{ITEF} transformation for all paired constructs and found out that (r^2) - values of each one correlation is roughly the same values as shown in Table II.

The Linear Regression analysis and Bivariate Correlations for each factor of IT flexibility within cloud computing and Aspects of ITEF: The linear regression and bivariate

correlations analyses were executed for every of the 45 paired constructs as shown in Table III (15 factors of IT flexibility within cloud computing times 3 aspects of ITEF). Also, discovered that *MODU1* * *ITEF2* ($r^2=.511$, $p<.001$) have the strongest correlation between all probably paired constructs at the level of factors of IT flexibility within cloud computing have been utilized in the research. The all pairs in terms of correlation values (r^2) are as shown in Table III. the paired of constructs relating two Sub-factors of Compatibility (*COMP*) variable make it to the list as their (r^2) values were lower than 0.150, whereas all paired constructs remaining relating Sub-factors of Modularity (*MODU*), *CONN1* (External Links in Applications), *COMP5*(Multiple Interface), *CONN2* (Systems/Apps Interconnectivity) and *MODU2*(Legacy Systems Along With New Apps) have been stronger correlations with each precise aspect of information technology effectiveness (*ITEF1*, *ITEF2*, *ITEF3*) that have been utilized in this Research. Also, *COMP1* (Integration Enterprise) have fewer correlations with each precise aspect of information technology effectiveness (*ITEF1*, *ITEF2*, *ITEF3*).

C. Test of Hypotheses

An assessment of the investigation findings has been executing to evaluation the researcher's hypotheses. The strength and direction of the relationships between the variables were an assessment by the (r^2) value of every correlation computation. The (r^2) values as shown in Table II represent the inter-scale correlation results for IV (*ITEF1*, *ITEF2*, *ITEF3*) which along with p-value have been used to accept, or reject nine hypotheses. The nine null hypotheses have been rejected because the p-value of .000 was less than the significance level of .05 to test [20].

TABLE I. THE CHI-SQUARE CROSSTABS, LINEAR REGRESSION AND BIVARIATE CORRELATION ANALYSIS RESULTS FOR FACTORS OF ITF WITHIN CLOUD COMPUTING AND ITEF

Variable	Pearson Chi-Square	Pearson's R	R-Square(r2)	Sig. (2-tailed) (p)
Connectivity * IT Effectiveness	646.441	.758	.574	.000 (<.001)
Modularity * IT Effectiveness	764.211	.772	.595	.000 (<.001)
Compatibility * IT Effectiveness	767.691	.741	.549	.000 (<.001)

TABLE II. THE CHI-SQUARE CROSSTABS, LINEAR REGRESSION AND BIVARIATE CORRELATION ANALYSIS RESULTS FOR FACTORS OF ITF WITHIN CLOUD COMPUTING VERSUS ASPECTS OF ITEF

Variable	Pearson Chi-Square	Pearson's Correlation (r)	R-Square (r2)	Sig. (2-tailed) (p)
Connectivity * ITEF1	335.729	.709	.502	.000 (<.001)
Connectivity * ITEF2	352.392	.711	.505	.000 (<.001)
Connectivity * ITEF3	310.497	.653	.426	.000 (<.001)
Modularity * ITEF1	349.114	.695	.483	.000 (<.001)
Modularity * ITEF2	428.361	.727	.528	.000 (<.001)
Modularity * ITEF3	358.983	.686	.470	.000 (<.001)
Compatibility * ITEF1	330.701	.674	.454	.000 (<.001)
Compatibility * ITEF2	359.974	.684	.467	.000 (<.001)
Compatibility * ITEF3	350.377	.667	.444	.000 (<.001)

TABLE I. THE LINEAR REGRESSION AND BIVARIATE CORRELATION ANALYSIS RESULTS FOR THE TOP TEN FACTORS OF ITF WITHIN CLOUD COMPUTING VERSUS ASPECTS OF ITEF

NO	Variable	Pearson's Correlation (r)	R-Square (r2)	Sig. (2-tailed) (p)
	MODU1 * ITEF2	0.715	0.511	.000 (<.001)
	CONN1 * ITEF2	0.66	0.436	.000 (<.001)
	COMP5 * ITEF1	0.657	0.432	.000 (<.001)
	MODU1 * ITEF3	0.635	0.403	.000 (<.001)
	COMP5 * ITEF2	0.627	0.393	.000 (<.001)
	CONN2 * ITEF1	0.615	0.378	.000 (<.001)
	CONN2 * ITEF2	0.615	0.378	.000 (<.001)
	MODU2 * ITEF1	0.614	0.377	.000 (<.001)
	COMP4 * ITEF3	0.613	0.376	.000 (<.001)
	CONN1 * ITEF1	0.609	0.371	.000 (<.001)
	CONN1 * ITEF3	0.606	0.367	.000 (<.001)
	MODU1 * ITEF1	0.602	0.362	.000 (<.001)
	CONN3 * ITEF1	0.6	0.360	.000 (<.001)
	CONN5 * ITEF1	0.592	0.350	.000 (<.001)
	COMP4 * ITEF1	0.588	0.346	.000 (<.001)
	CONN2 * ITEF3	0.584	0.341	.000 (<.001)
	MODU5 * ITEF3	0.575	0.331	.000 (<.001)
	MODU4 * ITEF2	0.574	0.329	.000 (<.001)
	CONN5 * ITEF2	0.572	0.327	.000 (<.001)
	CONN3 * ITEF2	0.57	0.325	.000 (<.001)
	MODU4 * ITEF1	0.567	0.321	.000 (<.001)
	MODU5 * ITEF2	0.56	0.314	.000 (<.001)
	MODU5 * ITEF1	0.553	0.306	.000 (<.001)
	MODU2 * ITEF2	0.545	0.297	.000 (<.001)
	MODU2 * ITEF3	0.534	0.285	.000 (<.001)
	CONN3 * ITEF3	0.532	0.283	.000 (<.001)
	COMP4 * ITEF2	0.526	0.277	.000 (<.001)
	COMP5 * ITEF3	0.52	0.270	.000 (<.001)
	MODU3 * ITEF2	0.518	0.268	.000 (<.001)
	COMP3 * ITEF3	0.518	0.268	.000 (<.001)
	MODU4 * ITEF3	0.515	0.265	.000 (<.001)
	COMP2 * ITEF3	0.511	0.261	.000 (<.001)
	CONN4 * ITEF2	0.508	0.258	.000 (<.001)
	CONN4 * ITEF1	0.497	0.247	.000 (<.001)
	COMP2 * ITEF2	0.496	0.246	.000 (<.001)
	COMP3 * ITEF2	0.496	0.246	.000 (<.001)
	CONN5 * ITEF3	0.494	0.244	.000 (<.001)
	MODU3 * ITEF3	0.49	0.240	.000 (<.001)
	COMP2 * ITEF1	0.479	0.229	.000 (<.001)
	CONN4 * ITEF3	0.475	0.226	.000 (<.001)
	MODU3 * ITEF1	0.455	0.207	.000 (<.001)
	COMP3 * ITEF1	0.435	0.189	.000 (<.001)
	COMP1 * ITEF2	0.425	0.181	.000 (<.001)
	COMP1 * ITEF1	0.373	0.139	.000 (<.001)
	COMP1 * ITEF3	0.34	0.116	.000 (<.001)

1) Hypothesis 1: CONN associated with ITEF1

H1₀: a factor of ITF (Connectivity) precise to cloud computing adoption was not positively associated with IT QoS, among IT companies.

H1₁: a factor of ITF (Connectivity) precise to cloud computing adoption was positively associated with IT QoS, among IT companies.

Finding 1: H1₀ Rejected

The factor of ITF (Connectivity) precise to cloud computing adoption did positively correlate with IT QoS. The values for CONN as shown in Table II confirmed a positive correlation between a factor of ITF (Connectivity) precise to cloud computing adoption and ITEF1. The values for CONN were $r=.709$, $r^2=.502$, $p<.001$; hence, the findings confirmed a positive correlation with IT QoS.

2) Hypothesis 2: CONN associated with ITEF2

H1₀: a factor of ITF (Connectivity) precise to cloud computing adoption was not positively associated with user satisfaction, among IT companies.

H1₁: a factor of ITF (Connectivity) precise to cloud computing adoption was positively associated with user satisfaction, among IT companies.

Finding 2: H2₀ Rejected

The factor of ITF (Connectivity) precise to cloud computing adoption did positively correlate with user satisfaction. The values for CONN as shown in Table II confirmed a positive correlation between a factor of ITF (Connectivity) precise to cloud computing adoption and ITEF2. The values for CONN were $r=.711$, $r^2=.505$, $p<.001$; hence, the findings confirmed a positive correlation with user satisfaction.

3) Hypothesis 3: CONN associated with ITEF3

H3₀: a factor of ITF (Connectivity) precise to cloud computing adoption not positively associated with information technology helpfulness to users, among IT companies.

H3₁: a factor of ITF (Connectivity) precise to cloud computing adoption was positively associated with information technology helpfulness to users, among IT companies.

Finding 3: H3₀ Rejected

The factor of ITF (Connectivity) precise to cloud computing adoption did positively correlate with IT helpfulness to users. The values for CONN as shown in Table II confirmed a positive correlation between a factor of ITF (Connectivity) precise to cloud computing adoption and ITEF3. The values for CONN were $r=.653$, $r^2=.426$, $p<.001$; hence, the findings confirmed a positive correlation with IT helpfulness to users.

4) Hypothesis 4: MODU associated with ITEF1

H4₀: a factor of ITF (Modularity) precise to cloud computing adoption was not positively associated with IT QoS, among IT companies.

H4₁: a factor of ITF (Modularity) precise to cloud computing adoption was positively associated with IT QoS, among IT companies.

Finding 4: H4₀ Rejected

The factor of ITF (Modularity) precise to cloud computing did positively correlate with IT QoS. The values for MODU as shown in Table II confirmed a positive correlation between a factor of ITF (Modularity) precise to cloud computing adoption and ITEF1. The values for MODU were $r=.695$, $r^2=.483$, $p<.001$; hence, the findings confirmed a positive correlation with IT QoS.

5) Hypothesis 5: MODU associated with ITEF2

H5₀: a factor of ITF (Modularity) precise to cloud computing adoption cloud was not positively associated with user satisfaction, among IT companies.

H5₁: a factor of ITF (Modularity) precise to cloud computing adoption was positively associated with user satisfaction, among IT companies.

Finding 5: H5₀ Rejected

The factor of ITF (Modularity) precise to cloud computing adoption did positively correlate with user satisfaction. The values for MODU as shown in Table II confirmed a positive correlation between a factor of ITF (Modularity) precise to cloud computing adoption and ITEF2. The values for MODU were $r=.727$, $r^2=.528$, $p<.001$; hence, the findings confirmed a positive correlation with user satisfaction.

6) Hypothesis 6: MODU associated with ITEF3

H6₀: a factor of ITF (Modularity) precise to cloud computing adoption was not positively associated with information technology helpfulness to users, among IT companies.

H6₁: a factor of ITF (Modularity) precise to cloud computing adoption was positively associated with information technology helpfulness to users, among IT companies.

Finding 6: H6₀ Rejected

The factor of ITF (Modularity) precise to cloud computing adoption did positively correlate with information technology helpfulness to users. The values for MODU as shown in Table II confirmed a positive correlation between a factor of ITF (Modularity) precise to cloud computing adoption and ITEF3. The values for MODU were $r=.686$, $r^2=.470$, $p<.001$; hence, the findings confirmed a positive correlation with information technology helpfulness to users.

7) Hypothesis 7: COMP associated with ITEF1

H7₀: a factor of ITF (Compatibility) precise to cloud computing adoption was not positively associated with IT QoS, among IT companies

H7₁: a factor of ITF (Compatibility) precise to cloud computing adoption was positively associated with IT QoS, among IT companies.

Finding 7: H7₀ Rejected

The factor of ITF (Compatibility) precise to cloud computing adoption did positively correlate with IT QoS. The values for COMP as shown in Table 2 confirmed a positive correlation between a factor of ITF (Compatibility) precise to cloud computing adoption and ITEF1. The values for COMP were $r=.674$, $r^2=.454$, $p<.001$; hence, the findings confirmed a positive correlation with IT QoS.

8) Hypothesis 8: COMP associated with ITEF2

H8₀: a factor of ITF (Compatibility) precise to cloud computing adoption was not positively associated with user satisfaction, among IT companies.

H8_a: a factor of ITF (Compatibility) precise to cloud computing adoption was positively associated with user satisfaction, among IT companies.

Finding 8: H8₀ Rejected

The factor of ITF (Compatibility) precise to cloud computing adoption did positively correlate with user satisfaction. The values for COMP as shown in Table 2 confirmed a positive correlation between a factor of ITF (Compatibility) precise to cloud computing adoption and ITEF2. The values for COMP were $r=.684$, $r^2=.467$, $p<.001$; hence, the findings confirmed a positive correlation with user satisfaction.

9) Hypothesis 9: COMP associated with ITEF3

H9₀: a factor of ITF (Compatibility) precise to cloud computing adoption was not positively associated with information technology helpfulness to users, among IT companies.

H9_a: a factor of ITF (Compatibility) precise to cloud computing adoption was positively associated with information technology helpfulness to users, among IT companies.

Finding 9: H9₀ Rejected

The factor of ITF (Compatibility) precise to cloud computing adoption did positively correlate with information technology helpfulness to users. The values for COMP as shown in Table II confirmed a positive correlation between a factor of ITF (Compatibility) precise to cloud computing adoption and ITEF3. The values for COMP were $r=.667$, $r^2=.444$, $p<.001$; hence, the findings confirmed a positive correlation with information technology helpfulness to users.

These findings are reliable with previous investigate been done by Lawal [19], Ness [10] and Chebrolu [12] which confirmed a positive correlation between factors of ITF (compatibility, modularity, and connectivity) within cloud technology and ITE. Setting a bar on the r^2 values from Table II as greater than 0.40, the conceptual model diagram is updated see Fig. 2. Similarly, depending on the values from Table II, and with a bar on the r^2 values as greater than 0.40, a minimized conceptual model diagram for Sub-Factors of ITF precise to Cloud Computing Adoption and aspects of ITE as shown in Fig. 3.

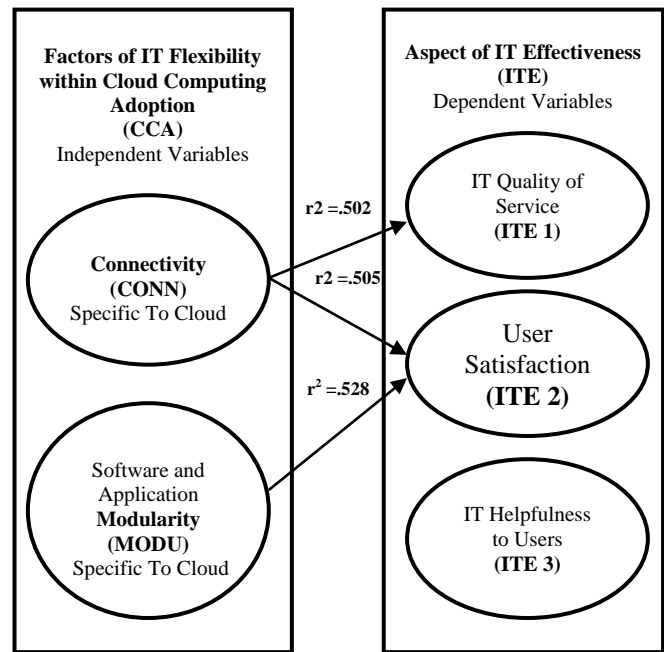


Fig. 2. Updated Conceptual Model for Factors of ITF Specific to the Cloud and Various Aspects of ITE with r^2 Values < 0.40.

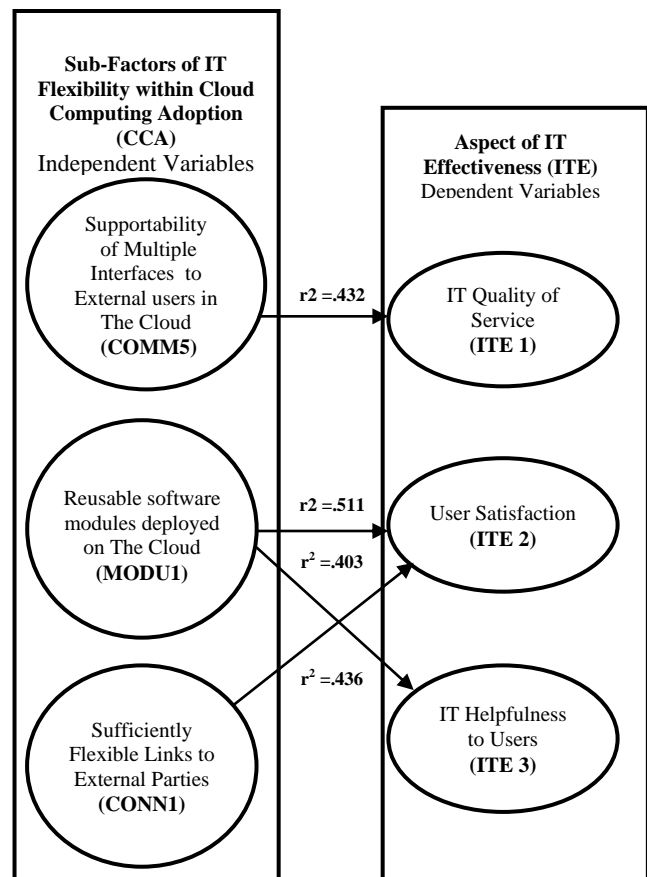


Fig. 3. Minimized Conceptual Model for Factors of ITF Specific to the Cloud and Various Aspects of ITE with r^2 Values < 0.40.

VI. SUMMARY

This paper presented new empirical evidence that correlation between factor of ITF Modularity (MODU) specific to cloud and User Satisfaction (ITEF2) has the highest correlation ($r=.727$, $r^2=.528$, $p<.001$) among five paired constructs at the level of cloud computing capabilities have been utilized in this research, followed by Connectivity (CONN) precise to cloud with User Satisfaction (ITEF2) ($r=.711$, $r^2=.505$, $p<.001$), Connectivity (CONN) precise to cloud with information technology QoS (ITEF1) ($r=.709$, $r^2=.502$, $p<.001$), Modularity (MODU) precise to cloud with information technology QoS (ITEF1) ($r=.695$, $r^2=.483$, $p<.001$) and Modularity (MODU) precise to cloud with IT Helpfulness To Users (ITEF3) ($r=.686$, $r^2=.470$, $p<.001$). Which are the three paired constructs with lower than 0.20 of their r^2 values? Correlation between Compatibility (COMP) precise to cloud with information technology QoS (ITEF1) has correlation ($r=.335$, $r^2=.189$, $p<.001$), Compatibility (COMP) with User Satisfaction (ITEF2) has correlation ($r=.425$, $r^2=.181$, $p<.001$) and Compatibility (COMP) with information technology Helpfulness To Users (ITEF3) has correlation ($r=0.34$, $r^2=.116$, $p<.001$). This paper presented new proof that several Factors of ITF precise Cloud Computing have been utilizing in this paper have a much higher impact on ITF than others have. Some authors have researched the impact of various constructs on ITE among IT companies, either as paired factors to evaluation business model and value through competitive benefit. On the other hand, this paper has been filled in the knowledge gap in the literature review because it concentrates on the impact of fifteen various aspects of cloud technology within IT companies.

VII. IMPLICATIONS

To determine the prioritization and dominance of modularity (MODU) precise to cloud over cloud connectivity (CONN) and compatibility (COMP) precise to cloud on several aspects of ITE (ITEF1, ITEF2, ITEF3), (see Table I). IT managers and IT executives could more effectively decide where, how and which Factors of ITF (Connectivity, Modularity, Compatibility) used of adoption of cloud computing toward assign financial resources for the implementation, maintenance, and deployment of their complex IT frameworks in their companies. The linear regression analysis has been used in this research confirmed that Modularity precise to the cloud is more dominant than connectivity precise to cloud additionally, connectivity more dominant than compatibility precise to cloud on different aspects of ITE. The implication of this investigate finding is that IT managers and IT executives should assign increasingly financial resources toward software and application modularity inside cloud than resources to connectivity and software and systems compatibility precise to cloud to enhancing ITE.

IT executives and managers should assign additional financial resources towards MODU1 (reusable software modules) and MODU2 (legacy systems along with new apps) which are the top two subfactors of ITF specific to the cloud which has a higher positive impact on different aspects of ITE

as listed in Fig. 2. The findings from this research represented only firms in the Hashemite Kingdom of Jordan; the results should be interpreted as representing the IT sector.

Lastly, since the participants were IT manager that is playing a CIO role in different IT companies, the research findings in this paper have contribution on the current knowledge of the relationships between Factors of information technology Flexibility precise Cloud Computing adoption (compatibility, modularity, connectivity), and several aspects of ITE has been used in this paper.

The findings addressed the benefits of used Factors and subfactors of ITF within Cloud Computing on aspects of ITE and would improve the decision making the procedure for IT executive and manager when taking into consideration the cloud computing adoption and its business models.

VIII. RECOMMENDATIONS

The study's recommendations are that IT executives and managers should assign increasingly financial resources toward software and application modularity inside cloud technology than resources to cloud connectivity and software and systems compatibility inside cloud in order to enhance their ITE. This research could be repeated with a quantitative method with the same variables on how a precise type of cloud service model IaaS, PaaS and SaaS or how a precise type of deployment model public, private and hybrid would impact on ITE. Additionally, the author recommends that this study be repeated with a similar quantitative correlative study to analyze the same variables by another type of business with more precise. IT managers could use this new knowledge and awareness when allocate financial resources and their human to enhancing their ITE and deliver services and solutions through the cloud to their business in a dynamic market.

IX. CONCLUSIONS AND FUTURE WORK

This study contributed to the limited literature regarding cloud computing adoption and implementation among IT Organizations in Jordan. The findings from the study provided statistical evidence that the combination of the three factors of ITF (compatibility, modularity, and connectivity), have a positive relationship with ITE.

The inferences of this study for researchers encompass the inclusion of other forms of ITF in future studies that could improve comprehension of the phenomenon, and enhance ITE. Further, the present research analyzed ITF and effectiveness, associated with cloud adoption and implementation from the perspective of IT companies. Within the Jordan, this study could also be extended by taking into consideration the perspective of cloud-based vendors and analyzing the challenges they encounter in deploying their solutions at IT companies. Also, this study was based on any of the cloud computing service models.

Additionally, the results of this research can be used in the educational, health, industrial and governmental sectors to improve performs.

ACKNOWLEDGMENT

We would like to thank Universiti Sultan Zainal Abidin for the financial support to this project under the Mentor-Mentee Grant (Unisza/Mentor mentee/2018/023).

REFERENCES

- [1] Pólkowski, Z. D. Z. I. S. L. A. W., et al. "Improving business processes by Cloud Computing in SMEs" *Zeszyty Naukowe Uczelni Jana Wyżykowskiego. Studia z Nauk Technicznych*(2017).
- [2] Gens, F. (2009). New IDC IT cloud services survey: Top benefits and challenges [Web log message]. Retrieved from <http://blogs.idc.com/ie/?p=730>
- [3] Ramzan, Muhammad, et al. "An Analysis of Issues for Adoption of Cloud Computing in Telecom Industries" *Engineering, Technology & Applied Science Research* 8.4 (2018): 3157-3161.
- [4] Suess, J., & Morooney, K. (2009). Identity management & trust services: Foundations for cloud computing. *EDUCAUSE Review*, 44(5), 24. Retrieved December 20, 2009, from ABI/INFORM Global. (Document ID: 1865415041).
- [5] Perez, J., Germain-Renaud, C., Kegl, B., & Loomis, C. (2009). Responsive, elastic computing. Paper presented at the GMAC '09: Proceedings of the 6th International Conference Industry Session on Grids Meets Autonomic Computing, Barcelona, Article (CrossRef Link).
- [6] Vouk, M.A. (2008). Cloud computing—Issues, Research, and Implementations. Paper presented at the ITI 2008: Proceedings of the 30th International Conference on Information Technology Interfaces, Cavtat, Croatia. 31-4. Article (CrossRef Link).
- [7] Skala, Karolj, et al. "Scalable distributed computing hierarchy: Cloud, fog and dew computing." *Open Journal of Cloud Computing (OJCC)* 2.1 (2015): 16-24.
- [8] Nikolov, Peter, Bert Armijo, and Vladimir Miloushev. "Globally distributed utility computing cloud." U.S. Patent No. 9,578,088. 21 Feb. 2017.
- [9] Duncan, N. B. (1995). Capturing flexibility of information technology infrastructure: a study of resource characteristics and their measure. *Journal of Management Information Systems*, 12(2), 37-57 Article (CrossRef Link).
- [10] Ness, L. R. (2005). Assessing the relationship among information technology flexibility, strategic alignment, and information technology effectiveness (Doctoral dissertation). Retrieved from ProQuest Dissertations and Theses database. (UMI No. 3178531)
- [11] Byrd, T. A. & Turner, D. E. (2000). "Measuring the Flexibility of Information Technology Infrastructure: Exploratory Analysis of a Construct," *Journal of Management Information Systems*, 17(1), 167-208. Article (CrossRef Link).
- [12] Chebrolu, S. B. (2010). Assessing the relationships among cloud adoption, strategic alignment, and information technology effectiveness. From ProQuest Dissertations & Theses database. (No. AAT 3426510).
- [13] Tallon, P.P., Kraemer K.L. (2003a). Investigating the relationship between strategic alignment and IT business value: The discovery of a paradox. University of California, Irvine. Retrieved March 12, 2004, [Online] Available: <http://www.crito.uci.edu/publications/pdf/AlignmentParadox.pdf>
- [14] Tallon, P. P., Kraemer, K. L., & Gurbaxani, V. (2000). Executives' perceptions of the business value of information technology: A process-oriented approach. *Journal of Management Information Systems*, 16(4), 145–173. Retrieved from http://www.jmis-web.org/issues/Spring_2000/index.html Article (CrossRef Link).
- [15] Fink, Lior, and Seev Neumann. "Exploring the perceived business value of the flexibility enabled by an information technology infrastructure." *Information & Management* 46.2 (2009): 90-99. Article (CrossRef Link).
- [16] Sultan, Nabil. "Cloud computing for education: A new dawn?" *International Journal of Information Management* 30.2 (2010): 109-116. Article (CrossRef Link).
- [17] Garrison, Gary, Robin L. Wakefield, and Sanghyun Kim. "The effects of IT capabilities and delivery model on cloud computing success and firm performance for cloud supported processes and operations" *International Journal of Information Management* 35.4 (2015): 377-393. Article (CrossRef Link).
- [18] Saleem I, Qureshi T.M., Mustafa S, Anwar F. and Hijazi T. (2011). Role of Information and Communicational Technologies in perceived Organizational Performance: An Empirical Evidence from Higher Education Sector of Pakistan. *Business Review*. 6(1): 81-93.
- [19] Lawal, HildaLyn. *Information Technology Flexibility and Effectiveness, Specific to Cloud Computing Adoption within Small and Medium Enterprises*. Northcentral University, 2014.
- [20] Norusis, M. (2008b). *SPSS Statistics 17.0 Statistical Procedures Companion*. Upper Saddle- River, N.J.: Prentice Hall.
- [21] Pekkarinen, S., & Ulkuniemi, P. (2008). Modularity in developing business services by platform approach. *The International Journal of Logistics Management*, 19(1), 84-103.
- [22] Saleem, D. I. (2011). Role of Information and Communicational Technologies in perceived Organizational Performance: An Empirical Evidence from Higher Education Sector of Pakistan. *Business Review*, 6(1), 81-93.
- [23] Serrano, N., Gallardo, G., & Hernantes, J. (2015). Infrastructure as a service and cloud technologies. *IEEE Software*, 32(2), 30-36.
- [24] Dahiya, D., & Mathew, S. K. (2016). IT assets, IT infrastructure performance and IT capability: a framework for e-government. *Transforming Government: People, Process and Policy*, 10(3), 411-433.
- [25] Benitez, J., Ray, G., & Henseler, J. (2018). Impact of information technology infrastructure flexibility on mergers and acquisitions. *MIS Quarterly*, 42(1), 25-43.
- [26] Hentschel, R., Leyh, C., & Baumhauer, T. (2019, January). Critical Success Factors for the Implementation and Adoption of Cloud Services in SMEs. In *Proceedings of the 52nd Hawaii International Conference on System Sciences*.
- [27] Isal, Y. K., Pikarti, G. P., Hidayanto, A. N., & Putra, E. Y. (2016). Analysis of IT infrastructure flexibility impacts on IT-Business strategic alignment. *Journal of Industrial Engineering and Management (JIEM)*, 9(3), 657-683.
- [28] Baysari, M. T., Lehnbohm, E. C., Li, L., Hargreaves, A., Day, R. O., & Westbrook, J. I. (2016). The effectiveness of information technology to improve antimicrobial prescribing in hospitals: a systematic review and meta-analysis. *International journal of medical informatics*, 92, 15-34
- [29] [1] Mjlae, S. A., Zarina, M., & Suryani, W. (2019). Impact Aspects of IT Flexibility Specific To Cloud Computing Adoption on IT Effectiveness. *Journal of Theoretical and Applied Information Technology*, 97(2), 1041–1059. Retrieved from <http://www.jatit.org/volumes/Vol97No3/28Vol97No3.pdf>

Assistive Technologies for Bipolar Disorder: A Survey

Yumna Anwar¹, Dr. Arshia Khan²

Department of Computer Science, University of Minnesota Duluth
Duluth, MN

Abstract—Bipolar disorder is a severe mental illness characterized by periodic manic and depressive episodes. The current mode of assessment of the patient’s bipolar state is using subjective clinical diagnosis influenced by the patients self-reporting. There are many intervention technologies available to help manage the illness and many researches have worked up on objective diagnosis and state prediction. Most of the recent work is focused on sensor-based objective prediction to minimize the delay between a relapse and the patient’s visit to the clinic for diagnosis and treatment. Due to the severity of the societal and economic burden caused by bipolar disorder, these researches have been given great emphasis. In this paper, we will start with a discussion of global severity of the disorder and economic and family burden inflicted due to it; we then talk about the existing mechanisms in place to identify the current state of the bipolar patient, then we go on to discussing the behavioral intervention technologies available and researched upon to help patients manage the disorder. Next, we mention the shift in focus of the current research, i.e. towards sensor based predictive systems for patients and clinical professionals, highlighting some of the preliminary researches and clinical studies and their outcomes.

Keywords—Bipolar disorder; mobile applications; electrodermal activity; heart rate variability; behavioral intervention technologies; depression; mania

I. INTRODUCTION

Patients suffering from bipolar disorder experience continuous swings in their mood and emotional state. There are 4 known bipolar states:

- 1) Euthymic
- 2) Manic
- 3) Depressive
- 4) Mixed

According to the DSM IV criteria [1], in a manic episode the patient has a “persistently elevated” mood; a state of very high self-esteem and grandiosity. They feel very energetic and feel rested after only a small amount of sleep. Their judgment is impaired, become reckless and they tend to be impulsive [2]. On the other hand, hopelessness, anxiety, anger, irritability, sadness, suicidal thoughts, minimized physical activity and social interaction are some of the common symptoms associated with depressive episodes [3]. In a mixed state, depression and mania exist simultaneously and the symptoms of both are observed. Recognizing a mixed state is difficult and sometimes is an intermediary state of an extreme manic and a depressive state [4]. Euthymic state, on the other hand, is the balanced state in which the patients experience the most stability in their mood

[5]. Euthymic state is characterized by a normal good quality and quantity of sleep and well balanced social and work life.

This survey paper starts with an overview of severity of bipolar disorder across the globe and its economic impact. It then discusses the applications and technology currently under use to assist bipolar disorder, the ongoing research for further advancement to reduce the gap and the evolution of these technologies over the past decade.

The rest of the paper is arranged as:

Section II mentions some worldwide statistics of the prevalence of the bipolar disorder, the mortality rates and socio-economic burden caused by it.

Section III discusses the current way of assessment of the bipolar patients and some commonly used rating scales.

Section IV introduces the concept of behavioral intervention technologies for bipolar patients and briefly discusses few of the related applications.

Section V moves on to a new focus of researches currently and sensor-based state prediction using biomarkers of bipolar disorder. Furthermore, it discusses four main areas within it; social and physical Activity, HRV, EDA and sleep. The subsections of each area discuss few of the research papers related to it.

Section VI talks about two projects largely contributing to this cause.

TABLE I. DEFINITION OF ABBREVIATIONS USED IN THIS SURVEY

Abbreviation	Definition
BD	Bipolar Disorder
HAMD	Hamilton Depression rating scale
HRV	Heart Rate Variability
EDA	Electrodermal Activity
SC	Skin Conductance
SMNA	Sudomotor nerve activity
IAPS	International Affective Picture System
QIDS	Quick Inventory of Depressive Symptomatology
YMRS	Young Mania Rating Scale
REM	rapid eye movement
NREM	Non-rapid eye movement
MONARCA	MONitoring, treAtment and pRediCtion of bipolar Disorder (Project)
PSYCHE	Personalized monitoring Systems for Care in mental Health (project)

Section VII examines the evolution of technologies to aid bipolar disorder and the change in focus of the researchers over the decade.

Section VIII is the discussion section with a brief summary.

Section IX highlights some of the future work and the challenges that prevent the implementation of sensor-based technologies.

II. SEVERITY ACROSS THE GLOBE

Bipolar disorder is one of the world's 10 most incapacitating disorders [6] and affects 5.7 million adults in the United States alone. According to a systematic review, the prevalence of bipolar disorder in UK, Germany and Italy is approximately around 1% [7]. World mental health survey initiative in 2011 reported from an aggregation from 11 countries, a lifetime prevalence of 0.6% and 0.4% for Bipolar type I and type II respectively [8]. On top of this worrying prevalence across the globe, the disability caused by it is also significant. On average the onset of Bipolar disorder is at age 20 years [8] [9] which results in more years of disability than any other major illness including cancer [8]. This not only inflicts a considerable economic but a social burden as well; with 93% of the caregivers of bipolar patients having reported to suffer from anxiety [10]. Patients with bipolar disorder tend to experience mild to severe restlessness and irritation. Caregivers are reported to have a great role in recognizing, intervening, and supervising in taking medication during these episodes [11].

A. Mortality Rate

Bipolar patients are at a high risk of suicide, 20 to 25% of individuals suffering with BD make suicidal attempts [12] [13]. They are also more likely to attempt suicide than any other depressed individual [3]. Alongside this, many studies have also indicated a simultaneous presence of another chronic diseases in patients suffering from bipolar disorder [7], which in turn increases the risk of mortality. Moreover, Comorbid conditions were observed worldwide in BP patients [8]. According to a 2007 report in UK, the death rate of bipolar patients was 18%, with an attempted suicide rate between 21%-54% [14].

B. Economic Burden

Bipolar patients require continuous treatments, both inpatient and outpatient, inflicting an annual cost of more than \$45 billion on the US economy in 1991 as estimated by one of the studies [15]. In 2009, another study [16] was conducted to include both the direct and indirect economic burden by bipolar disorder. Cost of treatment and utilization of health services is accounted as a direct cost while lost work time cost etc. is categorized as an indirect cost. The study realized the direct cost as over \$30 billion and the indirect cost as over \$120 billion, estimating the total minimum cost as approximately \$150 billion [16]. These large numbers have raised a serious concern, prompting the prioritization of researches on an alternate effective healthcare solution.

C. Caregivers Burden

Caregivers are the people who help the patients manage the illness by recognizing, intervening, and supervising in taking medication during their episodes. They are in most cases the partner, spouse or parent of the patient. In a survey conducted in

2016, amongst caregivers of bipolar disorder, it was reported that 49% of the caregivers had to make changes in their employment status because of the patients [11]. The level of distress was noted to be higher in females [17], with 72% of the total caregivers being females [11].

III. CURRENT SYSTEM IN PLACE

Patients' diagnosis of the bipolar disorder is made using diagnostic and statistical manual of mental disorders by American psychiatric association. On the other hand, the treatment of bipolar patients involves Pharmacotherapy and Psychotherapy. For the right medication and therapy, the current bipolar state of the patient has to be correctly identified. The current assessment system for bipolar patients includes a verbal interview with the psychiatrist who asks the patients to fill out questionnaires and then come up with a diagnosis of the current state accordingly.

The psychiatric interviews involve a verbal one-on-one between the patient and psychiatrist during which the psychiatrist asks questions and comes up with a diagnosis. During a psychiatric interview, a psychiatrist might also use a rating scale, the score of which would help them with the diagnosis. There are numerous rating scales for depression and mania that can be used by psychiatrist to evaluate the state of bipolar patient. One such scale is Hamilton Depression Rating Scale (HAMD), which was developed in 1957 and is highly preferred by psychiatrists [18]. 30-item Inventory of Depressive Symptomatology (IDS), and the 16-item Quick Inventory of Depressive Symptomatology Clinician rating (QIDS-C16) has also proven to have high psychometric usability [19], have the ability to assess wide range of depressive symptoms [20] and are commonly used, especially in clinical trials and researches. Young Mania Rating Scale (YMRS) is a commonly used scale in clinical settings to measure the severity of mania [20]. There are also other scales like the Suicide Probability Scale (SPS), but their capability to identify any future suicide attempts by the patients is unclear [20].

Apart from the psychiatrists rating scales, there are also self-reporting scales, one of which is QIDS-SR16, a quick inventory of depressive symptomatology version for self-reporting [19] [20]. There are also multiple mobile applications for self-management and logging that give feedback based on the daily mood assessment that the patient provides through the App. Some of these systems are discussed in a later section (IV).

IV. BEHAVIORAL INTERVENTION TECHNOLOGIES

There are many behavioral intervention technologies for both educational and intervention purposes for mental health. These behavioral intervention technologies include providing internet-based psychotherapies, web based and mobile based intervention and psychoeducation [21]. Studies have shown a clear long-term advantage of psychoeducation in terms of cost and better management of the disorder [22]. Psychoeducation for bipolar disorder includes giving patients in depth knowledge of the disorder, teaching them how to recognize the symptoms of each bipolar state and manage them accordingly. Internet has been identified as an essential source of information for caregivers and patients suffering from mental illnesses [23].

Hence the feasibility of such a system can be established for use in mental health care.

Web based intervention and psychoeducation technologies have a capacity to effectively aid bipolar and other mental disorders and improve their quality of life [21] [24] [25] [26]. MoodHwb [25] and Beating Bipolar [27] are some of the example technology. 'Beating bipolar' [27] is one of the web-based interventions for bipolar disorder. It contains educational and intervention content through an online program. Providing psychoeducation has encouraging results for long term management of bipolar disorder [27]. Although these web-based approaches have given promising results, additional research is still needed to establish the aggregate impact of this technology [27].

The prevalence of mobile phones and their constant connectivity with people nowadays has shifted the focus largely towards mobile technologies [21]. Live communication with therapist, reminders, logging self-reporting data are some of the other features on which work has been done previously [21]. eMoods Bipolar Mood Tracker app [28], Intellicare [29], PRISM [30], MMD [31], and MONARCA system [32] are some of the similar mobile based applications for aiding mental illnesses, especially mood disorder. Many studies have suggested that intervention with mobile based technologies can improve medication adherence in patients with serious mood disorder [33].

Personalized Real-Time Intervention for Stabilizing Mood (PRISM) [30] is one example of a mobile intervention system for bipolar disorder. Patients record their mood by responding to a set of questions. Then depending on the symptoms that are indicated by the patient, the app returns a self-management plan. Although interview with a clinician is independent, it helps in self-management of the diseases via psychoeducational intervention. There is clear evidence of the feasibility of using mobile devices, although more research is yet to be done on how effective they are [30].

Another example of such a mobile intervention is Mobile Mood Diary (MMD) [31]. It is inspired by the concept of a paper diary for bipolar patients for record keeping. With a less complex design to ensure adherence, the MMD System was developed as a javaME application which is easily downloadable on mobile phones. On a daily basis, the patients would enter mood, energy and sleep record through a series of step by step entry fields, which are then uploaded on the server. Summary with visualization would also be available for the patients to view. Both the perspectives of end user and the therapists were used to evaluate the usability of the system. A usability study and user trial were carried out to identify issues with the interface and working of the system for improvement. A 2-yearlong clinical evaluation was done using 9 bipolar patients in Ireland and the results of the total usage and adherence (65%) of the system by the patients over these 2 years was quite high, providing us strong evidence that such a mobile system is very engaging and suitable. Additionally, patients who are introvert and reticent about sharing their feelings, felt very comfortable reporting to a device. The 4 main benefits and reasons of using such a system are preference by youth, ease of use, privacy and timeliness [31].

A more advanced and a step ahead of just self-reporting applications is The MONARCA system [32]. Apart from using mobile phone application to record only self-reported mood data, MONARCA system also introduced activity monitoring through sensors in their system to set out early monitoring signs, along with visualization and coaching. The self-assessment consists of sections for Mood measurement, sleep quantity, Activity level and medicine adherence. Activity monitoring is done using phone sensors, such as accelerometer for physical activity and number of phone calls for social activity. Patients can get feedback from the applications through its graph visualization. The trigger feature of the application works using association rule mining. A 14-week feasibility trial was done to analyze the usability, suitability, usefulness and future compatibility of the system. The results of the trial showed that the average adherence to the system by the patients was over 80%. This result plus the usefulness survey conducted in this study holds promises for using such systems to assist and manage bipolar disorder [32].

V. ONGOING RESEARCHES TO INFER BIPOLAR STATE

Several researches have substantiated the possibility and applicability of systems to use certain biomarkers to identify the bipolar state in order to fill the gap caused by subjective data and delayed diagnosis. Some of the literatures on social interaction and physical motion like Heart rate variability, Electrodermal activity and sleep pattern for objective identification of bipolar states are discussed in the four subsections below.

A. Social Interaction and Physical Motion

Symptoms of Bipolar disorder are mainly indicated through the change in a patient's behavior [34]. The key point that a psychiatrist uses to assess a patient's state is their behavior which includes their physical activity and their social interaction; but all of that is based on the patient self-reporting, which is highly subjective. This is where the use of mobile devices and sensors can be very advantageous [34].

In one such study [35], the researchers devised a smartphone-based system to recognize the state and the subsequent change of states in a bipolar patient. Visiting a doctor late not only has financial consequences but also has a deleterious impact on the health of the patient. Keeping that in mind, this study introduces a system that collects social interaction, physical motion and travel pattern data of the patients from sensors to drive a forecast system to predict the state of the patient. The study involved patients of age 18 to 65+ who were diagnosed with ICD10 classification. They applied linear discriminant analysis to identify the three states (classes) namely, depressive, normal and manic. Moreover, after collecting phone call data, sound, acceleration data and location data, the datasets were split into training and test data. Using Weka, they performed Bayes Classification model separately on data from each sensor. The forecasting process involves calculating the distances from the initial state to the newly predicted state by each classifier, weighting each distance based on the number of available training points and finally calculating the centroid. The centroid delineates the predicted state of the patient. With the fusion of all the modalities, phone, sound, acceleration and location, the study resulted in an

average accuracy of 76 percent in state recognition [35]. The results though not being very high, still highlight a fine pattern between the attributes and the state change.

Acoustic voice analysis has also been something that has been greatly researched on for detecting mental disorder [58]. Some studies are also focused on analyzing voice to measure depression and mania in bipolar patients [36] [58]. In a 12 Week MONARCA study, text message, phone call and mobility data were collected from the smartphones of 28 participants. Voice features were obtained from the phone call data and Hamilton Depression Rating Scale (HAMD) and Young Mania Rating Scale (YMRS) were used to assess the patient's state. The average accuracy of classifying bipolar state using the voice feature was between 61%-74%, further indicating promising results for real-time objective data collection to aid bipolar patients [36]. In acoustic voice analysis, the actual content, the words or the language is unidentifiable and not important. Hence, there are less privacy and ethical issues with using this feature.

B. Electrodermal Activity

Electrodermal Activity (EDA) readings can be used to trace the emotional and cognitive state change and fluctuation. EDA has been shown to change along with the pathological mood states [37], hence proven to be a biomarker that can be used to track and predict Bipolar states.

In a Book published in 2016, "Advances in Electrodermal Activity Processing with Applications for Mental Health" [37], chapter 5 outlines experiments carried out on bipolar patients to specify how EDA changes with each mood state in order to prove EDA as a reliable biomarker to recognize bipolar state. 10 bipolar patients were recruited for an emotional elicitation protocol which involved a slideshow of emotionally negative evocative pictures from IAPS and some pictures from TAT [37]. International Affective Picture System (IAPS) is a database of pictures, developed by the Center for the Study of Emotion and Attention (CSEA) at the University of Florida, to evoke different emotions [38]. Thematic Apperception Test (TAT) is a set of ambiguous pictures and the participants are asked to tell a story about each picture and their response indicates certain psychometric characteristics because it evokes the subconscious of the participants [38].

Before each round of the experiment, a psychiatrist interviews the patient and assigns him/her a mood label. During the experiment, the patient's EDA signals were collected using BIOPAC MP150. After decomposition of EDA signal into phasic and tonic components, different features such as mean, maximum and standard deviation of phasic and tonic were extracted for analysis. EDA data collected from each round has a mood label associated with it for supervised learning. Afterwards, a K-Nearest Neighbor (k-NN) classification model was developed based on the data to identify different states. The results of the classification had an accuracy of over 80%. Further statistical analysis on the data gave evidence of how sympathetic activity decreases in a depressed patient represented by low EDA, and how phasic attributes are affected by mood change. A group of healthy participants were also examined as a control, confirming that analysis of

Electrodermal activity is feasible for identifying pathological mood in bipolar patients or other mental illnesses [37].

The Electrodermal activity signals that are received from the sensor have to go through a deconvolution process before features can be extracted for classification and prediction. Another preliminary study [39] as part of the PSYCHE project shows the correlation between Electrodermal activity and bipolar states, and also discusses the deconvolution analysis process.

Electrodermal activity signal has two components, tonic and phasic. Tonic is the skin conductance level and is the slow component while phasic is the skin conductance response and is the fast component [39]. Due to short intervals of the phasic component, there is overlapping of consecutive phasic. So in order to ensure proper decomposition of EDA signal into their respective components, a deconvolution process has been proposed [40]. Since the introduction of this process by Benedek, this process has been applied by many researches that involved EDA analysis. In this technique, Skin conductance (SC) is established as the convolved signal of sudomotor nerve activity (SMNA) and the impulse response (refer to equation 1 below).

$$SC = SMNA * IRF \tag{1}$$

The bi-exponential Impulse Response Function (IRF) is shown in equation 2 below:

$$IRF(t) = \left(e^{-\frac{t}{\tau_1}} - e^{-\frac{t}{\tau_2}} \right) \cdot u(t) \tag{2}$$

Sudomotor nerve activity (SMNA) is basically the driver tonic plus driver phasic. Therefore, deconvolution of the EDA signal with the bi-exponential Impulse Response Function (IRF) is done to get sudo motor nerve activity (SMNA) signal, and decomposition of which gives us the tonic and phasic as a separate entity (refer to Fig. 1).

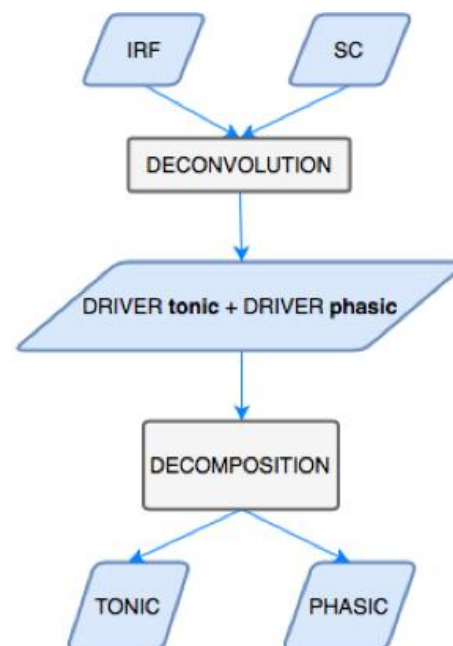


Fig. 1. Decomposition of Electrodermal Activity Signal.

It has been established that EDA collected from palms and feet is more reliable than any other part of the body [41] [42]. Taking this fact into account, the MONARCA project also introduced a smart sock that depicts an actual sock both in appearance and in comfort, and has electrodes embedded in it to measure Electrodermal activity. The project used the smart sock in a feasibility study involving healthy participants [42]. Further research on this textile involving Bipolar patients is underway.

C. Heart Rate Variability

Another physiological biomarker for identifying mood state and predicting mood change is heart rate variability. The mood changes in patients suffering from bipolar disorder are associated with dysregulation of the autonomic nervous system and analysis of the heart rate variability can give us a better understanding of it [43] [44]. Heart rate variability is a measure of the regularity of the heart rate and has been manifested to be a promising and suitable indicator to gauge the response of the autonomic nervous system.

A 14-week long research study [5] was carried out in the University hospital of Strasbourg and Geneva on 14 bipolar patients. Through the PSYCHE platform, using a sensorized t-shirt with ECG electrodes embedded in it, the researchers collected HRV data from the patients. Each patient was given different psychotropic medications which included mood stabilizers, antipsychotics, benzodiazepine-like and antidepressants. Psychiatrist interviews were done, and each patient's mood state was identified before each acquisition.

After the preprocessing of the ECG data, time domain, frequency domain, and non-linear features were extracted. Non-linear HRV features that were evaluated included sample entropy, approximate entropy, Poincare, and Detrended Fluctuation Analysis (DFA). After feature extraction, a $N \times M$ matrix of the features against the number of acquisitions were obtained. In order to reduce the dimensionality of the data, principal component analysis was applied. Because mood change in bipolar patients is dependent on the current mood (markov chain) [45], the current mood of the patient was also included as one of the features. The learning algorithm used was support vector machine (SVM) and it was trained and tested on the data of each participant individually, achieving an average prediction accuracy of 69%. It was also observed that non-linear features, Poincare SD1 and SD2, showed a more notable change with mood. Although the prediction accuracy of the system is not very high, it affirms the use of Heart rate variability as a biomarker for mood changes in patients suffering from bipolar disorder or other mood disorders.

Most of the researches are focused to a greater extent on identifying bipolar depression; however one study [46] specifically analyzes the HRV time, frequency and non-linear features in manic bipolar patients. 23 manic bipolar patients were examined, and their manic symptoms were evaluated using Young Mania Rating Scale (YMRS). The results of the study concluded an inverse relationship between HRV and the score from YMRS; meaning the more severe the mania, the lower the HRV. Nonlinear HRV features include complexity measure of the heart rate such as entropy and Correlation Dimension which was also shown to decrease in manic patients in the study [46].

D. Sleep Pattern

Along with heart rate variability, it has also been made evident that analysis of sleep cycle can help identify depressive state in bipolar patients [47]. In one of the European research studies [47], a sensor-based T-shirt was used to measure Electrocardiography signals (ECG) and body motion from 15 bipolar patients during night time. The study only focuses on predicting depressive state of the bipolar patient. Before every data acquisition the psychiatrist would assess the actual current state of the patient.

Using the collected data, the heart rate variability (HRV) and sleep stages were estimated for analyzing and predicting depressive episodes in Bipolar patients. The standard Time, frequency and non-linear features of HRV are all considered for analysis. As for sleep, the researchers used an already trained supervised Artificial Neural Network model for predicting the sleep stage (Wake, NREM, REM) when HRV and body activity data were provided to it. The following sleep related features were extracted for analysis in this study:

- 1) time spent in bed
- 2) sleep latency
- 3) total time spent in bed but not asleep
- 4) total sleeping time
- 5) sleep efficiency. sleeping time/ total time in bed.

It was observed that total sleep time and sleep efficiency differ appreciably in depressive and non-depressive state of the patients. In summary, the results of the study showed that a depressed state in a bipolar patient is characterized by a decreased HRV and increased sleep time and sleep efficiency [47]. The paper also asserts the possibility of using a home-based monitoring system for patients suffering from psychiatric disorders [47].

Disturbed sleep is a very common symptom of depression as proven by many studies [48] and hence it is a viable biomarker. While many studies have reported insomnia (loss of sleep) as being a symptom of mania [49] and hypersomnia as a symptom of a depressive state [48], one study has also highlighted that hypersomnia is an indication of relapse to mania in bipolar patients [50]. While the work on predictive systems using sleep cycle analysis has shown some hopeful results, research in this area still has a long way to go.

VI. TWO MAJOR EUROPEAN PROJECTS

A. MONARCA Project

MONARCA stands for MONitoring, treAtment and pRediCtion of bipolar Disorder. It is a big European project which is collaborating with University of Copenhagen on researches and trials towards cellphone based monitoring and predictive system for bipolar disorder using multiple parameters. A MONARCA system constitutes of a study as part of the project that developed a cell phone based self-reporting and monitoring application for bipolar patients to detect early warning signs and to give feedback [32], as discussed in section IV previously. The study conducted a trial to establish the usefulness of mobile phone-based system and the adherence of the patients towards such a system. Furthermore, it also monitored physical activity using accelerometer sensor in

mobile phone and social interactions by keeping track of the phone calls and messages. The project later also introduced some wearable sensors for motion and stress [41].

Literature [41] mentions a MONARCA wearable system constituting of a mobile phone device, a motion sensor to be worn on the wrist, and Electrodermal activity sensors embedded in a sock. Both the sensors were connected via Bluetooth to the mobile device to transfer data using social, physical and stress as three parameters. The system is set up to give early warning signs by comparing each parameter with the established baseline reading [41]. One aspect of this project involves using Electrodermal activity as discussed in section V.

B. PSYCHE System

PSYCHE [51] stands for “Personalized monitoring Systems for Care in mental Health”. It is a huge European project that aims towards portable sensor-based monitoring systems for bipolar patients using more than one parameter which is a shift of focus from current researches. The project model aims towards a portable, cost-effective, multi-parametric, and closed looped system with constant monitoring, feedback and alerts to the caregivers in case of emergency.

The project focuses on analyzing the following parameters from bipolar disorder patients:

- 1) heart rate variability
- 2) respiratory rate
- 3) activity and movement
- 4) voice analysis
- 5) social interaction
- 6) galvanic skin response
- 7) sleep cycle and pattern
- 8) Electrodermal activity
- 9) circadian rhythms

The primary focus is to confirm the hypothesis of the correlation between physiological changes and bipolar state, to identify the relevant parameters, use data mining to recognize pattern and develop algorithms and supporting tools for early identification. For data acquisition, the studies involved working with bipolar patients to collect data and evaluate their actual mood, which is done clinically using interviews and YMRS (Young mania rating scale) and QIDS-C16 (quick inventory of depressive symptomatology clinician rating) rating scales for assessing mood.

The development phase includes design and development of a comfortable and appealing garment with sensors imbedded in it, and a user interface for clinical professionals and patients [51]. Designing a user interface for bipolar patients is a challenging work that requires consideration of the patient’s interaction in both depressive and manic state. The PSYCHE study has been able to establish the relation between the autonomic nervous system parameters and the bipolar disorder, and the patient’s compliance to such a system.

VII. EVOLUTION

Management of the disorder by the bipolar patient mainly involves keeping record and self-recognizing symptoms to know exactly when they should get clinical help. There have

been many researches and developments on web based and mobile based intervention technologies to help the patients better manage the disorder. Their effectiveness depends on the patient’s choice and determination of the usage of the system. Initially these researches focused on providing training and education to the patients, self-assessment scales, and some had online psychotherapy features as well. With the prevalence of mobile phones, record keeping, and tracking applications were introduced. The inbuilt mobile sensors, such as accelerometer, were then also utilized by researchers to collect physical activity data to provide feedback.

Current system to manage, assess and correctly diagnose the bipolar state of the patient entirely depended upon self-reported data and verbal interviews by the psychiatrists. These systems’ reliance on subjective data and dependence upon if and when the patient would actually visit the clinician, is a prevalent research focus in sensor based objective data acquisition. The therapeutic effect of medications and therapies is most effective when given at early stages of depression or manic episodes [35]. Hence, majority of the researches in this 21st century is focused on prediction of the bipolar state using non-invasive sensor based objective data collection. Refer to Fig. 2 for the overview of the evolution based upon the literature discussed in this paper.

Researches on sensor based objective inference are underway but the accuracy isn’t high enough so that it can be deployed to clinics. Current assessment of the bipolar state of the patient for appropriate treatment still lacks objectivity. Apart from using sensors in clinical settings, technology is headed towards using wearable sensors along with smartphones for constant connectivity and a more patient centered system.

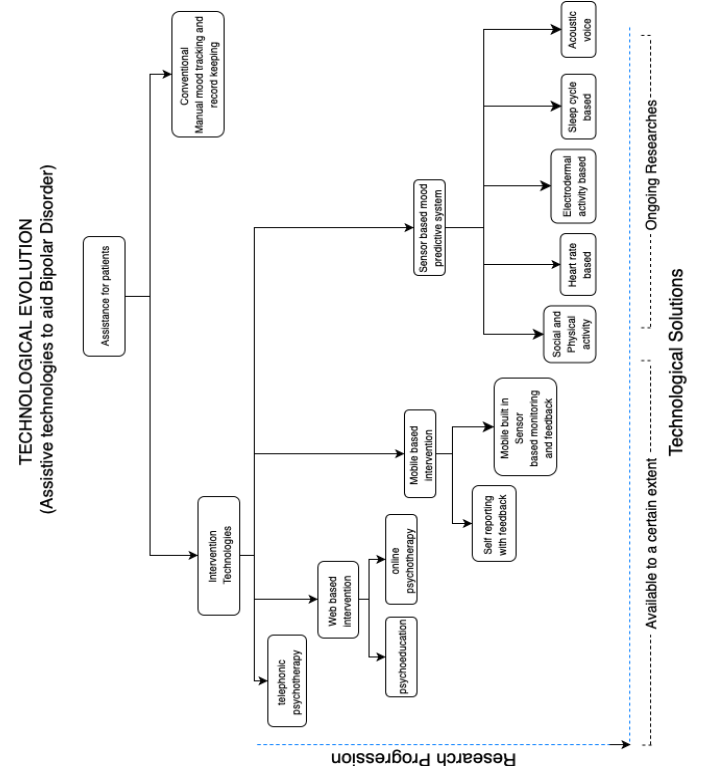


Fig. 2. Evolution of Technologies for Bipolar Patients.

TABLE II. SUMMARY OF THE LITERATURES DISCUSSED IN THIS PAPER

Study	Publishing year	Technology	Objective	Parameters	Findings
[27]	2011	Web-based	Intervention and education		Psychoeducation is good for long term management
[30]	2010	Mobile Application	Intervention, Self-management and education	Self-reported mood	feasibility of using mobile devices
[31]	2011	Mobile Application	Record keeping, summary and visualization	Self-reported mood, energy and sleep	Adherence of 65%. engaging and suitable especially for introverts.
[32]	2013	Mobile Application	Early warning sign, Feedback and visualization	Self-reporting, accelerometer, number of phone calls	Average Adherence of 80% by bipolar patients.
[35]	2015	Smartphone based system	Bipolar State prediction	phone call data sound acceleration location data	average accuracy of 76 percent in state recognition
[37]	2016	Sensor based (BIOPAC MP150.)	Identify bipolar state	phasic and tonic components of the EDA signal	classification had an accuracy of over 80%.
[42]	2011	Smart Textile	Feasibility study	EDA	Feasible. Yet to be tested on bipolar patients
[5]	2016	sensorized t-shirt with ECG electrodes	Bipolar state prediction	Nonlinear HRV features	average prediction accuracy of 69%
[46]	2010	Sensor Based (LifeShirt)	Correlation between HRV and bipolar Manic state	HRV time, frequency and non-linear features	HRV was shown to decrease in manic patients in the study
[47]	2015	sensor-based T-shirt	predicting depressive state of the bipolar patient	Sleep Features HRV features	depressed state in a bipolar patient is characterized by a decreased HRV, and increased sleep time and sleep efficiency
[41] [58]	2011-2015	mobile phone device, a motion sensor, HRV sensor, and Electrodermal activity sensors	early warning signs	social, physical and EDA data (for stress)	Feasibility assed and under develop
[36]	2016	Smart phones	Identify bipolar state	Voice features	average accuracy of 61-74 percent in state recognition

VIII. DISCUSSION

As discussed in the paper, up until now the diagnosis is entirely based on the feedback of the patient and the psychiatrist's understanding of it, both of which are subjective [55] [56]. Apart from the verbal, interview psychiatrist also makes use of the rating scales to gauge the bipolar state of the patients. These rating scales have also evolved overtime with the introduction of new and improved scales. However, according to a national survey in United Kingdom in 2002 [52], a study in 2006 [53] and another one in Korea in 2010 [18], it appears that more than half of the psychiatrists do not prefer using any scale of measure to assess the patients and their diagnosis is entirely based upon their understanding of what the patient reports (Fig. 3).

Moreover, for self-management, patients who adapt to new technologies have mobile and web intervention applications to benefit from. Self-management in general consists of: getting the right education for the illness, avoiding stress, finding relaxing activities, support groups, right sleep and diet, and tracking mood and symptoms [3]. If patients are able to identify

the early warning signs, it can lead to less frequent relapses. However, recognition of early warning signs by the patients has been scarcely reported [57]. Therefore, some of these applications aim at educating the patients to identify the early warning signs of relapses themselves. Adherence to such mobile applications by the patients has been established by many studies as discussed in Section IV.

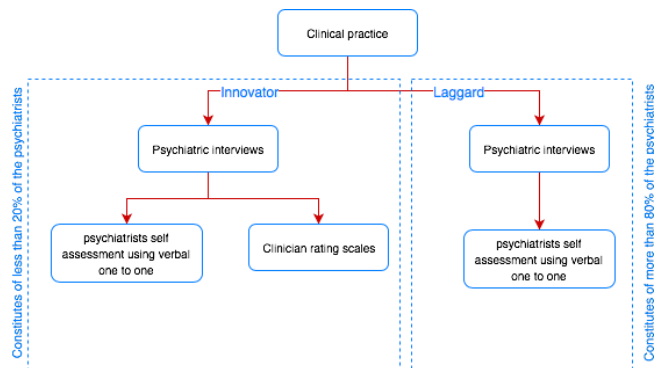


Fig. 3. Innovators and Laggards in Clinical Practice.

With the advancement of technologies, focus of researchers has been largely shifted towards objective monitoring and prediction of the bipolar state. Fig. 3 shows the evolution of these technologies that aid bipolar disorder and help patients self-manage the disorder. HRV, EDA, sleep, activity and acoustic voice are some of the biomarkers on which researches have been done and has shown promising results. Using a combination of these biomarkers to diversify and aim for a better accuracy for prediction is also an approach taken by some researchers [36] [59]. Along with the advancement of sensor-based predictive models as discussed in this paper, there has also been a progression towards smart textile. Smart textile is a technology in which the sensors are embedded into the garments and studies have shown that it increases user compliance, especially for mental health patients. It is also better if the sensors are as unnoticeable and unfelt as possible [41]. The sensor T-shirt by the PSYCHE project and the smart sock by the MONARCA project discussed earlier, are two of the examples of smart textile.

Though there are numerous researches on assistive and predictive technologies for bipolar disorder and they have evolved substantially over time with advancement of mobile, wireless and sensor technologies (Fig. 3), there are many challenges before such systems can be deployed and made available for patients and clinics to use. One major gap in the current research is that most of them focus on depressive state, but research on prediction and identification of manic state is very difficult to identify and often goes undiagnosed [46].

Table I gives a brief overview of the studies discussed in this literature. With the seriousness of the disorder across the globe and a dire need of a system to objectively identify a patient's bipolar state, researches are demonstrating promising results that can potentially address current gap between the diagnosis and treatment.

IX. FUTURE WORK

The main focus of research in the current decade is towards personalized monitoring systems as discussed in the previous sections. Such systems come under the category of Body Area Network (BAN), as it consists of sensors signaling physiological data from the patient [54]. An amalgamation of such a network with a smart mobile phone is the next generation of healthcare applications. Although with innumerable technological advances, there are still many challenges to tackle before such systems can be deployed and practically made available.

The first and the foremost challenge is to attain power efficiency. Devices in the system should consume less power so that battery recharging is as less often as possible. Wireless communication, such as Bluetooth, consumes a lot of power and hence low power operation is the biggest challenge [54] that needs to be addressed before a system can be deployed and made available for users. Future work and progress in the research on size reduction of the devices, security and privacy will enhance the feasibility and applicability of similar aforementioned systems [54] [41]. Along with technical challenges, there are also ethical and clinical dilemmas of using

mobile devices that are related to data confidentiality and network security that would need to be addressed [30].

REFERENCES

- [1] Psychiatric Association. Diagnostic and statistical manual of mental disorders, 5th ed. (DSM-5). Washington, DC: American Psychiatric Publishing; 2013.
- [2] B. Krans. Diagnosis guideline Kernel Description. url: <https://www.healthline.com/health/bipolar-disorder/bipolar-diagnosis-guide#mental-health-evaluation>.
- [3] Patel, Dupal, Kamal Singh Rathore, and Twinkal Patel. "BIPOLAR DISORDER—AN OVERVIEW."
- [4] Joyce, Peter R. 2008. "Classification of Mood Disorders in DSM-V and DSM-VI." Australian & New Zealand Journal of Psychiatry 42 (10): 851–62. doi:10.1080/00048670802363667
- [5] G. Valenza et al., "Predicting Mood Changes in Bipolar Disorder Through Heartbeat Nonlinear Dynamics," in IEEE Journal of Biomedical and Health Informatics, vol. 20, no. 4, pp. 1034-1043, July 2016. doi: 10.1109/JBHI.2016.2554546
- [6] Kupfer DJ. The Increasing Medical Burden in Bipolar Disorder. JAMA. 2005;293(20):2528–2530. doi:10.1001/jama.293.20.2528
- [7] Fajutrao L, Locklear J, Prialux J, Heyes A. A systematic review of the evidence of the burden of bipolar disorder in Europe. Clin Pract Epidemiol Ment Health. 2009;5:3.
- [8] Merikangas KR, Jin R, He J, et al. Prevalence and Correlates of Bipolar Spectrum Disorder in the World Mental Health Survey Initiative. Arch Gen Psychiatry. 2011;68(3):241–251. doi:10.1001/archgenpsychiatry.2011.12
- [9] Fuentes, Ileana, Alfredo Rizo-Méndez, and Adolfo Jarne-Esparcia. "Low compliance to pharmacological treatment is linked to cognitive impairment in euthymic phase of bipolar disorder." Journal of affective disorders 195 (2016): 215-220.
- [10] Baldassano, Claudia. "Reducing the burden of bipolar disorder for patient and caregiver." Medscape Psychiatry & Mental Health 9.2 (2004): 38-45.
- [11] Blanthorn-Hazell, Sophee, Alfredo Gracia, Jenna Roberts, Anca Boldeanu, and Davneet Judge. "A survey of caregiver burden in those providing informal care for patients with schizophrenia or bipolar disorder with agitation: results from a European study." Annals of general psychiatry 17, no. 1 (2018): 8.
- [12] Merikangas KR, Jin R, He J, Kessler RC, Lee S, Sampson NA, Viana MC, Andrade LH, Hu C, Karam EG, Ladea M, Medina-Mora ME, Ono Y, Posada-Villa J, Sagar R, Wells JE, Zarkov Z. Prevalence and Correlates of Bipolar Spectrum Disorder in the World Mental Health Survey Initiative. Arch Gen Psychiatry. 2011;68(3):241–251. doi:10.1001/archgenpsychiatry.2011.12
- [13] Novick DM, Swartz HA, Frank E. Suicide attempts in bipolar I and bipolar II disorder: a review and meta-analysis of the evidence. Bipolar Disord 2010; 12: 1–9.
- [14] Dutta R, Boydell J, Kennedy N, Van Os J, Fearon P, Murray RM: Suicide and other causes of mortality in bipolar disorder: a longitudinal study. Psychol Med 2007, 37(6):839-847.
- [15] Kleinman, L.S., Lowin, A., Flood, E. et al. Pharmacoeconomics (2003). "Costs of Bipolar Disorder" 21: 601. <https://doi.org/10.2165/00019053-200321090-00001>
- [16] Steven C. Dilsaver, An estimate of the minimum economic burden of bipolar I and II disorders in the United States: 2009, In Journal of Affective Disorders, Volume 129, Issues 1–3, 2011, Pages 79-83, ISSN 0165-0327, <https://doi.org/10.1016/j.jad.2010.08.030>.
- [17] Hirst M. Carer distress: a prospective, population-based study. Soc Sci Med. 2005;61(3):697–708.
- [18] Lee E. J., Kim J. B., Shin I. H., et al. Current use of depression rating scales in mental health setting. Psychiatry Investigation. 2010;7(3):170–176. doi: 10.4306/pi.2010.7.3.170
- [19] A.John Rush, Madhukar H Trivedi, Hicham M Ibrahim, Thomas J Carmody, Bruce Arnow, Daniel N Klein, John C Markowitz, Philip T Ninan, Susan Kornstein, Rachel Manber, Michael E Thase, James H Kocsis, Martin B Keller, The 16-Item quick inventory of depressive

- symptomatology (QIDS), clinician rating (QIDS-C), and self-report (QIDS-SR): a psychometric evaluation in patients with chronic major depression, *Biological Psychiatry*, Volume 54, Issue 5, 2003, Pages 573-583, ISSN 0006-3223.
- [20] Lam, Raymond W., Erin E. Michalak, and Richard P. Swinson. *Assessment scales in depression, mania and anxiety*. London: Taylor & Francis, 2005.
- [21] David C. Mohr, Michelle Nicole Burns, Stephen M. Schueller, Gregory Clarke, Michael Klinkman, *Behavioral Intervention Technologies: Evidence review and recommendations for future research in mental health*, *General Hospital Psychiatry*, Volume 35, Issue 4, 2013, Pages 332-338, ISSN 0163-8343, <https://doi.org/10.1016/j.genhosppsy.2013.03.008>.
- [22] JScottatall, "Long-term mental health resource utilization and cost of care following group psychoeducation or unstructured group support for bipolar disorders: a cost-benefit analysis", *J Clin Psychiatry*, 2009, Mar 10.
- [23] Meyer, Thomas D., Rebecca Casarez, Satyajit S. Mohite, Nikki La Rosa, and M. Sriram Iyengar. "Novel technology as platform for interventions for caregivers and individuals with severe mental health illnesses: A systematic review." *Journal of Affective Disorders* 226 (2018): 169-177.
- [24] Murray, Greg, Nuwan D. Leitan, Michael Berk, Neil Thomas, E. Michalak, Lesley Berk, Sheri L. Johnson et al. "Online mindfulness-based intervention for late-stage bipolar disorder: pilot evidence for feasibility and effectiveness." *Journal of Affective Disorders* 178 (2015): 46-51.
- [25] Jones, Rhys Bevan, Anita Thapar, Frances Rice, Harriet Beeching, Rachel Cichosz, Becky Mars, Daniel J. Smith et al. "A Web-Based Psychoeducational Intervention for Adolescent Depression: Design and Development of MoodHwb." *JMIR mental health* 5, no. 1 (2018).
- [26] Colom, Francesc. "Keeping therapies simple: psychoeducation in the prevention of relapse in affective disorders." *The British Journal of Psychiatry* 198, no. 5 (2011): 338-340.
- [27] D.J. Smith, et al. Beating bipolar: exploratory trial of a novel Internet-based psychoeducational treatment for bipolar disorder. *Bipolar Disord*, 13 (5-6) (2011), pp. 571-577
- [28] G. Technologies. (2013). *Emoods bipolar mood tracker (version 1.0)* [mobile software application]. [Online]. Available: <https://play.google.com/store/apps>
- [29] Mohr DC, Noth Tomasino K, Lattie EG, Palac HL, Kwasny MJ, Weingardt K, Karr CJ, Kaiser SM, Rossom RC, Bardsley LR, Caccamo L, Stiles-Shields C, Schueller SM. *IntelliCare: An Eclectic, Skills-Based App Suite for the Treatment of Depression and Anxiety*. *J Med Internet Res* 2017;19(1):e10
- [30] C.A. Depp, et al. Mobile interventions for severe mental illness: design and preliminary data from three approaches. *J Nerv Ment Dis*, 198 (10) (2010), pp. 715-721
- [31] M. Matthews and G. Doherty. "In the Mood: Engaging Teenagers in Psychotherapy Using Mobile Phones". In: *Proceedings of the SIGCHI Conference on Human Factors in Computing Systems*. CHI '11. Vancouver, BC, Canada: ACM, 2011, pp. 2947-2956. isbn: 978-1-4503-0228-9. doi: 10.1145/1978942.1979379. (cit. on p. 11).
- [32] J. E. Bardram, M. Frost, K. Sz'ant'o, M. Faurholt-Jepsen, M. Vinberg, and L. V. Kessing. "Designing Mobile Health Technology for Bipolar Disorder: A Field Trial of the Monarca System". In: *Proceedings of the SIGCHI Conference on Human Factors in Computing Systems*. CHI '13. Paris, France: ACM, 2013, pp. 2627-2636. isbn: 978-1-4503-1899-0. doi: 10.1145/2470654.2481364. url: <http://doi.acm.org/10.1145/2470654.2481364> (cit. on p. 12).
- [33] Rootes-Murdy, Kelly, Kara L. Glazer, Michael J. Van Wert, Francis M. Mondimore, and Peter P. Zandi. "Mobile technology for medication adherence in people with mood disorders: A systematic review." *Journal of Affective Disorders* 227 (2018): 613-617.
- [34] Venet Osmani, Alban Maxhuni, Agnes Gr'unerbl, Paul Lukowicz, Christian Haring, and Oscar Mayora. 2013. *Monitoring activity of patients with bipolar disorder using smart phones*. In *Proceedings of International Conference on Advances in Mobile Computing & Multimedia (MoMM '13)*. ACM, New York, NY, USA, , Pages 85 , 8 pages. DOI=<http://dx.doi.org/10.1145/2536853.2536882>.
- [35] A.Gr'unerbl,A.Muaremi,V.Osmani,G.Bahle,S.'Ohler,G.Tfoster,O. Mayora, C. Haring, and P. Lukowicz. "Smartphone-Based Recognition of States and State Changes in Bipolar Disorder Patients". In: *IEEE Journal of Biomedical and Health Informatics* 19.1 (Jan. 2015), pp. 140-148. Issn:2168-2194. doi:10.1109/JBHI.2014.2343154 (cit. on pp. 7, 9, 11).
- [36] Faurholt-Jepsen, Maria, Jonas Busk, Mads Frost, Maj Vinberg, Ellen M. Christensen, Ole Winther, Jakob Eyvind Bardram, and Lars V. Kessing. "Voice analysis as an objective state marker in bipolar disorder." *Translational psychiatry* 6, no. 7 (2016): e856.
- [37] Alberto Greco, Gaetano Valenza, Enzo Pasquale Scilingo, Alberto Greco, Gaetano Valenza, Enzo Pasquale Scilingo, "Advances in electrodermal activity processing with applications for mental health."
- [38] Lang, P.J., Bradley, M.M., & Cuthbert, B.N. (2008). *International affective picture system (IAPS): Affective ratings of pictures and instruction manual*. Technical Report A-8. University of Florida, Gainesville, FL.
- [39] A. Greco, A. Lanat`a, G. Valenza, G. Rota, N. Vanello, and E. P. Scilingo. "On the deconvolution analysis of electrodermal activity in bipolar patients". In: *2012 Annual International Conference of the IEEE Engineering in Medicine and Biology Society*. Aug. 2012, pp. 6691-6694. doi: 10.1109/EMBC.2012.6347529 (cit. on pp. 3, 4, 6, 8, 9, 11)
- [40] M. Benedek and C. Kaernbach, "Decomposition of skin conductance data by means of nonnegative deconvolution," *Psychophysiology*, vol. 47, no. 4, pp. 647-658, 2010.
- [41] A. Puiatti, S. Mudda, S. Giordano and O. Mayora, "Smartphone-centred wearable sensors network for monitoring patients with bipolar disorder," *2011 Annual International Conference of the IEEE Engineering in Medicine and Biology Society*, Boston, MA, 2011, pp. 3644-3647. doi: 10.1109/IEMBS.2011.6090613
- [42] C. Kappeler-Setz, J. Schumm, M. Kusserow, and B. Arnrich, *Towards Long Term Monitoring of Electrodermal Activity in Daily Life*, *UbiComp 2010*, Sep 26 Sep 29, 2010, Copenhagen, Denmark.
- [43] Malik M, Bigger JT, Camm AJ, Kleiger RE, Malliani A, Moss AJ, Schwartz PJ: Heart rate variability: Standards of measurement, physiological interpretation, and clinical use. *Eur Heart J* 1996; 17:354-381
- [44] Appelhans, B. M., & Luecken, L. J. (2006). Heart rate variability as an index of regulated emotional responding. *Review of General Psychology*, 10(3), 229-240.
- [45] G.Valenzaetal., "Wearable monitoring for mood recognition in bipolar disorder based on history-dependent long-term heart rate variability analysis," *IEEE J. Biomed. Health Informat.*, vol. 18, no. 5, pp. 1625-1635, Sep. 2014.
- [46] B. L. Henry, A. Minassian, M. P. Paulus, M. A. Geyer, and W. Perry, "Heart rate variability in bipolar mania and schizophrenia," *J. Psychiatr. Res.*, vol. 44, no. 3, pp. 168-176, Feb. 2010.
- [47] M. Migliorini, S. Mariani, G. Bertschy, M. Kosel, and A. M. Bianchi. "Can home-monitoring of sleep predict depressive episodes in bipolar patients?" In: *2015 37th Annual International Conference of the IEEE Engineering in Medicine and Biology Society (EMBC)*. Aug. 2015, pp. 2215-2218. doi :10.1109/EMBC.2015.7318831(cit. on p. 10)
- [48] D. Nutt, S. Wilson, and L. Paterson, "Sleep disorders as core symptoms of depression," *Dialogues Clin. Neurosci.*, vol. 10, no. 3, pp. 329-336, Sep. 2008.
- [49] Rate of switch from depression into mania after therapeutic sleep deprivation in bipolar depression. Colombo C, Benedetti F, Barbini B, Campori E, Smeraldi E *Psychiatry Res*. 1999 Jun 30; 86(3):267-70.
- [50] Kaplan K, McGlinchey EL, Soehner A, et al. Hypersomnia subtypes, sleep and relapse in bipolar disorder. *Psychol Med* 2014;17:1-13.
- [51] R. Paradiso, A. M. Bianchi, K. Lau and E. P. Scilingo, "PSYCHE: Personalised monitoring systems for care in mental health," *2010 Annual International Conference of the IEEE Engineering in Medicine and Biology*, Buenos Aires, 2010, pp. 3602-3605. doi: 10.1109/IEMBS.2010.5627469
- [52] Gilbody SM, House AO, Sheldon TA. Psychiatrists in the UK do not use outcomes measures. *National survey*. *Br J Psychiatry*. 2002;180:101-103.

- [53] Zimmerman M, McGlinchey JB. Why don't psychiatrists use scales to measure outcome when treating depressed patients? *J Clin Psychiatry*. 2008;69:1916–1919
- [54] E. Jovanov and A. Milenkovic, Body Area Networks for Ubiquitous Healthcare Applications: Opportunities and Challenges *Journal of medical systems*, Feb. 2011
- [55] G. Valenza et al., "Wearable Monitoring for Mood Recognition in Bipolar Disorder Based on History-Dependent Long-Term Heart Rate Variability Analysis," in *IEEE Journal of Biomedical and Health Informatics*, vol. 18, no. 5, pp. 1625-1635, Sept. 2014. doi: 10.1109/JBHI.2013.2290382
- [56] E. Vieta, M. Reinares, and A. Rosa, "Staging bipolar disorder," *Neurotoxicity Res.*, vol. 19, no. 2, pp. 279–285, 2011
- [57] Yves L. Coelho, Teodiano F. Bastos-Filho, A Bipolar Disorder Monitoring System Based on Wearable Device and Smartphone, *IFAC-PapersOnLine*, Volume 49, Issue 30, 2016, Pages 216-220, ISSN 2405-8963, <https://doi.org/10.1016/j.ifacol.2016.11.170>.
- [58] Gravenhorst, Franz, Amir Muaremi, Jakob Bardram, Agnes Grünerbl, Oscar Mayora, Gabriel Wurzer, Mads Frost et al. "Mobile phones as medical devices in mental disorder treatment: an overview." *Personal and Ubiquitous Computing* 19, no. 2 (2015): 335-353.
- [59] Khan, Arshia, and Yumna Anwar. "Framework to Predict Bipolar Episodes." In *Proceedings of SAI Intelligent Systems Conference*, pp. 412-425. Springer, Cham, 2018.

Hybrid Genetic-FSM Technique for Detection of High-Volume DoS Attack

Mohamed Samy Nafie¹, Hassan Abounaser³

Department of Computer Engineering
Arab Academy for Science, Technology and Maritime Transport (AASTMT), Cairo, Egypt

Khaled Adel²

Department of Computer Science
Ain Shams University
Cairo, Egypt

Amr Badr⁴

Department of Computer Science
Cairo University
Giza, Egypt

Abstract—Insecure networks are vulnerable to cyber-attacks, which may result in catastrophic damages on the local and global scope. Nevertheless, one of the tedious tasks in detecting any type of attack in a network, including DoS attacks, is to determine the thresholds required to discover whether an attack is occurring or not. In this paper, a hybrid system that incorporates different heuristic techniques along with a Finite State Machine is proposed to detect and classify DoS attacks. In the proposed system, a Genetic Programming technique combined with a Genetic Algorithm are designed and implemented to represent the system core that evolves an optimized tree-based detection model. A Hill-Climbing technique is also employed to enhance the system by providing a reference point value for evaluating the optimized model and gaining better performance. Several experiments with different configurations are conducted to test the system performance using a synthetic dataset that mimics real-world network traffic with different features and scenarios. The developed system is compared to many state-of-art techniques with respect to several performance metrics. Additionally, a Mann-Whitney Wilcoxon test is conducted to validate the accuracy of the proposed system. The results show that the developed system succeeds in achieving higher overall performance and prove to be statistically significant.

Keywords—Denial of Service (DoS); Evolutionary Algorithms (EA); Finite State Machine (FSM); Genetic Algorithm (GA); Genetic Programming (GP); Hill-Climbing Search

I. INTRODUCTION

In 1969, ARPANet invented the first link between two computers, which was the main predecessor of the Internet that appeared in 1983 [1]. Since then, computer networks have been in rapid development. Nowadays, they are continuously growing in size, complexity and efficiency, thus becoming one of the most important daily aspects of people's lives. For instance, people can use computer networks to send electronic e-mails, communicate via Voice over IP (VoIP) or transfer money via online bank portals instead of sending postal letters, making phone calls or going to the bank. Moreover, they can use it to access video streaming services, read news feeds, subscribe to online foreign exchange markets and many others things[2]. In addition to the basic services, new emerging technologies such as the Internet of Things (IoT)

and Software Defined Networks (SDN) make use of computer networks to accomplish their goals [3],[4].

Consequently, such vital services have to be available for the end-users, allowing them to acquire and exchange information in an agile, easy and pervasive way on a daily basis. From another perspective, a major security concerns is for such services to become unavailable in a way that can vastly and adversely affect users. Denial of Service (DoS) is one type of network attacks, which threatens the availability of the victim's network by disrupting it, hence disabling any legitimate users from reaching the desired services. Another form of DoS attack is the Distributed Denial of Service (DDoS). DDoS attacks are usually launched with the aid of botnets [5]. A botnet is a set of compromised hosts controlled by a malicious attacker, which are instructed to perform illegal and malicious actions.

To support the availability and resiliency of computer networks and protect them from DoS attacks, a network monitoring approach such as NetFlow can help by providing flow analysis rather than standalone packet analysis, grasping a wider picture of the network's behavior. NetFlow is a protocol that captures and collect the flow of data entering and exiting network devices such as routers and switches. A flow data includes both source and destination IP addresses and ports, and transport protocol type. The Internet Engineering Task Force (IETF) currently standardizes it under the name IP Flow Information Export (IPFIX) [6].

Since insecure networks are vulnerable to cyber-attacks that may lead to catastrophic damages, improving Intrusion Detection System (IDS) is one of the hot topics that are widely researched. Different techniques are used to enhance the detection rate of attacks. Some of these techniques are Statistical Analysis, Clustering, Soft Computing such as Artificial Neural Networks (ANN), Support Vector Machines (SVM), Evolutionary Algorithms (EA) and others [7]. Additionally, it is proven that hybrid classifiers are capable of boosting the weakness of the single classifiers, hence producing better overall outcomes. Therefore, a hybrid detection approach is preferred [8],[9].

Genetic Algorithm [10] and Genetic Programming [11] are well-known meta-heuristic evolutionary algorithms that encompass the behavior of the natural selection of the fittest [12]. Both operate on a population of randomly initialized individuals, named chromosomes. Each chromosome resembles a possible solution for the required objective. The basic genetic operators are selection, crossover and mutation. By applying these operators, there is a chance that the individuals will be enhanced with each generation, producing finer solutions. To evaluate the fitness of each individual, a fitness function that generates a fitness-based value is computed. A number of generations is sustained until the termination criteria is met.

Hill-Climbing is a variant generate-and-test heuristic algorithm which follows the approach of trial and error by starting with an arbitrary solution and keeps iterating by making incremental changes[13]. It continuously tests newly generated solutions until an optimal one is reached. Hill-Climbing is sometimes called greedy local search because it aims towards a better solution in hope of finding the optimal one. The Hill-Climbing technique has three different types known as Simple, Stochastic and Steepest-Ascent, and these are applicable to both discrete and continuous search spaces[14]. Each type differs in how it approaches the neighboring nodes during the testing phase.

Many expert systems used for DoS detection rely on a predetermined threshold of certain parameters to determine whether there is an attack occurring inside the network or not. These approaches can yield a higher false-positive rate as well as a low detection accuracy. Often, these values are interleaved and depend on the type of network; thus, the manual calibration of such values are exhaustive due to an extremely large search space[14],[15]. Hence, it is very important to find an effective technique capable of detecting the occurrences of high-volume DoS attacks[16]. In this research, a system combining different heuristic techniques along with a Finite State Machine is proposed to detect the occurrences of high-volume DoS attacks.

The rest of this paper is organized as follows. Section II is a review of related work in detecting denial of service and presents different anomaly classification techniques. Section III demonstrates the algorithms and techniques proposed by this research. In Section IV, the preparation details of the utilized dataset are explained, and the obtained results of the conducted experiments are discussed. Finally, Section V concludes this work.

II. RELATED WORK

Network reliability is important for both consumers and administrators. DoS attacks are common due to the fact that they can be easily launched in addition to their potential to cause catastrophic impacts on large scale networks[17]. Therefore, sophisticated and effective detection methods are considered as a priority to combat such attacks.

In [18], the authors have used supervised Artificial Neural Networks (ANNs) to detect the occurrences of DoS attacks. Each ANN is used to analyze the pattern of packet headers sent to a specific IP address if the number of packets is larger

than a certain threshold. The system then deduces the packet threat level based on the majority of votes among multiple trained ANNs. The authors created their own dataset and environment to simulate the attacks and they compared their results with Chi-squared, Probabilistic Neural Networks and SVM, and proved to provide better detection results.

In [19], the authors used Hidden Markov Models (HMM) to represent different states of the network according to various features and behaviors. The system is composed of multiple HMM for each feature vector, including source and destination ports, source and destination IP addresses, and length of packets. Based on the HMMs output, the system calculates the suspicion level for the packets. The authors generated their test suite using OpenFlow to evaluate the accuracy of detection. The system showed good results in flagging malicious packets. One advantage of this system is that HMM can readily adapt to changes that happen to the networks without re-training.

In [20], the authors proposed a system that uses a modification of Holt-Winters named Holt-Winters for Digital Signature (HWDS), which generates a Digital Signature of Network Segment using Flow Analysis (DSNSF) for seven analyzed dimensions of the IP flow. Their system compares the collected flows, which differ from the generated DSNSF, with signatures of known attacks such as DoS and DDoS. Finally, a game-theoretic approach is used to mitigate the impact of the attacks.

In [21], the authors also used the concept of DSNSF to encapsulate six analyzed dimensions for each IP flow. The system monitors the network and extracts traffic characterization to the standard IPFIX form. The authors have used unsupervised GA to generate the DSNSF from the network information. Afterwards, the DSNSF is passed to a Fuzzy Logic classifier that assigns an anomalous score for each dimension in the real collected DSNSF using a Gaussian membership function. The scores are aggregated and a flow is labeled anomalous if that total score surpasses a certain cutoff value. The authors compared their results with Outlier Detector, SVM, CkNN, and the system provided better results in terms of detection accuracy.

In [22], the authors proposed a hybrid classification technique based on Artificial Bee Colony (ABC) and Acritical Fish Swarm (AFS) to enhance the detection accuracy of IDS. Additional techniques such as Fuzzy C-Means Clustering (FCM) and Correlation-based Feature Selection (CFS) are employed to split the training dataset and remove insignificant features. CART technique is implemented to generate If-Then rules that distinguish the normal and malicious records. Finally, the proposed hybrid system is trained via the generated rules.

III. PROPOSED SYSTEM

This section aims to find an effective supervised-learning technique capable of automatically detecting the occurrences of high-volume DoS attack. To address this issue, a hybrid system of different heuristic techniques, along with a Finite State Machine (FSM) is proposed. The core of this system is a nested technique composed of a Genetic Algorithm (GA)

representing the outer layer and a Genetic Programming (GP) representing the inner layer. The GP technique is designed and implemented to evolve the detection model for the attacks whereas the GA technique is designed and implemented to optimize the coefficients of this model. In details, the role of the GP technique is to evolve a tree-based mathematical expression capable of detecting the occurrences of DoS attacks whereas the role of the GA technique is to fine-tune the coefficients of this expression. The system produces two final models; one is for classifying the DoS attack entries while the other is for classifying the legitimate ones.

Fig. 1 illustrates the structure of one GA chromosome and a set of assigned GP chromosomes. All GP nodes that have a letter k denote the used coefficients from the GA chromosomes, while those that have a letter v denote different features used from the provided dataset.

The system starts by generating and initializing a random population for the outer-layer GA and the inner-layer GP according to the specified sizes n_1 and n_2 respectively. The random population of the GA acts as a feed for the GP expressions, where each value inside the GA genes can be sourced to the GP chromosomes. This is governed as a multi-to-multi relationship where each gene value of each GA chromosome can be utilized multiple times inside the same GP. This happens across different GP chromosomes within the population and can be completely neglected.

Each GA chromosome is assigned with a number of GP chromosomes. Afterwards, the GP starts its own evolution process based on the previously assigned values from the GA and runs for a number of g_2 generations. The final fitness value for each iteration is calculated based on the best fitness value resulting from all the inner-layer GP chromosomes. The whole process is repeated for an overall of g_1 generations.

Fig. 2 illustrates the core operation which is described above for the proposed system and shows the interfacing between the outer-layer GA and inner-layer GP techniques. It also displays how the overall fitness value is calculated for each iteration.

A. Hill-Climbing

As previously mentioned, a reference point is required for the fitness function to be able to evaluate the fitness of GP chromosomes. Since there is no predetermined value to use, the Hill-Climbing technique is employed to calculate a pivot-point that acts as a reference value to overcome this issue. The algorithm utilizes an initial value, an acceleration factor, acceleration directions and step size parameters. The initial value is the starting point from where the search begins and the acceleration direction determines whether the search will accelerate, decelerate or stop. It also provides the direction of the search and whether the pivot-point should increase or decrease according to the selected acceleration factor. A step size decides how far the search should hop into the search space. A large step size helps in discovering a larger space, but it can delay the algorithm from reaching a stable point [23].

For each iteration, all the acceleration directions are tested by generating random chromosomes and evaluating them

using the testing dataset, then finally returning the best fitness. If the best fitness is accompanied with a stopping direction, then the step size would decrease which narrows the search plane, implying that the search is yielding positive results towards a satisfactory pivot-point. In contrast, if the stopping direction is not accompanied with the best fitness, then the step size increases according to both the acceleration direction and factor. This technique will run for a certain number of iterations until the final value is obtained.

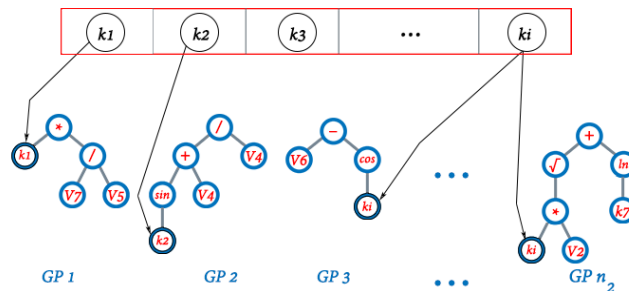


Fig. 1. Structure of GA and GP Chromosomes.

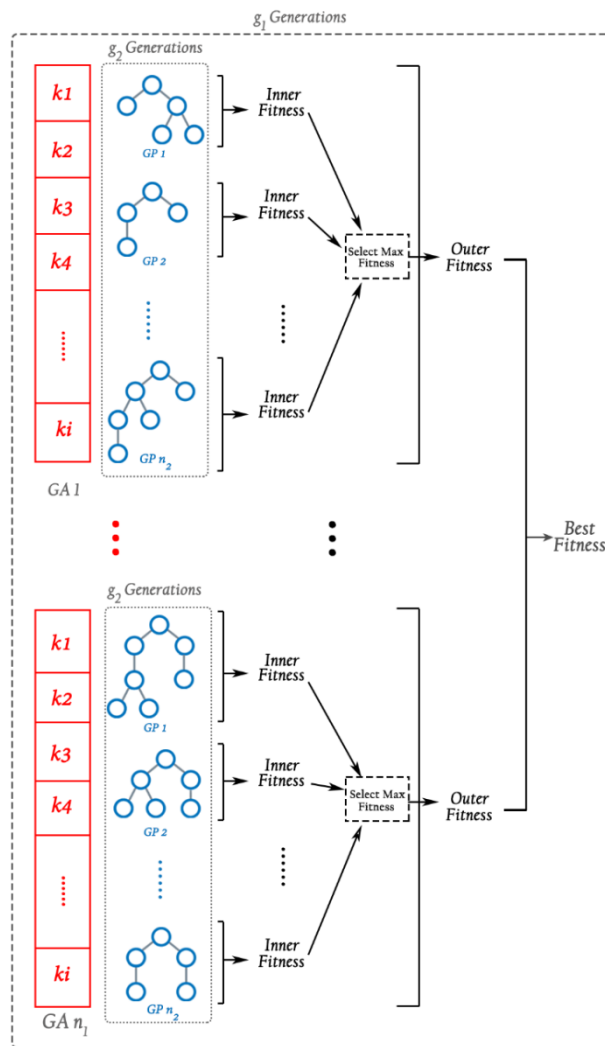


Fig. 2. Structure of the Proposed System. GA is Highlighted in Red and the GP is Highlighted in Blue.

B. Outer-Layer Genetic Algorithm (GA)

The chromosome consists of k genes; each one is a floating-point value. The crossover operator uses the standard single-point method, where two separating points are randomly assigned to the selected parents, and the genes between them are swapped. The selection operator uses the traditional roulette-wheel operator to select the fittest parents according to their fitness, in such a way that a parent chromosome with a higher fitness value will have a higher probability of being selected for crossover.

The mutation is carried in a non-uniform fashion as it depends on the value of best and average fitness of the current generation. The lower the average fitness of the population compared to the best fitness, the higher the mutation probability by a maximum of 50% probability. Non uniform mutation has proved to provide higher fitness values compared to the uniform fashion[24]. Elitism is also implemented and used to make sure that the fittest individual from a previous generation is transferred to the newer generation, so that the fitness value for the newest generation is either sustained or increased.

The objective of the of outer-layer GA is to fine-tune the performance of the inner-layer GP, in such a way that per each generation, a number of iterations for the inner-layer GPs are tested. The fitness function consists of a formula that selects the fittest individual from within the assigned GPs to each chromosome respectively.

C. Inner-Layer Genetic Programming (GP)

As mentioned earlier, the GP technique represents the core of the developed system along with the GA technique. It is designed and implemented to evolve a mathematical expression that can be used to classify the network traffic into DoS attacks, legitimate traffic or anomalous traffic. The tree structure of the inner-layer GP technique has a pre-determined depth d . Each GP chromosome is designed to encode a single tree representing a mathematical expression. Each gene represents a tree node that may hold a dataset feature, a mathematical operator or a coefficient value passed from the assigned GA chromosome of the currently evolving outer-layer GA generation.

A roulette-wheel operation is used to select two candidate parents that for the crossover operation. Then, according to a given probability value, the crossover operation will combine the genetic information in the parents to produce two new offspring. This is accomplished by generating a random cut-off point that is bounded by the tree dimension of the selected parents, around which, the two sub-trees are interchanged. Fig. 3 illustrates the crossover operation in inner-layer GP between the individuals GP_1 and GP_2 .

The mutation probability value is calculated in the same non-uniform fashion utilized by the GA; however, the mutation operator itself is completely different. It can be a simple mutation or a subtree mutation. Simple mutation involves the modification of an individual gene, where the contents can be altered or expanded. Subtree mutation creates a new subtree initialized and grown from the mutating gene, taking into account the maximum allowable depth. Both

mutation operators take into consideration the semantic and syntax limitations of the expression.

As for the fitness function, the fitness is computed based on the count of the correctly predicted entries. Each candidate model is compared to the pivot-point that has been previously calculated using Hill-Climbing technique. The system begins with classifying the DoS attacks aiming to produce a model for detecting them. If the evaluation of the mathematical model is found to be higher in value than the pivot-point, the system considers the entry to be an attack; otherwise, it is not. This prediction is compared to the expected label from the dataset. If it is correct, it is counted towards the fitness value, alternatively it is not counted. After the specified number of generations ends, the whole developed technique is repeated for the legitimate entries using the evaluation process. However, it differs in such a way that if the result of evaluating the mathematical model is found to be lower in value than the pivot-point, it is considered legitimate; otherwise, it is not.

D. Finite State Machine (FSM)

The finite state machine is responsible for interfacing all the outputs of the GP expressions into a single system developed to decide whether the output class is classified as attack, normal or anomalous. The FSM consists of three states corresponding to each of the output classes, along with an initial starting state. Each entry in the testing dataset is fed to the FSM. The FSM examines the entry by taking each attribute and assigning it to the corresponding parameter found in the GP expression. According to the evaluation of the expression against the previously found pivot-point, the FSM decides which state it will switch to. Fig. 4 illustrates the interfacing of the GP expressions into the FSM.

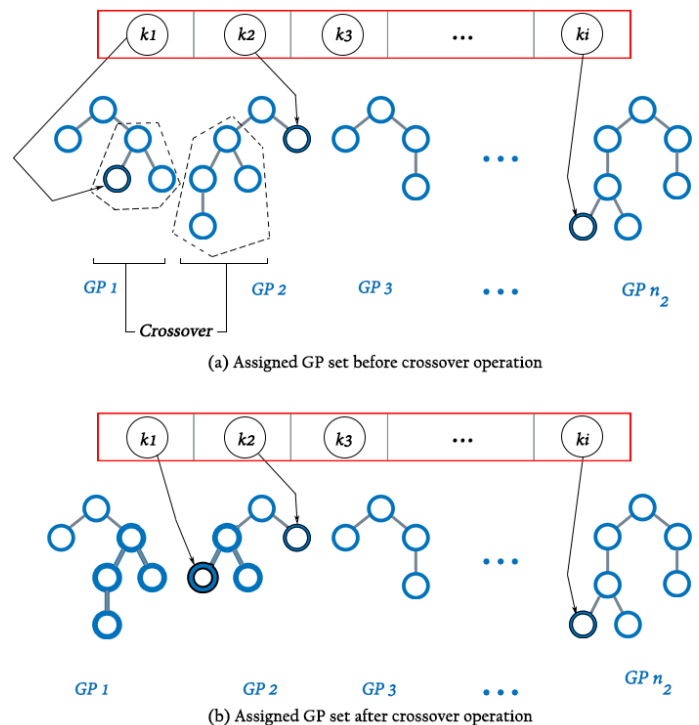


Fig. 3. Crossover Operation between two GP Chromosomes.

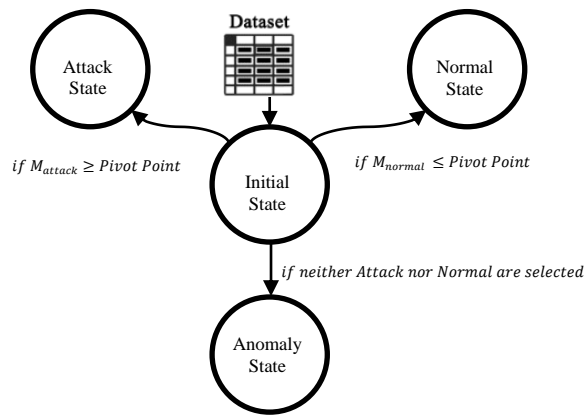


Fig. 4. Design of FSM.

IV. RESULTS AND DISCUSSION

The following results were obtained from a series of experiments conducted using the developed system described above to acquire an optimized detection model. The experiments were performed on an Intel Core i5-3750K overclocked at 4.2 GHz CPU, with a 64-bit edition of Windows 10 and 16GB of RAM. A Nvidia 1080 GTX GPU conjointly with AleaGPU[25] software was used to handle all the computation of fitness function evaluation utilizing the power of parallel computing using CUDA. The full code has been implemented using C# on Microsoft Visual Studio 2017 with the Accord.NET [26] framework installed.

A. Dataset Description and Prepration

The experiments are conducted on the following dataset named CICIDS2017, provided by the Canadian Institute for Cybersecurity (CIC), University of New Brunswick (UNB). The original dataset contains 12 different types of attacks and 80 extracted network features [27]. However, since this research mainly focuses on high-volume DoS attacks, which are labeled “Attack”, all other non-DoS attacks are out of our scope of research, and thus, they were removed from the dataset. The remaining DoS attack types are labeled “Anomaly”. They are Heartbleed, Slowloris, GoldenEye and slowhttptest. Finally, the legitimate traffic is labeled “Normal”.

For the system to work as intended, features fed to the system are required to be represented quantitatively. Volumetric features such as duration, number of packets and bytes are numerical; however, IP addresses and ports information are nominal. To extract the properties of these features, Shannon Entropy is employed. Shannon Entropy measures the uncertainty associated with the randomness of a variable. When the variable distribution is concentrated, the entropy value tends to be minimal, while it is completely zero when all the variables are same. In contrast, the value tends to be high in case of discrepancy and fluctuations. The Shannon entropy value is usually between zero and one[28]. Given a set of features $X = \{x_1, \dots, x_i, \dots, x_n\}$, the Shannon Entropy is defined by:

$$H(X) = - \sum_{i=1}^n P_i * \log_2(P_i)$$

where P_i is the probability of distribution of each feature from the set X . To calculate the probability of distribution, the frequency of occurrences of feature i is calculated by:

$$P_i = \frac{x_i}{\sum_{i=1}^n x_i}$$

Entries are aggregated based on the timestamp, source IP address, destination IP address, and source port in a similar way to how NetFlow aggregates data flows. Employing such an aggregation scheme creates an aggregated flow for each destination IP address in correspondence to every source IP juxtaposed with its source port for each time interval. This can help the system to effectively detect attacks[29]. Quantitative features are aggregated, while qualitative features are calculated separately. Table I shows the features used in the training process for each entry.

B. Performance Analysis

The results are obtained by running the dataset 5 times using 16 different configurations, and the output is then averaged to obtain a more accurate representation. The size of the GA chromosome utilized is 10 genes and the depth of the GP chromosomes utilized ranges between 3 and 5. The number of the generations for the outer-layer GA and inner-layer GP techniques are 25 and 50 respectively. Table II illustrates the number of training and testing entries in the dataset. Table III illustrates the settings used to train and test the system. Table IV lists the configurations for the common settings used to train and test the system. These configurations are sorted according to the number of GA and GP population sizes n_1 and n_2 respectively.

TABLE I. FEATURES USED IN THE TRAINING AFTER PRE-PROCESSING

Feature	Explanation
Duration	The duration of the flow activity in minutes.
# of source packets	Total number of packets sent from source IP address to a destination IP address.
# of destination packets	Total number of packets sent from destination IP address to a source IP address.
# of source bytes	Total number of bytes sent from source IP address to a destination IP address.
# of destination bytes	Total number of bytes sent from destination IP address to a source IP address.
IP Entropy	Shannon Entropy calculated for source IP address(es).
Port Entropy	Shannon Entropy calculated for destination port(s)
Source to Destination Packet Ratio	Ratio between total number of source packets to destination packets
Label	Attack, Normal, Anomaly

TABLE II. NUMBER OF TRAINING AND TESTING ENTRIES IN THE DATASET

Labels	Training Entries	Test Entries
Attack	110992	47568
Normal	257084	110180
Anomaly	13356	5724

TABLE III. LIST OF SETTINGS USED FOR TRAINING AND TESTING

Setting	GA / GP Crossover %	GA / GP Population Size
S1	30% / 30%	24 / 240
S2	30% / 30%	24 / 480
S3	30% / 30%	48 / 240
S4	30% / 30%	48 / 480
S5	30% / 60%	24 / 240
S6	30% / 60%	24 / 480
S7	30% / 60%	48 / 240
S8	30% / 60%	48 / 480
S9	60% / 30%	24 / 240
S10	60% / 30%	24 / 480
S11	60% / 30%	48 / 240
S12	60% / 30%	48 / 480
S13	60% / 60%	24 / 240
S14	60% / 60%	24 / 480
S15	60% / 60%	48 / 240
S16	60% / 60%	48 / 480

TABLE IV. LIST OF CONFIGURATIONS SHOWING THE COMMON SETTINGS

Configuration	Settings
C1	S1, S5, S9, S13
C2	S2, S6, S10, S14
C3	S3, S7, S11, S15
C4	S4, S8, S12, S16

Fig. 5 shows the convergence response for the training phase using the preselected configurations. Each one of these graphs illustrates the results for both normal and attack scenarios, showing the calculated fitness value across different generations. By inspecting the results, it is evident that those with a lower initial fitness value tend to converge faster than those with a higher initial fitness. This phenomenon is attributed to the fact that the system utilizes a non-uniform mutation function as already mentioned. Also, it is clear that the fitness values achieved after the run has finished is almost the same for all settings, which means that all settings are capable of properly training the system, but each with different performance. For instance, the settings with increased number of populations for both the GA and the GP yielded a fitness response with a higher initial value, which in turn, delivered better convergence output.

This trend can be associated with the fact that an elitism-based selection operator is performed by the system; therefore, those initially high values are always either improving or getting transferred to the newer generations. This way, starting with a relevant higher fitness value will positively influence the convergence performance. Table V shows the results of testing the proposed system. The testing phase involves testing the entries in the dataset against the output of the GA/GP and interfacing the output to the FSM, which is responsible for producing the final decision about whether the given entry signifies attacking, normal or anomalous behavior.

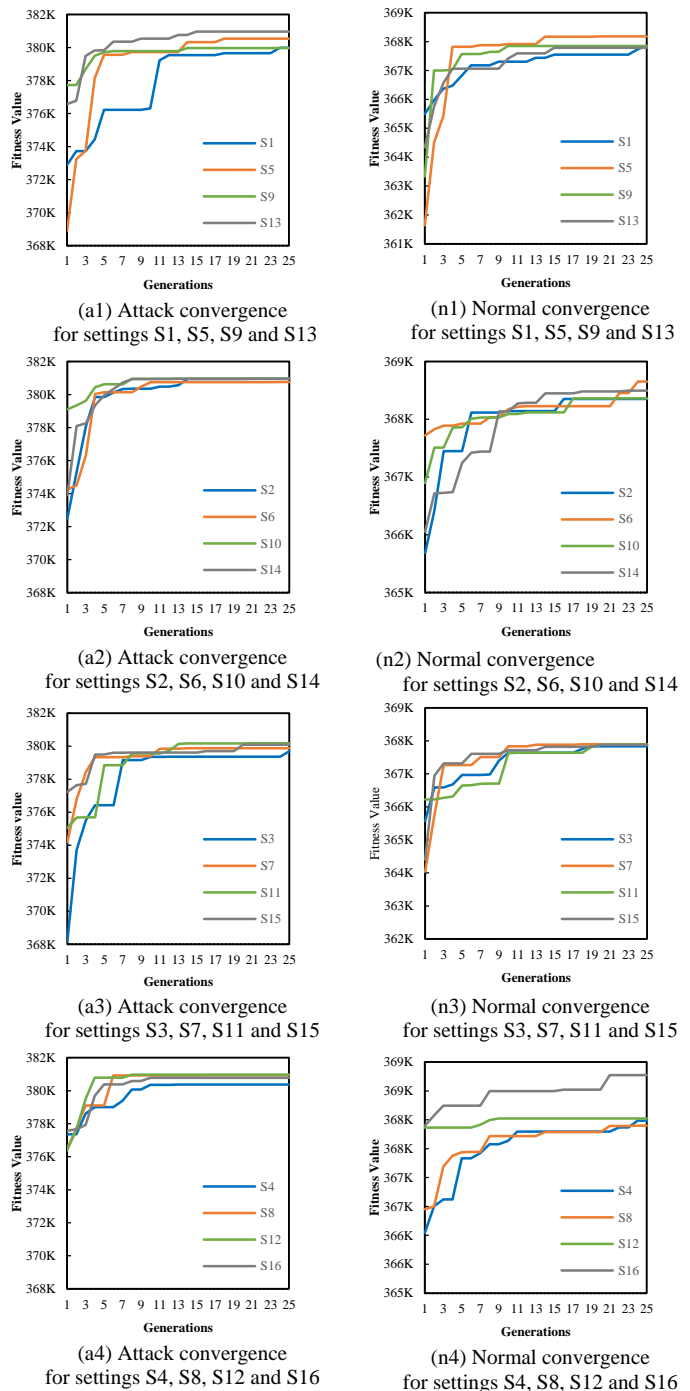


Fig. 5. The Convergence Performance for the Training phase using different Configurations.

By inspecting the relative standard deviation (RSD) and the mean fitness values, it is clear that almost all configurations have yielded very close final outputs. This means that varying the probability of crossover, mutation and the initial number of populations does not significantly affect the fitness value, but it mainly shapes the performance of the convergence process. Also, it is noticeable that setting S2 yielded the best testing accuracy while S11 yielded the worst results. This has occurred because the number of assigned GP chromosomes per GA chromosome were 20 GPs and 5 GPs

for the settings S2 and S11, respectively. It can be observed that the diversity of the GP population per GA chromosome had a role into the final accuracy of the training phase. Therefore, these two settings will be the subject of further testing below.

Interpreting the output of the inner-layer GP, which consists of mathematical formulas and a reference point, is another major issue as it is mainly used to validate the decision with the supervision labels. As already mentioned, the key was to determine a pivot-point value that can be used as the reference point. To solve this issue, a Hill-Climbing technique is employed and tested with the aforementioned two settings, S2 and S11 based on their accuracy results. The results are illustrated in Table VI.

We can infer two important pieces of information from the table above. The first one is the significance of the Hill-Climbing technique in calculating the pivot-point value. A continuous sweeping range of values was tested as starting points for the Hill-Climbing technique. The calculated points were generated based on the difference between the highest and lowest values initially computed for the 100-interval pivot-point. Therefore, three different pivot-points based on this value were included. It can be seen that the values around the 100-interval gave the most accurate results. Fig. 6 shows the convergence performance of the system using the three pivot-points for the already declared best and worst settings.

TABLE V. THE 5-RUN AVERAGE FITNESS AND THE RELATIVE STANDARD DEVIATION OF THE TESTING PHASE FOR EACH CONFIGURATION

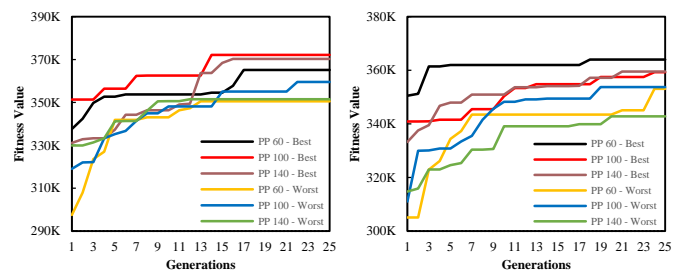
Config	Setting	Average Fitness	RSD (%)	Accuracy (%)
C1	S1	160.67K	0.621 %	98.318 %
	S5	161.09K	0.521 %	98.611 %
	S9	160.48K	0.383 %	98.175 %
	S13	160.88K	0.671 %	98.418 %
C2	S2	161.44K	0.289 %	98.761 %
	S6	161.28K	0.287 %	98.662 %
	S10	160.66K	1.090 %	98.283 %
	S14	161.31K	0.244 %	98.678 %
C3	S3	160.02K	0.840 %	97.889 %
	S7	160.39K	0.630 %	98.116 %
	S15	160.61K	0.513 %	98.252 %
C4	S4	160.78K	0.550 %	98.357 %
	S8	161.24K	0.242 %	98.639 %
	S16	161.34K	0.651 %	98.701 %

TABLE VI. OUTPUT ACCURACY USING DIFFERENT PIVOT-POINTS AND THE NUMBER OF GP GENERATIONS FOR THE BEST (S2) AND WORST SETTINGS (S11)

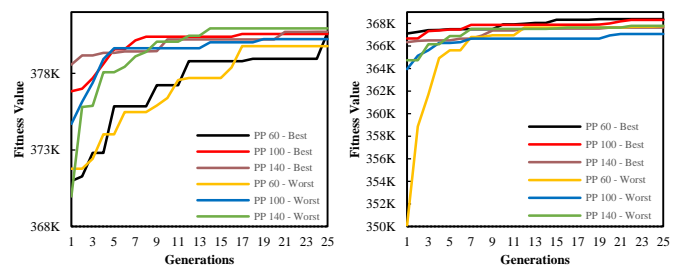
Pivot\GP Generations	1		25		50	
	Best	Worst	Best	Worst	Best	Worst
60	93.9%	87.5%	98.3%	98.1%	98.5%	98.3%
100	95.2%	90.6%	98.6%	98.1%	98.8%	98.3%
140	92.6%	87.0%	98.5%	98.0%	98.5%	98.2%

It is also worth mentioning that from all the runs that have been conducted, the *Port Entropy* were the most prominent feature appearing across all the produced models for the attack. This indicates that this feature has a special significance in the classification process. Entropy values tend to fluctuate higher during attacks, rendering the system more sensitive to such fluctuations[30].

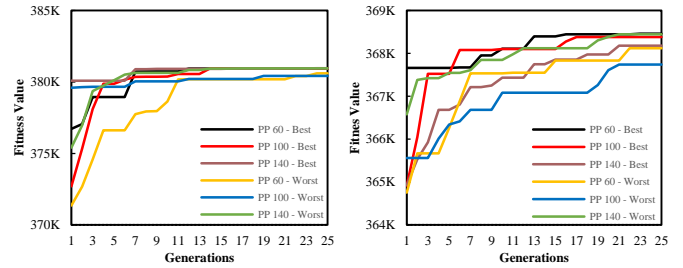
It is evident that the implementation of the Hill-Climbing method has helped in increasing the convergence performance. It can be seen from the graphs that the settings that were tested with the 100 pivot-point yielded a highest initial fitness value and continued to converge competitively quicker than the other two pivot-points, which means that the selection of the pivot-point is critical and can contribute to better results. To validate the results, a confidence interval metric based on a 95% confidence level is implemented. The confidence value is calculated based on the average accuracy of five different runs for each setting. It means that if the experiments are to be repeated, the output of the accuracy value will still fall between the calculated confidence interval ranges. Fig. 7 shows the results of implementing the confidence metric of detection accuracy for the attack, anomaly and normal classes.



(a1) Attack convergence with 1 inner-layer GP generations (a2) Normal convergence with 1 inner-layer GP generations



(a2) Attack convergence with 25 inner-layer GP generations (a2) Normal convergence with 25 inner-layer GP generations



(a3) Attack convergence with 50 inner-layer GP generations (a3) Normal convergence with 50 inner-layer GP generations

Fig. 6. Convergence Performance for the GP using the Three Pivot-Points with the Best (S2) and Worst (S11) Settings.

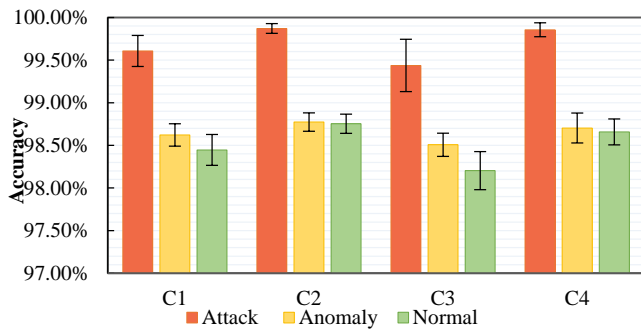


Fig. 7. Confidence Interval of 95% for the, Attack, Anomaly and Normal Labels.

It can be seen from the results in the figure above that the confidence interval for testing the developed system using the common settings C2 and C4 yielded the least error rates with 0.06% and 0.08% respectively for the attack detection. These two settings compared to the remaining settings, have the highest number of GP population, which means that the GP positively contributed to the consistency and coherence of the results, due to the higher diversity of the possible solutions, regardless of the final accuracy value.

C. Comparative Study

Supplementary tests were carried out to evaluate the performance of the developed system. The system is compared to four state-of-art supervised learning techniques. These techniques are Fuzzy Hybrid Genetic Based Machine Learning (FH-GBML)[31], Genetic Programming-based learning of Compact and Accurate Fuzzy rule based classification for High Dimensional Problems (GP-COACH) [32] and Genetic Programming with AdaBoost (GPBoost) [33]. All of the previously mentioned techniques are implemented in well-known data mining tools such as KEEL [34] and WEKA [35].

FH-GBML is a Fuzzy Rule-Based Classification System (FBRCS) that establishes a combination of Michigan and Pittsburgh style methods. Additionally, it implements Genetic Cooperative Competitive Learning (GCCL) [36]. The GCCL approach mainly encodes a single fuzzy rule per individual. The main idea of FH-GBML is to generate a random population of rule sets using the Pittsburgh approach followed by one iteration applying the genetic operators. Then a pre-defined probability is calculated to decide whether to perform a single Michigan iteration for the whole rule set or not. Those new rules generated by the Michigan iteration replace the original rule set. Finally, all the rule sets generated during the Pittsburgh process replace the whole population by applying Elitism. GFS-Adaboost is a similar system to FH-GBML but makes use of Adaboost to boost the fuzzy rules along with the iterative genetic algorithm tuning [37].

While FBRCS provides high accuracy, the generated rule sets are usually complex and substantial, which may render them impractical for systems where execution speed is a crucial factor. GP-COACH simplifies the generated rule sets with minimal loss in accuracy incorporating Genetic Programming.

GP-COACH aims to compress the rule set after the learning phase. It uses the GCCL approach while employing token competition to promote diversity. Rules are codified in a context-free grammar fashion that enables new children to be corrected, maintaining the validity of the population. The population is then evaluated according to a global fitness function that promotes both accuracy and interpretability.

GPBoost uses Genetic Programming in conjunction with a boosting algorithm known as AdaBoost. Boosting algorithms are suitable for binary classification problems because they are capable of finding highly accurate classifications by combining many weaker classifiers, each of which is accurate. In each iteration, the algorithm updates the weights of the training examples based on those which have been already classified correctly using the current classifiers. GP can provide reasonably accurate models, which can act as weak classifiers for AdaBoost. Combining boosting with GP always provides better results compared to the results obtained with standalone GP. In this version of GPBoost, AdaBoost is extended to support multiclass classifications [38]. Each algorithm has been run 5 times and the average accuracy value along with the 95% confidence interval are calculated. The parameters used for each algorithm are the ones recommended by their original authors.

Accuracy (Acc.), Sensitivity (Sen.) and Precision (Pre.) are used as performance metrics for attack (TK), normal (NR) and anomaly (AM) labels. These metrics are commonly used in the evaluation of binary classifications in soft computing, but can also be used for multi-class classifications[39]. Table VII presents the evaluation results for the proposed system, FH-GBML, GP-COACH, GFS-AdaBoost and GPBoost.

The developed system achieved the highest accuracy among all the labels compared to the other four techniques. It also achieved the highest recall value for the anomaly label, thus correctly detecting the highest number of anomaly instances. FH-GBML achieved a similar performance compared to our approach in terms of attack and normal instance classification; however, achieving a precision of 100% and sensitivity of 0% signifies that it failed to detect any anomaly instances. This also proves the $96.5 \pm 0\%$ confidence interval for the anomaly accuracy. Additionally, it is evident that all methods that implement fuzzy logic have the best confidence interval values for the attack label due to the ability of fuzzy systems to tolerate imprecisions and uncertainties [40]. GFS-AdaBoost has benefited from the

boosting, improving its ability to detect a few anomaly instances in comparison to the FH-GBML and GP-COACH which detected none.

GPBoost is the closest competitor to the proposed system in terms of design structure. It achieved lower scores than the proposed system in all classes. This implies that the outer-layer GA layer was successfully able to fine-tune the inner-layer GP expressions yielding better results. The use of FSM also decreased the total number of GP expressions required by one, in contrast to GPBoost that requires an expression for each label. GP-COACH has the lowest overall performance among all the tested techniques. It is apparent that it is the most sensitive method for attacks. This means it has a very low false negative rate. On the other hand, it achieved the lowest precision value indicating a high false positive rate.

To further validate the results of the proposed system, a Two-Sample Mann-Whitney-Wilcoxon (MWW) test is conducted. MWW is a nonparametric statistical test that is best suited for evaluating evolutionary algorithms due to their non-deterministic nature [41]. Table VIII shows that the proposed system has the best overall accuracy with a high confidence value, displaying statistically significant results ($P < 0.05$).

TABLE VII. COMPARISON BETWEEN ACCURACY, SENSITIVITY AND PRECISION OF EACH LABEL FOR THE DIFFERENT ALGORITHMS

Metric	Label	Proposed System	FH-GBML	GP-COACH	GFS-AdaBoost	GP Boost
Acc. (%)	TK	99.77 ± 0.3 %	99.48 ± 0.18 %	95.9 ± 0.25 %	97.21 ± 0.16 %	98.72 ± 1.04 %
	NR	98.63 ± 0.48 %	96.6 ± 0.25 %	95.28 ± 0.34 %	98.16 ± 0.73 %	97.09 ± 0.38 %
	AM	98.8 ± 0.24 %	96.5 ± 0 %	96.5 ± 0 %	97.16 ± 0.13 %	97.37 ± 0.31 %
Sen. (%)	TK	99.74 ± 0.02 %	99.76 ± 0.01 %	99.79 ± 0.02 %	99.65 ± 0.14 %	98.55 ± 2.2 %
	NR	98.93 ± 0.69 %	99.79 ± 0.05 %	95.95 ± 0.11 %	98.65 ± 0.54 %	98.8 ± 0.82 %
	AM	81.63 ± 8.31 %	0 ± 0 %	0 ± 0 %	21.82 ± 2.09 %	58.1 ± 6.63 %
Pre. (%)	TK	99.48 ± 1.01 %	98.49 ± 0.61 %	87.71 ± 0.45 %	91.49 ± 0.48 %	97.55 ± 1.92 %
	NR	98.98 ± 0.44 %	95.37 ± 0.3 %	96.76 ± 0.42 %	98.62 ± 0.58 %	96.98 ± 1.15 %
	AM	84.03 ± 4.27 %	100 ± 0 %	100 ± 0 %	88.07 ± 7.91 %	77.4 ± 11.99 %

TABLE VIII. OVERALL ACCURACY AND SIGNIFICANCE OF THE PROPOSED SYSTEM AND OTHER ALGORITHMS

Metric	Proposed System	FH-GBML	GP-COACH	GFS-AdaBoost	GP Boost
Overall Accuracy (%)	98.6 % ± 0.48 %	96.29 % ± 0.04 %	93.92 % ± 0.37 %	96.26 % ± 0.46 %	96.20 % ± 0.99 %
P-Value	-	< 0.05	< 0.05	< 0.05	< 0.05

V. CONCLUSION

In this research, a hybrid system consisting of Genetic Algorithms (GA), Genetic Programming (GP) and Finite State Machine (FSM) for the detection of high-volume DoS attacks along with anomalous DoS events was developed. Hill-Climbing was employed to search for a suitable pivot-point to be used for the evaluation of the GP expression. A synthetic dataset that mimics a real-world network traffic has been used to test the proposed system in comparison with several state-of-the-art techniques. The results show that the developed system achieved better overall performance in terms of accuracy, sensitivity and precision with 95% confidence intervals. MWW is applied for further validation, achieving a P-value of < 0.05 , rendering the proposed system statistically significant.

For future work, it is suggested to test the system with a larger dataset containing a larger number of attack labels and validate it by comparing it to more state-of-the-art techniques other than the ones used. A mitigation system applying the findings of the detection system should still be implemented into different types of networks, to assess how the system will perform when dealing with various types of network features and topologies. Also, the chromosomes of the GP can be further investigated in terms of mathematical formulation, which in turn, can establish a rigorous mathematical framework for the proposed system.

REFERENCES

- [1] L. Roberts, "The Arpanet and computer networks," Proc. ACM Conf. Hist. Pers. Work., pp. 51–58, 1986.
- [2] C. HAYTHORNTHWAITE, "Introduction: The Internet in Everyday Life," Am. Behav. Sci., vol. 45, no. 3, pp. 363–382, 2001.
- [3] T. Qiu, N. Chen, K. Li, M. Atiquzzaman, and W. Zhao, "How can heterogeneous internet of things build our future: A survey," IEEE Commun. Surv. Tutorials, vol. 20, no. 3, pp. 2011–2027, 2018.
- [4] E. Molina and E. Jacob, "Software-defined networking in cyber-physical systems: A survey," Comput. Electr. Eng., vol. 66, pp. 407–419, 2018.
- [5] N. Hoque, D. K. Bhattacharyya, and J. K. Kalita, "Botnet in DDoS Attacks: Trends and Challenges," IEEE Commun. Surv. Tutorials, vol. 17, no. 4, pp. 2242–2270, 2015.
- [6] A. Pras, R. Sadre, A. Sperotto, T. Fioreze, D. Hausheer, and J. Schönwälder, "Using NetFlow/IPFIX for network management," J. Netw. Syst. Manag., vol. 17, no. 4, pp. 482–487, 2009.
- [7] M. Ahmed, A. Naser Mahmood, and J. Hu, "A survey of network anomaly detection techniques," J. Netw. Comput. Appl., vol. 60, pp. 19–31, 2016.
- [8] A. A. Aburomman and M. B. I. Reaz, "A survey of intrusion detection systems based on ensemble and hybrid classifiers," Comput. Secur., vol. 65, pp. 135–152, 2017.
- [9] A. L. Buczak and E. Guven, "A Survey of Data Mining and Machine Learning Methods for Cyber Security Intrusion Detection," IEEE Commun. Surv. Tutorials, vol. 18, no. 2, pp. 1153–1176, 2016.
- [10] D. E. Goldberg and J. H. Holland, "Genetic Algorithms and," Machine Learning, vol. 3, no. 2–3, pp. 95–99, 1988.
- [11] J. R. Koza, "Genetic programming as a means for programming computers by natural selection," Stat. Comput., vol. 4, no. 2, pp. 87–112, 1994.
- [12] C. Darwin, The origin of species by means of natural selection: or, the preservation of favoured races in the struggle for life and the descent of man and selection in relation to sex. Modern library, 1872.
- [13] A. Rosete-Suárez, A. Ochoa-Rodríguez, and M. Sebag, "Automatic Graph Drawing and Stochastic Hill Climbing," Proc. of the {G}enetic and {E}volutionary {C}omputation {C}onf. {GECCO}-99, pp. 1699–1706, 1999.

- [14] S. Russell and P. Norvig, *Artificial Intelligence: A Modern Approach*, 3rd ed. Upper Saddle River, NJ, USA: Prentice Hall Press, 2009.
- [15] E. M. Knorr and R. T. Ng, "A Unified Notion of Outliers: Properties and Computation," in *Proceedings of the Third International Conference on Knowledge Discovery and Data Mining*, 1997, pp. 219–222.
- [16] J. Mirkovic and P. Reiher, "A taxonomy of DDoS attack and DDoS defense mechanisms," *ACM SIGCOMM Computer Communication Review*, vol. 34(2), pp. 39. <https://doi.org/10.1145/997150.997156>, ACM SIGCOMM Comput. Commun. Rev., vol. 34, no. 2, p. 39, 2004.
- [17] G. Fernandes, J. J. P. C. Rodrigues, L. F. Carvalho, J. F. Al-Muhtadi, and M. L. Proença, "A comprehensive survey on network anomaly detection," *Telecommun. Syst.*, vol. 70, no. 3, pp. 447–489, Mar. 2019.
- [18] A. Saied, R. E. Overill, and T. Radzik, "Detection of known and unknown DDoS attacks using Artificial Neural Networks," *Neurocomputing*, vol. 172, pp. 385–393, 2016.
- [19] T. Hurley, J. E. Perdomo, and A. Perez-Pons, "HMM-based intrusion detection system for software defined networking," *Proc. - 2016 15th IEEE Int. Conf. Mach. Learn. Appl. ICMLA 2016*, pp. 617–621, 2017.
- [20] M. V. De Assis, A. H. Hamamoto, T. Abrao, and M. L. Proença, "A game theoretical based system using holt-winters and genetic algorithm with fuzzy logic for DoS/DDoS mitigation on SDN networks," *IEEE Access*, vol. 5, pp. 9485–9496, 2017.
- [21] A. H. Hamamoto, L. F. Carvalho, L. D. H. Sampaio, T. Abrão, and M. L. Proença, "Network Anomaly Detection System using Genetic Algorithm and Fuzzy Logic," *Expert Syst. Appl.*, vol. 92, pp. 390–402, 2018.
- [22] V. Hajisalem and S. Babaie, "A hybrid intrusion detection system based on ABC-AFS algorithm for misuse and anomaly detection," *Comput. Networks*, vol. 136, pp. 37–50, 2018.
- [23] D. Yuret, "Massachusetts Institute of Technology From Genetic Algorithms To Efficient Optimization," *Artif. Intell.*, no. 1569, 1994.
- [24] M. Srinivas and L. M. Patnaik, "Adaptive probabilities of crossover and mutation in genetic algorithms," *IEEE Trans. Syst. Man, Cybern.*, vol. 24, no. 4, pp. 656–667, 1994.
- [25] QuantAlea AG, "Alea GPU." 2017.
- [26] C. R. Souza, "The Accord.NET Framework." São Carlos, Brazil, 2014.
- [27] I. Sharafaldin, A. Habibi Lashkari, and A. A. Ghorbani, "Toward Generating a New Intrusion Detection Dataset and Intrusion Traffic Characterization," *Proc. 4th Int. Conf. Inf. Syst. Secur. Priv.*, no. Cic, pp. 108–116, 2018.
- [28] K. Li, W. Zhou, S. Yu, and B. Dai, "Effective DDoS attacks detection using generalized entropy metric," in *International Conference on Algorithms and Architectures for Parallel Processing*, 2009, pp. 266–280.
- [29] T. Ding, A. Aleroud, and G. Karabatis, "Multi-granular aggregation of network flows for security analysis," *2015 IEEE Int. Conf. Intell. Secur. Informatics Secur. World through an Alignment Technol. Intell. Humans Organ. ISI 2015*, pp. 173–175, 2015.
- [30] J. David and C. Thomas, "DDoS attack detection using fast entropy approach on flow-based network traffic," *Procedia Comput. Sci.*, vol. 50, pp. 30–36, 2015.
- [31] H. Ishibuchi, T. Yamamoto, and T. Nakashima, "Hybridization of fuzzy GBML approaches for pattern classification problems," *IEEE Trans. Syst. Man, Cybern. Part B Cybern.*, vol. 35, no. 2, pp. 359–365, 2005.
- [32] F. J. Berlanga, A. J. Rivera, M. J. del Jesus, and F. Herrera, "GP-COACH: Genetic Programming-based learning of Compact and Accurate fuzzy rule-based classification systems for High-dimensional problems," *Inf. Sci. (Ny)*, vol. 180, no. 8, pp. 1183–1200, 2010.
- [33] A. T. R. P. Luzia Vidal de Souza and Anselmo C. Neto and Joel M. C. da Rosa, "We are IntechOpen , the world ' s leading publisher of Open Access books Built by scientists , for scientists TOP 1 % Control of a Proportional Hydraulic System," *Intech open*, vol. 2, p. 64, 2018.
- [34] A. F. Hernández, J. L. Uengo, and J. D. Errac, "KEEL: A software tool to assess evolutionary algorithms for Data Mining problems (regression, classification, clustering, pattern mining and so on)," *J. Mult. Log. Soft Comput.*, vol. 17, pp. 255–287, 2011.
- [35] E. Frank, M. A. Hall, and I. H. Witten, *The WEKA workbench. Online Appendix for "Data Mining: Practical Machine Learning Tools and Techniques"*, 4th ed. 2016.
- [36] H. Ishibuchi, T. Nakashima, and T. Murata, "Performance evaluation of fuzzy classifier systems for multidimensional pattern classification problems," *IEEE Trans. Syst. Man, Cybern. Part B Cybern.*, vol. 29, no. 5, pp. 601–618, 1999.
- [37] M. J. Del Jesus, F. Hoffmann, L. J. Navascués, and L. Sánchez, "Induction of fuzzy-rule-based classifiers with evolutionary boosting algorithms," *IEEE Trans. Fuzzy Syst.*, vol. 12, no. 3, pp. 296–308, 2004.
- [38] Y. Freund and R. E. Schapire, "Experiments with a New Boosting Algorithm," *Int. Conf. Mach. Learn.*, pp. 148–156, 1996.
- [39] M. Sokolova, N. Japkowicz, and S. Szpakowicz, "Beyond Accuracy, F-Score and ROC: A Family of Discriminant Measures for Performance Evaluation," in *AI 2006: Advances in Artificial Intelligence*, 2006, pp. 1015–1021.
- [40] L. A. Zadeh, "Fuzzy logic, neural networks, and soft computing," *Commun. ACM*, vol. 37, no. 3, pp. 77–84, 2002.
- [41] J. Derrac, S. García, D. Molina, and F. Herrera, "A practical tutorial on the use of nonparametric statistical tests as a methodology for comparing evolutionary and swarm intelligence algorithms," *Swarm Evol. Comput.*, vol. 1, no. 1, pp. 3–18, 2011.

Using Space Syntax and Information Visualization for Spatial Behavior Analysis and Simulation

Sheng-Ming Wang¹

Department of Interaction Design
National Taipei University of Technology
Taipei, Taiwan

Chieh-Ju Huang²

Doctoral Program in Design
National Taipei University of Technology
Taipei, Taiwan

Abstract—This study used space syntax to discuss user movement dynamics and crowded hot spots in a commercial area. Moreover, it developed personas according to its onsite observations, visualized user movement data, and performed a deep-learning simulation using the generative adversarial network (GAN) to simulate user movement in an urban commercial area as well as the influences such move might engender. From a pedestrian perspective, this study examined the crowd behavior in a commercial area, conducted an onsite observation of people’s spatial behaviors, and simulated user movement through data-science-driven approaches. Through the analysis process, we determined the spatial differences among various roads and districts in the commercial area, and according to the user movement simulation, we identified key factors that influence pedestrian spatial behaviors and pedestrian accessibility. Moreover, we used the deformed wheel theory to investigate the spatial structure of the commercial area and the synergetic relationship between the space and pedestrians; deformed wheel theory presents the user flow differences in various places and the complexity of road distribution, thereby enabling relevant parties to develop design plans that integrate space and service provision in commercial areas. This research contributes to the interdisciplinary study of spatial behavior analysis and simulation with machine learning applications.

Keywords—Spatial behavior; space syntax; information visualization; generative adversarial network (GAN); user movement

I. INTRODUCTION

The spatial movement of people has been presented in various forms in different fields. Approaches to demonstrating and discussing movement results are determined by the relationships perceived by researchers between people and spaces. In addition to the quantitative analysis of spatial data, this study discussed from a pedestrian perspective the relationship between crowds and spaces in commercial areas as well as observed the spatial behaviors of pedestrians onsite. Underpinned by a data-science-driven approach, this study simulated pedestrian movement in different scenarios. Through a simulation, this study determined the spatial differences of user movements in local and global environments in a commercial area, identified the key factors affecting pedestrian spatial behaviors, and discerned pedestrian accessibility within the space. Using a deformed wheel theory, we investigated spatial structures and their synergistic relationship with pedestrians. Moreover, we examined the differences of user movements in various areas and the complexity of space and

route distribution to provide recommendations on transport and spatial planning as well as to outline a design method for future integration between spaces and services in commercial areas. This study is to discuss the predictions of user spatial behavior and pedestrian movement simulations within the established business area. For the movement of hanging around and the consumption movement except walking are not discussed in this study.

In the following of this paper, we extracted the diverse elements of a city by space syntax, observed and collected pedestrians’ movement and behaviors from different groups in a commercial area, segmented personas, and then used a deep-learning GAN to integrate and analyze collected data and perform simulations. Then we discussed how data-science-driven concepts and data visualization could be used in the establishment of user movement and environmental behaviors in urban commercial areas. In the end of this paper, we tried to make the recommendations for further study.

II. LITERATURE REVIEW

A. Space Syntax and Deformed Wheel Theory

Urban space planning, which is focused on the relationship between spaces and people, may be analyzed using space syntax. Space syntax involves factors such as the main entrances and exits of cities, means of transport for cross-regional travel, and the structure of public spaces. Factors in the discussion of urban space planning include land use, urban functions, and the spatial behaviors of people in an area [1]. Hillier and Han [2] introduced the space syntax theory in “The Social Logic of Space”; it suggests that the movement scale of user activities and spatial distribution can be divided into the following basic elements: axial, convex, and isovist spaces. Space syntax emphasizes the patterns of pedestrian activities in a city, as well as relevant spatial measurements and relationships between spaces and social lives [3]. Space syntax presents graphic spatial data that are then used to discuss environmental factors influencing user’ spatial behaviors and experience. Such quantified data reveal the relationships among urban roads, blocks, and buildings [4]. Accordingly, space syntax provides attribute information that can be used in designs for solving or alleviating problems that exist in urban spaces [5].

Taiwanese studies using space syntax are predominantly related to urban planning and geographic environments; space syntax can be used to provide comprehensive and quantitative

analyses and recommendations for urban and route planning improvement in business activities. Therefore, this study used space syntax as a tool to analyze spatial behaviors and user movement, and then give service design suggestions in the future business environment.

The operation of an urban system can be interpreted using syntactic relation systems, such as symmetry–asymmetry, integration–segregation, the determination of control values, integration of features and control cores, and intelligibility and predictability [6] [7] [8] [9]. The fundamental concept of space syntax is that urban areas can all be represented using matrices of connected spaces; such matrices can be simulated and calculated using a computer and reveal space attributes using data [10]. The nature of space syntax is to show the interaction among and presentation of spatial patterns, user behaviors, and cultures [11]. Relationships between the spatial patterns of human settlements and activities are presented using business models, social structures, and ideologies [12]. Space syntax can predict the most crowded destinations, which should have the most highly integrated roads placed adjacent to them [13].

Space syntax is a digital tool that facilitates data quantification and provides spatial measurements of personal space and overall layout. It measures the connectivity between spaces as well as a space’s connectivity to the overall environment, and furthermore, it calculates the depth and spatial integration of a space. Depth is defined as the minimum steps required to reach a space from another, and connectivity refers to the number of spaces that a space is immediately connected to [14].

In quantitative studies, space syntax presents the spatial layout through topological distance and provides dynamic locations and distribution of people. More crucially, it reveals the walkability as well as pedestrians’ movement and route choices [15]. In space assessment, space syntax has three indicators of distance [16] [17] [18]:

- Topological distance: the route with the fewest number of turns.
- Geometric distance: the route with the smallest angle change.
- Metric distance: the route with the shortest length.

According to the theory of topological structures, space syntax contains three basic spatial elements for discussing the relationships among buildings, physical urban spaces, and their functions for activities ([19] Fig. 1):

- Convex space: a space where any two of its points are intervisible points.
- Axial space: a space formed by straight lines, such as roads.
- Isovist space: the total space that can be viewed from any point, in which the relationships between each connecting spatial element can also be viewed.

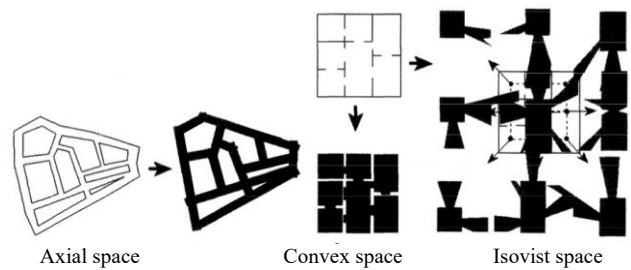


Fig 1. Models of Space Syntax’s Three Spatial Elements [20a].

Space syntax transforms physical spaces into topological structures that comprise nodes and lines. Fig. 2 depicts the process of using quantitative indicators to assess the structural characteristics of global or local spaces. These quantitative data are generated using the location of each spatial element and the connections between them in a system. Connected axial lines intersect at a node, which reveals the relationships among structural elements in a spatial system and enables investigation of the relative depth from one structural element to another.

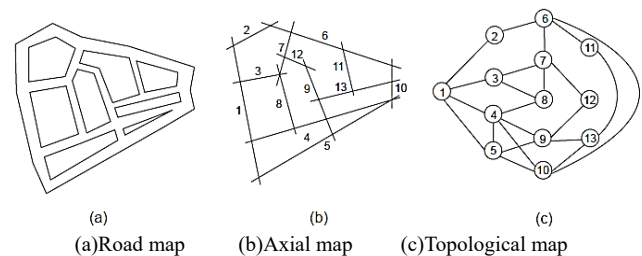


Fig 2. Spatial Transformation of Space Syntax [20b].

TABLE I. USER SEGMENTS EQUATIONS IN SPACE SYNTAX [21]

Mean Depth	$MD_i = \frac{1}{n-1} \sum_{j=1}^{n-1} d_{ij}, i \neq j$	M distance of the <i>i</i> -th axis from all the other <i>n</i> - 1.
	Basic centrality measure: it accounts for the distance between each axis and all the others, with the shallowest axis being the closest to all the others and the deepest being the farthest one. In a city with a perfectly circular axial map, the shallowest axis would be close to the center and the deepest would be on the perimeter.	
Connectivity	$C_i = k_i$	Number of axes connected to the <i>i</i> -th axis.
	Measures how much an axis is directly connected to the others. Axes with high C_i make it easier to pass through the areas.	
Global Integration	$RA_i = \frac{2(MD_i-1)}{n-2}$ $RA_N^D = \frac{2 \left\{ n \left[\log_2 \left(\frac{n+2}{3} \right) - 1 \right] + 1 \right\}}{(n-1)(n-2)}$ $RN = \frac{RA_N^D}{RA_i}$	Normalize <i>d</i> value of MD_i being $\min(MD_i) = 1$ and $\max(MD_i) = n/2$.
	RA expresses the centrality of an axis comparing its actual Mean Depth with the theoretical highest and lowest values that Mean Depth could have in the given graph. Compared to Mean Depth alone, Relativized Asymmetry is a normalization between 0 and 1.	
Control Value	$CTRL_i = \sum_{j=1}^{k_i} \frac{1}{C_j}$	Sum of the inverse values of C_j for the k_i axes connected to the <i>i</i> -th axis.
	Sum of the inverse values of C_j for the k_i axes connected to the <i>i</i> -th axis.	

Table I summarizes the Space Syntax measures analyzed in this research.

- Mean Depth (MD): This is a global indicator that measures the mean shortest route of each spatial element to other elements in a system through the relative depth between axial lines.
- Number of connections (Cn): This is a local indicator showing the number of elements adjacent to a particular element; a high CN value (a high number of immediately connected elements) indicates high accessibility and high publicness of that element.
- Global Integration (Rn): This is a global indicator; a higher RN value of an element indicates higher global integration of that element, namely it being more integrated in a spatial system. Specifically, this means that pedestrians can reach other roads in fewer steps from such an element.
- Control Value (CV): This is a local indicator revealing the extent to which adjacent elements control each other. A high number of elements adjacent to a particular result in high CVs of that element.

Deformed wheel theory in space syntax reveals the original structures of spaces that show the synergic relationships among the spaces. Deformed wheel is a semigrad or hub of lines near the central line that reveals a space's relevant information and characteristics. The spokes of a deformed wheel connect the center to the edge and form an enclosed space. The formation of a space comprises the following six steps:

- Place interaction: From the perspective of nodes and lines, a higher number and longer duration of user activities in a node indicate a lower number and shorter duration of people staying in the lines. By contrast, a higher number and longer duration of people staying in the lines indicate fewer and shorter durations of user activities in the node.
- Place identity: Place identity is related to people in a place. People coexist with places, and place identity emphasizes user in a place.
- Place release: This refers to unexpected and accidental events that elicit user enthusiasm and interests.
- Place realization: This refers to distinct events in a place that underlie its historical or cultural meanings.
- Place creation: This reveals the real needs of a place, such as its commercial or environmental characteristics.
- Place intensification: This denotes a place's features, which are formed through its design, policies, and city structure.

B. Simulation and Visualization of User Movement

Pedestrian movement is predominantly presented using spatial configuration variables, which represent the

characteristics of a road network. By overlaying pedestrian walking distribution on simulated traffic, conflicts between user and traffic can be identified and predicted on certain routes [22]. Accordingly, a quantitative analysis of space syntax provides insight into users' spatial behaviors as well as reveals connectivity among spaces through topological structures derived from axial maps, which also enables discerning the structures of movement networks. Thus, space syntax can be used to investigate how the structure of a spatial network affects people's movement in an urban environment or an indoor space.

To simulate and visualize user movement in commercial areas, this study employed a deep-learning generative adversarial network (GAN) to simulate a large amount of data using user movement data collected during our onsite observations. The study compared visualizations of the simulated data with space syntax results, discussed the similarities and differences between the two methods, and predicted future environmental behaviors of users.

Deep learning is a type of machine learning in artificial intelligence. Machine learning involves training large amounts of data through algorithms to establish mathematical models that facilitate data prediction. Using artificial neural networks (ANNs), which simulate the mechanism of human neural networks, deep learning increases the computational efficiency of central processing units and graphic processing units in computers and has developed rapidly with the increased prevalence of parallel computing. Data analysis of artificial intelligence is underpinned by data collection and algorithms that simulate user analysis patterns. Specifically, artificial intelligence entails a deep-learning mechanism fulfilled by computing.

The mechanism of a GAN comprises two deep-learning ANNs, namely a generator and a discriminator. The mutual learning between the two networks enables the GAN to simulate data that are comparable to the actual data [23]. Fig. 3 presents the mechanisms of a GAN. First, the generator generates random data and the discriminator uses the actual data to determine whether the generated data are flawed; subsequently, the generator corrects its network model accordingly. Through mutual learning and optimization of the model, the generator will be able to generate data that are highly comparable to the actual data. Therefore, when large amounts of simulated data are required under circumstances where few actual data are available, this algorithm may be employed.

This study employed a GAN because such a network can, using the existing actual data, simulate an unlimited amount of data that are similar to the actual data. Therefore, when large amounts of data are required yet only limited sample data are available, a GAN might be used to simulate logical data, as opposed to randomly simulated data. Thus, a GAN is useful for simulation analyses and prediction.

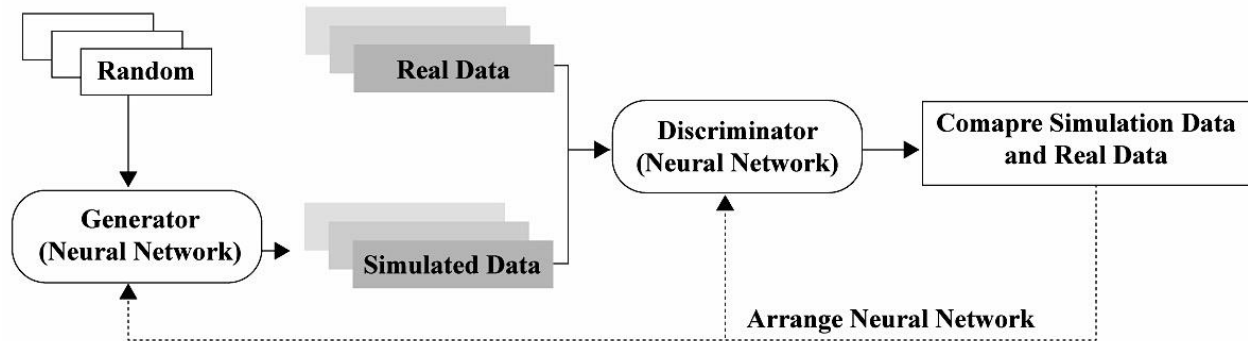


Fig 3. Mechanism of a GAN.

C. Research Site

This study focused on the Fengjia night market commercial area (the basic cartographic data are shown in Fig. 4), which is adjacent to Fengjia University and near downtown Taichung; thus, it has become a major tourist destination in Taichung. This commercial area plays a crucial role in the development of Taichung city and is often considered a highlight of a trip to central Taiwan. Fengjia night market, a combination of local culture and geography, has established connections with adjacent areas over more than 40 years of evolution; such an interaction between business and the university has created a unique marketing ecosystem in the region.

From the perspective of city-image design, the basic elements of a city image are edges, paths, nodes, districts, and landmarks [24]. Moreover, urban user activities start and grow outward from these elements. Therefore, this study defined the spatial structure and elements of the Fengjia commercial area from a city-image perspective. We conducted onsite observations to outline the commercial area's spatial structure. According to the observation results (Fig. 4), the section of Wenhua Road located at the upper-left corner (near MOS Burger) is divided into two parts by Fengjia University. We observed that the customer flow split when customers reach the dividing point, and incorporated this observation into our analysis and discussion. In Fig. 4, the major districts of commercial activities are distinguished from other regions; the borders represent the edges of Fengjia commercial area, namely the study's research site; and each line represents a path in this district. Visitors usually entered the commercial area through an entrance near McDonald's (Fengjia Road) or one near the food district on Wenhua Road, which is permits only pedestrian entry at night, whereas students of Fengjia University usually entered the night market through the university's main entranceway (Fengjia Road). The central road of the commercial area is constituted by a section of Fengjia Road between McDonald's and the university's main entranceway, and the intersections between the routes are the nodes where activities occur. The landmarks (represented by triangles) in this commercial area were the two ends of the Fengjia Road section, namely McDonald's and the university's main entranceway, and another university entranceway near MOS Burger. The three landmarks served as the starting points in our analyses.

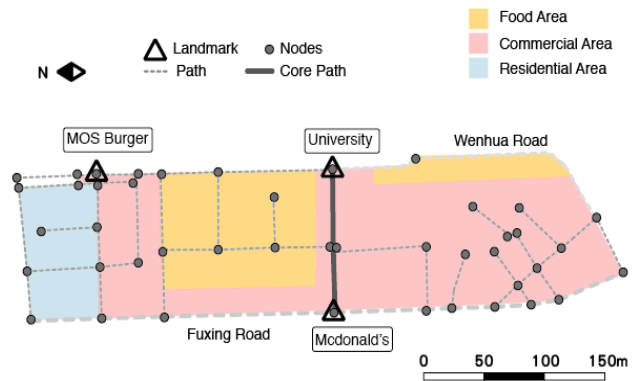


Fig 4. Map of the Fengjia Commercial Area.

This study compiled the locations of nodes and road sections and finalized 67 paths in the commercial area; the commercial area was separated into food, commercial, and residential districts, which were represented by different colors. The landmarks were determined as McDonald's, Fengjia University, and MOS Burger. To provide a clear demonstration of this area, the map is oriented horizontally with a north reference provided.

III. RESEARCH METHODOLOGY

A. Research Framework

According to our literature review, people are the foundational elements in the formation of cities; therefore, research that improves the understanding of and simulates user-behavior patterns and interactive experiences in urban spaces can contribute to the development and improvement of cities and commercial areas as well as improve related information services. Therefore, this study focused on these topics and proposed the research framework in Fig. 5. This study proposed an approach to extract the diverse elements of a city, observed and collected the movement and behaviors of user from different groups in a space, segmented personas, and used a deep-learning GAN to integrate and analyze collected data and perform simulations. Moreover, this study discussed how data-science-driven concepts and data visualization could be used in the establishment of user movement and environmental behaviors in urban commercial areas.

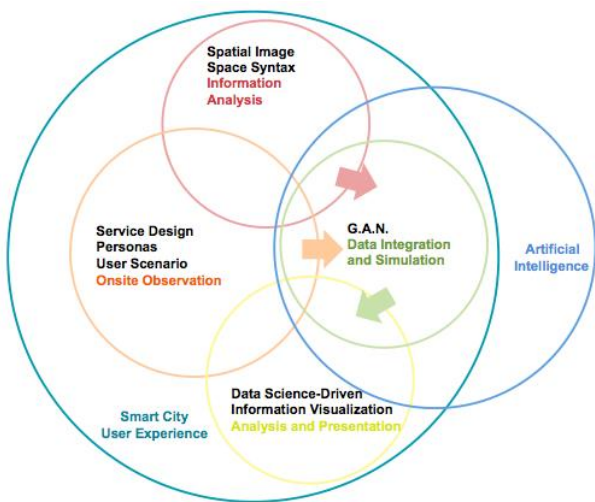


Fig 5. Research Framework.

B. Research Methodology and Assessment

This study focused on how user movement and a deformed wheel interacted differently in the visualized presentations of data yielded using space syntax and data simulation methods. Therefore, this study first observed user movement and behaviors in the research site, set research objectives, and obtained an overview of the research site using space syntax. Subsequently, this study used relevant software to analyze the axial lines and predict user movement in the research site. We defined personas according to our onsite observations and used these personas in space syntax for axial and isovist analyses of the research site, the results of which were used to predict hot spots where people predominantly gathered. From the deformed wheel perspective, the persona analysis results were used to discuss the dynamics of crowd behavior in different districts, which enabled us to identify crucial elements of service design as well as assessments. Finally, movement data of people with defined personas were inputted into simulation software to produce a large amount of user movement data. Subsequently, this study visualized these data and compared the visualization results with those generated using the deformed wheel theory; finally, it provided recommendations for service design and assessment methods that could be adopted in future research.

Mohammadi et al. [24] proposed the following GAN algorithm:

1) The discriminator (D) and generator (G) perform minimization and maximization algorithms simultaneously:

$$\min_G \max_D V(D, G) = \mathbb{E}_{x \sim p_{data}(x)} [\log D(x)] + \mathbb{E}_{z \sim p_z(z)} [\log(1 - D(G(z)))] \quad (1)$$

2) The weight of the discriminator is updated using the following equation:

$$\Delta_{\theta D} \frac{1}{m} \sum_{i=1}^m [\log D(x_i) + \log(1 - D(G(z_i)))] \quad (2)$$

3) The weight of the generator is updated using the following equation:

$$\Delta_{\theta D} \frac{1}{m} \sum_{i=1}^m [\log(1 - D(G(z_i)))] \quad (3)$$

4) GAN algorithm:

- Input: (Source, Destination), Training dataset
- For k = 1 to l do
- Draw m noise samples from $p_g(z)$
- Draw m real examples from $p_d(z)$
- Update the discriminator D based on (2)
- Draw m noise samples from $p_g(z)$
- Update the discriminator D based on (3)
- End for

This study visualized the large amount of data simulated from our experiment and analyses to identify differences between the simulated data and onsite observation results. Such data visualization facilitates interactions for user and reveals relevant information such as visitor backgrounds, purpose of visit, route taken, duration of stay, crowded areas, and distribution of business infrastructure. Moreover, we incorporated scenario simulation into the data visualization and used personas to simulate the spatial experiences for user with various needs and develop a decision support system.

IV. RESEARCH RESULTS AND DISCUSSION

A. Basic Analysis of Space Syntax

We labeled all the roads presented in Fig. 4 (see Fig. 6) and used a topological map to analyze the relationships among them (Fig. 7). According to the topological map, the Fengjia commercial area is divided into two main subareas by sections 1 and 2 of Fengjia Road. At deeper spatial layers are the food, commercial, and residential districts to the north, whereas a food-commercial hybrid district to the south is at a shallower layer because it has fewer roads and connections. Table II compiles locations of the commercial area's city-image elements, such as districts, landmarks, edges, and paths.

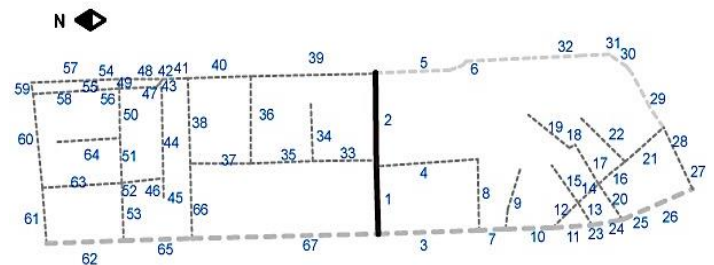


Fig 6. Road Labels in the Fengjia Commercial Area.

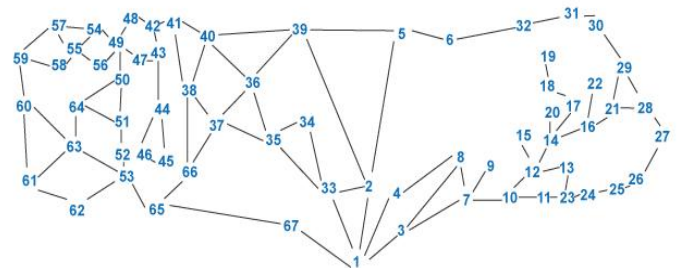


Fig 7. Topological Map of Roads in the Fengjia Commercial Area.

TABLE II. DISTRIBUTION OF CITY-IMAGE ELEMENTS IN THE FENGJIA COMMERCIAL AREA

	District	Landmark	Edge
Food Area A (Nearby MOS Burger)	33, 34, 35, 36, 37, 38, 39, 40, 66		39, 40
Food Area B (Food Street)	5, 6, 32, 31, 30,		5, 6, 32, 31, 30,
Commercial Area	1~29, 38, 41~53, 65~67	McDonald's: 1, 3, 67 Fang Chia University : 2, 5, 39 MOS Burger: 48, 49, 54	39, 5, 3, 7, 10, 11, 23~29, 41, 42, 48, 65, 67
Living Area	49~62		54, 57, 59~62,

TABLE III. SPACE SYNTAX MEASUREMENTS

Items	Paths	Max. Value	Min. Value	Average
MD	67	9.694	4.439	6.152
Rn	67	1.044	0.467	0.723
Cn	67	5	2	3.582

According to Table II, the top three landmarks are all located within the commercial district, which may be because the commercial district constitutes the largest area, and thus has the most roads passing through it. Food districts are distributed in two places; the one near MOS Burger has more roads passing through it than does the one on Wenhua Road.

Using space syntax theory, we incorporated relevant cartographic data into DepthmapX for calculation and analyses, which revealed layers of roads in the Fengjia commercial area; specifically, the mean depth, global integration, and number of road connections were revealed (Table III).

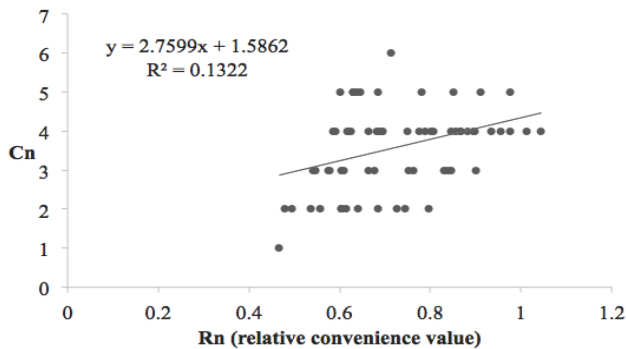


Fig 8. Distribution of RNs and Numbers of Connections.

The mean depth was 6.152, mean global integration was 0.723, and mean number of connections was 3.582. According to Fig. 8, RN and CN show synergy with a weak positive correlation ($R^2 = 0.1322$); a large R^2 (maximum = 1) implies that which user are more able to understand the spatial distribution within an area. Furthermore, high global integration would indicate a high number of connections; however, the positive correlation between them was weak and minor differences between the number of connections and RN was observed. The number of connections did not directly influence RN. Instead, it was because the Fengjia commercial area includes only short sections of roads and has a small area, thereby leading to a predominantly high RN.

The global integration values of roads are visualized in Fig. 9, where a red line represents a high RN and a blue line represents a low RN. In addition, Fig. 9 depicts the distribution of road RN values in the commercial area; the highest RN was observed at the middle section of Fuxing Road, with the RN decreasing toward the two ends. Overall, the RN decreased gradually upward from McDonald's, and roads with relatively high RN were located in the commercial district.

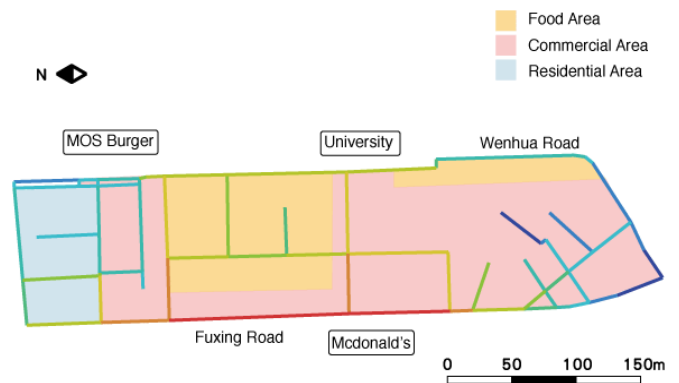


Fig 9. RN of Roads in the Fengjia Commercial Area.

B. Persona Design

1) *User segmentation per attribute*: This study recorded the stop points and observed purchasing behaviors of 65 people from 40 groups in the Fengjia commercial area during the night market's opening hours (6–8 PM). According to the onsite observation results, this study divided the research subjects into three segments and compiled these people's stop points as well as the routes they took. Subsequently, to analyze the distributions of RNs and customers from different segments in-depth, we divided the research subjects and defined each segment's purchase characteristics (Table IV).

TABLE IV. USER SEGMENTS

Segment	Numbers of groups and people	Spatial behaviors	Purchase characteristics
Locals	Six groups (Seven people)	Are familiar with the district distributions and routes and entering the commercial area from various entrances	Know what and how to purchase
Backpackers	30 groups (46 people)	Have researched the area, they know where to locate services they require, and enter the commercial area from various entrances	Have rough purchasing plans and are open to changes
Tour group travelers	Four groups (12 people)	Are unfamiliar with the area's spatial structure and enter the commercial area from the entrance near McDonald's on Fengjia Road	Are uncertain of what to buy, and thus explores the commercial area

- Segment 1: Locals consisting of six groups (one group comprised two people, with seven people in total);
- Segment 2: Backpackers consisting of 30 groups (46 people); and
- Segment 3: Tour group travelers consisting of four groups (12 people).

Table IV shows that the people most familiar with the area's spatial structure were locals (Segment 1), whereas the people least familiar with the spatial structure were tour group travelers (Segment 3). Regarding purchase characteristics, Segment 1 exhibited the most certain attitudes, whereas Segment 3 exhibited the most uncertain attitudes. Segment 2's spatial behaviors and purchase characteristics, namely familiarity with the area and certainty of purchases, were all between those of Segments 1 and 3. Accordingly, the characteristics of the three segments were distinct and their spatial behaviors revealed their distributions in the area.

2) *Persona and Spatial Behaviors*: The spatial behaviors (routes taken and stop points) of people from the three segments were inputted into the QGIS software package to identify hot spots. According to Fig. 10, locals (Segment 1) started their journey predominantly from entrances at the university's main entranceway or McDonald's and mainly proceeded north toward the yellow district (food district) or south toward the night market section on Wenhua Road.

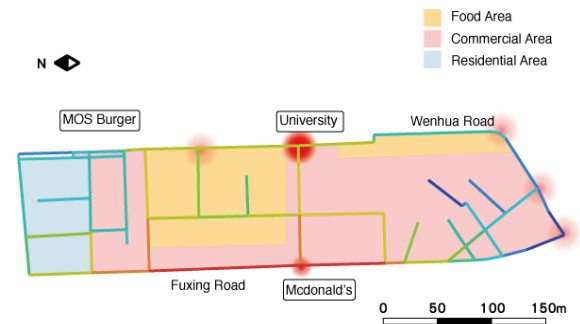


Fig 10. Space Syntax Analysis Map: Stop Points of Segment 1.

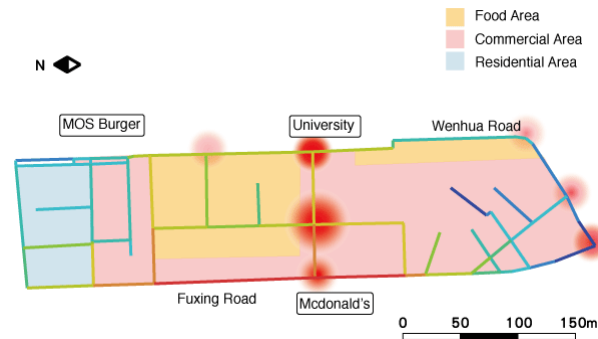


Fig 11. Space Syntax Analysis Map: Stop Points of Segment 2.

Backpackers (Segment 2; Fig. 11) started their journey mainly from road section with high RN (Fengjia Road) and moved south toward the yellow district, namely the night market section on Wenhua Road. The intersections of Fuxing Road and Wenhua Road became hot spots because they were adjacent to transport and parking spots.

Tour group travelers (Segment 3) predominantly stopped at places with high RN (Fig. 12); however, their stop points were scattered all throughout this area. They mainly spread along the roads from two landmarks, namely the night market entrance at the university's main entranceway and that near the McDonald's.

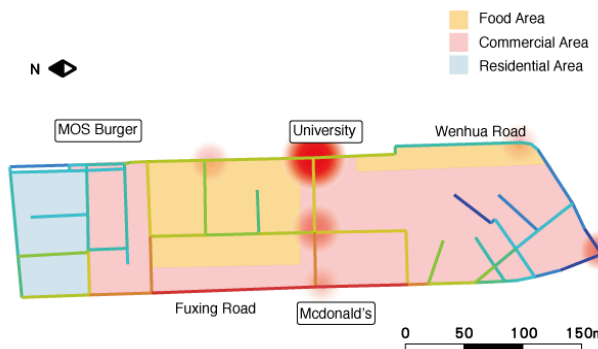


Fig 12. Space Syntax Analysis Map: Stop Points of Segment 3.

C. Crowd Behavior Analysis

Crowd behavior analysis involves using a computer to simulate pedestrian movement and crowd behavior in a space. It provides insights into pedestrian spatial behaviors, namely the relationship between space and pedestrian behavior and the interaction between space and pedestrians. According to the descriptions of user personas, pedestrians entered the Fengjia commercial area from various entrances; therefore, the crowd behavior we observed at different entrances was analyzed separately. Crowd density was presented using a color gradient from red (highest density) to blue (lowest density).

Fig. 13 presents the predicted crowd behavior without any focused entrance. The most crowded area (red section) is located at the center of Fengjia Road, with crowd density decreasing outward along the road.

Fig. 14 illustrates the predicted distribution of crowds using the entrance near McDonald's; the results were consistent with those shown in Fig. 14 (no focused entrance), which might be because the landmarks in this commercial were located at both ends of this road section. Accordingly, future research could use McDonald's as the main entrance to investigate crowd behavior and hot spots in this commercial area. In addition to McDonald's being a landmark, it was also a crucial indicator because it was located at the top of a key road in this area.

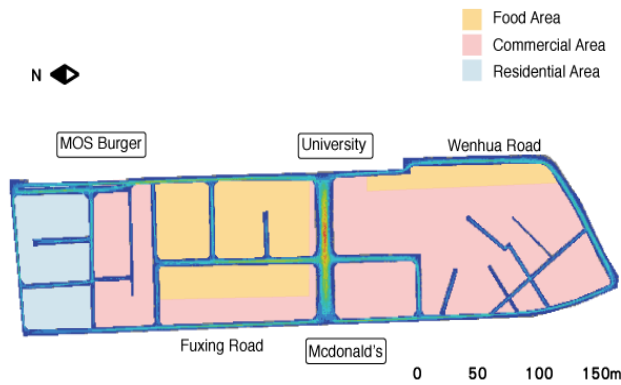


Fig 13. Predicted Crowd Behavior in the Fengjia Commercial Area without any Focused Entrance.

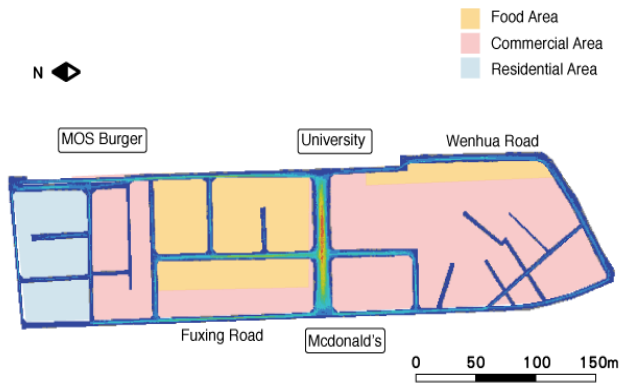


Fig 14. Predicted Crowd Behavior in the Fengjia Commercial Area: Using McDonald's as the Entrance.

Signage for Fengjia night market were provided at the intersection of Fuxing Road and Wenhua Road as well as near the parking lot located at the southern end of the commercial area. Fig. 15 illustrates the predicted crowd behavior of people entering the commercial area at the intersection of Fuxing Road and Wenhua Road; the most crowded area is on the section of Wenhua Road between the intersections with Fengjia Road and Fuxing Road. According to the night market's layout, this road section was one of two food districts in the commercial area. Food street vendors were located on both sides of this road section, which was adjacent to the commercial district; therefore, this road section exhibited the densest crowds. When we compared a panoramic photograph of the intersection of Fuxing Road and Wenhua Road with the map in Fig. 15, the right end of the panoramic photo indicated the entrance shown in Fig. 15. Because a signage for Fengjia night market was provided at this intersection, people driving there along Fuxing Road usually entered the commercial area from this entrance.

Fengjia University is a crucial landmark in this commercial area as well as a commonly used entrance into the commercial area for students. Fig. 16 presents the predicted crowd distribution in the commercial area of people entering from the university's main entranceway. Fengjia Road has the densest crowds, which is similar to the result when people enter through the entrance near McDonald's. This means that people entering the commercial area from the two ends of Fengjia Road mostly gathered along this section of road.

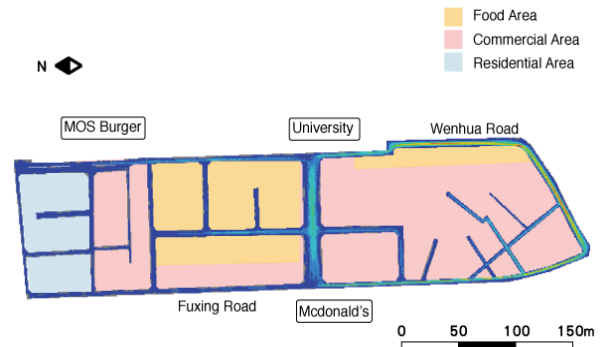


Fig 15. Predicted Crowd Behavior in the Fengjia Commercial Area: Intersection of Fuxing and Wenhua Roads as the Entrance.

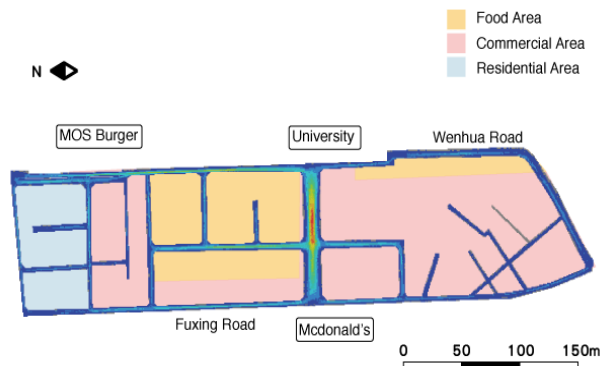


Fig 16. Predicted crowd behavior in the Fengjia Commercial Area: Fengjia University's Main Entranceway as the Entrance.

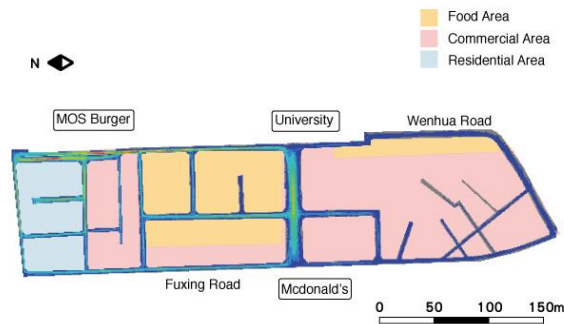


Fig 17. Predicted Crowd Behavior in the Fengjia Commercial Area: University Entranceway Near MOS Burger as the Entrance.

Another entranceway to Fengjia University is near MOS Burger located at the northern end of the commercial area (indicated by the red arrow in Fig. 17). Therefore, we also predicted the distribution of people entering the commercial area from the university entranceway near MOS Burger. According to Fig. 17, the most crowded area is on the Wenhua Road section near MOS Burger, and this road section passes through both food and residential districts. A reason might be that students at the university usually entered the commercial area through the university entranceway near MOS Burger. These maps of predicted crowd behavior can be used to plan and design services for students of the university.

D. User Movement Simulation and Visualization Analysis

1) *Collection cartographic data of the research site:* To record the road locations of pedestrians in the Fengjia commercial area, this study employed cartographic data provided by the Taiwan MAP Service (<https://maps.nslc.gov.tw/>) to pinpoint the locations of buildings, outline edges, and centerlines of the roads in the research site, as well as to define the site borders. Using digital cartographic data, Google Maps street view, and 360° panoramic photos and videos captured onsite, we produced a map of the research site with the edges and centerlines of roads indicated (Fig. 18 and 19). The blue-outlined road sections are those within the research site and the red lines are the road centerlines. According to our onsite observations, both vehicles and pedestrians are allowed on Fuxing Road and Xi'an Street; thus, the edges of the research site along the two sections of road were defined as being 3–5 m from buildings outward toward the roads. The remaining road sections were all only for pedestrian entry at night, and thus their road edges were defined as those shown in the cartographic data.

2) *Setting conditions for persona movement:* Following relevant studies related to GANs, which have predominantly adopted graphic data in their training processes, the present study collected graphic data of user movement, adapted its source code from another study [25], and employed a Keras-GAN. A sufficient amount of actual data is required before training a GAN; therefore, randomly simulated user movement data were produced before sufficient data were collected. According to the persona definitions in Table IV, we defined their spatial behaviors according to the characteristics

of the three segments (Table V), which served as the conditions and constraints used for subsequent simulations.



Fig 18. Road Edges and Centerlines in the Research Site.



Fig 19. Zoomed View of the Road Map.

TABLE V. SPATIAL BEHAVIOR SETTINGS OF PERSONAS

Segments	Max. walking distance per minute	Max. stopping time	Spatial behaviors
Locals	50 m	30 minutes	They know what to purchase, and thus tend to head to their destinations for purchases immediately after entering the commercial area and stop at shopping spots for relatively short durations.
Backpackers	40 m	120 minutes	They usually have planned their routes in advance according to shopping categories they are interested in. They orient themselves in this area after entry and make necessary changes to their plan. They stop at shopping spots for varying durations.
Tour group travelers	20 m	90 minutes	They are relatively open to what to purchase; bound to a tour group, they stop at limited places in the commercial area and for limited durations.

According to the purchase characteristics of the three customer segments and our onsite observations, the customers' spatial behaviors were defined as being distinct from one another. To generate pedestrian movement, we defined the maximum walking distance per minute and stopping durations in the commercial area of the three customer segments according to their spatial behaviors.

The interval between each two consecutive simulated positions of a pedestrian was determined at 1 minute in our simulation experiment. Therefore, in the commercial area, we recorded pedestrian positions, defined their maximum walking distance per minute, and tracked their movement sequences and directions to generate their movement tracks, which consisted of the recorded points. The largest point of each track indicated the position where the pedestrian spent the longest time during the recorded journey. For example, a recorded duration of 30 minutes yielded 31 points (including the starting point) on a pedestrian's movement track.

3) *User movement visualization and analysis:* According to the characteristics (Table IV) and spatial behaviors (Table V) of the customer segments, this study proceeded with data collection in the commercial area and finalized the sample size at 45 groups of people, with a total of 89 people; the sample comprised 32 groups of locals (55 people), 10 groups of backpackers (22 people), and three groups of tour group travelers (12 people). The main entrances of the commercial area comprised those at the three landmarks and one at the intersection of Wenhua Road and Fuxing Road. These graphic data were inputted into the Keras-GAN to simulate graphic user movement data; the process was as follows. The collected movement data were inputted in the Keras-GAN for training, and each training cycle involved 30 pictures. Fig. 20 presents the results at the 1000th training cycle, during which a large amount of noise was observed. Fig. 21 shows the results at the 1600th training cycle, during which the road edges became clearer and the simulated movement tracks were mostly located within the research site.

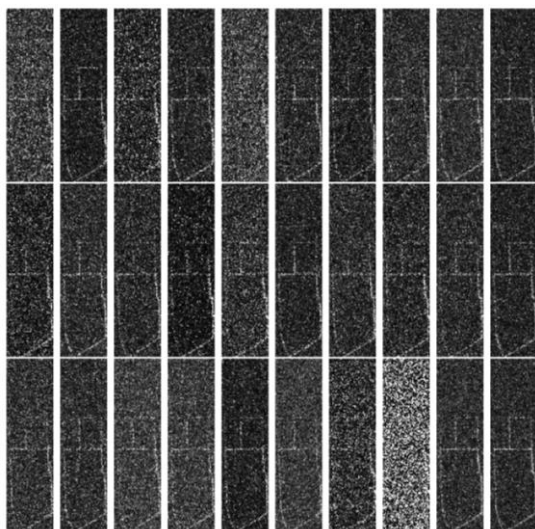


Fig 20. Simulated Results of Movement Tracks at the 1000th Training.

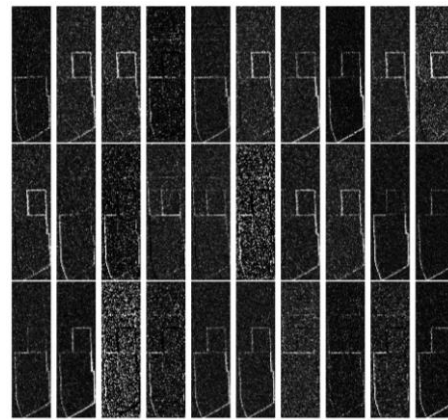


Fig 21. Simulated Results of Movement Tracks at the 1600th Training Cycle.

We continued the training and outputted a graphic result for each 100 training cycles. Fig. 22 presents the movement track results of the 2000th training cycle; the variation among the graphic results became smaller. Fig. 23 is the result of the 2400th training cycle, after which the movement track results started to converge. If the overfitting problem is encountered during ANN training, the ANN might produce pictures that are highly similar to the original inputs. Therefore, this study set the GAN's maximum training cycle to 2400.

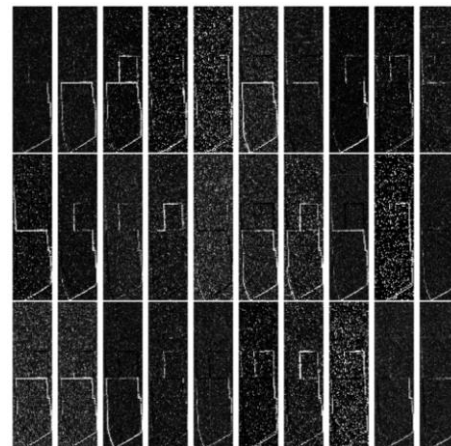


Fig 22. Simulated results of movement tracks at the 2000th training cycle.

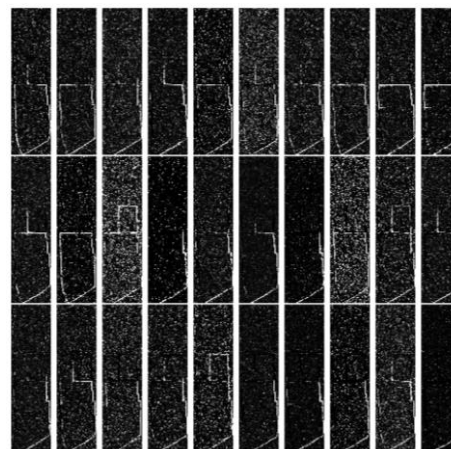


Fig 23. Simulated results of movement tracks at the 2400th training cycle.

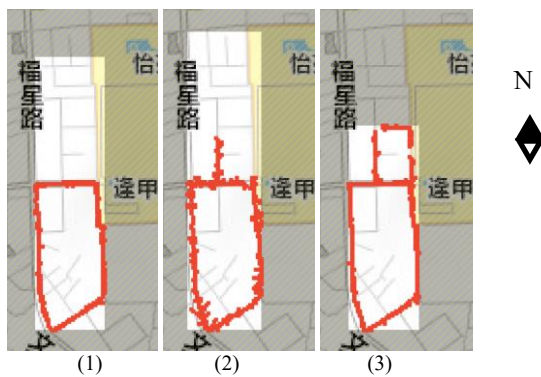


Fig 24. Pictures of the Three Most Common Movement Tracks Simulated During Training.

We extracted one simulated result every 100 training cycles between the 1600th and 2400th training cycles; the nine simulated results provided a total of 270 pictures of movement tracks, and the three pictures with the most occurrences were combined with the cartographic data for subsequent analyses. Fig. 24(1) shows that most pedestrian movement was concentrated at the south of the commercial area, namely from Fengjia Road southwards to the night market section on Wenhua Road and back to Fengjia Road through Fuxing Road. Fig. 24(2) presents a pedestrian movement track on Lane 20 of Fengjia Road (food district), in addition to that shown in (1). Fig. 24(3) includes both pedestrian movement tracks shown in (1) and (2) and shows an additional pedestrian movement track starting from Lane 20 of Fengjia Road through to Lane 127 of Wenhua Road and finally back to Fengjia Road.

The Keras-GAN-simulated movement results indicated that the pedestrian movement was predominantly concentrated at the south of the commercial area, despite it having four entrances at the McDonald's on Fengjia Road, the main entranceway of Fengjia University, the university entranceway near MOS Burger, and the intersection of Wenhua Road and Fuxing Road. Our onsite observations showed that the southern half of Wenhua Road constituted the main part of the night market, and therefore, most pedestrian movement tracks were observed in this part of the commercial area. Moreover, various food vendors operating along the northern part of Lane 20 of Fengjia Road to Lane 127 of Wenhua Road attracted people to walk around this area.

V. RESEARCH CONCLUSIONS AND RECOMMENDATIONS

This study used the global integration of space syntax to analyze hot spots where pedestrians most frequently stopped; the Keras-GAN to simulate three movement track graphic results; and the deformed wheel theory to investigate the relationship between the commercial area and pedestrians. The following conclusions were derived from the results:

1) *Global integration and movement track simulation results:* Global integration refers to the connectivity and integration of a road in a global space. Fig. 9 shows that road intersection with the highest global integration value is McDonald's. Similarly, the simulated movement results (Fig. 24) revealed that only one of the three road sections starting from McDonald's (northward along Fuxing Road) is

not among the most commonly occurring movement tracks, whereas the other two road sections from McDonald's are (toward Fengjia University to the east and southward along Fuxing Road). These results indicated that McDonald's as a landmark showed the highest connectivity with other roads within the commercial area; pedestrians had to pass the McDonald's when they entered and exited the area.

2) *Hot spot analysis of pedestrian segments and training results of the movement track simulation:* When we compared Fig. 10–12, which show the hot spots of different pedestrian segments, with Fig. 24, we observed the pedestrian hot spots to all be located on the most commonly occurring movement tracks in the simulation results. Therefore, the results of the movement track simulation and those of the pedestrian hot spots were positively correlated; future researchers who wish to analyze the movement tracks of different pedestrian segments more in-depth may also include predictions of pedestrian hot spot distributions in their research.

3) *Deformed wheel and movement track simulation results:* As previously described, deformed wheel theory is used to discuss the synergetic relationships between two spaces. According to Fig. 13–17, the Fengjia Road section is in the center of the commercial area, connecting roads on the commercial area borders, and thus integrates places near the borders. This result is consistent with that in Fig. 24, according to which Fengjia Road is where pedestrian movement is mostly concentrated. In addition, our onsite observations verified that Fengjia Road was the central road of the commercial area; specifically, this road divided the commercial area in the middle and connected the two food districts with the commercial district. Wenhua Road and Fuxing Road served as the commercial area borders, and their intersections with Fengjia Road were two main entrances of the commercial area. The section of Fengjia Road was short but served as a crucial hub of the commercial area, and thus should be seen as the primary focus of the area's service design. According to our onsite observations and the length and integration values of roads located in the northern part of the commercial area, namely the area to the north of Fengjia Road, only the food district had relatively dense crowds, whereas the other places in this area did not exhibit high spatial characteristics as a commercial area.

Overall, the global integration values and pedestrian hot spots in the Fengjia commercial area were highly mutually dependent; therefore, the global values of places in this commercial area may be incorporated into the spatial design for its service provision. The deep-learning simulation of pedestrian movement tracks and spatial characteristics revealed by space syntax could be used as a reference for each other. From the perspective of place creation in the deformed wheel theory, district layout greatly affected the affordances of roads in terms of service design. The southern part of the Fengjia commercial area was officially planned to be the main food district, and thus, frequent place interaction was observed along roads here. Regarding place identity and user behaviors in the night market, place creation on the road that constitutes the

commercial area's southern border facilitated the fulfillment of user needs in this part of the commercial area; this approach to user-need fulfillment is widely applied in urban planning. Moreover, place realization was observed on Fengjia Road; specifically, it is connected to Fengjia University's main entranceway and plays an essential role in the place identity of both the commercial area and the university.

Following are our recommendations for future studies discussing the relationship between and elements of persona-based movement track simulation and space syntax:

- Studies may consider examining whether tour group and backpackers stay overnight in the Fengjia commercial area. Those staying in hotels located in this commercial area will spend more time moving around the area, and thus will stop at more places than will those who do not stay overnight. A longer duration of user movement data collection will facilitate more comprehensive possibilities of simulated graphic results.
- This study inputted 45 groups of people (89 people) for GAN simulation, which included relatively limited data from tour group travelers (three groups; 12 people). Thus, future research may expand the sample size of tour group travelers. Moreover, future research may perform Keras-GAN simulations for the three personas separately to examine their movement simulation results individually.
- In this study, we did space syntax analysis and pedestrian movements simulation by GAN in a specific commercial area. There is currently no relevant overall application and interdisciplinary research. In the future, the relevant evaluation methods can be used to understand the practicality of each function in the cross-domain research from the professional perspective in order to extend service design for this research.

ACKNOWLEDGMENT

The authors acknowledge the technical support on GAN simulation application by Mr. Kai-Wan Cheng.

REFERENCES

- [1] Soufiane, F., Said, M., & Atef, A., "Sustainable urban design of historical city centers", *Energy Procedia*, vol. 74, pp. 301-307, 2015.
- [2] Hillier, B., & Hanson, J., *The Social Logic of Space*. Cambridge: Cambridge University Press, 1984.
- [3] Ratti, C., "Urban texture and space syntax: some inconsistencies", *Environment and Planning B: Planning and Design*, vol. 31, pp. 487-499, 2004.
- [4] Volchenkov, D., & Blanchard, P., "Scaling and Universality in City Space Syntax: between Zipf and Matthew", *Physica A*, vol. 387, pp. 2353-2364, 2008.
- [5] Zhao, J., & Künzli, O., "An introduction to connectivity concept and an example of physical connectivity evaluation for underground space", *Tunnelling and Underground Space Technology*, vol. 55, pp. 205-213, 2016.
- [6] Yesiltepe, D. & Kubat, A., "Impact of Bridges on Spatial Transformation of Urban Pattern: The case of Golden Horn, Istanbul", En 24th ISUF International Conference. Book of Papers. Editorial Universitat Politècnica de València. pp. 935-942. doi:10.4995/ISUF2017.2017.6059, 2018
- [7] Hillier, B., *Space is the Machine, A Configurational Theory of Architecture*. Cambridge University Press, 1986.
- [8] Daneshpour, S. A., Abbaszadegan, M., & Elahi, M., "The Morphology of Qom; The Study on Spatial Configuration Changes of The City (1956-2021)", *Space Ontology International Journal*, vol. 6, pp. 27-36, 2017
- [9] Önder, D. E., & Gigi, Y., "Reading urban spaces by the space-syntax method: A proposal for the South Haliç Region", *Cities*, vol. 27, pp. 260-271, 2010.
- [10] Choi, A.-S., Young-Ook Kim, Oh, E.-S., & Kim, Y.-S., "Application of the space syntax theory to quantitative street lighting design". *Building and Environment*, vol. 41, pp. 355-366, 2006.
- [11] Amorim, L. M. d. E., Filho, M. N. M. B., & Cruz, D., "Urban texture and space configuration: An essay on integrating socio-spatial analytical techniques." *Cities*, vol. 39, pp. 58-67, 2014.
- [12] Hanson, J., "Decoding Houses and Homes", Cambridge: Cambridge University Press, 1988.
- [13] Koohsari, M. J., Kaczynski, A. T., Giles-Corti, B., & Karakiewicz, J. A., "Effects of access to public open spaces on walking: Is proximity enough?", *Landscape and Urban Planning*, vol. 107, pp. 92-99, 2013.
- [14] Manzo, L. C., & Devine-Wright, P., *Place Attachment: Advances in Theory, Methods and Applications*. New York: Routledge, 2014.
- [15] Carpio-Pinedo, J., "Urban bus demand forecast at stop level: Space Syntax and other built environment factors", *Evidence from Madrid. Procedia - Social and Behavioral Sciences*, vol. 160, pp. 205-214, 2014.
- [16] Li, Y., Xiao, L., Ye, Y., Xu, W., & Law, A., "Understanding tourist space at a historic site through space syntax analysis: The case of Gulangyu, China", *Tourism Management*, vol. 52, pp. 30-43, 2016. Alfonso, M. A., "To Walk or Not to Walk? The Hierarchy of Walking Needs." *Environment and Behavior*, vol. 37, pp. 29, 2005.
- [17] Turner, A., "From axial to road-centre lines: a new representation for space syntax and a new model of route choice for transport network analysis" *Environment and Planning B: Planning and Design*, vol. 34, pp. 539-555, 2007.
- [18] Turner, A., Penn, A., & Hillier, B., "An algorithmic definition of the axial map", *Environment and Planning B: Planning and Design*, vol. 32, pp. 425-444, 2005.
- [19] Klarqvist, B., "A Space Syntax Glossary", *NORDISK ARKITEKTURFORSKNING*, vol. 2, 1993.
- [20] Jiang, B., Claramunt, C., & Klarqvist, B., "Integration of space syntax into GIS for modelling urban spaces", *Journal of Applied Gerontology*, vol. 2, 2000.
- [21] Enrico di, B., Luca, P., & Matteo, C., "A Multivariate Analysis of The Space Syntax Output For The Definition Of Strata In Street Security Surveys", *DEP - series of economic working papers*, 2011.
- [22] Lerman, Y., Rofè, Y., & Omer, I., "Using Space Syntax to Model Pedestrian Movement in Urban Transportation Planning", *Geographical Analysis*, vol. 46, 2014.
- [23] Arjovsky, M., Chintala, S., & Bottou, L., "Wasserstein GAN", Retrieved from arXiv:1701.07875, Retrieved Sep. 2018.
- [24] Lynch, K., *The Image of the City*. The Technology Press & Harvard University Press, 1960.
- [25] Mohammadi, M., Al-Fuqaha, A., & Oh, J.-S., "Path Planning in Support of Smart Mobility Applications using Generative Adversarial Networks", Retrieved from arXiv:1804.08396v1, Retrieved Mar. 2019.

Content based Document Classification using Soft Cosine Measure

Md. Zahid Hasan¹, Shakhawat Hossain², Md. Arif Rizvee³, Md. Shohel Rana⁴

Department of Computer Science & Engineering, Daffodil International University, Dhaka, Bangladesh^{1,3,4}

Department of Computer Science & Engineering, International Islamic University Chittagong, Chittagong, Bangladesh²

Abstract—Document classification is a deep-rooted issue in information retrieval and assumed to be an imperative part of an assortment of applications for effective management of text documents and substantial volumes of unstructured data. Automatic document classification can be defined as a content-based arrangement of documents to some predefined categories which is for sure, less demanding for fetching the relevant data at the right time as well as filtering and steering documents directly to users. For recovering data effortlessly at the minimum time, scientists around the globe are trying to make content-based classifiers and as a consequence, an assortment of classification frameworks has been developed. Unfortunately, because of using conventional algorithms, almost all of these frameworks fail to classify documents into the proper categories. However, this paper proposes the Soft Cosine Measure as a document classification method for classifying text documents based on its contents. This classification method considers the similarity of the features of the texts rather than making their physical compatibility. For example, the traditional systems consider ‘emperor’ and ‘king’ as two different words where the proposed method extracts the same meaning for both of these words. For feature extraction capability and content-based similarity measure technique, the proposed system scores the classification accuracy up to 98.60%, better than any other existing systems.

Keywords—Classification; similarity; feature extraction; cosine similarity; soft cosine measure; content; document

I. INTRODUCTION

Document classification refers to the way of storing similar documents together. This is considered as a major challenge for Information Retrieval in light of the fact that getting the right documents at the right time is hardly possible if the records are not legitimately classified and sorted out. Document classification can be done intellectually or automatically. Content-based document classification is an automatic arrangement of documents where the system goes through the entire content and groups them in light of the extracted features. There are several well-established algorithms for solving the content-based document classification problems. But none of these algorithms are fit for dealing with the similitude of the two words meaning the same. So, a much complex algorithm is required for considering the closeness of features in a vector space model (VSM) [1]. The framework proposed in this paper utilizes the Soft Cosine Measure for classifying text documents, which finds out the likeness of features of two documents. The proposed framework utilizes both Term Frequency (TF) [2] and Term Frequency-Inverse Document Frequency (TF-IDF) [3] to find the most important words in a text with the goal that, no vital

term is missed. As a result, the framework is capable of providing with the most precise outcomes. The performance accuracy of the proposed system is 11.2% superior to the most accurate document classifiers like Cosine Similarity [4]. The proposed system is tested 103 times and almost every time it classified documents correctly.

The paper is composed as follows: In Section 2, an investigation into the previous document classification frameworks is presented. Based on that investigation, a new classification framework, Soft Cosine Measure is proposed in Section 3. A data processing technique for the proposed classification method is described in Section 4. Section 5 describes the feature extraction techniques and Section 6 demonstrates the feature vector construction procedure. In Section 7, the implementation of Soft Cosine Measure for content-based document classification is outlined. A numerical study is provided in Section 8 and a detailed analysis of the system outcomes is done in Section 9. The paper is finished up in Section 10.

II. BACKGROUND STUDY

The evolution of document classification has started a long ago but still, it's a far away from getting saturated. Researchers have been applying various mathematical models to boost a sophisticated document classifier and, in that consequence, a number of documents classification frameworks have been established.

C. Goutte, L. Versoud, E. Gaussier, Eybens used Probabilistic Hierarchical Model for text categorization [5]. Probabilistic Hierarchical Model deals with classifying objects into similar categories where an object may coexist in multiple categories. For that purpose, the object-categories are organized in a hierarchical process where a clear dependency among the categories is visible. The final classification task is accomplished by providing some labels to the objects.

Evgeniy Gabrilovich and Shaun Markovitch argued to use C4.5 for text categorization [6] rather than traditional algorithms like Support Vector Machine (SVM). They showed that C4.5 is more capable of handling Redundant Features than SVM for categorizing texts into the preferred classes. Evgeniy Gabrilovich and Shaun Markovitch used Aggressive Feature Selection technique for developing a more sophisticated text categorization model. De Mello R.F., Senger L.J. and Yang L.T. (2005) introduced an Artificial Neural Network for content-based text classification [7]. The artificial neural network is much enough intelligent to cluster documents

without any previous domain knowledge. It uses document features to organize documents into proper clusters.

Y. H. Li and A. K. Jain conducted an experiment over Naive Bayes Classifier, Nearest Neighbor Classifier, Decision Trees and a Subspace Method [8] to find out the best-fit algorithm for document classification. The authors found that Naive Bayes and Subspace Method performed better than the other two classifiers on their data sets. They used the downloaded dataset for their experiments and their classification accuracy was approximately 83%. Authors also conducted an experiment to compare the performance accuracy among the Bayesian classifier, decision tree (ID3) and nearest neighbor with respect to the binary feature vector.

Shreyatakhatri proposed an improved K-means algorithm for Document Clustering [9]. In their experiment, they found that their proposed algorithm's accuracy was much better compared to current algorithms regarding time complexity and F-measure. On the other hand, Janani Balakumar proposed Enhanced Bisecting K-means (EBK) algorithm for clustering text document [10]. EBK is presented as an improved version of the Bisecting K-means clustering algorithm, capable of handling the limitations of Bisecting K-means algorithm while clustering documents into the assigned classes.

In 2017 S. Adinugroho, Y. A. Sari, M. A. Fauzi, and P. P. Adikara proposed a hybrid algorithm for clustering text documents correctly [11]. Their proposed algorithm consists of two prominent algorithms: Latent Semantic Indexing (LSI) and Pillar Algorithm. S. Adinugroho, Y. A. Sari, M. A. Fauzi, and P. P. Adikara used LSI to extract features and Pillar Algorithm to select seeds. A year back, in 2016, P. Bafna, D. Pramod and A. Vaidya proposed a new document clustering method, TF-IDF along with fuzzy k-means algorithm [12] to achieve the maximum clustering accuracy. The authors carried out a number of experiments on several datasets to verify the clustering accuracy of their proposed methodology. For that purpose, an approach for removing clamorous as well as less important data was followed by the authors. Hierarchical agglomerative clustering approach was applied in this experiment to optimize the system's performance.

Some researchers believe that Cosine Similarity secures the maximum accuracy in case of text document clustering. Lailil Muflikhah and B. Baharudin claimed that their proposed method performs better than all other clustering algorithms [13]. They calculated the performance of their system with f-measure some 0.91 and entropy about 0.51. They also claimed that the performance of their proposed system remains the same even if the system is applied to a huge amount of data. Baoli Li and Liping Han conducted a very deep analysis on cosine similarity for clustering text documents. Based on the experimental results, Baoli Li and Liping Han stated that cosine similarity is not always fit for document clustering tasks. Then they proposed Distance Weighted Cosine Similarity [14] for classifying text documents.

M. L. Aishwarya and K. Selvi proposed an intelligent similarity measure technique [15] to solve document clustering problems. They used the concept of the Neural Network algorithm to develop their intelligent similarity measure

approach. These researchers suggested Echo State Neural Network and Radial Basis Function to cluster documents if the tainting dataset contains irrelevant documents.

Unfortunately, none of these classifiers could overcome some common drawbacks which lead the scientist to develop a content-based document classification framework, a well more intelligent classification model, equipped for classifying any text documents just by experiencing its content.

III. METHODOLOGY

A. Soft Cosine Measure

Soft Cosine Measure, a new concept in classification tasks, considers the pairs of features [16] to discover the similitude between two word vectors in a vector space model (VSM) [17]. Although Soft Cosine Measure has derived from the Cosine Similarity, there is a major distinction between these two concepts. Cosine Similarity ordinarily considers the cosine of the angle between two non-zero vectors to discover the similitude between two documents [18] where Soft Cosine Measure calculates comparability between the features extracted from those documents. For, two N-dimension vectors α and β the Soft Cosine Similarity can be calculated as follows:

$$\text{Soft Cosine } (\alpha, \beta) = \frac{\sum_{i,j}^N s_{ij} \alpha_i \beta_j}{\sqrt{\sum_{i,j}^N s_{ij} \alpha_i \alpha_j} \sqrt{\sum_{i,j}^N s_{ij} \beta_i \beta_j}}$$

Where, $s_{i,j}$ = similarity (*feature_i*, *feature_j*)

If, $s_{i,i}=1$ and $s_{i,j}=0$ for $i \neq j$ then,

$$\begin{aligned} \text{Soft Cosine } (\alpha, \beta) &= \frac{\sum_{i,j}^N \alpha_i \beta_i}{\sqrt{\sum_{i,j}^N \alpha_i \alpha_i} \sqrt{\sum_{i,j}^N \beta_i \beta_i}} \\ &= \frac{\sum_{i=1}^N \alpha_i \beta_i}{\sqrt{\sum_{i=1}^N \alpha_i^2} \sqrt{\sum_{i=1}^N \beta_i^2}} \\ &= \frac{\alpha \cdot \beta}{\|\alpha\| \|\beta\|} = \text{Cosine Similarity.} \end{aligned}$$

So, when there is no similarity between the features of the objects, Soft Cosine Measure becomes proportional to the regular Cosine Similarity formula.

B. Data Processing

For obtaining a better classification model, the proposed framework needs to be trained with a legitimate set of pre-processed data. And to process data properly, the proposed system encounters a couple of steps as stated in Fig. 1.

C. Removing Punctuation

Removing punctuation is a vital task in natural language processing. There are quantities of approach to expel punctuation from a text. In the proposed system, a regular expression is used to dispose of all the punctuations.

D. Converting String into Lower Case Letter

For processing the data in the most convenient way, all the letters in a textual content are converted into the lower-case form.

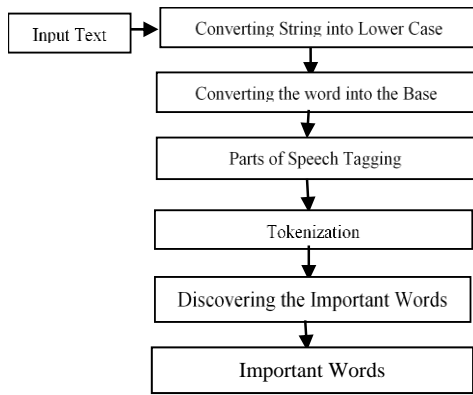


Fig. 1. Data Processing Diagram.

E. Converting the Word into the base form

A critical task in natural language processing is to convert all the words into their base form. This causes a framework to comprehend words regardless of whether they are in various structures. For instance, Table I represent some words in their base forms.

To convert the words into their base form, Streamer Porter Algorithm [19], [20] is used in this system.

F. Parts of Speech Tagging

The system proposed in this paper has used Latent Analogy [21] for tagging parts of speech. Only the noun and the verbs are used to train the system.

G. Tokenization

The process of breaking up the content into distinct meaningful units is recognized as tokenization. Tokenization is an important task for this system as the system makes the vector with some particular words or tokens.

H. Discovering the Important Words

All the words in a text file are not equally important for a specific purpose. So, researchers have taken this task as a challenge to find the important words out from a text document. As a result, various algorithms have been developed to discover the vital words from a text document. However, the proposed framework utilizes two most proficient algorithms to choose the important words: (TF) and TF-IDF as shown in Fig. 2.

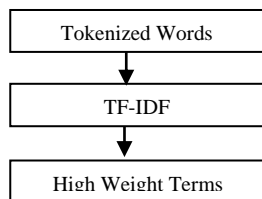


Fig. 2. Important Words Acquisition.

TABLE I. WORDS IN VARIOUS FORMS AND THEIR BASE FORM

Word in different Form	Base Word
ran, run, running, runs, runner	run
good, better, best	good

I. Term Frequency (TF) and Term Frequency-Inverse Document Frequency (TF-IDF)

Term Frequency [2] is the calculation of how many times each word appears in a text document. Term Frequency (TF) in documents can be calculated by using the logarithmic scale.

$$tf_{t,d} = \begin{cases} \log(1 + f_{t,d}), & \text{if } f_{t,d} > 0 \\ 0, & \text{otherwise} \end{cases}$$

where, t defines a term, d is the document and $tf_{t,d}$ is the frequency of the term in the documents.

Inverse Document Frequency [22], [23] is the calculation that determines whether a term is common or rare across all the documents. Inverse Document Frequency can be easily calculated by the following formula.

$$idf_{t,D} = \log \frac{|D|}{|d \in D: t \in d|}$$

where, d is a document and D is the set of documents.

Term Frequency-Inverse Document Frequency [3] calculates the high weighted terms in a set of documents.

$$tf - idf_{t,d,D} = tf_{t,d} * idf_{t,D}$$

where, t is a term, d is a document and D is a set of documents.

The implementation of TF-IDF mimics the following algorithm:

1. Set d ← Text Document, t ← a specific term; $t \in d$
2. Set n ← Number of times term t appears in d,
3. Set m ← Total number of terms in d;
4. Compute $X \leftarrow n \div m$;
5. Set N ← Total number of documents and M ← Number of documents with t; $M \in N$
6. Compute $Y \leftarrow N \div M$;
7. Set K ← Term Frequency Inverse Document Frequency
8. Compute $K \leftarrow X \times Y$;
9. Print K;

IV. FEATURE EXTRACTION

The basic convenience of Soft Cosine Measure over Cosine Similarity is its capability of computing similarity between two documents by using their inner features regardless of whether they have any physical comparability or not. For doing that, Soft Cosine Measure discovers features of each vital term in all the documents in a document set. For that purpose, it uses a dictionary that exposes all the possible words with the same meaning for a given word. This process is utilized at both the training and system handling time. The entire procedure is graphically spoken to in the accompanying segment.

A. Feature Extraction During System Training

For preparing the framework, vital terms are gathered from a substantial amount of datasets which indicates a solid plausibility of having duplicate terms. So, it becomes essential to extract feature at data processing time to remove redundant high weight terms. The imperative terms are principally put away in a cluster and the accompanying algorithm is utilized to evacuate all the redundant data.

1. start
2. set i to 0
3. if A[i+1]==A[i]
 - 3.1 remove A[i+1]
 - 3.2 else look for A[i] in lexicon and put all possible features of A[i] into B[j]
 - 3.2.1 set j to 0
 - 3.2.2 if A[i+1]==B[j]
 - 3.2.2.1 remove A[i+1]
 - 3.2.3 else set j to j+1;
 - 3.3 set i to i+1;
4. stop

B. Feature Extraction During Similarity Scoring

Feature extraction during classification is the key operation that enables the proposed framework to perform better than all other existing frameworks. This task is performed in accordance with the following algorithm (Fig. 3).

C. Feature Vectors Construction

In the wake of finding the essential words, the framework figures the Term Frequency for those words and builds the final vectors with the resultant numeric quantities. The following algorithm demonstrates the vector construction process.

1. start
2. declare high weight terms as $T_i; 1 \leq i \leq n$
3. declare the document as $d_i; 1 \leq i \leq n$
4. compute term frequency, TF for T_1 in document, d_1
5. extract features for T_1 in d_1
 - 5.1 add all TF for T_1
 - 5.2 rerun the sum
6. repeat step 4 for n times
7. store the result in a vector, V
8. repeat step 3 and 4 for n times
9. end

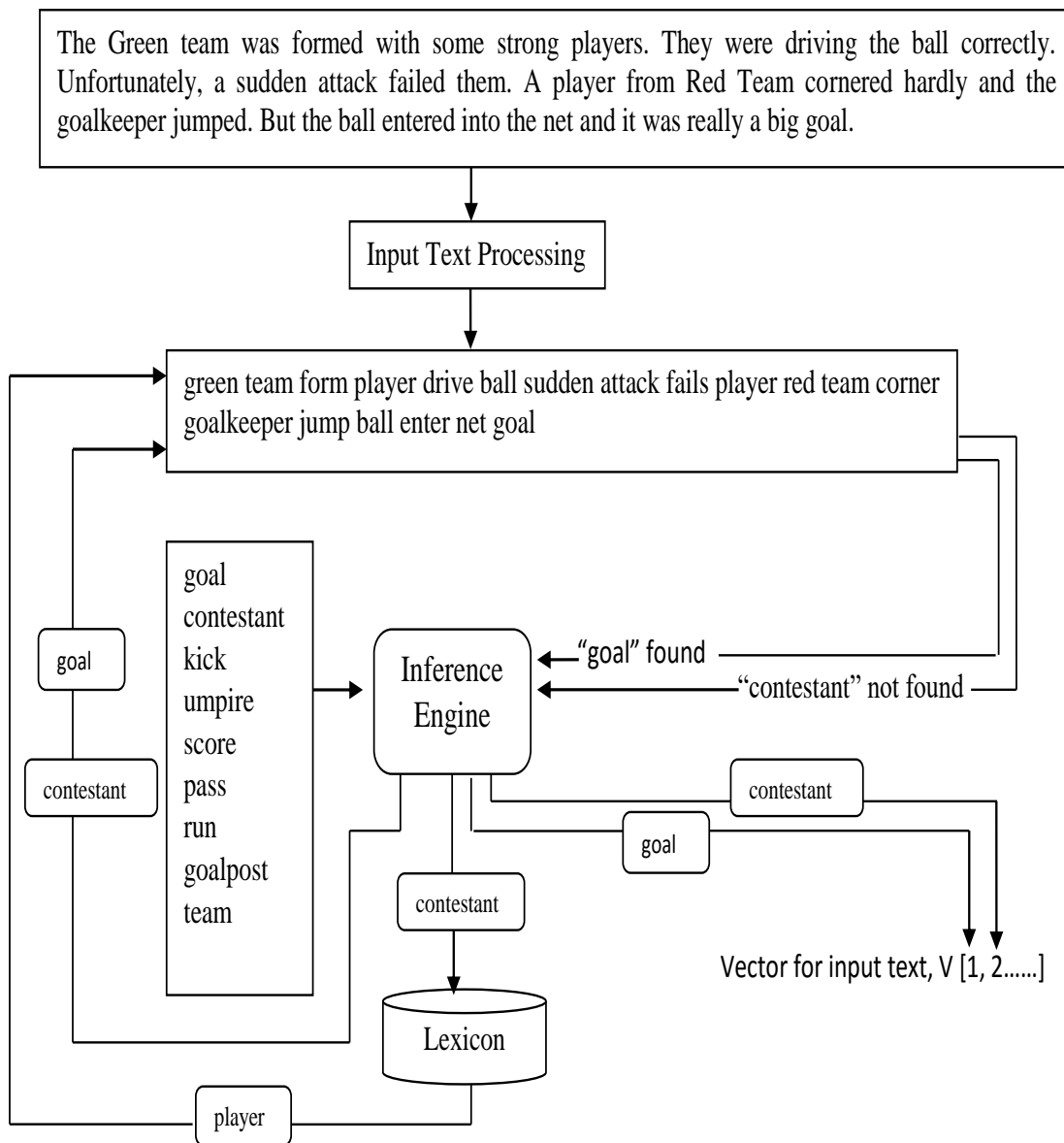


Fig. 3. Feature Extraction Procedure.

V. IMPLEMENTATION OF THE SYSTEM

Soft Similarity or Soft Cosine Measure classifies text documents in view of the content it bears. For that, only a cosine angle between the features of the trained data and the input data is estimated. The architectural design of how Soft Cosine Measure classifies the text documents is presented in Fig. 4.

Based on the similarity scores, performed by different text documents, the system classifies the documents into some predefined classes. A very straightforward algorithm for the proposed system is given below.

1. start
2. scan the input text, T
3. process T
4. extract the feature of T from the lexicon, D
5. make a feature vector, V_t
6. find the similarity score between V_t and V_i ; $\{V_t | V_i \in V; |V| = n\}$ where, $V =$ trained data vector and $n =$ number of classes
7. store the score in a list, L
8. repeat Step 6 and 7 for n times
9. find the biggest score from L
10. make the final decision to put T into S_t ; $\{S_t | S_t \in S; |S| = |V|\}$ S= set of classes.
11. end

Soft Cosine Measure considers the features in VSM which makes it equipped for figuring the likenesses between two documents regardless of whether they have any common word or not. It uses a lexicon to extract the features that are actually taken into account to quantify the similarity between the meaning of two words rather than the words themselves.

In the above figures, a very transparent comparison between Cosine Similarity and Soft Cosine Measure is stated. Fig. 5(a) exhibits a very big difference between Hi and Hello where in Fig. 5(b), Hi and Hello are considered as the words with the same meaning.

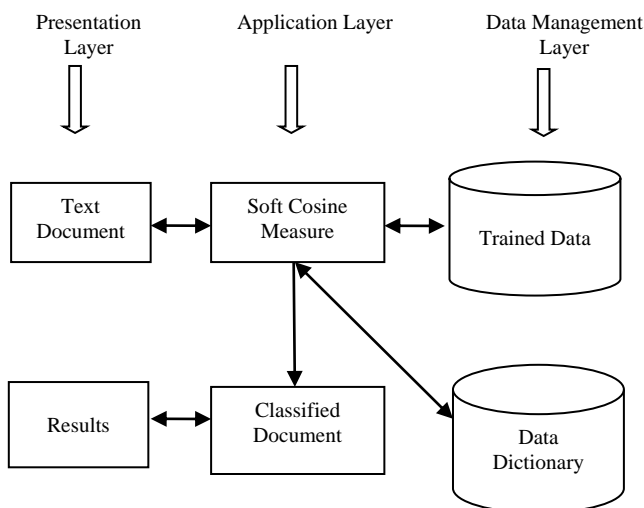


Fig. 4. System Architecture for Document Classification.

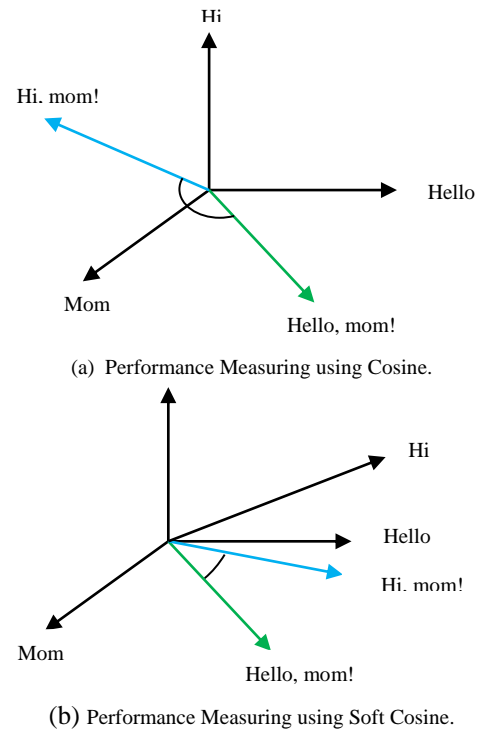


Fig. 5. Comparison between Cosine Similarity and Soft Cosine Measure.

VI. EXPERIMENTAL RESULTS

A number of experiments have been conducted over the proposed system and each of these experiments confirms that Soft Cosine Measure performs better than Cosine Similarity. The similarity scores of Cosine Similarity and Soft Cosine Measure between two sample documents are presented in Table II.

TABLE II. SIMILARITY SCORE COMPARISON BETWEEN CS AND SCM

Document 1	Document 2	Cosine Similarity Score	Soft Cosine Measure Score
Every Mom is the most amazing person for her children - she's their heroine. Mom always knows how her child feels and can help with any problem. Mom can make the most complicated braid and explain fractions; Mom can help to wake her child up in the morning and hug her tightly when she's sad.	Each Mom is the most stunning individual for her kids - she's their champion. Mother dependably knows how her kid feels and can help with any issue. Mother can make the most entangled mesh and clarify divisions; Mom can get her kid up toward the beginning of the day and embrace her firmly when she's pitiful.	0.5041	0.9997

They system is tested with different types and sizes of documents to observe its performance under different circumstances. Fig. 6 shows that Soft Cosine Measure performs 49.56% better than the Cosine Similarity. This experiment has been done with 50 distinct documents and for every document Soft Cosine Measure performs around 45% better than Cosine Similarity.

However, the proposed system has been tested for 114 times with 103 different documents to classify into five categories. Each time the system has classified 101 documents correctly which secures its accuracy rate up to 98.06% (Table III).

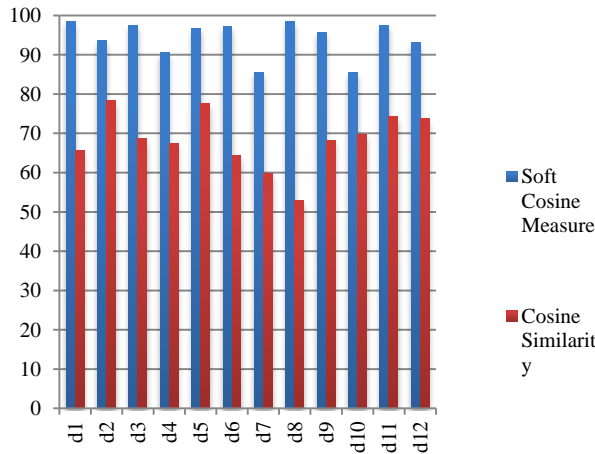


Fig. 6. Similarity Scores of Soft Cosine Measure and Cosine Similarity for 12 different Documents.

TABLE III. DOCUMENT CLASSIFICATION RESULTS OF SOFT COSINE MEASURE

Documents	System Selected Category	Actual Category	Remark
Doc1	History	History	✓
Doc 2	History	History	✓
Doc3	Literature	Literature	✓
.	.	.	.
.	.	.	.
.	.	.	.
.	.	.	.
Doc48	Comics	Comics	✓
Doc49	Politics	History	X
Doc50	Science	Science	✓
Doc51	Science	Science	✓
Doc52	Literature	Literature	✓
Doc53	History	Politics	X
.	.	.	.
.	.	.	.
.	.	.	.
.	.	.	.
Doc100	Comics	Comics	✓
Doc101	History	History	✓
Doc102	Literature	Literature	✓
Doc103	Politics	Politics	✓

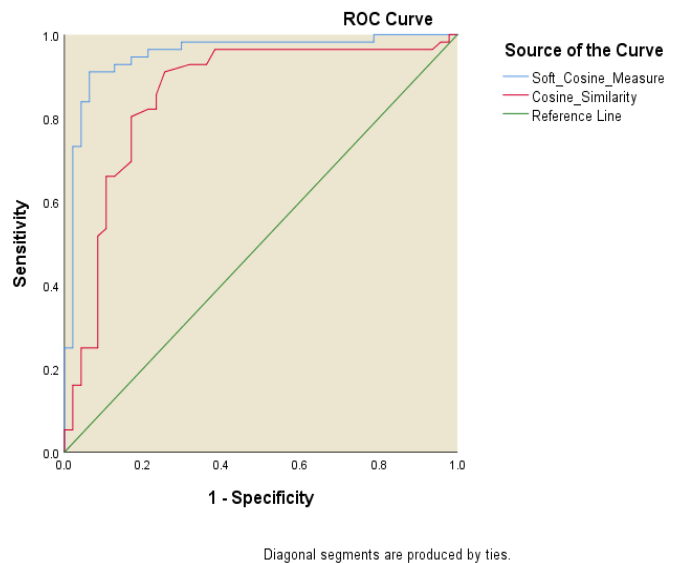


Fig. 7. ROC Curves Illustrate the Classification Accuracy of Soft Cosine Measure and Cosine Similarity.

Fig. 7 shows the ROC (Receiver Operating Characteristics Curve) curves where the blue curve represents the classification accuracy of Soft Cosine Measure and the red curve depicts the accuracy of Cosine Similarity. The AUC (area under the curve) of Soft Cosine Measure is 0.925 and AUC of Cosine Similarity is 0.840. So, it turns out to be evident that, the classification accuracy of Soft Cosine Measure is superior to the Cosine Similarity.

VII. RESULT ANALYSIS

Though document classification is a very important task in natural language processing for its extended use case, it is yet a big challenge to come across the most intense precision in document classification. Researchers have tried numerous strategies to locate the most extreme precision in content-based document classification. According to a contemporary research outcome [24], it has been clear to researchers that Support Vector Machine (SVM) provides the maximum accurate result than any other methods in document classification which is estimated 90.26%. But another recent research demonstrates that cosine similarity classifies content-based document more efficiently than SVM and its accuracy reaches up to 93.9% [4]. However, this research with adequate evidence clarifies that Soft Cosine Measure performs better than Cosine Similarity. A very straightforward comparison among different classification accuracy is given in Table IV.

TABLE IV. CLASSIFICATION ACCURACY OF DIFFERENT METHODS

Methodology	Accuracy (%)
SVM	90.26
Decision Tree	76.99
K Nearest Neighbor	84.60
Naive Bayes	84.70
Cosine Similarity	93.90
Soft Cosine Measure	98.60

VIII. CONCLUSION

Soft Cosine Measure is a state-of-the-art mathematical model that considers the features in a vector space model to quantify the comparability between two text documents. The proposed system uses this mathematical model to construct a content-based document classification framework. To classify any document the system considers the edge between the component vectors of the given documents and the readied data. The system secures its precision rate up to 98.6% which is vastly improved than some other existing framework. However, an improved feature extraction technique can increase the performance of Soft Cosine Measure up to 100%.

REFERENCES

- [1] D.L. Lee, HueiChuang, K. Seamons, "Document ranking and the vector-space model", IEEE Software, Volume: 14, Issue: 2, Mar/Apr 1997, DOI: 10.1109/52.582976
- [2] Mikio Yamamoto, Kenneth W. Church, "Using suffix arrays to compute term frequency and document frequency for all substrings in a corpus", Computational Linguistics archive Volume 27 Issue 1, March 2001, Pages 1-30, doi:10.1162/089120101300346787
- [3] Rung-Ching Chen, Jui-Yuan Liang, Ren-Hao Pan, "Using recursive ART network to construction domain ontology based on term frequency and inverse document frequency" Expert Systems with Applications, Volume 34, Issue 1, January 2008, Pages 488-501
- [4] Radhamothukuri, Nagaraju, M., DivyaChilukuri, "Similarity Measure For Text Classification", International Journal of Emerging Trends & Technology in Computer Science (IJETTCS), Volume 5, Issue 6, November - December 2016, ISSN 2278-6856
- [5] C. Goutte, L. Versoud, E. Gaussier, Eybens, "Method for Multi-class, multi-label categorization using probabilistic hierarchical modeling", U.S Patent 7 139 754 B2, Nov 21, 2006
- [6] Evgeniy Gabrilovich and Shaun Markovitch, "Text Categorization with many redundant features: Using aggressive feature selection to make SVMs competitive with C4.5", Proceedings of 21st International Conference on Machine Learning, 2004.
- [7] de Mello R.F., Senger L.J., Yang L.T. (2005) Automatic Text Classification Using an Artificial Neural Network. In: Ng M.K., Doncescu A., Yang L.T., Leng T. (eds) High Performance Computational Science and Engineering. IFIP—The International Federation for Information Processing, vol 172. Springer, Boston, MA.
- [8] Y. H. Li A. K. Jain, "Classification of Text Documents", The Computer Journal, Volume 41, Issue 8, 1 January 1998, Pages 537-546, https://doi.org/10.1093/comint/41.8.537
- [9] Shrivatsa Khatwal, Dr. Kunal Garg, "Document Clustering Using Improved K-Means Algorithm" International Journal of Engineering Research and General Science Volume 4, Issue 3, May-June, 2016 ISSN 2091-2730.
- [10] BALAKUMAR, Janani; VIJAYARANI, S.. An Improved Bisecting K-Means Algorithm for Text Document Clustering. International Journal of Knowledge Based Computer System, [S.l.], p. 32-37, dec. 2016. ISSN 2321-5623.
- [11] S. Adinugroho, Y. A. Sari, M. A. Fauzi and P. P. Adikara, "Optimizing K-means text document clustering using latent semantic indexing and pillar algorithm," 2017 5th International Symposium on Computational and Business Intelligence (ISCBI), Dubai, 2017, pp. 81-85. doi: 10.1109/ISCBI.2017.8053549
- [12] P. Bafna, D. Pramod and A. Vaidya, "Document clustering: TF-IDF approach," 2016 International Conference on Electrical, Electronics, and Optimization Techniques (ICEEOT), Chennai, 2016, pp. 61-66. doi: 10.1109/ICEEOT.2016.7754750
- [13] L. Muflikhah and B. Baharudin, "Document Clustering Using Concept Space and Cosine Similarity Measurement," 2009 International Conference on Computer Technology and Development, Kota Kinabalu, 2009, pp. 58-62. doi: 10.1109/ICCTD.2009.206.
- [14] Li B., Han L. (2013) Distance Weighted Cosine Similarity Measure for Text Classification. In: Yin H. et al. (eds) Intelligent Data Engineering and Automated Learning – IDEAL 2013. IDEAL 2013. Lecture Notes in Computer Science, vol 8206. Springer, Berlin, Heidelberg
- [15] M. L. Aishwarya and K. Selvi, "An intelligent similarity measure for effective text document clustering," 2016 International Conference on Computing Technologies and Intelligent Data Engineering (ICCTIDE'16), Kovilpatti, 2016, pp. 1-5. doi: 10.1109/ICCTIDE.2016.7725342
- [16] Sidorov, Grigori; Gelbukh, Alexander; Gómez-Adorno, Helena; Pinto, David. "Soft Similarity and Soft Cosine Measure: Similarity of Features in Vector Space Model" Computación y Sistemas 18 (3): 491–504. doi:10.13053/CyS-18-3-2043 Retrieved 7 October 2014.
- [17] Thomas Mikolov et al. Efficient Estimation of Word Representations in Vector Space. arXiv:1301.3781v3 [cs.CL] 7 Sep 2013
- [18] Li B., Han L. (2013) Distance Weighted Cosine Similarity Measure for Text Classification. In: Yin H. et al. (eds) Intelligent Data Engineering and Automated Learning – IDEAL 2013. IDEAL 2013. Lecture Notes in Computer Science, vol 8206. Springer, Berlin, Heidelberg
- [19] M.F. Porter, (1980) "An algorithm for suffix stripping", Program, Vol. 14 Issue: 3, pp.130-137, https://doi.org/10.1108/eb046814
- [20] Atharva Joshi et al, / (IJCSIT) International Journal of Computer Science and Information Technologies, Vol. 7 (1) , 2016, 266-26
- [21] Jerome R. Bellegarda, Part-of-Speech Tagging by Latent Analogy IEEE Journal of Selected Topics in Signal Processing Volume: 4, Issue: 6 Dec. 2010 ;DOI: 10.1109/JSTSP.2010.2075970
- [22] Church K., Gale W. (1999) Inverse Document Frequency (IDF): A Measure of Deviations from Poisson. In: Armstrong S., Church K., Isabelle P., Manzi S., Tzoukermann E., Yarowsky D. (eds) Natural Language Processing Using Very Large Corpora. Text, Speech and Language Technology, vol 11. Springer, Dordrecht, https://doi.org/10.1007/978-94-017-2390-9_18
- [23] Stephen Robertson, (2004) "Understanding inverse document frequency: on theoretical arguments for IDF", Journal of Documentation, Vol. 60 Issue: 5, pp.503-520, https://doi.org/ 10.1108/00220410410560582
- [24] Choudhury, S., Batra, T., Hughes, C., & LEMMATIZER, L. (2016). Content-based and link-based methods for categorical webpage classification.

Fuzzy Delphi Method for Evaluating HyTEE Model (Hybrid Software Change Management Tool with Test Effort Estimation)

Mazidah Mat Rejab^{1,4}, Nurulhuda Firdaus Mohd Azmi², Suriyati Chuprat³

Razak Faculty of Informatics and Technology, Universiti Teknologi Malaysia, Kuala Lumpur Malaysia^{1, 2, 3}

Faculty of Computer Sciences and Information Technology, Universiti Tun Hussein Onn Malaysia (UTHM), Batu Pahat, Johor¹

Abstract—When changes are made to a software system during development and maintenance, they need to be tested again i.e. regression test to ensure that changes behave as intended and have not impacted the software quality. This research will produce an automated tool that can help the software manager or a maintainer to search for the coverage artifact before and after a change request. Software quality engineer can determine the test coverage from new changes which can support cost estimation, effort, and schedule estimation. Therefore, this study is intended to look at the views and consensus of the experts on the elements in the proposed model by benefitting the Fuzzy Delphi Method. Through purposive sampling, a total of 12 experts from academic and industrial have participated in the verification of items through 5-point linguistic scales of the questionnaire instrument. Outcome studies show 90% of elements in the proposed model consists of change management, traceability support, test effort estimation support, regression testing support, report and GUI meet, the value threshold (d construct) is less than 0.2 and the percentage of the expert group is above 75%. It is shown that elements of all the items contained in the venue are needed in the HyTEE Model (Hybrid Software Change Management Tool with Test Effort Estimation) based on the consensus of experts.

Keywords—Fuzzy Delphi Method; software traceability; test effort estimation; regression testing; software changes

I. INTRODUCTION

The software application is present in every area of our life. The small and large system is developed using the software. Change is a part of everyday life. Software changes after some time. In today's competitive atmosphere, brand new needs are arising, and existing needs are altering swiftly. Changes are accomplished for various reasons, for example, to include new elements, to amend a few errors or to improve the product.

According to Vasa [1], "Software evolution or changes are direct consequences and reflections of ongoing changes in a dynamic real world". These changes are occurring very fast because of the competitive market. Enhancing software is a common necessity in business today as they encounter lots of need changes, prolonging software features and function, and including brand new modules. We cannot ignore the critically of software changes because real software system changes and becomes more complex over time [1]. A current report distributed by the Standish Group International [2] which involved 13522 software projects, Fig. 1 showed that out of the

reviewed projects just 29 percent were effective, 18 percent is considered as "failed" and 53 percent are viewed as "suspected" and the fundamental driver of the failed project is the prerequisite change. Lam [3] propose that changing necessity are the main issues of the re-building and maintenance activities. The majority of the previous study demonstrates that software maintenance activities are concerning adaptive and completeness maintenance close to 80%. For this aim, the company must get the opportunity to manage requirement adaptation as part of the border software evolution approach. One estimate expresses that 40% of the necessity requirement during software development [4].

Estimation is limited as the shrewd conviction of the quantum or field that should be performed and the essential material (in particular, HR, money related assets, material assets, and time assets) required playing out the work at a future date in a characterized domain for determined strategies. Test Effort Estimation that estimate of the testing length, exertion, cost and timetable for a specific programming test project in an individual domain for particular strategies, tool and methods [6]. The test effort is the foundation of the effort spent on test action and the effort spent on debug action [7].

Research objective for this study is:

- 1) To develop a software traceability model to reduce operational cost during regression testing using the Fuzzy Delphi Method.

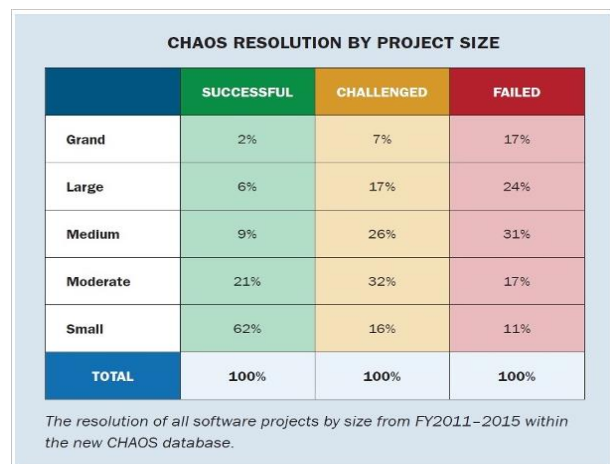


Fig. 1. CHAOS Resolution by Project Size 2011-2015 [5].

This study utilizes the FDM as an evaluation to evaluate the proposed model. This paper is organized as follows. Section I is an Introduction to the background of the problem, Section II introduces the process of the FDM to assess the expert consensus and lists the alternative options in the order of preference. Section III shows results and finding of an element in Hytee model. The conclusion of the research findings and future work of this research is presented in Section IV. The results are expected to provide an element to support in design and development of Hytee Model.

II. FUZZY DELPHI METHOD

A. Introduction

This research study is about implementing the Fuzzy Delphi Method in designing and developing a software traceability model with the test effort estimation during regression testing in software changes. The Delphi Method is an approach that has been used and widely accepted to collect data for a study based on the validation expert in the research study of Hsu [8]. The strength of this method has also produced a diversity technique in obtaining empirical data like the Fuzzy Delphi Method (FDM). Talking about FDM, it is a method of measurement based on the modification on the Delphi Method.

This method has been presented by Kaufman and Gupta in 1988 [9]. The Fuzzy Delphi Method (FDM) is a combination of the numbering of the fuzzy set method and Delphi itself [10]. This brings the meaning that this is not a new approach based on a classical Delphi method where the respondents involved must be from within the circle of experts who have experience in the context of the study. This improvement indirectly strives to make FDM as a measurement approach that is more effective, whereby FDM is able to resolve the issue of who has uncertainty for some issues of the research.

The review of previous literature shows that FDM is a combination of the traditional method of Delphi (Classic) and fuzzy set theory (Fuzzy). The fuzzy set theory was introduced by an expert in the field of mathematics in 1965 which Zadeh [11] worked, and it works as an extension of a classical set theory where each element in a set is assessed based on the set of binaries (Yes or No). Fuzzy set theory assessment also allows a gradual review of each element. Ragin [12] states that the value of numbering fuzzy consists of 0 to 1 or in the unit interval (0,1).

There are two mains in FDM which is Triangular Fuzzy Number and Defuzzification Process. Triangular Fuzzy Number is m is made up of the value of the m_1 , m_2 , and m_3 where m_1 represents the value of the minimum (smallest value), representing the most reasonable value m_2 (most plausible value) and m_3 is referring to the maximum value (but there is value). All three values in the Triangular Fuzzy Number this can be seen through Fig. 2 shows the graph that triangles mean against the value of triangular shows that all three of these values is also in the range of 0 to 1 and it coincided with fuzzy numbers [12].

B. Procedure in FDM

For further details on the findings using the Fuzzy Delphi approach method (FDM), there are procedures that must be compiled. Table I show about the procedures in FDM cover for seven steps.

C. The Number of Expert in FDM

The selection of the number of experts for the Fuzzy Delphi Method (FDM) is a total of 12 people. This is based on the view of Adler and Ziglio [13], who pointed out that the number of experts for the Delphi technique was as many as 10 to 15 people if the experts can get an agreement with each other. However, there is also an opinion stating that the minimum number of experts for the Delphi technique is five experts [14]. This matches the argument from Rowe and Wright [15] that the number of experts can start from 5 to 20 people based on their areas of expertise. On the other hand, Jones and Twiss [16] suggested the number of experts involved in the Delphi method approach is 10 to 50 experts.

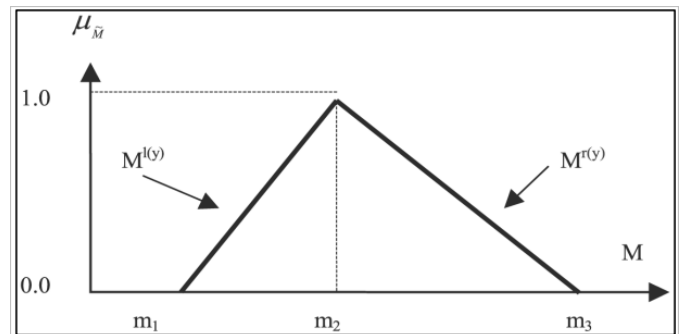


Fig. 2. Graph Triangle Min against the Value of Triangular.

TABLE I. PROCEDURES IN FDM

Step	Detail
1	Criteria to determine the experts involved in the study. <ul style="list-style-type: none"> ❖ Expert in FDM ➤ 10-15 expert (Adler & Ziglo, 1996) ➤ 10-50 expert (Jones & Twiss, 1978)
2	Convert all linguistic variables into a triangular fuzzy number
3	All data is scheduled to obtain the average value (m_1 , m_2 , m_3)
4	Determine the distance between the 2 numbers fuzzy to determine the value of the threshold, d $d \leq 0.2$, meaning that all the experts reach consensus.
5	Determine the consensus of the Group <ul style="list-style-type: none"> ❖ Value of the percent agreement of experts that must be equal to or more than 75.0%
6	Define Aggregate Fuzzy Evaluation by adding all fuzzy numbers
7	Data analysis using the average of fuzzy numbers or average response (Defuzzification Process)

The criteria and characteristics of this study involved software engineering specialists in software testing from the academic and industrial sector. Selection is also based on Berliner [17],[18] who argues that the expert is competent if they participated in a particular field consistently exceeding a period of 5 years. Nonetheless, there are other scholars pointing out that experts are highly skilled and experienced in the areas studied [19][20].

Based on Table II, the discussion for selection of the respondents for the design and development phase, the researcher lists down the criteria for selecting the experts, as below:

D. Questionnaire

This research uses the questionnaire as an instrument to get quantitative data for element requirements of Hytee Model. The questionnaire is aimed at in order to meet the criteria and conditions of the using the technique of fuzzy Delphi Method where this technique involves the use of a mathematical formula in order to obtain the consensus of experts. Instruments used by researchers is the instrument that has been modified based on the needs of the study researchers. The original of this questionnaire was adapted from the study of Ibrahim (2006) [21]. Table III shows the element in the questionnaire.

The process of data collection in the study is carried out using the Fuzzy Delphi approach between the processes involved in an interview for the Delphi technique while the questionnaire is analyzed with techniques of a fuzzy number. 5-point scale used Rahman, M. N. A. (2013) [23] to determine the expected kinds of video games against aspects of basic skills in the Malay language for foreign students to obtain consent or consensus of a group of expert. To facilitate experts, answer questionnaires, researchers have put the value of the scale of 1 to 5 to replace the Fuzzy value as shown in Table IV for linguistic scale 5 points follows;

TABLE II. CLASSIFICATION OF HETEROGENEOUS EXPERTS

Expert	Background	Number of Participants
Industry	Public Bank (System Analyst)	1
	Iris Berhad (It support)	2
	Mimos Berhad (Software Tester)	2
	Mesiniaga (It Engineer)	2
Government	It Officer (KPKT)	1
	It Officer (LGM)	1
	It Officer (MBPP)	1
Academicians	Lecture It (Polytechnic Penang)	2
Total		12

TABLE III. QUESTIONNAIRE IN FDM

Section	Element	Questionnaire
B	Change Management	B1: Do you agree that Hytee model support change management of software artifact? B2: Do you agree that change management support will help to save time? B3: Do you agree that Hytee model can help the current practice in after getting PCR B4: Do you agree that Hytee model provide appropriates content B5: Do you agree that Hytee model that the system and process developed to achieve the change are transparent
C	Traceability Support	C1: Do you agree that Hytee model provide traceability for requirement, test cases, and code C2: Do you agree that Hytee model it is easy to create traceability link between artifact C3: Do you agree that Hytee model it easy to locate test cases to the requirement or vice versa C4: Do you agree that developers get a benefit from requirements traceability when evolving and maintaining a software system? C5: Do you agree that Hytee model using top – bottom and bottom to up will help to find the bug?
D	Regression Testing Support	D1: Do you agree that Hytee model in regression testing provide the helpful function D2: Do you agree that Hytee model of RT function will help the user to save a time D3: Do you agree that Hytee model can help the current practice during RT D4: Do you agree that Hytee model provide appropriates content
E	Test Effort Estimation Support	E1: Do you agree that Hytee model provides a basis to cost estimation and plan schedules E2: Do you agree that Hytee model in test effort estimation support will help the user to estimate the cost after changes. E3: Do you agree that Hytee model in test effort estimation support provide appropriates content E4: Do you agree that Hytee model in test effort estimation support help the user save time /cost/skill E5: Do you agree that Hytee model in test effort estimation support will reduce <i>situational and human biases</i>
F	Report	F1: Do you agree that Hytee model produced the report is helpful F2: Do you agree that Hytee model provide the reports be invoked which identify the fields which have been modified F3: Do you agree that Hytee model these reports provide a complete record of all such changes
G	GUI	G1: Do you agree that Hytee model is user-friendly G2: Do you agree that Hytee model which the term in the prototype understandable G3: It helps me be more effective G4: Do you agree that Hytee model organization of information very clear

TABLE IV. LINGUISTIC VARIABLES FOR 5 POINT SCALE

Linguistic Variables	Likert Scale	Fuzzy Scale
Strongly agree	5	(0.9,1.0,1.0)
Agree	4	(0.5,0.7,0.9)
Neither agree	3	(0.3,0.5,0.7)
Disagree	2	(0.1,0.3,0.5)
Strongly disagree	1	(0.0,0.0,0.1)

III. RESULT AND FINDING

Data analysis is to follow the approach of Fuzzy\ Delphi through step 3 to 7 will answer questions the study disclosed. For viewing the degree of agreement among experts, the findings for each of the items were analyzed by a Threshold value (d) for two fuzzy numbers m = (m1, m2, m3) and n = (n1, n2, n3) are calculated using the formula:

$$d = \tilde{m}, \tilde{n} \sqrt{\frac{1}{3} [(m_1 - n_1)^2 + (m_2 - n_2)^2 + (m_3 - n_3)^2]}$$

It is supported by the Rahman, 2013 [22] and Jamil, 2013 [23] which States that in order to analyze the data, the distance between two Fuzzy number is calculated by measuring the average value of the deviation between the experts. Whereas the criteria used to assess the expert group consensus is based on the degree of agreement in excess of 75%.

In this study, one (1) is complied with because the value threshold for most of the subitem is ≤ 0.2, but only at part subitem only. However, the second condition (2) has also been observed because the expert group consensus is above 75%. Result value threshold ≤ 0.2, indicating that this study gets the value of the threshold exceeds 75% 77.8% by registering for a theme that includes a total of 5 subitems. This shows the degree of agreement among the experts has reached a consensus that good. Therefore, the second round for fuzzy Delphi is not needed because of data acquisition complies with both conditions.

Below show the findings for elements of Hytee model based on the consensus of experts. This data consists of the value of the threshold each element (d item), the value threshold constructs (d)

A. Change Management

Table V display findings for Change Management components for Hytee proposed model on the consensus of experts using the Fuzzy Delphi Method (FDM). The findings of this study show the value threshold (d) and the percentage of the expert group.

B. Traceability Support

Table VI display findings for Traceability Support components for Hytee proposed model on the consensus of experts using the Fuzzy Delphi Method (FDM). The findings of this study show the value threshold (d) and the percentage of the expert group.

TABLE V. CHANGE MANAGEMENT COMPONENTS

EXPERT		Change Management				
		B1	B2	B3	B4	B5
1	Expert 1	0.131	0.239	0.120	0.370	0.098
2	Expert 2	0.261	0.154	0.275	0.076	0.098
3	Expert 3	0.261	0.154	0.275	0.317	0.294
4	Expert 4	0.131	0.154	0.275	0.076	0.098
5	Expert 5	0.131	0.526	0.709	0.076	0.098
6	Expert 6	0.261	0.154	0.275	0.317	0.294
7	Expert 7	0.131	0.239	0.120	0.076	0.098
8	Expert 8	0.131	0.154	0.120	0.076	0.098
9	Expert 9	0.131	0.154	0.120	0.076	0.098
10	Expert 10	0.261	0.154	0.275	0.317	0.294
11	Expert 11	0.131	0.239	0.120	0.076	0.098
12	Expert 12	0.131	0.154	0.120	0.076	0.098
Threshold Value (d) of each item		0.174	0.206	0.234	0.161	0.147
The percentage of each item d ≤ 0.2		100.0	91.7	91.7	66.7	100.0
Average of fuzzy number (score fuzzy)		0.789	0.861	0.778	0.750	0.767

TABLE VI. TRACEABILITY SUPPORT COMPONENTS

EXPERT		Traceability Support				
		C1	C2	C3	C4	C5
1	Expert 1	0.186	0.261	0.196	0.261	0.163
2	Expert 2	0.186	0.131	0.196	0.131	0.228
3	Expert 3	0.186	0.131	0.196	0.261	0.163
4	Expert 4	0.186	0.131	0.196	0.131	0.228
5	Expert 5	0.495	0.261	0.196	0.131	0.163
6	Expert 6	0.206	0.131	0.196	0.131	0.163
7	Expert 7	0.206	0.261	0.196	0.261	0.163
8	Expert 8	0.186	0.131	0.196	0.131	0.228
9	Expert 9	0.186	0.131	0.196	0.131	0.228
10	Expert 10	0.206	0.131	0.196	0.131	0.163
11	Expert 11	0.206	0.261	0.196	0.261	0.163
12	Expert 12	0.186	0.131	0.196	0.131	0.228
Threshold Value (d) of each item		0.219	0.174	0.196	0.174	0.190
The percentage of each item d ≤ 0.2		91.7%	100.0%	100.0%	100.0%	100.0%
Average of fuzzy number (score fuzzy)		0.839	0.878	0.833	0.878	0.811

C. Regression Testing Support

Table VII display findings for Regression Testing Support components for Hytee proposed model on the consensus of experts using the Fuzzy Delphi Method (FDM). The findings of this study show the value threshold (d) and the percentage of the expert group.

D. Test Effort Estimation Support

Table VIII display findings for Test Effort Estimation Support components for Hytee proposed model on the consensus of experts using the Fuzzy Delphi Method (FDM). The findings of this study show the value threshold (d) and the percentage of the expert group.

TABLE VII. REGRESSION TESTING SUPPORT COMPONENTS

EXPERT		Regression Testing Support			
		D1	D2	D3	D4
1	Expert 1	0.065	0.249	0.141	0.108
2	Expert 2	0.326	0.145	0.251	0.284
3	Expert 3	0.065	0.249	0.141	0.108
4	Expert 4	0.326	0.145	0.141	0.108
5	Expert 5	0.065	0.833	0.432	0.401
6	Expert 6	0.065	0.145	0.251	0.108
7	Expert 7	0.065	0.145	0.251	0.108
8	Expert 8	0.065	0.145	0.141	0.284
9	Expert 9	0.065	0.145	0.141	0.284
10	Expert 10	0.065	0.145	0.251	0.108
11	Expert 11	0.065	0.145	0.251	0.108
12	Expert 12	0.065	0.145	0.141	0.284
Threshold Value (d) of each item		0.109	0.220	0.211	0.191
The percentage of each item $d \leq 0.2$		83.3%	91.7%	91.7%	91.7%
Average of fuzzy number (score fuzzy)		0.744	0.867	0.794	0.772

TABLE VIII. TEST EFFORT ESTIMATION SUPPORT COMPONENTS

EXPERT		Test Effort Estimation Support				
		E1	E2	E3	E4	E5
1	Expert 1	0.196	0.261	0.108	0.239	0.173
2	Expert 2	0.196	0.131	0.284	0.154	0.219
3	Expert 3	0.196	0.261	0.108	0.239	0.463
4	Expert 4	0.196	0.261	0.108	0.239	0.173
5	Expert 5	0.196	0.261	0.401	0.526	0.173
6	Expert 6	0.196	0.131	0.108	0.154	0.219
7	Expert 7	0.196	0.131	0.108	0.154	0.173
8	Expert 8	0.196	0.131	0.284	0.154	0.219
9	Expert 9	0.196	0.131	0.284	0.154	0.219
10	Expert 10	0.196	0.131	0.108	0.154	0.219
11	Expert 11	0.196	0.131	0.108	0.154	0.173
12	Expert 12	0.196	0.131	0.284	0.154	0.219
Threshold Value (d) of each item		0.196	0.174	0.191	0.206	0.220
The percentage of each item $d \leq 0.2$		100.0%	100.0%	91.67%	91.67%	91.67%
Average of fuzzy number (score fuzzy)		0.833	0.878	0.772	0.861	0.817

E. Report

Table IX display findings for Report components for Hytee proposed model on the consensus of experts using the Fuzzy Delphi Method (FDM). The findings of this study show the value threshold (d) and the percentage of the expert group.

F. Graphical user Interface

Table X display findings for Graphical User Interface components for Hytee proposed model on the consensus of experts using the Fuzzy Delphi Method (FDM). The findings of this study show the value threshold (d) and the percentage of the expert group.

TABLE IX. Report COMPONENTS

EXPERT		Report		
		F1	F2	F3
1	Expert 1	0.294	0.076	0.015
2	Expert 2	0.098	0.317	0.382
3	Expert 3	0.294	0.076	0.015
4	Expert 4	0.098	0.076	0.015
5	Expert 5	0.294	0.370	0.309
6	Expert 6	0.098	0.076	0.015
7	Expert 7	0.098	0.317	0.015
8	Expert 8	0.098	0.076	0.015
9	Expert 9	0.098	0.076	0.015
10	Expert 10	0.098	0.076	0.015
11	Expert 11	0.098	0.317	0.015
12	Expert 12	0.098	0.076	0.015
Threshold Value (d) of each item		0.147	0.161	0.070
The percentage of each item $d \leq 0.2$		100.0%	66.67%	83.33%
Average of fuzzy number (score fuzzy)		0.900	0.750	0.706

TABLE X. GRAPHICAL USER INTERFACE COMPONENTS

EXPERT		Graphical user Interface			
		G1	G2	G3	G4
1	Expert 1	0.141	0.261	0.239	0.108
2	Expert 2	0.251	0.131	0.154	0.284
3	Expert 3	0.251	0.131	0.154	0.284
4	Expert 4	0.141	0.131	0.154	0.108
5	Expert 5	0.432	0.261	0.526	0.401
6	Expert 6	0.141	0.131	0.154	0.108
7	Expert 7	0.141	0.261	0.239	0.284
8	Expert 8	0.251	0.131	0.154	0.108
9	Expert 9	0.251	0.131	0.154	0.108
10	Expert 10	0.141	0.131	0.154	0.108
11	Expert 11	0.141	0.261	0.239	0.284
12	Expert 12	0.251	0.131	0.154	0.108
Threshold Value (d) of each item		0.211	0.174	0.206	0.191
The percentage of each item $d \leq 0.2$		91.67%	100.0%	91.67%	91.67%
Average of fuzzy number (score fuzzy)		0.794	0.878	0.861	0.772

G. Result Consensus of the Expert

Requirement:

- 1) Triangular Fuzzy Numbers
 - a) Threshold value, $d < 0.2$
 - b) Percentage of Consensus Expert Group, $\% \geq 75.0 \%$
- 2) Defuzzification Process
 - a) Score Fuzzy (A) \geq Value α – cut = 0.5

Refer to Table XI, the Fuzzy Delphi Analysis of the present study has shown a satisfactory and good overall outcome.

From the findings, all the item meets the expert consensus $\geq 75.0 \%$. The first two elements, in change management and the report, has an average value of “d” threshold of less than 0.2. Accordingly, both have reached the percentage of expert consensus of more than 75%, and the defuzzification scores greater than 0.5, making them acceptable as antecedents for the customer engagement concept studied. This study for evaluation Hytee Model 2 item needs to revise again and update in the Hytee System. That action was done to able the whole % item “d” ≤ 0.2 has achieved the agreement of 78%, making this construct successfully maintained.

TABLE XI. RESULT OF A CONSENSUS OF THE EXPECT

No. Item/ Element		Triangular Fuzzy Numbers		Defuzzification Process				The Consensus of Experts
		The threshold value, d	Percentage of Consensus Expert Group,%	m1	m2	m3	Score Fuzzy (A)	
1	B1	0.174	100.0%	0.633	0.800	0.933	0.789	ACCEPT
2	B2	0.206	91.7%	0.750	0.883	0.950	0.861	ACCEPT
3	B3	0.234	91.7%	0.633	0.792	0.908	0.778	ACCEPT
4	B4	0.161	66.67%	0.583	0.758	0.908	0.750	REJECT
5	B5	0.147	100.00%	0.600	0.775	0.925	0.767	ACCEPT
6	C1	0.219	91.67%	0.717	0.858	0.942	0.839	ACCEPT
7	C2	0.174	100.00%	0.767	0.900	0.967	0.878	ACCEPT
8	C3	0.196	100.00%	0.700	0.850	0.950	0.833	ACCEPT
9	C4	0.174	100.00%	0.767	0.900	0.967	0.878	ACCEPT
10	C5	0.190	100.00%	0.667	0.825	0.942	0.811	ACCEPT
11	D1	0.109	83.33%	0.567	0.750	0.917	0.744	ACCEPT
12	D2	0.220	91.67%	0.767	0.892	0.942	0.867	ACCEPT
13	D3	0.211	91.67%	0.650	0.808	0.925	0.794	ACCEPT
14	D4	0.191	91.67%	0.617	0.783	0.917	0.772	ACCEPT
15	E1	0.196	100.00%	0.700	0.850	0.950	0.833	ACCEPT
16	E2	0.174	100.00%	0.767	0.900	0.967	0.878	ACCEPT
17	E3	0.191	91.67%	0.617	0.783	0.917	0.772	ACCEPT
18	E4	0.206	91.67%	0.750	0.883	0.950	0.861	ACCEPT
19	E5	0.220	91.67%	0.683	0.833	0.933	0.817	ACCEPT
20	F1	0.147	100.00%	0.800	0.925	0.975	0.900	ACCEPT
21	F2	0.161	66.67%	0.583	0.758	0.908	0.750	REJECT
22	F3	0.070	83.33%	0.517	0.708	0.892	0.706	ACCEPT
23	G1	0.211	91.67%	0.650	0.808	0.925	0.794	ACCEPT
24	G2	0.174	100.00%	0.767	0.900	0.967	0.878	ACCEPT
25	G3	0.206	91.67%	0.750	0.883	0.950	0.861	ACCEPT
26	G4	0.191	91.67%	0.617	0.783	0.917	0.772	ACCEPT

IV. CONCLUSION AND FUTURE WORK

It has concluded that all the elements in Hytee Model (except 2 elements) are maintained and certified of Hytee model based on the consensus of an expert. Using Fuzzy Delphi Method analysis, this study has proven the importance of element in Hytee Model. The findings of the study are in line with its purpose to answer the questions pertaining to the agreement of experts on an element into work developing proposed Hytee Model. The defuzzification process is greatly used to filter the priority of element. In change management, the contribution of this result to ensure the user understands the environment of change management. For traceability support the contribution of this study to prove the flow of the system using the traceability model. For regression testing support refer to Table VII is to show the function of regression testing in Hytee Model. In test effort estimation refer to Table VI show the user the result after all the flow of change of the error. For report and GUI refer to the table, we can see that the expert agree with the GUI of Hytee Model.

As future work, in this stage, the researcher will design the model based on the data from the Fuzzy Delphi Method discussion within the expert review. From elements of change management, traceability support, regression testing support, test effort estimation support, report and GUI, the findings it to continue to upgrade the proposed model to the actual model for improvement.

REFERENCES

- [1] Vasa, R., Schneider, J. G., & Nierstrasz, O. (2007, October). The inevitable stability of software change. In *Software Maintenance, 2007. ICSM 2007. IEEE International Conference on* (pp. 4-13). IEEE.
- [2] The Standish Group, Chaos, Standish Group Report, 2004
- [3] Lam, W., & Shankaraman, V. (1999). Requirements change a dissection of management issues. In *EUROMICRO Conference, 1999. Proceedings. 25th (Vol. 2, pp. 244-251)*. IEEE
- [4] Nurmaliani, N., Zowghi, D., & Powell, S. (2004). Analysis of requirements volatility during the software development lifecycle. In *Software Engineering Conference, 2004. Proceedings. 2004 Australian* (pp. 28-37). IEEE.
- [5] The Standish Group, Chaos, Standish Group Report, 2015
- [6] Bertolino, A. (2007, May). Software testing research: Achievements, challenges, dreams. In *2007 Future of Software Engineering* (pp. 85-103). IEEE Computer Society.
- [7] Aranha, E., & Borba, P. (2007, September). An estimation model for test execution effort. In *Empirical Software Engineering and Measurement, 2007. ESEM 2007. First International Symposium on* (pp. 107-116). IEEE
- [8] Hsu, C. C., & Sandford, B. A. (2007). The Delphi technique: making sense of consensus. *Practical assessment, research & evaluation*, 12(10), 1-8
- [9] Kaufmann, A., & Gupta, M. M. (1988). *Fuzzy mathematical models in engineering and management science*. Elsevier Science Inc.
- [10] Murray, T., Pipino, L., & Vangigch, J. (1985). A pilot study of Fuzzy set modification of Delphi. *Human-System Management*, 5(1), 6-80.
- [11] Zadeh L.A. (1965). *Fuzzy sets and systems*, System Theory (Fox J., ed.), Microwave Research Institute Symposia Series XV, Polytechnic Press, Brooklyn, NY, 29- 37. Reprinted in *Int. J. of General Systems*, 17, 1990, 129-138
- [12] Ragin, C. C. (2007). *Qualitative comparative analysis using fuzzy sets (fsQCA)*. In *Configurational comparative analysis*. London: Sage Publications.
- [13] Adler, M., & Ziglio, E. (1996). *Gazing into the oracle: the Delphi method and its application to social policy and public health*. London: Jessica Kingsley Publishers
- [14] Mahmud, R., Ismail, M. A., Mustapha, R., Din, R., & Yasin, R. M. (2006). Information and Communication Technology (ICT) Readiness among Malaysian Secondary School Teachers. *Asia-Pacific Collaborative Education Journal*, 2(1), 9-15.
- [15] Rowe, G., & Wright, G. (2011). The Delphi technique: Past, present, and future prospects – Introduction to the special issue. *Technological Forecasting and Social Change*, 78(9), 1487–1490
- [16] Jones, H. & Twiss, B.L. (1978). *Forecasting Technology For Planning Decisions*. New York: Macmillan
- [17] Berliner, D. C. (2004). Expert teachers: Their characteristics, development, and accomplishments. *Bulletin of Science, Technology and Society*, 24(3), 200-212.
- [18] Berliner, D. C. (2004). Describing the behavior and documenting the accomplishments of expert teachers. *Bulletin of Science, Technology & Society*, 24(3), 200-212.
- [19] Swanson, R. A., & Falkman, S. K. (1997). Training delivery problems and solutions: Identification of novice trainer problems and expert trainer solutions. *Human Resource Development Quarterly*, 8(4), 305-314.
- [20] Dalkey, N. C., & Helmer, O. (1963). An experimental application of the Delphi method to the use of experts. *Management Science*, 9(3), 458-467
- [21] Ibrahim, S. (2006). *A Document-based Software Traceability to Support Change Impact Analysis of Object-oriented Software*(Doctoral dissertation, Universiti Teknologi Malaysia).
- [22] Rahman, M. N. A. (2013). *Norlidah Alias, Saedah Siraj & Dorothy Dewitt. Model Homeschooling Berasaskan Teknologi di Malaysia: Pendekatan Interpretive Structural Modeling*.Mohd.
- [23] Jamil, M. R. M., Hussin, Z., Noh, N. R. M., Sapar, A. A., & Alias, N. (2013). Application of Fuzzy Delphi Method in educational research. Saedah Siraj, Norlidah Alias, DeWitt, D. & Zaharah Hussin (Eds.), *Design and developmental research*, 85-92.

Efficient MRI Segmentation and Detection of Brain Tumor using Convolutional Neural Network

Alpana Jijja¹, Dr. Dinesh Rai²
Computer Science and Engineering, Ansal University,
Gurugram, Haryana, India.

Abstract—Brain tumor is one of the most life-threatening diseases at its advance stages. Hence, detection at early stages is very crucial in treatment for improvement of the life expectancy of the patients. magnetic resonance imaging (MRI) is being used extensively nowadays for detection of brain tumors that requires segmenting huge volumes of 3D MRI images which is very challenging if done manually. Thus, automatic segmentation of the images will significantly lessen the burden and also improve the process of diagnosing the tumors. This paper presents an efficient method based on convolutional neural networks (CNN) for the automatic segmentation and detection of a brain tumor using MRI images. Water cycle algorithm is applied to CNN to obtain an optimal solution. The developed technique has an accuracy of 98.5%.

Keywords—Brain tumor; segmentation; convolutional neural network; water cycle algorithm

I. INTRODUCTION

Brain, the most important part has the most complex structure in the body. The presence of the skull around the brain hinders the study of its functions and also increases the complexity of diagnosing the diseases [1]. The brain is not prone to any particular diseases like the other parts of the body but can be triggered by the abnormal growth of cells in which there is a change in its behavior and structure. This abnormality is usually an indication of Brain Tumor. MRI is used for the detection of such tumors. With the improvements in technology, the segmentation of brain tumor and tissue has become an actively researched area [2]. The major issue in the segmentation of images is the clustering of feature vectors which are similar. Thus, extraction of acceptable features is the primary requirement for successfully segmenting the images. The useful feature extraction of images is a difficult task due to the intricacies in the structures of the various tissues in the brain [3]. The image segmentation is a significant building block in the studies related to brain tumor because, the extent of segmented brain tumor can remove the confusing structures from other brain tissues thus providing higher accuracy in the classification of the subtypes of the tumor and give information about the diagnosis and can also effectively monitor the growth, recurrence or shrinking of the tumors. The techniques of image segmentation can be classified as based on region/surface growing, edge detection, classifiers, quantization or feature clustering of vectors. The technique of vector quantization is an efficient model for the process of segmenting [4]. This technique will partition the n-dimensional vector space to M regions for optimizing the criterion function. The vector quantization involves two

processes of training and encoding, where training will determine the codebook vector set based on the input data probability while encoding will assign the input vectors to the vectors present in the codebook.

II. RELATED WORK

Segmentation of images in the applications such as detection of abnormality, surgical planning, post-surgery assessment in the medical field is a significant task. Hence, many methods have been proposed for segmentation [2] revisited the efficacy of two distinct texture features along with the application of the multimodal MR images for segmenting and classifying the pediatric brain tumors. The fractal feature of one of the texture is derived using Piecewise-Triangular-Prism-Surface-Area (PTPSA) algorithm and the other texture extraction uses fractional Brownian motion algorithm. The fusion of the features is achieved through a self-organizing map (SOM). The experimental results suggested that fusing the features of the intensity and fractal wavelet of the multimodal MR images gave better results when compared to that in images with a single modality. Mustaqeem et al., [5] developed and introduced an effective algorithm for detecting the brain tumor. The developed segmentation method was based on thresholding and watershed techniques. The images of the human brains obtained from the MRI scans were used for the segmentation process but this algorithm cannot be used in the segmentation of 3D images.

Padole & Chaudhari [6] developed a method for detecting the brain tumors from MRI images through component analysis. This method which can automatically detect the brain tumor surface area is a combination of Normalized cut (Ncut) and mean shift algorithms. Roy & Bandyopadhyay detected and measured the tumor from the brain MRI using symmetric analysis [7]. The very application of quantitative analysis of this method helps in the identification of disease status. El-Dahshan et al., reviewed the various classification and segmentation techniques and inferred that computer-aided diagnosis is the major issue of the MRI of the human brain [8]. Hence, the authors developed a hybrid intelligent machine learning method for automatically identifying the tumor through MRI brain. The images are segmented using a neural network which is coupled with a feedback pulse. The classification of the images to abnormal and normal is achieved with the help of a feed-forward neural network with backpropagation. The experiments are conducted on 101 images comprising 87 abnormal and 14 normal images from

the MRI dataset of a human brain. The results showed that this technique gave an accuracy of 99%.

Abdel-Maksoud et al., introduced an image segmentation technique that used the integration of K-means clustering and fuzzy C-means algorithm [9]. The stages of thresholding and segmentation at a set level helped in detecting the tumor accurately. The computational time was lower due to use of K-means clustering and accuracy was higher because of the use of fuzzy c-means. The performance evaluation of the suggested technique was processed by comparing it to the existing methodologies with respect to performance, processing time and accuracy. The results from the experiments proved the method's effectiveness in dealing with more number of problems related to segmentation by the improvement in the quality of segmentation and accuracy with minimum run time. Menze et al., [10] reported the outcomes of the Multimodal Brain Tumor Image Segmentation Benchmark (BRATS). A set of 65 multi-contrast MRI scans of various glioma patients was used as a dataset for around twenty segmentation algorithms for detecting the tumors. The authors found that separate algorithms were suitable for differentiated regions of the tumor and no particular algorithm was found best for all the subregions. Mahalakshmi & Velmurugan [11] developed an algorithm to detect brain tumor using particle swarm optimization. The algorithm comprises of four stages the conversion, implementation, selection, and extraction. The proposed PSO algorithm helps in determining the size of the MRI images of the brain. Elamri & Planque proposed a new algorithm for segmenting the Glioblastoma (GBM) tumor based on the 3D convolutional neural networks [12]. The authors proposed the generalization of CNN's to obtain 3D filters for increasing the robustness and conserving the spatial information. The presented CNN architecture also enabled the expansion of the effective size of data and reduction in the variance of the developed model and its accuracy was found to be 89%. Pereira et al., introduced an automatic technique for segmentation using convolutional neural networks (CNN) which explored small 3*3 kernels [13]. The use of these kernels allowed the deeper design of the architecture and had a positive impact against overfitting. By utilizing the intensity normalization as a preprocessing step along with augmentation of the data demonstrated the effectiveness of the segmentation for MRI images. This technique is validated using the BRATS 2013 database. The main problem of improvement in accuracy, still pertains in the above mentioned work. This can be solved by using optimized technique using WCA.

A completely automatic technique for segmenting the brain tumor which used deep convolutional networks based on U-Net was developed by Dong et al., [14]. The experiments were carried out on BRATS 2015 datasets consisting of both LGG as well as HGG patients. The results obtained from the experiments demonstrated that the proposed technique was effective. The technique was validated using the scheme of five-fold cross-validation. Using this technique, a model for segmenting the tumor images for specific patients can be generated without manually interfering. Havaei et al., [15] put

forward an automatic technique for segmentation of brain tumor using high capacity, flexible deep neural networks (DNN). This developed DNN technique uses both the global as well as the local contextual features at the same time. The difficulties with respect to the imbalance in the labels of the tumor are eliminated using a training procedure comprising two phases.

III. RESEARCH METHODOLOGY

The flow diagram for the proposed Brain Tumor image segmentation using Optimal Convolutional Neural Network (OCNN) is shown in Fig. 1. This proposed technique is implemented using MATLAB 14a software. The database contains grayscale images of the human brain. The images are preprocessed from the database using the technique of median filtering to remove the noise and reduce the distortions. The next step is the extraction of patches. A corner, edge or the uniform texture of the image can be considered as the patch. The extraction of patches helps in determining the parts of the brain where the abnormality is present. Further in patch pre-processing the values of standard deviation, variance, intensity etc. of the images which are under the training phase are obtained. The filtered images in which the tumors are present are detected, classified, and clustered using the CNN. Images were clustered using the K-means clustering technique and segmented using morphological segmentation. Water cycle optimization algorithm is applied to calculate the weight and bias factor that has a significant role in identifying and classifying of the tumors. The factors of weight and bias help in classifying the images with higher accuracy. Lastly, performance of this method is evaluated for different factors like specificity, accuracy, sensitivity, entropy, etc.

A. Image Preprocessing

Preprocessing enhances the quality of the images by eliminating noise and reducing the distortions of the input image. The current study uses a median filtering technique to preprocess the image. A median filter is a non-linear filter based on statistics. Subsequently the noisy value of the image is replaced by the median value of the neighboring mask. The pixels of the mask are ranked in the order of Grey levels, and the median value of the group is stored to replace the noisy value. The output of the median filtering is:

$$g(x, y) = \text{med} \{ f(x-i, y-j), i, j \in W \} \quad (1)$$

Where:

$f(x, y)$ = original image and $g(x, y)$ = output image

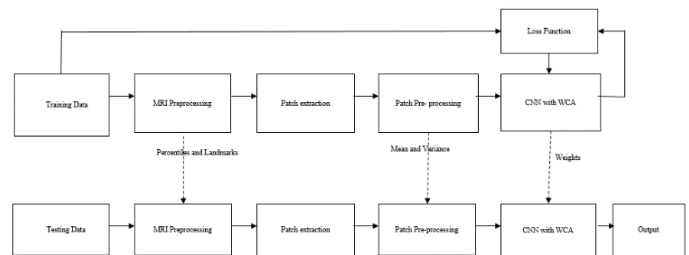


Fig. 1. Proposed Workflow Diagram.

$W = 2D$ mask whose shape can be square, circular, linear etc. The median filter will move throughout the image, pixel by pixel and replaces each value with the median value of the neighboring pixels. This matrix of neighbors is referred to as “windows”. The window will slide over the complete image pixel by pixel. The median value is derived by sorting all the values of the pixel from the window in the numerical order and then transposing the pixel under consideration to the median pixel value.

B. Convolutional Neural Networks (CNN)

Fig. 2 illustrates that CNN which is feed forward neural network and is widely used for image recognition. This is made up of neuron with learnable weights and biases. Each neuron receives several inputs, takes a weighed sum over them, pass it through activation function and responds with the output. CNN operates over volumes like neural networks where the input is a vector but in case of CNN the input is a multi-channeled image. CNN has overcome image segmentation challenges by automatically learning a hierarchy of increasingly complex features directly from data. The CNN basically is used in convolving the image with the kernels for the process of obtaining the feature maps. The weights in the kernels help in connecting each unit of the feature map to the previous layers. These weights of the kernels are utilized during training of the datasets for improving the attributes of the input [16]. The number of weights which have to be trained in the convolutional layers is lesser when compared to the fully connected (FC) layers because the kernels are common to all the units of one particular feature map. Some of the significant concepts with respect to CNN are discussed below.

- Initialization is the most significant step for accomplishing convergence. This process helps in maintaining the gradients at the required levels else there will be a chance of explosion of the gradients that are back propagated.
- The activation function is accountable for the data transformation in a nonlinear manner. There are various types of activation function of which the modified Rectifier linear units (ReLU) is used. It is defined as

$$f(x) = \max(0, x) + \alpha \min(0, x) \quad (2)$$

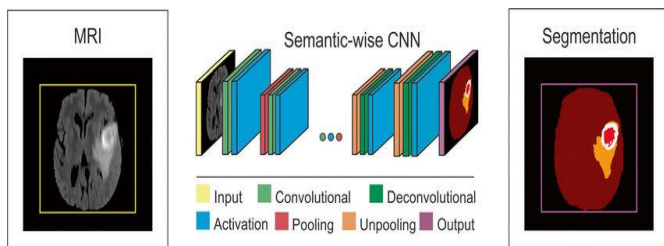


Fig. 2.

Architecture of CNN.

- In the feature maps, the process of pooling combines the feature that is nearby spatially. This sequence of redundant features helps in making the representation invariant in the case of small changes and also more compact. The computation load for the successive stages is also reduced.
- The overfitting is decreased with the help of regularization. In every step of training, it will eliminate the nodes of the network. In this way, all the nodes in the Fully Connected layer are forced to learn better representations and also prevent the co-adaptation of nodes.
- The number of parameters to train a fully connected network is much larger as compared to a CNN. In most images the nearby pixels are generally related but a fully connected neural network doesn't take this into account while a CNN takes into account relationship between space and pixel within an image.
- The loss function is the function (H) that has to be reduced during the training phase of the data. Categorical Cross-entropy is used in this study [17].

$$H = - \sum_{j \in voxels} \sum_{k \in voxels} C_j \log(\hat{C}_{j,k}) \quad (3)$$

The WCA off-late has been developed as the optimization technique which can be applied to various engineering design constrained optimization problems [18]. The fundamental concept which has been used in the development of this algorithm is based on the actual water cycle process. The WCA plays an important role in Identifying, detecting and classifying the images with tumors. The pseudocode for the WCA is given below [19].

IV. RESULTS AND DISCUSSIONS

The input to the proposed technique is the greyscale images obtained from the database related to brain tumor obtained from the internet. The images from the database are split into two sets of training and testing images. Totally 400 images of the brain MRI is used, out of which 300 images are considered for training and 100 images for testing. Fig. 3 shows the greyscale image of the human brain which is considered as an input obtained from the testing set of images. This image is preprocessed using the technique of median filtering to remove the noise and reduce the distortions present in the input image. Fig. 4 is filtered image of the test image.

The next step is the patch processing. A corner, edge or the uniform texture of the image can be considered as the patch. The size of each patch is 10px by 10px. Fig. 5 shows the patch processed image. This process is carried out to find the parts that have abnormalities. Further, the patch pre-processing is carried out to obtain the values of standard deviation, variance, intensity etc. of the images which are under the training phase.

```
Set user parameter of the WCA:  $N_{pop}$ ,  $N_{sr}$ ,  $d_{max}$  and  
Maximum_ iteration.  
Determine the number of streams (individuals) which flow  
to the rivers and sea  
Create randomly initial population. Define the intensity of flow  
streams flow to their corresponding rivers and sea  
While (t < Maximum_ iteration) for i =1: Population Size  
( $N_{pop}$ ) Stream flows to its corresponding rivers and sea  
Calculate the objective function of the generated stream  
    If  $F_{New\_Stream} < F_{river}$   
    River = New_ Stream;  
    If  $F_{New\_Stream} < F_{Sea}$   
    Sea = New_ Stream;  
    End if  
    End if  
    Calculate the objective function of the generated river  
    If  $F_{New\_River} < F_{Sea}$   
    Sea = New_ River;  
    End if  
    End for  
    For i= 1: number of rivers ( $N_{st}$ )  
    If (distance (Sea and River) <  $d_{max}$ ) or (rand < 0.1)  
    New streams are created end if  
    End for  
    Reduce the  $d_{max}$   
End while
```

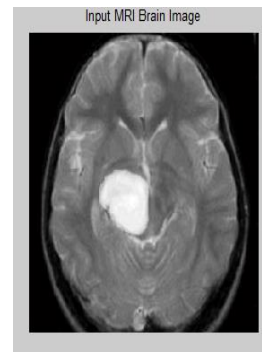


Fig. 3. Input image.

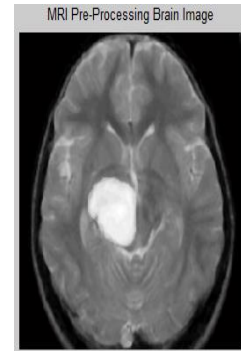


Fig. 4. Median Filter Image.

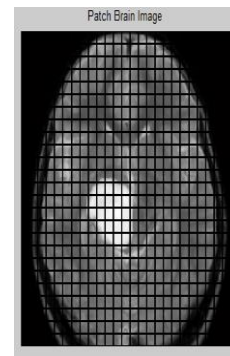


Fig. 5. Patch Image.

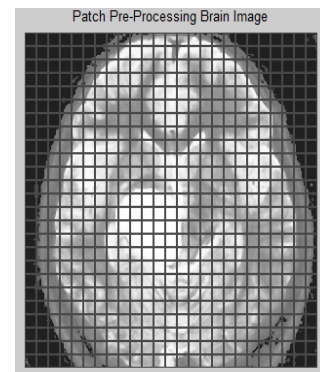


Fig. 6. Patch Pre-Processing Image.

Fig. 6 shows the patch preprocessed image. The final step is the cluster based segmentation of the tumor images using CNN. The CNN will classify the images based on various factors like intensity, shape etc. and detect the tumor. Fig. 7 is the clustered images to the brain showing various edges.

The brain tumors are usually formed by large connected regions. The final step of post-processing includes segmenting, detecting and extracting the tumor from the image and will remove any of the connected components however small the components are. At this stage, the tumor is detected along with the area that is covered by the disease. Fig. 8 shows the final output of CNN. Fig. 8a shows only the tumor part of the image and the Fig. 8b shows the color based segmented image.

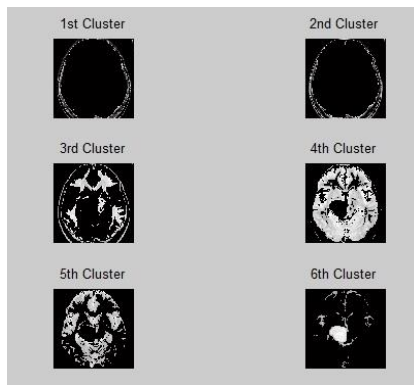


Fig. 7. Showing the Detection of the Tumor by Clustering.

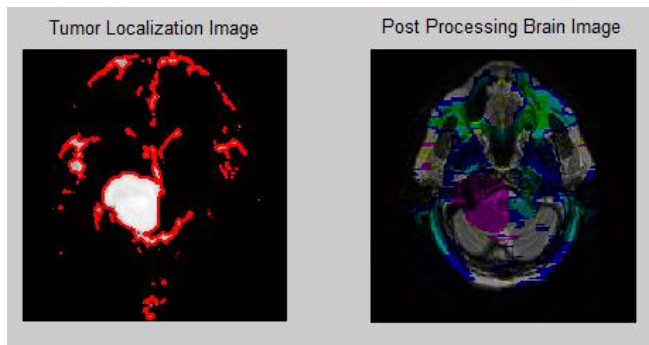


Fig. 8. (a) Localized Tumor Image (b) Post Processed Brain Image.

A. Performance Evaluation

The performance of the proposed technique is evaluated in terms of accuracy, sensitivity, and specificity where:

TP = True Positive

FN = False negative

The sensitivity is defined as the ability to determine the tumors correctly. It can be calculated using the following relation.

$$\text{Sensitivity} = \text{TP} / (\text{TP} + \text{FN})$$

The Specificity is defined as the ability for the correct determination of healthy cases. It can be calculated using the following relation.

$$\text{Specificity} = \text{TN} / (\text{TN} + \text{FP})$$

Accuracy is defined as the ability to differentiate healthy and unhealthy cases correctly can be calculated using the following relation.

$$\text{Accuracy} = (\text{TN} + \text{TP}) / (\text{TN} + \text{TP} + \text{FN} + \text{FP})$$

The performance metrics calculated for the tested images is tabulated in Table I. and Fig. 9 shows the plot for the sensitivity, specificity and accuracy parameters.

The comparative study in Table II examines the various automated segmentation techniques used by researchers on brain MRI. It has been observed that the proposed WCA algorithm has performed and overcome image segmentation challenges by automatically learning a hierarchy of

increasingly complex features directly from the data. In this algorithm is shown the calculation of cost sensitive feature selection using loss equation which balances accuracy and computational cost. Hence more modern techniques can be used to increase the accuracy by using deep learning methods along with increased sample data size.

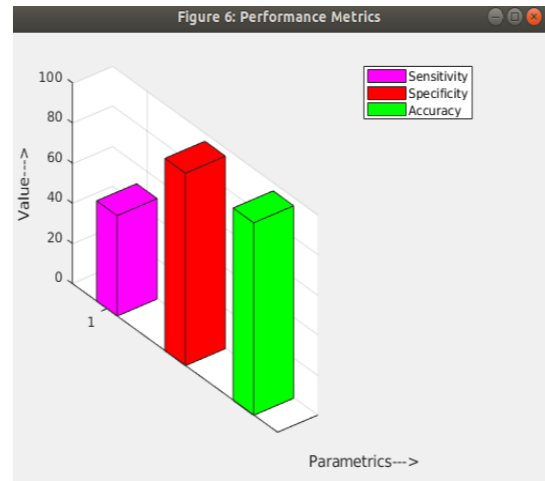


Fig. 9. Plot of Performance Metrics.

TABLE I. PERFORMANCE MATRIX

Parameter	Value
Tumor segment area	18.512
Tumor positive value	1
True negative value	60220
False positive value	886
Sensitivity	50
Specificity	98.55
Accuracy	98.54
MSE	9.82
PSNR	38.20
Entropy	0.771
Correlation	0.194
Structure similarity index	0.2108

TABLE II. COMPARATIVE SUMMARY OF DIFFERENT CLASSIFIER FOR SEGMENTATION ACCURACY

Title	Technique	Accuracy
Tumor segmentation from single contrast MR images of the human brain [20]	Random forest classification	83.00%
Detection of Brain Tumor in MRI Images, using Combination of Fuzzy C-Means and SVM [21]	Fuzzy c-means algorithm and SVM classifier	91.66%
An Automatic Brain Tumor Extraction System Using Different Segmentation Methods [22]	Fuzzy c-means algorithm	90.57%
Tumor detection and classification of MRI brain image using wavelet transform and SVM [23]	Wavelet transform and SVM classifier	86%
Proposed technique	CNN with WCA algorithm	98.50%

V. CONCLUSION

The current study developed an automated method for the segmentation and detection of a brain tumor. The greyscale images obtained from the database are preprocessed using median filtering to remove the noise and distortions that are present in the input image. The CNN is then used for clustering and segmenting the images and finally to detect the tumor. The WCA optimization algorithm is applied for optimal clustering of the images. The developed automatic image segmentation and tumor detection technique are found to have an accuracy of 98.5%, sensitivity of 50% and specificity of 98.5%. The comparison of the proposed technique with existing methods proves that the technique developed in this paper has the highest accuracy. The accuracy can be further improved using large datasets, however as compared to their imaging area, availability of dataset is not easily available. Thus sharing the data resources by different healthcare service providers may help to overcome this issue. There are unlimited opportunities to improve healthcare system by using more sophisticated filters in CNN. While the proposed model yields promising results, and leaves no room for errors. In surgical setting it is essential to remove as much of tumor mass as possible without damaging the surrounding healthy tissue. In future more work could be extended by developing more advanced patch extraction algorithm which will help in segmentation accuracy.

REFERENCES

- [1] Gondal and M. Khan, "A review of fully automated techniques for brain tumor detection from MR Images", *International Journal of Modern Education and Computer Science*, vol. 5, no. 2, pp. 55-61, 2013.
- [2] K. Iftakharuddin, K.M, "Techniques in fractal analysis and their applications in brain MRI", *Medical Imaging Systems Technology: Volume 1: Analysis and Computational Methods*, 2005, pp. 63-86.
- [3] Wang and D. Doddrell, "A segmentation-based and partial-volume-compensated method for an accurate measurement of lateral ventricular volumes on T1-weighted magnetic resonance images", *Magnetic Resonance Imaging*, vol. 19, no. 2, pp. 267-273, 2001.
- [4] Krishnamurthy, S. Ahalt, D. Melton and P. Chen, "Neural networks for vector quantization of speech and images", *IEEE Journal on Selected Areas in Communications*, vol. 8, no. 8, pp. 1449-1457, 1990.
- [5] Mustaqeem, A. Javed and T. Fatima, "An efficient brain tumor detection algorithm using watershed & thresholding based segmentation", *International Journal of Image, Graphics and Signal Processing*, vol. 4, no. 10, pp. 34-39, 2012.
- [6] V. Padole and D.S. Chaudhari, "Detection of the brain tumor in MRI images using the mean shift algorithm and normalized cut method", *International journal of Engineering and Advanced Technology*, pp. 52-56, 2012.
- [7] S. Roy and S. Bandyopadhyay, "Detection and quantification of brain tumor from MRI of brain and its symmetric analysis", *International Journal of Information and Communication Technology Research*, vol. 2, no. 6, pp. 477-483, 2012. [Accessed 30 March 2019].
- [8] E. El-Dahshan, H. Mohsen, K. Revett and M. Salem, "Computer-aided diagnosis of human brain tumor through MRI: A survey and a new algorithm", *Expert Systems with Applications*, vol. 41, no. 11, pp. 5526-5545, 2014. Available: 10.1016/j.eswa.2014.01.021.
- [9] Abdel-Maksoud, M. Elmogy and R. Al-Awadi, "Brain tumor segmentation based on a hybrid clustering technique", *Egyptian Informatics Journal*, vol. 16, no. 1, pp. 71-81, 2015.
- [10] Menze et al., "The multimodal brain tumor image segmentation benchmark (BRATS)", *IEEE transactions on medical imaging*, vol. 34, no. 10, pp. 71-81, 1993.
- [11] S. Mahalakshmi and T. Velmurugan, "Detection of brain tumor by particle swarm optimization using image segmentation", *Indian Journal of Science and Technology*, vol. 8, no. 22, 2015.
- [12] Elamri, and T.de Planque, "A new algorithm for fully automatic brain tumor segmentation with 3-D convolutional neural networks", 2016.
- [13] S. Pereira, A. Pinto, V. Alves, and C. A. Silva, "Brain tumor segmentation using convolutional neural networks in MRI Images," *IEEE Transactions on Medical Imaging*, vol. 35, no. 5, pp. 1240-1251, 2016.
- [14] H. Dong, G. Yang, F. Liu, Y. Mo, and Y. Guo, "Automatic brain tumor detection and segmentation using U-Net based fully convolutional networks," *Communications in Computer and Information Science Medical Image Understanding and Analysis*, pp. 506-517, 2017.
- [15] M. Havaei, A. Davy, D. Warde-Farley, A. Biard, A. Courville, Y. H. Tang, H. Lu, W. Liu, and X. Tao, "Tumor segmentation from single contrast MR images of human brain," *IEEE 12th International Symposium on Biomedical Imaging (ISBI)*, 2015.
- [16] K. O'Shea and R. Nash, "An introduction to convolutional neural networks" - arXiv preprint arXiv:1511.08458., 2015.
- [17] S. Cui, L. Mao and S. Xiong, "Brain tumor automatic segmentation using fully convolutional Networks", *Journal of Medical Imaging and Health Informatics*, vol. 7, no. 7, pp. 1641-1647, 2017.
- [18] H. Eskandar, A. Sadollah, A. Bahreininejad, and M. Hamdi, "Water cycle algorithm - A novel metaheuristic optimization method for solving constrained engineering optimization problems," *Computers & Structures*, vol. 110-111, pp. 151-166, 2012.
- [19] Sadollah, H. Eskandar, and J. H. Kim, "Water cycle algorithm for solving constrained multi-objective optimization problems," *Applied Soft Computing*, vol. 27, pp. 279-298, 2015.
- [20] M. Havaei, A. Davy, D. Warde-Farley, A. Biard, A. Courville, Y. H. Tang, H. Lu, W. Liu, and X. Tao, "Tumor segmentation from single contrast MR images of human brain," *IEEE 12th International Symposium on Biomedical Imaging (ISBI)*, 2015.
- [21] Parveen and A. Singh, "Detection of brain tumor in MRI images, using combination of fuzzy c-means and SVM," *2nd International Conference on Signal Processing and Integrated Networks (SPIN)*, 2015.
- [22] A. Kaur, "An automatic brain tumor extraction system using different segmentation methods," *Second International Conference on Computational Intelligence & Communication Technology (CICT)*, 2016.
- [23] R. Mathew assnd P. B. Anto, "Tumor detection and classification of MRI brain image using wavelet transform and SVM," *International*

Smartphones-Based Crowdsourcing Approach for Installing Indoor Wi-Fi Access Points

Ahmad Abadleh¹, Wala Maitah², Hamzeh Eyal Salman³, Omar Lasassmeh⁴, Awni Hammouri⁵
Department of Computer Science
Faculty of IT, Mutah University
Karak 61710, Jordan

Abstract—This study provides a new Crowdsourcing-based approach to identify the most crowded places in an indoor environment. The Crowdsourcing Indoor Localization system (CSI) has been one of the most used techniques in location-based applications. However, many applications suffer from the inability to locate the most crowded locations for various purposes such as advertising. These applications usually need to perform a survey before identifying target places, which require additional cost and time consuming. For example, Access Points (APs) installation can rely on an automated system to identify the best places where these APs should be placed without the need to use primitive ways to determine the best locations. In this work, we present a new approach for Wi-Fi designers and advertising companies to recognize the proper positions for placing APs and advertisement activities in indoor buildings. The recorded data of the accelerometer sensors are analyzed and processed to detect user's steps and thereby predict the most crowded places in a building. Our experiments show promising results in terms of the most widely used metrics in the subject as the accuracy for detecting users' steps reaches 95.8% and the accuracy for detecting the crowded places is 90.4%.

Keywords—Crowdsourcing; indoor localization system; accelerometer sensors; Wi-Fi access point; smartphones

I. INTRODUCTION

The extensive utilization of Smartphones and wireless network have magnified the importance of Indoor Positioning Service (IPS). Therefore, many approaches have been designed for providing users location services in a room or building level [1]. These approaches rely on off-the-shelf WiFi infrastructure and sensor mobiles. However, deploying Wi-Fi access points (WAP) are done on geographic base, which needs manpower and extra cost, rather relying on the crowded areas to determine the best places for installing them. Moreover, identifying crowded places help promotion companies to choose the best places to display their ads by most of the building visitors [1] [2].

Positioning system can be divided into two categories [3]: indoor positioning and outdoor positioning. The indoor positioning precision requirements are higher than that for outdoors. Global Positioning System (GPS) is the most popular system that establishes outdoor Positioning. However, GPS is not suitable for indoor localization, since the satellite signal cannot penetrate buildings walls or their roofs [4]. Indoor positioning system (IPS) is very useful to locate people or required objects within the building and in closed areas. In addition, indoor location-based services (ILBSs) have become

an essential part of people's activities in living, working, studying and shopping [5]. Indoor localization depends on infrastructures, such as ultra-wideband radio, Bluetooth and wireless access point [3][6].

One of the most common methods that use IPS approach is Crowdsourcing indoor positioning system [7]. Crowdsourcing is the most promising solution for solving the site survey problem in fingerprint technique. Crowdsourcing becomes a viable solution for collecting a large amount of data required to support location-based services (e.g., acceleration, a gyroscope and Received Signal Strength (RSS)).

Wi-Fi (Wireless Fidelity) is the most commonly used approach for indoor positioning. Wi-Fi is a good option for indoor positioning technology. This is due to the ubiquity of WAPs and embedded Wi-Fi connectivity in Smartphones. Indoor localization using Smartphones has been generally investigated; and its significance is consistently expanding as an after effect of the various applications that require indoor localization systems. Modern Smartphones have multiple sensors, which can be combined to obtain more precise indoor positioning results. These sensors are used to detect user phone proximity, for user activities such as, recognition, or indoor tracking and indoor localization. In general, the most popular approaches for indoor positioning are: cell of origin, triangulation, trilateration, and fingerprint. One of the most common methods that use the IPS approach is Crowdsourcing indoor positioning system. The main idea of the Crowdsourcing technique is to retrieve data from users in an indoor environment and store it in a database for future use. The larger the volume of data collected, the better the performance of the approach in terms of accuracy and efficiency [8].

One major issue in indoor environments is how to install Wi-Fi access points and where they should be placed. Typically, in any indoor environment, there are uncrowded places; hence, it would be helpful to have an approach that recognizes crowded areas for installing Wi-Fi access points to guarantee the best distribution of the network [9].

People spend most of their time indoors so indoor localization becomes an important issue. As the Wi-Fi spreads widely indoors, the network designers do not have some clear criteria on how to place the Wi-Fi access points. Thus, we proposed a new approach based on Smartphones and Crowdsourcing technique to automatically detect the best places where the access points must be placed inside the target building. Based on this base, our proposed approach collects

acceleration values of the building's visitors, which depend on their movements in the target building. These values are then smoothed to remove the noise and outliers' values, which resulted from irrelevant movements as well as the sensor sensitivity. Afterward, smartphones are exploited to detect user steps, time and stop location. These data are entered in the machine learning phase, Crowded Algorithm (CA), to label the most crowded places within the target building using KNN classifier, Naive Bayes and Random Tree.

To validate our approach, we carried out real experiments in the building of Information Technology faculty of 2291.04m². Our results show that our approach achieves high accuracy to detect crowded places in the target building. The average accuracy level for detecting crowded places is 96%; and the average accuracy levels for detecting user step and stopping time are (95.8%) and (90.3%), respectively.

The rest of the article is organized as follows. Section II presents the most recent and relevant research work in the subject. The proposed approach steps are detailed in Section III. In Sections IV and V, experimental results are presented and discussed, respectively. Finally, we conclude the article in Section VI.

II. RELATED WORK

GPS is the most effective positioning system for an outdoor environment. However, GPS is incapable of providing positioning services with sufficient localization accuracy in indoor environments due to the lack of Line of Sight(LOS) transmission channels between satellites and an indoor receiver [4]. In addition, it offers accurate positioning of the location for mobile device [3]. Wi-Fi technology is used to track and position the signal strength received by the end user's device. Smartphones, tablets and mobile devices have become more popular for outdoor and indoor seamless tracking and positioning [10]. In [11], Teuber increased the accuracy to 3m by applying minimal Euclidian Distance (ED) and fuzzy inference systems to determine the positions based on WLAN signal to noise ratio measurements. In [12], Chaudhary et al. proposed a system for indoor positioning based on RSSI values from AP's using RMSE algorithm (the number and positions of AP's play a major role in the tracking process the accuracy increases when the number of AP's is increased). The tracking and positioning are affected by the environmental factors and the acceptable error range, which gives importance for a crowded enclosed environment.

A. Indoor Positioning System Techniques

Indoor positioning system techniques have been developed rapidly throughout the last years. Multiple positioning methods can be applied for people's mobility tracking and positioning. CoO [13], Trilateration [14], Triangulation [15] and Fingerprinting [16] are typical and wide-spread methods. Indoor positioning localization techniques use signal metrics (e.g. AOA, TOA, TDOA, and RSS) and readings of Smartphone sensors to locate the position using either angle estimation or distance. Below, we present the indoor positioning techniques, the discussion of the limitations of these techniques and motions estimation in positioning systems [17].

CoO methods are used for people's tracking and positioning [13]. Each beacon (e.g. an AP or RFID reader) represents a cell/ polygon according to its RSSI distribution. The cell's size depends on the density of the beacons. The device held by the user can be detected by the closest beacon while the user walks through the area covered by the beacons. The hooked beacon locate the user's current position. The CoO is simple and less prone to environmental effects. In general, CoO is not used as other methods. This is because its low accuracy [13].

Triangulation depends on geometric properties of triangles to estimate the target location. Each direction is formed by the circular radius from a station to the mobile target. AOA methods should know the reference points and measured angles to derive the 2D of target location [15] [14]. One of these systems is Infrared Indoor Scout Local Positioning System (IRIS LPS) developed by [18]. The accuracy of the system about 8cm in near range and about 16 cm when covering 100m [18].

One of the advantages of the AOA-based technique is that the location estimation can be determined using fewer points. For finding direction, it requires directional antennas which means there is no need for time synchronization between measuring points [19]. Although AOA provides good accuracy, but it requires complex hardware and software, which increases the cost of the entire system.

The trilateration locates the object position by measuring its distance from multiple reference points. In trilateration, the "tri" says that at least three fixed points determine a position [14].

The main idea of fingerprint techniques is to collect a unique signature for each place in the interested area from a fingerprint database [16]. The location is determined by matching the measured fingerprint with those in the fingerprint database. Wi-Fi location of fingerprinting technique consists of two phases: the training phase and the positioning phase. To generate the database in a conventional way, (some reference points RPs) in the interested area are determined; and then locates a Smartphone at the location of one RP. Afterwards, RSS metrics in those RPs are measured for all Aps; and then RP characteristic feature is selected from these measurements and recorded in the database. A localization algorithm retrieves the fingerprint database and returns the matched fingerprints as well as the corresponding locations. The considerable manual cost, time-consuming, labor-intensive and vulnerable to environmental dynamics are the main drawbacks of fingerprinting-based methods; which can be solved by Crowdsourcing based approaches.

An IPS using RADAR signal was proposed in [10]. They provided a high degree of accuracy for locating and tracking users, which is about the size of a typical office room range 2 to 3 meters. An indoor positioning system with 0.45m of accuracy was developed by [20]. However, this approach requires a site survey at every location of interest to build a fingerprint database.

Crowdsourcing is an emerging field that allows solving difficult problems by collecting real data rather than trained set of data. Crowdsourcing stands as the only viable solution for collecting a large amount of data for individual's locations that are required to support location-based services; for instance,

RSS acceleration and gyroscope [21]. In Crowdsourcing, ordinary individuals and users benefit from the constructed localization systems by sharing their data with others to achieve a globally localization in indoor environment [7]. In UnLoc approach proposed by [22], the mobile sensors that sense the landmarks can recalibrate their location. They achieved higher than 95% of accuracy level in supporting room. In [23], Wu et al. proposed LiFS indoor localization system based on off-the-shelf Wi-Fi infrastructure and Smartphones. The calibration process of fingerprints in LiFS is crowdsourced and automatic. They conducted an empirical investigation to the suitability of Wi-Fi localization in order to get highly accurate indoor localization of Smartphones.

B. Motions Estimation

There are many investigations available to step detection for people movement. Various tools can be used for motion detection events such as, pedometer, gyroscope, and accelerometer. Pedometer or step counter is a portable device that counts each by detecting the motion of the person's hand or hips. This technology includes a mechanical sensor and software to count steps. The accuracy of step counters varies between devices since it depends on a fixed step length. The accuracy of the pedometer has error of 5% [24].

The Gyroscope is a device for measuring orientation based on the angular momentum principle. The spatial orientation of a solid object is based on three parameters: pitch, rotation around the x axis; roll, rotation around the y axis; azimuth rotation around the z axis [25]. Accelerometer is an electromechanical device that measures acceleration forces. Modern Smartphones have an accelerometer sensor that can be combined to measure the acceleration forces applied to the device on three axes (x, y, and z), as well as the force of gravity. The acceleration on (x, y) axes represents the change due to rotating or tilting the Smartphone; while the acceleration on z-axis represents the change due to vertical movements [26].

In indoor positioning using a Smartphone, built-in Smartphone accelerometer sensor offers the ability to physically measure the features dynamic motion, including the distance moved, orientation, steps, and the step length based on the periodic acceleration pattern of the user's gait. The proposed work in [27] used an inertial sensor to improve dead reckoning algorithm to help firefighters based on their location in the scene of fire accident. Accelerometers and gyros are applied to determine step, stride and heading. In [28], Hansson et al. used accelerometer and gyroscope to determine the users' motion. In their work, the accelerometer was used to count steps, and the gyroscope was used to detect the heading change. Their approach assumes that the step length, the initial position and heading are known. Moreover, they taken in account the step length and the error in counting the peaks. In this article, the proposed approach stored the Smartphone sensor data from the buildings visitors. The data from the accelerometer sensor will be used for detecting users' steps to address the most crowded places in a building.

Compared to the previous techniques, when we reassess our approach, we find that our method does not require any extra hardware or software. it is only based on the built-in sensors in the Smartphones. However, the previous methods

require the presence of Wi-Fi access points and some additional hardware and software requirements. Therefore, the current study achieves the objectives of detecting user steps; stopping time and identifying the crowded places in which Wi-Fi access points can be best deployed in the target building without any additional costs. Our proposed approach uses Crowdsourcing indoor localization for providing guidelines for Wi-Fi designers, which saves manpower and cost, and enables promotion companies to display their ads in the right place and at the right time.

III. THE PROPOSED APPROACH

Based on users' steps and time intervals, the stored data are clustered and classified using a machine learning algorithm. We made the flowing assumptions. Firstly, the mobile phone is at a static position placed in user's hand throughout the movement. Secondly, users must use a device equipped with some sensors such as accelerometer, which is rational since all the modern Smartphone are equipped with numerous sensors. Fig. 1 shows the block diagram of our proposed approach. It comprises of four stages. First, Crowdsourcing stage, pre-processing stage, step detection stage and crowded algorithm stage. Also, we rely on well-known classifiers to find the most crowded places.

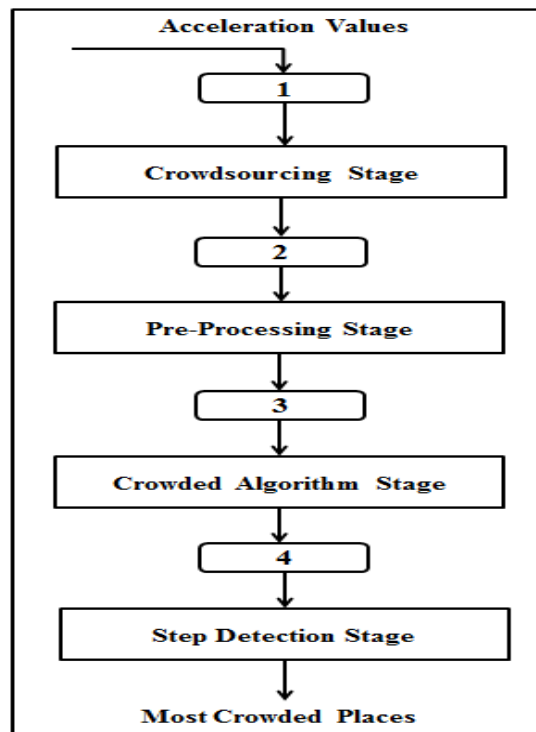


Fig. 1. Block diagram for the proposed approach.

A. Crowdsourcing Stage

The proposed approach uses Crowdsourcing method to collect acceleration values from buildings visitors Smartphones. An accelerometer is a sensor that measures user acceleration, which is the change rate in velocity of Smartphone. The measured acceleration includes gravity and the physical acceleration change of velocity. The acceleration on x, y axes

represents the change due to rotating or tilting the Smartphone, while the acceleration on z-axis represent the change due to vertical movements [29]. The raw data from the accelerometer are represented in a set of vectors: $Acc_i = \langle X_i, Y_i, Z_i \rangle$.

B. Pre-processing Stage

The magnitude value represents the vibration on the three axes coordinates calculated by Equation 1. To exclude the gravity force from the magnitude value, the average of magnitude for all values are computed. Then the average magnitude is subtracted from the magnitude value using Equation 2. During this stage a high pass filter is used to exclude the outliers' values and the Earth's gravity [30].

$$mag = \sqrt{X^2 + Y^2 + Z^2} \quad (1)$$

where X, Y and Z represent acceleration force along the x axis (including gravity) m/s^2 , y axis (including gravity) m/s^2 and z axis (including gravity) m/s^2 , respectively.

$$netmag = mag - avgmag \quad (2)$$

C. Step Detection Stage

In this approach, a new algorithm is proposed to detect the real peak that represents user steps and the stop time using an empirical threshold, since user visits different places in the environment. Our step detection algorithm involves the values of X, Y and Z measurement values as well as the time from the accelerometer sensor. Equation 1 is used to find the magnitude value of these readings. Afterwards, we calculate the threshold value by dividing the magnitude values into dynamic time windows and we find the average of (St.D) of each dynamic time window. When the value of the resulted St.D, for each time window, is greater than the grand St.D, it means a new step is detected. Algorithm 1 shows our proposed algorithm's steps.

Algorithm 1: Step Detection Algorithm

- 1 Collect accelerometer data including time: X, Y, and Z values.
 - 2 Calculate the magnitude value for each reading (x, y, z) using Equation 1.
 - 3 Divide into dynamic time window.
 - 4 Calculate standard deviation (St.D) of each time window.
 - 5 Calculate the threshold value, which is the average of standard deviation for each list of time windows.
 - 6 The step is detected if the standard deviation for a time window is greater than the overall standard deviation.
-

D. Crowded Algorithm Stage

The Crowded Algorithm (CA) is proposed to classify the data collected from step detection stage to make a model for the data that can be understood and analyzed and thus be able to determine the most crowded places. Then, it randomly splits the dataset into training data and test data. Firstly, the test data are created to test model's prediction on this subset. Secondly,

the training data is used for algorithm training whereas test data are to evaluate the efficiency of the algorithm. Finally, the classifier builds a model based on the training data in which it can predict a new test data. These data are entered to machine learning phase to label the most crowded places within the target building using KNN classifier [31], Naive Bayes [32] and Random Tree [33].

The accuracy of the learning algorithm is examined using the test data. It builds a model to calculate the distance between training data and input data, then predicts the class of the input data. This process is repeated on each derived subset to check whether all the data in the subset belong to the same class. Fig. 2 shows the block diagram for the CA.

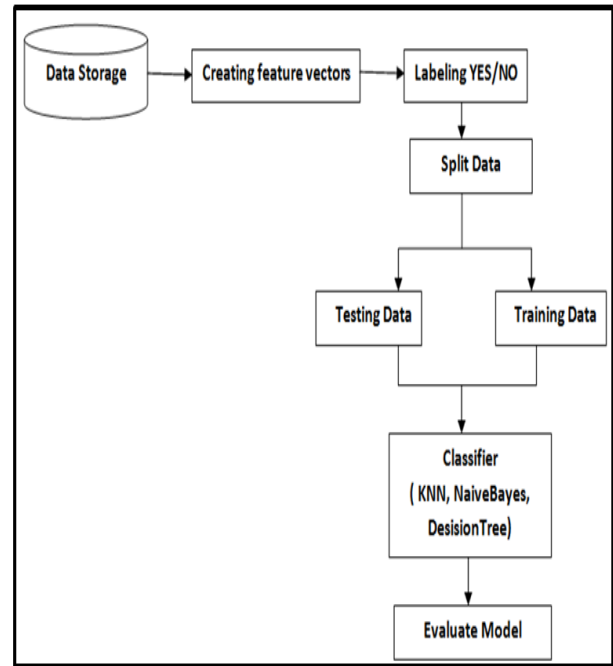


Fig. 2. Block diagram for the crowded algorithm.

IV. EXPERIMENTS AND RESULTS

The real experiments have been conducted in the faculty of Information Technology (IT) building at Mut'ah University. The layout of the environment setting is shown in Fig. 3, which represents an area of 2291.04m², 51.6m length by width of 44.4m, including more than 25 rooms.

To collect data from Smartphone sensor, we utilized two Android software applications equipped with accelerometer sensors, Samsung Galaxy J7Prime and Samsung Prime Plus, to conduct the real experiments. In addition, we used sensor manager. Most android devices have a built-in sensor that measure motion, orientation, and environmental conditions. Some of these sensors are hardware-based and some are software-based sensors. Whatever the sensor base is, android allows obtaining raw data from these sensors to be used in various applications.

A. Crowdsourcing Results

This experiment has been conducted in IT faculty corridors where untrained people of 56 volunteers were assigned to

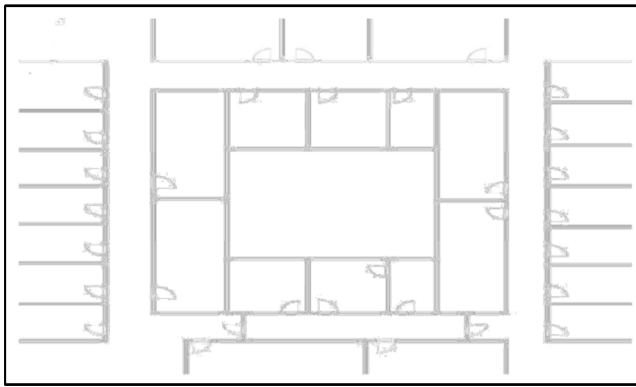


Fig. 3. Blueprint of IT faculty.

do their normal activities and movements while holding their smartphones. Their Smartphones collect accelerometer values along with user movement path. Fig. 4 shows an example of collected crowdsourcing data on 3-axis.

Values in Fig. 4 represents the movement dimensions of (x, y and z) measurements. During participant's tours, the accelerometer meter application records the acceleration values of their movements. Afterward, the collected data is examined to determine changing acceleration.

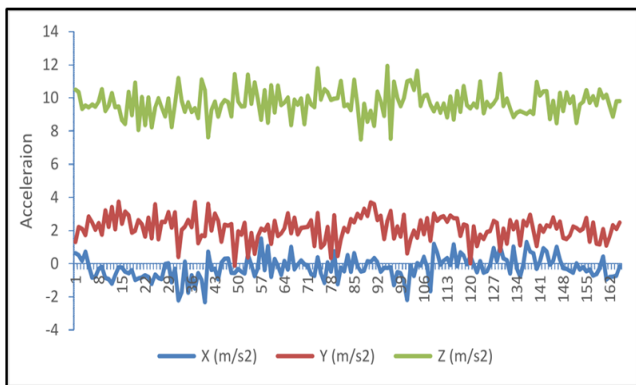


Fig. 4. An example of Crowdsourcing data on three axes.

B. Pre-processing Results

This step, as mentioned earlier, aims to purify the data collected from accelerometer using a high pass filter, based on Equations 1 and 2. Fig. 5 shows the results of our real experiments after applying the smoothing filter. Also, Fig. 5 shows the magnitude values. However, it needs to be purified to move to the next important stage, Step-Detection, which needs high purity data by removing gravity force using Equation 2.

C. Step-Detection Results

To validate our approach, different initial path points with three different scenarios have been experimented as follows:

- First scenario (specific path): Users were asked to move in a specific corridor, the initial point and the endpoints are known.

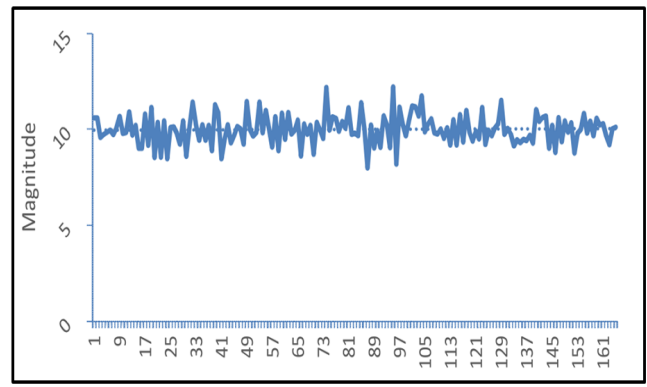


Fig. 5. Magnitude value.

- Second scenario (random path): Users were asked to choose any corridor to move in.
- Third scenario (landscape): Users were asked to be presented in 10 different locations, which have a landscape blueprint to determine the ability of our step detection algorithm at identifying the crowded places.

In the first scenario (specific path), at different speeds; users walked in a predetermined corridor, the starting point and the end point are known. This helps to detect the feasibility of the algorithm to identify crowded places through a path. Users are asked to start from interchangeable initial and endpoints, P1, P2 and P3, as shown in Fig. 6. Through the path shown in Fig. 6, the real steps, estimated steps and error ratio are obtained, as shown in Table I.

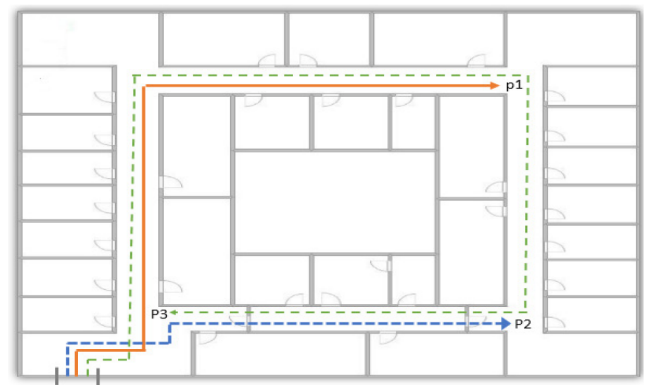


Fig. 6. Crowdsourcing_scenario 1.

Table I shows the results of each user after he has made three attempts to cross the corridor. The results show a good approximation between real and estimated steps. Such results indicate the accuracy of the algorithm in detecting the steps at an error rate of 5.6 for all users even when the distance is too long.

As for scenario 2 (random scenario), user picks his/her path starting from initial to endpoint. Fig. 7 shows the random scenario setting. In this scenario, users walk in a random path of their choice. However, we track their movement to determine the walking path. The result of this scenario is shown in the Table II which shows that our step detection algorithm proves accurate user step detection even if users

TABLE I. RESULTS OF SCENARIO 1.

User	Path	Real Steps	Estimated Step	Error Ratio
U1	1	81	83	2
U1	2	67	62	5
U1	3	210	202	8
U2	1	60	57	3
U2	2	51	51	0
U2	3	161	153	8
U3	1	58	57	1
U3	2	47	46	1
U3	3	170	161	9
U4	1	79	71	8
U4	2	63	56	7
U4	3	198	188	0
U5	1	57	55	2
U5	2	49	52	3
U5	3	161	150	11
U6	1	57	50	7
U6	2	49	45	4
U6	3	165	154	11
Average		99.05556	94.05556	5.55556

move in random paths; since the error ratio is not exceeded (4.1) on average.

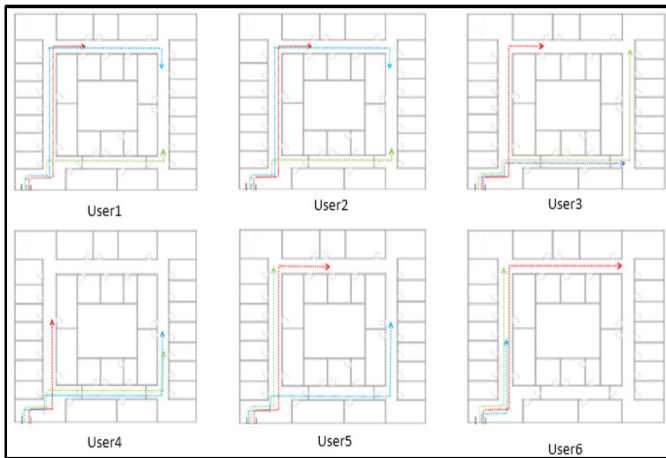


Fig. 7. Sample of Crowdsourcing_scenario 2.

Moreover, in this scenario, we have identified four random paths, C1, C2, C3 and C4, as well as the number of real steps to cross each corridor. Hence, the estimated steps in conjunction with real steps and the random path can determine the most crowded corridor. Therefore, the number of steps on each corridor gives the number of users. Table III shows the result of the step detection algorithms in terms of random paths.

As the step detection algorithm gives a high level of accuracy in both scenario 1 and scenario 2, the last scenario (i.e., landscape scenario) aims to examine the efficiency of our

TABLE II. RESULTS OF RANDOM SCENARIO.

User	Real Data (Steps)	Estimated data (Steps)	Error Ratio
R1_1	61	67	6
R1_2	106	99	7
R1_3	62	59	3
R2_1	60	70	10
R2_2	63	60	3
R2_3	110	106	4
R3_1	50	44	6
R3_2	63	58	5
R3_3	76	60	16
R4_1	70	69	1
R4_2	43	41	2
R4_3	72	78	6
R5_1	71	59	12
R5_2	76	63	13
R5_3	58	46	12
R6_1	63	55	8
R6_2	109	99	10
R6_3	32	28	4
Average	69.1666	64.5	7.111111

TABLE III. THE NUMBER OF STEPS IN EACH CORRIDOR.

Path	Real Data (Steps)	Estimated data (Steps)	Number of Steps	Number of Users
C1	60	62	881	18
C2	56	50	300	12
C3	51	47	377	10
C4	56	47	761	16

proposal under investigation in determining the most crowded sites. This is performed by asking user to spend some time nearby 10 landmarks, which have been identified in the target building blueprint (as shown in Fig. 8). Fig. 8 shows 10 locations, which have been identified in the different corridors of the target building. Many users are usually presenting in these places for certain activities. Based on the step detection algorithm and empirical stopping threshold, we can determine the duration of users stop. Tables III and IV show the results of landscape scenario.

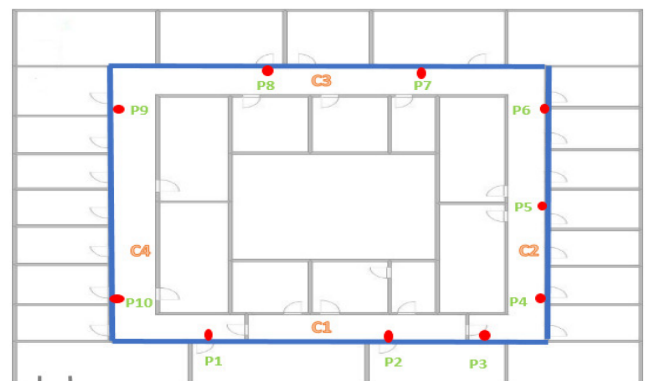


Fig. 8. Crowdsourcing_scenario 3; red points represents landscapes.

Tables III and IV represent the features that have been used in machine learning algorithms to identify the crowd places. Locations in Table IV are sorted ascending based on the number of users and the total time spent there. It shows that P9 is the most crowded location as the number of users is the most; while P6 is least crowded location as the number of users is the least.

TABLE IV. THE NUMBER OF STEPS IN EACH CORRIDOR.

Point	Number of Users	Total time(s)
P9	23	562
P8	12	555
P5	12	548
P2	16	545
P1	17	497
P10	15	392
P3	10	373
P7	7	106
P4	5	78
P6	4	39

D. Crowd Algorithm Results

In the proposed approach, a dataset from the experimental data is created comprising the features of points, Locations, users, stopping time, and labeled of required AP of YES /NO class for learning. Afterward, Weka tool has been used as a machine learning tool for this experiment using several classifying techniques, including k-Nearest Neighbor, Decision trees and Bayesian. The accuracy of the learning algorithm is examined using the test data as shown in Fig. 9.

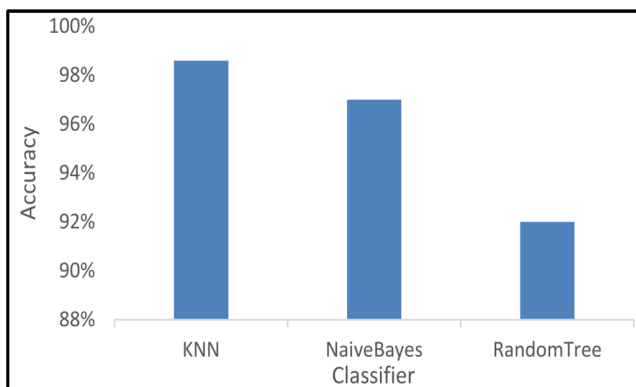


Fig. 9. Accuracy result.

V. ERROR ANALYSIS AND SYSTEM ACCURACY

To investigate the error rates and its effects in the challenge of the step-detection as well as for stationary detection, which is the ability of the approach to stationary detecting user estimated steps with the minimal error rate; we calculate the error rate for both the step-detection and stationary detection

using Equation 3. In addition, Equation 4 finds the error rate (Er) of step detection algorithm.

After determining the empirical threshold for the user movement, the error rate is calculated based on values that are not meeting the empirical threshold condition. Based on the empirical thresholds and Equation 3, the error rate is 4.2%. As for the accuracy of crowded places detection, the error rate is calculated based on values that are not satisfying the empirical threshold condition and Equation 4. Therefore, based on the empirical thresholds, the error rate is 9.6%, which implies that the accuracy of the system reached 90.4%.

$$StepAvgErr = AVG(RSs) - AVG(ESs) \quad (3)$$

$$ErrorRate = (Er_1 + Er_2 + +Er_n)/n \quad (4)$$

VI. CONCLUSION

In this article, we have proposed an automatic approach to detect the most crowded places inside a building. The proposed system utilizes accelerometer sensor data to detect user steps and predicts the most crowded places. Crowdsourcing methods are used to collect the acceleration data of Smartphone sensors. The experimental results show that the proposed approach achieves promising results by providing an accurate users steps detection reached (95.8%); and the accuracy of determining stopping time for user movement, which determines the most crowded places is 90.4%.

In the future work, we are going to extend the proposed approach to support more buildings such as circular buildings where the corners are not clear. More classifiers will be used as well as extensive experiments.

REFERENCES

- [1] P. Davidson and R. Piché, "A survey of selected indoor positioning methods for smartphones," *IEEE Communications Surveys Tutorials*, vol. 19, no. 2, pp. 1347–1370, Secondquarter 2017.
- [2] R. Zhang, A. Bannoura, F. Höflinger, L. M. Reindl, and C. Schindelhauer, "Indoor localization using a smart phone," in *2013 IEEE Sensors Applications Symposium Proceedings*, Feb 2013, pp. 38–42.
- [3] A. Abadleh, S. Han, S. J. Hyun, B. Lee, and M. Kim, "Ipls: Indoor localization using physical maps and smartphone sensors," in *Proceeding of IEEE International Symposium on a World of Wireless, Mobile and Multimedia Networks 2014*, June 2014, pp. 1–6.
- [4] H. Zou, B. Huang, X. Lu, H. Jiang, and L. Xie, "A robust indoor positioning system based on the procrustes analysis and weighted extreme learning machine," *IEEE Transactions on Wireless Communications*, vol. 15, no. 2, pp. 1252–1266, Feb 2016.
- [5] W. Win Myo, "A more reliable step counter using built-in accelerometer in smartphone," *Turkish Journal of Electrical Engineering and Computer Sciences*, vol. 12, p. 8, 11 2018.
- [6] B. Khan, R. Olanrewaju, F. Anwar, A. Najeeb, and M. Yaacob, "A survey on manets: Architecture, evolution, applications, security issues and solutions," *Indonesian Journal of Electrical Engineering and Computer Science*, vol. 12, pp. 832–842, 11 2018.
- [7] B. Lashkari, J. Rezaadeh, R. Farahbakhsh, and K. Sandrasegaran, "Crowdsourcing and sensing for indoor localization in iot: A review," *IEEE Sensors Journal*, vol. 19, no. 7, pp. 2408–2434, April 2019.
- [8] H. Mohammed, Y. Negash Shiferaw, and N. Teshale, *Survey on Indoor Positioning Techniques and Systems*, 07 2018, pp. 46–55.

- [9] Y. Gu, A. Lo, and I. Niemegeers, "A survey of indoor positioning systems for wireless personal networks," *Commun. Surveys Tuts.*, vol. 11, no. 1, pp. 13–32, Jan. 2009.
- [10] P. Bahl and V. N. Padmanabhan, "Radar: an in-building rf-based user location and tracking system," in *Proceedings IEEE INFOCOM 2000. Conference on Computer Communications. Nineteenth Annual Joint Conference of the IEEE Computer and Communications Societies (Cat. No.00CH37064)*, vol. 2, March 2000, pp. 775–784 vol.2.
- [11] A. Teuber, "Wlan indoor positioning based on euclidean distances and fuzzy logic," in *Hannoversche Beiträge zur Nachrichtentechnik: Proceedings of 3rd Workshop on Positioning, Navigation and Communication 2006 (WPNC 06)*, B. Eisfeller, Ed. Aachen: Shaker Verlag, 3 2006, pp. 158–168.
- [12] R. Chaudhary, D. Maduskar, and S. Tapaswi, "Optimization based qos aware routing algorithm in manet," in *2017 3rd International Conference on Advances in Computing, Communication Automation (ICACCA) (Fall)*, Sep. 2017, pp. 1–7.
- [13] M. Zhu, G. Retscher, and K. Zhang, "Integrated algorithms for rfid-based multi-sensor indoor / outdoor positioning solutions." Australia: SPACE Research Centre, School of Mathematical and Geospatial Sciences, RMIT University, 2012.
- [14] "Ieee transactions on systems, man, and cybernetics amp;mdash;part c: Applications and reviews publication information," *IEEE Transactions on Systems, Man, and Cybernetics, Part C (Applications and Reviews)*, vol. 37, no. 5, pp. C2–C2, Sep. 2007.
- [15] A. Azeez Khudhair, S. Jabbar, M. Qasim Sulttan, D. Wang, and M. Sulttan, "Wireless indoor localization systems and techniques: Survey and comparative study," *Indonesian Journal of Electrical Engineering and Computer Science*, vol. 3, pp. 392–409, 08 2016.
- [16] S. He and S. . G. Chan, "Wi-fi fingerprint-based indoor positioning: Recent advances and comparisons," *IEEE Communications Surveys Tutorials*, vol. 18, no. 1, pp. 466–490, Firstquarter 2016.
- [17] H. Lim, L. . Kung, J. C. Hou, and H. Luo, "Zero-configuration, robust indoor localization: Theory and experimentation," in *Proceedings IEEE INFOCOM 2006. 25TH IEEE International Conference on Computer Communications*, April 2006, pp. 1–12.
- [18] E. Aitenbichler and M. Muhlhauser, "An ir local positioning system for smart items and devices," in *23rd International Conference on Distributed Computing Systems Workshops, 2003. Proceedings.*, May 2003, pp. 334–339.
- [19] H. Liu, H. Darabi, P. Banerjee, and J. Liu, "Survey of wireless indoor positioning techniques and systems," *Systems, Man, and Cybernetics, Part C: Applications and Reviews, IEEE Transactions on*, vol. 37, pp. 1067 – 1080, 12 2007.
- [20] J. Chung, M. Donahoe, C. Schmandt, I.-J. Kim, P. Razavai, and M. Wiseman, "Indoor location sensing using geo-magnetism," in *Proceedings of the 9th International Conference on Mobile Systems, Applications, and Services*, ser. MobiSys '11. New York, NY, USA: ACM, 2011, pp. 141–154.
- [21] C. Laoudias, D. Zeinalipour-Yazti, and C. G. Panayiotou, "Crowd-sourced indoor localization for diverse devices through radiomap fusion," in *International Conference on Indoor Positioning and Indoor Navigation*, Oct 2013, pp. 1–7.
- [22] H. Wang, S. Sen, A. Elgohary, M. Farid, M. Youssef, and R. R. Choudhury, "No need to war-drive: Unsupervised indoor localization," in *Proceedings of the 10th International Conference on Mobile Systems, Applications, and Services*, ser. MobiSys '12. New York, NY, USA: ACM, 2012, pp. 197–210. [Online]. Available: <http://doi.acm.org/10.1145/2307636.2307655>
- [23] C. Wu, Z. Yang, and Y. Liu, "Smartphones based crowdsourcing for indoor localization," *IEEE Transactions on Mobile Computing*, vol. 14, no. 2, pp. 444–457, Feb 2015.
- [24] M. A. Solmon and M. Kosma, "Validating pedometer-based physical activity time against accelerometer in middle school physical education," vol. 5, no. 1. ICHPER-SD Journal of Research, 2010, pp. 20–25.
- [25] V. Marotto, D. Carboni, A. Serra, A. Manchinu, M. Sole, and T. Dessì, "Orientation analysis through a gyroscope sensor for indoor navigation systems," in *SENSORDEVICES 2013, The Fourth International Conference on Sensor Device Technologies and Applications*. IARIA, august 2013, pp. 85–90.
- [26] M. A.-n. Monteiro, C. Cabeza, and A. C. Marti, "Acceleration measurements using smartphone sensors: Dealing with the equivalence principle," *Revista Brasileira de Ensino de FÁsica*, vol. 37, 03 2015.
- [27] Z. Zhou, T. Chen, and L. Xu, "An improved dead reckoning algorithm for indoor positioning based on inertial sensors," in *2015 International Conference on Electrical, Automation and Mechanical Engineering*. Atlantis Press, 2015/07.
- [28] A. Hansson and L. Tufvesson, "Using sensor equipped smartphones to localize wifi access points," 2011, student Paper.
- [29] O. J. Woodman, "An introduction to inertial navigation," University of Cambridge, Research report 696, August 2007.
- [30] A. F. Olsen and J. Torresen, "Smartphone accelerometer data used for detecting human emotions," in *2016 3rd International Conference on Systems and Informatics (ICSAI)*, Nov 2016, pp. 410–415.
- [31] E. Fix and J. J. L. Hodges, "Discriminatory analysis: Nonparametric discrimination: Consistency properties," *International Statistical Review*, vol. 57, 12 1989.
- [32] I. Rish, "An empirical study of the naive bayes classifier," in *IJCAI 2001 workshop on empirical methods in artificial intelligence*, vol. 3, no. 22. IBM New York, 2001, pp. 41–46.
- [33] A. Cutler and G. Zhao, "Pert-perfect random tree ensembles," *Computing Science and Statistics*, vol. 33, 01 2001.

Data Citation Service for Wikipedia Articles

Arif Bramantoro¹, Ahmad A. Alzahrani²

¹Faculty of Computing and Information Technology Rabigh, King Abdulaziz University, Rabigh, Saudi Arabia

²Faculty of Computing and Information Technology, King Abdulaziz University, Jeddah, Saudi Arabia

Abstract—The citation of big scientific data is crucial not only for scientific activity but also for the scientific discovery and dissemination within scientist network. The main objective of this research is to develop a service-oriented data citation system using data mining techniques for Middle East and North Africa scientists. A novel service oriented framework is proposed to prototype the development of the system that includes query formalization, service discovery, service composition design, service selection, search space, and service optimization. In this research, Wikipedia scientific-related articles are connected with more than 35 petabyte Pangaea datasets. The output of this work is a web service that takes Wikipedia article information as an input and provides the possible relevant datasets (if exist) related to the article. The evaluation of this research is based on a quantitative assessment performed to the quality of web service metrics, such as number of access and bandwidth utilization; which shows that the framework is robust enough to handle both big data access and its citation.

Keywords—Scientific dataset; web services; wikipedia; pangaea; big data

I. INTRODUCTION

Scientific data residing in datasets are usually considered as a shared resource, so that world-wide scientific community can access these datasets for their relevant purposes. Similar to journal papers and conference papers, which are cited in scientific papers, datasets are also significant candidates for citations in scientific papers/articles. Data citation is the reference or link from one piece of content to other contents in the form of data or document. There are many big data centers in which these kinds of datasets reside. Pangaea is one of data publishers for scientific data, mostly from earth and environmental science. It is open to any scientists or projects who are willing to archive and publish data. This online scientific resource repository gives an access to huge number of (mostly free) datasets for more than 35 PB in size. Wikipedia, on the other hand, is a gigantic collaborative encyclopedia consisting of huge number of articles, including a scientific category. The scientific-related articles of Wikipedia, just like any other scientific articles, have a particular section of citations. However, data citations section is not provided in Wikipedia. This is because to find the relationship between Wikipedia articles and scientific big data is not an easy task.

Data mining technique to find the connection between the two huge resources of data i.e. Wikipedia and Pangaea, is proposed in this project. The application of data mining on these big data produces the relationship between a Wikipedia article and a Pangaea dataset. There might be a debate on whether Wikipedia articles can be easily connected to Pangaea datasets or not, but it certainly requires additional layers of work. It means that there must be an application of some

intelligent services, so that Wikipedia article can be linked to Pangaea dataset.

It is believed that the research approach adopted in this study constitutes an appropriate and important way to reach international audience by the help of web service, particularly used by scientists in Middle East and North Africa region. One can input information of Wikipedia article and the web service outputs the relevant Pangaea dataset, if exist, together with some statistical measures on its performance. This service is considered to be helpful for anyone who wants to enhance Wikipedia article by editing it and adding data citation for relevant data sets. In addition, this service is helpful for scientists to collect Wikipedia articles related to their research interests and downloading the cited scientific data according to their research purposes.

The main objective of this research is to develop an automatic service-oriented data citation system, utilizing the model produced by data mining techniques. In detail, the objectives are as follows:

- 1) To develop a robust mechanism to connect scientific-related articles with scientific dataset.
- 2) To provide service-oriented framework for citing large-scale data.
- 3) To give attribution of the contributors of scientific data and written web documents.

II. RELATED WORKS

Scientific data citation has been attracting many researchers not only in the field of computer science [1]. There have been enormous efforts in dealing with big data in e-science [2]. However, some challenges remain exist [3]. One of the challenges is dealing with data too big to analyze, as highlighted in [4]. To date, two technological breakthroughs are available to overcome this issue, grid computing [5] and MapReduce [6]. Because MapReduce is the latest technology and proven to be robust in archiving scientific datasets, it is necessary to utilize MapReduce to store big data of scientific dataset, before analyze it.

An automatic data citation idea has been previously proposed as a poster in [7]. Although it is still in the conceptual idea and no implementation yet, the authors in [7] give us a rough idea that automatic data citation is very important. In this research, it is necessary to implement the same idea to Wikipedia scientific-related articles by utilizing a robust data mining technique, i.e. association rule discovery, applied find the relationships between text attributes provided by Wikipedia articles and data attributes provided by scientific dataset.

Another similar effort of dealing with scientific workflow has been proposed in [8]. A novel rule based approach model

and infrastructure is considered as the best approach for handling a huge explosion in scientific data. This is due to the internal requirement in processing the streaming of scientific data, especially through social media and sensor. This approach is suitable for real time and emergency data, but not necessarily required for data citation. Data citation is mostly processed through metadata without mining the big scientific data.

The effort of utilizing Wikipedia articles to understand a better science has been done by Mietchen and others [9]. The authors created a bot that is able to search automatically the multimedia files of medical domain and upload these files to Wikipedia media repository. There are approximately more than ten thousands files attached to hundreds Wikipedia articles by the bot. It works by exploiting XML tag values of the files. Neither semantic capability nor data mining technique has been exploited by the bot.

The first definition of data service is coined in [10] which aims at seeking the technological trends in simple, united and cloud-based data service. The authors defined data services as the offsprings inherited from stored procedure in relational database management system that any programmers and database administrators are able to code both SQL queries and programming control logic in one place in order to provide both query and function optimization capability for getting at the data, as normally alleviated in procedural programming languages compilation. This stored procedure is used as an analog for data service since only stored procedure are able to get an access to important and sensitive data to some cases. The authors also characterized data service as a service based on a proprietary model. The advantage of this definition is that there will be more enhanced perspective of the data as well as more data oriented. In addition, the architecture is extended to fit the characteristics of data citation service.

Perhaps the most similar work to this research has been proposed in [11], which provides application-oriented search. The work is exploiting the use of scientific metadata generated by scientific experiment. With the power of indexing, the new search is not only relying on keyword based matching, but also semantic web and its ontology to increase the accuracy of searching. In this research, it is argued that the use of data mining technique is more appropriate to analyze the big scientific data. This is due to the need of Wikipedia articles in relating the scientific data. Indexing scientific metadata is not the focus in this research, but the scope is to analyze the relationship between big scientific data and Wikipedia articles.

III. SCIENTIFIC DATASET

“As research on so many fronts is becoming increasingly dependent on computation, all science, it seems, is becoming computer science” announced by the New York Times in a 2001 famous article [1]. Recently, many organizations have accumulated data from various sources like Web, network sensors and constructed large-scale data. Some organizations publish their data to public to facilitate activities of other organizations. For example, WDS (World Data System)¹, science data in a wide range of domains has been registered. Another example is Pangaea², a system which provides a part of science data

on WDS related to the earth and environment, contains 0.6 million datasets and 35 PB data in total. These 0.6 million datasets can be referenced by their DOIs for direct access and citation.

Pangaea is chosen in this research, because it is considered as the biggest repository for scientific data, focusing on earth and environmental science. This enables us to contribute to the local scientific society since earth and environmental data are usually specific to the geographical area. Another advantage is that Pangaea provides a comprehensive set of metadata to make us easier to identify and analyze datasets. For example, one of datasets residing at Pangaea has following title: “Contents of rare earth elements and some rock-forming chemical elements in bottom sediments from some deeps of the Red Sea.”

Fig. 1 depicts what type of information is available for a particular dataset. The attributes of the dataset are also present in the webpage³ from which snapshot is taken but they are not shown here in order to save space.

Wikipedia is a collaborative encyclopedia consisting of millions of articles. There are scientific-related articles that can be expanded by connecting them to relevant dataset residing at Pangaea. This makes the Wikipedia articles more informative and useful, such as connecting the dataset discussed above with relevant Wikipedia article. Since the dataset discusses about Red Sea Minerals, it requires a validation whether Wikipedia has such information in any of its articles or not. Further search reveals that there exists an article on red sea in Wikipedia in which a section is there that discusses about the minerals found in the depth of Red sea as illustrated in Fig. 2.

Another section of the article which discusses about the minerals in Wikipedia article is illustrated in Fig. 3. Hence, the relation between the Wikipedia article and scientific dataset can be in the form of one to one, one to many or many to many, that requires the flexibility of the system to cite on the fly.

After manually checking the two resources, it can be inferred that such dataset from Pangaea can be cited in the above Wikipedia article. However, there is an urgent requirement to have an automatic citation for millions of Wikipedia articles related to the big data of scientific dataset based on heterogeneous, loosely coupled and platform independent application by utilizing web service technology [12].

IV. METHODOLOGY

To achieve the research objective, the following steps are envisioned.

- Development of Corpus.
In this step, full Wikipedia articles are fetched as dumps into the database. Moreover the full metadata for every datasets from Pangaea is also downloaded. This corpus is expected to lead us to venue of Big Data.
- Preprocessing of Data.
Since the articles are in the form of text, lot of text processing techniques are applied to make it suitable

¹<http://www.icsu-wds.org>

²<http://www.pangaea.de>

³<http://doi.pangaea.de/10.1594/PANGAEA.774361>



PANGAEA®
Data Publisher for Earth & Environmental Science

Always quote citation when using data!

Data Description

Show Map Google Earth

Citation: Butuzova, GY, Lyapunov, SM (1995): Contents of rare earth elements and some rock-forming chemical elements in bottom sediments from some deeps of the Red Sea. *Geological Institute, Russian Academy of Sciences, Moscow*, doi:10.1594/PANGAEA.774361,
In Supplement to: Butuzova, Galina Yu; Lyapunov, Sergey M (1995): Rare earth elements in hydrothermal-sedimentary deposits from the Red Sea. *Translated from: Litologiya i Poleznyye Iskopaemyye, 1995, 1, 16-30, Lithology and Mineral Resources, N 1, 13-26*

Project(s): Archive of Ocean Data (ARCOD) a

Coverage: Median Latitude: 20.722289 * Median Longitude: 38.362489 * South-bound Latitude: 17.888300 * West-bound Longitude: 38.053333 * North-bound Latitude: 21.388300 * East-bound Longitude: 39.813300
Minimum DEPTH, sediment/rock: 1.1 m * Maximum DEPTH, sediment/rock: 10.6 m

Event(s): AK22-1996 a * Latitude: 21.283333 * Longitude: 38.053333 * Elevation: -2205.0 m * Location: Red Sea a * Device: Gravity corer (GC) a
PS-226 a * Latitude: 17.888300 * Longitude: 39.813300 * Elevation: -886.0 m * Location: Red Sea a * Campaign: PIKAR a * Device: Gravity corer (GC) a
PS-363 a * Latitude: 21.388300 * Longitude: 38.061700 * Elevation: -2085.0 m * Location: Red Sea, Atlantis II Deep a * Campaign: PIKAR a * Device: Gravity corer (GC) a



Fig. 1. Metadata of scientific dataset from Pangaea.

Red Sea

From Wikipedia, the free encyclopedia

Coordinates: 22°N 38°E

This article is about the body of water between Arabia and Africa. For other meanings, see Red Sea (disambiguation).

The **Red Sea**, or what is sometimes called the **Erythraean Sea**, is a **seawater inlet** of the **Indian Ocean**, lying between **Africa** and **Asia**. The connection to the ocean is in the south through the **Bab el Mandeb** strait and the **Gulf of Aden**. In the north, there is the **Sinai Peninsula**, the **Gulf of Aqaba**, and the **Gulf of Suez** (leading to the **Suez Canal**). The Red Sea is a **Global 200 ecoregion**. The sea is underlain by the **Red Sea Rift** which is part of the **Great Rift Valley**.

The Red Sea has a surface area of roughly 438,000 km² (169,100 mi²).^{[1][2]} It is about 2250 km (1398 mi) long and, at its widest point, 355 km (220.6 mi) wide. It has a maximum depth of 2211 m



Fig. 2. An example of Wikipedia article possibly corresponds to scientific dataset from Pangaea.

Geology

The Red Sea was formed by the **Arabian peninsula** being splitting from the **Horn of Africa** by movement of the **Red Sea Rift**. This split started in the **Eocene** and accelerated during the **Oligocene**. The sea is still widening, and it is considered that it will become an ocean in time (as proposed in the model of **John Tuzo Wilson**). In 1949, a deep water survey reported anomalously hot brines in the central portion of the Red Sea. Later work in the 1960s confirmed the presence of hot, 60 °C (140 °F), saline brines and associated metalliferous muds. The hot solutions were emanating from an active seafloor **rift**. The high salinity of the waters was not hospitable to living organisms.^[16] Sometimes during the **Tertiary** period, the **Bab el Mandeb** closed and the Red Sea evaporated to an empty hot dry salt-floored sink. Effects causing this would have been:

- A "race" between the Red Sea widening and **Perim Island** erupting filling the Bab el Mandeb with **lava**.
- The lowering of world **sea level** during the **Ice Ages** because of much water being locked up in the **ice caps**.

A number of volcanic islands rise from the center of the sea. Most are dormant. However, in 2007, **Jabal al-Tair Island** in the Bab el Mandeb strait erupted violently. An eruption among the nearby **Zubair islands** followed in 2011.^[19]

Mineral resources

In terms of mineral resources the major constituents of the Red Sea sediments are as follows:

- Biogenic constituents:
Nanofossils, **foraminifera**, **pteropods**, siliceous fossils
- Volcanogenic constituents:
Tuffites, **volcanic ash**, **montmorillonite**, **crystalite**, **zeolites**
- Terrigenous constituents:



Fig. 3. Another part of Wikipedia article that discuss the scientific dataset in detail.

for data mining techniques. The Wikipedia articles require special preprocessing in order to produce output that is used as input for next step.

Since there is no training data, association rule mining algorithms as well as different similarity measurement techniques are applied to find the related articles.

- Application of different Data Mining Techniques.
- Web Service for World Wide Audience.

A web service service is dedicated to the users who are interested in finding the relevant scientific datasets for a particular Wikipedia article. It has the functionality of providing the Wikipedia article information. The output of service is the relevant and related Pangaea datasets.

To realize the expected results, the following mechanism is proposed.

- 1) A properly archived corpus of Wikipedia articles and Pangaea metadata.
To obtain the corpus, an open source MapReduce based Hadoop archive system is employed.
- 2) An ordered association and relationship information between Wikipedia scientific-related articles and Pangaea big datasets.
To obtain the information, a robust data mining of Association Rule techniques are employed.
- 3) Scientific Data Citation Service for Wikipedia scientific articles, Pangaea big datasets, and the relationship information that supports platform independent, autonomous, dynamic, reusable, heterogeneous, self-contained and loosely-coupled system.
To develop the service, XaaS (Everything as a Service) techniques, including DaaS (Data as a Service), TaaS (Text as a Service), CaaS (Citation as a Service), and SaaS (Software as a Service) are employed.

The mechanism of XaaS is implemented in service-oriented framework to ease the prototyping of the data citation system development as proposed in Fig. 4. The framework starts with query formalization and decomposition to ease the search for scientific dataset. The service discovery follows the step by providing more semantic capability during the searching process in multi-ontological environment [13]. The design of service composition improves a simple pattern of searching into fully automatic composition. The service selection follows the process until it combines Wikipedia and Pangaea datasets. The searching space is eventually improved from simple search by utilizing the previous approach of service atomization [14]. Finally, the simulation is conducted in several stages during service optimization of first algorithm.

With this research, it is expected that in long term, there will be an increase of productivity of the scientists in the Middle East and North Africa regions in term of re-do experiments, fast and easy access to Wikipedia scientific-related articles and the corresponding Pangaea scientific datasets. It is also expected there will be an improved management for information services in the Kingdom due to integral administration of data citation as an information asset. This can be done through the expected results of this project that provides useful relationship information between Wikipedia articles and scientific data, in order to be utilized by the scientists.

The data are analyzed to mine the relationship between two different objects of properly archived corpus of Wikipedia articles and Pangaea metadata. The scientists can utilize the corpus for their research. For example, Wikipedia scientific article corpus is used for a layman-friendly guidelines about the research topics and the Pangaea metadata corpus is used for re-do their experiments.

An ordered association and relationship information between Wikipedia scientific-related articles and Pangaea big datasets are provided to the scientist to choose the right Pangaea datasets for particular Wikipedia scientific-related articles. The association and relationship information is ordered based on the degree of the relatedness between Wikipedia scientific-related articles and Pangaea big datasets, so that the scientists have a variety of options to choose the appropriate datasets for particular Wikipedia articles.

Scientific Data Citation Service for Wikipedia scientific articles, Pangaea big datasets, and the relationship information web services are provided to make the information publicly available and seamlessly integrated to any legacy systems. The relationship service between Wikipedia scientific-related articles and Pangaea big datasets is utilized by scientists to cite the most related datasets for the articles. Archive service of Wikipedia scientific articles are provided to scientists to search and access the required articles based on the datasets owned or accesses by scientists. Archive service of Pangaea big datasets are provided to scientists to search and access the required datasets based on the Wikipedia scientific articles written or accesses by scientists.

V. DATA MINING AND ITS ARCHITECTURE

This research proposes to utilize data mining concept in this research, due to the nature of big data. Data mining is able to identify what data are passed between services. Since there are several services in this research and collaboration amongst the services in one composition, the identification of data is non-trivial. Data citation service also requires data mining to know what services are available as well as what results are generated for particular sets of input values. More specifically, data mining enables user to trace the process that led to the aggregation of services producing particular output.

Data mining processes are combined in the form of graph, which is implemented later as rule or workflow. The graph contains hybrid data and services. There is no focus on this data mining technique, since all available data and services are grouped together depends on the aim of the model. For example, the Fig. 5 shows data citation service utilizing three data mining services and seven datasets. Based on the objective of the workflow, the data mining technique determines that there should be two groups of service S_2 and S_3 , before composed with service S_1 . The group of service S_2 are related with dataset D_1 and D_3 , whereas the group of service S_3 are correlated with data set D_3 , D_2 and D_2' (a complimentary of dataset D_2).

Different objective has different composition. Fig. 6 illustrates that similar workflow may have different data mining tools. All services and datasets are in the same group, except for all datasets complimentary, D_0' and D_2' .

To implement the data mining tools in data citation service, a data citation service architecture is designed to accommodate the nature of scientific services and dataset as illustrated in Fig. 7. This data citation service architecture is based on the basic data service architecture proposed in [10]. The architecture extension includes an enhancement of the traditional service where the operations of the service, i.e. inputs and outputs, are semantically unplugged to the clients; which has no data

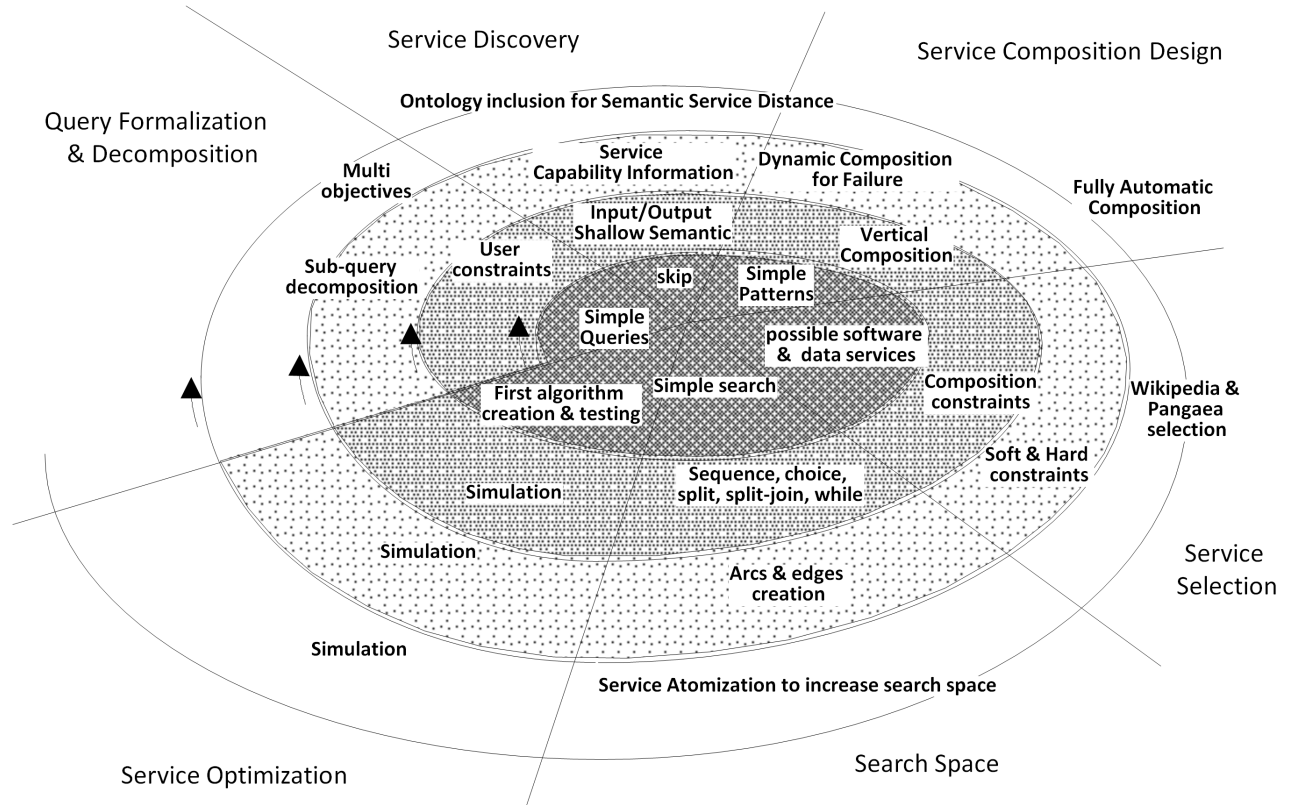


Fig. 4. Service-oriented framework for data citation system.

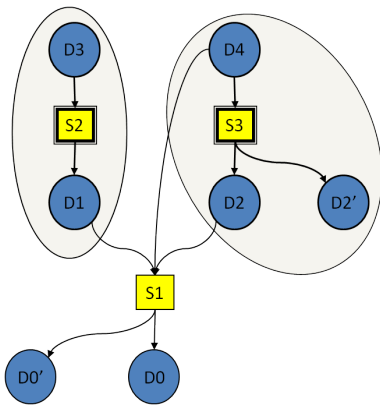


Fig. 5. Data citation service workflow 1.

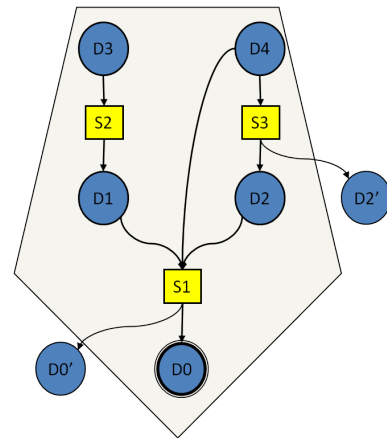


Fig. 6. Data citation workflow 2.

model inside. In data citation service architecture, both data and metadata are requested and published through various methods, such as XML, JSON, or atom publishing protocols. This architecture is proposed on top of the previous experience in combining two different architectures, such as workflow based services and pipelining based components [15].

Since this research is not only using the traditional datasets, the architecture aims at accommodating both relational data database and various data source, such as big data in Pangaea which has spatial and temporal information. Hence, the integration between the conventional database management

system and others are enabled through this architecture. The everything as a service are considered as functional datasets in order to be able to combined with relational datasets.

VI. DISCUSSION

Data citation services are openly published to the earth and environment scientists in north Africa and middle east countries. The right configuration is required to access the service. The example of the configuration of preprocessing filters and user defined index is illustrated in Fig. 8. This con-

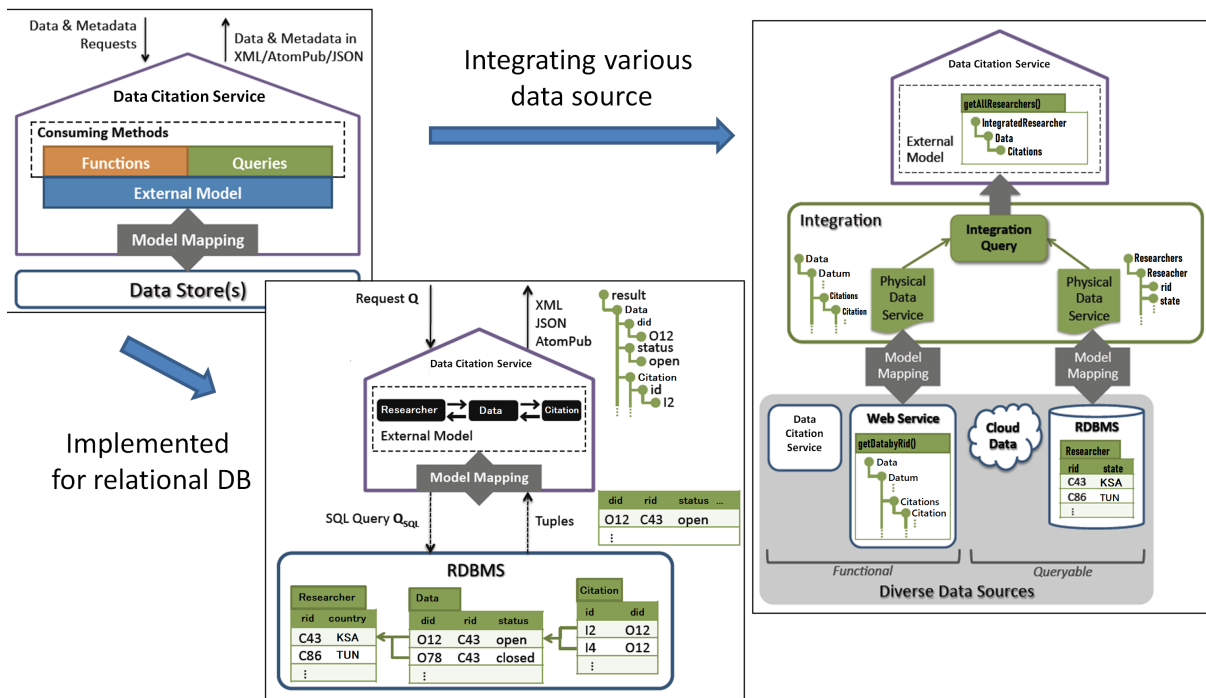


Fig. 7. Data citation service architecture.

figuration burdens the data center hardware due to the request of the dedicated resource allocation for each searching index. The structure includes HTML documents, structure analysis, parsing result, caller information, page ranking, evaluation of expression, system coordinate which includes latitude, longitude, and altitude.

percentage since there is an execution of several services in one workflow. There is a bottleneck to access the service due to the limitation of the data center hardware capability. There is also an excess of the internal university proxy to restrict the access, which is the base of future work to include a dedicated proxy to improve the access.

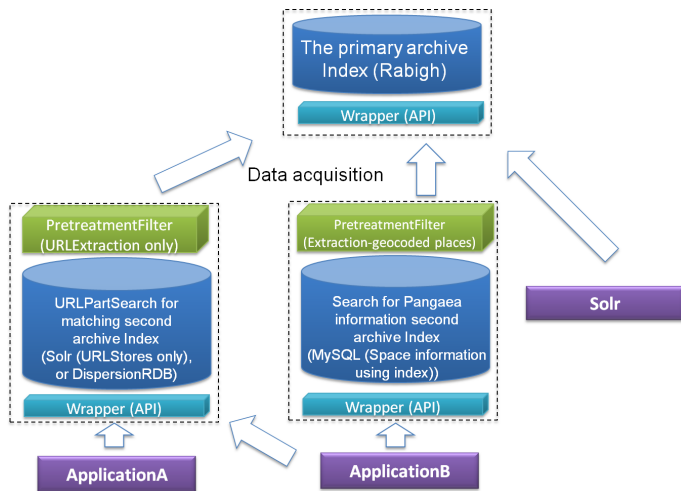


Fig. 8. Configuration example for data citation service.

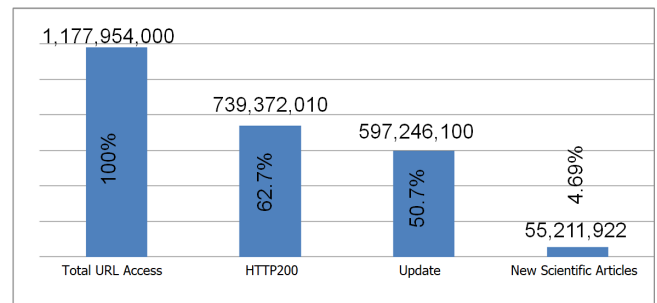


Fig. 9. Performance evaluation based on the number of access.

Fig. 9 represents the evaluation of the performance for data citation service. From total URL access, HTTP200 represents the most access by 62.7%, while updating the data citation holds 50.7%. It is interesting to note that there is a new articles related to scientific data written by the scientists through this citation enablement, although takes the portion of 4.69% only. In addition, the total access might not fully represent the total

Full bandwidth is assigned to data citation service, however not all accesses utilized fully the bandwidth. Fig. 10 represents the overall bandwidth utilization mainly on the processing time. It is interesting to note that the access of the scientific data in north Africa and middle east countries has a peak in working hours. This pattern reoccurs in any days, although there is a less amount of peak access during weekends. It infers that there is still a scientific activity beyond normal working hours, although not as much as the one during working hours.

VII. CONCLUSION

This research developed a service-oriented framework and architecture for data citation service. Through this framework

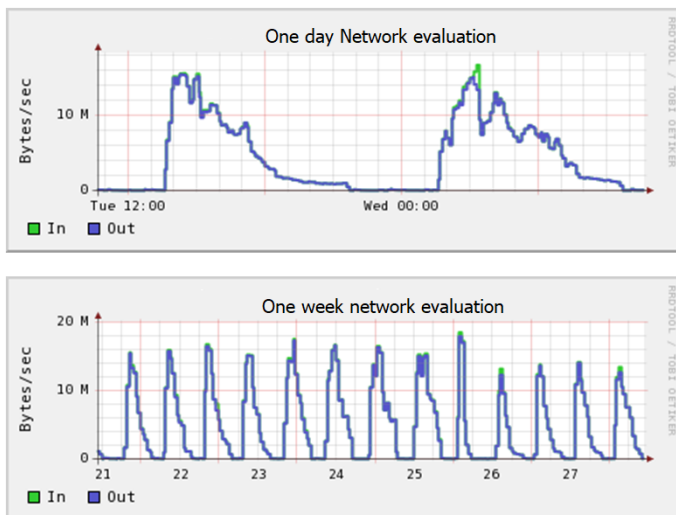


Fig. 10. Bandwidth evaluation.

and architecture, a robust mechanism is available for scientists, especially in the field of earth and environment, to relate scientific articles with scientific datasets as a big data. This framework enables the scientists; especially in Middle East and North Africa region, to cite their articles with worldwide big scientific data. In the evaluation, it is shown that the framework is robust and reliable enough to handle both big data access and its citation. It remains the future work on how to increase the relevance of the data citation, especially to attract more scientists in this region by utilizing a social media in collaborating the citation.

ACKNOWLEDGMENT

This work was funded by the Deanship of Scientific Research (DSR), King Abdulaziz University, Jeddah, Saudi Arabia, under grant no. 830 - 16 - D1439. The authors, therefore, gratefully acknowledge the DSR technical and financial support.

REFERENCES

[1] G. Johnson, "All science is computer science," *The New York Times*, vol. 25, pp. 1–5, 2001.

[2] M. Zhao, E. Yan, and K. Li, "Data set mentions and citations: A content analysis of full-text publications," *Journal of the Association for Information Science and Technology*, vol. 69, no. 1, pp. 32–46, 2018.

[3] S. B. Davidson, P. Buneman, D. Deutch, T. Milo, and G. Silvello, "Data citation: A computational challenge," in *Proceedings of the 36th ACM SIGMOD-SIGACT-SIGAI Symposium on Principles of Database Systems*. ACM, 2017, pp. 1–4.

[4] S. A. El-Seoud, H. F. El-Sofany, M. A. F. Abdelfattah, and R. Mohamed, "Big data and cloud computing: Trends and challenges," *International Journal of Interactive Mobile Technologies (IJIM)*, vol. 11, no. 2, pp. 34–52, 2017.

[5] I. Foster, C. Kesselman, J. M. Nick, and S. Tuecke, "Grid services for distributed system integration," *Computer*, no. 6, pp. 37–46, 2002.

[6] J. Dean and S. Ghemawat, "Mapreduce: simplified data processing on large clusters," *Communications of the ACM*, vol. 51, no. 1, pp. 107–113, 2008.

[7] E. Gonzales, X. Zhang, Y. Akahoshi, Y. Murayama, and K. Zettsu, "Data citation wiki for harnessing collective intelligence on document-to-data associations to interdisciplinary data access," in *23rd International CODATA Conference, Taipei, China, 2012*.

[8] Y. Murakami, M. Tanaka, A. Bramantoro, and K. Zettsu, "Data-centered service composition for information analysis," in *2012 IEEE Ninth International Conference on Services Computing*. IEEE, 2012, pp. 602–608.

[9] D. Mietchen, J. McEntyre, J. Beck, and C. Maloney, "Adapting jats to support data citation," in *Journal Article Tag Suite Conference (JATS-Con) Proceedings 2015*. Force11 Data Citation Implementation Group, National Center for Biotechnology Information (US), 2015.

[10] M. J. Carey, N. Onose, and M. Petropoulos, "Data services," *Communications of the ACM*, vol. 55, no. 6, pp. 86–97, 2012.

[11] C. Gupta and M. Govindaraju, "Framework for efficient indexing and searching of scientific metadata," in *Proceedings of the 2010 10th IEEE/ACM International Conference on Cluster, Cloud and Grid Computing*. IEEE Computer Society, 2010, pp. 553–556.

[12] H.-y. Paik, A. L. Lemos, M. C. Barukh, B. Benatallah, and A. Natarajan, "Web service composition: Data flows," in *Web Service Implementation and Composition Techniques*. Springer, 2017, pp. 193–202.

[13] A. Bramantoro, R. K. Alshammari, and A. O. Almagrabi, "Measuring business entities in multi-ontologies," *International Journal of Electronic Business*, vol. 13, no. 4, pp. 342–358, 2017.

[14] A. Bramantoro, T. Kamada, M. Tanaka, Y. Murakami, and K. Zettsu, "Towards service atomization for analyzing information," in *2012 IEEE 19th International Conference on Web Services (ICWS)*, June 2012, pp. 676–677.

[15] A. Bramantoro, U. Schäfer, and T. Ishida, "Towards an integrated architecture for composite language services and multiple linguistic processing components," in *International Conference on Language Resources and Evaluation*, 2010, pp. 3506–3511.

Software Abstractions for Large-Scale Deep Learning Models in Big Data Analytics

Ayaz H. Khan¹, Ali Mustafa Qamar², Aneeq Yusuf³, Rehanullah Khan⁴
College of Computing and Information Sciences^{1,3}
Karachi Institute of Economics and Technology, Karachi, Pakistan
College of Computer, Qassim University^{2,4}
Mulaidah, Saudi Arabia

Abstract—The goal of big data analytics is to analyze datasets with a higher amount of volume, velocity, and variety for large-scale business intelligence problems. These workloads are normally processed with the distribution on massively parallel analytical systems. Deep learning is part of a broader family of machine learning methods based on learning representations of data. Deep learning plays a significant role in the information analysis by adding value to the massive amount of unsupervised data. A core domain of research is related to the development of deep learning algorithms for auto-extraction of complex data formats at a higher level of abstraction using the massive volumes of data. In this paper, we present the latest research trends in the development of parallel algorithms, optimization techniques, tools and libraries related to big data analytics and deep learning on various parallel architectures. The basic building blocks for deep learning such as Restricted Boltzmann Machines (RBM) and Deep Belief Networks (DBN) are identified and analyzed for parallelization of deep learning models. We proposed a parallel software API based on PyTorch, Hadoop Distributed File System (HDFS), Apache Hadoop MapReduce and MapReduce Job (MRJob) for developing large-scale deep learning models. We obtained about 5-30% reduction in the execution time of the deep auto-encoder model even on a single node Hadoop cluster. Furthermore, the complexity of code development is significantly reduced to create multi-layer deep learning models.

Keywords—Big data; deep learning; deep auto-encoders; Restricted Boltzmann Machines (RBM)

I. INTRODUCTION

Big volumes of data have been started to accumulate based on the advancements in sensor technology, the Internet, social networks, wireless communication, and inexpensive memory in various formats such as numerical, textual, and image. Such a high volume of data can be analyzed using statistical and Computational Intelligence (CI) tools based on neuro-computing, fuzzy logic, clustering, Bayesian networks, Principal Component Analysis (PCA), etc. for an efficient data management by reducing its size and developing non-parametric models based on extracted information and its knowledge base [1]. These workloads are normally processed with a distribution on massively parallel analytical systems. GPUs (Graphics Processing Units), MICs (Many Integrated Cores) or FPGAs (Field Programmable Gate Arrays) etc. are available as co-processors to accelerate the required computations in various algorithms with the distribution of data among the processors and co-processors to support bigger workloads.

Deep learning can be considered as an extension to Machine learning methods for learning data representations [2]. In

the area of image classification, face detection and recognition, the features of an image can be represented in various ways based on pixel intensity values, set of edges, specific regional shapes. Deep learning provides efficient algorithms for unsupervised or semi-supervised feature learning and extraction. Several deep learning architectures including convolutional deep neural networks, Recurrent Neural Networks (RNN), and Deep Belief Networks (DBN) are applicable to the various fields of computer science such as speech recognition, computer vision, natural language processing, and bioinformatics to produce state-of-the-art analytical results. Deep learning is an active research area both in industry and academia to solve various practical examples such as image and speech recognition, neural machine translation, traffic management, and cancer detection. Furthermore, it has been successfully applied in task classification, object detection, motion modeling, dimensionality reduction, and network flow prediction [3]. Various software solutions have been provided in the market for deep learning using different parallel computing architectures including programming language extensions, libraries, frameworks.

In order to ease the development of deep learning models for big data analytics, there is a dire need of a software API with high level abstractions to create multi-layer deep learning models with the capability of processing big training data that is in high volume, velocity and variety. We explored several parallel algorithms, optimization techniques, tools and libraries related to big data analytics and deep learning on various parallel architectures. Based on our exploration and analysis, we identified the basic building blocks for the parallelization of the deep learning models and proposed a parallel software API using PyTorch, Hadoop Distributed File System (HDFS), Apache Hadoop MapReduce (MR) and MapReduce Job (MRJob) for developing large-scale deep learning models. We obtained about 5-30% reduction in the execution time of the deep auto-encoder model even on a single node Hadoop cluster. Furthermore, the complexity of code development is significantly reduced to create multi-layer deep learning models.

The rest of the paper is organized as follows: Section II presents a summary of the latest research trends in using deep learning approaches for big data analytics, Section III reviews the current software tools and libraries in the domain of deep learning, Section IV provides an in-depth analysis of the basic building blocks for deep learning in big data analytics, Section V explains the proposed API for the development

of deep learning models, whereas Section VI presents the evaluation of the proposed API in terms of performance and its usage. Lastly, Section VII concludes the paper and highlights future research directions.

II. LITERATURE REVIEW

Deep learning is a branch of Machine learning based on a set of algorithms that attempt to model high-level abstractions in data by using multiple processing layers, with complex structures or otherwise, composed of multiple non-linear transformations. Deep learning is part of a broader family of Machine learning methods based on learning representations of data. An observation (e.g. an image) can be represented in many ways, such as a vector of intensity values per pixel, or in a more abstract way as a set of edges, regions of a particular shape, etc. Some representations are better than others at simplifying the learning task (e.g., face recognition or facial expression recognition) from examples. In recent years, deep learning approaches have gained significant interest because while processing unstructured data, it doesn't require to label everything to discover patterns. It uses big data, and the computational power of the GPU to gain speed and accuracy [4]. One of the promises of deep learning is replacing handcrafted features with efficient algorithms for unsupervised or semi-supervised feature learning and hierarchical feature extraction. Deep learning can achieve outstanding results in various fields. However, it requires so significant computational power that massively parallel processors and/or numerous computers are often required for practical applications. Deep learning algorithms are based on distributed representations. The underlying assumption behind distributed representations is that the observed data is generated by the interactions of factors organized in layers. Deep learning adds the assumption that these layers of factors correspond to various levels of abstraction or composition. Varying numbers of layers and layer sizes can be used to provide different amounts of abstraction. Deep learning exploits this idea of hierarchical explanatory factors, where more abstract higher levels are learned from the lower level ones. Deep learning helps to disentangle these abstractions and pick out which features are useful for learning. For supervised learning tasks, deep learning methods obviate feature engineering, by translating the data into compact intermediate representations akin to principal components, and derive layered structures which remove redundancy in the representation. Many deep learning algorithms are applied to unsupervised learning tasks. This is an important benefit because unlabeled data is usually more abundant than labeled data. An example of a deep structure that can be trained in an unsupervised manner is a Deep Belief Network (DBN). A DBN is composed of a stack of Restricted Boltzmann Machines (RBMs). A core component of the DBN is a greedy, layer-by-layer learning algorithm, which optimizes the DBN weights at a time complexity linear to the size and depth of the networks. Separately and with some surprise, initializing the weights of an Multi-Layer Perceptron (MLP) with a correspondingly configured DBN often produces much better results than that with random weights. As such, MLPs with many hidden layers, or Deep Neural Networks (DNN), which are learned with unsupervised DBN pre-training followed by Back-Propagation fine-tuning is sometimes also called DBNs in the literature [4].

Several technologies and their correlations have been explored [5] to be useful in big data analytics for future volume prediction and deep knowledge of data. This helps in taking proactive and better strategic decisions in the business community focusing on unstructured data and open source technologies including Apache Flume, Apache Sqoop, Apache Pig, Apache Hive, Apache ZooKeeper, Mongo DB, Apache Cassandra, Apache Hadoop, MapReduce, Apache Splunk and Apache Spark. An in-depth analysis of different hardware platforms and related software frameworks suitable for big data analytics is presented in [6] based on various matrices, including fault tolerance, scalability, I/O bandwidth requirements, distributed and real-time processing. It has been found that the right choice of the platform should be based on proper investigation of the application/algorithm needs. The decision has to be made on the basis of the results' frequency requirements, the size of data to be processed, and the number of iterations to build a model. A case study of various implementations of K-means clustering algorithm has been presented taking consideration of various algorithmic and system level issues. The analytical results can be further strengthened by investigating other algorithms such as decision trees, nearest neighbors, page ranking, and etc. In order to develop highly scalable applications, a combination of multiple platforms can be utilized such as Hadoop as a horizontal scaling platform and GPUs as a vertical scaling platform to perform the analysis in real-time. Chen et al. [7] presented a review of technical challenges and the latest advances in the related technologies for the four phases of big data analytics that are data generation, data acquisition, data storage, and data analysis. Several open problems and future directions have been discussed in several representative applications such as enterprise management, Internet of Things (IoT), online social networks, medical applications, collective intelligence, and smart grid. An end-to-end big data benchmark, BigBench [8], has been proposed by addressing the variety, velocity, and volume aspects of big data systems in the domain of product retail businesses with physical and online stores. The benchmark contains the structured data adopted from the TPC-DS benchmark, semi-structured data captured from the user responses on the retailers' websites, and unstructured data captured from the online product reviews. The benchmark has been designed to generate the data upon a set of queries based on the source of data, types of query processing, and techniques used in analysis as three data dimensions. The response time feasibility of BigBench has been evaluated on Teradata Aster Database with 200 Gigabyte of big data set and executing queries developed using Teradata Aster SQL-MR. Further evaluation of the BigBench is planned to be done on one of the Hadoop eco-systems like HIVE.

Wang [9] proposed a method to process network traffic streaming data with unknown protocol using neural network and deep learning approaches. The proposed method can be applied on feature learning, protocol classification, anomalous protocol detection and unknown protocol identification. The method is beneficial in comparison to the traditional methods that have poor adaptation and are difficult to automate. Agneeswaran et al. [10] reviewed three generations of tools/paradigms for iterative machine learning algorithms in the context of big data analytics. The third generation tools/paradigms such as *Spark* and *GraphLab* were found to be the

most promising in the implementation of the large number of machine learning algorithms in terms of horizontal scalability. It has been identified that more sophisticated paradigms such as *Bulk Synchronous Parallel* (BSP) based paradigms and graph processing paradigms need to be considered in the implementation of a number of machine learning algorithms in addition to Hadoop's Map-Reduce paradigm for big data analytics. Bengio [11] examined the scalability issues of deep learning algorithms for larger models and datasets to develop more efficient and powerful inference and sampling procedures with reduced optimization difficulties. Enhancements in training deep learning algorithms have been achieved [12] using more sophisticated optimization methods including Limited memory BFGS (L-BFGS) and Conjugate Gradient (CG) with linear search instead of using Stochastic Gradient Descent Methods (SGDs) as the traditional approach. The experiments have been performed by considering both algorithmic extensions such as sparsity regularization and hardware extensions such as GPUs or Computer Clusters. The use of L-BFGS in convolutional network model obtained 0.69% set test error on the standard MNIST dataset which is a state-of-the-art result among other related algorithms. However, L-BFGS was found to be highly competitive to SGDs/CG for dimensional problems. Significant performance improvements of L-BFGS and CG over SGDs have been observed with the use of sparse auto-encoders on GPUs. The performance trend is almost linear to the number of machines in use of locally connected networks and convolutional networks. Furthermore, it has been found that Map-Reduce framework can also be utilized in the computation of gradients using L-BFGS for locally connected networks or other networks with a relatively small number of parameters.

In terms of statistical analysis, machine learning, pattern recognition, data fusion, data mining, and numerical analysis, big data infrastructure and analytics are directly related to the traditional data sciences [13]. However, deep analysis of big data requires the use of massively parallel computing concepts with large numbers of high-end servers. Such an analysis has been performed on US DoD (Department of Defense) big data for pattern recognition, anomaly detection and data fusion using various methods like Lexical Link Analysis (LLA), System-Self Awareness (SSA), and Collaborative Learning Agents (CLA) as an unsupervised learning or deep learning. In order to satisfy the needs of traffic flow prediction in real-world applications, deep architecture models have been applied [3] on big traffic data with inherently spatial and temporal correlations. In this method, feature extraction of the generic traffic flow has been done using stacked auto-encoder while training has been performed in a greedy layer-wise fashion. The performance evaluation has been performed on PeMS dataset to compare with the BP NN, SVM, and RBF NN models. The proposed method is found to be superior than the other competing methods. Further investigation can be performed using other deep learning algorithms for traffic flow prediction with the application on different public open datasets to examine their effectiveness. Deep learning on big data has been applied [14] for complex pattern extraction, data tagging, semantic indexing, simplifying discriminative tasks, and fast information retrieval on an un-labeled and un-categorized raw dataset. The study highlights the usefulness of deep learning in solving specific problems of big data analytics while suggesting improvements in deep learning to

```
import tensorflow as tf
import matplotlib.pyplot as plt

W = tf.Variable([0.3], dtype=tf.float32) #1
b = tf.Variable([-0.3], dtype=tf.float32) #2
x = tf.placeholder(tf.float32) #3
linear_model = W*x + b #4
y = tf.placeholder(tf.float32)

plt.scatter([1, 2, 3, 4], [0, -1, -2, -3]) #5
s = tf.Session()

init = tf.global_variables_initializer() #8
s.run(init) #9

squared_deltas = tf.square(linear_model - y)#10
loss = tf.reduce_sum(squared_deltas)#11

result = s.run(linear_model,{x: [1,2,3,4]})#12
result_loss = s.run(loss,{x: [1,2,3,4], y: [0,-1,-2,-3]})#12
print (result,result_loss)

plt.plot([1, 2, 3, 4], result*[0,-1,-2,-3], 'r')#13
plt.show()
```

Fig. 1. Tensor Flow Linear Regression Model

overcome the challenges in big data analytics. The work can be extended to focus on other aspects of big data analytics that are variety and velocity of data, large-scale models, and distributed computing.

III. EXISTING SOLUTIONS AND TOOLS

This section reviews mostly used software tools and libraries in the domain of deep learning.

A. TensorFlow

TensorFlow (TF) is the most popular deep learning package on github [15]. TensorFlow is an interface for expressing machine learning algorithms on heterogeneous distributed systems [16]. The intent behind its development was to create a framework that supports scalable machine learning and an easy to use programming paradigm. Before starting TensorFlow, Google had used DistBelief as their first-generation machine learning system. The old generation did not have support for a large portion of hardware. The second generation of machine learning framework, which is TensorFlow, does solve this problem and added more features. The advance in hardware, especially in GPU supported deep learning.

Fig. 1 shows a basic example of a linear regression model that takes a sample of training data and evaluates the model using a loss function. The loss function calculates the distance between the provided data and the model. Furthermore, TensorFlow provides *tf.train* API, which is an optimizer called gradient descent to reduce the loss in the model. TensorFlow operations have both CPU and GPU implementations; if TF finds a GPU device, then it automatically executes GPU implementations of the used operation instead of the CPU one. Moreover, it also provides an API function *device* to set a specific device for a certain code block.

B. PyTorch

PyTorch is a deep learning library for Python. It has been developed by Facebook and is mainly used for natural language processing. It has two high-level features: tensor computation

that comes with GPU acceleration and deep Artificial Neural Network (ANN) built with taped-based auto-grad system. In PyTorch, one can use the old python packages such as Numpy, cython, and Scipy to maximize the use of PyTorch. It provides *tensors* that can execute commands using either GPU or CPU, and speed up compute by a huge amount.

1) Advantages of using PyTorch:

- 1) The debugging process is easy, making it easier to understand and follow the code.
- 2) It has the same as well as some more features and layers that happen to be in Torch like (Grus, CONV1, 2, 3D; LSTMCONV 1, 2, 3D; LSTM, Unpool).
- 3) Could be a Numpy extension To GPUs.
- 4) It is fast and some consider it the fastest among other libraries *define by run* for example dynet and chainer.
- 5) With PyTorch, one can build a strong network structured by its computation.
- 6) In PyTorch, the overhead in the framework is minimal.
- 7) Making neural network is easy and requires no extensions.

PyTorch figured out a new way of building neural networks, using tape recorder and replay it. Other frameworks like Caffe, Theano, TensorFlow and CNTK use a static view. When they build a neural network, they have to use the same neural network and cannot change it; although they can but they have to start from the scratch. However, in PyTorch, there is a new way called *Reverse-mode auto-differentiation*, that allows the user to change the neural network and to modify without overheating or lags.

C. Caffe2

Caffe2 is a deep learning framework which is simple and helps to use the algorithms of new models. Using the GPU power, we can bring the creation to scale with Caffe2 libraries that support cross-platform operations. The operators are a basic computation unit of Caffe2. It is a flexible layers' version of Caffe since it comes with more than 400 different operators.

D. Comparison of Deep Learning Frameworks

TensorFlow is a powerful deep learning framework, with a lot of documentation and is good in visualization. Furthermore, it has the ability to build a strong model for many platforms. Therefore, TensorFlow is good in building a model for production, used to build models for mobile platforms, and has a good community support. On the other hand, PyTorch is relatively a newer framework and is growing up fast. For now, PyTorch is good for research and building products with the non-functional requirements, good for testing and debugging. PyTorch was designed with additional capabilities like the ability to trace and debug errors, and building a dynamic neural network. While the other frameworks like Tensorflow, Theano and Caffe use static neural networks, lack the ability to trace and debug errors, and may require more time in finding the errors. In addition, PyTorch is a new framework that happens to grow fast, and could in the near future use the same advantages as found in other frameworks, like having its own visualization. In short, PyTorch is a newer framework, that is more flexible than its competitors.

Caffe2 supports a large-scale deployment. It brings the Torch and itself together to support the multi-GPUs as it provides the same level of support. It can work on both single-host and multi-host GPUs workstations.

E. Customize Code Optimizations of Deep Learning Algorithms

Olas et al. [17], [18] presented the implementations of Restricted Boltzmann Machine (RBM) and Deep Belief Net (DBN) using Intel Xeon Phi CoProcessor (Many Integrated Core). The algorithms are fully implemented in C++ language using the OpenMP standard for parallelizing computation. The transformation of computations was performed in such a way that efficient implementations of matrix and vector operations available in the *BLAS* library can be utilized. For example, the operation of summing the elements of a matrix is replaced with a matrix-vector multiplication, where the vector contains all ones. All the codes are compiled using Intel C++ Compiler available in Intel Parallel Studio XE 2015 environment. Additionally, the Intel Math Kernel Library (MKL) is used for the efficient implementation of *BLAS* routines. Furthermore, in order to generate pseudo-random numbers in particular, the *SIMD-oriented Fast Mersenne Twister pseudo-random number generator VSL_BRNG_SFMT19937* is utilized.

IV. BUILDING BLOCKS FOR DEEP LEARNING IN BIG DATA ANALYTICS

Parallelism has been employed for many years, mainly in high-performance computing, but interest in it has grown lately due to the physical constraints preventing frequency scaling. As power consumption (and consequently generated heat) by computers has become a concern in recent years, parallel computing has become the dominant paradigm in computer architecture [19]. In addition, GPU development during the last few years has contributed to a growth in the concept of deep learning. Parallel computing in deep learning in its *natural form* would mean improvements in training time from months to weeks or days. Deep learning has many different algorithms such as auto-encoders, denoising auto-encoders, stacked denoising auto-encoders, Restricted Boltzmann Machines (RBM), Deep Belief Networks (DBN).

A. Restricted Boltzmann Machines (RBMs)

RBM was invented by Geoff Hinton. This algorithm can automatically find the patterns in data by reconstructing inputs. It is used in dimensional reduction, classification, regression, collaborative filtering, feature learning, and topic modeling. It is increasingly being used in supervised and unsupervised learning scenarios. The first layer of the RBM is called the visible or input layer, and the second is the hidden layer as shown in Fig. 2. Each circle in the graph represents a neuron-like unit called a node, and the calculations take place in the nodes. The nodes are connected to each other across layers, but no two nodes of the same layer are linked. As their name implies, RBMs are a variant of Boltzmann machines, with the restriction that their neurons must form a bipartite graph. By contrast, *unrestricted* Boltzmann machines may have connections between hidden units. Therefore, there is no intra-layer communication. This restriction allows for more efficient training algorithms than are available for the general

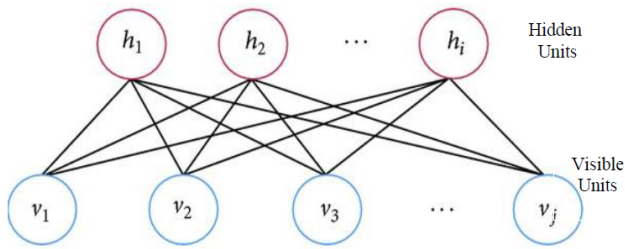


Fig. 2. Restricted Boltzmann Machine

class of Boltzmann machines, in particular the gradient-based contrastive divergence algorithm. Since the inputs from all visible nodes are being passed to all of the hidden nodes, RBM can be defined as a symmetrical bipartite graph [20].

1) *RBM Implementation Structure:* RBM consists of two steps. Each step has effect of different parameters:

- 1) n_{visible} : Number of visible units. It is used to train per one iteration train_X (column size)
- 2) n_{hidden} : Number of hidden units
- 3) train_n : Sets number or iteration number of train_X (row size)

a) *Training step (Contrastive Divergence function):*

Contrastive divergence is used to calculate the gradient (the slope representing the relationship between a network's weights and its error), without which no learning can occur. The parameters here are:

- 1) k : The number of times the contrastive divergence is run
- 2) train_x : Sample data used for training purpose
- 3) $\text{input}[j]$: or visible units is a sample from the training distribution (it's one row of train_x) for the RBM (vector size is # of n_{visible})
- 4) learning_rate : Like momentum, affects how much the neural net adjusts the coefficients on each iteration as it corrects for errors. This parameter helps to determine the size of the steps, the net takes down the gradient towards a local optimum. A large learning rate will make the net learn fast, and may overshoot the optimum. A small learning rate will slow down the learning, which can be inefficient.
- 5) N : sample row size (# of train_N). Samples will be processed row by row. Each iteration will process the complete number of column (size is # of n_{visible})

b) *Testing step (Reconstruction):* The dependent parameters here are:

- 1) test_x : Sample data that is used for testing purpose
- 2) reconstructed_x : variable which is used for sigmoid and the trained data

2) *Principal Factor Analysis on RBM:* We have applied Principal Factor Analysis (PFA), a well-known statistical method for finding the parameters that are affecting the performance of any system. For RBM implementation, the following factors (see Table I for execution times) were analyzed:

- 1) k : contrastive divergence steps

- 2) v : the number of visible neurons
- 3) h : the number of hidden neurons
- 4) N : training set dimension

Table II shows the ANOVA table as a result of Principal Factor Analysis of RBM factors. It shows that the factor, which strongly affects the performance of RBM is k , that represents the contrastive divergence steps. These steps are strongly sequential in execution. Therefore, parallelization will not benefit from this factor because of strong flow dependency of loop iterations. At the second level, the factor N (training set dimensions) is showing significant variations in execution time of RBM. Since the input samples (N) are processed independently in RBM storing the resulting weights on different indices, therefore, it is a good candidate for parallelization so as to gain significant performance improvement of deep learning models.

B. Deep Belief Nets (DBNs)

A Deep Belief Network (DBN) is a type of deep neural network, composed of multiple layers of latent variables (hidden units), with connections between the layers but not between units within each layer. As what has been introduced before, the most important use of RBM is as learning modules that are composed to form deep belief nets. RBMs are shallow, two-layer neural networks that constitute the building blocks of deep belief networks (see Fig. 3). It can be formed by *stacking* RBMs and optionally fine-tuning the resulting deep network with gradient descent and back-propagation. Therefore, DBN can be defined as a stack of Restricted Boltzmann machines (RBM). Each RBM layer communicates with both the previous and subsequent layers. The nodes of any single layer don't communicate with each other laterally. This stack of RBMs might end with a *Softmax*¹ layer to create a classifier, or it may simply help cluster unlabeled data in an unsupervised learning scenario. When trained on a set of examples in an unsupervised way, a DBN can learn to probabilistically reconstruct its inputs. The layers then act as feature detectors on inputs. After this learning step, a DBN can be further trained in a supervised way to perform classification. With the exception of the first and final layers, each layer in a deep-belief network has a double role: it serves as the *hidden layer* to the nodes that come before it, and as the input (or *visible*) layer to the nodes that come after. The reason of using DBN is to recognize, cluster and generate images, video sequences and motion-capture data. A continuous deep-belief network is simply an extension of a deep-belief network that accepts a continuum of decimals, rather than binary data [21].

MNIST is a good place to begin exploring image recognition and DBNs. The first step is to take an image from the dataset and to convert its pixels from continuous gray scale to binary. Typically, every gray-scale pixel with a value higher than 35 becomes a 1, while the rest are set to 0. The MNIST dataset iterator class performs this operation [21], [22].

¹*Softmax* is a function used as the output layer of a neural network that classifies input. It converts vectors into class probabilities. It normalizes the vector of scores by first exponentiating and then dividing by a constant.

TABLE I. RBM EXECUTION TIME (MSEC) WITH DIFFERENT PARAMETERS

v →		6			12			24		
		h			h			h		
k	N	3	6	12	3	6	12	3	6	12
1	1000	1.58	2.48	4.41	2.47	3.88	6.73	4.36	6.70	11.53
	2000	3.13	5.01	8.72	4.96	7.82	13.48	8.87	13.52	22.96
	3000	4.67	7.51	13.01	7.49	11.68	20.34	13.19	20.08	34.18
5	1000	4.76	7.11	11.94	8.01	11.51	18.46	10.85	14.73	22.59
	2000	9.45	14.20	23.88	15.87	22.98	29.17	21.77	31.07	44.91
	3000	14.24	21.33	35.72	23.91	34.69	40.10	32.80	46.56	67.24
10	1000	6.72	9.92	15.93	11.33	15.77	24.22	20.51	27.34	40.34
	2000	13.57	19.69	31.95	22.52	31.30	48.29	40.84	54.77	80.88
	3000	20.14	29.49	47.81	33.86	47.15	72.48	61.63	81.63	121.31

TABLE II. RBM PRINCIPAL FACTOR ANALYSIS - ANOVA TABLE

Main Effects	% Variations
k	41.65
v	17.60
N	25.83
h	15.07

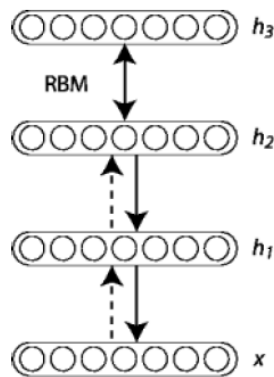


Fig. 3. Deep Belief Network

V. PROPOSED SOFTWARE ABSTRACTIONS FOR DEEP LEARNING MODELS

Based on our analysis of deep learning algorithms like RBM and DBN in Section IV-A2, it has been found that the performance of the algorithms is highly affected by the iterations on visible and hidden nodes which are strongly dependent on each other and are not suitable for parallel implementations. The only effective parallelization in these algorithms is to distribute the input samples among several workers (processes or threads) to obtain a significant speedup of deep learning model execution. Furthermore, there are several frameworks and available libraries that provide efficient implementation of these algorithms. In order to utilize these frameworks and libraries for developing large-scale deep learning models for big data analytics, we need to extend these tools to execute on multiple computing nodes where each node has a portion of input samples and runs the model in parallel. At the end, the final output of the learning process needs to be accumulated at the single (master) node. This requires an in-depth knowledge of writing parallel programs and concepts of data distribution. In order to ease the development of deep learning models for big data analytics, we propose a parallel software API as an extension of PyTorch with HDFS and MapReduce frameworks. The following sub-sections explain the tools used in the API, its process flow, usage and functions.

A. Used Tools

a) *PyTorch*: is a scientific computing library, which is developed as a GPU-enabled alternative for *Numpy*. It is a deep-learning platform that provides both speed and flexibility. Much like other deep-learning libraries, PyTorch makes use of *Tensors* for storing data and training of neural networks [23]. In addition to this, PyTorch makes it fairly simple to create *computational graphs*, an important aspect of neural networks. Furthermore, the PyTorch library comes with an autograd function, so as to automate the process of calculating the gradient descent, whilst training a network. It is important to note here that loading data into PyTorch is a difficult process. The data needs to be converted into a form that can be read by the library's *DataLoader* class. Moreover, the *CUDA* library also needs to be installed and enabled in PyTorch for GPU computations.

b) *Hadoop*: is an open-source and Java-based framework, which allows distributed processing of datasets, across a cluster of connected computers [24]. The core components of the framework include Hadoop Common, Hadoop Distributed File System (HDFS), Hadoop YARN and Hadoop MapReduce. In the following process, HDFS and MapReduce would be of key importance. One of the main reasons for Hadoop's popularity is its adherence to the principle that hardware failures of individual machines, within a cluster, should be handled automatically by the framework.

c) *MRJob*: is a module developed by *Yelp*, to create Hadoop MapReduce jobs in Python, instead of the conventional Java code [25]. As compared to other MapReduce libraries for Python, MRJob allows the users to keep the mappers and reducers, both, in a single class. Moreover, it allows users to define a multi-step mapper and switch input and output formats, with a single line of code.

B. API Process Flow

In order to develop a distributed neural network API, we constructed a simulation of a Restricted Boltzmann Machine, the most basic kind of neural network. Although the entire process was developed and tested using the MNIST dataset, the configuration of the network has been kept dynamic, so that the users of the API can alter the configurations as per their needs. It should be noted here that the API makes use of PyTorch and MRJob at the backend.

The API makes use of three modules, namely the *Neural Network Configuration* (NNC) module, *MapReduce Configuration* (MRC) module and the *Network Definition* (ND) module. The NNC module comprises of three classes, the

```
newnet=rbm(0.015, 0.8, 64)
MRDL.newnet=newnet
net=newnet.create_net(layer_count=4, node_seq=[784,500, 100, 10])
MRDL.net=net
MRDL.run()
iter1=newnet.combine_weights(MRDL.weights)
net=newnet.create_net(layer_count=4, node_seq=[784,500,100,10])
newnet.set_w(iter1, net)
```

Fig. 4. Code Example for Model Configuration of 784 → 500 → 100 → 10

net class, the *data_load* class and a *ToTensor* class, whereas the MRC module comprises of the *MR_dist* class and the ND module comprises of *RBM* class. It should be noted here that the *net* class inherits from PyTorch's *torch.nn.module* and overrides the feed-forward function.

Since everything has been well-defined and properly implemented throughout the API, the users just need to interact with the ND and MRC modules. The users need to create an object of the *rbm* class, to set the parameters for the network to follow. This includes the learning rate, the momentum and the batch size, respectively. Each of the three parameters need to be passed to the constructor of the class object. This object should be then passed to the *newnet* variable of the *MR_dist* class.

This would then be followed by defining the layers of the network, which can be done by calling the *create_net* function of the *rbm* class object, the number of layers and the list containing the number of nodes for each layer. This all should be passed as arguments to the function. The output of this function should be passed to the *net* variable of the *MR_dist* class.

It should be noted here that *create_net* function creates a new list, which contains the nodes of the network in linear configuration. Similarly, *Xavier* weights are specified for each layer, with the *relu* function being set as the default *gain* function. Furthermore, the feed forward function makes use of the logarithmic softmax function, as the default feed forward function.

The users then need to call the *run* function of the *MR_dist* class, which executes the distributed training of the RBM. Following the training, the users would need to combine the output from multiple reducers, for which they can call the *combine_weights* function of the *rbm* class object. The variable *weights* from the *MR_dist* class should be passed to the function as an argument. The user can then call the *set_w* function of the *rbm* class object, passing the output of the last function and the weights to be applied as arguments. This will create a network that has the trained weights and is ready to be used.

Note: The aforementioned process has been defined for a network of just 4 layers: 1 output, 2 hidden and 1 input layer. Subsequent hidden layers, if needed, can be added easily. For example, Fig. 4 shows the code for a configuration of 784 → 500 → 100 → 10.

In order to test the accuracy, the users would need to first call the *data_load* function of the *rbm* object and pass the path of the test data file as an argument. The output of this function should be saved in a variable. Finally, the users would just need to call the *test* function of the *rbm* object, passing the loaded data variable and the network as arguments to the function.

The results of the test would then be printed as output on the user screen.

The addition of a *data_load* class and a *ToTensor* class, to the NNC module was necessary, so as to ensure that all data passed into the network is in a consistent and specified format. As such, the data being passed to the API needs to be in CSV format and should contain a label column and adjoining value columns. The reasons to choose this format, as the default data format for the API include:

- The fact that most of the data available for training models can easily be found in CSV formats.
- It is easy to convert data from different sources to a CSV format.
- Hadoop reads a file line by line and does not split the data from the middle of a line.

The *data_loader* object can be created by passing the absolute path of the file, as an argument to the class object. Additional data can also be passed to the object, as well as any transformations that need to be applied to the data. It should be noted here that the *data_loader* class inherits from PyTorch's *torch.utils.data.Dataset*. Moreover, to make individual instances of the data fetchable, as label and corresponding value, the *__getitem__* function of the parent class is over-ridden. In addition to this, the *ToTensor* class is used as a transformation mechanism to convert all of the data which has been passed to a tensor for GPU computations.

Similarly, the *MR_Dist* class inherits from the MRJob class, from the MRJob module and over-rides the reducer and mapper functions. It is important to note here that since training and running the network requires multiple steps, a multi-step mapper was defined in the class. There are basically three steps involved as part of the mapper: the data splitting step, the data collection, loading and transformation step. Each of these three steps are defined as a separate function in *MR_Dist*.

This is followed by a reducer function, which basically trains networks on the split data and then collects the weights of the trained networks. As such, the *reducer* and the *steps* functions of the parent class are over-ridden, in the *MR_Dist* class. The user just needs to initiate an object of this class in the main program and MRJob would take care of the rest.

C. API Usage

In order to use the API, the user would have to follow the following steps (see Fig. 5):

- 1) Make sure that all of the data is in a CSV format, with a label's section and a values' section.
- 2) Create an object of the *rbm* class, from the ND module, passing the *learn_rate* (type float), momentum (type float) and *batch size* (type integer) as arguments.
- 3) Set the *newnet* variable in the *MR_dist* class equal to the newly created *rbm* object.
- 4) Create a neural network by calling the *create_net* function of the newly created *rbm* object and passing the number of nodes (*nodes*, of type list) and layers (*num_layers*, of type integer) in the arguments.
- 5) Set the *net* variable in the *MR_dist* class equal to the output of the previous function.

```

if __name__ == '__main__':
    newnet=rbm(0.015, 0.8, 64)
    MRDL.newnet=newnet
    net=newnet.create_net(layer_count=4, node_seq=[784,500,100,101])
    MRDL.net=net
    MRDL.run()
    iter1=newnet.combine_weights(MRDL.weights)
    net=newnet.create_net(layer_count=4, node_seq=[784,500,100,101])
    newnet.set_w(iter1, net)
    testdata=newnet.load_data(data_path='test.csv')
    newnet.test(loaded_data=testdata, nNet=net)

```

Fig. 5. Proposed API Usage Example.

- 6) Call the *run* function from the *MR_dist* class to begin training.
- 7) Call the *fetch_weights* function of the trained *rbm* object, to fetch the newly defined weights and store them in a variable.
- 8) Call the *combine_weights* function from the *rbm* object, passing the weights variable from the *MR_dist* class, as an argument.
- 9) Keep the data in your HDFS directory.
- 10) Run your Python script in Hadoop streaming, by typing 'python3 path_to_python_script path_to_data_file -r hadoop > path_to_output_file' in the terminal.

Once the script has finished running, the final network would be saved in the specified output directory and can be later viewed and used for future work.

D. API Functions

a) *Net.__init__(self, num_layers, nodes)*: This is basically the network initialization function and is used to create the neural network that would be later trained on some data. The argument *num_layers* identifies how many layers the RBM would have and what is the size of the *nodes* list. The *nodes* list in turn inputs how many nodes each of the layers is supposed to have. Once an object of this class is created, this function is called and a neural network, having the specified configuration, is created. The network is also assigned *Xavier Uniform* weights and the gain function for the entire network is set to the *Relu* gain function.

b) *Net.forward(self, x)*: This function overrides the default feed-forward function of the *torch.nn.module* class and returns the logarithmic softmax of the gain values, for the entire network. The function works by passing the training values, iteratively through the individual layers of the network and adjusts the weights, as needed.

c) *Data_load.__init__(self, file, direct, transform)*: This is the object initialization function for the *data_load* class. It takes as arguments the path of the CSV file to be read for the data, the path of any additional directories to use and the list of transformations to apply. The function then reads the CSV file and splits it into two variables: *X* and *Y*. The variables contain the training data and the corresponding label of the data respectively. It should be noted here that the first index of the CSV file is considered to be the label, while the remaining columns are classified as training data.

d) *Data_load.__len__(self)*: This function returns the number of data points present in the specified dataset.

TABLE III. HADOOP CLUSTER CONFIGURATIONS

Component/Configuration	Description/Value
Processor	Intel(R) Core(TM) i5-7300HQ @ 2.5 and 2.5 GHz
Memory	8 GB
Hard Disk	1 TB
Yarn CPU Cores	4
Yarn Memory	10240 MB
Scheduler Max Memory	8192 MB
Scheduler Min Memory	512 MB
Yarn Virtual Memory Check	Disabled
MapReduce CPU Cores	4
MapReduce Memory	4096 MB
Mapper Memory	2048 MB
Reducer Memory	2048

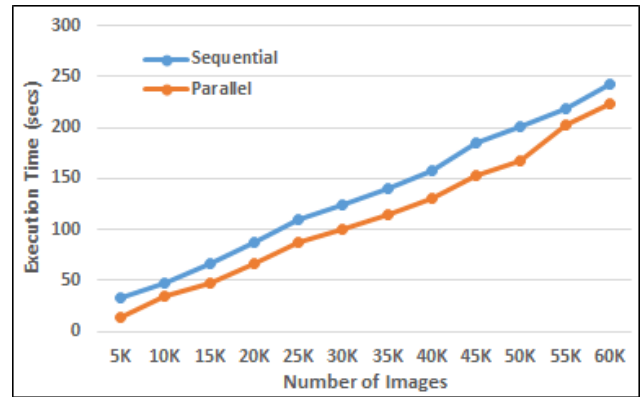


Fig. 6. Performance comparison of Deep Autoencoder using Proposed API

e) *Data_load.__getitem__(self, index)*: The function works to fetch a data point from an index, specified by the user, from the supplied data. The data is first selected from the variables *X* and *Y* and the list of specified transformations are applied on *X*. The updated label and data is then returned as a single tuple, representing the data and label, in respective order.

f) *ToTensor.__call__(self, sample)*: This function is initialized as soon as the class is called. The function takes a list of data as an argument and transforms it to a *tensor*, which is then passed through the neural network.

VI. API EVALUATIONS IN TERMS OF PERFORMANCE AND USAGE

In order to evaluate the performance of our proposed software API, we configured a single-node Hadoop cluster in a workstation with the configurations as shown in Table III.

Fig. 6 shows the execution time in seconds for both sequential (in PyTorch) and parallel implementations of deep autoencoder on MNIST dataset using the proposed software API with different number of input images for model training. The obtained results show significant improvement in performance (about 58%) for an input size of 5000 images while the improvement percentages are decreasing as the input size increases such that the performance improvement is only about 8% for an input size of 60000 images. The reason for this behavior is heavy read operations from permanent storage and extensive memory usage to store the input dataset into memory for processing. Therefore, if we extend the cluster configurations to have multiple data nodes then the input dataset will be distributed among several data nodes and the

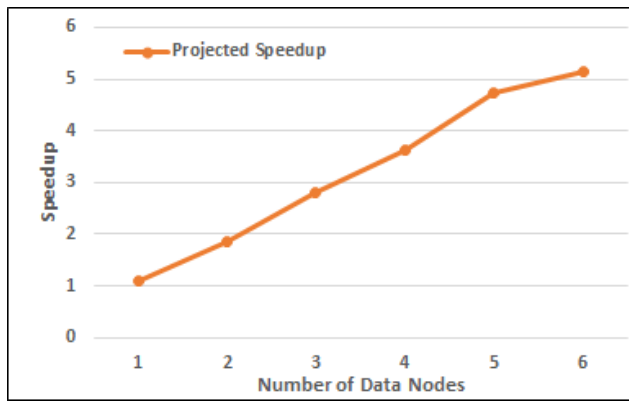


Fig. 7. Projected Speedup based on Parallel Time Estimation

training will be performed on each partition of the data in parallel. This would give more speedups as we increase the number of data nodes in the cluster. Fig. 7 shows the projected speedup estimating the reduction of execution time of parallel implementation based on the size of the data partition that each node will contain for processing.

Furthermore, the complexity of code development is significantly reduced to create multi-layer deep learning models. This is achieved by using a list of visible and hidden neurons provided by the user and `Net.__init__` function of the proposed API will generate the required PyTorch code to add layers into the model.

VII. CONCLUSION AND FUTURE WORK

In this paper, we proposed a software API for fast development of large-scale deep learning models for big data analytics. The idea was to analyze the datasets with a higher amount of volume, velocity, and variety. The API proposal is on the basis of our exploration of the latest trends in the development of parallel algorithms, optimization techniques, tools and libraries related to big data analytics and deep learning on various parallel architectures. Initially, we assumed the need of parallelizing the deep learning algorithms as basic building blocks for the parallel software API. However, with the statistical analysis of a deep learning algorithm (RBM), we found that the factors affecting the most on the performance of these algorithms are highly sequential in nature and parallelizing using these factors will not be beneficial because of strong flow dependencies in the code. Furthermore, there are several frameworks and available libraries that provide efficient implementations of these algorithms. Therefore, there is a need to extend these frameworks to do the model execution on multiple computing nodes, where each node has a portion of input samples and runs the model in parallel. Hence, in order to ease the development of deep learning models for big data analytics, we propose a parallel software API as an extension of PyTorch with HDFS and MapReduce frameworks. We obtained significant improvements in the deep learning models using the proposed API in reduction of the execution time and code complexity. We have evaluated the API by implementing a deep auto-encoder using MNIST dataset on a single node Hadoop cluster. In future, we plan to setup a multinode Hadoop cluster and run the implementation with various number of data nodes.

ACKNOWLEDGMENT

This work is supported by the Deanship of Scientific Research at Qassim University under the project no. 1374-coc-2016-1-12-S.

REFERENCES

- [1] B. K. Tannahill and M. Jamshidi, "Big data analytic paradigms-from PCA to deep learning," in *AAAI Spring Symposium - Technical Report*, vol. SS-14-04, 2014, pp. 84–90.
- [2] X.-W. Chen and X. Lin, "Big Data Deep Learning: Challenges and Perspectives," *IEEE Access*, vol. 2, pp. 514–525, 2014.
- [3] Y. Lv, Y. Duan, W. Kang, Z. Li, and F.-y. Wang, "Traffic Flow Prediction With Big Data : A Deep Learning Approach," *Intelligent Transportation Systems, IEEE Transactions on*, vol. 16, no. 2, pp. 865–873, 2015.
- [4] L. Deng and D. Yu, *Deep Learning: Methods and Applications*. NOW Publishers, May 2014.
- [5] J. Zakir, T. Seymour, and K. Berg, "Big Data Analytics," *Issues in Information Systems*, vol. 16, no. 2, pp. 81–90, 2015.
- [6] D. Singh and C. K. Reddy, "A survey on platforms for big data analytics," *Journal of Big Data*, vol. 2, no. 1, p. 8, 2014.
- [7] M. Chen, S. Mao, and Y. Liu, "Big data: A survey," in *Mobile Networks and Applications*, vol. 19, no. 2, 2014, pp. 171–209.
- [8] A. Ghazal, T. Rabl, M. Hu, F. Raab, M. Poess, A. Crolotte, and H.-A. Jacobsen, "BigBench," in *Proceedings of the 2013 international conference on Management of data - SIGMOD '13*. New York, New York, USA: ACM Press, 2013, pp. 1197–1208.
- [9] Z. Wang, "The Applications of Deep Learning on Traffic Identification," *Black Hat USA*, 2015.
- [10] V. S. Agneeswaran, P. Tonpay, and J. Tiwary, "Paradigms for Realizing Machine Learning Algorithms," *Big Data*, vol. 1, no. 4, pp. 207–214, 2013.
- [11] Y. Bengio, "Deep learning of representations: Looking forward," in *Lecture Notes in Computer Science (including subseries Lecture Notes in Artificial Intelligence and Lecture Notes in Bioinformatics)*, vol. 7978 LNAI, 2013, pp. 1–37.
- [12] Q. V. Le, A. Coates, B. Prochnow, and A. Y. Ng, "On Optimization Methods for Deep Learning," *Proceedings of The 28th International Conference on Machine Learning (ICML)*, pp. 265–272, 2011.
- [13] Y. Zhao, D. J. MacKinnon, and S. P. Gallup, "Big Data and Deep Learning for Understanding DoD Data," *CrossTalk*, vol. 28, no. 4, pp. 4–11, 2015.
- [14] M. M. Najafabadi, F. Villanustre, T. M. Khoshgoftaar, N. Seliya, R. Wald, and E. Muharemagic, "Deep learning applications and challenges in big data analytics," *Journal of Big Data*, vol. 2, no. 1, p. 1, 2015.
- [15] E. B. Yoav Shoham, Raymond Perrault and J. Clark, "The ai index 2017 annual report," Stanford, Review Report, 2017.
- [16] M. Abadi, P. Barham, J. Chen, Z. Chen, A. Davis, J. Dean, M. Devin, S. Ghemawat, G. Irving, M. Isard, M. Kudlur, J. Levenberg, R. Monga, S. Moore, D. G. Murray, B. Steiner, P. Tucker, V. Vasudevan, P. Warden, M. Wicke, Y. Yu, and X. Zheng, "Tensorflow: A system for large-scale machine learning," in *12th USENIX Symposium on Operating Systems Design and Implementation (OSDI 16)*, 2016, pp. 265–283. [Online]. Available: <https://www.usenix.org/system/files/conference/osdi16/osdi16-abadi.pdf>
- [17] T. Olas, W. K. Mleczko, R. K. Nowicki, and R. Wyrzykowski, *Adaptation of Deep Belief Networks to Modern Multicore Architectures*. Cham: Springer International Publishing, 2016, pp. 459–472.
- [18] T. Olas, W. K. Mleczko, R. K. Nowicki, R. Wyrzykowski, and A. Krzyzak, *Adaptation of RBM Learning for Intel MIC Architecture*. Cham: Springer International Publishing, 2015, pp. 90–101.
- [19] B. Barney, "Introduction to parallel computing," https://computing.llnl.gov/tutorials/parallel_comp/#Whatis, (Accessed on 01/31/2019).
- [20] "A beginner's tutorial for restricted boltzmann machines - deeplearning4j: Open-source, distributed deep learning for the JVM," <https://jrmerwin.github.io/deeplearning4j-docs/restrictedboltzmannmachine>, (Accessed on 12/31/2018).

- [21] “Deep-belief networks in java - deeplearning4j: Open-source, distributed deep learning for the jvm,” <https://mgubaidullin.github.io/deeplearning4j-docs/>, (Accessed on 12/31/2018).
- [22] “Deep learning tutorials — deeplearning 0.1 documentation,” <http://www.deeplearning.net/tutorial/>, (Accessed on 12/31/2018).
- [23] “What is Pytorch?” https://pytorch.org/tutorials/beginner/blitz/tensor_tutorial.html#sphx-glr-beginner-blitz-tensor-tutorial-py, (Accessed on 03/30/2019).
- [24] S. P. Bappalige, “An Introduction to Apache Hadoop for big data,” <https://opensource.com/life/14/8/intro-apache-hadoop-big-data>, (Accessed on 03/30/2019).
- [25] Yelp and Contributors, “Why mrjob?” <https://mrjob.readthedocs.io/en/latest/guides/why-mrjob.html#overview>, (Accessed on 03/30/2019).

Person Detection from Overhead View: A Survey

Misbah Ahmad¹, Imran Ahmed², Kaleem Ullah³, Iqbal Khan⁴, Ayesha Khattak⁵, Awais Adnan⁶

Center of Excellence in Information Technology

Institute of Management Sciences (IMSciences) Hayatabad, Peshawar (Pakistan)

Abstract—In recent years, overhead view based person detection gained importance, due to handling occlusion problem and providing better coverage in scene, as compared to frontal view. In computer vision, overhead based person detection holds significant importance in many applications including person detection, person counting, person tracking, behavior analysis and occlusion free surveillance system, etc. This paper aims to provide a comprehensive survey on recent development and challenges related to person detection from top view. To the best of our knowledge, it is the first attempt which provides the survey of different overhead person detection techniques. This paper provides an overview of state of the art overhead based person detection methods and guidelines to choose the appropriate method in real life applications. The techniques are divided into two main categories: the blob-based techniques and the feature-based techniques. Various detection factors such as field of view, region of interest, color space, image resolution are also examined along with a variety of top view datasets.

Keywords—Person detection; background subtraction; segmentation; blob based techniques; feature based techniques

I. INTRODUCTION

In video surveillance, one of the key tasks is to detect, identify, and monitor person in crowded and public scenes such as airports, train stations, and supermarkets. The problem of locating a person in the surveillance images and videos sequences from overhead view has been actively researched since last decades. Top view based person detection got importance, due to its better handling occlusion and providing wide coverage of the scene as compared to a frontal view. Overhead based person detection has many applications in various fields, however, the most significant is surveillance systems. Other applications include person detection in indoor and outdoor surveillance systems, person counting [1] (including pedestrian [2], [3], [4], & passenger counting in railway stations [5], shopping malls, airports, buses [6], person tracking [7], [8], [9], [6] [10], [11], behavioural understanding [12], action recognition, person posture characterization [13], crowd analysis [14], industrial work flow [15], [10], provision of large or more coverage area. Furthermore it is also helpful in search and rescue situations. Privacy issues can also be reduced by using an overhead camera because instead of face images overhead view of the person body is captured [16].

Detecting person in overhead videos and images is a challenging job because of the following factors: person body appearance, the wide range of poses, complex backgrounds, unconstrained illumination conditions and self-occlusion. For detecting the person in top view videos and images the understanding of the shape, structure and features of overhead viewed person body is mandatory. Once a person is detected the application system can be further improved.

A variety of top view person detection algorithms are available however these algorithms are still far from human ability to detect the person in images and videos just using a single clue.

One of the major hurdles in the person detection task is the flexible nature of person body, such as variation in poses, size, orientation and direction of person body. The variation in hair colour and texture, clothes colour and texture also add to the complexity. Similarly, the complex environment i.e. cluttered background, crowd, and lighting conditions, also create hurdles for researchers.

Various overhead person detection techniques have been developed in the last few years. In this paper, the significance of overhead view person detection techniques have been studied. To the best of our knowledge, this paper is the first review and survey that objects to cover the most significant advances reported in the literature until now.

From the broad literature of overhead person detection, a representative sample of papers have been selected. This paper classify developed techniques into two groups; blob based and features based.

As discussed earlier that task of person detection can be done using two different perspectives; frontal and overhead. The content of the paper and general frame work of overhead person detection has been summarized in Fig. 1. It can be seen that categorically the developed techniques are divided into two groups: Blob based techniques and feature based techniques.

The different detection factors including camera field of view (narrow or wide), the region of interest (person head, head-shoulder, whole overhead body), colour space (RGB, Depth, HSV & YCbCr), the device used for video and image recordings, recording environments (indoor and outdoor) are also shown in Fig. 1. Furthermore the challenges and applications of overhead based person detection are also depicted in Fig. 1.

The remainder of this paper is structured as follows: Section II begins by introducing the overhead based person detection techniques in general. It is divided into two subsections; the first reflects the different blob-based techniques used by most of the researchers. While the second discusses the features-based techniques. Different datasets used in the literature are also examined in Section II. The discussion on the existing techniques, dataset, issues related to the existing overhead based person detection are covered in Section III. Section IV concludes and summarize the paper and provide some future directions.

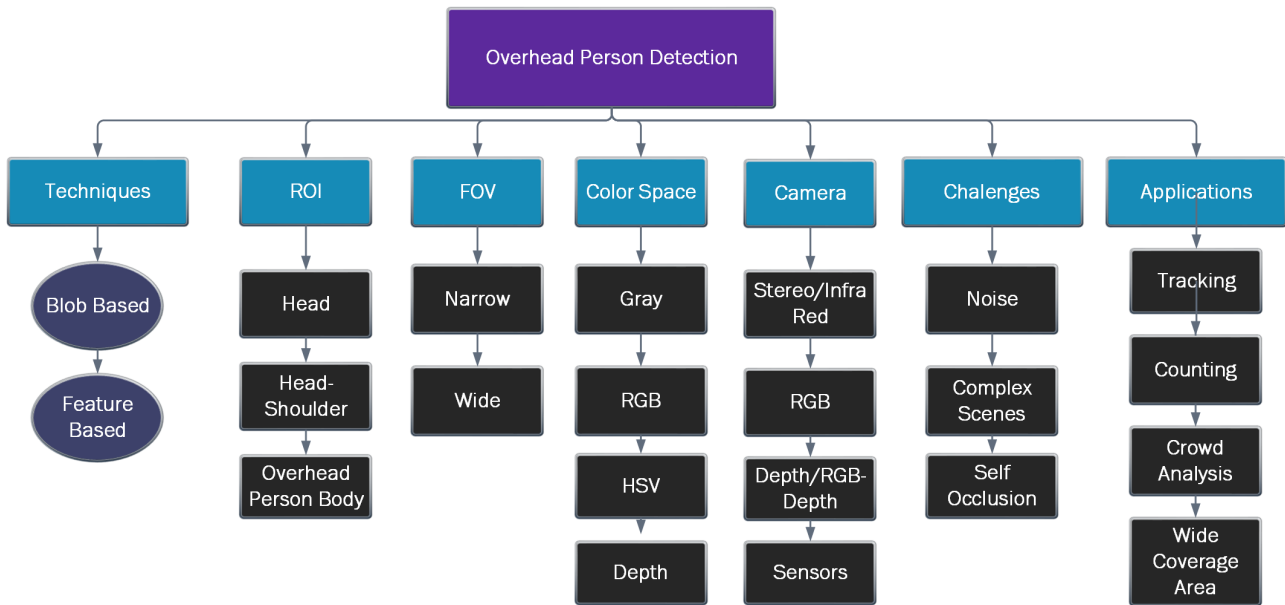


Fig. 1. Overview of the paper and general frame work of Person detection.

II. OVERHEAD BASED PERSON DETECTION TECHNIQUES

Locating a person in top view images and videos is merely a two step process; defining the ROI and localizing the person in the input image and video sequence. In overhead, the person in the image can be localized by its head, head-shoulder or sometimes, the whole overhead body is considered. In below Fig. 2 the overhead view of the person body can be clearly seen. As in the Fig. 2 it can be clearly perceived how the shape, size and body orientation of the person changes from an overhead view. In computer vision, it is important to understand how the person is detected in overhead images and videos. This chapter mainly focuses on algorithms which involved people detection in given overhead videos or images. This chapter broadly divides the relevant literature into two practices. In section, two different practices have been discussed, the first is based on simple blob based algorithms, while the second subsection discusses the feature based techniques used for person detection.

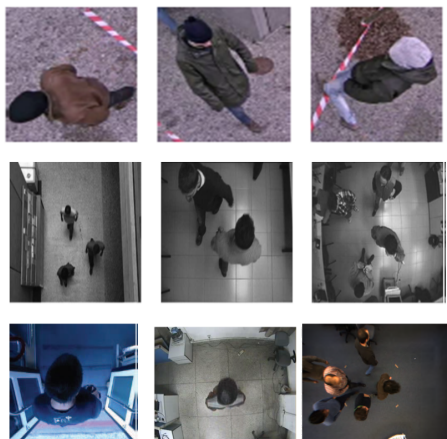


Fig. 2. Some of the images captured from Overhead surveillance cameras [3], [17], [18], [2].

A. Blob based Techniques

In this section, blob based techniques for overhead view person detection is debated. The general framework of blob-based techniques is shown in Fig. 3. These involve background subtraction, foreground extraction, segmentation and pre-processing techniques. Usually, in blob based techniques a foreground image is obtained from background subtraction. Different pre-processing techniques are also used to remove noise, shadow and illumination. A threshold is set to get the desired foreground image.

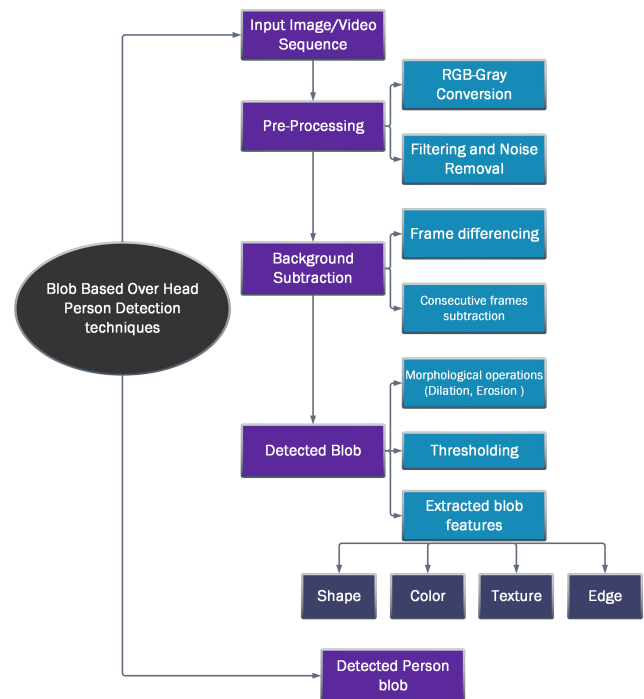


Fig. 3. Blob based Person Detection.

From the foreground image the blob is extracted which is further classified into categories like, a single person, number of the person or another object, etc. The classification is based on the shape, color, motion or other feature of the blob. The review of the techniques which detect a person from top view using blob and background subtraction based techniques is as follows:

Cohan et al. [19] and other studied out in this paper adopted a basic background subtraction and segmentation method to detect the person in overhead images. Table I illustrates that majority of the researcher adopted background subtraction and segmentation based methods to detect the individual in the overhead image and video sequences. In pre-processing, morphological operators including erosion and dilation are typically used by mainstream researchers to detect the required blob. For noise removing Gaussian and median filter methods have been used as revealed in Table I Connected component labeling method for blob extraction is used by [2], [20], [18] and [13] shown in Fig. 4. By examining Table I it can be clearly stated that after background subtraction maximum of the researchers used the extracted blob information to detect the person. The basic features of blob including shape, color, edges and size are considered.



Fig. 4. Connected Component Labeling Method used by [2], [18] and [13].

The blob shape feature is used by majority of the researchers as shown in Table I. Zhang et al. [7] considered the cylindrical shape blob to detect individual body in images. The author in [8] used the blob shape information to reconstruct the hemi ellipsoid head model of the person with the help of image stitching seen in Fig. 5(a). Ozturk et al. [21] used the elliptical shape blob to detect the person in input images (Fig. 5(b)).

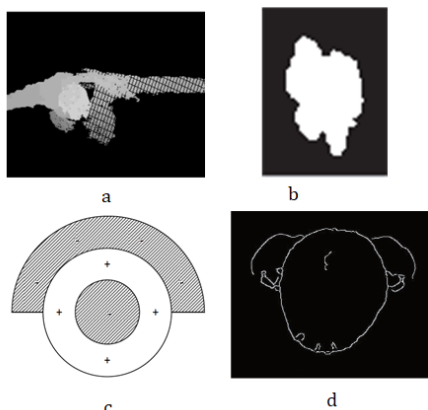


Fig. 5. Images of some shape based features [8], [21] used elliptical based shape, [16] two spherical bounds to detect the person.

Similarly [22] used Hough circle to detect the spherical blob in the image Fig. 5(c). The blobs are further divided into two sub-spherical bounds with a same central point. Inner spherical was used to detect a person head while the outer one was used to detect the head shoulder of the person as shown in Fig. 5(c). Nakatani et al. [16] used the shape information of hair whorl shape to detect the person in overhead images shown in Fig. 5(d).

Moreover blob color information is also considered by the researchers e.g. Cohan et al. [19] used color information to detect the human in topview images. Similarly, [17], [23], [16], [21], [24] also used color information to detect the person in overhead images.

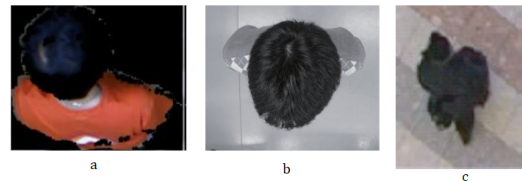


Fig. 6. Color information used by some of the discussed used by some of the authors a [23], b[16], c[21].

As seen in Fig. 7 some of the researchers [25], [7], [16], [21], [9] & [26] took advantage of the edge information of the blob to detect the person. Ozturk et al. [21] and Garcia et al. [9] used the Sobel edge method while Mukherjee et al. [26] used canny edge methods for detecting the person in overhead images as shown in Fig. 7(a), Fig. 7(b) and Fig. 7(c), respectively.

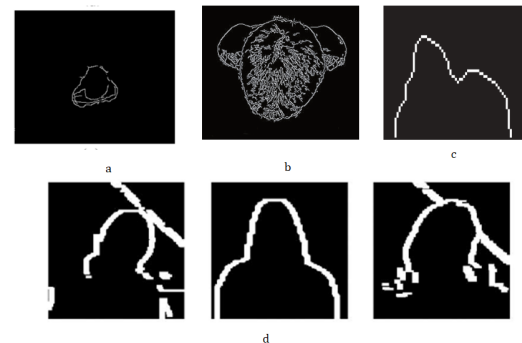


Fig. 7. Sobel edge detector used by [21] and [9], Canny Edge detector [26].

The texture information is also a significant factor, some of the work discussed in this paper also used texture feature to detect the person for example Cohan et al. [19], Chia et al. and Nakatani [16] used hair texture information to detect the person head in overhead images as shown in Fig. 8 below.



Fig. 8. Hair texture information used by [16] [24].

It can be seen from Table I that to detect the person in overhead images there exists a variation in region of interest ROI. Some of the researchers assumed the person head while others considered head-shoulder as ROI to detect the person. Few of them also considered whole overhead person body as ROI for detection. Some examples of considered ROI used by some of the researchers discussed in this paper has been depicted in Fig. 9. In first Row researcher [16], [9] considered Head as ROI. In the second row some [27], [25], [23] & [18] considered Head-shoulders as ROI. Some of them are discussed in this paper [1], [27], [21]& [28] also considered whole overhead body as ROI.

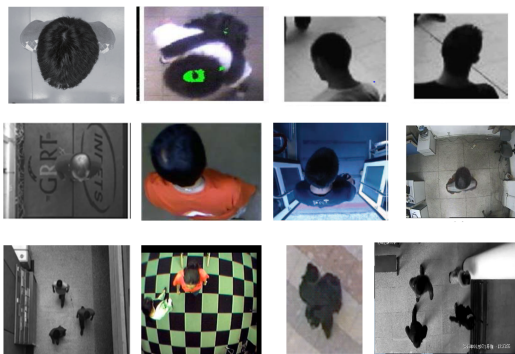


Fig. 9. The First Row shows Head as ROI [16], [9] the second row whose Head-shoulder [27],[25],[23] & [18] as ROI while the third in third row [1],[27],[21]& [28] whole overhead body has been considered as ROI, respectively.

Table I demonstrate that most of the researchers except [12], [16], [22], [22], [8] & [19] used overhead background subtraction methods for people counting. Authors in [25], [29], [28] & [18] have taken account of virtual lines for counting people in top-view images as shown in Fig. 10 below.

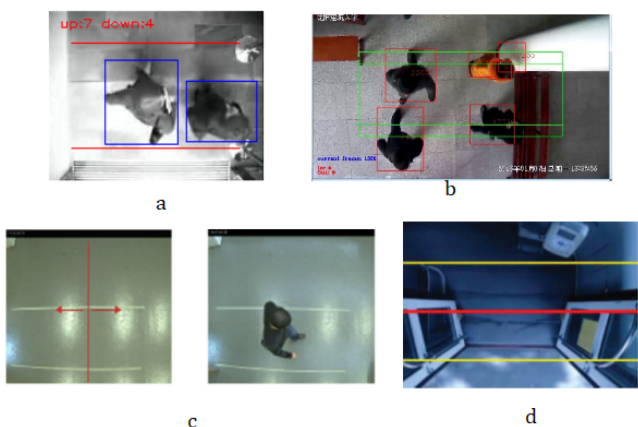


Fig. 10. Virtual lines used for person counting e.g (a) [25] (b) [28] (c) [29] & [18].

In the surveillance system, overhead person detection methods along with tracking has also been developed. For tracking the person, overhead images and video sequences has been considered. For tracking purposes different tracking algorithms are adopted as reflected in Table I.

Authors in [17], [1], [9], [4], & [23] used the Kalman filter whereas [8],[17], [24], [21], & [20] used a particle filter to track the person. Vera et al. [2] used Hungarian algorithm for person tracking. Moreover [24] used median filter and Velipasalar [27] considered mean shift algorithm for tracking. Burbano et al. [6] uses graph structuring based method for tracking people. Some of the examples of different tracking algorithm has been shown in Fig. 11.

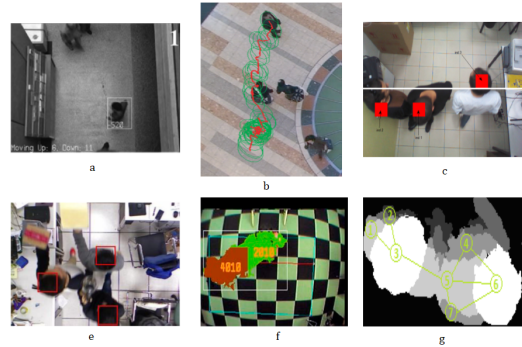


Fig. 11. Results of Different tracking algorithms used by authors discussed in this paper (a) Kalman filter [17], (b,c,d) particle filter [21], [17] [20] and (e) [27] uses mean shift tracking algorithm, (f) [6].

Majority of the work considered for this paper, used depth information to detect the person in images as depicted by Table I and Fig. 12. Few of them also considered RGB images. Authors in [17] and [21] have taken account of HSV model while only [12] used YCbCr model to detect the person in overhead images as shown in Fig. 12. For recording purposes, multiple researchers used variety of recording devices and sensors.

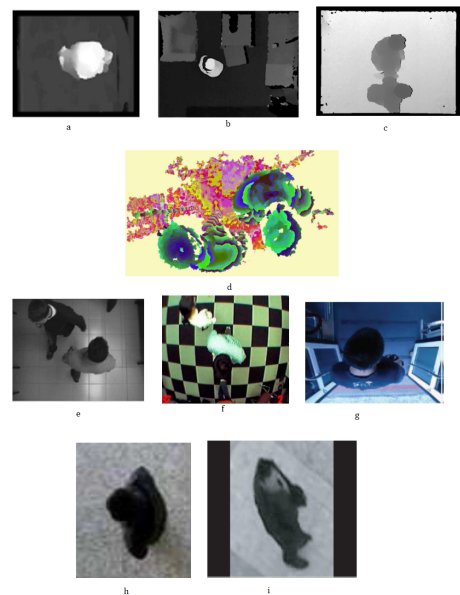


Fig. 12. First Row shows the example of depth images, (d)[30], third row contains images of RGB color space while last row include YCbCr [12]and HSV [21] color model, respectively.

TABLE I. BLOB BASED OVERHEAD PERSON DETECTION TECHNIQUES

S.No	Ref	Year	Purpose	Methodology	Field of View	Region of Interest	Color Space	Data Set	Number of Images/Videos
1	[19]	2000	Detection, Identification	BS, Segmentation, Gaussian Probability, Blob Color/Texture Features, Hair(Color, Texture), DTC, Bayesian Network	Narrow	Head	Gray	Indoor images, Low Resolution,	720
2	[17]	2005	Detection, Counting, Tracking	BS, Segmentation, Blob shape and color features, RGB-Gray conversion, Blob statistical features, Kalman Filter	Narrow	Overhead Body	RGB and HSV	Indoor images, 384 × 288	13138
3	[1]	2008	Detection, Counting, Tracking	BS, Segmentation, Binary Image Conversion, Morphological (Opening), Kalman Filter	Narrow	Head-Shoulder	Depth	Indoor	150 Sequences
4	[27]	2006	Detection, Counting	BS, Blob Statistical Features (Mean & Standard Deviation), Mean Shift Tracking Algorithm	Narrow	Overhead Body	RGB	Indoor, 320 × 240	6 Video Sequences (3-5 min)
5	[25]	2008	Detection, Counting	BS, Foreground Background Edge Model, RGB-Gray conversion, Canny edge detector, Bounding Box, Virtual lines for counting, Tracking (Mass Center)	Narrow	Overhead Body	RGB	Indoor, 320 × 240, 640 × 480	Multiple Video clips
6	[7]	2008	Detection, Counting	BS, Frame Differencing, blob based 3D human cylindrical model(Head, torso, leg) Camera Calibration, Matching Score(size, shape, visibility)	Narrow	Overhead Body	RGB	Indoor, Multiple Sensor Based Cameras , 320 × 240	38 hrs video clip 50fps
7	[12]	2012	Detection, Behaviour Understanding	BS, GMM, Geometric transformation, Hu moments, Behaviour feature (squat, stand, standing)	Narrow	Overhead body	YCbCr	Indoor images	300(100 sample of each posture)
8	[23]	2013	Detection, Counting	BS, segmentation, GMM, Blob color features, U-Disparity, Kalman & particle filter	Narrow	Head	RGB, Depth	Indoor RGB and Depth images	Video sequences
9	[8]	2014	Detection, Tracking	BS, Graph based segmentation, Image stitching, Head hemiellipsoid model, geodesic model distance map, particle tracking filter	Narrow	Head-shoulder	RGB, Depth	Indoor images	888
10	[16]	2012	Detection, Identification	BS, Shadow & Noise removal, Blob features (size, color), Hair (color, whorl)	Narrow	Head	Gray	Indoor images, 400 × 500	240

S.No	Ref	Year	Purpose	Methodology	Field of View	Region of Interest	Color Space	Data Set	Number of Images/Videos
11	[21]	2009	Detection, Tracking	BS, Blob shape features (Elliptical), Blob(color, orientation), Sobel edge detection, Morphological(opening), Median & particle filter	Narrow	Overhead	HSV	Indoor, 1440 × 1080 HD, Human Model(70 × 90)	Video clips
12	[9]	2011	Detection, Counting, Tracking	BS, Segmentation, Blob Shape, Gaussian Distribution, Morphological, Blob separation, Connected component labeling	Narrow	Head-Shoulder	RGB, Depth	Indoor RGB, Depth, Color images	Video clip (292 frames)
13	[2]	2016	Detection, Counting	BS, Segmentation, Blob Shape, Morphological(Filling), Camera Calibration, hungarian Tracking Algorithm	Narrow	Head	Depth, RGB	Indoor RGB & Depth images, 240 × 320	2384
14	[31]	2016	Detection, Counting	BS, Gaussian Smoothing, Virtual line	Narrow	Head	RGB, Depth	Indoor and Outdoor, 640 × 480, 320 × 240, 160 × 120	Video Sequences
15	[32]	2017	Detection	BS, Connected component morphological(opening), Blob(split merge)	Narrow	Overhead body	RGB, Depth	Indoor and outdoor images 640 × 480	Indoor = 33599 , Outdoor = 37799
16	[33]	2018	Detection, Counting	BS, Gaussian filter, MOG, ROC	Narrow	Overhead	RGB, Depth	Indoor images	4500 Sequences
17	[20]	2018	Detection, Counting, Tracking	BS, Depth images subtraction, Gaussian Filter, particle Filter	Narrow	Head-shoulder	Depth	Indoor images	
18	[26]	2011	Detection, Counting	Segmentation, Consecutive frame differencing, Aspatio-temporal background subtraction AMBS, Blob (shape,edge) features, Hough Circle, Canny edge detector, Optical flow(tracking)	Narrow	Head	RGB	Indoor, 480 × 640	Video Sequences (2000 & 5000) samples
19	[34]	2010	Detection, Counting	BS, Segmentation, Blob features(shape, size, velocity, orientation) extraction,spatial temporal map, linear regression model,optical flow	Narrow	Overhead body	RGB	Indoor&Outdoor 640 × 240&240 × 320	Video Sequences (30 min 25fps & 2hr 30fps)
20	[9]	2013	Detection, Counting, Tracking	BS, Segmentation, Equalized difference image, Dilation, Erosion, Circular patterns, Sobel Edge Detector, Kalman Filter	Narrow	Head	Gray	Indoor, 320 × 240	Video Sequence
21	[9]	2013	Detection, Counting	BS, For ground Extraction, Segmentation, Kalman Filter	Narrow	Head	RGB	Indoor	-

S.NO	Ref	Year	Purpose	Methodology	Field of View	Region of Interest	Color Space	Data Set	Number of Images/Videos
22	[35]	2014	Detection, Tracking	BS, MOG, Forgound Mask, Erode, Dilate, contour threshold	Narrow	Overhead body	RGB, YUV	Indoor 320 × 240	Video sequences
23	[5]	2014	Detection, Counting	BS, Segmentation, Head candidate detection, Local maxima detection	Narrow	Head	Depth	Indoor 640 × 480	500 images
24	[6]	2015	Detection, Counting, Tracking	BS, Light weight segmentation, Estimation of relative position & orientation, Blob size features, graph structure representation, camera calibration	Narrow	Head-shoulder	Depth	Indoor 640 × 480	
25	[14]	2015	Detection, Counting	Color Based BS, Segmentation, Morphological Operations (Dilation, Erosion), Local Minima estimation, Blob grouping	Narrow	Head-shoulder, torso, leg	Color Depth	Indoor	268 images
26	[28]	2016	Detection, Counting	BS, Forgound extraction, Blob merge-split, Gaussian model for noise removal, counting zone	Narrow	Overhead Body	RGB	Indoor 1080 × 720	HD Video Sequence
27	[4]	2016	Detection, Counting	Adaptive background model, Segmentation, Reconstruction of 3D points, Kalman Filter	Narrow	Body	Depth	Outdoor Thermal Images 640 × 480	Two Five min videos
28	[24]	2016	Detection, Counting	Color based BS, Water Filling, GMM, Detected Regions Shape, Color gradient model, Median filter	Narrow	Overhead body	Depth	Indoor	11890 images
29	[18]	2016	Detection, Counting	BS, Frame differencing, Morphological operations(Dilation, Erosion), Connected component labeling, Counting zone, Virtual line, Euclidean Distance	Narrow		Overhead Body RGB	Indoor 320 × 240	Video 30fps
30	[13]	2016	Detection, Action recognition	BS, Segmentation, Forgound extraction, Connected component labeling, Action recognition (sitting down, standing up, lying down, waking up, bending and falling on)	Narrow	Overhead Body	Depth	Indoor	Video sequence

B. Feature based Techniques

In recent decades, with the advancement of computer vision and machine learning, various feature based techniques gained importance due to their robustness and efficient detection accuracy. Some of the feature based techniques considered for overhead view person detection has been highlighted in Table II. The general frame work of feature based person detection is shown in Fig. 13 below.

These techniques operate on features extracted from overhead view videos and images. The extracted features are further used to classify person and non-person images. The extracted features contain shape (in the form of contours, edges, corners or other descriptors), color and texture (of hair or clothes), direction, orientation or motion information and sometimes combinations of these. Some used features based algorithms including SIFT and HOG algorithms to detect person in overhead view images as reflected in Table II. The images are often divided into samples for training and testing. These samples are further fed into machine learning classifiers i.e. SVM, adaboost, KNN.

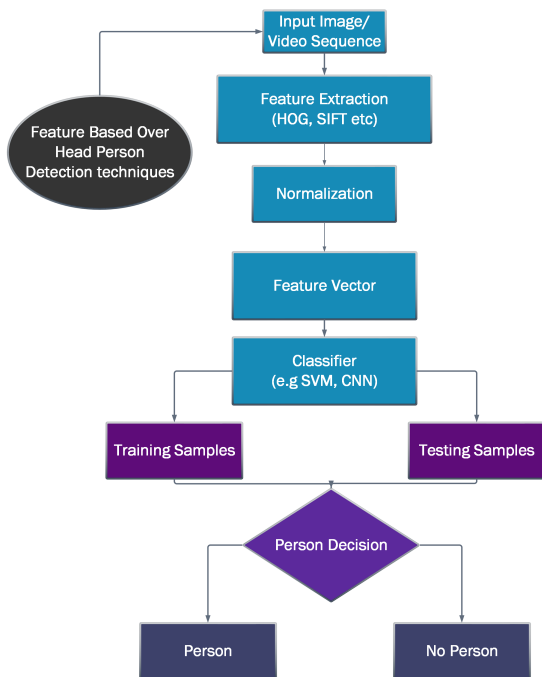


Fig. 13. General Frame Work of Feature based Person Detection.

One of the attractive, preferred and widely used feature based algorithm for person detection is Histogram of Oriented Gradient [36]. This feature based method counts occurrences of gradient orientation localized in image portion. For overhead person detection, Pang et al. in [37] proposed efficient HoG based features detection method for human detection as shown in Fig. 14. Pang et al. [38] proposed another human feature extraction technique using both top view images. The proposed method mainly focused on co-occurrence histograms of oriented gradients of HOG-based human detection method. Rauter et al. [11] proposed a method based on local ternary patterns features for human detection and tracking. The main features used for training SVM was human head and shoulder.

Ahmed et al. [15] used Rotated-HoG algorithm in

overhead images in industrial environment as shown in Fig. 14. Another robust algorithm is proposed by Ahmed et al. [39] in which wide angle lens camera is used for capturing overhead view images of person. The proposed algorithm used bounding boxes with variable size having different orientations. Features from detected windows or bounding box images were extracted using RHOG for building a learning or training model with the help of a linear Support Vector machine. [24] also used HOG features to detect after background subtraction to detect and count the people in complex environments.

Another popular feature based algorithm is SIFT [40]. Ozturk et al. [21] used optical flow of SIFT features to observe the orientation change of person body and head. From Table II it can be clearly comprehended that SVM is the most popular classifier. To detect a person in image Table II shows that scholars used a kernel or sample called detection window (as shown in Fig. 14). The size of the detection window varies with height and width of the person. Likewise [37] used 80×120 size detection window to detect person body in overhead images. The author in [15] used variable size detection window due to the variations in the size of the person as the distance of the person form the camera increases. The author in [11] used 64×128 size detection window along with CoHOG to detect person in overhead images. The authors in [41] and [3] used various size detection windows including 4×4 , 8×8 & 12×12 and 64×96 & 96×96 to detect head-shoulder and person body in overhead images, respectively.

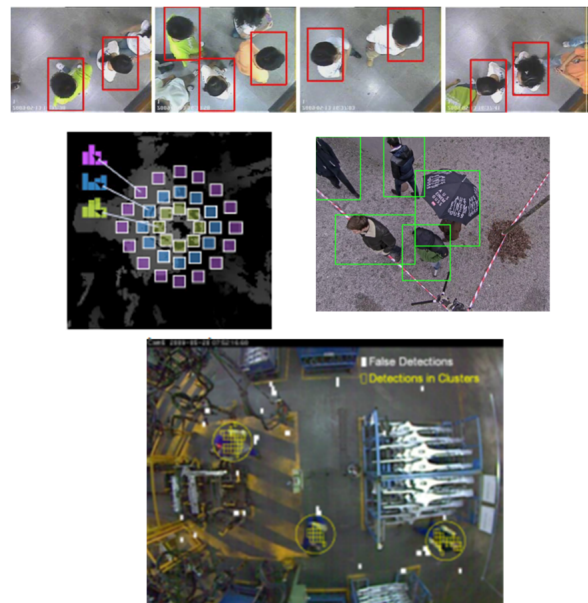


Fig. 14. Example of feature based person detection images taken from [37][41] [3], [15], respectively.

Table II shows that to reduce the feature vector after feature extraction [11] PCA has been used. To reduce feature vector size, [41] used statistical measurement, like mean and standard deviation. For normalization, non maxima suppression NMS was used which improved the performance of the proposed models. In feature based person detection techniques majority of the work consider in this chapter used Non Maxima Suppression in multiple ways (as shown in Table II).

TABLE II. FEATURE BASED OVERHEAD PERSON DETECTION TECHNIQUES

S.no	Ref	Year	Purpose	Methodology	Classifier	Field of View	Region of Interest	Color Space	Data Set	Number of Images/Videos
1	[21]	2009	Detection, Tracking	Motion Vector Detection, SIFT Optical Flow(Around head region) SOFV vector, particle filter.		Narrow	Overhead	HSV	Indoor, 1440 × 1080 HD, Human Mode(70 × 90)	Video clips
2	[37]	2011	Detection	HoG, Detection Window Size 80 × 120, Sub-cell based interpolation algorithm, Non-maximum suppression	SVM	Narrow	Overhead Body	RGB	Indoor and Semi outdoor images, 320 × 240	Almost 1000 images
3	[15]	2012	Detection	Rotated HoG, Variable Size Bounding Box, Non-maximum suppression, Disparity Check between actual and detected positions	SVM	Wide	Overhead body	RGB	Indoor, Industrial SCOVIS data set, 640 × 480	13000 images
4	[38]	2012	Detection	Co-HoG, Sliding Window, CoHOG feature vector is very large (200 000), Incremental principal component analysis (IPCA), non maximum-suppression, Detection Window: Size 64 × 128)	SVM	Narrow	Overhead body	RGB	Indoor images 320 × 240, INRIA + Overhead	6680 images
5	[11]	2013	Detection, Tracking	Depth map for local maxima Local Ternary patterns, Non-Maxima Suppression, Head trajectories	SVM	Narrow	Head-shoulder	Depth	Indoor images	30780 images
6	[24]	2016	Detection, Counting	HoG, Color gradient Model, Median filter	SVM & KNN	Narrow	Head	Depth	Indoor	15188 images & 11890 images
7	[41]	2016	Detection	SLTP and Rauter. Sliding detection window, Statistical Features 4 × 4, 8 × 8, $amd12 \times 12$	SVM	Narrow	Head-shoulder	Depth	Indoor	2382 images
8	[3]	2017	Detection	bounding box, Original Greedy Non-maxima suppression	CNN, R-CNN	Narrow	Overhead body	RGB-Depth	Indoor 800 × 600	850 images
9	[39]	2018	Detection	HoG, RHoG, Bounding box, 64 × 96, 96 × 96, Non-maxima suppression	SVM	Wide	Overhead body	RGB	Indoor SCOVIS industrial, 640 × 480	26032

To increase the accuracy and efficiency of the feature based person detection techniques. Christian Ertler et al. [3] suggested two extensions to the state of the art Faster R-CNN detection model. The RGB and depth representations were fused at different layers of the proposed model. Their experiment shows that the most eligible layer for the fusion was the mid layer.

III. DISCUSSION

The above discussion shows that most of the work done in literature is based on background subtraction techniques. Most of the researchers used simple background subtraction and segmentation methods to detect the ROI in overhead images including (person head, head shoulder and body). These techniques are effective but only on their own developed dataset. As seen in Table I that most of their researcher developed their own indoor based data set for overhead based person detection. Some of the data sets have been recorded in a constrained environment against simple backgrounds as seen in Fig. 10, Fig. 11 and Fig. 12, etc. Some detect the person in overhead images when the person lies exactly below the camera as shown in Fig. 7, Fig. 8 and Fig. 9. Mostly considered the basic blob features i.e. shape, texture, color and size information to detect the person in overhead images. The comparison of the accuracy of developed blob based techniques cannot be made as every method has been tested on their own developed data set according to environments requirement, illumination conditions and application needs.

Background subtraction based methods performed accurately but it mostly suffers from issues including gradual(day-night) and sudden illumination changes, background geometry (entrance of other objects in scene), camera related issues including (camera oscillation, noise, motion blur), shadow factors, same cloths colors as background and some time self occlusion of the own person body. Some feature based overhead person detection methods has also been discussed in this paper. Feature based methods, increases the accuracy and robustness of overhead based person detection methods. But because of the self generated data sets the accuracy of feature based method also cannot be more meaningful as they have also been recorded against simple backgrounds, low illumination condition. Some of the researcher used very complex industrial environment as shown in Fig. 14. With the recent trend of using a feature-based method to increase the efficiency of the algorithm and with the advancement of machine learning algorithms, this work can be extended and make more robust using deep learning. Feature based methods are robust but sometimes it increases the computation cost for researchers. Also, sometimes the size of feature vector is too large which creates complexity for the researchers.

In this paper, we consider methods used different recording devices for capturing topview images, some used single sensor based device e.g. Kinect, while others used multiple sensors. Majority of the researchers consider in this paper used narrow field of view as shown in Fig. 10, Fig. 11 and Fig. 12.

IV. CONCLUSION

In this paper, different overhead person detection methods found in the literature has been reviewed. Differ-

ent issues faced during topview person detection methods have also been discussed. The literature considered for this paper has been divided in to two categories based on blob and features. We have analyzed that most of the work considered for this paper is based on background subtraction and very few discussed feature based methods for overhead person detection. Different challenges and issues related to the data set are also pointed out including noise, complex and cluttered background and self occlusion. From above discussion, we concludes that overhead person detection is widely open to new research and development. The accuracy of discussed methods can not be evaluated because of self recorded datasets. The paper, also suggests new directions for future research. Some of the possible suggestion would be: The developed techniques should be implemented on same benchmark data set, most of the data set has been recorded in constrained environments and illumination conditions. Different feature based methods might be considered for future work. For feature classification advanced machine learning algorithms might be used which makes person detection more efficient and robust.

ACKNOWLEDGMENT

We are thankful to the Institute of Management Sciences and Higher Education Commission (HEC) Pakistan, funding for this research work via NRPU project under project number 5840/KPK/NRPU/RND/HEC/2016.

REFERENCES

- [1] T. Yahiaoui, C. Meurie, L. Khoudour, and F. Cabestaing, "A people counting system based on dense and close stereovision," in *International Conference on Image and Signal Processing*. Springer, 2008, pp. 59–66.
- [2] P. Vera, S. Monjaraz, and J. Salas, "Counting pedestrians with a zenithal arrangement of depth cameras," *Machine Vision and Applications*, vol. 27, no. 2, pp. 303–315, 2016.
- [3] C. Ertler, H. Posseger, M. Optiz, and H. Bischof, "Pedestrian detection in rgb-d images from an elevated viewpoint," in *22nd Computer Vision Winter Workshop*, 2017.
- [4] M. Kristoffersen, J. Dueholm, R. Gade, and T. Moeslund, "Pedestrian counting with occlusion handling using stereo thermal cameras," *Sensors*, vol. 16, no. 1, p. 62, 2016.
- [5] F. Malawski, "Top-view people counting in public transportation using kinect," *Challenges of Modern Technology*, vol. 5, 2014.
- [6] A. Burbano, S. Bouaziz, and M. Vasiliu, "3d-sensing distributed embedded system for people tracking and counting," in *2015 International Conference on Computational Science and Computational Intelligence (CSCI)*. IEEE, 2015, pp. 470–475.
- [7] Z. Zhang, P. L. Venetianer, and A. J. Lipton, "A robust human detection and tracking system using a human-model-based camera calibration," in *The Eighth International Workshop on Visual Surveillance-VS2008*, 2008.
- [8] T.-E. Tseng, A.-S. Liu, P.-H. Hsiao, C.-M. Huang, and L.-C. Fu, "Real-time people detection and tracking for indoor surveillance using multiple top-view depth cameras," in *2014 IEEE/RSJ International Conference on Intelligent Robots and Systems*. IEEE, 2014, pp. 4077–4082.
- [9] J. García, A. Gardel, I. Bravo, J. L. Lázaro, M. Martínez, and D. Rodríguez, "Directional people counter based on head tracking," *IEEE Transactions on Industrial Electronics*, vol. 60, no. 9, pp. 3991–4000, 2013.
- [10] I. Ahmed, A. Ahmad, F. Piccialli, A. K. Sangaiah, and G. Jeon, "A robust features-based person tracker for overhead views in industrial environment," *IEEE Internet of Things Journal*, vol. 5, no. 3, pp. 1598–1605, 2018.
- [11] M. Rauter, "Reliable human detection and tracking in top-view depth images," in *Proceedings of the IEEE Conference on Computer Vision and Pattern Recognition Workshops*, 2013, pp. 529–534.

- [12] Q. Lin, C. Zhou, S. Wang, and X. Xu, "Human behavior understanding via top-view vision," *AASRI Procedia*, vol. 3, pp. 184–190, 2012.
- [13] T.-W. Hsu, Y.-H. Yang, T.-H. Yeh, A.-S. Liu, L.-C. Fu, and Y.-C. Zeng, "Privacy free indoor action detection system using top-view depth camera based on key-poses," in *2016 IEEE International Conference on Systems, Man, and Cybernetics (SMC)*. IEEE, 2016, pp. 004 058–004 063.
- [14] D. Ryan, S. Denman, S. Sridharan, and C. Fookes, "An evaluation of crowd counting methods, features and regression models," *Computer Vision and Image Understanding*, vol. 130, pp. 1–17, 2015.
- [15] I. Ahmed and J. N. Carter, "A robust person detector for overhead views," in *Proceedings of the 21st International Conference on Pattern Recognition (ICPR2012)*. IEEE, 2012, pp. 1483–1486.
- [16] R. Nakatani, D. Kouno, K. Shimada, and T. Endo, "A person identification method using a top-view head image from an overhead camera," *JACIII*, vol. 16, no. 6, pp. 696–703, 2012.
- [17] L. Snidaro, C. Micheloni, and C. Chiavedale, "Video security for ambient intelligence," *IEEE Transactions on Systems, Man, and Cybernetics-Part A: Systems and Humans*, vol. 35, no. 1, pp. 133–144, 2005.
- [18] J.-W. Perng, T.-Y. Wang, Y.-W. Hsu, and B.-F. Wu, "The design and implementation of a vision-based people counting system in buses," in *2016 International Conference on System Science and Engineering (ICSSE)*. IEEE, 2016, pp. 1–3.
- [19] I. Cohen, A. Garg, and T. S. Huang, "Vision-based overhead view person recognition," in *Proceedings 15th International Conference on Pattern Recognition. ICPR-2000*, vol. 1. IEEE, 2000, pp. 1119–1124.
- [20] R. Iguernaissi, D. Merad, and P. Drap, "People counting based on kinect depth data," in *ICPRAM*, 2018, pp. 364–370.
- [21] O. Ozturk, T. Yamasaki, and K. Aizawa, "Tracking of humans and estimation of body/head orientation from top-view single camera for visual focus of attention analysis," in *2009 IEEE 12th International Conference on Computer Vision Workshops, ICCV Workshops*. IEEE, 2009, pp. 1020–1027.
- [22] T. Van Oosterhout, S. Bakkes, B. J. Kröse *et al.*, "Head detection in stereo data for people counting and segmentation," in *VISAPP*, 2011, pp. 620–625.
- [23] C. Wateosot, N. Suvonvorn *et al.*, "Top-view based people counting using mixture of depth and color information," in *The second asian conference on information systems, ACIS*. Citeseer, 2013.
- [24] C. Gao, J. Liu, Q. Feng, and J. Lv, "People-flow counting in complex environments by combining depth and color information," *Multimedia Tools and Applications*, vol. 75, no. 15, pp. 9315–9331, 2016.
- [25] S. Yu, X. Chen, W. Sun, and D. Xie, "A robust method for detecting and counting people," in *2008 International Conference on Audio, Language and Image Processing*. IEEE, 2008, pp. 1545–1549.
- [26] S. Mukherjee, B. Saha, I. Jamal, R. Leclerc, and N. Ray, "Anovel framework for automatic passenger counting," in *2011 18th IEEE International Conference on Image Processing*. IEEE, 2011, pp. 2969–2972.
- [27] S. Velipasalar, Y.-L. Tian, and A. Hampapur, "Automatic counting of interacting people by using a single uncalibrated camera," in *2006 IEEE International Conference on Multimedia and Expo*. IEEE, 2006, pp. 1265–1268.
- [28] J. Cao, L. Sun, M. G. Odoom, F. Luan, and X. Song, "Counting people by using a single camera without calibration," in *2016 Chinese Control and Decision Conference (CCDC)*. IEEE, 2016, pp. 2048–2051.
- [29] L. Del Pizzo, P. Foggia, A. Greco, G. Percannella, and M. Vento, "A versatile and effective method for counting people on either rgb or depth overhead cameras," in *Multimedia & Expo Workshops (ICMEW), 2015 IEEE International Conference on*. IEEE, 2015, pp. 1–6.
- [30] J. Nalepa, J. Szymanek, and M. Kawulok, "Real-time people counting from depth images," in *International Conference: Beyond Databases, Architectures and Structures*. Springer, 2015, pp. 387–397.
- [31] L. Del Pizzo, P. Foggia, A. Greco, G. Percannella, and M. Vento, "Counting people by rgb or depth overhead cameras," *Pattern Recognition Letters*, vol. 81, pp. 41–50, 2016.
- [32] V. Carletti, L. Del Pizzo, G. Percannella, and M. Vento, "An efficient and effective method for people detection from top-view depth cameras," in *2017 14th IEEE International Conference on Advanced Video and Signal Based Surveillance (AVSS)*. IEEE, 2017, pp. 1–6.
- [33] H. Song, S. Sun, N. Akhtar, C. Zhang, J. Li, and A. Mian, "Benchmark data and method for real-time people counting in cluttered scenes using depth sensors," *arXiv preprint arXiv:1804.04339*, 2018.
- [34] Y. Benabbas, N. Ihaddadene, T. Yahiaoui, T. Urruty, and C. Djeraba, "Spatio-temporal optical flow analysis for people counting," in *2010 7th IEEE International Conference on Advanced Video and Signal Based Surveillance*. IEEE, 2010, pp. 212–217.
- [35] L. Maddalena, A. Petrosino, and F. Russo, "People counting by learning their appearance in a multi-view camera environment," *Pattern Recognition Letters*, vol. 36, pp. 125–134, 2014.
- [36] N. Dalal and B. Triggs, "Histograms of oriented gradients for human detection," in *international Conference on computer vision & Pattern Recognition (CVPR'05)*, vol. 1. IEEE Computer Society, 2005, pp. 886–893.
- [37] Y. Pang, Y. Yuan, X. Li, and J. Pan, "Efficient hog human detection," *Signal Processing*, vol. 91, no. 4, pp. 773–781, 2011.
- [38] Y. Pang, H. Yan, Y. Yuan, and K. Wang, "Robust cohog feature extraction in human-centered image/video management system," *IEEE Transactions on Systems, Man, and Cybernetics, Part B (Cybernetics)*, vol. 42, no. 2, pp. 458–468, 2012.
- [39] I. Ahmed and A. Adnan, "A robust algorithm for detecting people in overhead views," *Cluster Computing*, pp. 1–22, 2017.
- [40] D. G. Lowe, "Object recognition from local scale-invariant features," in *iccv*. Ieee, 1999, p. 1150.
- [41] T.-W. Choi, D.-H. Kim, and K.-H. Kim, "Human detection in top-view depth image," *Contemporary Engineering Sciences*, vol. 9, no. 11, pp. 547–552, 2016.

Towards a Context-Dependent Approach for Evaluating Data Quality Cost

Meryam Belhiah¹, Bouchaïb Bounabat²
AL QualSADI Team-ENSIAS, Rabat IT Center
Mohammed V University in Rabat, Rabat, Morocco

Abstract—Data-related expertise is a central and determining factor in the success of many organizations. Big Tech companies have developed an operational environment that extracts benefit from collected data to increase the efficiency and effectiveness of daily operations and services offered. However, in a complex economic environment, with transparent accounting and financial management, it is not possible to solve data quality issues with “dollars” without justifications and measurable indicators beforehand. The overall goal is not to improve data quality by any means, but to plan cost-effective data quality projects that benefit the organization. This knowledge is particularly relevant for organizations with little or no experience in the field of data quality assessment and improvement. Indeed, it is important that the costs and benefits associated with data quality are explicit and above all, quantifiable for both business managers and IT analysts. Organizations must also evaluate the different scenarios related to the implementation of data quality projects. The optimal scenario must provide the best financial and business value and meet the specifications in terms of time, resources and cost. The approach presented in this paper is an evaluation-oriented approach. For data quality projects, it evaluates the positive impact on the organization’s financial and business objectives, which could be linked to the positive value of quality improvement and the implementation complexity, which could be coupled with the costs of quality improvement. This paper tries also to translate empirically the implementation complexity to costs expressed in monetary terms.

Keywords—Data quality improvement project; cost of data quality; data quality assessment and improvement; cost/benefit analysis

I. INTRODUCTION

Repositioning into a data-driven organization, or at least turning the data available into a real asset [1], inevitably imposes the need to improve their quality. Indeed, organizations tend to depend on their data to make informed decisions. In addition, quality customer data is the most essential component of a CRM. It is also worth mentioning the various innovative uses of information for increasing operational efficiency, offering better products and services, reducing costs and controlling risks. Research in the area of data quality has shown that non-quality absorbs a considerable margin of an organization’s revenue. In the United States and at the end of FY 2012, The Postal Service estimated the cost of processing addressed and undelivered mail at \$ 1.5 billion [2]. A report published in 2011 by Gartner reveals that approximately 40% of the value anticipated by business initiatives is not achieved due to poor data quality. Indeed, the

latter affects operational efficiency, productivity, decision-making and downstream analysis [3].

A plethora of research in the academic and industrial spheres provides approaches to measuring the costs of poor data quality as well as the financial value of the improvement initiatives. However, generic and tangible metrics, based on a cost-benefit analysis, which can be adopted by organizations operating in diverse contexts, are lacking. The work presented in this paper tries to evaluate the business value of data quality projects, using a cost-benefit analysis. This approach can assist beneficiary organizations in determining the optimal investment to be allocated to data quality improvement projects. This paper tries also to translate empirically the implementation complexity to costs, expressed in monetary terms.

The organization of this paper is addressed as follows: Section II presents data quality definitions and dimensions. Section III summarizes the literature in both academic and industrial area that is focused on measuring the business and financial value of data quality. Sections IV and V describe the main steps of our approach. In Section VI, the conclusions and future work are summarized.

II. DATA QUALITY: DEFINITIONS AND DIMENSIONS

A. Data Quality Definitions

Data Quality is largely conceived as a multidimensional concept. It is commonly defined as “the degree to which information meets the requirements and expectations of all stakeholders who need it to execute their process” [4]. This concept is echoed by the expression “Fitness for use” [5] [6].

Particular attention is given to the context in which the data quality is considered, since it cannot be evaluated and analyzed independently of the environment of the organization in question. The environment refers to the direct environment of the organization, namely: its customers, competitors, suppliers, etc. as well as its macro environment: technological, geopolitical, economic, social, legal, etc.

The data is created or collected, stored and manipulated by the Information System through the various business processes deployed. Given the variety of fields of application, the heterogeneity of information systems and the increasing volume of available data (social networks, open data, data retrieved from connected objects, etc.), various data quality issues have emerged.

B. Data Quality Dimensions

Data quality dimensions describe an aspect of the data that can be measured and evaluated against a reference quality level in order to characterize the current level of quality.

Initially, researchers identified 179 attributes of data quality [3]. As it is a high number of dimensions to work with, advanced statistical methods have been applied to reduce the number of dimensions, in a consequent way, to 15, broken down into four categories [4]; which are: (i) intrinsic, (ii) contextual, (iii) representation, and (iv) accessibility.

Intrinsic dimensions describe how the data has a quality in itself; in other words, the way in which data must be accurate, credible, objective and reputable. The contextual dimensions underline the requirement that the quality of the data must be taken into account in the context of the task at hand. The final categories, the representation and accessibility dimensions, emphasize the role of systems and tools to facilitate interactions between users and data.

In general, data quality dimensions are categories used to characterize the data and their fitness for use. These make it possible to characterize the current state of quality and to communicate around the desired state.

In concrete terms, this qualification makes it possible to:

- Act as a reference framework and guide to quality standards;
- Act as an instrument for segmenting efforts to improve DQ;
- Match the dimensions of the DQ with the needs of the organization;
- Prioritize improvement scenarios of the DQ.

In an economic context where financial resources are scarce, the goal is not to achieve superior data quality regardless of cost. Indeed, in addition to the characterization of quality levels, it is important to integrate the cost dimension into any strategy that aims at the improvement of data quality. This approach intends to give value to data quality initiative in monetary terms. As such, the problem of quality improvement is approached both efficiently and effectively.

III. MEASURING THE BUSINESS VALUE OF DATA QUALITY

One of the most important topics of data quality management is how to define and measure the value of the data. This section presents an overview of the work of leading experts, in both industry and academia, on how data closes or produces value.

A. Research in the Field of Industry

In “*Data Quality for the Information Age*”, Thomas Redman identifies several ways in which poor data quality affects an organization's bottom line. These include: customer attrition, incidental cost induction, decreased employee satisfaction, negative impact on the organization's reputation, negative impact on decision-making, induction of costs related to process reengineering and the negative impact on the organization's long-term strategy, to name a few. He also

emphasizes that the production and maintenance of quality data can be a unique source of competitive advantage [7].

In “*Improving Data Warehouse and Business Information Quality: Methods for Reducing Costs and Increasing Profits*”, Larry English focuses on the high cost of poor quality data. He cites examples of direct and indirect costs caused by inaccurate and incomplete data and false and misleading information. English also provides recommendations on how to measure the costs associated with poor data quality [8].

In “*Enterprise Knowledge Management: The Data Quality Approach*”, David Loshin describes the essential and incremental costs associated with poor data quality at the operational, tactical, and strategic levels. The categories identified form a framework that can be used to identify and evaluate the costs imputed to poor quality and to the same extent, the relative benefits of a high quality level within an organization. It defines incidental costs as those that are clearly identified, but that remain difficult to measure, such as the difficulty of making decisions as well as organizational conflicts. In contrast, essential costs such as customer attrition, scrap and rework and operational delays are costs that can be estimated and measured. Loshin also presents a process for using this framework to create an aggregated dashboard that “synthesizes the cost associated with poor data quality” [9].

In “*Executing Data Quality Projects: Ten Steps to Quality Data and Trusted Information (TM)*”, Dannette McGilvray introduces several techniques for measuring the impact of data quality issues in both quantitative and qualitative terms. For this, she presents a framework to facilitate this analysis. These techniques include:

- Collection and analysis of background and examples of the impact of poor data quality on the organization;
- Creating a repository of current and future uses of data;
- Analysis of data quality issues;
- Creating a benefit versus cost matrix to understand the effects of poor data quality;
- Classification of problems in order of importance, as well as plausible solutions.

The aim of this evaluation is to build an optimal business case and to guarantee the necessary support from the management to carry out a data quality improvement project. As a result, the decision-making process for investments related to this activity is improved [10].

In “*Information quality applied: Best practices for improving business information, processes and systems*”, Larry English provides a summary of the costs associated with poor information quality [11]. He presents well known cases that have been widely publicized:

- In 1999, NASA lost the \$ 125 million *Mars Climate Orbiter* spacecraft and all the knowledge this spacecraft had to collect;
- In 2000, the United States Supreme Court discredited the vote of 4.6 million voters because of data quality issues.

English consolidated a list of poor software and data quality costs including references from more than 120 organizations, for a total of \$ 1.25 trillion. English concludes that in many industries, these costs account for 20-25% of the company's operating revenues. These costs are broken down into the costs of recovery after a process failure and corrective actions.

“DAMA Book of Knowledge” uses a similar approach to describe the value of the data in terms of the benefits derived from the use of quality data and the costs associated with the deterioration of data. DAMA recommends assessing the effects of potential changes in revenue, cost and exposure to various risks [12].

According to the statistics collected by English, as well as the categories and techniques presented by Redman, Loshin and McGilvray, the first step in improving the quality of data within an organization is to understand its value. The business value of data can be either negative, through the costs generated by the poor quality, or positive through the benefits of a high quality level. The quality of the data therefore has a direct impact on the value of the data.

Other approaches in the industrial field have also addressed this issue [3] [13].

B. Research in the Academic Field

Industrial researchers have placed particular emphasis on assessing the positive impact of improving data quality. The different approaches mentioned above propose formulas for calculating the financial benefits that would potentially result from this improvement.

In addition to the references cited above, other research work in the academic field, focused on assessing the value of the data through the analysis of costs associated with poor quality and with improving data quality [14] [15] [16]. It would also be fair to say that research in the academic sphere has paid particular attention to the definition and evaluation of costs attributable to poor data quality.

However, these approaches offer few quantifiable measures or valuations to express these costs in monetary terms, thus qualifying the importance and priority of data quality improvement initiatives.

IV. PORTFOLIO DATA QUALITY ASSESSMENT FRAMEWORK

Among the 15 dimensions of data quality, this paper focuses on the dimension of accuracy. However, it should be recalled that this methodology is reusable and transferable to other data quality dimensions.

Portfolio Data Quality Assessment Framework (PortfolioDQAF) enables the identification of the most efficient data quality improvement projects, through the suggestion of two aggregate indicators of positive impact and implementation complexity. The goal of PortfolioDQAF is to:

- Evaluate the positive impact of data quality improvement on the overall organization's business objectives;
- Evaluate the complexity of data quality improvement actions;

- Recommend, through the analysis of a proposed cost of quality model, the optimal business case for improvement.

These results will make it possible to select data quality projects, based on the benefits provided to the organization, compared to the complexity of implementation.

A. Identifying the Business Objectives

In order to understand how execution performance and quality of business processes affect an organization's success, business objectives, and results, the following key factors are considered: operational efficiency, increased revenue, improved productivity, reduced costs, improved customer satisfaction, compliance with regulatory authorities, and improved decision-making.

B. Identifying Evaluation Factors

1) *Positive impact criteria:* The positive impact factor is dividable into several criteria. These are the success factors identified in the beginning of this section, augmented by other criteria such as:

- **The transversal nature of the process** - improvement of the quality of critical data used by a transversal process has more impact compared to a vertical process;
- **The nature of the data** - the data is classified into: (i) master data; (ii) transactional data; and (iii) historical data. It can be assumed that improving the quality of master data has more impact compared to improving transactional or historical data;
- **The frequency of access to the data** - if the critical data is used several times by the process, the improvement of its quality will yield a more positive impact;
- **The completion deadline** - like other technological projects, a short completion time for the project, allows for quick results. Indeed, the extended delays may induce the demotivation of the project team, the change in the scope of the project, the evolution of the regulations, among others.

2) *Implementation complexity criteria:* Similarly, the implementation complexity factor is split into several criteria. The following criteria concern the evaluation of the complexity of improving accuracy. These criteria originate from the literature review, but also from interviews with IT managers.

The criteria considered for the improvement complexity are:

- **Risk level** - a high level of risk is proportional to a considerable level of implementation complexity. Risks can include data loss, shutdown, systemic risks, chain reactions, and cost, delays, allocated resources overruns, etc.;

- **Existence of standards to validate data** - the existence of standards for verifying and validating data reduces the complexity of detecting erroneous values;
- **Existence of a data repository** - the existence of a reference data source, even outside the organization's IS, reduces the complexity of correcting inaccuracies at the data level, through a data-match;
- **Key identification potential** - the existence of a primary key / global identifier, that is consistent across different data sources, reduces the complexity of data cleansing, making it easy to confront and cross-check data;
- **Nature of data processing** - from a technical point of view, the accuracy improvement project may consist of automatic, semi-automatic or manual processes. Manual processing, depending on the volume of the data, corresponds to a high load and complexity;
- **Volume of data to be processed** - high data volume leads to high load and complexity.

C. Measuring Evaluation Factors

Due to the fact that each organization has specific aspects and sets of success factors, and in order to provide a generic approach that can be implemented without any adjustment, the third step of our approach introduces the context-aware and configurable weighting coefficients.

Following are few examples where using different weighting coefficients is relevant:

- Public organizations may have more concerns about increasing end-users satisfaction (citizens in this particular case), than increasing revenues;
- Healthcare actors may devote more attention to meeting regulatory driven compliance than to the other factors, while still important, owing to the fact that norms and standards are mandatory in the field of healthcare;
- Industrial companies may give the same importance to all the factors above.

1) *Setting the relative importance of the criteria:* For each criterion, a weighting coefficient is defined by the business managers, thus making it possible to express the importance of the contribution of each criterion to construct the aggregate impact factor. As cited before, the weights are specific to each organization and describe its context and strategy. Table I depicts the configuration canvas for positive impact calculation.

A similar canvas, represented by Table II, is adopted for evaluating implementation complexity. Unlike the analysis of the impact factor, the definition of the weighting factors of the implementation complexity factor is the responsibility of the IT managers.

2) *Measurement of the positive impact:* Business and IT managers, who are in charge of data quality projects, must:

- List all the key business processes;
- Configure the importance of each factor by acting on the associated weighting coefficient. The sum of all weighing coefficient must be equal to 100;
- For each factor in column 1, select the corresponding value in column 2 (each value is associated with a notation in column 3).

In the case of an organization with several key business processes, the positive impact of each process is calculated using the weighted sum formula below:

$$\sum_{i=1}^m (R_i * I_i) / \sum_{i=1}^m (I_i) \tag{1}$$

Where R_i is the rating for the factor “i” and I_i is the weighing coefficient that is associated with the factor “i”, that was previously defined by both business and IT leaders. The obtained score ranges between 0 and 5, where “0” refers to “unnoticed impact” and “5” refers to “high positive impact”.

3) *Measurement of the implementation complexity:* The implementation complexity will be calculated as follows:

$$\sum_{i=1}^m (R_i * C_i) / \sum_{i=1}^m (C_i) \tag{2}$$

TABLE I. CONFIGURATION CANVAS FOR POSITIVE IMPACT CALCULATION

Factor	Values	Rating (R)	Weighting coefficient (I)
Impact on daily operations	- True - False	1 0	
Impact on short-term business/financial objectives	- Increasing revenues	0.15	
	- Increasing productivity	0.15	
	- Reducing costs	0.15	
	- Increasing end-user satisfaction	0.15	
	- Meeting regulatory driven compliance	0.15	
- Other	0.15		
Impact on decision making	- True - False	1 0	
Impact on downstream analysis	- True - False	1 0	
Is the process cross-functional?	- True - False	1 0	
Reasonable deadline	- True - False	1 0	
Nature of Data	- Master data	4	
	- Transactional data	2	
	- Historical data	0	

TABLE II. CONFIGURATION CANVAS FOR COMPLEXITY CALCULATION

Factor	Values	Rating (R)	Weighting coefficient (IC)
Risk Level	- Severe/inacceptable - Major - Medium - Minor - Imperceptible	1 0,75 0,5 0,25 0	
Existence of standards to validate data	- False - True	1 0	
Existence of a data repository	- False - True	1 0	
Key identification potential	- False - True	0 1	
Nature of Data Processing	- Manual - Semi-automatic - Automatic	1 0.5 0.25	
Volume of Data	- Very large - Large - Medium - Minor	1 0.75 0.5 0.25	

Where R_i is the rating for the factor “i” and C_i is the weighing coefficient that is associated with the factor “i”, that was defined previously by both business and IT leaders. The obtained score ranges between 0 and 5, here where “0” refers to “minimal complexity” and “5” refers to “severe complexity”.

4) *Analysis and recommendation*: Fig. 1 depicts the main steps of the PortfolioDQAF approach:

- Identification of the key processes that contribute the most to the organization’s objectives and results;
- Measurement of the complexity of the improvement of the given objects;
- Recommendation of the optimal scenario for improving data quality.

Defining the key processes is therefore about defining who is involved in achieving the organization’s goals. These processes depend on the data needed to achieve these goals.

Fig. 1 depicts the phases of

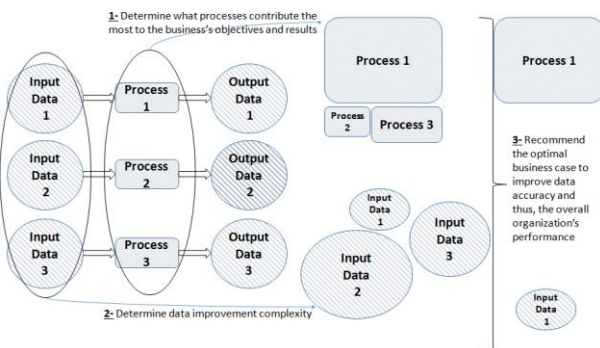


Fig. 1. Main Process [17].

The quantitative metrics of PortfolioDQAF approach correspond to the factors of positive impact and complexity of implementation. Each factor is expressed with a score, ranging from 0 to 5, corresponding to a level of impact or complexity.

The purpose of the next section is to translate empirically the implementation complexity to costs, expressed in monetary terms. Although this section does not claim to present a comprehensive cost theory, it attempts to introduce some elements that could be the starting point for a cost model for data quality.

V. TOWARDS A CONTEXT-DEPENDENT APPROACH FOR EVALUATING DATA QUALITY COST

As presented in Section IV, the objective of multi-criteria analysis of data quality improvement projects is to select a portfolio of projects, which produces the best cost-benefit ratio, according to several constraints. In this type of problem, there is uncertainty about the ROI of these projects. Non-linear programming helps to resolve the uncertain nature of this problem [18].

The classical Cost of Quality models are the PAF model (Prevention-Appraisal-Failure), which was first published by 1956 [19] and the Juran model [20]. In the context of data quality, reference books in terms of evaluation of data quality initiatives are [7] [8] [9].

Currently, the majority of models that measure the business value of data quality are developed in the context of the industry: [3] [13].

A. Definition of the Decision Problem

PortfolioDQAF approach qualifies the positive impact of data quality and its implementation complexity by quantitative indicators. It is now important to characterize the financial cost reflecting the implementation complexity.

Currently, there are little public information available that address the link between investment in terms of cost of data quality and expected quality levels, which makes this characterization difficult. It is however possible, from experience in the field of industry to make the following assumptions:

- The cost-quality curve of data would be convex;
- The improvement cost is equal to zero if the same level of data quality is maintained;
- The quality cost is exponentially high when approaching 100% accuracy. However the gradient becomes more important towards the maximum of the quality;
- The gradient would be a function of complexity.

This mathematical problem has a predictive model and the shape of the mathematical function is weakly defined.

To optimize this mathematical problem, the decision variables should be identified, as well as the constraints. The objective function is constructed from these same decision variables and constraints.

B. Definition of Decision Variables

To select projects, managers must make two independent but related choices:

- Which project portfolio can be selected for implementation? To model this decision, the following binary decision variables will be used: Y_i , where $i = 1, 2, 3$.
- Managers need to determine the optimal level of data quality that can be achieved. This variable will be characterized by the variables a_i , where $i = 1, 2, 3$.

C. Constraints Definition

In a real case scenario, this objective function would be subject to several constraints, among which:

- The sum of the costs of selected projects must not exceed the budget allocated to the data quality improvement program:

$$\sum_i Y_i * C_i \leq C \quad (3)$$

Where:

- C_i : corresponds to the cost associated with improving the accuracy of the business object I ,
- C : corresponds to the overall cost of improving data accuracy;
- Constraints on human resources allocated to projects.

D. Empirical Form of the Objective Function

The goal of managers is to minimize the costs associated with data quality improvement projects, while maximizing the expected impact of this improvement. This implies that the complexity factor composes the numerator and the positive impact factor is part of the denominator. The objective function is thus composed of:

- The positive impact factor;
- The implementation complexity factor;
- The initial accuracy of the business object;
- The target accuracy of the business object.

$$\min_i \sum Y_i * \frac{C_i * (a_i - a_{0i})}{I_i * (1 - a_i)} \quad (4)$$

Where:

- Y_i : is the binary variable that defines whether the business object i will be selected;
- C_i : refers to the complexity of implementing the business object i ;
- I_i : refers to the positive impact of the business object improvement i ;
- A_{0i} : refers to the initial accuracy of the business object i ;
- A_i : refers to the target accuracy of the business object i .

E. Identification and Resolution of Data Quality Issues

The final step in the business case consists of understanding the roots of data quality issues and how they can be addressed. Typically, this means reviewing the flow of information from the point of creation of the process-level data to detect when the error was introduced. Once the source of the data failure is identified, the data analyst can consider the alternatives to eliminate sources of errors, instituting preventive measures or corrective actions. Each of these alternatives will have an impact and will introduce a financial or other cost (organizational, risk, etc.), that can be measured, even conservatively, with the cost-benefit analysis proposed by PortfolioDQAF. The techniques in sections IV and V will prioritize actions that have an interesting cost-benefit ratio, subject to different financial and human constraints.

In addition, and with the objective of recommending the optimal scenario to improve the data accuracy and thus the overall performance of the organization, the model takes into consideration:

- The initial level of data quality (as-is);
- The positive impact of key processes that use the data to be improved;
- The complexity of implementing data quality improvement.

Depending on the values of these indicators and the target accuracy (to-be), one or more improvement scenarios should be considered.

A web platform has been developed to implement PortfolioDQAF approach and calculate the various metrics, automatically.

The main features of this application are:

- 1) Create the definition of business processes;
- 2) List all configured business processes;
- 3) Add new business objects (physically implemented by data objects), which are used by previously registered business processes;
- 4) List all registered business objects;
- 5) Evaluate data quality improvement projects.

VI. CONCLUSION AND FUTURE WORK

Data quality problems perfectly illustrate the key principle of any performance effort: "You can't control what you can't measure". This paper presents PortfolioDQAF approach, which is a metrics-based approach, to evaluate and analyze the positive impact and complexity of implementation of data quality improvement projects. This approach provides a factual basis for identifying and justifying investments in data quality. It is also a medium of communication between business managers and IT analysts. PortfolioDQAF develops a cost-benefit model, based on multi-criteria decision support analysis, to evaluate the portfolios of data quality improvement projects. It also introduces an approach to evaluate data quality cost.

It is possible to identify numerous research and future development, among which: (i) the generalization of PortfolioDQAF approach for more dimensions of data quality, in addition to accuracy. For instance, timeliness and consistency and (ii) the enrichment of the approach by an automated mechanism for reassessing cost progression as part of a continuous improvement of quality.

REFERENCES

- [1] Evans, Nina, Louis Fourie, and James Price. "Barriers to the Effective Deployment of Information Assets: The Role of the Executive Manager." *Proceedings of the European Conference on Management, Leadership & Governance*. Vol. 7. 2012.
- [2] Nixon, Ron. "Postal Service Reports Loss of \$15 Billion." *The New York Times*, *The New York Times*, 15 Nov. 2012, www.nytimes.com/2012/11/16/us/politics/postal-service-reports-a-nearly-16-billion-loss.html.
- [3] Gartner Group. *Measuring the Business Value of Data Quality*. 2011, https://www.data.com/export/sites/data/common/assets/pdf/DS_Gartner.pdf.
- [4] International Association for Information and Data Quality. 2013, <http://iaidq.org/main/glossary.shtml#I>.
- [5] Wang, Richard Y., and Diane M. Strong. "Beyond accuracy: What data quality means to data consumers." *Journal of management information systems* 12.4 (1996): 5-33.
- [6] Batini, Carlo, et al. "Methodologies for data quality assessment and improvement." *ACM computing surveys (CSUR)* 41.3 (2009): 16.
- [7] Redman, Thomas C., and A. Blanton. *Data quality for the information age*. Artech House, Inc., 1997.
- [8] English, Larry P. *Improving data warehouse and business information quality: methods for reducing costs and increasing profits*. Vol. 1. New York: Wiley, 1999.
- [9] Loshin, David. *Enterprise knowledge management: The data quality approach*. Morgan Kaufmann, 2001.
- [10] McGilvray, Danette. *Executing data quality projects: Ten steps to quality data and trusted information (TM)*. Elsevier, 2008.
- [11] English, Larry P. *Information quality applied: Best practices for improving business information, processes and systems*. Wiley Publishing, 2009.
- [12] DAMA, O. GUIA. "The DAMA guide to the data management body of knowledge." DAMA International (2012).
- [13] Laney, Douglas B. *Infonomics: how to monetize, manage, and measure information as an asset for competitive advantage*. Routledge, 2017.
- [14] Haug, Anders, Frederik Zachariassen, and Dennis Van Liempd. "The costs of poor data quality." *Journal of Industrial Engineering and Management (JIEM)* 4.2 (2011): 168-193.
- [15] Eppler, Martin, and Markus Helfert. "A classification and analysis of data quality costs." *International Conference on Information Quality*. 2004.
- [16] Kim, Won, and Byoungju Choi. "Towards Quantifying Data Quality Costs." *Journal of Object Technology* 2.4 (2003): 69-76.
- [17] Belhiah, Meryam, Mohammed Salim Benqatla, and Bouchaïb Bounabat. "Decision support system for implementing data quality projects." *International Conference on Data Management Technologies and Applications*. Springer, Cham, 2015.
- [18] Ragsdale, Cliff. *Spreadsheet modeling and decision analysis: A practical introduction to business analytics*. Nelson Education, 2014.
- [19] Feigenbaum, Armand Vallin. "Total quality-control." *Harvard business review* 34.6 (1956): 93-101.
- [20] Juran, J. M., F. M. Gryna, and R. Bingham. "Quality Control Textbook." (1975).

Towards Usability Guidelines for the Design of Effective Arabic Websites

Design Practices and Lessons Focusing on Font and Image usage

Abdallah Namoun¹

Department of Information Systems
Faculty of Computer and Information Systems
Madinah, Saudi Arabia

Ahmad B. Alkhodre²

Department of Information Technology
Faculty of Computer and Information Systems
Madinah, Saudi Arabia

Abstract—The Arabic websites constitute 1% of the web content with more than 225 million viewers and 41% Internet penetration. However, there is a lack of design guidelines related to the selection and use of appropriate font type and size and images in Arabic websites. Both text and images are vital multimedia components of websites and thereby were selected for investigation in this study. The herein paper performed an in-depth inspection of font and image design practices within 73 most visited Arabic websites in Saudi Arabia according to Alexa Internet ranking in the first quarter of 2019. Our exhaustive analysis showed discrepancies between the international design recommendations and the actual design of Arabic websites. There was a considerable variation and inconsistency in using font types and sizes between and within the Arabic websites. Arabic Droid Kufi was used mostly for styling page titles and navigation menus, whilst Tahoma was used for styling paragraphs. The font size of the Arabic text ranged from 12 to 16 pixels, which may lead to poor readability. Images were used heavily in the Arabic websites causing prolonged site loading times. Moreover, the images strongly reflected the dimensions of the Saudi culture, especially collectivism and masculinity. Current Arabic web design practices are compared against the findings from past studies about international designs and lessons aiming at ameliorating the Arabic web design are inferred.

Keywords—Arabic websites; design principles; font type; font size; readability; legibility; images; graphics; site performance

I. INTRODUCTION

There is growing evidence in the literature that web design and content significantly impact the perceived usability and acceptability of websites [1]. For instance, reference [2] stipulated that the visual appeal of websites affects users' perception of the website and that judgment is usually formed within the first 50 milliseconds of exposure. Actually, 70% of the web content is represented in the form of text or images which are considered the building blocks of any website [3]. Limited research efforts attempted to address the question of 'what is the optimal way to represent textual content and graphics within Arabic websites.

Both text typography [4] and images [5] are believed to enhance content understanding and predict user perception, acceptance and engagement. However, the factors that affect the acceptability of Arabic websites, which constitute 1% of

the web, remain unexplored. Font type and size influence reading speed and overall page appearance, whilst images and graphics impact the visual appeal of the site.

In this study, we are faced with two web design questions and research challenges. What font types and font sizes are used by major Arabic websites? Determining these typographical characteristics will assist us to understand the level of conformance to international design recommendations and best practices for web design. What types of images are used within the Arabic websites given the Saudi culture, values, and religious identity? The proverb says "a picture is worth a thousand words"; however, it is important to ensure that the images used in web design conform to the context and society where they are being introduced. Our inspection of images' characteristics will assist us in identifying the common practices within the Saudi environment.

Studies investigating the effects of fonts and images on user judgment and acceptance of Arabic websites are limited in the literature. To this end, it is crucial to first identify the common fonts and images being used by Arabic websites. This paper focuses on exploring the current practices adopted by designers for styling Arabic text with regard to the font type and size, as well as the genre of images incorporated within the Arabic websites. Such knowledge lays the foundations for further web design research.

The paper is divided into seven main sections. Section two sets the foundations of usability and web design and reviews past studies focusing on web typography and images. Section three describes the research methodology we adopted to answer the research questions. Section four presents the results of our in-depth inspection of current font and image practices. Section five discusses the findings and predicts potential implications. Section six and seven provide an outlook towards potential ways to enhance the Arabic web design.

II. PREVIOUS WORKS

A. Perceived Usability

Online companies that provide a rich user experience by accounting for website usability are more likely to succeed than those which do not [1], [6]. In other words, unusable websites drive customers away and cause them to look for alternative websites [7]. Perceived web usability is a quality

This research project is fully sponsored by the Deanship of Research, the Islamic University of Medina, KSA.

factor that refers to the empowerment of users to achieve their goals and needs by exploiting the design features of the website [6]. Perceived usability is believed to contribute towards accepting and using a particular technology; for instance, [8] demonstrated that perceived usability impacts the acceptance of educational technologies by teachers.

Perception of website usability has been linked to numerous factors including attractiveness, controllability, efficiency, learnability, and helpfulness [33]. Moreover, users' demographics are found to influence overall website perception. Further research reported a consolidated model of usability metrics and measurements [9]. This model encompassed 10 factors which are, in turn, divided into 126 metrics. The proposed quality in use integrated measurement model included efficiency, effectiveness, productivity, satisfaction, learnability, safety, trustfulness, accessibility, universality, and usefulness [9]. The readability of the text is indicated as one of the key metrics contributing to perceived usability.

B. Web Design and Content

So what actually affects web design quality and overall usability perception of customers? Research has indicated that various factors impact how users perceive and interact with online websites. Indeed, both web content and web design have been considered as critical factors leading to the success of websites and repeated customer visits [3], [1]. Author in [2] defined content as the information or services available on a particular website whilst design refers to the way this content is presented to the users. For example, [1] proposed a web usability assessment model that incorporates multiple factors such as navigation, content, and layout. Evidence in the literature confirms that when textual content is readable easily, the website receives higher usability by its viewers [10].

Authors in [10] and [11] carried out three website studies to explore the relationship between the perceived usability of websites, web design and performance. Findings showed that website success and satisfaction are highly correlated with the available content, navigational structure, interactivity, feedback, and site loading speed. Author in [7] presented an automated tool that checks the conformance of websites to design guidelines and predicts an overall website rating. The usability checks assess the quality of the web design by measuring aspects related to the text, links, graphics, as well as their formatting. However, the model neither investigated Arabic fonts nor the types of images used.

Author in [12] found that web design is a critical success factor for positive user experience and interaction on websites. Effective web design contributes towards user acceptance and empowers users to find relevant information easily in e-commerce sites. Moreover, visual appearance is found to significantly influence users' perceptions of business to consumer websites [13].

Author in [14] described a detailed framework to assess the usefulness of web content. A total of 18 content benchmarking criteria (e. g. text quality, scope, accuracy, uniqueness) were collated from existing works and expert reviews. In respect to screen appearance, the authors suggested using different

readable font sizes. Effective and easy navigational structures within a site are favored by website users than complex navigations [14].

C. Font Type and Size

Font type and font size influence the readability and legibility of text. Recent research, for instance [47], demonstrated that difficult to read fonts encourage the willingness to pay for the adventure tours. A strong link between visual attributes of travel text and intention to travel was established. In addition, [49] showed that users' judgment of memory retention will be higher as a result of increasing the font size. In smartphones, the big text was liked more than smaller text when styling brand names [50].

Author in [1] advocated using adequate font size for displaying information on websites. However, determining the appropriate font type and size for text on websites is not an easy task. In an eye-tracking experiment, [15] demonstrated through eye gaze data that the speed of online reading deteriorates in the presence of small font sizes. Only Helvetica and Georgia fonts were compared at varied sizes 10, 12, and 14 points. Surprisingly, no significant differences were detected between these sizes and between the serif and non-serif fonts in respect to reading speed.

In contrast, Serif fonts performed better than Sans Serif with respect to online readability [4] and information recall [16] whilst Sans Serif fonts were preferred over Serif fonts [4]. Font type Verdana at size 14 points ranked first amongst online readers and induced the lowest mental load.

Author in [10] carried out an experiment to compare eight famous fonts, namely Century Schoolbook, Courier New, Georgia, Times New Roman, Arial, Comic Sans MS, Tahoma, and Verdana at size 10, 12, and 14 points respectively. Although these varied sizes did not result in different reading efficiency, Times New Roman and Arial were read significantly faster than the other fonts. Moreover, font size 10 was read significantly slower than font size 12 and 14. In respect to legibility, Arial and Courier were perceived more legible than the remaining fonts. Size, however, did not seem to improve font legibility. In respect to attractiveness, Georgia was rated as the most attractive font amongst the candidate fonts. The overall ranking of fonts showed Verdana as the most preferred font, whereas Times New Roman was ranked as the least preferred font type.

In a relevant study, students aged between 10 and 12 years participated in a screen legibility experiment of Arabic characters [4]. Only two font types were investigated, mainly Arabic Traditional and Simplified Arabic in different sizes 10, 14, 16 and 18 points respectively. Results indicated that font size 16 and 18 were more readable than font size 10 and 14 by 9-12 years aged students. However, font size 10 triggered the highest number of errors. Nonetheless, [4] claim that font type did not influence the readability of the Arabic language.

For the English language, font size 10 and 12 points were found to be equally readable [10]. However, for the Arabic characters [17] suggested that text is more readable at font size 14 points. Moreover, [17] claimed that font types influence reading speed, which contradicts the findings of [4]. In fact,

author in [4] recommends using at least font size 18 point and over for efficient online reading of the Arabic text.

More recent research investigated how four fonts (i.e. Georgia, Verdana, Times New Roman, and Arial) impact online readability [18]. Verdana and Georgia were favored for computer displays while Times New Roman and Arial were favored for printed media. Reference [19] confirmed Verdana as a more suitable font type for showing English text on computerized screens.

D. Images

Author in [14] emphasized the need to use images and graphical elements to convey messages and improve the overall usability of websites. Moreover, the use of graphics enhances the aesthetics of websites and leads to user satisfaction [18]. Visual appeal was deemed as important as content for visual arts websites [3]. Graphics are known to improve the overall perceived attractiveness of websites and design considerations must be catered for different cultures [20].

Author in [21] compared three different e-commerce web designs, a website containing no human images, a website containing human images without faces, and a website containing images with human faces to explore how the use of images influence visual appeal of websites. The websites utilizing images with human faces were perceived as more appealing and trustworthy. Reference [22] emphasized the need to take cultural differences into consideration when embedding graphical components within e-commerce websites.

E. Design Guidelines

Author in [22] recommended the design of culturally sensitive websites, use of correct translation, employment of consistent colors, and minimization of animations. HHS design guidelines advised using at least font size 12 points and sticking to familiar fonts [23], [24]. For image usage, HHS design guidelines proposed to add images to the website and use images of people, but reduce their size so as not to slow down page loading. Reference [48] suggested the consideration of site loading time as a key usability metric as part of an evaluation framework of dual language websites.

F. The Research Gap

Research efforts tackling the usability of Arabic websites are limited. Some studies examined the performance of Arabic websites by inspecting the internal attributes of the HTML pages. For example, [25] compared three Arabic educational websites and reported technical issues related to the site loading speed as a direct consequence of the excessive number of HTML objects and images and their large size. Similarly, [26] inspected the number of HTML files, objects, images, CSS files, broken links and size of images on 9 websites using two specialized online tools. Other aspects reported included page loading time, HTML errors and browser compatibility.

Until today and despite the prevalence of the Arabic language on the web, there are still no systematic studies that examine the use of fonts and images on Arabic websites. This is the first research effort to review and analyze a large number of websites to identify the real practices pertaining to the usage of fonts and images on Arabic websites.

III. RESEARCH METHODOLOGY

Evaluation methods of websites' usability vary greatly in regard to the procedures, complexity, and accuracy [27]. Usability inspection is the second most used web usability evaluation method after user testing [27], [9]. In simple terms, usability inspection refers to the methods that are employed by an evaluator to inspect usability issues or features of a specific user interface [9]. In our case, we concentrate on two main design elements; firstly we inspect the quality of the typography of 73 Arabic websites and the genre of images used within these websites and secondly we verify the agreement of these design elements (i. e. typography and images) with the proposed international design guidelines. The steps of the evaluation we performed are depicted in Fig. 1.

This form of inspection is called 'perspective-based inspection' where the evaluator concentrates on particular design elements [28]. It is worthwhile to note that inspection differs from user testing for it does not involve actual users in the evaluation process. This makes it more favorable especially when the number of websites to test is large as is our case. Moreover, conducting usability inspection is still considered useful and more affordable than other evaluation techniques [29].

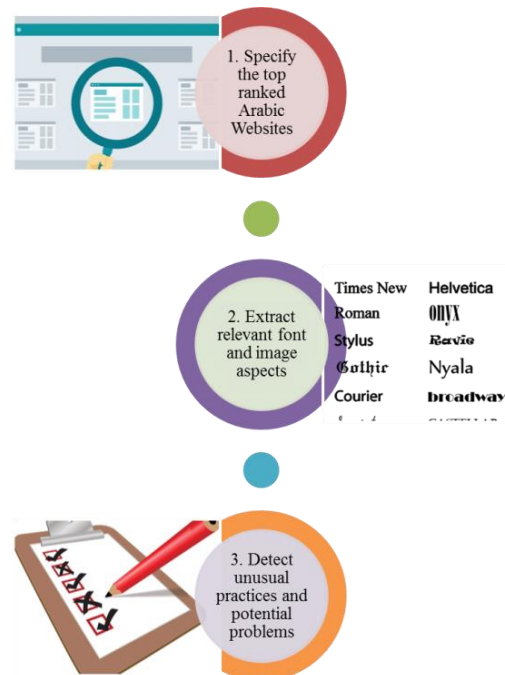


Fig. 1. Research Methodology.

IV. FONT AND IMAGE INSPECTION STUDIES

A. The Morphology of the Arabic Language

Before delving into the details of the studies conducted in this research, a brief introduction to the Arabic language is given. Arabic is one of the richest Semitic languages with more than 12 million unique words and 300 million speakers across the globe. Arabic is written from right to left. In essence, words are created from a set of 28 distinct letters, with 15 letters using dots, either above or below the letter (as depicted in Fig. 2). The Arabic letters use diacritics which create different meanings according to the context of use.

Table I demonstrates how applying well-known font types changes the look and feel and overall readability of the Arabic text. The selected fonts to showcase are the most used fonts as per our analysis below. This includes Times New Roman, Arial, Tahoma, Helvetica, Cairo, and Droid Arabic Kufi. All font types are applied to the same sentence and are sized to 8 points (~ 11 pixels).

B. Selection of the Arabic Websites

A total of 73 differing Arabic websites were selected and evaluated on several metrics with a focus on font and image characteristics as detailed below. The selected online websites for investigation were the most visited websites by users living in the Kingdom of Saudi Arabia according to the latest ranking (i.e. February 2019) of Alexa Internet [30]. Technically, Alexa ranks websites locally or globally using multiple Internet browsing and web traffic criteria, including the number of monthly unique visitors to the site, number of site views for the last three months, and average time spent viewing the website. The websites we decided to investigate were the most visited Arabic websites and included 52 local websites (71.23%) and 21 international websites (28.77%). This enabled us to learn about the font and image related design practices of both local (e. g. Souq, Alzubasher ... etc.) and international sites (e. g. Google, YouTube, Microsoft ... etc.). A selected sample of the tested Arabic websites is shown below in Fig. 3, Fig. 4, and Fig. 5.

Fig. 6 depicts the distribution of 73 top ranked Arabic websites according to their genre. Notably, Government websites were the most commonly visited websites among the Saudi population, with 14 websites. This was followed by news (13 websites), corporate (11), education (9), e-commerce (7), entertainment (5) and social media (4) websites. The remaining sites (12 websites) spread across diverse categories, such as charity, search engine, travel, and tourism, etc.

TABLE I. THE EFFECTS OF FONT TYPE ON THE READABILITY OF ARABIC TEXT

Font Type	Arabic Text (All sizes are set to 8 points, ~ 11 pixels)
Times New Roman	أثر نوع الخط على سهولة قراءة النص
Arial	أثر نوع الخط على سهولة قراءة النص
Tahoma	أثر نوع الخط على سهولة قراءة النص
Helvetica	أثر نوع الخط على سهولة قراءة النص
Cairo	أثر نوع الخط على سهولة قراءة النص
Droid Arabic Kufi	أثر نوع الخط على سهولة قراءة النص

خ	ح	ج	ث	ت	ب	أ
khah	hah	jeem	thah	teh	beh	alef
ص	ش	س	ز	ر	ذ	د
sad	sheen	seen	zain	reh	thal	dal
ق	ف	غ	ع	ظ	ط	ض
qaf	feh	ghain	ain	zah	tah	dad
ي	و	ه	ن	م	ل	ك
yeh	waw	heh	noon	meem	lam	kaf

Fig. 2. The Arabic Characters and their Pronunciation, Adopted from [34].

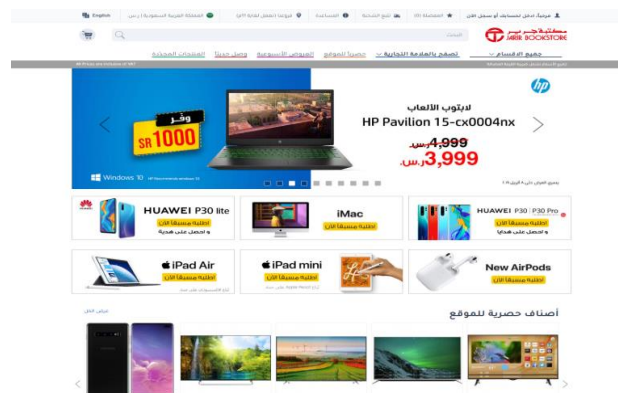


Fig. 3. Jarir Bookstore, An E-commerce Website.

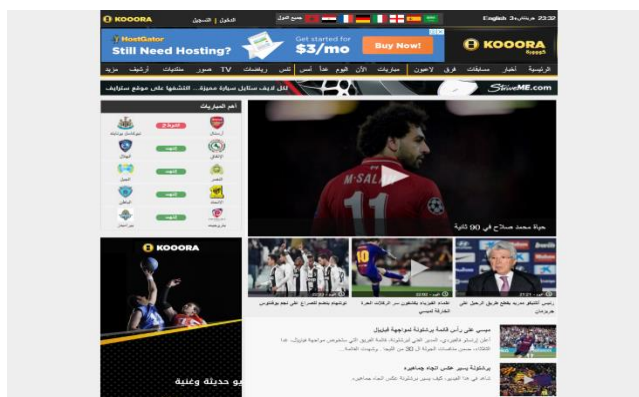


Fig. 4. Kooraa, A News Website.

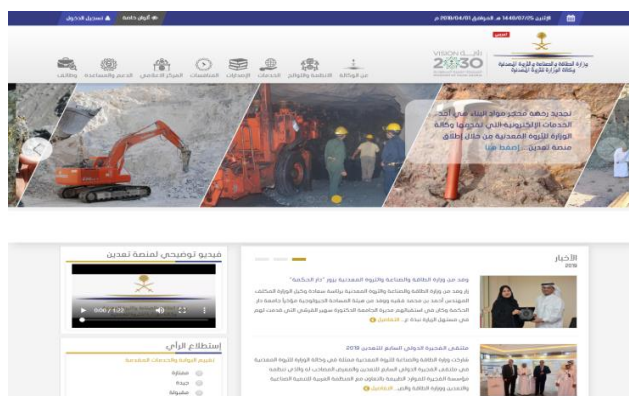


Fig. 5. Dmmr, A Government Website.

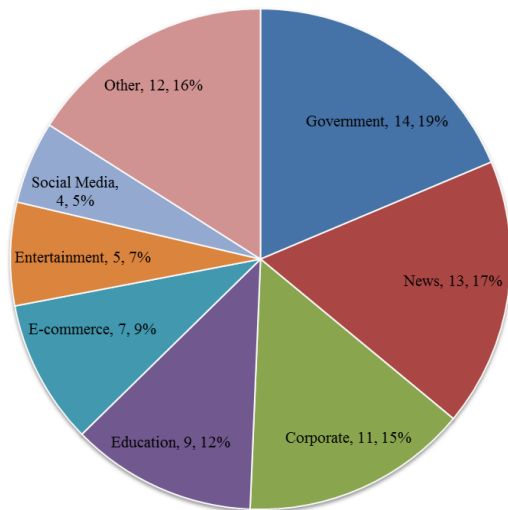


Fig. 6. The Categories of Arabic Websites Inspected and their Frequency (Labels: Site Category, Frequency, Percentage).

V. RESULTS

Our technical inspection focused on analyzing a set of characteristics that are related to font and image usage. Below we delve into the current practices of 73 top viewed Arabic websites.

A. Practices Pertaining to Font Type and Font Size

Chrome extension Font Face Ninja [31] was installed to detect and identify the fonts utilized to format the sample Arabic websites, with a particular emphasis on font aspects such as type and size (reported in pixels). In the inspection, we explored font styling pertaining to three key text elements namely, titles (or headings), navigation menus, and paragraphs.

Formatting text with a particular font size has a direct impact on the overall readability and legibility of text on computer screens. Our next analysis explored the various fonts and sizes applied to format the Arabic text. It is worth noting that approximately 40 websites (~55% of the websites) used different font types within their pages raising concerns about internal consistency.

The second observation we noticed is the large variability in the font's usage across the Arabic websites. In total, 39 different font types were utilized to style the titles of the 73 Arabic websites. The most frequent font type used for formatting titles was Droid Arabic Kufi (7 occurrences). When styling the navigation menus, 38 different font types were used, with Droid Arabic Kufi being the most frequent font. However, 35 different fonts were used to style the paragraphs of 73 Arabic websites, with Tahoma appearing more than the remaining fonts.

When font types were ordered according to their occurrence, six main types emerged as clear winners specifically; Droid Arabic Kufi, Tahoma, Arial, Cairo, Helvetica and Times New Roman (see Fig. 7). In respect to page titles and navigation menus, Droid Arabic Kufi, Tahoma and Helvetica were used more frequently. However, for styling paragraphs, Tahoma, Helvetica, Arial and Times New Roman were more dominant (see Fig. 7).

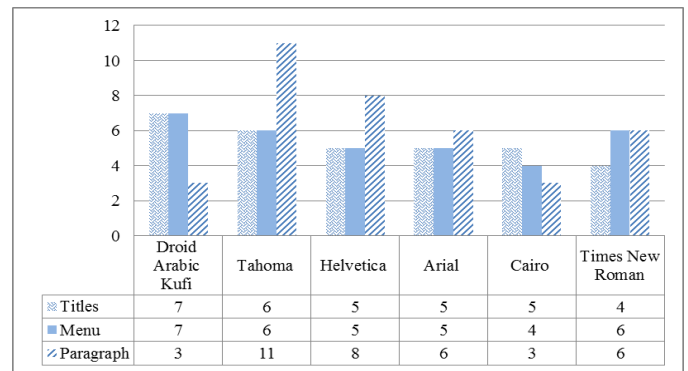


Fig. 7. The Most Frequently used Font Types in Arabic Websites.

With regard to the font size used for the titles, size 28 pixels (8 times), 24 pixels (7 times) and 30 pixels (6 times) emerged as the most recurring sizes. Due to the variability of font sizes used for styling the Arabic titles, we created a histogram with the bins ranging from 10 to 14 pixels, 15 to 19 pixels, 20 to 24 pixels, 25 to 29 pixels, 30 to 34 pixels, 35 to 40 pixels, and more than 40 pixels (see Fig. 8). The below chart shows that the majority of Arabic websites styled their titles using sizes ranging from 15 to 40 pixels. Font sizes less than 15 pixels or more than 40 pixels were scarce.

Less font size variability was identified in relation to the formatting of menus of Arabic websites. In total, only 10 font sizes were utilized in the 73 websites, with font size ranging from 11 pixels to 22 pixels. The most recurring font size for formatting navigation menus was 14 pixels (19 times ~ 26%), followed by 13 pixels font size (13 times ~ 18%) (see Fig. 9).

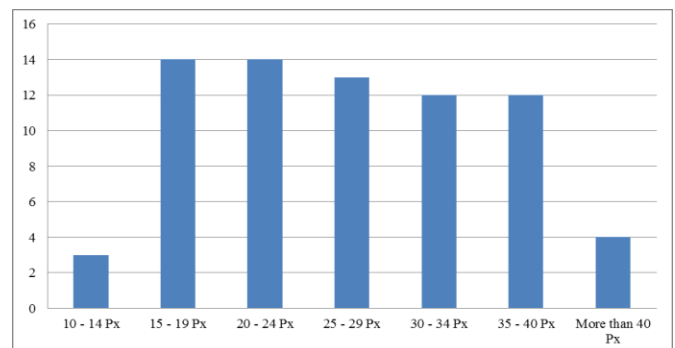


Fig. 8. The Frequency of Titles' Font Sizes (in Pixels) used in Arabic Websites.

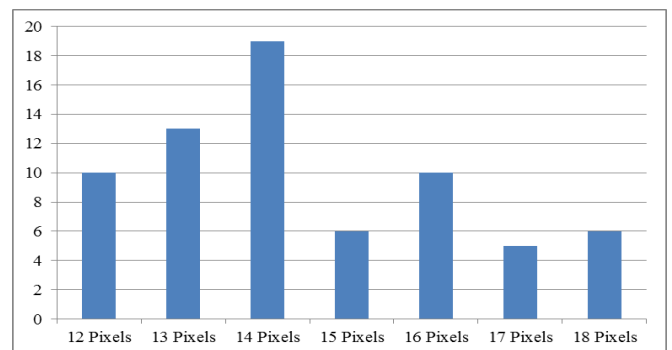


Fig. 9. The Frequency of Menu's Font Sizes (in Pixels) used in Arabic Websites.

When it came to formatting Arabic paragraphs, font size 14 pixels (~26%), 16 pixels (~19%), and 12 pixels (~18%) were more commonly used than the other sizes, as depicted in Fig. 10. Once again, 10 different font sizes, ranging from 12 to 26 pixels, were used to style the paragraphs of 73 websites. Only three websites used font sizes larger than 18 pixels to format the paragraphs.

B. Practices Pertaining to Images and Graphics

In respect to the use of images, the inspection looked into the content of the websites' images with regard to four major aspects, the use of images containing human faces, the gender portrayed in the images, the use of individuals or groups, and the conservatism or openness of the image content with respect to the Saudi values and Islamic religion.

Moreover, a technical analysis was undertaken to check the number of images incorporated in each site and their size since these aspects have a direct impact on the loading speed of the web pages. We have used website speed test [32] to gather data about several aspects of the images and learn how these images could be optimized to ameliorate the overall site performance. The results showed that all 73 Arabic websites included images. A total of 3486 images (mean= 47.75 per page) were reported and analyzed by a website speed test. These analyzed images were fetched mainly from the home pages.

The average number of images varied greatly between the site categories. News, entertainment, government and e-commerce websites used approximately 50 images or more on their home pages respectively (Fig. 11). This is an anticipated result. The average size of the images ranged between 135KB and 2900KB. Most of the Arabic websites used images greater than 1500KB in size (Fig. 12). Social media websites produced smaller sizes as the analysis focused on the home pages only.

Overall, 66 (90%) Arabic websites embedded images that contained humans and only 7 websites did not include images with humans in them (see Table II). Interestingly, the vast majority of these websites (52 websites) used images that are conservative in nature respecting the Islamic identity and cultural values of the Saudi society. Nonetheless, 14 websites used non-conservative images, for example, pictures of women wearing short clothes. These images are considered unacceptable Islamically and against the values of the Saudi culture. All non-human images were conservative in nature and did not portray things against the teachings of Islam or Saudi society.

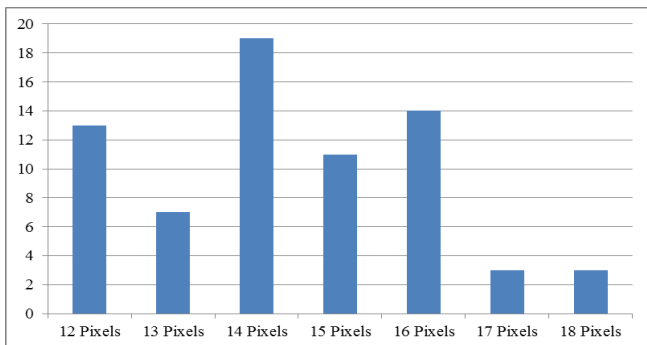


Fig. 10. The Frequency of Paragraph's Font Sizes (in Pixels) used in Arabic Websites.

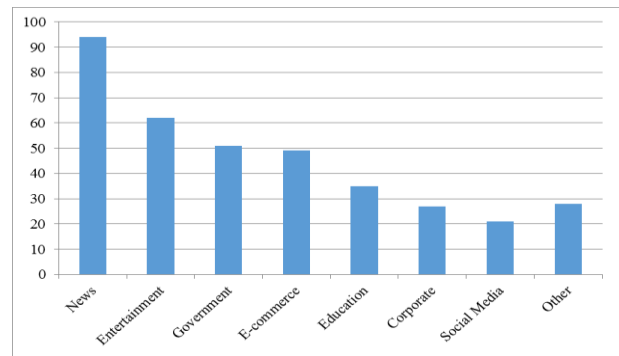


Fig. 11. Average Number of Images on Home Pages of the Arabic Websites.

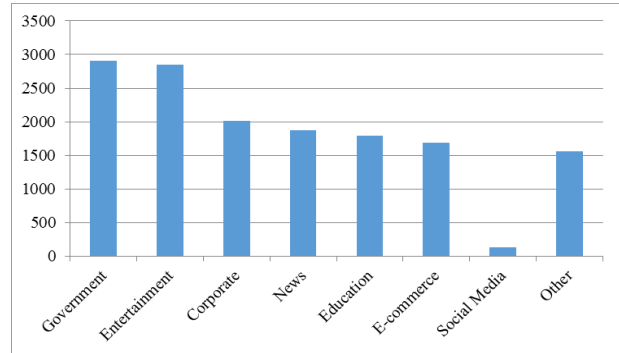


Fig. 12. Average Size of Images (in Kilobytes) on Home Pages of the Arabic Websites.

Moreover, 45 websites (out of 66) used images of men and women; this is approximately 68% of the websites including images containing humans (see Fig. 13). However, 21 websites (approximately 32%) used images of men only which shows that the masculinity in Saudi society still prevails. No website used images containing women alone.

TABLE II. THE TYPE OF IMAGES USED IN THE ARABIC WEBSITES

Type	Conservative	Open	Total
Images containing humans	52	14	66 (90.41%)
Images without humans	7	0	7 (9.58%)
	59 (80.82%)	14 (19.18%)	

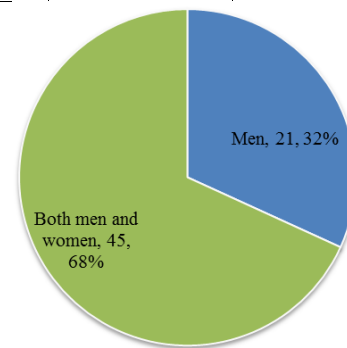


Fig. 13. The Frequency of Arabic Websites using Images Containing Men, Women or Both (Label: Gender, Frequency, Percentage).

48 Arabic websites (~72%) used a combination of images containing both individuals and groups of people (Fig. 14). This reflects the collective nature of Saudi society. In contrast, only 7 websites included pictures of individuals.

A total of 47 websites (~64%) incorporated some form of interactive animations ranging from rotating images, loading animations, to CCS animations (see Fig. 15). However, only 20 Arabic websites (~27%) incorporated videos.

C. The Performance of the Arabic Websites

We undertook a general site analysis to check the performance of the Arabic websites. To this end, GTmetrix¹ was used to collect useful data about the speed scores of the websites, the site loading time, and the total page size. The data were collected for all 73 Arabic websites and averaged per category as shown in Fig. 16 and Fig. 17. Site performance scores are rated as a relative percentage (100%) to the performance of other websites analyzed by GTmetrix in the last 30 days. Only social media and entertainment websites scored above than 70% of other sites. However, government, education, and news websites scored less than 50% of the other analyzed sites (see Fig. 16).

In respect to the site loading time, GTmetrix extracts metrics that capture the average time spent, in seconds, until the website ceases the data transfer process over the network and the onload events are launched on the designated website. The shorter this time is the better it is for the end user. Reduced loading time is also an indication of good implementation practices (e.g. fewer HTTP requests, compressed files...etc.). Author in [25] suggested that the site should take less than 3 seconds to load fully otherwise users might leave the site.

Our analysis showed that all categories took, on average, over 5 seconds to load except the social media sites (approximately 3 seconds). Social media loaded fast for they contain a low number of images on their homes pages prior to signing in. Interestingly, government, education, and news websites showed the worst performance taking 10 seconds or longer to fully load (as depicted in Fig. 17). The government websites contained large images as shown earlier in Fig. 12.

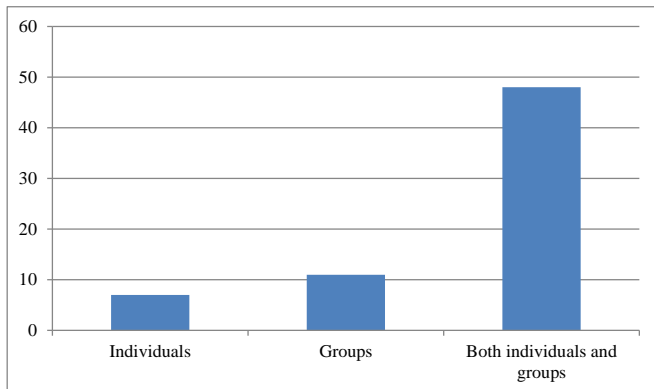


Fig. 14. The Frequency of Arabic Websites using Images Containing Individuals, Groups of People or Both.

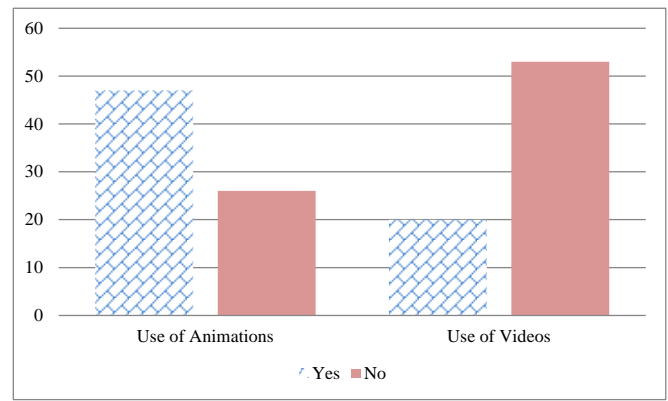


Fig. 15. The Frequency of Arabic Websites using Animations and Videos.

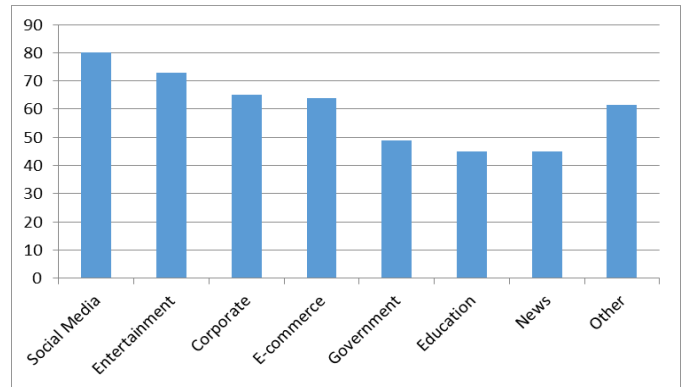


Fig. 16. Average Page Speed Score (as Percentage) per Site Category (High Scores are Better).

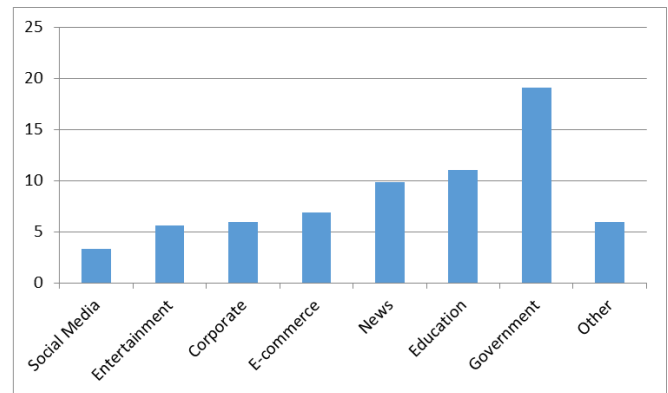


Fig. 17. Average Fully Loaded Time (in Seconds) per Site Category (More is Worse).

VI. DISCUSSION

Our comprehensive inspection of current practices concerning text formatting and image usage within the top visited Arabic websites in Saudi Arabia revealed various interesting findings. The usability inspection was performed to gather insights about the font types and sizes used to style Arabic text, especially that they could directly influence the legibility of text on websites.

¹ <https://gtmetrix.com/>

Let us review and attempt to answer the research questions posited in the introduction. What font types and font sizes are used by major Arabic websites? On the positive side, the selection of the Arabic websites included a large pool of websites, which were selected objectively by relying on Alexa Internet latest ranking. In effect, the inspection covered a total of 73 top viewed websites (52 local and 21 international) in Saudi Arabia. The websites' ranking is based on a set of metrics, primarily the average viewing time for the last three months.

Typically, a font has several characteristics including type, size, width, weight, and serifs [37], [46]. However, for the purpose of this research, we directed our focus towards two key font characteristics namely type and size. On the web, font type usually refers to the font family that represents a certain typeface, including all sizes and styles, for example, Arial and Verdana. To style a particular family type, the size of text may be increased or decreased using the font size attribute. There are different ways to resize the font including Ems (em), pixels (px), points (pt), and percent (%). In our font size analysis, we used pixels (px) as the sole measurement for the font since it is the main measurement unit for media shown on computer screens. Moreover, web designers usually use pixels as their key measurement unit for font size. Points, however, are used to measure font size for print media.

It is noted that more than half of the Arabic websites breached the principle of consistency when applying font types to the text. This means that multiple font types were used on the same web pages. Previous research, however, has already emphasized the role of consistency of user interface elements, such as font, in the overall usability of websites [35], [36]. On that basis, it is recommended that designers should adhere to the same font family to create attractive and consistent Arabic web designs.

Moreover, there was no evident consensus amongst the websites in favoring a particular font type in order to display the Arabic text. More than 35 font types were used by the selected 73 websites. There are various potential theories that could explain this staggering variability; firstly, the lack of research and thereby guidelines with respect to styling Arabic text to guide the effective design of Arabic websites; secondly, the weak conformance to international design practices and recommendations; thirdly, the lack of awareness that text formatting might ultimately impact text legibility and thereby readers' mental load and overall satisfaction.

Nonetheless, a pattern of font usage emerged within the Arabic websites; six font types recurred several times in the formatting of titles/headline, menus, and paragraphs. These font types were used differently according to the type of text element. For titles and menus, Droid Arabic Kufi, Tahoma, Helvetica, and Arial, emerged as favorites. It is no surprise that Droid Arabic Kufi came out as a winner for it is a unique font that reflects the Arabic calligraphy. This font gives a true feeling of the traditional Arabic scripts (Kufic scripts) that date back to the 7th century. For paragraphs, Tahoma, Helvetica, Arial and Times New Roman were used more frequently.

International recommendations suggest using font type Verdana since it is one of the most legible fonts as rated by

online readers of English websites [38]. Nonetheless, this font did not appear frequently in the Arabic websites that we tested. Moreover, other famous fonts that were found earlier to be legible or attractive by English readers, such as Georgia [18] and Courier [10], did not rank well in the Arabic websites. However, Arial emerged as one of the top six font types used by the Arabic websites. Previous research confirmed that font type Arial was read significantly faster and was perceived as legible [10].

Design guidelines have indicated that font size 12 points (~16 pixels) is the most suited size for displaying text on English websites [39]. This is somewhat disputable as subsequent research suggested the use of font size 14 points (~19 pixels) instead. For displaying the Arabic text, recommendations are inconclusive yet. For example, [17] proposed to use font 14 points (~19 pixels) whereas [4] argued that font size 16 (22 pixels) to 18 points (~24 pixels) must be used for better readability. These suggestions are in strike contrast with the current practices of the Arabic web design. More than 60% of the inspected websites used font size ranging between 12 pixels to 16 pixels (i.e. 9 points to 12 points) to style the paragraphs. Similarly, menu items are sized from 13 pixels to 14 pixels, which is still considerably illegible [17].

In respect to using images in web design, we aimed at answering the following question. What types of images are incorporated within the Saudi websites given the Saudi culture? All Arabic websites included images as part of their content. Authors in [40] and [41] suggested that graphics improve the overall attractiveness of websites. Moreover, 90% of the Arabic websites we tested included human images. This is known to improve user engagement, trust, and satisfaction [21]. However, 80% of the Arabic websites used conservative images that respect the Islamic identity and cultural values of the Saudi people. Research studies agree that web designs should adhere to the cultural values of its users to achieve success and acceptance [42], [43], [44]. Two-thirds of the websites used images of both genders. The remaining third, however, used images of men only. This could be explained by the masculine dimension of the Saudi society as indicated by Hofstede scores [45]. More than 80% of the websites included images containing groups of people. Again, this can be justified by the collectivism dimension of the Saudi society [45]. Finally, there was high usage of animations, possibly, in an attempt to engage web visitors and improve the aesthetics of the websites. Evidently, the high presence of images in these websites contributed to lower performance scores and increased site loading time. Optimization of images' size, using the appropriate image compression techniques, is therefore recommended as a result of our analysis.

VII. CONCLUSIONS

The 73 top viewed Arabic websites from local and international service providers, covering a wide range of areas in Saudi Arabia such as government, news, and e-commerce, were carefully inspected with a focus on the fonts applied to format the Arabic text and images incorporated to improve the overall site attractiveness. The Arabic websites suffered from inconsistency for they mixed font types on the same web pages. The added value of such practice is ambiguous and

invites the designers of Arabic websites to pay more attention to the application of fonts more consistently within and across pages.

Droid Arabic Kufi was dominant in formatting the titles and menus of the Arabic sites. This font type reflects the specific characteristics of the Arabic writing, especially that related to calligraphy. Nevertheless, Tahoma and Helvetica were also used frequently to style the titles and menus. Surprisingly, however, the analysis showed that famous fonts used to style English text, such as Tahoma, Helvetica, Arial and Times New Roman, are used to format the Arabic paragraphs. Nonetheless, a myriad of other font types was used to style the Arabic text, which shows that the Arabic websites still do not favor a particular font type to improve text legibility or attractiveness. Instead, web designers of Arabic websites seem to trust what international websites frequently use such as Helvetica and Arial. This might not be necessarily efficient for reading the Arabic characters and language. Arabic content on the web is still yet to find its appropriate font type and font size.

Images were extensively used in the Arabic websites, which may indeed increase user engagement and visual appeal. However, the high number of images resulted in lower website loading speed, which is a key quality factor in web design. The use of images in the Arabic websites revealed three main characteristics, masculinity, collectivism and conservatism. These characteristics are in agreement with the Saudi culture and its religious identity.

Despite the insights highlighted by the results, there are several qualifying limitations that have to be enumerated here. The aforementioned studies describe the current design practices pertaining to font and image usage within the Arabic websites and do not shed light on the rationale for their use nor do they test real users' perception and judgment towards these practices. In other words, usability inspection studies do not allow obtaining a deep understanding of the effects of certain design decisions on user judgment and satisfaction. Follow-up studies are recommended to gauge user views and acceptability towards font and image usage in the Arabic websites. The inspection raised several interesting observations, but more statistical analysis is needed to assert differences between website categories.

VIII. FUTURE RESEARCH DIRECTIONS

The herewith research provides a detailed outlook on the general practices of local and international websites in relation to the application of font and images in Arabic web design. To the best of our knowledge, this is the first study that investigates the use of font and images in Arabic websites extensively. Indeed, there is an overarching necessity to undertake more organized research focusing on these two important design elements. As part of a long-term agenda, we have already started to conduct a series controlled experiments in order to identify the most efficient Arabic font type and size to use in e-commerce websites as well as users' perception towards conservative and non-conservative images within fashion online stores and study how these images could influence customers' buying decisions. Researchers into the impact of typography on Arabic web usability should consider

using eye-tracking to collect objective measures about Arabic reading performance and mental load. However, for the use of images, more user testing is required to judge users' attitudes and acceptance towards the shift in using less conservative images, especially in Arabic e-commerce websites, where buying decisions are greatly driven by the display of products such as clothes. Other interactive media such as animations and videos and their effect on user judgment and website performance would also need to be examined in the future.

REFERENCES

- [1] E. Deborah, E-P. Rosen, "Website design: Viewing the web as a cognitive landscape", *Journal of Business Research*, Vol. 57, no. 7, pp. 787-794, 2004.
- [2] G. Lindgaard, G. Fernandes, & C. Dudek, J. M. Brown, "Attention web designers: You have 50 milliseconds to make a good first impression!", *Behaviour and Information Technology Journal*, vol. 25 no. 2, pp. 115-126, 2006
- [3] R. Sinha, M. Hearst, M. Ivory, and M. Draisin. "Content or graphics? an empirical analysis of criteria for award-winning websites", in Proc. Human Factors and the Web, 7th conference, Madison, WI, June 2001.
- [4] A A Abubaker, J Lu, "The optimum font size and type for students aged 9-12 reading Arabic characters on screen: A case study", *Journal of Physics: Conference Series*, 2012, available at: <https://iopscience.iop.org/article/10.1088/1742-6596/364/1/012115/meta>
- [5] M. Bernard, "Criteria for optimal web design (designing for usability)", available at: <http://psychology.wichita.edu/optimalweb/structure.htm>, 8. 7. 2004.
- [6] J. Nielsen, "Usability 101: Introduction to Usability, Available at: <http://www.nngroup.com/articles/usability-101-introduction-to-usability/>, 2012.
- [7] M. Y. Ivory, M. A. Hearst, "Improving website design", *University of California, Berkeley*, Vol. 01, Page no. 7, 2002.
- [8] H. Holden, R. Rada, "Understanding the Influence of Perceived Usability and Technology Self-Efficacy on Teachers' Technology Acceptance", *Journal Of Research On Technology In Education*, (International Society For Technology In Education), vol. 43, no. 4, pp. 343-367, 2011.
- [9] A. Seffah, M. Donyaee, K. R. B Kline, H. K. Padda, "Usability measurement and metrics: A consolidated model". *Software Quality Journal*. Vol. 14. pp. 159-178. Jun 2006.
- [10] M. Bernard, B. Lida, S. Riley, T. Hackler, K. Janzen, "A comparison of popular online fonts: which size and type is best?", *Usability News*. 2002 Jan; Vol. 4(No. 1) Online journal
- [11] J. W. Palmer, "Web site usability, design, and performance metrics", *Information Systems Research*; vol. 13, no. 2; pg. 15, Jun 2002.
- [12] C. Flavian, R. Gurra, C. Orus, "Web design: A key factor for the website success", *J. Systems and IT*. pp. 168-184. 2009.
- [13] J. Hu, K. Shima, R. Oehlmann, J. Zhao, Y. Takemura, KI. Matsumoto, "An empirical study of audience impressions of B2C web pages in Japan, China and the UK", *Electronic Commerce Research and Applications*. , vol. 3, no. 2, pp 176-89 Jun. 2004.
- [14] H. Shahizan, L. Feng, "Evaluating the Usability and Content Usefulness of Web Sites: A Benchmarking approach," *Journal of Electronic Commerce in Organizations*, vol. 3, no. 2, pg. 46, Apr-Jun 2005.
- [15] D. Beymer, D. Russell, P. Orton, "An eye tracking study of how font size and type influence online reading", *Proceedings of the 22nd British HCI Group Annual Conference on HCI 2008: People and Computers XXII: Culture, Creativity, Interaction Vol. 2*, pp. 15-18. Sept 2008.
- [16] M. Gasser, J. Boeke, M. Haffernan, R. Tan, "The Influence of Font Type on Information Recall", *North Am J Psychol*, vol. 7, no. 2, pp. 181-188, 2005.
- [17] A. Z. Alotaibi, "The effect of font size and type on reading performance with Arabic words in normally sighted and simulated cataract subjects", *Clinical and Experimental Optometry*, vol. 90, no. 3, pp. 203-206, 2007.
- [18] M. A. Zamzuri, A. Mohamad, W. Rahani, S. Khairulanuar, Z. I. Muhammad, "Reading on the Computer Screen: Does Font Type has

- Effects on Web Text Readability?", *International Education Studies*; Vol. 6, No. 3, pp. 26-35; 2013.
- [19] N. Hojjati, B. Muniandy, "The Effects of Font Type and Spacing of Text for Online Readability and Performance ", *Contemporary Educational Technology*, vol. 5, no. 2, pp. 161-174, 2014
- [20] A. Sears, J. A. Jacko, E. M. Dubach, "International Aspects of World Wide Web Usability and the Role of High-End Graphical Enhancements", *Int. J. Hum. Comput. Interaction*, vol. 12, no. 2, pp. 241-261, 2000.
- [21] D. Cyr, H. Larios, M. Head, B. Pan, "Exploring human images in website design: a multi-method approach", *MIS Quarterly* Vol. 33 No. 3, September 2009.
- [22] S. A. Becker and F. E. Mottay, "A global perspective on Web site usability," in *IEEE Software*, vol. 18, no. 1, pp. 54-61, Jan. -Feb. 2001.
- [23] N. Bevan, L. Spinhof, "Are guidelines and standards for web usability comprehensive?", *Proceedings HCI International 07*, Springer, pp. 407-419, July 2007.
- [24] N. Bevan, " Guidelines and Standards for Web Usability", *Proceedings of HCI International*, Lawrence Erlbaum, *The Management of Information: E-Business, the Web, and Mobile Computing*, vol. 2, July 2005
- [25] Mohamed Benaida and Abdallah Namoun, "Technical and Perceived Usability Issues in Arabic Educational Websites" *International Journal of Advanced Computer Science and Applications(IJACSA)*, vol. 9, no. 5, 2018.
- [26] S. H. Mustafa, L. F. Al-Zoua'bi, "Usability of the Academic Websites of Jordan's Universities, An Evaluation Study", 9th International Arab Conference for Information Technology(ACIT2008).
- [27] A. Fernandez, E. Insfran, S. Abrahão, "Usability evaluation methods for the web: A systematic mapping study". *Information & Software Technology*. Vol 53, pp. 789-817, Aug 2011.
- [28] T. Conte, J. Massolar, E. Mendes, GH. Travassos, "Web usability inspection technique based on design perspectives", *IET software*. Apr, vol3 no. 2, pp. 106-23. Apr. 2009.
- [29] R. Otaiza, C. Rusu, S. Roncagliolo, "Evaluating the usability of transactional web sites", In *2010 Third International Conference on Advances in Computer-Human Interactions*, pp. 32-37, Feb. 2010. K-S. Kang, B. Corbitt, "Effectiveness of Graphical Components in Web Site E-commerce Application-A Cultural Perspective", *EJISDC*, vol. 7, no. 2, pp. 1-6. 2001.
- [30] "Top Sites in Saudi Arabia", available online at: <https://www.alexa.com/topsites/countries/SA>, last visit: 30. 3. 2019.
- [31] "Fontface Ninja", available online at: <https://fontface.ninja/>, last visit: 30. 3. 2019.
- [32] "Website Speed Test Image Analysis Tool", available online at: <https://webspeedtest.cloudinary.com/>, last visit: 30. 3. 2019.
- [33] S. Mentese, A. h. Turan, "Assessing the usability of university websites: An empirical study on Namik Kemal University". *Turkish Online Journal of Educational Technology*. Vol. 11, pp 61-69, Jul 2012.
- [34] A. El-Sawy, M. Loey and H. El-Bakry, "Arabic Handwritten Characters Recognition Using Convolutional Neural Network," *WSEAS Transactions on Computer Research* ,vol. 5, pp. 11-19, 2017.
- [35] S. Steinau, O. Díaz, J.J. Rodríguez, F. Ibáñez, "A Tool for Assessing the Consistency of Websites", *INICEIS* (pp. 691-698). 2002.
- [36] E. Shawgi, N. A. Noureldien, "Usability measurement model (umm): a new model for measuring websites usability", *International Journal of Information Science*, vol. 5. no. 1, pp. 5-13, 2015.
- [37] T. Rabinowitz, "Exploring typography", Cengage Learning; 2015.
- [38] J. Banerjee, D. Majumdar, D. Majumdar, "Readability, Subjective Preference and Mental Workload Studies on Young Indian Adults for Selection of Optimum Font Type and Size during Onscreen Reading", *Al Ameen Journal of Medical Sciences*. 4, pp. 131-143, Jan. 2011.
- [39] M. Bernard, M. Mills, "So, What Size and Type of Font Should I Use on My Website?", *usability news*, , Vol. 2, no. 2, July 2000.
- [40] Y. -C. Lin, C. Yehb, C. Wei, " How will the use of graphics affect visual aesthetics? A user-centered approach for web page design , "et al. / *Int. J. Human-Computer Studies* vol. 71, pp. 217–227, 2013.
- [41] D. Willis, " Effects of using enhancing visual elements in Web site design", *American Communication Journal*, vol 3, no. 1, 1999, available at: <http://ac-journal.org/journal/vol3/iss1/articles/Willis.htm>.
- [42] N. Tsiriktsis, " Does Culture Influence Web Site Quality Expectations? An Empirical Study", *Journal of Service Research*. Vol 5, no. 2, Nov 2002.
- [43] R. Fletcher, "The impact of culture on web site content, design, and structure: An international and a multicultural perspective". *Journal of Communication Management*, vol. 10, no. 3, Jul. 2006.
- [44] A. Marcus, E-W. Gould. "Crosscurrents: cultural dimensions and global Web user-interface design. " *ACM Interactions*, pp 32-46, vol. 7, no. 4, Jul. 2000.
- [45] "Hofstede Insights", available online at: <https://www.hofstede-insights.com/>, last visit: 30. 3. 2019.
- [46] J. Janbi, "Classifying Digital Arabic Fonts Based on Design Characteristics", 2018 21st Saudi Computer Society National Computer Conference (NCC), Riyadh, pp. 1-6. April 2018.
- [47] Y. Huang, J. W. Wenjie Shi, "The impact of font choice on web pages: Relationship with willingness to pay and tourism motivation", *Tourism Management*, vol. 66, pp. 191-199, June 2018.
- [48] M. A. Ababtain, A. R. Khan, "Towards a Framework for Usability of Arabic-English Websites", *Procedia Computer Science*, vol. 109, pp. 1010-1015, 2017.
- [49] C. Yang, T. S. T. Huang, D. R. Shanks, "Perceptual fluency affects judgments of learning: The font size effect", *Journal of Memory and Language*, vol. 99, pp. 99-110, April 2018.
- [50] J. Grobelny, R. Michalski, "The role of background color, interletter spacing, and font size on preferences in the digital presentation of a product", *Computers in Human Behavior*, vol. 43, pp.85-100, 2015.

Digital Certificate Exchange of Agricultural Products using SOAP Web Services

Miyanda Chilikwela¹

Department of Electrical and Electronics Engineering
University of Zambia, Lusaka, Zambia

Jackson Phiri²

Department of Computer Science
University of Zambia, Lusaka, Zambia

Abstract—Developing countries have continued to experience a number of challenges in managing import and export certificate for various goods. In this paper, we are proposing a model for digital certificate exchange in an effort to improve the security levels of data exchange among the government organizations and the business community. With the increase of various information systems being used in many organizations, data exchange between systems has become critical. The model developed uses SOAP web services for data exchange and RSA encryption for secure data exchange. Ministry of Agriculture is responsible for the issuance of import and export certificates in Zambia while Zambia Revenue Authority is responsible for ensuring that goods imported or exported out of the country have a valid certificate that is authentic. The results show that the model provides a secure and timely exchange of information between the ministries and the government agencies.

Keywords—Digital; certificate; Rivest, Shamir and Adleman (RSA); Simple Object Access Protocol (SOAP); web service; model

I. INTRODUCTION

The government of the republic of Zambia has appointed the Ministry of Agriculture (MOA) and other related ministries to oversee the import and export of certain controlled products such as food through the issuance of import and export certificates prior to the importation or exportation of goods [1]. The ministries are responsible for ensuring that the products imported or exported have a valid certificate prior to importation or exportation [2]. There are various agencies that are tasked to ensure that the certificates issued are valid at the time of import or export. Such agencies include Zambia Revenue Authority (ZRA) which is mandated to collect taxes on behalf of the government [3]. The authority depends on the certificates presented to them by would be exporters or importers during the importation or exportation of goods.

The certificates presented are sometimes forged or expired certificates. This results in the importation or exportation of food stuff that don't meet health requirements. This consequently has adverse effects on health. The lack of secure data exchange results in forged certificates being presented to the authority at the boarder points and loss of government revenue [4]. Therefore a proposed model which uses SOAP web services in the exchange of information between government agencies and ministries will be used as a means of data exchange. The model is based on ISO 27001 standard to ensure that data being exchanged is secure. This paper is structured as follows: Section II looks at the literature review,

followed by Section III which shows related works. Section IV focuses on the methodology, Section V looks at the security mechanism. And finally in Section VI, the findings are presented and conclude the paper in Section VII.

II. LITERATURE REVIEW

A. Ministry of Agriculture

The ministry is mandated to design, implement and manage the Governments activities in the agricultural sector. The purpose of the ministry is to facilitate and support the development of a sustainable, diversified and competitive agricultural sector that assures food and nutrition security, contributes to job creation and maximizes the sector's contribution to Gross Domestic Product. The ministry is mandated under the Control of Goods Act to ensure that controlled goods being imported or exported into the country meet the stated requirements as per the law [1].

B. The Control of Goods Act

The control of goods act is an act that provides regulation of the sale, distribution, purchase and disposal of unmanufactured or manufactured products or poultry and animal. The act controls the import and export of controlled products such as poultry or animal and other products [2].

C. Web Services

A web service is any service that is available over the Internet, uses a standardized (Extensible Markup Language) XML messaging system, and is not tied to any one operating system or programming language specification. Web services use Hyper Text Transfer Protocol (HTTP) for data exchange. Web services employ a variety of technical standards such as XML, Simple Object Access Protocol (SOAP), Web service Description Language (WSDL), Representational State Transfer (REST) and Universal Description, Discovery and Integration (UDDI) [5] [6]. Fig. 1 shows data exchange between different systems.

D. SOAP Web Services

SOAP is a protocol based on XML for exchanging information between computers. Because SOAP is platform-independent it enables applications or systems written in different programming languages to be able to communicate. The WSDL is an XML vocabulary used to describe SOAP-based web services. XML is a language that uses XML tags to describe the data being exchanged [5].

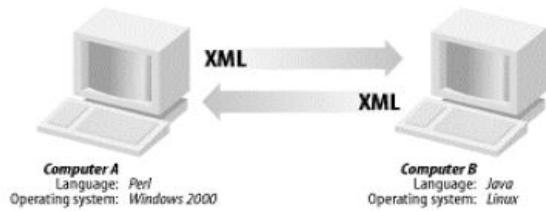


Fig. 1. Web Service [5].

E. ISO 27001 Standard

ISO stands for International Standard Organization; it was formulated to provide a model for establishing, implementing, operating, monitoring, reviewing and maintaining an Information Security Management System (ISMS). The standard emphasizes implementation of operating controls that manage an organization's information security risks in the context of the organization's overall business risks among others. This includes measures or controls put in place by an organization to safeguard itself from different types of threats. The control objective: "to maintain the security of information and software exchanged within an organization and with any external entity" seeks to ensure that information being exchanged is secure during transmission. This includes all forms of controls put in place to safeguard data in transit against cyber-attacks [6] [7].

F. Encryption

Encryption refers to the art of protecting information by converting the information into an unreadable format. The encrypted text is called cipher text [8]. Encryption algorithms can be categorized into two types, namely Symmetric and Asymmetric keys encryption. Encryption where one key is used to encrypt and decrypt data is known as Symmetric keys encryption. In Asymmetric keys, two keys are used; private and public keys [8] [9]. There are many cryptography algorithms used to secure information such as RSA, 3DES, Blowfish, AES, DES, Paillier and ElGamal. The user who wishes to implement encryption needs to find the best security algorithm which consumes less computational power and provides high security [10] [11].

G. RSA Encryption

Rivest, Shamir and Adleman (RSA) introduced RSA algorithm in 1977. RSA is an asymmetric algorithm that uses the public key for encryption and the private key for decryption as shown in Fig. 2 [12]. RSA key generation is generated as follows.

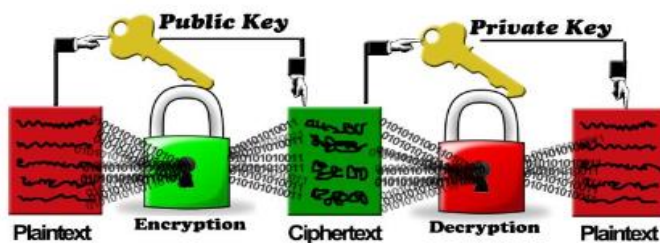


Fig. 2. RSA Encryption and Decryption [14].

Taking two large prime numbers (P and Q), Computing N by using the given formula ($N=P*Q$), Choose the public key exponent E such that $1 < E < (N)$ and, E and (N) are co-prime. Finally determine the private key exponent D through the given formula. $D * E = 1 * \text{mod} ((N))$. The public key consists of (N, E) and the private key consists of (N, D) [13].

Current usage of RSA: Pretty Good Privacy (PGP) is a freeware that provides encryption and authentication for email and file storage applications across multiple platforms and uses RSA algorithm for transporting the key. Google's G Suite, is a brand of cloud based services that provides collaboration tools, products such as Gmail, Hangouts, Calendar [13].

Strengths of RSA: The strengths of RSA lies in the use of large random prime numbers to calculate the modulus. It is difficult to computationally factor large integers into primes. Keys of size 2048 bits provide best security. It is widely used for secure communication channel and for authentication to identify service provider [13] [14].

Husam Ahmed Al Hamad alludes to the use of XML for exchange and integration of data between heterogeneous applications and systems. XML represents data using tags called elements. Each data component to be exchanged is represented by a tag. The author suggests that XML has become a standard data format that is widely used by many organizations and a common language for data transmission over the Internet [15].

Marcelo arenas pontificia and Leonid Libkin discuss the use of XML to exchange data due to the increased need for exchange of data in various formats. The advantages of XML that makes it suitable for data exchange include the format of XML document is not rigid, can easily add additional information using the elements [16].

Cui-xiao Zhang, Ying-xin hu, Guo-bing Zhang and Jin Sha define web services as a technique to achieve data exchange. The authors further state that web services not only provide the possibility of data exchange, but also provide the technique supporting data integration, data collection and data sharing between different systems. Web services provide a valid technique support for system integration [17].

P. Dinesh, P. J. Charles and S. BrittoRamesh narrate that web services is a self-contained, self-describing and modular applications that can be described, published, located and invoked over a network. Web services provide means for data exchange that can be written in a different programming language from that of the exchanging parties [18].

Douglas Harris, Latifur Khan, Raymond Paul and Bhavani Thuraisingham discuss that data integration has been at the core of research until recently where brute force integration techniques that consisted of techniques such as gateways and translators were used between multiple data management. Standards such as Remote Database Access (RDA) were developed initially for client- server interoperability. Later object-based wrappers were used to encapsulate the multiple systems including the legacy systems. The authors allude that common representation of the data remained a challenge [19].

Rajdeep Bhanot and Rahul Hans carried out an analysis on various encryption algorithms based on different parameters. The authors proceeded to compare the algorithms to choose the best algorithm. They defined RSA as the most important public-key cryptosystem. The RSA algorithm can be used for digital signatures and public key encryption. The security is based on the difficulty of factoring large integers [8].

III. RELATED WORKS

Rajan Datt, N.N. Jani, Rasendu Mishra, Ajay Patel designed a model using web services to exchange data between the heterogeneous databases. The findings of this study are that web services are being employed as a means of exchanging data between heterogeneous databases. The model developed does not secure data being transmitted over the web. It is on this basis of limitation that this research is being conducted [20].

Aftab Ahmed Chandio, Dingju Zhu, Ali Hassan Sodhro and Muhammad Umer Syed proposed a system for the University of Sindh based on the Service Oriented Architecture (SOA) with web services. The system solves the problem that frequently occurs in the process of no-dues verification of a student from different departments. No security mechanisms were implemented to safeguard the data whilst in transmit over the web despite the websites being used within the organization. This limitation provides the basis for this research [21].

P. Dinesh, P. J. Charles and S. BrittoRamesh reviewed related works based on the studies of ten different authors. Their works review different security mechanisms that can be employed in web services. They further outlined that public key infrastructure security mechanism provides device and service authentication [18]. This research seeks to implement asymmetric type of encryption.

Vu Van Tan, Dae-Seung Yoo, and Myeong-Jae Yi designed and implemented a web application-based OPC (Openness, Productivity, and Connectivity) technique to exchange data between the measurement and control systems on the plant floor with XML for slow process monitoring and control systems. The solution fully applies technologies such as OPC, XML, and links to the Internet [22].

Memorie Mwanza and Jackson Phiri conducted a research study on fraud detection on bulk tax data using Business Intelligence (BI) data mining tool. The authors outlined that ZRA like many other revenue authorities in Africa, has been affected by fraud mechanisms employed by tax payers. They identified BI as a technique that can be used to detect tax frauds, non- fillers and non- compliant tax payers. They further alluded that data mining is a significant technique that can be used to overcome the challenges of fraud detection and anomalies that arise in tax administration [23].

Jackson Phiri and Tiejun Zhao study was on identity attributes using quantitative analysis and developed an identity attribute metric model. The study focused on various sources of information such as first name, last name, email address and date of birth that can be obtained from various forms i.e public services, health care systems. The model seeks to improve the robustness of most identity systems [24].

IV. METHODOLOGY

Qualitative research was primarily used to gather information on the import and export of agricultural products. Techniques such as observations and record sampling were employed. Activities involved mapping of the current business process that highlights the process flow from import application to actual importation of products in part (a). The proposed business process is then highlighted in part (b) below. The model is developed in java based on the proposed business process as shown in part (d). To evaluate data exchange, an application for a certificate is approved and data is electronically submitted on the customs processing system for import approval at the border office.

The following activities were carried out in the methodology:

A. Mapping of Current Business Process Flow

The interaction of the importer/exporter in the importation and exportation of goods includes various business processes from MOA and ZRA. Fig. 3 below shows the use case diagram and interaction of the actors in the current business process.

- Current business Process

The current business process flow for the importation and exportation of goods is described below as shown in Fig. 4.

An importer or exporter obtains an application form from MOA. He/she fills in the form and submits it to the Senior Agribusiness Officer at MOA. The officer verifies the quantity applied for importation or exportation. The quantity applied for depends on the product being imported or exported. If the verification results are successful, the importer or exporter is advised to make a bank deposit for the certificates applied for. The importer or exporter makes a bank deposit and presents the bank deposit slip to the Officer at MOA. The officer proceeds to approve and issue the certificates based on the quantity applied for. The certificate issued is only valid for 30 days from the time of issuance there after it is deemed as invalid.

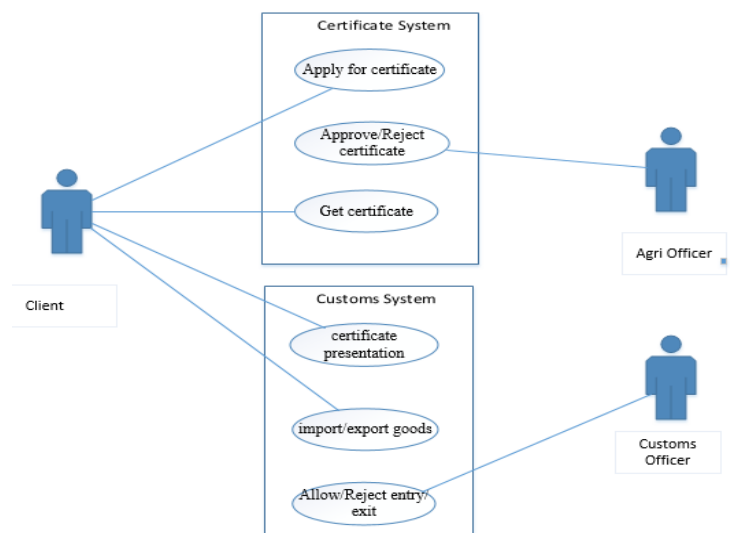


Fig. 3. Use Case Diagram of Current Business Process.

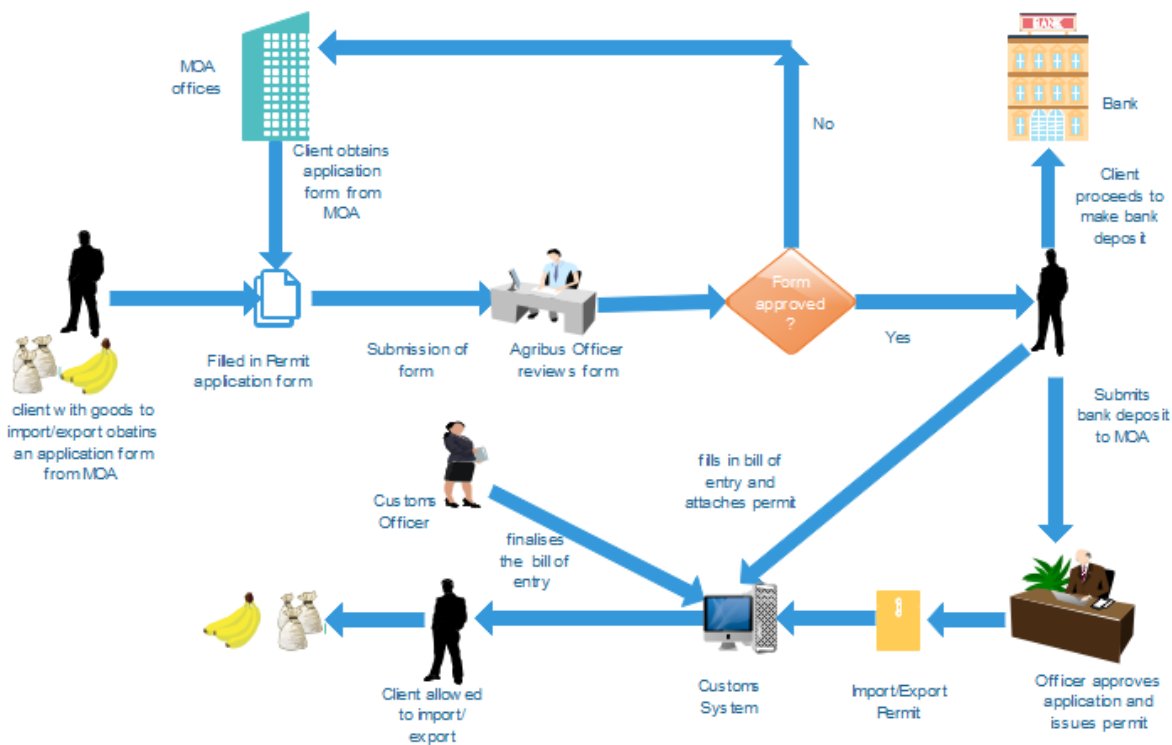


Fig. 4. Current Business Process.

The importer or exporter proceeds with the clearing process on the customs system. He/she scans the certificate(s) and attaches the certificates to the bill of entry on the customs system. Then he/she finally registers the bill of entry as a submission to import or export goods. The customs officer scrutinizes the bill of entry on the customs systems. If the attached certificates are not valid the importer/exporter is asked to obtain valid certificates from MOA.

The certificate presentation by the importer/exporter and the validation process by the customs officers is manually done.

According to the Control of Goods Act [2], a potential importer/exporter who wishes to import or export goods needs to obtain a valid import or export certificate prior to the importation or exportation. The steps followed are:

- 1) The applicant applies for a certificate to import or export
- 2) If the applicant meets the requirements, the applicant pays the required amount.
- 3) Client is issued with import or export certificate.
- 4) Client presents the certificate at any of the customs boarder offices in the country.
- 5) ZRA customs officer checks if the certificate is valid

If it's valid, client is given the opportunity to export or import their goods.

- Challenges of the Current Business Process

The paper based system that is used for the exchange of certificate data between the government agencies has the following challenges:

- 1) Certificates presented at the boarder offices may not be genuine (counterfeit certificates).
- 2) Loss of government revenue because some clients use old certificates during importation or exportation.
- 3) Lack of physical presence of trained man power from Ministry of Agriculture at all boarder offices in the country.
- 4) Customs officers are not trained to validate the authenticity of the certificate thus they are unable to identify potential culprits.
- 5) Importation or exportation of banned goods that may pose health challenges.

B. Proposed Business Process

An importer or exporter applies for a certificate on the certificate processing system website. The officer then verifies the quantity applied to be imported/exported. The importer or exporter is advised to make a bank deposit for the certificates applied for. The importer or exporter makes a bank deposit and presents the bank deposit slip to the cashier at MOA. The cashier inputs the bank deposit slip details and submits the application. The Agribusiness Officer proceeds to approve the certificate, clicking the approval button invokes the web service as shown in Fig. 5. The SOAP request message with the certificate details is created as shown in Fig. 6. Once the SOAP request message is created, it is encrypted and sent to the Customs System. The SOAP request message is received on the customs system where the message is decrypted and a SOAP response message is sent to the certificate system. The client uses the digital certificate received on the Customs system to frame the bill of entry.

- How it works

The development and implementation of the soap web service included the following activities:

1) Creation of a user requirements document that defined data to be exchanged between parties.

To develop, implement and use soap web services, a contract (WSDL) needs to exist between the two parties that need to exchange data. The contract defines the data elements to be exchanged, the purpose and function of its operations, messages that need to be exchanged in order to engage the operations, a set of conditions under which the operations are provided and information about how and where the service can be accessed. The user requirements document is signed by both parties.

2) Development of a SOAP web service by both parties based on WSDL.

The web server and web client was developed in java programming language. The system that provides a resource becomes a client and the system that utilizes the resources sent is the server. The Certificate Processing System is the client while the Customs System is the server. The Customs System has a web service that defines the data it is expecting to receive. The Certificate Processing system has a web client that sends certificate data to the Customs Processing System.

```
public static void main(String args[]) {  
  
    SwInfoDetails sw = new SwInfoDetails();  
    sw.SendPermitDetails(15);  
  
}
```

Fig. 5. Java Code.

The sw object shown in the fig above contains data that is sent from the Certificate Processing System. The object contains data such as the goods code, description, permit number and importer/exporter code as shown in Fig. 6. Once the object is compiled it creates a SOAP request message as shown in Fig. 6. The message contains the data elements generated from the client.

1) The SOAP request is successfully sent to Customs System where it is saved on the database and a SOAP response is sent back to the client as shown in Fig. 7.

2) SOAP response message sent back to Certificate Processing System.

Fig. 8 shows the SOAP response message that is generated on the server side once the SOAP request message is received from the client. The certificate number is used on the customs processing system when importing or exporting goods.

C. Security Mechanism

The SOAP request message is encrypted using RSA encryption. To encrypt the data, there is need to have a public/private key pair. The key pair consists of the public key and the private key. To generate the key pair, a keystore is created using the keytool JDK utility as shown in Fig. 9 below. This file has both per-store and per-key passwords which provides additional security to the key pair.

```
<S:Envelope xmlns:S="http://schemas.xmlsoap.org/soap/envelope/">  
<S:Body><ns2:swSubmit  
xmlns:ns2="http://www.asycuda.org"><ns2:swInfo>  
<ExpCode></ExpCode>  
<ImpCode>1000001420</ImpCode>  
<ImpNam>JONES MWANGALA</ImpNam>  
<CuoCod>VFL</CuoCod>  
<RefNbr>I201803VFL0003</RefNbr>  
<GoodsItems>  
<GoodsCode>10051000000</GoodsCode>  
<GoodsDescription>Maize seed</GoodsDescription>  
<Quantity>458</Quantity>  
<Weight>458</Weight>  
<Value>4544 ZMK</Value>  
<Unit> </Unit>  
<QuotaUsed>0.0</QuotaUsed>  
<QuotaBalance>458.0</QuotaBalance>  
<PerNbr>I201803VFL000310051000</PerNbr>  
<PerValidFrom>14-Mar-18</PerValidFrom>  
<PerValidTo>13-Apr-18</PerValidTo>  
<Origin>AE</Origin>  
</GoodsItems>  
<Agencies>  
<AgencyName>Ministry of Agriculture</AgencyName>  
<AgencyDetails>Ministry of Agriculture</AgencyDetails>  
<Status>Processed</Status>  
<Comment>ok</Comment>  
</Agencies>  
<Agencies>  
<AgencyName>Ministry of Agriculture</AgencyName>  
<AgencyDetails>Ministry of Agriculture</AgencyDetails>  
<Status>Processed</Status>  
<Comment>okay</Comment>  
</Agencies>  
</ns2:swInfo>  
</ns2:swSubmit>  
</S:Body>  
</S:Envelope>
```

Fig. 6. SOAP Request Message.

SINGLE WINDOW PERMIT						
Importer No. 1000001420	Customs Office CHR	Registration Date 22/01/2018				
JONES MWANGALA		Single Window App. ID I201801CHR0001				
Exporter No.	Reference No. 2018 2					
Hs.code	Goods.Desc	Per No	Origin	Valid From	Valid To	Qty
10051000000	Maize seed	I201801CHR0...	ZA	22-Jan-18	21-Feb-18	6,000

Fig. 7. Digital Certificate Data on Customs System.

```
<S:Envelope xmlns:S="http://schemas.xmlsoap.org/soap/envelope/">  
<S:Header/>  
<S:Body><ns2:swSubmitResponse  
xmlns:ns2="http://www.asycuda.org">  
<ns2:swSubmitResult>  
<result>E</result>  
<errorCode>0</errorCode>  
<ErrorDescription>Permit Sent Successfully</errorDescription>  
</ns2:swSubmitResult>  
</ns2:swSubmitResponse>  
</S:Body>  
</S:Envelope>
```

Fig. 8. SOAP Response Message.

```
C:\keystore>keytool -genkeypair -alias mykey -storepass s3cr3t -keyalg  
RSA -keystore keystore.jks
```

Fig. 9. Keystore Generation.

```
C:\keystore>keytool -export -file miyanda.cer -alias mykey -storepass s3cr3t -
keystore keystore.jks
Certificate stored in file <miyanda.cer>
```

Fig. 10. Key Pair.

The key pair is generated as shown in Fig. 10. The key store directory contains the miyanda.cer file which contains both the public and private key as shown in Fig. 11.

keystore.jks	6/18/2018 4:48 PM	JKS File	3 KB
miyanda.cer	6/18/2018 4:53 PM	Security Certificate	1 KB

Fig. 11. Keystore Directory.

The miyanda.cer file below in Fig. 12 shows the encryption algorithm, and the signature hash algorithm.

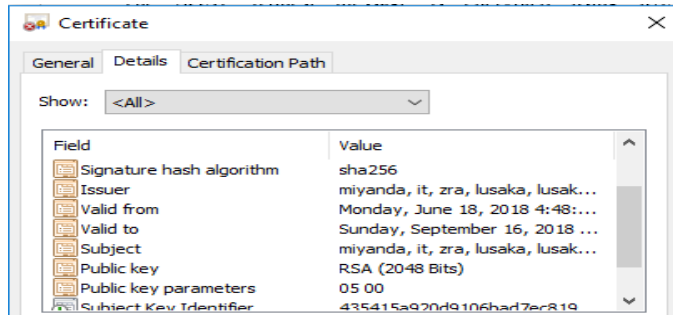


Fig. 12. Certificate Contents.

Fig. 13(a) below shows the flowchart for the generation of the keystore using keytool JDK utility.

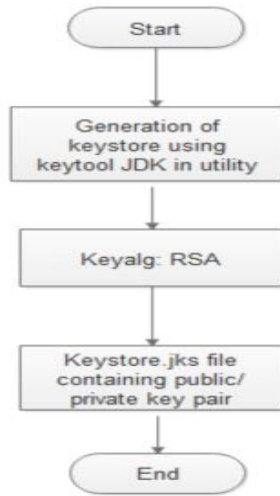


Fig. 13 (a). Flowchart for Keystore Generation.

Algorithm for the generation of encrypted SOAP request using the public key is as follows:

Algorithm 1: At Client Side

Input: SOAP request message

Processing: encryption of SOAP request message using public key

Output: encrypted SOAP request message

Fig. 13(b) shows the flowchart for the generation of encrypted SOAP request message.

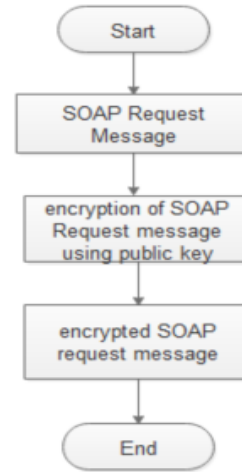


Fig. 13 (b). Flowchart for Encryption of SOAP Request.

Algorithm 2: At Server Side

Input: encrypted SOAP request message

Processing: decryption of SOAP request message using private key

Output: decrypted SOAP request message in customs processing system

Fig. 13(c) below shows the flowchart for the decryption of the encrypted SOAP request message.

Fig. 14 shows the proposed business process.

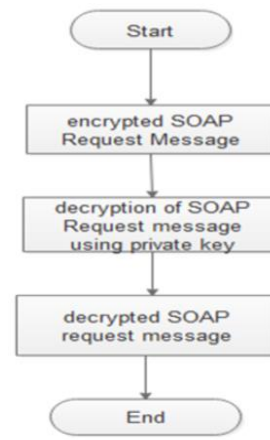


Fig. 13. (c) Flowchart for Decryption of SOAP Request.

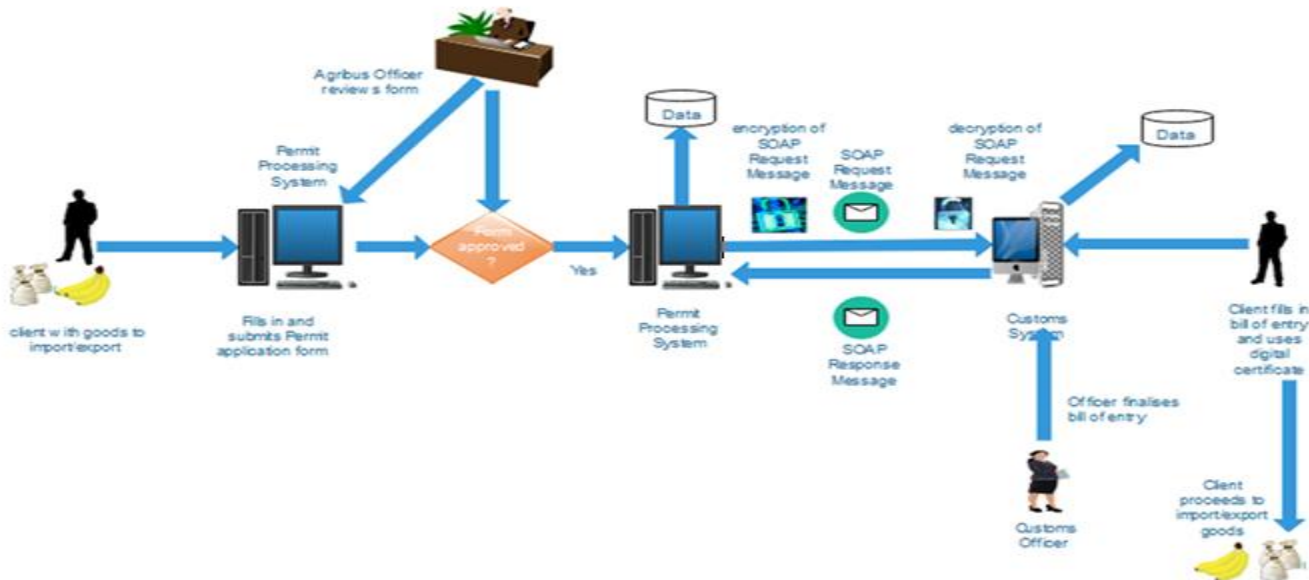


Fig. 14. Proposed Business Process.

D. Proposed SOAP Web Service Model

To achieve secure data exchange between MOA and ZRA the following model is proposed.

- 1) The client applies for a certificate through the electronic Certificate Processing System.
- 2) MOA approves the clients certificate.
- 3) Upon approval of the certificate, the data about the certificate is encrypted and sent to ZRA's system via SOAP web services.
- 4) The client then finds the approved certificate on the Customs Processing system and uses the certificate to declare the goods to be imported or exported.

Components of the SOAP web service model

1) *Certificate processing system:* The application system used for processing of certificates is developed in Java programming language. The MOA has a web service client written in java programming language that will invoke the web service at ZRA. The web service will only be invoked once the certificate has been approved. Once the certificate is approved a SOAP request message will be sent to the Customs Processing System.

2) *Customs processing system:* The system used for declaring goods to be imported or exported is developed in java programming language. The authority has a web service server written in java programming language. The server will be receiving certificate data sent in XML format from MOA certificate processing system. The system will respond with an appropriate SOAP response.

3) *The SOAP web service:* The web service model is written in java programming language and consists of XML tags that define the data being exchanged. The SOAP web service has a WSDL that defines the standard data that is being sent from one system to the other. The web service model defines the expected request and response. Fig. 15 shows the WSDL of the SOAP web service. The WSDL is the contract that shows the data to be exchanged between the two systems. It shows the individual fields to be exchanged.

4) *Database systems:* The database management system being used by both parties is Oracle 11g. The certificate processing system will store certificate data in the database. Once the SOAP request is sent to the Customs Processing System. The certificate data is stored in the oracle database for the customs processing system.

5) *Web:* The web is an interconnection of specially designed web pages. These web pages are specially formatted using HTTP. The SOAP request is moved via the web from one system to the other.

V. SYSTEM ARCHITECTURE

The architecture has five main components these are (Fig. 16):

- 1) The Certificate Processing System
- 2) The SOAP web server and the database storage
- 3) The web
- 4) The Customs System
- 5) The SOAP web client and the database storage

The SOAP request is sent via the web to the Customs System where it is saved to the database and a SOAP response is sent back to the Certificate Processing System.

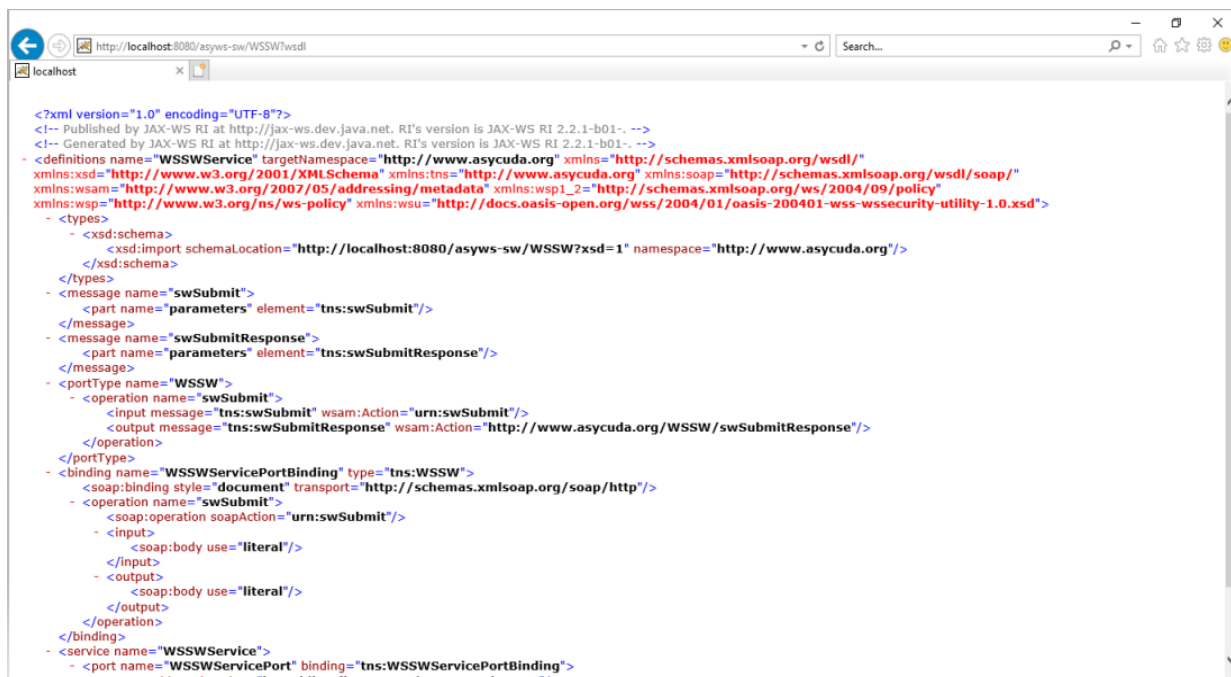


Fig. 15. SOAP Web Service (WSDL).

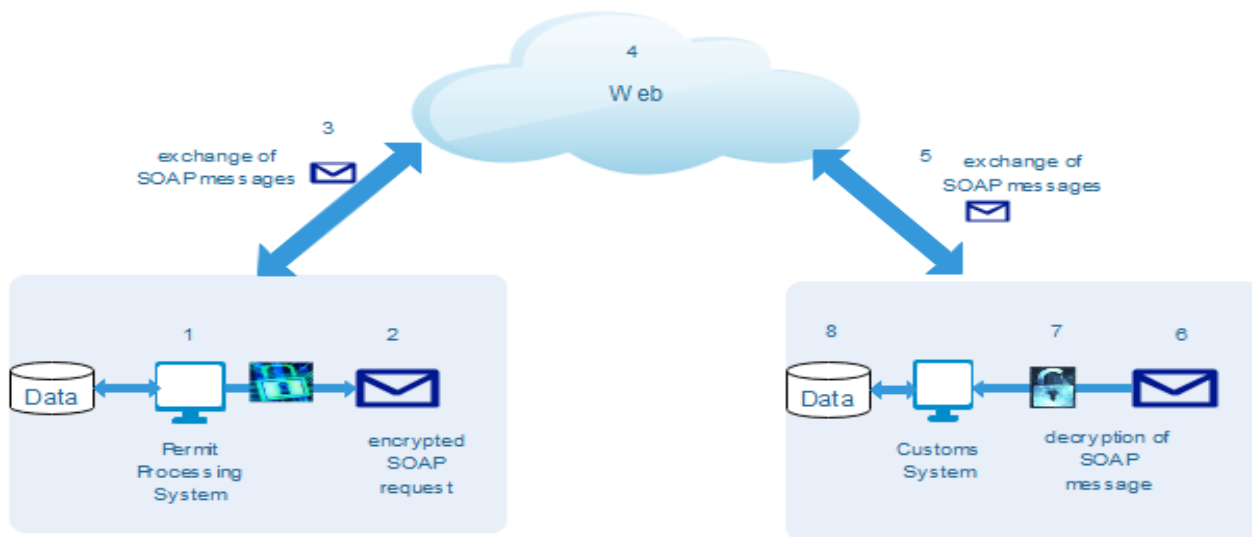


Fig. 16. System Architecture.

VI. RESULTS AND DISCUSSION

In the prototype developed, an application for a permit was submitted on the Certificate Processing System which was approved. Once the officer clicked the approval button the web service is invoked and a SOAP request message is generated as shown in Fig. 17. The SOAP request is encrypted and converted to an object as shown in Fig. 18.

The encrypted SOAP request is transmitted via the web and reduces the chances of data alteration, data theft because the data is encrypted using a public key. The recipient of the data uses the private key to decrypt the data. The importer/exporter uses the received digital certificate to frame an entry on the customs processing system as shown in Fig. 19.

```
public static byte[] encrypt(String soapRequest, PublicKey publicKey) throws Exception {
    Cipher encryptCipher = Cipher.getInstance("RSA");
    encryptCipher.init(Cipher.ENCRYPT_MODE, publicKey);
    //byte[] cipherText = encryptCipher.doFinal(soapRequest.getBytes());
    return encryptCipher.doFinal(soapRequest.getBytes());
}
```

Fig. 17. Java Code with Encryption of SOAP Request

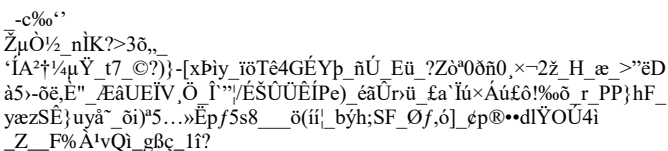


Fig. 18. Encrypted SOAP Object.

Importer No. 100001420 JONES MWANGALA	Customs Office CHR	Registration Date 22/01/2018				
Exporter No.	Reference No. 2018 2	Single Window App. ID I201801CHR0001				
Hs.code 10051000000	Goods.Desc Maize seed	Per No I201801CHR0...	Origin ZA	Valid From 22-Jan-18	Valid To 21-Feb-18	Qty 6,000

Fig. 19. Received digital certificate

This ensures that only approved certificates from the Certificate Processing System are used during importation and exportation. Clients will no longer present physical documents at the customs boarder offices. This solves the challenges of invalid certificates, forged certificates and prevents unauthorized entry of banned goods. It's important to note that a weak key generation makes RSA very vulnerable to attacks therefore care must be taken to ensure that two large random prime numbers are used to calculate the modulus.

The model can be used as a baseline model for the exchange of data/information between government agencies that wish to share information between different information systems. This model can be used as an aid to e-government. The RSA security algorithm implemented helps to achieve data confidentiality, integrity and availability of data.

VII. CONCLUSION

In this paper, a secure SOAP web service model has been developed. The model is used for certificate data exchange between heterogeneous systems. The model helps to solve the data security challenges being faced by many governments and organizations. The model can be used as a framework for implementation of e-government especially that the model provides a cheaper platform for data exchange.

Future work includes the exploration of penetration tests to ensure data being exchanged over the web is secure from cyber -attacks. The research can be carried out to ascertain the extent of accessing the SOAP data request being exchanged while it's in transit over the web using various packet sniffer tools.

ACKNOWLEDGMENT

The authors would like to thank the Zambia Revenue Authority (ZRA) and Ministry of Agriculture (MOA) for the support given during this research. Appreciation also goes to staff at the University of Zambia for the support rendered during the research.

REFERENCES

[1] "http://www.agriculture.gov.zm/," [Online]. [Accessed 18 July 2018].
[2] G. o. t. R. o. Zambia, "http://www.parliament.gov.zm/sites/default/files/documents/acts/Control%20of%20Goods%20Act.pdf," Government of the Republic of Zambia. [Online].

[3] Z. R. Authority, "https://www.zra.org.zm/main.htm?actionCode= show HomePageLnclck," [Online].
[4] "http://www.times.co.zm/?p=95579," [Online].
[5] M. Z. Gashti, "Investigating Soap and Xml Technologies in Web Services," Journal on Soft Computing, vol. 3, no. 4, 2012.
[6] "Information technology — Security techniques — Information security management systems — Requirements," 2005.
[7] "www.iso.org," [Online].
[8] R. Bhanot and R. Hans, "A Review and Comparative Analysis of Various Encryption Algorithms," International Journal of Security and Its Applications, 2015.
[9] P. Mahajan and A. Sachdeva, "A Study of Encryption Algorithms AES, DES and RSA for Security," Global Journal of Computer Science and Technology Network, Web & Security, 2013.
[10] A. A. Hasib and A. A. Haque, "A comparative study of the performance and security issues of AES and RSA cryptography," in Proceedings. -3rd International.Conference. Convergence. Hybrid Information. Technology, 2008.
[11] R. H. Rathod and C. Dhote, "Comparison of symmetric key encryption algorithms," International Journal of Research in Information Technology (IJRIT), 2014.
[12] R. R. S. A. A. L, "A method for obtaining Digital Signatures and Public Key cryptosystems," Communication of the ACM, 1983.
[13] S. Nisha and M. Farik, "RSA Public Key Cryptography Algorithm—A Review," International journal of scientific & technology research, 2017.
[14] T. Bala and Y. Kumar, "Asymmetric Algorithms and Symmetric Algorithms: A Review," International Conference on Advancements in Engineering and Technology.
[15] H. A. Hamad, "Xml based data exchange in the heterogenous Databases (XDEHD)," International Journal of Web & Semantic Technology, 2015.
[16] M. Arenas and L. Libkin, "XML Data Exchange: Consistency and Query Answering".
[17] C.-x. Zhang, Y.-x. Hu, G.-b. Zhang and S. Jin, "Data Exchange based on Web Services," International Journal of Computer Science and Network Security, 2006.
[18] P. Dinesh, P. J. Charles and S. BrittoRamesh, "Security Issues in Web Services," International Research Journal of Engineering and Technology, 2016.
[19] D. Harris, L. Khan, R. Paul and T. Bhavani, "Standards for secure data sharing across organizations," Dallas, 2007.
[20] R. Datt, N. N. Jani, R. Mishra and P. Ajay, "Data Exchange Model Using Web Service For Herogeneous Databases," International Journal Of Advanced Research In Engineering And Technology, vol. 6, no. 4, 2015.
[21] A. A. Chandio, D. Zhu, A. H. Sodhro and M. U. Syed, "An Implementation of Web Services for Inter-Connectivity of Information Systems," International Journal of Computing and Digital Systems, 2014.
[22] V. V. Tan, . D.-S. Yoo and M.-J. Yi, "Efficient Web Service Based Data Exchange for Control and Monitoring Systems," International Journal of Information Technology, 2008.
[23] M. Mwanza and J. Phiri, "Fraud detection on bulk tax data using business intelligence data mining tool: A case of Zambia revenue authority," International Journal of Advanced Research in Computer and Communication Engineering, vol. 5, no. 3, pp. 793-798, March 2016.
[24] J. Phiri and T. Zhao, "Identity Attributes Quantitative Analysis and the Development of a Metrics Model using Text Mining Techniques and Information Theory," Proceedings of IEEE International Conference on Information Theory and Information Security, pp. 390-393, 2010.

New Approach based on Model Driven Engineering for Processing Complex SPARQL Queries on Hive

Mouad Banane¹, Abdessamad Belangour²
Ben M'sik Faculty of Science, Hassan 2 University
Casablanca, Morocco

Abstract—Semantic web technologies are increasingly used in different domains. The core technology of the Semantic Web is the RDF standard. Today with the growth of RDF data it requires systems capable of handling these large volumes of data and responding to very complex requests at the join level. Several RDF data processing systems have been proposed, but are not dedicated to handling complex SPARQL queries. In this paper we present a new approach based on model driven engineering for processing complex SPARQL queries using one of the big data processing tools named Hive. We evaluate our system using three datasets from LUBM Benchmark. The results of this evaluation show the performance, and the scalability of our approach, also give very interesting results when it is compared with existing works.

Keywords—SPARQL; big data; model driven engineering; RDF

I. INTRODUCTION

Since its appearance in the early 1990s, the web has profoundly transformed contemporary society. It is now ubiquitous in our lives, whether in the way we communicate, work, play, buy products, and so on. It is now the most used application of the Internet to create, share and use information.

Victim of its success, the web has become a huge reservoir of information that sometimes makes finding information difficult, especially when it comes to finding reliable and relevant information. Faced with this problem, web inventor Tim Berners-Lee came up with the idea of adding "semantics" to web documents [1]. This idea considers the semantic web as an evolution of the web that would allow the available data (content and links) to be more easily usable and interpretable by both human and machine.

In the Semantic Web, information contained in resources such as web pages, databases, services ... will be available and understandable not only for men but also for machines, programs or IT agents. The Semantic Web is designed so that the content of resources on the Web can be made semantically "understandable" and accessible by software. Resources available on the Internet such as documents, images, services or even physical resources that are not on the Internet but their references are available such as physical books, people have an associated semantics. Thanks to this semantics, the organization, the backup, the search for information could be realized, processed automatically by software. The semantics of the content of resources in the Semantic Web must, therefore, be made explicit and available to the machines in a formal and standardized representation. Standardization can

help different programs to interoperate or exchange data. The way to represent semantics in the Semantic Web is to use the RDF standard. Today the amount of RDF data continues to grow in a very remarkable way, it is no longer possible to store all linked data sets on a single machine while being able to evolve requests from multiple and varied users. Thus, such volumes of data have raised the need for distributed storage architectures and query processing frameworks. The arrival of Hadoop and especially its MapReduce framework greatly improved the development of massively parallel applications. Nevertheless, the MapReduce API does not allow complex operations making the development of large programs a difficult task for intermediate programmers. To overcome the limitations, higher level languages have been developed as Hive, providing a declarative way of writing programs that are then automatically translated into MapReduce jobs.

As part of model-driven software engineering, model transformation is an increasingly important activity in the development cycle: code generation, maintenance, code optimization, aspect composition, reverse engineering, etc. Thus, model transformation languages represent prime components of a development environment. The basic object of these languages is the model that requires the definition of new operators, among others, construction, navigation, composition, comparison and evaluation.

On the other hand, the explosion of Web data offers a new challenge to manage them. For the management of these large volumes of data we present a new technique of RDF data queries based on the principle of meta-models that allows to transform a given SPARQL queries into a Hive program. To evaluate the SPARQL2Hive approach we use The Lehigh University Benchmark LUBM [2], the results show the efficiency of SPARQL2Hive when the amount of RDF data is very important.

The outline of the paper is as follows: Section 2 exposes some existing related works on this topic. Section 3 describes semantic web technologies RDF and SPARQL, and also Hive. Section 4 presents our main contribution SPARQL2Hive. Section 5 evaluates and analyzes our approach with the Lehigh University Benchmark. Finally, we conclude in Section 6.

II. RELATED WORK

Recently, many research efforts have been devoted to developing a new scalable RDF data volume management system, such as Jena-HBase [3]: a distributed RDF triplestore based on HBase [4] the NoSQL database management system

The schema of this system consists of two parts storage and querying, it stores the RDF documents in HBase tables, and for querying this data this system uses the Jena Framework to execute the SPARQL queries. PigSPARQL [5] is an RDF data manipulation system, the principle of PigSPARQL is the translation of SPARQL queries into an executable program of PigLatin [6] language of Apache Pig [7], the translation process starts with the analysis than a compile step of algebra, then optimization of algebra before it is translated into PigLatin, this program will be transformed into a Job MapReduce. The work in [8, 9] presents comparative studies of existing systems based on NoSQL technology and which propose the management of large volumes of RDF data according to the NoSQL models: key/value model, document model, column model, and graph model. From us we have presented a new, more detailed [10] study and brings together about all Distributed RDF Stores based on NoSQL. Galarraga et al. present [11] an evolutionary system that is based on a technique for optimization in the case of large volumes of RDF data.

III. PRELIMINARIES

A. RDF

Developed by the W3C as part of the Semantic Web activities, RDF is not strictly speaking a metadata schema. It constitutes a structured data description model inspired by the logic of first-order predicates and graph theory.

Its genericity and flexibility provide an interoperable framework for describing all types of resources in a networked environment such as the Web. RDF is a model that allows expressing assertions in a very simple model comparable to a simple sentence: [subject] [predicate] [object]. Each assertion forms a triple whose different components are expressed as a URI. The interest of RDF lies in the fact that it is possible to exploit RDF triplets without conversion and whatever the vocabulary used, unlike XML for which it is necessary to convert the data if they do not. Do not use the same scheme. Thus, it does not require the different producers to agree strictly on a metadata structure. The expression "social contract written by john jack rousseau" can be expressed by writing an RDF triple, which can be represented as a subject-predicate-object graph (Fig. 1):

B. SPARQL

To enable the construction of RDF data queries, the W3C has developed the SPARQL standard. It is both a protocol, a query language, and a formalism for the expression of results. SPARQL queries are used to dynamically query data in RDF without downloading all raw data.

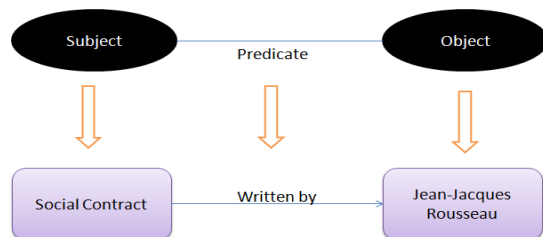


Fig. 1. Example of a RDF Triple.

With RDF and the SPARQL language, it is possible to query the structured information contained in the metadata without having a lower common denominator. As there are many data warehouses structured according to RDF, it is mostly possible to build web or mobile applications with RDF data linked together by URIs. These URIs take mostly the form of URLs, i.e. web addresses. This is the principle of linked data.

C. Model Driven Engineering

In Model Driven Engineering (MDE) [12], a formalism, or modeling language, in which a model is expressed, is described by a meta-model. The meta-model has the particularity of containing all the concepts necessary to create models in a domain, a particular context: the meta-model is at the heart of the MDE. More precisely, the role of a meta-model is to define, as a minimum, the abstract syntax of a formalism, by defining concepts and relations between them [13].

For example, the meta-model of a programming language represents its grammar, the meta-model of an XML file represents its DTD (Document Type Definition). In MDE everything is model, a meta-model is also a model, described according to a certain formalism: the meta-meta-model.

In a MDE context, we call model transformation any program whose inputs and outputs are models. We also speak of "source model" and "target model". Depending on whether a transformation outputs a model or code, it will be referred to as "Model To Model" ("M2M") or "Model To Text" ("M2T"). However, let us nuance this definition, because from a rigorous point of view, in MDE, "everything is model".

IV. SYSTEM ARCHITECTURE

In this section, we present a meta-modeling of our approach. The Metamodel describes our approach independently of the source and target models used. Then, we illustrate the two meta-models of Hive and SPARQL with the case of the transformation of a query of the SPARQL language into a HiveQL program.

The aim of the SPARQL2Hive approach is to transform a given model, expressed in a formalism: SPARQL standard of the Semantic Web into another model expressed in another formalism: Hive tool for the management of Big Data. Fig. 2 illustrates the different stages of operation of our approach. The source model contains a set of elements to transform. We randomly assign a transformation possibility for each element of the source model.

We evaluate, via an objective function, the quality of the proposed transformation. Finally, the last step is to refine the solution or proposed solutions and iterate the different steps until converging towards an acceptable solution (target model of good quality).

We use the principle of model-driven engineering to realize this transformation of SPARQL to Hive, the help is to first realize the two metamodels SPARQL and Hive then in the second stage we propose a transformation between its two meta-models using transformation languages like ATL [14,15].

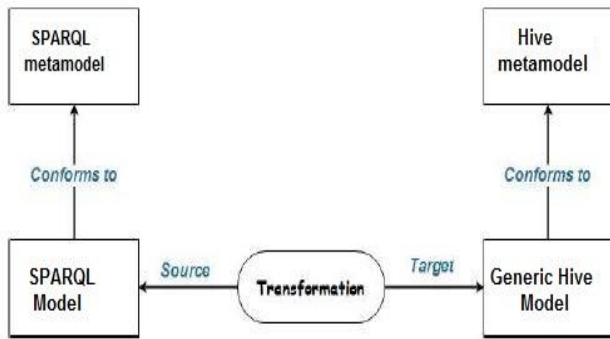


Fig. 2. System Architecture.

A. SPARQL Metamodel

The structure of a SPARQL query is very similar to that used in the SQL language, so a SPARQL query can be a SELECT, ASK, CONSTRUCT query. A SELECT query, of the interrogative type, is used to extract from the RDF graph a subgraph corresponding to a set of resources that satisfy the conditions defined in a WHERE clause. But a CONSTRUCT request, of constructive type, generates a new graph which completes the interrogated graph. In addition, a SPARQL query can have other purposes than providing a set of matches to the variables specified in the SELECT. Indeed, in the SPARQL language, it is possible to ask if a request has at least one solution. To do this, the SELECT is replaced by an ASK.

The SELECT clause contains as SQL: SELECT, FROM and WHERE, There are also other elements in the SPARQL language that make it possible to specify prefixes (PREFIX), conditions (FILTER), disjunctions (UNION), filters on the production of results (LIMIT and OFFSET). Fig. 3 presents the SPARQL meta-model. Fig. 4 presents the Hive meta-model.

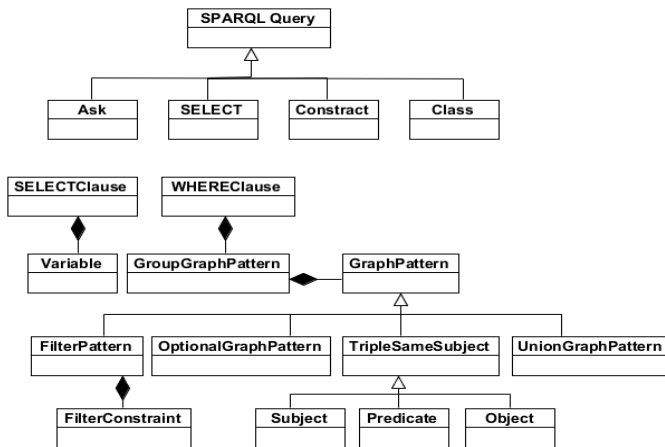


Fig. 3. SPARQL Meta-Model.

B. Hive Meta-model

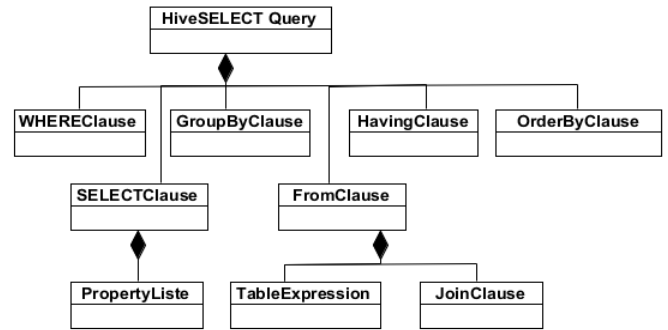


Fig. 4. Hive Meta-Model.

C. Transformation

After the creation of the OMG MDA standard, many tools based on this approach have emerged, such as Atlas Transformation Language (ATL) [15] for model transformation. This language is close to the standard QVT (Query, View, Transformation), proposed by the OMG. This resemblance is historic since ATL is the first attempt to implement QVT [15]. ATL is now one of the most mature model transformation languages, so naturally we chose this language. Fig. 5 shows our transformation engine.

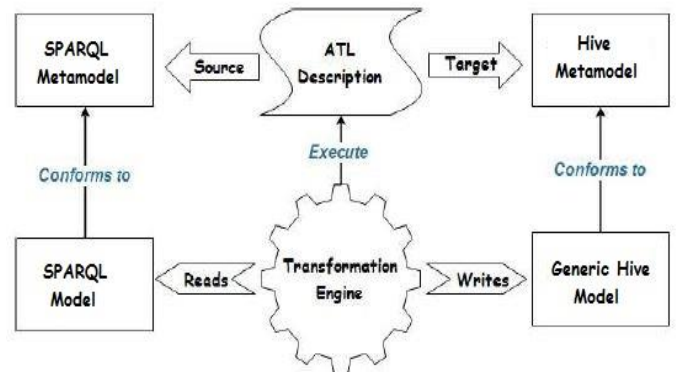


Fig. 5. Transformation Engine.

An ATL program consists of rules that specify how the elements of the target model should be created based on the elements in the source model. These rules are always established according to the following schema:

```

rule Nom_de_la_regle
from
    i: Nom_MM_Source!Nom_Meta-Classe_Source

to
    o: Nom_MM_Cible!Meta-Classe_Cible
    Attribut1 <- i.AttributA,
    Attribut2 <- i.AttributB+i.AttributA,
    
```

- Rule, from and to are the language instructions.

- i (resp., o) is the name of the variable that in the body of the rule represents an instance of the source (or target) meta-class in the source (or target) model.
- *Attribute1,2* (respectively A, B) are the attributes of the target meta-class (or source) of the target (or source) meta-model.

The exclamation point is used to specify which meta-model belongs to a meta-class. A translation into everyday language would give:

The Rule *rule* creates for each instance i identified in the source model an instance o of the target meta-class in the target model, giving *Attribut1* the value of *AttributA* and *Attribut2* the value of the sum *AttributA* plus *AttributB*.

ATL makes it possible to factorize the rules with the use of helper, which one can assimilate to functions.

The execution of this transformation gives the result obtained in the following figure (Fig. 6).

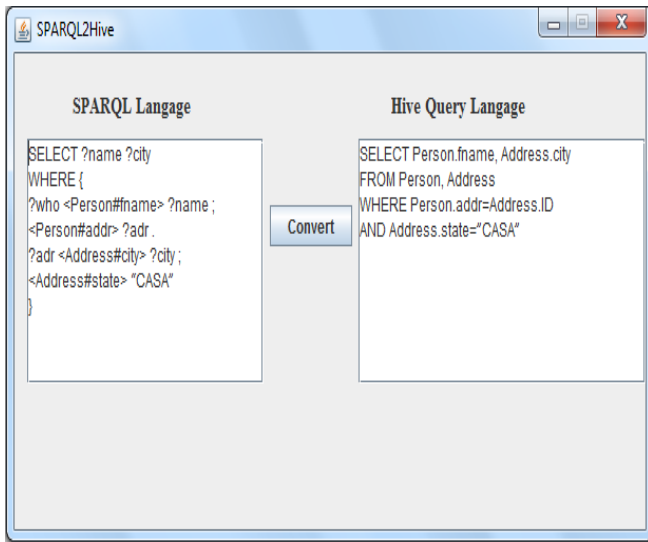


Fig. 6. Conversion Example of SPARQL Query to HiveQL.

V. EVALUATION

To evaluate our approach, we performed a validation using the LUBM Benchmark [16], we execute LUBM queries on three datasets of different sizes to better analyze our SPARQL2Hive system. We present, in the first subsection, the context of our experiments. Then we will analyze the results obtained. Finally, we will evaluate the impact of the size of the sample database on the quality of model transformation.

SPARQL2Hive is implemented on the Hadoop 3.xy version and the Hive 3.1.0 version on a machine with a 2.3 GHz Intel Xeon processor; this machine can store up to 4 TB of hard disk storage and RAM storage of 16 GB. LUBM1, LUBM2 and LUBM5 these three datasets used in this experiment, they have the following triplets' number: 138 million triples, 275M and 689M and the sizes of these three datasets are: 11.4 GB, 22, 77 GB and 56, 8 GB. The results obtained for the loading time of these three games to give are presented in Table I:

TABLE I. LOADING TIME

Dataset	LUBM1	LUBM2	LUBM5
Loading Time(ms)	1,26	3,05	7,9

TABLE II. SYSTEM RUNTIME FOR LUBM QUERIES (MS)

Queries	LUBM1	LUBM2	LUBM5
Q1	481	537	752
Q2	429	516	641
Q3	535	583	633
Q4	509	621	627
Q5	743	797	851
Q6	657	720	773
Q7	678	736	794
Q8	179	216	201
Q9	129	130	142
Q10	181	237	252
Q11	121	135	150
Q12	83	103	126
Q13	376	405	451
Q14	325	361	404

Table II illustrates the results of running the 14 LUBM queries on the three instances of this Benchmark.

We compare our SPARQL to Hive system with Jena by always using the three datasets LUBM1, LUBM2, LUBM5, generally on the majority of the queries; SPARQL2hive is more powerful than Jena at the runtime of LUBM Benchmark queries. Figures 7, 8, 9, 10, 11, 12, 13, 14, 15, and 16 show the results of this comparison for all LUBM queries.

The results obtained after this experiment show the SPARQL2Hive efficiency when the RDF data volume is very large, SPARQL2Hive does not take a lot of time to load the data. Because it performs a simple translation of a given SPARQL query into a program Hive [17], Query Language. But with the Jena Framework, the operation becomes a little complicated because the request goes through a set of steps, which takes a lot of time, especially for loading data, preparing data for recovery, more than Jena uses a lot of resources such as RAM.

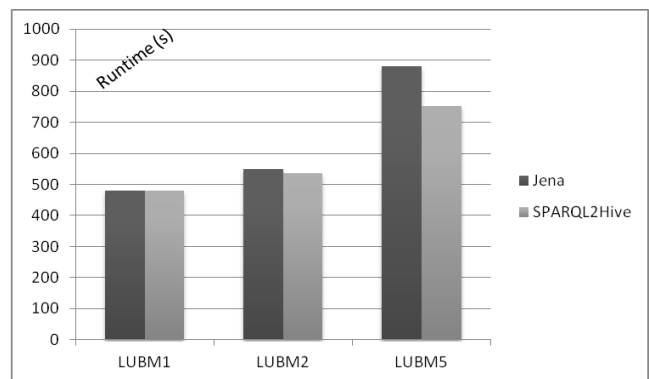


Fig. 7. LUBM Q1 Runtime.

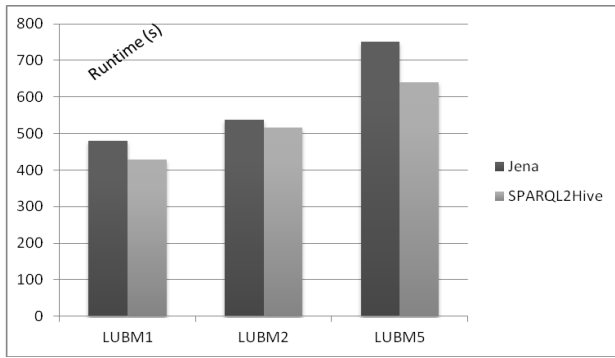


Fig. 8. LUBM Q2 Runtime.

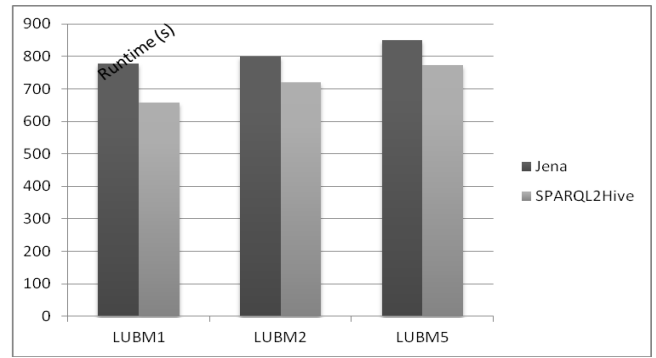


Fig. 12. LUBM Q6 Runtime.

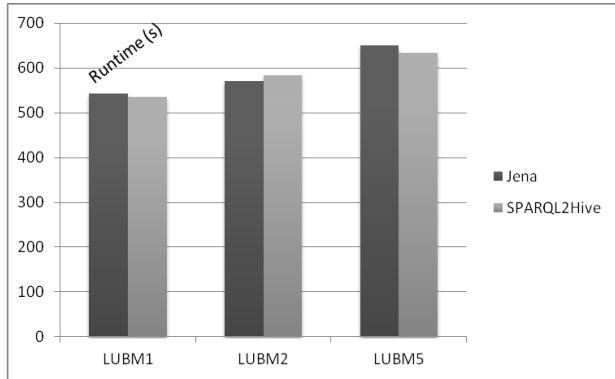


Fig. 9. LUBM Q3 Runtime.

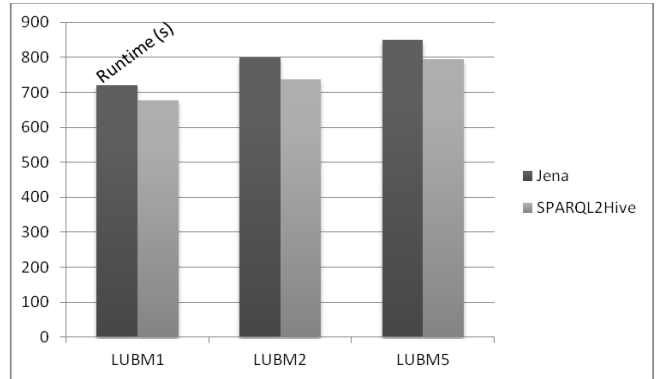


Fig. 13. LUBM Q7 Runtime.

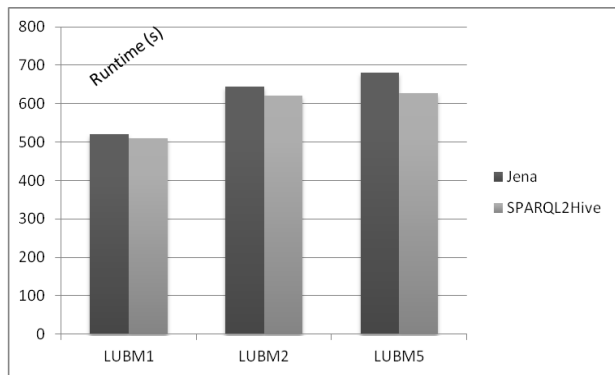


Fig. 10. LUBM Q4 Runtime.

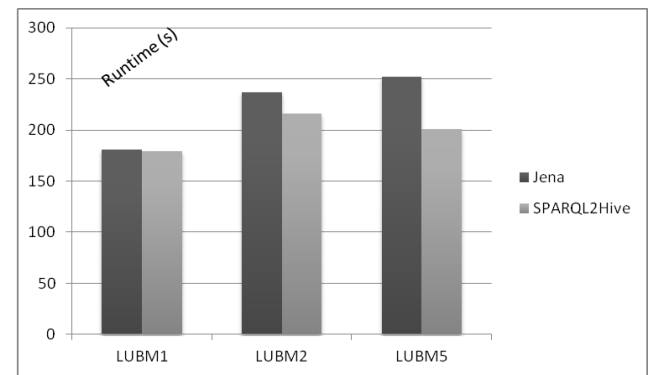


Fig. 14. LUBM Q8 Runtime.

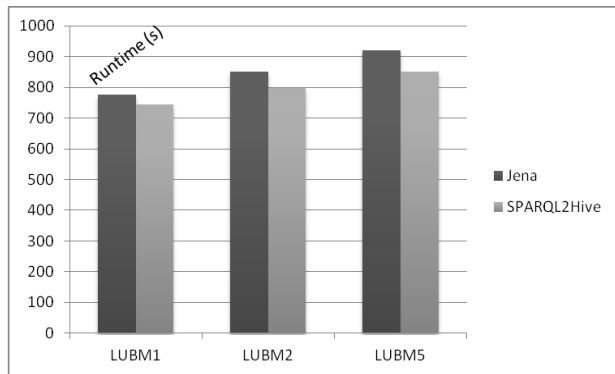


Fig. 11. LUBM Q5 Runtime.

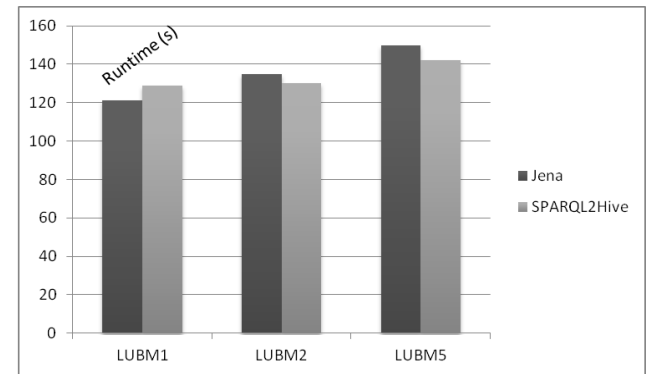


Fig. 15. LUBM Q9 Runtime.

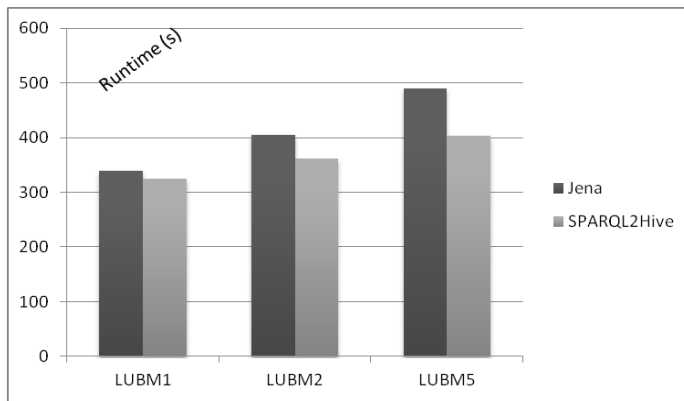


Fig. 16. LUBM Q14 Runtime.

VI. CONCLUSION AND FUTURE WORK

The explosion of RDF data offers a new challenge for researchers to manage these large volumes of RDF data, searches are oriented towards Big Data storage systems like HBase, and for management we find query systems like Hive. In this work, we presented SPARQL2Hive a system based on the principle of meta-models for transforming a SPARQL query into a HiveQL program. In our future work we are going to work on RDF data management in real time, we combine the solution to present in this work with a streaming system like Spark streaming and Storm.

REFERENCES

- [1] Schmidt, M. (2018). Foundations of SPARQL query optimization. PhD Thesis, Albert-Ludwigs-Universität Freiburg (Germany).
- [2] Chebotko, A., Lu, S., Jamil, H. M. et Fotouhi, F. (2006). Semantics Preserving SPARQL-to-SQL Query Translation for Optional Graph Patterns. Technical Report TR-DB-052006-CLJF.
- [3] V. Khadilkar, M. Kantarcioglu, B. Thuraisingham, et P. Castagna, « Jena-HBase: A Distributed, Scalable and Efficient RDF Triple Store », p. 4
- [4] Azqueta-Alzúaz, Ainhoa, et al. "Massive data load on distributed database systems over HBase." Proceedings of the 17th IEEE/ACM International Symposium on Cluster, Cloud and Grid Computing. IEEE Press, 2017.
- [5] Schätzle, Alexander, Martin Przyjaciél-Zablocki, and Georg Lausen. "PigSPARQL: Mapping SPARQL to pig latin." Proceedings of the International Workshop on Semantic Web Information Management. ACM.
- [6] Fuad, Ammar, Alva Erwin, and Heru Purnomo Ipung. "Processing performance on Apache Pig, Apache Hive and MySQL cluster." Proceedings of International Conference on Information, Communication Technology and System (ICTS) 2014. IEEE.
- [7] I. Kurtev, « State of the Art of QVT: A Model Transformation Language Standard », in Applications of Graph Transformations with Industrial Relevance, vol. 5088, A. Schürr, M. Nagl, et A. Zündorf, Éd. Berlin, Heidelberg: Springer Berlin Heidelberg, 2008, p. 377-393.
- [8] Banane, M., Belangour, A., & Labriji, E. H. (2018). RDF Data Management Systems Based on NoSQL Databases : A Comparative Study, 58(2), 98–102
- [9] Banane M., Belangour A., El Houssine L. (2019) Storing RDF Data into Big Data NoSQL Databases. In: Mizera-Pietraszko J., Pichappan P., Mohamed L. (eds) Lecture Notes in Real-Time Intelligent Systems. RTIS 2017. Advances in Intelligent Systems and Computing, vol 756. Springer, Cham.
- [10] Banane M., Belangour A. (2019) A Survey on RDF Data Store Based on NoSQL Systems for the Semantic Web Applications. In: Ezziyyani M. (eds) Advanced Intelligent Systems for Sustainable Development (AI2SD'2018). AI2SD 2018. Advances in Intelligent Systems and Computing, vol 915. Springer, Cham
- [11] Galárraga L., Hose K., Schenkel R.: Partout: A distributed engine for efficient RDF processing. Proceedings of the companion publication of the 23rd international conference on World Wide Web companion, International World Wide Web Conferences Steering Committee, 2014, p. 267-268
- [12] Da Silva, Alberto Rodrigues. "Model-driven engineering: A survey supported by the unified conceptual model." Computer Languages, Systems & Structures 43 (2015): 139-155.
- [13] Boussaïd, Ilhem, Patrick Siarry, and Mohamed Ahmed-Nacer. "A survey on search-based model-driven engineering." Automated Software Engineering 24.2 (2017): 233-294.
- [14] ATLAS group, LINA & INRIA: ATL: Atlas Transformation Language, User Manual, Nantes, January 2005,
- [15] F. Jouault et I. Kurtev, « Transforming Models with ATL », in Satellite Events at the MoDELS 2005 Conference, vol. 3844, J.-M. Bruel, Éd. Berlin, Heidelberg: Springer Berlin Heidelberg, 2006, p. 128-138.
- [16] Y. Guo, Z. Pan, and J. Heflin. LUBM: A benchmark for OWL knowledge base systems. J. Web Sem., 3(2-3):158–182, 2005
- [17] Du, Dayong. Apache Hive Essentials. Packt Publishing Ltd, 2015.

Improved Cryptanalysis of Provable Certificateless Generalized Signcryption

Abdul Waheed¹

School of Electrical and Computer Engineering
Seoul National University Korea Republic of
Department of Information Technology
Hazara University Mansehra, KP

Nizamud Din³

Department of Computer Science
University of Chitral, KP

Arif Iqbal Umar⁵

Department of Information Technology
Hazara University Mansehra, KP

Jawaid Iqbal²

Department of Information Technology
Hazara University Mansehra, KP

Shahab Ul Islam⁴

Department of Computer Science
IQRA National University

Noor Ul Amin⁶

Department of Telecommunication
Hazara University Mansehra, KP

Abstract—Certificateless generalized signcryption adaptively work as certificateless signcryption, signature or encryption scheme having single algorithm for suitable storage-constrained environments. Recently, Zhou et al. proposed a novel Certificates generalized scheme, and proved its ciphertext indistinguishability under adaptive chosen ciphertext attacks (IND-CCA2) using Gap Bi-linear Diffie-Hellman and Computational Diffie-Hellman assumption as well as proved existential unforgeability against chosen message attacks (EUF-CMA) using the Gap Bi-linear Diffie-Hellman and Computational Diffie-Hellman assumption in random oracle model. In this paper, we analyzed Zhou et al. scheme and unfortunately proved IND-CCA2 insecure in encryption and signcryption modes in defined security model. We also present a practical and improved scheme, provable secure in random oracle model.

Keywords—Digital signature; certificateless encryption; certificateless generalized signcryption; malicious-but-passive KGC; random oracle model

I. INTRODUCTION

Diffie-Hellman [2] introduced the concept of trapdoor one way function, while the concept of encryption and digital signature using public key approach were realized by Rivest, Shamir and Adleman [3], within Public Key Infrastructure (PKI). PKI has centralized and hierarchical infrastructure, consists of trusted third party provides solution for proving public keys authenticity. It most commonly use in scalable communication environment, but having limitations such as high cost, storage cost, difficult to verify, revoke of certificates and its distribution. To make certificate management more simple for public key in PKI Shamir [4] introduced notion of Identity Based Encryption (IBE), later on Boneh Franklin [5] realized in 2001 using Weil pairing. IBE has limitations having lacking of scalability and compromising Private Key Generator (PKG), which lead to compromise whole system and over authority of PKG. Riyami and Paterson [6] first time gave Certificateless Public Key Cryptography (CL - PKC) concept, a more flexible infrastructure in-between PKI and IBE. The role of PKG split between user and Key Generation Center (KGC). User identity and associated public key used for composition of key pair. It does not require pricey infrastructure like PKI and cope the limitations of

IBE. An alternative to sign-then-encrypt approach, Zheng [7] first proposed a novel and efficient crypto primitive named signcryption in PKI, while Barbosa and Farshim [8] first coined the concept of certificateless signcryption.

Signcryption is efficient when combined authenticity and confidentiality are required. However, in scenario where one or both of authenticity and confidentiality is required separately or simultaneously a signature or encryption or signcryption will be used, which is optimal in memory constrained environments like smart card, sensor networks, etc. This problem was addressed by Han [9] and proposed generalized signcryption (GSC) adaptively works as a signature (if authentication mandatory), encryption scheme (if confidentiality mandatory), or signcryption (if authentication+confidentiality mandatory) scheme within one algorithm. Kushwah and Lal [10] proposed ID Based generalized signcryption (GSC) scheme within a security model for the first time. Huifang et al. [11] first proposed certificateless generalized signcryption (CLGSC) scheme, and introduced CLGSC formal definition and security model. But Kushwah and Lal [12] proved scheme [11] Type I insecurity and introduced new efficient and secure CLGSC scheme. Ji et al. [13] introduced new CLGSC scheme based on [8], and later on [14] proved scheme [8] insecure against IND - CCA2 and EUF - CMA, and thus scheme [13] insecurity also proved indirectly. Au et al. [15] introduced Type - II adversary a novel approach known as "Malicious-but-Passive Key Generation Center" (MP - KGC). Hwang et al. [16] proposed certificateless scheme only for encryption purpose but Xiong et al. [17] proposed certificateless scheme for the purpose of only signature and Weng et al. [18] proposed certificateless signcryption scheme secured against MP - KGC. Zhou et al. [1] introduced a formal security model for new CLGSC (N - CLGSC) scheme and claimed its security against MP-KGC attacks.

In 2013 [19] the concept of heterogeneous signcryption firstly adopted which provided inter-operable environment for communications between sender and receiver and thus in 2016[20] Li et al. introduced heterogeneous signcryption two way communication for PKI and Identity Based Cryptography(IBC) environment but faced heavy cost in the form of pairing. After that IBC to Certificateless (CLC)

scheme also presented in 2017[21] and that same year Wang et al.[22] introduced *ID* based to *PKI* in standard model scheme. These above few heterogeneous schemes found in literature but the generalized form still missing.

We analyzed Zhou et al. [1] *CLGSC* scheme and unfortunately proved *IND – CCA – II* insecure in encryption and signcryption modes in their defined security model. We provided a fix to Zhou et al. *N – CLGSC* and proposed an improved *N – CLGSC(IN – CLGLSC)* scheme. The improved scheme is efficient and secure compare with Zhou et al. *N – CLGSC* and few others found in literature.

Remaining sections of this paper is organizes as: Section 2 gives preliminaries overview and security model. Section 3 presents of Zhou et al. scheme review. Section 4 presents attacks on stated scheme. Section 5 presents attacks over improved scheme. Security and cost analysis are presented in Section 6 and at the end Section 7 conclude paper.

II. PRELIMINARIES

Definitions evoke in following are used in proposed scheme [1].

Let $(G_1, +)$ and $(G_2, +)$ be two additive cyclic group having P_1 and P_2 elliptic curve points generator defined over finite field of order n . Let $G_T(G_1, *)$ be a multiplicative cyclic subgroup of finite field.

A bilinear group description $\Gamma(G_1, G_2, \hat{e}, G_T)$ where $\hat{e} : G_1 \times G_2 \rightarrow G_T$ is able to compute efficient group laws and non degeneracy of bilinear mapping.

Let a bilinear group plan Γ , such that \mathcal{GBDH} assumption is hold if advantages of probabilistic polynomial time(\mathcal{PPT}) intruder defined is considered negligible as below.

$$\text{Adv}_{\Gamma}^{\mathcal{GBDH}}(A; q_{\mathcal{DBDH}}) = \Pr[T := \hat{e}(P, P)^{\tilde{x}\tilde{y}\tilde{z}} | \tilde{x}, \tilde{y}, \tilde{z} \leftarrow Z_p; T \leftarrow A^{O_{\Gamma}(T, \tilde{x}P, \tilde{y}P, \tilde{z}P)}] \quad (1)$$

By O_{Γ} point to the Decisional Bilinear Diffie Hellman oracle is used for tuple $(\tilde{x}P, \tilde{y}P, \tilde{z}P, T)$. The result is 1, if the statement $T := \hat{e}(P, P)^{\tilde{x}\tilde{y}\tilde{z}}$ hold else 0 otherwise, and $q_{\mathcal{DBDH}}$ represents number of queries in $eq(1)$.

Let a bilinear group plan Γ such that in presence of Decisional Bilinear Diffie Hellman oracle assumption if the advantage of \mathcal{PPT} attacker defined under below probability is consider negligible.

$$\text{Adv}_{\Gamma}^{\mathcal{CDBDH}}(A, q_{\mathcal{DBDH}}) = \Pr[Q = \tilde{x}\tilde{y}P | \tilde{x}, \tilde{y} \leftarrow Z_p, Q \leftarrow A^{O_{\Gamma}(\Gamma, \tilde{x}P, \tilde{y}P)}] \quad (2)$$

O_{Γ} and $q_{\mathcal{DBDH}}$ define as above.

Let a bilinear group plan Γ , such that the assumption of Computational Diffie Hellman (\mathcal{CDH}) is hold if the advantage of any \mathcal{PPT} attacker defined under below probability is negligible.

$$\text{Adv}_{\Gamma}^{\mathcal{CDH}}(A) = \Pr[Q = \tilde{x}\tilde{y}P | \tilde{x}, \tilde{y} \leftarrow Z_p; Q \leftarrow A(\Gamma, \tilde{x}P, \tilde{y}P)]. \quad (3)$$

A. Framework of *N-CLGSC*

The *N – CLGSC* defined using five Probabilistic Polynomial Time (\mathcal{PPT}) and one Deterministic Polynomial Time (\mathcal{DPT}) algorithms.

- 1) *Setup* (1^k): Its is a \mathcal{PPT} algorithm executed by \mathcal{KGC} , which takes security parameter (1^k security parameter key and public key pair (m_{pk}, m_{sk}) , with global parameters $params$.
- 2) *Extract-partial-private-key* ($ID, m_{sk}, params$): This \mathcal{PPT} algorithm executed by \mathcal{KGC} , which takes user identity $ID_i \in \{0, 1\}^*$, $params(m_{sk}, params)$ as input, and returns *partial-private-key* D_i .
- 3) *Generates user keys* ($ID, params$): This \mathcal{PPT} algorithm executed by user, which takes $(ID_i, params)$ as input and returns a secret key and public key pairs (x_i, P) .
- 4) *Set-private-key* ($D, x, params$): This \mathcal{PPT} algorithm executed by the user, takes $(ID_i, x_i, params)$ as input and returns full private key S_i .
- 5) *GSC*(m, S_A, ID_s, D_B, ID_B): This \mathcal{PPT} algorithm executed by the user and run in three modes: signature, encryption and signcryption.

- **Signature only mode:** If sender sign message $m \in M$ without definite receiver, it takes inputs (S_A, m, ID_{ϕ}) , with null receiver identity ID_{ϕ} , and returns $\sigma = GSC(m, S_A, ID_{\phi}) = sign(m, S_A)$.
- **Encryption only mode:** If Alice confidentially sends message m to receiver Bob, it takes inputs (m, S_{ϕ}, D_B, ID_B) , with null sender identity S_{ϕ} , and returns $\sigma = GSC(S_{\phi}, m, D_B, ID_B) = encrypt(m, D_B, ID_B)$.
- **Signcryption only mode:** If Alice transmits a message m in an authenticated and confidential way to receiver, it takes inputs (m, S_A, ID_B) , and returns $\sigma = GSC(m, S_A, ID_A, D_B, ID_B) = signcrypt(m, S_A, ID_A, D_B, ID_B)$

- 6) *UGSC*(σ): This \mathcal{DPT} algorithm runs by receiver it takes received σ as input and validate if it is true then decrypts or unsigncrypts and returns message (m) , otherwise return false \perp .

B. Security Analysis

Confidentiality

The *N – CLGSC* notion is captured here to represent two games between challenger (\mathcal{C}) and adversary (\mathcal{A}). First for adversary-I ($\mathcal{A-I}$) and second for adversary-II ($\mathcal{A-II}$).

1) *GAME 01:* (*IND – CLGSC – CCA2 – I*) :

- **Initialization:** Challenger \mathcal{C} start this algorithm and take security parameters k as input and returns $params$ as output to adversary $\mathcal{A-I}$.
- **Find stage:** At this level adversary $\mathcal{A-I}$ makes few oracles adaptively.
- **Challenge:** $\mathcal{A-I}$ selects m_0 and m_1 equal length two distinct messages, ID_A^* is sender's *ID* and ID_B^*

receiver's ID using which he/she makes challenges. Adversary \mathcal{A} -I must have no private key for extraction query on ID_B^* , and also $ID_B^* \neq ID_\phi$ for confidentiality game. Challenger \mathcal{C} selects a bit $\lambda \in \{0, 1\}$ randomly, and runs GSC algorithm with message m_λ using ID_A^* and ID_B^* and returns output (σ^*) as a ciphertext to \mathcal{A} -I.

Guess stage: Just like find stage \mathcal{A} -I makes few queries adaptively. For private key extraction corresponding to ID_B^* does not allow to make UGSC query on ciphertext (σ^*) using private keys of sender and receiver ID_A^* and ID_B^* respectively until to replace with public keys (PK_A^*, PK_B^*) after a challenge. Eventually, \mathcal{A} -I wins the game after output a bit $\hat{\lambda}$ and if $\lambda := \hat{\lambda}$.

Advantage of adversary \mathcal{A} -I define as;

$$Adv_{\mathcal{A}-I}^{IND-CLGSC-CCA2-I} := 2Pr[\lambda := \hat{\lambda}] - 1$$

Note: In above game, we consider only encryption mode of $CLGSC$ where sender private key ID_A^* is equal to zero therefore in challenge phase algorithm runs in only encryption mode. For encryption and signcryption only modes use same confidentiality game.

A *New - CLGSC* scheme is secure against $IND - CLGSC - CCA2 - I$ in encryption only mode or signcryption only mode if it is secure for all Probabilistic Polynomial Time PPT adversary \mathcal{A} -I and game winning consider negligible.

2) **GAME 02 ($IND - CLGSC - CCA2 - II$):** Here in this game k represents security parameters and \mathcal{C} represents simulator.

Simulator \mathcal{C} executes \mathcal{A} -II using input 1^k and *master key gen*. A master key pair (M_{SK}, M_{PK}) set *params* generated by adversary \mathcal{A} -II provides M_{SK} and *set params* to \mathcal{C} without making query to any oracle.

\mathcal{C} executes \mathcal{A} -II on 1^k again with different tag makes above query adaptively and \mathcal{A} -II select two equal length messages (m_0, m_1) and ID_A^*, ID_B^* on which makes challenges. For the purpose of extraction query on ID_B^* \mathcal{A} -II must have no choice to make private key.

\mathcal{C} selects a bit $\lambda \in \{0, 1\}$ randomly, and also runs \mathcal{A} -II using challenged ciphertext σ^* with guess where;

$$\sigma^* \leftarrow GSC(m_\lambda, ID_A^*, ID_B^*)$$

Like step 2 \mathcal{A} -II makes queries again adaptively. Extraction and UGSC query on ciphertext σ^* not allowed. Eventually, \mathcal{A} -II wins the game after output a bit $\hat{\lambda}$ and if $\lambda := \hat{\lambda}$. Advantages of \mathcal{A} -II's is define as;

$$Adv_{\mathcal{A}-II}^{IND-CLGSC-CCA2-II} = 2Pr[\lambda = \hat{\lambda}] - 1$$

Note: At step second in above algorithm, if sender ID_A^* vacant, it will be run in encryption only mode else it will be run in signcryption only mode, for both modes share similar confidentiality game.

$CLGSC$ scheme is to be secured against $IND - CLGSC - CCA2 - II$ in encryption only mode or signcryption only mode if it is secure for all Probabilistic Polynomial

Time PPT adversary \mathcal{A} -II, and consider it negligible to win game.

3) **Unforgeability:** For $EUF - CMA$ the $CLGSC$ security notion is captured here using following two games between challenger (\mathcal{C}) and adversary (\mathcal{A}).

4) **GAME 03 ($EUF - CLGSC - CMA - I$):**

- **Initialization:** This phase is similar to game 01.
- **Queries:** Adversary \mathcal{A} -I makes polynomial time above phases oracles adaptively.
- **Forgery:** \mathcal{A} -I produces (ID_A, ID_B, σ) without exposed private key ID_A where $ID_A = ID_\phi$ for unforgeability game. If final results of UGSC $(\sigma, ID_B, S_B, PK_B, ID_A, PK_A)$ is not \perp \mathcal{A} -I succeed to win game. The advantage of \mathcal{A} -I defines from the probability of their wining.

Note: In above game, we consider $CLGSC$ signature only mode and signcryption only mode. If in forgery phase the sender ID_B^* vacant then algorithm runs in signature only mode else runs in signcryption only mode and that is why we consider similar game for both modes.

A $CLGSC$ scheme $EUF - CLGSC - CMA - I$ is to be declared secure in signature only mode or in signcryption only mode if it secure against all types of PPT adversary \mathcal{A} -I and consider negligible to win the game.

5) **GAME 04 ($EUF - CLGSC - CMA - II$):**

- 1) This phase is similar to game 02.
- 2) challenger \mathcal{C} again invokes \mathcal{A} -II on 1^k with tag *forge*. \mathcal{A} -II makes above oracles polynomial time adaptively.
- 3) At final stage \mathcal{A} -II produces output (ID_A, ID_B, σ) without exposed private key ID_A where $ID_A = ID_\phi$ for unforgeability game.
- 4) If result of UGSC $(\sigma, ID_B, S_B, PK_B, ID_A, PK_A)$ is not \perp then \mathcal{A} -II succeed to win the game. \mathcal{A} -II advantage defines from the probability of victory.

Note: At step 2 of above algorithm, if sender ID_B^* vacant then it will be run in signature only mode else it runs in signcryption only mode and we consider same game for both type modes.

The scheme $N - CLGSC$ will be $EUF - CLGSC - CMA - II$ secured in signature only mode or in signcryption only mode if it is secure for all type of PPT adversary \mathcal{A} -II and consider it negligible to win this game.

III. REVIEW OF ZHOU ET AL. N-CLGSC

In this section of paper, we review Zhou et al. scheme, which has the following algorithms:

- **Setup (1^k):** Given (1^k) , the Key Generation Center chooses two groups $(G_1, +)$ and $(G_2, *)$ having generator P of prime order n , using a bilinear map such that $\hat{e} : G_1 \times G_1 \rightarrow G_2$, 4 hash functions as; $H_1 : \{0, 1\}^* \rightarrow G_1, H_2 : \{0, 1\}^* \rightarrow \{0, 1\}^k, H_3 : \{0, 1\}^* \rightarrow G_1, H_4 : \{0, 1\}^* \rightarrow G_1$, KGC selects random integer $s \in Z_q^*$

and computes $P_{Pub} = sP$ and then defines function like $f(ID_i)$, if $ID_i \in \varphi$, $f(ID_i) = 0$ else $f(ID_i) = 1$ KGC publishes, $\{G_1, G_2, e, q, f(\cdot), P, P_{Pub}, H_1, H_2, H_3, H_4\}$ as system parameters.

Note: At initial stage it is also possible that KGC be malicious.

- **Extract partial private key:** For the given i th user identity ID_i , KGC computes partial private key as $D_i = sQ_i = sH_1(ID_i)$.
- **Generate user keys:** The i th user chooses random integer $x_i \in \mathbb{Z}_q^*$ and computes public key as $PK_i = x_iP$
- **Set private key:** The i th user sets $SK_i = \langle x_i, D_i \rangle$ as a private key.
- $N - CLGSC(m, D_A, ID_A, ID_B, PK_B, PK_A)$:
 - 1) Computes $f(ID_A), f(ID_B)$
 - 2) Chooses random number $r \in \mathbb{Z}_q^*$ and then computes $U = rP$
 - 3) Computes $w := \hat{e}(P_{Pub}, QB)^{rf(ID_B)}$
 - 4) Computes $h = f(ID_B)H_2(w, U, r, PK_B, PK_B, PK_A, ID_A, PK_A, PK_B)$ item Computes $V := h \oplus m$
 - 5) Computes $H = H_3(U, V, ID_A, ID_B, PK_A, PK_B)$
 - 6) Computes $'H = H_4(V, U, ID_A, PK_A, ID_B, PK_B)$
 - 7) Computes $W = f(ID_A)D_A + rH + f(ID_A)x_A$
 - 8) At the end returns c as ciphertext $= (U, V, W)$
- $UGSC(U, V, W, ID_A, ID_B, PK_A, x_B)$:
 - 1) Computes $f(ID_A), f(ID_B)$
 - 2) Computes $H = H_3(U, V, ID_A, PK_A, ID_B, PK_B)$
 - 3) Computes $'H = H_4(U, V, ID_A, ID_B, PK_A, PK_B)$
 - 4) If $\hat{e}(P, W) = \hat{e}(P_{Pub}, QA)^{f(ID_A)} \hat{e}(H, U) \hat{e}(PK_A)$, $'H^{f(ID_A)}$ else return \perp .
 - 5) Computes $w = \hat{e}(U, D_B)^{f(ID_B)}$
 - 6) Computes $h = f(ID_B)H_2(U, w, x_B, U, ID_A, PK_A, ID_B, PK_B)$
 - 7) Computes $m = V \oplus h$
 - 8) Returns m

A. Adaptation

$N - CLGSC$ work adaptively and impeccably switches on user inputs to three different modes according to the applications need without any other additional operation.

- **Signature only mode:** When $ID_A \neq \varphi$, and $f(ID_A) = 1$ as well as $f(ID_B) = 0$, $V = m \oplus h = m$, $c = (U, m, W)$.

- **Encryption only mode:** When $ID_A = \varphi$, and $ID_B \neq \varphi$ then $f(ID_A) = 1$ as well as $f(ID_B) = 0$, $W = rH$, and $c = (U, V, W)$.
- **Signcryption only mode:** When $ID_A \neq \varphi$, and $ID_B \neq \varphi$ then $f(ID_A) = 1$ as well as $f(ID_B) = 1$, $W = D_A + r.H + x_A$ 'H and $c = (U, V, W)$.

IV. CRYPTANALYSIS OF N-CLGSC

In this section of the paper, we presented attack and proved Zhou et al. scheme ($N - CLGSC$) insecure against $IND - CCA2$ under encryption and signcryption only modes and working securely in signature only mode.

• Encryption only Mode

Setup:- Let k represent security parameter and \mathcal{C} represents a simulator and executes \mathcal{A} -II using 1^k and a master-key-generator. \mathcal{A} -II generates a master key pair (M_{SK}, M_{PK}) and params and atedthcalA-II and M_{SK} to \mathcal{C} without making any query to oracle.

Phase 1: Not to ask any queries.

Phase 2: \mathcal{A} -II selects $(m_0$ and $m_1)$ two equal length messages and ID_A^* and ID_B^* to make challenges. For the purpose of extraction query on $ID_B^* := ID_A^*$ \mathcal{A} -II must has no choice to make private key. \mathcal{C} randomly chooses a bit $\lambda \in \{0, 1\}$ and \mathcal{A} -II runs a challenge where ciphertext σ^* and a tag guess where;

$$\sigma^* \leftarrow GSC(m_\lambda, ID_A^*, ID_B^*)$$

- 1) Computes $U^* = r^*P$
- 2) Computes $w^* = \hat{e}(P_{Pub}, QB)^{r^*f(ID_B)}$
- 3) Computes $h^* = f(ID_B, H_2, U^*, w^*, r^*, PK_A, PK_B)$
- 4) Computes $V^* = m_\beta^* \oplus h^*$
- 5) Computes $H^* = H_3(U^*, V^*, ID_B, PK_A, PK_B)$
- 6) Computes $'H^* = H_4(U^*, V^*, ID_B, PK_A, PK_B)$
- 7) Computes $W^* = 0.ID_A + r^*, H^* = r^*H^*$
- 8) Returns ciphertext $c^* = (U^*, V^*, W^*)$

Sent $c^* = (U^*, V^*, W^*)$ to \mathcal{A} .

Upon receipt of the challenge ciphertext $c^* = (U^*, V^*, W^*)$, \mathcal{A} computes

- 1) Computes $H^* = H_3(U^*, V^*, ID_B, PK_A, PK_B)$
- 2) Computes $r^* = \frac{W^*}{H^*}$
- 3) Chooses another equal length message m^+ as that of m_β^*
- 4) Computes $V^+ = V^* \oplus m^+$
- 5) Computes $H^+ = H_3(U^*, V^+, PK_A, ID_B, PK_B)$
- 6) Computes $W^+ = r^*H^+$

\mathcal{A} can legally queries $c^+ = (U^*, V^+, W^+)$ to \mathcal{C} , as $c^* = c^+$. \mathcal{C} will certainly return $m_\beta^* \oplus m^+$ to \mathcal{A} and \mathcal{A} can compute $m_\beta^* = m_\beta^* \oplus m^+ \oplus m^+$, guess the β and wins the game. Hence it is proved that $N - CLGSC$ insecure against $IND - CCA2$ in encryption only mode.

• Signcryption only Mode

In this section of the paper, we presented an attack and proved that Zhou et al. provable certificateless generalized

signcryption scheme ($N - CLGSC$) is not $IND - CCA2$ secure in signcryption mode also.

Setup: Same as in encryption mode.

Phase 01: Same as in encryption mode.

Phase 02: \mathcal{A} -II provides (m_0, m_1) two equal length messages and sender's identity ID_A^* and receiver's identity ID_B^* use for challenge. \mathcal{A} -II not to be allowed for private key extraction query on ID_B^* , as $ID_B^* = ID$ using for confidentiality game. The challenger \mathcal{C} picks a bit $\beta \in \{0, 1\}$ randomly and runs \mathcal{A} -II takes a challenged ciphertext σ^* as input a challenged ciphertext $\sigma^* \leftarrow GSC(m_\beta, ID_A^*, ID_B^*)$.

- 1) Computes $U^* = r^*P$
- 2) Computes $w^* = \hat{e}(P_{Pub}, QB)^{r^*f(ID_B)}$
- 3) Computes $h^* = f(ID_B, H_2)(U^*, w^*, r^*, PK_A, PK_B, ID_B)$
- 4) Computes $V^* = m_b^* \oplus h^*$
- 5) Computes $H^* = H_3(U^*, V^*, PK_A, ID, PK_B)$
- 6) Computes $\hat{H}^* = H_4(U^*, V^*, PK_A, ID_B, PK_B)$
- 7) Computes $W^* = f(ID_A).D_A + r^*H^* + f(ID_A)x_A \hat{H}^*$
- 8) At the end send ciphertext $c^* := (V^*, U^*, W^*)$

to \mathcal{A} . On the receiving challenged ciphertext $c^* = (U^*, V^*, W^*)$, In above generalized signcryption process $H^* = \hat{H}^*$ as $H_3 : \{0, 1\}^* \rightarrow G_1, H_4 : \{0, 1\}^* \rightarrow G_1$ and $H^* = H_3(U^*, V^*, PK_A, ID_B, PK_B), \hat{H}^* = H_4(U^*, V^*, PK_A, ID_B, PK_B), \mathcal{A}$ computes

- 1) Computes $(r^* + x_A) H^* = r^*H^* + x_A' H^* = W^* - f(ID_A).D_A$
- 2) Computes $H^* = H_3(U^*, V^*, PK_A, ID, PK_B)$
- 3) Computes $(r^* + x_A) = \frac{(r^* + x_A) \hat{H}^*}{H^*}$
- 4) Chooses another equal length message m^+ as that of m_β^*
- 5) Computes $V^+ = V^* \oplus m^+$
- 6) Computes $H^+ = H_3(U^*, V^+, PK_A, PK_B, ID_B)$
- 7) Computes $W^+ = ID_A + (r^* + x_A)H^* = ID_A + r^*H^* + x_A H^*$

\mathcal{A} can legally queries $c^+ = (U^*, V^+, W^+)$ to \mathcal{C} , as $c^* = c^+$. \mathcal{C} will certainly return $m_\beta^* \oplus m^+$ to \mathcal{A} and \mathcal{A} can compute $m_\beta^* = m_\beta^* \oplus m^+ \oplus m^+$, guess the β and wins the game.

Hence here also proved insecurity of $N - CLGSC$ under $IND - CCA2$ in signcryption only mode.

V. IMPROVED N-CLGSC

This section represents improved scheme, we proposed an Improved scheme ($IN - CLGSC$) scheme, comprises on the following algorithms:

- **Setup (1^k):** Given (1^k) , two groups $(G_1, +)$ using generator P and $(G_2, *)$ respectively to be chosen by KGC using prime order n , a bilinear map \hat{e} , and 4 hash functions such that; $H_1 : \{0, 1\}^* \rightarrow G_1, H_2 : \{0, 1\}^* \rightarrow G_1, H_3 : \{0, 1\}^* \rightarrow G_1, H_4 : \{0, 1\}^* \rightarrow G_1, KGC$ selects a random integer $s \in Z_q^*$ as a master key and computes $P_{Pub} = sP$ and then defines like function $f(ID) \mid if ID \in \varphi, f(ID) = 0$ else $f(ID) =$

1. KGC publishes following system parameters as $G_1, G_2, q, f(\cdot), P_{Pub}, e, H_1, H_2, H_3, H_4$.

- **Note:** At the initial stage it is also possible that KGC be malicious.

- **Extract partial private key:** Given the i th user identity ID_i , KGC computes partial private key as $D_i = sQ_i = sH_1(ID_i)$.

- **Generate user keys:** Given i th user partial private key D_i and identity ID_i chooses random integer $x_i \in Z_q^*$ and thus computes public key $PK_i = x_i P$.

- **Set private key:** The i th user sets $SK_i = \langle x_i, D_i \rangle$ as a private key.

- $IN - CLGSC(m, D_A, ID_A, ID_B, PK_B, PK_A,):$

- 1) Computes $f(ID_A), f(ID_B)$
- 2) select a random integer value $r \in Z_q^*$
- 3) Computes $U := r.P$,
- 4) Computes $w := \hat{e}(P_{Pub}, QB)^r f(ID_B)$,
- 5) Computes $h := f(ID_B)H_2(U, w, r.PK_B, ID_A, PK_A, ID_B, PK_B)$
- 6) Computes $V := m \oplus (ID_A || ID_B) \oplus h$
- 7) Computes $H := H_3(U, V, w, ID_A, PK_A, ID_B, PK_B)$,
- 8) Computes $\hat{H} := H_4(U, V, ID_A, PK_A, ID_B, PK_B)$,
- 9) Computes $W := f(ID_A)D_A + r.H + f(ID_A)x_A' H$
- 10) At the end returns ciphertext $c = (U, V, W)$ forward to receiver.

- $U - IN - CLGSC(U, V, W, ID_A, ID_B, PK_A, x_B)$

- 1) Computes $f(ID_A), f(ID_B)$,
- 2) Computes $w := \hat{e}(U, D_B), f(ID_B)$,
- 3) Computes $H := H_3(U, V, w, ID_A, ID_B, PK_A, PK_B)$
- 4) Computes $\hat{H} := H_4(U, V, ID_A, ID_B, PK_A, PK_B)$
- 5) If $\hat{e}(P, W) := \hat{e}(P_{Pub}, Q_A) f(ID_A) \hat{e}(U, H) \hat{e}(PK_A, \hat{H})$, $f(ID_A)$ else returns \perp .
- 6) Computes $h := f(ID_B)H_2(U, w, x_B, U, ID_A, PK_A, ID_B, PK_B)$
- 7) Computes $m := V \oplus (ID_A || ID_B) \oplus h$
- 8) Returns m .

A. Variation

$IN - CLGSC$ works adaptively and impeccably switches on inputs of users, to three different modes according to the applications need without any other additional operation.

- **Signature only mode:** when $ID_A \neq \varphi$, and $ID_B = \varphi$ then the value of $f(ID_A) = 1$, and $f(ID_B) = 0, V = mh = m, c = (U, m, W)$.
- **Encryption only mode:** when $ID_A = \varphi$, and $ID_B \neq \varphi$ then the value of $f(ID_A) = 0$, and $f(ID_B) = 1, W = r.H$, and $c = (U, V, W)$.
- **Signcryption only mode:** when $ID_A \neq \varphi$, and $ID_B \neq \varphi$ then the value of $f(ID_A) = 1$ and $f(ID_B) = 1, W = D_A + r.H + x_A' H$, and $c = (U, V, W)$.

VI. ANALYSIS OF IN-CLGSC

This section of paper provides detail analysis. First part is correctness then security and cost analysis of our $IN - CLGSC$ scheme.

A. Correctness

The correctness proofs of Zhou et al. $N - CLGSC$ and $IN - CLGSC$ are same. As the proofs had not discussed in the existing scheme but here we demonstrate correctness proofs also as;

- Signcryption only mode

If ID , and $f(ID_A) = 1$ then

$$\begin{aligned} \hat{e}(P, W) &= \hat{e}(P, D_A + r.H + x'_A H) \\ &= \hat{e}(P, D_A) \hat{e}(P, r.H) \hat{e}(P, x'_A H) \\ &= \hat{e}(P, s.Q_A) \hat{e}(r.P, H) \hat{e}(x_A P, \hat{H}) \\ &= \hat{e}(sP, Q_A) \hat{e}(U, H) \hat{e}(PK_A, \hat{H}) \\ &= \hat{e}(P_{Pub}, Q_A) \hat{e}(U, H) \hat{e}(PK_A, \hat{H}) \\ &= \hat{e}(P_{Pub}, Q_A), f(ID_A) \hat{e}(U, H) \hat{e}(PK_A, \hat{H}), f(ID_A) \end{aligned}$$

- Encryption only mode

If $ID_A = \varphi$, and $f(ID_A.h) = 0$ then

$$\begin{aligned} \hat{e}(P, W) &= \hat{e}(P, r.H) \\ &= \hat{e}(rP, H) = \hat{e}(U, H) = 1. \hat{e}(U, H).1 \\ &= \hat{e}(P_{Pub}, Q_A), f(ID_A) \hat{e}(U, H) \hat{e}(PK_A, H), f(ID_A) \end{aligned}$$

- Signature only mode

If $ID_A \neq \varphi$, and $f(ID_A) = 1$ then

$$\begin{aligned} (P, W) &= \hat{e}(P, D_A + r.H + x'_A H) \\ &= \hat{e}(P, D_A) \hat{e}(P, r.H) \hat{e}(P, x'_A H) \\ &= \hat{e}(P, sQ_A) \hat{e}(rP, H) \hat{e}(x_A P, \hat{H}) \\ &= \hat{e}(sP, Q_A) \hat{e}(U, H) \hat{e}(PK_A, \hat{H}) \\ &= \hat{e}(P_{Pub}, Q_A) \hat{e}(U, H) \hat{e}(PK_A, \hat{H}) \\ &= \hat{e}(P_{Pub}, Q_A), f(ID_A) \hat{e}(U, H) \hat{e}(PK_A, \hat{H}), f(ID_A) \end{aligned}$$

B. Security Analysis

Confidentiality proof of $IN - CLGSC$

Theorem 01 : Against above proposed (signcryption or encryption only mode) scheme if \mathcal{PPT} adversary $\mathcal{A-I}$ has non negligible advantage to win game ($IND - CLGSC -$

$CCA2 - I$) in random oracle model then $\mathcal{A-I}$ must be used algorithm B to solve a hard $GBDH$ problem as;

$$Adv_{CLGSC}^{IND-CCA2-I}(\mathcal{A-I}) \leq q_T Adv_{\Gamma}^{GBDH}(B, q_D^2 + 2q_D q_2 + q_2) + q_{SC}(q_{SC} + q_D + q_3 + 1)/2^k \quad (4)$$

Where $q_T = q_1 + q_x + q_{SK} + 2q_D + 2q_{SC} + 2$. Here $q_1, q_2, q_3, q_x, q_K, q_{SC}$ and q_D represents maximum queries which an adversary could place to H_1, H_2, H_3 , for full and partial private keys extraction as well as for, GSC and $UGSC$ oracles.

Theorem 02 : Against above proposed (encryption or signcryption only mode) scheme if \mathcal{PPT} adversary $\mathcal{A-II}$ has non negligible advantage to win game ($IND - CLGSC - CCA2 - II$) in random oracle model then $\mathcal{A-II}$ must be used algorithm B to solve a hard CDH problem as;

$$Adv_{CLGSC}^{IND-CCA2-II}(\mathcal{A-II}) \leq q_T Adv_{\Gamma}^{CDH}(B) + q_{SC}(q_{SC} + q_D + q_3 + 1)/2^k \quad (5)$$

Where $q_T = q_{PK} + q_{SK} + 2q_D + 2q_{SC} + 2$. Here q_{PK} represents maximum queries which an adversary can place multiple request for public key oracles.

C. Unforgeability of Proof $IN-CLGSC$

Theorem 03 :

$$Adv_{CLGSC}^{EUF-CMA-I}(\mathcal{A-I}) \leq q_T Adv_{\Gamma}^{GDH}(B, q_{2D} + 2q_D q_2) + (q_{SC}(q_{SC} + q_D + q_3 + 1) + 2)/2^k \quad (6)$$

where $q_T = q_1 + q_x + q_{SK} + 2q_D + 2q_{SC} + 1$ and various q' s are as .Against above proposed (signature or signcryption only mode) scheme if \mathcal{PPT} adversary $\mathcal{A-I}$ has non negligible advantage to win game ($EUF - CLGSC - CMA - I$) in random oracle model then $\mathcal{A-I}$ must be used algorithm B to solve a hard GDH problem as:

$$Adv_{CLGSC}^{EUF-CMA-I}(\mathcal{A-I}) \leq q_T Adv_{\Gamma}^{GDH}(B, q_{2D} + 2q_D q_2) + (q_{SC}(q_{SC} + q_D + q_3 + 1) + 2)/2^k \quad (7)$$

where $q_T = q_1 + q_x + q_{SK} + 2q_D + 2q_{SC} + 1$ and various q' s are as .

Theorem 04 : Against above proposed (signature or signcryption only mode) scheme if \mathcal{PPT} adversary $\mathcal{A-II}$ has non negligible advantage to win game ($EUF - CLGSC - CMA - II$) in random oracle model then $\mathcal{A-II}$ must be used algorithm B to solve a hard CDH problem as:

$$Adv_{CLGSC}^{EUF-CMA-II}(\mathcal{A-II}) \leq q_T Adv_{\Gamma}^{CDH}(B) + (q_{SC}(q_{SC} + q_D + q_3 + 1) + 2)/2^k \quad (8)$$

Where $q_T = q_{PK} + q_{SK} + 2q_D + 2q_{SC} + 1$ and few others q' s are as discussed before.

Note:The proofs of above theorems are similar to discussed in [4].

D. Cost Analysis

In public key cryptography, the standard notion of computational cost is the number of major operations like the elliptic curve scalar point multiplication (*ECPM*) in G_1 , the modular exponentiation computation ($M - Exp$) in G_2 and the pairing computation (*PC*). The communication overhead is the ciphertext size in bits.

The security and cost comparison of proposed and existing schemes (only four *CLGSC* schemes are there in existing literature up-to date) are presented in the following Tables 1 and 2.

TABLE I. SECURITY COMPARISON

Scheme	Security		
	IND-CCA2	EUFCMA	M-PKGC
Huifang et al.[11]	No	Yes	No
Kushwah and Lie. [12]	Yes	Yes	No
Zhou et al.[1]	No	Yes	No
Proposed IN-CLGSC	Yes	Yes	Yes

VII. CONCLUSION

Zhou et al. recently proposed a new certificateless generalized signcryption scheme and proved its security against *IND - CCA2* and *EUFCMA* in presence of Malicious-but-Passive Key Generation Center in random oracle model. We analyzed Zhou et al. scheme and unfortunately proved *IND - CCA2* insecure in encryption and signcryption modes in their defined security model. We also presented an improved scheme, provable secure in presence of Malicious-but-Passive Key Generation Center in random oracle model. The improved scheme is same cost as Zhou et al. scheme and feasible for scarce resource environment.

REFERENCES

[1] C. Zhou, W. Zhou, and X. Dong, "Provable certificateless generalized signcryption scheme," *Des. Codes, Cryptogr.*, vol. 71, no. July 2012, pp. 331-346, 2014.

[2] W. Diffie and M. Hellman, "New directions in cryptography," *IEEE Trans. Inf. Theory*, vol. 22, no. 6, pp. 644 - 654, 1976.

[3] R. L. Rivest, a. Shamir, and L. Adleman, "A method for obtaining digital signatures and public-key cryptosystems," *Commun. ACM*, vol. 21, no. 2, pp. 120-126, 1978.

[4] A. Shamir, "Identity-based cryptosystems and signature schemes," *Adv. Cryptol. CRYPTO 84, LNCS*, vol. 196, pp. 47-53, 1985.

[5] D. Boneh and M. Franklin, "Identity-Based Encryption from the Weil Pairing," in *Advances in Cryptology CRYPTO 2001, LNCS*, 2001, vol. 2139, pp. 213-229.

[6] S. S. Al-Riyami and K. G. Paterson, "Certificateless Public Key Cryptography," in *Advances in Cryptology-ASIACRYPT 2003, 2003*, pp. 452-473.

[7] Y. Zheng, "Digital signcryption or how to achieve cost (signature & encryption) <= cost (signature)+ cost (encryption)," in *Advances in Cryptology, CRYPTO'97, 1997*, pp. 165-179.

[8] M. Barbosa and P. Farshim, "Certificateless Signcryption," in *ACM symposium on Information, computer and communications security ASIACCS '08, 2008*, pp. 369-372.

[9] Y. Han, X. Yang, P. Wei, Y. Wang, and Y. Hu, "ECGSC: Elliptic Curve based Generalized Signcryption," in *Ubiquitous Intelligence and Computing, LNCS-4159, 2006*, pp. 956-965.

[10] S. Lal and P. Kushwah, "ID based generalized signcryption," in *Cryptology ePrint Archive, Report 2008/084. http://eprint.iacr.org (2008)*, 2008, pp. 1-26.

[11] J. Huifang, H. Wenbao, and Z. Long, "Certificateless generalized signcryption," in *Cryptology ePrint Archive, Report 2010/204. http://eprint.iacr.org, 2010*.

[12] P. Kushwah, "Efficient Generalized Signcryption Schemes," *Theor. Comput. Sci.*, vol. 412, no. 45, pp. 6382-6389, 2011.

[13] L.-D. Liu, H.-F. Ji, W.-B. Han, and L. Zhao, "Certificateless Generalized Signcryption Scheme," *Phys. Procedia*, no. 33, pp. 962 - 967, 2012.

[14] C. P. R. S. Sharmila Deva Selvi, S. Sree Vivek, "Cryptanalysis of Certificateless Signcryption Schemes and an Efficient Construction without Pairing," in *Information Security and Cryptology, LNCS Volume 6151, 2010*, pp. 75-92.

[15] M. H. Au, Y. Mu, J. Chen, D. S. Wong, J. K. Liu, and G. Yang, "Malicious KGC attacks in certificateless cryptography," *ASIACCS 2007 Proc. 2nd ACM Symp. Information, Comput. Commun. Secur.*, pp. 302-311, 2007.

[16] Y. H. Hwang, J. K. Liu, and S. S. M. Chow, "Certificateless public key encryption secure against malicious KGC attacks in the standard model," *J. Univers. Comput. Sci.*, vol. 14, no. 3, pp. 463-480, 2008.

[17] H. Xiong, Z. Qin, and F. Li, "An Improved Certificateless Signature Scheme Secure in the Standard Model," *Fundam. Informaticae*, vol. 88, no. 1-2, pp. 193-206, 2008.

[18] J. Weng, G. Yao, R. H. Deng, M. R. Chen, and X. Li, "Cryptanalysis of a certificateless signcryption scheme in the standard model," *Inf. Sci. (Ny)*, vol. 181, no. 3, pp. 661-667, 2011.

[19] Li, Fagen, Hui Zhang, and Tsuyoshi Takagi. "Efficient signcryption for heterogeneous systems." *IEEE Systems Journal* 7.3 (2013): 420-429.

[20] Li, Fagen, Yanan Han, and Chunhua Jin. "Practical access control for sensor networks in the context of the Internet of Things." *Computer Communications* 89 (2016): 154-164.

[21] Niu, Shufen, et al. "An Efficient Heterogeneous Signcryption Scheme from Certificateless to Identity-based Cryptosystem." *MATEC Web of Conferences*. Vol. 139. EDP Sciences, 2017.

[22] Caifen, Wang, et al. "Efficient Heterogeneous Signcryption Scheme in the Standard Model." *Journal of Electronics & Information Technology* 39.4 (2017): 881-886.

TABLE II. COST COMPARISON

Scheme	Computational Cost						Cipher text Size
	<i>CLGSC</i>			<i>CLUGSC</i>			
	<i>ECPM</i>	$M - Exp$	<i>PC</i>	<i>ECPM</i>	$M - Exp$	<i>PC</i>	
Huifang et al.[11]	3	2	0	1	1	2	$ m +2 G_1 + ID + G_2 + P $
Kushwah and Lie. [12]	2	3	0	1	3	2	$ m +2 G_1 + ID + G_2 $
Zhou et al.[1]	1	4	0(+1)	0	1	4(+1)	$ m +2 G_1 $
Proposed IN-CLGSC	1	4	0(+1)	0	1	4(+1)	$ m +2 G_1 $

Efficient Energy Utilization in Cloud Fog Environment

Babur Hayat¹, Muhammad Nauman Ali², Sheraz Yousaf³, Mudassar Mehmood⁴, Hammad Saleem⁵
University of Lahore, Gujrat Campus

Abstract—Cloud computing provides various kind of services like storage and processing that can be accessed on-demand when required. Despite its countless benefits, it incorporates some issues too that limits the full adaption of cloud and enjoy its various benefits. Mainly the issue faced during the adaptability of cloud infrastructure is high latency and unawareness of location. To overcome these issues the concept of fog computing is introduced to reduce the load on the cloud and improve the allocation of resources. The fog provides the same services as the cloud. The main features of fog are; location awareness, low latency, and mobility. However, increasing the use of IoT devices, also increase the usage of Cloud. Fog environment. So, much usage of fog getting attention of researcher about energy consumption. In this paper, we try to solve the problem of energy consumption in terms of resources allocation by applying the load balancing algorithms and compare its result with the energy models.

Keywords—Energy efficiency; fog computing; cloud computing; load balancing; resources allocation

I. INTRODUCTION

The readers have to know about cloud computing, fog computing, and load balancing algorithm to understand the problem. So, cloud computing is a network or pool of physical and virtual resources over the internet, rather than personal hardware and soft- ware. We simply say that cloud is a delivery of computing services such as network, storage, database, and software over the internet. Need to pay for access the cloud services for using purpose. The architecture of cloud computing is -referred to its components and sub components. Fog architecture is described as in Fig. 1.

It can describe in four layers. First one is Front-end, it consists of the client-side devices. The second one is the back end, it consists of the servers that providing the services mean where the data is stored. It contains the cloud resource that demanded by the user. The third one the median between client and server it consists of software, web browser or the virtual session. It can be also called the middle-ware. And the fourth one is consists of the cloud-based delivery and networks. There are different cloud base deliveries Software as a Service (SaaS), Development as a Service (DaaS), Data as a Service (DaaS) and Platform as a service (PaaS). In SaaS, the client did not need to install any specific software required to connect to the server. Software service is already installed on the server side. Development as a service (Daas) is consisting of development tools. Data as a Service (Daas) is also considered as the subset of software in which cloud data is accessed by using APIs. Platform as a Service is service provide by cloud computing and it provides the service like as Platform and database as a service.

Fog computing extends the concept of cloud computing that contributes a productive solution to manage the fastly growing smart devices by simply adding the data to the edge of the network. Fog computing is introduced to reduce the load on cloud computing and fog have some features which are location awareness, low latency, and response faster compare to cloud. Fog is placed at the edge of networks and provides the fast transfer of cloud service and its appropriate architecture divided it in three-layer. The bottom most layer is consist of a client device that needed the service to utilize. It consists of mobile devices, clients, robots and any device that needed the cloud services and can connect to the fog computer. The Middle layer is consisting of the network that is used by server and clients to share services. The network layer consists of components like as router, switches, gateways and base station. And the third is the server layer mean cloud layer that provides the services.

Load balancing algorithms that can be used to intelligently to balance the load of client access requests across servers pool. The load balancing has some functions it distributes client requests or network load efficiently across multiple servers, ensures high availability and reliability by sending requests only to servers that are online, and provides the flexibility to add or subtract servers as demand dictates. The main problem in the server now a days are load and its distribution. Some node is too busy to process the data and some are not utilizing their resource. In load balancing, technique data is the load of data divided between the server in proper manners that every server should utilize its maximum resource and avoid latency. And there many load balancer algorithm that manage the load in an efficient way that is the Routers and Switches that intercept the data to a target server and redirect the traffic or send it to servers that are available [4]. The load has dynamic nature mean it varies with time so it depends on the end user client request. So when some server is overloaded we use load balancing technique to utilize the unutilized server. There are several factors should be considered for the load balancing that is the total load, scalability of servers, throughput, a performance of the system, interaction between the servers, amount of work to be transferred and selection of best nodes. The load can be a network, virtual or CPU load and load balancing can also be done through in many ways like as dynamic or static and centralized and non-centralized. In the static technique, we have a record of the past load and we apply the technique on the basis of the previous record while in dynamic load balance we focus on the current data and processed on the current based. So, dynamic is better than the static.

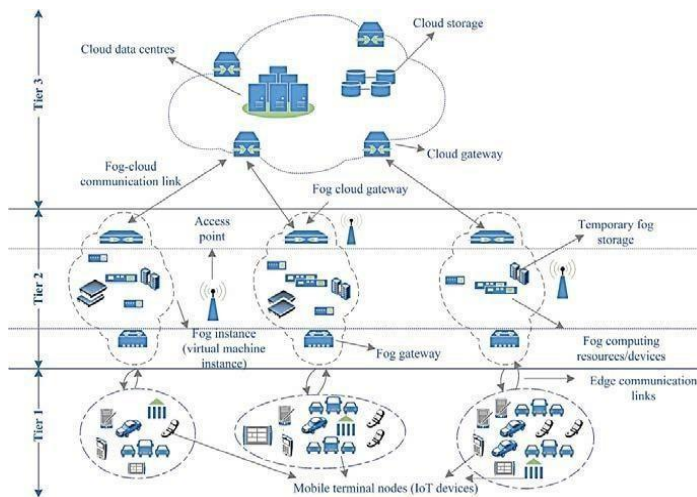


Fig. 1. Fog Architecture [3].

As we maintain the work burden on the cloud by adding the fog in the network but the as with the increasing rate of IoT devices we have to reduce the energy consumption on the fog computing. When the end user request for the resource from fog, during that time energy consumption can reduce by efficient allocation of re- source and here we are trying to solve the problem of resource utilization with respect to energy consumption. The energy consumption is based mostly on two things. The type of data to process and the requests and the energy consumption at the request level further is divided into three types. First is when the request is sent by the end user to the fog or received by fog. The second one is when the request is then processed by the fog and the third one is when fog requests the data from the cloud. Our focus is on the energy consumption of fog when it processes the request.

A. Motivation

Information technology plays an important role in computing. With the increase in the number of IoT devices, the request of resources increases on the cloud-fog [1]. So request response time, resources utilization and energy consumption have been critical issues nowadays. Fog computing act as a mid-layer between the end user and cloud that allocate the resources according to the request of the users which is closer to the end user to optimize the response time [2]. On the other hand, load balancing is one of the important technique to allocate the resources and optimize the response time. And we want to improve resources allocation for reducing energy consumption by using load balance techniques.

II. RELATED WORK

The authors in [5], used matching game formulation to minimize the energy consumption in fog computing. In this formulation, matching game acts as a player between fog and devices.

According to authors the outcome of this model matching game that explained as a task of devices. The matching game scheme obtained the performance through effective coordination between fog and devices that connect with one

another and choose their methodology dependent on the current conditions, the usage of the Fog content accessibility and the resource allocation management and putting away to get better execution. The authors say in this work proposed a matching game approach to deal with accomplishing low-energy utilization in IOT and fog condition. The authors made utilization of cache technology and fog computing to enhance energy efficiency.

The authors in [6], introduced an investigation of fog computing as an answer for expanding the demand for IoT gadgets and focus on the energy utilization, quality of services. The authors contributing to investigating an issue of energy utilization of the fog computing with regards to IOT applications and proposed an energy-delay solution for the cloud-fog is an efficient computing model where resource, storage, and network infrastructure can be shared as a service through the internet. For this purpose the authors adopt the two optimization method which is BIP algorithm and improved the GA to solve the problem.

In [7], the authors propose a cloud and fog based condition for the management of energy. The goal of the author's energy cost minimization, carbon release minimization and to adjust to risky transmission supportable sources are destinations of this work. The authors developed a cloud-fog based structure for the viable management of the purchases request. Fog gives low idleness benefits as it is put near the end customer layer and can respond rapidly to customers' request. MGs are set near each fog which fulfills the power essentials by keeping up the supportability of structures. Response time and request changing time are enhanced using the BA. In this paper [8], the authors' cloud-fog based condition for effective energy management is proposed. Simulation in Cloud Analyst is performed to look at and analyze the execution of load balancing algorithms like Round Robin, Throttled, and Weighted Round Robin. Simulations results demonstrated that Throttled load balancing algorithm gives preferred reaction time over RR and WRR.

The authors in [9], consider the layer of architecture consists of edge, fog and cloud layers. At different layers, processing and forwarding data by devices power are consumed differently. The problem arises here how to identify which machine learning steps to be performed at which layer to minimize the energy consumption. The authors proposed fog based Ubicomp system consisting of edge, cloud and fog layer. An Ubicomp system which is consists of different units which is sensing, communication, processing, and storage. The authors present fog based architecture of Ubicomp system and analyze the energy consumption on the edge, fog and cloud devices by complete the system. Ubicomp has different devices which are sensing, processing devices and relay devices. The relay device forwards the data within the same layer and other layers in the network. The sensing devices can collect the data on edge devices from different sensor and total data transmitted by a sensor for Ubicomp application. The Ubicomp applications also divide machine learning steps into data processing step and machine learning steps for figuring the results through processing devices.

The authors in [10], concentrated on a cloud-fog based model is proposed for resource management in SG. The objective of this study is the efficient utilization of re-sources. The authors inspected the advantages and opportunities of cloud-fog to help resource management in the SG. In addition, a model is proposed to interface these spaces. The authors play out the assessment regarding processing time, reaction time and cost minimization. Later on, the authors intend to improve the usage of cloud-fog based SG, which incorporate more services and features. As the cloud and fog advance quickly engaged with SG to build productivity, there is a requirement for devices to analyze and study the advantage of the innovation. Summary of related work is described in Table I [10]:

In [11], the authors talked about resources allotment in the cloud-fog condition. The proposed system IST effectively assigns the resources to DCs and satisfies the DS request. The authors focus is around the allotment of VMs to DCs. The effectiveness of IST is figured by looking at the response time and Cost. It very well may be seen from the finished up results that the expense of the fog and cluster is nearly the equivalent. The response time of IST is same as the response time of the RR algorithm. Minimal effort and response time show the unwavering quality of this framework. Later on, the authors to crossover RR and IST process the execution of the present situation and furthermore in the wake of rolling out improvements in the present as well.

In [12], the authors plan to think about different energy effective procedures for the cloud which utilizes resources allotment and solidification to accomplish the equivalent. Further, the authors attempt to change the current procedure by including an additional parameter. The fundamental point of the author's works creates viable approaches and algorithms for virtualized data farms. Furthermore, attempt to reduce energy utilization with boosting the resource usage. The authors propose to include an additional parameter viz. time alongside cost, which may bring about boosting resources usage and limiting the number of running servers. The proposed thought is yet to be executed and tried in different constant or reenactment condition before its wide acknowledgment.

In [13], the authors focused issues of migrating virtual machines (VMs) among various physical hosts is crucial for resource use and carbon dioxide (CO₂) minimization in cloud data centers. The proposed method CPU Utilization Variance (CUV) depends on choosing the best VMs from over utilized

servers and moving them into different servers to spare the used resources and not to damage the SLA built up between clients and cloud service provider. Server link is a methodology used to reduce the total number of utilizing servers that an organization requires. Static VM combination techniques are not recommended to implement the experiments, in this way unique consolidation strategies should be utilized to enhance the resources use. In this paper, the proposed procedure is executed on a large scale server farm made out of 800 physical hosts. The results obtained by CloudSim apparatus are as far as energy utilization in KW/hour, execution in Million Instructions for every Second (MIPS), a number of VM relocations and SLAV. The recreation results demonstrate that CUV algorithm has a number of VM allocations and energy utilization superior to in future, the authors intend to build up the proposed algorithm to get the finest results of performance and SALV normal results. The authors implement all investigations in real cloud organization using nearly open- source apparatuses like OpenStack which these days have a critical use in distributed computing situations.

In [14], the authors discuss the load management algorithms that are often used in cloud computing. After that, the authors perform an experiment by using one load balance technique on a VM in cloud computing. The method is tested in a cloud computing condition. It has two options to test the first option is to use real tests like Amazon EC2, and the second is to use a simulation tool to simulate the cloud environment. In this paper, it can be seen that load balancing is an essential viewpoint on the execution of existing distributed computing. Since a load of the demand from clients is specifically and moving. What's more, after that from this examination, the authors presume that the throttled algorithm utilized in load balancer in cloud computing recreations utilizing Cloud Analyst is the typical response rate is still inside the ordinary range among user-base 1 and the other. Be that as it may, in regards to the base normal and greatest response.

The world is distributed in regions shown in Fig. 2, and the every region has its own id given in Table II [14]. **Paper Organization:** The remaining part of this paper is divided in a category as: In Section 3, literatures has been discussed. Section 4 discussed the load balancing algorithm, Section 5 discussed the proposed approach, Section 6 discussed the experiment, evaluation setup and Section 7 discussed conclusion.

TABLE I. SUMMARY OF RELATED WORK

Authors	Proposed Algorithm	Infrastructure	Evaluation Process	Method Proposed for	
				Energy Efficiency	Resources Allocation
Assila et al.[5]	Matching Game	Fog	Cloud Analyst	Yes	Yes
Meberk et al.[6]	IGA	Fog	System	Yes	No
Zafar et al.[7]	BA	Cloud-Fog	Cloud Analyst	Yes	Yes
Nacem et al.[8]	RR,WRR,Throttled	Cloud-Fog	Cloud Analyst	Yes	No
Saraswat et al.[9]	ML	Cloud-Fog	Mathematical Analysis	Yes	No
Zahoor et al.[10]	RR,PSO,Throttled	Cloud-Fog	Cloud Analyst	No	Yes
Sharif et al.[11]	IST	Cloud-Fog	Cloud Sim	No	Yes
Patel et al.[12]	MaxUtil	Cloud	Theoretical Analysis	Yes	Yes

TABLE II. REGION DISTRIBUTION

Region	Region Id
North America	0
South America	1
Europe	2
Asia	3
Africa	4
Oceans	5

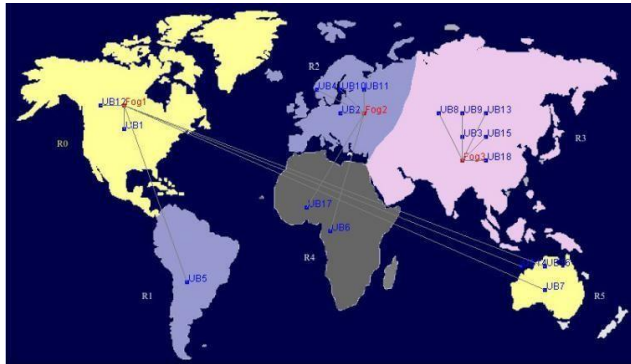


Fig. 2. Regions

III. LOAD BALANCING ALGORITHMS

Load balancing algorithms have an important role in the cloud fog environment. These algorithms are used to distribute the resource Received by the data center efficiently. In this paper, three load balancing algorithm are considered which are described are as follows:

1) *Round Robin (RR)*: Round Robin is a time-sharing technique. It stores the entry of the user request with respect to arrival time in the table. It equally shares the time among the virtual machine. That makes the balance between the virtual machines.

2) *Throttle (TT)*: Throttle working is different from the round robin. It checks the type of request and analyzes the virtual machines. And allocate the resource to that machine which has the capacity to full fill the task efficiently. This algorithm saves the state of every virtual machine in the table. The request received by the data center, it sends it to the load balancer. The load balancer checks the type of request and the virtual machines available to perform this task. If any machine is available then allocate the task to a virtual machine else it has to wait for the virtual machine.

3) *Active VM*: In the Active VM, the request received by the data center is stored in the queue. The data center checks the availability of the virtual machines. If the virtual machine available, then assigns the task to it and request removed from the queue. When the task is completed by the virtual machine, it will be available to perform another task.

We use these benchmarks because we want to compare our pro-posed algorithm performance with the previous algorithms results.

IV. PROPOSED APPROACH

The energy consumption in fog is on three steps: 1) Receiving re- quest from end user, 2) Process the request, 3) Send request to cloud for resource but we focus on the second one which processing of the request. When request is received by the fog it check the VM’s and send request to selected VM to process request. Our contribution here is to manage the sending of data for processing to VM’s. We improve the Active VM load balance algorithm by adding threshold and sorting to manage this request, and consume less energy. This algorithm will check the VM distance, latency, processing speed and load then send request to the appropriate one. From this approach all virtual machines are utilized and burdens divided among the all machines which reduce the energy consumption. Before our algorithm the other only provide the list machine, the virtual machine was not managed in any order. So a machine on top can used more than one time as non-utilize machine will be not utilized until the first one complete its capacity. But in our Algorithm as a request is sent to the fog it receives and checks the status of the Virtual machines and takes account of those machines that’s lies between the fixed thresholds, then machines are sorted according to their status and the request is process with which have low load of data. As the algorithm checks the status of every VM on every request the sorting of the VM give the less consumed VM and the system utilize it. Which puts the non-utilize virtual machine on top. A request received by fog. Firstly, it checks the type of data or service requested. Then check the machine which relates to it, then check each virtual machine status and compare the latency ratio and available virtual machines, then send the request to the appropriate one which has less burden and consume less time. In this scenario, we can say that more time saved and the less energy consumed as shown in Fig. 3.

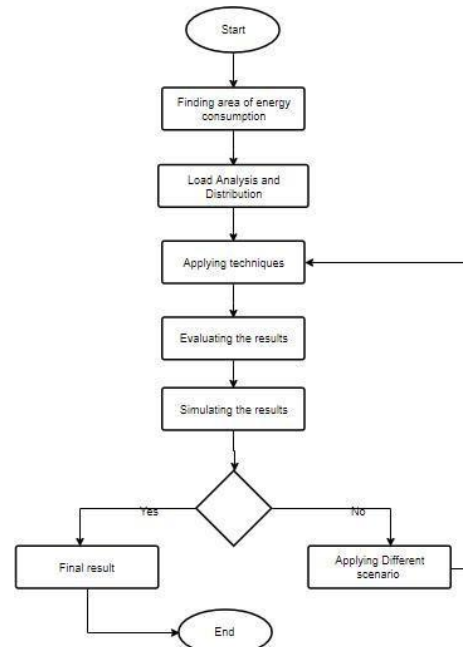


Fig. 3. Proposed Work.

A. Algorithm

The main working of the IAVM is discussed above, the pseudocode of the algorithm describes the working of the main part of algorithm.

Algorithm 1 IAVM

```

1: VMlist
2: Calculate :Load ,VmCapacity
3: VM List VirtualMachines
4: while(VMlist!=null):
5: if VM list < threshold then
6: VM Stack virtualmachine
7: close;
8: VM Stack.sort()
9: allocatedVm(VMStack.index)
    
```

In the first step, the load and capacity of every virtual machine are stored in the virtual machine list. Then a threshold sets to save those virtual machines into the stack that's been able to perform the given task, after that the virtual machines in the stack are sorted according to their capacity and availability. In the end, the resource is allocated to the virtual machine on the top and to other respectively.

V. EVALUATION AND EXPERIMENTS

We perform the experiments on the different simulator to test our assumptions. The example of one test that we performed is given below. We created six fog nodes on different location and they all are connected and each fog node contains the 6 virtual machine. We set the request sent to each server after five minutes. The size of the single request is 100 bytes and the request size varies after some time. Three algorithms are used to compare which are RR,

Throttle and Active VM: After saving the configuration we put the simulator for the simulation of result for 24 hours and save the results after simulation. Simulators evaluation is described in Table III.

The facts about the experiment are:

$$\text{Energy} = \text{No. of KWh} \times \text{Cost of one kWh.}$$

TABLE III. SIMULATORS EVALUATION

Simulation Time	24 Hours.
Service Broker Policy	Closest Data Center

Cost model is described in Table IV [7]:

Data center hardware is mentioned below in Table V [12]:

Data center virtual machine specification is described below in Table VI [7]:

TABLE IV. COST MODEL

VM cost	0.1 per hour.
Memory Usage Cost	0.025 per second.
Data Storage Cost	0.05.
Storage Cost	0.05.

TABLE V. DATA CENTER HARDWARE CONFIGURATION

Processors on physical machine	2.
Processing power	75 MIPS.
Storage devices	75 GB.
Memory	1 GB.
Internal bandwidth	5000 Mbps.

TABLE VI. DATA CENTER VIRTUAL MACHINE SPECIFICATION

RAM	512 MB.
Storage	5 GB.
Architecture	x86.
Operating system	Linux.
Virtualization technique	Xen.
Bandwidth	5000 MBPS.

Firstly, we check the Service response time by performing the experiments on the Cloud Analyst. There are many tests that are performed and in each test, the data on every machine varies with time and simulate these results and to compare our result with previous studies. We compare our algorithm with the different load balancing algorithm.

1) Cost: We test the cost analysis by varying different parameter. The experimental results show that if the cost of the data centers the same for all then the total cost is the same for the improved algorithm and comparative algorithms. But if we make difference in the cost of the data center, then the cost of the RR and Throttle is increased but the total cost of the IAVM is decreased. So, it proves that our algorithm is cost efficient.

2) Response time and energy: After cost analysis we check the SRT (Service Response Time) and the NL (Network Latency). We perform our experiments on the cloud analyst. And for energy we perform experiment on ifogsim shown in Fig. 4 [11].

In both experiment we varies the parameter that effect the performance like as number of machine, data load and data center cost. The overall results shows that the new purposed algorithm performs best in most of scenarios. The result can be seen in Fig. 5 and 6 [11].

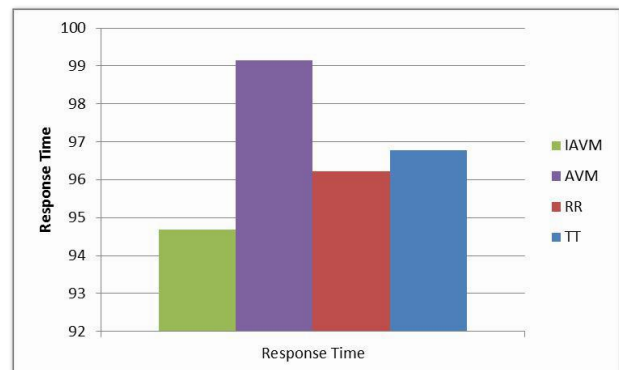


Fig. 4. Avg Response Time.

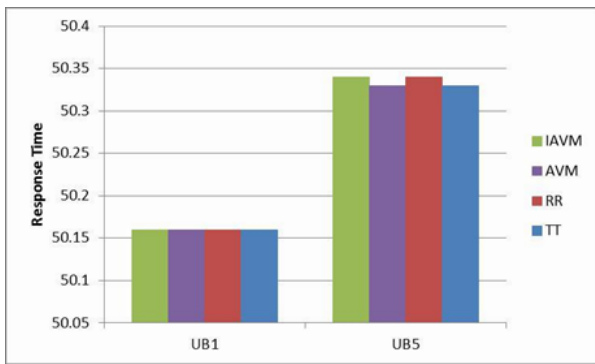


Fig. 5. Response time for user base 1 and 5.

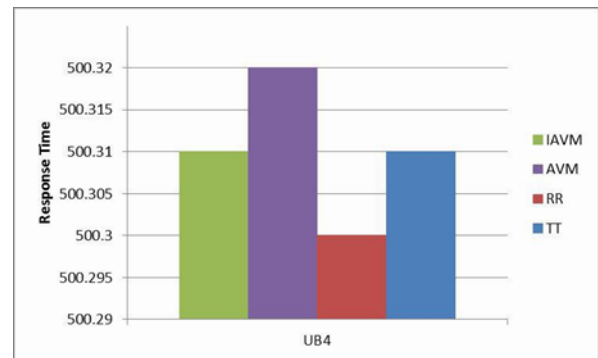


Fig. 8. Response Time for user base 4.

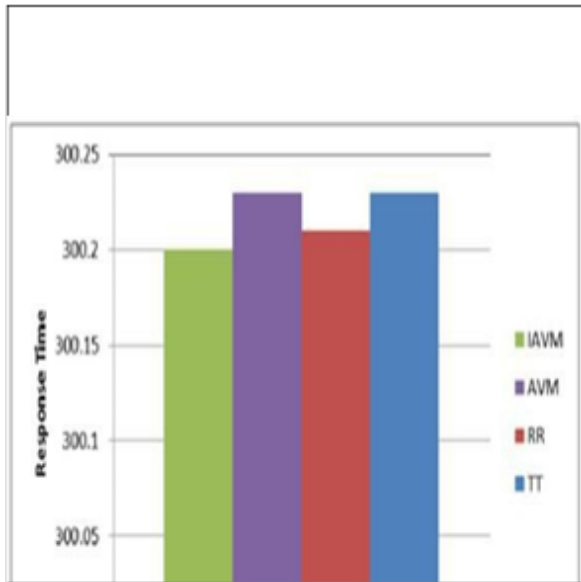


Fig. 6. Response Time for user base 3.

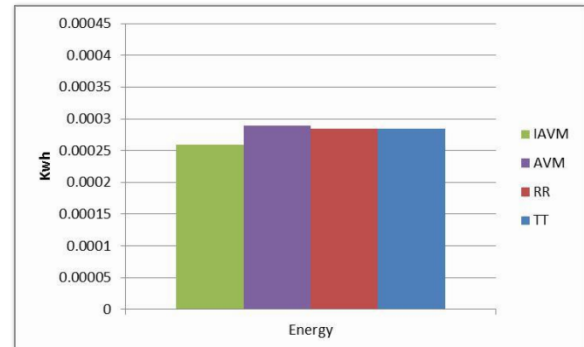


Fig. 9. Energy Consumption.

VI. CONCLUSION

Due to the most advantages, the fog computing is becoming famous and the increase in the IoT devices increase the load on the fog computing. Due to the more the more processing, the power and energy consumption in cloud fog environment have become an issue due to the ecological and economic reasons. In this paper, we have presents an algorithm which distributes the resource in fog computing efficiently and minimizes the energy consumption in the cloud fog environment. The research results show that the purposed algorithm performs better than other. This paper will be helpful for efficient use of the resource in the cloud fog environment, which improve its performance in minimizing the energy consumption in Fog computing.

REFERENCES

- [1] Okay, F. Y., Ozdemir, S. (2016, May). "A fog computing based smart grid model." In Networks, Computers and Communications (ISNCC), 2016 International Symposium on (pp. 1-6). IEEE
- [2] Chiang, M., Zhang, T. (2016). "Fog and IoT: An overview of research opportunities." IEEE Internet of Things Journal, 3(6),854-864
- [3] Naas, M. I., Parvedy, P. R., Boukhobza, J., Lemarchand, L. (2017, May). iFogStor: "an IoT data placement strategy for foginfrastructure. In Fog and Edge Computing (ICFEC)", 2017 IEEE 1st International Conference on (pp. 97-104). IEEE
- [4] Verma, M., Yadav, N. B. A. K. (2015). "An architecture for load balancing techniques for Fog computing environment." International Journal of Computer Science and Communication, 8(2),43-49.
- [5] Assila, B., Kobbane, A., Walid, A., & El Koutbi, M. (2018, May). "Achieving low-energy consumption in fog computing environment: A matching game approach." In 2018 19th IEEE Mediterranean Electrotechnical Conference (MELECON) (pp. 213- 218). IEEE.
- [6] Mebrek, A., Merghem-Boulahia, L., & Esseghir, M. (2017, October). "Efficient green solution for a balanced energy consumption and delay in

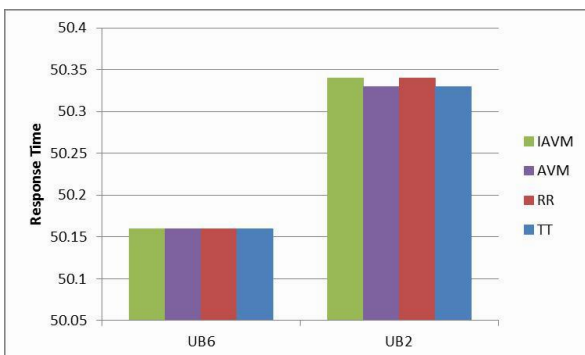


Fig. 7. Response Time for user base 2 and 6.

- the IoT-Fog-Cloud computing." In Network Computing and Applications (NCA), 2017 IEEE 16th International Symposium on (pp. 1-4). IEEE.
- [7] Zafar, F., Javaid, N., Hassan, K., Murtaza, S., Rehman, S., & Rasheed, S. (2018, September). "Resource Allocation over Cloud-Fog Framework Using BA." In International Conference on Network-Based Information Systems (pp. 222-233). Springer, Cham.
- [8] Naeem, M., Javaid, N., Zahid, M., Abbas, A., Rasheed, S., & Rehman, S. (2018, September). "Cloud and Fog Based Smart Grid Environment for Efficient Energy Management." In International Conference on Intelligent Networking and Collaborative Systems (pp. 514-525). Springer, Cham.
- [9] Saraswat, S., Gupta, H. P., & Dutta, T. (2018, January). "Fog based energy efficient ubiquitous systems." In Communication Systems & Networks (COMSNETS), 2018 10th International Conference on (pp. 439-442). IEEE.
- [10] Zahoor, S., Javaid, N., Khan, A., Muhammad, F. J., Zahid, M., & Guizani, M. (2018). "A cloud-fog-based smart grid model for efficient resource utilization." In 14th IEEE International Wireless Communications and Mobile Computing Conference (IWCMC-2018).
- [11] Sharif, M. U., Javaid, N., Ali, M. J., Gilani, W. A., Sadam, A., & Ashraf, M. H. (2018, September). "Optimized Resource Allocation in Fog-Cloud Environment Using Insert Select." In International Conference on Network-Based Information Systems (pp. 611-623). Springer, Cham.
- [12] Patel, K., Patel, N., & Patel, H. (2016, March). "Efficient Resource Allocation Strategy to Improve Energy Consumption in Cloud Data Centers." In Proceedings of the Second International Conference on Information and Communication Technology for Competitive Strategies (p. 76). ACM.
- [13] Selim, G. E. I., El-Rashidy, M. A., El-Fishawy, N. A. (2016, February). "An efficient resource utilization technique for consolidation of virtual machines in cloud computing environments." In Radio Science Conference (NRSC), 2016 33rd National (pp. 316-324). IEEE.
- [14] Ramadhan, G., Purboyo, T. W., Latuconsina, R. (2018). "Experimental Model for Load Balancing in Cloud Computing Using Throttled Algorithm." International Journal of Applied Engineering Research, 13(2), 1139-1143.